International Journal of Engineering Works (IJEW)

OPEN ACCESS

ISSN E 2409-2770
ISSN P 2521-2419

IJEW

VOL. 6-2019

Printable Version Vol. 6 Issue 01-12, Page: 01-575

Managing Editor: Dr. Irfan Jamil
Chief-In-Editor: Prof. Isak Karabegovic

www.ijew.io/

https://www.ijew.io/rss/2020

Editorial Board

Table of Content

Minimization of Losses and Improving Stability of High Tension Network using Load Flow Analysis
Vol. 6, Issue 07, PP. 235-243, July 2019

A Survey Report on MultiiLevel-Inverter Topologies
Vol. 6, Issue 07, PP. 228-234, July 2019

Energy Efficient and CO2 Absorbing Concrete Material
Vol. 6, Issue 07, PP. 224-227, July 2019

Insulated Concrete Blocks Using Plastic Waste and Steel Fibers
Vol. 6, Issue 07, PP. 221-223, July 2019

Application of Polyvinyl Acetate (PVAc) in Dye Sensitized Solar Cells (DSSC) as Electrolyte in The Presence of Acetonitrile as Highly Soluble Organic Solvent And KI Iodide As Inorganic Redox Salt
Vol. 6, Issue 07, PP. 217-220, July 2019

Modeling and Simulation of a Novel Module for Thermoelectric Power Generation from Solar Photovoltaic Panels
Vol. 6, Issue 06, PP. 212-216, June 2019

Pyrolysis of Chickpeas Waste and Peanut Shells for the Production of Oil and its Analysis
Vol. 6, Issue 06, PP. 208-211, June 2019

Production of Liquid and Solid Fuel by the Technique of Microwave Pyrolysis of Scrap Tires and its Analysis
Vol. 6, Issue 06, PP. 202-207, June 2019

Impact of Urban Infrastructure Development on Power Loss of Solar Photovoltaic Modules
Vol. 6, Issue 06, PP. 196-201, June 2019

Novel Control Technique for Control of Circulating Current in Modular Multilevel Converters
Vol. 6, Issue 06, PP. 192-195, June 2019

Energy Audit: A Case Study of UET Jalozai Campus
Vol. 6, Issue 05, PP. 187-191, May 2019

Denoisation of ECG Signal using JADE and FAST ICA Comparison
Vol. 6, Issue 05, PP. 182-186, May 2019

Power Quality Enhancement in Distribution System using Dynamic Voltage Restorer
Vol. 6, Issue 05, PP. 176-181, May 2019

Conventional and Rubberize Concrete Cylinders Filled with PVC Tube
Vol. 6, Issue 05, PP. 172-175, May 2019

Enhance and Maintain Efficiency of Solar Panel using Auto Cleaning System
Vol. 6, Issue 05, PP. 159-163, May 2019

Enhancement of Dynamic Performance of Transmission Line using Static Synchronous Series Compensator
Vol. 6, Issue 05, PP. 164-171, May 2019

Research on Charging and Discharging of Lithium Ion Battery based on Temperature Controlled Technique
Vol. 6, Issue 05, PP. 153-158, May 2019

Techniques to Mitigate Problem of Partial Shading and Soiling on PV Module: A Review
Vol. 6, Issue 05, PP. 148-152, May 2019

IJEW 国际工程期刊 International Journal of Engineering Works انجینیرنگ کاموں کا بین الاقوامی جرنل

Welcome to

Online Manuscript Submission

If you are a first time users, please visit the submission home (www.ijew.io) and read the information before registering for an account. If you are an experienced user, please log in and proceed the steps. If you experience any problems, please send email info@ijew.io.

About the IJEW:

International Journal of Engineering Works (IJEW) is the official, monthly peer-reviewed journal affiliated Kambohwel Publisher. IJEW serves as an international forum for sharing ideas and deliver information between all engineering studies and reflecting common challenges in engineering and technology professional academic sectors including industries.

Bibliographic Information:

ISSN: 2409-2770 (Online)

ISSN: 2521-2419 (Print)

Int.j.eng.works

DOI Prefix: 10.34259

Journal DOI: 10.34259/ijew

Managing Editor: Dr. Irfan Jamil

Cheif-In-Editor: Prof. IsK karabegovic

www.ijew.io

IJEW

Contact Info

+92-333-5244035

+92-061-6520357

info@ijew.io

International Journal of Engineering Works
ISSN-p: 2521-2419
ISSN-e: 2409-2770
Vol. 6, Issue 01, PP. 1-5, January 2019
https://www.ijew.io/

Millimeter Wave Antenna Using Microstrip Patch

Muhammad Nauman[1], Syed Waqar Shah[2], Bilal Mehmood[3], Faizan Alam[4]
engr.nauman001@yahoo.com[1], waqar.shah@uetpeshawar.edu.pk[2], bilal1208@gmail.com[3], faizan.alam100@yahoo.com[4]
[1,2,3,4]University of Engineering and Technology Peshawar, Pakistan

Received: 06 December, Revised: 12 December, Accepted: 01 January

***Abstract*—** This paper is propose to design a MM-Wave antenna using Microstrip patch for 5G communication. The proposed antenna is design by using CST Studio. This simulation tool enables us to anlyze and record different parameters of the antenna in ral time simulation like the gain, effieciency, bandwidth, return losses directivity and many other parameters as well. The 5th Generation of communication technology is most probable being implemented in 2020 around the globe. The work done in this field of communication is so far up to smaller, compact, efficient and less coastly antennas whicn can provide high bandwidth with high gain. The goal of this work is to design an antenna with more greater bandwidth which can be utilize for 5th generation communication in the futurea and by varying the design of the patch it is seen that different parameters of the antenna also improved.

***Keywords*—** MM-Wave Antennna using Microstrip patch, high bandwidth, CST Studio, 5G Communication, High frequency

I. Introduction

Modern age is the age of communication especially wireless communication. With the beginning of 21st century wireless communication has seen unexpected modifications. If we study mobile phone services of last fifteen years we will come to know that there is a tremendous change in their services regarding data rate, size, graphics and other quality services without compromising on the performance of the wireless communication. The rapid increase of smart phones and high data rate with high bandwidth is creating unprecedented challenges for wireless services providing companies to overcome the bandwidth issue and also other security issues. As we know that now a day's wireless communication companies are trying their best to provide high quality services regarding bandwidth and data rate with the minimum possible cost.

Wireless services provider's needs to tackle the ever growing exponential rate of data rate to the consumer and also the increase in traffic predicted. As we know that first generation cellular networks were the basic analogue system only design to provide the voice communication services. The digital modulation, time division and code division multiple access and the importance of efficient spectral efficiency is realized in the second generation of cellular network system.

High speed packet access (HSPA) and wideband code division multiple access (W-CDMA) is introduced in the third generation of cellular communication in which high internet speed with multimedia functions like video calling and online streaming is required. In third generation wireless communication system frequency spectrum ranges from 700MHz to 2.6GHz. High speed download packet access (HSDPA) and high speed upload packet access (HSUPA) both are also a feature of 3G cellular communication which helps and improves the protocols utilization of WCDMA and provide us a better telecommunication system [3].

There is a lot of engineering efforts to develop more power efficient RFIC's upto 60GHz and industrial standards is also develop such as Wireless HD technology, ECMA-387 etc, integrated circuit transceivers are also available for some of the standards to achieve their targets of high gain and efficiency. Many of these technologies were also use for millimeter wave (MM-Wave) spectrum [2].

II. Literature Review

An antenna is the interference among radio waves propagating through space and electric currents moving in a conductor used with a transmitter and receiver. In the transmitter side transmitter a radio transmitter supplies an electric current to the antenna terminal and that antenna converts that electric current into and electromagnetic wave and radiates it while at receiver ends an antenna catches some of that radiated power of the electromagnetic wave in order to produce an electric current at its terminal which is feed to the receiver for amplification. Antennas are fundamental device for radio communication, cell phones, television broad casting, satellite communication, and so many other communication systems [1].

An antenna is an array of elements that is connected electrically to the transmitter and receiver. In the process of transmission an oscillating current is applied to the antenna by a transmitter in result it generates oscillating electric and magnetic field around the elements of antenna. As we know that these fields are time-varying and it radiates energy away from the antenna into the space as a transverse electromagnetic field wave.

At receiver end oscillating electric and magnetic field of an incoming radio wave exerts force on the electron of antenna elements causing them to move back and forth as a result creates an oscillating current in the antenna.

There are mainly two types of antenna i.e. Omni-directional antenna and directional antenna [4]. Omni-directional antenna transmits and receives waves in all horizontal directions equally while in directional antenna it mostly transmits waves in a specified direction. One of the best features of antenna is that if an antenna is design for transmission it will be the same for receiving.

A typical micro-strip patch antenna is usually rectangular or square. For certain reasons, such a design has advantages but the shape of the patch is not limited to a these shapes and may differ according to the application it is used for. Some of the paper present circular antennas with coaxial feed and show good results for a specific frequency range. In [6], a tri-band patch antenna for Wi-Max applications has been proposed. The three operating frequencies of the antenna are 2.4, 5.2 and 5.8 GHz and have a very large impedance bandwidth ranging from 3.1 to 9.0 GHz. This shows that the typical monopole antennas used for wideband applications have some drawbacks. Figure 2 shows a typical rectangular micro-strip patch antenna for a single band.

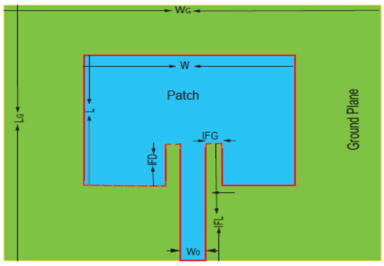

Figure 1: A typical Rectangular Micro-strip patch antenna

In figure 1, the blue region shows the patch. This square patch antenna has a feed line at the bottom and the width and length of the antenna is mentioned as 'w' and 'l' in the figure. Some other important parameters such as Wg, Lg IFL, IFG, IFD and W0 represent the dimensions that are important for the antenna to acquire maximum radiation. Wg and Lg however represent the width and length of the entire antenna respectively. Keeping in mind these parameters, the center frequency, bandwidth, and gain etc can be adjusted.

In a micro-strip patch antenna, the width of the antenna is given by

$$W = \frac{C}{2f_0\sqrt{\frac{\varepsilon_r+1}{2}}} \tag{1}$$

Given the center frequency, we can calculate the width of the patch by using equation (1).

A. MICROSTRIP PATCH ANTENNA

It all began in the early fifty's when Deschamps gave the idea for Microstrip radiator. But Gutton and Baissinot French technicians were the first who generate a patented archive on Microstrip patch antenna in 1955. Howell and Munson was the first two scientists who implemented Microstrip patch antenna practically [6].

The first most application of Microstrip patch antenna was implemented in missile called sidewinder at data link side designed by Munson. After that it was used in a semi active detective side seeker sprint missile.

Great developments is seen the applications and implementation of patch antenna in 1960's and 1970's. After that it starts functioning on high frequencies and with solid state equipments. Munson was working as a defence officer in the ball Aerospace laboratory at the time of cold war so he would have access to all of the advance facilities [7].

B. BASIC OPERATION OF PATCH ANTENNA

A patch antenna usually operates at three different stages i.e. one is the patch element which is the radiating element of the antenna lying at the top of the antenna substrate, while the feed line is at one end of the patch of antenna which provides power to the antenna and at the end ground plane lies on which substrate is put on top of it. In order to vary different properties and circuitry of the antenna like gain, bandwidth, efficiency, far field regions, spectrum etc the dielectric constant and its thickness must be change[8].

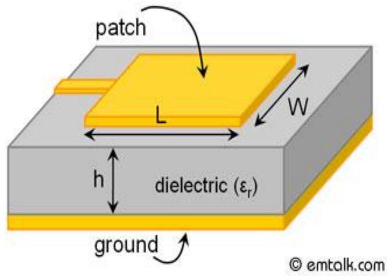

Figure 2 Basic Patch Antenna

These different parameters are discuss below

- ***Dielectric Constant*:** The bandwidth of the antenna depends on the dielectric constant of the antenna substrate if the permittivity of the antenna dielectric is low then it will has a wider value of impedance bandwidth with smaller value of excitation wave of antenna surface.
- ***Thickness of Antenna Substrate*:** It has a direct relationship with the bandwidth of the antenna and inversely proportional to the coupling level of the antenna. If the substrate of the antenna is thick it means it will has a wider bandwidth and similarly with a small value of coupling level of the antenna.
- ***Patch Length*:** The frequency at which antenna resonates is determined by the length of the patch of the antenna.
- ***Patch Width*:** The width of the patch is inversely related to the resonance frequency of the antenna.

C. INVERTED-F ANTENNA

Simple F-antenna is basically derived from the basic quarter wave monopole antenna. It was first invented in the 1940. In inverted-F antenna the feed line does not connected directly to the base but an intermediate point along with the length of the antenna and the ground and base are connected with one another. The benefit of doing such geometry is that it the input impedance of the antenna is completely dependent on the distance of the feed line from the ground end and the area between the feeding point and ground plane is behaving like a short circuit stub. In simple we can match the antenna input impedance with the system impedance by simply adjusting the position of the feed point [9].

After that inverted-L antenna in which the feed line is bent over and goes parallel along with the ground plane and it is a simple monopole antenna. The main two advantages of inverted-L antenna are that it is shorter in length and is compatible with most of the devices. But the most important drawback of the inverted-L antenna is low impedance of the antenna just a few ohms.

The inverted-F antenna has the advantages of both antennae i.e. the F-antenna and the inverted-L antenna collectively which is the compactness of inverted-L antenna and impedance matching of F-antenna [13]. The inverted-F antenna is that type of antenna which is used in the communication systems. It has basic two parts one is the monopole antenna and other one is the ground plane which is grounded at one end and they both are parallel to one another. This antenna is being powered (feed) by an intermediate point at a distance from the grounded end. Such a design is smaller and compatible. Also the manufactures can control the impedance matching by simply varying the feeding point distance without the need of extra impedance matching components [8].

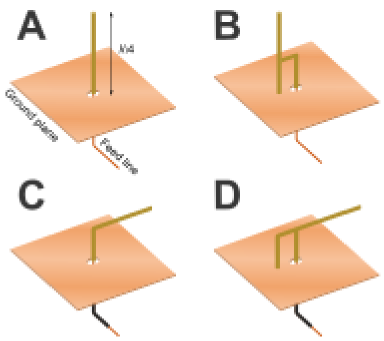

Figure 3 Inverted F-Antennas

A: Quarter Wave Monopole antenna
B: Intermediate Fed Quarter Wave Monopole Antenna
C: Inverted-L Antenna ***D: Inverted-F Antenna***

D. PLANAR INVERTED F-ANTENNA

The planar inverted-F antenna or PIFA is the advancement in the inverted-F antenna used in wireless circuitry implemented on the Microstrip. This format is compatible with the modern communication devices. PIFA can be implemented as the classic inverted-F antenna on one side of the circuit where the ground plan is being removed from beneath [6].

Another method is of the patch antenna. In this method one fringe or some transitional point is being grounded through pins or through ground plane. If patch of the antenna is short it means antenna will have wider bandwidth compare to thin line type due to greater radiation area. Mostly PIFA is printed on their own board or on some dielectric material hooked with the main board [14].

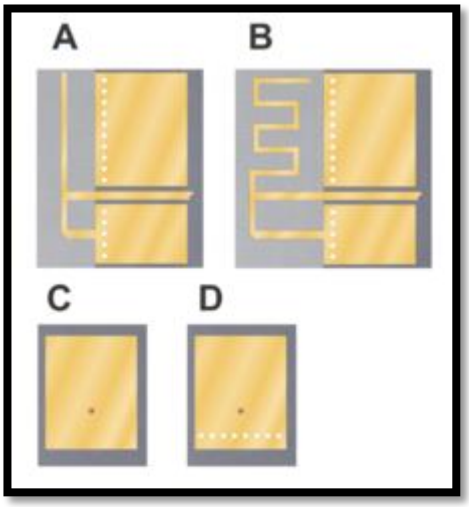

Figure 4 Planar Inverted F-Antennas

A: Printed Inverted F-Antenna
B: Meandered Printed Inverted F-Antenna
C: Patch Antenna
D: Planar Inverted F-Antenna (PIFA)
Board without Ground Plane
Board with Ground Plane
Antenna Feed Pin ***Ground Pin***

III. COUPLED MICROSTRIP PATCH ANTENNA

Both designing and functionality of Microstrip patch antenna were rapidly elaborating and improving in 1970's while in 80's the array antenna element structure and its architecture is completely changing in terms of both designing and modelling. Another research was also on going at that time to improve other qualities of antenna like bandwidth, efficiency, gain, spectrum etc [8].

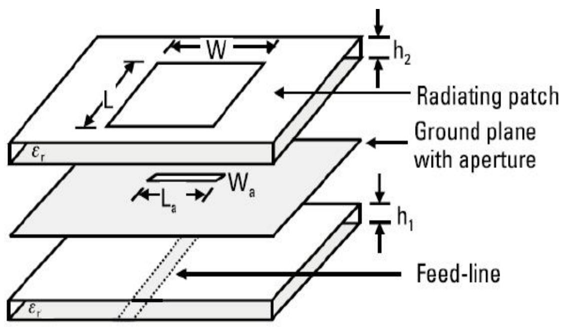

Figure 5 Coupled Microstrip Patch Antenna

A. MULTI-BAND ANTENNAE

A multiband antenna consist of four different patches i.e. a ground patch , first radiating patch, second radiating patch, and last one is the connecting patch. The function of the connecting patch is that it connects the two radiating patches with the ground patch and also with the feeding source. These all patches and feeding source collectively form a loop antenna as shown in figure.

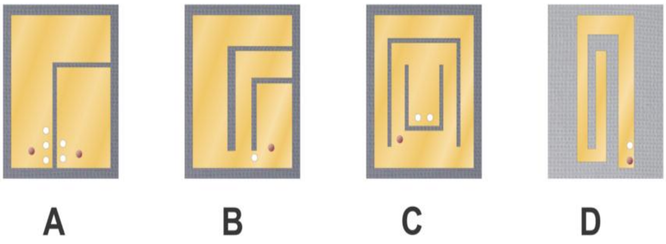

Figure 6 Inverted Multi-Band F-Antenna

A multiband antenna is design to perform different operation at same time at different resonating frequencies. A multiband antenna has the features of different antennas together. The need for multiband antenna is due to the need of greater bandwidth and different features of communication devices like video calling and surfing at same time or surfing at very high data rate etc [15]. A multiband antenna is composed of printed antenna and decoupling network. One of the key characteristic of the antenna is radiation efficiency or simply called antenna efficiency is defined as the ratio of the radiated power of antenna to the input power of the antenna. Antenna having high efficiency has most of input power radiated while a low efficiency antenna absorb its input power mostly as losses or reflect it because of the mismatch impedance.

$$\varepsilon_R = \frac{P_{radiated}}{P_{input}}$$

B. MILLIMETER WAVE SPECTRUM (Releasing THE 3 to 300 GHz spectrum)

Before the millimeter wave spectrum all communication like Amplitude Modulation / Frequency Modulation Radio, HD Television, Cellular Communication, satellite communication, GPS etc all are using a narrow frequency spectrum known as the sweet spot because of its favourable propagation characteristics in commercial wireless application and that sweet spot of frequency ranges from 300MHz to 3GHz respectively. The area of radio frequency spectrum greater then 3GHz is still not completely explored for commercial wireless operations. However a small portion of above 3GHz is being utilized for short range and fixed wireless communication. For example 3.1GHz to 10.0GHz is being used in personal area network as UWB for high data rate. There is another band in the range of 57GHz to 64GHz also called oxygen absorption band is used in some local area networks to provide data rates in gigabits for confidential purposes and security and also for some priority operations. Also LMDS which is local multiple distribution system is using a frequency band between 28GHz to 30GHz for fixed broadband and point to multipoint technologies for high data rate [2].

The spectrum range up to 252GHz is suitable for mobile communication and there is a tremendous feature of millimeter waves that they are absorbed in oxygen and water vapours in the atmosphere. The frequency range of 57 – 67 GHz is oxygen absorption and 164-200 GHz is the water vapour absorption by the atmosphere. We simply exclude these two bands from the wireless communication as the communication in these bands is very much limited. Millimeter wave broad band spectrum promises us to provide a band up to 100GHz for mobile communication which is 200 times greater spectrum than we are currently using for wireless communication [3].

C. FREE SPACE PROPAGATION OF MILLIMETER WAVES

The transmission losses in the millimeter wave are measured as free space losses. One of the greater delusion of wireless engineers is that the free space losses of a wave depends on the frequency of the wave i.e. greater frequency will propagate less compare to smaller frequency. The logic behind that delusion is some engineer’s textbook that path loss of transmission loss is calculated at specific frequency between two isotropic antennas is lamda by two ($\lambda/2$). Whose area aperture effectiveness increases with the wavelength and decreases with the carrier frequency [2].

An antenna with more apertures has bigger gain than a smaller antenna because with larger aperture the antenna will abduct more energy from the radio wave that passes compare to a smaller antenna.

IV. PENETRATION AND OTHER LOSSES OF MILLIMETER WAVES

As the spectrum of millimeter waves are from 3-300GHz and the penetration losses and other losses like atmospheric gases and water vapours losses are not greater than a few dBs per kilometre excluding the bands of oxygen absorption and water vapour absorption. As we know that the losses occurs due to reflection and diffraction completely depends on the nature of material and surface area. But as reflection and diffraction minimize the range of the millimeter waves and also it entertain and helps in the communication without line of sight or non line of sight communication. The signals of millimeter waves do not penetrate easily among the solid material compare to low frequency signals.

Table Material and Their Losses at 1 to 2 GHz

Material	**Loss**
Porous concrete	6.5 dB
Reinforced Glass	8.0 dB
Concrete (30 cm)	9.5 dB
Thick Concrete Wall (25cm) with Large Glazed Panes	11.0 dB
Thick Concrete Wall (25cm) without Large Glazed Panes	13.0 dB
Thick Wall (>25cm)	15.0 dB
Tile	23.0 dB

The above mention table of losses is only for frequency of 1 to 2Ghz respectively.

CONCUSLION

The main theme behind this research is to design and antenna small and compact which can eliminate future bandwidth and high frequency issues most probably of 5G communication and also analyze its different parameters like return losses, radiation pattern , gain etc. The design antenna can provide performance that support the proposed structure but the performance of the antenna can also improved further with fine tunning and material whose relative permittivity is low.

REFERENCES

[1] Rappaport, Theodore S., Shu Sun, Rimma Mayzus, Hang Zhao, Yaniv Azar, Kevin Wang, George N. Wong, Jocelyn K. Schulz, Mathew mimi, and Felix Gutierrez Jr. "Millimeter wave mobile communications for 5G cellular: It will work!." IEEE access 1, no. 1 (2013): 335-349.

[2] Rappaport, Theodore S., Shu Sun, Rimma Mayzus, Hang Zhao, Yaniv Azar, Kevin Wang, George N. Wong, Jocelyn K. Schulz, Mathew Samimi, and Felix Gutierrez Jr. "Millimeter wave mobile communications for 5G cellular: It will work!." IEEE access 1, no. 1 (2013): 335-349.

[3] Rappaport, Theodore S., Shu Sun, Rimma Mayzus, Hang Zhao, Yaniv Azar, Kevin Wang, George N. Wong, Jocelyn K. Schulz, Mathew Samimi, and Felix Gutierrez Jr. "Millimeter wave mobile communications for 5G cellular: It will work!." IEEE access 1, no. 1 (2013): 335-349.

[4] Rappaport, Theodore S., Shu Sun, Rimma Mayzus, Hang Zhao, Yaniv Azar, Kevin Wang, George N. Wong, Jocelyn K. Schulz, Mathew Samimi, and Felix Gutierrez Jr. "Millimeter wave mobile communications for 5G cellular: It will work!." IEEE access 1, no. 1 (2013): 335-349.

[5] Zhao, Hang, Rimma Mayzus, Shu Sun, Mathew Samimi, Jocelyn K. Schulz, Yaniv Azar, Kevin Wang, George N. Wong, Felix Gutierrez, and Theodore S. Rappaport. "28 GHz millimeter wave cellular communication measurements for reflection and penetration loss in and around buildings in New York City." In Communications (ICC), 2013 IEEE International Conference on, pp. 5163-5167. IEEE, 2013.

[6] Zhao, Hang, Rimma Mayzus, Shu Sun, Mathew Samimi, Jocelyn K. Schulz, Yaniv Azar, Kevin Wang, George N. Wong, Felix Gutierrez, and Theodore S. Rappaport. "28 GHz millimeter wave cellular communication measurements for reflection and penetration loss in and around buildings in New York City." In Communications (ICC), 2013 IEEE International Conference on, pp. 5163-5167. IEEE, 2013

[7] Rappaport, Theodore S., Shu Sun, Rimma Mayzus, Hang Zhao, Yaniv Azar, Kevin Wang, George N. Wong, Jocelyn K. Schulz, Mathew Samimi, and Felix Gutierrez Jr. "Millimeter wave mobile communications for 5G cellular: It will work!." IEEE access 1, no. 1 (2013): 335-349.

[8] MacCartney, George R., Junhong Zhang, Shuai Nie, and Theodore S. Rappaport. "Path loss models for 5G millimeter wave propagation channels in urban microcells." In Globecom, pp. 3948-3953. 2013.

[9] Yngvesson, K. Sigfrid, T. L. Korzeniowski, Y-S. Kim, Erik L. Kollberg, and Joakim F. Johansson. "The tapered slot antenna-a new integrated element for millimeter-wave applications." IEEE Transactions on Microwave Theory and Techniques 37, no. 2 (1989): 365-374.

IJEW 国际工程期刊 International Journal of Engineering Works انجینئرنگ کاموں کا بین الاقوامی جرنل

International Journal of Engineering Works
ISSN-p: 2521-2419
ISSN-e: 2409-2770
Vol. 6, Issue 01, PP. 6-11, January 2019
https://www.ijew.io/

Modeling of Multi Junction Solar Cell and MPPT Methods

Rabia Bibi[1], Aftab Ahmad[2], Asfandyar Ali[3], Juveria Anwar[4], Tanvir Ahmad[5]
[1,3,4,5]USPCAS-E University of Engineering and Technology, Peshawar
[2]Pakistan Institute of Engineering and Applied Sciences
rabiakhan1294@yahoo.com[1]
Received: 06 December, Revised: 13 December, Accepted: 01 January

***Abstract*—** Multi Junction solar cells (MJSC) have gotten high attention in the concentrated PV systems because of its superior performance and high efficiency. MJSC have increased the concentration capacity of solar panels with a level greater than ever before. Compared to conventional silicon photovoltaic cell, MJSC have augmented 39.5% efficiency under similar atmospheric conditions. In this research work, two tasks have been performed, one is modeling and simulation of single, double and triple junction solar cell and the second one is modeling of MPPT methods. Graphical Results of MJSC modeling show approximately three times increase in power with using triple junction solar cell compared to conventional single junction solar cell. Constant voltage and perturb & observe maximum power point tracking (MPPT) techniques, that automatically adjust the switch duty cycle of converter are presented. Very simple and inexpensive analog PWM controllers are employed to continuously track the maximum power point of solar cell as the irradiance changes. The switch duty cycle is formed such that it automatically adjusts itself to produce maximum power as solar cell voltage changes. LTspice simulations are presented to demonstrate the effectiveness of proposed MPPT algorithms. Perturb & Observe method has a fast response, it takes 0.05s and gives smooth output initially. Constant voltage method takes 0.08s for simulation and it gives huge output initially. So perturb and observe method doubles the efficiency.

***Keywords*—**maximum power point tracking(MPPT); PWM; constant voltage; perturb & observe; multi junction solar cell;

I. Introduction

Renewable energy provides a better and clean alternative to fossil fuels. Solar energy is one of the most important renewable energy resources. It provides energy by capturing the solar radiation and converting it into electric energy by either running a steam turbine or by using photovoltaic cells. Photovoltaic cells are portable, easy assembly and flexible to suit most applications. Photovoltaic systems can be used in standalone and grid connected configurations [1]. Grid connected solar photovoltaic has reached 303 GW globally [2]. But photovoltaic systems also have some problems associated with it: Variability and lower efficiency. Electric power generated by solar arrays is continuously changing with weather conditions and solar irradiance and the V-I characteristic of photovoltaic panels have non linear dependence on irradiance and temperature [3]. In the V-I curve there is only one maximum power point and it changes continuously with the weather conditions. To extract maximum power from the solar panel the controller must set the panels to operate at this point thus increasing the efficiency of the system. These controllers are called maximum power point trackers (MPPTs). There are several techniques in literature to find the maximum power point for PV systems which include: incremental conductance method, perturb and observe method, fixed duty cycle method and constant voltage method [3]. If the MPPT controller could track the maximum power point accurately, the solar panels will be operating at its higher efficiency.

Perturb and observe, constant voltage and incremental conductance methods are the most commonly used algorithms used in MPPT controllers. Perturb and observe method employs the trial and error methodology and changes the terminal voltage and current of solar panels and compares the power output with the previous iteration. If the power increases it further changes the voltage and current in the directions otherwise it changes in the opposite direction until maximum power point is reached [4]. Constant voltage and constant current MPPT methods are simple and efficient.

Apart from MPPT, various issues also appear for solar cell itself like now, silicon the most prominent semiconductor due to its large vacancy in nature, cause it economical in designing and making the device. But, the silicon PV cell's efficiency is significantly low. Multi Junction solar cells (MJSCs) have gotten high attention in the concentrated PV systems because of its superior performance and high efficiency. MJSCs have increased the concentration capacity of solar panels with a level greater than ever before. Compared to conventional silicon photovoltaic cell, MJSC have augmented 39.5% efficiency under similar atmospheric conditions [5]. In this research work, two tasks have been performed, one is modeling and simulation of single, double and triple junction solar cell and the second one is modeling of MPPT methods.

Normally nowadays, the trend is towards microprocessor based tracking of MPPT which is expensive. In this paper, a simple, inexpensive and analog PWM controlling constant voltage and perturb & observe MPPT algorithms are developed in LTspice software.

II. GENERAL SCHEME OF PHOTOVOLTAIC (PV)

Fig. 1 describes the process of PV system.

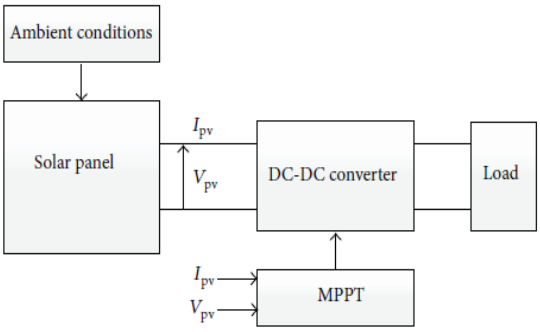

Fig. 1.General scheme of photovoltaic system

A. Simulation of Solar Cell

Solar cell model is simulated in LTspice as shown in fig. 2 to analyze its characteristics curves. Current-Voltage (I-V) and Power-Voltage (P-V) curves are called characteristics curves of PV cell. These curves are non linear in nature and shown in fig. 3. Results of simulation shows single junction solar cell gives maximum power of 2mW with V_{oc} of 0.31V and I_{sc} of 10mA.

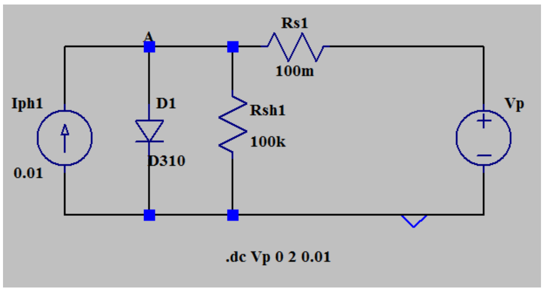

Fig. 2.LTspice model of solar cell

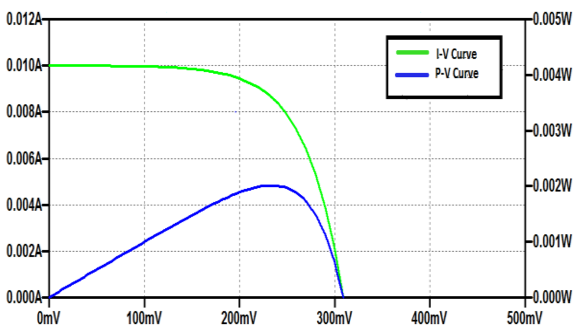

Fig. 3. I-V and P-V Curves of Solar Cell

B. Simulation of Double Junction Solar Cell

Fig. 4 shows circuit of double junction PV cell in which top layer is InGaP and bottom layer is InGaAs. The sub-cells are assembled in series with reduced energy gaps.

Table 1. Values of parameters for double junction InGaP/InGaAs solar cell

Parameter Value	**Top layer InGaP**	**Bottom layer InGaAs**
E_g(eV)	1.976	1.519
I_{sc}(mA)	6.5	7.8
N	1.97	1.75

Table 1 presents the values of parameters used in double junction solar cell modeling [5]. E_g is the activation energy or band gap energy of a diode and N is ideality factor. Fig. 5 shows that double junction of InGaP/InGaAs solar cell gives maximum power of 3.4mW with V_{oc} of 0.75V and I_{sc} of 6.5mA.

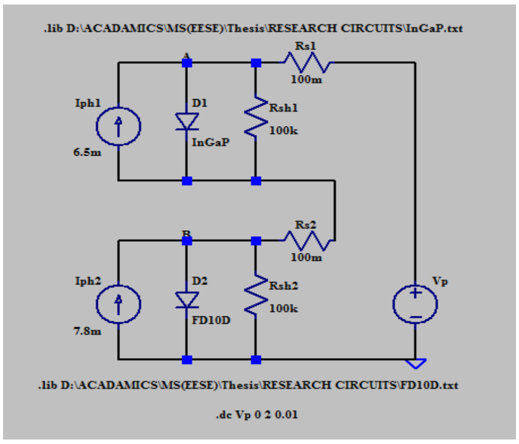

Fig. 4.LTspice model of double junction solar cell

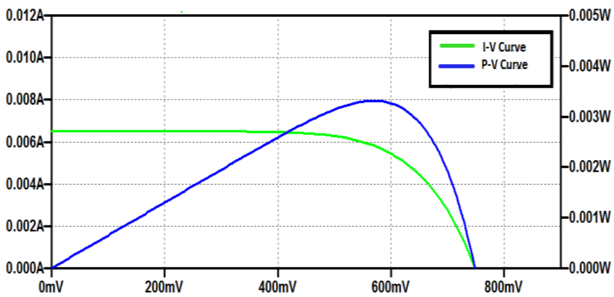

Fig. 5. I-V and P-V Curves of double junction Solar Cell

C. Simulation of Triple Junction Solar Cell

Bandgap variety isn't demonstrating the adequate decision. A perfect triple junction could deliver energy viably with composition of 1.976, 1.519 & 0.744 eV materials [5]. Consequently, AlAs is examined contain much big energy bandgap and could be replaced by InGaP. On account of that a three junctions PV cell designed by stacking InGaP, InGaAs, and Ge all together with measurement.

Table 2. Values of parameters for triple junction InGaP/InGaAs/Ge solar cell

Parameter Value	**Top/first layer InGaP**	**Second layer InGaAs**	**Third layer Ge**
E_g(eV)	1.976	1.519	0.744
I_{sc}(mA)	6.5	7.8	10.5
N	1.97	1.75	1.96

Fig. 6 shows spice model of this triple junction solar cell combination. Table 2 demonstrates the parameter's values utilized in triple junction cell modeling [5].

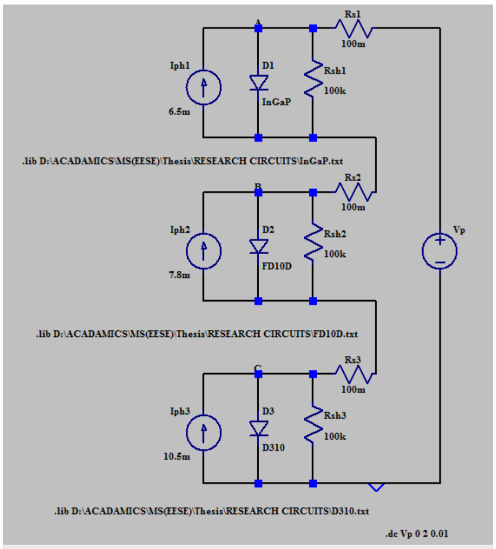

Fig. 6.LTspice model of triple junction solar cell

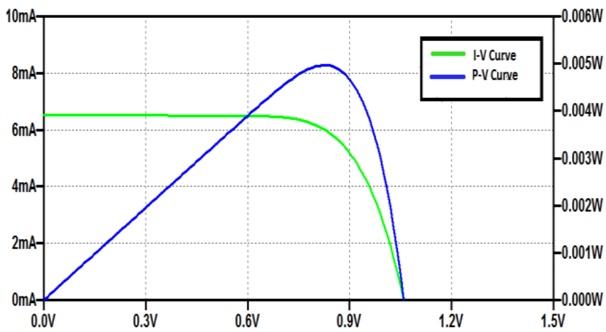

Fig. 7. I-V and P-V Curves of triple junction Solar Cell

Fig.7 shows that triple junction of InGaP/InGaAs/Ge solar cell gives maximum power of 5mW with V_{oc} of 1.05V and short-circuit current, I_{sc} of 6.5mA. This shows that power generated by triple junction solar cell is approximately three times greater than power generated by single junction solar cell.

III. MPPT METHODS

It is mandatory to get much accessible energy as could be expected from the PV cell to limit the energy price figure of PV system. An MPP tracker is utilized to discover the point when the MPP occurs. Various MPPT methods have been suggested by researchers but in this research, two widely used techniques are carried out for modeling.

A. Constant Voltage (CV) Method

This is the easiest MPPT method. The operating voltage of the panel is maintained close to a reference value, Vref. The value of reference voltage depends on the data provided by the manufacturer. In case of constant voltage method energy efficiency is increased as compare to no MPPT technique but it is used for optimization of only one ambient conditions. For other values of sun irradiance and temperature conditions, operational point will not overlap with maximum power point of IV curve. Thus by adjusting the duty cycle we can move operating point towards the MPP [6]. Fig. 8 shows block diagram of this method.

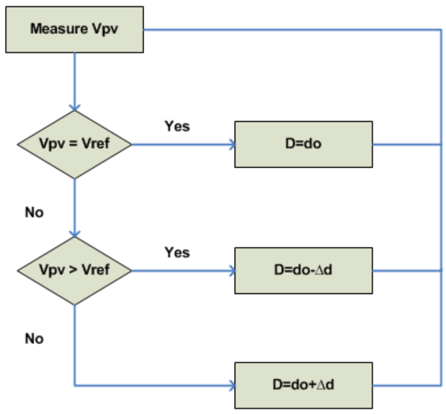

Fig. 8.*Block diagram of CV method*

1) LTspice model of CV method

Fig. 9 shows spice model containing solar cell, constant voltage MPPT method and boost converter with a resistive load.

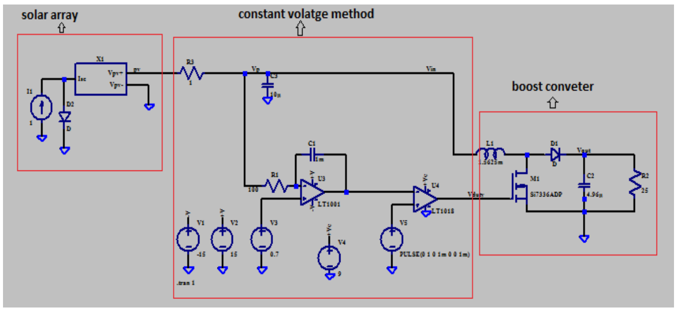

Fig. 9.*LTspice model of CV method*

In this method, PV cell output goes to boost converter as well as to integrator. Op-amp being used as an integrator holds the PV voltage. Capacitor in an integrator, initially charges and then supply voltage to the comparator, which is further compared with sawtooth signal to gives pulse width modulation (PWM) signal for the MOSFET gate switch present in boost converter. As PV voltages is changed, Duty cycle of PWM is changed and this set maximum power to the load.

2) Simulation Results

Constant voltage method model is simulated in LTspice. Simulation results shows variation of current and voltages of boost converter which include PWM, inductor current, input and output voltages.

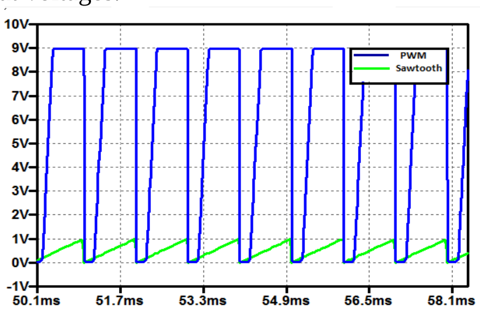

Fig. 10.*Generating PWM for switch with constant voltage method*

PWM generation is shown in fig. 10. When PV voltage is higher than saw tooth, comparator gives high and when low than it gives 0. Output voltage from solar array is shown in fig. 11 which is 1V while fig. 12 shows output of boost converter which is initially 5V and then goes to steady state which is 3.5V. The simulation time taken by constant voltage method is 0.08s. Fig. 13 shows inductor current of boost converter which works in CCM because does not go to zero.

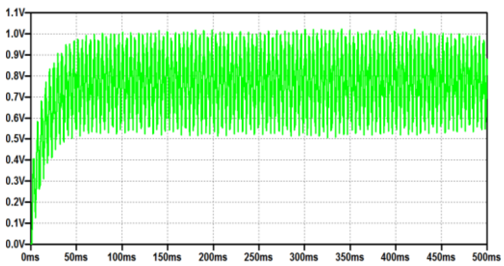

Fig. 11.*Output voltage from solar cell*

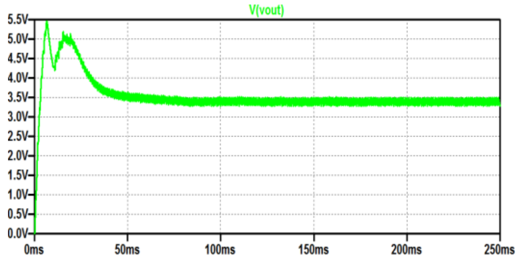

Fig. 12.*Output voltage from boost converter*

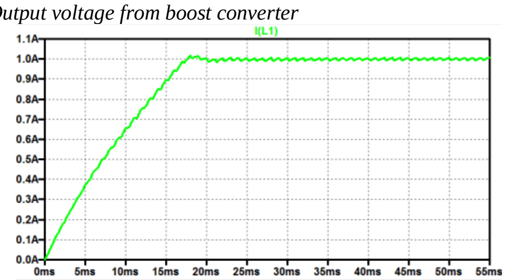

Fig. 13.*Inductor current of boost converter*

B. Perturb and Observe (P&O) Method

The algorithm starts by setting the computed maximum power P_{MAX} to an initial value (usually zero). Then at specific intervals, the actual PV current and voltage are measured and the current value of PV power, P_{ACT} is calculated. Then P_{ACT} and P_{MAX} are compared. If P_{MAX} is less than P_{ACT}, it is stored in the P_{MAX} as the new value. At every moment the P_{ACT} is computed, and the comparison is constantly carried out. The point when both are equal will be the point at which maximum power can be delivered to the load. The input impedance should be equal to the load impedance for maximum power transfer across the load. Fig. 14 shows block diagram of this method.

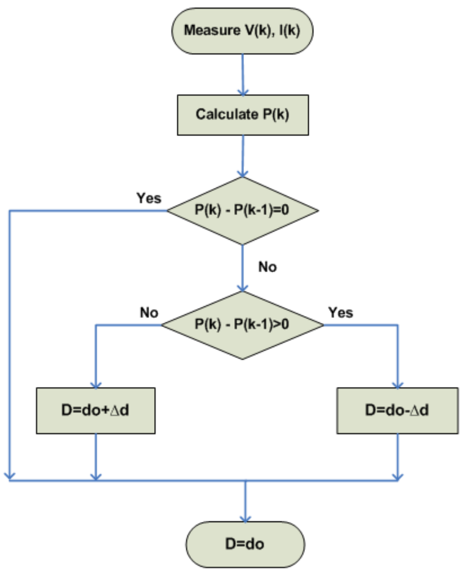

Fig. 14.*Block diagram of P&O method*

1) LTspice model of P&O method

Fig. 15 shown is spice model of Perturb and Observe MPPT method. In this method, Solar cell gives voltage Vp to boost converter and also Vp and Ip goes to M2 MOSFET which gives product of these two called power. After that this power goes to hold circuit which holds the previous value and then comparator compares the past and present value of power. The comparator output goes to circuit which determine the direction of power that either it is increasing or decreasing. It produces signal CNT which goes to Switches that produces the PWM signal for boost converter and it controls the power to a maximum level.

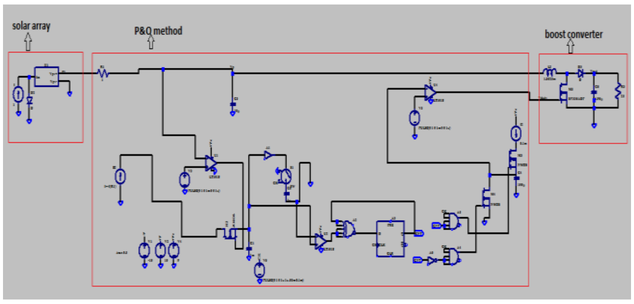

Fig. 15.*LTspice model of P&O method*

2) Simulation Results

Following waveforms are the simulation results of perturb and observe MPPT method. Fig. 16 shows the PWM signal which is the result of comparison of PV signal and sawtooth waveform. Fig. 17 shows output voltage of boost converter which shows that P&O method gives smooth output and takes less time, 0.05s which is approximately half of the time taken by CV method. Fig. 18 shows the variation in inductor current used in boost converter. One drawback is that this method adds oscillation to the inductor current.

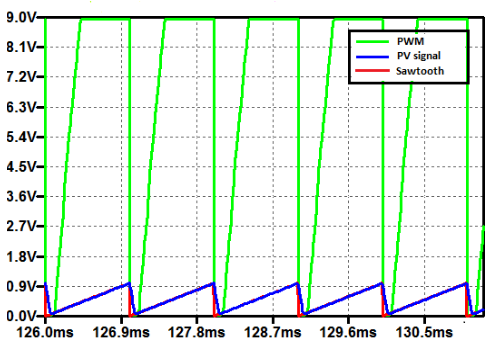

Fig. 16.*Generating PWM for switch with P&O method*

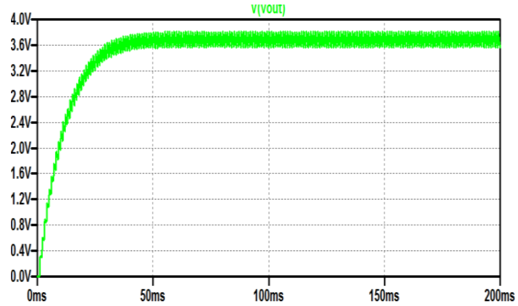

Fig. 17.*Output voltage from boost converter*

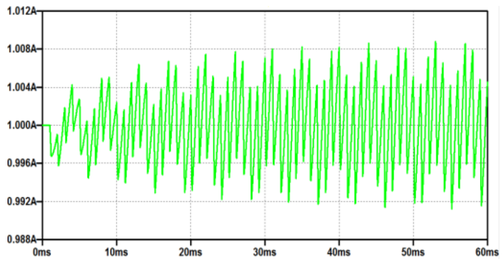

Fig. 18.*Inductor current of boost converter*

CONCLUSION

In this paper, two widely used MPPT methods, Constant Voltage and Perturb & Observe MPP algorithms were simulated in LTspice software. A simple and analog model of these algorithms is developed which is inexpensive compared to microprocessor based which are often expensive. Constant voltage method is easy to implement but reference voltage needs to be changed automatically. Perturb and Observe method is fast, accurate, medium implementation but it adds oscillations to the output. Perturb & Observe method has a fast response, it takes 0.05s and gives smooth output initially. Constant voltage method takes 0.08s for simulation and it gives huge output initially. So perturb & observe method increases the efficiency two times.

Apart from MPPT, the output power of triple junction PV cell is compared with single junction conventional silicon solar cell. Comparison shows approximately three times increase in power delivered from conventional silicon cell. This gigantic rise in output energy of Photo-voltaic verifies the supremacy of suggested technique that will be translated to significant cost depletion of the produced kWh.

ACKNOWLEDGMENT

A part of this work was carried out at Arizona State University (ASU) in the United State under the supervision of Dr. Bertan Bakkaloglu. The authors would like to acknowledge the efforts of the team at ASU who gave time to this research work. Also to USAID who funded this research work.

REFERENCES

[1] Kaundinya, D.P., P. Balachandra, and N. Ravindranath, "Grid-connected versus stand-alone energy systems for decentralized power—A review of literature". Renewable and Sustainable Energy Reviews, p. 2041-2050, 2009. **13**(8):

[2] Sawin, J.L., et al., "Renewables 2017 Global Status Report", 2013.

[3] Rezk, H. and A.M. Eltamaly, "A comprehensive comparison of different MPPT techniques for photovoltaic systems", Solar energy, **112**: p. 1-11,2015.

[4] Femia, N., et al., "Optimization of perturb and observe maximum power point tracking method", IEEE transactions on power electronics, **20**(4): p. 963-973, 2005.

[5] H. Rezk and E.-S. Hasaneen, "A new matlab/simulink model of triple-junction solar cell and mppt based on artificial neural networks for photovoltaic energy systems," *Ain Shams Engineering Journal*, vol. 6, no. 3, pp. 873–881, 2015.

[6] Liu, B., et al. "Analysis and improvement of maximum power point tracking algorithm based on incremental conductance method for photovoltaic array", Power Electronics and Drive Systems, PEDS'07. 7th International Conference on. 2007. IEEE,2007.

[7] Mohamed A. El-Sayed, Steven Leeb, "Evaluation of maximum power point tracking algorithms for photovoltaic electricity generation in Kuwait", international conference on renewable energies and power quality (icrepq'14), April 2014.

[8] A. M. Atallah, A. Y. Abdelaziz, and R. S. Jumaah, "Implementation of perturb and observe mppt of pv system with direct control method using buck and buckboost converters," Emerging Trends in Electrical, Electronics & Instrumentation Engineering: An international Journal *(EEIEJ)*, vol. 1, no. 1, pp. 31–44, 2014.

[9] Kennedy A. Aganah, Aleck W. Leedy, "A Constant Voltage Maximum Power Point Tracking Method for Solar Powered Systems", March 2011.

[10] Bibi Rabia, " Design of multi junction solar cell MPPT controller in LTspice", MS thesis.

International Journal of Engineering Works
ISSN-p: 2521-2419
ISSN-e: 2409-2770
Vol. 6, Issue 01, PP. 12-26, January 2019
https://www.ijew.io/

Analysis of Non-Standardized Traffic Calming Devices under Local Conditions of Pakistan

Saira Ramzan[1], Muhammad Jawed Iqbal[2]
[1,2]National Institute of Transportation, National University of Science & Technology, Islamabad
saira10engineer@gmail.com[1], drjawediqbal@scee.nust.edu.pk[2]
Received: 03 January, Revised: 16 January, Accepted: 21 January

***Abstract*—**The paper presents the issues regarding traffic calming devices in Pakistan. The problem is that no comprehensive analysis of the impacts of the traffic calming devices had been done previously.

The paper proposed answer to three questions: 1) What are the current practices of traffic calming devices in Pakistan 2) What guidelines and standard exist for installation of these devices? 3) What are the suitable measures for the execution of traffic calming devices?
To achieve these goals field survey and questionnaire survey was conducted in order to evaluate the current condition of traffic calming devices and to know the perception of general public about device suitability, quality and their agreement. Different agencies were visited which look after it and interviewed different officials to inquire about the design and maintenance of calming devices.
The major findings were: 1) Traffic calming devices are not constructed according to standard dimensions and there is lot of variations in implementation 2) Regulations regarding design, construction and installation of traffic calming devices are established at local level. 3) Suitable measures are suggested for the installation of traffic calming devices.

***Keywords*—** Traffic calming devices, Speed hump, Speed bump, Speed table, Steel stud

Abbreviations
TCD: Traffic calming device

I. Introduction

The term 'Traffic calming' has become the buzzword in the last decade throughout the nation. Speedy vehicles through residential areas, in an attempt to find ways to avoid congested arterial roadways, has become an issue for the safety of children. For that reason, traffic calming, specifically speed humps, are being installed as a solution to control these issues. For improving safety and quality of life of residents many countries have adopted different physical devices to prevent vehicular traffic in the occupant’s area. Traffic calming create the roads that are safer for pedestrian, bicyclist and public transport. But in many cases traffic calming devices are installed randomly without study where no proper design and particularly no reflectors, marking and advance warning signs are used. These devices are mostly constructed in a way that may cut the path of water over the pavement surface. So installation of these devices may create negative effects due to uncontrolled deceleration and acceleration of vehicular movements on the service level of roadway and it may be a factor in reducing the service life of pavement.

The use of traffic calming devices is not considered good engineering practice. As no study on this issue have been found till date so the prime objectives of the study are to find out:

1. Current practices of traffic calming devices in Pakistan.
2. Guidelines available for the implementation of traffic calming devices.
3. Departments involved in traffic calming planning and implementation and to recommend suitable measures to counter the negative impacts of traffic calming devices.

Based on literature research, these appeared to be key questions which had not been addressed before in any case study or survey. So the objective of the current study is to obtain the information on traffic calming devices with respect to above concerns. The viewpoint of road users, residents, traffic engineers and officials is taken into consideration. The review is not technically oriented as it does not include engineering aspects or scientific research methodology but the focus of study is to identify the ways by which these calming devices have been used in residential areas. Community acceptance and factors having effect on it are evaluated.

The study depends on three main sources of information: 1) field survey 2) a survey carried out via questionnaire 3) in depth interviews with agency personnel.

Following the introduction, the literature is described having focus on the countries which have documented experience with traffic calming devices. Most of the documentation came from United States.

II. LITERATURE REVIEW

TABLE I SUMMARY OF FINDINGS ABOUT TRAFFIC CALMING DEVICES

	Area	Year	Device	Results
1	Spain	2018	Speed kidney	The design of speed kidney moderates the speed and minimizes the emergency response delays and the maintenance, inconvenience caused to the passengers, damages to the vehicles, the noise and vibrations. [1]
2	Indonesia	2018	Speed hump	Speed reduction mean for standard speed hump is substantially larger than speed reduction mean for non-standard speed hump. [2]
3	Bangladesh	2018	Speed hump	Proper placement and dimension of the speed humps is an imperative requirement to be solved by government by providing guidelines, standards, and policy. [3]
4	Spain	2018	Various devices	Women have highest road traffic incident (RTI) rate in case of minor injuries while men have highest RTI in case of serious and fatal injuries. Motorcycles are most risky mode of transport while public transport is safest. [4]
5	Egypt	2017	Speed hump	Pavement conditions are greatly influenced by existence of speed humps and their characteristics. [5]
6	India	2016	Speed hump	Speed hump could harm the bicyclists, unless proper considerations for bicyclists are made. [6]
7	Lithuania	2016	Speed hump, Speed bump, Raised crosswalk	Fatal and injury accidents decreased by 60%. Injured decreased by 63% People killed decreased by 82%. [7]
8	China	2014	Speed hump	By comparing body acceleration, wheel ground adhesion index and wheel load the best speed limit range of the speed hump can be determined. [8]
9	Malaysia	2013	Speed hump	Speed hump significantly reduces the speed and capacity of road. [9]
10	Thailand	2013	Speed hump	Speed hump profile can be estimated correctly by using quarter car model. [10]
11	South Africa	2012	Speed hump	Vehicle speed changes significantly with speed hump but their resultant highway capacity loss is also significant. [11]
12	Sweden	2011	Speed hump	Distance between speed hump and pedestrian crossing should be 10m or equal to length of two cars. [12]
13	Chile	2010	Speed hump	Seating in a motor vehicle, especially on the last row in a bus, may cause severe traumatic spine injuries as it passes over a speed hump. [13]
14	North America	2009	Various devices	Speed is most significant issue for installing a TCD. Community support is most important factor for the selection of TCDs. [14]
15	China	2008	Speed hump	Small inclinations should be added to the top of the hump for best performance. Response of optimal hump is smooth, gentle and symmetric at speeds different from the design speed. [15]
16	United States (Illinois)	2008	Speed hump	Speed humps are the most turbulent TCDs to the emergency vehicles response time. [16]
17	Turkey	2005	Speed bump	Speed bump should be build regarding testing standards. Drivers should be educated and strongly warned on the potential hazards of traversing past such measures too fast. [17]
18	United States (Iowa)	2002	Speed hump	Optimum spacing of speed humps/tables is 220-285 feet for temporary speed humps. [18]
19	United States (Oregon)	2000	Speed hump	An average delay to emergency response is 3.6 seconds per speed hump. Design, construction and placement of TCDs is done at local level. [19]

III. METHODOLOGY

This research was based on information from following three sources.

First: The first phase was to collect field data of traffic calming devices on different local roads, collectors, and major arterials of Lahore city. So a thorough field survey was conducted. By using personal knowledge, an initial list of about 120 spots was generated which were reported to have tried traffic calming in the last few years. From this list, one in three was selected randomly to be surveyed, managing to successfully conduct a survey in 37 of the 40 spots thus selected. Hence the sample included 37 spots reporting active traffic calming installations or planning programs.

Total eleven sites on local road, twenty-one sites on collectors, and five sites on arterial road, were selected. The objective was to collect data from different locations to compare the different info regarding traffic calming devices. Continuance of field survey was one month. All data were collected on day time. Photographs of the calming devices were also taken.

Two: Questionnaire survey of a large volume of residents was conducted who were living along these study streets and using these traffic-calming devices. The duration of questionnaire survey was from 1st June up to 30th June 2018 on the selected survey locations. The objective of the opinion survey was to know the demand of road users of different ages, genders, classes and professions regarding traffic calming. A total of three road categories were selected to obtain a clear picture that are arterial, collector, and local road.

Third: In-depth interviews were conducted with number of officials working in agencies to determine the extent to which these agencies have involved themselves in traffic calming. The agencies selected for interviews were the 6 largest in the Lahore. For the selected agencies, the officials were interviewed who assigned to handle traffic calming or to work on neighborhood issues. If there was no such assignment, the head of the section was interviewed that works most closely with local government's transportation programs. All persons thus identified were provided with a brief description of the study and were invited to participate in a detailed interview on their experiences with traffic calming. For those who agreed to participate, an interview was scheduled. The vast majority of the interviewees were traffic engineers or engineers in transportation or public work departments. In a very small number of cases interviewees were from other departments. In some agencies more than one person was interviewed.

- ***Interview guide***

For the interview, a list of questions was used as a guide. The interview format was one of a structured conversation rather than questionnaire administration; the aim was holistic understanding of the locality's traffic calming experience rather than for a detailed accounting of actions taken, devices used, or reactions to the experience. As a result, the interviews did not always cover every single question in equal detail, but did identify the main issues as each interviewee saw them. Most interviews took about thirty minutes, with a few considerably shorter and several longer discussions.

IV. DATA ANALYSIS

A. Data analysis from field survey

Three categories of road (Arterial, collector, local) in Lahore city are considered to investigate the effects of traffic calming devices. The sites are located in twenty-three of Lahore total communities. Locations are given in Table II. The sites in table are selected based on pedestrian generation, traffic flow and population density.

TABLE II LIST OF LOCALITIES & SITES SURVEYED DURING RESEARCH

Sr. #	Localities	Sites Included
1	Gulberg IV	Site-1
2	Model Town	Site-2, 13
3	Nisar Colony	Site-3, 11
4	Officers Colony	Site-4, 12
5	Walton Cantt Board Officers Housing Society	Site-5
6	DHA, Phase I	Site-6, 7
7	New Muslim Town	Site-8, 9
8	Main Gulberg	Site-10
9	Askari 11	Site-14,15,16,17,18,19
10	DHA, Phase VI	Site-20, 21, 22
11	Paragon City	Site-23
12	Gulberg III	Site-24
13	Mian Mir Colony	Site-25
14	Valencia	Site-26
15	Judicial Colony	Site-27
16	Agrics Town	Site-28
17	Garhi Shahu	Site-29, 30
18	Mughal Pura	Site-31
19	Dharampura	Site-32
20	Saddar	Site-33
21	Green Town	Site-34
22	Wapda Town	Site-35
23	Johar Town	Site-36, 37

These 37 sites are located in twenty-three of Lahore total communities. These sites exact location is presented in fig 1.

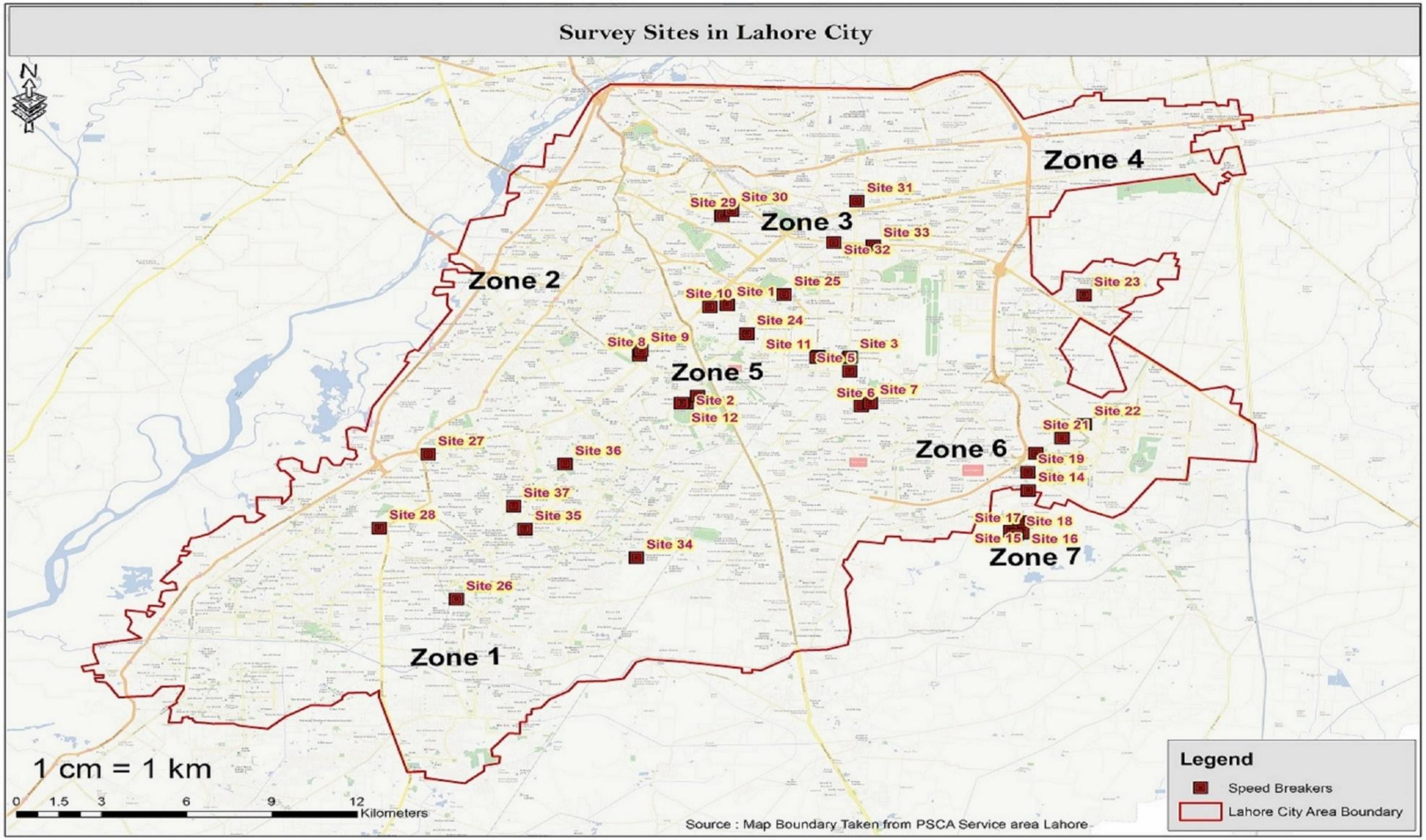

Figure 1. Location map of study sites in Lahore district

An inventory of traffic calming devices is done and more than 90 devices installed are found. For the analysis, only vertical traffic calming devices implanted on the roads of Lahore are selected. The sites irrelevant to research are rejected.

Tendency of traffic calming devices

The type of traffic calming devices which are found during investigation by their type consist of speed table, speed bump, speed hump and steel studs. From the field survey the tendency of used devices in Lahore city is found as shown in table III and fig 2.

TABLE III. TENDENCY OF TRAFFIC CALMING DEVICES

Traffic Calming Device	%age of the Devices Used
Sinusoidal speed hump	10.9
Circular speed hump	41.8
Parabolic speed hump	4.5
Flat-topped speed hump	5.5
Speed hump (Inappropriate shape)	5.5
Speed Table	10.9
Speed bump	13.2
Steel Studs	7.7

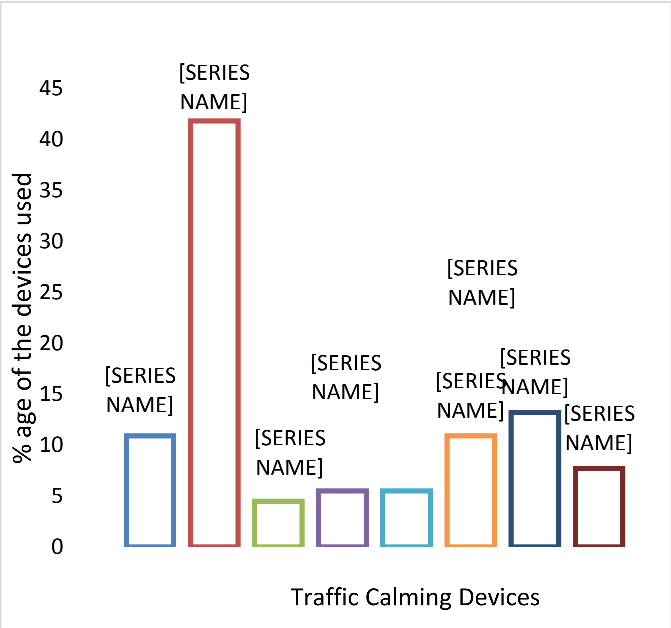

Figure 2. Trend of traffic calming devices used in the city

Four typical design profiles of speed humps are found in Lahore city that are sinusoidal, circular, parabolic and flat-topped.as shown in the following figures.

Figure 3. Speed humps at four leg intersection (Muslim Town)

Reflectors and Marking

Table IV lists the survey locations and number of calming devices on each site investigated in the study. Status of calming devices regarding reflectors and marking is also presented in the table.

TABLE IV REFLECTORS & MARKINGS USED ON TRAFFIC CALMING DEVICES

Site No.	Site Name	Calming Device	# of Calming devices	Reflectors	Marking
Site-1	Syed Maratib Ali road	Steel studs	1	✗	✗
Site-2	Model Town Circular road	Circular speed humps at junction	2	✓	✓
Site-3	Tufail road	Circular speed humps at junction	2	✓	✗
Site-4	Walton road	Parabolic speed hump at junction	1	✓	✓
Site-5	Walton road	Speed table	1	✓	✗
Site-6	Street 1	Flat-topped speed hump	1	✗	✗
Site-7a	Street 10	Circular speed hump	1	✓	✗
		Circular speed hump	1	✗	✗
		Circular speed hump	1	✗	✗
Site-7b	Street 7	Speed hump (Inappropriate shape)	1	✗	✗
Site-8a	Service Road	Sinusoidal & flat-topped speed humps at junction	2	✗	✗
Site-8b	Service Road	Steel studs	3	✗	✗
Site-9a	Main Abdul Waheed st & Ayoubia Market road	Parabolic, Circular, Sinusoidal &Flat-topped speed humps at junction	4	✗ 1 hump has reflectors	✗ 1 hump has marking
Site-9b	Ayoubia Market road	Steel studs	1	✗	✗
Site-10a	Zahoor Ilahi road	Speed table	1	✗	✗
Site-10b	Zahoor Ilahi road	Sinusoidal speed hump	1	✗	✗
Site-11	Khursheed Alam road	Circular speed hump at junction	1	✓	✗
Site-12	Shami road	Circular speed hump at junction	1	✓	✗
Site-13a	Model Town Ferozpur link road	Circular speed humps at junction	4	✓	✓
				1 hump has no reflectors	
Site-13b	Model Town Ferozpur link road	1 Sinusoidal & 3 Circular speed humps at junction	4	✓	✓
				2 hump have no reflectors	
Site-14	Askari 11 Underpass	Speed bump	4	✗	✓
Site-15	Street 31-40	Speed bump	5	✗	✓
Site-16	Service Road	Flat-topped speed hump	1	✗	✗

Site No.	Site Name	Calming Device	# of Calming devices	Reflectors	Marking
Site-17	Service Road	Circular speed humps	2	✖	✔
				✖	✖
Site-18	Service Road	Circular speed humps	4	✔	✔
Site-19	Service Road	Speed bump + Speed stud	1	✖	✔
Site-20	Shabir Sharif Road	Speed table	1	✔	✖
		Speed bump	1	✖	✖
Site-21	Shabir Sharif Road	Speed table	2	✔	✖
Site-22	Shabir Sharif Road	Speed table	2	✔	✖
		Speed table + Speed studs	2	✔	✖
Site-23	Main Boulvard	Sinusoidal speed hump + Steel Studs	1	✖	✔
		Steel studs	1	✖	✖
		Sinusoidal speed hump	1	✔	✖
Site-24	Sir Syed Road	Flat-topped speed hump	1	✖	✖
		Speed bump	1	✔	✖
		Speed table	1	✖	✖
Site-25	Jail Road	Speed hump (Inappropriate shape)	1	✖	✖
Site-26	Valencia main Blvd	Circular speed hump	3	✔	✔
Site-27	Local Street	Sinusoidal speed hump	4	✖	✔
Site-28	Agrics Town Rd	Circular speed hump	5	✖	✔
Site-29	Davis Road	Circular speed hump + Steel studs	2	✖	✔
Site-30	Durand Road	Circular speed hump	2	✖	✔
Site-31	Shalimar Link Road	Parabolic speed hump	1	✖	✖
Site-32a	Allama Iqbal Road	Steel studs	1	✖	✖
Site-32b	Allama Iqbal Road	Circular speed hump	1	✖	✖
Site-33	Zarrar Shaheed Road	Parabolic speed hump	1	✖	✖
Site-34	Madar-e-Millat Road	Circular speed hump	1	✖	✔
Site-35	Wapda Avenue	Circular speed hump	1	✔	✔
Site-36	Shadewal Road	Speed hump (Inappropriate shape)	1	✖	✖
Site-37	Service Road	Speed hump (Inappropriate shape)	2	✖	✖

Material used for traffic calming devices

The following graph shows the percentage proportion of the material used for calming devices.

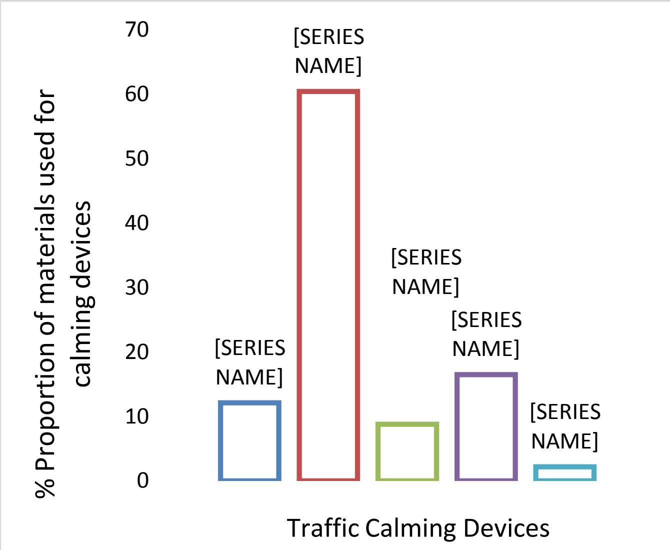

Figure 4. Material used for traffic calming devices

Condition of traffic calming devices

Most of the traffic calming devices were found in good conditions. Following table and graph shows the percentage proportion of the good, normal and poor devices.

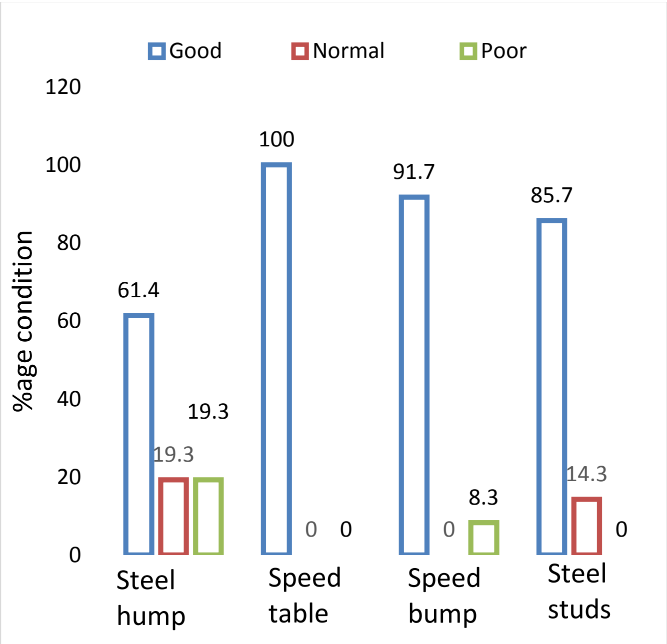

Figure 5. Condition of traffic calming devices

B. Data analysis from questionnaire survey

According to the capacity and function, roads are divided into different categories roads that are arterial, collector and local road. The sample was taken non-statistically due to limited availability of resources, budget and manpower. Sample size is denoted by "n".

TABLE V SAMPLE SIZE n

Sample size (n)	
Arterial	70
Collector	130
Local	200
Total	**400**

Survey was categorized according to four groups that are gender, age, vehicle type and profession. The characteristics of study group is presented in the following table.

TABLE VI CHARACTERISTICS OF STUDY GROUP

	N (%)		N (%)
Gender		**Age**	
Female	22.97	Less than 25	42.40
Male	75.97	Greater than 25	56.54
Vehicle Type		**Profession**	
Car/Taxi	29.33	Driver	21.20
Bus	22.97	Police	35.34
Truck	2.47	Student	25.44
Motor Bike	41.34	Transport Operator	3.53
Cycle	2.83	Others	13.43

From opinion survey, it is found that respondents have vast variation in the response. The comparison of respondent's perception is provided in following table.

TABLE VII COMPARISON OF RESPONDENTS PERCEPTION

Question: 1

Aspect	Road Classification	Proportion (%)				
		Very good	Good	Fair	Poor	Very poor
Public acceptance	Arterial	17.1	45.7	28.6	2.9	5.7
	Collector	15.3	47.8	23.9	13	0
	Local Road	15.4	55.5	20.8	6.4	1.98
		15.5	53	22.3	7.1	2.1

Question: 2

Aspect	Road Classification	Proportion %		
		Reduced safety	No change	Increased safety
Effect of speed breaker on traffic safety	Arterial	31.4	2.9	65.7
	Collector	30.4	8.7	60.9
	Local Road	25.2	4.5	70.3
		26.9	4.95	68.2

Question: 3

Aspect	Road Classification	Proportion %	
		Yes	No
User satisfaction of material used	Arterial	68.6	31.4
	Collector	58.7	41.3
	Local Road	74.3	25.7
		71	28.97

Question: 4

Aspect	Road Classification	Proportion %				
		Strongly disagree	Disagree	Ambivalent	Agree	Strongly Agree
Speed breaker damages the vehicles?	Arterial	14.3	25.7	14.3	25.7	20
	Collector	6.5	23.9	19.6	36.95	13
	Local Road	9.9	42.1	10.4	28.2	9.4
		9.9	37.1	12.4	29.3	11.3

Question: 5

Aspect	Road Classification	Proportion %			
		Fatal	Major	Minor	No accident
Any accident occurred due to speed breakers?	Arterial	5.7	20	45.7	28.6
	Collector	8.7	8.7	36.9	45.7
	Local Road	4.9	11.9	34.7	48.5
		5.7	12.4	36.4	45.6

Question: 6

Aspect	Road Classification	Proportion %				
		Strongly disagree	Disagree	Ambivalent	Agree	Strongly Agree
Congestion due to traffic calming device	Arterial	2.9	31.4	11.4	51.4	2.9
	Collector	8.7	34.8	15.2	41.3	0
	Local Road	3.5	51.5	10.9	30.7	3.5
		4.2	46.4	11.7	34.9	2.8

Question: 7

Aspect	Road Classification	Proportion %				
		Strongly disagree	Disagree	Ambivalent	Agree	Strongly Agree
Traffic diversion to another street	Arterial	54.3	0	14.3	31.4	0
	Collector	10.9	23.9	19.6	43.5	2.2
	Local Road	8.4	55.9	11.4	20.8	3.5
		14.5	43.8	13.1	25.8	2.8

Question: 8

Aspect	Road Classification	Proportion %				
		Very much	Somewhat	Not so much	Not at all	No comment
User friendliness w.r.t dimensions	Arterial	8.6	25.7	37	17.3	11.4
	Collector	6.5	30.5	37	6.5	19.5
	Local Road	7.9	30.2	12.9	12.9	36.1
		7.8	29.7	19.8	12.4	30.3

Question: 9

Aspect	Road Classification	Proportion %			
		Noise	Air	Vibration	All
Environmental effect of traffic calming devices	Arterial	14.3	17.1	14.3	54.3
	Collector	26.1	13	19.6	41.3
	Local Road	36.6	6.9	10.5	46
		32.1	9.2	12.4	46.3

Question: 10

Aspect	Road Classification	Proportion %	
		Yes	No
Fuel consumption due to traffic calming device	Arterial	71.4	28.6
	Collector	76.1	23.9
	Local Road	80.2	19.8
		78.4	21.6

C. Data analysis from agency representatives

Comments of officials and my observations are presented in the following table.

TABLE VIII AGENCIES VISITED DURING RESEARCH

Sr. #	Agency	Officer Name	Designation	Comments	Observations
1	**The Urban Unit (UU)**	Zuhair Aslam	Senior Specialist Transport Planning & Management	Urban Unit has initiated the development of the Punjab Geometric Design Manual (PGDM). The Manual is expected to provide guidelines for provincial departments, development authorities and local governments towards using standardized roadway design procedures and guidelines meeting the expectancy of the local drivers, and thus contributing towards provision of safe roadway designs.	PGDM Manual has been developed through a long consultative process involving technical experts to ensure the quality and value for its use. The Manual is a dynamic document and current edition is still a draft document that requires continuous review and feedback by the stakeholders on a regular basis which will be incorporated in the final document.
		Dr. Syed Murtaza	Transport Planner	Currently there is no policy which is followed for the construction of speed breakers	
2	**National Engineering Services Pakistan (NESPAK)**	Arshad Malik	Prinicipal Engineer (Highway Section)	NESPAK has received many requests from general public and officials for the installation of calming devices throughout the city. But currently there is no policy which is followed. NESPAK follows design standards of OMAN.	NESPAK officials have limited knowledge and guidance to make decisions to implement traffic calming devices.
3	**Traffic Engineering & Planning Agency (TEPA)**	Waqar Aslam	Senior Traffic Engineer	According to official, Calming devices should be installed only when it is unavoidable. Agency only offer technical help in the construction of devices. Speed table is better than any other traffic calming measures because it causes less damage to vehicles. TEPA does not recommend traffic calming devices even though the request may be valid.	TEPA did not use proper design specifications for the installed traffic calming devices.
4	**City District Govt. Lahore (CDGL)**	Muhammad Tariq Effendi	Metropolitan Officer (Infrastructure)	26 Roads are in the jurisdiction of CDGL and we only look after the calming devices at these 26 roads. There is no policy for installation of calming devices. We suggest calming devices when we get intimation from TEPA or CTP. Speed table should be installed instead of any other traffic calming device.	CDGL had passed many resolutions against dangerous and illegally constructed traffic calming devices in the city but unfortunately concerned authorities of road department failed to implement such bill passed by the elected representatives so far.
5	**City Traffic Police (CTP)**	Athar Ismail	Superintendent of Police (SP)	We do not install or deal with any traffic calming device. Only two speed humps were suggested in the start of ring road because pressure from the community was increasing for installation.	LRA approved the use of speed hump without analyzing the impact they may have upon vehicles speed or safety.
6	**Lahore Development Authority (LDA)**	-	-	-	No official available dealing with traffic calming.

CONCLUSION

D. Conclusion from field survey

Tendency of traffic calming devices

Among all types of TCDs installed in city, the most commonly used are the speed humps because of its low cost and effectiveness in reducing speed. Speed humps are of various shapes are found that includes sinusoidal speed hump (10.9%), circular speed hump (41.8%), parabolic speed hump (4.5%), flat-topped speed hump (5.5%) and speed humps of inappropriate shape (5.5%). Speed bumps are 13.2 %, speed tables are 10.9% and steel studs are 7.7%.

Reflectors and marking on traffic calming devices

Most of the calming devices do not have marking and reflectors so far. Reflectors should be installed on all calming devices implanted on arterials connecting major roads of the city in order to avoid road mishaps, which are increasing day by day.

Material used to construct traffic calming devices

In Lahore, 60.4% traffic calming devices are constructed by asphalt and concrete and 12.1% are made up by rubber. While traffic calming devices constructed by metals, tuff tiles or cement are of 8.8%, 16.5 % and 2.2% respectively.

Condition of traffic calming devices

It is necessary to ensure good quality of TCDs in order to avoid any mishap. In Lahore 61.4 % speed humps are in good condition while speed table, speed bump and steel stud are in good conditions with 100%, 91.7% & 85.7% respectively. According to survey, 19.3% speed humps and 8.3 % speed bumps are in poor conditions because of non-availability of reflectors, marking and poor material used.

E. Conclusion from questionnaire survey

Public acceptance

Question one of the questionnaire survey was to ask about acceptance each resident have for traffic calming devices. Survey found that 9.2% residents opposed to the traffic calming devices and 90.8% residents were in favor (15.5% public marked it very good, 53% marked it good while 22.3 % people marked it fair). So overall public supports traffic calming devices because maximum percentage of people marked these measures positively.

Safety

Question two of survey asked whether residents perceived an increase in safety due to installation of calming devices. Lahore city reported mixed results. Some respondents (26.9%) reported that by using these devices traffic has not always slowed enough to satisfy residents. While most respondents (68.2%) felt that traffic calming is largely successful. Other respondents (4.95%) agreed that there were no changes regarding safety.

User satisfaction for material used for calming devices

For the question which deals with the suitability of material used for the traffic calming devices at roads, high proportion (71%) of respondents stated their agreement that the devices material is suitable, while on the contrary low proportion (28.97%) of respondents stated that they are not satisfy with the material used for calming devices as it is dissatisfactory & trouble causing for travelers according to them.

Damage to vehicles

Question four was to ask the residents whether calming devices damage the vehicles or not. 47% respondents were either disagreed or strongly disagreed with the point that traffic calming is causing damage to the vehicles when passing over it, while 12.4% were ambivalent. Rest of the respondents were agreed that calming devices damage the vehicles as the suspension of the vehicles is not normally made according to these non-standardized devices which can cause damage to them.

Accident occurrence

Prime focus of traffic calming devices is to reduce fatal incidents & injuries. Response from respondents revealed that 5.7% people faced fatal accidents, 12.4% faced major accidents and 36.4% faced minor accidents due to calming devices. Remaining 45% people faced no accident. Respondents said that vehicles swung out of control after hitting the calming device at high speed.

Congestion

It is surprising to know that most of the respondents (50.6%) in all road categories stated that the calming devices do not cause congestion. While remaining 37.7% were agreed over this point and 11.7% were ambivalent.

Traffic diversion

Common response to this question was that the calming devices do not divert the traffic. 58.3% respondents were disagreed, 28.6% agreed that there was diversion of traffic. While remaining 13.1% were ambivalent.

User friendliness w.r.t dimensions

From the survey results, 37.5% of total respondents stated that calming devices are user friendly with respect to dimensions. 42.7% respondents declared it non user friendly.

Environmental effect

Along with positive impacts, environmental problem is always one of the major concerns of traffic calming devices. Almost all the road users were agreed to the point that traffic calming devices are causing environmental problem as these are increasing noise, air pollution and vibration of vehicles.

Fuel consumption

From the data analysis, it can be shown that most of the respondents (79%) stated that the implantation of calming devices has increased fuel consumption.

F. *Conclusion from agencies dealing with traffic calming devices*

Public acceptance

After visiting several agencies and conducting interviews, it is clear that no agency has formulated traffic calming policy till time. None of them defined that what types of traffic calming devices can be used. No agency indicated the departments that should be consulted before the installation of these devices and what studies need to be conducted before and after the implementation. No one gathered and analyzed data on the traffic complaint or evaluated the suitability of the requested device or where it can be used.

The answer to the question whether planning organizations are involved in traffic calming or providing any technical assistance was that there is very little such activity to date. Almost all interviewee claimed to be doing absolutely nothing related to traffic calming. Urban Unit has put out guidelines on traffic calming as part of its management program but it is also in review process. Almost every interviewee stated that they were not aware of the diversion issue and did not consider it before installing a device and had even never studied the traffic on alternate routes before and after installation of a calming device to check for diversion.

Many of interviewee were unfamiliar with the details of department's budget and were unsure how projects and programs had been funded. They did not remember the details or have access to a detailed accounting.

RECOMMENDATIONS

Based on the research, the undermentioned factors have been found that should be considered in the policy:

Public education:

There should be awareness campaigns organized by the agencies to give the knowledge about traffic calming to the residents that will help them in the selection of suitable device. The knowledge includes effect of calming device height, signage, markings, spacing etc.

Involvement of the Public:

Traffic calming devices should be installed only after getting consent and opinions from the occupants which are directly affected by these devices. Common people can be involved by many ways like public events, meetings, leaflets and walkabouts.

Standard application process:

There should be a proper way to request for a traffic calming device installation. For this purpose, there should be at least one organization in the city which will specifically deal with the said purpose.

Evaluation process:

After getting request, the concerned official will visit the location to check the validity of the request received.

Approved devices:

Concerned department should check out whether the desired device should be approved or not. There should be testing process to come to know the possible pros and cons of the alternate devices before taking decision.

Installation process:

There should be a sequence that which request should be addressed firstly. These sequence can be made based on the severity of the need and availability of funds.

Funding source:

Who will provide funds for the desired project?

Detailed map for emergency routes:

A map depicting all emergency service routes should be drawn by the help of traffic engineers and emergency department's personnel. The devices which have high impact on response time should not be installed on these routes. The map updation should be done on regular basis.

Future development:

A survey should be conducted to know the opinions of residents about the installed devices to develop a guideline for future installation.

REFERENCES

[1] A. Garcia, A. T. Moreno, M. A. Romero, "Technological development and validation of speed kidney, a new traffic calming device," Journal of the Transportation Research Board, December 2011.

[2] L. S. Putranto, and K. Kurniawan, "Effect of type of road humps on vehicular speeds on residential roads," 2018.

[3] F. Rahman, T. B. Joewono, and S. Al Masum, "Application of traffic calming devices in developing countries: learning lesson from bangladesh. Journal of Transportation Technologies," vol. 8, p. 119, 2018.

[4] G. González-Sánchez, E. Maeso-González, M. I. Olmo-Sánchez, M. Gutiérrez-Bedmar, A. Mariscal, and A. García-Rodríguez, "Road traffic injuries, mobility and gender. Patterns of risk in Southern Europe," Journal of Transport & Health, 2018.

[5] T. A. Abdel-Wahed, I. H. Hashim, "Effect of speed hump characteristics on pavement condition," 2017.

[6] T. Patel, and V. Vasudevan, "Impact of speed humps of bicyclists. Safety Science," vol. 89, pp. 138-146, 2016.

[7] L. Jateikiene, T. Andriejauskas, I. Lingyte, and V. Jasiuniene, "Impact assessment of speed calming measures on road safety," Transportation Research Procedia, vol. 14, pp. 4228-4236, 2016.

[8] L. Song, G. Feng, X. Guoyan, D. Nenggen, "The best speed limit range for road hump," April 2015.

[9] S. M. Ghaemi and M. A. Sahraei, "Determining the Impact of road humps on road capacity," 2013.

[10] A. Kanjanavapastita, and A. Thitinaruemitb, "Estimation of a speed hump profile using quarter car model," Social and Behavioral Sciences, vol. 88, pp. 265 – 273, 2013.

[11] J. Ben-Edigbe and N. Mashros, "Extent of highway capacity loss resulting from road humps," IACSIT International Journal of Engineering and Technology, vol. 4, April 2012.

[12] C. Johansson, P. Rosander, and L. Leden, "Distance between speed humps and pedestrian crossings: Does it matter?," Accident Analysis & Prevention, vol. 43, pp. 1846-1851, 2011.

[13] J. J. Zamorano, B. A. Marre, F. Ilabaca, A. U. Bacciarini, "Speed hump spine fractures injury mechanism and case series," Journal of Spinal Disorders & Techniques, December 2010.

[14] F. Rahman, A. Kojima, and H. Kubota, "Investigation on north american traffic calming device selection practices," IATSS research, vol. 33, pp. 105-119, 2009.

[15] P.Y. Zhua, J.P. Hesslingb and D.S. Liua, "Optimal road hump for comfortable speed reduction," vol. 7130, 2008.

[16] R. R. Jaeger, "Traffic calming-speed humps, effect on emergency response times," 2008.

[17] S. Aslan, O. Karcioglu, Y. Katirci, H. Kandis, N. Ezirmik, and O. Bilir, "Speed bump–induced spinal column injury," The American Journal of Emergency Medicine, vol. 23, pp. 563-564, 2005.

[18] D. Smith, S. Hallmark, K. Knapp, and G. Thomas, "Temporary speed hump impact evaluation," July 2002.

[19] T. Robertson, "Speed hump impacts on emergency response times eugene fire and emergency medical services," https://www.hsdl.org/?abstract&did=4174, 2000.

国际工程期刊
International Journal of Engineering Works
انجینرنگ کاموں کا بین الاقوامی جرنل

International Journal of Engineering Works
ISSN-p: 2521-2419
ISSN-e: 2409-2770
Vol. 6, Issue 01, PP. 27-32, January 2019
https://www.ijew.io/

Evaluation of Ramp Metering Control on Urban Expressway in Cairo

Salma H.Abu-Bakr[1], Hatem Abdel-Latif[2], Khaled El-Araby[3], Mohamed Shawky[4]
[1,2,3,4]Faculty of Engineering Ain Shams university
salma.hussein@eng.asu.edu.eg[1]
Received: 03 January, Revised: 16 January, Accepted: 21 January

***Abstract*—** Uncontrolled on-ramp merging section is considered as a bottleneck at several locations on urban expressways in Greater Cairo Region (GCR). This study aims to evaluate the impacts of applying ramp metering control on the traffic performance at three critical on-ramp sites on the 6th of October corridor using VISSIM. The simulation models were calibrated using the traffic data collected during peak period. Two different control strategies were tested; fixed-time ramp metering and actuated control for both mainline and on-ramp traffic, and compared to "no control" using average speed, average vehicle delay and on-ramp queue length as performance measures. The results indicated that fixed-time ramp metering could improve the overall traffic performance at merging sections by increasing the speed up to 100% and reducing the average vehicle delay up to 50%. However, fixed-time ramp metering control results in on-ramp queue spillback onto adjacent roads at some sites due to insufficient ramp storage length and huge on-ramp volumes. In this case, the actuated control strategy showed significant improvements on traffic performance at both the mainline and on-ramp, in addition to the whole system by increasing the speed by 25%, reducing the average delay by 11%, and reducing the queue length by 35%.

***Keywords*—** Ramp metering, Microsimulation, VISSIM, Fixed-time control

I. INTRODUCTION

As other crowded big cities around the world, Greater Cairo Region (GCR), the capital of Egypt, roadway network is suffering from severe traffic congestions especially during peak periods. Traffic congestions at GCR cost nearly 4% of the Gross Domestic Product (GDP) according to the World Bank study 2013 [1]. Although the Egyptian Government has done great efforts to solve the traffic congestions during recent years, by constructing new roads, bridges, and new metro lines, main roads still suffer severe recurrent traffic congestions, especially at on-ramp merging sections on urban main roads. The 6th of October corridor is considered as one of the major urban corridors in GCR with a length of 20.5 km linked the east to the west regions of GCR and has 23 entry and exit. Recurrent traffic congestions are frequently observed at on-ramp merging sections on this corridor due to uncontrolled on-ramp merging traffic onto the mainstream. Currently, at some on-ramp sites, the Cairo traffic police department applies a manual control strategy by allocating a policeman at the on-ramp to control the entry traffic onto the mainline based on his own limited vision and judgment. Despite ramp metering control strategies have shown significant improvements on traffic operation around the world, no studies were conducted to test the efficiency of applying such control systems on urban expressways in GCR. Accordingly, this study mainly aims to evaluate the effectiveness of applying ramp metering control system at some on-ramp sites on the 6th of October corridor . In addition, the study aims to find the optimal signal timing of the on-ramp metering system and the best control scenario.

II. LITERATURE REVIEW

Ramp Metering is considered as the most effective traffic control management system that controls the entry traffic volumes onto freeways, or urban expressways to alleviate traffic congestions at merging sections [2]. Ramp meter is a special traffic signal placed at on-ramp to control the entry traffic volumes from on-ramp onto the mainline [3]. The main objectives of applying ramp metering control system are to improve traffic operation on freeways and enhance the traffic safety [4]. It aims to regulate the rate by which entry vehicles are allowed to enter the freeway by optimizing the use of available gaps between vehicles on the mainline of the freeway to keep the flow under its capacity [5]. Ramp metering also aims to break up the platoons of on-ramp vehicles tends to enter the mainline. The first implementation of ramp metering control was in 1963 on Chicago's Eisenhower Expressway in Illinois, where a policeman controlled the entering traffic by releasing one or more vehicles to enter at a predetermined rate [6].

Based on the entry mode, ramp metering strategy is classified into three modes: single lane one car per green, single lane multiple cars per green, and dual lane [7]. For dual lane entry, the on-ramp consists of two lanes and each lane has a signal controller with one car per green or multiple car per green. There are two operational ramp metering control strategies to determine the metering rates based on its response to real-time traffic conditions at the merging section: pre-timed (fixed) ramp metering control system and responsive ramp metering control system. In pre-timed ramp metering control, the metering rate is determined based on historical traffic data, regardless the fluctuation in traffic condition during operation time [8]. Fixed-time ramp metering control is effective in case of recurrent traffic congestion [9]. The metering rates in responsive control are calculated using algorithms. The responsive ramp metering control system are classified into two types: local (isolated) and coordinated ramp metering control. Local ramp metering control use the traffic data such as Demand/Capacity [10], and ALINEA algorithm [11] from detectors in the vicinity in a specific algorithm to find the optimum entry rate of traffic form the on-ramp. The coordinated ramp metering control algorithms use traffic data from detectors on a set of consecutive ramps to set the rate, such as BOTTLENECK algorithm [12] to control a set of on-ramps along the study corridor.

Several prior studies have been conducted to evaluate the benefits of different ramp metering control strategies in improving traffic performance [13], [14], [15], [16] and traffic safety [17], [18] by using both field test and microscopic/macroscopic simulation techniques. For example, [19] tested the impacts of applying fixed-time ramp metering control strategy on the traffic efficiency and equity on an urban freeway in Istanbul, Turkey, using VISSIM microsimulation. A set of fixed timing signal scenarios were evaluated to indicate the optimal fixed-time cycle length. The results concluded that fixed-time cycle length with 15 seconds showed the best results in improving the network efficiency by increasing the speed by 52% and reducing the network travel time, delay and number of stops by 32%, 60%, and 80%, respectively. Also, ramp metering could provide equity concerns for the ramp travelers when taking the spot speed in consideration. [20] used microsimulation AIMSUN to evaluate the effects of two ramp metering control strategies (including fixed-time control and one responsive control) on Shahid Kharrazi Freeway in Isfahan city at three demand levels (80%, 100%, and 110). The results concluded that didn't show any significant improvements for 100% demand level, while it improved traffic operation at 110% demand level. Also, they concluded that ramp metering showed negative effects at low demand level.

III. Case Study Selection and Data Collection

Three on-ramp sites along the 6^{th} of October corridor with different geometric configurations were selected as a case study: Ramsis on-ramp (site 1), Abdel-Monem Riyadh on-ramp (site 2), and Al-Gazera on-ramp (site 3). The study sites were selected such that they suffer severe recurring traffic congestions during peak periods. Figure 1 shows the location of the three study sites along corridor. Each site includes a single lane on-ramp with 5 m, 5.5m and 6m width at site-1, site-2, and site 3, respectively. Due to the lane width of the on-ramps and mainlines, an additional lane always occurs during peak periods on each on-ramp and the mainline segments, as well, resulting from the drivers' behavior in Cairo that doesn't discipline the designed lane width. Only, at Ramsis on-ramp, the lane width is narrowed to 3 m just before entering the mainline, so it was considered as a dual-lane ramp which turns into a single lane before merging. Moreover, the max on-ramp storage length at each site is 160 m for site-1, 190 m for site-2, and 155 m for site-3. At sites (1) and (2), manual controlling by a policeman at on-ramp traffic is taken place during peak hours. At site-3, bottleneck mainly occurred downstream on-ramp due to the existence of a nearby off-ramp that creates a weaving section, in addition to the merging traffic. Traffic data were collected using video records technique and the traffic volumes were collected manually through the video records during peak hours. The maximum hourly mainline volumes were 3712, 3450, and 5402 veh/hr, at site-1, site-2, and site-3 respectively, while the cross ponding on-ramp traffic volumes were 1468, 1610, and 1490 veh/hr at site-1, site-2, and site-3, respectively.

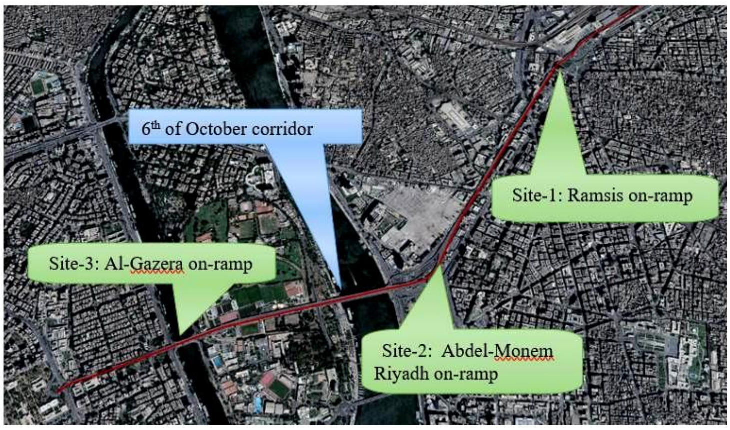

Figure 1. the 6th of October corridor layout with selected sites

IV. Developing of Microscopic Simulation Modeling

A. Model development

Microscopic simulation modeling technique is used to achieve the objectives of the study. The microscopic software package "PTV VISSIM-10" was used in modeling each on-ramp site and evaluating different control strategies. VISSIM is defined as a microscopic, behavior based and time step oriented simulation tool used for modeling urban streets, freeways, multimodal transport operations, and pedestrian flows [24]. It applies psychophysical car following models developed by Wiedemann: Wiedemann 99 and Wiedemann 74. For the network coding, each link in the network was specified to "Urban motorized" link type, while the links in the merging area were specified to a new introduced link type "Merging".

B. Models calibration and validation

Each simulation model was calibrated using traffic data set of one hour by adjusting the values of specific Vissim parameters until the model replicates the real traffic conditions. Geoffrey E. Haver (GEH) index was used in models calibration to compare between simulated S and observed V traffic volumes for both mainline and on-ramp directions. The GEH is calculated using the following equation [21] :

$$GEH = \sqrt{\frac{2*(S-V)^2}{(S+V)}}$$

Where S is the simulated traffic volume and V is the observed traffic volume. The simulation model is considered accurately reflect the prevailing conditions on the network, if more than 85 % of the GEH values are less than 5 [22]. All the calculated GEH values were found to be less than 5 for all sites with average values of 1.33, 1.96, and 0.94 for site-1, site-2, and site-3, respectively. Table 1 shows the final calibrated values of each simulation model parameters. In general, the calibrated values are the same for all simulation models, except the values of maximum deceleration for cooperative braking and min headway parameters of the "Merging" driver behavior type which they are same for site-2 and site-3 only.

TABLE I. CALIBRATED VALUES OF VISSIM PARAMETERS FOR EACH SIMULATION NETWORK

Parameter	Calibrated value	Applied sites
Car following model parameters (a_x, $b_{x\ add}$, $b_{x\ mult}$)	0.7m, 0.3m, 0.3m	site-1,site-2, site-3
Safety distance reduction factor	0.1	site-1,site-2, site-3
Min. headway for urban motorized	0.5 m	site-1,site-2, site-3
Min. headway for Merging	0.2 m	site-2, site-3
Max. deceleration (Own) for urban motorized	-5 m/sec^2	site-1,site-2, site-3
Max. deceleration (Trailing) for urban motorized	-4 m/sec^2	site-1,site-2, site-3
Max. deceleration (Own) for Merging	-6 m/sec^2	site-1,site-2, site-3
Max. deceleration (Trailing) for Merging	-6 m/sec^2	site-1,site-2, site-3
Max. deceleration for cooperative braking for urban motorized	-6 m/sec^2	site-1,site-2, site-3
Max. deceleration for cooperative braking for Merging	-6 m/sec^2	site-1
	-9 m/sec^2	site-2, site-3

The calibrated models were validated using another traffic data set by applying GEH statistics approach and ensuring the occurrence of bottlenecks on the mainline segments through visual inspection. All the GEH values for validation were less than 5 with average values of 1.17, 2.28, and 1.44 for site-1, site-2, and site-3, respectively. From the GEH values, the models are well calibrated and can be used for analysis.

V. DESIGN OF THE TESTED SCENARIOS AND RESULTS

Two different control strategies were tested: ramp metering strategy and actuated signal control strategy. The effectiveness of both control strategies was evaluated and compared to "no control" scenario as baseline scenario. A number of performance measures were used to evaluate the examined control scenarios such as average speed and average vehicle delay on the whole system (including corridor and the on-ramp), average speeds of mainline segments (upstream and downstream), and average on-ramp queue length.

A. Ramp metering control strategy evaluation

1) Design of fixed-time control scenarios

All the tested on-ramp sites suffer from recurrent congestions during study peak period with no variation in traffic volumes, so fixed-time ramp metering control strategy was proposed to be applied. A set of scenarios were designed based on the number of vehicles allowed to enter onto the mainline per green (entry mode) to find the optimum signal timing. As mentioned earlier, all studies on-ramps operate as dual lane ramps during peak periods. Therefore, they were considered as dual-lane ramps in the evaluation study to replicate the actual situation. Traffic signal was added at each lane such that the red-green cycles never occur at the same time. The proposed control scenarios for fixed-time ramp metering strategy at the selected sites and the signal display at each lane are listed in TABLE II.

TABLE II. THE PROPOSED SCENARIOS FOR FIXED SIGNAL TIMING

Control scenario no.	Cycle length (sec)	No. of vehicles per green per lane	Lane 1	Lane 2
No control				
1	6	1	2G+1AR+2R+1AR	2R+1AR+2G+1AR
2	8	1	2G+2AR+2R+2AR	2R+2AR+2G+2AR
3	10	1	2G+3AR+2R+3AR	2R+3AR+2G+3AR
4	10	2	4G+1AR+4R+1AR	4R+1AR+4R+1AR
5	12	2	4G+2AR+4R+2AR	4R+2AR+4G+2AR
6	14	2	4G+3AR+4R+4AR	4R+3AR+4G+3AR
7	16	2	4G+4AR+4R+4AR	4R+4AR+4G+4AR
8	14	3	6G+1AR+6R+1AR	6R+1AR+6G+1AR
9	16	3	6G+2AR+6R+2AR	6R+2AR+6G+2AR

*G=Green, R=Red, AR=All Red (all intervals are in second)
* 2G+1AR+2R+1AR means 2 seconds green to allow one vehicle to enter from lane-1, 1 second all-red, 2seconds red and 1 second all-red.

2) Simulation results of fixed-time scenarios

TABLE III. summarizes the performance results of fixed-time scenarios at site-1. The results indicated that all scenarios significantly improved the traffic performance, only scenarios no. 4, 8, and 9 showed reduction in the speed and increase in the vehicle delay compared to "no control". Scenarios with one and two cars per green with long cycle length, showed better results in improving traffic conditions on mainline and whole system compared to "no control" scenario and other control scenarios with short cycle length and same entry mode. On the other hand, all control scenarios increased the on-ramp queue length with no significant difference between the queue length under different scenarios, except scenarios no. 8 & 9 with 3-cars per green that showed significant reduction in the on-ramp queue length. Accordingly, scenario no. 3 with cycle length of 10 seconds and one car per green can be considered as the optimum control scenario as it showed the best whole system performance by increasing the speed by 38% and reducing the average vehicle delay by 38%.

TABLE III. PERFORMANCE RESULTS FOR FIXED SIGNAL TIMING SCENARIOS AT SITE-1

Control scenario	Whole system		Mainline upstream speed (km/h)	Mainline downstream speed (km/h)	On-ramp queue length (m)
	Speed (km/h)	Vehicle delay (sec/veh)			
no control	13.5	64.7	11	15	162.0
1	14.5	56.7	20	16	167.0
2	18.0	41.7	37	24	168.0
3	18.6	40.1	43	28	168.1
4	12.8	65.7	13	16	153.0
5	15.0	54.1	21	18	167.0
6	17.2	44.4	29	21	167.3

7	17.9	41.8	35	24	167.6
8	12.5	68.0	12	15	127.0
9	13.2	64.6	13	16	139.5

The simulation results of implementing fixed-timing signal control scenarios at site-2 are listed inTABLE IV. It is observed from the table that all control scenarios improved the traffic performance better than "no control". For the same entry mode, the increase in the speeds and reduction in the delay increased as the cycle length increase. It is also revealed from the table that ramp queue length exceeded the ramp storage length under all control scenarios with no significant difference between the queue lengths. Finally, scenario no.3 with cycle length of 10 seconds and one car per green is considered as the optimum scenario in term of increasing the whole system speed by 100% and reducing the vehicle delay by 50%.

TABLE IV. PERFORMANCE RESULTS FOR FIXED SIGNAL TIMING SCENARIOS AT SITE-2

Control scenario	Whole system		Mainline upstream speed (km/h)	Mainline downstream speed (km/h)	On-ramp queue length (m)
	Speed (km/h)	Vehicle delay (sec/veh)			
no control	8.2	113.4	6.5	9.1	200
1	9.9	96.4	10.0	10.6	206.3
2	14.7	64.6	24.4	13.0	206.8
3	16.4	57.1	38.7	16.4	207.1
4	8.6	109.5	8.2	9.7	198.8
5	10.1	94.3	9.7	10.5	206.2
6	13.2	72.9	15.2	11.4	206.6
7	14.3	66.7	21.9	12.4	206.7
8	8.5	109.1	7.8	9.5	199
9	9.3	102.3	8.8	10.0	200

For site-3, the mainline downstream segment is considered as a weaving segment, so the impact of ramp metering control was evaluated on the traffic performance on the weaving segment as well. The simulation results for each performance measure are listed in TABLE V. The results concluded that all fixed-time ramp metering control scenarios improved the traffic performance on whole system and the weaving segment, as well. Moreover, it is noticed that fixed-time ramp metering control increased average speed on mainline upstream segment compared to "no control", especially scenarios with long cycle length. Regarding the on-ramp queue length, all scenarios increased the queue length compared to "no control" without exceeding the ramp storage. The best whole system performance was provided in case of scenario no. 3 with 10 second cycle length and one car per green, so it is considered as the optimum signal timing control scenario. It improved the system performance by increasing the speed with 62% and reducing the average vehicle delay by 49%.

TABLE V. PERFORMANCE RESULTS FOR FIXED SIGNAL TIMING SCENARIOS AT SITE-3

Control scenario	Whole system		Mainline upstream speed (km/h)	Mainline downstream speed (km/h)	On-ramp queue length (m)
	Speed (km/h)	Vehicle delay (sec/veh)			
no control	12.4	66.7	6.8	10.9	115.1
1	16.4	47.1	19.8	12.1	152.7
2	19.1	36.9	30.7	16.3	153.2
3	20.1	34.1	35.1	19.5	153.5
4	13.5	60.5	9.2	10.6	144.6
5	15.3	52.2	15.3	11.2	152.4
6	17.8	41.5	23.4	13.6	153.0
7	19.4	35.4	32.6	16.7	153.1
8	13.6	60.9	9.0	10.6	124.2
9	14.1	58.0	10.5	10.5	115.1

B. Actuated control strategy for mainline and on-ramp traffic

1) Actuated control scenarios design

An actuated control strategy for mainline and on-ramp traffic with three different control methods were developed and evaluated. In the actuated control system, traffic signals and detectors are allocated at the on-ramp lanes and the mainline lanes upstream the on-ramp (see Figure 2. The main idea of this control strategy is to transfer the queue formed on the on-ramp to the mainline upstream segment when the on-ramp storage length can't accommodate the on-ramp queue and there is a sufficient storage space on mainline upstream segment. Occupancy rate at the mainline and on-ramp is used as the main performance measure to adjust the green and red duration of each signal groups to maintain the occupancy rate on both mainline and on-ramp less than or equal pre-defined critical values. The Occupancy rate is defined as the time percentage that the detector is occupied by a vehicle [21]. The occupancy rates are obtained from the installed detectors upstream the merging section and on-ramp as shown in Figure 2.

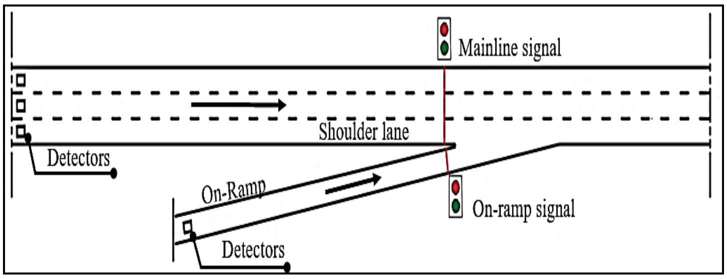

Figure 2. layout for the actuated control system components

The actuated control strategy has three main parameters that should be calibrated before applying any of the control methods: cycle update, mainline critical occupancy$(\hat{O}_m)$, and On-ramp critical occupancy $(\hat{O}_r)$.

At the beginning of each cycle update, the ramp occupancy(O_r) is firstly checked by comparing its vale with the predefined critical value $(\hat{O}_r)$ then the steps, illustrated in TABLE VI. , are proceeded based on the applied logic.

TABLE VI. ACTUATED CONTROL STRATEGY STEPS BASED ON THE APPLYING LOGIC

Control logic	If $(O_r) > (\hat{O}_r)$	If $(O_r) < (\hat{O}_r)$
Logic 1	Check the mainline occupancy • If $(O_m)> (\hat{O}_m)$, keep both signals groups green. • Else, Turn mainline signals into red.	Check mainline occupancy • If$(O_m)> (\hat{O}_m)$, Turn on-ramp signals into red • Else, keep both signals groups green.
Logic 2	Turn mainline signals into red	
Logic 3	Turn mainline signals into red	Keep both signals groups green

The three actuated signal logics were applied and evaluated at site-2 as there is a sufficient storage space on the mainline upstream segment of 400 m length that could accommodate the formed mainline queue. The 400 m is the distance on the mainline between the on-ramp and the upstream off-ramp to Ramsis. The mainline detectors were placed at 400 m upstream the merging area, while the on-ramp detectors were placed at the entrance of the ramp to make use of the whole ramp length. The calibrated values of cycle update, mainline and on-ramp critical occupancies were set by 10 seconds, 0.8, and 0.6, respectively. Each control logic was programmed using VisVap interface [25] to be simulated in VISSIM and compared to “no control” scenario in terms of the performance measures.

2) Simulation results of actuated control strategy

Performance results were obtained for each actuated control logic at site-2 in addition to the “no control” scenario and listed inTABLE VII.

TABLE VII. PERFORMANCE RESULTS FOR ACTUATED SIGNAL STRATEGY AT SITE-2

Control logic	Whole system		Mainline upstream speed (km/h)	Mainline downstream speed (km/h)	On-ramp queue length (m)
	Speed (km/h)	Vehicle delay (sec/veh)			
No control	8.2	113.4	6.5	9.1	200.0
Control logic-1	10.3	101	8.8	12.1	129.9
Control logic-2	9.9	102.1	8.7	12.9	122.1
Control logic-3	9.9	101.9	8.7	11.4	117.2

It is observed from the table that there was no significant difference between the simulation results of the control logics in increasing the speeds on the whole system and the mainline segments and reducing the average vehicle and delay. The on-ramp queue length was less than the on-ramp storage length (190 m) under all actuated control logics. Actuated control logic-1 could be selected as the best actuated control logic as it increased the mainline segments and whole system speeds by 25%, reduced the whole system delay by 11%. It also reduced the on-ramp queue length by 35% to reach 113m which is less than ramp storage length.

VI. CONCLUSION AND SUMMARY

The aim of this paper is to investigate the feasibility of applying ramp metering control strategy on congested urban expressways in Greater Cairo Region (GCR) and define the optimum cycle length and control strategy. Microscopic simulation models were developed using VISSIM microsimulation approach and the models were calibrated to reflect actual conditions. Three on-ramp merging sections were selected along the 6th of October corridor, as a case study. Both fixed signal timings scenarios and actuated traffic control strategies with different signal timing scenarios were evaluated and compared to “no control” scenario.

The simulation results indicated that fixed-time ramp metering control strategy in general improved the traffic performance at all examined merging sites. Despite the differences in the geometric layout and traffic volumes of the three sites, the optimum fixed-time scenario was the same at all sites: scenario no.3 with cycle length of 10 seconds and one car per green at all sites. It showed significant increase in the system speeds and reduction in the average vehicle delay, although it increased the queue length compared to “no control”. On the other hand, all three actuated control logics improved traffic performance on the whole system and on the on-ramp at site-2 and also prevent ramp queue spilling back onto adjacent roads. Actuated control logic-1 is considered as it showed the best performance compared to no control and other actual control logics.

Over all, the findings of this study proved the importance of applying ramp metering control system based on the recommended signal timing at the examined sites, instead of the manual control strategy that is currently used, to mitigate the recurrent traffic congestions at on-ramp sections and weaving sections during peak periods on urban expressways in GCR network roads.

Since this paper focused on studying the impacts of fixed-time ramp metering control strategy on the traffic performance, it is recommended to study the impacts of ramp metering control strategies on the traffic performance and traffic safety.

REFERENCE

[1] Bank, W., Cairo Traffic Congestion Study : Final Report. 2013.

[2] Hall, R., Handbook of transportation science. Vol. 23. 2012: Springer Science & Business Media.

[3] Arnold, E., Ramp metering: A review of the literature. Technical report. 1998, Virginia Transportation Research Council, Charlottesville, VA (United States).

[4] Sisiopiku, V.P., A. Das, and A. Sullivan, Applications of Freeway Ramp Metering in Alabama (No. UTCA Report 04203). 2005, University Transportation Center for Alabama.

[5] Piotrowicz, G. and J. Robinson, Ramp Metering Status in North America: 1995 Update. 1995: U.S. Department of Transportation.

[6] Jacobson, L., et al., Ramp management and control handbook (No. FHWA-HOP-06-001). 2006, United States. Federal Highway Administration.

[7] Bertini, R.L., et al., Using Archived Data to Measure Operational Benefits of ITS Investments: Ramp Meters. 2004: Portland State

University, Center for Transportation Studies, Research Report, p.15. p. 15.

[8] Zhang, M., et al., Evaluation of On-ramp Control Algorithms. 2001, Institute of Transportation Studies, Research Reports, Working Papers, Proceedings qt83n4g2rq, Institute of Transportation Studies, UC Berkeley.

[9] Ahn, S., et al., Evaluating benefits of systemwide adaptive ramp-metering strategy in Portland, Oregon. Transportation Research Record: Journal of the Transportation Research Board, 2007(2012): p. 47-56.

[10] Masher, D.P., et al., Guidelines for design and operation of ramp control systems. 1975, Stanford Research Institute, Menid Park, CA.

[11] Papageorgiou, M., H. Hadj-Salem, and J.-M. Blosseville, ALINEA: A Local Feedback Control Law for On-ramp Metering. Transportation Research Record, 1991. 1320, 58-64(1).

[12] Jacobson, L.N., et al., Real-time Metering Algorithm for Centralized Control. 1989: Washington State Transportation Center.

[13] Chu, L., et al. DEVELOPMENT OF A SIMULATION LABORATORY FOR EVALUATING RAMP METERING ALGORITHMS. in Transportation Research Board 81st Annual Meeting. 2002.

[14] Abdelfatah, A., A. Ramadan, and G. Darwish, Utilizing Vissim to Evaluate Ramp Metering Performance. International Journal of Traffic and Transportation Engineering, 2012. 1(1): p. 1-6.

[15] POORJAFARI, V. and W.L. YUE, Investigating the Impacts of Fixed-Time Ramp Metering through Microsimulation. Journal of the Eastern Asia Society for Transportation Studies, 2013. 10: p. 1824-1835.

[16] Janota, A., et al., Ramp-Metering Algorithms Evaluated within Simplified Conditions. Civil and Environmental Engineering, 2017. 13(2): p. 112-119.

[17] Lee, C., B. Hellinga, and K. Ozbay, Quantifying effects of ramp metering on freeway safety. Accident Analysis & Prevention, 2005. 38(2): p. 279-288.

[18] Abdel-Aty, M., A. Dhindsa, and V. Gayah, Considering various ALINEA ramp metering strategies for crash risk mitigation on freeways under congested regime. Transportation research part C: emerging technologies, 2007. 15(2): p. 113-134.

[19] Kesten, A.S., M. Ergün, and T. Yai, An analysis on efficiency and equity of fixed-time ramp metering. Journal of Transportation Technologies, 2013. 3(02): p. 48.

[20] Mirbaha, B. and G. Eftekhari, Comparing Methods of Ramp Metering for On-Ramps to Improve the Operational Conditions at Peak Hours. International Journal of Transportation Engineering, 2018. 5(3): p. 301-318.

[21] Hall, F.L., Traffic stream characteristics. Traffic Flow Theory. US Federal Highway Administration, 1996.

International Journal of Engineering Works
ISSN-p: 2521-2419
ISSN-e: 2409-2770
Vol. 6, Issue 01, PP. 33-38, January 2019
https://www.ijew.io/

Novel Design of Optical Nano-Antennas to Enhanced Light-Absorption In Thin Film Solar Cell

Fazal E Subhan[1], Adnan Daud Khan[2], Fazal E Hilal[3]
[1, 2, 3] University of Engineering and Technology Peshawar, Pakistan, U.S Pakistan Center for Advanced Studies in Energy (USPCAS-E)
fsubhan@asu.edu[1], adnan.daud@uetpeshawar.edu.pk[2], fazal.hilal@gmail.com[3]
Received: 14 January, Revised: 21 January, Accepted: 22 January

***Abstract*—** We propose a novel design of enhanced light-absorption schemes for thin-film solar cells based on optical Nano-Antennas whose parameter governing the features of localized surface Plasmon's resonance and their effect on photosensitive possessions of the materials. The procedure of our design is based on excitation of collective modes of the optical Nano-Antennas whose electric field is localized between contiguous medium, collective modes is very productive to harness the long range of energy from solar spectrum with different and emerging material used in thin-film solar cells. We demonstrated theoretically substantial enhancement of solar-cell absorption spectral density in the whole spectrum range of the solar-cell operation equated to conventional structures commissioning anti-reflecting coating. We have been used COMSOL Multiphysics environment which is based on numerical finite element method (FEM). This approach is paramount substitute of anti-reflection coating and texturing in thin-film solar cells. Owing to less material usage along with efficient novel broad band light-harvesting structures, thin-film solar cells technically well-suited for large area fabrication techniques.

***Keywords*—** Localized Surface Plasmon Resonance, Nano-Antenna, Ligth Management Scheme, Thin Film Photovoltaics

I. INTRODUCTION

The modern world going towards advancement in the arena of thin film solar cells (TFSC) technology for large-area panel production to harvest the solar energy, further efficiency enhancement and reduction in cost. The cost of thin film solar cell as compared to other solar cells is quite less due to fewer materials' usage, as the material cost is around 40% of the total solar panel module, rapid payback and minor extent of toxic waste [18-20].

The thin film photovoltaics technology is the promising green energy technology which is the remedy of energy shortage and environmental delinquent. TFSC energy generation deals declining greenhouse gas releases and improve ecological co-benefits in the protracted term. In the first-generation solar cell, the bulk silicon material used which purification around 99.99% owing to these processing complexities cost of the solar cell technology is comparatively higher than fossil fuel technology. The thin-film technology is very promising technology to contribute in the energy mix of the globe to achieve the energy demand in a clean and green manner [28, 30, 35].

In TFSC the depth of the active layer is shortened, though the absorption is not taken place effectively at low energy photon in visible and infrared spectrum which is quite optimum energies near to the bandgap energy of the photovoltaics. To produce efficient thin film solar cells of a very small thickness around 120-150 nm, conventional texturing technique is quite unmanageable to employee upon the expose active surface of photovoltaic. However, for sake of more thin structure the anti-reflecting coating (ARC) would also be replaced by a novel design of light-harvesting structures which have the broad band spectrum and material independence properties [2-11]. Since anti-reflecting coatings has uni-spectral property and cannot prevent the transmission and refection of light through at very thin photovoltaic layer.

The operation band of TFSC according to their band gap energy can be tuned for localized surface Plasmon resonance (LSPR) upon changing the following parameter of the Nano-Antennas used in the novel design of light-trapping structure for TFSC [22-24]:

- Size of the Nano-Antenna
- Shape of the Nano-Antenna
- Local dielectric medium or environment or background medium
- Polarization of incident wave

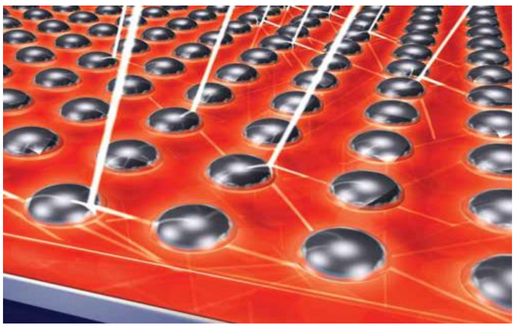

Figure 1. Optical Nano-Antenna Array [54]

In this work we demonstrated the various conceivable mechanism of absorption enhamcment of thin film GaAs solar cell by using a Nano-Antenna of different materials i.e gold (Au) and silver (Ag) and deployment methods, such as single and dimer optimized configurations to excite higher order plasmonic modes for better abosption efficiency in TFSC.

II. LITERATURE REVIEW

The thin-film photovoltaics to become an effective solution to the manufacturing and processing cost of first-generation photovoltaics a novel and alternate technique of improving the efficiency by increasing the absorption in active region of thin-film photovoltaics is desirable. The utmost encouraging technique is to achieve the plasmonic miracle of metallic nanostructures for improve performance, such as silver aluminum, copper and gold. The implementation of subwavelength metallic nanostructures which localized the electromagnetic radiation incident to very small region of plasmonic Nano structure. Furthermore, the other means of energy carried in the absorbing layer is scattering, the light is efficiently catch by activating into lateral waveguide modes [4, 8]. Together, these significantly improve the light absorption in active material and enhance the power conversion efficiency (PCE) of thin film solar cell.

A. Physics of Photonics

The photonics field is deal with interaction of light with matter, matter may be semiconductor, conductor and insulator. The field of plasmonic deal only interaction of light with metal. The interaction of light with Nano-Metal particle whose size is very less than size of wavelength of operational band then collective oscillation of electron taken place at the surface of these Nano-Particle called surface plasmon resonance. These surface plasmon is further categorized in to two category (i) Polariton moving surface plasmon resonance (ii) LSPR. In this work we will be observed the phenomena of LSPR to enhance the near-field of Nano-Antenna which intensity will be more than the incoming light intensity and yield to light-absorption in TFSC which results in photo-current and efficiency enhancement.

There are four noble metal gold (Au), silver (Ag,), copper (Cu) and aluminum (Al) [37] used to which exhibits a property of absorption and scattering due to collective oscillation of free electron which also form of LSPR. The LSPR or dipole modes depends on the following parameters such as (i) size of a Nano-particle, (ii) shape of Nano-particle, (iii) local dielectric medium and (iv) polarization of incident wave. LSPR is also highly depends upon the density of free electron in the Nano antenna or particle, these electronic densities for different noble metallic materials displays the sort of optics, which resembles to the resonance, Aluminum particle suitable for ultra-violet spectrum, gold visible, silver ultra-violet, copper visible range [3]. However, the operational spectrum is altering from blue-shift to the red-shift and vice versa by varying the embedded medium, shape and scope. In most of the previous work we observed that by employing silver Nano-particle directly on to a high index substrate such as transparent conductive oxide (TCO) and silicon dioxide SiO2 coating the LSPR is red-shifted in the direction of the near-IR region, growing light harvesting at those specific frequencies. To broaden the operational spectrum of solar cell high index medium or high size particle is used. In TFSC concentrated solely to grab the more energy content of solar spectrum which is long wavelength as, where all noticed a significant drop in photocurrent and light as compared to short wavelength, whose photo absorption and current below the LSPR for gold (Au) and silver (Ag) noble metal Nano-particles [33, 42, 48].

Previous work [49] display that if the LSPR is blue-shifted extreme enough, the improvement in photo absorption leads over the greater part of the operational sun spectrum, instead of show decreases at shorter wavelengths. The trade-off is condensed enhancements at longer wavelengths, but however, this method allows for an overall improvement in solar cell light absorption. The short-circuit current and external quantum efficiency (EQE) is highly improved by utilizing the red-shift response Nano-particle with high index medium to broaden the operational spectrum. The material selection for Nano-particle keep the cost and desired operational spectrum is very challenging. The cheap material is silver, but it is likely unstable and get oxidize quickly and narrower peak of absorption than gold is exceptionally steady and demonstrates the reverberation crest more extensive than silver. Conversely, copper is less expensive than silver, and more absorbing than gold but high losses occur as compare to other metal. Aluminum shows LSPR response in the UV range and having very weak oxidation than other plasmonic metal.

B. Higher-Order Modes Excitation for Enhanced Absorption

Confinement of photon energy in photovoltaic layer can also achieve effectively by excite higher order modes in Nano-antenna structure using two kind of excitation techniques for higher order modes.

i) Use cluster of Nano-Antennas
ii) Symmetry breaking

As there is two kind of modes bright mode and dark mode and overlapping of these modes enhance near field energy [51, 53] which improve the efficiency of TFSC. Array or cluster or structure of Nano-antennas is used to excite higher order modes which yield surface enhance ramen scattering (SERS) [33, 34, 36]. The various structure for higher order modes excitation includes such as Nano-particle dimmer [38], dolmen Nano-structure [40], metal Nano-shell [41], coupled Nano-rods [42], the stoutest structures nanoparticle oligomers [44].

The Pentamer and heptamer structure which is special types of oligomers structure is very efficient structure for SERS. In these different metal and high index dielectric core-shell structure the distance between two Nano-particle in the array is play a vital role in the excitation of higher order modes. As the gap between two Nano-particle increases they become independent and less chances of higher order modes excitation. The radius and index of dielectric is taking part in modes excitation where the process of hybridization of the Plasmon's of inward center and external shell decides the operational full frequencies of the complex nanostructure [46]. The interaction of hybridize dipole mode with stray modes can be achieved.

These hot-spot and field generated by the Nano-antennas will be much stronger than the incoming field due to LSPR and SERS which improve further the generation of photocurrent and increase sensitivity to the operational band [50].

Symmetry breaking in metal-dielectric (core-shell) Nano-particle properties is significantly change with the geometry due to dependence of fundamental dipole mode with surface of Nano-particle [32, 53]. Symmetry breaking alter the connections between plasmon modes which is hybridized dipole mode and stray modes and provide growth to SERS, and completely novel plasmonic feature is achieved. There are three alternates of a core–shell nanoparticle which near field strength is different from each other that is Nano-shells, Nano-eggs and Nano-cups. Nano-shells, comprising of a round high file dielectric center covered with a thin metal shell, change to Nano-egg by balancing the center inside the shell. Balances of the center more than the profundity of the shell layer, where the center cuts the shell, result in Nano-cups. Due to symmetry breaking, the modes are highly mix and results in quadrupole mode (Dipole active quadrupole mode), octupole (Dipole active octupole mode) and other higher order modes. In TFSC technology the TCO, ARC and Nano-antenna are used as core-shell structure and employee the symmetry breaking and cluster of Nano-antenna for short-circuit current density and efficiency improvement by increase absorption enhancement [53].

III. SIMULATION MODEL

We have been investigated the various mechanism of plasmoic Nano-structure encompassed of Au and Ag nanospheres on top of GaAs solar cell for absorption enhamcement with presence of embedded medium SiO2. The various size and cluster of nanpsphere are chosen such that the most absorbing one has easily found out among the optimized scenario's. The improved absorption, well-defined as :

$$\bar{A}\,(\lambda) = P_{ABS\text{-}GaAs}(\lambda)\,/\,P_{Source}(\lambda) \qquad (1)$$

Where as the PSource(λ) is the incident power from the sun source of photon flux of AM1.5G, PABS-GaAs(λ) is the power absorbed in the GaAs solar cell while λ is the wavelength around the air and GaAs. The power defined in (1) is tells us how much power is scattered out of plasmonic layer and absorbed in active layer. However, in order to find the absorbed power in the active bulk of photovoltaic layer with better matching between air and thin photovoltaic layer the equation will be turned out to the following equation:

$$\bar{A}_{GaAs}(\lambda) = P_{Trans\text{-}GaAs}(\lambda)\,/\,P_{Source}(\lambda) \qquad (2)$$

Where $P_{Trans\text{-}GaAs}(\lambda)$ is the power which transpassing the Nano-partical laid on front-surface and captivated in GaAs layer. There are two principal loss mechanism which reduce the absorption in the active bulk layer that's power absorbed in the plasmonic layer and scattered out power. In order to get more power absorbed in the GaAs layer local field in active layer vicinity and path length enhamcement is best approach to reduce the effects of loss mechanism. The model we propose included back reflector of Au and Ag according to plasmonic partical selection, prevent the transmittance of light out of GaAs absorbing layer and enhances the path length.

$$\bar{A}_{eff}\,(\lambda) = P_{ABS\text{-}GaAs}(\lambda)\,/\,P_{Trans\text{-}GaAs} \qquad (3)$$

The enhanced absorption effeicincy of the model were measured using (3) and considerd various stratagem such as clustering and Nano-partical size optimization methods.

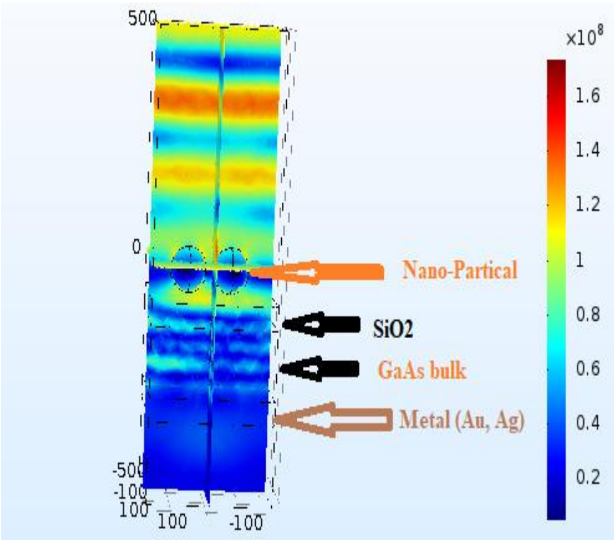

Figure 2. COMSOL simulation model ofpPlasmonic solar cell

Th simulation model developed in the COMSOL Multiphysics software which is very effective numerical simulation software built on finite element method (FEM), which precisely disentangles electromagnetics problem at very Nano-scale. The simulation in COMSOL Multiphysics will be carried out by the radio frequency (RF) module. Many Research group around the globe working on the Nano-device have been employed this software for design and simulation. The simulation in software accomplished usually by constructing a 3D simulation Planetary, which is consist of a perfectly matched layer (PML), boundaries were comsisted of perfectly electric conductor (PEC) and perflectly megnatic conductor (PMC) and oriented according to plane wave polarization, an embedding medium and spherical volume of far field layers. The two port network of simulation model were built for plane wave excitation injection and reception in order to get the absorption values for various model configuration for simulations.

We built and performed, plasmonic layer arrangement in single and array configuration using Au and Ag meta-material overhead of SiO2 , GaAs substrate and back reflector respectively in COMSOL environment as shown in fig.2. The dielectric function of Ag, Au and GaAs are based on already measured data from Nanohub [search]. The absorbed power in the different layer were monitored to get optimum novel shape for enhanced backscatterd light absorption in active photovoltaic layer.

IV. RESULTS AND DISCUSSION

First, we investigated the absorption of our proposed model by plane wave excitation of wavelength range from 300-1100 nm on GaAs and SiO2 in absence of plasmonic Nano-antenna. The gold (Au) single Nano-partical was then laid on top of GaAs and SiO2 with 150 nm and 50 nm respectively, while varying the size of partical, we observed that partical size below 30nm were not so effective to enhance absotion in active bulk by back scattering power. However, Au Nano-antenna with size 50 nm and 70 were stood up finest in the wavelength rangle from 300-650 nm. The operational band of Au partical is widend and easily tunable for higher order plasmonic modes by varying size and shape, as we did by optimized size for more absoption .Owing to norrow band features of SiO2 ARC this Au plasmonic partical with size above 50 nm with enhaced surface plasmone resonace make absorption efficiency Āeff (λ) high enough to substitute the ARC for thin film photovoltaics as can be readly seen in fig. 3. The Au partical size 15 nm and 70nm observed enhanced efficiency 15% and 33% accordingly compare to lone ARC layer.

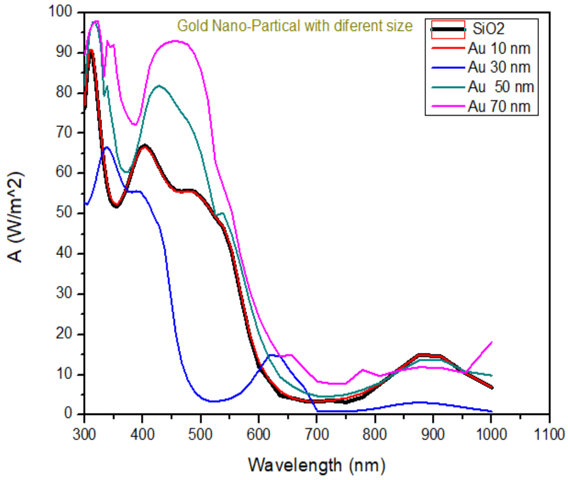

Figure 3. Different size gold Nano-antenna

The profound operational band of Au partical mostly lies in ultra-voilet wavelength range , hot spot and near field generation were achived by SERS and LSPR responses which improved further the absorption efficiency.

Fig. 4 shows the absorption efficiency Āeff (λ) of Au partical with different cluster size such as, dimer, trimer, tetramer and pentamer. The higher absorption efficiency were achived at greater cluster size due to excitation of higher modes from individual partical LSPR and SERS distribution and field interferences. The spacing and size of partical in cluster decides the net absorption efficiency. In order to observed the effect of number of partical in cluster, we kept the size of partical 30 nm persistent and were varying the cluster size increased to get notice the effect. In the array configuration we noticed, it seems that the main machinery contributing to the heightened absorption is the growth in array size. As the Au partical is blue shifted, so the dipole, quadrapole and hexapole of absorption peak at wavelength 300 nm, 450 nm and 550 nm were observed respectively, in different cluster configuration. The 10% increase observed enhanced efficienced 10% from dimer to pentamer cluster configuration.

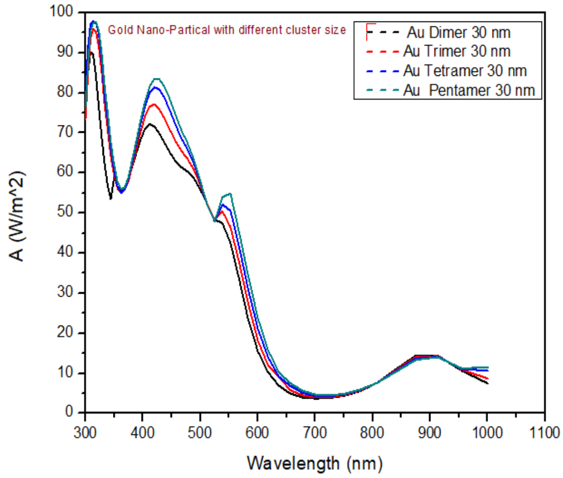

Figure 4. Gold Nano-antenna with different cluster size

The retort of absorption efficiency $\bar{A}_{eff}$ (λ) can also be shifted either red or blue by using different material. In fig. 5 the silver (Ag) Nano-partical have used to get red-shifted broad band region. The Ag partical is more broad capricious LSPR and SERS response compare to Au partical owing to the fact that Au is more stable partical. The red-shifted higher order LSPR modes makes Ag a very desirable plasmonic Nano-partical to harness the visible range of solar spectrum for GaAs. With increase in partical size the higher order excitation were detected and the most prominent size were again 50 and 70 nm.

The average 10% and 30% enhanced absorption efficiency above ARC layer were pragmatic in wavelength range 500-1100 nm of partical size 50 and 70 nm repectively.

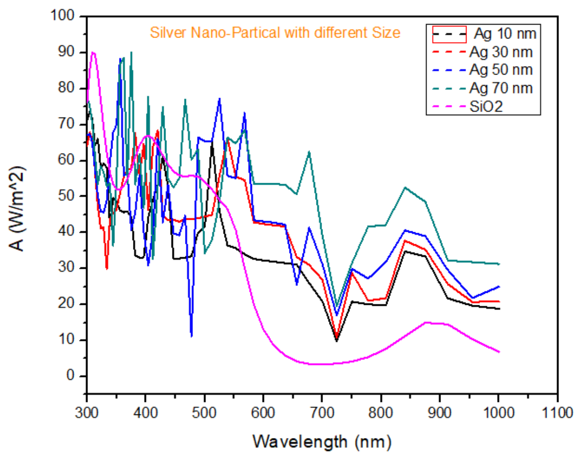

Figure 5. Different size silver Nano-antenna

Due to angular back scattered light of Ag partical in longer wavelength region enhanced the absorption efficiency and path length for higher short circuit current density.

Fig. 6 shows the absorption efficiency $\bar{A}_{eff}$ (λ) of Ag partical with different cluster size such as, dimer, trimer, tetramer and pentamer. In order to observed the effect of number of partical in cluster, we kept the size of partical 50 nm persistent and were varying the cluster size increased to get notice the effect of different array configuration. The shifting from dimer to pentamer in Ag array configuration the significant absorption efficiency difference among array configuration were not observed. However, the wavelength range from 500-1100 nm seems a very prominent absorption efficiency regime under each array configuration. In this long wavelength range around 30% increase observed from dimer to pentamer configuration.

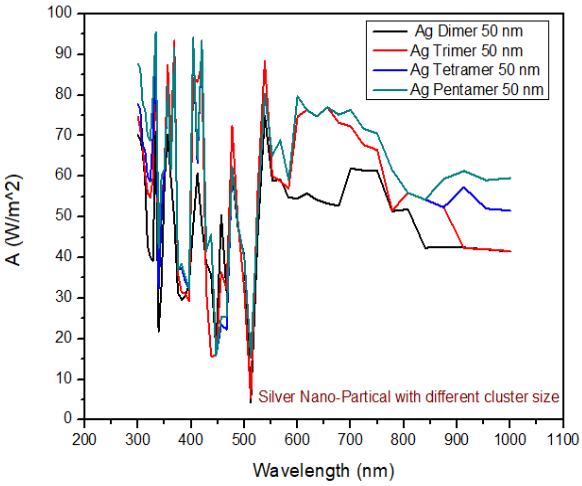

Figure 6. Silver Nano-Partical different with cluster size

The shift to longer wavelength of the absorption peak in case of Ag Nano-partical is associated with partical and cluster size. In order to get optimized broad band spectrum we used to keep the partical size 50 nm, instead of 30 nm as was in case of Au partical. The higher order modes were observed more in Ag as compare to Au due to material nature. The angular back scattering field modified a lot the absorption in GaAs layer. The excitation of higher order modes and peak shifting can also be done through embedded medium, in our case was SiO^2. In over-all comparison both plasmonic partical at different cluster configuration the Au and Ag gives us optimum absorption efficiency at shorter wavelength and longer wavelength respectively. Moreover, in single spherical consideration Au and Ag have given us blue-shifted and red-shifted responses respectively. However, these responses may pron to changes under different parameter variation which mentioned earlier.

CONCUSLION

In summary we have suggested and analyzed the different approaches of light-traping leading to improved absorption in thin film GaAs layer of 150 nm. Our novel model can be employed in a variety of thin film solar cell technologies in the ultra-voilet, visible and infrared band region. More significantly, the proposed light-traping structure is broad band and shows us the desired operational band material and cluster configuration. The presence of anti-reflection coating also effect the collective excitation modes of these Au and Ag Nano-antennas. We have demonstrated that our single and cluster Au and Ag nano plasmonic partical are noticbly better light absorption efficiency than sole anti-reflecting coatings in broad band operational region.

REFERENCES

[1] Eriksen, Emil H., et al. "Particle-particle interactions in large, sparse arrays of randomly distributed plasmonic metal nanoparticles: a two-particle model." Optics Express 25.16 (2017): 19354-19359.

[2] Senthil Kumar, N., et al. "Green mediated synthesis of plasmonic nanoparticle (Ag) for antireflection coating in bare mono silicon solar cell." Journal of Materials Science: Materials in Electronics (2018): 1-10.

[3] Catchpole, KR and, Albert Polman. "Plasmonic solar cells." Optics express 16.26 (2008): 21793- 21800.

[4] Dunbar, Ricky B., Thomas Pfadler, and Lukas Schmidt-Mende. "Highly absorbing solar cells—a survey of plasmonic nanostructures." Optics express 20.102 (2012): A177-A189.

[5] Heidarzadeh, Hamid, et al. "Plasmon-enhanced performance of an ultrathin silicon solar cell using metal-semiconductor core-shell hemispherical nanoparticles and metallic back grating." Applied optics 55.7 (2016): 1779-1785.

[6] Al-Adhami, Yasir, and Ergun Ercelebi. "A Plasmonic Monopole Antenna Array on Flexible Photovoltaic Panels for Further Use of the Green Energy Harvesting." Progress in Electromagnetics Research 68 (2018): 143-152.

[7] Garcia, Miguel A. "Surface Plasmon's in metallic nanoparticles: fundamentals and applications." Journal of Physics D: Applied Physics 44.28 (2011): 283001.

[8] Diukman, Iddo, and Meir Orenstein. "How front side plasmonic nanostructures enhance solar cell efficiency." Solar Energy Materials and Solar Cells 95.9 (2011): 2628-2631.

[9] Rockstuhl, Carsten, and Falk Lederer. "Photon management by metallic Nano-discs in thin film solar cells." Applied Physics Letters 94.21 (2009): 213102 .

[10] Dunbar, Ricky B., Thomas Pfadler, and Lukas Schmidt-Mende. "Highly absorbing solar cells—a survey of plasmonic nanostructures." Optics express 20.102 (2012): A177-A189.

[11] Jiao, Hongfei, et al. "Ultra-broadband perfect absorber based on successive Nano-Cr-film." Advances in Optical Thin Films VI. Vol. 10691. International Society for Optics and Photonics, 2018.

[12] Xu, Zhenhe, et al. "Harvesting Lost Photons: Plasmon and Up conversion Enhanced Broadband Photo Catalytic Activity in Core@ Shell Microspheres Based on Lanthanide- Doped NaYF4, TiO2, and Au." Advanced Functional Materials 25.20 (2015): 2950-2960.

[13] Lu, Zelin, et al. "Plasmonic-enhanced perovskite solar cells using alloy popcorn nanoparticles." RSC Advances 5.15 (2015): 11175-11179.

[14] Saravanan, S., et al. "Efficiency improvement in dye sensitized solar cells by the plasmonic effect of green synthesized silver Nano-particles." Journal of Science: Advanced Materials and Devices 2.4 (2017): 418-424.

[15] Lee, Kwang-Sup, et al. "Feature issue introduction: organic and polymeric materials for photonic applications." Optical Materials Express 7.7 (2017): 2691-2696.

[16] Ren, Wenzhen, et al. "Broadband absorption enhancement achieved by optical layer mediated plasmonic solar cell." Optics express 19.27 (2011): 26536-26550

[17] Navab, Arvin Attari, et al. "Hydrothermal synthesis of TiO2 Nano-rod for using as an electron transport material in perovskite solar cells." AIP Conference Proceedings. Vol. 1920. No. 1. AIP Publishing, 2018.

[18] Atwater, Harry A., and Albert Polman. "Plasmonics for improved photovoltaic devices." Nature materials 9.3 (2010): 205.

[19] Kato, Kazuhiko, et al. "A life-cycle analysis on thin-film CdS/CdTe PV modules." Solar Energy Materials and Solar Cells 67.1-4 (2001): 279-287.

[20] Bloss, W. H., et al. "Thin- film solar cells." Progress in Photovoltaics: Research and Applications 3.1 (1995): 3-24.

[21] Fischer, Holger, and Olivier JF Martin. "Engineering the optical response of plasmonic Nano-antennas." Optics express 16.12 (2008): 9144-9154.

[22] Cao, Wei, et al. "Localized surface Plasmon resonance of single silver nanoparticles studied by dark-field optical microscopy and spectroscopy." Journal of applied physics109.3 (2011): 034310.

[23] Feng, Chuanzao, Yizhi Yang, and Yingjie Tan. "Design of broadband metamaterial near-perfect absorbers in visible region based on stacked metal-dielectric gratings." Materials Research Express (2018).

[24] Lang hammer, Christoph, et al. "Localized surface Plasmon resonances in aluminum Nano disks." Nano letters 8.5 (2008): 1461-1471.

[25] Abbey, Grant P., et al. "Structural characteristics of Au-GaAs nanostructures for increased plasmonic optical enhancement." Quantum Dots and Nanostructures: Growth, Characterization, and Modeling XIII. Vol. 9758. International Society for Optics and Photonics, 2016.

[26] Qian, Jun, et al. "Nano sphere-in-a-Nano egg: damping the high-order modes induced by symmetry breaking." Nanoscale research letters 10.1 (2015): 17.

[27] Akimov, Yu A., Wee Song Koh, and Kostya Ostrikov. "Enhancement of optical absorption in thin-film solar cells through the excitation of higher-order nanoparticle Plasmon modes." Optics express 17.12 (2009): 10195-10205.

[28] Chu, Steven, and Arun Majumdar. "Opportunities and challenges for a sustainable energy future." nature 488.7411 (2012): 294.

[29] Akimov, Yuriy A., and Wee Shing Koh. "Design of plasmonic nanoparticles for efficient subwavelength light trapping in thin-film solar cells." Plasmonics 6.1 (2011): 155-161.

[30] Kamat, Prashant V. "Meeting the clean energy demand: nanostructure architectures for solar energy conversion." The Journal of Physical Chemistry C 111.7 (2007): 2834-2860.

[31] Makarov, Sergey V., et al. "Light- Induced Tuning and Reconfiguration of Nanophotonic Structures." Laser & Photonics Reviews (2017).

[32] Knight, Mark W., and Naomi J. Halas. "Nano shells to Nano eggs to Nano cups: optical properties of reduced symmetry core–shell nanoparticles beyond the quasistatic limit." New Journal of Physics 10.10 (2008): 105006.

[33] Sakir, Menekse, et al. "Fabrication of Plasmonically Active Substrates Using Engineered Silver Nanostructures for SERS Applications." ACS applied materials & interfaces 9.45 (2017): 39795-39803.

[34] Roelli, Philippe, et al. "Molecular cavity optomechanics as a theory of plasmon-enhanced Raman scattering." Nature nanotechnology 11.2 (2016): 164-169.

[35] Serrano, Elena, Guillermo Rus, and Javier Garcia-Martinez. "Nanotechnology for sustainable energy." Renewable and Sustainable Energy Reviews 13.9 (2009): 2373-2384

[36] Oldenburg, Steven J., et al. "Surface enhanced Raman scattering in the near infrared using metal Nano shell substrates." The Journal of chemical physics 111.10 (1999): 4729-4735.

[37] Ferry, Vivian E., et al. "Light trapping in ultrathin plasmonic solar cells." Optics express 18.102 (2010): A237-A245.

[38] Wang, Hui, et al. "Symmetry breaking in individual plasmonic nanoparticles." Proceedings of the National Academy of Sciences 103.29 (2006): 10856-10860.

[39] Ge, Lixin, et al. "Unidirectional scattering induced by the toroidal dipolar excitation in the system of plasmonic nanoparticles." Optics Express 25.10 (2017): 10853-10862.

[40] Takei, Hiroyuki, Michael Himmelhaus, and Takayuki Okamoto. "Absorption spectrum of surface-bound cap-shaped gold particles." Optics letters 27.5 (2002): 342-344.

[41] Charnay, Clarence, et al. "Reduced symmetry metallodielectric nanoparticles: chemical synthesis and plasmonic properties." The Journal of Physical Chemistry B 107.30 (2003): 7327-7333.

[42] Liu, Jingquan, et al. "Anisotropic optical properties of semitransparent coatings of gold Nano caps." Advanced Functional Materials 16.11 (2006): 1457-1461.

[43] Lim, S. H., et al. "Photocurrent spectroscopy of optical absorption enhancement in silicon photodiodes via scattering from surface Plasmon polaritons in gold nanoparticles." Journal of applied physics 101.10 (2007): 104309.

[44] Chong, Katie E., et al. "Observation of Fano resonances in all- dielectric nanoparticle oligomers." Small 10.10 (2014): 1985-1990.

[45] Sakir, Menekse, et al. "Fabrication of plasmonically Active Substrates Using Engineered Silver Nanostructures for SERS Applications." ACS applied materials & interfaces 9.45 (2017): 39795-39803.

[46] Prodan, Emil, et al. "A hybridization model for the Plasmon response of complex nanostructures." science 302.5644 (2003): 419-422.

[47] Beck, F. J., A. Polman, and K. R. Catchpole. "Tunable light trapping for solar cells using localized surface Plasmon." Journal of Applied Physics 105.11 (2009): 114310.

[48] Temple, T. L., et al. "Influence of localized surface Plasmon excitation in silver nanoparticles on the performance of silicon solar cells." Solar Energy Materials and Solar Cells 93.11 (2009): 1978-1985.

[49] Villesen, Thorbjørn Falk, et al. "Aluminum nanoparticles for plasmon-improved coupling of light into silicon." Nanotechnology 23.8 (2012): 085202.

[50] Dodson, Stephanie, et al. "Optimizing electromagnetic hotspots in plasmonic bowtie Nano antennae." The journal of physical chemistry letters 4.3 (2013): 496-501.

[51] Makarov, Sergey V., et al. "Light- Induced Tuning and Reconfiguration of Nano photonic Structures." Laser & Photonics Reviews (2017).

[52] Katyal, Jyoti, and R. K. Soni. "Localized surface Plasmon resonance and refractive index sensitivity of metal–dielectric–metal multilayered nanostructures." Plasmonics 9.5 (2014): 1171-1181.

[53] Yu, Yiling, et al. "Dielectric core–shell optical antennas for strong solar absorption enhancement." Nano letters 12.7 (2012): 3674-3681.

[54] Photo courtesy: www.ecn.nl, "Plasmonic solar cell".

FAZAL E SUBHAN received B.Sc. degrees in Electrical Engineering from the University of Engineering and Technology, Peshawar, Pakistan, in 20015. He's currently perusing his Master degree in Renewable Energy Engineering from U.S Pakistan Center for Advanced Studies in Energy, UET, Peshawar, Pakistan. He has been to Arizona State University (ASU), USA in 2018 as a Research Exchange Scholar for semester long duration. He worked in Holman Research Group which is member of Quantum Energy and Sustainable Solar Cells Technologies (QESST), Eyring Energy Material (EEM), Nano Fabrication (NanoFab) and Optoelectronics and energy material lab in school of Electrical, Computer and Energy Engineering at Ira. A Fulton school of Engineering ASU, USA. He got certificates of "Technology Entrepreneurship and Innovation" and "Energy Policy and Sustainability" from ASU.

His research interests included optoelectronic modeling of photovoltaic devices, photonics Nano-technology for light management in third generation solar cell, renewable energy materials & technology modeling, smart energy grid, power electronics and electrical machinery.

.

International Journal of Engineering Works
ISSN-p: 2521-2419
ISSN-e: 2409-2770
Vol. 6, Issue 01, PP. 39-43, January 2019
https://www.ijew.io/

Performance Evaluation of Nickle Platinum Novel Electrocatalysts for Proton Exchange Membrane Fuel Cell

Shahbaz Ahmad[1], Dr. Saim Saher[2], Mushtaq Ahmed[3], Abid Ullah[4]
[1,2,3,4]U.S Pakistan Center for Advanced Studies In Energy (U.S PCAS-E), UET Peshawar
khan908020@gmail.com[1], sahmad19@asu.edu[1], s.saher@uetpeshawar.edu.pk[2], mushtaqkhattak113@gmail.com[3]
adhchem@gmail.com[4]
Received: 15 January, Revised: 21 January, Accepted: 23 January

Abstract—Among different types of fuel cells, the proton exchange membrane fuel cell (PEMFC) represents promising technology due to its lower operating temperature and higher efficiency. PEMFC can bring revolution in automobile industry by providing power to drive by consuming less fuel in a environmental friendly way. However, right now the main hurdle for its commercialization is the sluggish oxygen kinetics or slow reduction of oxygen at respective electrodes. To accelerate the sluggish oxygen reduction reaction (ORR) different types of expensive noble Pt alloys has been used as catalyst at cathode. The use of Pt based catalysts increases the cost of PEM fuel cell production therefore extensive research has been carried out to explore and develop different kinds of low costcatalysts as an alternative option. This study involves fabrication and testing of Ni-Pt ZIF as substitute electrocatalyst for cathode in PEM fuel cell. Ni-Pt has found to be a good substitute with a peak power density of 450 $mW.cm^{-2}$ at temperature of 75℃ with Nickle to Platinum ratio of 9:1.

Keywords— PEMFC, ORR, ZIF, Electrocatalyst

I. Introduction

Fuel Cells are electrochemical devices to convert chemical energy resulting from oxidation process to electrical energy [1]. Fuel Cells are highly efficient conversion devices with theoretical efficiency of 83%, however, typically their value ranges between 40-60 % [2]. Due to mechanical stability and zero emission power source, protom membrane fuel cell (PEMFC) is seeking much attention in recent years [3]. PEM fuel cell is one of the most efficient contestants for power hotspots and electric drive vehicles. PEM fuel cel is also known as polymer electrolyte membrane fuel cell is fabricated from proton-conducting polymer electrolyte membrane, usually a perflourinated sulfonic acid polymer [4]. On respective electrodes usually two types of chemical reactions which are also known as oxidation-reduction (redox) reactions take place.

Oxidation process occurs at anode in which hydrogen molecule loses its two conducting electrons that flows through outer circuit producing electric current. Reduction process takes place at cathode which is complex phenomena. Reduction reaction occurs in three modes in which either one, two or four electrons transfer takes place thus forming hydrogen oxide, hydrogen per oxide ions or water molecule. In order to have clean energy both of contributing elements (H_2 and O_2) should be pure so that the end product obtained is pure water with no environmental hazards. In order to have complete reaction usually the four electron pathway is desired to make water molecule [5]. Overall reactions are represented as under.

Reaction at anode

$$2H_2 \rightarrow 4H^+ + 4e^-$$

Cathode Reaction

$$O_2 + 4H^+ + 4e^- \rightarrow 2H_2O$$

Overall Reaction

$$2H_2 + O_2 \rightarrow 2H_2O$$

The performance of PEM fuel cell is evaluated through the kinetics of electrocatalytic reactions that involves transfer of electrons from hydrogen to oxygen, which is also knows oxygen reduction reaction (ORR) [6]. The working of the PEMFC is presented in Fig. 1.

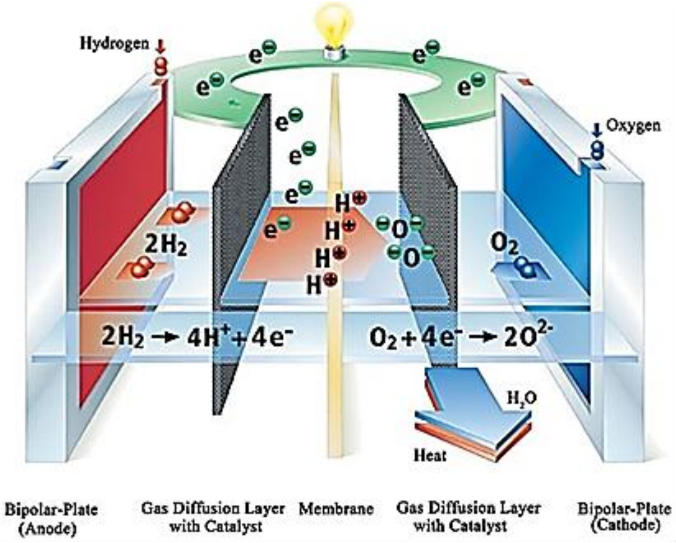

Fig.1 Schematic figure of PEMFC

A. Research Problem

In commercialization of low temperature fuel cells such as PEM fuel cell, the primary need is to develop a highly porous material which is low cost, durable and highly active. To accelerate the sluggish oxygen reduction reaction (ORR) different types of noble Pt alloys has been used as catalyst at cathode which has adversely affected the electrochemical performance of fuel cells due to its high loading effects [7]. Under these circumstances extensive studies has been carried out to explore and develop non noble Pt less catalysts as an alternative option. Among them the most interested compounds that have been developed are Zeolitic imidazolate framework (ZIF) based electroatalysts. ZIF's are porous crystalline materials which forms a connection between inorganic metals and polymer crystalline materials. They are also known as porous coordination polymers (PCPs). ZIF's has gained interest in field of energy storages devices because of its unique porous structure which can store potential electrons and act as high power density materials, high surface area, organic-inorganic hybrid nature and versatility [8].

Both the anode and cathode electrodes consist of highly dispersed Pt-based catalysts loading on carbon support to promote the hydrogen oxidation reaction (HOR) and oxygen reduction reaction (ORR). The reaction rate of the HOR on Pt is sufficiently fast, therefore the required amount of Pt loading at the anode can be less than 0.05 $mg.cm^{-2}$. However, at the cathode, the sluggish reaction kinetics of the ORR requires a much higher Pt loading (~0.4 mg/cm2) to achieve appropriate fuel cell performance [9]. Pt-based precious metal catalysts still suffer from several critical problems, such as high cost, poor stability, crossover effect, and CO poisoning [10]. Reducing Pt loading or even completely replacing it with a low cost transition metal based catalyst without compromising the performance is a major challenge faced by the application of this promising technology.

B. Research Objective

The main hurdle in commercialization of PEM fuel cells are high cost of carbon supported Pt catalyst used in cathode which accounts for almost 60% of total fuel cell stack cost [11] and insufficient durability which occurs due to sluggish oxygen reduction reaction. Among existing fuel cell technologies PEMFC are most studied in recent years because of low working temperature, high power density and quick startup but problem is high cost of Platinum loading which are much required at cathode side for proper cell performance. Researchers and scientists around the world are trying to come up with new techniques to decrease the platinum loading like platinum nano-particles on carbon surface, or replacing the platinum group metal (PGM) with other metals like transition metals and alloys. This research is dedicated to study effect of transition metals such as Nickel based electrocatalyst and its combinations with low content PGM to achieve comparable performance with respect to Pt electrocatalysts alone.

II. METHODOLOGY

A. Preparation of sample

Nickle Platinum ZIF was prepared according to liturature [12]. According to this method 27.5g of 2-methylimidazole (2-MIM) was mas mixed in 100 ml of deionized (DI) water in one beaker with constant stirring while in another beaker 1.2 g of Nickel (II) nitrate hexahydrate which is a precursor of Nickle was dissolved in 15 ml of DI water . The solution was stirred contantly until green color was formed. Both of the solutions were mixed togetter under continuous stirrering for 6 hours at ambient temperature and pressure. After the complete reaction the solution was centrifuged three times while with mixing with fresh water to remove unreacted immadazole precipitate. After washing, the sample was dried overnight in oven at 80 ℃.

B. Addition of Platinum

Before pyrolysis of sample 10% of chloroplatinic acid (H_2PtCl_6) aas added to the dried sample . The sample yield was 500 mg in which 10 ml of H_2PtCl_6 solution was added.

C. Pyrolysis

After the addition of chloroplatinic acid, the sample was heated up at 350 ^oC for 1.5 h then the temperature is raised to 800 ^oC at a ramp rate of 5 ^oC per minute for 3.5 h in Helium and Argon atmosphere reflux. After preparing the black sample, it is cooled down to ambient temperature automatically. The sample was washed in 0.5M H_2SO_4 solution for 10 h. the catalyst which is prepared were accumulated by high centrifugation, recurrently cleaned with DI water and dehydrated at 100 ^oC under vacuum for 2-3 hour.Finally Ni-Pt ZIF was ready for testing. The final yield of the product was 100 mg. The block diagram of process is represented in Fig. 2.

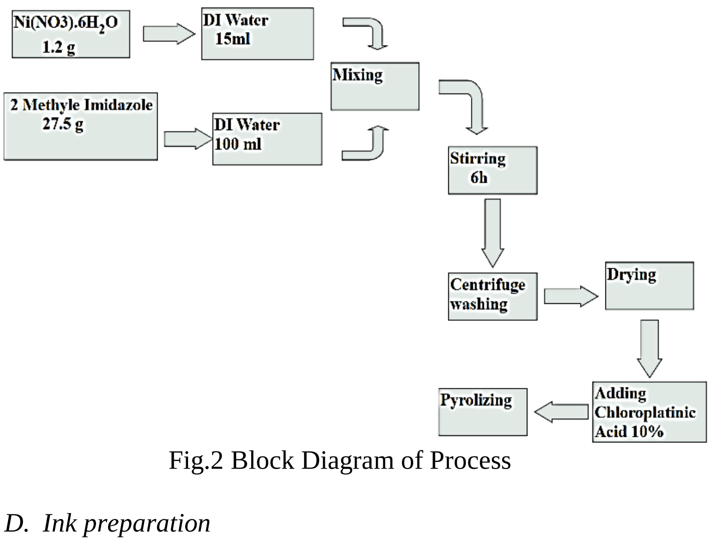

Fig.2 Block Diagram of Process

D. Ink preparation

In order to test our synthesized material it has to sprayed on nafion membrane to make membrane electrode assembly (MEA) out of it. In order to make ink of it 50mg of a Ni-Pt catalyst was mixed with 2.25ml of isopropyl alcohol and

0.3ml of nafion ionomer (20%wt). The ink was aggetated following by sonication of 10 mins for three time.

E. Membrane electrode assembly MEA)

MEA is a core component of a fuel cell which assists to produce electrochemical reaction that gives us free electron. MEA is made of polymer electrolyte membrane on which is sprayed on either side to make cathode and anode and this membrane is sandwich between two gas diffusion layers (GDL). GDL is typicaaly made of porous carbon fibers array. Its function is to create electrically conducting pathway for the collection of current. Loading on cathode side is typically higher then anode because the fuel (Hydrogen) passes through membrane and meet oxidant (Oxygen) at cathode side. In this research nafion membrane is used as polymer electrolyte membrane.

E.1. Material Loading

Area of material loading on nafion membrane is 1×1 inch^2. Weight of membrane before and after loading was recorded. As presented in table1 are the weights of MEA for pre and post weights of MEA before and after spray loading of catalyst.

Table 1. Loaded content

No	Ni-Pt MEA		
	Weight before loading (gm)	***After Anode Loading (gm)***	***After Cathode loading (gm)***
1	0.2559	0.2567	0.2617

F. Testing

Finally the product made was tested in a fuel cell test station which consist of an expandable research test cell and data acquisition center. The test cell consist of MEA slots with small openings in which hydrogen (H_2) and oxygen (O_2) gases or Air is supplied and silicon sheet with square opening in which MEA and GDL is placed all these components are sandwiched between bipolar anode and cathode plates. The purpose of silicon sheet is to insulate both plates so that short circuit won't occur. As shown in fig. 3 is complete model of a expandable research test fuel cell [13].

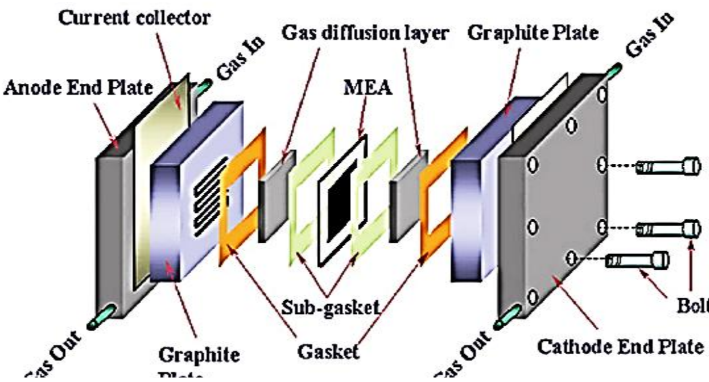

Fig.3 Expandable Research test fuel cell

III. RESULTS AND DISCUSSION

The oxygen reduction reaction (ORR) activities of Ni-Pt catalyst were evaluated through single MEA fuel cell test. In order to make it commercialized, it has to be tested under different parameters resembling the commercial fuel cell stack. In order to evaluate results first we tested MEA made of commercial platinum inside test station to check its performance parameters such as open circuit voltage (OCV), current density and peak power density [14]. Fig. 4 and 5 presents the polarization and power density graph of commercial standard platinum and nickel platinum respectively.

Fig. 4 shows us that commercial grade platinum has peak power density of 800 mW.cm^{-2} at current density of 1800 mA.cm^{-2} with OCV of 0.97 V. As the cell is connected to the external load it begins to draw current and subsequently power density increase until a point where concentration losses occur. The decrease in OCV is due to activation, ohmic and concentration losees occurs inside cell and circuit [15]. For a commercial grade platinum the slope will be always smooth as compare to other materials due to the presence of higher active sites [16]. Readings were taken at three different temperatures and in full humidified environment.

Fig.5 is polarization and power density curve for nickel platinum catalyst which shows almost same OCV of 0.975 V at current density of 16 mW.cm^{-2} . The peak power obtain for this catalyst is 450 mW.cm^{-2} at temperature of 75℃ at current density of 850 mA.cm^{-2} which is almost half as compare to commercial Platinum. A limiting current of 1400 mA.cm^{-2} has been recorded for this catalyst.

The governing equtions for calculating Power is given by [16].

$$P = \frac{V_b^2 RL}{(Rint + RL)^2} \tag{1}$$

V_b = fuel cell battery voltage (V)

R*int* = effective internal resistance of a fuel cell (Ω)

RL = load resistance (Ω)

Open Circuit voltage OCV of fuel cell is calculated through Nerst Equation [17].

$$E = E^{\circ} - \frac{RT}{nF} lnQ_C \qquad (2)$$

s

E = cell potential (V) under specific conditions

E^{o}= cell potential at standard conditions

R = ideal gas constant = 8.314 J/mol-K

T = temperature in (kelvin)

n = number of moles of electrons transferred

F = Faraday's constant = 95,484.56 C/mol

lnQ_c = the natural log of the reaction quotient

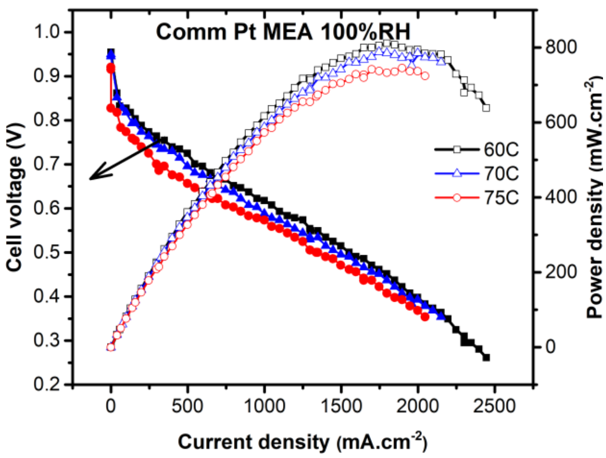

Fig. 4 The single fuel cell current-voltage polarizations curve. Test conditions: Nafion membrane, Catalyst =comm Pt/C cathode loading ~ 0.7 mg cm^{-2}, anode loading 0.5 mg cm^{-2}, cell area = 1×1 $inch^2$, T = 60℃,70℃,75 ℃ PO_2 = PH_2 = 1.0 bar, 100% Relative humidity.

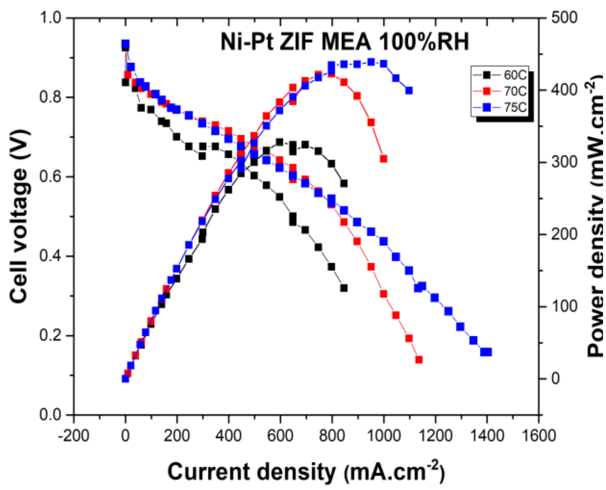

Fig. 5 The single fuel cell current-voltage polarizations curve. Test conditions: Nafion membrane, Catalyst = Ni-Pt , comm Pt/C cathode loading ~ 5 $mg.cm^{-2}$, anode comm Pt/C loading 0.8 $mg.cm^{-2}$, cell area = 1×1 $inch^2$, T = 60 ℃,70 ℃, 75 ℃ PO_2 = PH_2 = 1.0 bar, 100% Relative humidity.

Comparing both values of Fig. 4 and Fig. 5, we found that by reducing the amount of platinum in our catalyst from 90% to 10% has only reduced the peak power density by 40% while keeping the OCV constant. from Our investigation finds out that the reduction in peak power of catalyst as compare to commercial platinum is due to the limitation of active sites in this catalyst. The ORR activity mainly depends on the number of free electrons present on the surface area of the catalys which is called active sites. The reduction in cost of catalyst is significant as compare to the total power density drop.

IV. Conclusion

In summary Nickel (ii) nitrate hexahydrate has been successfully use as precursor to synthesized Ni-Pt ZIF. The well designed Ni-Pt ZIF with control structure morphology has been synthesized with control parameters which has shown much better electrochemical performance as compare to other metal ZIF's being synthesized. The reduction in cost of this catalyst as compare to commercial platinum is very significant relative to the peak powers. The performance parameters of this catalyst can be enhanced by the addition of other transition metals which subsequently can create more active sites thus facilitating ORR activity.

We believe that the proposed methodology will open up another road for the structure and blend of ZIF-based models, which will expand the broad utilizations of ZIFs; what's more, the as acquired Ni-Pt ZIF-based nanostructures will be magnificent materials for different applications such as catalysts, sensors and energy storage and conversion devices.

V. Acknowledgment

The authors wish to thank the researchers whose literature has been cited in this article and acknowledge Advance Materials for Energy Laboratory (Pakistan) for providing materials and experimental setups used in this study. Research leading to this article was supported by the research grants of U.S.-Pakistan Center for Advanced Studies in Energy (USPCAS-E), University of Engineering and Technology (UET) Peshawar, Fuel Cell and Batteries Lab of Arizona State University (ASU), and U.S. Agency for International Development, USAID (AID-391-A-14-000007).

References

[1] Novel materials for solid oxide fuel cell technologies: A literature review. Fellipe Sartori da Silva, Teofilo Miguel de Souza J. Clerk

[2] Maxwell, A Treatise on Electricity and Magnetism, 3rd ed., vol. 2. Oxford: Clarendon, 1892, pp.68–73.

[3] K. Elissa Thermodynamics of Fuel Cells, Springer, 1st Edition, 2008.

[4] Analysis performance of proton exchange membrane fuel cell (PEMFC) A. N. A. Mubin1, M. H. Bahrom1, M. Azri1, Z. Ibrahim1, N. A. Rahim2 and S. R. S. Raihan2

[5] RYAN O'HAYRE, Fuel Cell Fundamentals, Springer, Third edition, 2013.

[6] Chaojie Song and Jiujun Zhang, Electrocatalytic Oxygen Reduction Reaction, Springer, 2012, 89-34.

[7] A. J. Appleby, J. Electroanal. Chem., 1993, 357, 117–179.

[8] Recent Progress on MOF-Derived Nanomaterials as Advanced Electrocatalysts in Fuel Cells Zhongxin Song, Niancai Cheng, Andrew Lushington and Xueliang Sun H. A. Gasteiger, S. S. Kocha, B. Sompalli and F. T. Wagner, Appl. Catal., B, 2005, 56, 9–35

[9] QLongZhu, RuqiangZou, QiangXu, Metal Organic Frameworks for energy applications, Chem., 2017, 52-77.

[10] Rabis, A.; Rodriguez, P.; Schmidt, T.J. Electrocatalysis for polymer electrolyte fuel cells: Recent achievements and future challenges. Acs Catal. 2012, 2, 864–890.

[11] Cheng, N.; Mu, S.; Pan, M.; Edwards, P.P. Improved lifetime of PEM fuel cell catalysts through polymer stabilization. Electrochem. Commun. 2009, 11, 1610–1614.

[12] Madhu Sudan Saha, Vladimir Neburchilov, Dave Ghosh and Jiujun Zhang Nanomaterials-supported Pt catalysts for proton exchange membrane fuel cells, Wires Energy and Environment, Vol. 2, 2012, 32-45.

[13] Alexeyeva et al. Electro reduction of oxygen on nitrogen-doped carbon nanotube modified glassy carbon electrodes in acid and alkaline solutions. Journal of Electro analytical Chemistry, (2010), 169-175.

[14] http://www.northerngraphite.com/about-graphite/graphite-growth-markets/fuel-cells/

[15] Non-Precious Metal Catalysts Prepared By Zeolitic Imidazolate Frameworks: The Ligand Influence to Morphology and Performance.

[16] https://www.zswbw.de/fileadmin/user_upload/PDFs/Vorlesungen/est3/FCF_A4.pdf

[17] The power performance curve for engineering analysis of fuel cells Jay B. Benziger ∗ , M. Barclay Satterfield, Warren H.J. Hogarth, James P. Nehlsen, Ioannis G. Kevrekidis. Journal of Power Sources 155 (2006) 272–285.

[18] http://www.chem.tamu.edu/class/fyp/stone/tutorialnotefiles/electro/nernst.htm.

Shahbaz Ahmad did his bachelors in Mechancial Engineering from from University of Engineering and Technology (UET) Peshawar,Pakistan in 2016. Presently, he is enrolled in Masters in Renewable Energy Engineering from U.S Pakistan Center for Advanced Studies In Energy (U.S PCAS-E), UET Peshawar. Also, he has completed semester long training at Arizona State University (ASU) USA as a research scholar. His area of interest includes renewable energy resourses such as Fuel Cell ahd Hydel Energy, Mechanical Engineering Design and IC engines.

IJEW 国际工程期刊 International Journal of Engineering Works انجینرنگ کاموں کا بین الاقوامی جرنل

International Journal of Engineering Works
ISSN-p: 2521-2419
ISSN-e: 2409-2770
Vol. 6, Issue 02, PP. 44-49, February 2019
https://www.ijew.io/

Performance Enhancement of Heterogeneous Cellular Networks Using Vertical Handover

Saad Iqbal[1], Alamgir Khan[2], Hassan Wasim Khan[3], Imraan Khan[4], Fazal Muhammad[5]
[1,2]Telecommunication Engineering, University of Engineering and Technology Peshawar, Pakistan
[3,4]University of Engineering and Technology Mardan, Pakistan
[5]City University of Science and Information Technology Peshawar, Pakistan
saadiq839@gmail.com[1], alamgir_uet@outlook.com[2], hassanwasimkhan@gmail.com[3],
imran@uetmardan.edu.pk[4], fazal.muhammad@cusit.edu.pk[5],
Received: 18 January, Revised: 31 January, Accepted: 05 February

***Abstract*—** In seamless and fast mobility, smooth handover is one of the major challenges in small cell heterogeneous cellular networks. This paper focuses on the phenomenon of vertical handover for wireless heterogeneous networks. This class of networks can be grounded on the parameter values such as bandwidth availability, received signal strength, call request/served per unit time (mean), power dissipation, consumption of power, duration of mobile station presence, network security, cost of the network and velocity of the mobile station. The proposed system, in this paper, is characterized on the basis of four network parameters which are scrutinized as per a pre-defined criterion. Thereafter, vertical handover occurs at the most suitable among the available four networks. In order to achieve the objective, various parameters are applied for the vertical handover decision and implementation. Furthermore, the final decision is taken on the basis of individual network's call blocking probability considering the aforesaid parameters.

***Keywords*—** Handover, Cellular Networks, HetNets, 3G, 4G, GSM, WLAN, QoS, RSS.

I. Introduction

Today's technological world is going towards swift development and express of evolution in wireless networks. In these advancements, trial and errors have been a common practice, resultantly; researchers have pinpointed various challenges in assembling different networks. For instance, the fourth generation (4G) of cellular networks integrate a huge amount of heterogeneous cellular networks (HetNets) [1]. This serves as a step towards universal seamless access; however, this does not mean that the issues encountered in the field of seamless mobility have all been met [2].

A quick scrutiny of the literature available in the domain of seamless mobility reveals that among many other areas to refine, one significant sub-domain is that of efficient handovers. Talking more specifically, one can tell that there is a need of efficient schemes to enable vertical handover among different types of radio technologies such as cellular, wireless area network (WAN), wide local area network (WLAN) [2],[3]. This handover bears emphasis because it acts as the decision-point for a mobile node in such HetNets. In the traditional cellular network like global system for mobile communication (GSM) authors compared different parameters in specific order using pre-defined threshold for handover decisions [3].

Furthermore, it encompasses multiple interfaces in order to select the best available link in all possible alternatives for mobile nodes connecting the network in real time. A survey with a scheme for the IEEE 802.11 protocol which modifies the distributed coordination function (DCF) admittance technique in the variance phase carry numerous levels of priorities in such a way that the user mobility is encouraged in WLANs [4],[5]. Different types of algorithms that are purely based on network technique (classical) and many other concentrates on the idea of Markov process outcome [6].

When it comes to maintaining quality of service (QoS) based connections between networks, there is a variety of parameters that need to be considered; for example, pre-defined QoS standards and minimum call dropping ratios. It is customary to mention here that the call dropping ratios are usually calculated after the undesired handover during which the call-in process may be affected and the chances of dropping increases abruptly. This undesired handover directly affects the scenario of ongoing connection of the transmission. One of the most important terms to be considered in handover is the enhancement of QoS. For instance, applications such as unicast and multicast video streaming and web browsing come with strict QoS requirements. In order to ensure quality, vertical handover concentrates on minimizing the ping-pong effect. This minimization helps in reduction of interruption in processing calls and provides an increase in throughput during the handover [7],[8].

In the light of the above-mentioned facts, one can state that the main challenge in upcoming networks would be quick handover in IP-based networks. Researchers have also anticipated this quick handover as a high transmission, packet loss small handover [9]. In the initial discovery stage, the connections of mobile nodes made up with various interfaces have to go through a decision-making. This decision-making takes into account the network's suitability for usage and the presence of services in network. In the second stage namely the system discovery, the mobile node seeks the network to which it may connect. This pursuit followed by the network selection depends upon many factors like jitter, access cost, available bandwidth, transmit power, delay, the user's preferences and current updated status of the mobile device. In the third stage, the need for re-routing from the network in use to the new one occurs. This requires the node to deal with authorization as well as authentication; it transfers the user information accordingly. A study of the recent literature shows that different types of vertical handover decisions scheme have been worked out. The networks in 4G HetNets are managed by distinct operators or in other words the service providers. The distribution of sustained services for mobile nodes is a principal complication for the fixed grid wavelet network (FGWN). This ensures the necessity to accord seamless handover while working in environment like this [10] - [13].

In this regard, the handover serves as the main practice for maintaining ongoing call connections. It also aids in providing the best QoS packages and fulfilling the requirement for more stable services. However, the traditional handover of GSM based networks lacks when it comes to keeping trade-off between smooth handover and mobility. Fortunately, this glitch has been dealt with in 4G by introducing the idea of vertical handover based on received signal strength (RSS) values and services like class mapping [14]. A comparison between vertical and horizontal handovers reveals that vertical handover is likely to happen between radio access technologies (RATs) also called inter-system handover while horizontal handover is an intra-system means it occurs within the same network technology.

Apart from improved handover, the other notable advancements in 4G networks are that of data rate services (high) and global roaming (nonpareil) [15]. Nevertheless, in the current scenario, vertical handover decision is dependent upon the available bandwidth, access network, the available internet service provider (ISP) imposed to the specific network connection, power usage needs, and the battery status of concerned mobile device. The mechanism for vertical handover seems to be recommended for the users of mobile devices gaining a low-level control overhead. It would also be able to control connections acting as sources of packet loss and minimize transfers in times of delay as well. Vertical handover can be illustrated by categorizing it into three discrete steps; 1) handoff decision, 2) system discovery and 3) handoff execution [16].

The rest of the paper is organized as follows. Section II describes our system model. This is followed by Section III that highlights the background knowledge related to the topic. Furthermore, Section IV presents the proposed algorithm for our work. Section 5 shows the discussion of our experimental results. Finally, Section VI concludes the paper.

II. SYSTEM MODEL

In this work, we have taken four networks into consideration. One of them is the global system for mobile communication (GSM); while others are worldwide interoperability for microwave access (WiMAX), wireless local area network (WLAN) and code division multiple access as implemented in 3G (WCDMA/3G). All of these networks are different from one another and we look at various parameters of all these networks. After examining different parameters of these networks, a case study is presented that focuses on a scenario where disturbance is caused due to low level of signal or no network availability. Because of this, the proposed system goes through the aforementioned three steps of vertical handover to the desired network according to the proposed model.

A. *Global System for Mobile Communication*

GSM, abbreviated as global system for mobile communication is a communication system that works on the phenomenon of circuit switching shown in Figure 1. at the operating frequency of 900 MHz or 1800 MHz GSM, although obsolete now, is a standard that is elaborated by ETSI (european telecommunications standards institute) and is used to mark out second generation 2G protocols that are held by mobile phones. It is used for transferring of voice data in communication systems that is based on wireless technology.

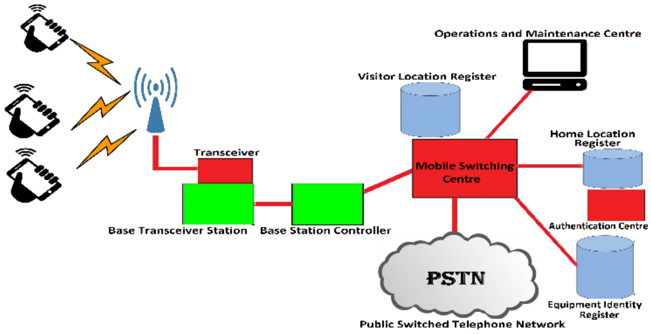

Figure 1. Architecture of GSM Based Cellular Network

The structure of this network is designed in terms of different sections named as base station subsystem (explains the idea of base stations and the controllers used in it), network and switching subsystem (the part identical to fixed network – also known as core network), general packet radio service GPRS core network (the non-obligatory part that allows packet based internet connections) and operational support system (for network preservation).

B. *Worldwide Interoperability for Microwave Access*

Worldwide interoperability for microwave access (WiMAX) is used for long-range wireless networks. WiMAX is linked with wireless metropolitan access network and is adapted at 802.16 standard of institute of electrical and electronics engineering (IEEE). The specialty of WiMAX is its high speed – long-range data network as compared to Wi-Fi (wireless fidelity). It has the ability to hold up both the broadband (mobile) and node (fixed) access. While focusing on mobile broadband, different sections combine to make WiMAX. These are mobile station (user's device), connectivity service network (used for connection of IP to user's device) and access service network (contains base stations, gateways and works for radio access).

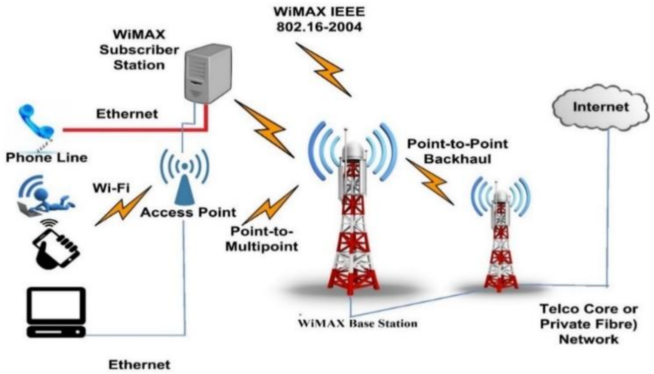

Figure 2. Illustration of WiMAX Connecting Both Fixed and Mobile Nodes

C. *Wireless Local Area Network*

Commonly known as wireless fidelity (Wi-Fi) is a type of wireless network that usually works for short ranges as depicted in Fig.3. IEEE has given it a standard of 802.11 and its basic idea is to provide connection to a number of daily use devices like laptops, mobiles, printers etc. The standard 802.11 establishes connection in two modes of operation. Ad hoc mode (support of access point is not required and communication of devices is direct) and Infrastructure mode (access point is required for communication of Wi-Fi nodes).

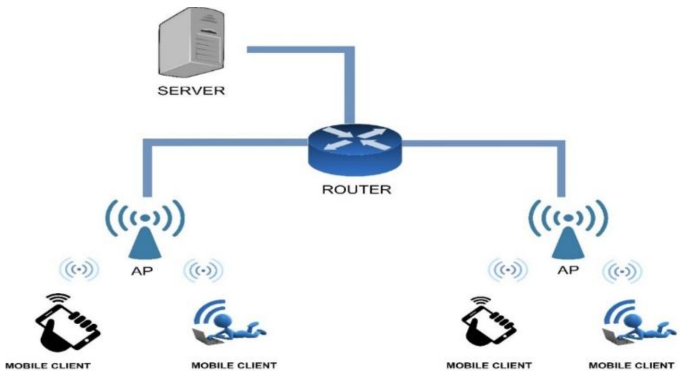

Figure 3. A Small Infrastructure Mode WLAN

D. *Wide Band Code Division Multiple Access*

Wide band code division multiple access – 3G network standard is a third-generation network (WCDMA/3G) as shown in Figure 4. and serves as an updated version to the typical 2G/CDMA network. It comes with two versions called as UMTS (universal mobile telecommunications systems) and HSPA (high speed packet access) and both use WCDMA as the prime multiple access technique. WCDMA is responsible to manage the traditional voice and text services as well as high speed multimedia messaging service (MMS) /data services. 3G uses different air interfaces; however, its standards are similar as 2G/ GSM and enhanced data for GSM evolution (EDGE). It has the ability to switch between GSM and EDGE. The transition of network from GSM to 3G does not require large investments due to the introduction of general packet radio services (GPRS) and EDGE.

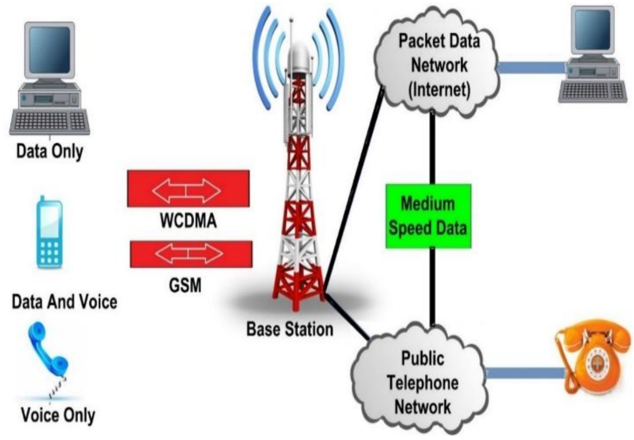

Figure 4. Illustration of the Entities Inside a 3G Network

III. HANDOVER MANAGEMENT STRATEGY

To maintain uninterrupted connection for active mobile node, the connection has to smoothly move from one access network to another. Referring to handover management strategy shown in Figure 5. the work at hand considers a systematic handover process that consists of a variety of steps:

A. *Stage 1:*

Initiative: is setting up the threshold values, which helps to select the best available network in the process of handover.

Informative: is the collection of information data in order to initiate handover. This term can also be defined as system discovery and can be related to initiative stage.

B. *Stage 2:*

Conclusion: is the stage where the decision and execution of handover process takes place. Moreover, the requirements and needs for performing the handover are indicated and the choice of best available network is taken into account.

Evaluation via Dynamic Call Blocking Probability: is the stage where the blocking probabilities of the available networks are observed, because performing handover would be based on the call blocking probability of the networks under consideration.

C. *Stage 3:*

Handover Operation: is the stage where the process of handover actually takes place according to the requirements of the system and selects the best available network that is based on the handover algorithm.

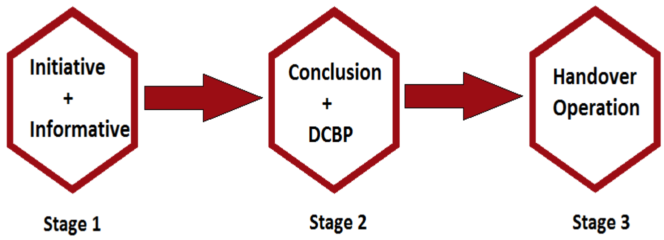

Figure 5. Handover Management Strategy

IV. MATHEMATICAL MODEL

Commencing with Stage 1 – handover informative, we collected the basic information given below, required to handle vertical handover. Furthermore, we pre-defined the number of total evaluation networks (NEN) presently available to be 4.

The available bandwidth of currently connected network ID 1 is Bx = 900 MHz. Furthermore, received signal strength (RSS) of currently connected network is set as RSS = -55dB.

RSS value can be obtained by values of effective isotropic radiated power (EIRP) and path loss (ήo) [16] as follows:

$$RSS = EIRP - ήo, \tag{1}$$

where EIRP can be mathematically represented as:

$$EIRP = Ptrans+Ga, \tag{2}$$

where Ptrans shows antenna power and Ga is antenna gain. Similarly, in order to model the path-loss [17] we used the following mathematical expression

$$ήo = 34.4\ (dB)+20\log [f(MHz) + \log [d\ (km)], \tag{3}$$

where 34.4 is proportionality constant, f is frequency of mobile node and d is distance between mobile node and base station (BS).

The estimated time for which a mobile node stay in the network coverage is 10ms. Battery power of mobile node currently connects with network 50 Wh. The mean number of request arrivals per unit time is, λ=10. where λ is the number of call per unit time.

Furthermore, average number of calls serving in certain time frame are shows as =3.

Using values of the above-mentioned parameters, we calculate weightages for each of the networks considered in our proposed system. For this, power dissipation in network is assumed as 20 Wh.

The process was repeated for the second, third and fourth networks with respective network IDs 2, 3 and 4. This can be seen in Table I given below. In the Stage II respectively i.e. handover decision, we compared these parameters values with the pre-defined threshold values. It is customary to mention here that the threshold values were those that defined the handover decision and also the best network for handover. If any network had values greater than these pre-defined thresholds, the mobile node would jump to that network and continue communication with good quality.

The value of bandwidth threshold, Bxi, is 1800 MHz. Similarly, the pre-defined threshold for RSS is set as - 65 dBm.

It is noteworthy here that the RSS mentioned here is the signal strength measured at receiver side and its values is always negative on the logarithmic scale. Table II gives the values we considered during the work.

TABLE I. NETWORK PARAMETER VALUES

S No:	Parameter	GSM Network ID 1	WLAN Network ID 2	WiMAX Network ID 3	3G Network ID 4
1	Available Bandwidth (Bx)	900 Mhz	2400 Mhz	5000 Mhz	2100 Mhz
2	Received signal level (RSS)	-55 dBm	-70 dBm	-60 dBm	-65 dBm
3	Estimated Time for MS (TE)	10 ms	15 ms	10 ms	10 ms
4	Power Dissipation in Network (Pj)	20 Wh	30 Wh	40 Wh	40 Wh
5	Lambda (λ)	10	5	10	10
6	Call served per unit time (mu)	3	2	4	4
7	Battery Power of MS (P)	50 Wh	50 Wh	50 Wh	50 Wh
8	Velocity of MS (V)	2 m/s	2 m/s	5 m/s	3 m/s

TABLE II. SHEET FOR RANGE RSS

RSS Value in dBm	**Scale**
Up to -65 dBm	Excellent
-75 to -95	Normal
-65 to -75	Good
<-95	Worst

Thresholds for estimated time mobile node stays in the network coverage and transmit power are given by the following set of values:

TEi=5ms

10 Wh

TABLE III. THRESHOLD PARAMETER VALUES

S No.	Parameter	Threshold
01.	Current Available Bandwidth (Bxi)	1800 MHz
02.	Received Signal level (RSSi)	-65 dBm
03.	Estimated Time MS will be in present network (TEi)	5ms
04.	Power Dissipation in Network(Pji)	50 Wh
05.	Battery Power Of MS (Pi)	10 Wh
06.	Velocity Of Mobile Station (Vi)	3 m/s

Once the thresholds were defined, we evaluate the initial step that is basically decision algorithm to look for the worthy enough network in the other present networks with values more than threshold. For this, we considered the following relation:

$$\alpha=\tau-\mu, \quad (4)$$

where *'τ'* is available network value and *'μ'* is the threshold value. Threshold velocity (V) of the mobile station is 3.

$$\Phi=[Bx\text{-}Bxi\ (\alpha)]\ [RSS\text{-}RSSi\ (\alpha)]\ [TE\text{-}TEi\ (\alpha)]\ [V\text{-}Vi\ (\alpha)]\ [P\text{-}Pi\ (\alpha)]\ [Pj\text{-}Pji\ (\alpha)], \quad (5)$$

The threshold of Phi Φ is network value - threshold value

If is equal 1 it means we have the network to be consider for operation of vertical handover either value comes 0 it means no other network having the value greater than the predefine threshold and should not be consider for operation. Thus, the mobile node will remain connect in the same network.

For Φ =0 is assumed that no network was available for handover at the moment. Greater will be the value of Φ, the greater was the probability of finding a good QoS network using dynamic call blocking probability (DCBP) based vertical handover and is given as

$$i = \frac{\lambda}{\odot} \quad (6)$$

$$\text{DCBP}=\frac{i^B}{B!} \quad (7)$$

V. SIMULATION RESULTS

In Fig. 6, vertical handover decision function graph is shown, as we can see from the Figure 6., the point is on Network with ID 3 means vertical handover was successfully completed and newly selected network is 4G. This has been implemented based on parameters values according to DCBP which clearly identify the network with good parameters. From Figure 6., we can see EVHDF (extended vertical handoff function) which conclude the systematic algorithm for all the selected pool of network, this decision will be based on DCBP function.

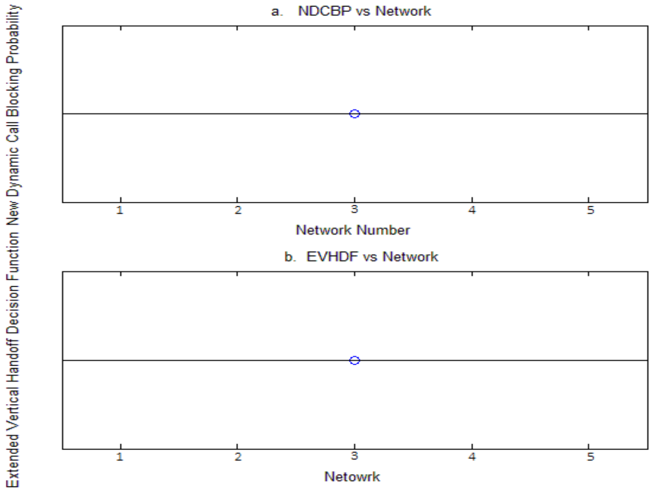

Figure 6. Handover decision

CONCUSLION

In this paper, we presented a comparative analysis of vertical handover that explain the notion of vertical handover and its implementation. The process of vertical handover mainly depends on available networks in surrounding environment in HetNets. In this paper, we considered four different networks that were available to the mobile nodes. These networks available to mobile node are used for the benefit of users through handover management. This was further enhanced by selecting pre-defined threshold as compared with standards for switching mobile nodes from connected network to the best available network. In the results, we observed parameters of four different networks and compared them with pre-defined threshold for an accurate analysis of the vertical handover process. The proposed model identifies the available network with best parameter values in a well-scrutinized manner.

REFERENCES

[1] F. Muhammad, Z. H. Abbas, and F. Y. Li, "Cell Association with Load Balancing in Non-uniform Heterogeneous Cellular Networks: Coverage Probability and Rate Analysis," IEEE Transactions on Vehicular Technology,, vol. 66, no.6, pp. 5241–5255, Jun. 2017.

[2] Nasser, N., Hasswa, A., & Hassanein, H. (2006). Handoffs in fourth generation heterogeneous networks. IEEE Communications Magazine, 44(10), 96-103.

[3] Hasswa, A., Nasser, N., & Hassanein, H. (2007). A seamless context aware architecture for fourth generation wireless networks. Wireless Personal Communications, 43(3), 1035-1049.

[4] Ghaderi, M., & Boutaba, R. (2006). Call admission control in mobile cellular networks: a comprehensive survey. Wireless communications and mobile computing, 6(1), 69-93.

[5] Deng, D. J., & Yen, H. C. (2005). Quality-of-service provisioning system for multimedia transmission in IEEE 802.11 wireless LANs. IEEE Journal on Selected Areas in Communications, 23(6), 1240-1252

[6] Singhrova, A., & Prakash, N. (2007, September). A review of vertical handoff decision algorithm in heterogeneous networks. In Proceedings

of the 4th international conference on mobile technology, applications, and systems and the 1st international symposium on Computer human interaction in mobile technology (pp. 68-71). ACM.

[7] Joe, I. A Mobility-based Prediction Algorithm for vertical handover in hybrid wireless network (2010).

[8] Enrique Stevens-Navarro and Vincent W.S. Wong, Comparison between Vertical Handoff Decision Algorithms for Heterogeneous Wireless Networks, 2006 IEEE.

[9] Singhrova, A., & Prakash, N. (2012). Vertical handoff decision algorithm for improved quality of service in heterogeneous wireless networks. IET communications, 6(2), 211-223.

[10] Zhu, F., & McNair, J. (2004, March). Optimizations for vertical handoff decision algorithms. In Wireless Communications and Networking Conference, 2004. WCNC. 2004 IEEE (Vol. 2, pp. 867-872). IEEE.

[11] Chen, W. T., & Shu, Y. Y. (2005, March). Active application oriented vertical handoff in next-generation wireless networks. In IEEE Wireless Communications and Networking Conference, 2005 (Vol. 3, pp. 1383-1388). IEEE.

[12] Zhang, W. (2004, March). Handover decision using fuzzy MADM in heterogeneous networks. In Wireless communications and networking conference, 2004. WCNC. 2004 IEEE (Vol. 2, pp. 653-658). IEEE.

[13] Song, Q., & Jamalipour, A. (2005, May). A network selection mechanism for next generation networks. In IEEE International Conference on Communications, 2005. ICC 2005. 2005 (Vol. 2, pp. 1418-1422).

[14] Pawar, P., Wac, K., Van Beijnum, B. J.,Maret, P., van Halteren, A., & Hermens, H. (2008, March). Context-aware middleware architecture for vertical handover support to multi-homed nomadic mobile services. In Proceedings of the 2008 ACM symposium on Applied computing (pp. 481-488). ACM.

[15] Dekleva, S., Shim, J. P., Varshney, U., & Knoerzer, G. (2007). Evolution and emerging issues in mobile wireless networks. Communications of the ACM, 50(6), 38-43.

[16] Chen, W. T., Liu, J. C., & Huang, H. K. (2004, July). An adaptive scheme for vertical handoff in wireless Overlay networks. In Parallel and Distributed Systems. ICPADS 2004. Proceedings. Tenth International Conference on (pp. 541-548). IEEE.

[17] Isabona, Joseph & Bright, Chinule & Gregory Peter, Isaiah." Radio Field Strength Propagation Data and Pathloss calculation Methods in UMTS Network." (2013).

Saad Iqbal, Department of Telecommunication Engineering, University of Engineering and Technology Peshawar, Pakistan.

International Journal of Engineering Works
ISSN-p: 2521-2419
ISSN-e: 2409-2770
Vol. 6, Issue 03, PP. 50-70, March 2019
https://www.ijew.io/

Effects of Additive Concentrations on Cement Rheology at Different Temperature Conditions

Ikpeka Princewill Maduabuchi[1], Odo Jude Emeka[1], Benedict Ugochukwu Wisdom[1], Utojiuba Ifeanyi Davida[1], Uzuegbu Godson Chizirim[2]
[1]Department of Petroleum Engineering, Federal University of Technology, Owerri
[2]Haliburton Oil Services
Received: 29 December, Revised: 06 January, Accepted: 12 February

Abstract— Cement slurries are designed to achieve zonal isolation; improve rheological properties and displacement efficiency of cementing system. Oil well cement slurries depend on temperature, additive concentrations; quality and quantity, to contribute to the placement and success of cementing operation. This study aims at analysing the effects of cement slurry additive concentration on rheology at different temperature conditions. Three additive concentrations were varied; Retarder, Fluid Loss Additive and Dispersant. Using full factorial design, 27 experiments were carried out to analyse the effect of these additives at different temperatures. Rheological properties like plastic viscosity, yield stress, shear rate and shear stress were experimentally determined at different temperatures and concentrations of additives. A simple cement slurry design which consists of: Dyckerhoff Class G, Fluid Loss Additive, Retarder, Dispersant, Defoamer and Drill Water, was used for the laboratory experiments. The slurry was conditioned in accordance with the procedure set out in API RP 10B-2. Linear regression was then used to build models describing the effect of temperature and additive concentration on plastic viscosity and yield point of the cement slurry. Ms-Excel plots were used as a tool in presenting the relationships between Shear Stress and shear rates at varying temperature conditions. Results from the analysis reveal that for a Temperature increase of 125% and Retarder concentration increase of 200%, there were significant decline in Plastic viscosity (-41%) and Yield point (-44%). Whereas increasing the Fluid loss additive by 100% caused a significant increase in Yield point (+51%) and relatively insignificant increase in Plastic Viscosity (+4.4%).

Keywords— Oil Well Cementing, Class G Cement Slurry design, Cement rheology, Effect of temperature on cement slurry, Cement additive concentration.

I. INTRODUCTION

In drilling engineering, cement is used for a number of different reasons; cementing protects and seals the wellbore. Most commonly, cementing is used to permanently shut off water penetration into the well. Part of the completion process of a prospective production well, cementing can be used to seal off annulus after a casing string has been run in the wellbore and it is also used to plug a well to abandon it. Additionally, cementing is used to seal a lost circulation zone or an area where there is a reduction or absence of flow within a well. In directional drilling, cement is used to plug an existing well, in order to run a directional well from that point.

Rheology is the study of flow of matter, primarily in liquid state, the relation of flow/deformation behaviour of fluids with its internal structure, under applied forces which is routinely measured using a rheometer. Rheology describes the relationship between force, deformation and time. Rheology is an extremely important property of drill-in-fluids, workover and completion fluids, cements and specialty fluids. A rheometer is a laboratory device used to measure the flow response of a liquid to applied forces (i.e. it measures the rheological properties of the fluid). A rotational or shear rheometer measures applied shear stress. Mud rheology is measured on a continual basis while drilling and adjusted with additives or dilution to meet the needs of the operation. In water-base fluids, water quality plays an important role in how additives perform.

The particle size distribution (fineness) is an important parameter with respect to cement reactivity and slurry rheology. The development of compressive strength is often dependent on cement surface area; cements with narrow particle size distributions tend to develop higher compressive strength (Michaux et al., 1990). The rheological behaviour of cement depends on different factors such as: water-to-cement ratio, size and shape of cement grains, chemical composition of the cement, type and amount of additive, mixing and testing procedures, temperature and pressure.

Most fluids exhibit a shear-rate dependent viscosity which is non-trivial to characterize, but for fluids such as cement slurries, the viscosity is not only a function of shear rate currently applied, but also of the past shear history. They exhibit a time dependent behaviour which is more difficult to characterize (Nelson and Guillot, 2006).

A sound knowledge of rheology of cement slurry is required for a successful cementing operation for the following reasons;

i. Evaluation of slurry mixability (i.e to understand the interaction between different ingredients in a material to get an insight into its structure) and pumpability (i.e to evaluate the capability of a slurry or paste to transport large particles (e.g, some lost circulation materials and fibers).
ii. Determination of appropriate flow regime for placement of cement slurry (i.e to control the quality of a raw material by measuring its rheological properties.
iii. Determination of the displacement rate required to achieve optimum mud removal.
iv. Determination of pressure versus depth relationship during and after cement slurry placement.
v. The acceptance/rejection of a product can be determined based on rheological results.
vi. To evaluate how the temperature profile affects the placement of slurry.

Temperature can have drastic effect on cement slurry rheology but the extent of this effect is highly dependent on the type of cement and the additives. Water-cement ratio is the ratio of the weight of water to the weight of cement used in a concrete mix. A lower ratio leads to a higher strength and durability but may make the mix difficult to work with and a higher ratio leads to segregation of the sand and aggregate components from the cement paste. Cement hardens/sets as a result of the chemical reaction between cement and water. When Portland cement reacts with water, the system cement plus water undergoes a net volume diminution. This is an absolute volume decrease, and occurs because the absolute density of the hydrated material is greater than that of the initial reactants. Despite the decrease in absolute volume, the external dimensions of the set cement or the bulk volume remain the same or slightly increase (Arnoldus M.A and Ade L., 2016). The water-to-cement ratio required to wet the cement particle and prepare a pumpable slurry is directly related to the surface area. (Shuker et al, 2014).

1.2 Statement of problem

In Oil Well drilling, one of the goals of a good well completion is a successful cementing job. To avoid bad cementing jobs, the cement system must be designed to be pumped under conditions such as can be anticipated within the pressure and temperature conditions of the downhole strata. (Michaux M. et al, 1990). Designing cement slurry can be quite tricky because there are varying elements that can easily alter the cement properties. Modelling cement behaviour is also quite challenging because of the need to simulate down-hole conditions in the laboratory. How do we ascertain the effect of some of these elements on the cement slurry design? Although there are existing models to help achieve good slurry design, these models are built on fundamental relationship between shear rate, shear stress, time, temperature and pressure.

1.3 Aim of study

The primary objective of this study is to analyse the rheology of cement (class G) under various conditions of Temperature and additive concentration. Other objectives include:

i. To study the effect of varying retarder concentration on overall cement rheology
ii. To study the effect of varying dispersant concentration on overall cement rheology
iii. To study the effect of varying fluid loss additive concentration on overall cement rheology
iv. To study the behaviour of the cement slurry with varying temperatures

1.4 Significance of study

This study helps in modelling the flow regime which helps the cement or mud engineer also known as the mixer to know what proportion of different components to use to understand the rheology of cement. The study also helps to predict cement rheology under various conditions of Temperature and additive concentration..

II. Previous Works on Cement Rheology

Doherty D.R. et al., (2010), in his research on “pushing Portland cement beyond the norm of extreme high temperature”, designed a high temperature cement that can be applied when extracting energy contained within coal in a process known as Underground Coal Gasification (UGC). Modified Bingham equations were generated that characterised the results obtained from the experiment carried out. The flow regime both in the drill pipe and at the annulus was predicted with densities obtained from the laboratory; therefore, at these different conditions of varying temperature, water-cement ratio and additive concentration, the flow regimes were predicted so as to know at what condition to pump cement downhole.

Olowolagba, K. and Brenneis C. (2010) researched on “Techniques for the study of foamed cement technology”. They presented methods and laboratory equipment that enable a more accurate assessment of foamed cement used to provide zonal isolation in oil and gas wells by analysing rheology-testing results using the “bob and sleeve” conventional rotational viscometer and the Fann Yield Stress Adapter (FYSA). After analysing the viscosity plot, it was noticed that the bob and sleeve viscometer does not accurately measure the viscosities of the foamed cement at the different foam qualities. Also, rheology measured with FYSA showed higher YPs and also higher and stable viscosities at low shear rates compared to the bob and sleeve.

Kelessidis V.C et al., (2014) carried out a research on “Comprehensive assessment of additive and class G cement properties affecting rheology, fluid loss, setting time and long term characteristics of elastic cements”. The aim was to present a comprehensive laboratory assessment of the properties of two different non-foamed cement slurries, by combining initial tests, such as rheology, fluid loss, and thickening time, with strength, ultrasonic and advanced Nuclear Magnetic Resonance (NMR) measurements, at both room and elevated pressure and temperature. To achieve the objective, the cement microstructure was correlated with the mechanical properties of cement at borehole conditions, acquiring critical information for designing better sheath integrity. A very good correlation was found between the microscopic NMR data that probe the evolution of the average pore size and consequently the kinetics of hydration with macroscopic comprehensive strength data.

Haichuan L. et al., (2015), in a research on "Cement slurries with rheological properties unaffected by temperature", tend to resolve the problem of varying rheological properties with a change of temperature. Cement slurry with temperature-insensitive viscosity was being prepared by adding a type of thermo-sensitive viscosity controller (TVC). The experiment showed that the cement slurry had relatively temperature-stability rheological properties and shows very little thermal thinning between 20 and 120oC. In addition, the thermally-stable-viscosity cement slurry had good stability and a performance that can meet the demands of well cementing.

Bakirov D.L et al., (2016), in a research on "Cement for temperature range 160-300oC" made a study concerned with thermal resistant cements designed for cementing the casing strings with thermal gas treatment of the formation drilled in the Srende-Nazymkoe Field of the JSC RITEK. Methods were studied to increase thermal resistance of plant-manufactured cements and methods to augment the strength of the cement stone formed at hardening temperatures of up 90oC. Further modifications of the cements ThermoLight-9 (300) and ThermoLight-4 (160), which were resistant to thermal treatment, having the ultimately low thermal conductivity were produced. The parameters of the developed cements were stable and predictable both in atmospheric and barothermal conditions. The developed cements had an increased WOC (48hours) required for the formation of the right crystalline structure.

Okoro O. Nwakpu G., (2017), made a research on "determination of cement rheology and flow regime prediction" to determine the flow parameters of class E and G cement samples, also, created a model that relates the shear stress of cement slurry with its velocity gradient. Modified Bingham equations were generated that characterised the results obtained from the experiment carried out. The flow regime both in the drill pipe and at the annulus were predicted with densities obtained from the laboratory, therefore, at these different conditions of varying temperature, water-cement ratio and additive concentration, the flow regimes were predicted so as to know at what condition to pump cement downhole. It was concluded that additive concentration and temperature have effects on the rheology of cement i.e. the higher the temperature, the higher the plastic viscosity, and the higher the yield point, also, at lower temperature, the yield point was directly proportional to additive concentration and at lower temperature, the yield point was inversely proportional to the concentration of additive. It was stated that Rheology is also dependent on the ratio of water to cement, i.e. at low and high water-cement ratios, the plastic viscosity was high.

III. MATERIAL AND METHOD

Seven (7) different cement slurries were prepared for this study. The first case was assumed to be the base case, whereas the remaining six (6) composed of varying concentrations of the first sample and they were labelled Recipe 1-6. The Cement slurries used for this study consist of:

i. Dyckerhoff Class G
ii. Fluid Loss Additive
iii. Retarder
iv. Dispersant
v. Defoamer
vi. Drill Water

Apparatus used in the laboratory experiments include: sieve, weighing scale, mixing blender, Fann viscometer, atmospheric consistometer and measuring cylinder.

The following are the laid down procedures involved in carrying out the experiment:

i. The cement and additive were sieved and weighed using a sieve and weighing scale respectively. Whereas, the volume of water was measured using the measuring cylinder.
ii. The slurry was formed by mixing the cement, water and additive to form a homogenous substance, using the mixing blender.
iii. The slurry (i.e. cement, water and fluid loss additive) was conditioned, following the correct mixing procedure (refer to API RP 10B-2).
iv. The slurry was conditioned following the procedure set out in API RP 10B-2 to ensure that the atmospheric consistometer is at 80˚F prior to commencing conditioning.
v. The slurry was conditioned for 30 min ± 30s at test temperature. In this case 80oF, 130oF and 180oF.
vi. When the slurry was conditioned, the bob, sleeve and thermo-cup were pre-heated to test temperature.
vii. With the Fann viscometer turning at 3 rpm, the cup was raised until the liquid level covers the scribed line on the rotating sleeve.
viii. Then the dial readings were recorded on the paperwork 10 seconds after continuous rotation.
ix. Immediately the speed was changed and the remaining dial readings were taken 10 seconds after each speed change.
x. Also dial readings were read and recorded in ascending then descending order as shown: 3 – 6 – 30 – 60 – 100 – 200 – 300 - 600 – 300-200 – 100 – 60 – 30 – 6 – 3

3.1 Design of Experiment

The full factorial design was used to determine the number of experiment to be carried. The number of experiment to be carried out is given by equation (1):

$$No\ of\ experiment = L^K \tag{1}$$

Where:

L = Level (3 levels: Base Case, Additive Concentration 1, and Additive Concentration 2)

K = no of factors (Temperature, Concentration)

$No\ of\ experiment = 3^2 = 9$

Thus nine (9) experiments were performed each for each additive concentration. Since three (3) additive concentrations were studied, a total of 27 experiments were conducted as shown in table 2.

Table 1 - Design of Experiment

S/N	Temperature Factor	Retarder Concentration	Fluid Loss Additive Concentration	Dispersant Concentration
1	0	0	0	0
2	1	0	0	0
3	2	0	0	0
4	0	1	1	1
5	1	1	1	1
6	2	1	1	1
7	0	2	2	2
8	1	2	2	2
9	2	2	2	2

IV. Results

Results from the 27 laboratory experiments are presented in tables 2 to table 8.

Slurry Details;

Density: 15.8ppg

BHCT: 80degF, 130degF and 180degF

Table 2: Base Case

Concentration	Material	S.G	Test Amount
100%BWOC	Dyckerhoff Class G	3.18	781.17g
0.5% BWOC	Fluid Loss Additive	1.37	3.91g
0.1% BWOC	Retarder	1.16	0.78g
0.05% BWOC	Dispersant	0.92	0.39g
0.02 GPS	Defoamer	1.28	1.28g
44.69 L/100Kg	Drill Water	1.00	348.44g

Rheology Result;

Temp(^{o}F)	600rpm	300rpm	200rpm	100rpm	6rpm	3rpm
80	400	241	181	111	14	9
130	318	192	144	90	12	8
180	280	170	129	81	12	8

Table 3: Recipe 1

Concentration	Material	S.G	Test Amount
100%BWOC	Dyckerhoff Class G	3.18	781.01g
0.5% BWOC	Fluid Loss Additive	1.37	3.91g
0.2% BWOC	Retarder	1.16	1.56g
0.05% BWOC	Dispersant	0.92	0.39g
0.02 GPS	Defoamer	1.28	1.28g
44.62 L/100Kg	Drill Water	1.00	347.81g

Rheology Result;

Temp(^{o}F)	600rpm	300rpm	200rpm	100rpm	6rpm	3rpm
80	322	188	136	79	8	6
130	275	158	118	71	8	5
180	240	145	109	67	8	5

Table 4: Recipe 2

Concentration	Material	S.G	Test Amount
100%BWOC	Dyckerhoff Class G	3.18	780.85g
0.5% BWOC	Fluid Loss Additive	1.37	3.90g
0.3% BWOC	Retarder	1.16	2.34g
0.05% BWOC	Dispersant	0.92	0.39g
0.02 GPS	Defoamer	1.28	1.28g
44.55 L/100Kg	Drill Water	1.00	347.19g

Rheology Result;

Temp(^{o}F)	600rpm	300rpm	200rpm	100rpm	6rpm	3rpm
80	318	180	131	76	8	5
130	268	156	116	69	8	5
180	234	140	106	67	8	5

Table 5: Recipe 3

Concentration	Material	S.G	Test Amount
100%BWOC	Dyckerhoff Class G	3.18	780.4g
0.75% BWOC	Fluid Loss Additive	1.37	5.85g
0.1% BWOC	Retarder	1.16	0.78g
0.05% BWOC	Dispersant	0.92	0.39g
0.02 GPS	Defoamer	1.28	1.27g
44.59 L/100Kg	Drill Water	1.00	347.26g

Rheology Result;

Temp(^{o}F)	600rpm	300rpm	200rpm	100rpm	6rpm	3rpm
80	562	366	279	174	26	17
130	480	320	244	156	25	16
180	456	290	224	143	25	16

Table 6: Recipe 4

Concentration	Material	S.G	Test Amount
100%BWOC	Dyckerhoff Class G	3.18	779.63g
1.0% BWOC	Fluid Loss Additive	1.37	7.80g
0.1% BWOC	Retarder	1.16	0.78g
0.05% BWOC	Dispersant	0.92	0.39g
0.02 GPS	Defoamer	1.27	1.27g
44.48 L/100Kg	Drill Water	1.00	346.09g

Rheology Result;

Temp(^{o}F)	600rpm	300rpm	200rpm	100rpm	6rpm	3rpm
80	U2R	514	397	259	41	27
130	U2R	450	350	229	40	27
180	U2R	430	331	211	37	24

N/B: U2R means **Unable to Read** because the slurry was too viscous.

Table 7: Recipe 5

Concentration	Material	S.G	Test Amount
100%BWOC	Dyckerhoff Class G	3.18	780.92g
0.5% BWOC	Fluid Loss Additive	1.37	3.90g
0.1% BWOC	Retarder	1.16	0.78g
0.15% BWOC	Dispersant	0.92	1.17g
0.02 GPS	Defoamer	1.28	1.28g
44.64 L/100Kg	Drill Water	1.00	347.91g

Rheology Result;

Temp(°F)	600rpm	300rpm	200rpm	100rpm	6rpm	3rpm
80	340	198	144	87	14	10
130	276	172	129	80	14	10
180	240	150	112	72	13	10

Table 8: Recipe 6

Concentration	Material	S.G	Test Amount
100%BWOC	Dyckerhoff Class G	3.18	780.54g
0.5% BWOC	Fluid Loss Additive	1.37	3.90g
0.1% BWOC	Retarder	1.16	0.78g
0.3% BWOC	Dispersant	0.92	2.34g
0.02 GPS	Defoamer	1.28	1.28g
44.56 L/100Kg	Drill Water	1.00	347.11g

Rheology Result;

Temp(°F)	600rpm	300rpm	200rpm	100rpm	6rpm	3rpm
80	280	156	110	61	6	4
130	206	118	86	50	6	4
180	186	106	78	46	5	4

V. Analysis and Discussion

5.1 Effect of Retarder Concentration on Cement Slurry Rheology at Specified temperatures: 80°F, 130°F &180°F

There were significant changes in the shear stress- shear rate plot @ 80oF, 130oF, and 180oF for the base case (Fig 1) compared to recipes 1&2 (Fig A.1 & A.2 in the appendix section). It was observed that increasing the concentration of the additive (retarder) above 0.1% (base case), there will be no significant change in the shear stress- shear rate plot at different temperatures.

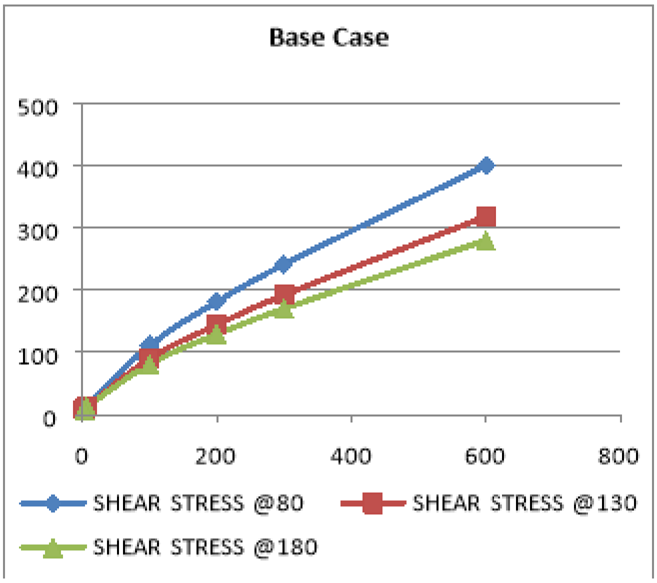

Figure 1: Graph of Shear stress against Shear rate for Base case @ 80°F, 130° F, & 180°F

However, when the concentration and temperature of the retarder is increased, there will be a corresponding decrease in shear stress at constant shear-rate.

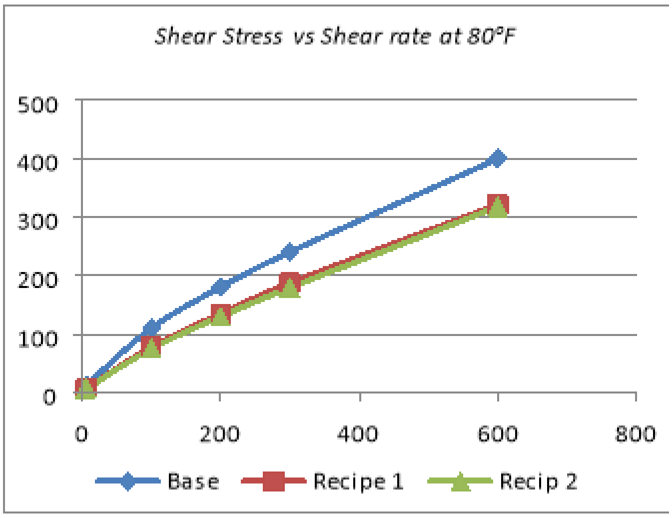

Figure 2: Graph of Shear stress against Shear rate for base case, recipe 1 & recipe 2 @ 80°F

A plot of shear stress vs shear rate as shown in Figure 2 revealed decreasing effect of retarder concentrations on cement rheology. This flow behaviour is consistent even with increase in Temperature as shown in Fig A.3 and A.4 in the appendix section. At each temperature, there was change in shear-stress-shear rate plot in base case, recipe 1& 2 (i.e. increasing the temperature, reduces the shear-stress at constant shear-rate).

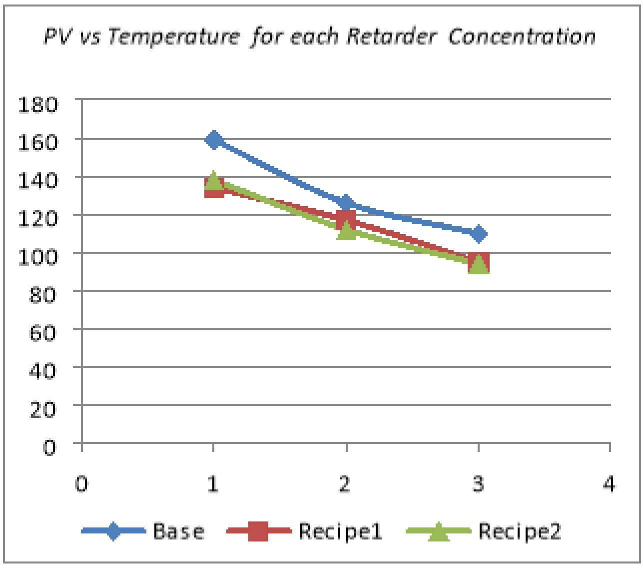

Figure 3: Graph of Plastic viscosity against Temperature for base case, recipe 1 & recipe 2

An increase in temperature will cause a corresponding decrease in plastic viscosity. As concentration increased 0.1%, there was no significant change between recipe 1&2 compared to the base case, as shown in Figure 3.

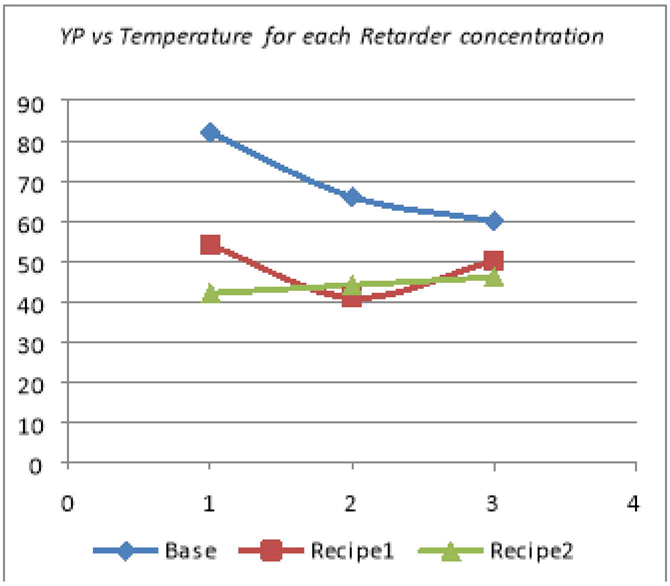

Figure 4: Graph of yield point against temperature for base case, recipe 1 & recipe 2

The plot in Figure 4 represents the relationship between yield point and temperatures at 80oF, 130oF and 180oF for base case, recipe 1 & recipe 2. From the plot, an increase in temperature and concentration will cause a decrease in the yield stress, thereby reducing the force required to cause the cement slurry to flow.

5.1.1 Regression Analysis

Table 9: Factorial design for analyzing effect of retarder concentration

S/ N	Retarder Concentration (%)	Temperature Factor (%)	Plastic Viscosity (%)	Yield Point (%)
1	0	0	0	0
2	0	62.5	-20.75	-19.51
3	0	125	-30.82	-26.83
4	100	0	-15.72	-34.15
5	100	62.5	-26.42	-50
6	100	125	-40.25	-39.02
7	200	0	-13.21	-48.78
8	200	62.5	-29.56	-46.34
9	200	125	-40.88	-43.9

$$PV = -0.0535 \times RC - 0.2214 \times TF - 4.9956 \quad (2)$$

$$YP = -0.1544 \times RC - 0.07152 \times TF - 14.3644 \quad (3)$$

Where:
PV – Plastic Viscosity
YP – Yield Point
RC – Retarder Concentration
TF – Temperature Factor

5.2 Effect of Fluid Loss Additive Concentration on Cement Slurry Rheology at Specified temperatures: 80°F, 130°F &180°F

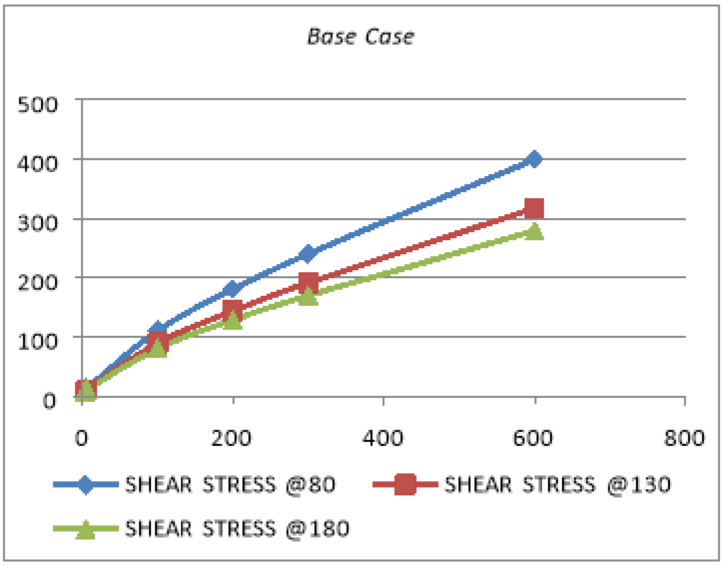

Figure 5 Graph of Shear stress against Shear rate for Base case @ 80°F, 130° F, & 180°F

From Figure 5 showing the effects of fluid loss additive on shear stress- shear rate for base case, recipes 3&4 (Fig A.5 and

A.6 in the appendix section), at different temperatures, it can be deduced that an increase in the concentration of fluid loss additive for each case will cause a significant increase in shear stress at constant shear rate thereby making the fluid more viscous to flow at constant temperatures. Moreover, it was observed that the increase in the shear stress curve for each case @ 80oF was significantly higher compared to temperatures at 130oF and 180oF i.e. shear stress will be higher at lower temperature than at higher temperature.

For recipe 4, the fluid was too viscous to flow, as a result, shear stress at 600rpm could not be recorded as well as plastic viscosity and yield point.

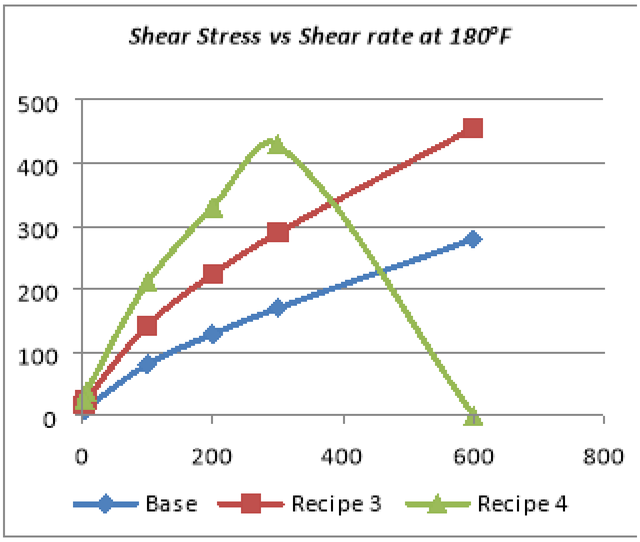

Figure 6. Graph of Shear stress against Shear rate for base case, recipe 3 & recipe 4 @ 180°F

Figure 6, describes the shear stress- shear rate relationship for each case at temperatures of 180oF. There was a noticeable decline in the plot for Recipe 4 at shear rate of 300rpm because the cement slurry at that concentration was too viscous to flow. Decreasing the temperature increases the shear stress for each case. Moreover, increasing the concentration increases the viscosity of the cement slurry. The relationship at 80 oF and 130 oF are shown in Fig A.7 and A.8 in the appendix section.

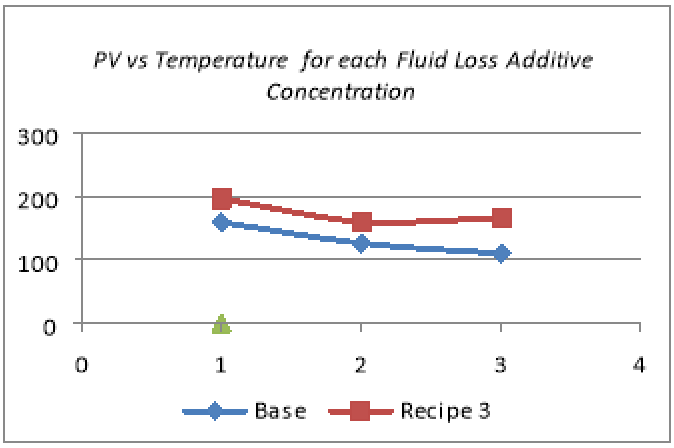

Figure 7 Graph of Plastic viscosity against Temperature for base case, recipe 3 & recipe 4

This graph above shows the relationship between plastic viscosity and temperature for each case. It was observed that plastic viscosity is inversely proportional to the temperature (i.e an increase in temperature will cause a decrease in the plastic viscosity). Plastic viscosity for Recipe 4 was not determined due to the viscometer's inefficiency to read the value of shear stress at 600rpm because the concentration was too high as well as the viscosity.

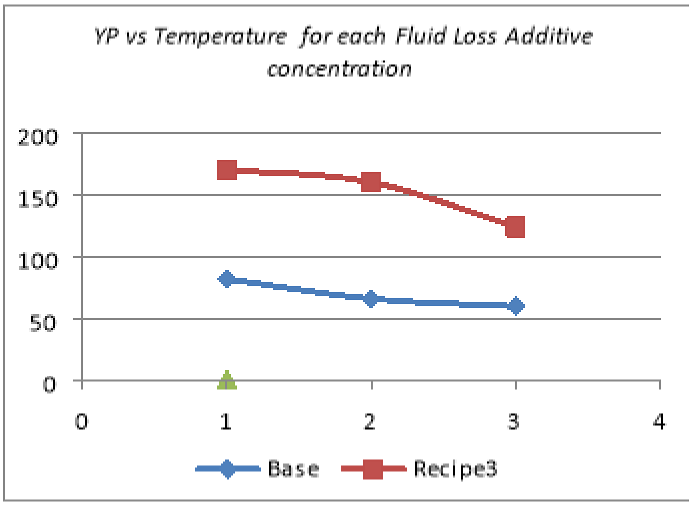

Figure 8. Graph of Yield Point against Temperature for base case, recipe 3 & recipe 4

Figure 8 shows the relationship between yield point and temperature for each case, yield point also decreases with an increase in temperature.

5.2.1 Regression Analysis

Table 10: Factorial design for analyzing effect of Fluid Loss Additive concentration

S/ N	Fluid Loss Additive Concentration (%)	Temperatur e Factor (%)	Yield Point (%)	Plastic Viscosit y (%)

1	0	0	0	0
2	0	62.5	-19.51	-20.75
3	0	125	-26.83	-30.82
4	100	0	170.32	23.27
5	100	62.5	95.12	0.63
6	100	125	51.22	4.4
7	200	0	N/A	N/A
8	200	62.5	N/A	N/A
9	200	125	N/A	N/A

$$PV = 0.2662 \times FLAC - 0.1988 \times TF - 4.7675 \quad (4)$$

$$YP = 1.21 \times FLAC - 0.5837 \times TF - 21.0358 \quad (5)$$

Where:
PV – Plastic Viscosity
YP – Yield Point
FLAC – Fluid Loss Additive Concentration
TF – Temperature Factor

* N/A – At higher concentrations of Fluid loss Additives the slurry was too thick to take readings of PV and YP

5.3 Effect of Dispersant Concentration on Cement Slurry Rheology at Specified temperatures: 80^oF, 130^oF &180^oF

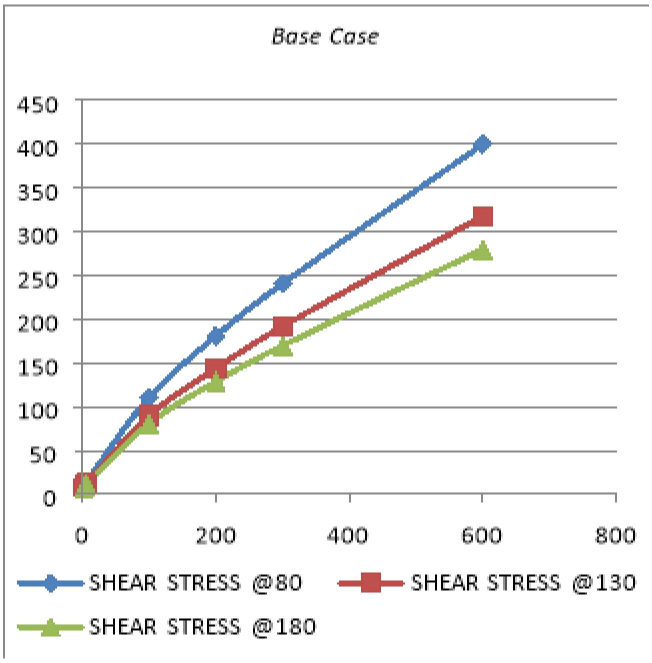

Figure 9. Graph of Shear stress against Shear rate for base case @ 80oF, 130o F, & 180oF

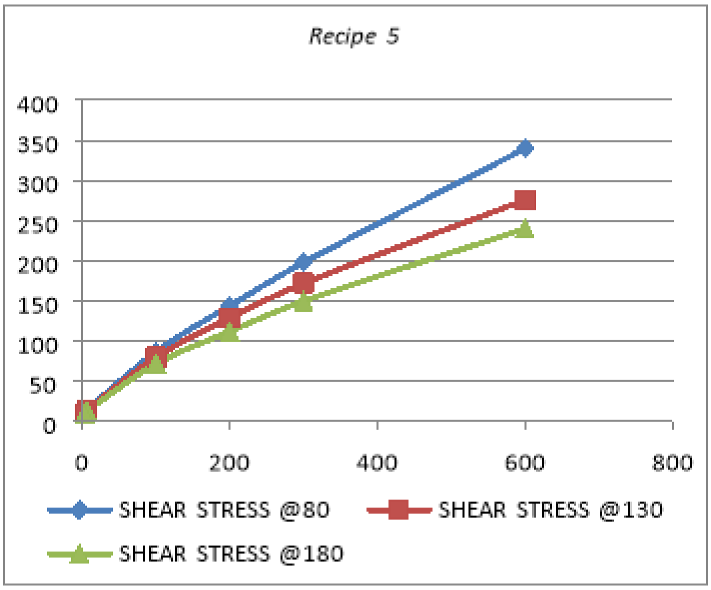

Figure 10. Graph of Shear stress against Shear rate for Recipe 5 @ 80^oF, 130^o F, & 180^oF

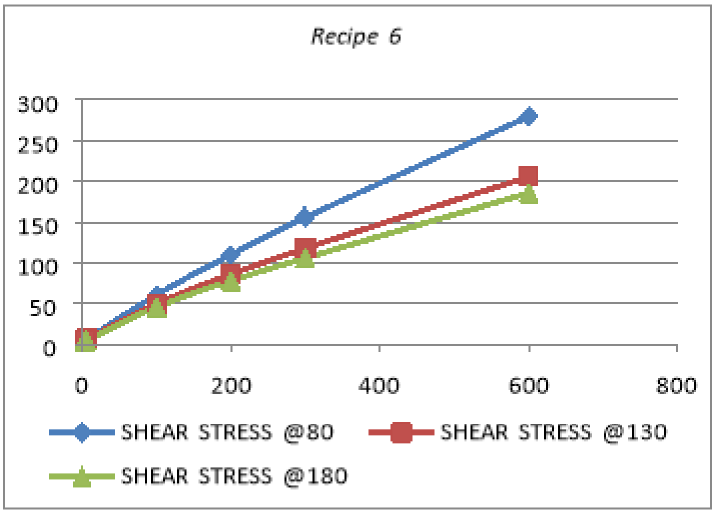

Figure 11. Graph of Shear stress against Shear rate for Recipe 6 @ 80^oF, 130^o F, & 180^oF

The charts (Figure 9, 10 & 11) show the relationship for each case at different temperatures. Increasing the concentrations of the additive at constant temperatures, the shear stress decreases as well thereby reducing the viscosity of the cement slurry. From the above, there was a more significant change in the shear stress- shear rate plot between temperature @ 80oF and that @ 130oF and 180oF for recipe 6 compared to other cases.

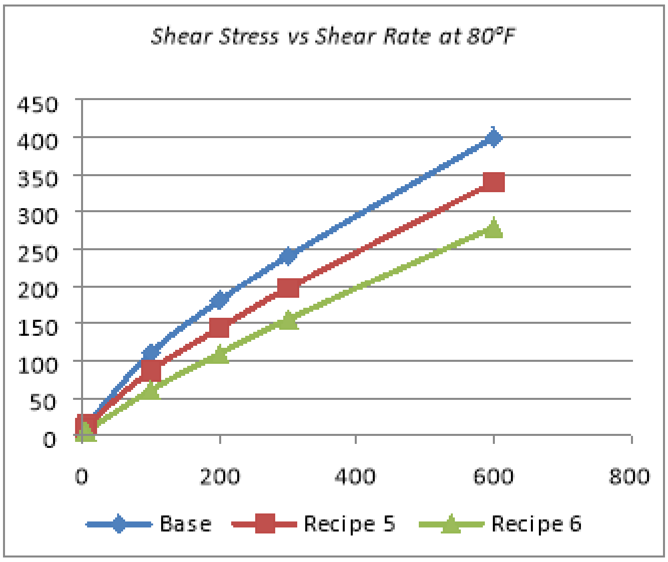

Figure 12. Graph of Shear stress against Shear rate for base case, recipe 5 & recipe 6 @ 80°F

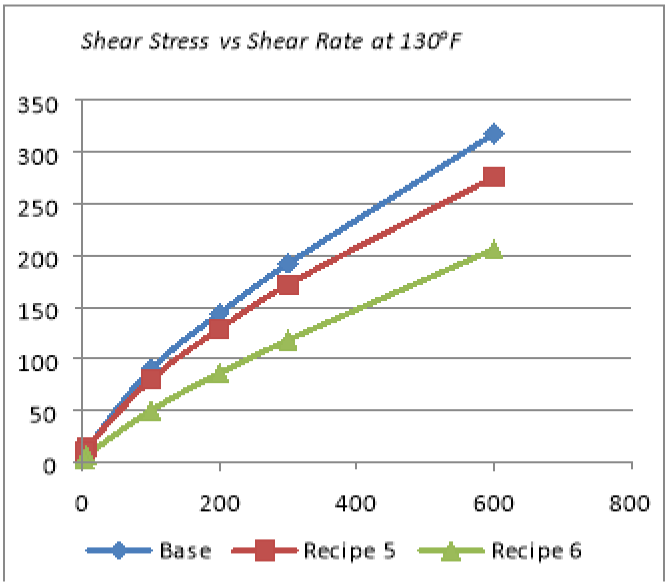

Figure 13. Graph of Shear stress against Shear rate for base case, recipe 5 & recipe 6 @ 130°F

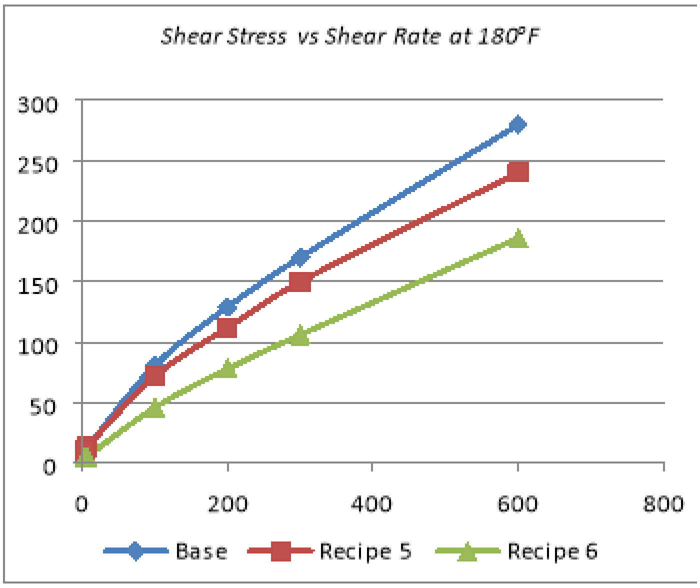

Figure 14 Graph of Shear stress against Shear rate for base case, recipe 5 & recipe 6 @ 180°F

From the above Figure (Fig 12, 13 and 14), the shear stress reduces with an increase in concentration and temperature.

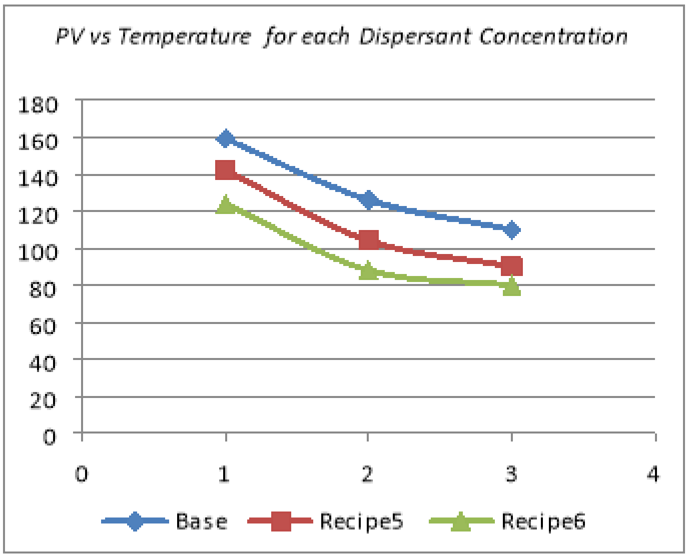

Figure 15. Graph of Plastic viscosity against Temperature for base case, recipe 5 & recipe 6

The above Figure (Fig 15) shows the relationship between plastic viscosity and temperature. Increase in temperature causes a corresponding decrease in plastic viscosity.

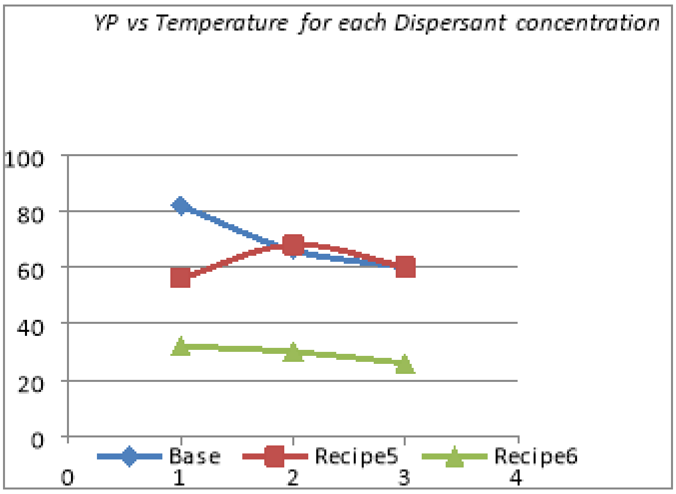

Figure16. Graph of Yield point against Temperature for base case, recipe 5 & recipe 6

The graph above (Fig 16) shows the relationship between yield point and temperature for different cases (base case, Recipe 5 and Recipe 6). For the base case, an increase in temperature causes a corresponding decrease in yield point, therefore the resistance to flow will decrease with an increase in temperature.

For recipe 5, there was an increase in yield point as the temperature was initially increased @ 130^{o}F. This shows that maximum stress required for fluid flow was attained at that temperature and concentration of additive and above that temperature, yield point was decreased; reducing the resistance to flow.

For recipe 6, there was a slight decrease in yield point as temperature was increased.

5.3.1 Regression Analysis

Table 11: Factorial design for analyzing effect of Dispersant concentration

S/N	Dispersant Concentration (%)	Temperature Factor (%)	Plastic Viscosity (%)	Yield Point (%)
1	0	0	0	0
2	0	62.5	-20.75	-19.51
3	0	125	-30.82	-26.83
4	100	0	-10.69	-31.70
5	100	62.5	-34.59	-17.07
6	100	125	-43.40	-26.83
7	200	0	-22.01	-60.98
8	200	62.5	-44.65	-63.41
9	200	125	-49.69	-68.29

$$PV = -0.12243 \times DC - 0.2664 \times TF - 0.585 \quad (6)$$

$$YP = -0.2317 \times DC - 0.0586 \times TF - 7.315 \quad (7)$$

Where:
PV – Plastic Viscosity
YP – Yield Point
DC – Dispersant Concentration
TF – Temperature Factor

Conclusion

From the above experimental results and analysis in chapter four, it has been demonstrated that the rheological properties of OWC slurries are highly dependent on temperature; both shear stress, yield stress and plastic viscosity increased nonlinearly with corresponding temperature. The following conclusions can be drawn:

i. An increase in the concentration and temperature of the retarder will cause a corresponding decrease in shear stress at constant shear-rate.
ii. An increase in temperature will cause a corresponding decrease in plastic viscosity and yield stress when retarder is added to the cement slurry.
iii. It can be deduced that an increase in the concentration of fluid loss additive for each case will cause a significant increase in shear stress at constant shear rate thereby making the fluid more viscous to flow at constant temperatures.
iv. An increase in temperature will cause a corresponding decrease in the plastic viscosity and yield point when a fluid loss additive is added to the slurry.
v. Increasing the concentrations of the dispersant at constant temperatures, the shear stress decreased; thereby reducing the viscosity of the cement slurry.
vi. Increase in temperature causes a corresponding decrease in plastic viscosity and yield point, thereby decreasing the resistance to flow.

It should be noted that this study and its findings are valid for the oil well cement and the additives used. Other cement/additive combinations can exhibit different characteristics. Even additives from the same category, but different source, could behave differently, and thus need to be investigated separately.

References

[1] Michaux M. Nelson EB, Vidik B (1990). Chemistry and Characterization of Portland Cement In Well Cementing. Elsevier Science Publishers Amsterdam 8-25.

[2] Nelson, E. B., and Guillot, D. 2006. Well Cementing, second edition. Schlumberger.

[3] Arnoldus M.A and Ade L. (2016). Compressive and Shear Bond Strength of Oil Well Cement with Calcium Carbonate and Silica Fume. Department of Civil Engineering, Faculty of Engineering.

[4] Shuker MT, Memon KR, Tunio SQ, Memon MK (2014) Laboratory Investigation on Performance of Cement Using Different Additives Schemes to Improve Early Age Compressive Strength Research. Journal of Applied Sciences Engineering and Technology 7: 2298-2305.

[5] API RP 10B-2, Recommended Practice for Testing Well Cements. 2013. Washington, DC: API

[6] Doherty D.R. et al., (2010). Pushing Cement beyond the Norm of Extreme High Temperature. Paper IADC/SPE 134422 Presented at the IADC/SPE Asia Pacific Drilling Technology Conference and Exhibition

held in Hochi Minh City, Vietnam, 1-3 November 2010. https://doi.org/10.2118/134422-MS

[7] Olowolagba K. and Brenneis C. (2010). Techniques for the Study of Foamed Cement Technology. Paper SPE 133050 presented at the SPE production and Operations Conference and Exhibition Held in Tunis, Tunisia, 8-10 June 2010. https://doi.org/10.2118/133050-MS

[8] Kelessidis V.C, Fraim M., Fardis M., Karakosta E., Diamantopoulos G., P. Arkoudeas, S. ElHardalo , L. Lagkaditi, G. Papavassiliou, 2014. Comprehensive Assessment of Additive and Class G cement Properties Affecting Rheology Fluid Loss, Setting Time and Long Term Characteristics of Elastic Cements. Paper SPE 167731 presented at the SPE European Unconventional Conference and Exhibition Held in Vienna, Austria, 25-27 February 2014. https://doi.org/10.2118/167731-MS

[9] Haichuan L., Chengbin X., Yonghui G., Lirong L., Haijin Z., (2016). Cement Slurries with Rheological Properties Unaffected By Temperature. Paper SPE 178922. https://doi.org/10.2118/178922-PA

[10] Bakirov D.L., Burdyga V. A., Svyatukhova S.S., Melekhov A.V., Kafarova I.V., Sledkov V.V., Shadchnev A.N., Shtyfel A.P., Yakunin S.A., Chudinov V.A., (2016). Cement fir Temperature range 160-300o C. Paper SPE -181935-MS Presented at the SPE Russian Petreoleum Technology Conference. https://doi.org/10.2118/181935-RU

[11] Okoro O., Nwakpu G. (2017). Undergraduate Thesis presented to Department of Petroleum Engineering, Federal University of Technology Owerri.

APPENDIX 1

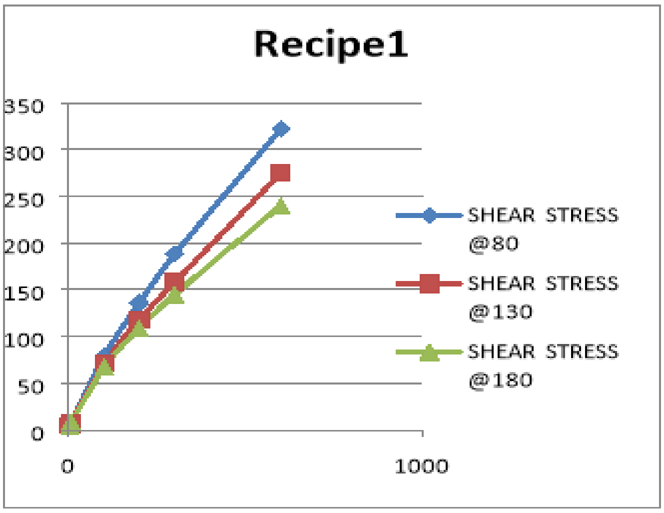

FIG A.1. Graph of Shear stress against Shear rate for Recipe 1 @ 80^oF, 130^o F, & 180^oF.

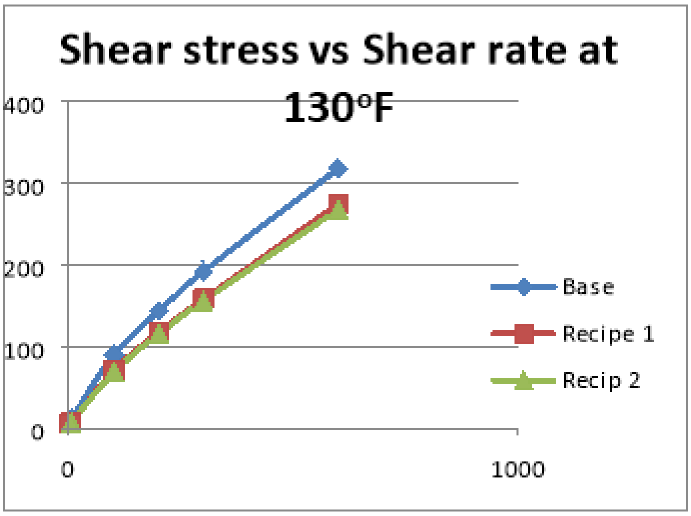

FIG A.3. Graph of Shear stress against Shear rate for base case, recipe 1 & recipe 2 @ 130^oF

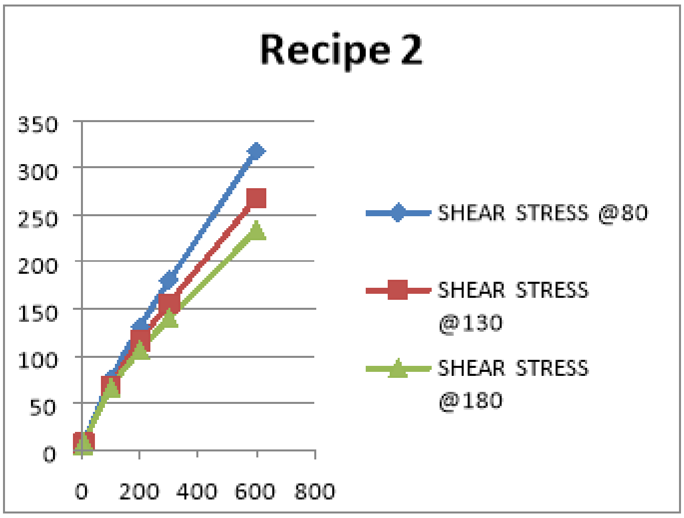

FIG A.2. Graph of Shear stress against Shear rate for Recipe 2 @ 80^oF, 130^o F, & 180^oF

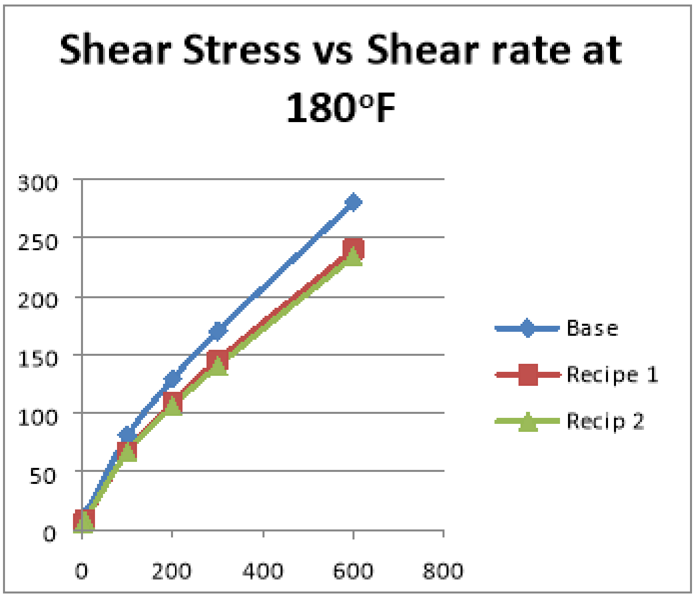

FIG A.4. Graph of Shear stress against Shear rate for base case, recipe 1 & recipe 2 @ 180^oF

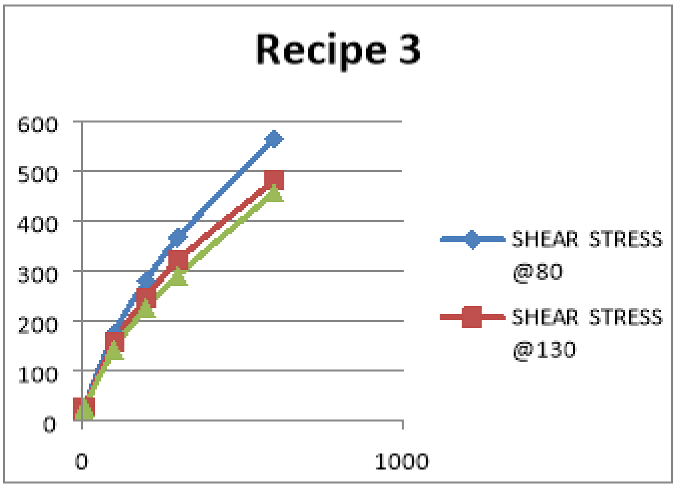

FIG A.5 Graph of Shear stress against Shear rate for Recipe 3 @ 80°F, 130° F, & 180°F

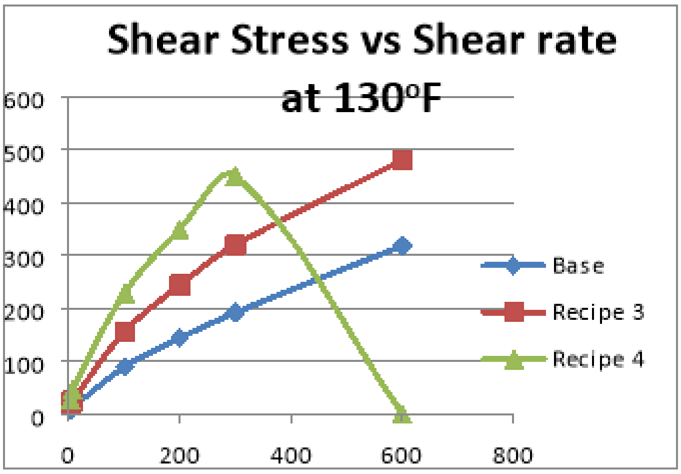

FIG A.8. Graph of Shear stress against Shear rate for base case, recipe 3 & recipe 4 @ 130°F

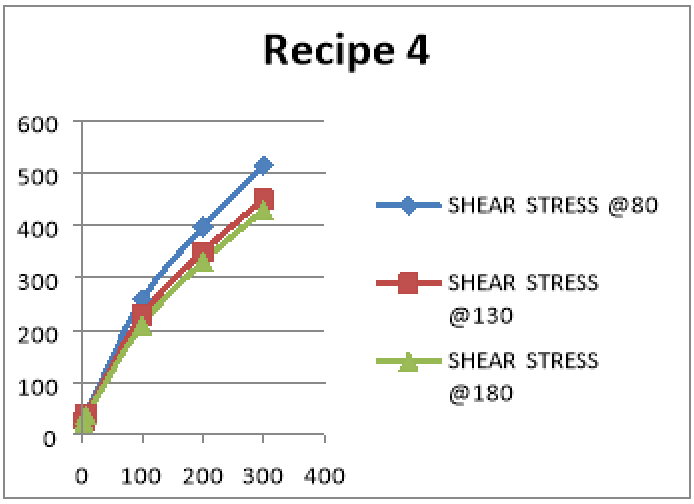

FIG A.6. Graph of Shear stress against Shear rate for Recipe 4 @ 80°F, 130° F, & 180°F

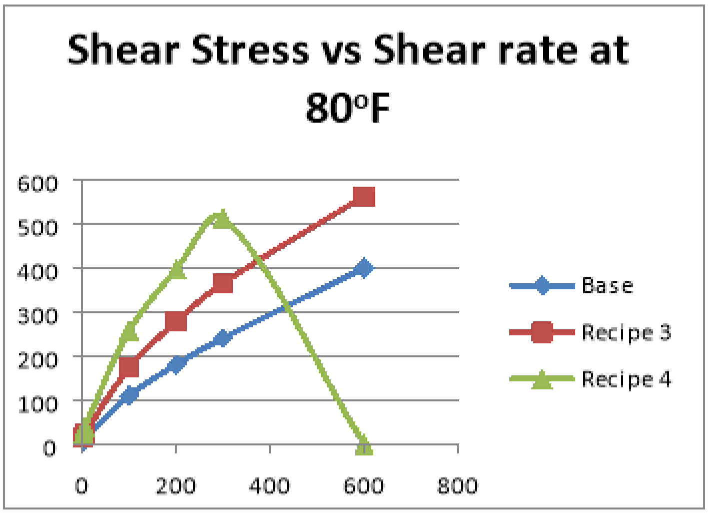

FIG A.7. Graph of Shear stress against Shear rate for base case, recipe 3 & recipe 4 @ 80°F

APPENDIX 2

RETARDER - LINEAR REGRESSION ON PV

Regression Statistics	
Multiple R	0.96987286
R Square	0.940653365
Adjusted R Square	0.920871154
Standard Error	3.725926184
Observations	9

	Coefficients	*Standard Error*	*t Stat*	*P-value*	*Lower 95%*	*Upper 95%*	*Lower 99.0%*	*Upper 99.0%*
Intercept	-4.995555556	2.483950789	-2.011133062	0.09101153	-11.07356418	1.08245307	-14.20462431	4.213513204
X Variable 1	-0.053466667	0.01521103	-3.514993189	0.01259483	-0.090686716	-0.01624662	-0.109860465	0.002927132
X Variable 2	-0.221386667	0.024337648	-9.096469281	9.9127E-05	-0.280938746	-0.16183459	-0.311616745	-0.131156589

RESIDUAL OUTPUT

Observation	*Predicted Y*	*Residuals*	*Standard Residuals*
1	-4.995555556	4.995555556	1.548170953
2	-18.83222222	-1.917777778	-0.59433787
3	-32.66888889	1.848888889	0.572988538
4	-10.34222222	-5.377777778	-1.666625314
5	-24.17888889	-2.241111111	-0.694541995
6	-38.01555556	-2.234444444	-0.692475931
7	-15.68888889	2.478888889	0.768231627
8	-29.52555556	-0.034444444	-0.010674666
9	-43.36222222	2.482222222	0.769264659

PROBABILITY OUTPUT

Percentile	*Y*
5.555555556	-40.88
16.66666667	-40.25
27.77777778	-30.82
38.88888889	-29.56
50	-26.42
61.11111111	-20.75
72.22222222	-15.72
83.33333333	-13.21
94.44444444	0

RETARDER - LINEAR REGRESSION ON YP

Regression Statistics	
Multiple R	0.846218653
R Square	0.716086009
Adjusted R Square	0.621448013
Standard Error	10.12531664
Observations	9

	Coefficients	Standard Error	t Stat	P-value	Lower 95%	Upper 95%	Lower 99.0%	Upper 99.0%
Intercept	-14.3644444	6.750211093	-2.127999295	0.077423	-30.88161596	2.15272708	-39.3903662	10.66147731
X Variable 1	-0.15446667	0.041336432	-3.736816626	0.009659	-0.255613272	-0.0533201	-0.30771851	-0.00121482
X Variable 2	-0.07152	0.066138291	-1.081370543	0.321068	-0.233354569	0.09031457	-0.31672295	0.173682955

RESIDUAL OUTPUT

Observation	Predicted Y	Residuals	Standard Residuals
1	-14.3644444	14.36444444	1.638134621
2	-18.8344444	-0.675555556	-0.077040985
3	-23.3044444	-3.525555556	-0.402057639
4	-29.8111111	-4.338888889	-0.494810929
5	-34.2811111	-15.71888889	-1.792596727
6	-38.7511111	-0.268888889	-0.030664339
7	-45.2577778	-3.522222222	-0.401677502
8	-49.7277778	3.387777778	0.386345333
9	-54.1977778	10.29777778	1.174368167

PROBABILITY OUTPUT

Percentile	Y
5.555555556	-50
16.66666667	-48.78
27.77777778	-46.34
38.88888889	-43.9
50	-39.02
61.11111111	-34.15
72.22222222	-26.83
83.33333333	-19.51
94.44444444	0

DISPERSANT LINEAR REGRESSION ON PV

Regression Statistics	
Multiple R	0.976752
R Square	0.954044
Adjusted R Square	0.935662
Standard Error	3.954388
Observations	8

	Coefficients	Standard Error	t Stat	P-value	Lower 95%	Upper 95%	Lower 99.0%	Upper 99.0%
Intercept	-0.585	2.887877	-0.20257	0.847455	-8.00852	6.838523	-12.2293	11.05933

X Variable 1	-0.12243	0.018407	-6.65112	0.001159	-0.16974	-0.07511	-0.19664	-0.04821
X Variable 2	-0.26636	0.029451	-9.04427	0.000276	-0.34207	-0.19065	-0.38511	-0.14761

RESIDUAL OUTPUT

Observation	*Predicted Y*	*Residuals*	*Standard Residuals*
1	-0.585	0.585	0.175041
2	-17.2325	-3.5175	-1.05249
3	-33.88	3.06	0.915601
4	-12.8275	2.1375	0.639574
5	-29.475	-5.115	-1.53049
6	-46.1225	2.7225	0.814615
7	-25.07	3.06	0.915601
8	-41.7175	-2.9325	-0.87745

PROBABILITY OUTPUT

Percentile	*Y*
6.25	-44.65
18.75	-43.4
31.25	-34.59
43.75	-30.82
56.25	-22.01
68.75	-20.75
81.25	-10.69
93.75	0

DISPERSANT LINEAR REGRESSION ON YP

Regression Statistics	
Multiple R	0.872783
R Square	0.76175
Adjusted R Square	0.66645
Standard Error	12.48488
Observations	8

	Coefficients	*Standard Error*	*t Stat*	*P-value*	*Lower 95%*	*Upper 95%*	*Lower 99.0%*	*Upper 99.0%*
Intercept	-7.315	9.117664	-0.80229	0.458805	-30.7527	16.1227	-44.0787	29.44872
X Variable 1	-0.23171	0.058114	-3.98714	0.010456	-0.38109	-0.08232	-0.46603	0.002615
X Variable 2	-0.05855	0.092982	-0.62965	0.556568	-0.29757	0.180472	-0.43346	0.316371

RESIDUAL OUTPUT

PROBABILITY OUTPUT

Observation	Predicted Y	Residuals	Standard Residuals
1	-7.315	7.315	0.693257
2	-10.9742	-8.53583	-0.80896
3	-14.6333	-12.1967	-1.1559
4	-30.4858	-1.21417	-0.11507
5	-34.145	17.075	1.618231
6	-37.8042	10.97417	1.040043
7	-53.6567	-7.32333	-0.69405
8	-57.3158	-6.09417	-0.57756

Percentile	Y
6.25	-63.41
18.75	-60.98
31.25	-31.7
43.75	-26.83
56.25	-26.83
68.75	-19.51
81.25	-17.07
93.75	0

FLUID LOSS ADDITIVE **LINEAR REGRESSION ON YP**

Regression Statistics	
Multiple R	0.960076
R Square	0.921745
Adjusted R Square	0.869576
Standard Error	27.7878
Observations	6

	Coefficients	*Standard Error*	*t Stat*	*P-value*	*Lower 95%*	*Upper 95%*	*Lower 99.0%*	*Upper 99.0%*
Intercept	21.03583	21.22328	0.991168	0.394671	-46.5061	88.5778	-102.927	144.9991
X Variable 1	1.21	0.226886	5.333064	0.012886	0.487946	1.932054	-0.11522	2.535223
X Variable 2	-0.58372	0.222302	-2.62579	0.078609	-1.29119	0.123746	-1.88217	0.714728

RESIDUAL OUTPUT

Observation	*Predicted Y*	*Residuals*	*Standard Residuals*
1	21.03583	-21.0358	-0.9773
2	-15.4467	-4.06333	-0.18878

PROBABILITY OUTPUT

Percentile	*Y*
8.333333	-26.83
25	-19.51

3	-51.9292	25.09917	1.166083		41.66667	0
4	142.0358	28.28417	1.314055		58.33333	51.22
5	105.5533	-10.4333	-0.48472		75	95.12
6	69.07083	-17.8508	-0.82933		91.66667	170.32

FLUID LOSS ADDITIVE **LINEAR REGRESSION ON PV**

Regression Statistics	
Multiple R	0.952713
R Square	0.907661
Adjusted R Square	0.846102
Standard Error	7.54893
Observations	6

	Coefficients	*Standard Error*	*t Stat*	*P-value*	*Lower 95%*	*Upper 95%*	*Lower 99.0%*	*Upper 99.0%*
Intercept	-4.7675	5.765591	-0.82689	0.468931	-23.1162	13.58118	-38.4438	28.90879
X Variable 1	0.266233	0.061637	4.319392	0.022865	0.070078	0.462389	-0.09378	0.626248
X Variable 2	-0.19876	0.060391	-3.29119	0.046037	-0.39095	-0.00657	-0.5515	0.153981

RESIDUAL OUTPUT | PROBABILITY OUTPUT

Observation	*Predicted Y*	*Residuals*	*Standard Residuals*		*Percentile*	*Y*
1	-4.7675	4.7675	0.815323		8.333333	-30.82
2	-17.19	-3.56	-0.60882		25	-20.75
3	-29.6125	-1.2075	-0.2065		41.66667	0
4	21.85583	1.414167	0.241846		58.33333	0.63
5	9.433333	-8.80333	-1.50552		75	4.4

6	-2.98917	7.389167	1.263672	91.66667	23.27

Authors Bio:

Ikpeka Princewill is a researcher and Lecturer at the department of Petroleum Engineering, Federal University of Technology Owerri. His core area of research include: Reservoir Characterization for conventional and unconventional systems, Building numerical reservoir models and assessing field development strategies for various reservoir systems, Drilling Fluid flow modelling, Natural Gas Production Optimization Studies. He holds a B.Eng and MSc degree in Petroleum Engineering and is currently studing for his PhD.

Odo Jude is a lecturer at the department of Petroleum Engineering, Federal University of Technology owerri. Over the years,he has demonstrated a range of experience in Natural Gas processes,monitoring,evaluation and measurements,Laboratory Analysis using Dean-Stack Distillation. He holds a B.Eng and MSc degree in Petroleum Engineering.

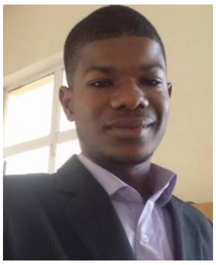

Uzuegbu Godson is an experienced Cementer with Haliburton Oil Services. He holds a B.Eng in Petroleum Engineering

Bennedict Ugochukwu and **Utojiuba Ifeanyi** are graduates of Petroleum Engineering, Federal University of Technology Owerri.

IJEW 国际工程期刊 International Journal of Engineering Works انجینرنگ کاموں کا بین الاقوامی جرنل

International Journal of Engineering Works
ISSN-p: 2521-2419
ISSN-e: 2409-2770
Vol. 6, Issue 03, PP. 71-77, March 2019
https://www.ijew.io/

Control Strategy for Distribution Static Compensator based on Instantaneous Reactive Power Theory for Power Quality Improvement in Distribution System

Umar Farooq[1], Kaleem Ullah[2], Dr. Muhammad Naeem Arbab[3]
[1,2,3]Department of Electrical Engineering, University of Engineering and Technology Peshawar, Pakistan
ixumer@gmail.com[1]
Received: 21 February, Revised: 01 March, Accepted: 03 March

Abstract: Nonlinear loads inject harmonics in the power system and distorts the load current waveform. These load current harmonics ultimately give rise to harmonics on the supply side and hence can affect the neighboring consumers. Custom power technology is employed to avert issues of power quality on the source side. Among numerous custom power tools, Distribution Static Compensator (D-STATCOM) is considered to be an effectual Shunt Active Power Filter to banish current harmonics, providing a good balance between cost and performance. A control strategy based on Instantaneous Reactive Power (IRP) theory for D-STATCOM is discussed in this paper. D-STATCOM is controlled to compensate for reactive power and to discard the objectionable harmonics injected in the distribution system by nonlinear load. Anti-harmonics current is inserted in the grid lines by the mentioned Shunt Active Power Filter, which nullify the harmonics introduced by the nonlinear load. To be used for the nullification of current harmonics, D-STATCOM is connected parallel with the load. Moreover, the power factor of the system is ameliorated along with a significant decrease in Total Harmonic Distortion (THD) in the source current. The model is simulated in MATLAB/SIMULINK in order to investigate the performance and efficiency of the propounded system. The simulation results reveal expeditious dynamic response and high precision of D-STATCOM in achieving the desired goals.

Keywords: Distribution Static Compensator (D-STATCOM), Power Quality, Instantaneous Reactive Power (IRP) Theory, Custom Power.

I. INTRODUCTION

The term power quality is more frequently utilized these days in the power industry and both the power providers as well as the cessation users are equally perturbed about it. The quality of power distributed to the end users is of great paramount and depends on all the three parameters i.e. voltage, current and frequency. Power quality is considered to be affected if there occurs a deviation in any of the above mentioned parameters of the distributed power i.e. frequency voltage or current, from the nominal values.

Reasons of these deviations may include the presence of a variety of loads in the electric power network or the happening of faults in the exposed network. Majority of the loads in our system have inductive nature such as industrial load, motors, fans etc. These loads draw reactive power with a lagging power factor and hence affect the source power factor by incrementing reactive burden on the source [1]. This will augment losses within the distribution network and essentially lessen active power flow capacity in the network. A poor power factor causes terrible voltage regulation with a rise in the load current since load current and power factor has an indirect relation. A load with poor power factor will draw higher current as compared to a load with good power factor, even if power rating of both loads is same. Consequently a low power factor implicatively insinuates more sizably voluminous machine size, more voltage drops, more sizably voluminous conductor size and low efficiency. common feeder. These voltage/current harmonics may affect the normal operation of the appliances and ultimately may result in the breakdown of the equipment [2].

Custom power device technology is utilized to rectify problems of power quality in the distribution network [3]. A Distribution Static compensator (D-STATCOM) is a member of custom power device family utilized for harmonics banishment, reactive power redress and load balancing in the distribution system [4]. Several control strategies are implemented to extract reference signals for D-STATCOM including Instantaneous Reactive Power (IRP) theory [5], Modified Power Balance Theory [6], Synchronous Reference Frame (SRF) theory [7] and neural network predicated technique [8]. Among all these mentioned techniques, IRP theory and SRF theory are widely employed [9]. This paper utilizes IRP theory as a control strategy for D-STATCOM in MATLAB/SIMULINK and results are analyzed.

II. SYSTEM CONFIGURATION

A simplified system model is show in fig.1. The distribution feeder shown in the figure represent the secondary side of distribution transformer which supplied the load. Rs reflects resistance of the source and distribution line. Similarly, Ls reflects inductance of the source and the line. For elimination of current harmonics, D-STATCOM is connected parallel with the load wherein the harmonics are banished by injecting compensating current identical to harmonic-frequency components of current. Consequently, the source current will be sinusoidal with no harmonics at PCC.

D-STATCOM accommodates a three phase voltage source inverter (VSI) which can be realized by six IGBT switches

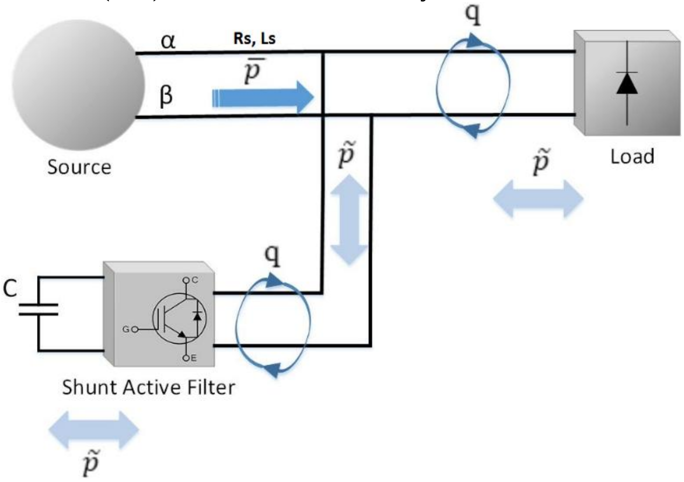

Figure 1: System Configuration

forming three legs [10]. A capacitor is applied at the DC side of voltage source inverter (VSI) whose purpose is to hold the voltage at a delegated degree to carry out switching of IGBTs. The DC capacitor being a voltage source plays a vital role satisfying reactive power demand of the load. DC capacitor voltage is kept constant by means of employing a PI controller. D-STATCOM is connected with the distribution line through interfacing inductance Lf to clear out excessive frequency additives of compensating current [11]. A complete system model is shown in fig. 2.

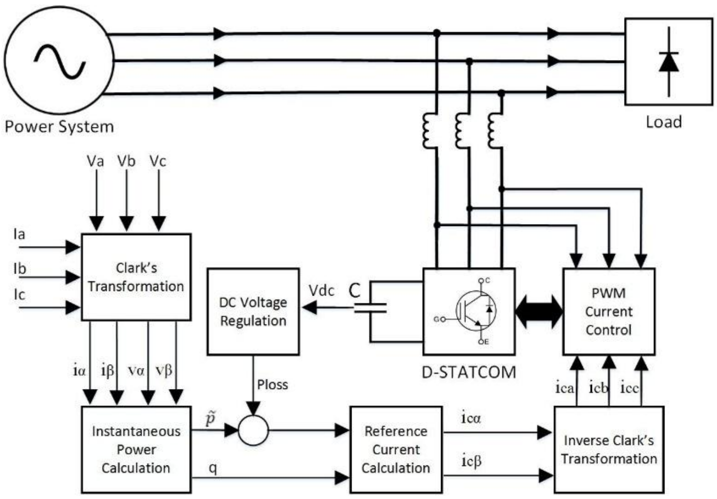

Figure 2: Complete System Model

The model is simulated for both linear and nonlinear load. Linear load is modelled using R-L load whereas nonlinear load is modelled by means of connecting three phase diode rectifier with the power lines. Reference current signals are extracted through instantaneous reactive power (IRP) theory and then pulse width modulation (PWM) technique is implemented using these reference current signals to trigger the IGBTs. Hysteresis based PWM current controller is used which is fed with the reference currents to sway the compensating current contemporary to observe these reference currents. A working model of D-STATCOM with instantaneous reactive power theory simulated in SIMULINK is manifested in fig. 3.

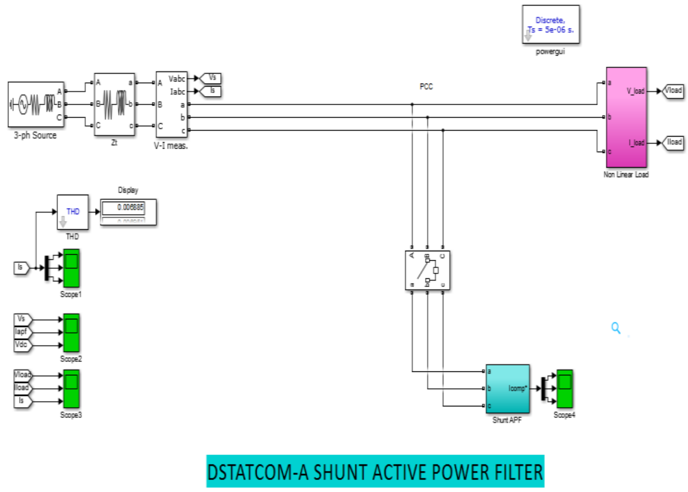

Figure 3: System Configuration in SIMULINK

III. CONTROL ALGORITHM

After the text edit has been completed, the paper is ready for the template. Duplicate the template file by using the Save As command, and use the naming convention prescribed by IJSEI for the name of your paper. In this newly created file, highlight all of the contents and import your prepared text file. You are now ready to style your paper; use the scroll down window on the left of the MS Word Formatting toolbar.

A. IRP Theory

Akagi was the first to instigate the conception of instantaneous reactive power theory [12]. This theory possess flexibility and can be utilized in both transient state as well as steady state. IRP theory or p-q theory transmute three phase quantities to α-β-0 stationary orthogonal coordinates and then computation of instantaneous power is realized on these axes [13],[14]. Zero sequence component may subsist in a three phase 4 wire distribution system because there exists a system ground. However zero sequence component cannot be realized in a three phase 3 wire system, ergo transformation is done to α-β frame. Figure 4 displays the block diagram representation of IRP theory.

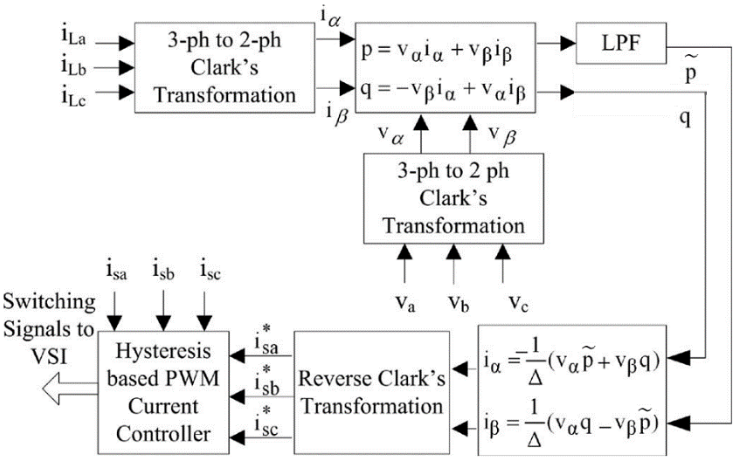

Figure 4: Block diagram representation of IRP theory

The system three phase instantaneous voltages are stated as

$$v_a = V_{max}\, Sin(\omega t)$$

$$v_b = V_{max}\, Sin(\omega t - 2\pi/3)$$

$$v_c = V_{max}\, Sin(\omega t + 2\pi/3)$$

Similarly, the instantaneous load currents can be stated as under

$$i_a = \sum i_{an}\ Sin\{n(\omega t) - \ \theta_{an}\}$$

$$i_b = \sum i_{bn}\ Sin\{n(\omega t - 2\pi/3) - \ \theta_{bn}\}$$

$$i_c = \sum i_{cn}\ Sin\{n(\omega t + 2\pi/3) - \ \theta_{cn}\}$$

The instantaneous currents and voltages are set on a, b and c axes whose amplitudes change with respect to time. These voltage and current quantities are transmuted to α-β frame from a-b-c axes using Clark's transformation as given below

$$\begin{bmatrix} 1 & -\frac{1}{2} & -\frac{1}{2} \\ 0 & \frac{\sqrt{3}}{2} & -\frac{\sqrt{3}}{2} \end{bmatrix} \begin{bmatrix} v_\alpha \\ v_\beta \end{bmatrix} = \sqrt{\frac{2}{3}} \begin{bmatrix} v_a \\ v_b \\ v_c \end{bmatrix}$$

$$\begin{bmatrix} 1 & -\frac{1}{2} & -\frac{1}{2} \\ 0 & \frac{\sqrt{3}}{2} & -\frac{\sqrt{3}}{2} \end{bmatrix} \begin{bmatrix} i_\alpha \\ i_\beta \end{bmatrix} = \sqrt{\frac{2}{3}} \begin{bmatrix} i_a \\ i_b \\ i_c \end{bmatrix}$$

Instantaneous three phase power on a-b-c axes is given by

$$p = v_a * i_a + v_b * i_b + v_c * i_c$$

Similarly, instantaneous powers can be translated onto α-β frame as follows

$$p = \ v_\alpha * i_\alpha + v_\beta * i_\beta$$

$$q = \ -v_\beta * i_\alpha + v_\alpha * i_\beta$$

Expressing in matrix form as

$$\begin{bmatrix} p \\ q \end{bmatrix} = \begin{bmatrix} v_\alpha & v_\beta \\ -v_\beta & v_\alpha \end{bmatrix} \begin{bmatrix} i_\alpha \\ i_\beta \end{bmatrix}$$

Both active and reactive powers can be splitted into two constituents

Active power: $p = \bar{p} + \tilde{p}$

Reactive power $q = \bar{q} + \tilde{q}$

$\bar{p}$ and $\bar{q}$ represents average (dc) components of real and imaginary powers whereas the swaying components are represent by $\tilde{p}$ and $\tilde{q}$ respectively. $\bar{p}$ corresponds to the actual active power flow from source towards load. $\bar{q}$ shows the fundamental component of reactive power that sway between the phases. No power transfer between source and load is implied by this component. $\tilde{p}$ is oscillating active power that flows due to the harmonic current. $\tilde{q}$ corresponds to the oscillating component of reactive power ascribable to current harmonics.

For current harmonics abstraction and reactive power redress, $\tilde{p}$, $\bar{q}$ and $\tilde{q}$ should be used for the determination of reference current for gating VSI. Accordingly, the reference compensating current signals in α-β frame can be written as

$$\begin{bmatrix} i_{s\alpha}^* \\ i_{s\beta}^* \end{bmatrix} = \frac{1}{\Delta} \begin{bmatrix} v_\alpha & v_\beta \\ v_\beta & -v_\alpha \end{bmatrix} \begin{bmatrix} -\tilde{p} \\ -q \end{bmatrix}$$

Where

$$\Delta = \ v_\alpha^2 + \ v_\beta^2$$

These reference compensating currents can be retransformed to a-b-c coordinates utilizing inverse Clarke's transformation.

$$\begin{bmatrix} i_{sa}^* \\ i_{sb}^* \\ i_{sc}^* \end{bmatrix} = \begin{bmatrix} 1 & 0 \\ -\frac{1}{2} & \frac{\sqrt{3}}{2} \\ -\frac{1}{2} & -\frac{\sqrt{3}}{2} \end{bmatrix} \begin{bmatrix} i_{s\alpha}^* \\ i_{s\beta}^* \end{bmatrix}$$

B. PI Controller

The AC source satisfies the active power requirement of the load as well as some losses e.g. switching losses in DSTATCOM [15]. If switching losses are not provided by the source, it would be provided by the dc capacitor itself and its voltage would drop down perpetually. Consequently, the reference current for triggering VSI contains two components, one is for emolument of reactive power and harmonics and others is for emolument of these losses. PI controller is used for voltage regulation as its main feature is to diminish steady state error. PD controller improves the speed and transient response of the system. PD or PID is not used because they may cause system instability.

The switching loss component is computed by comparing a set value of dc bus voltage $V_{dc\ ref}$ with observed dc voltage V_{dc}

$$v_{diff\,(x)} = v_{dc\ ref\,(x)} - v_{dc\,(x)}$$

The above difference gives the error signal which gets processed by PI controller as shown in fig. 5.

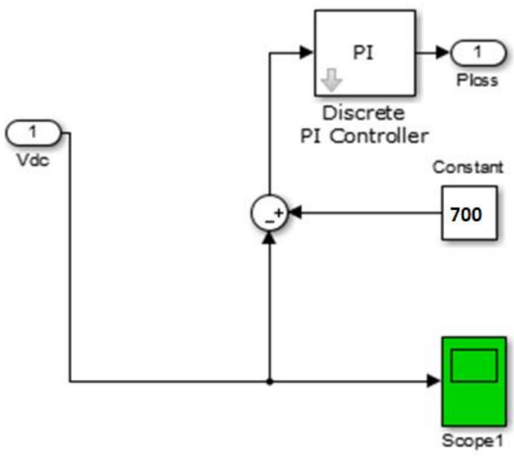

Figure 5: Voltage error signal processing by PI controller

At the xth sampling moment, PI controller gives output $I_{p(x)}$ as

$$I_{p(x)} = I_{p(x-1)} + K_p\left(v_{diff\,(x)} - v_{diff\,(x-1)}\right) + K_i v_{diff\,(x)}$$

Where

K_p = Proportional gain
K_i = Integral gain

PI controller outputs the loss component P_{loss} which is added with $\overline{p}$ i.e. the real power drawn by the load, so that the source furnish this component along with the real power of the load.

C. Hysteresis Current Controller

The reference compensating current signals obtained by means of IRP theory are now utilized for triggering the VSI. Sundry current controllers are available for controlling D-STATCOM such as PI controller, Hysteresis current controller [16], Predictive current controller [17], Sliding mode controller [18], Delta modulation controller [19] etc. Hysteresis current control provides the best balance as it can be facilely implemented with enhanced current controllability and fast response. Hysteresis current controller is elucidated in fig 6 with the help of a block diagram.. $\boldsymbol{i_f^*(t)}$ is the reference line current of D-STATCOM whereas $\boldsymbol{i_f(t)}$ is the real-time line current. Triggering pattern of VSI is decided by Hysteresis current controller upon comparing both of these currents.

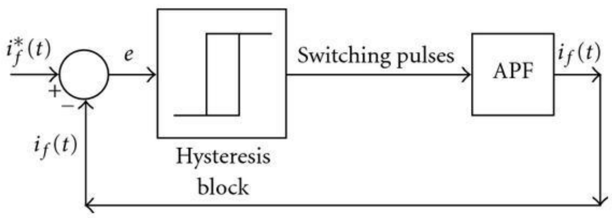

Figure 6: Block diagram of hysteresis based current controller

IV. SIMULATION RESULTS

The efficacy of D-STATCOM with the implementation of IRP theory for current harmonics abstraction, reactive power redress, load balancing, and power factor improvement is analyzed by simulating the model in SIMULINK. The efficiency of D-STATCOM for both unbalanced linear and nonlinear loads is promised by the simulation results. Difference parameters are investigated by exhibiting their waveforms afore and after emolument.

A. Current Harmonics Elimination

The load and source current prior to and after application of compensation is manifested in fig. 7 below.

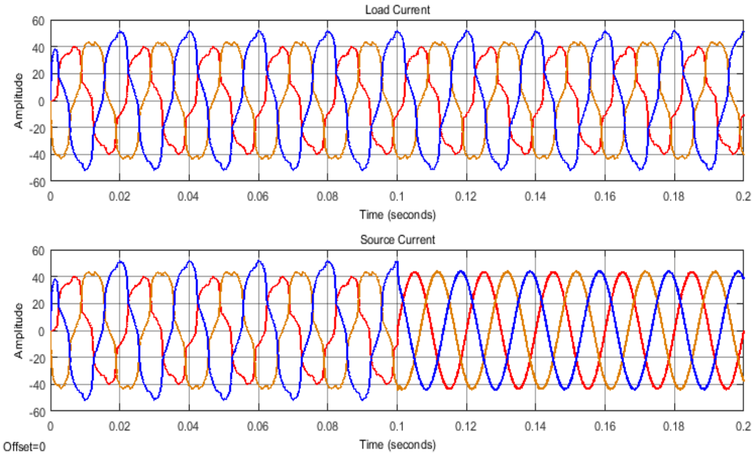

Figure 7: Pre/Post compensation Load and Source current

The deformation of load current waveform is caused by the presence of nonlinear load. It can be seen that before inserting D-STATCOM in the circuit, source current is affected by the harmonics introduced by nonlinear load, but the source becomes sinusoidal after connecting D-STATCOM at 0.1 sec since the compensating current after 0.1 sec is provided by the D-STATCOM. Figure 8 shows the three separate phases of source current.

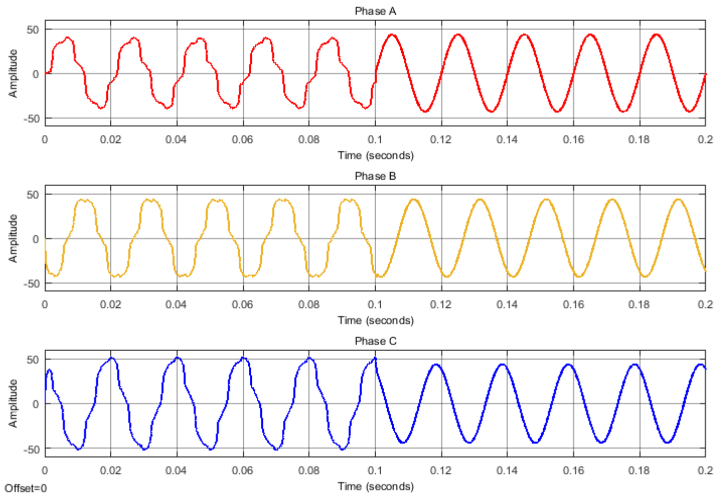

Figure 8: Three phase source current

The source current is outstandingly improved by reducing THD from 20% to 0.78%.

B. Reactive Power Compensation

The real and imaginary powers required by load are displayed in figure 9. Due to existence of current harmonics, both powers are oscillating. The instantaneous power supplied by the source is shown in fig. 10. After connecting the shunt active filter at 0.1 sec, the source only satisfies the active power requirement of load along with switching losses. Whereas the reactive power as well as oscillating active power is supplied by the D-STATCOM.

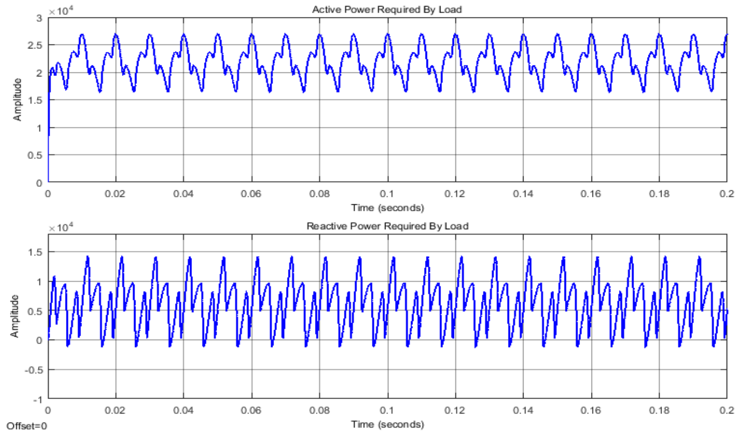

Figure 9: Active and Reactive power drawn by load

The reactive power compensation capability of D-STATCOM is clearly demonstrated in fig. 10.

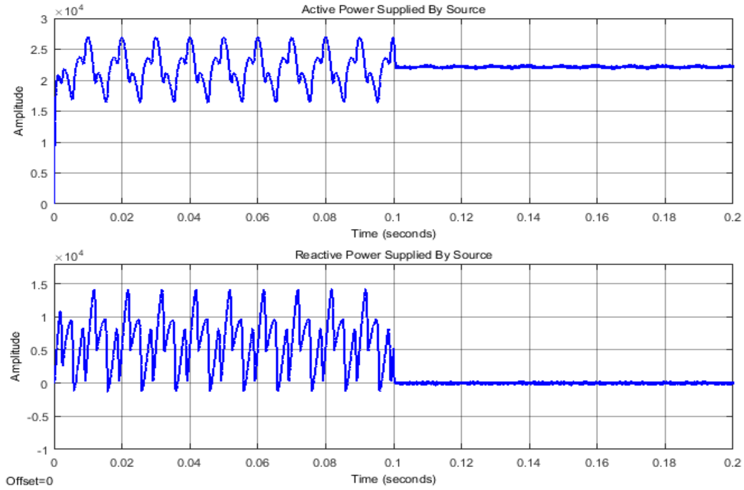

Figure 10: Active and Reactive power supplied by source

C. Power Factor Improvement

After inserting D-STATCOM in the circuit at 0.1 second, it furnishes the reactive power to the load. Therefore, the source is relieved from reactive power burden thereby improving source power factor to unity.

Figure 11 displays the waveforms for Red phase of source current and source voltage. Before compensation, the presence of inductive load determine the source power factor to be 0.8 lagging. However after inserting D-STATCOM at 0.1 second, the source power factor becomes unity as is obvious from the figure below, although the load power factor remains the same.

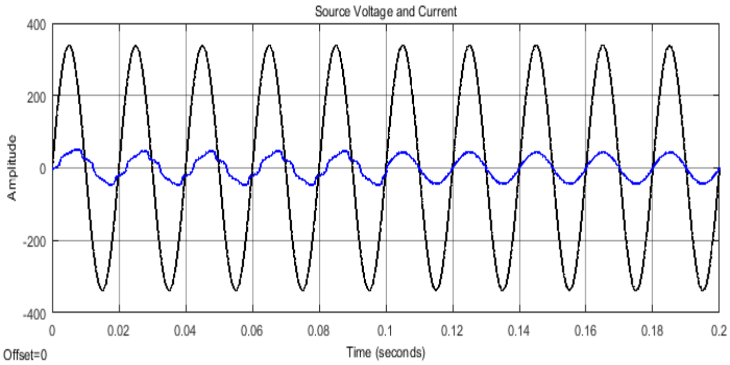

Figure 11: Power factor improved by compensation

D. Load Balancing

Load balancing achieved by compensation is shown in fig. 12. Unbalanced current flows in all the three phases due to unbalanced load before compensation. After compensation, the current in all phases become equal.

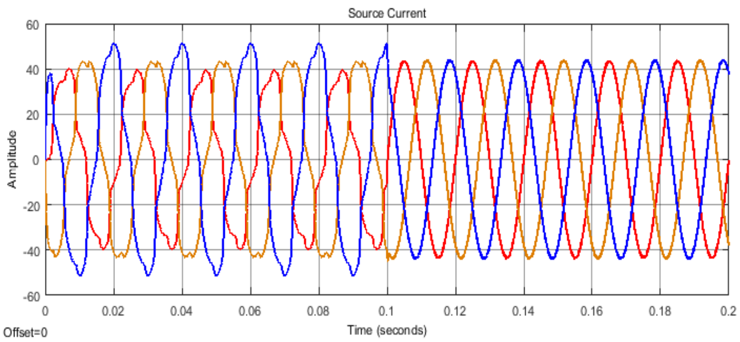

Figure 12: Load balancing achieved by compensation

E. Compensating Current

Fig. 13 illustrates that the compensating current provide by the D-STATCOM before 0.1 second is zero. After connecting it at 0.1 second, it provides the required compensating current for power factor improvement.

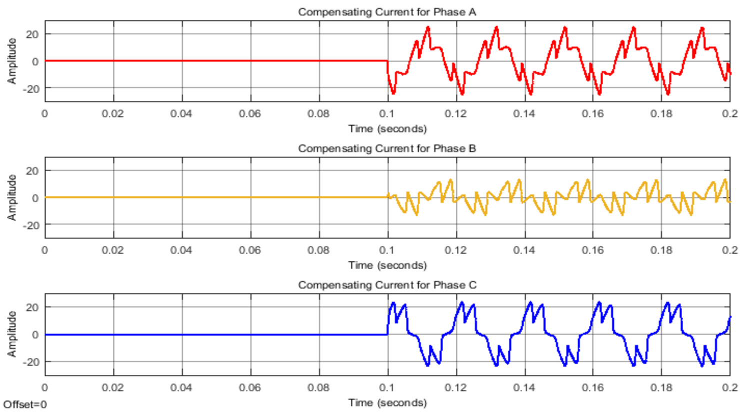

Figure 13: Compensating current provided by D-STATCOM

F. DC Bus Voltage

PI controller has proved its efficacy by maintaining the DC bus voltage at 700 V for proper switching of VSI as shown in fig. 14.

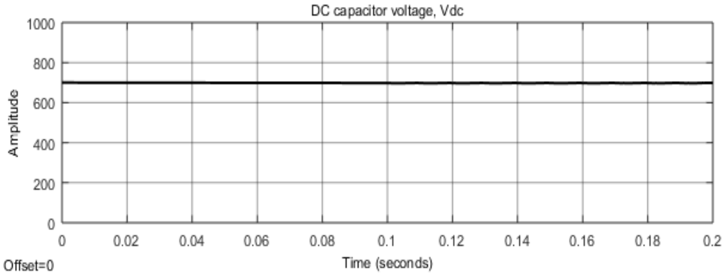

Figure 14: DC link voltage of D-STATCOM

CONCLUSION

The performance of D-STATCOM has been studied in this paper with implementation of IRP theory for generating reference current signals. Simulation results has proved the performance to be cop-acetic for reactive power emolument, current harmonics elimination, power factor amelioration and load balancing. As compared to other reactive power controlling contrivances, D-STATCOM has quite expeditious replication for reactive power compensation. The source current was improved remarkably by diminishing its THD down to a level of 0.78% to meet IEEE 519 standard for harmonics under non-ideal voltage conditions. Similarly, the regulation of DC bus voltage at a level specified by the reference value is swimmingly achieved for better performance of the shunt active filter.

REFERENCES

[1] W. Jewell, “Electrical power systems quality”, 2nd edition, IEEE Power and Energy Magazine, Vol. 99, Issue 5, Sept.-Oct. 2003.

[2] P. Reveulta, S. Litran, J. Thomas, “Active Power Line Conditioners”, 1st Edition, Academic Press, 2015.

[3] M. L. Crow, ”Power quality enhancement using custom power devices”, IEEE Power and Energy Magazine, Vol. 2 , Issue 2 , Mar-Apr 2004.

[4] Y. Pal, A. Swarup, B. Singh, “A Review of Compensating Type Custom Power Devices for Power Quality Improvement”, Power System Technology and IEEE Power India Conference, Oct 2008.

[5] M. Ucar, E. Ozdemir, “Control of a 3-phase 4-leg active power filter under non-ideal mains voltage condition”, Electric Power Systems Research, Vol. 78, Issue 1, pp. 58-73, 2008.

[6] B. Singh, S. Kumar, “Modified Power Balance Theory for control of DSTATCOM”, International Conference on Power Electronics, Drives and Energy Systems (PEDES), Dec. 2010.

[7] B. Singh, P. Jayaprakash, D. P. Kothari, “New control approach for capacitor supported DSTATCOM in three-phase four wire distribution system under non-ideal supply voltage conditions based on synchronous reference frame theory”, International Journal of Electrical Power & Energy Systems, Vol. 33, Issue 5, pp. 1109-1117, 2011.

[8] B. Singh, P. Jayaprakash, S. Kumar, D. P. Kothari, “Implementation of Neural-Network-Controlled Three-Leg VSC and a Transformer as Three-Phase Four-Wire DSTATCOM”, IEEE Transactions on Industry Applications, Vol. 47, Issue 4, July-Aug.2011.

[9] B. Singh and J. Solanki, “A Comparision of Control Algorithms for DSTATCOM,” IEEE Transactions on Industrial Electronics, Vol 56, Issue 7, pp. 2738-2745, 2009.

[10] S. R. Arya, B. Singh, R. Niwas, A. Chandra, K, Al-Haddad, “Power

Quality Enhancement Using DSTATCOM in Distributed Power Generation System", IEEE Transactions on Industry Applications, Vol. 52, Issue 6, Nov.-Dec. 2016.

[11] K. Padiyar, "FACTS Controllers in Power Transmission and Distribution", New Age International, 2007.

[12] H. Akagi, Y. Kanazawa, and A. Nabae, "Instantaneous Reactive power compensators comprising Switching Devices without Energy Storage Components,"IEEE Transactions on Industry Applications, vol.IA-30, no. 3, pp. 625-630, 1984.

[13] H. Akagi, E. H. Watanabe, and M. Aredes, "Instantaneous Power Theory and Applications to Power Conditioning", Hoboken, NJ: Wiley, 2007.

[14] Herrera RS, Salmeron P, Kim H, "Constraints of instantaneous reactive power p-q theory", IET Power Electronics, Vol. 7, Issue 9, 2014.

[15] Singh B, Solanki J, "Mitigation of power quality problems using distribution static synchronous compensator: a comprehensive review", IET Power Electronics, Vol. 8, Issue 7, 2015.

[16] C. Harkare, P. Kapoor, "Study and Simulation of Current Controlled PWM Inverters and their applications", Internation Journal on Recent and Innovation Trends in Computing and Communication, vol. 3, no. 2, pp. 138-142, Feb. 2015.

[17] K. Venkatraman, M. P. Selvan, S. Moorthi, "Predictive Current Control of Distribution Static Compensator for Load Compensation in Distribution System" IET Generation, Transmission and Distribution, vol. 10, no. 10, pp. 2410-2423, July 2016.

[18] M. A. E. Alali, J-P Barbot, "A First Order Sliding Mode Controller for Grid Connected Shunt Active Filter with a LCL Filter" IFAC-PapersOnLine, vol. 50, no. 1, pp. 14812-14817, July 2017.

[19] P. D. Ziogas, "The delta modulation technique in static PWM inverters", IEEE Trans. Ind. Appl., vol. IA-18, no. 2, pp. 199-204, 1981.

IJEW 国际工程期刊 International Journal of Engineering Works انجینیرنگ کاموں کا بین الاقوامی جرنل

International Journal of Engineering Works
ISSN-p: 2521-2419
ISSN-e: 2409-2770
Vol. 6, Issue 03, PP. 78-83, March 2019
https://www.ijew.io/

Technical Analyses of MHP ELCS; An Analysis of KPK MHP Project, Pakistan

Waqar Ahmad Dawar[1], Dr. Tanvir Ahmad[2].
[1,2]US Pakistan Center for Advance Studies in Energy, University of Engineering and Technology, Peshawar
waqardawar018@gmail.com[1], tanvir.ahmad@uetpeshawar.edu.pk[2]
Received: 14 February, Revised: 01 March, Accepted: 04 March

***Abstract*—**Energy is the basic requirement for the development of a country. Pakistan is fronting meaningful contests in the sector of energy on the way to conference the demand which is significantly increasing annually. The government of Pakistan have initiated various renewable energy projects for the provision of electrical energy particularly to the rural areas where population is less, and extension of main grid-system is not fiscally and technically practicable due to huge rate asset essential for transmission network. In electrical power system the users need uninterrupted power supply at rated frequency and voltage. Due to existence of different kinds of loads having different structure and load demand the frequency and voltage of micro hydro plant (MHP) may not be continuous. To keep these constraints in the specified boundaries appropriate control approach must be recognized for the system. Frequency is maintained by eliminating the difference among generation and load demand through Electronic load controller (ELC). ELC function is to dump extra power into dummy loads, when consumers switch their loads off, maintaining system frequency constant. The purpose of this research paper is to analyses the connected MHP ELCs in KPK via considering the case study of Ashran Valley District Swat and Tehsildar kali district Mardan to know the impacts of voltage, frequency and power factor of these MHP ELCs likewise to recommend for improvement. Comprehensive literature review was carried out to achieve these goals. The real time data was collected using the site observation, and the analyses of real time data (voltage, frequency and power factor) of MHPs ELCs are analyzed through Microsoft Excel software. This research work concludes that these MHPPs requires proper management, quality work and skillful operators to have a sustainable and reliable system for the community.

Keywords— Micro hydro system, Electronic load controller, Dummy load, Microsoft Excel

I. Introduction

Any nation that want to advance their living standards and raise their economy must have secure and sustainable energy system. Since our environment suffers from gas emission, the use of clean and renewable energy sources is one of the best solutions that would help limiting the global warming effect [1]. In a suitable location micro-hydro power is one of the most cost-effective and reliable renewable energy technologies. It has several advantages over solar and wind power, with a prominent level of predictability. Micro hydropower system is one of the most environmentally benevolent energy conversion options available. Unlike large-scale hydro power, it does not attempt to interfere significantly with river flows. Micro-hydro power plants (MHPP) are usually built on mountains to provide electricity for rural communities.

However, they are mostly isolated from national electric grid. In addition, variations of the consumed power on the load side cause deviations between the produced and the consumed power, which causes variations of both MHPP frequency and voltage outputs [2].

Thus, MHPP that work in isolated mode require the mixture of good and price moderate control system to ensure the stability of both MHPP frequency and voltage with changing load demand. MHPP is a nonlinear and non-stationary multivariable system whose characteristics vary significantly with unpredictable load on it. Generally, two main control strategies could be used to automatically control the rotational speed of the generator shaft, and thus the frequency of the voltage waveform. The turbine speed can remain constant either by acting on the gate opening position (mechanical regulation of the turbine water flow) or by using an electronic load controller (ELC).

First, triggering the gate opening position aims to produce just the necessary power according to the connected load [3]. However, this speed governor must be slow to avoid the water hammer effect, and so, it takes a considerable time to stabilize the turbine speed when a load disruption occurs. It becomes insufficient in case of large load variations [4]. Moreover, the cost of such governor is often dearer than the cost of the generator [5].

The accepted alternative to the speed governor is the ELC which maintains the speed of the set by adjusting an electrical ballast load connected to the generator terminals through a power electronic system [1,5]. Typically, the cost of the ELC is about one tenth that of the speed governor and so the economic advantage of the ELC is double, because of the lower capital cost of the governor and of the turbine. Pakistan power sector is an emerging market. For years the matter of balancing the supply and demand for electricity has remained an unsolved issue [6]. For these reasons government of KPK is deploying different projects of micro hydro power for the electrification of those rural areas where there is no access to the national grid.

The purpose of this research paper was to analyses the connected MHP ELCs in KPK via considering the case study of Ashran valley district swat and Tehsildar kali district Mardan to know the impacts of voltage, frequency and power factor of these MHP ELCs. Different site visits were conducted for the data collection of MHP ELCs.

II. Standard Techniques of ELC's

A. *Binary Load Regulation*

The dump/ballast loads are created from a swapped mixture of binary procedure of individual resistive load in binary loads regulation. A switching choice was made to attach the suitable grouping of load phases, in reply to an alteration in the user load. In transient period only the switching action happen, afterward complete "system" voltage was functional toward the novel segment of the dump loads then later harmonic were not formed through this technique in the solid states. Steady states swapping relay contains a zero-voltage switching circuit which eliminates the harmonics distortion related thru the transient switching period [7]. Solid state relay has higher prices than the TRIACS as individually it comprises navigation electronics. To gain the even adjustment, all the ballast loads must have precisely the accurate capacity. System cannot adjust evenly, and stages b/w ballast load grouping stay too big thru less number of ballast loads.

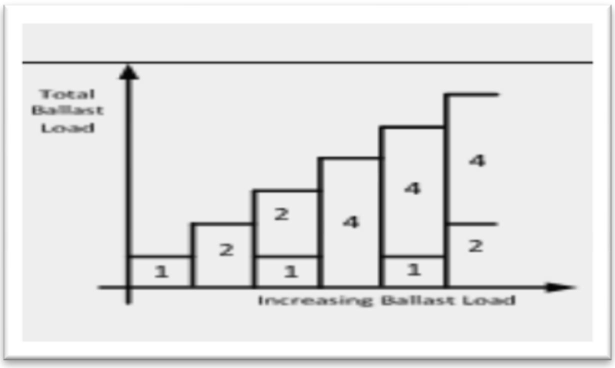

Figure.1 Principle of binary loads

The load share supported by apiece of the stages is in the proportion of "1: 2: 4: 8" and once "switched" in order, the dump load displays a stepped feature, realize figure 1. The addition of all the dump load ladders are identical to (or somewhat larger than) the esteemed production of the generator. In reply to a verdict to adjust the level of the dump load a switching order is done to choose a novel mixture of the load stages. The switching action is for a temporary period solitary, subsequently complete scheme voltage is functional toward the novel portion of the dump load and later harmonics are not formed entirely in the steady state situation.

B. *Pulse width modulation*

Pulse width modulation (PWM) is a variation method utilized to translate a communication into a pulsating indicator. The modulation method could be utilized to translate data for transmission purposes. The key use of PWM technique is to permit the control of the power provided to "electrical devices", specifically to inertial loads such as motors [8]. Pulse width modulation is usually utilized method for modifying voltage's indicator. The advanced transistors like MOSFET or IGBT was utilized by PWM, to set up a pulsation indicator. Generally, in PWM the signal is either 1 (on) or 0 (of). PWM technique utilized the thickness of pulses signals to govern the middling voltages signals (realize picture 2). Width is described as the duty cycle at the time when the signal is on. Thru changing the duty's cycles, it's out-put voltages signals are altered. Meanwhile that voltages levels are comparative towards the powers, in ELC circuit it will be monitoring the power to the ballast loads.

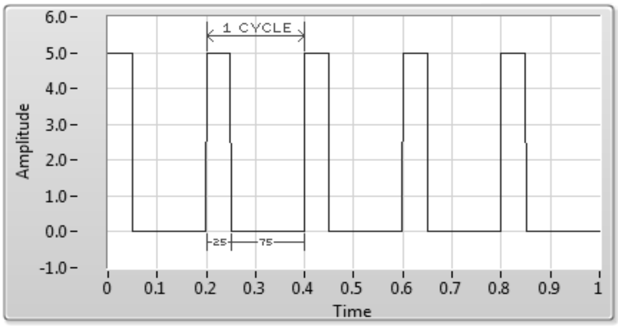

Figure.2 Principle of PWM at 25% duty cycle

For case: The generator voltage level surges, after the feeding load declines. The power "must" be abstracted to the ballast loads to preserve a continuous voltage level. By rising the duty cycle of the signal this process can be attained. The power abstracted to the ballast loads rises as the middling voltage signal rises. To deliver stability to the system the frequencies of the pulse width modulation signals must remain arranged greater than the alteration of that systems. To control advanced power transistors like MOSFET and IGBT, PWM has a benefit with a simple electronic circuit. Drawbacks of PWM consist of tall prices, reduced convenience and sensitivity of the power transistors [9].

C. *Controlled Bridge Rectifier*

To proficiently transform the fluctuating current into Direct Current (DC) bridge rectifier practices four otherwise extra diodes in a bridge circuit construction.

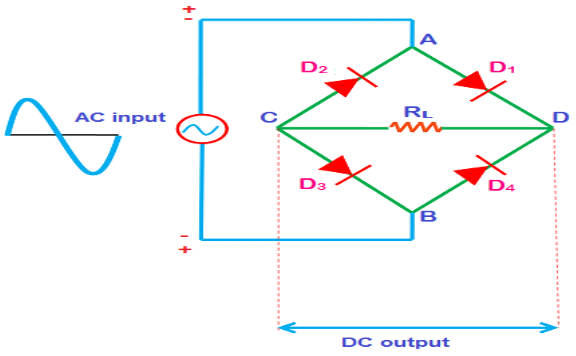

Figure.3 Controlled bridge rectifier

The construction of bridge rectifier is done through 4 diodes i.e. D4, D3, D2, D1 besides resistor load R-L [10]. These diodes are linked inside a locked circle formation to proficiently transform the fluctuating current into DC. This key benefit of tie path formation is, that we don't need luxurious centres tapped transformers, thus deducting its magnitude besides price. AC input signal is functional crossways the two ends B & A and the DC output signal is gained across the resistor load RL which is linked between the ends D & C. The diodes D1, D2, D3, D4 are organized in succession with solitary two diodes permitting electric current throughout individually half cycle. For illustration, diodes D3 and D1 are well thought-out as one couple which permits electric current throughout the +ve semi cycle while diodes D4 and D2 are well-thought-out as additional pair which permits electric current throughout the negative semi cycle of the AC input signal.

D. *Phase Angle Regulation*

The dump load includes a forever linked, solo resistible loads circuit of scale identical towards the complete loads valued out-puts of the generators. The firing angle of a power electronics switching device is regulated, such as a TRIAC due to the alteration in user load and, accordingly varying the level of the voltage nourished and the power degenerate by the dump load [11]. This method makes known to unwanted harmonics against the electrical system with all power electronic switching of this flora. The different form of the voltage waveform of the dump load is specified in below figure.

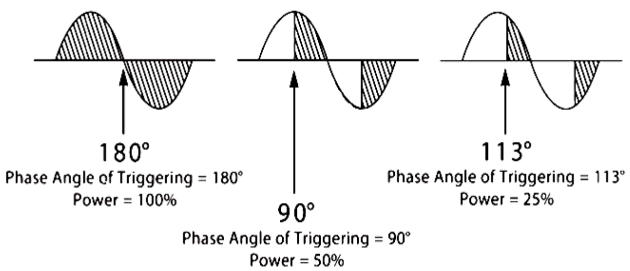

Figure.4 Phase angle control voltage-waveform

"It must be distinguished that these chopped-sine waveforms are unendingly existing for all phase angle control apart from complete dump load". The existence of the harmonics might be the reason of "overheating" of electrical apparatus linked to the generator and the system, generally responded thru the "derating" of the plant [12]. In sure cases, "high neutral currents" might be formed owing to the TRIACS switching at irregular periods in reply to disturbed loads [11].

III. METHODOLOGY

To communicate the difficulties and research questions in the way of MHP projects existing rural zones, simple approach was followed. For collecting useful information relating to such systems, different site visits were conducted to different areas in the Khyber Pakhtunkhwa province, Pakistan which includes Charsada district, Mardan district, Abbottabad district and Upper Dir District. The Tehsildar kali Mardan district was recognized for the case study to understand the influence of frequency of these MHP Electronic load controller (ELC). Using the site observation, real time data was collected, and analyses was done through Microsoft Excel software.

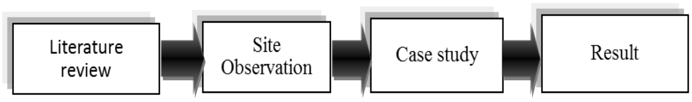

Figure. 5 Research Methodology steps

IV. RESULT AND ANALYSES

A. *Case study of Tehsildar kali and Tableeghi Markaz*

The installed capacity of Tableeghi Markaz and Tehsildar kali was 30 KW each, but the output power delivered by Tableeghi Markaz was 10 KW and 14 KW for Tehsildar kali maximum. The users linked to the Tehsildar kali MHPP ELC are currently 28, including one mosque and 27 residents. Electricity bills were collected by the concerned operator, as billing meter were installed at each user premises. Turbine belt was the main issue of the Tehsildar kali MHP ELC which cost them Rs 6500 by replacing them twice. ELC was used for the frequency control purpose of existing MHPs.

The aim of ELC was to balance the power generated through turbine and the power consumed by the user. The case study of these MHP ELC was passed out to analyses the diverse parameter of the system with the change of load. The data for the calendar year cannot altogether due to the unavailability of data storing system, so only real time data was collected available on the ELC panel screen to show the response of frequency with the load alteration.

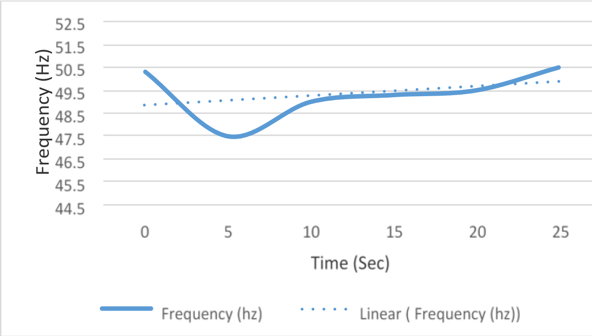

Figure. 6 Frequency response to the load variation with time

The above figure 6 shows the response of Tehsildar kali MHP frequency once load abruptly oscillates. To recover the frequency to its original state ELC use the dummy loads to balance the power generated through turbine and the power consumed by the user. ELC done the alteration by diverting the surplus power to the dummy load. The procedure of deviation was done through the thyristor switch, measured thru the ELC main panel based on the variation of frequency on the system. ELC has very fast recovery time and can handle the large load variation within 10 ms.

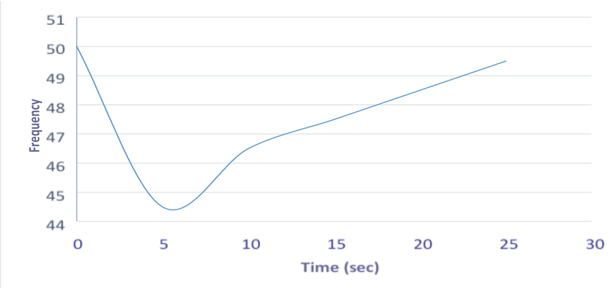

Figure. 7 Frequency variation with 20% increase in load with respect to time

The above figure 7 shown us that when 20% load is increased on the turbine, frequency of the system abruptly changes from its normal state, to control that frequency variation ELC used dummy load of water heater to reestablish the frequency to its original value. As we know that the standard frequency recovery time is 10 ms but in the above figure the situation is quite diverse and obviously seen that the frequency recapturing time is 15-20 ms because of not using the standard rating dummy load according to standard technique and use of local made turbines.

B. *ELC Technique of ballast load Tehsildar kali*

The ballast load used in Tehsildar kali MHP for ELC was water heater as given in the above figure 8, was not in good health because 3 of the resistor coil was broken due to heat, which need continuous water flow to prevent from drying and overheating.

Figure. 8 Water heater Tehsildar kali Mardan

The chances of erosion are also there because of that, heater water tank might leak, and overheating may occur. Due to all these facts ELC operation was not at their standard rating.

C. *Tableeghi Markaz ballast load*

The technique of ballast resistive loads used by Tableeghi Markaz can be seen from the below figure 9, which is against the standard procedure of ELC. First of all, these dummy resistive loads were not according to the rated capacity of MHP turbine and are local made. There are the chances of short circuit any time and the damage probabilities of apparatus as well the injury of living being is sure, because of these high resistive loads are hook with the iron metal.

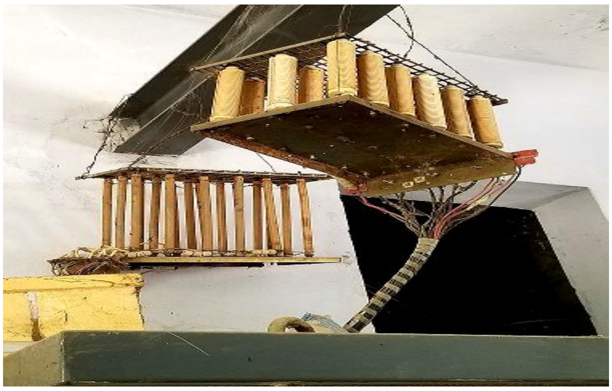

Figure. 9 Tableghi Markaz Mardan dummy resistive load

Due to all these facts ELC operation was not at their standard rating and cannot adjust the load deliberately due the derated capacity of the dummy load.

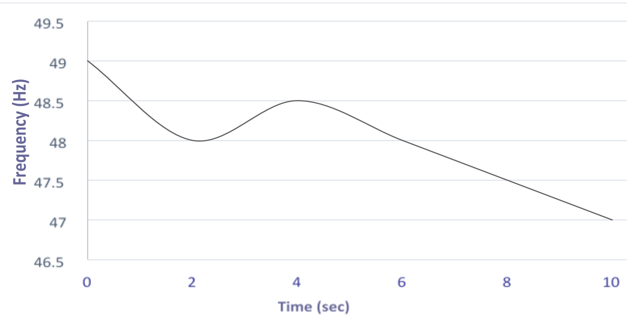

Figure. 10 Tableeghi Markaz frequency with load alteration

We can clearly see from the above figure 10 that the Mardan Tableeghi Markaz MHP frequency is unstable and undershoot with the load variation and due to the poor ELC technique with derated capacity of resistive loads, frequency does not come to its original value. The dummy resistive loads used by Mardan Tableeghi Markaz MHP is local made having no standard capacity rating, which does not adjust the surplus power deliberately.

D. *Standard dummy loads*

Two types of dummy frame have been followed as standard, closed type with wired mesh screen to defend the element from external substances and open type without screen. The heater type used is tubular air heater, which make it less maintenance requirements, longer lifetime and easy in installation comparing to water heater type. Air heater type does not need forced air convection (fan/blower), only install it in place with good air circulation for heat evacuation i.e. windows. The standards versions of ELC comes with open types ballast frame. The rated total power of the ballast normally overrated 10-30% of design turbine power in case of bigger turbine output then design and longer life time of element.

Tubular air heater is industrial standard heater which normally used on heating and drying process. Usual lifetime about 15 years and should be more in ballast load application, meanwhile it's not fully used at all time. Avoid dummy load from water splash, rain and combustible material. It should be out of reach of children and access of public. Never replace damaged dummy element with other type of dummy or distinct size of power. It might disturb the stability and safety of the plant.

CONCUSLION

The intention of this thesis was to technically analyze the installed MHP ELCs in KPK via considering the case study of Tehsildar kali district Mardan and Ashran valley district swat to understand the influences of frequency, voltage and power factor of these MHP ELCs also to endorse for enhancement. Broad literature revision was passed out to achieve these goals. The literature section offerings a summary and important matters of diverse exploration revisions for electronic load controller. SE-IG is located to be idyllic like they remain rough, low-priced and consumer kindly. IGBT is favored on thyristor because ELC built with IGBT's takes healthier voltage directive then built on thyristors. This is understood, as of the present works, for modelling ELC there are diverse key procedures. literature section defines phase by phase progress in E-L-C that delivers appropriate procedures and orientations for the scholars anticipating doing extra homework in "small hydro power generation". The below efficiency action of the system is because of the turbine design. i.e. Tehsildar kali 30 KW unit runs at about 12 KW. The mechanical gear at Tehsildar Kali MHPPs for intake gate was not operating suitably. Regular substitution of belt, bearing triggering slowdowns throughout highest demand in summertime. Standard and excellent quality machineries should be used for the consistent working of these projects. Appropriate training and knowledge should be given to the operator about the MHP ELCs components there caring and reparation.

The key benefit of PWMs iss thats its needs a simple's electronics circuit fors navigating thee switchings devices. tThe drawback iss thee highs dissipations inn thee controllers meanwhile thee voltages of generator must bee rectifieds first earlier its cann goo too thee powers transistors itselff. Therefore, theree iss requirement forr as big heats sinks. Binarys load regulation has numerous drawbacks suchs ass thee numbers off ballast loadss respectively through itss networks, cables besides switchings devices. To gain the even adjustment, all the ballast loads must have precisely the accurate capacity. System cannot adjust evenly, and stages b/w ballast load grouping stay too big thru less number of ballast loads.

In summary, together the controllers attain equally regulation and voltage control. Grounded onn thee availedd outcomes, thee binarys load scheme iss aa healthier technique forr executing thee inductions generators controllers. Level thru thee complication plus cost, itt iss nott exaggerated bye thee flora off thee loads linked, thee voltages settles down backs too itss references voltages withh an alteration inn loads plus waveforms distortions iss nots produceds. Noo harmonics filters iss essential forr binarys controllerss then may remain needed byy as purelys PWMs controllers.

ACKNOWLEDGMENT

I would adore to express my heartfelt appreciation to my supervisor professor Dr. Tanvir Ahmad, first for bestowing to supervise my project, as well for his endless assistance throughout the research stage. I am appreciative for his leadership, motivation besides wisdom also for being not solitary my advisor but too the inspiration behindhand my research.

I am grateful to USPCAS-E, UET Peshawar for providing me an occasion to achieve my master's degree. I am thankful to the USAID supported scheme of advanced schooling "US Pakistan Center for Advanced Studies in Energy" for the assistance in conduction of research. I am grateful to the Sarhad Rural Support Program (SRSP) and Pakhtunkhwa Energy Development Organization (PEDO) for their benevolent aid.

REFERENCES

[1] Salhi I, et al. Modeling and regulation of a micro hydroelectric power plant. In: IEEE international symposium on industrial electronics (ISIE'08). Cambridge, UK, July 2008. p: 1639–44.J. Clerk Maxwell, A

Treatise on Electricity and Magnetism, 3rd ed., vol. 2. Oxford: Clarendon, 1892, pp.68–73.

[2] Laboratory of Electric Systems and Telecommunications, Cadi Ayyad University, BP 549, Av Abdel Karim Elkhattabi, Gueliz, Marrakesh, Morocco b CReSTIC, Reims University, 9, rue de Québec B.P. 396, F-10026 Troyes cedex, FranceK. Elissa, "Title of paper if known," unpublished.

[3] Hanmandlu M et al. Proposing a new advanced control technique for micro hydro power plants. Electric Power Energy Syst 2008;30:272–82.

[4] Chennani M et al. Study of the regulation of a micro hydroelectric power plant prototype. Int Sci J Alternative Energy Ecol 2008;5(6):79–84.

[5] Henderson DS. An advanced electronic load governor for control of Micro hydroelectric power generation. IEEE Trans Energy Convers 1998;13(3):300–4.

[6] Junaid Riaz, Majid Baseer., Technical Challenges and Issues Faced During the Installation of Micro Hydro Power Plants in Pakistan.

[7] International Journal of Electrical, Electronics and Data Communication, ISSN: 2320-2084 Volume-3, Issue-6, June-2015, 200.

[8] R. Armstrong-Evans, "EVANS Electronic load governing", Evans Engineering, 2016. [Online]. Available: http://evansengineering.co.uk/controlsystems.cfm. [Accessed: 23- Jun-2016].

[9] Jan Portegijs. The 'humming bird' electronic load controller/induction generator controller. http : //microhydropower.net/mhp group/portegijs/humbird/humb main.html, 2012.

[10] www.elprocus.com/bridge-rectifier-circuit-theory-with-working-operation/.

[11] "G.P. Electronic Load Controllers for Small Hydro", G.P. Electronics.

[12] BARNES, R., 1989, lEE Power Engineering Journal, Vol 1 No k 11-15.

Waqar Ahmad Dawar: The author was born in KPK province, District North Waziristan Agency, Pakistan in the year of 1991. He did his matriculation from Islamia collegiate school, Peshawar, Pakistan. Afterwards, He pursued his Higher secondary education in Pre-Engineering from Government College Peshawar, Pakistan. After that He did his bachelor's Degree in Electrical Power Engineering from COMSATS Abbottabad, Pakistan. Currently, He is enrolled in MS, Electrical Energy System Engineering from USPCAS-E UET Peshawar, Pakistan.

The author started his professional career as an Internee at Rawat Laboratories, Islamabad. Later, he joined Faisalabad Electric Supply Company, as a Trainee Engineer. Currently working as a Research Associate in a joint research program on distributed energy technologies with social science and hydrological research with Arizona State University, USA.

IJEW 国际工程期刊 International Journal of Engineering Works

International Journal of Engineering Works
ISSN-p: 2521-2419
ISSN-e: 2409-2770
Vol. 6, Issue 03, PP. 84-89, March 2019
https://www.ijew.io/

Modeling of Cascaded H-Bridge Multi-level Inverter Having Low Total Harmonic Distortion by using Equal Phase Distribution Method

Muhammad Salman[1], Abdul Basit[2], Aemal Ahmad[3], Zeeshan Saeed Shah[4], Kamran Alam[5]
[1,2,3,4,5]US Pakistan Center for Advanced Studies in Energy, University of Engineering and Technology Peshawar, Pakistan
12ktete0236@uetpeshawar.edu.pk[1], abdul.basit@uetpeshawar.edu.pk[2], aemalahmad@hotmail.com[3], zshah1@asu.edu[4], kalam3@asu.edu[5]
Received: 12 February, Revised: 01 March, Accepted: 05 March

***Abstract*—** Multi-level inverters' popularity over traditional inverters can be attributed to its low total harmonic distortion. Multi-level inverter is used both for high and low power applications. This study uses Equal phase method to analyze the total Harmonic distortion of 3, 5, 7 and 9 levels by using Cascaded H-Bridge configuration for such analysis. The total harmonic distortions of three, five, seven and nine levels are analyzed, studied and finally their output is compared through fast Fourier transform. Results are acquired by simulating Cascaded H-Bridge Multi-level inverter with MATLAB/Simulink. Simulation results reveal that total Harmonics Distortion reduces as voltage level is increased. Total harmonic distortion for 3, 5, 7 and 9 levels is 41.42, 39.46, 39.40 and 22.50 percent respectively.

***Keywords*—** Cascaded H-Bridge, Equal Phase method, MATLAB/Simulink, Switching Angle, Total Harmonic distortion (THD).

I. INTRODUCTION

Power electronics interface is needed to synchronize the power of renewable energy sources with that of grid in order to meet the requirement of grid integration. Different kind of grid tied inverters solves the issue of synchronization each associated with certain level of THD. Multi-level inverter (MLI) proves a good candidate with the ability to harness high quality waveform with low THD. The output waveform of multilevel inverter is much better because of multiple voltage levels if compare to two levels inverter which has such distortion comparatively higher. Also, there is no need of output filter for removing these distortions. With low switching frequency and absence of large output filter it is advantageous in minimizing cost, complexity and power losses. MLI uses many different topologies: Diode clamped MLI, flying capacitor MLI, H-Bridge MLI [1]. Total harmonic distortion can be reduced by varying pulse widths and phase delays of any level of inverter [1]. Total harmonic distortion of single phase 3-level and 5-level is analyzed by varying loads such as R-loads and RL loads. Both type of power i.e. active and reactive power is calculated and compared [2].

Multi-level inverter is better in terms of electromagnetic compatibility, low switching losses and high voltage capability. In recent years MLI got much higher consideration [3]. Multi-level inverter synthesizes voltage from different dc sources and separates them in case of cascaded H-bridge.

Three different topologies presented here: diode clamped, flying capacitor and cascaded H-Bridge; their functions, features, applications, configurations, operating principles and performances are discussed [3]. Multilevel inverter besides reducing harmonics and EMI also decreases the dv/dt stress on switches without the use of high frequency switching and thus lowering switching loses [4].

When these three configurations are compared, harmonic content in cascaded H-Bridge multilevel inverter is much lower as compared to diode clamped and flying capacitor, also the output waveform in cascaded H-Bridge is much better and more sinusoidal than the other two topologies under discussions. Harmonic contents decreases by increasing the output levels [5].

Different methods can be used to calculate the switching angles of multilevel inverter. Output voltage depends on firing of switching angles. For m level 2(m-1) switching angles are needed [5].

Devising of line voltage THD of MLI is proposed by analytical algebraic method with uneven dc generators. The conventional technique works in more of an approximate fashion, ignoring high order harmonics and formulating the THD with limited number of low order harmonics. Nine equations of a line voltage for five level inverters are presented to formulate a line THD and consider harmonics up to 10^6th order. The proposed model is based on speed, accuracy and simplicity and found accurate [6].

A model of three phase 5 level hybrid inverter with three cascaded H-Bridges and different DC sources is proposed [1]. The control signal is given through digital technique by FPGA controller. The prototype has been tested with different types of load such as 18W fluorescent lamp, induction motor of 1 HP and RL load. The results are obtained in terms of total harmonic distortion. Results show that THD voltage is between 15.6% and 18.3% for output line-line and phase voltages having 5 levels, the output waveform of phase current is close to sinusoidal such that its THD current is between 2.7% and 4.2%. Nine levels inverter are simulated by using cascaded H-Bridge configuration and grid simulator. Sampling method of pulse width modulation is validated in this paper [7]. Two carrier frequencies are chosen 600 Hz and 2 kHz for experimental work.

A 13-level inverter is simulated with equal distribution of switching angle arrangement. As the name suggest it has 13 levels of output and consist of three cascaded H-Bridges per phase [10]. The proposed method has advantage of equal load distribution on each transistor thus preventing overheating.

By using different level of MLI, reduction in THD is studied in this paper. In second section of paper methodology has been discussed for different configurations in different levels of inverter. Equal phase method is used for measuring switching angles. In third section of paper simulation results are presented. Three, five, seven and nine levels inverter is simulated and results are gathered for discussions. In fourth section paper is concluded by comparing the THD of 3, 5, 7 and 9 level of inverter based on total harmonic distortion.

II. METHADOLOGY

Application of Multi-level inverter lies high voltage direct current. HVDC can be converter through MLI. Two level inverter has limitations for high power and high voltage applications. We cannot rely further on conventional two-level inverter. We have to switch to multi-level inverter for these applications. Two different electrically operated schemes can be connected by using MLI. The most appropriate topology is cascaded H-Bridge which allows to add up the voltages. The switches current and voltage stresses can be minimized by using this topology.

Total harmonic distortion has inversely relation with the voltage levels. Increasing voltage levels results in large number of components which hence increases the price and complexity but we have to compromise between smooth waveform and price [8]. Table 1 shows the number of switches and components used in different topologies of multi-level inverter [9].

Three level inverter has one H-Bridge and four main switches with a freewheeling diode. Five level inverter has two H-Bridges. Seven level inverter has three H-Bridges. Nine level inverter has four H-Bridges. We can synthesize three output levels in three level inverters as V, 0. –V. Five level inverter can synthesize five output voltage levels as shown in fig 1. Seven level inverter has seven output voltage levels i.e. -3V, -2V, -V, 0, V, 2V, 3V. Output of nine level inverter is shown in fig 2.

Fast Fourier transform is used for analyzing the total harmonic distortion. Cascaded H-Bridge has been used as it has less number of switches and also it does not require any clamping devices like capacitor and diodes [1].

Firing angles are formulated through Equal phase method. Switches are given a specific firing angles with a known pulse width. We need 2(m-1) switching angles for m level. There is increase of of power by (m-1) time of 2-level inverter in multi-level inverter [2].

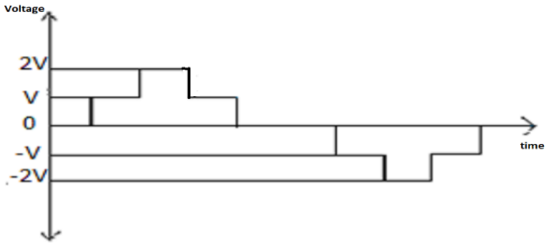

Figure 1. Output waveform of five level inverter

TABLE I. COMPARISON OF COMPONENTS OF 7 LEVEL INVERTER

Type of multilevel inverter	**Number of switches**	**Clamping diodes**	**Flying Capacitors**
Flying capacitor	12	-	15
Diode clamped	12	30	-
Cascaded H-Bridge	12	-	-

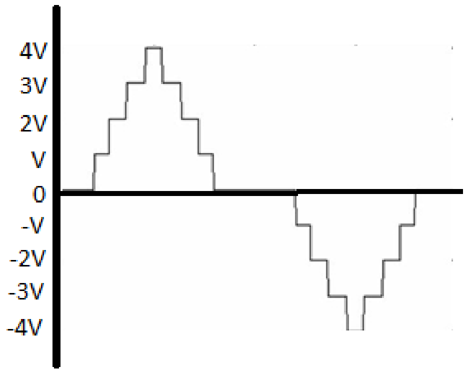

Figure 2. Output waveform of Nine level inverter

Main switching angles in the first quarter ( ) are

$$a_1,\ a_2, a_3,\cdots\cdots \tag{1}$$

In second quarter switching angles ( ) are

$$a_{(m+1/2)} = \pi - a_{\left(m-\frac{1}{2}\right)}, \pi - a_{\left(m-\frac{2}{2}\right)}, \cdots\cdots, \pi \tag{2}$$

Switching angles in the third quarter ( ) are

$$a_m = \pi + a_1, \pi + a_2, \cdots\cdots, \pi + a \tag{3}$$

Switching angles in the fourth quarter ( ) are

$$a_{(3m-1/2)} = 2\pi - a_{\left(m-\frac{1}{2}\right)}, \cdots\cdots, 2\pi - a_1 \tag{4}$$

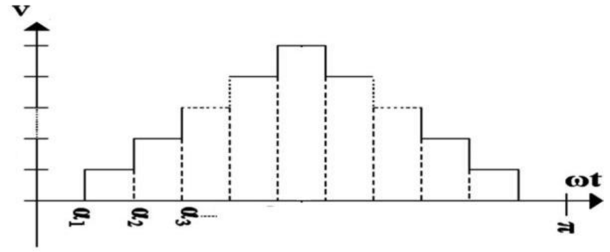

Figure 3. Multilevel output waveform

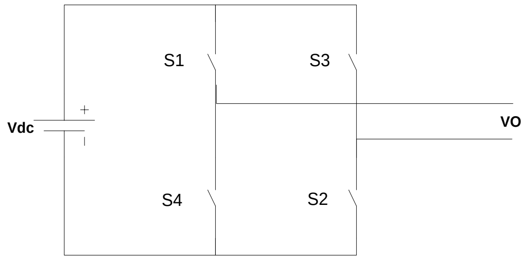

Figure 4. Simulink model of three level H-Bridge inverter

A. *Equal Phase Method:*

Equal phase distribution has been used for obtaining the switching angles. By using equal distribution method, the problem of unbalance loading in cascaded H-Bridge configuration is solved which increases the life time and prevent the switches from overheating. The main switching angle is obtained from:

$$a_i = i \times 180/m \qquad (5)$$

Where m is the level of output voltage and i = 1, 2, 3…, m-1/2

III. SIMULATION RESULTS

3, 5, 7 & 9 level inverter is simulated using MATLAB/Simulink. The firing angles for switches correspond to a particular triggering pulse are provided using equal phase method from timing table. Total harmonic distortion is analyzed based on these simulation results.

A. *Three Level Inverter*

Equal phase method is used for Switching. In Fig 4 three level inverter has been shown by using four mosfets as switches to form an H-Bridge configuration. Output waveform can be seen in Figure 5. Total harmonic distortion has been analyzed here by using fast Fourier transform analysis and results are compared. In Fig 6 percentage of THD is shown, clearly limiting it to 41.42%, for equal phase method. In the positive half cycle S1 & S2 are closed keeping S3 & S4 open at the same time and thus providing a positive voltage at output. In the negative half cycle S1 & S2 are open to provide negative voltage at output whereas S3 & S4 are closed. Triggering pulses are provided from table 2 where control of multilevel inverter is given showing how to create a PWM signal for switches to operate and synthesize desirable output.

TABLE II. TIMING DIAGRAM OF THREE LEVEL INVERTER

Phase	0	V	0	-V	0
Switching Angle	60	120	240	300	360
Phase Delay	0.0033	0.0066	0.0133	0.0166	0.02
S1 & S2		30%			
S3 & S4				30%	

Fourier expansion of output voltage of squared natured waveform has three components: fundamental component, desired component and harmonic component. Magnitude of fundamental component depends directly on input dc voltage.

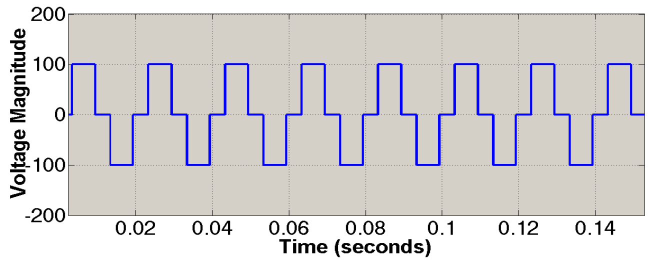

Figure 5. Output waveform of three level inverter

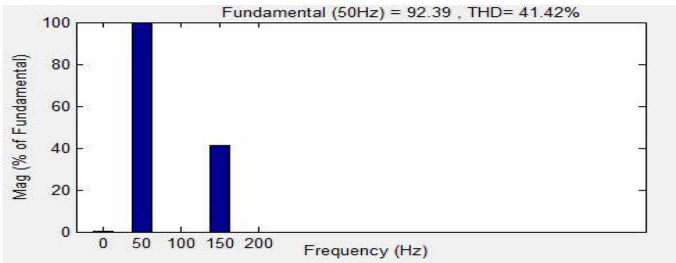

Figure 6. Total harmonic distortion percentage of three level inverter

B. *Five Level Inverter*

For five levels inverter, there are two bridges connected in series to make two H-Bridges interconnection having two separate DC sources. Equal phase method has been used for switching angles calculation. Eight mosfets are used to form two H-Bridge configuration as can be seen in Fig 8. THD as Fig 9 indicates is 39.46%.

For positive cycles S1, S2 & S6 are closed giving +V voltage. In order to get 2V, switch S5 will be closed with other switches. For negative switches S3, S7 & S8 are closed which gives –V, whereas for getting -2V switch S4 will be operated with other switches. Table 3 shows the timing table with firing angles and phase delays given.

Magnitude of fundamental component is inexorable, leaving no control to user, though constant, throughout the cycles. Magnitude of harmonic component depends in inverse fashion on order of harmonics. For square waveform results in odd harmonics.

TABLE III. TIMING TABLE OF FIVE LEVEL INVERTER

Phase	0	V	2V	V	0	-V	-2V	-V	0
Switching angles	36	72	108	144	216	252	288	324	380
Phase delay	0.002	0.004	0.006	0.008	0.012	0.014	0.016	0.018	0.02
S1, S2 & S6			30%						
S5			10%						
S3, S7 & S8							30%		
S4							10%		

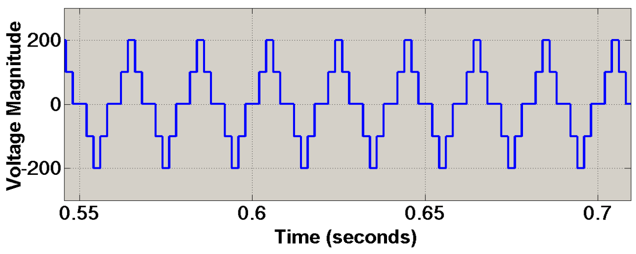

Figure 7. Output waveform of five level inverter

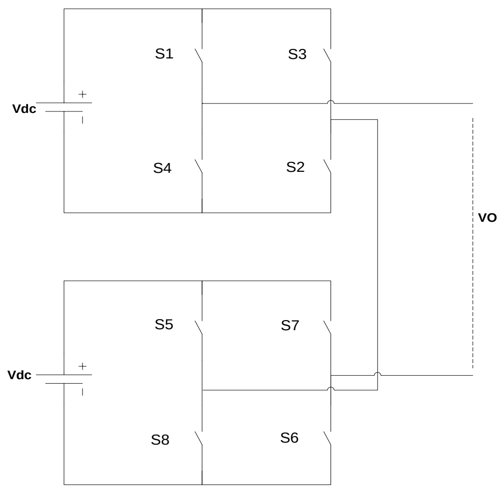

Figure 8. Simulink model of five level inverter

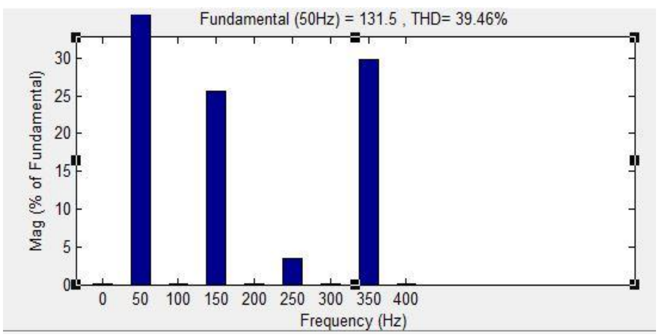

Figure 9. Total harmonic distortion percentage of five level

C. Seven Level Inverter

Three H-Bridges are connected with three distinct DC generating units in series in case of seven level inverter. Equal phase method is used to calculate bridges switching angles and fast Fourier transform is used to measure THD. Twelve mosfets are used as a switch with triggering pulses generated by PWM generator in seven level cascaded H-Bridge configuration.

As discussed earlier, triggering pulses are given from PWM generator. Four switches S1, S2, S6 and S10 are used to operates for getting +V while other four switches S3, S7, S11 and S12 are used to operates for -V. Similarly, remaining switches are used for both positive and negative voltages like S9 for 2V, S5 for 3V, S4 for -2V and S8 for getting -3V. Fig 10 shows output waveform of 7 level inverter and THD is 26.78% shown in fig 11.

Phase delays and firing angles given to each switch is shown in table 4.

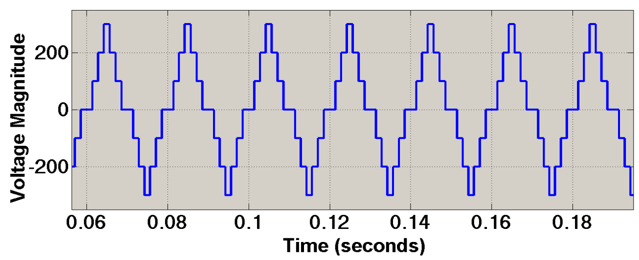

Figure 10. Output waveform of seven level inverter

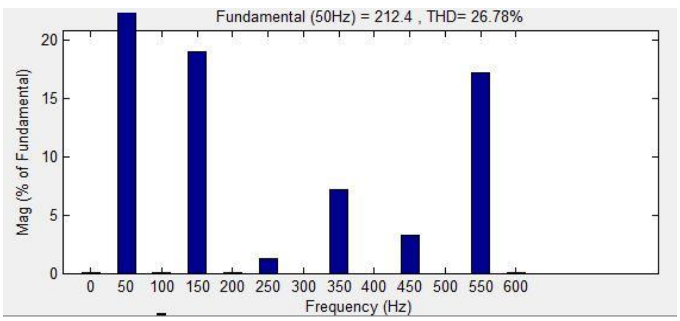

Figure 11. Total harmonic distortion percentage of seven level

TABLE IV. TIMING TABLE OF SEVEN LEVEL INVERTER

Phase	**0**	**V**	**2V**	**3V**	**2V**	**V**	**0**	**-V**	**-2V**	**-3V**	**-2V**	**-V**	**0**
Switching angles	25.71	51.42	77.14	102.86	128.58	154.29	205.71	231.42	257.14	282.86	308.58	334.29	360
Phase Delay	0.0014	0.0028	0.0042	0.0056	0.0071	0.0085	0.0114	0.0128	0.0142	0.0157	0.0171	0.0185	0.02
S1, S2, S6 & S10				35.70%									
S9				21.42%									
S5				7.14%									
S3,S7, S11&S12										35.70%			
S4										21.452%			
S8										7.14%			

TABLE V. TIMING TABLE OF NINE LEVEL INVERTER

Phase	0	V	2V	3V	4V	3V	2V	V	0	-V	-2V	-3V	-4V	-3V	-2V	-V	0
Switching angles	20	40	60	80	100	120	140	160	200	220	240	260	280	300	320	340	360
Phase delay	0.0011	0.0022	0.0033	0.0044	0.0055	0.0066	0.0077	0.0088	0.011	0.012	0.013	0.014	0.015	0.016	0.017	0.018	0.02
S1,S2,S6,S12& S14					38.88%												
S13					27.77%												
S9					16.66%												
S5					5.55												
S3,S7,S11, S15&S16													38.88%				
S4													27.77%				
S8													16.66%				
S12													5.55				

D. Nine Level Inverter

In this type of inverter, 4 H-Bridges connected in series with 4 separate DC generating units. Again, equal phase method is used to calculate switching angles. Fig 12 shows output waveform of nine level. From figure 13, we can see that Total harmonic distortion should be less than the seven-level inverter.

S1, S2, S6 & S14 are closed for positive voltage switches which gives +V, however, other switches are open. Similarly, S3, S7, S11, S15 and S16 are closed for negative cycle which gives –V. Switch 13 is closed for getting 2V. Control of nine level inverter is shown in table 5.

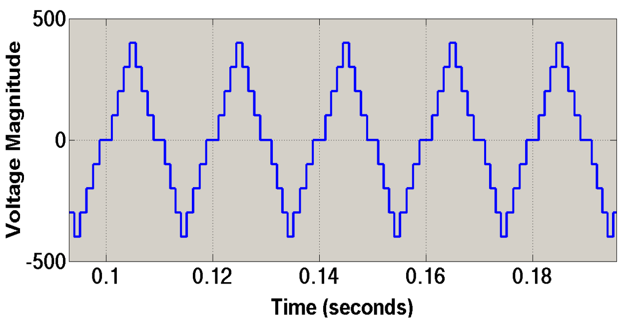

Figure 12. Output waveform of nine level inverter

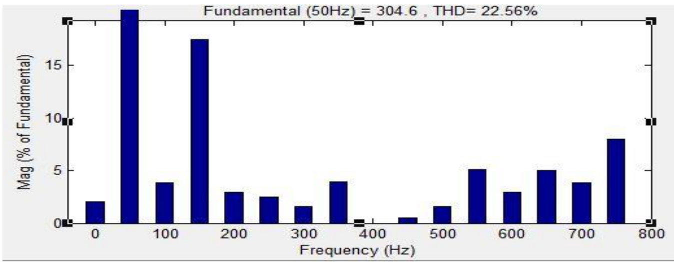

Figure 13. Total harmonic distortion percentage of nine level

TABLE VI. COMPARISON TABLE OF TOTAL HARMONIC DISTORTION

Total Harmonic Distortion percentage comparison of different level of inverter by Equal Phase Method		
S.NO	***Levels of Inverter***	***THD %***
1	3 level	41.42
2	5 level	39.46
3	7 level	26.78
4	9 level	22.56

IV. CONCLUSIONS

In this paper it is concluded that with the increases in the levels of output voltages the output waveform gets smoother and more sinusoidal. It is observed from the above results that with the increase of levels total harmonic distortion reduces.

Total harmonic distortion has inverse relation with number of levels of output voltage as shown in Table VII.

Cascaded H-Bridge configuration is more feasible to implement as compared to ‘diode clamped’ and ‘flying capacitor’ because of few numbers of components and reduced complexity.

Results show that the total harmonic distortion in 3, 5, 7 and 9 level inverters decrease as the number of levels increase. Both Harmonics and dv/dt stresses reduce.

ACKNOWLEDGMENT

I am thankful to the faculty of US Pakistan Center for advanced studies in Energy for guidance and USAID for the support.

REFERENCES

[1] Thongprasri, P. "A 5-level three-phase cascaded hybrid multilevel inverter." *International Journal of Computer and Electrical Engineering* 3.6 (2011): 789.

[2] Singh, Gurcharan, and Vijay Kumar Garg. "THD analysis of cascaded H-bridge multi-level inverter." *Signal Processing, Computing and Control (ISPCC), 2017 4th International Conference on*. IEEE, 2017.

[3] Gaikwad, Asha, and Pallavi Appaso Arbune. "Study of cascaded H-Bridge multilevel inverter." *Automatic Control and Dynamic Optimization Techniques (ICACDOT), International Conference on*. IEEE, 2016.

[4] Karnik, Neha, Deepshikha Singla, and P. R. Sharma. "Comparative analysis of harmonic reduction in multilevel inverter." *Power India Conference, 2012 IEEE Fifth*. IEEE, 2012.

[5] Jalakanuru, Nageswara Rao, and Meseret Yenesew Kiber. "Switching Angle Calculation By EP, HEP, HH And FF Methods For Modified 11-Level Cascade H-Bridge Multilevel Inverter."

[6] Singla, Deepshikha, P. R. Sharma, and Narender Hooda. "INTERNATIONAL JOURNAL OF ENGINEERING SCIENCES & MANAGEMENT." Int. J. of Engg. Sci. & Mgmt.(IJESM) 1.1 (2011): 64-76.

[7] Leonard, J., et al. "Experimental PWM method validation of a 9-level 4.16 kV series connected H-bridge grid simulator." *Power and Energy Conference at Illinois (PECI), 2016 IEEE*. IEEE, 2016.

[8] Farokhnia, Naeem, et al. "Calculating the formula of line-voltage THD in multilevel inverter with unequal DC sources." *IEEE Transactions on Industrial Electronics* 58.8 (2011): 3359-3372.

[9] Lai, Jih-Sheng, and Fang Zheng Peng. "Multilevel converters-a new breed of power converters." *Industry Applications Conference, 1995. Thirtieth IAS Annual Meeting, IAS'95., Conference Record of the 1995 IEEE*. Vol. 3. IEEE, 1995.

[10] Tapuchi, Saad, et al. "Equal Switching Distribution Method for Multi-Level Cascaded Inverters." *Energy and Power Engineering* 5.09 (2013): 560

国际工程期刊
International Journal of Engineering Works
انجینئرنگ کاموں کا بین الاقوامی جرنل

International Journal of Engineering Works
ISSN-p: 2521-2419
ISSN-e: 2409-2770
Vol. 6, Issue 03, PP. 90-93, March 2019
https://www.ijew.io/

Efficiency of Silver Nanoparticles in third Generation Solar Cells

Misbah Faiz[1], Engr. Dr. Adnan Daud Khan[2]
[1,2]U.S.Pakistan Center for Advanced Studies in Energy, University of Engineering and Technology, Peshawar.
misbah_faiz@hotmail.com[1], adnan.daud@uetpeshawar.edu.pk[2]
Received: 21 February, Revised: 01 March, Accepted: 06 March

Abstract— Immense energy is required for the production of first generation solar cells and they also tend to be rigid. There are lower efficiencies of the second generation solar cells than the first generation solar cells. On the other hand, the durability and efficiency of the third generation solar cells is more than the first generation solart cells. Moreover, the third generation solar cells are not available commercially and this area of solar cells requires more research and development. The current research works makes use of silver nanoparticles to enhance the efficiency of third generation solar cells. Silver nanoparticles were first made and then the solar cells were fabricated. Titanium and platinum electrodes were used. The titanium electrode was immersed in the silver nanocluster solution for 12 hours after which the electrodes were then clipped together. Solar simulator was used in the research work for testing the efficiency of the solar cells. The efficiency was calculated to be 3.46%. The results of the research work suggest that silver nanoparticles can essentially enhance the efficiency of third generation solar cells.

Keywords— Nanoparticles, solar cells, third generation, silver nanoparticles, dye sensitized solar cells.

I. Introduction

As there is economic growth, there is also an increase in the demand of energy. The world is highly dependent on the fossil fuels (86.4%) [1] and this has enhanced the emission of the greenhouse gases. Innovation and creativity is required for solving the problem of climate change. Renewable energy sources need to be developed to reduce the dependence on the fossil fuels.

There has been immense development of the environmental issues associated with the fossil fuels, therefore, there have been increased research and development in the alternative resources of power. One of this is to convert the sunlight into useable power source through the photovoltaic cells. The greatest potential in the renewable energy has been shown by solar energy [3]. In one hour, 6.12 x 10^17 KJ of solar energy hits the earth [3]. Therefore, we can see the abundance of this energy resource and it has gained the eyes of the researchers as a huge area of interest. The real challenge is to harness the solar energy to its full potential and then distributing the energy to the needed areas. Photovoltaic makes use of semiconductor materials and converts sunlight into electricity. For this purpose, usually silicon-based p-n junctions are used [4]. However, these tend to have high cost and the conversion efficiency is only 27% that too in ideal conditions [5]. On the other hand, these also have low operation cost and are highly reliable.

The photovoltaic technology of crystalline silicon constitutes the first-generation solar cells. The advance in the technology of thin film and amorphous silicon are classified under the second-generation solar cells. Lastly, organic solar cell, quantum dots, and organic dyes are classified as the third-generation solar cells. The efficiency of these cells has been increasing with time [6].

Third generation solar cells make use of small molecules, polymers or nanoparticles. Research is also undergoing on the perovskite solar cells and quantum dots. These have huge potential and have shown record efficiencies of 20% [2]. As a result, experiments are being performed on the third-generation solar cells and various materials are being used for testing their efficiency.

An emerging family of model compounds include monodisperse thiolate protected metal nanoclusters which are also known as the nanoclusters [2]. Researchers have been engaged in profound studies due to the discrete size and well-denned structures of the nanoclusters. This has enabled the researchers to study the physical and chemical properties of the nanoclusters in detail. Favorable properties of the silver nanoclusters can be used for the light harvesting applications. The current research work makes use of silver nanoclusters to test their efficiency in the third-generation solar cells. Silicon based solar cells are being used for commercial purposes as they have the characteristics of longevity and durability. The performance of the first-generation solar cells is usually 15-20% [2]. These solar cells have a good performance and the stability of these cells is also high. However, the first-generation solar cells require immense energy for their production and are also rigid. Moreover, third generation solar cells are more durable and efficient than the first-generation solar cells. On the other hand, the third-generation solar cells are not commercially available in the market as they are in the research and development phase and more research is required in this field. Moreover, third generation solar cells are currently expensive to be made commercially available. Furthermore, there is also a dire need to reduce the cost and test their efficiency to make them a viable option for the masses.

The objective of the research study is to produce Ag44(SR)30 and to test efficiency of silver nanoparticles in third generation solar cells.

II. LITERATURE REVIEW

The structural characterization in full have only been characterized for Silver thiolate nanoclusters [7]. There have been various reports of silver thiolate nanoclusters, however, these tend to be unstable and are polydisperse. Silver nanoclusters are of great importance as they have rare and attractive properties related to optical. These include various absorption peaks and a wide range of wavelengths are covered by these i.e. 350-950nm. These properties help in providing a material for light harvesting photovoltaics. However, the previous studies have reported nanoclusters that are prone to the oxidation which is a drawback of the previous studies [8]. The emerging model compounds include atomically monodisperse thiolate and they are considered one of the most important class of thiolates. These have well defined structures and the size is discrete which has enabled the researchers to envision a lot of researcher and engage then in studies. The advantageous physical properties include magnetism, nature of the interface of thiol-metal and chirality [9]. The most significant factor of the nanoclusters are the macroscopic sized crystals.

A great number of gold nanoclusters have been reported so far [10]. However, silver nanoclusters have not been explored greatly. [11] reports nitro group as the anchoring groups for organic dyes. The nitro group was designed, and synthesized in the research work. Furthermore, the research study also applies nitro group in the dye sensitized solar cells. As the voltage was reversed, an unusual change in the color was reported.

Thiolate-protected noble metal molecular nanoparticles have been used in the research study of [12]. These are a promising class for the nanomaterials. However, the different applications have not been materialized to the full extent. Thiolate protected noble nanoparticles have not been materialized to the full extent as the ligand exchange strategies do not widely exist. Thiolate had been used in the research study for preserving the nature of the particles and the native ligands have been replaced which contain various functional groups. Therefore, smooth thin films were created with the help of the research study and therefore creating pathway for the solution processed devices and their integration.

[12] report synthesis of the thiol-protected silver nanoclusters as well. The nanoclusters tend to be highly stable in this manner and the research reports highly stable nanoclusters as compared to the previous studies. Such nanoclusters are produced that are stable for at least 9 months under the room temperature and the degradation in these 9 months is very less. Mass spectrometry was used and ultracentrifugation was used in the research work. Spectrum charge state nanoclusters were produced in the research study and there are various unique features in the absorption spectrum. The research study also identifies the protocol to transfer the nanoclusters. Solid state films were fabricated in the research work of [Ag44(SR)30]m. The distinct features were retained in the research study. X-ray diffraction was used in the research work to study the films and photoelectron spectroscopy was also used for the investigation of the atomic composition, structure of the valance band and crystallinity. The pathway to the crystallization of [Ag44(SR)30]m is paved in the research study.

III. FABRICATION OF SILVER NANOPARTICLE BASED SOLAR CELL

5,5’ -dithiobis (2-nitrobenzoic acid) (DTNBA) was stirred with Sodium hydroxide (NaOH) aqueous solution. DTNBA amount taken for the experiment was 9.91mg and 25mmol. Amount of NaOH used in the experiment was 20mL and 1 M of NaOH aqueous solution. The solution was stirred, the orangish solution turned to dark yellow which indicated the disulfide bond yielding cleavage to MNBA i.e. 5 mercapto-2-nitrobenzoic. The MNBA solution was then added with AgNO3. 8.5mg, 50mmol and 5mL of AgNO3 was taken. As they were mixed, the color turned to greenish yellow which indicated that Ag-S complex was formed. For reduction of the complex, NaBH4 solutions was taken. The amount of NaBH4 was 1mg, 2mL. The color changed to dark brown and slowly and gradually it further changed to dark red. The color changed to dark red after 6 hours of stirring. Precipitation was performed to purify the clusters with methanol. Centrifugation was performed at 9000 rpm. The process was repeated 4 times till the supernatant turned colorless. Fig. 1 shows the spectrophotometer plot of the silver nanoparticles. The figure presents the absorbance (Y-axis) and wavelength (x-axis). The four peaks in the graph shows the presence of silver nanoparticles.

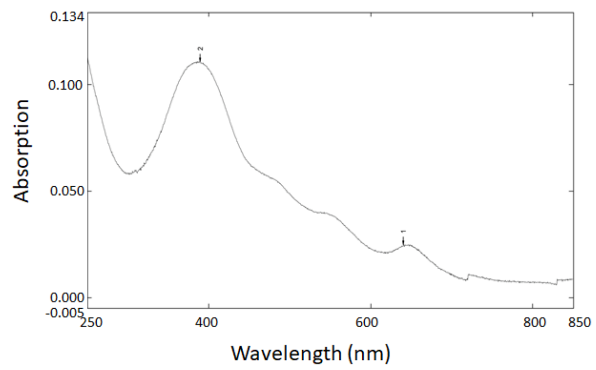

Figure 1. Spectrophotometer plot

Fig. 2 represents the solar cell area used in the research. It is necessary to sensitize titanium dioxide as it does not absorb visible light which is needed for the solar cells. The titanium dioxide was sensitized by immersing it in silver nanoclusters for 12 hours. The titania electrode, after taking it out from the silver nanoclusters, was dried with the help of a blowdryer.

Multimeter was used to identify the conductive side of the TCO glass plates. TCO glass plates tend to be conductive only on one side. By placing the probes of the multimeter on the glass plates helped to determine the conductive side. Pre-made

Titania electrodes were ordered. Firing process was run before the usage of the electrodes. This ensured to remove any moisture from the ambient air.

Titanium dioxide does not absorb the visible light therefore, it is necessary to sensitize the titanium dioxide which is a white semiconductor. The titania electrode was stained in silver nanoclusters for 12 hours. The titania electrode had titania paste deposited on the electrode. After that, the electrode was removed and rinsed with the help of ethanol. The rinsing process was not mixed with the stained solution so that the solution can be used again. Gasket is put on both the electrodes. Iron is applied on the gasket sealing so it melts.

The platinum electrode and the titania electrode's active sides are put together. The stained titania face the platinum side. The electrodes were sealed together and the electrolyte was injected via the hole that is drilled in the cathode. This approach gives linger lasting solar cells than the open cell approach. The electrodes are sealed together with the help of a gasket. The electrodes were put in such a manner that there is room for electrical contacts. The gap between the electrodes is filled with an electrolyte. The electrolyte used is Spirometal. Complete filling is performed with the help of observation and examination. Most of the cavity is filled with electrolyte. Excess electrolyte is wiped off and the glass is cleaned. After filling the electrolyte, the hole is sealed with the help of a sealing cap. Iron is applied on the sealing cap so it melts and tightly fits.

IV. CHARACTERIZATION OF SILVER NANOPARTICLE BASED SOLAR CELL

Solar simulator was used for the purpose of finding the efficiency of the cells. The solar simulator of Kethlink company has been used. Solar simulator was set under 1 sun conditions (1000 W/square m). Kickstart software was used for the purpose of finding the efficiency and the I-V curve. Fig. 3 shows the I-V curve obtained form the solar simulator.

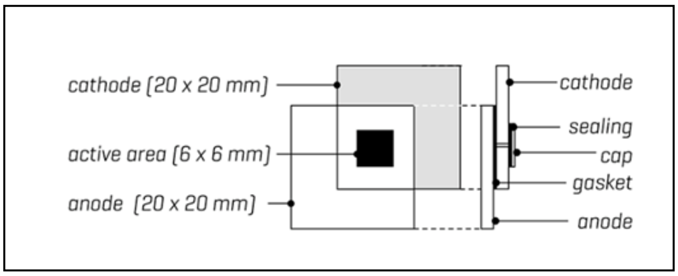

Figure 2. Solar cell area

The fill factor refers to the maximum power that is obtainable and is calculated using the product of I(sc) and V(oc). It represents the overall behavior of the solar cell. The fill factor represents the quality of the solar cell. The I-V curve also represents the fill factor. Fill factor is impacted due to the losses of the diode, resistances. The fill factor is calculated from the following formula:

$$FF = P_m/(V_{oc} x I_{sc}) \quad (1)$$

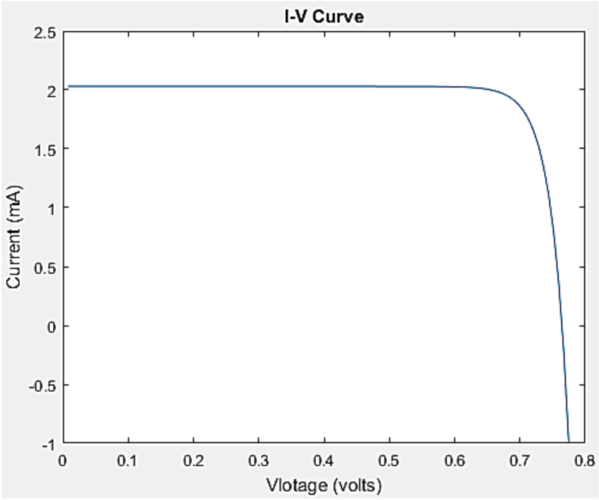

Figure 3. I-V curve

FF= 88%

The efficiency of the solar cell is calculated from the following formula:

$$\eta = \frac{V_{oc} I_{sc} FF}{P_{in}} \quad (2)$$

Efficiency = 3.46%

CONCUSLION

The results indicate that silver nanoclusters can be used in third generation solar cells. The efficiency obtained from the results in 3.46%, however, the efficiency can be further improved. Normal PV cells that are operating in the market (first generation solar cells) have typically efficiency of 20%. Measures can be taken to improve the efficiency of the third-generation solar cells making use of silver nanoclusters. There were a few limitations in the research study. Firstly, the nanoclusters were made in the city of Lahore and then they were taken to Peshawar for development of the solar cell. This might have resulted in some degradation of the nanoclusters. Moreover, another limitation is that there might have been some influence of unintended impure particles when transferring the solution in beakers and during the experiment which might have hindered the results.

The current research work has provided the researchers more insights regarding the efficiency of silver nanoparticles. Future work can be carried out on both silver nanoparticles and gold nanoclusters and under the same conditions, the performance of both can be compared. Different electrolytes can be used and the efficiency of both the nanoparticles can be compared under the same conditions. Dye sensitized solar cells can also be made and the performance of dye sensitized and nanoclusters can be compared which will give detailed insight regarding the phenomenon.

REFERENCES

[1] “http://www.ncpre.iitb.ac.in/page.php?pageid=46&pgtitle=World-Energy-Scenari.” .

[2] D. Kislov, "Effect of Plasmonic Silver Nanoparticles on the Photovoltaic Properties of Graetzel Solar Cells", Physics Procedia, vol. 73, pp. 114-120, 2015.

[3] “http://www.zmescience.com/ecology/renewable-energy-ecology/national-renewable-energy-us- 31072012/.” .

[4] M. C. Scharber, D. Mühlbacher, M. Koppe, P. Denk, C. Waldauf, A. J. Heeger, and C. J. Brabec, “Design Rules for Donors in Bulk-Heterojunction Solar Cells—Towards 10 % Energy-Conversion Efficiency,” Advanced Materials, vol. 18, no. 6, pp. 789–794, 2006.

[5] A. Slade and V. Garboushian, “27.6% efficient silicon concentrator solar cells for mass production,” in Technical Digest, 15th International Photovoltaic Science and Engineering Conference, Beijing, 2005.

[6] “http://www.nrel.gov/pv/thin_fiml/docs/kaz_best_research_cells.ppt.” .

[7] H. Yang, J. Lei, B. Wu, Y. Wang, M. Zhou, A. Xia, L. Zheng and N. Zheng, Chem. Commun., 49, 300–302, 2013

[8] O. M. Bakr, V. Amendola, C. M. Aikens, W. Wenseleers, R. Li, L. Dal Negro, G. C. Schatz and F. Stellacci, Angew. Chem.121, 6035–6040, 2009

[9] P. D. Jadzinsky, G. Calero, C. J. Ackerson, D. A. Bushnell and R. D. Kornberg, Science, 318, 430–433, 2007

[10] O. A. Wong, C. L. Heinecke, A. R. Simone, R. L. Whetten and C. J. Ackerson, Nanoscale4, 4099–4102, 2012

[11] Cong,J., Yang,X., Liu,J., Zhao,J., Hao,Y., Wang,Y & Sun,L. Nitro group as a new anchoring group for organic dyes in dye-sensitized solar cells, 48, 6663-6665, 2012

[12] Saravanan, S., Kato, R., Balamurugan, M., Kaushik, S., & Soga, T. Efficiency improvement in dye sensitized solar cells by the plasmonic effect of green synthesized silver nanoparticles. Journal Of Science: Advanced Materials And Devices, Vol. 2, No. 4, 418-424, 2017.

IJEW 国际工程期刊 International Journal of Engineering Works انجینرنگ کاموں کا بین الاقوامی جرنل

International Journal of Engineering Works
ISSN-p: 2521-2419
ISSN-e: 2409-2770
Vol. 6, Issue 03, PP. 94-97, March 2019
https://www.ijew.io/

Enhancing the Absorption and Power Conversion Efficiency of Organic Solar Cells

Waqas Farooq[1], Aimal Daud Khan[2], Mahmood Khan[3*], and Javed Iqbal[4]
[1,2,3,4] Sarhad University of Science & Information Technology, Peshawar 25000, Pakistan
waqasfarooq.ee@gmail.com[1], aimaldawoodkhan@gmail.com[2], mahmood.ee@suit.edu.pk[3], Javed.ee@suit.edu,pk[4]
corresponding author*: mahmood.ee@suit.edu.pk
Received: 03 March, Revised: 08 March, Accepted: 11 March

***Abstract*—** Optimizing the thickness of organic solar cells (OSCs) is a potent way to enhance the power conversion efficiency (PCE). In the present work, we have investigated a novel structure in which poly (9, 9-dioctylindenofluorene-*co*-benzothiadiazole) (PIF8BT): *N′*-bis (1-ethylpropyl) -3, 4, 9, 10-perylene tetracarboxy diimide (PDI) is used as a photoactive absorber layer. The influence of window layer material such as Zinc oxide (ZnO) and titanium dioxide (TiO_2) with various electrode materials including Indium tin oxide (ITO), Fluorine tin oxide (FTO), aluminum(Al) Silver (Ag) and Gold (Au) with different combinations have been investigated with the objective to enhance the absorption and PCE of the cell. Extracted results shows that the proposed scheme of the structure with ITO/Al as top and bottom electrode holds the highest performance parameters including J_{sc}*=9.26* (mA/m^2), V_{oc}*=0.59* (V), *FF=68.86*% and η*=3.86*% respectively as compared to different electrode combination and window layers with the same photoactive absorber material(PIF8BT:PDI). This indicates that the proposed structure can be a good choice for replacing less efficient in-organic cell.

***Keywords*—** Organcis solar cells, Bulk Heterojunction, PIF8BT:PDI, Buffer layer, Power Conversion Efficiency**.**

I. Introduction

Organic photovoltaic (OPV) continue to be the most emerging technology due to the rapid increase in the demand of sustainable clean energy. Today the depletion of fossil fuel and rapid increase in the population is of great concern. And to counter this problem with renewable sustainable energy source without effecting the environment is of main consideration by utilizing non-toxic material to fulfill the global energy demand and to minimize the energy crisis [1]. Conventional silicon (Si)-technology can be replaced by the OPV, as the OPV provide a striking potential for the replacement of non-organic former technology [2-4]. In order to penetrate in the market, the main seeking promise of OPV is reduced cost linked with its manufacturing. The incomparable properties of OPV materials provide a broad pathway scope for more novel possibilities such as, solution process facile fabrication over larger area, tunable opto-electronic properties, high mechanical flexibility and chemical customization. [5-7]. In contrast to this, the limitations for OPV in order to commercialize for potential applications is its low efficiencies extracted so far[8]. The recent years reported an efficiency of 11%, [9] it is tacit that OPV need to be optimized with improved performance with high conversion efficiency in order to captivate industrial point of interest and ensure commercially reliable technology. Also, air and moisture de-stabilize the OPV based devices, which need to be stabilize under ambient conditions in order to obtain better performance[10].

For a typical OPV bulk heterojunction (BHJ), a photo absorber (active layer) is placed between two conductive electrodes in which the top electrode is mostly transparent conductive oxide(TCO) i.e., indium tin oxide (ITO) or Fluorine tin oxide (FTO) and bottom electrode is metal like Aluminum (Al), Magnesium (Mg) and calcium (Ca). The photons first incident on the anode side TCO, which give rise to exciton generation, and then propagate towards D/A in the absorber layer. As the number of photons is increases with the rise in sunlight intensity, the excitons get separated and collected at the top and bottom electrode [11-13].

Herein, we investigated a novel structure in which PIF8BT: PDI is used as an active absorber layer. The complete simulated structure consist of ITO/PEDOT: PSS/PIF8BT: PDI/Al. The influence of different electrode materials on the proposed structure is tested and scheme for best electrode selection on top and bottom surface is investigated.

II. Device Modelling

The proposed investigated OSC structure is depicted Figure 1. The structure consist of four effective layers in which indium tin oxide (ITO) is used as top electrode. After the ITO layer, buffer layer (BL), PEDOT: PSS is placed which is also known as Hole transporting layer (HTL) and electron blocking layer(EBL). PEDOT: PSS has excellent stability, mechanical flexibility and highly conductivity [14-16]. Below the (BL) layer, PIF8BT: PDI is introduced as a photoactive layer with variable thickness. Different window layers including zinc oxide (ZnO) and titanium dioxide

(TiO2) is used as these window layers has high transparency, larger exciton binding energy and can enhance transmittance [17, 18].

All the simulations are performed in the GPVDM a free source solar cell simulator. The advantage of this software compared to other [19, 20] is that it can calculate both the optical and electrical property of the cell more precisely. In our investigation, we investigated both the electrical and optical model on the proposed structure which include poison equation (1), Drift diffusion model by equation (2, 3) and continuity equations (4, 5) for electron-hole. Whereas, for recombination of carrier Shockley-Read-Hall (SRH) is used in 1D- and time domain [21-23]

$$\frac{d}{d_x}\ \varepsilon_o\varepsilon_r.\ \frac{d_\varphi}{d_x}=q\left(n-p\right) \tag{1}$$

$$J_n=q\mu_c n\frac{\partial E_c}{\partial x}+qD_n\frac{\partial n}{\partial x} \tag{2}$$

$$J_p=q\mu_c p\frac{\partial E_v}{\partial x}-qD_p\frac{\partial p}{\partial x} \tag{3}$$

$$\frac{\partial J_n}{\partial x}=q\left(R_n-G+\frac{\partial n}{\partial t}\right) \tag{4}$$

$$\frac{\partial J_p}{\partial x}=q\left(R_p+G+\frac{\partial p}{\partial t}\right) \tag{5}$$

The more detail analysis on the above equations can be found in [24-27].

III. Results and Discussion

In order to optimize the thickness of the absorber layer with special emphasis on improving the performance parameters with improved η is main consideration. We have investigated a structure in which PIF8BT: PDI is used as an absorber layers and effect of thickness on high temperature on the performance of the cell is studied. In our proposed structure PIF8BT: PDI is used as a main absorber material in which ITO and Al is used on top and bottom electrode respectively. For hole transport material, PEDOT: PSS layer is utilized. However, different window and electrode material is tested on the proposed structure and comparison of the performance parameters with different combination schemes is analyzed for better performance of the cell.

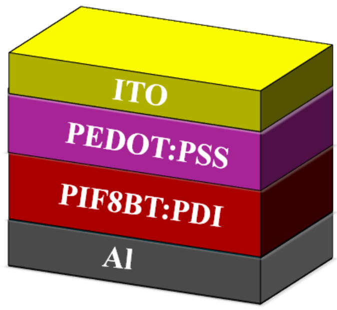

Figure 1. Schematic of proposed structure based on PIF8BT: PDI absorber material.

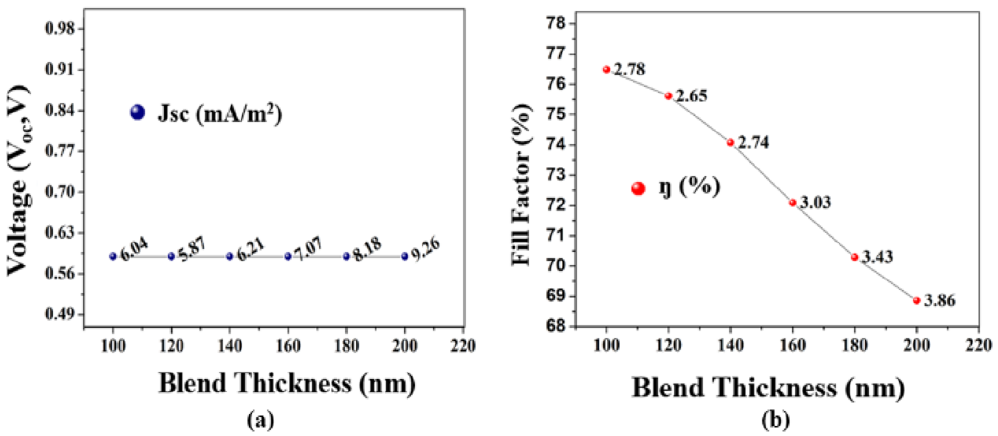

Figure 2. Influence of blend thickness on (a) V_{oc} and J_{sc}, (b) FF and η

To investigate proposed structure (illustrated in Fig. 1), we have first varied the thickness of the absorber layer (PIF8BT: PDI) and observed the influence of thickness on the Voc, Jsc, FF and η. The reason for varying the absorber layer thickness is that this layer plays a key role in the overall cell performance[28, 29]. The photon is absorbed and electron-hole pair is generated in this absorber layer[30]. Fig. 2(a) shows the variation of Voc and Jsc as the dependent of thickness. It is visible from the fig. 2(a) that when the thickness of the absorber layers increases the Jsc also increases This rise in Jsc is due to the fact when the absorber layer thickness is increases large amount of photon is absorbed which results in the greater value of Jsc [31]. The Jsc increases from 6.04 (mA/m2) to 9.26 (mA/m2) when thickness varied from 100 (nm) to 200 (nm). The fig. 2(a) also indicates that Voc is not much effected with the increase in the thickness. Fig. 2(b) shows FF and η as a function of thickness, as the Voc and Jsc has relation with FF and η [32] therefore, by increasing the thickness of the absorber layer the η also increases. This rise in η is due to the larger amount of photons absorption in the active region which results in the greater number of excitons which enhances the η. The best optimum thickness for extracting the highest η of the investigated proposed structure is 200(nm). At 200(nm) the efficiency recorded to be 3.86%. However, different window layer materials is tested on the proposed structure and recorded parameters are summarized in table I.

Table I. Extracted performance parameter of PIF8BT: PDI with different windows layers.

Window Layers	V_{oc} (V)	J_{sc} (mA/m^2)	***FF %***	***η %***
ZnO	0.59	8.68	69.16	3.58
TiO_2	0.59	8.37	69.31	3.45

The recorded parameters in table I. are less compared with our extracted results and its observed that windows layers has not much contributed to the conversion efficiency and shows a decrease in the performance parameters as compared to our proposed reference cell extracted results.

The same structure is tested with different top and bottom electrode to check the best compatibility with our proposed investigated cell in order to enhance η.

Table II. Extracted performance parameter of PIF8BT: PDI with different top and bottom electrode.

ELECTRODES	V_{oc} (V)	J_{sc} (mA/m^2)	***FF %***	***η %***
ITO/Ag	0.59	9.45	68.71	3.89
FTO/Al	0.59	8.70	69.09	3.50
FTO/Au	0.59	8.68	69.31	3.59
FTO/Ag	0.59	9.42	68.74	3.80

From table II. We can observed that recorded *η* is almost equivalent to the reference proposed structure and ITO/Ag has the closest value of *η* in comparison with the ITO/Al (proposed scheme). The reason for selecting ITO/Al is that it gives us almost the same *η* i.e., 3.86 % as that with ITO/Ag (3.89%) and FTO/Ag (3.80%). Also the price of (Al) is less compared to (Ag) so opting the ITO/Al for top and bottom electrode will be the best option in order to enhance *η* with making the cost of manufacturing less.

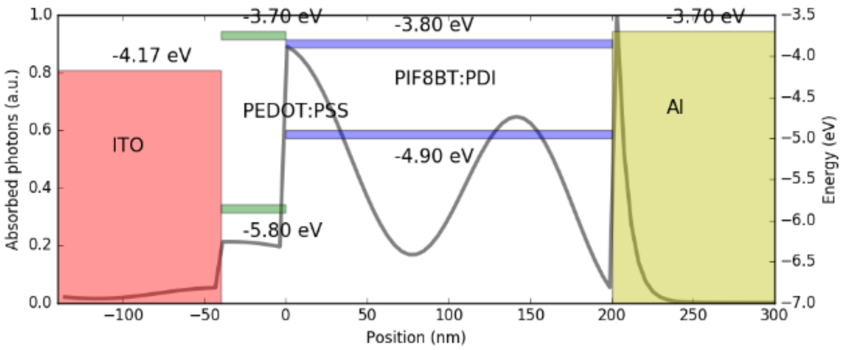

Figure. 3. Photon absorption –localization energy variance of investigated OSC

Fig. 4 Shows the peaks for the absorption of photons in each material. It is visible from the graph that the peak is increases from 0(nm) to 200(nm) in which absorber material is positioned. The rise in the aluminum (Al) layer indicates that some amount of photons are also absorbed in the Al layer.

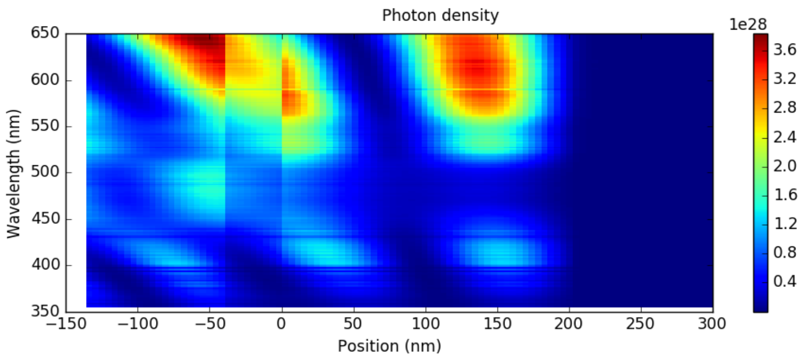

Figure 4. Photons distribution –localization energy variance of investigated OSC

The Fig. 4 Shows distribution of photons in the different material of the cell, and its visible from the figure that the photons are distributed randomly from 350 (nm) wavelength to 650 (nm) wavelength.

CONFLICT OF INTEREST

The authors hold no conflict of interest.

CONCUSLION

In summary, we investigated a novel organic material in which PIF8BT: PDI is used as active material. Our extracted results provide a new pathway for exploring new electrode materials incorporating with the novel organic material for η enhancement in the OSCs. Moreover, our work also highlighted the influence of window layer on the cell performance with different electrode combinations. Our recorded results shows a brand new avenue for improving the absorption and power conversion efficiency of OSCs which can be prefer for future applications.

REFERENCES

[1] J. Conti, "International energy outlook 2016 with projections to 2040. 2016, USDOE Energy Information Administration (EIA)," Washington, DC (United States)

[2] D. Wöhrle and D. Meissner, " Organic solar cells," Advanced Materials, 1991. 3(3): p. 129-138.

[3] S. E. Shaheen, C. J. Brabec and N. S. Sariciftci, "2.5% efficient organic plastic solar cells," Applied Physics Letters, 2001. 78(6): p. 841-843.

[4] S. Mori, H. Ohoka, H. NAakao, T. Gotanda, Y. Nakano, H. Jung, A. Iida, R. Hayase, N.Shida, M.Saito, K. Todori, T. Asakura, A. Matsui and M. Hosoya, "Organic photovoltaic module development with inverted device structure," MRS Online Proceedings Library Archive, 2015. 173

[5] G. Li, R. Zhu and Y. Yang," Polymer solar cells. Nature photonics," 2012. 6(3): p. 153.

[6] R.Po, A. Bernardi, A. Calabrese, C. Carbonera, G. Corso and A. Pellegrino," From lab to fab: how must the polymer solar cell materials design change?–an industrial perspective," Energy & Environmental Science, 2014. 7(3): p. 925-943.

[7] M. C. Scharber and N. S. Sariciftci, "Efficiency of bulk-heterojunction organic solar cells," Progress in polymer science, 2013. 38(12): p. 1929-1940.

[8] [8] M. A. Green, "Corrigendum to 'Solar cell efficiency tables (version 49)'[Prog. Photovolt: Res. Appl. 2017; 25: 3–13]," Progress in Photovoltaics: Research and Applications, 2017. 4(25): p. 333-334.

[9] S. Holiday, R. S. Ashraf, A. Wadsworth, D. Baran, S. A. Yousaf, C. B. Nielson, C. H. Tan, S. D. Dimitrov, Z. Shang, N. Gasparini, M. Alamoudi, F. Laquai, C. J. Brabec, A. Salleo, J. R. Durrant and I. McCulloch, " High-efficiency and air-stable P3HT-based polymer solar cells with a new non-fullerene acceptor," Nature communications, 2016. 7: p. 11585.

[10] S. Cavaliere, S. Subianto, L. Savych, D. J. Jones and J. Roziere, " Electrospinning: designed architectures for energy conversion and storage devices," Energy & Environmental Science, 2011. 4(12): p. 4761-4785.

[11] H. L. Yip and A. K,-Y. Jen, " Recent advances in solution-processed interfacial materials for efficient and stable polymer solar cells," Energy & Environmental Science, 2012. 5(3): p. 5994-6011.

[12] N. Marinova, S. Valero and J. L Delgado, " Organic and perovskite solar cells: working principles, materials and interfaces," Journal of colloid and interface science, 2017. 488: p. 373-389.

[13] A. D. Khan and A. D. Khan, " Optimization of highly efficient GaAs–silicon hybrid solar cell," Applied Physics A, 2018. 124(12): p. 851.

[14] J. Ouyang, "Solution-processed PEDOT: PSS films with conductivities as indium tin oxide through a treatment with mild and weak organic acids," ACS applied materials & interfaces, 2013. 5(24): p. 13082-13088.

[15] D. J. Lipomi, J. A. Lee, M. Vosgueritchain, B. C. -K. Tee, J. A. Bolander and Z. Bao, " Electronic properties of transparent conductive films of PEDOT: PSS on stretchable substrates," Chemistry of Materials, 2012. 24(2): p. 373-382.

[16] U. Lang, N. Naujoks and J. Dual, " Mechanical characterization of PEDOT: PSS thin films," Synthetic Metals, 2009. 159(5-6): p. 473-479.

[17] D. C. Look, " Recent advances in ZnO materials and devices," Materials Science and Engineering: B, 2001. 80(1-3): p. 383-387.

[18] N. R. Mlyuka, G. A. Niklasson, and C. G. Granqvist, " Thermochromic multilayer films of VO2 and TiO2 with enhanced transmittance," Solar Energy Materials and Solar Cells, 2009. 93(9): p. 1685-1687.

[19] J. Pala, M. Mordiya, D. Virpariya, A. Dangodara, P. Gandha, C. R. Savaliya, J. Joseph , T. Shiyani, D. Dhruv and J. H. Markna," Analysis and design optimization of organic dye sensitized solar cell based on simulation," in AIP Conference Proceedings. 2017. AIP Publishing.

[20] R. Stangl, C. Leendertz and J. Haschke, " Numerical simulation of solar cells and solar cell characterization methods: the open-source on demand program AFORS-HET," in Solar Energy. 2010, IntechOpen.

[21] H. Movla, " Optimization of the CIGS based thin film solar cells: Numerical simulation and analysis," Optik, 2014. 125(1): p. 67-70.

[22] M. Burgelman, J. Verschraegen, S. Degrave and P.Nollet, "Modeling thin-film PV devices," Progress in Photovoltaics: Research and Applications, 2004. 12(2-3): p. 143-153.

[23] H. Mohd. Zuhair, I. Saad, A. Roystone, A. M. Khairul, B. Ghosh and N. Bolong, " Enhancing efficiency of organic solar cells by interfacial materials modification," in 2017 IEEE Regional Symposium on Micro and Nanoelectronics (RSM). 2017. IEEE.

[24] R. C. I. MacKenzie, T. Kirchartz, G. F. A. Dibb and J. Nelson, " Modeling nongeminate recombination in P3HT: PCBM solar cells," The Journal of Physical Chemistry C, 2011. 115(19): p. 9806-9813.

[25] R. Hanfland, M. A. Fischer, W. Brütting, U. Würfel, and R. C. I. MacKenzie,"The physical meaning of charge extraction by linearly increasing voltage transients from organic solar cells," Applied Physics Letters, 2013. 103(6): p. 063904.

[26] F. Deschler, D. Riedel, B. Ecker, E. Hauff, E. D. Como and R. C. I. MacKenzie, "Increasing organic solar cell efficiency with polymer interlayers," Physical Chemistry Chemical Physics, 2013. 15(3): p. 764-769.

[27] R. C. I. MacKenzie, C. G. Shuttle , M. L. Chabinyc and J. Nelson, "Extracting microscopic device parameters from transient photocurrent measurements of P3HT: PCBM solar cells," Advanced Energy Materials, 2012. 2(6): p. 662-669.

[28] M. Lenes and L. J. A. Koster, "Thickness dependence of the efficiency of polymer: fullerene bulk heterojunction solar cells," Applied physics letters, 2006. 88(24): p. 243502.

[29] D. H. Apaydın, D. E. Yıldız, , A. Cirpan and L. Toppare, "Optimizing the organic solar cell efficiency: role of the active layer thickness" Solar Energy Materials and Solar Cells, 2013. 113: p. 100-105.

[30] M. C. Hanna and A. J. Nozik, "Solar conversion efficiency of photovoltaic and photoelectrolysis cells with carrier multiplication absorbers," Journal of Applied Physics, 2006. 100(7): p. 074510.

[31] S. Fabiano, Z. Chen, S. Vahedi, A. Facchetti, B. Pignataro and M. A. Loi, "Role of photoactive layer morphology in high fill factor all-polymer bulk heterojunction solar cells," Journal of Materials Chemistry, 2011. 21(16): p. 5891-5896.

[32] K.Vandewal ,A.Gadisa ,W.D. Oosterbaan, S.Bertho ,F.Banishoeib ,I. V.Severen ,L.Lutsen ,T.J. Cleij,D.Vanderzande and J.V. Manca, "The relation between open-circuit voltage and the onset of photocurrent generation by charge-transfer absorption in polymer: fullerene bulk heterojunction solar cells," Advanced Functional Materials, 2008. 18(14): p. 2064-2070.

International Journal of Engineering Works
ISSN-p: 2521-2419
ISSN-e: 2409-2770
Vol. 6, Issue 03, PP. 98-105, March 2019
https://www.ijew.io/

Statistical Determination of Climate-Specific Defects and Degradation Modes in PV Modules

Shakeel Ahmed[1], Abdul Basit[2], Fahim-ur-Rehman[3]
[1,2,3]US Pakistan Center For Advance Studies in Energy, University of Engineering and Technology, Peshawar
shakeel.engr2014@gmail.com[1], abdul.basit@uetpeshawar.edu.pk[2], engr.fahimkhattak@gmail.com[3]
Received: 14 February, Revised: 09 March, Accepted:13 March

Abstract—In the last decade, there has been a dramatic increase in the numbers of photovoltaic (PV) Systems as the world shifts toward clean and sustainable energy resources. Seeing this rise in the Solar PV market, multiple new manufacturers are seeking entry into the marketplace and the need to identify the good performance modules from the bad becomes an absolute necessity. The Performance and reliable operation of PV Modules depend on many factors including materials, manufacturing processes and environmental constraints. Even best quality PV modules and systems degrade with time. The degradation rate largely depends on field conditions and manufacturers, as well as test engineers are highly interested in accurate performance modeling of the field installed PV modules. Thus two factors have been seen to give good indications of the degradation: the Performance Ratio and the Performance Index. As a power plant in Pakistan is analyzed for its degradation using these two factors in this paper, an indication on its possible lifetime can be predicted. The performance ratio method indicated at degradation of .61% while the performance index method indicated a degradation of 1.09%.

Keywords— Performance Ratio, Performance index, Degradation Rate

I. Introduction

Pakistan is a developing country and its energy crisis is one of the most burning issues it faces as there is a lack of supply of continuous energy. At the same time, increasing fuel prices is an integral factor leading to excessive load shedding. In Pakistan, sustainable energy is still immature on the commercial & industrial scale. By the end of 2050 large number of countries will set milestones of reaching 20-30% of their energy demand by utilizing renewable energy [1]. Solar energy is one of the most promising technologies among all renewable technologies. Pakistan in particular receives enough solar irradiation to fulfil its required energy demand. A large number of companies are investing in Pakistan's solar market as it is anticipated that a rush of large scale PV installation will be seen in the future. This then leads to the need of having highly precise energy forecasting and modeling methods of how these solar power plants will generate energy. Studies have indicated that relatively accurate energy Prediction can be done by calculating the trend of degradation rates of photovoltaic modules technologies and existing PV power plants [2]. This will be helpful for manufacturers as the climate specific degradation trends can be reviewed and be implemented in producing better and reliable modules. Also such forecasting studies will aid the investors have a better idea of what to expect from existing and future solar power plants. Solar energy is expected to play an important role in the energy mix of future energy scenario in Pakistan and hence, one has to see whether the country has a favorable environment where this technology can flourish. Hence this simulation can cater to the ever-increasing demand for solar energy solutions and provide an idea on the economics involved.

Performance of PV system mainly depends upon the global irradiation, selected PV technology, operating module temperature and other climatic factors [3]. Performance ratio (PR) and Performance index (PI) are key parameters to define the performance of the whole system. These indicators tell how effectively solar energy is being converted into electricity. According to the IEC 61724 standards [4] [5], PR is defined as a ratio of system yield (Y_f) to the reference yield (Y_r) at standard testing conditions or STC [6].

$$PR = Y_f / Y_r \tag{1}$$

Since,

$$Y_f = \tau_R * \sum P_A / P_o * \eta_{load} \tag{2}$$

$$Y_r = \tau_R * (\sum G_I / G_{I,}\ ref) \tag{3}$$

Where,

$\tau_R * \sum P_A$ = daily array energy of the system

Po = rated array power

η_{load} = efficiency with which the energy from all sources is transmitted to the loads.

$\tau_R * \sum G_I$ = daily energy incident on the system

Performance index is a more accurate dimensionless indicator that accounts for temperature, wiring and module mismatch losses.

$$PI = Actual\ Energy / Adjusted\ Energy \quad (4)$$

Where,

Actual Energy = measured energy at any given time
Adjusted Energy = Rated Power x Loss Adjustments

When substituting in the actual loss factors that can be derived for PV systems, Equation 4 can be modified to that of Equation 5, as shown below. [7]

$$PI = (Actual\ Energy * rated\ irradiance) / (Rated\ power * Actual\ Isolation * TA * DA * SA * BOSA) \quad (5)$$

Where,
Rated Irradiance = 1000 W/m^2 for flat plate modules Rated Power = nameplate power of the array
Actual Insolation = total energy incident on the plane of array TA = Temperature Adjustment DA = DegradationAdjustment
SA = Soiling Adjustment
BOSA = Balance of System Adjustment

A systematic approach for economics analysis of a project mainly depends upon the total power delivered to the load and parameters i.e. NPV, IRR, benefit-cost ratio, Equity & simple payback period.[8][9] These parameters indicate the feasibility of the system. In this paper, techno-economic analysis of an on-grid PV system is done.

II. Power Plant Description

In the Islamic republic of Pakistan, the first on-grid photovoltaic solar power plant was commissioned near the main entrance of the government office towards the west of planning commission building, located at Islamabad with an installed capacity 178.08 kW. The project was titled “Introduction of clean energy by solar electricity generation system” and was started on May 29, 2012 & supported by Japan international cooperation agency (JICA).

A. Site and Climatic Condition

The Photovoltaic power plant is installed in Islamabad with an area of around 4108 m2 .This system is connected to the 400V side of the incoming 11kV feeder of IESCO. The remaining surplus power is flowing to the grid network of IESCO. The site specific information along with the component specification is shown in the table 1 below.

TABLE I. General Description of PV Power plant

Longitude Latitude Altitude	73.0667◦E 33.7167◦N 750 m
Avg. ambient temperature	46.6 ◦C
Maximum wind speed	20.58 m/s
Average humidity	88%
Average daily Solar Insolation	5.24 kW/m^2/day
PV MODULE SPECIFICATION	
No. of Panel/module	848 PV Solar Panel
No. of Solar Cell in each module	72 cells
Type of Module	Monocrystalline
Module Surface Area	1.28296 m^2
Total Module Area	1088 m^2
Total Land Area Used	2300 m^2
Panel Frame	Aluminum
Module eff	16.4%
PV ARRAY	
No. of sub-array	36
Module in a string	8
Total No. of strings	106
Modules in sub-array	24 x 35 set 8 x 1 set
Total PV capacity	178.08kW

III. Statistical Analysis

Before you begin to format your paper, first write and save the content as a separate text file. Keep your text and graphic files separate until after the text has been formatted and styled. Do not use hard tabs, and limit use of hard returns to only one return at the end of a paragraph. Do not add any kind of pagination anywhere in the paper. Do not number text heads-the template will do that for you.

A. Methodology

The Power plant was evaluated for performance and degradation rate calculations using two different methods. The Daily data was used which was then used to generate monthly values for both PR & PI determination.

1) Performance Ratio (PR) Analysis:
For the system under consideration, PR values were calculated by using kWh data and calculating expected energy. The Plane of array data was given by the authority of power plant and temperature model of PVSYST was used [10]. Figure 1 shows the steps followed in measuring the degradation rate. Data with irradiance values less than 50 W/m2 was filtered out. As needed, the obvious outliers were removed for a better year to year fit. The monthly average values were used as available for the PR values. The corresponding slopes for each month versus the number of years in operation was used to determine the degradation rates for each of the 12 months of the year.[7]

2) Performance Index (PI) Analysis:
PI is considered to be more accurate than PR as it incorporates the losses in the system in its measurement. For this system, the kWh data to measured energy data have been corrected for irradiance, temperature, and Module mismatch and inverter efficiency while calculating the PI values.[7] The module mismatch and the ohmic losses in the string was

assumed at 3% and 2% respectively. In PVSYST, the ohmic losses were kept at 1.5%. Figure 2 shows the methodology of PI method.

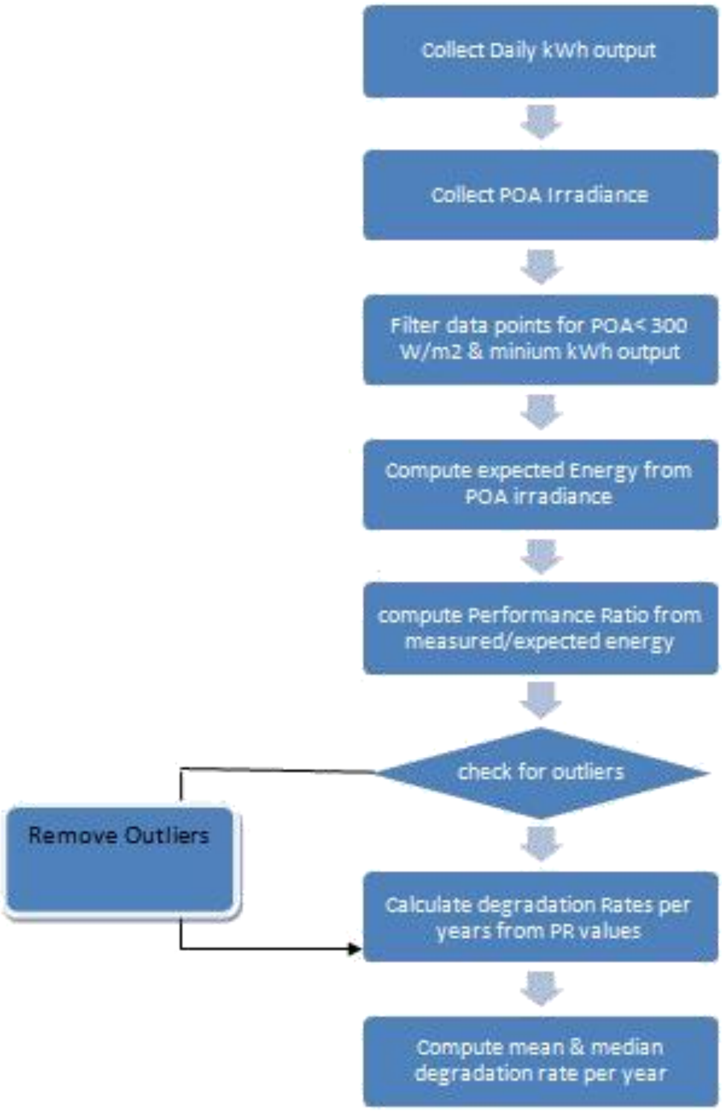

Fig.1 PR Methodology Flow Chart

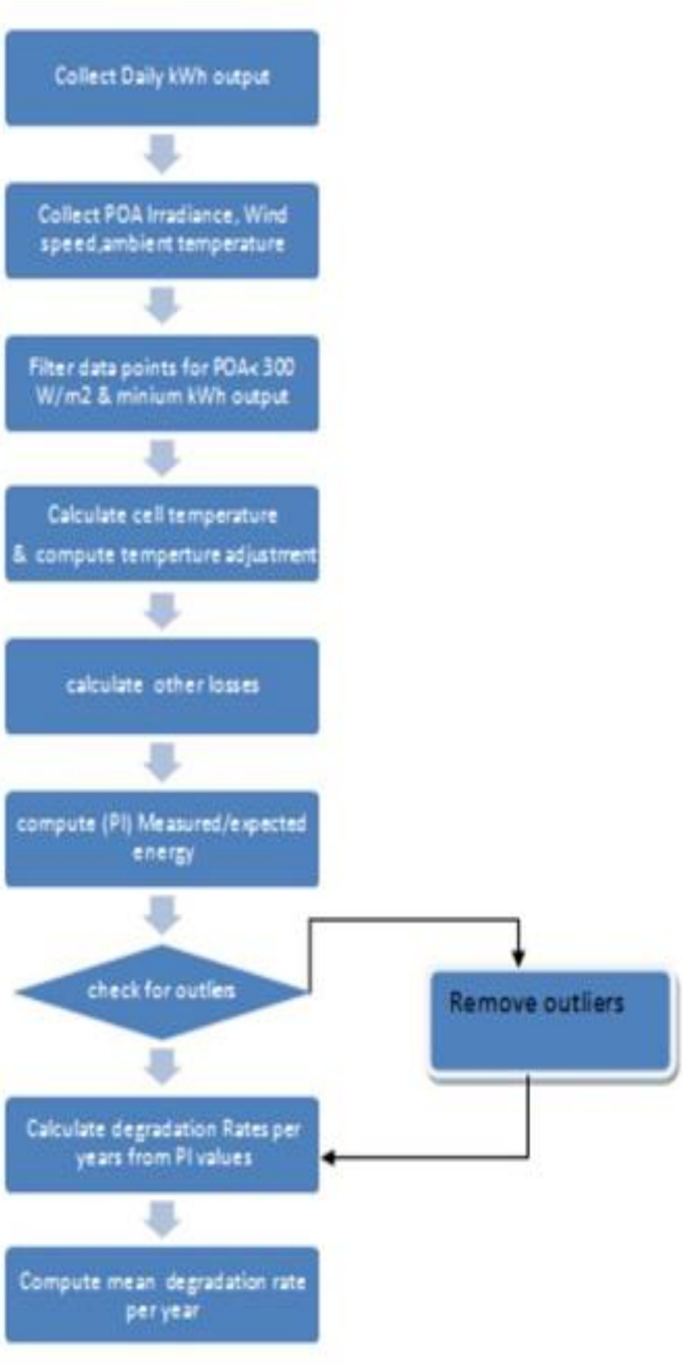

Fig.2 PI Methodology Flow Chart

IV. Results and Discussions

Performance of a system mainly depends upon variation of the solar irradiation and variety of other parameters. The metrological parameters i.e. solar irradiation, ambient temperature, and wind speed as average of every 10 minutes interval are used. Figure 3 shows the average monthly power generation from 2013 to 2016 with variation in solar irradiation.

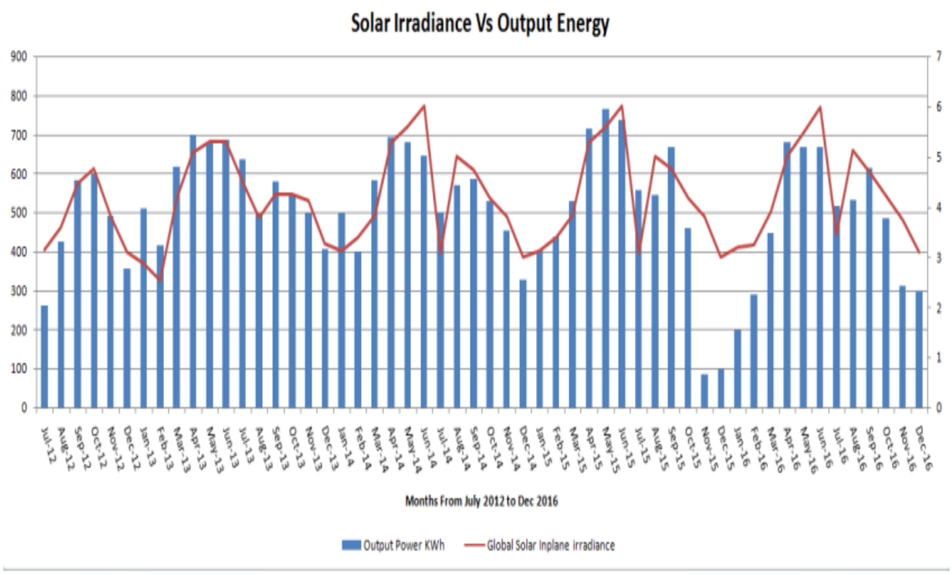

Fig.3 Solar Irradiance

From the figure 4 below, it can be seen that performance ratio of the summer months (April - August) was reduced due to the hot weather conditions leading to decrease in the module performance. From the plot it is shown that PR in year 2012 is less, this could be due to possible low irradiance conditions or component malfunctioning and replacement. The degradation rate of each month was calculated by taking slope of each PR value as shown in the table.2. The Degradation rates are shown in table

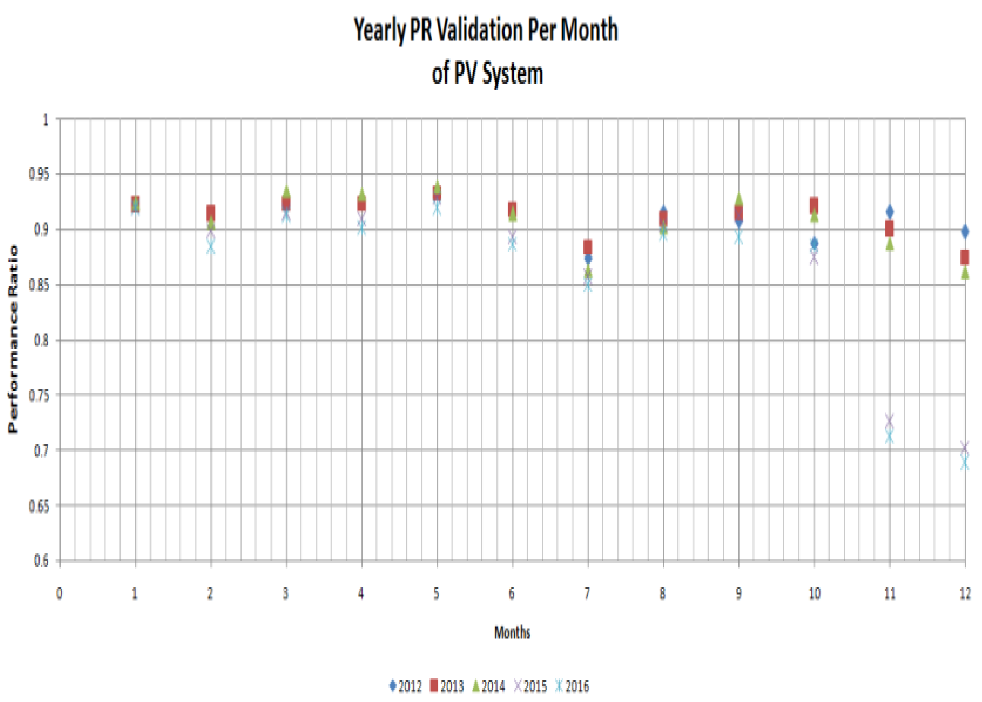

Fig.4: Monthly Average PR

Following the findings of Shrestha et al, the months with the least variation in irradiance values were considered. Hence the months of May-September were considered and the average of these months were considered as the true degradation rate. A value of 3.9% was seen to be the calculated degradation rate using the PR values determined from the measured values. The onsite degradation in the module level is hardly seen as the plant in consideration is relatively new which is verified by the IV values measured.

TABLE II MONTHLY AVERAGE DEGRADDATION RATE FROM PR

PR MONTHLY DEGRADATION RATE						
MONTHS	2012	2013	2014	2015	2016	DERGR-ADATION RATE
Jan		0.922	0.924	0.919	0.919	-0.13%
Feb		0.914	0.907	0.898	0.884	-0.99%
March		0.923	0.935	0.915	0.913	-0.49%
April		0.923	0.932	0.909	0.901	-0.87%
May		0.932	0.939	0.928	0.919	-0.49%
June		0.917	0.914	0.893	0.887	-1.13%
July	0.873	0.884	0.863	0.857	0.850	-0.73%
Aug	0.916	0.909	0.902	0.904	0.895	-0.48%
Sept	0.907	0.914	0.929	0.912	0.893	-0.30%
Oct	0.887	0.921	0.913	0.875	0.885	-0.50%
Nov	0.915	0.900	0.887	0.726	0.713	-5.79%
Dec	0.898	0.874	0.862	0.702	0.689	-5.89%

A. *Performance Index (PI)*

The performance index (PI) was used to correct for irradiance losses and other system losses (inverter efficiency losses, mismatch of the module losses, temperature loss, and wiring losses). The following plot shows that there is very less variation for the summer months that is, May-August as the PI values are calculated using the corrected vales for the high temperature months.

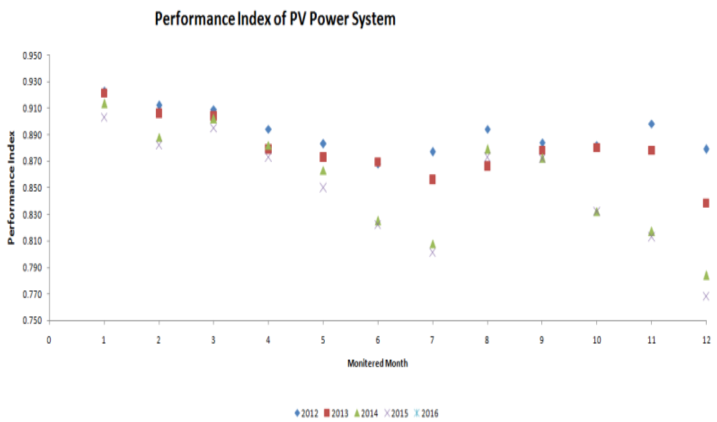

Fig. 5. Monthly Average PI

As in the case of PR, the same months with least variations in irradiance were considered and the average values were used for the determination of the degradation rates. The value thus attained is 5.83%, which show that the losses already included for the PI calculation are an accurate representation of the general losses seen by the PV system.

TBBLE III MONTHLY PI DEGRADATION

Monthly PI Degradation						
Month	2012	2013	2014	2015	2016	Degra-dation Rate
Jan		0.923	0.921	0.913	0.903	-0.68%
Feb		0.912	0.906	0.888	0.882	-1.08%
March		0.909	0.904	0.902	0.895	-0.44%
April		0.894	0.879	0.882	0.873	-0.60%
May		0.883	0.873	0.863	0.850	-1.09%
June		0.868	0.869	0.825	0.822	-1.82%
July	0.899	0.877	0.856	0.808	0.801	-2.65%
Aug	0.878	0.894	0.866	0.879	0.873	-0.25%
Sept	0.885	0.884	0.878	0.872	0.872	-0.38%
Oct	0.898	0.882	0.880	0.832	0.832	-1.82%
Nov	0.913	0.898	0.878	0.817	0.813	-2.81%
Dec	0.899	0.879	0.838	0.784	0.768	-3.57%

CONCLUSION

From the results that were discussed previously, important conclusions for failure analysis modes of modules can be drawn. The occurrences of failure modes in the power plant installed at PRL-ASU were determined. The FMEA technique was implemented on each module separately to rank the failure modes according to their impact on the performance and safety of the specific site. Weld bond weariness/breakdown with/without gridlines/metallization contact fatigue was found most dominant failure mode in PV modules. The rise of approx. 20% to 40% in series resistance even in the best modules is generally associated with failures. The degradation and weld bond weariness issues in due course could lead to breakdowns and hotspot and burning of backsheet, which could be proved catastrophic to plant.

From the analysis and result discussion of photovoltaic system performance evaluation, some conclusions are drawn. The performance models used, performance Ratio, performance index and kilowatt hour methods, which also showed difference in the calculated degradation rates. Since it is known that the best method to calculate is I-V method. Hence, after comparing different calculated values of degradation rates from this research with the values of I-V method of state-of-the-art systems of same climatic conditions found in literature, performance index degradation rate is chosen most accurate for both systems installed in Islamabad. The degradation rate of systems in Islamabad is calculated 1.09% per year. The degradation rates could be attributed to an improvement in the quality of modules that are being installed in newer system.

The trend and rate of degradation for crystalline silicon PV systems was found linear. The graphs presented in earlier sections help support the idea of linearity in the degradation rate. Prospect of solar industry seems promising in Pakistan due to good profile of the existing photovoltaic systems performance. Overall performance ratio o the PEC systems is 86.01. Comparison of these values with the other state-of-the-art- systems were made which proves that the performance of system is viable for future solar energy prospect.

ACKNOWLEDGEMENT

We would like to acknowledge Assistant Professor Dr. Abdul Basit for his valuable knowledge and experience which helped us in achieving this milestone. We are thankful to our fellow students, faculty and all the staff members of United States Pakistan Center for Advanced Studies in Energy at UET Peshawar for their support in this work. We are also thankful to USAID for providing us financial support in our MS studies.

REFERENCES

[1] D. C. Jordan and S. R. Kurtz, "Photovoltaic degradation rates - An Analytical Review," Prog. Photovoltaics Res. Appl., vol. 21, no. 1, pp. 12–29, 2013.

[2] Z. Campeau, M. Mikofski PhD, E. Hasselbrink PhD, Y.-C. Shen PhD, D. Kavulak PhD, A. Terao PhD, R. Lacerda, W. Caldwell PhD, M. Anderson PhD, Z. Defreitas, D. Degraaff PhD, A. Budiman PhD, and L. Leonard, "SunPower Module Degradation Rate," p. 61, 2013.

[3] K. Sakuta, T. Sugiura, N. Van Der Borg, K. Van Otterdijk, S. Gmbh, A. Ohrberg, and D.- Emmerthal, "International Energy Agency Pvps Task 2: Analysis of the Operational Performance of the Iea Database Pv Systems," no. May 2000, pp. 3–7, 2000.

[4] A. Chaita and J. Kluabwang, "Performance Evaluation of 3 . 5 kWp Rooftop Solar PV Plant in Thailand," vol. II, no. 3, pp. 988–991, 2016.

[5] P. P. G. A. E. Fernandez and E. M. F. Almonacid, "Photovoltaic systems installed at the University of Jaen," pp. 169–172.

[6] B. Decker and U. Jahn, "Performance of 170 grid connected PV plants in northern Germany - Analysis of yields and optimization potentials," Sol. Energy, vol. 59, no. 4–6–6 pt 4, pp. 127–133, 1997.

[7] K. Padmavathi and S. A. Daniel, "Performance analysis of a 3MWp grid connected solar photovoltaic power plant in India," Energy Sustain. Dev., vol. 17, no. 6, pp. 615–625, 2013.

[8] L. M. Ayompe, a. Duffy, S. J. McCormack, and M. Conlon, "Measured performance of a 1.72 kW rooftop grid connected photovoltaic system in Ireland," Energy Convers. Manag., vol. 52, no. 2, pp. 816–825, 2011.

International Journal of Engineering Works
ISSN-p: 2521-2419
ISSN-e: 2409-2770
Vol. 6, Issue 03, PP. 106-112, March 2019
https://www.ijew.io/

Optimization of off Grid Solar-Gas Generator Hybrid Power System for Rural Area of District Karak, Pakistan

Shifaat Ur Rehman[1], Tanvir Ahmad[2], Rizwan Kamal[3], Muhammad Ilyas[4]
[1,2,3,4]US Pakistan Center For Advanced Studies in Energy, University of Engineering and Technology, Peshawar, Pakistan
shifaatqurtuba@gmail.com[1], tanvir.ahmad@uetpeshawar.edu.pk[2], rkrizwan891@gmail.com[3], milyas0009@gmail.com[4]
Received: 28 February, Revised: 08 March, Accepted: 18 March

***Abstract*—** The environmental impact of using conventional thermal energy sources for generating electricity and fossil fuel's depletion fear are two major factor pushing world towards alternative energy resources. Pakistan is blessed with high potential of solar energy but hight initial cost and unpredictable nature of solar energy makes it uneconomical. Because of the shortfall and due to the bad geographical location, most of the rural areas in Pakistan have no access to central grid.Although some of the remote community is served by the local fuel generator for just a couple of hour at night, but increasing rate of fuel is issue which makes this system non-economical and also have harmful effect on the surrounding to emit carbon dioxide and carbon mono oxide gases. To decrease dependency on hydrocarbon base generator and cope the unpredictable nature of Photovoltaic (PV) system, an off grid hybrid solar-gas generator with battery storage is presented in this research work for the electrification of rural areas of Pakistan. Purpose of this research work is to model optimize and stable system with minimum net present cost and low cost of electricity using HOMER software.

***Keywords*—** Solar PV, Gas Generator, Hybrid Power System, HOMER, Net Present Cost.

I. Introduction

Energy particularly electricity plays an important role in the economic growth of any country. Electricity has become so important that life without electric energy is difficult to imagine, because it is used to run everything in our everyday life, i.e. light, appliances, cooling and heating for homes and business. No one thinks about electricity as long as it is available. But when outage happens in power system, the importance of electricity is realized. However, lots of people around the world do not have access to reliable electrical energy.

In many developing countries, the access to the central power grid is problematic due to the bad geographical location or location with less community. Solution for such problem is either installation of decentralized local generating units based on conventional energy sources or on renewable resource such as hydro, solar wind etc. The need to improve the performance of these systems generates an interest in hybrid generating power system that comprises many power generating sources. Such systems are good, technically and economically to provide reliable power supply for independent consumers.

In Pakistan, the urban community has access to electricity while rural areas are affected badly. Out of total population round about 27% population have no access to electricity [1]. As electricity is an important tool in every field of life such as health care, education, transportation, communication, high standard of life and economic growth. Unfortunately, in Pakistan so many remote areas have no access to main grid station to get benefit from the use of electricity. That area which has access to electricity is facing high load shedding or electricity is served irregularly. The main hurdle in developing remote and rural areas is the non availability of electricity. Reason behind this problem is low population in remote areas where grid extension proves very expensive. Therefore these areas remain out from grid extension.

Because of increase in population day by day and increase in the need of energy, its demand is increasing. In Pakistan, demand for electrical energy is increasing drastically. The total installed capacity is 25,000MW and shortfall is between 5,000MW-6,000MW [2]. In Pakistan, energy is generated generally from the conventional source like fossil fuels 14,635 MW (64.2%) of total out of which form oil (35.2%) and gas (29%), hydro 6611 MW of total (29%) and nuclear 1322 MW of total (5.8%) [2].These figures clearly show that, in Pakistan, major part of energy is generated from fossil fuels. The excessive use of fossil fuels will finally cause the depletion of these resources one day due to which it is necessary to search for alternative sources of energy to fulfill the energy demand of the world. [3].

One of the major harms with Pakistan's power system is ineffective operational system and high losses in transmission and distribution network. To solve this problem, it is requisite to generate electricity near the community without using complex network of transmission and distribution system [4]. There are some remote and rural areas which have great renewable resources potential [5]. In Pakistan rural area are blessed with renewable energy resources like biomass, hydro, solar and wind [6]. Now a days the renewable energy which is catching the attention in the world is mostly the solar energy

[7], as it can be catch easily, economical to generate electrical energy from solar energy and every where available [8].

The southern parts of KPK, rural sindh and Baluchistan have highly solar potential [6]. Solar energy is a gift of energy

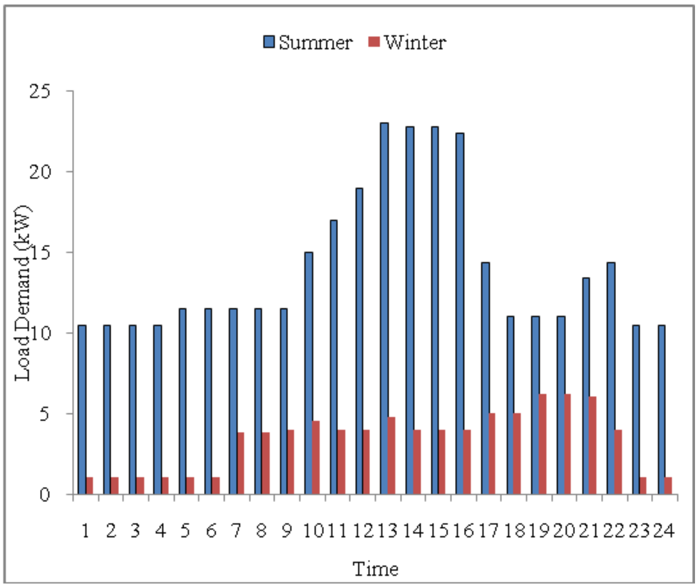

Figure 1. Seasonal Load Profile of Study Area

source because it is free available. Utilization of solar has become significantly attractive and cost effective [3]. However one drawback in getting solar energy is its unpredictable nature, dependency on weather and non availability at night. It is practical that a standalone Photovoltaic system is not able to provide a constant supply of power as it changes seasonally and periodically [9].

To solve the problem of load shedding people are using hydrocarbon based generators (natural gas) which is non-economical due to increasing rate of hydrocarbon fuels and also have harmful effect on the surrounding to emit carbon dioxide and carbon mono oxide gases. To decrease the dependency on hydrocarbon based generator, people are using standalone photovoltaic system in homes and irrigation. But the problem with PV system is its dependency on weather. On the basis of availability of solar potential and the trend of gas engine usage in karak, a hybrid system of PV/gas generator can be used for continuous and sustainable generation.

II. PROPOSED LOCATION

In Pakistan the rural areas are badly affected by load shedding. District karak is one of those affected areas. It is in between Peshawar and D.I.Khan on main Indus highway 140 Km from Peshawar. The latitude and longitude of karak is 33.1105° N, 71.0914° E repectively [10]. The total population of karak counted in the 1998 census was 431,000 [11] that increased to 706,299 by census 2017 [12]. In district karak several natural resources have been discovered such as oil, gas, and uranium. According to a report the average daily production of gas is 80 million cubic feet and oil is 7000 barrels [13]. Being very important for the economy of Pakistan, the people of karak are facing 20-22 hours daily load shedding [14].

III. METHODOLOGY

This portion discusses in detail the method followed in this research work. To know about the load, a survey was conducted to collect the data. The resource potential of study area has been collected from different sources. Finally HOMER pro software is used to modle the optimized solar-gas generator hybrid power system.

A. *Load Assessment*

The electric loads in villages are mostly consisting of lights, fans, TV, water pumps and school loads [15]. The study area has 80 households with an average 8 members per family, 4 general stores, 4 mosques and 2 schools.

During winter season and some part of spring season, fans and freezer are not used . Since fans and freezer add major loads in the system, therefore the load profile is separated into two seasons i.e. winter and summer as shown in fig.1. To know about the load, a survey was conducted to collect the data. The load of mosques consists of fans and lights which are used five times a day during prayer times. During summer the fajar prayer timing is 05:00 a.m to 06:00 a.m, zuhar prayer timing is 01:00 p.m to 03:00 p.m, while asar, Maghrib and isha timing are 05:00 p.m to 08:00 p.m. The load of houses consists of fans, lights, freezers and iron. In summer the peak load (23 kW) is in mid of the day where mostly all fans are used along with freezers. In summer school timing is from 07:00 a.m to 12:00 noon. These are primary school which consists of 4 rooms. In every room there are fans and lights. . Fans are use during day time while lights are used during night time. In general stores the fans are on during day time from 09:00 a.m to 01:00 p.m and 03:00 p.m to 05:00 p.m. The whole load of the village combine together give peak hour at mid of the day.

In winter the load is very low because the fans and freezers are not used. Whole night only few security lights are on. During day time there is no need of lights in homes, mosques, general stores and schools.

B. *Resource Assessment*

Anything that has the ability to generate electric or thermal power is term as resource. Recourse may be renewable energy resource that includes (solar energy, wind energy, hydro and biomass) or any generator that make use of any fuel to run and generator electrical power. Renewable energy resources are mostly depending on the geographical location and weather condition. The solar energy depends strongly on the latitude and climate condition. The wind energy depends on atmospheric and geographic condition. The hydro energy depends on the pattern of rainfall and topography of that location, and the biomass energy resource mainly depends on biological productivity of the location. Moreover, the renewable energy resources have the nature of seasonal unevenness. These unpredictable natures of renewable energy resources effect the cost of renewable power system. Therefore it is very important to model the renewable energy resources carefully. The main focus is on solar energy, therefore in this paper, solar resource along with gas potential is discussed.

1) Solar potential of study area

For modeling a power system comprising a PV array, it is necessary to provide the solar data of that location. The solar data includes the solar radiations and clearness index. Solar radiation may be the direct radiation or indirect radiations. The solar data can either be in the form of hourly average solar radiation (Kw/m2) or monthly or yearly average solar radiation.

The clearness index is defined as the ratio of the solar radiation that strikes the surface of earth to the solar radiation that strikes the top of the atmosphere. It defines how clear the atmosphere and this constant number are ranging between 0 and 1.

Solar data obtained from NASA surface meteorology and solar energy database as shown in fig. 2.

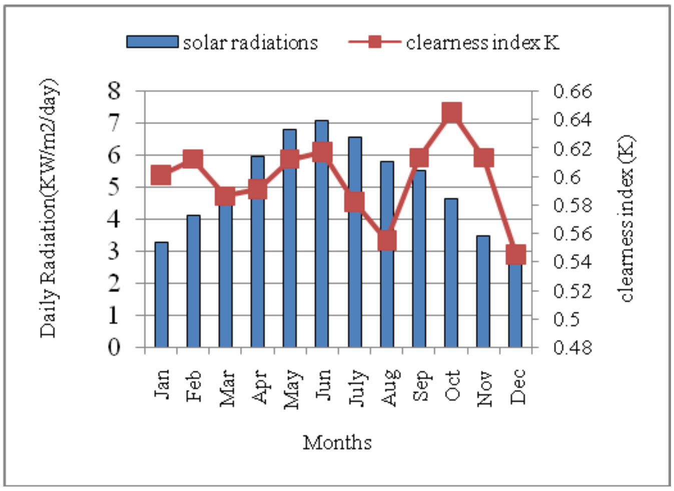

Figure 2. Average Solar Radaition and Clearness Index of Study Area

2) Gas Potential of Study Area

District karak is blessed with so many natural resources. Recently oil and gas reservoir has been found in different location of district karak such as makori, nashpa banda, and gurguri and lachi circle. Many national and international companies and Oil and Gas Development Company Limited (OGDCL) are exploring gas and oil in different areas of karak. Until now, the area of nashpa and gurguri are explored whereas other areas are on the way to be explored. In nashpa banda karak, 8 wells have been explored by OGDCL where as well number 9 is under process. Recently (in 2018) well number 8 has been explored and tested by the production department of OGDCL. According to the daily morning report (DMR) generate every day by the production department of nashpa oil field karak; the average gas production of nashpa from all 8 wells is 80 million cubic feet per day which varies day by day. Besides natural gas, there is also LPG reservoir mix with natural gas. To extract LPG from natural gas, LPG recovery plant has been installed recently which is inaugurated by ex prime minister of Pakistan Shahid Khaqan Abbasi on March 8, 2018.

C. Components Assessment

In HOMER software, components mean anything that can generate, convert or having the ability to story energy. There are different built-in components in HOMER software. There are renewable energy resources components that include PV, wind turbine, hydro and biomass. It has the option of generators that run on different fuels, grid which is dispatchable energy source component, converter and electrolyzer. Converters are an electrical component that can convert alternating current (ac) to direct current (dc) or dc to ac. Electrolyzer is used to converts electricity into hydrogen. This is done through a chemical process called the electrolysis of water. Another component is a reformer, which is used to generate hydrogen gas from natural gas by reforming process. The hydrogen gas produce during the process of electrolyzer and reforming can be stored and used as a fuel when needed in the system. To store energy for future use, there are components i.e. batteries and hydrogen storage tank. Since the performance of each component and their costs has an important role in the cost optimization and designing of a system, therefore the different data related to the component used in the system is carefully selected. HOMER software use different set of performance and cost parameters in order to characterize each component. The component of interest has been covered in the given section.

Solar PV is a renewable source component used in this paper. The derating factor of PV, which is the real output of PV as compare to the rated output, is considered 80%. This is because in real world when PV is operating then temperature, dust and many other factors affect the output. The solar panels are fixed with the slope of 350. The capital cost of solar panel is considered 1,06,000/- Pakistani Rupees (PKR/kW) while operating and maintenance cost is 6000 PKR/kW.

Next power generating component is gas generator. The initial capital cost, maintenance cost and fuel cost of generator play important role in the designing of hybrid system and cost optimization, therefore all the parameters related with generator should be specified carefully. The initial capital cost is 91,500 PKR for 5kW generator while operating and maintenance cost is 10,000 PKR.

Battery is used to store energy from PV system. It is cheaper to use batteries than generator for long term, although it needs regular maintenance. HOMER analyzes different combination of system and consider batteries when need. In this work 60 Ah, 12 V Lead Acid batteries with initial cost of 34,500 PKR/battery and replacement cost of 30,000 PKR/battery are used.

Another component used is converter. It converts ac to dc or dc to ac. To convert ac to dc is rectification while dc to ac is inversion. In modeling electrical power system, the size of converter needs to be defined. The converter size is either inverter capacity or rectifier capacity which is the maximum power produce by converting ac or dc. So the important parameters are these efficiencies that are constant. We consider converter as an inverter in this work. The initial capital cost of inverter is 38000 PKR/kW with 90% efficiency.

The price of gas varies with the passage of time therefore sensitivity variables are added on gas price and they are 27 PKR/m3 and 29.7 PKR/m3 to inspect the cost with each gas price.

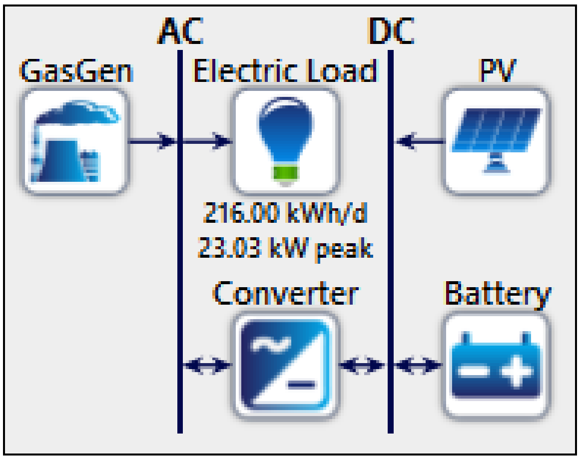

Figure 3. Schematic Diagram of Hybrid System

IV. SIMULATIONS AND RESULTS

We have simulated our model using HOMER software. Our model consists of Solar PV, Gas Generator, Batteries and converter and the peak demand is 23.03 kW with average energy demand of 216 kWh/day as shown in fig. 3. The HOMER software performs simulation for the whole year (8,760 hours). The simulation results comprise different combinations of each source, with net present and initial cost of each of them, cost of energy (COE), and carbon di oxide (CO_2) emission in each combination. Since the price of gas changes with time due to which the net present cost, cost of energy and other costs changes. As discussed earlier, HOMER can do sensitivity analysis on the bases of which a sensitivity variable is added for gas price. It is assumed that a 10% increase in gas price occurs, so sensitivity variable Rs. 27 and Rs. 29.7 is added. On the basis of gas prices, we discuss two cases each with different scinarios.

A. Case #1

In this case we simulated our system with gas price 27 PKR/m^3 and obtained different combinations. Two most expensive and two most optimal system are being discussed, the detail of which are given below.

1) Scenario 1(PV, Batteries, Inverter)

In this scenario, the total demand is met by the combination of PV's with batteries in backup. During day time, there is solar radiation and PV directly met the demand to some extent. As there no sunlight during nights, so batteries will be needed to charge in day time from PV. In order to meet demand at day time and charge batteries to use in night, a very huge PV system will be needed. Therefore in this scenario 125 kW PV, string of 312 batteries and 49.4 kW converter is used.

This system generates 2, 08,235 kWh/year. Throughput of batteries is 38,566 kWh/year while the losses in batteries are 8618 kWh/year. The minimum power production is 0Kw while maximum power production is 127 kW.

Although there is no CO2 in this system, but the costs are too high to make this system the most expensive one.

The initial capital cost, which is the combination of cost of PV, Batteries and inverter is 25.9 million PKR. The operation and maintenance cost is 9.7 million PKR. The replacement cost is 7 million PKR. As a result the net present cost of whole system is 40.6 million PKR as shown in fig. 4.

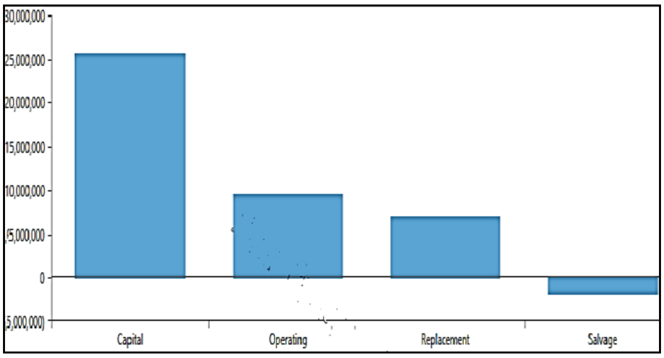

Figure 4. Cost Summary of PV System

2) Scenario 2 (Gas Generator only)

In this scenario, the total demand is met by gas generator only. The generator is to run day and night to meet demand load. The minimum electrical output is 2.6 kW and maximum output is 23 kW as shown in fig. 5.

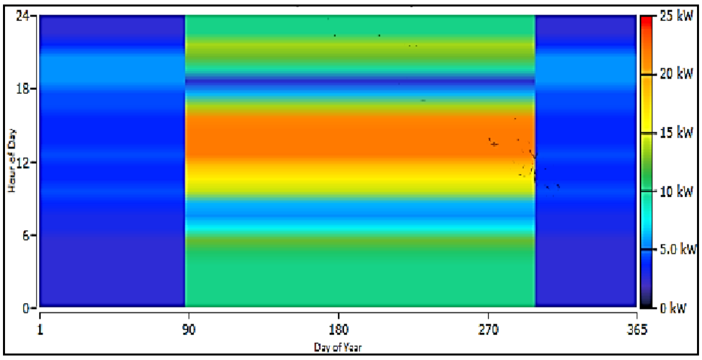

Figure 5. Gas Generator Power Output

Average of 95.5 m3/day gas is consumed as result 80,942 kwh/year energy is generated. The energy cost and net present cost in this case is almost three time less than first scenario.

The initial capital cost is this case is Rs. 475,800. Operation and maintenance cost is Rs. 136,656/year and fuel cost is Rs.941, 252/year. The operating cost which is the maintenance cost plus fuel cost is Rs. 1.08 million. Cost of energy in this case is Rs. 14.14.But still this case is considered as the second most expensive system due to constant usage of gas.

3) Scenario 3 (PV, Gas Generator and Inverter)

This is the second most optimal system. In this scenario, there is no battery to be charged, therefore at night time gas generator will meet the demand. At day time PV is contributing in power production, since there is no battery the contribution of PV is very small. The rated capacity of PV is 0.657 kW and Gas generator is 25 kW. Out of total energy, 1.35% of energy is generated by PV and 98.65% is by Gas generator.

4) Scenario 4 (PV, Gas Generator, Batteries, Inverter)

This scenario consists of 11.3 kW PV and 19 kW gas generators with 16 batteries and 6.47 kW converters. In this case 23.2 % of total energy is generated by PV (orange color) system while 76.8% is generated by gas generator (green color) as shown in fig .6.

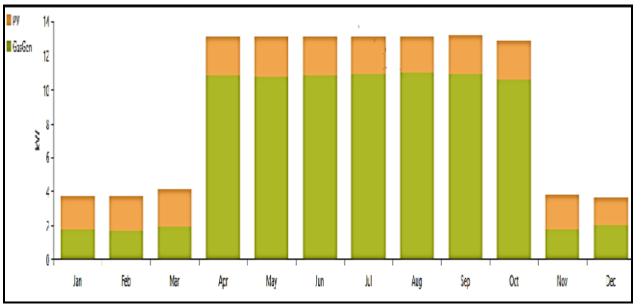

Figure 6. Monthly Average Production of PV and Gas Generator

When demand is low at day time, PV will charge batteries until they get fully charged. These batteries will meet the demand at night time or at peak. When they get discharge, gas generator will meet the demand. The initial capital cost of this system is highest of all because of PV system, but net present cost and operating & maintenance cost is lowest of all.

The initial capital cost is 2.34 PKR million, operation and maintenance cost is 142,540 PKR/year, fuel cost is 655,599PKR/year and replacement cost is 480,000 PKR twice in year, which is the cost of batteries to be replaced. At the end of project the salvages is 434, 003 PKR which is the price of batteries to be sold. The cost of energy of this system is lowest which is 12.65 PKR. The CO_2 emission is lowest i.e.46,873 kg/year expect in the case when there is only PV system which is the most expensive one.

Hence this system is considered as the most optimal system.

B. Case # 2

In this case we simulated our system with 10% increase in gas price and obtained different combinations. The detail of different scenarios are given below.

1) Scenario 1 (PV, Batteries and Inverter)

Since this scenario has no gas generator, therefore the sensitivity variable has no effect on the cost of energy, net present cost and other costs. This scenario is same as the one discuss in case #1 scenario 1. This is the expensive one.

2) Scenario 2 (Gas Generator only)

In this scenario, the total demand is met by gas generator only. The generator is to run day and night to meet demand load. The CO_2 emission is same as in case 2 scenarios 2, because in both cases only generator is used to meet the load. Due to increase in gas price the operating cost, net present cost and cost of energy increased as shown in fig. 7.

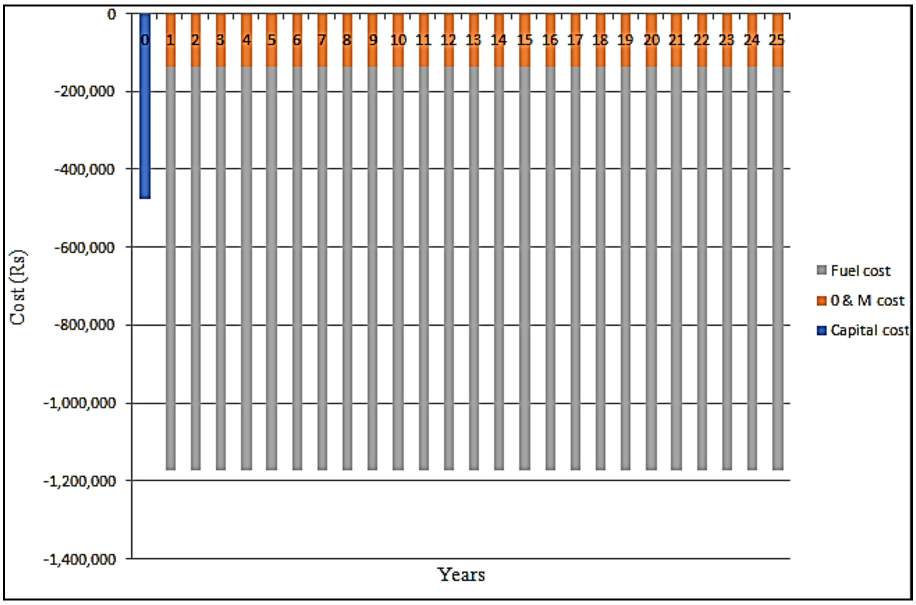

Figure 7. Cash flow of Gas Generator System

The initial capital cost is this case is 475,800 PKR while Operation and maintenance cost is 136,656 PKR/year. These costs are same as in the system discussed in case 1 scenario 2. Fuel cost is 1,035,378 PKR/year which is increased by 94,000 PKR as compare to case 1 scenario 2. The operating cost which is the maintenance cost plus fuel cost is 1.17 million PKR. Cost of energy in this case is 15.33 PKR.

Average of 95.5 m3/day gas is consumed as result 80,942 kwh/year energy is generated. The minimum electrical output is 2.6 kW and maximum output is 23 kW.

The fuel consumed and energy generated remain the same in both cases when only generated is used.

3) Scenario 3 (PV, Gas Generator and Inverter)

This is the second most optimal system. Compare to the scenario 3 of case 2 the initial capital cost is same because both scenarios has same PV and gas generator. The rated capacity of PV is 0.657 kW and Gas generator is 25 kW. Out of total energy, 1.35% of energy is generated by PV and 98.65% is by Gas generator. But due to change in gas price the net present cost increased by 1.2 million PKR, cost of energy is increased by 1.17 PKR and operating cost increased by 90,000 PKR.

4) Scenario 4 (PV, Gas Generator, Batteries, Inverter)

This scenario consists of 11.3 kW PV and 19 kW gas generators with 13 batteries and 6.33 kW converters. In this case 23.2 % of total energy is generated by PV system while 76.8% is generated by gas generator.

The average monthly production of this system is same as the one discussed in case 1 scenario 4. When demand is low at day time, PV will charge batteries until they get fully charged

Table 1 summary of Scenarios

		PV kW	Gas Generator kW	Batteries	Inverter kW	Initial capital cost (PKR)	NPC (PKR)	COE (PKR)	CO_2 (kg/Year)	Remarks
Case1	1	125	--	312	49.4	25.9m	40.6m	39.85	0	Most expensive scenario
	2	--	26	--	--	475,800	14.4m	14.14	67,306	Second expensice scenario
	3	0.654	25	--	0.467	544,602	14.2m	13.92	65,803	Second optimal scenario
	4	11.3	19	16	6.47	2.34m	12.9m	12.68	46,813	Most optimal scenario
Case2	1	125	--	312	49.4	25.9m	40.6m	39.85	0	Most expensive scenario
	2	--	26	--	--	475,800	15.6m	15.33	67,306	Second expensive scenario
	3	0.654	25	--	0.467	544,602	15.4m	15.09	65,803	Second optimal scenario
	4	13.3	19	13	6.33	2.24m	13.8m	13.52	47,219	Most optimal scenario

These batteries will meet the demand at night time or at peak. Compare to case 1 scenario 4, the number of batteries and converter size is decreased due to which initial capital cost is decreased.

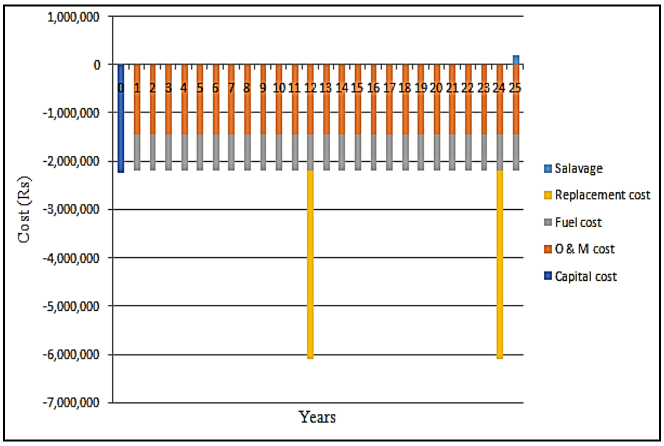

Figure 8. Cash flow of Hybrid Powe System

Fig. 8 shows that initial capital cost is 2.34 million PKR, operation and maintenance cost is 142,540 PKR/year, fuel cost is 726,371 PKR/year and replacement cost is 390,000 PKR twice in year, which is the cost of batteries to be replaced. At the end of project the salvages is 200, 058 PKR which is the price of batteries to be sold. The cost of energy of this system is lowest which is 13.52 PKR. The CO2 emission is lowest i.e. 47,219 kg/year expect in the case when there is only PV system which is the most expensive one.

The detail of both cases along with different scenario is given in table 1, which shows that in each case the scenario which consist of hybrid system i.e. Solar PV, Gas Generator, Batteries and Inverter is the most optimal system for rural areas.

CONCLUSTION

The objective of this project is to give an idea that renewable energy is very important to provide electricity to remote areas. Making a hybrid system of renewable energy sources and other power sources is economical and decrease the cost of energy rather than investing in only hydrocarbon base generator.

Load changes whole day in locality. More power is needed during evening and mid of the day. During day time solar irradiance is quite enough to meet the demand. Since there is no sunlight during night or evening to generate electricity, solutions are needed to fulfill the demand. First is to use battery bank in the system. During peak sun hours, batteries will get charge from solar system when solar energy is more than the demand. These batteries can meet the demand at night because at night time the demand is usually low. This option can decrease the cost per kWh because gas generator is not use to run. The second option is to run gas generator when load is high. This project is designed and simulated for different scenarios using all the components of different combinations. These scenarios are compared in order to get the best and optimal system. By comparing the net present cost and cost of energy it is concluded that the most optimal system is hybrid power system consisting PV, gas generator, string of batteries and inverter. This system reduces the carbon emission to the environment.

The results of this study show that a standalone hybrid power system is cheaper and good for remote areas. It encourages the private investors and local community members, especially in Pakistan, to make use of renewable energy because it is sustainable energy.

ACKNOWLEDGMENT

I would like to express my sincere gratitude to my supervisor Dr. Tanvir Ahmad for his expert guidance, constructive comments, suggestion and encouragement without which this work could not have been completed.

I am very grateful to United States Pakistan Center for Advanced Studies in Energy (USPCAS-E) at UET Peshawar and all the staff members of US-Aid Pakistan for providing me the opportunity to continue my education and complete my M.Sc in Electrical Energy Systems Engineering.

REFERENCES

[1] International Energy Agency, 'sWEO – Energy Access Database', 2016

[2] https:en.wikipedia.org/wiki/electricity_sector_in_pakistan

[3] Current status of research on optimum sizing of stand-alone hybrid solar-wind power generation systems by Wei Zhou, chengzhi Lou, zhongshi li, lin lu, hongxing yang (applied energy 87(2011) 380-389)

[4] "Chaos in power: Pakistan's electricity crisis" Development Research Group, The World Bank I.N. Kessides / Energy Policy 55 (2013) 271–285

[5] R. Szweda. "Renewable energy applications in the Indian subcontinent," photovoltaics bulletin, vol. 2003, pp. 7-9 2003

[6] Prospects for harnessing renewable energy sources in Pakistan by S.M Hasnain and B.M Grabs

[7] A. Bhomik, et al., "Renewable energy for sustainable development in India: Review on status, potential and policies," 2012

[8] I. Dinecr, "Renewable and sustainable development: a crucial review," Renewable and sustainable review, vol 9, pp.157-175, 2000

[9] [9] Yang HX, Zhou E, Lu, L, Fang ZH. Optimal sizing for standalone hybrid solar-wind system with LPS technology by using genetic algorithm, Sola energy 2008; 82(4):354-67

[10] http://www.fallingrain.com/world/PK/03/Karak.html

[11] 1998 District Census report of Karak Census publication. 97. Islamabad: Population Census Organization, Statistics Division, Government of Pakistan. 2000.

[12] "Pakistan Bureau of Statistics Census 2017" (PDF). www.pbscensus.gov.pk. Retrieved 26 September2017.

[13] "Vast reserves of oil, gas in Karak". DAWN.COM. 20 December 2009. Retrieved 27 September 2017

[14] http://www.pbs.gov.pk/content/district-glance-karak

[15] "Photovoltaic Application in Rural Area of the Developing World" by Gerald Foley

Authors Detail:

Shifaat Ur Rehman has received BS degree in Electrical Engineering from University of Engineering & Technology Peshawar KP, Pakistan in 2014. Currently pursuing MS degree in Electrical Energy System Engineering from US Pakistan Center for Advanced Studies in Energy(USPCAS-E), University of Engineering & Technology Peshawar. He has availed exchange program to the partner university of USPCAS-E Arizona State University (ASU), USA in 2016, as a research scholar. He has good hands on experience in the field of renewable energies especially PV reliability.

Tanvir Ahmad has received PhD degree with specialization in Wind Farm Coordinated Control and Optimization from School of Engineering and & Computing Science, Durham Universtiy, UK in 2017. He is currently working as a Assistant Professor at US-Pakistance Center for Advance Studies in Energy, University of Enegineering and Technology Peshawar, Pakistan. Tanvir's main research interests involve Smart Control of power system based on Artificial Intelligence (AI) and heuristic based optimization techniques, Energy Management Systems, Energy Auditing, Socio-Technical models for Energy Systems, Data Analytics for efficient utilization of Renewable Energy, Wake Flow Models and Wind Deficit Models.

Rizwan Kamal has received B.Sc Electrical Engineering degree from department of Electrical Engineering University of Engineering and Technology Peshawar, Pakistan in 2014. He is currently pursuing M.Sc degree in Electrical Energy Systems Engineering from United States Pakistan Center for Advanced Studies in Energy (USPCAS-E) at University of Engineering and Technology Peshawar. He worked on first hybrid renewable energy system of Pakistan which is consist of solar PV, Micro-hydro and Biomass resources installed at Sakhakot, Malakand division KP, Pakistan.

Muhammad Ilyas has received B.Sc Electrical Engineering degree from department of Electrical Engineering University of Engineering and Technology Peshawar, Pakistan in 2015. He is currently pursuing M.Sc degree in Electrical Energy Systems Engineering from United States Pakistan Center for Advanced Studies in Energy (USPCAS-E) at University of Engineering and Technology Peshawar. He worked on Efficiency Improvement of Small Scale Hydro Power Plants for the potential sites in KPK, Pakistan.

IJEW 国际工程期刊 International Journal of Engineering Works انجینرنگ کاموں کا بین الاقوامی جرنل

International Journal of Engineering Works
ISSN-p: 2521-2419
ISSN-e: 2409-2770
Vol. 6, Issue 04, PP. 113-119, April 2019
https://www.ijew.io/

Bandwidth Improvement and Reduced Size MPA Design using HIS

Muhammad Saleem Khan[1], Irfan Khattak[2], Muhammad Salman Khan[3], Asaf Khan[4]
[1,2,3,4]Universitivy of Engineering and Technology Peshawar Pakistan
saleemkk51@yahoo.com[1] , m.i.khattak@uetpeshawar.edu.pk[2], engrcalman.khan@yahoo.com[3], asafkhan@yahoo.com[4]
Received: 09 March, Revised: 22 March, Accepted: 28 March

Abstract— Recently, there has been extensive research on high impedance structure (HIS) and their applications in microstrip antennas and transmission lines. These periodic structures have unique property of preventing the propagation of electromagnetic waves for specific frequencies and directions which are defined by the shape, size, symmetry, and material used in their construction. These structures also facilitate in bandwidth enhancement of planar antennas. In this article, a mizrostrip patch antenna (MPA) is designed to operate at 3.5 GHz. Then a mushroom type HIS ground plane is designed in the operating band of MPA which is further integrated. Aim of this configuration is to enhance bandwidth of the MPA through incorporation of HIS plane, Bandwidth of the MPA is evaluated with and without HIS plane. All the designs and simulations are carried out in CST microwave studio.

Keywords— Microstrip patch antenna, high impedance surface, substrate, bandwidth

I. INTRODUCTION

Multiple elements fashioned from composite materials, like plastic or metals, are assembled and arranged in a repeating patterns result in Metamaterials. Metamaterials do not exist naturally and their electromagnetic properties as well as performance is superior and different from their base materials [1]. This change of properties like permittivity, permeability, refractive index etc. of the host material occurs due to the cutoffs or inclusions of integral elements. Therefore, for achieving a particular electromagnetic performance such materials can be well-thought-out. Metamaterials type Single Negative [2, 3], Double Negative [4, 5] and Electromagnetic Band Gap of planar type structures [6] are in demanding study since 1990s. Sievenpiper [7] introduced mushroom type 2- Dimensional EBG surfaces composed of a regular pattern array of unit cells in a 2 dimensional pattern. The unit cell is sandwiched in between of-patches (conducting) and ground (conducting) with a dielectric substrate. To connect the top metal patches to the ground vias are used to form a mushroom like structure.

For a desired bandwidth, AMC ground plane finds their application and to overpower surface waves propagation. The characteristic properties of AMC ground plane will effect by the dimensions of the EBG unit-cell and substrate thickness. The unit cell is of rectangular or square type. Mushroom, loop, or spiral may be used as the resonating element. It has been observed that on PEC or conventional EBGs, sense of polarization of incident plane wave reverses resulting in polarization mismatch between-reflected and incident wave. To sidestep this mismatch in several applications [8-11], Polarization dependent EBGs (PDEBGs) are introduced.

In modern wireless communication system, Microstrip patch antenna is considered a smart solution because of their several advantages. It consumes small volume, planarly configurable, mechanically robust and having lightest weight as compared to other antennas. Also its integration is easy with microwave integrated circuits (MICs). Besides various advantages of microstrip patch antennas, main drawbacks are narrow bandwidth, low gain and surface wave excitation. Several techniques can be used to overcome these main issues [12]. First of all, the choice of using a thicker substrate having low dielectric constant is best but the antenna size will increase and thus it will not remain a low-profile. The use of multi resonator stack configuration is another possible solution but again resulting to a large thickness prototype [13, 14]. To minimize the surface waves, electromagnetic band-gap structures are used. The use of EBGs is considered to be a best solution for improving MPA performance among antenna research community [15–17].

Metamaterials like Frequency selective surfaces (FSS) [18–20], which provide either AMC or EBG behavior, is alternative solution to microwave circuits and antenna problems. This option has been used in previous works [20–29].

L probe and U slot have been used by Shakelford et al. [30] in designing a small Microstrip patch antenna. Different designs have been proposed by these authors who utilized various techniques for size reduction: make use of a microwave substrate material, addition of a shorting wall and a shorting pin. A significant improvement in bandwidth is observed in all the designs.

Another method employed by researchers is using compound techniques [31]. These techniques include adjusting the patches displacement, setting two pairs conducting bars loading a capacitive disk on the top of probe and the lower patch as parasitic radiator. A new type of stacked MPA is studied using these compound techniques and the frequency bandwidth has been remarkably improved. In [32], the bandwidth of an aperture coupled MPA has been studied and improved by using an appropriate impedance matching network using filter design techniques. The initial useful antenna characteristics were maintained for the proposed new feed configuration.

The use of two triangular structures for MPA to improve the bandwidth has also been studied [33] in which two separate triangular patches are used to form patch antenna with a small spacing left between the two triangular patches. A full-wave technique in spatial-domain together with the closed-form Green's function is employed for obtaining the S-parameters of MPA and measurement results confirm a considerable improvement in bandwidth.

In the design of patch antenna, the use of unbalanced structures to improve VSWR characteristic has also been studied previously [34]. Similar to [33], a full wave spatial domain MoM technique together with the closed-form Green functions have been working for characterizing high-frequency S-parameters of Microstrip discontinuities. The obtained results(numerical) are compared with existing measurement data which show a decent agreement to each other. To improve the bandwidth of patch antennas, electromagnetic bandgap (EBG) structures [35] is using different shapes and sizes of EBG. These structures have led to considerable improvement in patch antennas bandwidth. In this article, design of Microstrip antenna along with high impedance structure is demonstrated. Main goal is to improve bandwidth of microstrip patch antenna designed for 3.5 GHz through incorporation of mushroom type high impedance surface (HIS) which is also designed to operate in the same band as that of MPA. The designed HIS ground plane is integrated with MPA and then the integrated design is evaluated for operating band.

Sequence of the paper is as following. Section II mainly deals with theory of MPA and discusses its different pros and cons. Section III deals with design parameters of HIS. Section IV presents design of MPA for 3.5 GHz, design of HIS plane for 3.5 GHz and their integration as well alongwith discussion of results. At the end conclusion of the research work is presented.

II. Microstrip Patch Antenna

The basic layered structure with two parallel conductors detached by a thin dielectric substrate is shown in the Figure 1. The upper conductor called patch with a length that is an appreciable fraction of a wavelength (λ), approximately half a wavelength (λ/2).

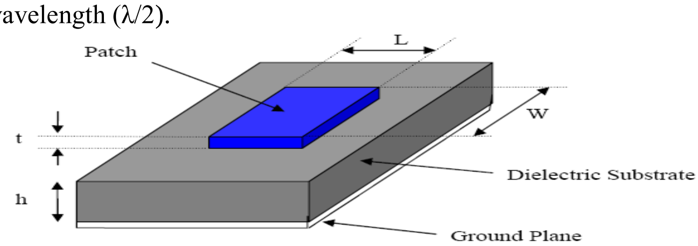

Figure 1. Microstrip patch antenna [36]

The upper conductor patch is generally made of copper and can take any possible shape as shown in Figure 2.

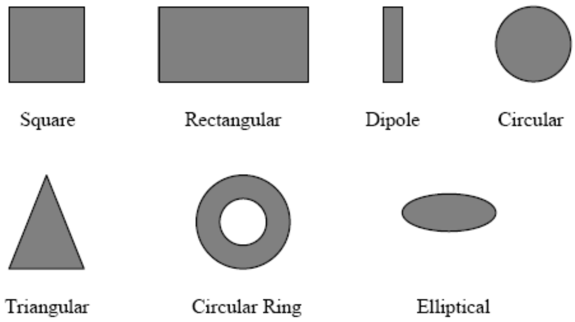

Figure 2. Geometrical shapes and sizes of patch [36]

On the dielectric substrate, the radiating patch and feed lines are usually photo etched. Because of the fringing fields between the ground plane and the patch edge, micro strip patch antennas radiate primarily. Some advantages of MPA discussed by [36] and Kumar and Ray [37] are:

- Low volume and Light weight and lowest fabrication cost.
- Planar configuration and different types polarization support.
- Integration with microwave integrated circuits (MICs) is easy
- Multiple Frequency band operations
- Robust mechanically.

Disadvantages discussed by Kumar and Ray in [37] and Garget al. in [12] are:

- Narrow BW and low efficiency
- Low Gain
- Unnecessary radiation from feeds and junctions
- Power handling capacity is low

The discussion of losses is worth to note here. Different types of losses associated to patch antenna are conduction losses, radiation losses, dielectric and surface wave excitation losses. The quality factor (Q) of Microstrip patch antennas is very high which denote losses of patch antenna. For very thin substrates, all types of losses can be neglected. However, when thickness of the substrate increases, an increasing fraction of the total power delivered by the source goes into a surface wave. This unwanted power loss in surface wave contribution is considered since it is ultimately scattered at the dielectric bends and causes degradation in antenna characteristics.

III. High Impedance surface

This article specifically talks about the use of EBG by utilizing its high impedance feature for achieving size reduction in terms of substrate height when incorporated to MPA. Rahmat Samii [38] describes EBG as a periodic or a periodic configuration of multi dimension having power to stop or enhance the transmission of electromagnetic waves in a certain frequency range with no conditional limit of incident angel and polarization. Bandgap is the frequency range in which the surface waves are suppressed. Substrate thickness and dimensions of the EBG unit-cell affect the band gap characteristic. The unit cell may be either square or rectangular in shape. The mushroom, loop, or spiral may be the resonating element. Rahmat-Samii [39] and Sievenpiper [40] designed several kinds of EBG and HIS configuration which were further used and find its application in a variety of low profile linear and circularly polarized antennas. HIS design by Sievenpiper is shown below in Figure 3 and 4.

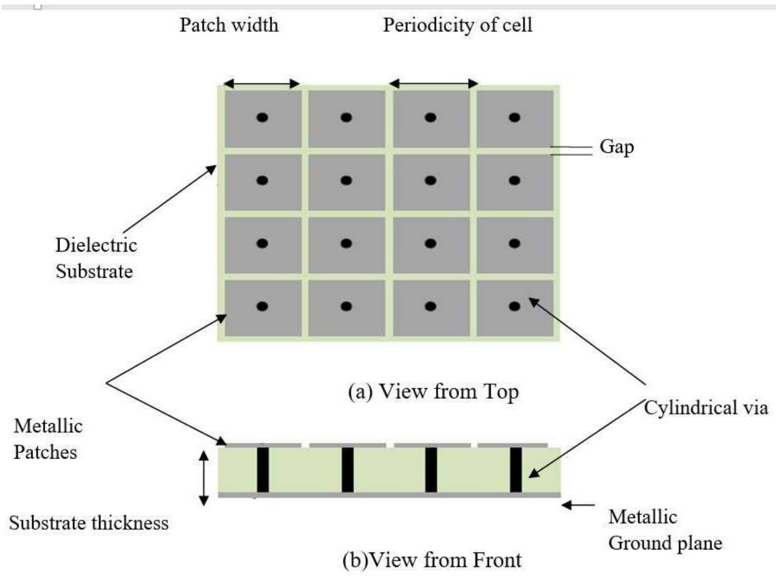

Figure 3. High impedance Surface (Sievenpiper) (a) Top-View (b) Front-View

Planar structures give in-phase reflection and suppress surface propagation in a particular frequency band. Additionally, the antenna currents are in-phase with the image currents, therefore both constructively interfere and provide better antenna performance[41].

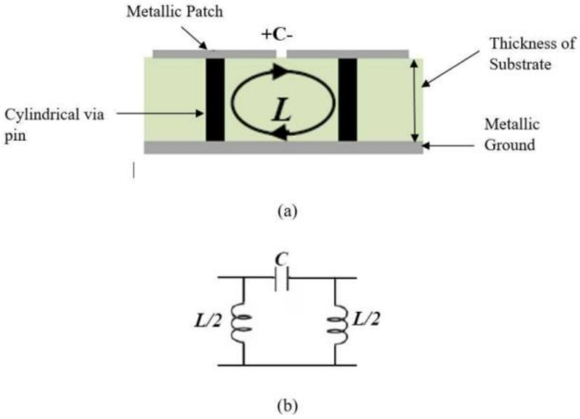

Figure 4. Equivalent circuit (LC) model (a) Front-View (b) Equivalent resonant circuit (LC)

To explain operation of HIS, consider Figure 4. It can be seen that HIS behavior is just parallel resonant circuit. The charge distribution among neighboring cells correspondent to capacitance C while the current flow through metallic via from top and bottom results to inductance L.
Following formula determines L and C values [39].

$$C = \frac{W(\varepsilon_0+\varepsilon_r)}{\pi}\cos$$

Here
W = Width of the patch
g = Gap between two adjacent patches
Ɛr = EBG substrate relative permittivity
h= Thickness of the substrate used
 = Medium permeability

Following equation expressed resonant frequency

From above equation the Frequency Band Gap (BW) can be come near to as

E

Here **η** is the intrinsic impedance of free-space = 120π

By suppressing surface waves, these assemblies are very co-operative just in case of planer antennas resulting in directivity, efficiency of the antenna and achieving high gain [42-43]. EBGs can also be utilized for GPS applications [44-45]. It has been observed that when EM wave in plane orientation incident on Perfect Electric Conductor or planner EBGs, sense of polarization reverses resulting in mismatching in polarization. In order to side-step this kind of mismatch, PDEBGs (Polarization dependent EBGs) in several applications are introduced [46-47].

IV. Results and Discussions

Planar antennas are normally desired in most of wireless communication systems. MPA is one of widely used planner antenna which is desired in several applications. In this research we will mainly focus on MPA design which will further be evaluated for bandwidth enhancement through incorporation of HIS.

Here MPA is designed for 3.5GHz having structural configurations and dimensions as depicted in Figure 5.

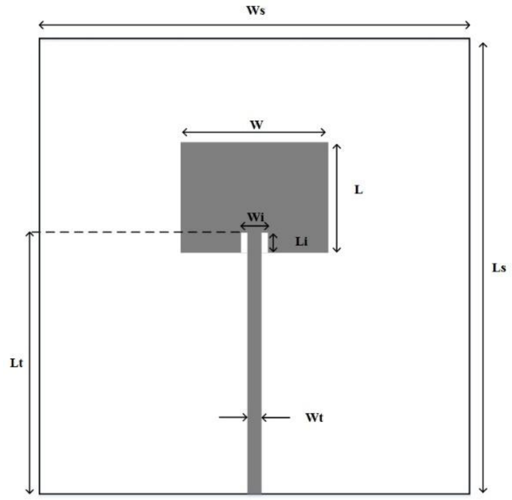

(a)

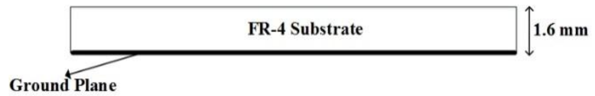

(b)

Figure 5. Illustration of geometry for Microstrip Patch antenna (a) Top View (b) Side View

TABLE I: DIMENSIONS FOR MPA

Dimension	Value (mm)
Ws	130
Ls	130
W	20
L	18
Wt	2.5
Lt	60
Wi	7
Li	5.5

Here FR4 material is used for substrate of the antenna. Ws and Ls are width and length of the substrate material. Similarly patch element of the antenna has length L and width W. microstrip line having 50-ohm impedance is used to excite the antenna that has length Lt and width Wt. For matching purpose an inset cut of Li x Wi is made in patch of the antenna. This modeling and designing is performed in CST microwave studio. Operating band of the antenna is given in Figure 6.

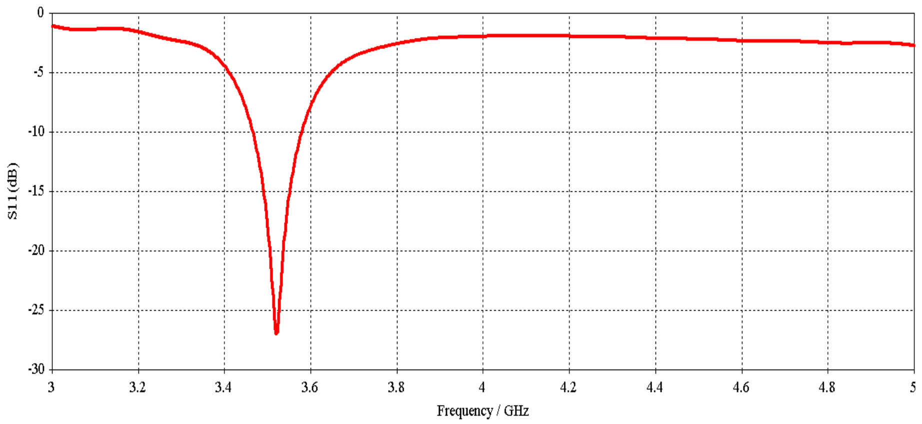

Figure 6. MPA response designed for 3.5 GHz

Here we can see that MPA is resonating at 3.5 GHz having -27 dB return loss value. Bandwidth of the antenna is 116 MHz ranging from 3.463 GHz to 3.5803 GHz.

Next step is design of high impedance surfacein the operating band of MPA. For this purpose mushroom type high impedace surface is modeled and designed in CST microwave studio. Here a via less design is utilized for the sake of simplicity. Unit cell along with in-phase reflection response of the HIS plane is given in Figure 7

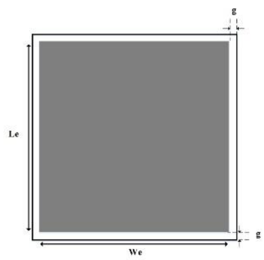

(a)

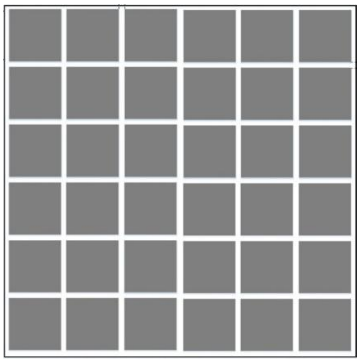

(b)

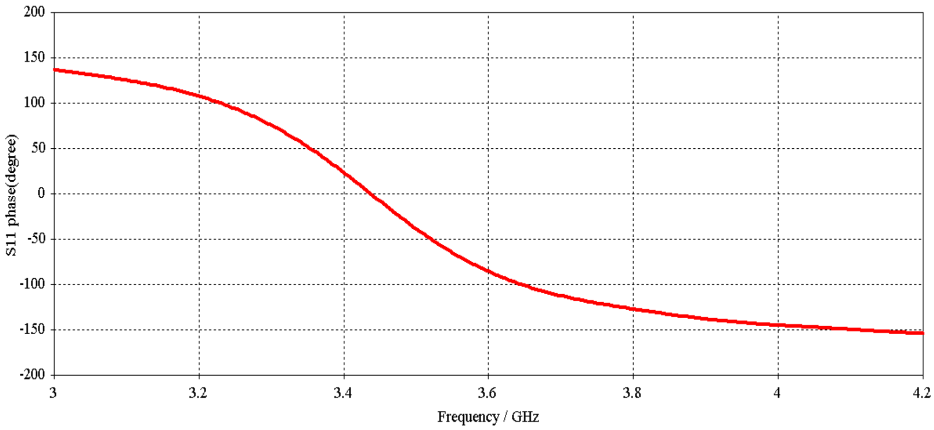

(c)

Figure 7. HIS Ground plane with results (a) Unit Cell (b) Configuration of 6x6 patch HIS ground plane (c) In-phase reflection response of HIS plane

Dimension of unit cell is 18 mm x 18 mm having a gap of 0.125 mm which is utilized to form a 6 x 6 patches of HIS ground plane. Reflection phase response as depicted in Figure 7 show that in-phase reflection occurs near 3.45 GHz.

After design of HIS plane, the MPA was integrated to it. For this purpose, ground plane of MPA was removed and replaced with the HIS ground plane thus forming the integrated antenna. Upon exciting the integrated antenna, a wide band frequency response was observed as can be seen in Figure 8.

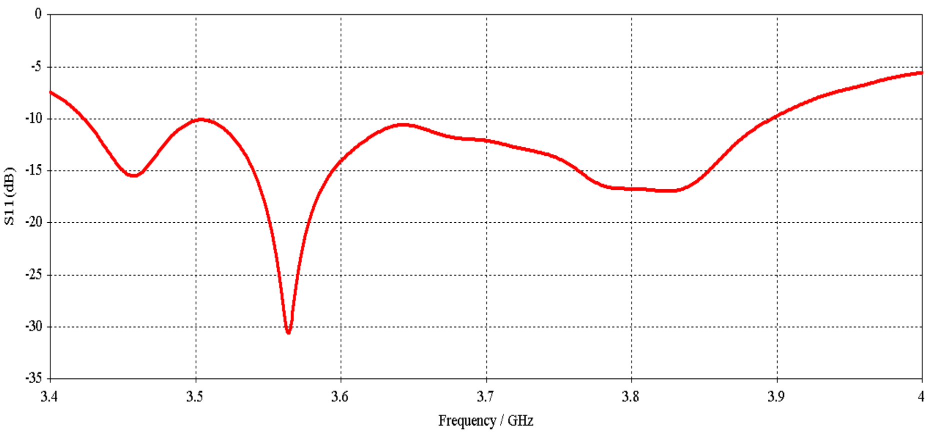

Figure 8. Operating band of integrated antenna

As can be seen that integrated antenna for 3.5 GHz has operating bandwidth of 485MHz ranging from 3.4221GHz to 3.9077GHz. Hence 318.1 % increase in operating bandwidth is observed as compare to bandwidth of MPA which is only 116MHz before integration.

CONCUSLION

This article discusses microstrip patch antenna design issue and its resolution through incorporation if high impedance structure. The aim is to counter narrow bandwidth, being a critical design constraint of MPA, through integration of HIS ground plane to the antenna. For this purpose, MPA is initially designed to operate at 3.5 GHz. The antenna is resonating at 3.5 GHz with a return loss value of -27 dB and a bandwidth of 116 MHz ranging from 3.463 GHz to 3.5803 GHz is observed. Afterwards, HIS ground plane was designed in the operating band of MPA which shows in-phase reflection at 3.45 GHz. This HIS was utilized as ground plane of MPA to form the integrated design. It has been observed that integrated antenna was also resonating at 3.5 GHz with a bandwidth of 485 MHz ranging from 3.4221GHz to 3.9077GHz. Hence 318.1 % increase in operating bandwidth is observed as compare to bandwidth of MPA which is only 116MHz before integration.

REFERENCES

[1] A. Pirhadi, F. Keshmiri, M.Hakkak, and M. Tayarani, "Analysis and design of dual band high directivity EBG resonator antenna using square loop FSS AS superstrate layer," Progress in Electromagnetics Research, vol. 70, pp. 1–20, 2007.

[2] A. Sihvola, "Electromagnetic emergence in metamaterials", Advances in Electromagnetics of Complex Media and Metamaterials, vol. 89, pp. 1-17, 2003.

[3] J. Zehentner and J. Machac, "Volumetric single negative metamaterials", Proceedings of Metamaterials Congress, pp. 22–24, 2007

[4] N. Engheta, "Metamaterials with negative permittivity and permeability: background, salient features, and new trends", IEEE MTT-S International Microwave Symposium Digest, pp. 187-190, 2003.

[5] N. Engheta, "Design, fabrication, and testing of double negative metamaterials", IEEE Transactions on Antennas and Propagation, vol. 51, issue. 7, pp. 1516-1529, 2003

[6] W. R. Ziolkowski and N. Engheta, "Metamaterials: Physics and Engineering Explorations", John Wiley & Sons, Inc., 18 September 2006.

[7] D. Sievenpiper, "High Impedance Electromagnetic Surfaces", Ph.D. dissertation, Electrical Engineering Department, University of California, Los Angeles, 1999.

[8] P. Kovács, Z. Raida, M. Martínez-Vázquez, "Parametric study of mushroom-like and planar periodic Structures in terms of simultaneous AMC and EBG Properties", Radio Engineering, vol. 17, no. 4, pp. 19-24, December 2008.

[9] S. K. Hampel, O. Schmitz, O. Klemp, and H. Eul, "Design of Sievenpiper HIS for use in planar broadband antennas by means of effective medium theory", Adv. Radio Sci., pp. 87-94, 2007.

[10] F. Yang and Y. Rahmat-samii, "Reflection phase characterisation of EBG ground plane for low profile wire antenna applications", IEEE Transactions on Antennas and Propagation, vol. 51, no. 10, October 2003

[11] D. F. Sievenpiper, J. H. Schaffner, H. J. Song, R. Y. Loo, "Two-dimensional beam steering using an electrically tunable impedance surface", IEEE Transactions on Antennas and Propagation, vol. 51, no. 10, pp. 2713-2722, October 2003.

[12] G. Poilasne, "Antennas on High impedance ground planes: on the importance of the antenna isolation," Progress in Electromagnetics Research, vol. 41, pp. 237–255, 2003.

[13] S. Zhu and R. Langley, "Dual-band wearable textile antenna on an EBG substrate," IEEE Transactions on Antennas and Propagation, vol. 57, no. 4, pp. 926–935, 2009.

[14] M. Mantash, A. C. Tarot, S. Collardey, and K. Mahdjoubi, "Dual-band antenna for WLAN application with EBG," in the 4th International Congress on Advanced Electromagnetic Materials in Microwaves and Optics, pp. 794–796, Karlsruhe, Germany, September 2010.

[15] M. Mantash, A. C. Tarot, S. Collardey, and K. Mahdjoubi, "Dual-band CPW-fed G-antenna using an EBG structure," in Antennas and Propagation Conference (LAPC), pp. 453–456, Loughborough, UK, 2010.

[16] Shakelford, A., Lee, K.F., Luk, K.M.," Design of small-size wide-bandwidth microstrip patch antennas," Antennas and Propagation Magazine, IEEE, vol. 45, Issue 1, pp. 75-83, Feb. 2003.

[17] Ting-Hua Liu and Wen Xun Zhang, "Compound techniques for broadening the bandwidth of microstrip patch antenna," Microwave Conference Proceedings, vol. 1, pp. 241-244, Dec. 1997.

[18] AdilenaSlavova, A. Abdel Rahman and A.S. Omar, "Broadband bandwidth enhancement of an Aperture coupled microstrip patch antenna," Antennas and Propagation Society International Symposium, vol. 4, pp. 3737-3740, June 2004.

[19] Tao Yuan, Jian-Ying Li, Le-Wei Li, Lei Zhang, and Mook-Seng Leong, "Improvement of Microstrip Antenna Performance Using Two Triangular Structures", Digest of 2005 IEEE Antennas and Propagation Society International Symposium, vol. 1A, pp. 301-304, 3-8 July 2005.

[20] J.Y. Li, Zaw-ZawOo, and Le-Wei Li, "Improvement of characteristics of microstrip antennas using unbalanced structures," IEEE Antennas and wireless Propagat. Lett, vol. 1, pp. 71-73, 2002

[21] E. Yablonvitch, "Photonic band-gap structures," J. Opt. Soc. Amer. B, Opt. Phys. , vol. 10, no. 2, pp. 283-295, Feb 1993.

[22] Balanis, C.A., Antenna Theory: Analysis and Design, John Wiley & Sons, Inc, 1997.

[23] Kumar, G. and Ray, K.P., Broadband Microstrip Antennas, Artech House, Inc, 2003.

[24] Cisco, "Antenna Pattern and Their Meaning," Copyright © 1992–2007 Cisco Systems, Inc.

[25] B. Jecko, T. Monediere, L. Leger, "High Gain EBG Resonator Antenna", 18th International Conference on Applied Electromagnetics and Communications, ICECom 2005, pp. 1-3, 12-14 Oct. 2005 12] R. Garg, I. Bhartia, I. Bahl, and A. Ittipiboon, Microstrip Antenna Design Handbook, Artech House, Boston, Mass, USA, 2001.

[26] G. Kumar and K. C. Gupta, "Directly coupled multiple resonator wide-band microstrip antenna," IEEE Transactions on Antennas and Propagation, vol. 33, no. 6, pp. 588–593, 1985.

[27] F. Yang, X. X. Zhang, X. Ye, and Y. Rahmat-Samii, "Wide-band E-shaped patch antennas for wireless communications," IEEE Transactions on Antennas and Propagation, vol. 49, no. 7, pp. 1094–1100, 2001.

[28] E. Rajo-Iglesias, L. Incl´an-S´anchez, and O. Quevedo-Teruel, "Back radiation reduction in patch antennas using planar soft surfaces," Progress In Electromagnetics Research Letters, vol. 6, pp. 123–130, 2009.

[29] Z. Duan, S. Qu, and Y. Hou, "Electrically small antenna inspired by spired split ring resonator," Progress In Electromagnetics Research Letters, vol. 7, pp. 47–57, 2009.

[30] F. Yang and Y. Rahmat-Samii, "Electromagnetic Band-Gap Structures in Antenna Engineering", The Cambridge RF and Microwave Engineering Series, Cambridge University Press, Cambridge, Mass, USA, 2008.

[31] M. E. De Cos, F. L. Heras, and M. Franco, "Design of planar artificial magnetic conductor ground plane using frequency selective surfaces for frequencies below 1GHz," IEEE Antennas and Wireless Propagation Letters, vol. 8, pp. 951–954, 2009.

[32] O. Luukkonen, C. R. Simovski, and S. A. Tretyakov, “Grounded uniaxial material slabs as magnetic conductors,” Progress in Electromagnetics Research B, no. 15, pp. 267–283, 2009.

[33] H. Shaban, H. Elmikaty, and A. A. Shaalan, “Study the effects of electromagnetic band-gap (EBG) substrate on two patch microstrip antenna,” Progress in Electromagnetics Research B, vol. 10, pp. 55–74, 2008.

[34] F. Yang and Y. Rahmat-Samii, “Reflection phase characterizations of the EBG ground plane for low profile wire antenna,” IEEE Transactions on Antennas and Propagation, vol. 51, no. 10, pp. 2691–2703, 2003.

[35] J. R. Sohn, K. Y. Kim, H. S. Tae, and J. H. Lee, “Comparative study on various artificialmagnetic conductors for low-profile antenna,” Progress in Electromagnetics Research, vol. 61, pp. 27–37, 2006.

[36] S. Chaimool, K. L. Chung, and P. Akkaraekthalin, “Bandwidth and gain enhancement of microstrip patch antennas using reflective metasurface,” IEICE Transactions on Communications, vol. E93-B, no. 10, pp. 2496–2503, 2010.

[37] J. Liang and H. Y. D. Yang, “Radiation characteristics of a microstrip patch over an electromagnetic bandgapsurface,”IEEE Transactions on Antennas and Propagation, vol. 55, no. 6, pp. 1691–1697, 2007.

[38] D. Sievenpiper, L. Zhang and E. Yablonovitch, “High-Impedance Electromagnetic Ground Planes”, IEEE MlT-S Digest, vol. 4, pp. 1529-1532, 1999.

[39] Qian Y., Coccioli R., Sievenpiper D., Radisic V., Yablonovitch E., and Itoh T., “A Microstrip Patch Antenna using novel photonic bandgap structures”, Microwave J., vol 42, pp. 66-76, Jan 1999.

[40] Z. Duan, D. Linton, W. Scanlon, and G. Conway, “Using EBG to Improve Antenna Efficiency in Proximity to the Human Body”, Institution of Engineering and Technology Seminar on Wideband, Multiband Antennas and Arrays for Defence or Civil Applications, pp. 173-180, London, 13-13 March 2008.

[41] X. L. Bao, G. Ruvio, M. J. Ammann, and M. John, “A novel GPS patch antenna on fractal Hi-Impedance surface Substrate”, IEEE Antenna and Wireless Propagation Letters, vol. 5, 2006.

[42] R. Baggen, M. Martínez-Vázquez and J. Leiss, “Low Profile GALILEO Antenna using EBG Technology”, IEEE Transactions on Antennas and Propagation, vol. 56, no. 3, pp. 667-674, March 2008.

[43] F. Yang, Y. Rahmat-Samii, “Polarization-Dependent Electromagnetic Band Gap (PDEBG) structures: designs and applications”, Microwave and Optical Technology Letters, vol. 41, issue. 6, pp. 439–444, June 20, 2004.

[44] Y. Fu and N. Yuan, “Surface-wave bandgap of Polarisation dependent Electromagnetic bandgap Structures”, Microwave and Optical Technology Letters, vol. 49, issue 4, pp. 946–949, 26 February 2007.

[45] D. Yan, Q. Gao, C. Wang, C. Zhu, N. Yuan, “A novel polarisation convert surface based on artificial magnetic conductor”, Asia-Pacific Microwave Conference Proceedings, APMC 2005, vol. 3, pp. 4-7, December 2005.

[46] P. J. Ferrer, B. Kelem and C. Craeye, “Design of broadband transpolarizing surfaces”, Microwave and Optical Technology Letters, vol. 48, no. 12, pp. 2606-2611, December 2006.

国际工程期刊
International Journal of Engineering Works
انجینیرنگ کاموں کا بین الاقوامی جرنل

International Journal of Engineering Works
ISSN-p: 2521-2419
ISSN-e: 2409-2770
Vol. 6, Issue 04, PP. 120-125, April 2019
https://www.ijew.io/

Speed and Direction Control of a DC Motor using Dual Converter Technique

Obaid Hussain[1], Sohail Gul[2], Dr. Muhammad Naeem Arbaab[3], Amjad Khan[4]
[1,2,4]PG Research student, Dept. of EEE, University of Engineering and technology Peshawar, KP, Pakistan,
[3]Research Scholar, Dept. of EEE, University of Engineering and technology Peshawar, KP, Pakistan
Received: 10 March, Revised: 28 March, Accepted: 01 April

***Abstract*—**This Paper presents the basic concept and methodology variable levels of DC voltage as well as reversal of polarity (without changing terminals physically). The circuit has been designed for this purpose can break into two parts: Dual H-bridge Converter and Microcontroller. Dual H-bridge converter is available in the form of L293D IC and L298N.The total power loss of existing system i.e. 8051 microcontroller with L293D was 1.7365W. While the total power loss of PIC microcontroller with L293D was1.56165W So, We have chosen proposed Atmega328 I.C because the power loss has been reduced to 1.560115w. The Microcontroller Atmega328is programmed with C++ language. The Atmega328 microcontroller provides pulses to the gate of the NPN and PNP transistor for the required output DC voltage and polarity, which runs the DC motor.column.

***Keywords*—** Machines, Motors, Speed Control, H-bridge Convertor, Micro Controller.

I. INTRODUCTION

The major trouble in the advance power industries is to construct technical methods, algorithms, technologies, ideas for the design of procedure control systems which must be able to evolve, self-develop, self-organize, and self-evaluate and to self-improve. Speed and direction rheostat of a DC motor is needed and helpful in steel industries, cement industries and paper mills etc. it plays a significant part in the atomization of aforesaid industries. This paper provides speed as well as direction control of DC motor with higher efficiency. The simulated result is synchronized with the experimental results. Owing to ease of control and wide range applications of a DC motor, it becomes inherently recommended and used machine. Besides, a DC motor also rids the mechanism from the requirement of any power circuit switching.

Employing Pulse Width Modulation for the control mechanism of a DC motor is one of the several techniques available and commonly used for motor speed control. It is achieved through controlling the armature voltage. Either clockwise or anti-clockwise, both speeds can be controlled by the introduction of a microcontroller in the assembly. A wide and orderly arranged array of solar cells is often termed as a Solar panel. It is responsible for changing Sun's energy into electrical energy which can then be used in almost an unlimited number of ways. A very high percentage in terms of efficiency can also be achieved when, though complex in nature, solar panels are perfectly aligned with the Sun, that is to say always facing towards the Sun. This research paper aims at furnishing a procedure for development of a hardware for maximum exposure of the PV panel to the Sun in a solar day by tracking the position of Sun at all times. The design indulges an 8051 microcontroller, a DC motor and a light sensor assembled on a single board. The output of the scheme is calculated to be 32.17 % more than the usually placed static flat solar panels. The L293D dual H-bridge converter controls the direction operation of the attached DC motor .

The highly trendy procedure of automation is currently going above the charts in usage by finding its applications in mega industries, factories, state of the art and tech facilities to homes. This research paper furnishes, based upon temperature variation, a cutting-edge mechanism regarding the control of speed of a DC motor. An interfacing was achieved through Lab VIEW owing to the dependence of motor speed on the variation in ambient temperature.

The temperature sensor that was utilized in this research paper is an LM35. Designing of the computer code and its execution, both the steps are carried out in the LABVIEW software. This software was already laden into an Arduino board in the first place. The Maker Hub makes possible the communication amid Lab VIEW software and the hardware board that is Arduino Uno board. For the starters, Pulse Width Modulation technique has been utilized for the generation of a duty cycle by changing the pulse width, for a range of temperatures. Next, generation of mean values of voltage for a duty cycle was carried out. Then, these generated voltage values are applied onto the DC motor so as to achieve the variation in the speed of the DC motor. The speed parameter regarding the DC motor has been controlled by the help of the program written in Lab View. It aimed at either increasing or decreasing the speed, depending upon the temperature.

This research paper furnished a practical and logical system for the speed control of a DC motor. Simulink (a tool in MATLAB) along with Arduino were utilized for the achievement of the speed control of a motor. This research paper work also furnishes a duo of Arduino board basics and PI controller of Simulink (used in a closed loop). It also describes the basics of coding program in Arduino Amalgamated with a

Simulink coder. Finally, the results of using a PI controller for DC motor speed will also be furnished towards the later stages device.

II. SYSTEM DESCRIPTION

The block diagram of the system is shown below. In the following block diagram DC motor can be operated by powering it through the battery storage or the mains via an adaptor. TON and TOFF are displayed along with frequency and the duty cycle on an LCD. There are also two relays for causing the current direction to swing from one phase to another. Just keeping one relay ON will cause the current to remain in one phase only, that is to say that current will remain either positive or negative. It therefore causes the motor to run in either one direction or the other. The desired speed of the motor can be achieved through the control mechanism through the analog pin A0. The PWM is controlled through the potentiometer using pot.

Here, the employment of the H-Bridge converter (L293D) is done so as to provide DC motor with 12V dc with at least 5V. Transistors in the bridge mechanism can be turned ON and OFF by the help of the input voltage. This technique is therefore much more unswerving and competent. The two motor pins, located on the outer area of the Atmega328, namely M1 and M2 are connected to two separate relays. Only the PWM control pin is the one that is in connection with both the relays. Pressing the "A" key causes motor to run in anti-clockwise direction, "C" causes it to run in clockwise direction. Whereas pressing the "S" key turns OFF both of the relays, thereby halting any supply of power to the DC motor. As a result, the DC motor stops.

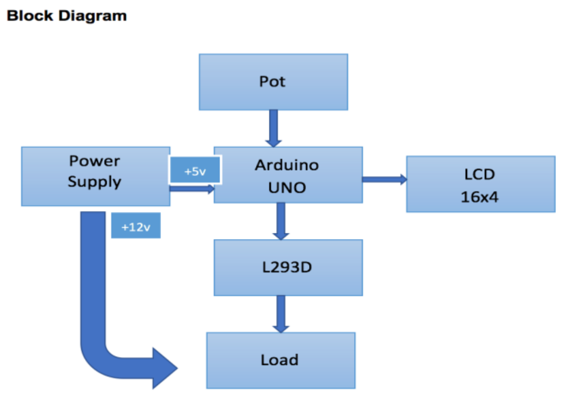

Figure 1. Block Diagram

III. SIMULATION RESULTS

A. Potentiometer

A maximum amount of current will flow towards the load when the resistance of the potentiometer is at its maximum and vice versa. The basic code is written in the C language, conversion to hexadecimal format has been carried out in the Arduino.

B. Micro-Controller

It is responsible for the control mechanism of the direction and speed of the DC motor. Micro controller is connected with the set of relays, a dual H-bridge converter and a speed controlling potentiometer.

C. Dual H-bridge Converter (L293 D)

This IC is responsible for driving the motor. It comes with an array of 4 high current diodes and a half H driver built inside of it. The aim of having this circuitry is to control not one but two motors simultaneously. The output current is rated at 600 mA, while voltage is maintained in a range of a minimum of 4.5 V to a maximum of 36 V.

This is a motor driver IC in which half H driver with quadruple High current is designed for controlling two motors at a time. It Provides drive currents of 600 mA that are bi-directional and the value of voltage is in the range of 4.5v - 36v.

D. DC Motor

A permanent 12 V DC motor has been employed. Variation in the speed of Dc motor is controlled by the variation in voltage. The Dc motor draws around 100mA of current. Stepper motor can also be used instead of the DC motor.

The frequency of the Pulse Width Modulation signal on a large amount of the pins is around0.490 KHz. Pin 5 and pin 6 are the ones on a UNO board that give access to a frequency as an input for the system which is rated at around0.980 KHz. The below figure is showing that duty cycle is 0% due to which output voltage is zero and no current will flow through the dc motor in fig.3.

In this image fig.4, we have seemed that the duty cycle is now 50% adjusted by potentiometer so that output voltage i.e. 12v is 50% off and 50% on and only 50% current of the peak current has been supplied to the dc motor.

In the above image fig.5, we have seen that the duty cycle is now 100% adjusted by potentiometer so that output voltage i.e. 12v is 0% off and 100% on and now 100% current peak current has been supplied to the dc motor.

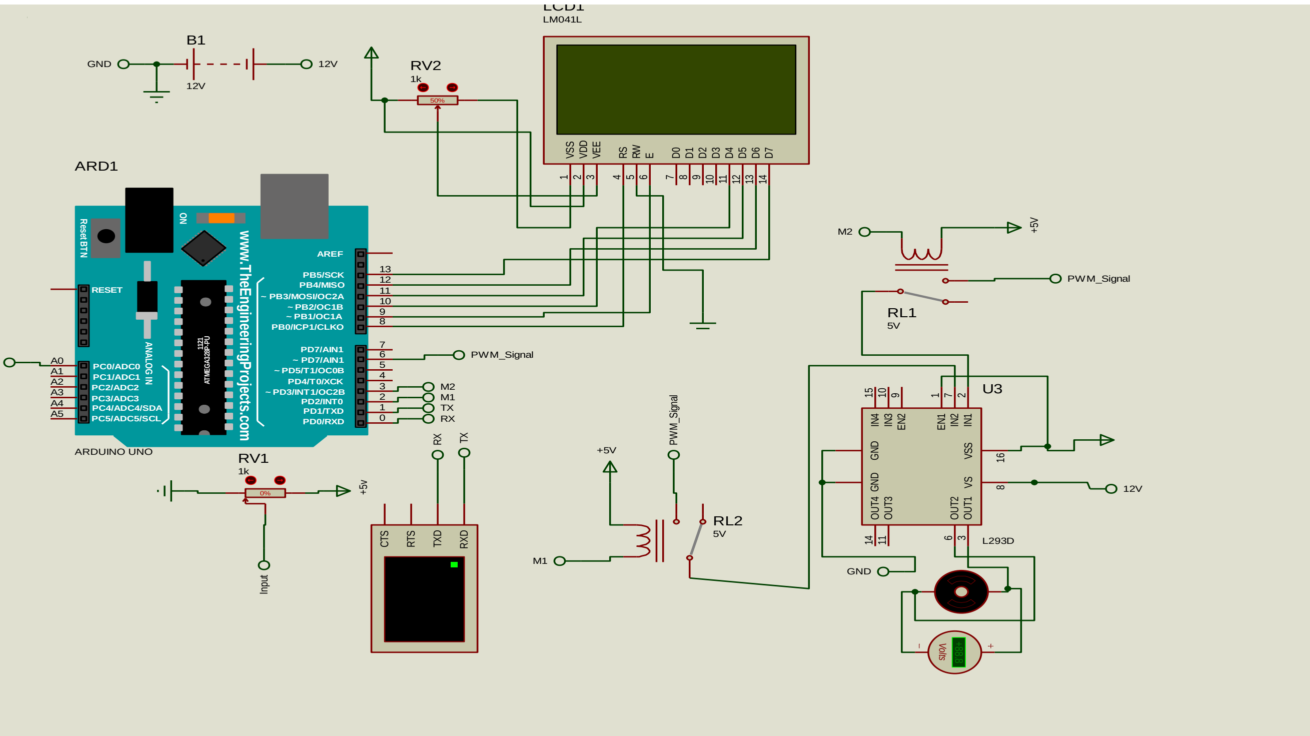

Figure 2. Complete Simulation Diagram

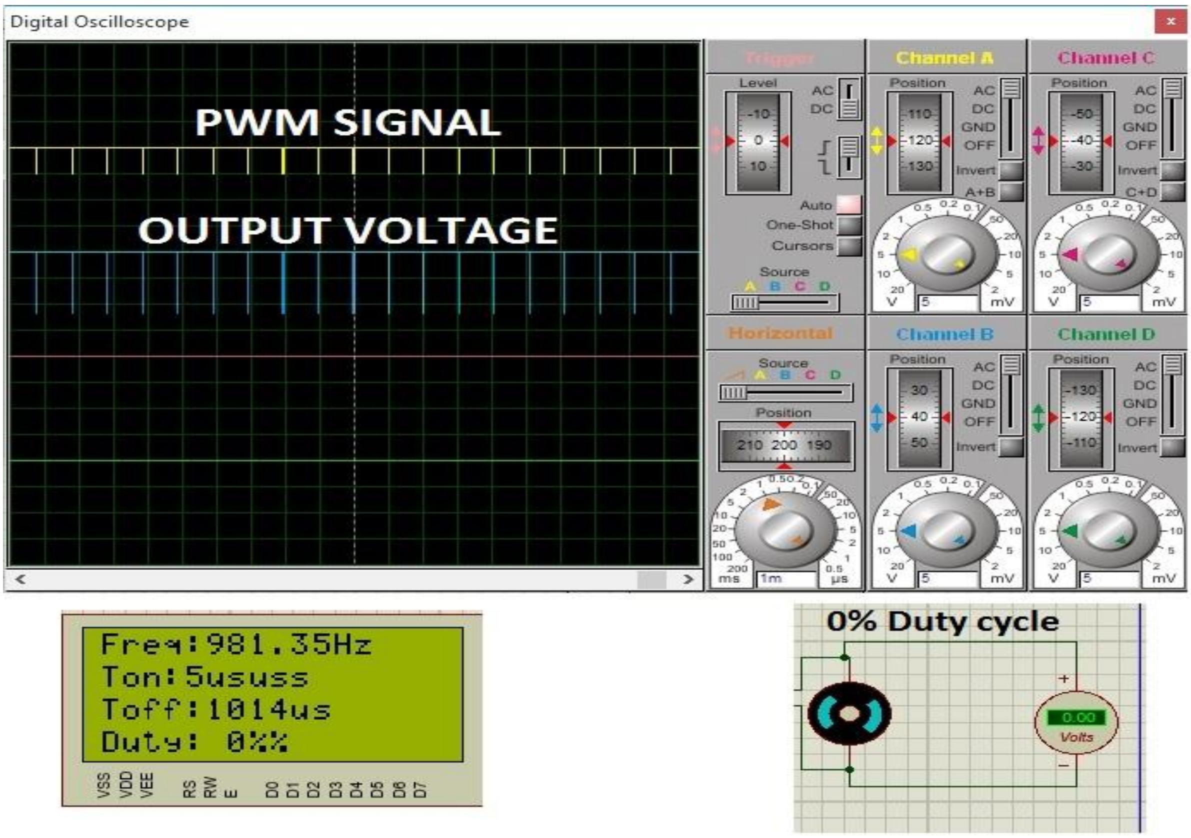

Figure 3. Figure of Motor is off at zero Duty Cycle

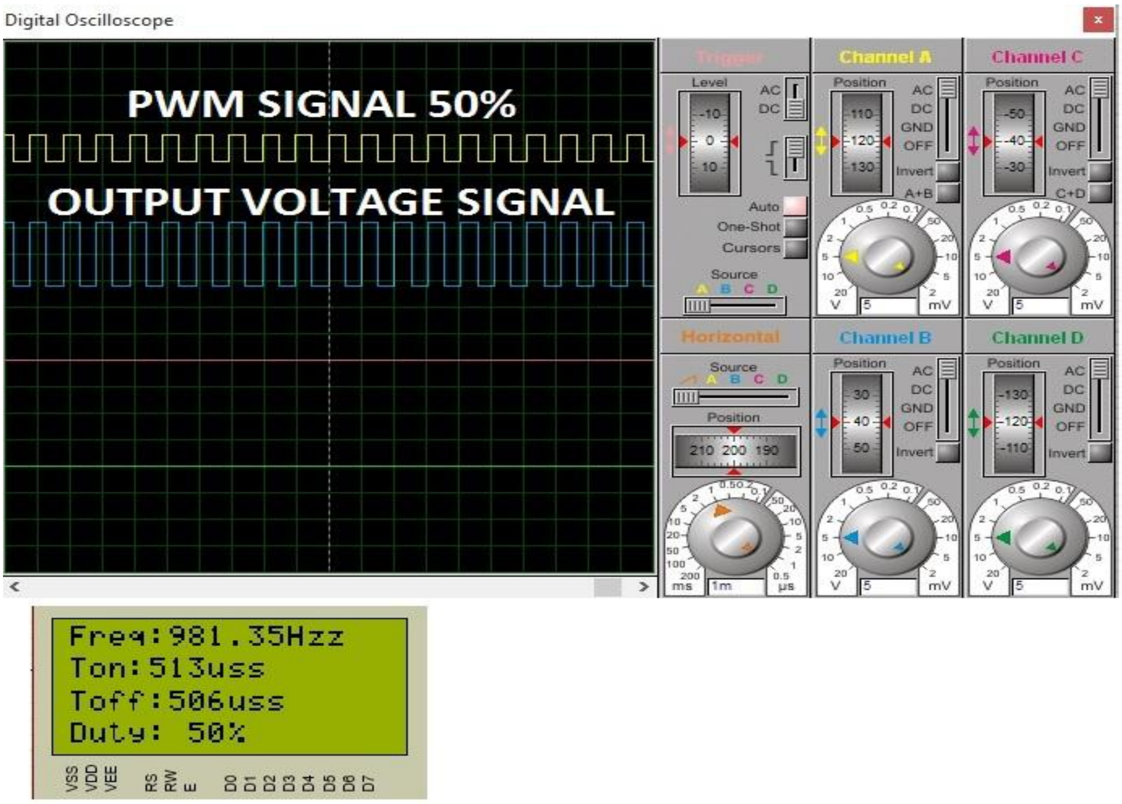

Figure 4. Figure of Motor is half on and half off at 50% Duty Cycle

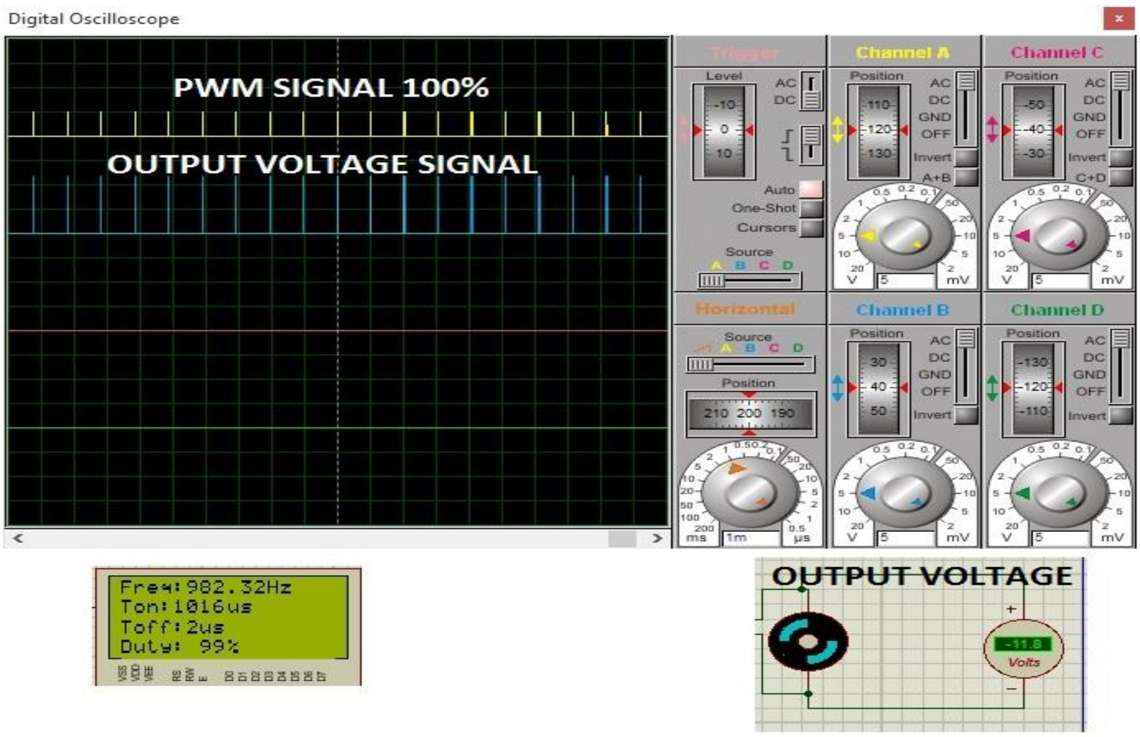

Figure 5. Figure of Motor is fully on at 100% Duty Cycle

E. Why Arduino Uno Atmega 328

Dual H-bridge Converter (L293D) Power consumption is Voltage drop = 2.6v, current = 0.6 so power loss is 1.56w.

We did not choose 8051 microcontroller and PIC microcontroller because of their high costs. System designing complexity and power losses are higher as compared to the Arduino UNO (Atmega 328) and are as given below the cost of a PIC microcontroller is Rs 200 along with pick it program burner (2000), Adapter (150) and wires/crystal/ PCB (100) due to which cost of the system will increase to $24 and

Power consumption is 3.3v, 0.5mA, 1.65mW.

While 8051 microcontroller costs are Rs. 180 along with programming kit which costs Rs. 800, an adapter that is available for Rs 150, 100 pieces of wires/crystal/PCB for about Rs 100. So, the total cost increased to $12. In addition, system designing and complexity are also complicated. Therefore, after this cost analysis, we have decided to go for ARDUINO UNO (Atmega328) Microcontroller and the cost is $6 including the adapter. The power consumption is (5V and 0.023mA) = 0.115mW.

Parameters	**8051 MICROCONTROLLERS**	**PIC-MICROCONTROLLER**	**ARDUINO UNO ATMEGA 328**
Power loss	82.5mW	1.65mW	0.115mW
Total cost	12 dollars	24 dollars	6 dollars
Libraries	Less libraries	Less libraries	Vast number of libraries
Prototype	Slow prototype	Slow Prototype	Quick Prototyping
Oscillating Crystal	External	External	Mounted on board
Programming Language	Assembly Language	C/C++	C/C++
System Design	Complex	Complex	Simple

IV. SCOPE

Converter-controlled electrical machine drives are very important in modern industrial applications. Some examples in the high-power range are metal rolling mills, cement mills, and gas line compressors. In the medium-power range are textile mills, paper mills. Machine tools and computer peripherals are examples of converter-controlled electrical machine drive applications in the low-power range. The dual H-bridge converter normally provides the variable dc output voltage i.e. 12v to change the direction of dc motor in forward and reverse direction using Atmega328 I.C mounted on Arduino UNO developing board. The drive system efficiency is high because the converter operates in switching mode using power semiconductor devices. Speed and direction rheostat of a DC motor is needed and helpful in steel industries, cement industries and paper mills etc. it plays a significant part in the atomization of aforesaid industries. This paper provides speed as well as direction control of DC motor with higher efficiency. The simulated result is synchronized with the experimental results. Owing to ease of control and wide range applications of a DC motor, it becomes inherently recommended and used machine. Besides, a DC motor also rids the mechanism from the requirement of any power circuit switching.

A. Future Work

In future, we can also employ the PID controller so as to control the speed of the motor in the efficient way.

CONCLUSION

Dual H-bridge convertor is the most efficient and effective for the sake of controlling the rotor speed and maintaining the direction of rotation of rotor in a DC motor. We have selected Atmega328 which is mounted on ArduinoUNO developing board has less power loss if we compared it with 8051 microcontroller and PIC microcontroller. In addition, the system i.e. Atmega328 (ARDUINO UNO) with LT93D H-bridge reduced the complexity of the system as well as the cost.

REFERENCE

[1] Asha K R, SuhadaTasleemP"RealS Time Speed Control of a DC motor by Temperature Variation using LabVIEW and Arduino" 2017 International Conference on Recent Advances in Electronics and Communication Technology, 16-17 March 2017

[2] Mario Gavran*, MatoFruk** and GoranVujisić" PI controller for DC motor speed realized with Arduino and Simulink" 22-26 May 2017

[3] L.Boaz1, S.Priyatharshini2 "DC Motor Direction and Speed Control byArduino through RF Wireless Technique" International Journal of Innovative Research in Computerand Communication Engineering ,Vol. 4, Special Issue 2, April 2016.

[4] Lei Zhao, ChuangyuXu, XuemeiZheng and Haoyu Li "A Dual Half-Bridge Converter with Adaptive EnergyStorage to Achieve ZVS over Full Range ofOperation Conditions" Energies Article, 28 March 2017.

[5] ShashiBhushan Kumar, Mohammed Hasmat Ali*, AnshuSinha, "Design and Simulation of Speed Control of DC Motor by Artificial Neural Network Technique" International Journal of Scientific and Research Publications, Volume 4, Issue 7, July 2014.

[6] Oun Lee, Shin-Young Cho, and Gun-Woo Moon "Phase-Shifted Dual H-Bridge Converter with a Wide ZVS Rangeand Reduced Output Filter" IEEE, 2012.

[7] Zhe Zhang and Michael A. E. Andersen "Interleaved Boost-Half-Bridge Dual–Input DC-DCConverter with a PWM plus Phase-Shift Control forFuel Cell Applications" IECON, IEEE, 2013.

[8] WasanPhetphimoon "Modeling and Simulation of Bidirectional Half Bridge DC-DC Converter" ELEKTRO, IEEE, 2016

[9] G.SUDHA1, "Performance Based Comparison Between Various Z-N Tuninng PID And Fuzzy Logic PID Controller In Position Control System Of Dc", International Journal on Soft Computing (IJSC) Vol.3, No.3, August 2012.

[10] Manoj Kushwah1 and Prof. Ashis Patra2, "Tuning PID Controller for Speed Control of DC Motor Using Soft Computing Techniques-A Review" Advance in Electronic and Electric Engineering, Volume 4, Number 2 (2014), pp. 141-148.

[11] J. C. Basilio and S. R. Matos, "Design of PI and PID Controllers With Transient Performance Specification",," IEEE Trans. Education, vol. 45, Issue No. 4, 2002, pp. 364- 370

[12] AdityaPratap Singh, "Speed Control of DC Motor using PID Controller Based on Matlab" International Conference on Recent Trends in Applied Sciences with Engineering Applications, Vol.4, No.6, 2013.

[13] Rahul Malhotra1, Narinder Singh2, Yaduvir Singh3, "SOFT COMPUTING TECHNIQUES FOR PROCESS CONTROL

APPLICATIONS” International Journal on Soft Computing (IJSC), Vol.2, No.3, August 2011.

[14] MdAkram Ahmad, PankajRai, “Speed control of a DC motor using Controllers” Automation, Control and Intelligent Systems,2014; 2(6-1): 1-9

[15] Ramesh Chandra Chourasia, Mukesh Kumar, “Speed Control of S.E.D.C. Motor by Using Pi and Fuzzy Logic Controller” International Journal of Soft Computing and Engineering (IJSCE),Volume-3, Issue-2, May 2013.

[16] J. C. Basilio and S. R. Matos,“Design of PI and PID Controllers With Transient Performance Specification”, ,” IEEE Trans. Education, vol. 45, Issue No. 4, 2002, pp. 364- 370.

[17] ShashiBhushan Kumar, Mohammed Hasmat Ali*, AnshuSinha, “Design and Simulation of Speed Control ofDC Motor by Artificial Neural Network Technique” International Journal of Scientific and Research Publications, Volume 4, Issue 7, July 2014.

[18] KapinjayUcharia, Himmat Singh, “International Journal of Scientific Engineering and Technology” Volume No.3 Issue No.3, pp : 235 – 239 1 March 2014.

[19] AdityaPratap Singh, “Speed Control of DC Motor using Pid Controller Based on Matlab” Innovative Systems Design and Engineering, Vol.4, No.6, 2013 - Selected from International Conference on Recent Trends in Applied Sciences with Engineering Applications.

[20] P. M. Meshram, Rohit G. Kanojiya “Tuning of PID Controller using Ziegler-Nichols Method for Speed Control of DC Motor” IEEE-International Conference On Advances In Engineering, Science And Management (ICAESM -2012) March 30, 31,2012 117.

Obaid Hussain Shah received the B.Sc degree from the Department of Electrical and Electronics, University of Engineering and Technology CECOS Peshawar, Khyber Pakhtunkhwa, Pakistan, in 2013.He is doing his Master from the UET Peshawar with specialization in Electrical Power. His research interests are to design and simulate the Speed and Direction Control of DC Motor Using Dual Converter Technique. His email address is obaidshah891@gmail.com.

Sohail Gul received the B Tech degree from the Department of Electrical and Electronics, University of Engineering and Technology Peshawar, Khyber Pakhtunkhwa, Pakistan, in 2009.He is doing his Master from the SARHAD University with specialization in Electrical Power. His research interests are to design and simulate the Speed and Direction Control of DC Motor Using Dual Converter Technique. His email address is sohailgul4@gmail.com.

Dr Muhammad Naeem Arbab received the B.Sc degree from the Department of Electrical and Electronics, University of Engineering and Technology Peshawar, Khyber Paktun Khwa, Pakistan, in 1989 and M.S. and Ph.D. degrees from University of Manchester, UK. He is currently a professor in Department of Electrical Engineering of UET Peshawar. His email address is mnarbab@yahoo.com

Amjad khan received the B.Sc degree from the Department of Electrical and Electronics, University of Engineering and Technology Peshawar, Khyber Pakhtunkhwa, Pakistan, in 2013.He also received Master from the same University with specialization in Electrical Power. Now he is doing PhD from the same university His research interests are in to power system Analysis, control and designing. His e-mail address is k_amjad461@yahoo.com.

International Journal of Engineering Works
ISSN-p: 2521-2419
ISSN-e: 2409-2770
Vol. 6, Issue 04, PP. 126-131, April 2019
https://www.ijew.io/

Novel Light Trapping in Thin Film Solar Cells with Nano Particles and Integrated Diffraction Grating

Fazal E Hilal[1], Adnan Daud Khan[2], Muhammad Noman[3], Fazal E Subhan[4], Mohsin Hamid[5], Aimal Daud Khan[6]
[1,2,3,4,5]University of Engineering and Technology Peshawar, Pakistan, U.S Pakistan Center for Advanced Studies in Energy (USPCAS-E)
[6]Sarhad University of Science and Information Tecnology (SUIT)
fazal.hilal@gmail.com[1], adnan.daud@uetpeshawar.edu.pk[2], muhammad.noman@uetpeshawar.edu.pk[3], fsubhan@asu.edu[4], mohsinhamid66@gmail.com[5], aimaldawoodkhan@gmail.com[6]
Received: 26 March, Revised: 03 April, Accepted: 05 April

Abstract— To over come the lower absorption of solar radiation in thin film solar cell a novel technique of combining metallic grating and metallic nano particle is presented. The increase in absorption is associated with localized surface Plasmon's resonance that depends on many factors ranging from the size of nano particle to its shape, material of nano particle, polarization of light and the medium of enviroment in which the solar cell is placed. The solar cell is designed in COMSOL Multiphysics environment which uses the numerical finite element method (FEM). The enhancement of absorption of spectral density in the solar radiation is demonstrated, theoretically. The collective oscillaton of the metallic nano particles and metallic grating produces individual electric field thus interacting with each other to produce higher modes of excitation. This collective mode supports the dark modes of nano partiles which is very useful for harnessing the long range of radiation. To reduce reflection from the top of solar cell, anti reflection coating is provided at the top whereas the back of solar cell is made of metallic reflector aluminium. The different simulations reveals that the antireflection coating has negligent effect on the absorption of solar cell by using the integrated structure of metallic grating and nano particles. Moreover, this approach is suited for thin film solar cell which will absorb more radiations due to the multiple peaks in the spectrum of the aforementioned proposed structure.

Keywords— Thin Film Solar Cells, Light Trapping, Anti Reflective Coating, Localized Surface Plasmon Resonance, Nano Particles, Grating.

I. INTRODUCTION

Photovoltaic (PV) is the process of converting light into electricity by utilizing solar cells. When light strikes a semiconductor material, photons are absorbed inside the semiconductor and create electron-hole (e-h) pairs which are directed to negative and positive terminals of the cell. Photovoltaic impact was first discovered by a French physicist, Becquerel, in 1839, while conducting various experiments using metal cathodes in an electrolyte. In 1877, Adams and Day concluded that the emanated selenium anodes produced electricity. In 1904, Albert Einstein clarified the hypothesis of the marvel behind PV impact, which was tentatively demonstrated by Robert Millikan in 1916. Decades after revelation of Jan Czochralski's technique to develop mono crystalline silicon, in 1954, Bells' research center designed designing the first crystalline silicon solar cell with 6% efficiency. In early days, solar cell efficiency was very low because of a lesser amount of absorption of light and amount of reflected light from the solar cell. To overcome these problems antireflection coating (ARC) was used, but it also contained many shortcomings. The concept of surface texturing was bobbed up as a result, which further enhanced the efficiency of solar cells.

In the last decade, many ligh-trapping strategies have been explored, among which a run of the mill case is utilizing a pyramidal surface texture [1]. But, such technique is feasible for solar cells which have thicker light absorber layer than the spectrum of visible light. The enhanced light catching is adjusted by the surface roughness. It is almost an indistinguishable request from the film width and by the enhanced surface recombination, because of the bigger surface area. Lately, much consideration has been given to light coupling in solar cells with the plan of improving absorption and henceforth photogeneration inside the cell [2,3]. Empowering light catching into the light absorbing layer solar cell having less width and has reliably drawn an expanding measure of consideration. Nanostructures made of metals, which support surface plasmons are employed nowadays [4]. Electron motions which proliferate along the border amid a metal and a semiconductor or dielectric material, is known as surface plasmons. In addition, electromagnetic field is unequivocally bound at the metal/dielectric or semiconductor edge, with their power having an exponential reliance on the separation far from the interface by surface plasmons. In this manner, through excitation of SPs, near-field electromagnetic field boosting and the upgraded scattering cross area (SCS) can be attained [14-21]. Larger electrical field will lead to more absorption and a bigger SCS will divert the falling sunlight amount into the retaining layer. These two things will bring about a substantially more light retention in a considerably more slender semiconductor layer. Thus, both restricted or localized surface plasmons (LSPs) are [5] energized in metallic nanoparticles and surface plasmon polarizations (SPPs) [6] proliferating at the occasional metal/semiconductor boundaries have been so far generally examined with zealous interests in making high efficient thin film solar cells [7-10] Due to less consumption of the absorber material the thin film solar cell can overcome the high cost of solar cells. Thus it can be considerd as a cheaper renewable energy resource which can contribute significantly to the energy mix of the world [11,12, 13,22].

The longer wavelength radiations require more diffusion depth in order to be absorbed in the solar cell. Thin film has less absorber material and thus it has small diffusion length. So,the longer wave length radiations are transmitted therein rather than absorption which leads to absorption loss of the radiations. To overcome the smaller diffusion length of thin film solar cell, light trapping techniques and light management are highly encouraged. Conventional technique like texturing is not suitable for thin film solar cell because the thickness of the thin film solar cell is few microns. However, texturing also require the removal of few micron materials which will be horrible scenario for TFSC and will lead to the stability issues of the solar cells [23]. The anti reflection coating (ARC) can be replaced by novel nano materials which can further enhance the absorption of solar cell by local surface plasmon resonance leading to the broad band spectrum of the solar cell [24-26]. Owing to uni-sepctral property of ARC, it can not completely prevent the reflection and transmission through the absorber layer of solar cell, which is very thin in case of thin film solar cell. The operational band of TFSC can be tuned using surface Plasmon resonance (LSPR). Moreover, the LSPR depends on the following properties of the nano material.

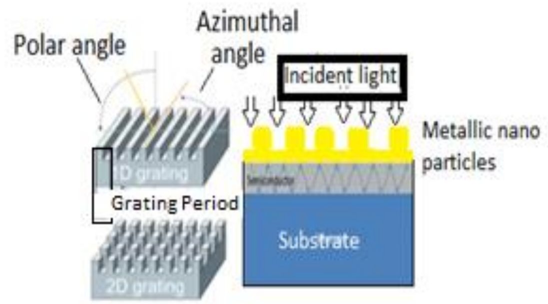

Figure 1. Left side Grating and right side metallic nano particles on top of solar cell

- Size, shape and number of the nano particles
- Distance between nano particles
- Refractive idex of environment around the solar cell
- Material of absorber layer in the solar cell
- Polarization of incident radiation

The grating period and the thickness of the grating material also influence the absorption of radiation in solar cell. The grating period and nano particles on the top of solar cell is shown in Figure 1. In this paper, we used the approach of combing metallic nano particles and metallic grating to enhance the absorption of silicon solar cell. There are many parameters which govern the tuning of the surface plasmon resonance to the operational bandwidth of thin film solar cell. The individual dimensions of the metallic nano structure have been considered herewith. Also, the individual grating period of the metallic grating and the grating structure dimension are stated. After that, the optimized structure, metallic nanostructure and grating are selected. Lastly, the grating and nanoparticles are coupled."

II. LITERATURE REVIEW

Solar power is free and clean wellspring of endless power that can be collected to help the energy shortage on planet earth. Solar cells have lower efficiency, which is a major obstacle in its way. An extensive research is conducted in this field to expand the proficiency of Solar PV modules to its hypothetical cut-off, given by Shockley-Quiesser. When sunlight interact with PV module, the first loss occurs at the front glass surface, that is reflection which is around 8-9% of the total light, which implies that even 8-9% of the light does not enter the PV panel. To limit reflection losses, diverse arrangements were proposed by various analysts. Reflection from glass Surface of PV panel can be limited by either surface texturing that creates roughness in the surface, which helps in the trapping of light, or by utilizing antireflective coatings [27]. Needle-like structures on melded silica substrate were made by Park et al [28] that showed a wide antireflective impact with a normal transmittance of 98.5%. Similarly, a surface was made by texturing and accomplished a normal transmittance of 94.4% by Son et al [29]. However, these procedures include various advances, are costly, and don't promptly scale to substantial substrates. Different size layers of silica particles on top were kept individually on double layer TiO2 and SiO2 antireflection coating (ARC) by Watanabe et al [30]. These layers were of 100nm, 200nm and 300nm. The small layer molecule covering that is 100nm demonstrated increase in efficiency of 7.1 % as compared to double covering alone. Composite films of zinc sulfide and magnesium fluoride were sputtered by Jung et al [31] on three layer anti reflection coating of gallium arsenide substrate and the improvement in efficiency was achieved. Lesser absorption of light is a major drawback in thin film solar. This problem is encountered especially at larger wavelengths and henceforth, effective light trapping designing is required [32]. The other approach for light absorption upgrade is to limit the reflection from the top surface that can be accomplished by progressive difference in refractive index, called reflectivity. Total internal reflection (TIR) can confine light inside the solar cell. On the off chance, that light is totally randomized into the solar cell, the mean path length of light within the cell material an be improved by a factor of 4n2, where n represents the refractive index of the medium in which light is trapped [33]. To start with thoughts to utilize the diffractive properties of gratings for light trapping in solar cells were planned by Sheng [34]. Plasmonics was intended for collective oscillation of the free electrons gas density by David Pines in 1956 [35]. In plasmonics, interaction of light and nano size metals particles are studied. During last five years or in the previous couple of years, plasmonics has been shown widely in solar cell applications; in any case, the idea of light absorption boost because of the scattering properties of little metal nanoparticles (MNPs) supporting surface plasmons was just presented with the 1998 spearheading work of Stuart [36]. Thin film solar cell perfomance can be enhanced by light trapping prompting decrease of the material utilization took after by the cost of green power generation [37,38]. Thin film plasmonic solar cells (TFSC) has three advantages due to three independent impacts: expanded semiconductor assimilation (enhanced Jsc), diminished non-raditative recombination (enhanced Voc), and diminished sheet resistance (enhanced FF) [39]. By introducing metallic resonators in solar cells higher excitation modes can be obtained which can also increase the bandwidth capacity of the MPAs. The response of every resonator is specific for a specific frequency and does not depend on the response of other resonators [40,41]. To keep away from expanded manufacture costs, straightforward templating strategies and less expensive metals like copper and Aluminium ought to be considered for substantial scale selection of these ideas. Localized surface plasmon resonance is caused by the metallic grating structure because it is energized when strike by photons. The optical path length of photons in the absorbing layer is delayed which leads to greater absorption [42-45]. Another type of solar cell based on Gallium arsenide by fusing a nanoparticles of silver in a periodical way was designed by Hong et al [46] wherein they observed improved light absorption because of the surface plasmon actuated by metal nanoparticles. As compared to planar solar cells, gallium arsenide based solar cells can bring about 31 % change in short-circuit current. By plasmonic back grating, more than 80% of the incident radiation above bandgap of GaAs using layer of just 200 nm can be achieved. The change in the open circuit voltage is obtained by decreasing the bulk recombination current when the solar cell becomes very thin. Providing the condition that open circuit voltage ramps more quickly than the short circuit current falls so thinner layers will deliver more productive cells. The fill factor is enhanced by the consolidation of metallic scatters which diminish the sheet resistance of a top surface-passivating layer [47].

A. Photonics

Photonics is the branch of physics which deals with the interaction of light and matter, while, plasomonic is the interaction of electromagnetic wave with metallic nano particles. In this research paper, effect of surface plasmon resonance on the absorption of light in solar cell is observed. Surface plasmon resonance (SPR) is observed due to the interaction of light and metallic nano particles. Noble elements like gold (Au), silver (Ag), copper (Cu), aluminium(Al) can generate surface plasmon resonance and can absorb more light in solar cell by scattering and absorbing more light [48]. Surface plasmon resonance depends on the geometry of nano particles, the medium surrounding the solar cell and the nano particle and the polarization of the incoming radiation. The plasmon resonance also depends on the number of electrons present in the nano particle. So, the electronic densities of different elements are different. Therefore, aluminium, silver, gold and copper will have different shape of surface and amplitude of surface plasmon resonance. Gold (Au) nano particles are suitable for the visible range of spectrum, aluminium and silver nano particles are suitable for the ultra-violet region while copper support surface plasmon resonance in the visible range [49]. If LSPR is shifted towards the blue region of spectrum, then the absorption of light in solar cell is significantly ameliorated [50].

B. Higher-Order Modes Excitation for Enhanced Absorption

The energy of photons can also be trapped in the absorber layer of solar cell by exciting darker modes of the nano particles which are placed at the solar cell. This can be achieved either by symmetry breaking of the nano particle or placing the nano particles in the form of cluster. There are two modes of the interaction of light with different materials. The one is the bright mode and the other is darker mode. So each nano particle and the material of solar cell will have different modes of bright and dark modes. The interaction of bright mode of the nano particle with the dark mode of solar cell material will excite the dark mode of solar cell material. Thus, this process can excite the higher modes that will lead to field enhancement of the nano particle and hence absorption of the solar cell will be improved that will result into the better current density of the solar cell [51,52]. By placing nano particles in cluster or in array form on the solar cell will lead to more Raman scattering that will also excite the dark modes resulting into higher absorption of photons [53,54].

Symmetry breking of the nano particle and the absorber layer can also excite the dark modes. The electron distribution of nano particle is disturbed, when the symmetry of nano particles is broken. Therefore, the interaction of the resulted nano particle with light will be different. Surface plasmon resonance in the desired range of spectrum can be achieved by manipulating the symmetry of nano particle [55].

III. SIMULATION MODEL

A silicon solar cell is made silicon solar cell having thickness of absorber layer 300 nm, silicion dioxide layer 40 nm and gold reflector 40 nm respectively. After this simple block shape metallic grating and metallic nano particle of spherical shape are introduced separately in the solar cell. The effect of these structures for different dimensions of metallic grating and nano particles is investigated individually. In the last simulation, the effect of both metallic gratting and metallic nano structure on absorption enhancement is explored. The different size of grating and nano particle is selected such that one can easily calculate the best case scenario for both structures. The enhanced absorption is given by

$$\bar{\mathbf{A}}\ (\boldsymbol{\lambda}) = \mathbf{P}_{\text{ABS-Silicon}}(\boldsymbol{\lambda})\ /\ \mathbf{P}_{\text{Source}}(\boldsymbol{\lambda}) \tag{1}$$

Where,

$P_{Source}(\lambda)$ = Incident power from the sun source of photon flux having air mass (AM) 1.5G,

$P_{ABS\text{-}Silicon}$ (λ) = Power absorbed in the silicon solar cell while λ is the wavelength of the surrounding medium of the solar cell's environment.

The above equation tells about how much the additional structure introduced in the solar cell has scattered the light and how much light is absorbed in the active region. For finding the power which is absorbed in the bulk region of the absorber layer with improved matching between thin film of silicon and air the equation (I) takes the form

$$\bar{A}_{Silicon}(\lambda) = P_{Trans\text{-}silicon}(\lambda) \,/\, P_{Source}(\lambda) \qquad (2)$$

Where,

$P_{Trans\text{-}silicon}(\lambda)$ = Power that passes from the geometry of nanostructures placed at the top of solar

and $P_{Source}(\lambda)$ = Incident power from the sun source of photon flux having air mass(AM) 1.5G,

IV. Results and Discussion

The model we suggested has a back reflector made of gold which help the solar cell to over come the transmission losses and improve the absorption efficiency of solar cell.

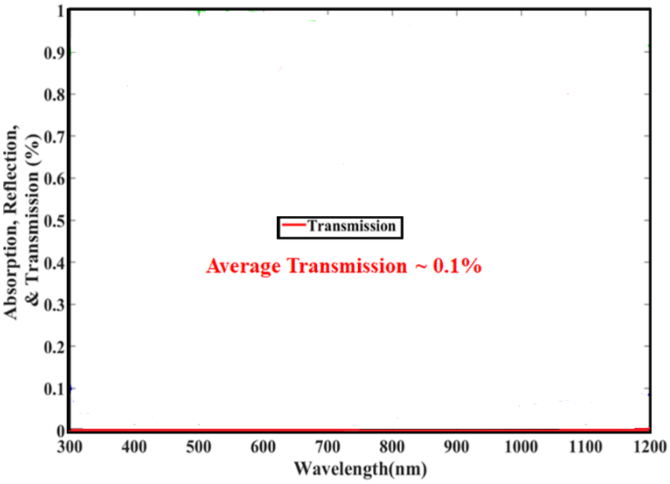

Figure 2. Approximately zero transmission due to Gold reflector

The diferent size of spherical nano particles when palced at the top of solar cell has different absorption efficiencies. The larger the size of nano particle, more will be the efficiency of absorpting solar radiation. When more than one nano particle is placed at the top of solar cell then there will be more absorption of light. The absorption is further improved when the distance between nano particles is reduced which is due to the fact that there will be the interaction of fields of the light absorbing nano particles and hence will lead to near field enhancement. The spherical shape of nano particle is taken because of its ability of not depending or very less dependence on the polarization of electro-magnetic radiation.

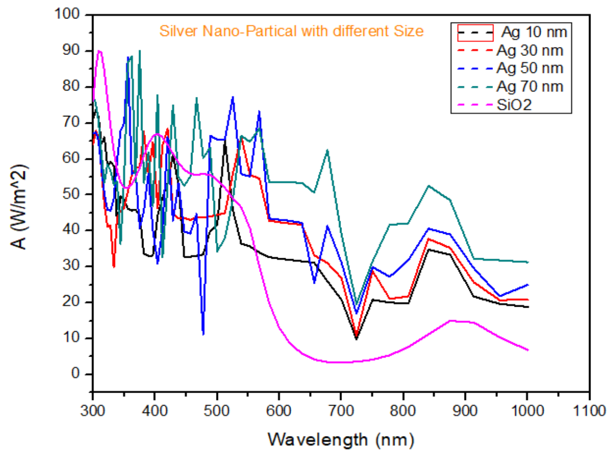

Figure 3. Silver nano particles of different raddi

Materials for nano particles having spherical shape of silver and gold has separately tested in the simulations. Both materials show higher absorption than the solar cell that has only anti reflective coating of silicon dioxide. When the size of the silver nano particle is increased then the absorbtion is also increased which can be noted from figure 3.

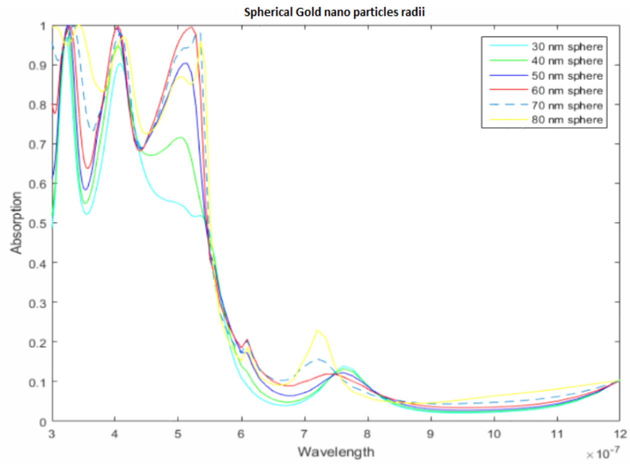

Figure 4. Gold nano particles of different raddi

The size of gold nano particle relation versus absorption is shown in Figure 2. Both Figure 3 and Figure 4 shows the dependence of absorption of electromagnetic waves on the size of nano particle.When both nano particles and grating are introduced at the top of solar cell then the absorption is surpassed than that of the individual nano particles imparted in the solar cell and the grating applied at the top of solar cell which is shown in Figure 5.

By reducing the distance between nano particles and the grating structures the absorption is further improved. Grating and nano particle made of gold lead to more absorption than that of aluminnium grating and nano particles. Also, in the Figure 5, it is shown that the more nano particles integrated with the grating will lead to further enhance absorption. The sky blue line is of grating and 2 spherical nano particles which are all made of gold shows less absorption than the dark blue grating and 6 spherical nano particles that are all made of gold. Furthermore, grating and 6 spherical nano particles made of aluminium also shows more enhanced absorbtion than that of separate nano particles.

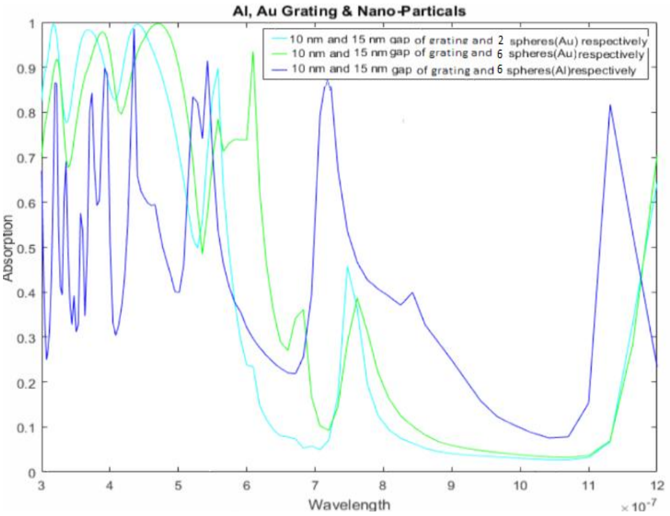

Figure 5. Integrated Grating and Spherical nano particles

CONCUSLION

The novel idea of integrating nano particles and metallic grating in solar cell provides better absorbtion of light than solar cells which have only nano particles or grating in them for light absorption. By changing the materials of nano particles, the spacing between them and size of each individual nano particle we can excite the spectrum of our interest in solar cell that will lead to better absorption of light.

REFERENCES

[1] M. Green, "Lambertian light trapping in textured solar cells and light-emitting diodes: analytical solutions", Progress in Photovoltaics: Research and Applications, vol. 10, no. 4, pp. 235-241, 2002.

[2] H. Atwater and A. Polman, "Plasmonics for improved photovoltaic devices", Nature Materials, vol. 9, no. 3, pp. 205-213, 2010.

[3] V. Ferry, J. Munday and H. Atwater, "Design Considerations for Plasmonic Photovoltaics", Advanced Materials, vol. 22, no. 43, pp. 4794-4808, 2010.

[4] W. Barnes, A. Dereux and T. Ebbesen, "Surface plasmon subwavelength optics", Nature, vol. 424, no. 6950, pp. 824-830, 2003.

[5] C. Rockstuhl, S. Fahr and F. Lederer, "Absorption enhancement in solar cells by localized plasmon polaritons", Journal of Applied Physics, vol. 104, no. 12, p. 123102, 2008.

[6] H. Lu and W. Wang, "Surface plasmon resonance absorption of composite films doped with metal nanoparticles", Optical Engineering, vol. 56, no. 6, p. 067110, 2017.

[7] X. Li, "Plasmonic nanostructures for custom photonic devices", SPIE Newsroom, 2014.

[8] P. Spinelli and A. Polman, "Light Trapping in Thin Crystalline Si Solar Cells Using Surface Mie Scatterers", IEEE Journal of Photovoltaics, vol. 4, no. 2, pp. 554-559, 2014.

[9] C. Fei Guo, T. Sun, F. Cao, Q. Liu and Z. Ren, "Metallic nanostructures for light trapping in energy-harvesting devices", Light: Science & Applications, vol. 3, no. 4, pp. e161-e161, 2014.

[10] H. Tran, V. Nguyen, B. Nguyen and D. Vu, "Light trapping and plasmonic enhancement in silicon, dye-sensitized and titania solar cells", Advances in Natural Sciences: Nanoscience and Nanotechnology, vol. 7, no. 1, p. 013001, 2016.

[11] Chu, Steven, and Arun Majumdar. "Opportunities and challenges for a sustainable energy future." nature 488.7411 (2012): 294.

[12] Kamat, Prashant V. "Meeting the clean energy demand: nanostructure architectures for solar energy conversion." The Journal of Physical Chemistry C 111.7 (2007): 2834-2860.

[13] Serrano, Elena, Guillermo Rus, and Javier Garcia-Martinez. "Nanotechnology for sustainable energy." Renewable and Sustainable Energy Reviews 13.9 (2009): 2373-2384

[14] Senthil Kumar, N., et al. "Green mediated synthesis of plasmonic nanoparticle (Ag) for antireflection coating in bare mono silicon solar cell." Journal of Materials Science: Materials in Electronics (2018): 1-10.

[15] Heidarzadeh, Hamid, et al. "Plasmon-enhanced performance of an ultrathin silicon solar cell using metal-semiconductor core-shell hemispherical nanoparticles and metallic back grating." Applied optics 55.7 (2016): 1779-1785.

[16] Al-Adhami, Yasir, and Ergun Ercelebi. "A Plasmonic Monopole Antenna Array on Flexible Photovoltaic Panels for Further Use of the Green Energy Harvesting." Progress in Electromagnetics Research 68 (2018): 143-152.

[17] Jiao, Hongfei, et al. "Ultra-broadband perfect absorber based on successive Nano-Cr-film." Advances in Optical Thin Films VI. Vol. 10691. International Society for Optics and Photonics, 2018.

[18] Saravanan, S., et al. "Efficiency improvement in dye sensitized solar cells by the plasmonic effect of green synthesized silver Nano-particles." Journal of Science: Advanced Materials and Devices 2.4 (2017): 418-424.

[19] Sakir, Menekse, et al. "Fabrication of Plasmonically Active Substrates Using Engineered Silver Nanostructures for SERS Applications." ACS applied materials & interfaces 9.45 (2017): 39795-39803.

[20] Katyal, Jyoti, and R. K. Soni. "Localized surface Plasmon resonance and refractive index sensitivity of metal–dielectric–metal multilayered nanostructures." Plasmonics 9.5 (2014): 1171-1181

[21] Ge, Lixin, et al. "Unidirectional scattering induced by the toroidal dipolar excitation in the system of plasmonic nanoparticles." Optics Express 25.10 (2017): 10853-10862.

[22] N.-N. Feng, J. Michel, L. Zeng, J. Liu, C.-Y. Hong, L. C. Kimerling, and X. Duan, "Design of Highly Efficient Light-Trapping Structures of Thin-Film Crystalline Silicon Solar Cells," IEEE Trans. Electron. Dev. 54(8), 1926–1933 (2007).

[23] H. Sai, Y. Kanamori, K. Arafune, Y. Ohshita, and M. Yamaguchi, "Light trapping effect of submicron surface textures in crystalline Si solar cells," Prog. Photovoltaics 15(5), 415–423 (2007).

[24] V. E. Ferry, M. A. Verschuuren, H. B. T. Li, E. Verhagen, R. J. Walters, R. E. I. Schropp, H. A. Atwater, and A. Polman, Light trapping in ultrathin plasmonic solar cells, Opt. Express 18, A237 (2010).

[25] V.Ferry,L.Sweatlock,D.Pacifici,andH.Atwater,Plasmonicnanostructured esign for efficient light coupling into solar cells, Nano Lett. 8, 4391 (2008).

[26] V. E. Ferry, J. N. Munday, and H. A. Atwater, Design considerations for plasmonic photovoltaics, Adv. Mater. 22, 4785 (2010)

[27] D. Bouhafs, "Design and simulation of antireflection coating systems for optoelectronic devices: Application to silicon solar cells", Solar Energy Materials and Solar Cells, vol. 52, no. 1-2, pp. 79-93, 1998.

[28] K. Park, H. Choi, C. Chang, R. Cohen, G. McKinley and G. Barbastathis, "Nanotextured Silica Surfaces with Robust Superhydrophobicity and Omnidirectional Broadband Supertransmissivity", ACS Nano, vol. 6, no. 5, pp. 3789-3799, 2012

[29] J. Son, S. Kundu, L. Verma, M. Sakhuja, A. Danner, C. Bhatia and H. Yang, "A practical superhydrophilic self cleaning and antireflective surface for outdoor photovoltaic applications", Solar Energy Materials and Solar Cells, vol. 98, pp. 46-51, 2012.

[30] T. Yang, X. Wang, W. Liu, Y. Shi and F. Yang, "Double-layer anti-reflection coating containing a nanoporous anodic aluminum oxide layer for GaAs solar cells", Optics Express, vol. 21, no. 15, p. 18207, 2013

[31] Jung, S., Kim, Y., Kim, S. and Yoo, S. (2011). Design and fabrication of multi-layer antireflection coating for III-V solar cell. Current Applied Physics, 11(3), pp.538-541

[32] Saravanan, S. and Dubey, R. (2017). Grating influence study of GaAs solar cell structures. Nanosystems: Physics, Chemistry, Mathematics, pp.503-506.

[33] T. Markvart, "Beyond the Yablonovitch limit: Trapping light by frequency shift", Applied Physics Letters, vol. 98, no. 7, p. 071107, 2011

[34] Y. Shi, X. Wang, W. Liu, T. Yang and F. Yang, "Light-absorption enhancement in thinfilm silicon solar cells with front grating and rear-located nanoparticle grating", physica status solidi (a), vol. 212, no. 2, pp. 312-316, 2014.

[35] S. Castelletto and A. Boretti, "Noble Metal Nanoparticles in Thin Film Solar Cells", Nanoscience and Nanotechnology Letters, vol. 5, no. 1, pp. 36-40, 2013.

[36]] C. Joshi, Y. Shim, T. Bigioni and J. Amar, "Critical island size, scaling, and ordering in colloidal nanoparticle self-assembly", Physical Review E, vol. 90, no. 3, 2014.

[37] A. Baca, M. Meitl, H. Ko, S. Mack, H. Kim, J. Dong, P. Ferreira and J. Rogers, "Printable Single-Crystal Silicon Micro/Nanoscale Ribbons, Platelets and Bars Generated from Bulk Wafers", Advanced Functional Materials, vol. 17, no. 16, pp. 3051-3062, 2007

[38] J. Yoon, A. Baca, S. Park, P. Elvikis, J. Geddes, L. Li, R. Kim, J. Xiao, S. Wang, T. Kim, M. Motala, B. Ahn, E. Duoss, J. Lewis, R. Nuzzo, P. Ferreira, Y. Huang, A. Rockett and J. Rogers, "Ultrathin silicon solar microcells for semitransparent, mechanically flexible and microconcentrator module designs", Nature Materials, vol. 7, no. 11, pp. 907-915, 2008.

[39] W. Chen, A. Cardin, M. Koirala, X. Liu, T. Tyler, K. West, C. Bingham, T. Starr, A. Starr, N. Jokerst and W. Padilla, "Role of surface electromagnetic waves in metamaterial absorbers", Optics Express, vol. 24, no. 6, p. 6783, 2016.

[40] G. Wang, M. Liu, X. Hu, L. Kong, L. Cheng and Z. Chen, "Multi-band microwave metamaterial absorber based on coplanar Jerusalem crosses", Chinese Physics B, vol. 23, no. 1, p. 017802, 2014

[41] S. Liu, J. Zhuge, S. Ma, H. Chen, D. Bao, Q. He, L. Zhou and T. Cui, "A bi-layered quad-band metamaterial absorber at terahertz frequencies", Journal of Applied Physics, vol. 118, no. 24, p. 245304, 2015.

[42] C. Sun and X. Wang, "Efficient Light Trapping Structures of Thin Film Silicon Solar Cells Based on Silver Nanoparticle Arrays", Plasmonics, vol. 10, no. 6, pp. 1307-1314, 2015.

[43] S. Saravanan, R. Dubey, S. Kalainathan, M. More and D. Gautam, "Design and optimization of ultrathin crystalline silicon solar cells using an efficient back reflector", AIP Advances, vol. 5, no. 5, p. 057160, 2015.

[44] Sangjun Lee and Sangin Kim, "Optical Absorption Characteristic in Thin a-Si Film Embedded Between an Ultrathin Metal Grating and a Metal Reflector", IEEE Photonics Journal, vol. 5, no. 5, pp. 4800610-4800610, 2013.

[45] L. Zhu, M. Shao, R. Peng, R. Fan, X. Huang and M. Wang, "Broadband absorption and efficiency enhancement of an ultra-thin silicon solar cell with a plasmonic fractal", Optics Express, vol. 21, no. 3, p. A313, 2013.

[46] L. Hong, Rusli, X. Wang, H. Zheng, L. He, X. Xu, H. Wang and H. Yu, "Design principles for plasmonic thin film GaAs solar cells with high absorption enhancement", Journal of Applied Physics, vol. 112, no. 5, p. 054326, 2012.

[47] D. Bouhafs, "Design and simulation of antireflection coating systems for optoelectronic devices: Application to silicon solar cells", Solar Energy Materials and Solar Cells, vol. 52, no. 1-2, pp. 79-93, 1998

[48] Ferry, Vivian E., et al. "Light trapping in ultrathin plasmonic solar cells." Optics express 18.102 (2010): A237-A245.

[49] Catchpole, KR and, Albert Polman. "Plasmonic solar cells." Optics express 16.26 (2008): 21793- 21800.

[50] Temple, T. L., et al. "Influence of localized surface Plasmon excitation in silver nanoparticles on the performance of silicon solar cells." Solar Energy Materials and Solar Cells 93.11 (2009): 1978-1985.

[51] Dodson, Stephanie, et al. "Optimizing electromagnetic hotspots in plasmonic bowtie Nano antennae." The journal of physical chemistry letters 4.3 (2013): 496-501.

[52] Katyal, Jyoti, and R. K. Soni. "Localized surface Plasmon resonance and refractive index sensitivity of metal–dielectric–metal multilayered nanostructures." Plasmonics 9.5 (2014): 1171-1181.

[53] Sakir, Menekse, et al. "Fabrication of Plasmonically Active Substrates Using Engineered Silver Nanostructures for SERS Applications." ACS applied materials & interfaces 9.45 (2017): 39795-39803.

[54] Roelli, Philippe, et al. "Molecular cavity optomechanics as a theory of plasmon-enhanced Raman scattering." Nature nanotechnology 11.2 (2016): 164-169.

[55] Katyal, Jyoti, and R. K. Soni. "Localized surface Plasmon resonance and refractive index sensitivity of metal–dielectric–metal multilayered nanostructures." Plasmonics 9.5 (2014): 1171-1181.

Fazal E Hilal received B.Sc. degree in Electronics Engineering from the University of Engineering and Technology (UET) , Peshawar, Pakistan, in 2016. He is currently perusing his Master degree in Renewable Energy Engineering from U.S Pakistan Center for Advanced Studies in Energy, UET, Peshawar, Pakistan.
His research interests includes optoelectronic modeling of photovoltaic devices, photonics nano-technology for light management in third generation solar cell, renewable energy materials & technology modeling, smart grid and power electronics.

IJEW 国际工程期刊 International Journal of Engineering Works انجینئرنگ کاموں کا بین الاقوامی جرنل

International Journal of Engineering Works
ISSN-p: 2521-2419
ISSN-e: 2409-2770
Vol. 6, Issue 04, PP. 132-142, April 2019
https://www.ijew.io/

Productive Lithology Discrimination in Structurally Complex Area by Means of AVO/AVA Synthetics and Petrophysical well log Analysis, A Case Study from Khipro Block, Southern Indus Basin, Pakistan

Manaf Muhammad[1], Haris Ahmad Khan[2], Shaukat Khan[3], Faisal Rehman[4]
[1,3,4]Department of Earth Sciences, University of Sargodha, Sargodha, Pakistan
[2]Department of Earth Sciences, Bahria University, Karachi, Pakistan
faisal.rehman@uos.edu.pk[4]

Received: 15 February, Revised: 07 March, Accepted: 02 April

Abstract**—**In this study, AVO/AVA Synthetics and petrophysical well log analysis was carried out to discriminate between the reservoir and non-productive lithology for two wells Naimat Basal 01 & Siraj South-01. Synthetic AVO/AVA traces of Naimat Basal 01 & Siraj South-01 were generated. The behavior of the theoretical and NMO corrected synthetics for Naimat Basal 01 has a weak response, while Siraj South-01 indicated a clear sharp anomaly. AVA synthetic created for well Naimat Basal-01 and Siraj South-01 using Zoeppritz equation clearly indicated amplitude variations. On the basis of AVO/AVA anomalies petrophysical well log analysis was carried out for Naimat Basal-01 from 2600-3550 m depth. The two zones interval 3395m- 3411m and 3480m-3497m were studies in detail which confirmed the results obtained from AVO/AVA synthetics and 3395-3411m and 3480-3497m may be good reservoir zone for the hydrocarbon accumulation.

Keywords**—** AVO/AVA Synthetics, Petrophysics, Reservoir Evaluation.

I. INTRODUCTION

Basic AVO theory is widely used as a tool in lithology identification, hydrocarbon detection, and fluid parameter analysis, by means of basis that seismic amplitudes across the interfaces are influenced by the difference in the physical characteristics immediately above and below the interface [1-2]. The dissimilarity in transmission and reflection coefficients with an increase in offset and angle of incidence (AVA) is often referred to as offset-dependent reflectivt property and primary root for amplitude-versus-offset (AVO) analysis. Conventional AVO (amplitude variation with offset) analysis is based on the well-known Knott-Zoeppritz equations [3-4]. Shear velocity measurements are essential since AVO seeks to employ the elastic nature of seismic wave propagation. Measurements of very slow shear waves using Dipole source shear logging increases the range of applicability and possibility for greater reliability in AVO interpretation [5]. The offset is a simple function of angle in relatively simple geologic settings, however, a more rational V (z,m) will make a complex relation Between offset and incidence angle. In such cases, amplitude variation with an angle (AVA) is a preferable alternative to AVO analysis [6]. The modeling exercises provide valuable information on how to obtain a better fit with the measured data (iterative method with perturbation of the reservoir/seal properties). Data with different sample support should be integrated properly, with appropriate up- and down-scaling [7].

AVO analysis is commonly used in hydrocarbon exploration being considered as potent demarcation tool for lithologies and type of fluid present in within the reservoir achieved by investigating the Primary wave reflections output at the interface of the target zone and adjoining sediment [8]. We must also realize that AVO models are highly susceptible to small changes in the input parameters, in particular, Poisson's ratio. And unfortunately, Poisson's ratio is one of the parameters we know the least about.

The third cause for concern is the Domenico effect-a small amount of gas has almost the same effect on amplitude as does a large amount of gas. Therefore, when we see an increase or decrease in amplitude due to the presence of gas, we generally cannot predict the quantity of gas present.

Another limitation to the method is the homogeneity of the model, both laterally and vertically, versus the in homogeneity of the subsurface. We naturally would like every relationship between an AVO response and a rock property to be linear and unique, but this is not often the case.. Thus, using a single velocity versus density trend for the shale in the model did not reflect the true complexity of the area. Another reason for the failure of the "AVO response for a sand package depends not only on the degree of shaliness but also the shale distribution within the sand package" [9].

The fundamental objective of the evaluation of petrophysical parameters is to arrive at accurate estimates of in-situ permeability and porosity in which measurement of these parameters is impossible. In such cases, the values for these parameters can be determined through petrophysical correlations with those in similar oil reservoirs to be used in combination with information on their formation lithology in order to evaluate their average hydrocarbon saturation percentage and their approximate reserve volume. The adverse effects of estimation errors cause higher venture risks and therefore the need for an estimation method that guarantees the minimum estimations errors possible [10-11].

Evaluation of oil reservoirs and their portrayal are crucial tools in the oil industry, especially for the appropriate discovery of reservoirs and their economic assessment. Parameters such as porosity, permeability, and formation structure are amid the most key features of reservoirs whose fortitude is difficult, more complications being introduced into the process by their heterogeneity. Functional management strategies can only be effective when the detailed spatial distribution of the reservoir petrophysical parameter is available [12].

In clastic reservoir during the evaluation, the occurrence of shale or clay within the sand is a factor to be judged precisely. The presence of shale influence formation properties and response of the logging tool. The limestone and dolomite are a typical example of, non-clastic carbonates reservoirs. Around carbonate rocks constitute 50 percent of the reservoir in the world. The response of well logging tool is principally dependent upon matrix chemical nature and fluid type in pores. The reservoir characterization aims to infer the petrophysical properties distribution at field scale spatially. Porosity and permeability of formation are linked through a broad relationship. The utilization of rock physics theory and data is actually observed in petrophysical interpretation for reservoir geophysics observations [13].

II. Ease of Use

After the fragmentation of Gondwanaland in Carboniferous to Early Permian [14], India started to move rapidly northward relative to Australia and Antarctica [15] till establishment of its initial collision with Kohistan Island arc and Eurasian Plate in Late Cretaceous [16-19], marked by the exposures of ophiolites along the southern margin of Kohistan Island arc [19-21] The ongoing convergence after the initial collision caused deformation, crustal shortening and surface uplift which developed the Himalayas, Indus basin and Pakistani Fold and Thrust Belt [15 and 19].

Indus Basin which is tectonically divided into three Sub Basins, Sargodha High (Precambrian Indian Shield) which is considered to be the main controlling feature that divides the Indus basin into two Basins Upper Indus Basin from Lower Indus Basin. Another major Feature which rose through Jurassic and Cretaceous age is Jacobabad High, divides the Lower Indus Basin further two sub-basins Central Indus Basin and Southern Indus Basin [22].

Hydrocarbon Production Contribution of Southern Indus Basin includes:

- Sui Main Limestone (54%),
- Lower Goru (14%),
- Habib Rahi Limestone and Pab Formation (13%).

Study area Co-ordinates (Latitude: 25˚45′ to 25˚57′ North Longitude: 68˚36′ to 68˚54′ East) falls in Southern Indus Basin and geographically in Sanghar Distt., Sindh province of Pakistan (Fig.1). Southern Indus Basin which is highly effected (tilted Faulted Blocks) because of extensional tectonic activities cause Indo-Pak divergence from Gondwanaland in early Paleozoic [23].

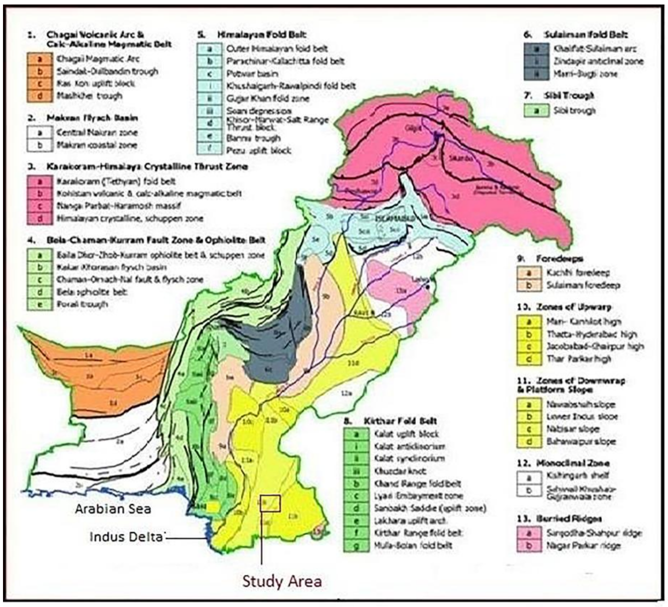

Figure 1. Study area location on tectonic map of Pakistan (modified after Faisal et al., 2013.

Cretaceous age Sembar is the main potential source rock of study area, deposits under restricted environment which is suitable for significant accumulation of Organic Matter [24]. Sands of Lower Goru formation overlying the sembar source rock is our main focus, where the Trapping mechanism is tilted fault blocks, faulted gentle role-overs and Stratigraphic traps. Sealing intervals are present for all potential reservoirs in the platform area, especially intra-formational shale for Lower Cretaceous reservoirs [25].

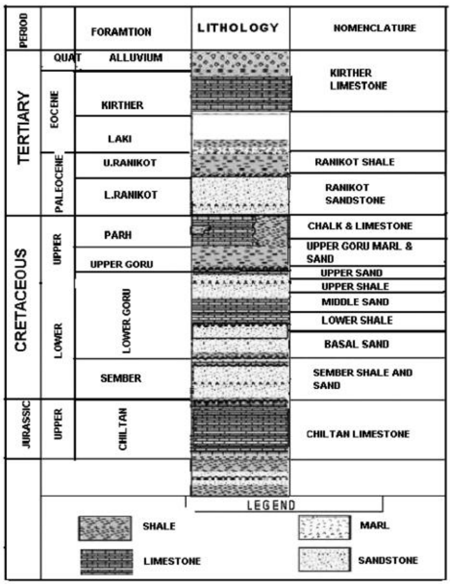

Figure 2. Generalized stratigraphic column of the area (Khipro)

The rate of success compared with other basins of Pakistan is highest because small tilted faulted blocks of Lower Goru Reservoir in this region are targeted progressively [26]. The Figure 2 is a generalized stratigraphic chart for the study area.

III. Prepare Your Paper Before Styling

A. *AVO/AVA Synthetics*

Amplitude determination of reflected and transmitted plane waves at the planar boundary of two elastic media in welded contact for all incidence angles is done using Zoeppritz's equations [27]. Two wells of the Khipro area were selected. Naimat Basal-01(latitude 25□47’37.69” N and Longitude 68□41’47.34” E) and Siraj South-01 (Latitude 25.51’33.34” N and Longitude 68.43’01.51” E). Fort both well AVO/AVA Synthetics were generated using Zoeppritz Equation (Fig.3, 4, 5, 6).

On the basis of anomaly indicated by AVO/AVA Synthetics Naimat Basal-01 was selected for further analysis.

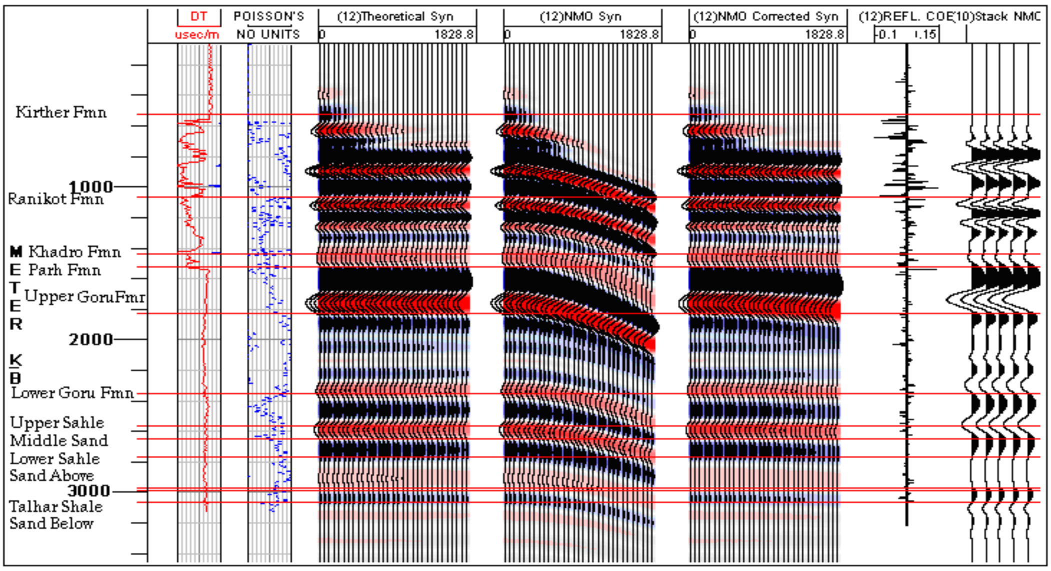

Figure 3. AVO synthetic has been created for well Siraj South 01 using Zoeppritz Equation

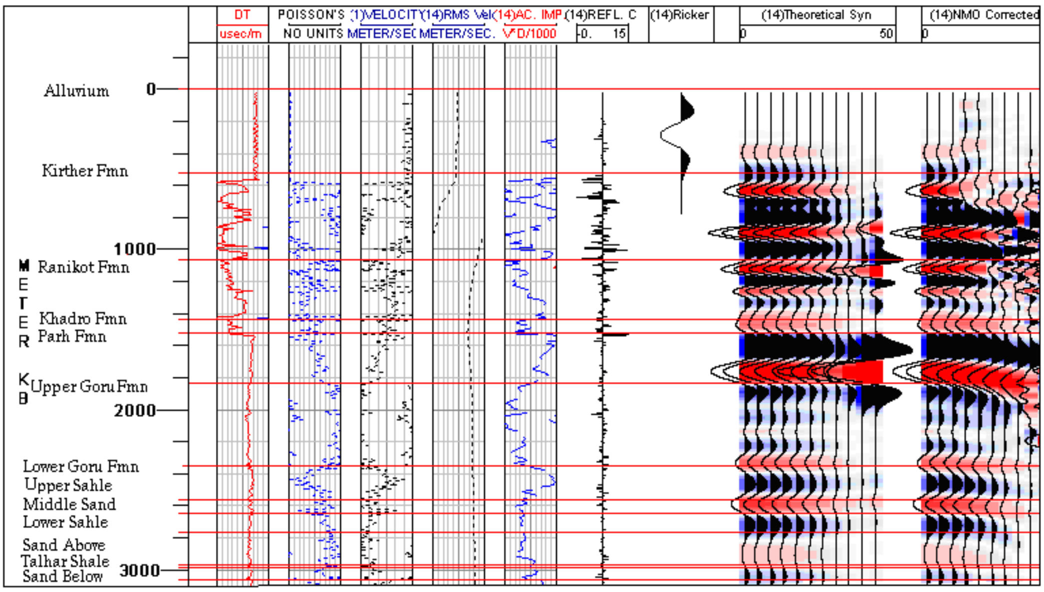

Figure 4. AVA synthetic has been created for well Siraj South 01using Zoeppritz equation

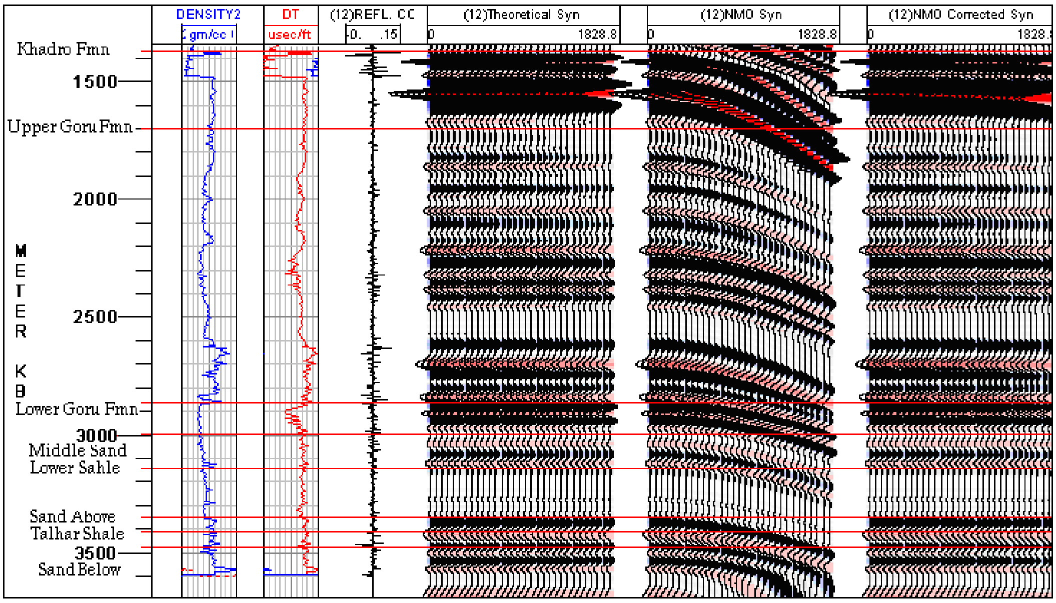

Figure 5. AVO synthetic created for well Naimat Basal 01 using Zoeppritz

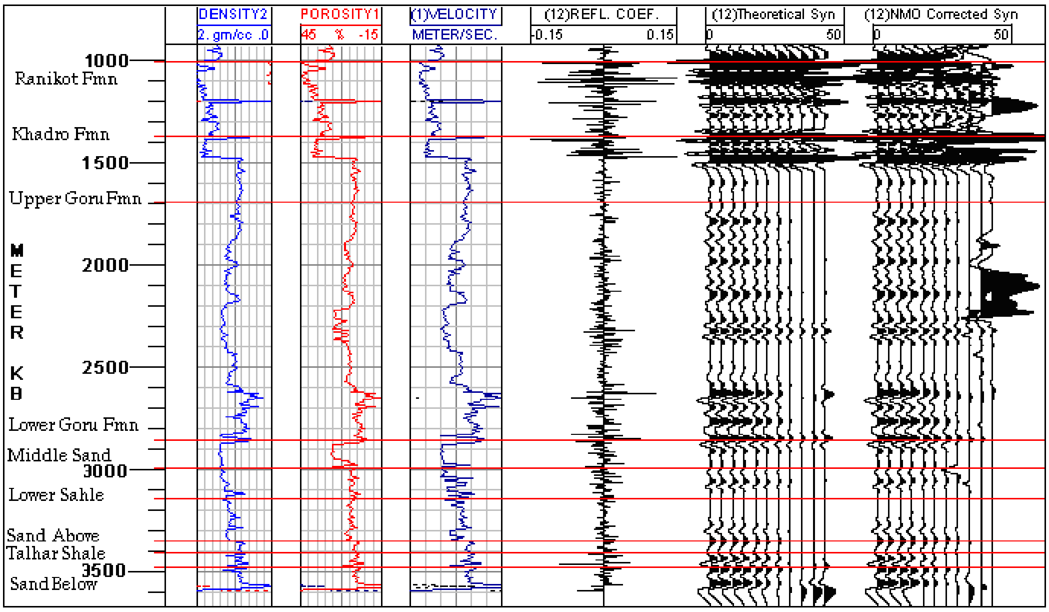

Figure 6. AVA synthetic has been created for well Naimat Basal using Zoeppritz equation

B. Petrophysical Parameters Evaluation

The well logging is the mainstream tasks for any well post drilling to resolve from log measurements the shale volume, porosity, permeability, and water saturation [28]. A detailed petrophysical analysis for Naimat Basal_01 was preformed from depth 2800m to 3550 m.

The first step from where we start Petrophysical analysis, Shale volume curve have been generated on the basis GR log. This curve supposed to be helpful in separating the reservoir and non-reservoir zones. Other logs like NPHI, RHOB together use to target porous lithologies then PEF & DT use to confirm the lithology type. After that Resistivity log is used to target the porous and highly resistive zones within the interpreted lithologies. Lithology plot in last track represented by various standard colors (Fig.7). Yellow and Green illustrating sandstone and shale intervals respectively because only two lithology exists in studied interval due which to delimit the intermediated zone between sand and shale has been represented as silt. After Separating the shale and sand intervals, named according to the General Stratigraphic Section. On the basis of the interpreted section, the well was divided into 6 major zones (Fig.7) representing intervals from 2805m to 3000m, 3000m to 3186m, 3186m to 3354m, 3354 m to 3412 m, 3412m to 3480m and 3480 to 3550m (Table.1). The overall impression of the interpreted section is alternating layers of sandstone and shale, the shale volume in sandstone ranges from 10 to 30 (above 30 Vsh was neglected for reason not to be selected for reservoir zone).

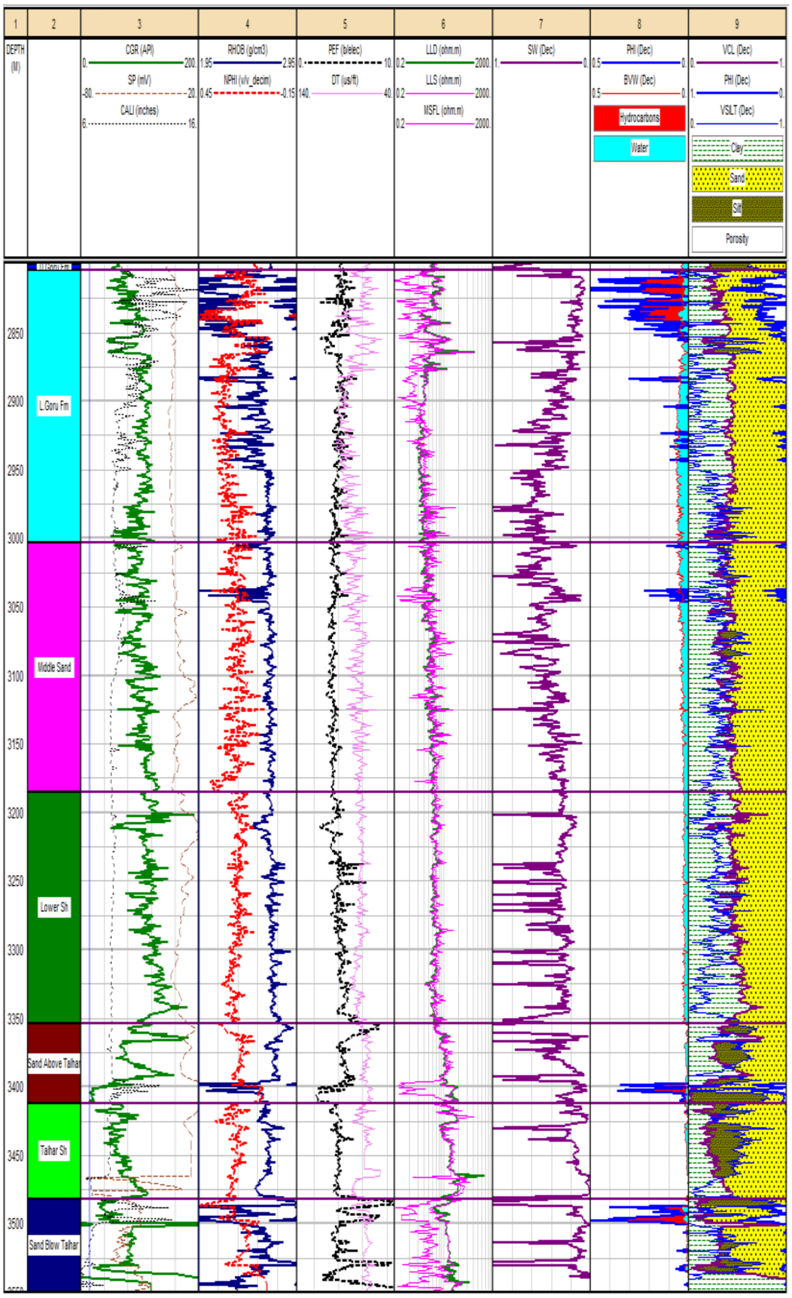

Figure 7. General Log plot for analyze the behavior of basic curves (3rd track Gamma-ray, Caliper and Spontaneous Potential, 4th track Neutron and Density, 5th track Photoelectric Factor and sonic, 6th track Saturation of water, 7th track resistivity logs, 8th track Porosity and Bulk volume of water and 9th track interpreted lithology track).

The porosity measurement and density contrast also indicate the fluid type but also the effect of Vsh on porosity (Fig. 7). On plotting the cross plot, it can clearly be seen that the output trend of the data points is linear and in increasing order. Most of the data points are blue in color, showing the respective depth range between 2800m to 3500 meters. It can also be noted that for the rocks having high density and the low porosity values showing very compact rocks. Where ever the higher denser rocks having high values of porosity can act as reservoir rocks (Fig. 8). This plot representing low GR Value with yellow color, we consider only those yellow clusters on this plot which falls in density rang of sandstone with high neutron porosity values. Similarly, the low denser and highly porous rocks may show the presence of shale contents. For the reservoir zone, one usually concerned with higher values of porosity and the respective higher values of the densities. Two zones Sand above Talhar thickness (3354m–3412m) and Sand below Talhar thickness (3480m – 3550m) has been picked for detail investigation for possible hydrocarbon accumulation (Fig. 9 and 10). After that generating a cross plot of NPHI vs RHOB specifically for depth ranges from 3398m to 3406m & 3487m to 3499m. Which indicates the cluster lies in a rage of Sandstone. Then resistivity curves image of the same area also placed over cross plot to select the zone where hydrocarbon can possibly accumulate (Fig.11 and 12).

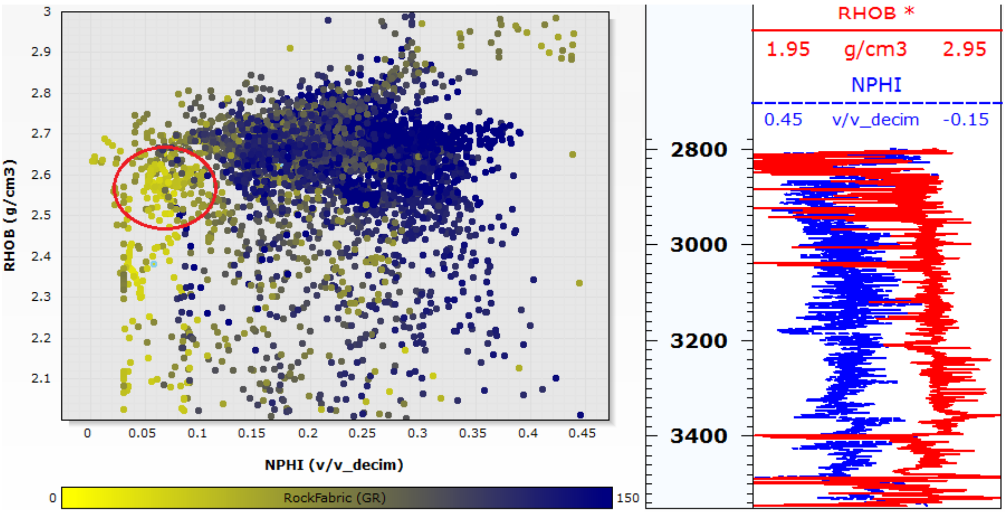

Figure 8. Cross Plot of Porosity Vs Density and GR color Scheme use to target the Low gamma ray value with high density and low porosity. Red circle indicating the best

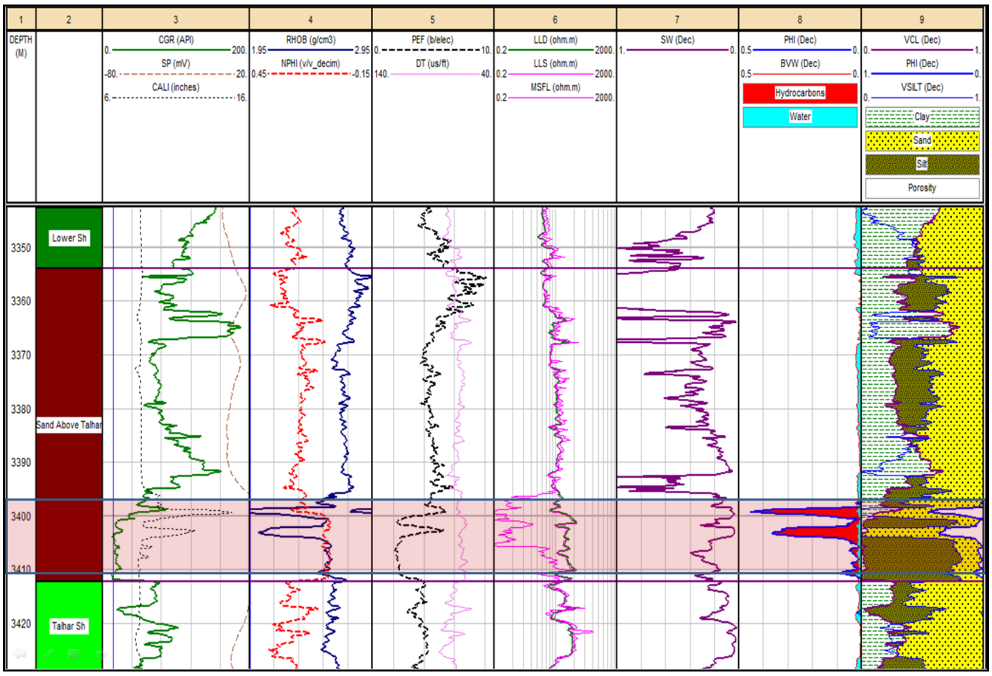

Figure 9. 1st Interpreted interval which fits on possible condition of reservoir. Resistivity curves separation provides the strong evidence about the existence of movable hydrocarbon accumulation. In 8th track aqua color representing pore spaces filled with water and red color representing the pore spaces filled with hydrocarbons

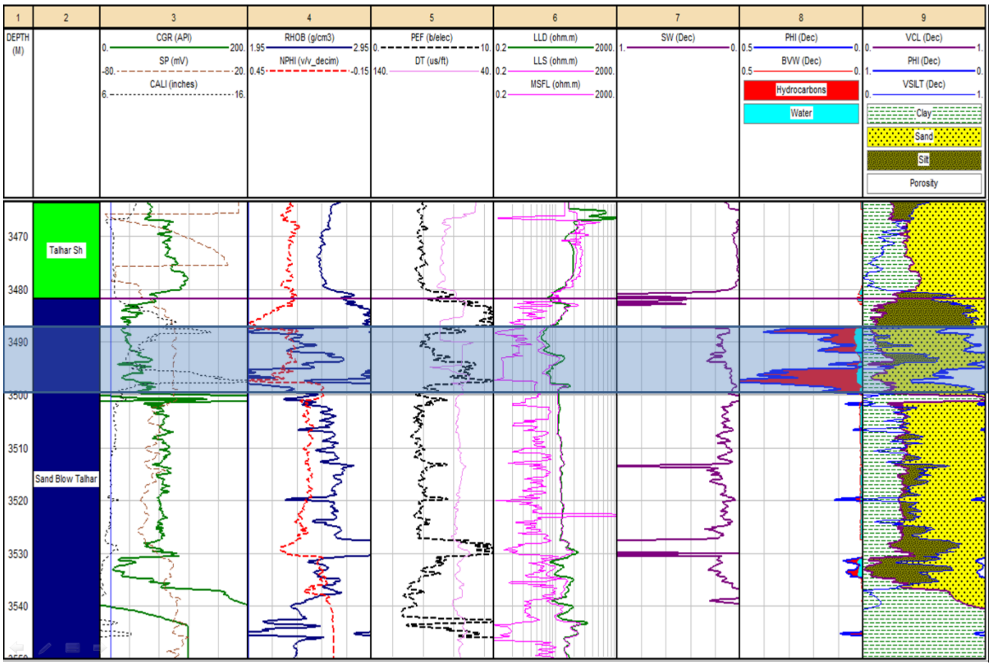

Figure 10. 2nd interpreted interval which also fits on possible condition of the reservoir. Resistivity curves separation provides strong evidence about the existence of movable hydrocarbon accumulation. In 8th track aqua color representing pore spaces filled with water and red color representing the pore spaces filled with hydrocarbons

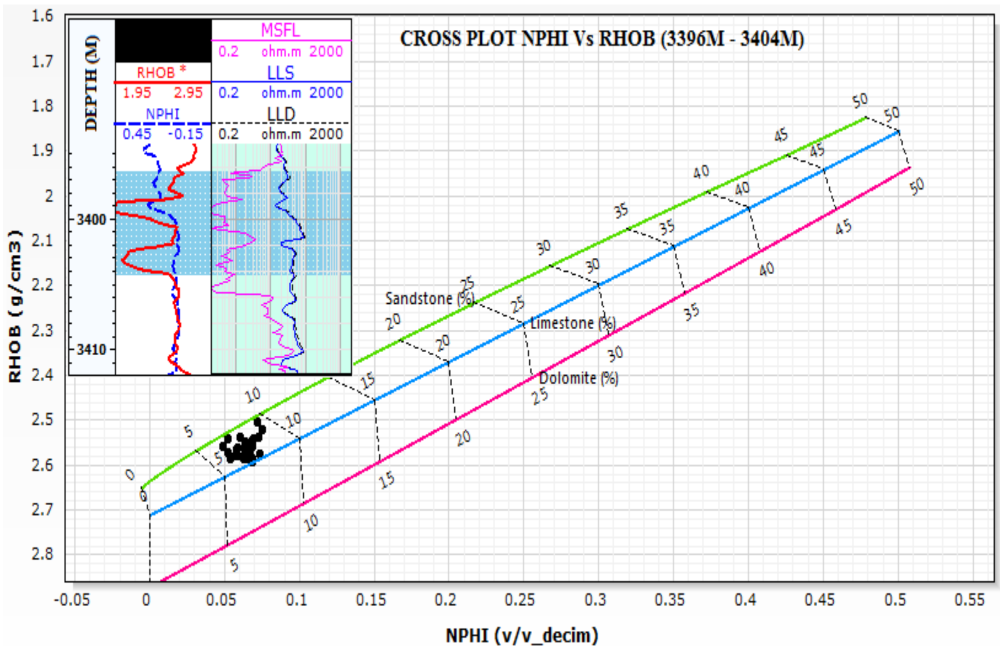

Figure 11. 1st interval (3396M – 3404M) cross plot between NPHI Vs RHOB which confirm the target zone exist in range of sandstone, and Resistivity separation clearly visible in left top resistivity curve plot

On the second step the picket plot was generated The picket plot It is a plot which is made on a logarithmic scale taking the values of true receptivity on the x-axis and the values of density porosity on the y-axis. A best-fit regression line of 100% value through the cluster of the points gives us the water saturation line represented by blue color (Fig.13). Sw curve is also generated but the main purpose of Pickett plot is to find the water saturation of specific zone plotted against Porosity and Resistivity (LLD) with four lines of water saturation in the plot. These lines (Sw lines) have been represented as percentages of 25, 50, 75 and 100. Objective is to find the area where there is a possibility of hydrocarbon. Most of the porous area of the well lies in the region having water saturation 100%, and rest of the area lies at 75% and between 50% to 60% water saturation as which in represented by colors, red and green representing most of the area less resistive because of high water saturation. Line that shows the value of water saturation as 50% to below is our focused zone where value of resistivity and porosity is high i.e. Initially interpreted two zones highlighted in (Fig 9 and 10) also highlighted in picket plot to calculate saturation of water exist which falls within the range of 40 to 100 ohm.m resistivity, 15 to 20 % saturated with water and 10 to 60 ohm.m resistivity, 30 to 35 % saturated with water (Fig.14 and15). In highlighted zones (Fig 9 and 10) red color filled between porosity and Bulk volume of water curves which indicating the presence of movable hydrocarbons.

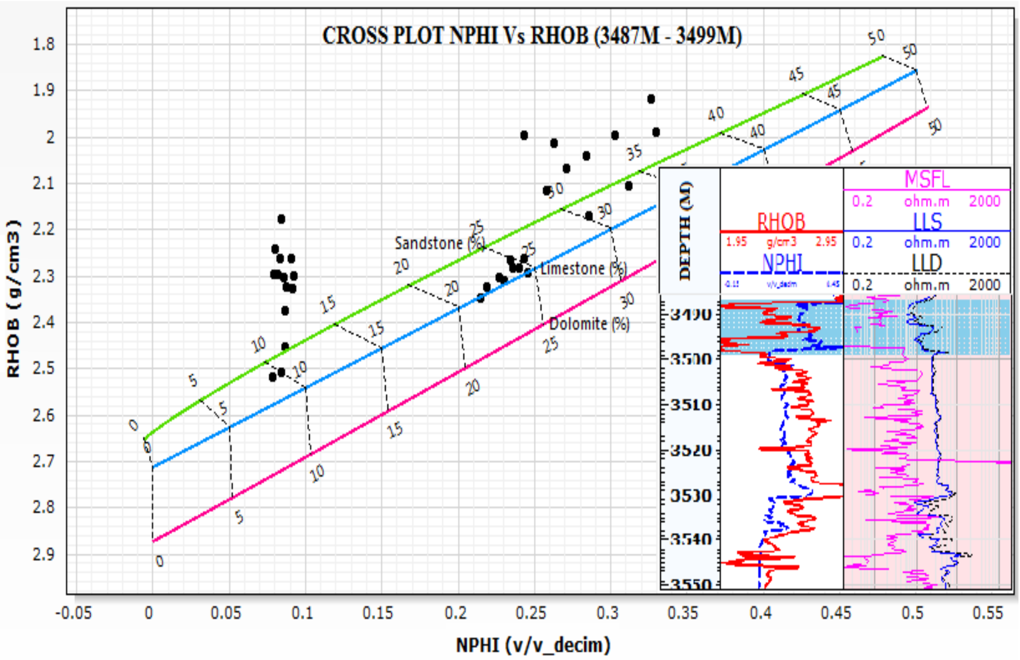

Figure 12. 2nd interval (3487M – 3499M) cross plot between NPHI Vs RHOB which shows the disperse values with in sandstone zone and below density value with high porosity ranges 10% to 30% and Resistivity separation clearly visible in right bottom resistivity curve plot.

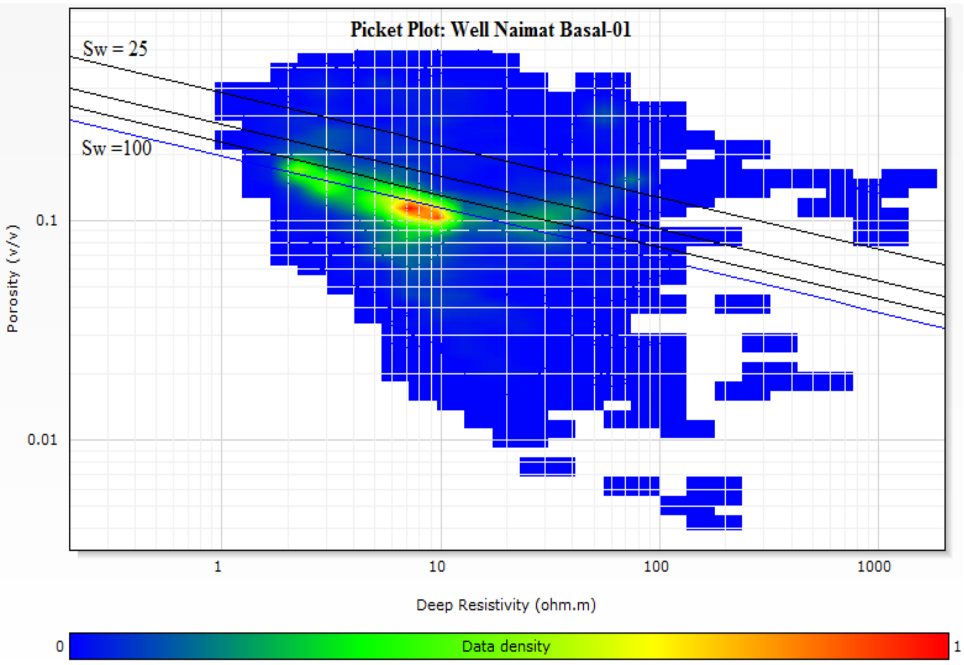

Figure 13. Picket plot between LLD and Porosity for water saturation. Color scheme use to find the general trend of data which lies above 75% water saturation.

Permeability calculated by using
Top Depth: 2805 meter
Bottom Depth: 3550 meter

The depth from 3395-3411 and 3480-3497 may be good reservoir zone for the hydrocarbon accumulation. To the oil and gas operator, reserves are volumes of crude oil, natural gas, and associated products that can be recovered profitably in the future from subsurface reservoirs.

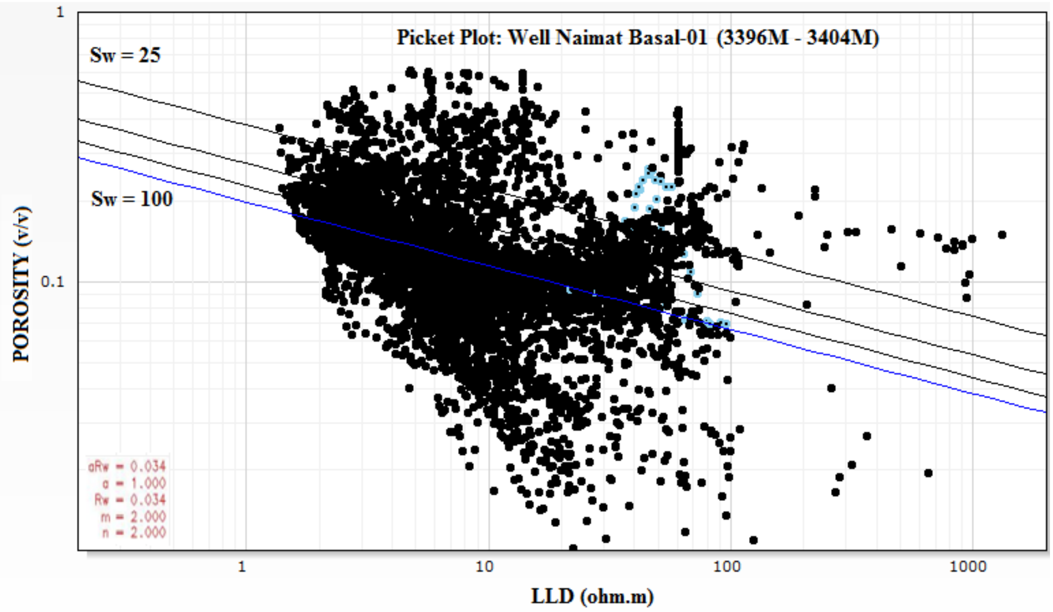

Figure 14. Interactively selected 1st interval in log plot is also highlighted in picket plot with sky blue color representing Sw ranges between 10% to 20%.

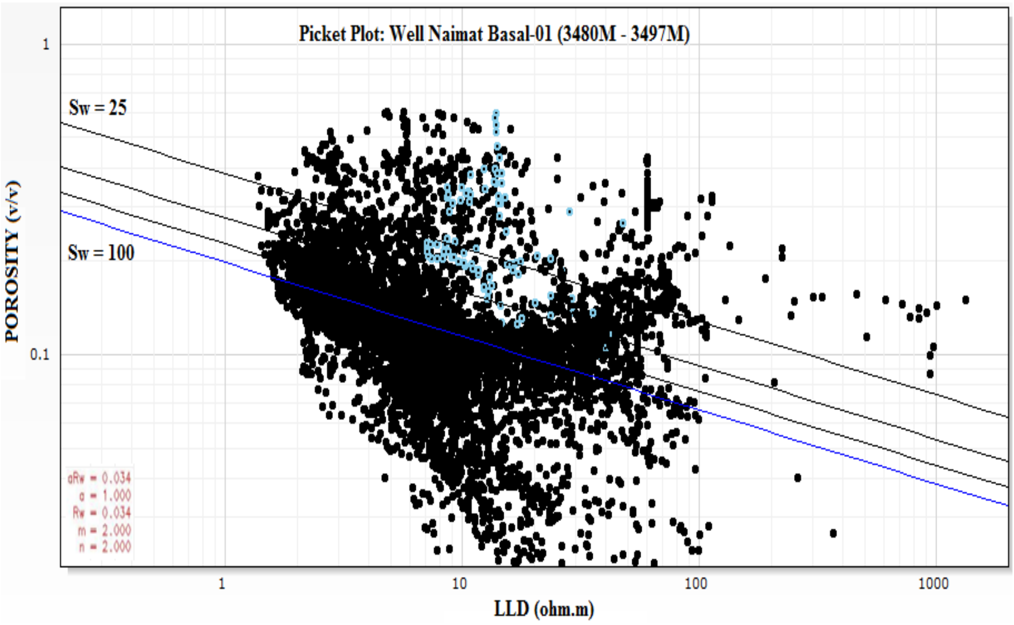

Figure 15. Interactively selected 2nd interval in the log plot is also highlighted in the picket plot with sky blue color representing Sw ranges between 10% to 30%.

Conflict of Interest

The authors declare no conflict of interest.

Concuslion

- This part must be writtern a refine and summary of your results and macth with your experiements works The behavior of the theoretical and NMO corrected synthetics created for well Naimat Basal 01 using Zoeppritz's Equation indicates very small variation along (Fig 1) the formation tops, marked. It is very difficult to analyze the amplitude variation because of strong reflectivity. The sharp reflection only observed along the Basal Sand but the amplitude variation is very difficult to analyze.
- There is a sharp fluctuation in amplitude with depth in AVO synthetic created for well Siraj South 01 based on Zoeppritz equation particularly the amplitude variation at the level of Basal Sand. This is directly giving a hint of the presence of hydrocarbon.
- AVA synthetic created for well Naimat Basal-01 and Siraj South-01 using Zoeppritz equation clearly indicate amplitude variations, both in the theoretically and NMO corrected synthetics. AVA has more implications to the structurally complex areas, rather than the AVO synthetics. Both of these have been created with different equations. The clear phase reversal can be seen at two different reflectors in AVA trace at 20' angle of incidence in the encircled zone. This usually acts as hydrocarbon indicator or gives a hint of the presence of some anomaly.
- Volume of clay and sand curve plot in trak 9th as well as trak 8th Porosity and Bulk volume of water curve interpretation assist to target movable hydrocarbon location is represented by red color in fig.A. These zones are also marked as an anomalous location in AVO & AVA section.
- Keeping in mind about anomaly synthetic of Naimat Basal-01 has been generated which perfectly ties with an interval having hydrocarbon indications.
- Two Intervals studied precisely, where in 1st interval 3395m- 3411m having very low density is underestimated because of bad hole condition. But resistivity shows a clear indication of hydrocarbon existence. On the other hand in 2nd interval 3480m-3497m low high-density value which is underestimated also because of repeated disturbance in hole size and hydrocarbons.

References

[1] Smith, G.C., and P.M. Gidlow. Weighted stacking for rock property estimation and detection of GAS. Geophysical Prospecting, 1987. 35(9): 993-1014.

[2] Zhang, H., and R.J. Brown. A review of AVO analysis: CREWES Research Report. 2001. 358

[3] Knott, C.G., III. Reflexion and refraction of elastic waves, with seismological applications." The London, Edinburgh, and Dublin Philosophical Magazine and Journal of Science, 1899. 48(290): 64-97.

[4] Zoeppritz, K. Erdbebenwellen VIII B. Uber Reflection and Durchgang seismischer Wellen durch Unstetigkeitsflachen. Gottinger Nachrichten.1919.1: 66-84.

[5] Leaney, S.W., W.E. Borland. AVO and anisotropy from logs and walkaways. AAPG International Conference and Exhibition, Kuala Lumpur, Malaysia. 1994

[6] Gratwick, D., Amplitude analysis in the angle domain: SEP, 2001. 108: 45-62.

[7] Veeken, P.C.H., and Marianne Rauch-Davies. AVO attribute analysis and seismic reservoir characterization. First Break. 2006. 24(2): 41-52.

[8] Tsa, C.C., C.S., Liu, P., Schnurle. Application of AVO method to analyze the seismic characteristics of gas hydrate offshore Southwestern Taiwan. 2007.

[9] Hilterman, F., Is AVO the seismic signature of lithology? A case history of Ship Shoal - South Addition. The Leading Edge (1990). 9(6). 15-22.

[10] Beucher-Darricau, H., B. Doligez, and J.M., Yarus. Modeling complex reservoirs with multiple conditional techniques: A practical approach to reservoir characterization, in T. C. Coburn, J. M. Yarus, and R. L. Chambers, eds., Stochastic modeling and geostatistics: Principles, methods, and case studies, volume II: AAPG Computer Applications in Geology 2006. 5: 289-299.

[11] Valizadeh Alvan, H., Uncertainty of Estimated Petrophysical Parameters of Ahvaz Oil Reservoir. J, Adv Sci Eng Res. 2011. 1:165-176.

[12] Ehinola, O. A., et al., Geology, geochemistry and biomarker evaluation of Lafia-Obi coal, Benue Trough, Nigeria. Fuel, (2002). 81(2) 219-233.

[13] Aigbedion, I., and S.E.. Iyayi. Formation evaluation of Oshioka field using Geophysical well logs." Middle-East J. Sci. Res. 2007. 2(3-4): 107-110.

[14] Searlc, M.P., Geology and Tectonics of the Karakoram Mountains. Chichester (John Wiley and Sons Ltd.), 1991. 358.

[15] [15] Powell, C.M., A speculative tectonic history of Pakistan and surroundings: Some constraints from the Indian Ocean." In: Farah, A. & DeJong, K. A. (eds.) Geodynanmics of Pakistan. Geol. Surv. Quetta, Pak. 1979. 1-451.

[16] Khan, S.D., et al., Did the Kohistan-Ladakh island arc collide first with India?." Geological Society of America Bulletin, 2009. 121(3-4): 366-384.

[17] Valdiya, K.S., Emergence and evolution of Himalaya: reconstructing history in the light of recent studies. Progress in physical geography. 2002. 26(3): 360-399.

[18] Chaudhry, M.N., M. Ghazanfar, J.G. Ramsay, D.A. Spencer and M. Qayyumm. Northwest Himalaya – A Tectonic subdivision. 175-184, Feburary 1994 In; (Eds: Ahmed, R and Shiekh, A.M) Geology in South Asia-1: Proceeding of First South Asia Geological Congress. Islamabad, Pakistan:

[19] Burg, J.P., J.L., Bodinier, S.H., Chaudhry and H., Dawood. Infra-arc mantle-crust transition and intra-arc mantle diapirs in the Kohistan complex (Pakistani Himalaya): petro-structural evidence." TERRA NOVA-OXFORD 1998. 10: 74-80.

[20] Khan, M.A., S., Rehman, M., Fahad ullah and N., Ahsan. Geochemistry and tectonic environments of Babusar amphibolites in southeast Kohistan, Pakistan. Geol. Bull. Punjab Univ 2009. 44: 105-116.

[21] Khan, M.A., S., Rehman and N., Ahsan. Geology and geochemistry of Sumal amphibolites, Kamila amphibolite unit, southeast Kohistan, Pakistan. Int. J. Agric. Appl. Sci, 2012. 4(2): 99-111.

[22] Qadri I.B., Petroleum geology of Pakistan: Pakistan Petroleum Limited. Karachi, Pakistan. 1995.

[23] Zaigham, N.A., and K.A., Mallick. Prospect of hydrocarbon associated with fossil-rift structures of the southern Indus basin, Pakistan."AAPG bulletin. 2000. 84(11): 1833-1848.

[24] Faisal, M., F.,Rehman, S., Rehman and N., Ahsan. Better perceptive and enhanced visualization of seismic profiles for the exploration of hydrocarbon using a seismic and synthetic seismogram modeling of Khipro Block, Southern Indus Basin, Sindh Province, Pakistan." Energy Sources, Part A: Recovery, Utilization, and Environmental Effects, 2013. 35(22): 2101-2112.

[25] Ahmad, Z., G. Akhter, F., Bashir, M.A., Khan, and M., Ahmad. Structural interpretation of seismic profiles integrated with reservoir characteristics of Bitrism block (Sind Province), Pakistan." Energy Sources, Part A: Recovery, Utilization, and Environmental Effects. 2009. 32(4): 303-314,

[26] Jamil, A., A., Waheed, et al., Pakistan's Major Petroleum Plays - An overview of dwindling reserves. AAPG, 2012. 1-14.

[27] Haase, A.B., Modelling of linearized Zoeppritz approximations. AVO model. CREWES Research Report. 2004. 16:1-4

[28] Naji, H.S., et al., Sedimentology and quantitative well logs petrophysical parameters, Lower Qishn Clastic reservoir, Masila Oilfield, Yemen." JKAU: Earth Sci. 2010. 21(1): 53-77.

International Journal of Engineering Works
ISSN-p: 2521-2419
ISSN-e: 2409-2770
Vol. 6, Issue 04, PP. 143-147, April 2019
https://www.ijew.io/
https://doi.org/10.34259/ijew.19.604143147

L Shaped via based Mushroom type High Impedance Structure

Touseef Ahmad
Universitivy of Engineering and Technology Peshawar, Pakistan
touseefkhattak2013@gmail.com
Received: 27 March, Revised: 03 April, Accepted: 08 April

***Abstract*—**High-impedance Electromagnetic Band-Gap structures (EBG) surfaces have the capability to forbid flow of EM waves in a given band which and therefore surface waves in case of planar antennas like mictostrip antenna can be minimized with this characteristics of EBG plane. Shape, size, symmetry, and material used in their construction defines their operating band. In this research, a novel compact EBG structure also called high impedance structure (HIS) is proposed. The design is achieved through incorporation of 'L' shaped via to conventional mushroom type EBG/HIS instead of straight vias. The design includes distribution of square patches over substrate material below which there exists a ground plane. Vias passing through the substrate connecting square patches and the ground plane are also part of its design It has been observed that operating frequency of L shaped via based EBG is much lower than that of conventional mushroom type EBG/HIS having straight vias. Alternatively, we can say that size reduction has been achieved through incorporation of L shaped via to the EBG/HIS resulting in 62.5 % of size reduction. All the designs and simulations are carried out in CST microwave studio.

***Keywords*—** Microstrip patch antenna, high impedance surface, substrate, bandwidth.

I. Introduction

One of emerging materials that has been engineered artificially is metamaterial. By definition these surfaces satisfy two conditions, i.e they are purely artificial and do not exist naturally, and secondly EM properties possessed by these structures is superior and different from their parent elements [1]. EM and optical characteristic offered by these artificial materials are very much unique as well as different from their constituents. This phenomenon is achieved through inclusion, discontinuities and pattern of host material due to which their EM fields interact differently resulting in modification of EM properties like of host materials permittivity (ε), permeability (μ), refractive index (n) etc of constituent materials. As these materials provides control over EM properties therefore some desired electromagnetic and optical performance can be achieved through them.

Since 1990s, rigorous analysis has been carried out for Single Negative (SNG) [2], Double Negative (DNG) metamaterials [3, 4] and planar Electromagnetic Band Gap (EBG) structures [5]. Sievenpiper in [6] introduced 2D mushroom type EBG surfaces that were structured through array of unit cells distributed in periodic manner. This unit cell is composed of square patch placed over dielectric substrate below which there exist ground plane. A conducting cylindrical pin connects the square patch with ground plane which is passing through the substrate hence forming mushroom like configuration. These periodic structures possess the ability of suppression of propagation of surface energy waves along with in-phase reflection in a given frequency band. In-phase reflection characteristics enable these structures to have image currents and antenna current both with same phase that results in constructive interference resulting in better antenna performance. If we look into the structural configuration of high impedance structure, we will see that its composition incudes two-dimensional lattice of resonating elements that form basic two dimensional stop band filter to forbid flow of surface currents.

As explained, high-impedance Electromagnetic Band-Gap structures (EBG) surfaces have the capability to forbid flow of EM waves in a given band which is another important feature. Surface waves in case of planar antennas like mictostrip antenna can be minimized with the help of EM wave suppression characteristics of EBG plane. An initial research on EBG structure at microwave frequencies was conducted by Prof. E. Yablanovitch and his research group in [7], which explained many of its properties (surface current suppression and zero reflection phase) using an effective surface impedance model. Since then, theory and practical applications of EBG structure has become an extensive research area due to its unusual properties and design flexibilities. Consequently, numerous of EBG structures have been successfully employed to realize novel high performance devices such as filters, waveguides, antennas, etc. [8], [9], [10].

Low profile wire antennas with EBG ground are studied in [11], [12], [13]. In [14] and [15], EBG structure is employed to on-body antennas to reduce sensitive absorption rate (SAR). Other applications of EBG structures such as Multi-band antenna, LTCC and bandwidth enhancement are introduced in [16], [17] and [18], respectively.

Another area of EBG structure research is focused on characteristics of its unique properties, providing simple and fast design approaches. [19] presents a study on in-phase reflection and wave suppression characteristics of EBG structure. In [20], a method of designing controlled bandwidth EBG structure is demonstrated. Spectral domain method is explained in [21] to prove that capacitive surfaces can perform perfect magnetic conductors in a relative low frequency range. Requirement for miniaturization exists in every design whether it is related to antenna, amplifiers, filters or some other RF components. Therefore, EBG structure with compact size is required in several applications. Several attempts have been carried out in different articles [22-24]. Edge located via based mushroom type EBG was presented in [25] for demonstrating reduction in size of the EBG. Another design introduced in [26] used helical shaped via in their design for size compactness of EBG plane.

In this research, a novel compact EBG structure is proposed. The design is achieved through incorporation of 'L' shaped via to conventional mushroom type EBG instead of straight vias. The design includes distribution of square patches over substrate material below which there exists a ground plane. Vias passing through the substrate connecting square patches and the ground plane are also part of its design. Geometrical shape of via can vary response of the EBG. In our case straight via is modified and transformed into L shaped via. This modification is carried out by moving both ends of straight via over square patches in opposite direction. Band gap response and parametric study of the newly designed L shaped based EBG is studied. A comparison between conventional mushroom type EBG & L shaped EBG is also carried out in order to analyze the benefit of L shaped EBG.

Sequence of the paper is as following. Section II mainly deals design parameters of HIS. Section III presents design of L shaped via base mushroom type HIS alongwith discussion of results. At the end conclusion of the research work is presented.

II. HIGH IMPEDANCE SURFACE

Square patch EBG structures is the conventional design which is also termed as high impedance structures (HIS) that was proposed by Sievenpiper [27-31] which finds application in variety of low profile efficient antennas. Rahmat Samii [32] describes EBG as a periodic or a periodic configuration of multi dimension having power to stop or enhance the transmission of electromagnetic waves in a certain frequency range with no conditional limit of incident angel and polarization. Bandgap is the frequency range in which the surface waves are suppressed. Substrate thickness and dimensions of the EBG unit-cell affect the band gap characteristic. The unit cell may be either square or rectangular in shape. The mushroom, loop, or spiral may be the resonating element. Rahmat-Samii [33] and Sievenpiper [34] designed several kinds of EBG and HIS configuration which were further used and find its application in a variety of low profile linear and circularly polarized antennas. HIS design by Sievenpiper is shown below in Figure 1 and 2.

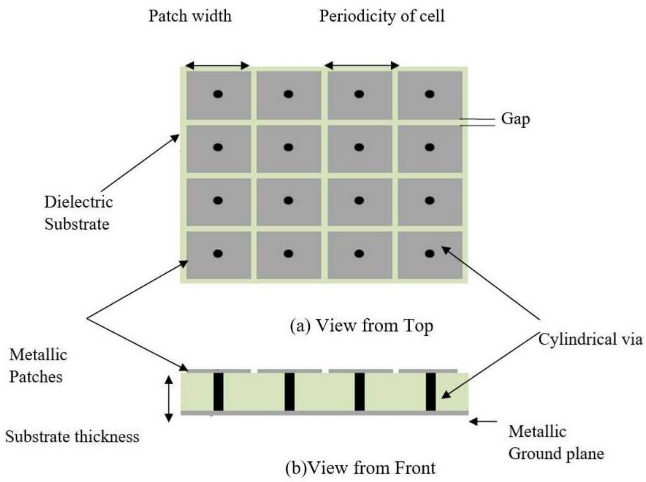

Figure 1. High impedance Surface (Sievenpiper) (a) Top-View (b) Front-View

Planar structures give in-phase reflection and suppress surface propagation in a particular frequency band. Additionally, the antenna currents are in-phase with the image currents, therefore both constructively interfere and provide better antenna performance[35].

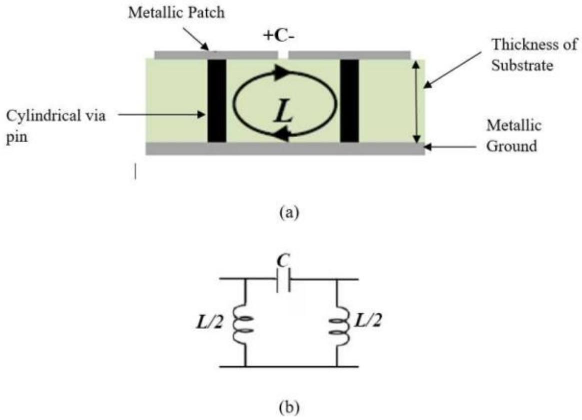

Figure 2. Equivalent circuit (LC) model (a) Front-View (b) Equivalent resonant circuit (LC)

To explain operation of HIS, consider Figure 4. It can be seen that HIS behavior is just parallel resonant circuit. The charge distribution among neighboring cells correspondent to capacitance C while the current flow through metallic via from top and bottom results to inductance L.

Following formula determines L and C values [33].

$$C = \frac{W(\varepsilon_0 + \varepsilon_r)}{\pi}\cosh^{-1}\left(\frac{2W+g}{g}\right)$$

$$L = \mu h$$

Here

W = Width of the patch
g = Gap between two adjacent patches

ε_r = EBG substrate relative permittivity
h= Thickness of the substrate used
μ= Medium permeability

Following equation expressed resonant frequency f_r

$$f_r = \frac{1}{2\pi\sqrt{LC}}$$

From above equation the Frequency Band Gap (BW) can be come near to as

$$BW = \frac{\Delta\omega_0}{\omega_0} = \frac{1}{\eta}\sqrt{\frac{L}{C}}$$

Here η is the intrinsic impedance of free-space = 120π

By suppressing surface waves, these assemblies are very co-operative just in case of planer antennas resulting in directivity, efficiency of the antenna and achieving high gain [36-37]. EBGs can also be utilized for GPS applications [38-39]. It has been observed that when EM wave strike Perfect Electric Conductor or planner EBGs, sense of polarization reverses resulting in mismatching in polarization. In order to side-step this kind of mismatch, PDEBGs (Polarization dependent EBGs) in several applications are introduced [40-41].

III. Results and Discussions

This section represents the design of mushroom type EBG with L shaped vias. The design includes distribution of square patches over substrate material below which there exists a ground plane. Vias passing through the substrate connecting square patches and the ground plane are also part of its design. Geometrical shape of via can vary response of the EBG. In our case straight via is modified and transformed into L shaped via. This modification is carried out by moving both ends of straight via over square patches in opposite direction. Figure 3 shows this transformation.

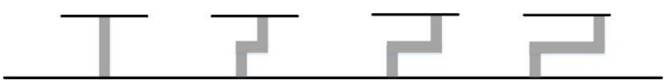

Figure 3. Transformation of Straight Vias to L shaped Vias

Structural configuration of designed mushroom type EBG with L shaped vias is given in figure 4.

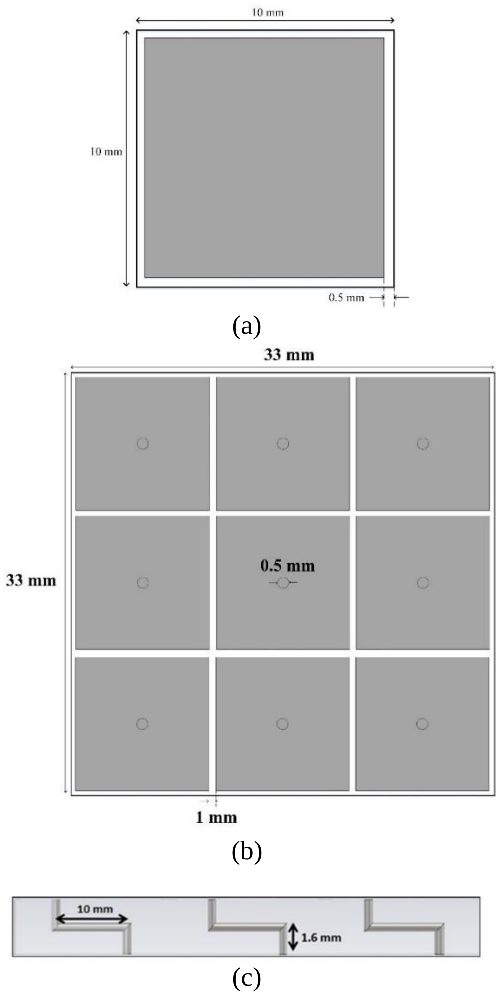

Figure 4. Mushroom type EBG with L shaped Vias (a) Unit Cell Model (b) Top view of 3x3 EBG plane (c) Side View of 3x3 EBG plane

Here FR-4 substrate is used for the design of EBG having dielectric constant of 4.3 with thickness of 3.2 mm. Dimension of square patch is 10 mm x 10 mm and a total of nine patches are taken for the design. Gap between square patches is 1 mm and radius of connecting vias is taken to be 0.25 mm. Overall dimension of 3 x 3 patch mushroom type EBG is 33 mm x 33 mm.

To evaluate band gap behavior of the EBG, suspended microstrip line technique is utilized. For this purpose, a microstrip line is placed over the EBG ground plane and excited on both of its port thus forming a to port network. Coupling between the two port of transmission line i.e S21or S12 will show the band gap response of the EBG. As surface impedance of EBG plane is very high, therefore propagation of EM waves will be blocked in side band gap and similarly EM wave transmission will be high in rest of the band. Hence reduction if S21 will be observed within bandgap.

To analyzer bandgap response of the mushroom type EBG with L shaped, a microstrip line having length of 33 mm and width of 2 mm is placed over 3 x 3 patch mushroom type EBG with L shaped vias and excited. The configuration of design is given in figure 5.

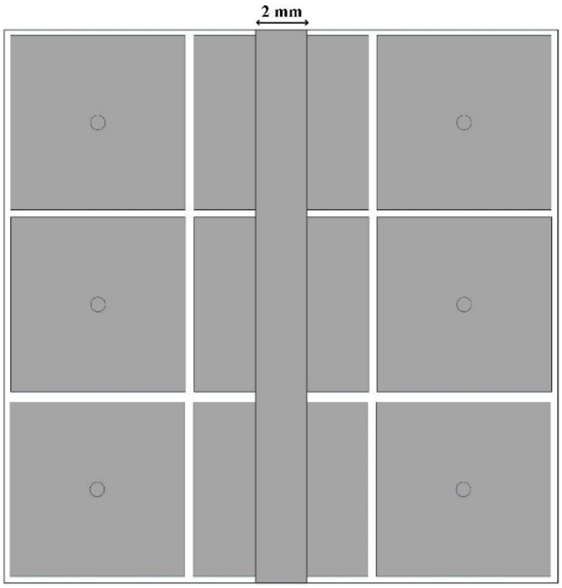

(a)

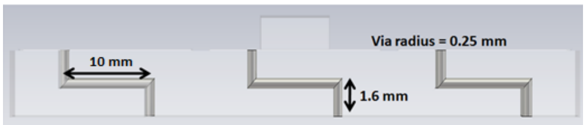

(b)

Figure 5. Suspended transmission line over Mushroom type EBG with L shaped Vias (a) Top View (b) Side View

Frequencies, having S21 less than -10 dB, are defined as the band gap normally. Simulated S21 of mushroom type EBG with L shaped vias is presented in figure 6. This can be seen that value of S21 decreases to –40 dB near 1.3 GHz having -10 dB stop band of 112 MHz ranging from 1.253 GHz to 1.366 GHz.

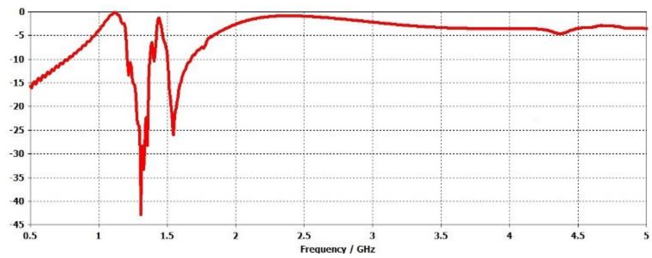

Figure 6. S21/Band gap for Mushroom Type EBG with L shaped Vias

Afterwards conventional mushroom type EBG having straight vias is also designed. In this case all the parameters are kept same as that of mushroom type HIS with L shaped via except configuration of the via. It was observed that its operating frequency band is centered at 2.1135 GHz having -10 dB stop band of 310 MHz ranging from 1.9559 GHz to 2.2659 GHz as depicted in figure 7.

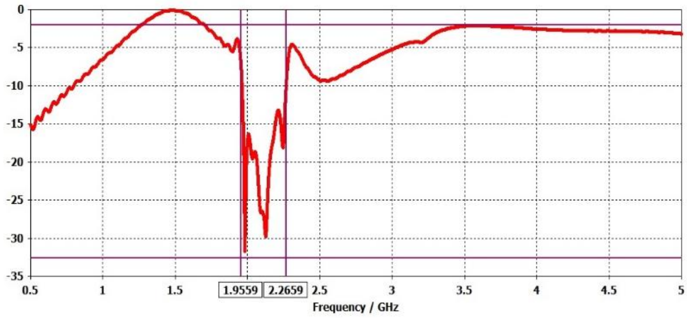

Figure 7. S21/Band gap for Mushroom Type EBG with Straight Vias

From these results we can clearly see that operating frequency of L shaped via based EBG is much lower than that of conventional mushroom type EBG. Alternatively, we can say that size reduction has been achieved through incorporation of L shaped via to the EBG resulting in 62.5 % of size reduction.

CONCUSLION

This article discusses miniaturization of conventional mushroom type EBG/HIS. Desired response is achieved through modification of via configuration of HIS. For this puspose the straight vias of HIS plane is replaced with L shaped vias. It has been observed that band gap of conventional mushroom type HIS with straight via is centred at 2.1135 GHz having -10 dB stop band of 310 MHz ranging from 1.9559 GHz to 2.2659 GHz. Wheras band gap of mushroom type HIS with L shaped vias was centred at 1.3 GHz having -10 dB stop band of 112 MHz ranging from 1.253 GHz to 1.366 GHz. Hence 62.5 % reduction is operating band of mushroom type HIS was observed through incorporation of L shaped vias i.e 62.5 % size reduction is achieved.

REFERENCES

[1] A.Sihvola,―Electromagnetic emergence in metamaterials‖, Advances in Electromagnetics of Complex Media and Metamaterials, vol. 89, pp. 1-17, 2003.

[2] J. Zehentner and J. Machac, ―Volumetric single negative metamaterials‖, Proceedings of Metamaterials Congress, pp. 22–24, 2007

[3] N. Engheta,―Metamaterials with negative permittivity and permeability: background, salient features, and new trends‖, IEEE MTT-S International Microwave Symposium Digest, pp. 187-190, 2003.

[4] N. Engheta,―Design, fabrication, and testing of double negative metamaterials‖, IEEE Transactions on Antennas and Propagation, vol. 51, issue. 7, pp. 1516-1529, 2003.

[5] W. R. Ziolkowski and N. Engheta, ―Metamaterials: Physics and Engineering Explorations‖, John Wiley & Sons, Inc., 18 September 2006.

[6] D. Sievenpiper, ―High Impedance Electromagnetic Surfaces‖, Ph.D. dissertation, Electrical Engineering Department, University of California, Los Angeles, 1999.

[7] D. Sievenpiper, L. Zhang, R. F. J. Broas, N. G. Alexopolous, E. Yablonovitch,, "High-Impedance Electromagnetic Surfaces with a Forbidden Frequency Band," IEEE Transactions on Microwave Theory and Techniques, vol. 47, no. 11, pp. 2059-2074, 1999.

[8] Y. J. Lee, J. Yeo, R. Mittra, W. S. Park, "Application of Electromagnetic Bandgap (EBG) Superstrates With Controllable Defects for a Class of Patch Antennas as Spatial Angular Filters," IEEE

Transactions on Antennas and Propagation, vol. 53, no. 1, pp. 224-235, 2005.

[9] S. G. Mao, M. Y. Chen, "Propagation Characteristics of Finite-Width Conductor-Backed Coplanar Waveguides with Periodic Electromagnetic Bandgap Cells," IEEE Transactions on Microwave Theory and Techniques, vol. 50, no. 11, pp. 2691-2703, 2002.

[10] F. Yang, Y. Rahmat-Samii, "Reflection Phase Characterizations of the EBG Ground Plane for Low Profile Wire Antenna Applications," IEEE Transactions on Antennas and Propagation, vol. 51, no. 10, pp. 677-682, 2003.

[11] F. Yang, Y. Rahmat-Samii, "A low-profile circularly polarized curl antenna over an electromagnetic bandgap (EBG) surface," Microwave and Optical Technology Letters, vol. 31, no. 4, pp. 264-267, 2001.

[12] Z. Li, Y. Rahmat-Samii, "PBG, PMC and PEC ground planes: A case study of dipole antennas," in IEEE Antennas and Propagation Society International Symposium, 2000.

[13] T. H. Liu, W. X. Zhang, M. Zhang, K. F. Tsang, "Low profile spiral antenna with PBG substrate," Electronics Letters, vol. 36, p. 779–780, 2000.

[14] [14] S. Bashir, M. Hosseini, R. M. Edwards, M. I. Khattak, L. Ma, "Bicep Mounted Low Profile Wearable Antenna Based on A Non-Uniform EBG Ground Plane – Flexible 60 EBG Inverted-L (FEBGIL)," in Loughborough antennas and propagation conference, Loughborough, 2008.

[15] N. Chahat, M. Zhadobov, R. Sauleau, K. Mahdjoubi, "Improvement of the On-Body Performance of a Dual-Band Textile Antenna Using an EBG structure," in Loughborough antennas and propagation conference, Loughborough, 2010.

[16] J. H. S. D. Sievenpiper, "Textured Surface Having High Electromagnetic Impedance in Multiple Frequency Bands". United States Patent US 6,483,481 B1, 19 November 2002.

[17] R. Li, G. DeJean, M. M. Tentzeris, J. Papapolymerou, J. Laskar, "Radiation-Pattern Improvement of Patch Antennas on a Large-Size Substrate Using a Compact Soft-Surface Structure and Its Realization on LTCC Multilayer Technology," IEEE Transactions on antennas and propagation, vol. 53, no. 1, pp. 200-208, 2005.

[18] R. Diaz, V. Sanchez, E. Caswell, A. Miller, "Magnetic Loading of Artificial Magnetic Conductors for Bandwidth Enhancement," 2003.

[19] Aminian, F. Yang, Y. Rahmat-Samii, "In-phase Reflection and EM Wave Suppression Characteristics of Electromagnetic Band Gap Ground Planes," IEEE Antennas and Propagation Society International Symposium," 2003.

[20] [20] Aminian, Y. Rahmat-Samii, "Bandwidth Determination for Soft and Hard Ground Planes: A Unified Approach in Visible and Surface Wave Regions," in IEEE Antennas and Propagation Society International Symposium, 2004.

[21] [21] F. Bilotti, L. Vegni, "Radiating Features of Capacitive and Inductive Surfaces," Microwave and Optical Technology Letters, vol. 39, no. 2, pp. 117-121, 2003.

[22] Stylianos D. Assimonis, Traianos V. Yioultsis, and Christos S. Antonopoulos, "Design and Optimization of Uniplanar EBG Structures for Low Profile Antenna Applications and Mutual Coupling Reduction," IEEE Transaction on antennas and propagation, vol. 60, no. 10, Oct. 2012, pp. 4944-4949.

[23] S. Zhang, B. Kiong Lau, Y. Tan, Z. Ying, and S. He, "Mutual Coupling Reduction of two PIFAs with a T-Shape Slot Impedance Transformer for MIMO Mobile Terminals," IEEE Transaction on antennas and propagation, vol. 60, no. 3, March 2012, pp. 1521-153l.

[24] A. M. Abdelreheem, and M. A. Abdalla, "A Novel Bilateral UC-EBG Structure," IEEE Antenna and Propagation Society International Symposium pp. 1780-81, July 2014, pp. 1780-1781.

[25] Eva Rajo-Iglesias, Member, IEEE, Luis Inclán-Sánchez, José-Luis Vázquez-Roy, Member, IEEE, and Enrique García-Muñoz, "Size Reduction of Mushroom-Type EBG Surfaces by Using Edge-Located Vias" IEEE MICROWAVE AND WIRELESS COMPONENTS LETTERS, VOL. 17, NO. 9, SEPTEMBER 2007.

[26] Wenquan Cao Bangning Zhang Tongbin Yu Daosheng Guo Aijun Liu "Helical-Via-Type Mushroom EBG Structure for Size Reduction" IEEE Antenna and Propagation Society International Symposium pp. 1780-81, June 2015, pp. 1347-1349

[27] D. Sievenpiper, ―High-Impedance Electromagnetic Surfaces with a Forbidden Frequency Band‖, IEEE Transactions on Microwave Theory and Techniques, vol. 47, pp. 2059-2073, November 1999.

[28] D. Sievenpiper, L. Zhang and E. Yablonovitch, ―High-Impedance Electromagnetic Ground Planes‖, IEEE MlT-S Digest, vol. 4, pp. 1529-1532, 1999.

[29] D. Sievenpiper, R. Broas and E. Yablonovitch, ―Antennas on high-impedance ground planes‖, IEEE MTT-S, International Microwave Symposium Digest, vol. 3, pp. 1245-1248, 1999.

[30] D. Sievenpiper, ―High Impedance Electromagnetic Surfaces, Ph.D. dissertation, Electrical Engineering Department, University of California, Los Angeles, 1999.

[31] F. Yang, Y. Rahmat-Samii, ―Electromagnetic Band Gap Structures in Antenna Engineering‖, The Cambridge RF and Microwave Engineering Series, October 2008.

[32] B. Jecko, T. Monediere, L. Leger, "High Gain EBG Resonator Antenna", 18th International Conference on Applied Electromagnetics and Communications, ICECom 2005, pp. 1-3, 12-14 Oct. 2005

[33] D. Sievenpiper, L. Zhang and E. Yablonovitch, "High-Impedance Electromagnetic Ground Planes", IEEE MlT-S Digest, vol. 4, pp. 1529-1532, 1999.

[34] Qian Y., Coccioli R., Sievenpiper D., Radisic V., Yablonovitch E., and Itoh T., "A Microstrip Patch Antenna using novel photonic bandgap structures", Microwave J., vol 42, pp. 66-76, Jan 1999.

[35] Z. Duan, D. Linton, W. Scanlon, and G. Conway, "Using EBG to Improve Antenna Efficiency in Proximity to the Human Body", Institution of Engineering and Technology Seminar on Wideband, Multiband Antennas and Arrays for Defence or Civil Applications, pp. 173-180, London, 13-13 March 2008.

[36] X. L. Bao, G. Ruvio, M. J. Ammann, and M. John, "A novel GPS patch antenna on fractal Hi-Impedance surface Substrate", IEEE Antenna and Wireless Propagation Letters, vol. 5, 2006.

[37] R. Baggen, M. Martínez-Vázquez and J. Leiss, "Low Profile GALILEO Antenna using EBG Technology", IEEE Transactions on Antennas and Propagation, vol. 56, no. 3, pp. 667-674, March 2008.

[38] F. Yang, Y. Rahmat-Samii, "Polarization-Dependent Electromagnetic Band Gap (PDEBG) structures: designs and applications", Microwave and Optical Technology Letters, vol. 41, issue. 6, pp. 439–444, June 20, 2004.

[39] Y. Fu and N. Yuan, "Surface-wave bandgap of Polarisation dependent Electromagnetic bandgap Structures", Microwave and Optical Technology Letters, vol. 49, issue 4, pp. 946–949, 26 February 2007.

[40] D. Yan, Q. Gao, C. Wang, C. Zhu, N. Yuan, "A novel polarisation convert surface based on artificial magnetic conductor", Asia-Pacific Microwave Conference Proceedings, APMC 2005, vol. 3, pp. 4-7, December 2005.

[41] P. J. Ferrer, B. Kelem and C. Craeye, "Design of broadband transpolarizing surfaces", Microwave and Optical Technology Letters, vol. 48, no. 12, pp. 2606-2611, December 2006.

International Journal of Engineering Works
ISSN-p: 2521-2419
ISSN-e: 2409-2770
Vol. 6, Issue 05, PP. 148-152, May 2019
https://www.ijew.io/
DOI:10.34259/ijew.19.605148152

Techniques to Mitigate Problem of Partial Shading and Soiling on PV Module: A Review

Aemal Ahmad[1]*, Muhammad Arif Khattak[2], Muhammad Zeeshan[3], Muhammad Salman[4], Kamran Alam[5]
[1,2,3,4,5]U.S.-Pakistan Center for Advanced Studies in Energy (USPCAS-E), University of Engineering and Technology Peshawar, Pakistan
*Corresponding author: Aahmad14@asu.edu[1]
Received: 09 April, Revised: 17 April, Accepted: 24 April

***Abstract*—** Power output of a pv module strongly depends on the irradiance it receives. There are many factors which limit this irradiance and badly effect power output of solar PV module. The most prominent are soiling and shading due to surrounding environment. The most damaging one is the exposure of different cells to different irradiances which is called partial shading. The subject of partial shedding and its effects on Photo Voltaic (PV) system are receiving much attention of researchers. In order to model PV system in such conditions, and design a PV system that is immune and tolerant to the problem being addressed, several research articles have been reviewed in this study. Different techniques have been summarized and briefly described here, giving an insight to model PV system and mitigate the problem, with different tested configurations that are more effective in such conditions.

***Keywords*—** Shading, Optical losses, Solar PV.

I. Introduction

There has been a tremendous shift from Carbon fuels consumptions to renewable energy which is environmentally friendly. This give a top spot to solar energy in today's widely used renewable energy sources, which is abundant, free and of extremely large potential. Transformation of this solar energy could be done in many ways but the most user friendly and affordable solution is photovoltaic systems. Photovoltaic modules used for this purpose can be managed easily and the end user is able to extract power of it by installing and managing simply without a lot to worry about maintenance. Whereas harnessing from other renewable energy sources involve complex systems that need an organized structure and deep knowledge to interact with such systems.

With the advent of latest inverter technology local consumer is able to connect its solar PV system to grid and thus can sell extra power to power utility companies. This benefit has increased PV system penetration in both rural as well as urban areas. Limited and costly lands in urban area result in too densely located houses and offices with PV modules on their roof top very nearly placed. Such environment is surrounded with tall buildings, chimneys, trees,dust, birds' droppings that blocks sunlight from equally falling on every module or even each cell in a same module. Single PV cell when receives solar irradiance give current and voltage. At temperature of 25oC and 1.5 AM illuminations single silicon solar cell give 0.5 to 0.6 V across its two terminals. [1]. All the application involving electricity consumption required a voltage higher than one cell can provide. However, it can be made useful if many such cells are cascaded together in series and parallel configuration based on the need and demand of required load and application. In order to optimize the performance of pv module cells need to be electrically matched with same currents and voltages across each cell terminal for both series and parallel combinations [2]. Even if diligence is practiced in connecting the cells together still the problem exists if different cells receive different intensity of lights. If all the cells receive equal intensity light then no such problem arise but that is the ideal condition which is not always the case. In a situation when sunlight is blocked from a cell or group of cells then hotspot is created. Such cells start acting as a load thereby consuming some power from nearby cells. This can further aggravate the problem by heating those cells which receive little or no sunlight and thus limiting the power from those cells which receive enough sunlight and thus causing partial shading to happen.

`Power output of the whole PV system is reduced when system is exposed to partial shading. It is hard to track the absolute maximum power point when partial shading causes the system to detect many local maximum power points. Such shortcomings make the need to bring immunity in PV system more important in order to improve the power output of such systems. Such design needs to disconnect those cells that receive lesser light in order to avoid those cells from limiting their power that generate enough power if isolated from shaded cells. This will bring extra safety feature to the PV module by saving module from heating up too high. This is the common objective to mitigate partial shading problem which can be achieved through number of techniques. However, all techniques follow the same basic rule to bypass these shaded cells.

The first step is to model the PV system properly and then predict the shading patterns the module or group of modules is exposed to. Then bypassing those shaded cells are of much importance through bypassing devices by keeping power loses in these devices to the minimum. These cells can be bypassed in number of ways. The use of bypass diodes has attracted quite attention and that's why all commercially available modules practice this technique [3].

This paper investigates and reviews different techniques, modelling of cells and modules, different shading conditions, effectiveness of different techniques against different shades.

In Section 2 circuit modeling has been discussed and also a brief overview of the tools and software's used by different studies. Section 3 analyses different studies done by different researchers and their contributions to mitigate the problem of partial shading.

II. CIRCUIT MODLING

In order to model PV circuit first single PV cell is modeled either with single or two diode model. A set of equations is used to model behavior of single PV cell and different elements of basic electrical circuits, such as resistors in series and parallel and diodes are used. The easiest way is to model cell with single diode as it almost gives nearly same responses as two diode model could provide with ease and simplicity in its design [2] [4] [5]. Series Rs and Shunt resistance Rp is also included in the model by most studies to consider the losses attached to them. The equivalent circuit of PV cell can be seen in Figure.1 [2]. Where Jphoto , Jdark represent photocurrent and saturation current density respectively. Vout represents cell's terminal voltage.

In order to meet current and voltage requirements modules are formed by interconnecting these cells in series and parallel fashions.

1 represent the principle equation of fig 1 as mentioned by [5] is:

$$J_{out}=J_{photo}-J_{sat}\{\exp[q\,(V+J_{out}Rs)/nkT]-1\}-V+J_{out}R_s/R_{sh} \quad (1)$$

q Represents electronic charge 1.6×10-19 C

k is Boltzmann constant = 1.38×10-23 J/K

T the cell temperature in K

In order to make such study easier simulations has been preferred because it saves time with the ease to simulate the varying uncontrolled environmental conditions of different temperatures and irradiances. Further, such simulation software's can enhance the study by observing different shades patterns. Different tools have been used in different studies: [5]–[8] uses LTspice, some authors have used Pspice [6], [7], Matlab and Simulink is also used to study PV cells [8], few studies prefer Python for simulation when these modules are exposed to different shading condition[9], [10]

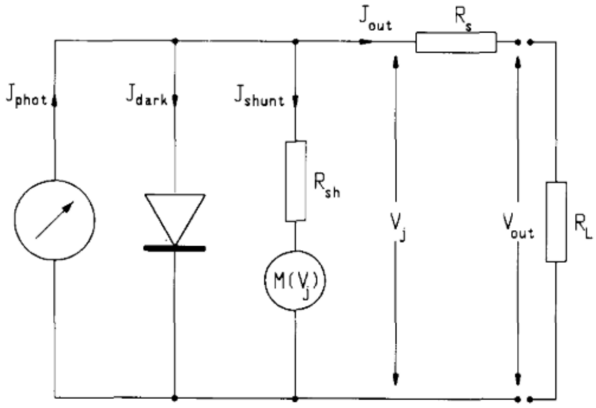

Figure 1. Solar Cell equivalent Circuit

III. TECHNIQUES TO OVERCOME SHADING

Number of techniques are currently being studied in order to solve the problem of partial shading. The most prominent and prolific one is the use of bypass diode. In such technique diodes are connecting across a cell or group of cells called strings and bypass them when they no more generate power or generate less power than other strings in the same modules [3]. Integrated diode in each cell is also used by [11]. Evidently, literature has also some studies which consider that bypassing of shaded cells can be done if cell junction breakdown voltage is controlled and reduced having the same effect as of bypass diodes [2]. Application of Power MOS Switches with cool bypass switch (CBS) is also proposed as can be seen in the study carried out by [12] bringing power losses from 4W to few mWs by replacing Schottky diode with these CBS switches. Series parallel paths in a module can enhance immunity against partial shading, such claim is proved by a study in which full and halved cells are compared [13].

[14] studies shading's effects for photovoltaic (PV) module and photovoltaic-thermal (PVT) where simulation has been done with LTspice and then results are validated with experimental study, Solarus AB module is studied and investigated for this purpose. Temperature affects maximum power Pmax , maximum voltage Vmax and open circuit voltage Voc greatly whereas temperature affects maximum current Imax and short circuit current Isc little when it is prone more to irradiance[14]. [15] studies different shading patterns for a single cell experimentally. The same study suggests that monocrystalline module is not as much affected by partial shading as do multi crystalline silicon cells [15].

For an array having many connected modules in series, if a cell or number of cells get shaded then the power output will depend on string size. Otherwise, the shaded cell will dissipate nearly twice the power produced by module if it is not bypassed with diode or any other bypassing device [16]. For every 1 A decrease in current for each cell, maximum power reduced by 0.4 W with a decrease in Voc and temperature rise for all shading conditions [7]. Power decreases by 11-12% when there is a rise of 25o C in temperature [7]. When a cell is completely shaded, then module with more bypass diodes is more efficient then the one having little number of diodes [17].

However, number of diodes is not always immunity measuring factor i.e. when part of a module is shaded by a constantly moving shadow of certain pattern, then efforts are needed to configure bypass diodes in effective way [17]. The best practice is to consider a diode configuration that is more shade resilient for a shade pattern already known and can be predicted. In [7], bypass diodes and blocking diodes' effects has been studied for an array with 3 rows and 20 modules in total when subjected to four different shading patterns.

In [4] effects a module with single and multiple shaded cells has been investigated, and IV curves are studied after exposing cells to shading and changes in IV curves are noted. [4] is used by author to diagnose fault in PV power generating system. Therefore, those primary factors can be observed which contribute to these losses upon observing the changes that occur in characteristics of IV curves [4]. Another study suggested by [18] is "hotspot prevention technique" in order to detect faults in case of partial shading. "Active fault tolerant control" can also be used to detect faults by observing and detecting closely positive peaks, and the contribution of non-uniform shadow in appearance of hotspot [18].

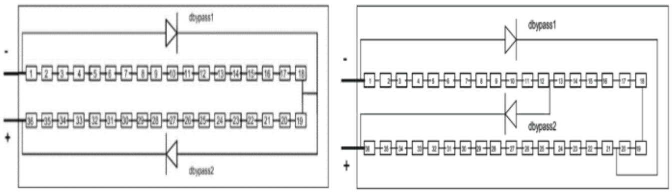

Figure 2. Equivalent circuit of PV module with two bypass diodes. (a)Non-overlapped cells (b) overlapped cells

In [19] PV cells and modules are modeled and simulated with PSPICE and then impacts on these designs are noted for different possible configurations of bypass diodes. Simulation results are compared with experimental result in [19]. In the same study two bypass diodes' model has been compared for 36 cells: One with overlapping cells and another without overlapping cells as shown in fig 2 [19]. Different observations have been made, for single and two shaded cells with overlapping and non-overlapping diodes [19]. Such study is useful in deciding an optimized configuration of bypass diodes, an expression has also been proposed that can help in deciding number of cells that could be protected by single bypass diode [19].

In [11], shading patterns has been observed for two types of cell structures: Type A and Type B. Type A has diode integrated in its cell while type B does not have such integrated diode. The tolerance of both types is experimentally quantified. When single cell is shaded with less than 10% shade, both types almost perform in similar way [11]. As shading keep on increasing Type A perform better and more resilient to shade i.e. 50% shading of a single cell contribute 40 % loss in type B system while the same shading adds losses to only 4% in type B system [11]. For 100% shade, the losses in system A are 20 times lower than that of system B [11].

[20] explains the minimum distance and tilt angle that is needed among PV modules in an array as shown in fig 3 in order to avoid shade of one row over another.

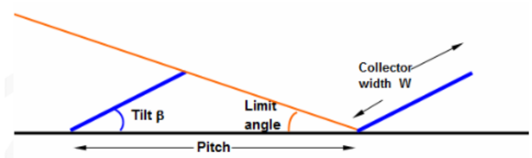

Figure 3. Reprensentation in row arrangement

W = row active width

β = plane tilt angle

P= pitch between rows.

LimAngle = ArcTan (W · cos β / (P – sin β))

Occupation ratio = OR = W / P

Occupation ratio does not depend on limit angle; it depends on tilt angle though [20].

In fig 4 comparison of different shadows can be seen on full and half cells. It is proved by [13] that 72 cells module is not affected by direction of shading. However, halved cells' module has improved result for shade moving vertically but this same module performance is exacarbated for shade that moves in X-direction [13]. Another such study uses half cells which shows that short circuit current increases to 3% and fill factor increases to nearly 1.48 percent while a decrease in losses has been noted from 8W to 2W due to decrease in series resistance value [21]. Furthermore, this study suggests use of single bypass diode across two strings of half cells [21]. The direction of moving shade has no such impact on module of standard cells [21]. However, half cells' module shows different behaviour to vertical and horizontal shade with better immunit for horizontal shades [21]. Half-cells module have the potential of minimizing losses due to shading to 50 percent at partial shading condition[21].

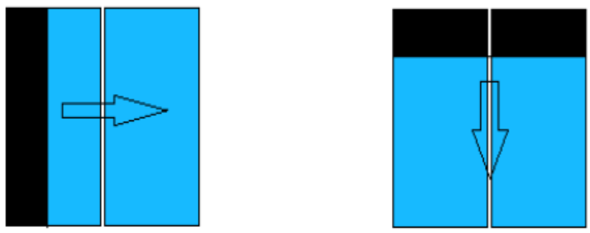

Figure 4. Effect of shadow on Full and Halved cells from two directions: (a) X direction (b) Y direction

PV industry has categorized Cells into two different categories according to reverse breakdown voltage: Type A and Type B. For type A, reverse breakdown voltage of cell is greater than maximum power point (MPP) of string, whereas for Type B it is the other way [22]. In heavy shaded condition type B does not perform good, such as illumination level of 0 W/m2 [22]. Type A also perform worst for illumination level equal to MPP power when it dissipates power equal to MPP power [22]. The cell dissipate different power related to its breakdown voltage; for lower reverse breakdown voltage less power is dissipated during mismatch. [22] experimenatlly prove the effectiveness of "open circuit protection" based on hotspot detection.

In [23], 52 different module cofingurations are studied based on simulation for shading patterns that are static and predictable, for number of bypass diodes with many parallel paths. For uniform illumination nearly each configuration behave in similar way, but those with more blocking diodes increases loses[23]. For variable illumination different parameters needs to be considered which affects the yield in a different way such as how PV modules are orientated? number of paths in parallel and number of bypass diodes. Configurations having shortest branches in the direction of movement of shade is better in its perforamnce than the rest [23]. As the number of bypass diodes increases energy yield increases. Two configurations stand out in its performances against 3 diodes series connected PV panel : the one with 5 parallel branches for landscape orientation, and another with 42 branches for portrait orientation[23]. Another such study supports the same idea of relationship between panel configurations and its effects; otuput power is reduced to 16.54% for series configuration and 6.03% for parallel configuration under same level of shading condition [24]. Another study based on static dispersion positioning (SDP) in order to reduce those partial shading loses that closely depend on direction of shading [25]. This technique without bringing any change in electrical configuration distributes partial shading effects in whole array. In [25] this technique is compared with all known topologies and based on the results this technique proved better in its performance, with 13% improvement.

In [26], bypass diode is replaced with NMOS-based Integrated Modular Bypass (NIMBUS). NIMBUS is a smart switch that detect a failing cell when subjected to shading, and then activated upon requirement. It has small losses attached to them as compared to conventional diode [26]. Such switches can be combined together in parallel in order to handle larger current than that could be handled by single NIMBUS [26]. The optimum number of cells are grouped together, and with buck converter in place current is increased whenever there is a shade for a particular group [27]. This architecture is tested for different shading patterns and the result are quite attractive with 47% and 13.4% increase in average energy generation from that of series and parallel connected cells respectively [27].

Conclusion

This paper presents in depth review of mitigating the problem of partial shading. Different studies suggest different methods and techniques to overcome the problem of partial shading. This review includes the information of simulation tools used in any study and wherever applicable their experimental data too. For already known shading patterns, a specific kind of modules should be used particular to that shading pattern and direction. Efforts are needed to solve the addressed problem with a solution, which is neither expensive nor complex without dissipating too much power.

AAcknowledgment

The authors wish to thank the researchers whose literature has been cited in this article and author providing materials and experimental setups used in this study. Research leading to this article was supported by the research grants of U.S.-Pakistan Center for Advanced Studies in Energy (USPCAS-E), University of Engineering and Technology (UET) Peshawar, Photovoltaic Reliability Lab (PRL ASU).

References

[1] "Module Circuit Design | PVEducation." [Online]. Available:https://www.pveducation.org/pvcdrom/modules/module-circuit-design. [Accessed: 02-Jun-2018].

[2] J. W. Bishop, "Computer simulation of the effects of electrical mismatches in photovoltaic cell interconnection circuits," vol. 25, pp. 73–89, 1988.

[3] C. Gonzalez and R. Weaver, "Circuit design considerations for photovoltaic modules and systems," in 14th Photovoltaic Specialists Conference, 1980, pp. 528–535.

[4] H. Kawamura, K. Naka, N. Yonekura, S. Yamanaka, H. Kawamura, and H. Ohno, "Simulation of I 2 V characteristics of a PV module with shaded PV cells," vol. 75, pp. 613–621, 2003.

[5] S. Guo, F. J. Ma, B. Hoex, A. G. Aberle, and M. Peters, "Analysing solar cells by circuit modelling," Energy Procedia, vol. 25, pp. 28–33, 2012.

[6] M. Lotfi, D. Zohir, and A. Electronic, "Modeling , Simulation and Implementation of PV Cell / Modules Using PSpice," vol. 9, no. 3, pp. 1–5, 2017.

[7] R. Rathee, V. Khanna, and B. K. Das, "Spice Based Modelling and Simulation to Study the Effects of Partial Shading on PV Array Characteristics," vol. 2, no. 5, pp. 68–73, 2013.

[8] R. P. Vengatesh and S. E. Rajan, "Analysis of PV module connected in different configurations under uniform and non-uniform solar-radiations," Int. J. Green Energy, vol. 13, no. 14, pp. 1507–1516, 2016.

[9] B. B. Pannebakker, A. C. De Waal, and W. G. J. H. M. Van Sark, "Photovoltaics in the shade : one bypass diode per solar cell revisited," no. May, pp. 836–849, 2017.

[10] E. Science and C. Details, "Master Thesis – Final Report."

[11] S. Cells and R. December, "shadow tolerance of modules incorporating i n t e g r a l the module or array . It is not surprising that this causes the rapid overheating of the cell and module destruction . The standard technique to protect against the destructive effects of partial s," vol. 19, pp. 109–122, 1987.

[12] S. Pennisi, F. Pulvirenti, and A. La Scala, "Low-Power Cool Bypass Switch for Hot Spot Prevention in Photovoltaic Panels," vol. 33, no. 6, pp. 880–886, 2011.

[13] F. Lu, S. Guo, T. M. Walsh, and A. G. Aberle, "Improved PV Module Performance Under Partial Shading Conditions," Energy Procedia, vol. 33, pp. 248–255, 2013.

[14] S. K. Nashih, C. A. F. Fernandes, J. P. N. Torres, J. Gomes, and P. J. Costa Branco, "Validation of a Simulation Model for Analysis of Shading Effects on Photovoltaic Panels," J. Sol. Energy Eng., vol. 138, no. 4, p. 044503, 2016.

[15] W. B. Xiao, F. Y. Hu, H. M. Zhang, and H. M. Wu, "Experimental investigation of the effects of partial shading on photovoltaic cells' electrical parameters," Int. J. Photoenergy, vol. 2015, 2015.

[16] A. Mermoud and T. Lejeune, "Partial shadings on PV arrays: By-pass diode benefits analysis," Eur. Photovolt. Sol. Energy Conf., pp. 6–10, 2010.

[17] S. Guo, T. M. Walsh, A. G. Aberle, and M. Peters, "Analysing Partial Shading of PV Modules by Circuit Modelling § L voltage [V]," pp. 2957–2960, 2011.

[18] M. Bressan, A. Gutierrez, L. G. Gutierrez, and C. Alonso, "Development of a real-time hot-spot prevention using an emulator of partially shaded PV systems," Renew. Energy, 2018.

[19] S. Silvestre, A. Boronat, and A. Chouder, "Study of bypass diodes configuration on PV modules," Appl. Energy, vol. 86, no. 9, pp. 1632–1640, 2009.

[20] A. Mermoud, "Optimization of row-arrangement in PV Systems, shading loss evaluations according to module positioning and connexions," 27th Eur. Photovolt. Sol. Energy Conf., no. September, pp. 24–28, 2012.

[21] H. Hanifi and J. Schneider, "reduced shading effect on half-cell modules – measurement," no. February 2018, 2015.

[22] K. A. Kim and P. T. Krein, "Reexamination of Photovoltaic Hot Spotting to Show Inadequacy of the Bypass Diode," vol. 5, no. 5, pp. 1435–1441, 2015.

[23] B. Lefevre, S. Peeters, J. Poortmans, and J. Driesen, "Predetermined static configurations of a partially shaded photovoltaic module," 2016.

[24] A. K. Tripathi, M. Aruna, and C. S. N. Murthy, "Performance of a PV panel under different shading strengths," Int. J. Ambient Energy, vol. 0, no. 0, pp. 1–6, 2017.

[25] P. R. Satpathy and R. Sharma, "Power loss reduction in partially shaded PV arrays by a static SDP technique," Energy, vol. 156, pp. 569–585, 2018.

[26] P. Bauwens and J. Doutreloigne, "NMOS-Based Integrated Modular Bypass for Use in Solar Systems (NIMBUS): Intelligent Bypass for Reducing Partial Shading Power Loss in Solar Panel Applications," 2016.

[27] M. Architecture, "Improvement of Shade Resilience in Photovoltaic Modules Using Buck Converters in a Smart," 2018.

[28] anocomposites, ACS Appl. Mater. Interfaces 6 (2014) 1415–1423.

IJEW 国际工程期刊 International Journal of Engineering Works انجینئرنگ کاموں کا بین الاقوامی جرنل

International Journal of Engineering Works
ISSN-p: 2521-2419
ISSN-e: 2409-2770
Vol. 6, Issue 05, PP. 153-158, May 2019
https://www.ijew.io/
DOI:10.34259/ijew.19.605153158

Research on Charging and Discharging of Lithium Ion Battery based on Temperature Controlled Technique

Muhammad Fahad Ali[1], Shi Linjun[2], Irfan Jamil[3], Muhammad Aurangzeb[4]
[1,2,3,4]College of Energy and Electrical Engineering, Hohai University, Nanjing, China
fadi@hhu.edu.cn[1]

Received: 11 January, Revised: 12 March, Accepted: 25 April

***Abstract*—**With the development of technology and the growing problems of environmental protection and energy shortage, renewable and clean energy power generation is receiving more and more attention. However, due to the randomness and volatility of renewable energy, it has a certain impact on the power grid. Hence, efficient energy storage technology is urgently needed to solve this problem. Therefore, battery energy storage system (BESS) has become one of the hot topic for research. Currently most of the electric energy is being stored in battery storage system. The main tasks of this paper are as follows: firstly, introduce and analyze lithium ion battery storage system and its characteristics, especially the operating temperature ranges of the optimal charging and discharging curves. Secondly, analyze the charge and discharge curve of lithium ion battery in the range of minus 40 degrees Celsius to plus 40 degrees Celsius by simulating temperature dependence model in MATLAB. And through observation, it was found that Lithium Ion Battery has better charge-discharge properties during operation in the range of zero degrees to 40 degrees Celsius. Thirdly, a temperature controlled topological method is proposed to make the lithium ion battery to operate in three temperature ranges respectively: 10 to 20 degrees Celsius, 20 to 30 degrees Celsius and 30 to 40 degrees Celsius. Based on MATLAB and GUI, a program for comparing the charge and discharge performance of lithium-ion battery in different temperature ranges was developed. The conclusions of this paper were verified by the analysis of charging and discharging in these temperature ranges. Finally, an android application is designed to upload battery voltage, temperature and circuit control status in real time. In conclusion, this paper provides some technical support for charging and discharging application of lithium battery energy storage system

***Keywords*—** Battery Energy Storage System (BESS), lithium ion battery(Li-ion), temperature control circuit, charge, discharge, temperature ranges

I. INTRODUCTION

Lithium Ion battery charger system technology is currently being incorporated in urban industrial areas to maintain with these demands lot of work is on towards [1]. Batteries are extremely convenient energy devices which employed in our daily life, in energy storage, lighting, household appliances and portable electronic devices [2],[3].Temperature plays a significant role in lithium ion batteries and their performance; cycle lifetime and safety depend highly on the temperature range. So, its operating temperature needs to be well controlled for better performance.[4],[5].Operation at higher temperatures may cause catastrophic failures, thermal runaway and may ignite fire or explosion. Different operating temperatures will also cause the difference in behavior of its operation like due to high temperature the resistance may increase which cause the change in charging and discharging characteristics of the battery[6]. So, to overcome these issues special cooling systems and protections are used to control the temperature hence increase the safety and increase the efficiency of battery. LIB's usability can be increased if its operation temperature range is extended by using modern technology.

In this paper authors have presented a temperature controlled circuitry for the charging and discharging of lithium ion battery. It's a new technique which enables the lithium ion battery to charge and discharge in specific temperature range and by analyzing its performance in that specific temperature range authors have concluded that If we make the lithium ion battery to operate in the temperature range of 20 ^{o}C to 30 ^{o}C for both charging and discharging then we get the better battery performance. To develop this circuitry, I have used various components integrated together centrally controlled by Arduino Uno.

II. LITERATURE REVIEW/ METHODOLOGY

All the battery technologies, that is, lead, nickel, lithium, and sodium-can avail different and important functions to the network thus introducing a variety of application and financial benefits.

Until recently, BESS technology that was considered economically feasible was based on lead-acid battery technology. However, recent improvements in the valve regulated lead-acid (VRLA) batteries and other types of batteries contributed towards their emergence as important energy storage components in consumer system

A. Lead Acid Battery

This type of energy storing system is marginally economical, despite having substantial maintenance and space requirements. This BESS has a characteristically shorter life, which decreases significantly once the battery's charge reaches

30%. [7] This characteristic causes a reduction in energy density thus increasing capital costs linked with this BESS. This energy storing system is mainly used in uninterrupted power supply (UPS) and in renewable and distributed power system. The main strengths associated with this system is that it has long life span, and the technology is commercially available. The key limitations linked with this system are frequent maintenance, limited portability and it is expensive as compared to conventional options.[8]

The electrolyte between the rods contains aqueous ions of H+ and SO4-2. Further, conduction mechanism at the surface of the rod involves redox reaction, where charges are transferred from ions in the solution to the conducting electrons in the electrodes. Chemical reaction that takes place during its functioning are as follows;

$$\mathrm{Pb} + \mathrm{SO}_4^{-2} \rightarrow \mathrm{PbSO}_4 + 2\mathrm{e}^-$$

Further, charged sulfate and hydrogen ions diffuse towards the lead-oxide molecules on the surface of the anode. Lead atoms become ionized and bond with sulfate ions, thus releasing two water molecules. This reaction, is as follows;

$$\mathrm{PbO}^2 + \mathrm{SO}_4^{-2} + 4\mathrm{H}^+ + 2\mathrm{e}^- \rightarrow \mathrm{PbSO}_4 + 2\mathrm{H}_2\mathrm{O}$$

The reactions above cause electrodes to be coated with lead sulfate and reduce the concentration of the acid electrolyte.[9]

Lead acid batteries are commonly used in cars as a starter. Lead acid batteries are effective in extreme conditions. Constant current charging for lead acid batteries is a set voltage of 2.40V/Cell at normal temperature of surroundings. This voltage is directly related to the temperature and it is set higher in cold environment and set to lower in warm environment.

Cold environment has some side effects for lead acid batteries like if the surrounding temperature is below 0oC and it causes the freezing of lead acid battery then it can cause permanent damage to lead acid battery. Special care must be taken in such areas and should keep the battery fully charged because in a discharge state the electrolyte in lead acid battery has characteristics resemble with water and it may freeze quicker as compared to the charged state. [10]

B. Vanadium Redox Flow Battery

Vanadium redox flow batteries (VRFB) are electricity storage system that has numerous potential applications within deregulated and decentralized energy networks.This system mainly comprises of two main elements; a) the cell stack, on which chemical energy is changed to electricity in a reversible reaction, and b) the tanks containing electrolyte where the energy is stored [11].

The vanadium redox flow battery uses vanadium on the positive and negative electrodes. One benefit of its design is that the battery's capacity does not decrease when the positive and negative electrolytes are mixed through the membrane. [20] [24] Further, the electrode reactions in the vanadium redox flow system are as follows;

Reactions taking place at the anode

$$\mathrm{VO}^{2+}(\mathrm{tetravalent}) + \mathrm{H}_2\mathrm{O} \leftrightharpoons \mathrm{V0}_2{}^+ + 2\mathrm{H}^+ + \mathrm{e}^-: \mathrm{E}^0 = 1.00\mathrm{V}$$

Reactions taking place at the cathode

$$\mathrm{V}^{3+}(\mathrm{trivalent}) + \mathrm{e}^- \leftrightharpoons \mathrm{V}^{2+}(\mathrm{bivalent}): \mathrm{E}^0 = -0.26\mathrm{V}$$

Operating temperature has a deep effect on the electrochemical process of VRFB. During the electrochemical process of charging and discharging, Operating temperature affects the electrode kinetics and transport properties.[12] Additionally, the reaction rates of hydrogen and oxygen evolution and vanadium crossover also depends on the operating temperature. Temperature affects the performance of VRFB in such a way that its voltage performance is best in conditions where temperature is increased from 15°C to 55°C. Beyond or less than this temperature will affect the efficiency of VRFB. Average charge voltage of VRFB decreases with temperature while the discharge voltage increases. Increasing operating temperature reduces both the charge and discharge overpotentials and thus favors the voltage efficiency[13]

C. NiCad Battery

The abbreviation of nickel – cadmium batteries came from the chemical symbols of nickel (Ni) and cadmium (Cd). It is a rechargeable battery mostly used in computers, camcorders, versatile drills, and other small battery-fueled gadgets, having an effective and even power release.[14][15]

Nickel based batteries have a great market in worldwide. Ni-based battery cells typically comprise of a Nickel Oxyhydroxide (NiOOH) cathode, a separator between the terminals and a basic electrolyte – for the most part potassium hydroxide – though the anode comprises of various minerals, contingent upon the Ni-based battery cell compose.[16][17]

The voltage of Ni-based batteries is 1.2V/cell and the real sorts are NiCd, NiMH and NiFe battery cells

Like other batteries, nickel based batteries also get affected by the operating temperature range Permissible range for charging nickel based batteries is 0°C to 45°C and for discharging the range is -20 °C to 65°C.[18] It is highly recommended that if charging is required to be done below freezing point then charge current must be 0.1C. [19][20]

D. Analysis of Lithium ion battery temperature dependant model

From the analysis done by using MATLAB Simulink standard model for charging and discharging at different temperatures it is observed that the battery will perform well when it is made functional above 0 oC. During the temperature above 0 oC the charging and discharging cycles of lithium ion battery gives the graph which is more near to the graph of a standard battery B (Blue) as shown in the figure below where Battery A(Yellow) is being operated in the conditions where temperature does not go below 0 oC and beyond 40 oC, so its operating temperature is kept between 0 oC to 40 oC. While Battery C (Red) is being tested for the conditions where temperature does not increase from 0 oC and decrease from -40 oC i-e between 0 oC to -40 oC .The model has been run for 4000 seconds during which the battery gets discharge first and then gets charge.

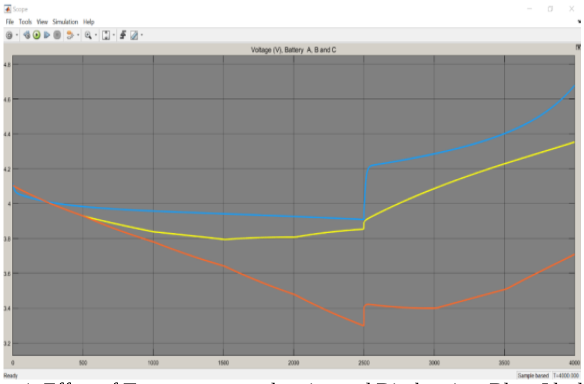

Figure 1: Effect of Temperature on charging and Discharging, Blue=Ideal State, Yellow= Battery A, Red = Battery

So considering this fact I decided to make a temperature control circuit which will control the temperature of battery to make it work in the specified temperature range and gives the output in the form of graph on MATLAB. Also, I divided the temperature ranges into three to observe the lithium ion battery Charging/Discharging best performance in specified temperature ranges which are 10-20 ^{o}C, 20-30 ^{o}C and 30-40 ^{o}C.

TABLE I. MBIENT TEMPERATURE, INTERNAL TEMPERATURE AND VOLTAGE COMPARISON OF BATTERY A.B AND C

Time	Battery A			Battery B	Battery C		
Seconds	Ambient Temp in °C	Internal Temp in °C	Voltage V	Voltage V	Ambient Temp in °C	Internal Temp in °C	Voltage V
0	0	18	4.18	4.2	0	18	4.19
500	5	12	3.95	4.0	-5	11	3.94
1000	10	9	3.86	3.9	-10	06	3.75
1500	20	10	3.78	3.88	-20	0	3.63
2000	30	14	3.79	3.85	-30	-8	3.42
2500	40	20	3.85	3.82	-40	-17	3.40
3000	40	28	4.15	4.25	-30	-24	3.42
3500	40	33	4.2	4.3	0	-21	3.49

III. METHODOLOGY

A. *Design Background*

From the analysis done by using MATLAB Simulink standard model for charging and discharging at different temperatures it is observed that the battery will perform well when it is made functional above 0 oC. During the temperature above 0 oC the charging and discharging cycles of lithium ion battery gives the graph which is more near to the graph of a standard battery so considering this fact It is decided to make a temperature control circuit which will control the temperature of battery to make it work in the specified temperature range and gives the output in the form of graph on MATLAB. Also, to observe the lithium ion battery Charging/Discharging best performance, temperature is divided into three ranges, which are 10-20 oC, 20-30 oC and 30-40 oC.

B. *Temperature Control Circuitry for Lithium Ion Battery.*

To control the temperature of lithium ion battery and to make it work in a specified temperature ranges following circuit is designed in Porteous software.

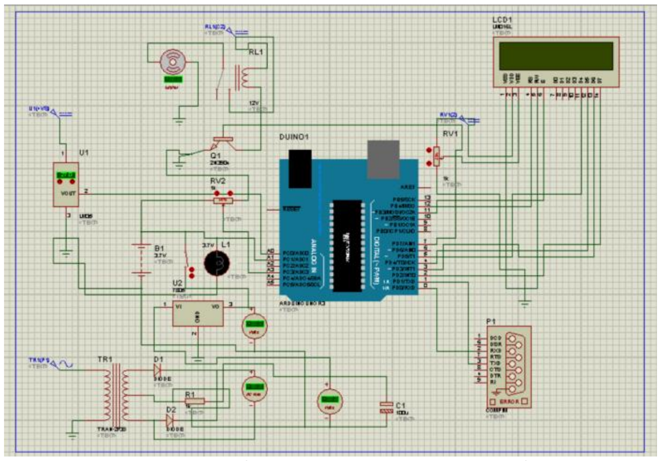

Figure 2: Proteous Model of Temperature Control Circuitry for Lithium Ion Battery

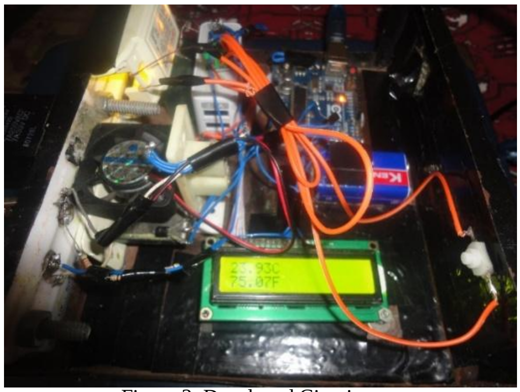

Figure 3: Developed Circuit

Figure 4: Developed Circuit

IV. RESULTS AND DISCUSSION.

For experimentation a rechargeable lithium ion battery of 3.7 V, 1050mAh is selected and placed it in circuit for charging and discharging analysis. A 4W LED is selected as load and observed the process of charging and discharging on different temperature ranges which are as follows

Charging at:

- 10 to 20 °C
- 20 to 30 °C
- 30 to 40 °C

Discharging at:

- 10 to 20 °C
- 20 to 30 °C
- 30 to 40 °C

A. *Charging Graphs*

1. Between Range of 10-20 °C

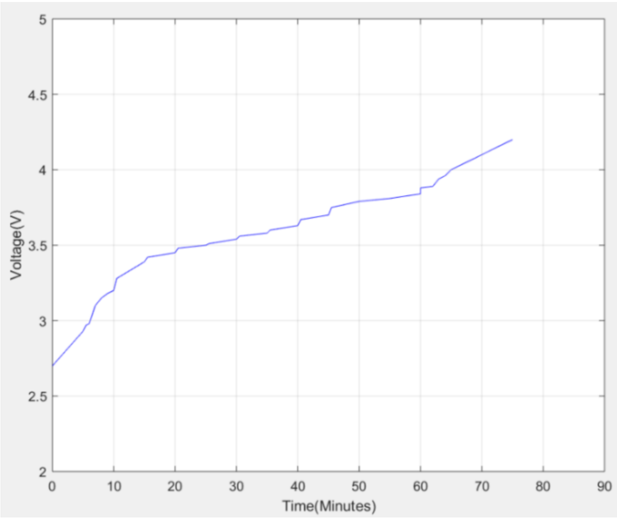

Figure 5: Graph of Charging Between temperature range of 10 to 20 °C.

2. Between Range of 20-30 °C

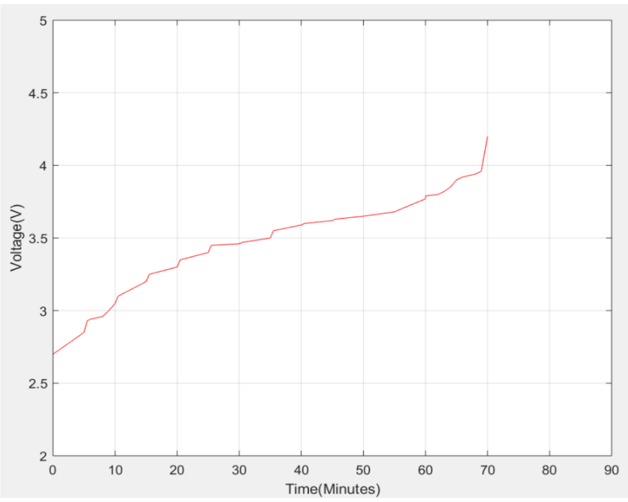

Figure 6: Graph of Charging Between temperature range of 20 to 30 °C

3. Between Range of 30-40 °C

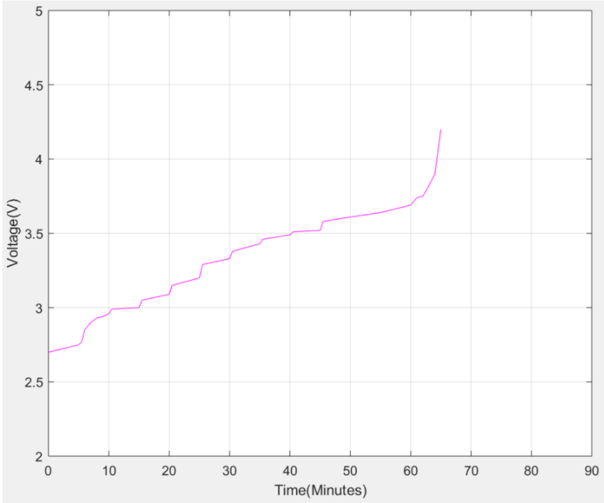

Figure 7: Graph of Charging Between temperature range of 30 to 40 °C

4. Comparison between three ranges:

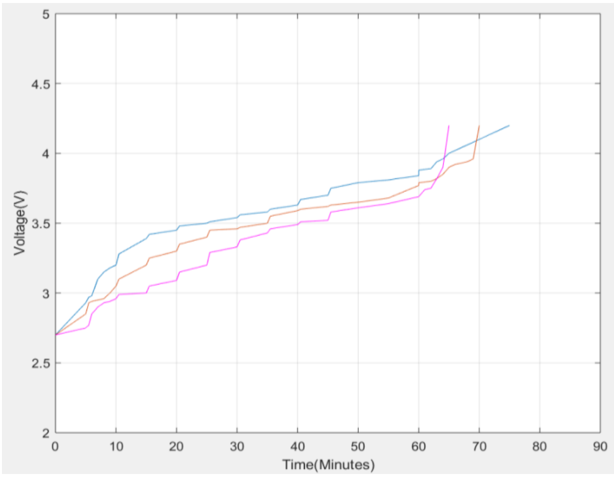

Figure 8: Comparison of All three temperature ranges

Following table shows the comparison of all three ranges.

TABLE II. COMPARISON OF THREE CHARGING CURVES

10-20 °C			20-30 °C			30-40 °C		
Time (minutes)	**Voltage (V)**	**Temp °C**	**Time (minutes)**	**Voltage (V)**	**Temp °C**	**Time (minutes)**	**Voltage (V)**	**Temp °C**
0	2.7	13	0	2.7	24	0	2.7	31
10	3.20	13	10	3.05	24	10	2.96	35
20	3.45	15	20	3.30	23	20	3.09	33
30	3.54	14	30	3.46	26	30	3.33	30
40	3.63	18	40	3.59	28	40	3.49	34
50	3.79	20	50	3.65	27	50	3.61	39
60	3.84	17	60	3.77	30	55	3.64	40
70	4.19	20	65	3.95	30	60	3.69	39
75	4.3	20	70	4.3	29	65	4.2	40

From above graph its observed that when the battery is being operated at elevated temperatures i-e between 30 to 40 °C it takes little less time to get charge as compared to the comparatively lower temperature and there is a sharp rise of voltage level near 100%SOC.Fast charging can be achieved on elevated temperatures but continuous operation on elevated temperatures is harmful for the life cycle of battery and it may harm the internal structure of battery also. While its observed from the above graphs that when battery is operated between 20-30 °C temperature range it achieves highest voltage point a little earlier as compared to 10-20 °C and also 20-30 °C is very close to room temperature. So, it can be said that battery may have longer life and faster charging at the temperature range of 20-30 °C.

B. Discharging Graphs

1. Between Range of 10-20 °C

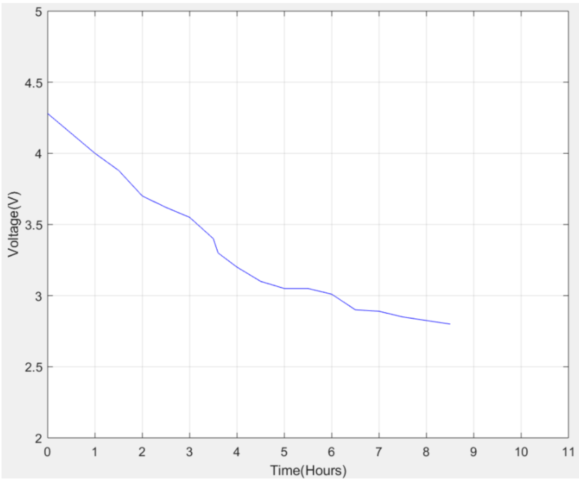

Figure 9: Graph of Discharging Between temperature range of 10 to 20 °C

2. Between Range of 20-30 °C

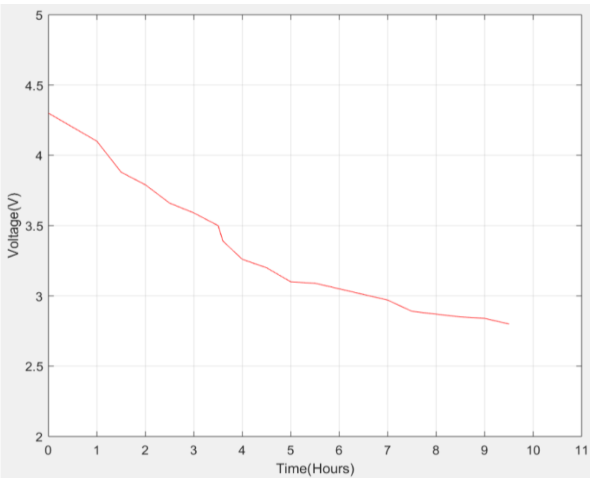

Figure 10: Graph of Discharging Between temperature range of 20 to 30 °C

3. Between Range of 30-40 °C

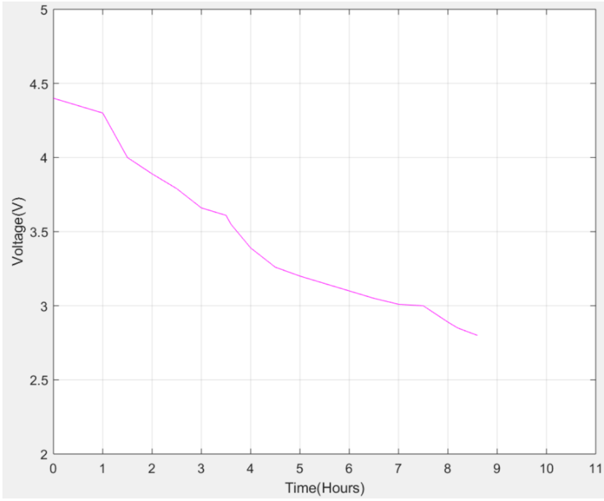

Figure 11: Graph of Discharging Between temperature range of 30 to 40 °C

4. Comparison between three ranges:

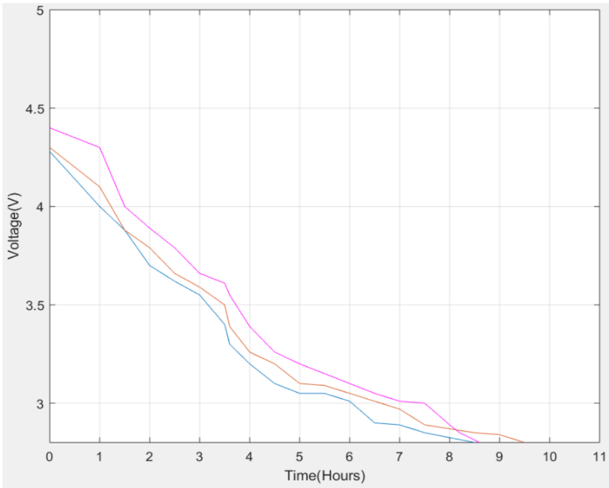

Figure 12: Comparison of all three discharging curves

From Above 4 figures it can be can seen that the discharging of lithium ion battery at three temperature ranges i-e 10-20 °C, 20-30 °C and 30-40 °C. and the 4th graph is the comparison graph of all these three temperature ranges graphs. According to the comparison of three discharging graphs at three different temperature ranges its analyzed that when battery is operating between 20-30 °C it gives the maximum discharging time as compared to the 10-20 °C and 30-40 °C. Infact during 30-40 °C it goes a sudden discharge at the extreme end. So, it can be said that if the battery temperature is maintained between 20-30 °C during discharging, maximum output can be obtained and it will also make the operating life of lithium ion battery longer. Following table shows the comparison of all three discharging curves.

TABLE III. COMPARISON OF ALL THREE DISCHARGING CURVES

10-20 °C			20-30 °C			30-40 °C		
Time (h)	Voltage (V)	Temp °C	Time (h)	Voltage (V)	Temp °C	Time (h)	Voltage (V)	Temp °C

0	4.28	15	0	4.3	22	0	4.4	31
1	4.0	12	1	4.1	23	1	4.3	33
2	3.70	10	2	3.79	25	2	3.89	35
3	3.55	15	3	3.59	27	3	3.66	36
4	3.20	19	4	3.36	29	4	3.39	38
5	3.05	20	5	3.10	30	5	3.20	40
6	3.01	16	6	3.05	28	6	3.10	39
7	2.89	18	7	2.97	26	7	3.01	36
8	2.85	17	8	2.88	23	8	2.89	36
8.5	2.80	20	9	2.84	21	8.5	2.75	35
-	-	-	9.5	2.80	24	-	-	-

CONCLUSION

This work used to investigat efficiency of charging and discharging for battery level with temperature range. The circuit developed, makes the battery to operate between the temperature range of 10 to 40 ^{o}C. And after analyzing the charging/discharging performance of a lithium ion battery in these temperature ranges authors have come to a conclusion that as far as charging is concern the battery will be charged quickly at the elevated temperatures but continuous operation at elevated temperatures is not feasible for the battery life and it may harm the battery so after graphic analysis for battery charging, 20-30 ^{o}C is found to be the best suitable temperature range and for discharging, the battery can be operated between 10-20 ^{o}C it also gives good results in this temperature range but it may give better results if its been operated between 20-30 ^{o}C range. By keeping the operational range of lithium ion battery in these temperature ranges, performance and life of Lithium ion battery can be enhanced.

REFERENCES

[1] F. Ausfelder, "Energy Storage Systems: The Contribution of Chemistry". Jun.-2017.

[2] [M. Singh, L. A. Lopes, and N. A. Ninad, "Grid forming Battery Energy Storage System (BESS) for a highly unbalanced hybrid mini-grid," *Elecric Power Systems Research*, vol. 127, pp. 126–133, 2015.

[3] K. Divya and J. Østergaard, "Battery energy storage technology for power systems—An overview," Electric Power Systems Research, vol. 79, no. 4, pp. 511–520, 2009.

[4] Y. Parvini and A. Vahidi, "Maximizing charging efficiency of lithium-ion and lead-acid batteries using optimal control theory," *2015 American Control Conference (ACC)*, 2015.

[5] T. Sasaki, K. Enomoto, T. Shigematsu, H. Deguchi, "Evaluation Study about Redox Flow Battery Response and its Modeling," CEPSI Fukuoka (2002)

[6] X. Luo, J. Wang, M. Dooner, J. Clarke, Overview of current development in electrical energy storage technologies and the application potential in power system operation, Appl. Energy 137 (2015) 511–536.

[7] A. Oberhofer, "Energy Storage Technologies & Their Role in Renewable Integration". Jun. - 2012.

[8] A. Joseph and M. Shahidehpour, "Battery storage systems in electric power systems," *2006 IEEE Power Engineering Society General Meeting*, 2006.

[9] M. Beaudin, H. Zareipour, A. Schellenberg, and W. Rosehart, "Energy Storage for Mitigating the Variability of Renewable Electricity Sources," *Energy Storage for Smart Grids*, pp. 1–33, 2015.

[10] Association Of European Automotive And Industrial Battery Manufacturers, "Energy Storage for Smart Grids," 2015.

[11] H. Zhang, "Redox Flow Battery for Energy Storage," 2010.

[12] L. Lu, X. Han, J. Li, J. Hua, M. Ouyang, A review on the key issues for lithium-ion battery management in electric vehicles, Power Sources 226 (2013) 272e288.

[13] S. Teleke, M. E. Baran, S. Bhattacharya, A. Huang, ―Rule Based Control of Battery Energy Storage for Dispatching Intermittent Renewable Sources, IEEE Trans. Sustainable Energy, vol. 1, no. 3, pp. 117–124, Oct. 2010

[14] Ahmad Rahmoun, Helmuth Biechl, Modeling of Li-ion Battery using equivalent circuit diagrams, ISSN 2012

[15] U. Rudez and R. Mihalic, "Revealing Disturbance Localization Issues in Large Power Systems," *Engineering and Industry Deregulated Electricity Market Issues in South Eastern Europe*, 2015

[16] X. Luo, J. Wang, M. Dooner, and J. Clarke, "Overview of current development in electrical energy storage technologies and the application potential in power system operation," *Applied Energy*, vol. 137, pp. 511–536, 2015.

[17] S.teleke, M.E. Baran, S. Bhattacharya, A. Huang, "Rule Based Control of Battery Energy Storage for Dispatching intermittent Renewable Sources", *IEEE Trans Sustainable Energy, Vol 1,no.3, pp.117-124, oct 2010.*

[18] I. Plitz, A. D. Pasquier, F. Badway, J. Gural, N. Pereira, A. Gmitter, and G. G. Amatucci, Applied Physics A, A82, 615- 626 (2006).

[19] M. Singh, L. A. Lopes, and N. A. Ninad, "Grid forming Battery Energy Storage System (BESS) for a highly unbalanced hybrid mini-grid," *Electric Power Systems Research*, vol. 127, pp. 126–133, 2015.

[20] Y. Parvini and A. Vahidi, "Maximizing charging efficiency of lithium-ion and lead-acid batteries using optimal control theory," *2015 American Control Conference (ACC)*, 2015.

Muhammad Fahad Ali received his degree of BE Electronics Engineering from National University of Sciences and Technology (NUST) in 2013. He is currently pursuing Masters degree in Electrical Engineering from College of Energy and Electrical Engineering at Hohai University Nanjing, China. His area of specialization is in Battery Energy Storage System, its utilization in Renewable Energy Plants and house hold equipments. He has worked on Infrared based tracking system and Development of boost converter with coupled inductors for PV system applications.

International Journal of Engineering Works
ISSN-p: 2521-2419
ISSN-e: 2409-2770
Vol. 6, Issue 05, PP. 164-171, May 2019
https://www.ijew.io/
https://doi.org/10.34259/ijew.19.605164171

Enhancement of Dynamic Performance of Transmission Line using Static Synchronous Series Compensator

Muhammad Ali[1], Prof. Dr. Naeem Arbab[2], Muhammad Daniyal[3]
[1,2,3]USPCAS-E, University of Engineering & Technology, Peshawar.
engr.muhammadali78@yahoo.com[1], mnarbab@yahoo.com[2], engr.daniyal11@gmail.com[3]
Received: 16 April, Revised: 26 April, Accepted: 30 April

***Abstract*—**Static synchronous series compensator (SSSC) belongs to the facts family. It controls the flow of power in transmission line. The SSSC is a voltage source inverter connected in series with the transmission line and injects the voltage in quadrature with line current. Demand of power is growing day after day. Installation of new transmission lines is difficult because of environmental factors. The power flow capacity of existing transmission line has to be increased which is done by using compensation devices. The main reason behind poor performance of transmission system is the power flow capacity of existing transmission line under dynamic situations subjected to disturbances. FACTS technology opens new opportunities for controlling power and increases the usable capacity. It enhances corresponding power to flow through such lines under normal and contingency conditions. Recently new advancement in FACTS technology has introduced devices for reactive power compensation.

In this paper, a case study is discussed and test system is simulated in MATLAB/Simulink under normal conditions and also under fault conditions to improve the transient stability of the system. A 132kv transmission line coming from Kohat grid station to tall grid station has been selected as a test system which is suspected to overloaded conditions due to which voltage stability could not be maintained especially during the months of June, July and August. Static synchronous series compensator (SSSC) is installed near the Kohat bus. The results of current, voltage, active power and reactive power have been analysed with and without SSSC in the test system. Results shown that the stability of power system, voltage profile and power flow capability enhances by using SSSC. Also by using SSSC the oscillations were damped very quickly as compared to the circuit without using SSSC and the stability is maintained.

***Keywords*—**Flexible Alternating Current Transmission System (FACTS), Static Synchronous Series Compensator (SSSC), MATLAB/Simulink Software, Per Unit (Pu), Peshawar Electric Supply Company (PESCO).

I. INTRODUCTION

The modern power system covers a large area, and has a large number of buses, load and generators. In addition, the production plants available are often not close to the load centers and therefore power must be transmitted over long distances. To respond to the day by day increasing electrical load and industrialization new lines should be added to the system to fill the gap between generation and consumption, but because of the cost, the installation of new lines is mostly restricted [1]. Therefore, power system companies are forced to rely on the infrastructure already existing instead of constructing new transmission lines. In order to maximize the efficiency of production, transport and distribution of electrical energy, the transmission networks are very often pushed to their thermal and physical limits, which cause power disruption and individual power outages and could lead to failure of the entire system. With such an increased stress on the transmission lines of existing system, use of different methods of compensation becomes important [2].

Electric power system ability to damp system oscillation after occurrence of major fault is called stability of power system. After the occurrence of fault, there is disturbance in power system until the oscillations are damped out. Any change in voltage or frequency in AC power system leads to disturbance [3]. Part of the system where fault has occurred should be disconnected to avoid system break down. Eventually to avoid whole system break down or disturbance in system, voltage and frequency should be observed and controlled accurately. A very common type of fault is short circuit fault which restrain the voltage of grid thus causing oscillations by disturbing the rotating machines in jurisdiction of fault. In order to avoid system instability these oscillations need to be damped out. Voltage stability, frequency stability and inter area stability are of major concern in AC electric power system [4]. When electric power system does not fulfill the demand of reactive power, voltage instability is caused. Healthy voltage profile must be maintained and must constantly be delivered to load. But there is always a diversity factor i.e. variation in demand time to time so power system's reactive power demand also changes that is the reason why voltage instability is caused in power system which effects the quality of power transmitted.

A. Flexible Alternating Current Transmission System

The long established techniques for solving these difficulties; usually we use mechanically and fixed switched shunt and series capacitors, synchronous generators and reactors. Due to slowly response, damage of mechanical components, derived response has not been effective. Power electronic converters are created with the innovation of Thyristor devices. It is based controller that provides unwrinkled, continues, at a great rate and able to be done again performance for control of power system. FACTS family is an implementation of power electronic devices to electrical transmission systems. FACTS are AC transmission systems that Composed of other static controllers and power electronic controller. Current rating has enhanced to larger values for Thyristor in the last years. It made power electronics able and thousands MW high power applications.

FACTS devices has their speed and resilience are capable to supply the transmission system with a few benefits. Examples are Transient stability enhancement, voltage stability and control, power oscillation damping. The chosen device sort and rating and the specific voltage level, a transmission capability improvement of up to 40% to 50% may be obtained by FACTS elements. Now days the fundamental abstractions to the integration of these promising innovations are Cost, complexity and reliability issues.

FACTS technologies give solutions to today's power system. It increases power flow transfer capability. It also enhances voltage profile continues control, enhancing damping of system, minimizing losses etc. FACTS devices has its real time operating control with high power electronics based equipment. FACTS controllers two groups which is based upon various technical methods, resulting in controllers capable to solve transmission problems [5].

B. Static Synchronous Series Compensator (SSSC)

The static synchronous series compensator (SSSC) is a series device of the Flexible AC Transmission Systems (FACTS) family using power electronics to control power flow and improve transient stability on power grids. In place of using capacitor and reactor banks, a SSSC use self-commutated voltage-source switching converters to synthesize a three-phase voltage in quadrature with the line current. The main interest is to use the SSSC for controlling flow of power (active and/or reactive) in transmission lines, whereas the SSSC is mainly recommended for damping electromechanical oscillations. Thus, the SSSC control system may be made by a compensation control loop, to accomplish its steady-state function, and by a fast response control, to act during electromechanical transients [6].

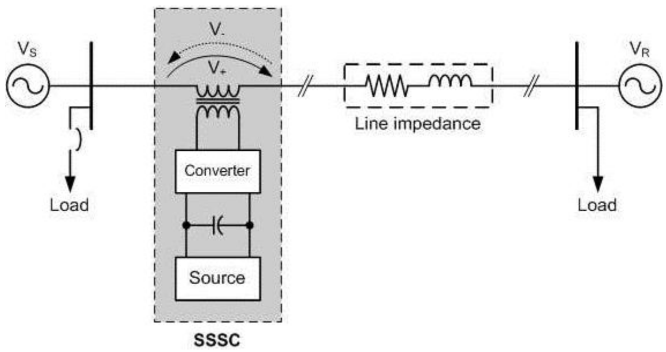

Figure 1. Static synchronous series compensator (SSSC) [6]

II. RELATED WORK

The long transmission lines connected to the weak grid system will result in system instability. Work has been done to enhance the transmission line flow limits and the system stability. The first swing and subsequent stability limit of oscillation of a system with SSSC and STATCOM is discusses in [7] one at a time. In both cases the stability of the system was greatly increased. STATCOM improved first swing limit of stability more affectively shown by Results, however in the subsequent swings SSSC was more affective. This paper is deficient in system response in Transient condition.

Moreover, in [8] the some technical issues that include sub synchronous resonance, protective equipment's and reliability of capacitors are discussed. Traditionally used series capacitor could not eliminate these technical problems, so a new series compensation device called static synchronous series compensator was used in transmission line to remove those problems, that device consist of synchronous voltage source, voltage source converter employing IGBT or gate turn off relying upon power requirements. The basis for superior operation and performance of static synchronous series compensator was proffered by voltage source nature.

About real and reactive power to enhance the amount of power delivered by the transmission line, authors also discussed [9] about compensation methods. Performance of power system is made better by using series compensation technique which enhances the power flow. In future some more wok can be done in this paper to model SSSC in such a way to control true power and reactive power flow in the system.

The SSSC were brought in contact with electrical parameters of the line in paper [10]. It was straight forward from the results that PI and PID (fuzzy logic controlled devices) provided by FACTS family (SSSC) has developed method used for control to great extent.

The requirement of real and reactive power flow in the transmission line for the reason of compensation and increase of the capacity of power transferred by a line when IPF Controller acted as standalone as SSSC. In this paper [11] a test case was presented and from the numerical results performance and eligibility of compensation device on transmission line was demonstrated.

The SSSC was modeled and simulated in research paper [12], SSSC inserted voltage is sinusoidal and variable in magnitude is shown from result. The inserted volts are in phase quadrature with the transmission line amps. The line is in series with the capacitive reactance and inductive reactance. The operation and working of a novel control scheme designed both for SSSC and STATCOM described by the Authors in [13]. The scheme was based on a design which composed of 48-pulse GTO voltage source inverter. Authors studied voltage stability and compensation of reactive power in the electric grid network. The designed scheme containing SSSC and STATCOM in the power system was simulated and complete digital simulation was performed.

Phase-lead characteristics are provided by 2 stage block in paper [14], for the compensation of the output signals which lag behind the input signal. Block three is a high pass filter also called wash out block. Volts Vabc and amps Iabc respectively are taken as input by power oscillation damping controller and are converted into power. The switch remains unclosed when the fault does not occur but when fault occurs then the switch closes. An error signal is produces after the oscillations are damped out, and at the end both error signals are added.

Two area 11-bus test systems is used in paper [15], so we have two areas which are zone-1 and zone-2, these are used to check the efficiency of the series compensator, the FACT family device which is used for series compensation is static synchronous series compensator, it is connected between bus-9 and bus-10. Volts sources of (13.8) kilo Volts are attached to a (290) kilo meter line with the help of three-phase transformer, this step up transformer has an output voltage of 500KV and power in area-1 and area-2 are 1000MVA and 4200MVA respectively. Loads in both area-1 and area-2 are 30KW which are such designed that the true power flow on the line is from zone-1 to zone-2. The true power and reactive power used by the connected load is a function of the system volts.

III. PRINCIPAL OF SERIES COMPENSATION

The voltage source VC is connected at the intermediate point of a transmission line. As shown in figure2 represents an ideal series compensator.

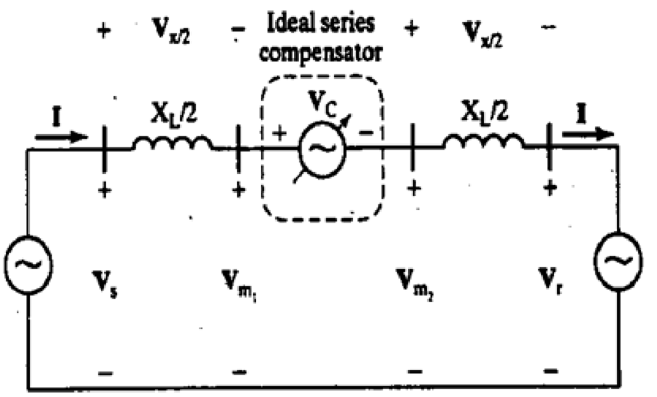

Figure 2. Ideal Series compensator in transmission line

In transmission line current flowing is given by:

$$I = \frac{Vs - Vr - Vc}{jX} \tag{1}$$

Voltage source can only supply or absorb reactive power in transmission line as series compensator cannot supply or absorbed real power [4]. It is replaced by capacitive or inductive impedance shown in equation 3.3

$$Xeff = X - Xcomp \tag{2}$$

Xcomp represents inductive or capacitive impedance, X represents total impudence of transmission line Xeff represents the effective impedance. Current leads voltage by 90oinductive mode. Power is not absorbed/generated by the voltage source (VC) installed in inductive and capacitive modes. Capacitive mode of compensation is commonly used. Compensation cost for series capacitor is less than shunt capacitor. The cost per unit VAR of shunt capacitor is half as compared to series capacitor. Series capacitor rating will nearly be 10% of shunt capacitor rating [16].

IV. CONCEPT OF SERIES CAPACITIVE COMPENSATION

Basic principle of series capacitive compensation is to decrease the overall series impedance of the line as shown in Equation 1, power is inversely proportional to impedance (X), as overall impedance of the circuit decreasing power flow increases. In Figure 3 (a) series compensated line with two identical sections is represented. Magnitude of voltage across inductor is assumed to be equal. Let us suppose that magnitude of voltage across inductor for same end voltages is increased by the magnitude of the compensation voltage developed across series capacitor, resulting in an increase in transmission line current.

$$P = V2\sin \delta / X \tag{3}$$

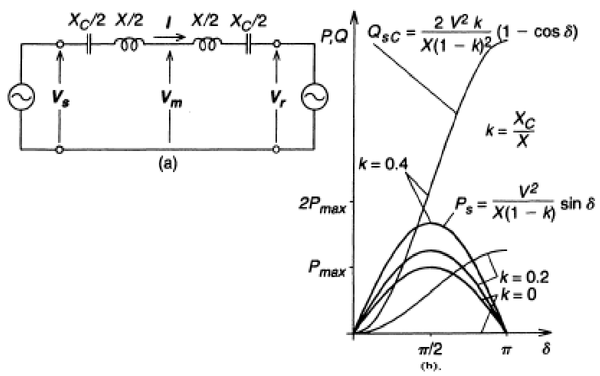

Figure 3. (a) Two machine power system with series capacitive compensation. (b) Real power and series capacitor reactive power vs angle characteristics

For series capacitive compensation Equation 4.3 becomes:

$$X_{eff} = X - X_c \tag{4}$$

Or

$$X_{eff} = (1\text{-}k)\ x0 \le k<1. \tag{5}$$

In Equation 4.6 ‘K’ shows the degree of compensation. Thus by changing K we can control the flow of power. After compensation the current equation is given in Equation 4.7.

$$1 = \frac{2V}{(1-k)} \text{ x } \sin\frac{\delta}{2} \tag{6}$$

The real power is given as:

$$P = V_{m1} = \frac{V^2}{1-K}\sin\delta \tag{7}$$

The reactive power supplied by the series capacitor can be expressed as follows:

$$Q_c = I^2Xc = \frac{2V^2K}{X(1-k)^2}\ 1 - \cos\delta \tag{8}$$

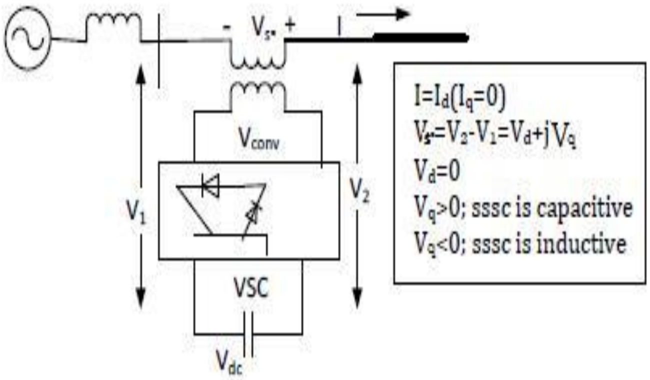

Figure 4. Connection of SSSC with transmission line [17]

Above figure.4 shows how SSSC is connected with the transmission line in the power system, to connect SSSC in series with the transmission line coupling transformer is used, capacitor is connected on the DC side of the circuit and is kept charged by drawing small power from the system, the control block is DC to AC converter, it may be IGBT or GTO. Basic equation of power flow is given as:

$$P = \frac{V_s V_r}{XL} \sin(\delta s\text{-}\delta r) = \frac{V2}{XL} \sin\delta \tag{9}$$

$$Q = \frac{Vs\, Vr}{XL} (1\text{-}\cos(\delta_S\text{-}\delta_R) \tag{10}$$

SSSC has the ability of emulating a compensating reactance Xq (both inductive and capacitive) in series to the transmission line inductive reactance XL, Therefore, the expressions for power flow becomes:

$$P_q = \frac{V^2}{X_{eff}} \sin\delta = \frac{V^2}{XL(1-\frac{x_q}{X_L})} \sin\delta \tag{11}$$

$$Q_q = \frac{V^2}{X_{eff}}(1\text{-}\cos\delta) = \frac{V^2}{XL(1-\frac{x_q}{X_L})}(1 - \cos\delta) \tag{12}$$

The reactance of the transmission line between sending and receiving ends Xeff. In above equations, it also comprise of emulated variable reactance Xq inserted by the injected voltage source of the SSSC.

V. Modeling of Circuit in MATLAB

A detailed model has been designed and developed in MATLAB/Simulink. The results of system with and without SSSC have been analyzed. The Model was selected from Kohat area as currently that area is facing the low voltage issues especially during peak load in month of June, July and August. Using SSSC we achieved an improved voltage profile, power flow and better transient stability of system.

A. *Case Study*

In this article the case study is Kohat, Gurguri and Tall 132 kV grid station as shown in figure 5. During peak load especially in the month of June, July and August, the grid faces low voltage problems due to which the system become overloaded as shown in table 1. In transmitted power after occurrence of major faults the problem of Transient stability can become the limiting factor. To enhance the power transfer capability and to increase voltage stability during overloaded and fault conditions SSSC is installed near Gurguri grid station. By increasing the voltage stability at the consumer end, the possibilities of blackouts have been reduced in the mentioned area. Furthermore, the forced load shedding, which is considered as a big loss for the utility companies has been avoided.

Test system has been simulated in MATLAB/Simulink at overloaded conditions. The outputs have been analyzed for the test system with and without SSSC in the circuit as shown in figure 6 and figure 7 respectively.

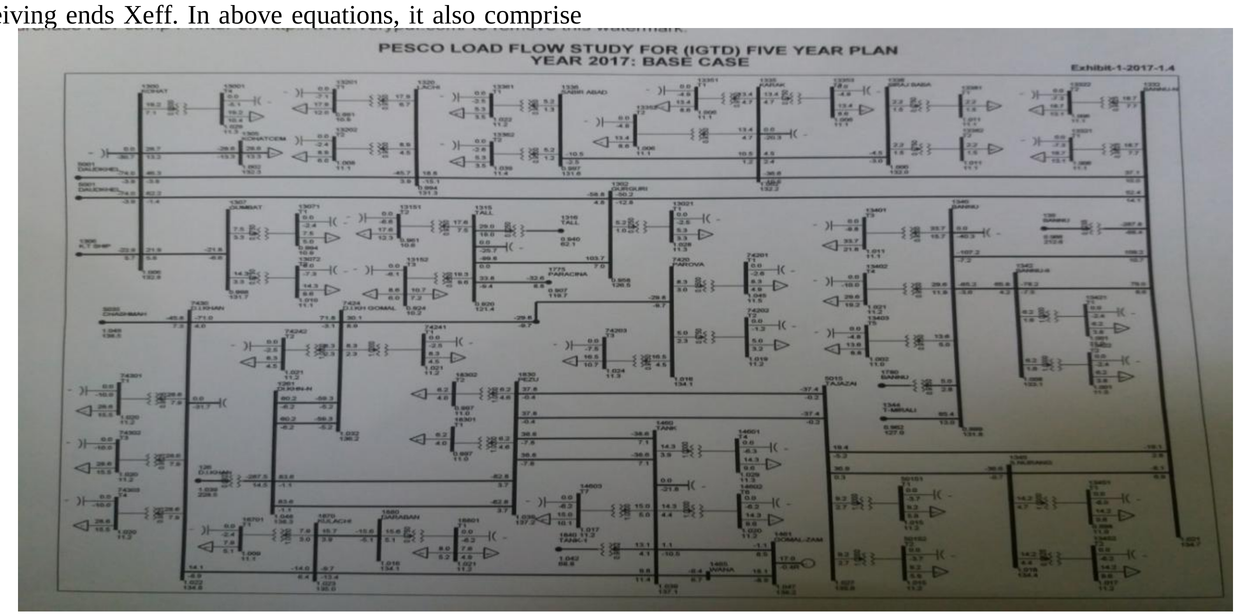

Figure 5. Test System

B. System without SSSC

In this system Three-phase programmable voltage source is modeled as 132kv Kohat grid station here in MATLAB/Simulink. Configuration of which is shown below in figure 6, Three buses are used in the test system i.e. Kohat Bus, Gurguri Bus and Tall Bus which are modeled as Three-phase V-I measurement. The transmission line between the grids is modeled by distributed line parameter block. The results are analyzed under overloaded condition.

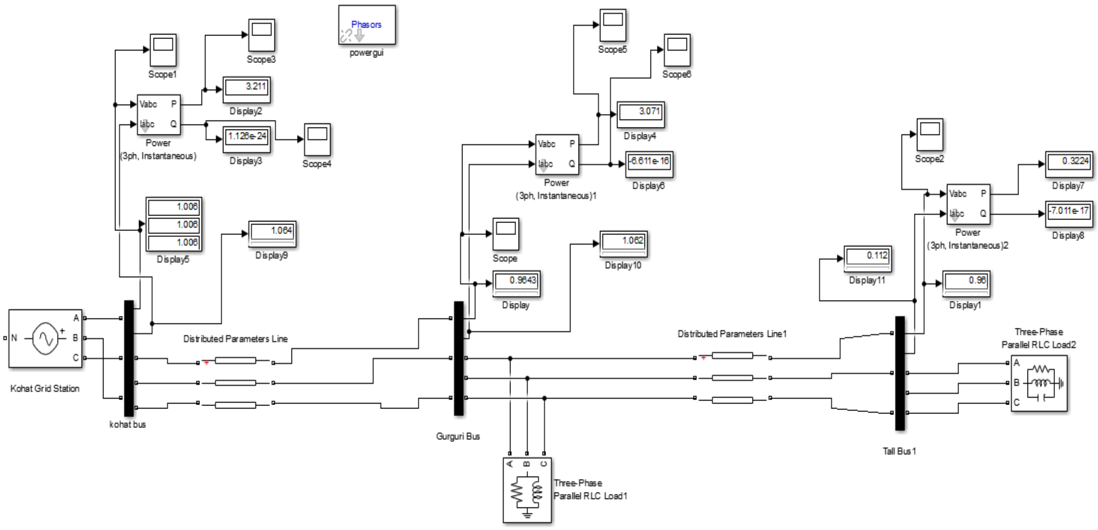

Figure 6. Simulink model of test system without using SSSC

C. Syste using SSSC

Now SSSC is installed near Kohat bus in 132kv transmission line coming from Kohat to Gurguri as shown in figure 7, as the line length is in range of medium transmission line so SSSC can be installed and used to fulfill the need of the test system. In Simulink test system is simulated with SSSC and the results are analyzed.

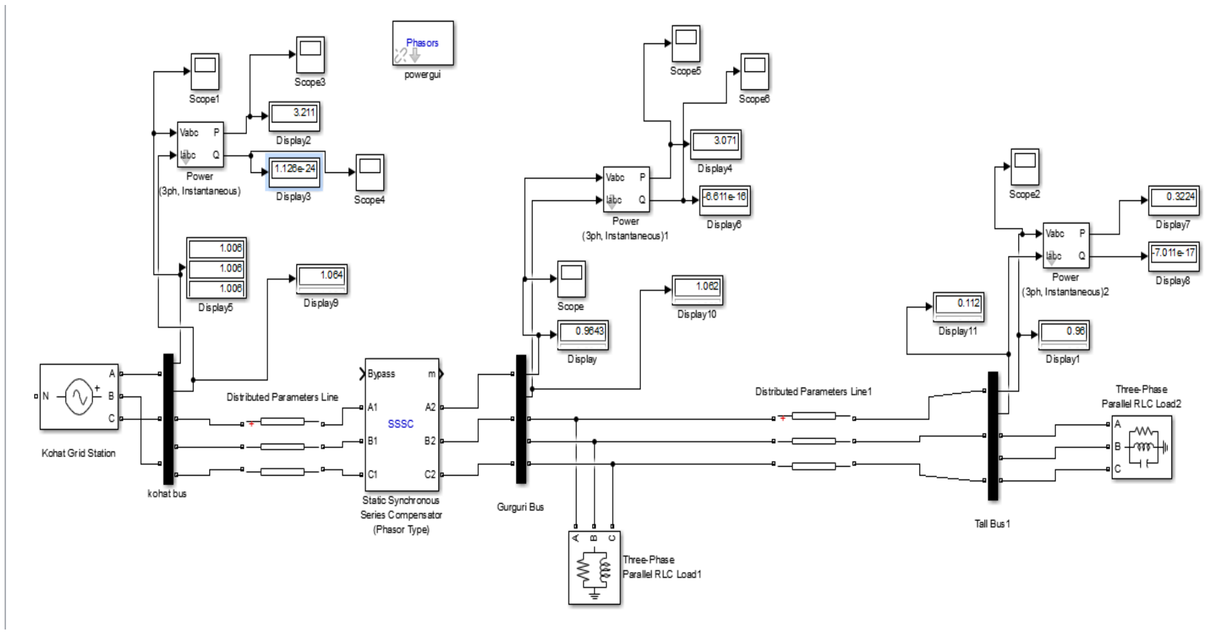

Figure 7. Simulink Model of test system using SSSC

D. *Discussion on Results*

The results of simulation without SSSC are shown in Table 1. The below data is for the months of June, July and august in overloaded conditions at peak load. The data is in terms of different parameters consists of voltage (pu), current (pu), Active power (pu) and reactive power(pu) respectively. All these values are taken before the installation of SSSC at peak load. Test system is simulated with SSSC in MATLAB/Simulink and the results are shown in Table 2.The same parameters were again tested and analyzed on the same conditions after the installation of SSSC. The obtained data clearly shows that there is a significant increase in the values of voltage (pu), current (pu), Active power (pu) and reactive power (pu) after the installation of SSSC.

TABLE I. TEST SYSTEM WITHOUT SSSC AT PEAK LOAD

Bus	Voltage (pu)	Current (pu)	Active Power (pu)	Reactive power (pu)
Kohat bus	1.008	1.021	1.202	0.9597
Gurguri Bus	0.9425	1.035	1.208	0.8253
Tall Bus	0.9180	0.1872	0.2011	0.1923

TABLE II. TEST SYSTEM WITH SSSC AT PEAK LOAD

Bus	Voltage (pu)	Current (pu)	Active Power (pu)	Reactive Power (pu)
Kohat Bus	1.064	1.064	3.211	2.972
Gurguri Bus	0.9643	1.062	3.071	2.958
Tall Bus	0.960	0.112	0.3224	0.1988

It is clear from the results that voltage profile is improved at Kohat and Gurguri bus and the active and reactive power flow is enhanced. All the values are given in per unit and according to PESCO 0.95pu in the healthy voltage limit below which the system gets overloaded. During peak loads the voltage level at Kohat and gurguri bus goes below healthy voltage limit thereby increasing current in the circuit which increases losses. Under these conditions the system becomes overloaded which lead to forced load shedding. In order to reduce these losses and increase the flow of power, series compensator SSSC is included in the system model simulation which shows that voltage profile is improved and goes above 0.95 per unit for both Kohat and Gurguri bus thus increase in flow of active and reactive power in the system.

Figure 8 and Figure 9 shows the result of active power and reactive power respectively for the test system without using SSSC.

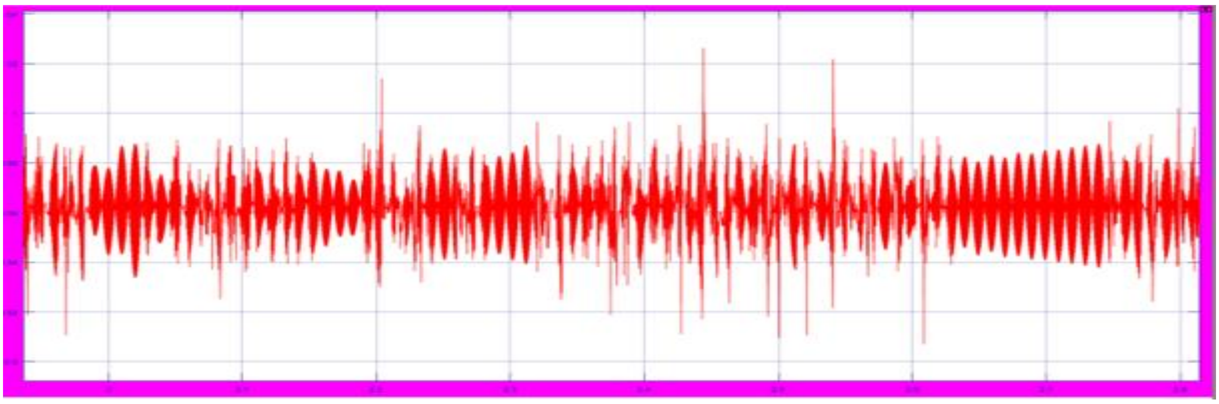

Figure 8. Reactive power flows in test system without using SSSC under overloaded condition

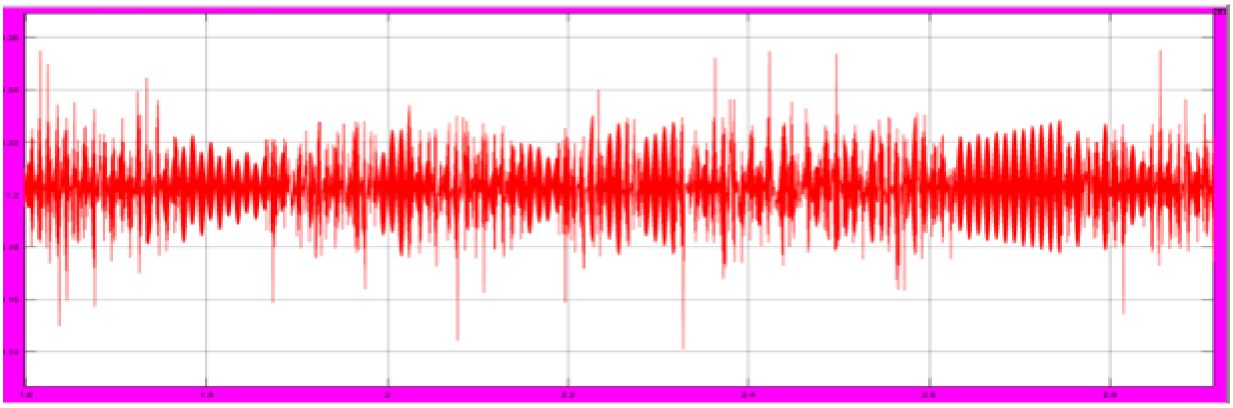

Figure 9. Active power flows in test system without using SSSC under overloaded condition

Figure 10. Active power flows in test system with using SSSC under overloaded condition

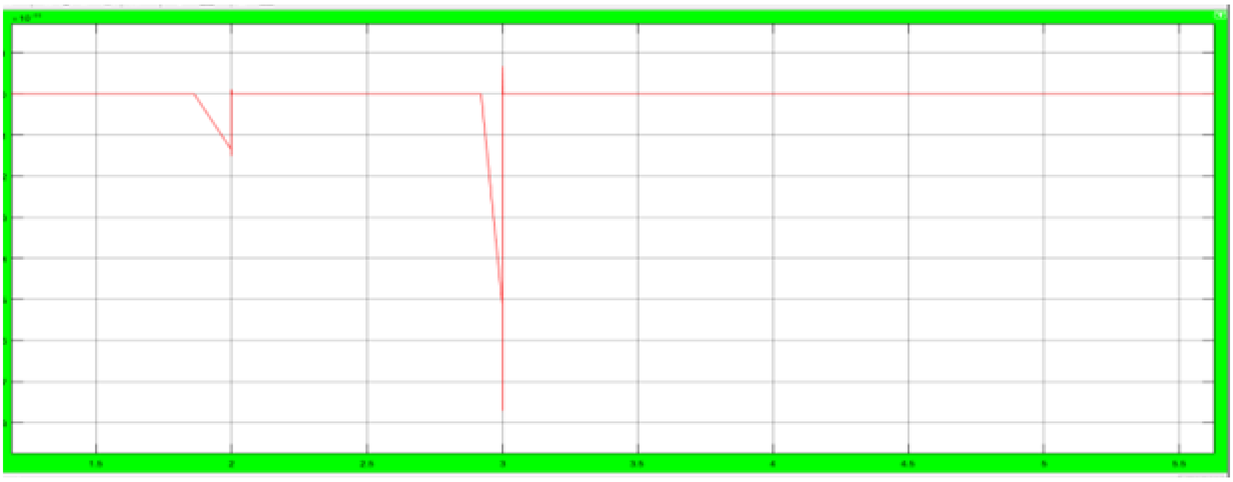

Figure 11. Reactive power flows in test system with using SSSC under overloaded condition

Figure 8 and figure 9 shows that during overload conditions oscillation go on increasing and the system destabilizes at the end which leads to force load shedding and due to this losses occur both to utility and customer.

Figure 10 and Figure 11 shows the result of active power and reactive power respectively for the test system with using SSSC.

After compensation techniques used, now in overloaded condition the series compensator provide reactive power to transmission line which increase the flow of active power in transmission line from generating station. in figure 8 and figure 9,the oscillation when rise up, the control system of SSSC detects and in milliseconds required voltage is provided which is in line qudrature with transmission line current and overall voltage level gets improved and system reaches to stability very quickly as can be seen in figure 10 and 11 a straight line after oscillation. Oscillations are damped very quickly and system becomes stable.

Acknowledgement

This project consumed huge amount of work, research and dedication. Still, implementation would not have been possible if I did not have a support of Prof. Dr. Naeem Arbab, Engr. Muhammad Daniyal and PESCO. Therefore I would like to extend my sincere gratitude to all of them.

Concuslion

SSSC has recently become the most effective and important device for the compensation of reactive power in power system. Installation of the new transmission lines are generally not economical. Furthermore, it is also a very time consuming method due to which power flow can be interrupted and can be very costlier in the urban areas. SSSC becomes the only way left to increase the power flow and to improve voltage stability in an economical way. A case study has been selected from Kohat area which is in PESCO. There is a 132Kv transmission line coming from Kohat to Gurguri. During over loaded conditions voltage stability is not maintained especially during the months of June, July and august. Losses increases and force load shedding is usually carry out which is big loss to the power supply companies. In this research paper SSSC is used to achieve voltage stability and enhance power flow in the network. The test model is implemented in MATLAB/ Simulink for two different scenarios. In both the Scenarios, with and without SSSC, the result of current, voltage; active power and reactive power have been analyzed. In first portion test system was simulated in overloaded condition. After simulation results it was clear that voltage profile has been improved greatly by using SSSC in the circuit. Power flow capacity has also been enhanced using SSSC. In second portion the test system was simulated under a common three phase short circuit fault and the result shows that by using SSSC the oscillation was damped very quickly as compared to the circuit without using SSSC and the stability was also maintained. Even though the obtained model results were very satisfactory. But still there is room to improve the current model response. The static synchronous series compensator (SSSC) is capable of controlling the flow of power at a desired point on the transmission line by injecting a fast changing voltage in series with the line and it keeps the constant power flow under fault conditions. SSSC can be implemented on more complex networks in Pakistan in future. Voltage profile and power flow control will be examined in MATLAB/Simulink. Location of SSSC should be optimized for network through further studies of system. It might be possible to build a hierarchical control scheme in order to achieve better control of oscillations and, for example, optimization of power flow, especially in case of multiple contingencies. Future research in this direction would provide more insight into these possibilities.

REFERENCES

[1] Prof.R.M. Malkar, Prof.V.B.Magdum, "Recent Trends in Real and Reactive Power flow Control with SVC and STATCOM Controller for transmission line," IJAIEM, March 2016.

[2] M.Maheskumar, "A study of reactive power compensation in power system and its compensation techniques" International journal of innovations in engineering and technology, 2016.

[3] S.S.Patil, Manasa.N.R, P.Anaji, "Power Quality Improvement using SSSC" International Journal of Emerging Research in Management &Technology, May 2016.

[4] Y.H.Song and A.T.Johns, "Flexible ac transmission systems (FACTS)," The Institution of Electrical Engineers 1999.

[5] N.G.Hingorani and L.Gyugyi, "Understanding FACTS: concepts and technology of flexible AC transmission systems," IEEE Press, 2000. B

[6] K S Apremeya, Veena "*Voltage Profile Improvement of Transmission Line Using SSSC*" International Journal of Scientific Development and Research (IJSDR) Volume 2, Issue 1 January 2017.

[7] M.H.Haque"Stability Improvement by Facts devices: A Comparison between STATCOM and SSSC"IEEEPower Engineering Society Meeting, 2005.

[8] G.Saraswathi, Dr.N.Visali, B.N.Reddy, "*Power flow improvement using Static Synchronous Series Compensator (SSSC)*" International Joural of Engineering Studies and Technical Approach.

[9] Sedighizadeh, M.Toulabi, M.S.Rezazadeh, A.Khatibi, *"Damping Improvement by SSSC and STATCOM in a Part of Iran Electrical Network"* 43rdUniversities Power Engineering International Conference, 2008.

[10] A.Haleem, R.Malgireddy, *"Power Flow Control with Static Synchronous Series Compensator (SSSC)"* Proc. of the International Conference on Science and Engineering (ICSE 2011)

[11] P.Dhoble, A.Bhandakkar, "Review of Active Reactive Power Flow Control Using Static Synchronous Series Compensator (SSSC)" INTERNATIONAL JOURNAL OF INNOVATIVE RESEARCH & DEVELOPMENT, April, 2013.

[12] Zenk, H. Akpinar, A.S. "PI, PID and Fuzzy Logic Controlled SSSC Connected To a Power Transmission Line, Voltage Control Performance Comparison" 4th Intl Conference on Power Engineering, Energy and Electrical Drives, 2013.

[13] A.A.Nimje, C.K.Panigrahi and A.K.Mohanty, *"Enhanced power transfer capability by using SSSC"* Journal of Mechanical Engineering Research Vol. 3 (2), pp. 48-56, February 2011.

[14] Sen, K.K. "SSSC, Theory, Modeling and Application" IEEE Transactions on Power Delivery" (Volume: 13, Issue: 1) Pages 241 – 246.

[15] M.S.E.Moursi and A.M.Sharaf"Novel Controllers for the 48-Pulse VSC STATCOM and SSSC for Voltage Regulation and Reactive Power Compensation" IEEE TRANSACTIONS ON POWER SYSTEMS, VOL. 20, NO. 4

[16] Rizan A. Ali, Ergun Ercelebi "*Improve Power Stability & Damping Oscillation in Multi Machine System Using (SSSC) with POD Controller"* International Journal of Computing, Communications & Instrumentation Engineering (IJCCIE) Vol. 3, Issue 2 (2016).

[17] P. Dhoble, A. Bhandakkar "*Active Reactive Power Flow Control Using Static Synchronous Series Compensator (SSSC)"* IOSR Journal of Electrical and Electronics Engineering (IOSR-JEEE) e-ISSN: 2278-1676,p-ISSN: 2320-3331, Volume 7, Issue 6 (Sep. - Oct. 2013)

[18] S.S.Patil, Manasa.N.R, P.Anaji "*Power Quality Improvement using SSSC*" International Journal of Emerging Research in Management &Technology ISSN: 2278-9359, May 2016

[19] M.Thangavel, S.Shiny Jasmine "Enhancement Of Voltage Stability And Power Oscillation Damping Using Static Synchronous Series Compensator With SMES" International Journal of Advanced Research in Technology Vol. 2 Issue 3, March 2012.

Muhammad Ali belongs to Peshawar, Pakistan. He is graduated from University of Engineering and Technology (UET) Peshawar as an Electrical Engineer in 2014. He has completed his MS Electrical Energy System Engineering from USPCAS-E, UET Peshawar and successfully defended his research thesis.

IJEW 国际工程期刊 International Journal of Engineering Works انجینئرنگ کاموں کا بین الاقوامی جرنل

International Journal of Engineering Works
ISSN-p: 2521-2419
ISSN-e: 2409-2770
Vol. 6, Issue 05, PP. 159-163, May 2019
https://www.ijew.io/
DOI:10.34259/ijew.19.605159163

Enhance and Maintain Efficiency of Solar Panel using Auto Cleaning System

Sana Akbar[1], Dr.Tanvir Ahmad[2]
[1,2] Department of Electrical Energy Systems Engineering, US Pakistan Centre for Advanced Studies in Energy, University of Engineering and Technology Peshawar, Pakistan
sana.mohammadzai@gmail.com[1], tanvir.ahmad@uetpeshawar.edu.pk[2]
Received: 15 April, Revised: 26 April, Accepted: 29 April

***Abstract*—**The conventional sources of energy are depleting rapidly. Which lead the world towards the trend of renewable energy sources. Among renewable energy sources solar PV is one of the major sources of energy. This technology of solar PV faces many challenges. Among these challenges dust accumulation on surface of solar panel is a major problem which leads to sharp decline in solar panel output power and hence efficiency. Different studies suggest that the efficiency of solar panel can be reduced by half of its maximum efficiency if not cleaned for a month. To tackle this problem of dust accumulation, in this thesis an automatic cleaning mechanism has been designed which automatically detects dust accumulation on the surface of solar panel and clean it using a vacuum blower. In this experimental setup a solar panel of 40 watts along with 2 DC motors of 12V supply. The vacuum blower slides over the surface of the solar panel using a cart in backward and forward direction for a few seconds. The supply used for this dc motor and hence the vacuum blower is made from the lead acid battery charged from the same solar panel. The maximum output efficiency of the panel is declined to 70% when dust is accumulated on its surface. Arduino microcontroller is used for triggering the motor and hence the vacuum blower. As vacuum blower is used for cleaning purpose, so this method is free from water wastage. Results showed that the efficiency can be improved to 18-20% after one round of cleaning using this automatic cleaning system.

***Keywords*—** Solar Panel, Efficiency maintaining, Cleaning, Hardware, arduuino.

I. INTRODUCTION

In today's world, energy is divided into two forms, renewable energy resources (RES) e.g. Wind, solar, geothermal etc. and nonrenewable also known as conventional energy resources i.e. coal, fuel, gas etc. While back in 19th century, after industrial revolution, fossil fuels (like coal and oil) were commonly used to generate energy. It is a fact, that fossil fuels are depleting quotidian due to profligate use besides that they are proved to be harmful for greenhouse as they release CO_2 which directly effects Ozone layer and it is noted that world's temperature is increased about 0.9 Celsius by 1880 [1]. According to NASA's research an increase of 1 Degree Celsius is enough to warm all oceans, lands and atmosphere [1]. Keeping in mind the environmental impacts and energy crisis of 1973 world needed to change their primitive energy production methods. Thus, the new and better era for search of energy resources started, where environmentally friendly, clean and sustainable energy resources were required which must be competent to completely supplant fossil fuels. As a result of this search RES were tested and accepted by society as they fulfill all the demands and requirements. Solar panels can generate electricity without any waste or pollution, or dependence on the Earth's natural resources once they are constructed. They have no moving parts, so modules are very reliable and have a long-life span. Solar panels are relatively easy to install and are very low maintenance.

A useful characteristic of solar photovoltaic power generation is that it can be installed on any scale as opposed to conventional forms of power generation that require large scale plant and maintenance. Solar panels can be installed to generate power where it is needed, which removes the need to transport and distribute electricity over long distances to remote areas.

A. *Background of using Solar Energy*.

Sun is the only and powerful gift of nature to humanity due to which live exist but from study material solar energy was used by humans as early as 7th century B.C. when history tells us that humans used sunlight to light fires with magnifying glass materials.

In the late 1700s and 1800s, researchers and scientists had success using sunlight to power ovens for long voyages. They also harnessed the power of the sun to produce solar-powered steamboats. Ultimately, it's clear that even thousands of years before the era of solar panels, the concept of manipulating the power of the sun was a common practice. In 1953, Calvin Fuller, Gerald Pearson, and Daryl Chapin, discovered the silicon solar cell. This cell produced enough electricity and was efficient enough to run small electrical devices. The New York Times stated that this discovery was "the beginning of a new era, leading eventually to the realization of harnessing the almost limitless energy of the sun for the uses of civilization. [2]"

The period from the 1970’s to the 1990’s saw quite a change in the usage of solar cells. They began showing up on railroad crossings, in remote places to power homes, Australia used solar cells in their microwave towers to expand their telecommunication capabilities. Even desert regions saw solar power bring water to the soil where line fed power was not an option.

Today we see solar cells in a wide variety of places. You may see solar powered cars. There is even a solar powered aircraft that has flown higher than any other aircraft Sun is the only and powerful gift of nature to humanity due to which live exist but from study material solar energy was used by humans as early as 7th century B.C. when history tells us that humans used sunlight to light fires with magnifying glass materials. except for the Blackbird. With the cost of solar cells well within everyone’s budget, solar power has never looked so tempting.

The main research question which we want to solve are 1) How to achieve maximum level of output from solar panel? 2) How to maintain efficiency of solar panel at maximum level? 3) Find the best way of cleaning solar panel to maximize its performance.?

B. Organization of paper.

This paper follows standard organization having introduction, literature review, methodology, results and conclusion. Section 1 is Introduction, which delineates a brief background and evaluation of solar energy and solar panel. Section 2 is Literature review about the studies which are been done and what new this work is offering. Section 3 is about methodology. Design parameters and control strategy is delineated. Section 3 is followed by result chapter i.e. Section 4 in this portion results are explained one by one with brief explanations and it is tried to elucidate that how by optimizing fatigue and structural loads power can be maximized. And in Section 5 we concluded the whole project that what we achieved which we planned. And Section 6 and Section 7 are about limitation of a system and future work.

II. Literature Review

As gathering of dust on the solar PV panel lessens its transmittance which brings about the decrease of the power yield, in this manner bringing about loss of energy age. This specific issue is likewise in charge of the short life expectancy of numerous interplanetary investigation missions, for example, Mars Exploration Mission of Curiosity Rover as the power yield from their solar PV panels decreases after some time as a result of the gathering of clean. At a state of time thickness of dust increments to level where control yield decreases to the degree which can’t bolster its fundamental capacities. Promote this issue has likewise brought about colossal losses for the solar PV influence plant administrators which experience the ill effects of lessened influence yield considering regular dust accumulation [3].

A. Manual cleaning.

Traditionally cleaning framework was done physically. The manual cleaning has weaknesses like danger of staff mishaps and harm of the boards, development troubles, poor upkeep and so on. The programmed tidy cleaning arrangement of solar PV has taken to defeat the troubles emerge in the conventional cleaning and furthermore creates a viable, non-grating cleaning and keeps away from the inconsistencies in the efficiency due to the affidavit of clean [4].

B. Automated cleaning.

Cleaning development for solar panel exhibit can propel viability of intensity made and secure the solar PV cell. The strategies for dust clearing, for instance, common methods, mechanical cleaning, self-cleaning Nano-film, and electrostatic method are discussed [5] [6]. This is supposed to help scrutinizes with picking up a broad insight of self-cleaning system for sun-based boards and other optical contraptions. The reason for this task is to build up a programmed self-cleaning system for cleaning the sunlight-based board with the goal that the procedure can turn out to be more dependable and quicker, therefore expanding the power yield of the sun powered power plant [7]. Distinctive advancements being made far and wide for self-cleaning of sun-oriented PV are discussed underneath [4] [8].

C. Natural cleaning of dust.

Regular methods are used to oust the cleaning, for instance, wind control, gravitational energy and the scour of the water [9], [10]. The surface of solar panel can be cleaned if its orientation can be swung to upright or sideways in morning, night time and stormy weather. In any case, changing position of the solar panel is incredible. troublesome [9].

Cleaning impact of rainfall is to be viewed as computing yearly losses because of the defilement. In any case, surveying this effect is troublesome. There are two imperative variables to be featured. One is the measure of rain falling on the double, and the other worldly event of rain. The purging impact of rain in two imperative determinants the measure of rain fell on one event, and the recurrence of the rainfall. During raining period, the dust accumulation is negligible because of frequent raining but during summer dry period dust removal by natural means become rare. For this situation, the purging impact of rain is negligible. As the level of radiation and long stretches of daylight in the late spring semester are the greatest, this is path ruining of boards caused the heavy losses in power age amid this time of year. The force of ruining of PV modules is the best on summer dry period. Amid the late spring half-year, the most noteworthy power age, and consequently the soil amid this period causes critical losses [4] [11].

D. Mechanical evacuation of residue.

The mechanical systems [15] empty the residue through scrubbing, vibration and ultrasonic drive. The scrubbing procedures unsoiled the sun-controlled cell with the help of a sweeper or brush which was driven by a motor, construction wise like windscreen-wiper of a car. In any case, immediately, owing to the little dimensions and the sturdy adhesively of the residue, this technique for dust removal is wasteful. Likewise, the loathsome working conditions of the sun powered PV makes the upkeep of the machine troublesome. By then, because of significant zone of the sun based solar panel show, that the machine used for cleaning is competent. Taking everything into account, the glass surface of the solar panel potentially was hurt by the brush while rubbing Expelling the cleans using vibration and other methods using ultrasonic is furthermore a generous mechanical cleaning [14]. The main consideration of this method is the methodology used for driving, the repeat and the eventfulness of the sun-controlled cell. [13] Williams R. Brett and his gathering considered the shuddering depiction of oneself cleaning sun powered boards with piezoceramic incitation. Their examination is still at the basic period of examination [9].

E. Self-Cleaning Nano-film.

When exterior of the sun-controlled panel display is anchored with a pellucid layer of Nano-film, it will remain tidy [13]. The composition of self-cleaning Nano-film is super hydrophilic material or super hydrophobicity material. It suggests oneself cleaning segment of the Nano-film incorporate two approaches [9].

TiO_2 is a champion among the most well-known super Hydrophilic material which has both hydrophilic and moreover photocatalytic characters. There are two stages in this cleaning strategy. Foremost is the is the photocatalytic methodology, the splendid radiance descends on the surface of TiO_2 film, both reacts and the dirt ruptures apart [14]. After that as a result of the hydrophilic thought of TiO_2 disseminates the water on to the surface of the sun-oriented board and flush the clean. Regardless, the above-mentioned technique isn't such outstanding in light of the way that sun powered power plants are generally arranged in the dry locale where precipitation is uncommon and unusual in nature [8].

Super-hydrophobic are those materials which indicate abnormal state of aversion to the water atoms. For instance, leaves of lotus plant which are have less wettability. As of late parcel of studies have been directed to recreate the hydro-phobic nature by framing small scale structures or Nano-structures [15]. These structures are outlined with the end goal that they make a contact edge of more than 150. Subsequently, the water beads that fall on these sorts of surface move off the surface, conveying natural and inorganic clean particles with them. In this manner cleaning the surface. Be that as it may, there is still a great deal of suspicion in the utilization of super hydrophobic material in self-cleaning application [16]. It is proposed that future examinations ought to be led to check the attainability of these kinds of materials in genuine world [8] [17].

F. Electrostatic removal of dust.

Electrostatic dust removal is a model electric system. After conducting research Clark P E, MiNET to F an and Keller J prescribed there might be two probable instruments of elements charging on surface of the moon. 1) Triboelectric charging, 2) Photoelectric effect using UV light. Consequently, assuming there is a high gradient on the exterior of the solar panel, the charged and uncharged dust particles will be pulled to the sheets in light of the electrostatic forces. At the end the solar panel will charge the particles and they will have comparative electric charge and electrostatic force of abhorrence. Ultimately, the perfect elements will drift apart the solar panel. Regardless, this strategy can't be used as a piece of PV structure, in perspective of the influencing of rainfall on earth. The well known the electric powered dust cleaning advancement relies upon the electric window adornment thought made by F.B. Tatum and associates at NASA in 1967 and also made by Masuda at the University of Tokyo in the 1970s[18]. The mentioned approach is seemed to elevate, and transfer charged and uncharged dust elements by means of electrostatic and dielectrophoretic powers [11]. Starting late, various investigators have engrossed the ways in which this development been associated for astronomical applications on the moon and Mars. Electrify window trimmings contain a movement of identical terminals introduced in a dielectric surface, transversely over which these movements are conveyed in the anode potential outcomes figure 1 [9]. At instant when the terminals interface with a multiple-stage AC voltage, a voyaging ripple galvanic shade be energized (appeared as figure 2 [19]. With the appropriate repeat and adequacy circumstances, the excited elements won't be permitted to store, anyway will be assigned to pass aside the outward after the electric field. Thusly, the exterior will remain free of particle oath [4].

G. Electrodynamic screens method.

In this paper author proposed for Electrodynamic Screens (EDS) process for cleaning of solar PV panels. Straightforward Electrodynamic Screens (EDS), comprising of lines of straightforward parallel cathodes inserted inside straight- forward dielectric film can be utilized for clean expulsion [14]. At the point when the anodes are stimulated by staged potential, the tidy elements on the SPV exterior of the film turn out to be electrostatically charged and are evacuated by the voyaging wave created by connected electric field [19]. More than 90% of stored tidy is evacuated inside two minutes, utilizing a little portion of the vitality delivered by the boards. Method proposed in this paper is useful for dry climatic, yet it has requirements in muggy conditions [20].

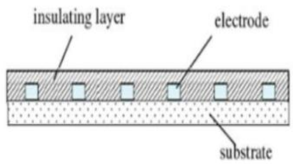

Figure.1

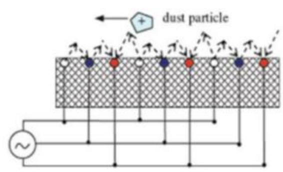

Figure.2

Clean isn't the main factor, different variables like flying birds dropping, water stains and so on comes into picture which diminishes the proficiency of the PV boards, where the previously mentioned procedure would not be effective [9][21]. All the methods discussed have certain merits and demerits. Therefore, in this thesis a different method is proposed for design of automatic cleaning system for solar panel using vacuum blower. The vacuum blower used will be power efficient and, in this way, we can avoid huge wastage of water used in other cleaning methods.

III. METHODOLOGY

Several methods for cleaning of solar panels are discussed in the previous section. Each method has its own merits and also some demerits due to which they are not feasible enough to be used. In this project an auto-cleaning system for solar panels is designed using vacuum blower to cope the problem of dust accumulation on solar panel in an efficient way. In this section detailed design of the prototype is discussed.

A. Block diagram.

According to block diagram a detection device is used to detect dust accumulation on surface of solar panel. Light sensors are mostly used. This light sensor is further connected to a microcontroller. Microcontroller is programmed in such a way that a predetermined threshold value is set. Whenever this threshold value is exceeded it activates the cleaning mechanism, vacuum blower in this case which cleans the surface of solar panel.

B. System components.

The components used in design of this prototype is 1) Light detection Sensor: for detecting sun light. 2) Solar panel. 3) Arduino. 4) DC motor drive: L293D IC package of 12V is used. 5) Cleaning mechanism: Vacuum blower with dc motor drive. 6) Cart: for sliding the vacuum blower over the solar panel. 7) Software proteus: For simulations.

C. Light detection sensor.

There is no built-in sensor in proteus, so a light sensor is designed with the help of components in proteus library. A sunlight detection sensor is used to find either there is sunlight around the solar panel or not. If there is solar radiation but efficiency of solar panel(voltage) is below a specific value, the threshold then it means that there is dust accumulation on solar panel. Microcontroller will trigger the vacuum blower for cleaning the solar panel. But if there is no sunlight that is output of the light sensor is below a specific threshold value, then it will indicate that its cloudy weather or night time so, it means this is not the case of dust accumulation and no triggering of vacuum blower. Output of light intensity sensor is also taken in volts.

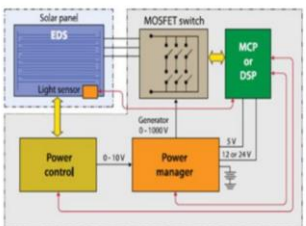

Figure 3. Block Diagram of EDS/PV array system [4].

Figure 4. Block diagram of Auto Cleaning Mechanism

There are two circuit components of light detection sensor. 1) LDR: Light dependent resistor is used for irradiance strength estimation. LDR is a light dependent resistor, its resistance varies as irradiance strength changes. Due to resistance variation output voltage will vary and in this way changes in solar radiations can be measured 2) RESISTOR: A 10K ohm resistor is used with LDR and output voltage is taken across this resistor. 3) VOLTAGE SOURCE: A voltage source B1 of 12V is used, which gives a maximum output of 11V with 10K ohm resistor.

D. Solar panel.

A solar panel is also modeled in proteus as there is no built-in solar panel in proteus library. It is only a logical model for implementation of basic idea, for detail and accurate measurements the above system can be implemented in hardware.

E. Arduino microcontroller.

Arduino UNO R3 is used as microcontroller for triggering the cleaning mechanism. The Arduino Uno R3 is a microcontroller board in view of a remount able, double inline-bundle (DIP) ATmega328 AVR microcontroller. It consists of 20 hi-tech input/yield pins (of which 6 pins can be used as PWM output and 6 can be utilized as simple sources of info [22].

F. L293D H-Bridge IC drive.

L293D is a dual H-connect engine motorist coordinated loop (IC). Engine drivers go about as current and flow speakers since they take a low-ebb and flow control flag and give a higher-ebb and flow flag. This high current pulse is used to operate the machines [23]. L293D composed of two inherent H-connect source circuits. In the genuine procedure of working, both the DC machines can be operated all the time, both in advancing and backward movement. The machine activities of two motors can be managed through input at pins logic 2 and 7 and 10 and 15. Information logic 00 or 11 will seize the comparing machine logic 01 and 10 will turn it in clockwise and anticlockwise directions individually. Empower pins 1 and 9 (comparing to the two engines) must be high for motor to start operating. At the extremity when an empower input is high, the interconnected machine will start operation. Afterward, the output stops self-motivated and work in phase with their data sources. Also, when the source input is low, that driver is debilitated, and their outputs are low and in the high-impedance state.

We are using small machines which could be handle by L293D IC which have its own optocoupler with H-Bridge connection for driving and isolating motor from Arduino microcontroller.

G. Vacuum blower.

A vacuum blower with simple dc motor-driver of 12V is used for cleaning purpose. Actual ratings of dc motor to be energy efficient, will depend on practical scenario of solar panel and its output voltage. For simulation purpose motor drive of 12V DC is used. It is connected to two output pins of L293D, pin no 3 and 6.

H. Cart.

Vacuum blower is mounted on a cart which can move forward and backward on the solar panel surface, the cart is also connected to the two output pins of L293D that is pin no 11 and 14. Dimensions of cart depends on actual size of solar panel used for observation purpose.

I. Proteus.

The Proteus Design Suite is an exclusive programming device software applied primarily for electronic outline robotization. The invention is employed principally by electronic plan engineers and professionals to make representations and electronic designs for buildup printed circuit sheets. Proteus design environment is a developer application used for simulations and design implementation in soft-ware. It tends to be bought in several combinations, depending upon the extent of plans to be developed and the provisions for microcontroller modernization. All PCB Project objects integrate an auto switch and essential combined mode SPICE reenactment potentials of plans and as the outline duration of a PCB set-up venture. It is in this manner a focus part and is merged with all element designs. The previously mentioned venture is reproduced in Proteus8.TIMER. In addition to the light detection sensor a timer is also inserted in the project model to enhance the efficiency and reliability of the dust cleaning system of the solar panel.

J. Detail chart flow.

Figure 5 is given the detailed flow chart of the working sequence of the simulation model. According to the flow chart there is cleaning mechanism, which depends on light intensity and hence the dust accumulated on surface of solar panel. The sunlight intensity sensor will monitor the intensity of sunlight continuously. Arbitrary values are chosen for Lux and voltage of 70 for the solar panel under observation. If the output of light sensor is less than 70, then there will be no triggering of cleaning mechanism and cycle will go to an end. Because it means there is no sunlight and efficiency are declined because of shading or cloudy weather and there is no dust accumulation impact. If this output of light sensor is greater than 70 and output voltage of solar panel is less than 70, then it means there is sunlight, but dust is accumulated on the surface of solar panel so output voltage and hence efficiency of solar panel is declined. Microcontroller will trigger the cleaning mechanism and it will operate until efficiency(voltage) of solar panel goes to its nominal values. The blower is mounted on the cart and will move backward and forward with a specific time delay of 2sec and 3 sec respectively. This cart movement delay will depend on solar panel size and dimensions in practical real word application. If the solar panel is lengthy and wide then this time delay will increase and vice-versa.

K. System simulation model in proteus:

All the circuit is divided into four main blocks as shown in figure 6 the first block (left-top in 3.9) is LDR as light sensor for reference voltage and to find either it is sunny day or not. and second block is solar panel, if there is sunny day but output of solar panel is less than Light sensor so it's mean that the panel want to be clean which is what decide by Arduino module and all the cleaning algorithm is program in third block (second and third block is shown right-top and left bottom section of 3.9.) and the last block are output module when panel need to be clean then Arduino activate blower

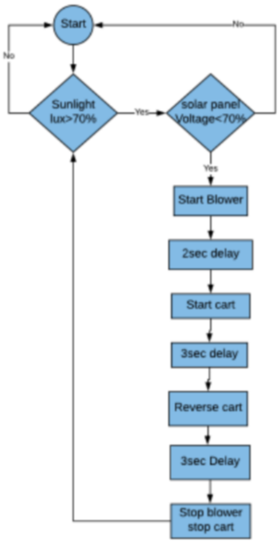

Figure 5. Block diagram of Auto Cleaning Mechanism

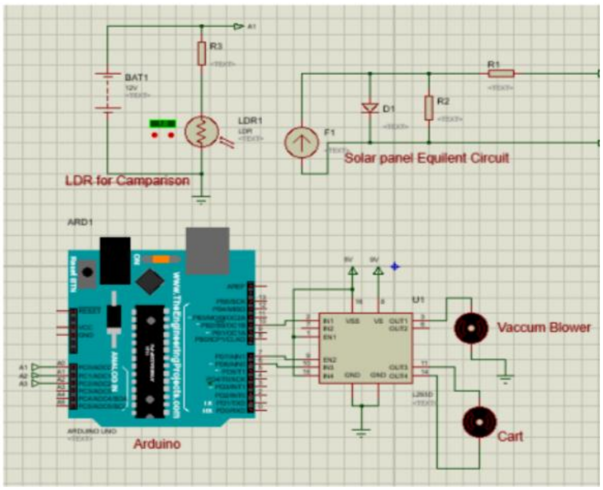

Figure 6. System Simulation Model in Proteus

IV. Results and Discussion

A. *Effects of dust accumulation on different electrical parameters of solar panel.*

An indoor experimentation was steered to find the effects of dust accrual on surface of solar panel.

The above figure 7 show voltage characteristics of the solar panel under observation. First the data of clear surface of solar panel is taken which gives a maximum voltage of 18.86 volts for a maximum luminous intensity of 21500 W/m2. The table given below shows the data collected during experiment using clear solar panel.

Power generated by the solar panel is given by P=VI. At clear surface maximum yield was obtained from the solar panel. But as layers of dust started to accumulate on surface of solar panel the area under the curve gets smaller and smaller. Hence power generated gets lessen and lessen. Figure 8 shows the data of dusty panel.

Figure 8 show us that due to dust accumulation there is a slight reduction in panel's voltage and hence power. The maximum voltage obtained in this case is 18.32 volts at maximum lux of 21500 W/m2. The table given below illustrate the data for dusty panel collected during experiment.

B. *Effects of dust on voltage of solar panel.*

Accrual of dirt on exterior of PV panel also leads to a decline of efficiency of the solar PV. Efficiency of PV array is observed on the basis of voltage variation of clear and dusty panel.

$$n = \frac{V_p x I_P}{P_s x A}$$

Vp and Ip are voltage and current of solar panel, whereas Ps is the power generated and A is the surface area of the solar panel. A comparison is made between clean and dusty panel voltage on the basis of experimental data collected during performance. The graph below shows that there is a slight reduction in panels voltage due to dust accumulation on surface of solar panel.

This reduction in panel voltage can lead to a decline of panel's efficiency up to 40-50% in worst cases. This can lead to loss of power which is an enormous amount. The table below shows data collected during experiment for clear and dusty panel.

The maximum efficiency can be achieved that is of 90% for improving that efficiency from 71% reduced by dust on maximum luminous intensity i-e on sunny day.

C. *Prototype analysis.*

The prototype designed in this thesis can be used to clean surface of solar panel and efficiency of solar panel can be enhanced up to 18%. A solar panel of 40 watts (20 volts) is used which can give maximum output of 36 watts as efficiency of most panels is 18-16%. If the power of solar panel is declined from 20 watts to 18 watts there is 10% decrement in output power of the solar panel.

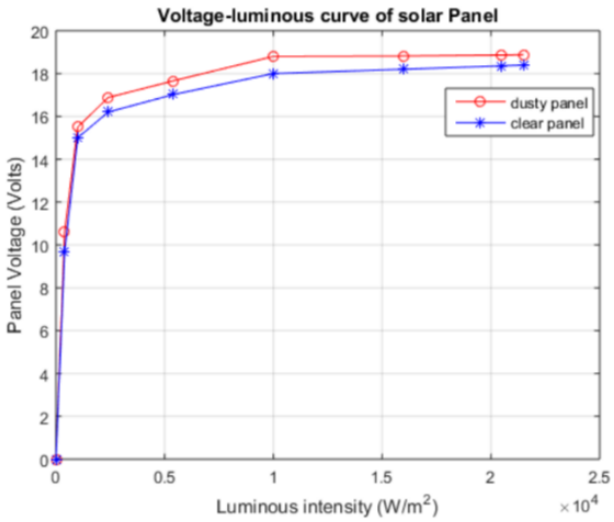

Figure 7. Voltage-Luminosity Graph of PV

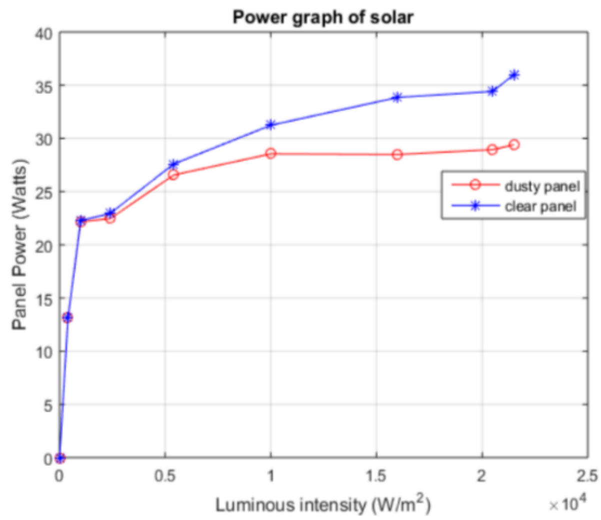

Figure 8. Power-Luminosity Graph of PV

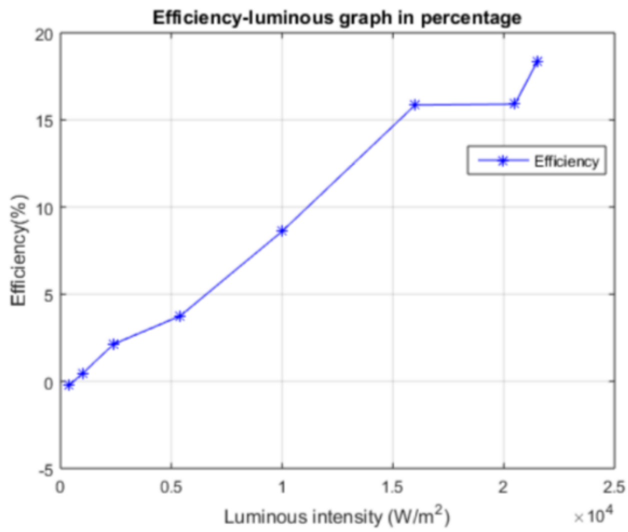

Figure 9. Efficiency-Luminosity Graph of PV

Figure 10. Prototype Analysis

But due to dust this reduction is decline to 30%. With the help of this prototype the 30% loss in output power of the solar panel can be avoided or can be reduced to a small value. Motor of cart and blower combinedly consumes 35 watts, but the duration of its operation is very small i-e 6 seconds. Length of the solar panel and the belt used for sliding the blower is 1m. As mentioned above the time of operation for the blower and cart is 6 seconds so power consumed during this short duration of time is negligible. Therefore, the power required from the solar panel to operate this prototype is not a problem.

CONCUSLION

It was shown during experimental analysis of this thesis that soiling has a negative impact on overall performance of the solar panel under examination. Graphical data collected during observation shows that output power of the PV panel can be declined up to 70% in the absence of the auto cleaning system designed specifically in this thesis for cleaning the solar PV. By practicing the auto cleaning system, which will detect if there is dust accumulation on the surface of solar panel and clean automatically the soiling effect, the overall output power and hence efficiency of the solar panel can be improved up to 18-20%. Beside improvement in output power and efficiency of the solar panel, there are certain other advantages of using auto cleaning system for the solar panels. Firstly, this mechanism of cleaning the solar PV is economical as no money has to be paid to companies or no labor force is required. Secondly in this method a vacuum blower is used for cleaning the solar panel so there is no wastage of water and this method can be very useful in arid zones where there is scarcity of water. Another advantage is that it is an automatic system so it is time efficient, there is no wastage of time. As soon as dust accumulation is detected on the surface of solar PV, the cleaning mechanism will start to operate until efficiency of the solar panel is restored to its nominal value. Besides the periodic cleaning of solar panel will results in good transmittance and full utilization of solar energy during peak sun shine hours. As no brushing and rubbing is used in this cleaning method so no deterioration of the solar panel surface. Finally, this method of cleaning the solar panel using vacuum blower is environmentally friendly and will prolong the lifespan of solar panel by preventing shading impact of solar panel. Note that the motor used for operating the vacuum blower is energy efficient as the kwh ratting of this motor is with cart is $5.82\text{x}10^{-5}$ KWh (as they operate only for 6 seconds) is very less as compare to solar panel i-e $3.6\text{x}10^{-2}$KWh. It is clear that the financial profit of improved production and protecting the lifetime of the panels significantly compensates the cost of regular maintenance of the PV modules surface.

LIMITATION

Limitation of our project are as follow;

- It is not so helpful for mud removal because of we used vacuum blower but if we use water spray along with brushes this limitation can be overcome.
- For more dusty areas the dust accumulation on panel is high so dust accumulation is directly related to cleaning mechanism due to which power consume by cleaning mechanism is more but this is probabilistic and operating only for 6seconds as per time so the power consumption is not so high to make panel overloaded.
- This project is only feasible for large scale solar parks.

FUTURE WORK

The prototype designed in this thesis is the basic design for solving the problem of dust accumulation on solar panel. Further changes can be made to this prototype to rectify it further and hence to improve its efficiency. Following work can be done in future to enhance efficiency of the above-mentioned prototype.

- Vacuum blower of low ratting can be designed to lower the power consumption from the solar panel.
- Additional development will optimize the system to be smaller, lighter, easier to assemble in higher volume and more user-friendly.

REFERENCES

[1] M. Carlowicz, “World of change: global temperatures: feature articles,” 2010.

[2] D. M. Chapin, C. Fuller, and G. Pearson, “A new silicon p-n junction photocell for converting solar radiation into electrical power,” Journal of Applied Physics, vol. 25, no. 5, pp. 676–677, 1954.

[3] K. K. Ilse, B. W. Figgis, V. Naumann, C. Hagendorf, and J. Bagdahn, “Fundamentals of soiling processes on photovoltaic modules,” Renewable and Sustainable Energy Reviews, vol. 98, pp. 239–254, 2018.

[4] M. A. Saini, A. Nahar, A. Yadav, D. S. Shekhawat, et al., “Solar panel cleaning system,” Imperial Journal of Interdisciplinary Research, vol. 3, no. 5, 2017.

[5] M. R. Maghami, H. Hizam, C. Gomes, M. A. Radzi, M. I. Rezadad, and S. Hajighorbani, “Power loss due to soiling on solar panel: A review,” Renewable and Sustainable Energy Reviews, vol. 59, pp. 1307–1316, 2016.

[6] G. Aravind, V. Gautham, T. Kumar, and B. Naresh, “A control strategy for an autonomous robotic vacuum cleaner for solar panels,” arXiv preprint arXiv:1412.0591, 2014.

[7] I. A. (US), Annual Energy Outlook 2012: With Projections to 2035. Government Printing Office, 2012.

[8] Y.-B. Park, H. Im, M. Im, and Y.-K. Choi, “Self-cleaning effect of highly water-repellent microshell structures for solar cell applications,” Journal of Materials Chemistry, vol. 21, no. 3, pp. 633–636, 2011.

[9] G. He, C. Zhou, and Z. Li, “Review of self-cleaning method for solar cell array,” Procedia Engineering, vol. 16, pp. 640–645, 2011.

[10] A. G. He, “Review of self-cleaning method for solar cell array,” School of Mechanical and Power Engineering, Chongqing University of Science and Technology, Chongqing 401331, China.

[11] C. Calle, J. McFall, C. Buhler, S. Snyder, E. Arens, A. Chen, M. Ritz, J. Clements, C. Fortier, and S. Trigwell, “Dust particle removal by electrostatic and dielectrophoretic forces with applications to nasa exploration missions,” in Proc. ESA Annual Meeting on Electrostatics, vol. 2008, ESA Minneapolis, MN, 2008.

[12] M. H. M. S. SATISH PATIL, “Design and implementation of microcontroller based automatic dust cleaning system for solar panel,” , Industrial Automation and Robotics, Department of Mechanical Engineering, SJC Institute of Technology, Chickamauga, Karnataka Assistant Professor, Department of Mechanical Engineering, SJC Institute of Technology, Chickamauga, Karnataka, june 1996.

[13] T. Sarver, A. Al-Qaraghuli, and L. L. Kazmerski, “A comprehensive review of the impact of dust on the use of solar energy: History, investigations, results, literature, and mitigation approaches,” Renewable and sustainable energy Reviews, vol. 22, pp. 698–733, 2013.

[14] M. Mazumder, M. N. Horenstein, J. W. Stark, P. Girouard, R. Sumner, B. Henderson, O. Sadder, I. Hidetaka, A. S. Biris, and R. Sharma, “Characterization of electrodynamic screen performance for dust removal from solar panels and solar hydrogen generators,” IEEE Transactions on industry applications, vol. 49, no. 4, pp. 1793–1800, 2013.

[15] L. Nelson and C. Hansen, “Evaluation of photovoltaic system power rating methods for a cadmium telluride array,” in Photovoltaic SpecialistsConference (PVSC), 2011 37th IEEE, pp. 002316–002321, IEEE, 2011.

[16] L. Nelson, M. Frichtl, and A. Panchula, “Changes in cadmium telluride photovoltaic system performance due to spectrum,” IEEE Journal of Photovoltaics, vol. 3, no. 1, pp. 488–493, 2013.

[17] J. Zhu, C.-M. Hsu, Z. Yu, S. Fan, and Y. Cui, “Nanodome solar cells with efficient light management and self-cleaning,” Nano letters, vol. 10, no. 6, pp. 1979–1984, 2009.

[18] M. Aoyoma and S. Masuda, “Characteristics of electric dust collector based on electric curtain,” in Proceedings of the General Conference of the Institute of Electronic Engineers in Japan, vol. 821, 1971.

[19] G. Liu and J. Marshall, “Particle transport by standing waves on an electric curtain,” Journal of Electrostatics, vol. 68, no. 4, pp. 289–298, 2010.

[20] S. Patil and H. Mallaradhya, “Design and implementation of microcontroller based automatic dust cleaning system for solar panel,” Int J Eng Res Adv Technol, vol. 2, pp. 187–190, 2016.

[21] M. G. Hudedmani, G. Joshi, R. Umayal, and A. Revankar, “A comparative study of dust cleaning methods for the solar pv panels,” Advanced Journal of Graduate Research, vol. 1, no. 1, pp. 24–29, 2017.

[22] H.-S. Juang and K.-Y. Lurrr, “Design and control of a two-wheel selfbalancing robot using the arduino microcontroller board,” in Control and Automation (ICCA), 2013 10th IEEE International Conference on, pp. 634–639, IEEE, 2013.

[23] C. Ryan, F. Vignola, and D. McDaniels, “Solar cell arrays: degradation due to dirt,” Proceedings of the American section of the international solar energy society, pp. 234–237, 1989.

International Journal of Engineering Works
ISSN-p: 2521-2419
ISSN-e: 2409-2770
Vol. 6, Issue 05, PP. 172-175, May 2019
https://www.ijew.io/
https://doi.org/10.34259/ijew.19.605172175

Conventional and Rubberize Concrete Cylinders Filled with PVC Tube

Faizullah Jan[1], Amjad Naseer[2] Muhammad Fahadullah[3], Hammad Akbar[4]
[1,2,4]University of Engineering and Technology Peshawar, Pakistan
[3]City University of Science and Information Technology (CUSIT) Peshawar
engrfaizullahjan@gmail.com[1], amjad_naseer@yahoo.com[2], engr.fuzi@gmail.com[3], hamadakbar10@gmail.com[4]
Received: 26 April, Revised: 02 May, Accepted: 03 May

***Abstract*—** The use of composite materials poly-vinyl chloride (PVC) in construction were studied. The use of PVC plastic pipe for concrete tubing is an alternative to use instead of concrete encased in steel tube and hence improve strength, ductility, durability, economical and environmental friendly. The key application of PVC tubing was its use in high aggressive environments and stop the penetration of chlorine and carbon dioxide directed towards core concrete and defect core concrete. Although the use of PVC as a composite materials in aggressive environments are efficient but PVC behave like brittle materials. The main parameters discussed are geometric and materials properties of thin PVC, stay-in-place formwork, PVC tubing from conventional concrete and rubberize concrete, confinement.

***Keywords*—** Polyvinyl Chloride, Rubberize Concrete, PVC Jacket, Composite Structure And External Confinement.

I. Introduction

Maintain the fortification and durability of new RC structures in aggressive and saline environments are a challenge for designers and engineers. There are many techniques used for protection of concrete and its reinforcement from harsh and aggressive environments. The use of PVC tubing is an effective, easy, economical way to protect reinforced concrete from chlorination and carbonation. PVC tube prevents construction practices from expensive curing process, protect concrete and its reinforcement by deter core concrete from moisture which have a role in setting and hydration of plastic concrete, make concrete impermeable and give lateral confinement to concrete. PVC tubing is state of the art new confining technique for structural engineers to overcome the exposing of core concrete to saline environments. This research study includes the parameters of PVC plastic tube encased conventional and rubberize concrete that influences the performance of composite materials structures.

A. Poly-vinyl Chloride (PVC) Tube

PVC is a polymer found universally having certain excellent applications in construction industries. The PVC deformation mechanism is still not clarify [1]. Research has been carried out to examine the short and long term ageing behaviour of FRP and PVC in 28 different organic compounds with extreme aggressive environmental condition for 112 days. Due to chemical reactions FRP degraded and PVC shows good performance as compared with FRP and are not degraded [2]. Observation based on stress degradation, PVC fatigue and crack growth expansion the design life of PVC can exceeded 100 years [3-7]. Due to its good mechanical stability and molecular structure PVC has a wide role in commercial usage [8]. Toughness due to fracture depends upon the molecular structure of polymers [9]. PVC tube filled with water test under concentrically indirect axial load to determine the slenderness behavior both experimentally and theoretically [11]. Due to use of polymer alloys Indulin Lignin the mechanical properties of PVC tube can also be enhanced [12]. The impact behaviour of PVC was found to increase incorporating chlorinated polyethylene (CPE) and acrylonitrile-butadiene-styrene (ABS) sub-polymers [13]. The geometrical and mechanical properties influences the deformation of buckling and axial capacity of non-metallic and metallic tubes [15, 16]. When PVC was compared with metallic steel tubes, PVC is lighter in weight as compared to steel tube, more economical and its thermal conductivity are 0.40-0.55 % lower as compared to steel tube [5, 18].

B. Crumb Rubber Concrete (CRC)

Crumb rubber concrete obtained from truck scrape tyres and replace a percentage of fine aggregate in making concrete. Due to huge amount of scrape tyres used in land infill make environmental concerns each year [34]. When tyre build up stocks exposed to fire then it is difficult to extinguish and release harmfull chemicals to environment [35]. Tyre store deposits reduce biodiversity due to soluble noxious chemicals [36]. If we used scrap tyres in conventional concrete to replace natural assets it will reduce demands on land infill and environmentally friendly [6]. However the rubberize concrete (crumb rubber concrete-CRC) has low tensile and compressive strength. CRC has also low modulus of elasticity as compared with conventional concrete [37,38]. The advantage of CRC over conventional concrete are better energy dissipation, ductility, make it more durable with good toughness and impact resistance [39, 40]. Despite its good mechanical properties its an another way to dispose off hazardous waste by replacing with natural resources in concrete and make it environmentally-friendly.

C. Non-Metallic PVC Jacket

PVC encasement provides a protection jacket to its infill concrete. In a research study the tubular concrete sunken into concentrated sea water having twenty times more concentrated than natural sea water for 180 days [19]. The post observation of experiments reveal that there is no major change in chemical composition and microstructure when exposed to harsh saline environments. The above mention studies indicates the performance of PVC in construction industry.

II. GEOMETRIC AND MATERIALS PROPERTY OF PVC TUBE

The geometrical properties of PVC tube from existing research studies are shown in TABLE I.

TABLE I. PROPERTIES OF PVC TUBE

Authors	**t mm**	**D mm**	**D/t**	**E Mpa**	**F_y MPa**	**F_u MPa**	υ
Alves and Martins [1]	1.7	40	23.53	2450		54	0.34
Kwon and Truss [9] UPVC	14.5	150	10.34	3100	45	45	
UniOPVC	5	160	32	4100	65	101	
BiOPVC	5	160	32	3800	65	94	
Kurt [20]	4.8	76	15.83	2760		40.90	
	6.4	100	15.60	2760		40.90	
Saadoon [21]	3.2	110	34.40	2770		49.60	
	5.3	110	20.75	2770		49.60	
Rahai et al. [22]	4.3	90	20.93	3000		55	
						88	
Wang and Yang [18]	3.7	110	29.73	3000	45		
	5.2	110	21.15				
	8.5	110	12.94				
Ma et al. [23]	4.5	200	44.44			44	0.36
Jiang et al. [24]	4.5	200	44.44			42.50	0.36
Wu et al. [25]	4.5	200	44.44		44		0.36
Oyawa et al. [26]	2.5	110	40	3380	39.96		0.38
	3	83	27.66	3380	39.96		0.38
	2.5	55	22	3380	39.96		0.38
Xue et al. [27]	2.3	75	32.60	3075		20.20	
	3		36.66	3315		19.56	
Chen at al. [28]	3	32	10.66	2520		107	0.36
	2	50	25				
	2.3	75	32.60				
Fakharifar and Chen [29]	7.1	166	23.38	4030	41.30	50.36	0.419

PVC tensile strength have been obtained from PVC coupon test in axial direction as shown in Figure (a). The uniaxial and biaxial oriented PVC (UniOPVC & BiOPVC) pipes were tested in tangential direction as shown in Figure (b) and concluded that UniOPVC and BiOPVC shows good behaviour in post-yielding load [9]. The critical buckling load was determined [1] as shown in Figure 1(a) and further investigated that additional instability (additional folds) were produced due to deformations [24]. The axial deformation curves was shown in Figure 1 (b).

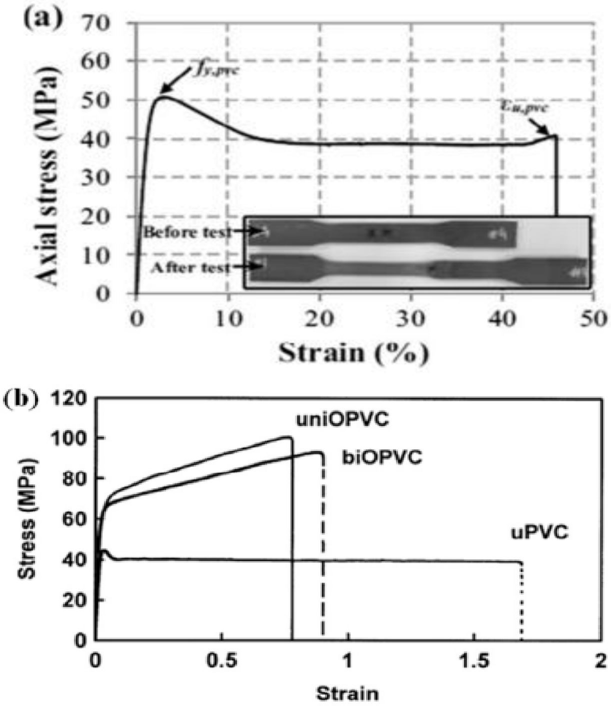

Figure I. (a), (b) Tensile stress-strain curve of coupon test: (a) axial direction [29] (b) tangential direction [9].

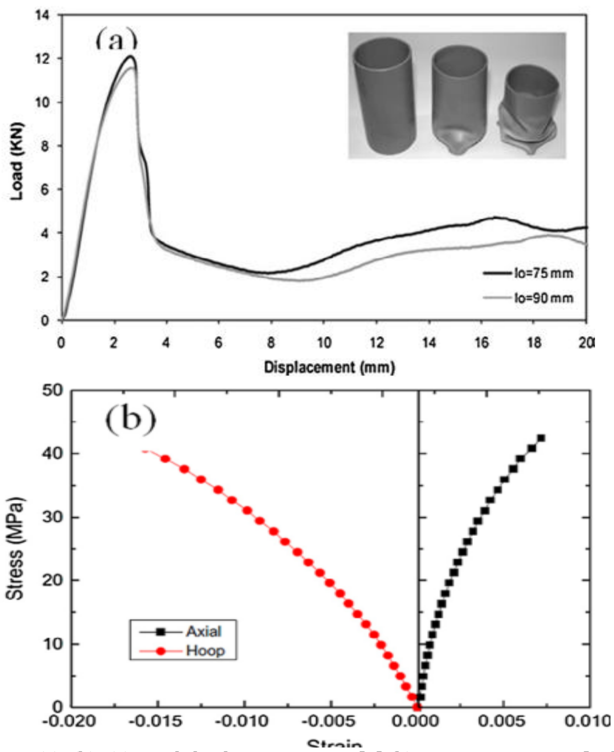

Figure 1 (a), (b): (a) Load-displacement curve [1] (b) Stress-strain curve [24]

The cost ratio of PVC compared with steel are half and very much less than FRP. PVC undergo longer deformation due to its good elastic properties. Being a low stiffness, modulus of elasticity of PVC (Ep) are lower than 50 % of modulus of elasticity of steel. The nominal confining ratio (flu/fuc) ratio of schedule-40 PVC pipe filled with concrete is 0.08 [29], where flu = lateral confinement pressure and fuc = Unconfined concrete strength. This level of confinement is 50 % of confinement provided by 1 layer of CFRP wrap from concrete cylinder. However the combine use of CFRP and PVC resists to local buckling between PVC and core concrete due to wrapping of CFRP [30, 31].

III. AXIAL DEFORMATION CAPACITY

Rubberize concrete slightly increase the peak strength with a decrease in ultimate drift ratio when concrete confined with PVC tube as compared with conventional unconfined concrete [16]. Concrete cylinder confined with PVC exhibit brittle behavior with a sudden loss of axial load capacity, by introducing an energy impact medium rubberize concrete enhances the load-deformation behavior with strain-softening in second part of the stress-strain curve [29]. Axial load capacity of short concrete columns were increased by 3.3% and its behaviour is similar to that of column internally confined with spiral reinforcement, while the columns fail due to hoop tension and axial compressive stresses [20]. The strength and deformation capacities of 12 concrete short columns after tested in axial compression show virtuous retort when paralleled with control specimen [21]. Mechanical characteristics of PVC confined concrete columns with partial replacement (20%-30%) of blended silica fumes were also evaluated [24]. The strength of PVC confined concrete columns were increased with 1.18%-3.65% when compared with control specimen [25].

IV. SEISMIC PERFORMANCE

Composite materials are frequently used in civil engineering construction and industries. Composite materials enhances the seismic performance of civil engineering structures. Cyclic test were performed on rubberize concrete confined with PVC tube, it was recommended that PVC is the best substitute instead of metallic steel tubes to resist seismic forces [32]. The seismic performance of PVC confined concrete tube and steel tube confinement were calculated and observe shear diagonal compression failure. It was also investigated that column confinement with PVC and steel tubes exhibits large axial deformation capacity and high ultimate strength, however the ductility could reduce with the increase in thickness of PVC tube [32]. Concrete columns filled with PVC tube yields good strength and ductility, also the wrapping of CFRP from PVC confined concrete enhance the strength and ductility and shows good hysteresis behaviour under reverse cyclic loadings [35].

CONCUSLION

PVC tube act as pre-installed protection jacket for core concrete. PVC used in research shows high ductility, good bearing capacity, used in normal and saline environment, good thermal and electrical conductivity, time saving, economical, light weight and more durable. The ductility and strength depends upon the compressive strength of core concrete, tube geometry, thickness of tube and slenderness ratio.

REFERENCES

[1] L.M. Alves, P.A.F. Martins, Cold expansion and reduction of thin-walled PVC tubes using a die, J. Mater. Process. Technol. 209 (9) (2009) 4229–4236.

[2] T.A. Ranney, L.V. Parker, Susceptibility of ABS, FEP, FRE, FRP, PTFE, and PVC Well Casing to Degradation by Chemicals, Special Report, 95-1: US Army Corps of Engineers, 1995.

[3] A. Boersma, J. Breen, Long term performance prediction of existing PVC water distribution systems: 9th International Conference PVC: Brighton: England (2005).

[4] J. Breen, Expected lifetime of existing water distribution systems-management summary, TNO Report MT-RAP-06-18692/MSO, published by TNO Science and Industry (2006).

[5] R. Nowack, O.I. Otto, E.W. Braun, 60 jahre erfahrungen mit rohr-leitungen aus weichmach-erfreiem polyvinylchlorid (PVC-U), KRV Nachrichten (1995) 1– 95.

[6] S. Burn, P. Davis, T. Schiller, Long-term performance prediction for PVC pipes, American Water Works Association AWWARF; Report 91092F (2006).

[7] S. Folkman, Validation of the long life of PVC pipes, in: Proceedings of the 17th Plastic Pipes Conference PPXVII. Chicago; Illinois: USA (2014).

[8] M.V. Titow, PVC Technology, Springer, 1984.

[9] J.A. Kwon, R.W. Truss, The work of fracture in uniaxial and biaxial oriented unplasticised polyvinylchloride pipes, Eng. Fract. Mech. 69 (5) (2002) 605–616.

[10] M.M. Carroll, Polyvinylchloride (PVC) pipe reliability and failure modes, Reliab. Eng. 13 (1) (1985) 11–21.

[11] M. Motavalli, M. Farshad, P. Flueler, Buckling of polymer pipes under internal pressure, Mater. Struct. 26 (6) (1993) 348–354.

[12] S.E.l. Raghi, R.R. Zahran, B.E. Gebril, Effect of weathering on some properties of polyvinyl chloride/lignin blends, Mater. Lett. 46 (6) (2000) 332–342.

[13] L. Zhou, X. Wang, Y. Lin, J. Yang, Q. Wu, Comparison of the toughening mechanisms of poly(vinyl chloride)/chlorinated polyethylene and poly(vinyl chloride/acrylonitrile–butadiene–styrene copolymer blends, J. Appl. Poly. Sci. 90 (4) (2003) 916–924.

[14] M.P. Kruijer, L.L. Warnet, R. Akkerman, Analysis of the mechanical properties of a reinforced thermoplastic pipe (RTP), Compos. Part A: Appl. Sci. Manufact. 36 (2) (2005) 291–300.

[15] A.A.N. Aljawi, Finite element and experimental analysis of axially compressed plastic tubes, Belgium Soc. Mech. Environ. Eng. 45 (1) (2000) 3–10.

[16] A. Mamalis, D. Manolakos, M. Loannidis, P. Kostazos, C. Dimitriou, Finite element simulation of the axial collapse of metallic thin-walled tubes with octagonal cross-section, Thin-Walled Struct. 41 (10) (2003) 891–900.

[17] Yu. K. Morozov, E.V. Ashraf, K. Shankar, Buckling behavior of reinforced thermo-plastic pipes under combined external pressure and bending: 8th Australian congress on applied mechanics (ACAM8) 2014: Melbourne.

[18] J.Y. Wang, Q.B. Yang, Investigation on compressive behaviors of thermoplastic pipe confined concrete, Constr. Build. Mater. 35 (2012) 578–585.

[19] P.K. Gupta, V.K. Verma, Study of concrete-filled unplasticised poly-vinyl chloride tubes in marine environment, Proc. Inst. Mech. Eng. Part M J. Eng. Maritime Environ. (2014). 1475090214560448.

[20] E.C. Kurt, Concrete filled structural plastic columns, Proceedings ASCE104 ST1 (1978) 55–63.

[21] A.S. Saadoon, Experimental and Theoretical Investigation of PVC-Concrete Composite Columns (Doctoral dissertation), University of Basrah, Iraq, 2002.

[22] A.R. Rahai, M.M. Alinia, S.M.F. Salehi, Cyclic performance of buckling restrained composite braces composed of selected materials, Int. J. Civ. Eng. 7 (1) (2009) 1–8.

[23] S. Ma, S. Jiang, Study on behavior of concrete-filled CFRP-PVC tubular slender columns under axial compression, China Civ. Eng. J. 1 (2014) 99–106.

[24] S. Jiang, S. Ma, Z. Wu, Experimental study and theoretical analysis on slender concrete filled CFRP–PVC tubular columns, Constr. Build. Mater. 53 (2014) 475–487.

[25] W. Wu, Q. Lin, S. Jiang, Study on the behavior of concrete-filled FRP-PVC tubular flexural members, Eng. Mech. 32 (6) (2015) 104–110.

[26] W.O. Oyawa, N.K. Gathimba, G.N. Mang'uriu, Innovative composite concrete filled plastic tubes in compression: The 2015 World Congress on Advances in structural engineering and mechanics (ASEM15) Incheon, Korea, 2015.

[27] J. Xue, H. Li, L. Zhai, X. Ke, W. Zheng, B. Men, Analysis on influence parameters and mechanical behaviors of embedded PVC pipe confined with reinforced high-strength concrete columns under cyclic reversed loading, Xi'an University of Arch. & Tech. (natural science edition), 48(1), 2016.

[28] Y. Chen, R. Feng, L. Xiong, Experimental and numerical investigations on steel– concrete–PVC SHS joints under axial compression, Constr. Build. Mater. 102 (2016) 654–670.

[29] M. Fakharifar, M.G. Chen, Compressive behavior of FRP-confined concretefilled PVC tubular columns, Compos. Struct. 141 (2016) 91–109.

[30] H. Toutanji, M. Saafi, Durability studies on concrete columns encased in PVC– FRP composite tubes, Compos. Struct. 54 (1) (2001) 27–35.

[31] J.G. Teng, Y.M. Hu, Suppression of local buckling in steel tubes by FRP jacketing, in: Proceedings, Second International Conference on FRP Composites in Construction, Adelaide, Australia 2004.

[32] A. Rteil, K. Soudki, D. Richardson, Flexural behavior of OctaformTM forming system, ACI SP 257 (9) (2008) 133–148.

[33] A.H. Chahrour, K.A. Soudki, J. Straube, RBS polymer encased concrete wall. Part I: experimental study and theoretical provisions for flexure and shear, Constr. Build. Mater. 19 (7) (2005) 550–563.

[34] K.G. Kuder, R. Gupta, C.H. Jones, R. Hawksworth, S. Henderson, J. Whitney, Effect of PVC stay-in-place formwork on mechanical performance of concrete, J. Mater. Civ. Eng. 21 (7) (2009) 309–315.

[35] N. Wahab, K.A. Soudki, Flexural behavior of PVC stay-in-place formed RC walls, Constr. Build. Mater. 48 (2013) 830–839.

International Journal of Engineering Works
ISSN-p: 2521-2419
ISSN-e: 2409-2770
Vol. 6, Issue 05, PP. 176-181, May 2019
https://www.ijew.io/
https://doi.org/10.34259/ijew.19.605176181

Power Quality Enhancement in Distribution System using Dynamic Voltage Restorer

Abdullah Taj[1], Muhammad Naeem Arbab[2]
[1,2]University of Engineering and Technology, Peshawar
engr_alitaj91@yahoo.com[1], mnarbab@gmail.com[2]
Received: 23 April, Revised: 02 May, Accepted: 16 May

***Abstract*—**The applications of Power quality at industrial and commercial scale is very important to be assured for the customer. But due to some reasons the load power system destructed like Sags of voltage, destruction of harmonics, irregularity in the voltage waveform and transient. Sensitive devices of power may also be harshly effected by voltage sags and change in the harmonics. Due to increase the heat in the power system devices and electrodes problem of harmonics could occur that may lead to failure of different speed drives and spin pulses in motors. The necessary requirement in the power system is decrease in harmonics. The use of DVR (Dynamic Voltage Restorer) in the power system devices is the source of reduction of this problem. To overcome the disturbance of voltage Sag and harmonics, it is the efficient and economical solution. Reduction of Total Harmonic Distortion (THD) will increase the quality performance of power system. Dynamic Voltage Restorer is used in this paper. Reduction in % THD and voltage sag are successfully corrected by using DVR on MATLAB/SIMULINK Software Package.

***Keywords*—**Dynamic Voltage Restorer (DVR), Total Harmonics Distortion (THD), voltage source inverter, Voltage sag.

I. INTRODUCTION

Nowadays industrial devices are typically based on the electronic devices such as PLC, microprocessors, computer, adjustable speed drives and inductive loads are very sensitive to disturbances such as voltage sag, swells and harmonics. Total harmonic distortion or THD of the signal is the measurement of the harmonic distortion present and is defined as the ratio of the sum of power of all harmonic components to the power of the fundamental frequency. THD is used to characterize the linearity of the audio system sent the power quality of the electrical system.

Harmonics have frequencies that have integer multiples of the waveform's fundamental frequency. For example, given a 50Hz fundamental waveform, the 2nd, 3rd, 4th, and 5th harmonic components will be the 100Hz, 150Hz, 200Hz and 250Hz respectively.

Thus harmonic distortion is the degree to which a waveform deviates from its pure sinusoidal values as a result of the summation of all these harmonics elements. Power quality problems have focused much attention in recent years as voltage sag is widely recognized as the most severe problem to the industrial loads affecting the power quality and performance [1].

THD is the summation of all harmonic components of the voltage or current waveform compared against the fundamental component of the voltage or current wave.

$$THD = \frac{\sqrt{(V2 + V3 + V4 + \cdots)}}{V1} X\ 100\%$$

The formula shows the calculation offer THD on a voltage signal. The end result is the percentage comparing the harmonies components to the fundamental component of the signal. The higher the percentage, the more distortion that is present on the main signal.

Voltage sag depends upon the duration and the magnitude of the rms voltage. Voltage total harmonic distortion plays an important role in a power system to maintain its quality and according to IEEE 519-1992 standards, total harmonic distortion should be equal or less than 5.0% of the fundamental frequency. IEEE standard 1152-1995 defines the sags root mean square (RMS) voltage variation with a magnitude between 0.1 pu and 0.9 pu of nominal voltage and duration typically ranging from a 0.5 second to sixty seconds. This voltage sag can cause undesirable function of the industrial machines and can eventually shutdown of machines, resulting in substantial productivity losses. By installing a custom power device, voltage mitigation or compensation can be achieved to reduce or cancel out the disturbances at the load end [2].

The usage of sensitive devices in chemical plants could effected by the drop of voltage and swell of voltage that leads to stoppage and failure of system. Because of these problems in the system the problem of tripping of breakers and blow fuses may occur with the disturbance of high currents. The interruption in the system and damage of equipment takes high cost from customers due to the various changes in the quality of system [3, 4]. The use of voltage sags is important in the common circulation systems rather than increase in voltage. The stimulation of big capacitor and switching off of a big inductive load is the main reason of voltage swells [5].

The sensitive devices are much vulnerable to small variations in the voltage that are due to severe change in the voltage sags. The changes in the magnitude of voltage supply in the phase shift is not the cause of voltage sags in the system. When the value of voltage become low there are changings that not remain permanent and get back to original position. By the failure of circuit and energization of transformer the resultant voltage become decreases as the short-term variation cause the generation of voltage sags on line. The serious destruction of widespread variety of devices is due to these short-term changes in the system [6].

The extent of voltages at the time of sags and interval could decide the specification of voltage sags. In practical way, the production duration of voltage sags is not much harming as the after the production loss may occur due to voltage sags. The problems of manufacturing lost, destruction of device, fear of breakage and restarting again could cost millions of dollars to be repaired because of voltage sags [7].

There are various custom power devices obtainable each with its own limitations and advantages for voltage reduction compensation such as DSTATCOM, SMES, DVR and SVC. DVR is a controlled voltage source inserted in between the network and a sensitive load voltage through a transformer inserting voltage into the distribution line to accurate any disturbance disturbing the sensitive load voltage. DVR with lead acid battery is a finest and attractive technique to deliver excellent dynamic voltage mitigation capability as compared to shunt connected devices. The main function in the power system is voltage source inverter with DVR to inject the desire three phase voltage to the load [4-5].

II. EXISTING SECONDARY DISTRIBUTION NETWORK IMPLEMENTATIONS & RESULTS

Power quality in distribution system is very important in commercial and industrial applications. The paper is basically for a specific case (A well-known public sector mechanical industry). We have taken one of the inductive load i.e. L_NF1 load and added the three phase fault at the 11kv feeder line to analyze the behavior in the distribution system as shown in Table I.

Unfortunately, sudden faults occur in power system which create disturbance and affect the Load voltage form are sags, transient, total harmonic distortions and notching. Out of these sag voltage and harmonics have severe impact on sensitive devices. Total harmonic distortion i.e. 6.29%, 9.61% and 6.54% on L_NF1 load in power systems result in increased heating in the equipment and conductors, misfiring in variable speed drives, and torque pulsations in motors. Reduction of harmonics is considered desirable.

TABLE I. ACTUAL NFS SHOP LOAD OF HMC INDUSTRY

NFS SHOP

S.No	Load	KW	KVA	KVAR
1	L_NF1	55	71.42857	45.57456
2	L_NF2	45	65.21739	47.20496
3	L_NF3	50	73.52941	53.91266
4	L_NF4	55	78.57143	56.11122
5	L_NF5	90	120	79.37254
6	L_NF6	110	139.2405	85.36931

The figure 1 shows the three phase existing distribution system with NFS load. The 11KV, 50Hz three phase supply is step down 11kV/380V. The Three phase fault has been applied at 11kv feeder line to create a voltage sag and the fault resistance is 50 ohm. The voltage sag event has occurred on the 11kv feeder line for a period of 0.05 to 0.185 sec, the fault has reduced the three phase non-ferrous load voltage from 300 peak voltage to 124.1v, 125.8 and 133.2 which can disturb the L_NF1 load may cause system failure .In addition, the total harmonic distortion (THD) has increased to 6.29%, 9.61% and 6.54% due to voltage sag [8-9].

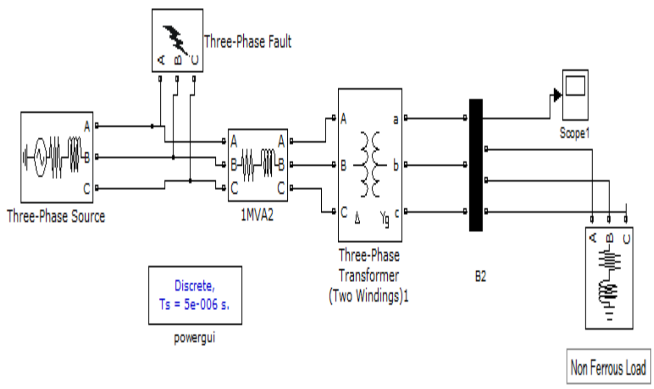

Figure 1 Simulation of Three phase Distribution system

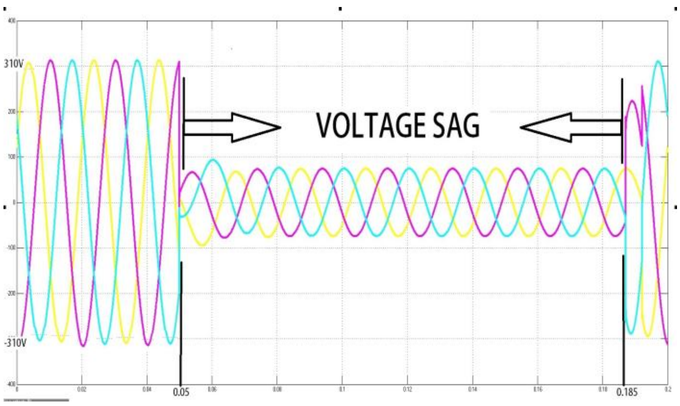

Figure 1.1 Load Voltage during Fault without DVR

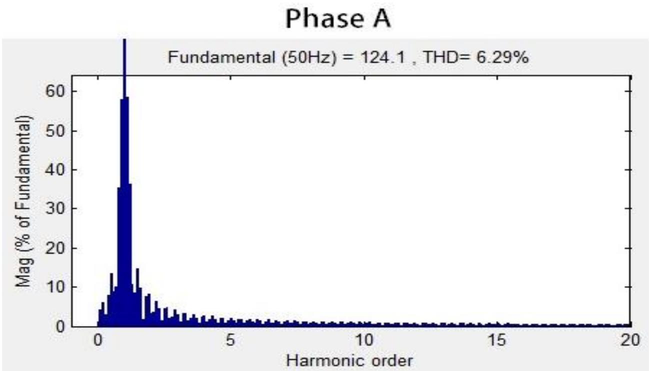

Figure 1.3(A) % THD during fault on L_NF1 Load

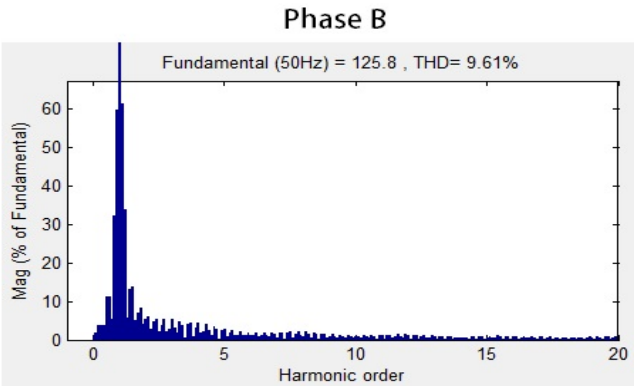

Figure 1.3(B) % THD during fault on L_NF1 Load

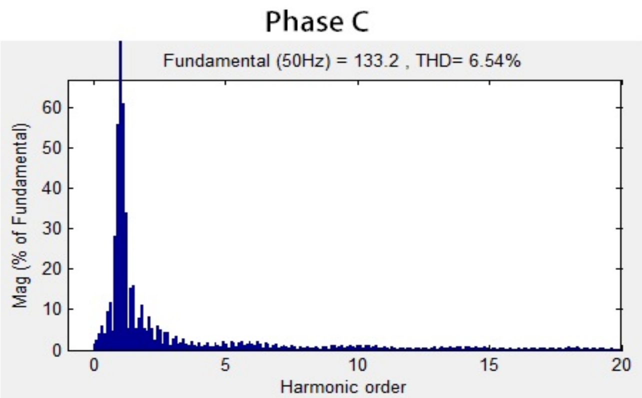

Figure 1.3(C) % THD during fault on L_NF1 Load

III. PROPOSED SECONDARY DISTRIBUTION NETWORK IMPLEMENTATION & RESULTS

Generally, DVR is used to transmit the voltages for the compensation as a necessary method in the DC side in which inverter is the source of transformation of value to the injected transformer before the filter. The fundamental role of DVR in the existence voltage sag is to add the values that are missing in the cycle by using a bunch of injection transformer. At the time of disturbance by voltage sag 3-phase injection voltage is the source of mitigation of this problem at secondary supply by means of amplitude of power. The defense of turbulences in the AC secondary source system through the voltages of various varieties done by production of voltages of identical values by means of inverter. The ejection of same voltages at the intermediate values of voltage done by using the faster transformer [8]. The mandatory parameters are shown in the Table II .

TABLE II. PROPOSED SECONDARY DISTRIBUTION NETWORK WITH DVR PARAMETER

S.No	Parameters	Values
1.	Source Supply Voltage	3.00-Phase 11.1kv,50Hz
2.	Injection transformer Turn ratio	1:1, 380/380v
3.	Inductive Load	55KW, 47KW
4.	Invertor	Carrier.Frequency = 1080.00, Sample.time = 20-6
5.	Filter inductance and resistance	1 ohm, 200-6
6.	Battery Voltage	1K
7.	Three Phase Fault Resistance	50ohm

Figure 2 shows that we have proposed the DVR which is coupled in series with the inductive load. There are two bus bars i.e. B1 and B2 and these bus bars are used for measuring input and voltage output. DVR control unit is monitoring the input and output voltage continuously via bus bar to prevent the system from any bad event. In addition, to test the performance of the DVR, the behavior of the system is examine at 11kv feeder line by adding 3-phase fault block. The 3-phases system having voltage sags of simulation with range 0.05 to 0.185 seconds. We have seen that the voltage sag event has been occurred. At this scenario, the DVR responded very well and corrected the voltage sag problem in millisecond.

Figure 2.1 is showing the injection voltages has been added at the distribution side. The inductive load is joint with the injection transformer and within the step-down transformer. PWM is the suitable way for the DVR in the existence of voltage sags to put voltage injection.

At voltage peak range the inductive load will be controlled and the mitigation of disturbance of voltages fully is elaborated in figure 2.2. The addition of total harmonic distortion percentages (THDV) as component of DVR cause the change in the voltage as shown in figure 2.3.

Furthermore, figure 2 showing the both uncompensated and compensated systems. Through the influence of variation in the storage means of power and energy cause load voltage's unsettling influence of total harmonics. The scope of capacity of energy at optimal level select the value such as 1000v showed the precise working ability of energy source. For both devastations, like existing harmonics and compensate voltage sags DVR is suitable to mitigate them in the resultant study. In conclusion, the objectives of DVR in the system to remove the harmonics issue fully from the load side and has been maintenance achieved [10-11].

The presented system in the study showed the similarity of both series of active power filters and the equivalent circuit of the DVR. Hence, DVR could give flawless and quick transient reply like power filter use to di by not regulating any additional necessities.

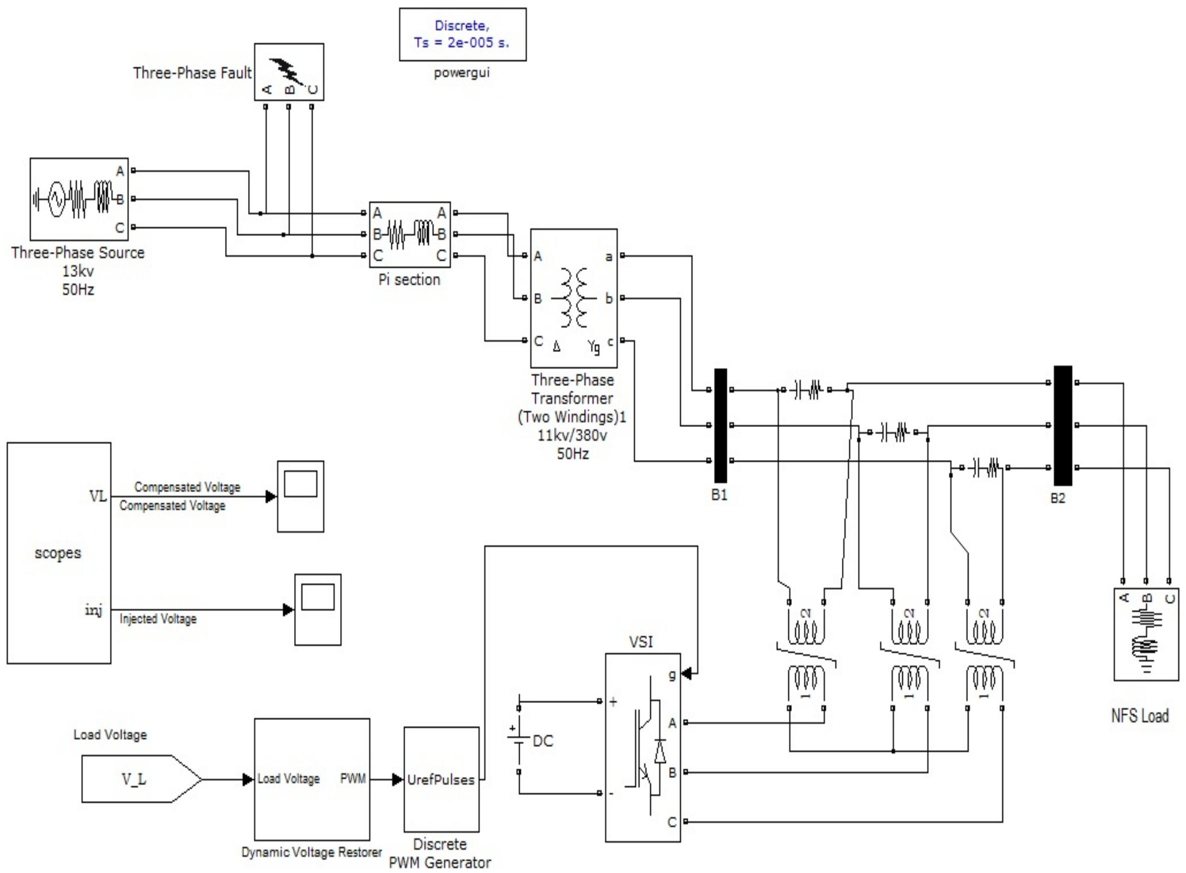

Figure 2 Proposed Secondary Distribution Network with DVR Circuit Diagram

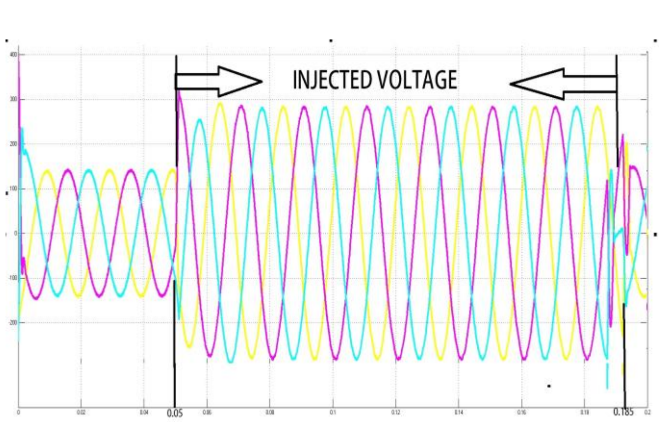

Figure 2.1 Injected Voltage via Injection Transformer in Secondary distribution Network

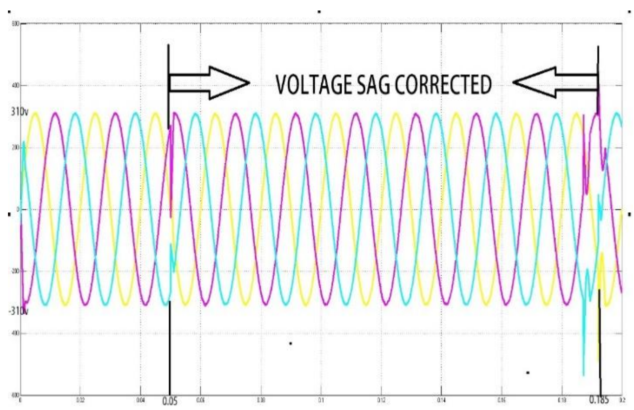

Figure 2.2 After Compensation (Sensitive Load Votlage)

The disturbance of Harmonics distortion removed in the end results of simulation model by using DVR. As shown in figure 2.3(A), 2.3(B) & 2.3(C) to reduce the harmonic distortions in 3-phase system FFT analysis is used.

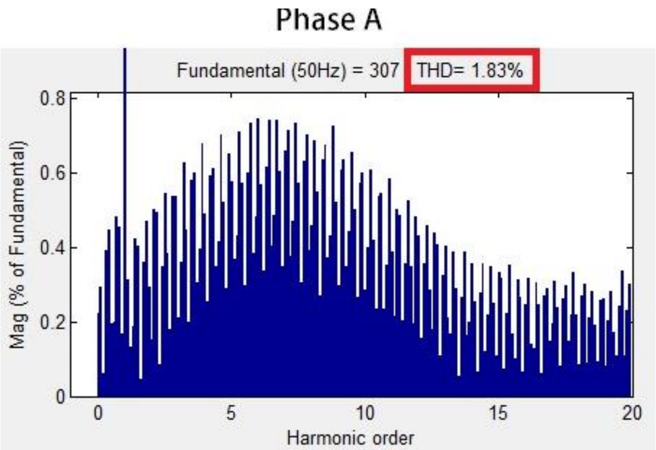

Figure 2.3(A) FFT analysis of the sensitive load voltage with DVR

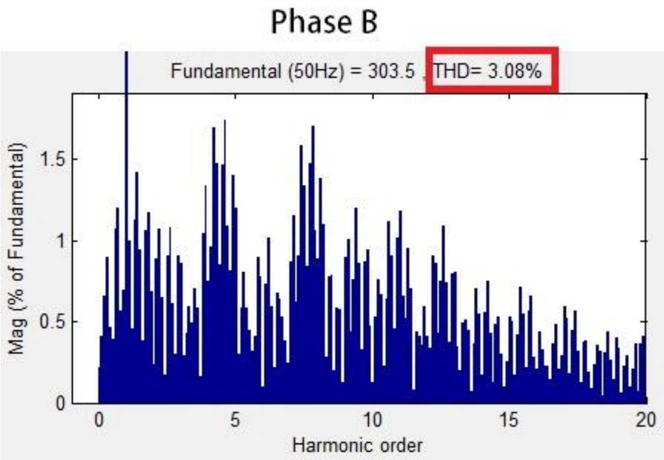

Figure 2.3(B) FFT analysis of the sensitive load voltage with DVR

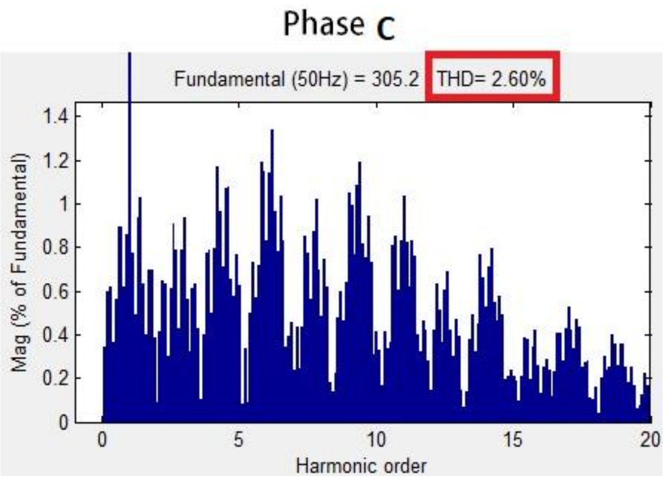

Figure 2.3(C) FFT analysis of the sensitive load voltage with DVR

IV. EXISTING & PROPOSED SECONDARY DISTRIBUTION NETWORK COMPARISON

Within the time 0.051 - 0.1851 sec a 50 Ω fault is embedded by utilizing 11.11kv feeder as a fault of 3.00-phase secondary distribution network for a short period of time, this faulty condition is achieved first when no DVR was exist in the framework When there is no DVR put into the system and the voltage range of load point of 100V is dependent on 310V supply then %age of THD increased in the presence of voltage sag. After the joining of DVR in the arrangement of second reenactment the system is same as examined above with the entire disposal of voltage droops. The upkeep of rms voltage at the load scope of 310v with the markdown in the issues at rate THD with DVR framework is appeared in figure 2.4. By utilizing MATLAB for the reduction or compensation of voltage swells/sags to enhance compel, Dynamic Voltage Restorer (DVR) is predicted and made. The proposed framework is beneficial system to repay the issues of voltage sags and THD in almost no time seconds for example milliseconds as emerge from the present arrangement of MATLAB in which the high range reduction of THD present in the structure has been finished [12-13].

To manufacture the nearness time of structure and to moderate the stinging conditions the delicate weight sides utilized the skilled proposed framework.

TABLE III. WITHOUT COMPENSATION & WITH COMPENSATION (SENSITIVE LOAD THD)

S.No	Secondary Three Phase Paramters	Without Compensation. THD%	With Compensation THD%
1	Phase(A)	6.29%	1.83%
2	Phase(B)	9.61%	3.08%
3	Phase(C)	6.54%	2.60%

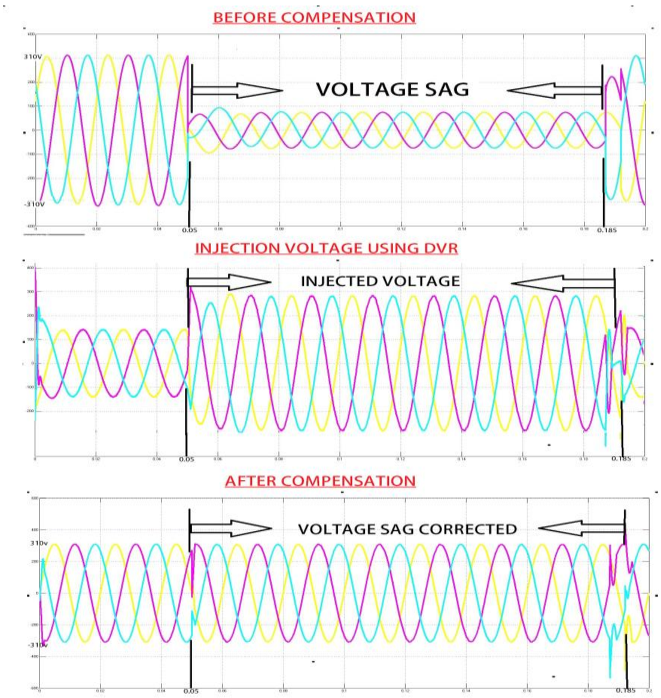

Figure 2.4 Without Compensation and with Compensation (Inductive Load)

V. SCOPE OF WORK

This Paper is on total harmonic distortion due to the production of voltage sag in one of the most industrious public-sector of Pakistan. The distribution system in the commercial and industrial applications are much imperative in terms of power quality. To analyze the behavior in the distribution system, the addition of the 3-phase fault at the 11kv feeder line and inductive load of L_NF1 load was taken.

Unfortunately, there are following disturbances to the load voltage including sags, transient, total harmonic distortions and notching that create unexpected faults in power system. The sensitive devices are most vulnerable to these voltage sag and harmonics. The failure of various speed drives and spin pulses in motors occur due to the hormonic distortion on L_NF1 load as a result of increase in the heat of power system. The power system should solve the problem of harmonics [14].

To overcome this problem, proposed Dynamic Voltage Restorer (DVR) has been used in the existing test system. It is an economic and effective solution for the protection of sensitive loads from harmonics and sags. In this paper, modeling, analysis and simulation of DVR has been used to enhance the performance of DVR by reducing Total Harmonic Distortion (THD). By using DVR on MATLAB/SIMULINK Software Package the percentage reduction of THD and voltage sag become successful [15].

CONCLUSION & FUTURE WORK

To proceed with the typical estimation of voltage for looking the viability of DVR to controller the load a supply of voltages infused in the present voltage sags mutilations, 3-staged framework that created voltage sags in variable conditions of the time space of DVR reproduction process. In conclusion, the DVR prove to be an effective system to remove the harmonics and voltage sags issues for simulation model. In the assumption the DVR is an efficient system to accurately restore the voltage of 310V in the presence of voltage sag. This projected system is easy and cost effective. It is nothing else but DVR.

Moreover, in future, the proposed system DVR can be improved using PID, Fuzzy Logic and SMC controllers can be used to get optimal values so that we can enhance efficiency of the Dynamic voltage restorer to mitigate the THD.

REFERENCES

[1] A. Teke, "MODELING OF DYNAMIC VOLTAGE RESTORER", Master of Science, UNIVERSITY OF ÇUKUROVA, Adana, September 2005.

[2] M.D. STUMP, G.J. KEANE, and F.K.S. LEONG, "The Role of Custom Power Products in Enhancing Power Quality at Industrial Facilities", IEEE Energy Management and Power Delivery, 1998, 2: PP. 507-517.

[3] A. Ghosh and G. Ledwich, "Power Quality Enhancement Using Custom Power Devices," Kluwer Academic Publishers, 2002.

[4] R. Buxton, "Protection from voltage dips with the dynamic voltage restorer," IEE Half Day Colloquium on Dynamic Voltage Restorers – Replacing Those Missing Cycles, 1998, pp. 3/1- 3/6.

[5] N.G. Hingorani, "Introducing Custom Power in IEEE Spectrum," 32p, 1995, pp. 4l-48.

[6] M.H.J. BOLLEN," Voltage Sags in Three Phase Systems. IEEE Power Engineering Review", 2001, 21(9): 8-11

[7] Sanjay Haribhai chaudhary ,Mr.Gaurav Gangali "Mitigation of voltage sags and swell using DVR".IOSR,vol 8,issue 4 (Nov-dec 2013).

[8] "Power Quality Improvement and Sag Voltage Correction by Dynamic Voltage Restorer" Shady Hossam Eldeen Abdel Aleem (1*), Ahmed Mohammed Saeed., International Review of automatic control.

[9] P. Boonchiam and N. Mithulananthan, "Understanding of Dynamic Voltage Restorers through MATLAB Simulation", Thammasat Int. J.Sc. Tech., Vol. 11, No. 3, July-Sept 2006.

[10] Geeta V. Awad "Simulation Model of Three Phase Dynamic Voltage Restorer for Voltage Compensation" 2016 International Conference on Electrical Power and Energy Systems (ICEPES)

[11] "Simulation of dynamic voltage restorer (DVR) to mitigate voltage sag during three-phase fault" Rakeshwri Pal and Dr. Sushma Gupta, 2016 International Conference on Electrical Power and Energy Systems (ICEPES).

[12] Taheri, A., Saki, M., Sheikholeslami, A., Samani, A.G., "Dynamic Voltage Restorer Using Sliding Mode Control to Improve Power Quality in Distribution System'', International Conference on Environment and Electrical Engineering (EEEIC),IEEE 2012.

[13] Venmathi M. and Ramesh L., "The impact of Dynamic Voltage Restorer on voltage sag mitigation," Sustainable Energy and Intelligent Systems (SEISCON 2012), IET Chennai 3rd International on, pp.1-7, 27-29 Dec. 2012.

[14] Benachaiba C. and Ferdi B., "Power Quality Improvement Using DVR," American Journal of Applied Sciences, vol. 6, no. 3, pp. 396-400, 2009.

[15] Omar R. and Rahim N.A., "Modeling and simulation for voltage sags/swells mitigation using dynamic voltage restorer (DVR)," Power Engineering Conference, 2008. AUPEC '08. Australasian Universities, vol. 1, no. 5, pp. 14-17, Dec. 2008.

Abdullah Taj is a student of University of Engineering and Technology, Peshawar, studying MS Electrical Power Engineering. Research area of interest is Power Quality enhancement. Control System and Electrical Transmission & Distribution. Email: engr_alitaj91@yahoo.com.

Professor Dr. Muhammad Naeem Arbab is a Professor in University of Engineering and Technology Peshawar in Electrical Department. He got his Ph.D. from UK and author of two engineering books i.e., High Voltage Engineering and Electrical Power Generation and published more than 25 Research Papers.
Email: mnarbab@gmail.com.

International Journal of Engineering Works
ISSN-p: 2521-2419
ISSN-e: 2409-2770
Vol. 6, Issue 05, PP. 182-186, May 2019
https://www.ijew.io/
https://doi.org/10.34259/ijew.19.605182186

Denoisation of ECG Signal using JADE ICA and FAST ICA Comparison

Syed Muhammad Ali Shah[1], Dr. Syed Waqar Shah[2]
[1,2]University of Engineering and Technology Peshawar
smasofficial@outlook.com[1], waqar.shah@uetpeshawar.edu.pk[2]
Received: 30 April, Revised: 06 May, Accepted: 15 May

***Abstract*—**Electrocardiograph signal is effective tool in diagnosis of cardiac related diseases and plays an important role in biomedical research. To diagnose the cardiac disease, the signal must be recorded properly. The addition of artifacts like Persistent noises, Burst noises and their types play an important in making it difficult to interpret and analyses the electrocardiograph signal. A Blind source separation (BSS) related technique named Independent Component Analysis (ICA) is the right solution for it. In this paper, different ICA Algorithms like JADE, FAST are used to de-noise the ECG signal from the artifacts and a comparison between both is shown which is done on the basis Performance Index (PI) using a dsp ICALAB toolbox in MATLAB.

***Keywords*—**Blind Source Separation, Electrocardiography signals, Independent Component Analysis, Performance Index, Signal to Interference ratio

I. INTRODUCTION

An ECG signal is a vital mechanism for analyzing the problem of cardiac. It is storage of imbalances of different electrical potential generated by heart beats with reference to time. ECG is an important and vital tool from the point of view of functionality and circulatory system. Premature diagnosis of cardiac irregularities can help saving one's life and a proper treatment will lead to a quality life. As ECG is primary source of any disorder that initiates from heart and a lot of work is already done on it but still it is famous issue for various researcher. By in large the ECG signal with its heart rate depicts the healthiness situation inside the heart [1].

II. CHARACTERISTICS OF ECG SIGNALS

The characteristics of ECG Signal can best be explained by the peaks in the graph.The graphical form of electrical action of the cardiac is known as Electrocardiography signal shown in Figure 1. Mainly two things in this figure need to be noticed. One is about the electrical movements observed though the muscles of heart and second is the period of the tramp the electrical waveform across the heart.

The nominal limit (0.05 – 100) Hz where the frequency of the electrocardiograph signal lies. The signal is further categorized on the basis of their discontinuity level like peaks sometimes called valleys named as P, Q, R, S, T. Occasionally, with very rare case the U peak also appears. A person health is only detected or the indicator to check one's health is to check whether the P wave, T wave and QRS complex interval is there or not? These indicators are the essence of the electrocardiograph waveform as the T wave and QRS complex interval show the activities involves in the ventricular portion and P wave which shows atrial activities

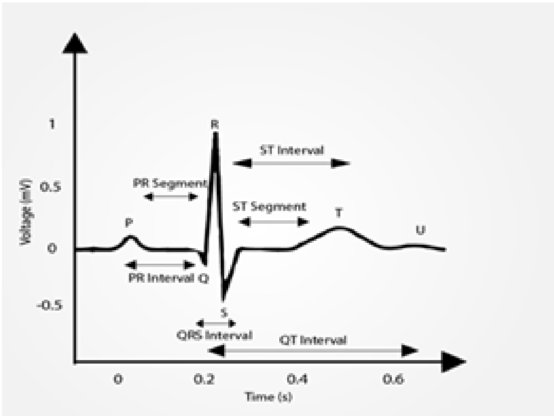

Figure 1 Characteristics of ECG Signal [9]

Basically the deep analysis of ECG signal shows that the waveform is divided into three parts, one is middle part the QRS complex interval (which is surely the identity of this signal) and the part before and after the QRS complex part is somewhat inverted replica with first having magnitude lesser than the last one [3].

TABLE I. DIFFERENT PARTS OF THE ECG SIGNAL WITH THEIR VOLTAGES [10]

INTERVAL	DURATION (sec)
P-R	0.12-0.20
Q-T	0.35-0.44
S-T	0.05-0.15
P wave	0.11
QRS	0.09

Out of these QRS complex interval is of great importance in any machine which is used for the analysis of the electro cardiograph signal. If the QRS complex is identified in the oscilloscope which is basic of the most of the cardiac checkups. The below table explains the duration of each particular interval in the ECG signal [11]

III. Noise affected the ECG signals

There are two mainly two types of noise that affect the ECG signal. One is Persistent noise and another is Burst noises [7].

A. Persistant Noises

These noises come up with the electrocardiograph signal with variation of range of frequencies. Their limit of intensity is dissimilar but the time-based distribution is same. Due to having a variety of frequency ranges their types are categorize on the basis of frequency range.

- Power Line Interference Noise
  This type of noise comes from the interference of wires that carries the biomedical signals, normally in this case for medical equipment. The signal faced interference with 50 Hz or 60 Hz frequency, mostly in the case in which the electromagnetic creates the disturbance to the line which has to analyze in monitoring room and comes from examination box [8]

- Baseline Wander (BW)
  This type of noise is due the impedance involved in the contact of the electrode terminal and human skin and also main cause involves the breathing and maneuvering initiated by patient[10]. These noises lie in the range less than unity Hz but considering electrocardiograph signal it may varies to long range. It is one of the leading noise in the reception of electrocardiograph signal with different monitoring system [12]

- Electromyography Noise
  Though electromyography is used for recording the movement of skeletal muscles and it is a bio signal but it also acts as noise to other bio signal like ECG signals. These muscles when contracts and relaxes in the tertiary of cardiac, their movement or activity is being recorded by the terminals and acts as a noise in the way of desired ECG signals. The muscles contraction and relaxation provide necessary level of the noise which is added to our desired signal but also the reading equipment terminals quality also play important role in it. The electromyography noise is random in nature and studies have proved that its distribution is Gaussian in nature which greatly dependent upon environmental condition

B. Burst Noises

This type of noise is due to production of noise through the leads of the equipment for measuring ECG signal. They are white gaussian in nature and have arbitrary range of frequency.

- Contact Noise or Electrode popup
  The main reason of this type of noise is disconnection of the contacts between the probe of the electrode and the human skin. The loss of connection amongst the parties will lead to affect the reading system which results in greater noise in ECG signal. The major factors of electrode or contact noise are the location of electrode with reference to heart and the medium of propagation between them and they play their part in the artifacts because of capacitive coupling nature of the ECG signal. The level of conductivity between the human skin and the electrode have also their importance as low level of conductivity will lead to low values of signal to noise ratio meaning greater amount of noise involved in the signal.

- Patient Electrode motion artifact
  These types of burst noise are produced by the motions of electrode causing changes to baseline. Normally, the main causing of this type of burst noise are movement by patient like respiration, shuddering etc [13]

- Instrumentational Noise
  This type of burst noises is due to the electrical hardware which is utilized in ECG estimations moreover contributes noise. The main causes of this type of noise includes probes of electrodes, A-D converters, cables, signal amplifiers or signal processor. One thing should be noted here that it is almost impossible to eradicate this type of burst noise but it can be minimized by utilizing the machines of better quality with cautiously developing the circuits

IV. Independent Component Analysis

Independent Component Analysis is a technique that can be used for removing artifacts from the noisy ECG signal. In this thesis we will compare the different algorithms of ICA for removal of noise from ECG signal [4].

A. JADE ICA

An ICA algorithm named Joint Approximation Diagonalization of Eigen matrices which works on retrieval of source signals using good advantage of moments of order fourth from the original source signal.[14]

Its working is based on calculating the P matrix, which leads to finding the signal z = P x [10]. Furthermore, the calculation of cumulates which are related to whitened mixtures are processed. By using the joint diagonalization, λiVi is used find out the R rotation matrix. For rotation matrix R conditions like keeping the diagonal behavior of cumulants as much, orthogonal optimization is achieved which is the basic working of JADE algorithms [15]. The JADE algorithms operates mostly on difficulties of low dimensions and there is no legal requirement of adjusting the variable. These all factors makes the JADE ICA fast to calculate the un mixing matrix [9].

B. FAST ICA

Another famous and well organized algorithms for Independent Component Analysis is FAST ICA. This fixed point iteration algorithms deals statistical independence as a factor of non gaussianity with capitalizing on non gaussainity [7].

This algorithm basically works on iteration for finding the more of variable which are non gaussainity in nature and that can be obtained from estimation of Newton iteration [2]. As this algorithm is associated to series of fixed point algorithms and with w weight vector is explained as follow.[12]

1. Let $w^+ = E\{xg(w^T x)\} - E\{g'(w^T x)\}w$
2. Let $w = w^+ / \|w^+\|$
3. If not converged go back to one

Some of the key features of FAST algorithm is explained below which differ it from rest of the algorithms.

1. The algorithm has linear convergence, while have on issue of gradient it has cubical. This convergence makes the algorithm a fast algorithm which is further proved from testing on the real data.

2. Under the supposition of ICA generalized model (in quadratic no step size is needed). In contrast to algorithm constructed on gradient algorithms. Which shows dissimilarities as compared to other ICA algorithm which show it convenience for implementation.

3. The algorithm uses non linearity to search out any independent component related only to non gaussian distribution which is the unique quality of this algorithm which is not present in others, While the others works on the principle of digs out first the prohability density function and then search the independent components [18]

4. One of the factor which enhance the process, is by choosing appropriate value of non-linearity. Precisely algorithms having low variance and robustness are mostly preferable and actually ideal characteristics are showed up by the two linearities.

V. RESULT AND DISCUSSION

ECG is an apparatus or tool in sensing the nature of the disorder related to cardiac. Also, the behavior of electrocardiograph signal (bio signals), being a non-stationary signal show lot of variety in domain of time. So, because of this reason the identification of heart disorder is a bit tricky to find but there is some irregular interval which would rather help the cause [6].

Furthermore, for an ECG signal to be analyzed efficiently things like signal variation, signal shape and heart rate should be taken into account and deeply studied. Independent Component Analysis is a technique that can be used for removing artifacts from the noisy ECG signal. In this thesis we will compare the different algorithms of ICA for denoisation of ECG signal [5].

It includes the results of the overall theory discussed before about the simulated signals, how the noise being added and how then finally the denoised signal is retrieved using ICA Algorithms.[11] The whole process is about the taking the data from the MIT-BIH Arrhythmia Database (PhysioNet) and then some noise is being added to the signal using MATLAB. Then the process is forwarded to ICALAB. A signal processing toolbox used in MATLAB for denoisation of different things using different ICA Algorithms. Where the original ECG signal retrieved which makes our whole process complete.[13]

Figure 2 show the original signal ECG signal which is taken from MIT-BIH source

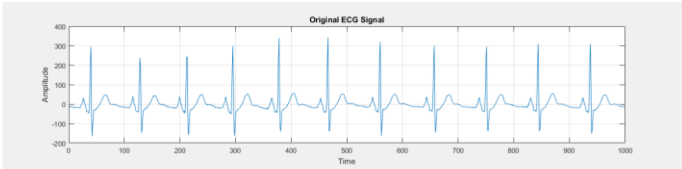

Figure 2 Original ECG Signal [9]

Figure 3 shows the noised version of Figure 2. The noise is been added in the original signal. 10dB in the first figure, 15db in the second figure and 20dB in the third figure.

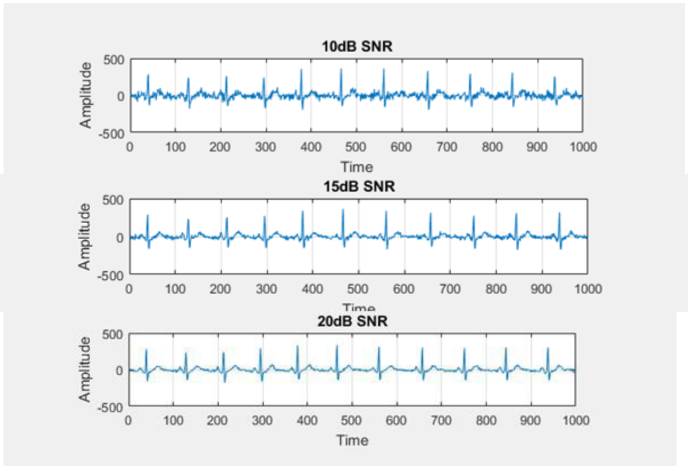

Figure 3 ECG noised signal with 10dB,15dB and 20dB [9]

The noised signal is then processed using two of the algorithms of ICA i.e. FAST and JADE and the de noised is shown using ICALAB tool box. The Figure 4 shows the denoised version of Figure 3 using FAST ICA. Figure 5 shows the denoised version of Figure 3 using JADE ICA.

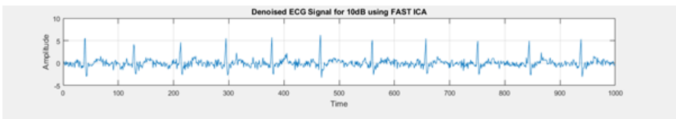

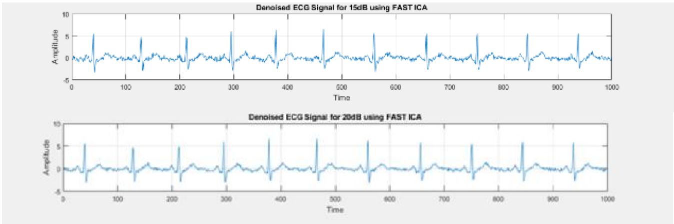

Figure 4 ECG de noised signal using FAST ICA [9]

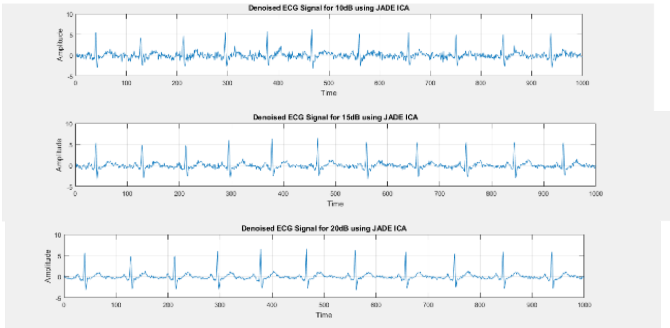

Figure 5 ECG de noised signal using JADE ICA [9]

Finally, the whole comparison is described in a tabular form to make a comparison of both the algorithms applied in this thesis. After applying the whole process with 10dB, 15dB and 20dB on the both the algorithms i.e. FASTICA and JADEICA. FAST ICA algorithm is found to be the better one in terms of their performance index that is being observed on the ICALAB toolbox used in MATLAB [15]

TABLE II. TABLE 1 PERFORMANCE INDEX WITH DIFFERENT NOISES OF FAST ICA [9]

S.No	Algorithms	Noise (dB)	Performance Index
1	FAST ICA	10	0.357305
2		15	0.391784
3		20	0.430206

TABLE III. TABLE 3 PERFORMANCE INDEX WITH DIFFERENT NOISES OF JADE ICA [9]

S.No	Algorithms	Noise (dB)	Performance Index
1	JADE ICA	10	0.294056
2		15	0.319209
3		20	0.33043

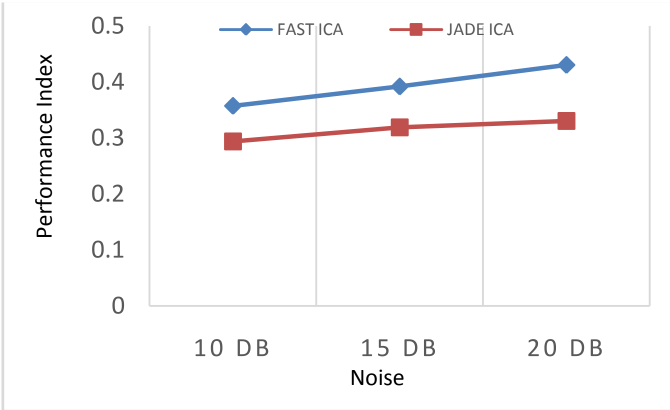

Figure 6 Graphical comparison of FAST and JADE Algorithms [9]

The Figure 6 shows the graphical comparison between the two algorithms of ICA and it is clearly shown in the figure that FAST ICA shows better performance in the circumstances

CONCUSLION

In this research paper, a comparative ¬analysis of two ICA algorithm namely JADE and FAST were analyzed on the basis of their performance index. The Signal to interference ratio is the main source of performance index in this research.

Different types of artifacts have contaminated the ECG signal like Types of Burst noises and Persistent noises. This result explore that Fast ICA is better than Jade ICA under the circumstance discussed in this research paper.

FUTURE WORK

FAST ICA as compared to JADE ICA shows better performance in the thesis, but one thing is observed that It memory used by FAST ICA is higher than JADE ICA. Although it is outweighed by its performance [16]

On the Other hand, JADE shows low performance in this scenario but balance by its low memory usage. According to the above two point, future work can be done on either JADE ICA to increase its performance as its memory utilization is better or to research on FAST ICA to make it use on low memory as its performance is better in this case [17]

REFERENCES

[1] Keshavamurthy T G, Dr. M.N.Eshwarappa, "Review Paper on Denoising of ECG Signal", Second International Conference on Electrical, Computer and Communication Technologies (ICECCT), 2017.

[2] Prof. Alka S. Barhatte, Dr. Rajesh Ghongade, Sachin V. Tekale, "Noise Analysis of ECG Signal Using Fast ICA", Conference on Advances in Signal Processing (CASP), 2016

[3] Shudong Tian, Jun Han, Jianwei Yang, Lijun Zhou, Xiaoyang Zeng, "Motion Artifact Removal Based on ICA for Ambulatory ECG Monitoring", IEEE 11th International Conference on ASIC (ASICON), 2015

[4] Mayank Kanaujia, Dr. Geetika Srivastava, "ECG Signal Decomposition Using PCA and ICA", National Conference on Recent Advances in Electronics & Computer Engineering RAECE, 2015

[5] Bhargav Bhatt, M.Ramasubba Reddy, “ICA Based Flow Artifact Removal from ECG During MRI”, International Conference on Advances in Computing, Control, and Telecommunication Technologies, 2009

[6] H.P. Kasturiwale, C.N. Deshmukh, “Quality Assessment of ICA Algorithms for ECG Signal Analysis”, Second International Conference on Emerging Trends in Engineering and Technology ICETET, 2009

[7] Uzzal Biswas, Anup Das, Saurov Debnath, Isabela Oishee, ”ECG Signal Denoising by Using Least-Mean-Square and Normalised-Least-Mean-Square Algorithm Based Adaptive Filter”, 3rd International Conference On Informatics, Electronics & Vision, 2014

[8] Deepak Vala, Tanmay Pawar, V. K. Thakar, “Motion Artifact removal in Ambulatory ECG Signal using ICA”, International Journal on Recent and Innovation Trends in Computing and Communication Volume: 2, 2014

[9] Syed Muhammmad Ali Shah, Dr. Syed Waqar Shah, "Comparative Analysis of ICA Algorithm for Denoisation of ECG Signal",A Thesis submitted to HEC Pakistan by Student from UET Peshawar

[10] Mrinal Phegade, P. Mukherji, “ICA Based ECG Signal Denoising”, International Conference on Advances in Computing, Communications and Informatics (ICACCI), 2013

[11] Baby Paul, P. Mythili, “ECG Noise Removal using GA Tuned SignData Least Mean Square Algorithm”, IEEE International Conference on Advanced Communication Control and Computing Technologies (ICACCCT), pp. 100 - 103, 2012.

[12] Mohammed Assam Ouali and Kheireddine Chafaa, “SVD-Based Method for ECG Denoising”, IEEE International Conference on Computer Applications Technology (ICCAT), pp. 1 - 4, 2013.

[13] Lukas Smital, Martin Vitek, Jiri Kozumplik, and Ivo Provaznik, “Adaptive Wavelet Wiener Filtering of ECG Signals”, IEEE Transactions On Biomedical Engineering, Volume 60, Issue 2, pp. 437 - 445, 2013.

[14] Ali Marjaninejad, Farshad Almasganj and Ata Jodeiri Sheikhzadeh, “Online Signal to Noise Ratio Improvement of ECG Signal based on EEMD of Synchronized ECG Beats”, IEEE 21th Iranian Conference on Biomedical Engineering (ICBME), pp. 113 – 118, 2014.

[15] Gholam-Hosseini H, Nazeran H and Reynolds K J, “ECG noise cancellation using digital filters,” Proc 2nd lnt Conf Bioelectromagnetism, p.151-152 (1998).

[16] Zhang D., “Wavelet approach for ECG baseline wander correction and noise reduction,” IEEE-EMBS 2005. 27th Annual International Conference of the IEEE, p.1212-1215 (2005).

[17] Y. Der Lin and Y. Hen Hu, “Power-line interference detection and suppression in ECG signal processing,” IEEE Trans. Biomed. Eng., vol.55, p.354-357 (2008).

[18] Phegade, Mrinal and P. Mukherji, “ICA based ECG signal denoising,” Advances in Computing Communications and Informatics (ICACCI), 2013 International Conference on IEEE, p.1675-1680 (2013).

International Journal of Engineering Works
ISSN-p: 2521-2419
ISSN-e: 2409-2770
Vol. 6, Issue 05, PP. 187-191, May 2019
https://www.ijew.io/
https://doi.org/10.34259/ijew.19.605187191

Energy Audit: A Case Study of UET Jalozai Campus

Zafar Ullah Khan[1], Noor Muhmmad[2], Dr. Muhammad Naeem Khan[3]
[1,2,3]US-PCASE UET Peshawar
Lab Engineer (zafar.ullah@uetpeshawar.edu.pk)[1], Professor (Naeem.khattak@uetpeshawar.edu.pk)[3]
Received: 08 May, Revised: 13 May, Accepted: 15 May

Abstract— Pakistan is facing a decade long worst crises of energy. The demand supply gaps, heavy dependence on imported fossil fuel and inefficient consumption patterns are major thematic reasons of crises. Energy conservation is a low hanging fruits which can be materialized to answer the crises. This is a joint academia and industry projects, where detailed energy audit of educational facility of University of Engineering and Technology Jalozai Campus was carried. The significant energy consumer areas of educational building like lighting, Heating and cooling system and generation plants were deeply investigated. In additions, the male and female boarding houses were audited. Based on Illumination Engineering Standards and ASHRAE level III benchmarking, various energy conservations measures were recommended including efficient lighting system, installation of occupancy sensors, office appliances scheduling and transition towards energy efficient fans. The suggested recommendations implementations are capable to save a 22.3% of electricity in the facility. The economic analysis shows a payback period six to eighteen months for various conservation measures. In addition, a behavioral training and mobilization drive is highly recommended to build the conservation culture on gross root level as integrated part of societal practices and cultural values.

Keywords— Energy Audit, Energy, Lux Meter, Lighting, Generation, Consumption

I. Introduction

The concept of energy conservation becomes popular during Arab Oil embargo of 1970 and further highlighted during recent focus on sustainability. The global agenda of sustainable development emphasize equally on energy access and energy conservation. On one hand, technological research is focused on efficiency targets whereas on other energy audit is utilized to save energy in existing facilities. Energy Audit is basically the inspection, monitoring and analysis of energy flow, for the energy conservation of domestic, industrial or commercial facility, to minimize the energy consumption of the system.

China is at the top having highest energy consumption growth rate of 5.5% per year followed by United States consuming 25% of the world total energy. Industrial sector is the top consumer accounting 37% of the world total energy consumption [1]. The total energy consumption in industrial sector in 2006 was 51,275ZW and it is expected to rises up to 71,961ZW in 2030 with an annual growth of 1.4% [1, 2]. In US 33% of the total energy is used by industries where as in china, according to the data available for 2003, 70% of the total energy is used by the industrial sector with an annual growth of 5% which is five times more than the normal growth. Only China alone is accounting for 23% of the world total industrial energy consumption [1, 2].

Pakistan energy demand is rapidly increasing because of urbanization and industrialization. Pakistan primary energy supply in the financial year 2017 was 92.9 MTOE [3]. It consists of 47.5% of natural gas, 30.5% of oil, and 10.9% of hydel, 9.2% of coal,1.2% nuclear and 0.7% LPG [3]. In the coming fifteen years the demand will increase to 122 MTOE, thus increasing the annual energy import bill to more than US $41 billion compared to the total current annual energy import bill of US $7.5 billion in 2008 [4]. To meet this galloping energy demand is a herculean task for the government. In Pakistan 43% of the total annual energy consumption is used by industry, 29% by transportation, 20% by domestic and 8% by others [4,5].

In 2011, Energy Conservation Centre (ENERCON) prepared the first national policy for energy conservation. They find that Pakistan need to improve the existing system taking Energy Conservation Measures (ECM) in various areas like power transmission and distribution, load management, power plants, and more importantly the end user. Overall saving of 25% of the total industrial consumption can be achieved through energy auditing. For financial year 2008, a saving of 8.4 MTOE was estimated which is approximately 15% of the total primary energy consumption [6]. It is forecasted that electricity and natural gas saved through continuous energy auditing and conservation is equal to the generation capacity of 3710 MW and 3060 MW correspondingly [6,7]. A total reduction of 51% in the annual fuel import is estimated. However there are many barriers to energy auditing and conservation such as lack of knowledge, management, policy and financial resources. According to report of SAARC a total investment of US $ 8.16 billion is required for energy efficiency sector from 2010-2019 in Pakistan [4].

A report from USAID office of energy , environment and technology entitled “Prompting energy efficiency in the reforming electricity market” has assessed the energy efficiency potential in developing and reconstructing countries and come up with the following informative conclusions [6];

1. Energy efficiency has the potential to reduce total forecast demand for power in said countries by 5% to 10%, equivalent to 220 – 440 GW new installed capacity and 1000 – 2000 billion kwh/year.
2. Energy efficiency measures cost less than half that of new supply, equivalent to;
    - Initial cost saving of at least $140 -280 billion in capital investments
    - Significant saving's in avoided operating costs

According to International Environmental Agency (IEA) 5% of emission of the world is taking place from steel and iron industry. US are the third largest steel making country with a production of 80.5 million tons in 2010 [1].A research for reducing energy consumption and carbon dioxide emissions in US steel and iron sector was carried proposing three different scenarios to achieve 20% reduction in annual emission. These scenarios are; investment in national energy efficiency measures, energy efficiency measures along with commodity trading with china and India and energy efficiency measures along with carbon trading with and India [6].

University of Engineering and Technology, Peshawar (UET-P) is one of the prominent institutes of Khyber Pakhtunkhwa. University of Engineering and Technology Jalozai is a campus of UET-P located southward on Pabbi-Cherat road at 12 Km from main Grand Truck road of district Nowshera. The campus total is spreader over an area is 402 acres whereas covered areas with educational facility is about 1021,233 sq.ft. Currently the campus includes Electrical, Civil, Mechanical and Industrial department's blocks and three hostels.

II. METHODOLOGY

This section describes the instrumentation and measurement techniques relevant to energy audit activities. An energy auditor must have a basic understanding of measurement techniques and instrumentation in order to be knowledgeable about the purchase or rental and use of the equipment [9,10]. Both the correct instrument and its correct use are fundamental requirements for obtaining useful measured data[15].

The auditor's Toolbox

The following sections include details of the instruments commonly found in the energy auditor's toolbox:

- Electric power meter
- Combustion analyzer
- Digital thermometer
- Infrared thermometer
- Psychomotor (humidity measurement)
- Airflow measurement devices
- Tachometer
- Ultrasonic leak detector
- Lux meter

Instruments used during Audit in UET Jalozai

The following are the instruments used during audit in University of Engineering and Technology Jalozai campus.

- Lux Meter
- Clamp meter
- Power factor meter
- Power quality manager
- Digital Millimeter
- Temperature Indicators

Energy Audit Methodology

Three steps to be taken for the energy audit methodology.

Data collection:

The first step of the energy audit is data collection. Different type of tools is used in the comprehensive data collection such as measurement, observation and interrogati ng the crucial persons [11,12].

Detail analysis:

The second step is the detail analysis of the energy audit where diverse instruments are used for extensive analysis of energy flow in the buildings [13].

Recommendations:

Based on real time analysis of energy flows, various energy conservation measures are recommended to optimize energy consumption patterns of the facility.

Energy audit of lighting and cooling system:

Lighting is providing in the indoor, outdoor, commercial building, industries for the relaxed working environment. The main objectives are to deliver essential lighting for the final installed load for example maximum lighting at the lowest power consumption[14,16].

Purpose of the Performance Test:

Most of the lights required in interior for meeting normal luminance of the horizontal plane, either through the inside or in the exact area within the interior share with common lighting of its lower value.

Main purpose of this test is to analyze the installed valve in terms of lux/watt/m² for the installation of common lights.

Lumen:

Lumen is the unit of light flow. The total lights production of the lamp is measure the lumen rating. General measurement of light output is lumen.

Lux:

Lux is the unit to measure the luminance of the surface. One lux is equal to the one lumen per square meter.

Circuit Watt:

The circuit watt is the total power drawn by the lamp in a lighting circuit underassessment.

Installed Load Efficacy:

Installed load effectiveness is to provide maintained average illuminance on the horizontal plane per circuit watt with the interior of general lighting. Unit: lux per watt per square meter (lux/W/m²)

Lamp Circuit Efficacy:

Amount of light emitted by the lamp for each watt of the power consumed by the lamp circuit. For example control gear losses. This is the meaningful measurement for those lamp that need the control gear.

Lighting System:

The hostel and departments was segmented into many sub groups which utilizes lighting system. These include the Offices, Class Room, Staff Room, Resident Rooms, Warden Lodges, Mosques, Washrooms, Mess and canteen, Common room, Study room, Corridors, Lounges.

The fixtures in this area include compact fluorescent light (CFL), Incandescent bulb and fluorescent fixture of varying size. Below Table I and Table II shows the properties of lights and recommendations and light level for different work space

TABLE I. TABLE 1: PROPERTIES OF LIGHTING APPLIANCES (IES-2010)

Lamp Type	Lumen Output (initial)	(maintained)	Burning Life Hours
Light Emitting Diode (LED)	150 +	150 +	60,000 +
Low-Pressure Sodium (LPS)	147	147	10,000
High-Pressure Sodium (Clear) (HPS)	105	77	12,000
Pulse Start Metal Halide (MH)	98	59	6,000
Standard Metal Halide (MH)	96	60	6,000
T8 Fluorescent (FL)	93	84	7,500
Induction Fluorescent (Sylvania Icetron) (IFL)	83	62	10,000
T12 High-Output (800 ma) Fluorescent (FL)	79	64	7,500
T12 Cool-White Fluorescent (FL)	74	59	7,500
Compact Fluorescent (PL)	68	54	5,000
Tungsten Halogen (Quartz) (TH)	19	17	2,000
Incandescent (standard) (INC)	14	12	1,000

TABLE II. TABLE 2: RECOMMENDATIONS AND LIGHT LEVEL FOR DIFFERENT WORK SPACE (IES-2010)

Activity	Illumination (lux, lumen/m2)
Public areas with dark surroundings	20 - 50
Simple orientation for short visits	50 - 100
Working areas where visual tasks are only occasionally performed	100 - 150
Warehouses, Homes, Theaters, Archives	150
Easy Office Work, Classes	250
Normal Office Work, PC Work, Study Library, Groceries, Show Rooms, Laboratories	500
Supermarkets, Mechanical Workshops, Office Landscapes	750
Normal Drawing Work, Detailed Mechanical Workshops, Operation Theatres	1,000
Detailed Drawing Work, Very Detailed Mechanical Works	1,500 - 2,000
Performance of visual tasks of low contrast and very small size for prolonged periods of time	2,000 - 5,000
Performance of very prolonged and exacting visual tasks	5,000 - 10,000
Performance of very special visual tasks of extremely low contrast and small size	10,000 - 20,000

III. RESULTS AND DISCUSSION

This section delineates the results of the energy audit activities undertaken during the course of the research. This section is organized such that the current energy consumption for the utility supplied electricity and gasoline generator electricity for all the buildings i.e. the three hostels, Civil Engineering department and the Electrical energy department is presented. Following this the same results are simulated while retrofitting low energy consumptive technology. The overall energy consumption for the aforementioned buildings using utility power is given in the table III, detailing the energy used in lighting, cooling and miscellaneous electricity consumption equipment. Figure 1 gives the percent consumption of the energy in the lighting, cooling, and miscellaneous sources.

TABLE III. TABLE 3 TOTAL POWER CONSUMPTION THROUGH ELECTRICITY

Lightening power consumption KWH/Year	172668.2
Fans and cooling power consumption KWH/Year	184116.6
Miscellaneous Power consumption KWH/year	174600
Total Power Consumption KWH/year	531384.8

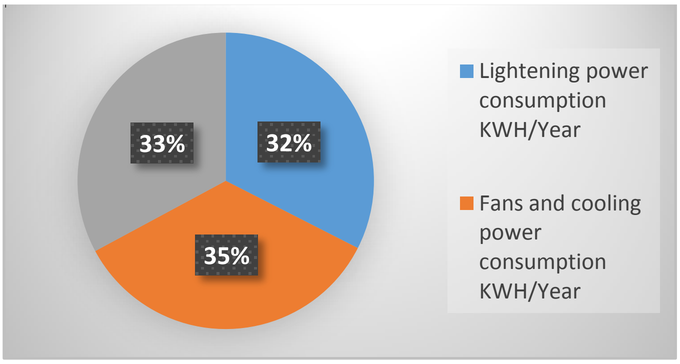

Figure 1. Percentage of total power consumption of electricity

Total power consumed by the hostel and departments for the session 2017-18 using gasoline in generator as a power source is 542049.12 KWH/year. In which major contribution to power consumption is by the cooling system 201892.32 KWH/year as shown in the Table IV.

TABLE IV. TOTAL POWER CONSUMPTION THROUGH GENERATOR

Lightening power consumption KWH/Year	167836.8
Fans and cooling power consumption KWH/Year	201892.3
Miscellaneous Power consumption KWH/year	172320
Total Power Consumption KWH/year	542049.1

Accordingly the percent energy consumption for each of the three mentioned sources i.e. cooling, lighting, and miscellaneous sources is given in the pie chart in Figure 2.

Figure 2. Retrofit of Lighting suggestions

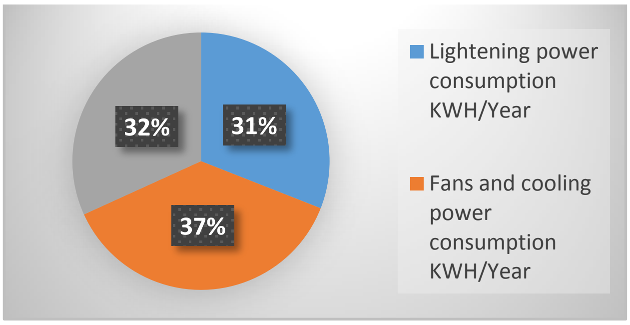

Figure 3. Percentage of total power consumption of Gasoline

The departments' and hostels' lighting system consist of fluorescent tubes, incandescent bulb and mostly CFL. We have suggested retrofitting according to figure 3 given below.

Similarly alternative less energy intensive suggestions have been made for cooling and miscellaneous energy consumption equipment as shown in the figures 4 and 5.

Figure 4. Retrofit of Fans

In addition Use of sensors for automatic lighting control system in washrooms, corridors, staff rooms and in offices to control and detect the actual requirements of lights[17]. It was also recommended to switch off the lights in unused area by installing automatic sensors and control system to save sustainable amount of energy.

Based on the recommended retrofitting appliances and sensor placement the simulation shows savings in energy consumption and pursuant capital savings for both the gasoline generator electricity consumption and the utility energy consumptions. The results from the retrofitting of appliances is given in the form of energy and capital savings as shown in the Tables V and Table VI for the utility and gasoline electricity provision respectively.

TABLE V. FISCAL SAVINGS FROM RETROFITTING APPLIANCES FOR UTILITY ELECTRICITY

Total Saving from electricity as source for replaced lights in KWH/Year	91601.84
Total saving from electricity as source replaced for fans in KWH/Year	217851.2
Total energy saving from electricity KWH/year	309453
PKR/KWH	15.5
Saved amount PKR/year	4796522

TABLE VI. FISCAL SAVINGS FROM RETROFITTING APPLIANCES FOR GASOLINE ELECTRICITY

Total saving from generator as source for replaced lights in KWH/year	86601.34
Total saving from generator as source for fan in KWH/year	26995.20
Total energy saving from generator as resource KWH/year	113596.54
Total saving from generator as resource MJ/year	408947.54
Conversion factor MJ/liter of Gasoline	35.00
Total gasoline used liters/year	11684.22
PKR/liter of gasoline	100.00
Total amount saved PKR/year	1168421.5 5

The overall amount saved through energy audit from both energy resources is PKR 5964943.674. The overall amount distribution is given in the table VII below.

TABLE VII. THE OVERALL AMOUNT DISTRIBUTION

Total saving from electricity PKR/year	Total saving from Gasoline PKR/year	Overall saving PKR/year
4796522.12	1168421.554	5964943.674

These results are only from the two engineering departments and three hostels. The whole of university could also be audited to give a more detailed analysis and more capital saving could be achieved.

CONCUSLION

The energy audit of a large buildings can allow national level analyses and considerations on the strategies for a smart planning of improvements. This research identified key energy efficiency improvement areas in a university in KP, Pakistan. The significant energy usage areas were identified in form of lighting, cooling/heating and other miscellaneous energy consumption appliances. The energy bills of the university, especially the gasoline consumption charges in times of load shedding from national utility have been significantly high. This research identified areas for improvement and recommended alternative appliances with lower energy intensity and the simulation of energy consumption with these appliances would prove extremely beneficial in terms of energy bills and environment. Overall the recommended energy appliances will result in benefit of PKR 5964943.674.

ACKNOWLEDGMENT

The research is supported by USAID funded Energy Center. I am very much thankful to USAID and USPCASE UET Peshawar for giving us the opportunity to complete our post graduation. I am grateful to my supervisor Dr. Muhammad Naeem Khan and respected teacher Dr. Abdul Basit for their help and support throughout my research.

REFERENCES

[1] U.S Energy Information Administration. International Energy Outlook 2009: World Energy and economic Outlook; 2009,

[2] United Nations Industrial Development Organization (UNIDO). Policies for promoting industrial energy efficiency in developing countries and transitioneconomies; 2008

[3] Hydro Carbon Development Institute (HDIP), Pakistan Energy Year Book, 2017

[4] SAARC Road Map For Energy Conservation And Energy Efficiency In Pakistan

[5] Abdul Raheem et. Al, Renewable energy deployment to combat energy crisis in Pakistan , Energy, Sustainability and Society ,2016

[6] ENERCON, Pakistan Energy Conservation Potentials, 2014

[7] Energy conservation and emission reduction through electric motors in industrial sector of pakistan. Sindh University Research Journal - SURJ (Science Series), [S.l.], v. 46, n. 1, mar. 2014. ISSN 1813-1743. Available at: <http://sujo.usindh.edu.pk/index.php/SURJ/article/view/1818>. Date accessed: 15 April 2019.

[8] USAID Energy Efficeny Initivitaie Prompting energy efficiency in the reforming electricity market, 2013

[9] Kim, H.Y.; Kang, H.J. A Study on Development of a Cost Optimal and Energy Saving Building Model: Focused on Industrial Building. Energies 2016, 9, 181.

[10] Hu, M. Cost-Effective Options for the Renovation of an Existing Education Building toward the Nearly Net-Zero Energy Goal—Life-Cycle Cost Analysis. Sustainability 2019, 11, 2444.

[11] Hinge, A.; Bertoldi, P.; Waide, P. Comparing commercial building energy use around the world. In Proceedings of the 2004 ACEEE Summer Study on Energy Efficiency in Buildings, Pacific Grove, CA, USA, 22–27 August 2004.

[12] Aljami, A. Energy audit of an educational building in a hot summer climate. Energy Build. 2012, 47, 122–130.

[13] Desideri, U.; Leonardi, D.; Arcioni, L.; Sdringola, P. European project Educa-RUE: An example of energy efficiency paths in educational buildings. Appl. Energy 2012, 97, 384–395.

[14] Bourdeau, M.; Guo, X.; Nefzaoui, E. Buildings energy

[15] consumption generation gap: A post-occupancy assessment in a case study of three higher education buildings. Energy Build. 2018, 159, 600–611.

[16] Lin, B.; Zhang, Z.; Ge, F. Energy Conservation in China's Cement Industry. Sustainability 2017, 9, 668.

[17] Zhu, P., Gilbride, M., Yan, D. et al. Build. Simul. (2017) 10: 799 https://doi.org/10.1007/s12273-017-0408-6

[18] Thollander, P.; Danestig, M.; Rohdin, P. Energy policies for increased industrial energy efficiency: Evaluation of a local energy programme for manufacturing SMEs. Energy Policy 2007, 35, 5774–5783.

Zafar Ullah Khan

The author was born in KPK province, District Lakki Marwat, Pakistan in the year of 1991. He is currently serving as Lab Engineer at USPCAS E UET Peshawar. He did his Bachelors Degree in Electrical Power Engineering from COMSATS Abbottabad, Pakistan. Currently, He is enrolled in MS, Electrical Energy System Engineerning at USPCAS-E UET Peshawar, Pakistan.

The author has experience in energy efficiency, renewable energy system design and integration. He has worked as Assistant Engineer at KPOGDCL KP, Pakistan for two years. In addition to this he has completed various workshops and trainings on energy auditing and conservation.

IJEW 国际工程期刊 International Journal of Engineering Works انجینئرنگ کاموں کا بین الاقوامی جرنل

International Journal of Engineering Works
ISSN-p: 2521-2419
ISSN-e: 2409-2770
Vol. 6, Issue 06, PP. 192-195, June 2019
https://www.ijew.io/
https://doi.org/10.34259/ijew.19.606192195

Novel Control Technique for Control of Circulating Current in Modular Multilevel Converters

Farhan Ali[1], Dr Tanvir Ahmad[2], Asif Khan[3], Saad Rashid[4]
[1,2,3,4]US Pakistan Centre for Advance Studies in Energy, University of Engineering and Technology Peshawar, Pakistan.
farhann_ali42@yahoo.com[1], tanvir.ahmad@uetpeshawar.edu.pk[2], asifengruet@outlook.com,[3] saad.789@outlook.com[4]
Received: 11 May, Revised: 20 May, Accepted: 25 May

Abstract**—**Modular multilevel converters are the prominent candidates for high voltage direct current transmission systems. They offer high flexibility, modularity and flexibility in their operation. The main problem of multilevel converters are the circulating current in the converter and arm's voltage balancing in steady state and dynamic state. An easy and flexible control scheme is introduced in this study which eliminates the even order harmonics in the circulating current and reduces the circulating current. The model is implemented in Simulink/Matlab and the results confirm the efficiency of the proposed model. , the response of the controller is also presented in result section, which manifest its ability to control the current and eliminate the even order harmonics.

Keywords**—** Modular Multilevel converters, circulating current, Even order harmonics, repetitive controller, arm voltages.

I. Introduction

Energy is the first and foremost need of mankind. Man has needed energy since the beginning in one form or another. The need for energy increased with the advent of industrialization with more energy being needed to cope with the increased demand. Energy is often generated at remote places and then connected to residential and domestic load centers. With the increased demand, efforts started to minimize the losses in energy transmission. The shift from alternating current transmission to direct current transmission system was the culmination of these efforts. At load centers, a modular multilevel converter, converts power from ac to dc which is then transmitted over a long distance. At the receiving end, another modular multilevel converter, converts power back to ac power. A modular multilevel converter consist of six arms, two for each phase of a three phase system. These converters, however, suffer from the problems of voltage balancing among the arms and circulating current flow in the converter. A study in [1] shows the existence of circulating current in modular multilevel converters. This circulating current affects the performance and efficiency of the converters [2] [3]. Another drawback of modular multilevel converters is the arm voltage balancing as shown in [4]. Variations in voltages of two arms of same phase and between different phases deteriorates the efficiency of the converter [5].

Numerous schemes have been proposed to address these shortcomings. In [6] [7] controls loops are employed to control the internal circulating current and balance the arm's voltages. Another study in [8] uses a single loop to overcome the drawbacks of a two loop control scheme. This scheme, while reducing the complexity of the system, has a trade off with the overall cost of the system. Another approach to deal with circulating current and arm's voltage balancing employs sampling and sorting algorithms [9]. These simple techniques, however, fail to perform in high voltage applications. Another method to control the circulating current employs the control over harmonics in circulating current for its control [10] [11]. Arm's voltage balancing in [12] by employing voltage correcting modules in converter. A divide and conquer approach is followed in [13] to control the internal circulating current in the converter. Moreover, actuators and sensor delays can also be employed to control the circulating current in modular multilevel converters [14]. For improving the steady state and dynamic response of the modular multilevel converter a scheme is adopted in [3]. For balancing the arm's voltages, a scheme is proposed in [5] that preserves the capacitor voltage in sub module when arm's power is varied and simultaneously maintains AC and DC output performance. Arm's voltages can also be balanced by selecting an optimum value for the capacitor of sub module [15]. Redundant voltage levels are employed in [2] to balance the arm's voltages. The arm's voltages and circulating current are also affected when the load is varied or when the load is unbalanced. A study in [15] deals with arm's voltage balancing in unbalanced load conditions..

II. Multilevel Converter and Its Model

Modular multilevel converters were first introduced in [16] and has ever since then been extensively used in energy transmission system and STATCOMS. A three phase modular multilevel converter has six arms, two for each phase. A typical modular multilevel converter is shown in Figure 1. The sub module of the converter acts as a controlled voltage source. Each of the sub module operates in one of three states, i.e.

State 1, state 2, and dead state as shown in Figure 2 The position of the switches Determine the state of the sub modules as shown in Table 1 Using the switching states, an individual sub module can be inserted or removed from the multilevel converter to increase or decrease the overall voltage of the converter. The voltages of the upper and lower arm are given as

$$V_{ug} = n_{ug}\frac{V_{cug}}{N} \tag{1}$$

$$V_{lg} = n_{lg}\frac{V_{clg}}{N} = \left(N - n_{ug}\right)\frac{V_{clg}}{N} \tag{2}$$

The upper arm voltage is denoted by Vcug , given by 1 and the lower arm voltage is denoted by Vlg as show in equation 2. The number of sub modules placed or removed in a phase leg are denoted by nug and nlg for upper and lower arm respectively. Similarly the current of the converter can be divided into three parts

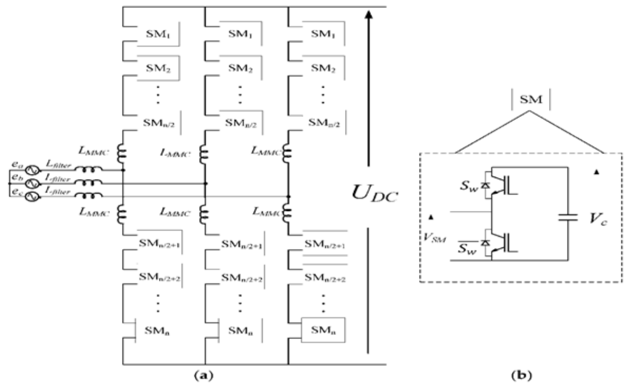

Figure 1. Figure.1 (a)Model of Multilevel Converter (b) sub module of converter

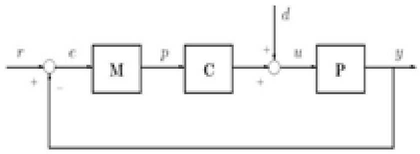

Figure 2. Basic Repetitive controller

$$i_{ug} = \frac{i_g}{2} + \frac{i_{dc}}{3} + i_{zg} \tag{3}$$

$$i_{lg} = -\frac{i_g}{2} + \frac{i_{dc}}{3} + i_{zg} \tag{4}$$

Where iug represent the current of the upper arm and ilg represent the current of the lower arm. The circulating current flowing through each is given by Izg. This circulating current is limited to the arms of converter and has no bearings on the converter output voltage but can significantly deteriorates the efficiency of the converter. This circulating current also leads the voltage imbalance between the upper arm and lower arm. Circulating current consist of a dc component and a differential component which are given by

$$i_{zg} = \frac{i_{ug} + i_{lg}}{2} - \frac{i_{dc}}{3} \tag{5}$$

TABLE I. SWITCHING STATE OF THE SUB MODULE

Mode	S_1	S_2	I	V_{out}	dV_c/dt
1	Off	On	>0	V_c	>0
2	Off	On	<0	V_c	<0
3	On	Off	>0	0	0
4	On	Off	<0	0	0

III. METHODOLOGY

The proposed scheme for the control of circulating current in modular multilevel converter employs an even harmonic repetitive controller that minimized the even order harmonics and circulating current in the converter. The proposed model consist of a repetitive controller with proportional integral controller. A repetitive controller is a simple controller that is used to track and eliminate a periodic signal in a system. Figure 2 shows a basic repetitive controller. A simple repetitive model consist of a plant, compensator and internal model each represented by transfer function P, C, and M respectively. The circulating current in modular multilevel converter also follows a periodic sequence. The Icr in modular multilevel converter consist of two parts as shown in equation 5. The differential current is made of a circulating current component and a dc component. In practical application the dc component is preferred for the stable operation of mmc and for minimizing the losses within mmc. By adjusting the voltage in upper and lower arm the differential component of the circulating current can be controlled. For the control of dc component a novel control scheme is presented here which consist of a combination of even harmonic repetitive controller and a PI controller. The overall control scheme of the proposed model is shown in Figure 3.

The proposed model uses PI controller as a primary mechanism of harmonic suppression of Icr. The Icr reference consist of a dc component, due to total energy, and a fundamental component, due to differential energy. The harmonics of the capacitor easily affects the dc component of the reference current, therefore a moving average filter (MAF) in the path of dc current reference. The arrangement is shown in figure 3.

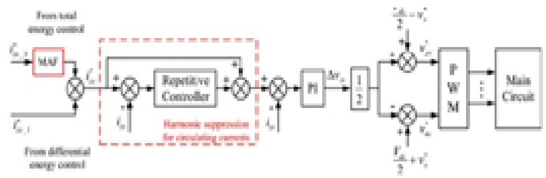

Figure 3. Overall control for internal circulating current

The transfer function of proportional resonant controller is given by

$$PI(s) = \frac{\{K_p + K_i\}}{s} \tag{6}$$

The Icr equations derived in equation 3 and 4 are used for the derivation of the plant, given by

$$G(s) = \frac{1}{2Ls} + 2R \tag{7}$$

The repetitive controller and the PI controller can be combined in different ways to achieve the desired results. In the proposed model we have combined both the systems as shown in Figure 4.

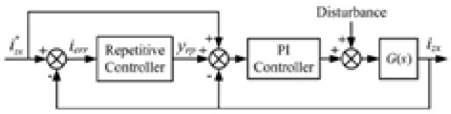

Figure 4. Proposed Repetitive control

IV. SIMULATION RESULTS

The proposed model was simulated in Simulink/Matlab. Tabe II shows the specification of the devices used in the converter.

TABLE II. PARAMETERS OF THE CONVERTER FOR PROPOSED MODEL

Voltage of dc link	240 V
Output voltage amplitude	100 V
Load Resistance	50 ohm
Load inductance	7 mH
Output voltage frequency	50 Hz
Sub modules per arm	17
Inductance of arm	4 mH
Resistance of arm	0.5 Ohm
Sub module capacitance	500 micro farad
Gain of Proportional controller	Kp = 4, Ki = 8
Repetitive controller gain	0.7
Switching frequency	2 kHz

The higher number of levels in the MLCR serve two purposes, i.e. the total harmonic distortion of the system is reduced and the output voltage approaches a sinusoidal waveform. The bode plot of the PI controller is shown in Figure 5.

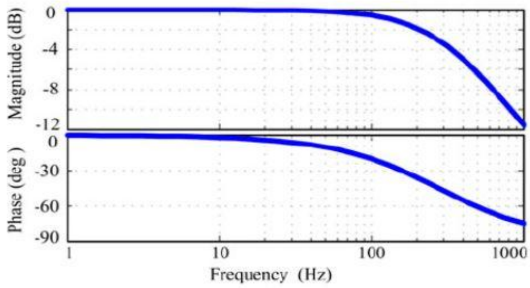

Figure 5. Bode plot of PI Controller

The controller provides unity gain from zero frequency up to the cut off frequency. The frequency is most desirable for the design of the repetitive controller. The cut off frequency of the proportional integral controller needs to be lower than the fundamental frequency in order to remain in the upper portion of the gain curve. From system stability point of view the roots of the controller must be at the origin of unity circle. In the given setup with gain of repetitive controller and PI controller adjusted, the roots lies near to origin as shown in Figure 6.

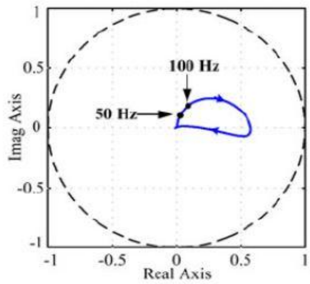

Figure 6. Nyquist Plot of proposed controller

When the system is configured in such a way, it successfully eliminate the even order harmonics from the circulating current. The even order harmonics are shown in Figure 7 without the even harmonics repetitive controller.

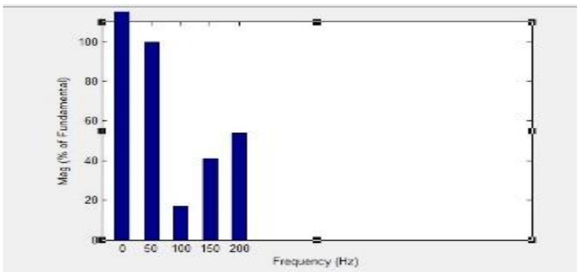

Figure 7. Even order harmonics without proposed controller

The harmonics are very high without the even harmonic repetitive controller. When the controller is inserted in the control loop, the even order harmonics are greatly reduced as shown in Figure 8.

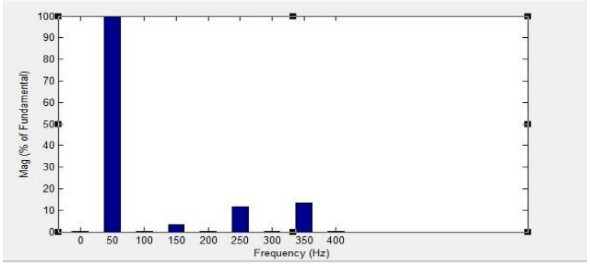

Figure 8. Even order harmonics with the repetitive controller

CONCLUSION

Modular multilevel converters are the prominent candidates for higher power transmission in future. The robustness and flexibility of the modular multilevel converters also make it the prominent candidate for industrial use. The overarching problem of circulating current can be controlled by using repetitive controllers that are easy to implement and offers increased flexibility in their control. The proposed scheme efficiently reduces the circulating current and even order harmonics as can be seen in the results. The effect of the controller on output voltage is also insignificant as the control is very simple and flexible.

REFERENCES

[1] L. A. a. H. P. N. A. Antonopoulos, "On dynamics andvoltage control of the modular MLCR," in 13th Eur. Conf. Power Electron. Appl., , Sep. 8–10, 2009,..

[2] J. P. S. C. R. P. J. Z. a. V. G. A. G. Konstantinou, "Control of CCRs in Modular MLCRs Through Redundant Voltage Levels," IEEE Transactions on Power Electronics, vol. 31, no. 11, pp. 7761-7769, Nov. 2016..

[3] Y. W. a. R. Marquardt, "Novel Control Scheme for the Internal Energies and internal circulating current of Modular multilevel converters," in International Exhibition and Conference for Power Electronics, Intelligent Motion, Renewable, PCIM Europe, 2017.

[4] H. L. Z. W. a. T. W. Y. Ma, "Capacitor voltage balancing control of modular MLCRs with energy storage system by using carrier phase-shifted modulation,," in IEEE Applied Power Electronics Conference and Exposition (APEC), , Tampa, FL,, 2017.

[5] T. J. S. a. R. E. B. J. D. Stringfellow, "A new arm voltage balancing technique for the control of modular multilevel converter," in 41st Annual Conference of the IEEE Industrial Electronics Society, Yokohama, 2015.

[6] J. P. S. C. J. Z. G. K. a. V. G. A. R. Picas, "Optimal injection of harmonics in CCRs of modular MLCRs for capacitor voltage ripple minimization," in IEEE ECCE Asia Downunder, Melbourne, VIC, 2013.

[7] P. W. Z. C. H. Z. Y. L. a. Y. L. Z. Li, "An Inner Current Suppressing Method for Modular MLCRs," IEEE Transactions on Power Electronics, vol. 28, no. 11, pp. 4873-4879, 2003.

[8] T. G. a. U. K. M. B. S. Riar, "Model Predictive Direct Current Control of Modular MLCRs: Modeling, Analysis, and Experimental Evaluation," IEEE Transactions on Power Electronics, vol. 30, no. 1, pp. 431-439, 2015.

[9] A. L. a. R. Marquardt, ""An innovative modular MLCR topology suitable for a wide power range," in IEEE Bologna Power Tech Conference Proceedings, 2003.

[10] Y. C. C. T. J. Y. a. X. Y. B. Chen, "Analysis and Suppression of Circulating Harmonic Currents in a Modular MLCR Considering the Impact of Dead Time," IEEE Transactions on Power Electronics, vol. 30, no. 7, pp. 3542-3552, 2015.

[11] A. A. D. S. K. I. M. V. a. H. P. N. L. Angquist, "Open-Loop Control of Modular MLCRs Using Estimation of Stored Energy," IEEE Transactions on Industry Applications, vol. 47, no. 6, pp. 2516-2524, 2011.

[12] B. S. R. a. U. K. Madawala, "Decoupled Control of Modular MLCRs Using Voltage Correcting Modules,," IEEE Transactions on Power Electronics,, vol. 30, no. 2, pp. 690-698, 2015.

[13] M. A. P. D. A. J. R. E. a. J. R. R. Lizana, "Decoupled Current Model and Control of Modular MLCRs," IEEE Transactions on Industrial Electronics, vol. 62, no. 9, pp. 5382-5392, 2015.

[14] S. L. a. M. D. P. Münch, "Modeling and current control of modular MLCRs considering actuator and sensor delays," in 35th Annual Conference of IEEE Industrial Electronics , Porto, 2009.

[15] Z. K. e. al, "Optimal submodule capacitor sizing for modular MLCRs with common mode voltage injection and CCR control," in IEEE Energy Conversion Congress and Exposition (ECCE), Cincinnati,, 2017.

[16] Y. e. a. Zhou, "Analysis and control of modular MLCRs under unbalanced conditions," IEEE Transactions on Power Delivery , pp. 1986-1995, 2013.

[17] A. L. a. R. Marquardt, "An innovative modular MLCR topology suitable for a wide power rang," in IEEE Bologna Power Tech Conference Proceedings, 2003.

International Journal of Engineering Works
ISSN-p: 2521-2419
ISSN-e: 2409-2770
Vol. 6, Issue 06, PP. 196-201, June 2019
https://www.ijew.io/
https://doi.org/10.34259/ijew.19.606196201

Impact of Urban Infrastructure Development on Power Loss of Solar Photovoltaic Modules

Shah Naveed[1], Saddam Ali[2], Dr.Saim Saher[3]
[1]Research Scholar, [2]Research Associate, [3]Assistant Professor US-Pakistan Centre for Advanced Studies in Energy, University of Engineering and Technology Peshawar, Pakistan,
snaveed1@asu.edu[1], saddam.ali@uetpeshawar.edu.pk[2], s.saher@uetpeshawar.edu.pk[3]
Received: 20 May, Revised: 24 May, Accepted: 02 June

***Abstract*—** Solar photovoltaics pose as a major technology in shifting reliance from non-renewable to renewable energy resources. Soiling is a key issue which is further escalated by dust blowing as a result of road infrastructure development in urban environments. The Peshawar Bus Rapid Transit Corridor (BRT) project provided a chance to carry out this study aimed at corelating scale of infrastructure development with heightened PV losses and formulating ways to cope with the problem. A site offering an urban topography located at a distance of 1.2 km away from the BRT route was identified. The soiling station at this site was operated for one month and the data was processed to identify the prevailing soiling loss trends. The soiling station recorded losses in excess of 20% within the first 2 weeks of operation. It was found that clouds and strong winds had no significant role in retarding the losses. However, frequent rainwater cleaning at one instant reversed the losses back to 0%. It was thus established that cleaning the modules with water on a two week basis during large scale road development works in and around urban areas could keep the losses within a bearable limit.

***Keywords*—** Solar Photovoltaics, Soiling losses in PV, Road infrastructure development, Peshawar Bus Rapid Transit Corridor, Soiling loss mitigation.

I. INTRODUCTION

Public infrastructure development is a significant contributor to economic growth whereas acquiring self-sufficiency and sustainability in energy resources is the key to maintaining the growth [1,2]. The industrial revolution resulted in a sustained and substantial increase of GDP per capita in real terms. However, the unprecedented deployment of fossil fuels it accompanied resulted in dwindling of conventional energy resources and a massive infusion of harmful emissions resulting in global warming and health problems [3]. It is reported that Pakistan on average loses 4-6% of its GDP annually due to insufficiency of adequate infrastructure [4]. Currently, Pakistan ranks 9th in the Belt and Road Infrastructure Development Index and the goal of this research is to contribute towards attaining sustainable growth through minimizing PV losses due to soiling resulting from such fast-paced infrastructure development [5]. The quest for urban infrastructure development has an inherent issue of increasing pollution that results in impacting the performance of solar PV power production adversely. To maintain a sustainable growth, it is needed to minimize these effects by devising effective coping procedures.

Pakistan's energy demand is rapidly increasing because of urbanization and industrialization. Pakistan's primary energy supply in the financial year 2017 was 92.9 MTOE [6]. It consisted of 47.5% of natural gas, 30.5% of oil, and 10.9% of hydel, 9.2% of coal,1.2% nuclear and 0.7% LPG [6]. In the coming fifteen years the demand will increase to 122 MTOE, thus increasing the annual energy import bill to more than US $41 billion compared to the total annual energy import bill of US $7.5 billion in 2008 [7]. To meet this galloping energy demand is a significant challenge for Pakistan and increasing reliance on renewable energy resources is a feasible solution. Reducing any setbacks faced by solar PV due to soiling losses is therefore a key goal.

The 21st century saw initiation of a remarkable research effort into renewable and green energy technologies as a means of mitigating the impending consequences. Studies suggest that renewables could contribute 20 to 50% of energy supplies in the second half of the century. Solar PV is one of the most widely applied technologies for power generation. The average power available at the earth's surface in the form of solar radiation is more than 1500 times the entire global power demand [8]. Solar technologies can be classified into solar thermal and solar electric or PV systems. PV systems make use of photo-electric effect to harvest energy from a photon to drive DC electric charges around the circuit. Presently almost 87% of the PV cells are fabricated using Silicon [9]. The power output and efficiency of PV systems are key to determining cost per watt. Greater the output lesser will be the cost. Among the factors impacting the yield of PV modules, the irradiance fluctuation is the most pertinent to the overall power output [10]. PV modules have a capacity factor of 15 to 25% depending on the location of installation. The downtime can be further exacerbated by the losses in irradiance due to shading caused in most powerplants by soil accumulation on the modules as dust particles sit on them [11].

Transportation development projects in urban settings are to reduce congestion, excessive fuel consumption resulting from traffic jams, and travel time as well as to increase connectivity, safety, environmental conservation, and economic activity. New road development projects may have many advantages in terms of boosting social and economic growth by increasing mobility and enhancing services availability. However, letting the unintended consequences go unnoticed would be a serious misrepresentation of facts. The immense rapid urbanization and pressure on urban transport sometime result in conception of road infrastructure development projects in urban centres without prior due diligence to all the factor that could generate a negative result. Our focus here is on investigating the performance degradation of PV modules in the immediate vicinity of these project sites because of the increased soiling losses resulting from accumulation of dust particles on PV panels after emanating from these sites.

The soiling problem in context of PV module performance studies arises from shading due to factors such as dust accumulation, snow, and bird droppings on the module surface. The most common and dominating among these factors is dust accumulation. Dust is a generic term for particulate matter with a diameter of less than 500 µm or 0.5 nm [12]. The degree of dust accumulation depends on factors such as climatic, location-based meteorological, environmental, and nearby ongoing construction scale conditions. The importance of soiling losses investigation and mitigation is derived from the understanding that around 75% of world population resides in countries that constitute the EPIA's designated 66-country sunbelt as shown in figure 1 [13]. Majority of these regions are widely prone to the existence of desert areas and have significant pollution indices. Moreover, the geographically dictated need to configure the PV modules at flat tilt angles in these areas results in robust soiling impact on PV module performance [14].

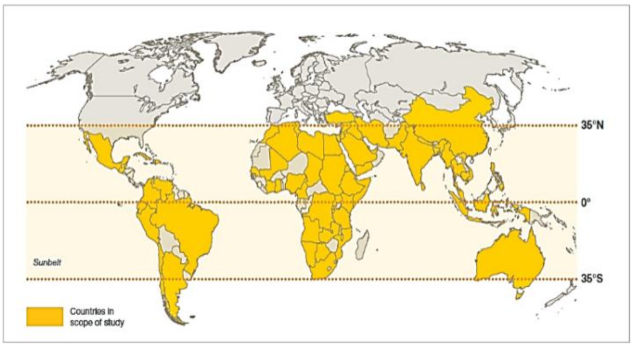

Figure 1. Focus countries of the Sunbelt; EPIA [13]

This study focused on the impact of increased dust accumulation resulting from the construction phase of the Peshawar Bus Rapid Transit Project (BRT) on PV performance. The BRT project is aimed at providing the local population with a sustainable urban transport system. The 26 km long integrated bus transit corridor system once operational will directly benefit 0.5 million people in terms of shorter travel times, lower vehicle operating costs, better air quality, and environmental conservation through reduced carbon emissions. A complete restructuring of the corridor with the provision of BRT dedicated lanes, 31 stations, 2 depots, mixed traffic lanes, sidewalks, and a proper drainage system are some of the major components that required immense excavation, construction, and remodeling works [15]. Such large-scale infrastructure development works always come with the infusion of huge concentrations of dust particles into the air for an extended period of time. The BRT route has been divided into three reaches and Reach 3 which stretches from Aman Chowk to Hayatabad is particularly affected by astonishing levels of dust blowing in the area. The existing PV installations in the vicinity of the route are affected adversely by unimaginable levels of soiling. This state of affairs prompted the study to probe into the soiling losses caused by such large-scale infrastructure development in the area.

II. Methodology

A. Site identification:

A portion of area along the BRT Reach 3 was identified that could provide the opportunity to investigate the impact of increased soiling on PV performance of the modules installed in a nearby urban area as shown in figure 2. The results from the soiling station output voltage data were then utilized to find out what mitigation approaches can be employed to curb the soiling losses in the face of similar scale urban infrastructure development activities.

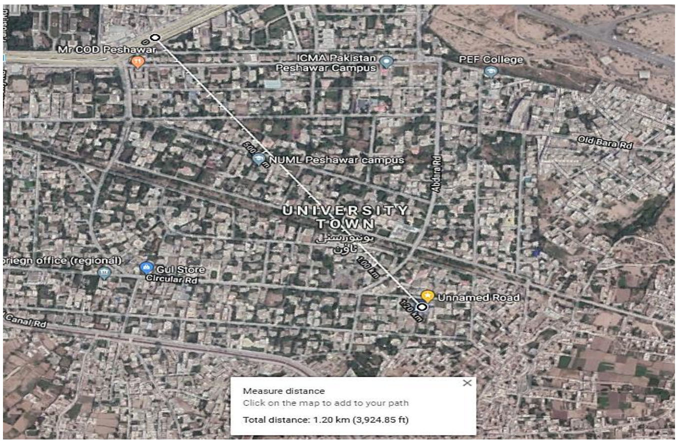

Figure 2. Soiling station installation site in urban area 1.2km away from the BRT route

One of the two identical half cells of the soiling station at the site was cleaned manually at 12pm every day and the other was left uncleaned for the whole month. The module voltage readings were compiled for the month of August 2018 and employed in subsequent analyses. The soiling loss factor (SLF) was calculated for the site at noon every day and the entire data resulted in a total of 31 SLF values for the course of the study. The SLF values along with rain gauge readings helped in understanding the observed trends.

B. Data Collection and Analysis

The soiling station was operated for the time span of the study. Transparent hatch was employed for the cleaned modules and was opened manually at 12pm every day to take readings. The time for taking readings was 2-3 minutes during which the hatch stayed open and the maximum window for human error was kept at 5 minutes with a ± 2.5 minute uncertainty. The reason for not automating the hatch-opening process was to avoid any unwanted deviations and discrepancies in the form of system break down and the technical assistance mandatory otherwise and cost incurred in the event of a fault was also a reason for carrying out the operation manually.

C. Data Collection Period

The data collection period was decided to be from August 1, 2018 to August 31, 2018. This period of time provided the opportunity to investigate soiling losses with the onset of vigorous construction activities undertaken around that month. This month also provided the opportunity to investigate any effect of rainwater cleaning during the monsoon season observed throughout the first 2 weeks of the month. Data was compiled daily from 6am to 7pm and the most important data points were those at noon.

D. Data Plots

The data thus obtained was plotted subsequently. Five data plotting intervals were employed for the site in such a manner that the first interval spanned the first three days of the month and the remaining four intervals spanned seven days each in an orderly manner. These plots helped tremendously in understanding the effects of meteorological phenomena such as clouds, rain, and storm on the voltage output of the PV half cells used. The peak values at noon for both the cleaned and soiled panels were used to calculate the soiling loss factor for the entire period on daily basis.

E. Soiling Loss Factor Calculation

The outdoor soiling data from the soiling station obtained between August 1, 2018 and August 31, 2018 was processed to calculate the daily Soiling Loss Factor. The output voltage from both the soiled and the clean half cells was used in the calculation and the August 1 data was utilized in SLF normalization. The normalized SLF values were then used to calculate daily percentage soiling losses at the site. Finally, the SLF values were compared along with rain data against time to reveal any important trends and findings.

III. Results and Discussion

The output voltage versus time graphs for both the soiled and clean half cells were plotted as shown in figures 3-7, and the peak voltage values of the individual plots were utilized to determine the soiling loss factor (SLF) values for each day. The first peak value obtained for the soiled panel was around 0.0843V and that for the clean module was 0.0921V on August 1. These values were used to calculate SLF for day 1 which was later used for normalization of data from the station and calculating normalized SLF values for the subsequent days throughout the study.

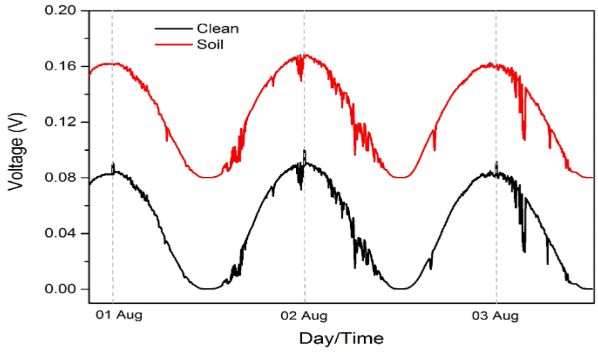

Figure 3. Output of clean and soiled panels during 1-3 August 2018

The offset of 0.08 V was added to the soiled panel data to plot the soiled panel voltage values over the clean panel voltage values in the same graph. On the noon of August 2, the peak value for the soiled module was 0.0782V and that for the cleaned module was 0.09V which resulted in the normalized SLF to drop to 0.95 from 1. This trend continued throughout the study with the SLF values dropping with time as evident from the data recorded for the first week as given in table 1 and was challenged only in the event of adequate rain.

TABLE I. SLF VALUES AND PERCENTAGE SOILING LOSSES DURING THE FIRST WEEK

Date	**1-Aug**	**2-Aug**	**3-Aug**	**4-Aug**	**5-Aug**	**6-Aug**	**7-Aug**
S (Soiled Module)	0.08	0.08	0.07	0.07	0.07	0.07	0.07
C (Clean Module)	0.09	0.09	0.09	0.09	0.09	0.09	0.09
S/C	0.92	0.87	0.82	0.84	0.80	0.78	0.77
Sf/Cf (First day)	0.92	0.92	0.92	0.92	0.92	0.92	0.92
SLF (Normalized)	**1**	**0.95**	**0.9**	**0.92**	**0.87**	**0.85**	**0.84**
% Soiling losses	0	5	10	8	13	15	16

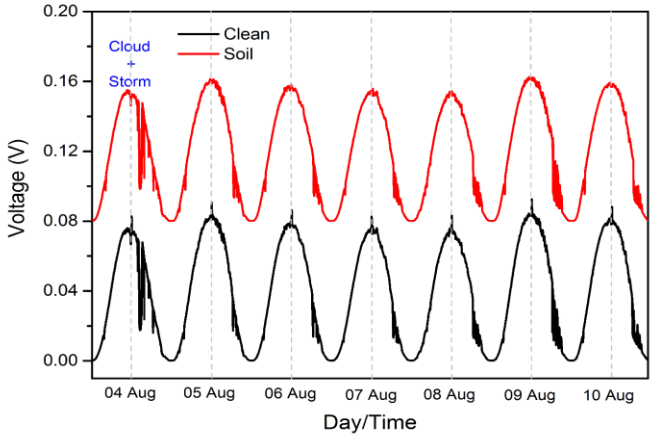

Figure 4. Output of clean and soiled panels during 4-10 August 2018

On August 4 the region witnessed clouds and storm as specified in figure 4. The soiled panel performed slightly better than it had the previous day. The reason behind this minor recovery is the storm which may have taken away the loosely adherent dust particles from the panel surface. Nevertheless, the previous trend continued and the SLF values kept decreasing during the subsequent days. This showed that the events of clouds and storm did not have any significant effect on the relative performance of the soiled and the clean solar PV panels. In other words, clouds and storm did not affect soiling losses to a significant extent. The small betterment in the soiled panel performance can only be due to the action of the winds alone since clouds alone do not bring about any such change. In the presence of clouds, both the soiled and the clean panels received the same number of photons. The reduced irradiance levels under cloud cover do not affect the SLF values since it in itself is a ratio of the clean and soiled panels outputs operating under the same conditions of irradiance.

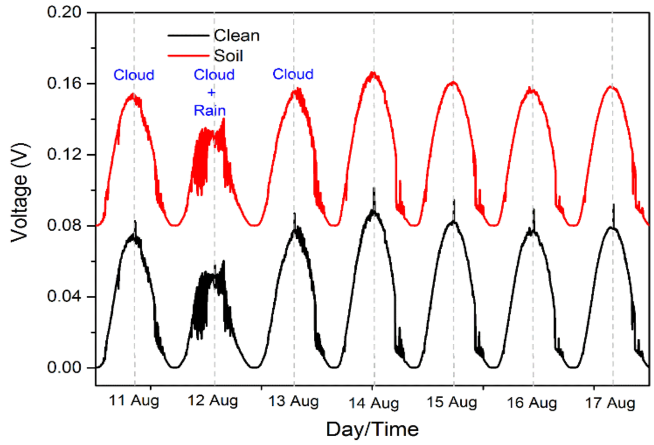

Figure 5. Output of clean and soiled panels during 11-17 August 2018

There were again clouds on August 11 but the peak values for both the panels did not deviate from the previous trend. However, the event of rain on August 12 resulted in a notable effect on the soiled PV panel performance as evident from the depressions in both the respective curves for that day in figure 5. The rainwater cleaning of the soiled PV panel resulted in enhanced performance and regaining the SLF value near to 1.

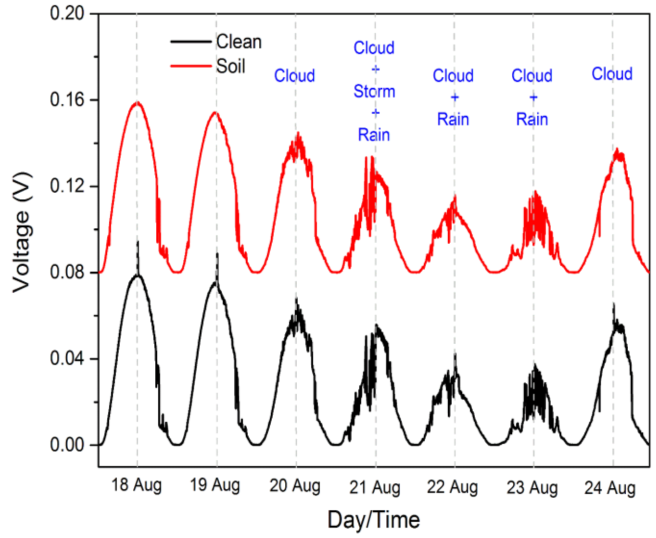

Figure 6. Output of clean and soiled panels during 18-24 August 2018

In the following 8 days until 21 August there was no rain and the declining SLF trend was back in action as evident from figure 6. The output of the soiled module kept decreasing and the gap in the peak values of the clean and soiled modules kept on increasing. This resulted in gradual increase in percentage soiling losses. Even the presence of clouds on 20 August did not impact this declining trend in the SLF values as described earlier.

The last day of the third week observed clouds and rain accompanied by strong winds. This time the rain gauge measurement showed 3 mm of rain on 21 August and the following two days having 4 mm rainfall each. The persistent cloud cover present at noon from 21-23 August resulted in reduced PV performance for both the soiled and cleaned panels. However, the relative difference in the performance of the cleaned and the soiled modules was reduced remarkably. The soiled panel surface was relieved of the accumulated dust by repeated rainfall until it was completely free of the particulate matter building up for the previous three weeks of the study. This in turn resulted in increasing of the SLF value. This time the base line of no soiling loss was achieved on August 24 and both the soiled and the clean panels recorded the same ratio of peak values of output voltage as observed on day 1. The percentage soiling losses were thus back to 0%.

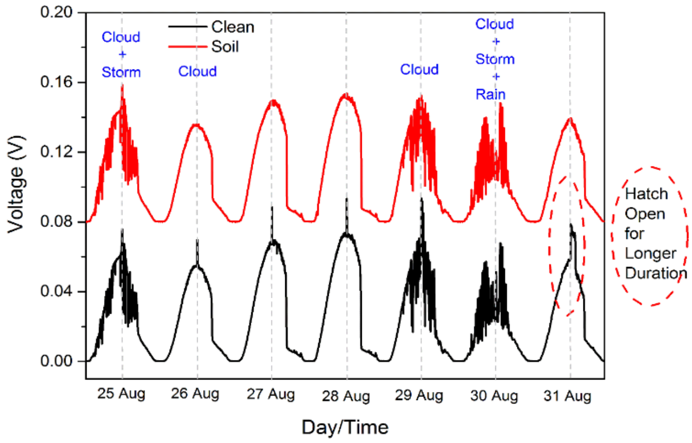

Figure 7. Output of clean and soiled panels during 25-31 August 2018

There were clouds on 24 August and both clouds and strong winds on 25 August, but the event of rain did not take place as specified in figures 6 and 7. The SLF values started declining with the passage of time and soiling losses became apparent on 28 and 29 August. The next day it rained for 3 mm and it was enough to easily reverse the SFL declining trend. This made it obvious that the rain frequency had a huge impact towards reducing the soiling losses by natural cleaning of the soiled panel. Also, the clean module hatch remained open beyond the stated error window of 5 minutes on the final day of the study for some unavoidable reasons and the resulting plot shape strayed to some extent as can be seen in figure 7.

TABLE II. THE EFFECT OF RAIN ON SLF VALUES AND PERCENTAGE SOILING LOSSES

Date	Rain (mm)	SLF	% Soiling loss
11-Aug-18		0.8	20
12-Aug-18	3	0.97	3
13-Aug-18		0.96	4
20-Aug-18		0.82	18
21-Aug-18	2	0.96	4
22-Aug-18	4	0.98	2
23-Aug-18	4	1	0
24-Aug-18		0.97	3
29-Aug-18		0.85	15
30-Aug-18	3	0.96	4
31-Aug-18		0.94	6

By looking at the values in table 2, recorded for the day before, during, and the day after an event of rain, it becomes obvious that rainwater cleaning of the modules contributed significantly towards decreasing soiling losses to some extent. It is notable that soiling losses dropped from 20% to just 3% on 12 August as a result of only 3 mm of rainwater cleaning effect. Moreover, three consecutive events of rain on 21, 22, and 23 August took the SLF back up to 1 which means all the soiling losses were virtually reversed to 0%. Finally the 3mm rain on August 30 had an impact in the same fashion which resulted in soiling losses to get reduced from 15% to 4%. The percentage SLF values and the corresponding percentage soiling losses at noon every day for the entire study period are represented in figure 8.

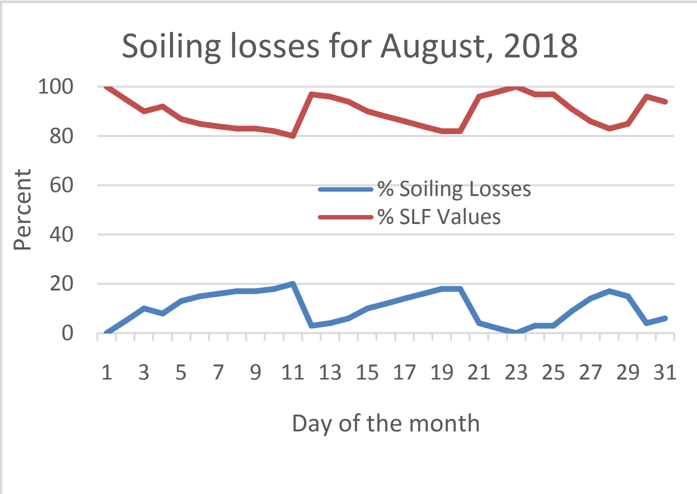

Figure 8. Percentage SLF values and the corresponding percentage soiling losses for the entire study period

CONCUSLION

The findings of the study showed that the site under consideration would have likely faced more than 20% soiling losses after the 12th day of installation, if there had been no rain. It is thus easy to assume that any urban PV installations experiencing road infrastructure development activity comparable in scale to the Peshawar BRT might easily experience soiling losses in excess of 20% towards the end of every two weeks operation cycle beginning with the cleaning of the panel surface. It therefore becomes necessary to clean the modules at least every fortnightly. The data showed that urban areas with low altitude PV installations reveal a continuous increase in soiling losses over time thus in case of no rain the cleaning of solar PV with water has to be scheduled at least every 2 weeks.

In conclusion, the soiling data approaching the 20% maximum soiling loss baseline for the present study within the first 2 weeks of installation is a stark indicator that such large-scale urban infrastructure development activities have a negative impact on solar PV performance. Hence, procedures such as dust control and other environmental protection safeguards must be followed in conjunction with optimal site selection for future PV plants installations in urban areas.

ACKNOWLEDGEMENT

The author is thankful for the funding provided for this study by the United States Agency for International Development (USAID) through the USPCAS-E, UET Peshawar. Gratitude also goes to Dr. Saim Saher for his help and guidance throughout this study.

REFERENCES

[1] Tanveer A, Manan N., “Impact of Infrastructure on Economic Growth of Pakistan.” Journal of Economic Research,Edition 1, 2016.

[2] B. Srinivasu, P. Srinivasa Rao, “Infrastructure Development and Economic growth: Prospects and Perspective”. Journal of Business Management & Social Sciences Research, Vol. 2, No. 1, 2013.

[3] P. Vries, Encyclopaedia of the Modern World, Vol. 4. Oxford University Press, 2008, pp. 158-161.

[4] State Bank of Pakistan, "The Pakistan Infrastructure Report", State Bank of Pakistan Infrastructure Task Force, 2018.

[5] The News International, "Pakistan ranked 9th in infrastructure development index", 2017.

[6] Chaudhry, M.A., Raza, R. and Hayat, S.A., 2009. Renewable energy technologies in Pakistan: prospects and challenges. Renewable and Sustainable Energy Reviews, 13(6-7), pp.1657-1662.

[7] International Energy Agency (IEA), Global Energy & CO2 Status Report (2017).

[8] J. Goldemberg et al., “World energy assessment: Energy and the Challenge of Sustainability”. New York, NY: United Nations Development Programme, 2000, p. 239.

[9] Module 7, Renewable energy technologies, Sustainable energy regulation and policymaking for Africa - TRAINING MANUAL, 2018.

[10] S. Canada, “Quality Assurance: Impacts of Soiling on Utility Scale PV System Performance”. SolarPro Magazine no. 6.3, pp. 14-20, 2013.

[11] K. Menoufi, “Dust accumulation on the surface of Photovoltaic Panels: Introducing the Photovoltaic Soiling Index (PVSI)”, MDPI Sustainability Journal, 2017.

[12] T. Sarver, A. Al-Qaraghuli and L. Kazmerski, "A comprehensive review of the impact of dust on the use of solar energy: History, investigations, results, literature, and mitigation approaches", Renewable and Sustainable Energy Reviews, vol. 22, pp. 698-733, 2013.

[13] European Photovoltaic Industry Association, "Unlocking the Sunbelt Potential of Photovoltaics", 2010.

[14] T. Weber, N. Ferreti, F. Schenider, A. Janker, M. Trawney and J. Berghold, "Impact and Consequences of soiling and cleaning of PV modules", NREL Photovoltaic Reliability Workshop (PVMRW), Denver, 2015.

[15] Peshawar Development Authority, "LARP Implementation Monthly Progress Report May 2018", Government of Khyber Pakhtunkhwa, 2018.

Shah Naveed: The author was born in Pakistan in the year 1992. He holds a bachelors degree in Mechanical Engineering from University of Engineering and Technology Peshawar. He also has completed a certificate course in Technology Entrereneurship from Arizona State University. The author cherishes his experience working at the Engineering Research Centre and the Macro Technology Works at the ASU, USA. Currently, he is pursuing masters degree in Materials for Energy Storage and Conversion at the US-Pakistan Centre for Advanced Studies in Energy, UET Peshawar, Pakistan.

IJEW 国际工程期刊 International Journal of Engineering Works انجینیرنگ کاموں کا بین الاقوامی جرنل

International Journal of Engineering Works
ISSN-p: 2521-2419
ISSN-e: 2409-2770
Vol. 6, Issue 06, PP. 202-207, June 2019
https://www.ijew.io/
https://doi.org/10.34259/ijew.19.606202207

Production of Liquid and Solid Fuel by the Technique of Microwave Pyrolysis of Scrap Tires and its Analysis

Kaleemullah[1], Ben Haoxi[2]*, Zhihong Wu[3]
[1,2,3]Key Laboratory of Energy Thermal Conversion and Control of Ministry of Education, School of Energy and Environment, Southeast University, Nanjing, China Nanjing, China
kaleemullahkatpar45@gmail.com[1], benhaoxi@gmail.com[2], 18915408402@163.com[3]
corresponding author*: benhaoxi@gmail.com
Received: 27 April, Revised: 21 May, Accepted: 12 June

Abstract— The discussion in this paper is about the possible use of microwave pyrolysis technique as an energy-capable alternative to present heating techniques in biomass waste processing and treatment for renewable energy system. The wreck tires have relevant disposal or recycling issues under environment and financial and sustainable modes. These techniques can be a challenging for manufacturing and intellectual learning researches. In this competition, pyrolysis is a latest, strong substitute to the reprocessing of useless tires, until unless it will be possible to produce value adding results. In any case, upgrades in warmth exchange innovation are fundamental to enhance the plenitude of the procedure. Here we are describing the usage of microwave radiation (MW) as one of the most beneficial heating skills for pyrolysis. Whereas, there are different techniques for the process of the waste tires in previous era, such as crushing to get crumbs and rubber powder, burning them in cement furnaces for thermal power generation, re-stepping, decomposition by chemicals Heat degradation of rubber materials. The important and valuable chemicals in commercial use are derived from oils which are obtained from pyrolysis process by subjecting the pyrolytic oils to a fraction distillation at a temperature of about 207 ° C (under atmospheric) pressure for the product of at least one commercially valuable Chemical to isolate at least one commercially valuable chemical. Some of the selected chemicals from the group, consisting of paraffin, naphenes, olefins and flavorings. Particularly valuable chemicals that can be extracted from ripe pyrolytic oils are benzene, toluene, xylene, styrene and lime dl. The distillation fraction, which boils above 204 ° C, can be used as an extension oil in the production of various rubber and plastic parts. An improved process for producing the carbon black by microwave pyrolysis (MWP) of used rubber tires is also revealed. The recovered products which have high commercial value indicates advantage over traditional, more destructive disposal methods, and it also advice the very great capability for measuring the process and feedback to the commercial as well as industrial level.

Keywords— Pyrolysis, Microwave Heating, Pyrolytic Oil, Biomass, Renewable Energy, waste Tires. Rubber.

I. Introduction

Pyrolysis is a process that has an vital prospective within the biomass refinery so that it can convert Bearable, by heating the lignocellulosic biomass raw material between 400° C to 600°C or more, supplying fuel and chemical substances in the absence of oxygen[1, 2]. The natural lower thermal conductivity of biomass means that conduction is the rate-determining step, and heating times can be of the order of several minutes[3].It is imperative that we use appropriate technologies for the upgrading of resources from unconventional sources such as waste to alleviate the energy crisis and slow environmental degradation, which, in turn, will be the percentage of buried Reduce waste[4]. The term “pyrolysis” can be explained as a thermal degradation while oxygen is not present which alters a raw material into various reactive intermediate products such as solid (char), liquid (heavy molecular weight) and gaseous products (light molecular weight gases) [5]. The power conversion of the waste tires with pyrolysis has been tested in step with the working conditions parametrically [6].

The understanding of the pyrolysis process is a complicated one since many factors have to be considered, such as raw material composition and experimental conditions. In terms of its physical form (structural arrangements, thermal conductivity and specific heat) and chemical characteristics (organic and inorganic composition), the proficiency of MP procedures depends enormously on the idea of the material being prepared. Therefore, not all materials present a similar dielectric conduct, and along these lines, not all materials are also heated by microwaves[7]. While the period of the MP, it is necessary to accentuate that not only the receptor will captivate microwave energy to yield heat; the solid excess formed in the process also donates to the concluding pyrolysis temperature. Microwave (MW) is a standout amongst the utmost encouraging heating skills for pyrolysis because of its capacity of warming rapidly and legitimately any MW engrossing material Polymers don't be able to assimilate MW and transform them into warmth.

The aim of this chapter is to emphasize the principles of MP and to show recent research on the application of this technology to waste treatment. As an introduction to the topic, a brief background on the pyrolysis process and the fundamentals of microwave irradiation as an energy source are presented.

A. *Essential features of pyrolysis*

- Very high heating and heat transfer rates, which require a finely ground feed.
- Deliberately controlled response temperature of around 600C in the vapor stage
- Stay time of pyrolysis vapors in the reactor less than 1 sec
- Extinguishing (fast cooling) of the pyrolysis vapors to give the bio-oil item

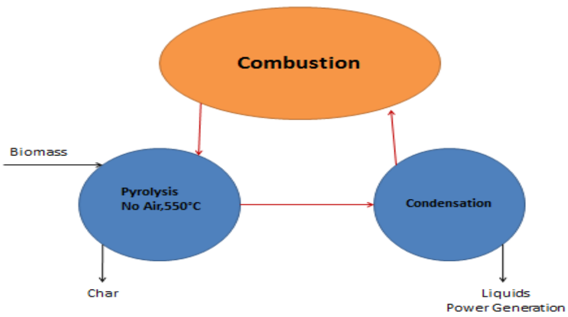

Figure 1. Biomass Liquefaction via Pyrolysis

B. *Sufficient level MW Pyrolysis*

The pyrolysis can be relatively small and untraceable, which lowers the cost of transporting and handling energy resources from biomass. Heat transfer has a critical area because the process is compromised and a sufficient level of heat transfer is provided to meet the heat demand of the process. Biomass pyrolysis offers an adaptable and alluring method for changing over natural issue into vitality items which can be effectively utilized for the generation of warmth, power and synthetic substances.

A wide scope of biomass feedstocks can be utilized in pyrolysis forms[8]. The pyrolysis procedure is subject to the dampness substance of the feedstock, which should to be about 10%. At high dampness substance, large amounts of water are delivered and at lower levels there is a hazard that the procedure just creates dust rather than oil.. High-dampness squander streams, for example, slime and meat handling squanders, require drying before exposing to pyrolysis.

C. *Pyrolysis Process*

It is the thermal transformation of raw resources just like fuel and wastes in a closed system, without delivering extra external components in particular oxygen the presence of which modifies the alignment of the acquired product. The pyrolysis is one of the secondary fuel conversion procedures; since in this method we can notice the conversion of one fuel form into another generally the other form is not so difficult to work with. After the pyrolysis process is concerned to the solid energy, it is called “gasification”, in the situation of liquid or gas fuels “cracking”.

In exercise the methods of thermal conduct of waste frequently run by a small quantity of the air. Ultimately this leads to a fractional gasification. It can be presumed that pyrolysis arises in the interior sector of the bed. These methods are habitually called as “quasi-pyrolysis”. Below are the three dissimilar substrates that can be positively used in a method of pyrolysis are shortly defined.

D. *Types of Pyrolysis*

Pyrolysis can also be based on the environment called oxidative pyrolysis, hydro-pyrolysis, vapor pyrolysis, catalytic pyrolysis and vacuum pyrolysis, as well as according to the heating system such as microwave or plasma pyrolysis. Other reactive types just like the AR and the rotary kon (mostly it is used for the construction of liquid, because of the large heating rate and the steam siding less period), can similarly be used for quick pyrolysis.

E. *Tire composition*

Tires are made of rubber (60–65 wt%), carbon black (CB) (25–35 wt%) and the rest consists of accelerators and fillers, which are added during the manufacturing process[10]. The rubbery materials are present in the form of CxHy with some fibrous materials and they are considered thermoset polymers. Vehicle tires (both passenger and truck) are mainly a blend of natural (NR) and synthetic rubber (SR) such as butyl rubber (BR) and styrene–butadiene copolymer (SBR). The NR comes from the Hevea tree, whilst the SR is generally derived from petroleum- based products. NR has unique elastic properties and it is an essential element of a tire[11]. Rubber comprises elastomeric polymers characterized by the presence of a network structure that can be temporarily deformed when subjected to external forces. According to the International Rubber Study Group 24.37 million tons of rubbers were produced in 2010. Of this amount, 10.38 million tons (42%) were NR and the remaining 13.99 million tons (58%) were SR. The materials of modern pneumatic tires are synthetic rubber, natural rubber, fabric and wire, along with carbon black and other chemical compounds. They consist of a tread and a body. The tread provides traction while the body provides containment for a quantity of compressed air. Before rubber was developed, the first versions of tires were simply bands of metal fitted around wooden wheels to prevent wear and tear. Early rubber tires were solid (not pneumatic). Pneumatic tires are used on many types of vehicles, including cars, bicycles, motorcycles, buses, trucks, heavy equipment, and aircraft.[11] Metal tires are still used on locomotives and railcars, and solid rubber (or other polymer) tires are still used in various non-automotive applications, such as some casters, carts, lawnmowers, and wheelbarrows.

F. *Pyrolysis technologies with respect to different Experimental materials*

1) *Materials*

The crude material is a blend of light obligation vehicles non-destroyed waste tires with piece sizes differing from 2 to 10 cm. Prior to investigation, the tire pieces were cleaned and dried at room temperature in a well-ventilated zone.

2) Analyses of Tires

The fundamental examination has taken place on a C, H, N, S-O Analyzer (Flash EA 1112 Series), with detection perimeter of 0.05%wt, however for higher heating rate (HHV) measurements a PARR 6200 Calorimeter was used.

3) Laboratory Scale Reactor Experiments

The pyrolysis trials were performed at500°C by fluctuating the warming rate inside the scope of 5–15°C/min. Before each test the reactor was inserted with nitrogen. Utilizing a gas-chromatograph with warm conductivity indicator (TCD/GC), the gas has been dissected at each 20min amid the warm scope of tires debasement. The analysis shows that the gases are mainly formed starting from 400°C and the major mixtures are H2 (25–29%vol) and CH4 (22–25%vol). The strong and condensable items yields are resolved and the gas yield is determined by distinction[13].

G. *Previous Studies and researches on tire pyrolysis*

Henne and Midgley considered the damaging refining of elastic in a progression of 18 papers amid the late 1920s and mid-1930s. They explored that isoprene and dependent were the commanding results of the elastic refining. From a mechanical perspective, a few creators called attention to that pyrolysis of WT was first endeavored by the US Bureau of Mines in a joint effort with the Firestone Company in the US in the mid-1970s. A 10 tire for each day lab unit was created with a generation of 3.9 l of fluid. 3.1 kg of roast, 1.3 kg of gas and 1 kg of steel and scorch per tire pyrolysed.

From a modern perspective, a few creators called attention to that pyrolysis of scrap tires was first endeavored by the US Bureau of Mines as a team with the Firestone Company in the US in the mid-1970s. A 10 tire for each day research facility unit was created with a generation of 3.9 l of fluid. 3.3 kg of char.

II. EXPERIMENTS, PROCESS AND RESULTS

The examples are squandering tire powders which are broadly accessible in China. Table I gives the estimated and ultimate investigation. The warming rate in the test are 10°C/min, 20°C/min and 40°C/min individually. The starting temperature is room temperature and the last temperature is set to be 600°C or 800°C. The tire is warmed within the sight of nitrogen gas.

Table I: Immediate and Decisive examination

Immediate examination				Qb,ad
Mad%	Aad%	Vad%	FCad%	(J/g)
0.81	7.42	64.69	27.17	39565
Decisive Examination				
Cad%	Had%	Nad%	Sad%	Oad%
81.84	6.06	1.79	1.64	0.48

A. *Illustration of pyrolysis*

The pyrolysis of discarded tire is explained as the next process:

$$a(s)\rightarrow b(s)+c(g) \tag{1}$$

However s is solid and is gas. The above equation is summarized by that the discarded tire, “a” converted into a solid which is represented as “b”, and a gas which is represented as “c” during the pyrolysis. The gassy section, c, was separated by nitrogen gas while the analysis was going on, which avoid the changeable response took place and confirmed the matching of permanent response with the research.

The weight loss rate can be distinct as:

$$\frac{d\alpha}{dt}\ Kf(= kf(\alpha) \tag{2}$$

where α is the proportion of weight cost at time t and is distinct as:

$$\alpha=W0-\frac{Wt}{Wo}-W\infty \tag{3}$$

where W0 is the early load, Wt is the weight at time t and W∞ is the weight when the reaction stops. Where as the rate constant k has a closely proportional to the temperature T and according to the Arrhenius's law it can be formulated as:

$$k=A\exp(-\frac{E}{RT}) \tag{4}$$

whereas

A = factor of frequency

E = activation energy

R i= gas constant

T = total temperature

The heating rate β was set as unceasing in the experimentation, β=dTdt.

Familiarizing β and equation (4) into equation (1) yields:

$$\frac{d\alpha}{f(\alpha)}=\frac{A}{\beta}\cdot\exp(-\frac{E}{RT})dT \tag{5}$$

Differential and integral are the two procedures to answer the equation.

The differential technique uses the DTG data right to define f(α), where as the integral process links the integration of equation (5) and the TG data to resolve f(α).

Define G(α)=∫α0dαf(α) and yields:

$$G(\alpha)=A\beta\int_{T_0}^{T}\exp\left(-\frac{E}{RT}\right)dT \tag{6}$$

While T_0 = initial temperature of pyrolysis. Integrate equation (6) among 0～αand 0～T correspondingly described as:

$$\int_0^\alpha \frac{d\alpha}{f\alpha}=G(\alpha)=\frac{A}{\beta}\int_{T0}^{T}\exp\left(-\frac{E}{RT}\right)dT \tag{7}$$

Coats and Redfern [15] derived the integration of the right hand side of equation (7)

According to temperature calculation method [16] and we get:

While $\ln\left[\frac{G(\alpha)}{T^2}\right]$ is related to $\frac{1}{T}$ with the slope $-\frac{E}{RT}$ and intercept, $\ln\frac{AR}{\beta E}$

The relating connection coefficient was taken as a list for assurance of sensible component work. The gas-strong response instrument work with a most extreme connection coefficient was chosen as the component work for tire pyrolysis. The initiation vitality E and the recurrence factor A were then determined by the direct line work.

B. Process

The process of pyrolysis of excess tire experiences numerous phases at a given heating rate. Figure 2 and Figure 3 clearly describes the thermogravimetric and the resulting thermogravimetry shape parallel to the method of pyrolysis of the excess tire fine particles, illuminating its quantity loss fraction and mass loss rate vs. temperatures[14]. The heating rate is set to be β=10,20 and 40°C/min and the tire precipitate size is 60,200 and 200 mesh. At the point when the temperature expanded from room temperature to under 200°C, weight reduction was watched. The marginally variety of the mass misfortune at the beginning period of the TG profile was because of the arrival of the dampness in the tire From that point forward, the TG bend kept level until about 200°C. At the point when the temperature surpassed about 200°C, mass misfortune started, which was because of the warm deterioration of the blend of oil, plastifiers and different added substances, At the point when the temperature expanded from 200°C to about 400°C, the nonstop contribution of vitality activated critical tire pyrolysis responses. Therefore, a greatest mass misfortune rate top was seen at 381.3°C on the DTG bend for 100-work tire powder at warming rate of 10°C/min, as appeared by Fig 2. In the meantime, unpredictable parts started to dissipate which brought about a weight reduction of around 15% on the TG bend. At the point when temperature expanded from 400°C to 480°C, concentrated vanishing of the volatiles occurred and created a high weight reduction with a most extreme rate at 453.5°C on the DTG bend.

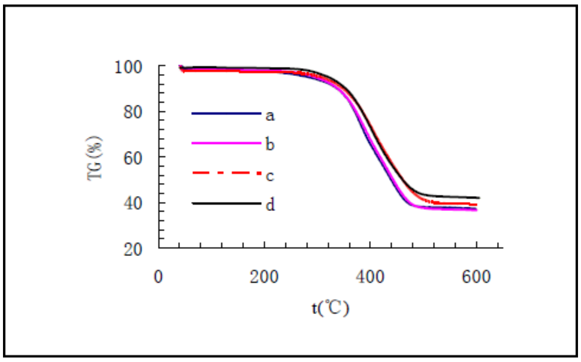

Figure 2. TG bend for 100 lattice tire dust at dissimilar heating amount (a: 10 'C/m, b: 20°C/m, c:40°C/m, d: 60 mesh, 40°C/m)

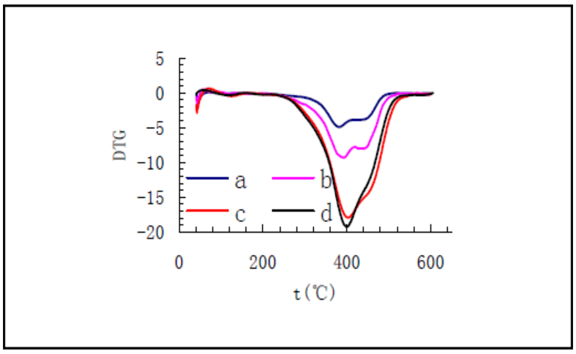

Figure 3. DTG bend for 100 mesh tire dust at unlike heating rate (a: 10°C/m, :20°C/m, c:40°C/mn, d: 60 mesh, 40°C/m)

These are the main steps of the tire pyrolysis method, which result as the arrival of unstable and dampness at lower temperature and the warm disintegration of common elastic and the decay of polybutadiene and polybutadiene-styrene elastic at higher temperature, individually.

C. Results

The publications relating to the pyrolysis of used tyres in terms of the reactors used by their authors, the efficiency of these reactors and the proportion of pyrolytic products obtained: liquid, gas and solid residue, mainly Oil or charcoal.

The present examination the TG aftereffects of 60 work tire powder at a warming rate of β=10∘C/min to demonstrate the weight reduction rate work, f(α). The examination was performed under states of low warming rate and little measure of test, along these lines the impact of warmth exchange and dissemination could be overlooked. The test information in the fundamental scope of 0.1⩽ α ⩽0.9 was utilized to figure model. Where as α <0.1 or α >0.9, the proportion of sign to clamor of the gadget was exceptionally little and the dependability of the test information diminished. While, at early process and conclusion of the pyrolysis, the response has much contrast with the primary response. At the point when pyrolysis temperature is less and higher than 385.3°C, it was named the low and high temperature organize separately. Moreover the weight reduction of tire pyrolysis was separated into a low temperature organize and a high temperature arrange by the point where the incline of the TG bend changed.

D. Some Results and discussion from previous experiments conducted by different institutes

1) The Reaction of MW on tire chips

The harmful reaction of MW radiation on the tire chips is reported in Figure 4. The pictures describe the progressive decomposition of tires to carbon particles partially coated with polymeric matrix and finally carbon particles only, when all surrounding organic molecules were pyrolyzed[15]. The presence of residual polymer or not fully pyrolyzed matrix was confirmed by FTIR (Fig. 4b). These pictures describe the technical availability to pyrolyze the whole tire without any previous treatments.

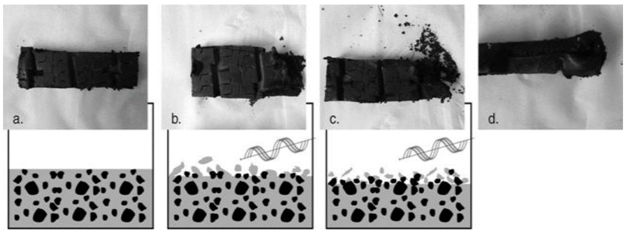

Figure 4. Tire chip when dissimilar MW irradiation period: (a) Tire piece effected (b) Tire piece effected after 60sec of irritation, (c) Tire piece effected after 90sec of irritation, it flakes if held, (d) Swell influence of a treated tire piece, cross sight

Table II. Pyrolysis products

No: of Entries	MW (P)	Tire (M) (g) (kW)	(kW/kg2)P/M2	TIR(K)	T EXT (K)	Time (m)	Solids%	Liquid %	Gas%
1		1501.1	1.3	533	787	70	50.7	39.3	9.0
2	3	64.1	730.1	453	617	47	47.5	30.1	22.3
3	3	233.3	55.1	522	764	39	43.2	42.6	14.2
4	4.7	212.8	106.0	546	814	15	40.6	43.1	16.2
5	6	202.8	137.6	573	872	14	41.6	31.5	27.3
6	3.	502.8	11.9	513	744	59	40.6	44.0	13.5
7	1.6	252.1	23.6	523	766	100	65.0	20.7	14.2

T^{IR}_{max}: max: temperature spotted by IR thermometer;

T^{EXT}_{max}: max: temperature concluded.

2) *Revenues of products*

The consequences of tests completed at various MW power and mass of tire pieces are accounted for in Table III as shown above

The ratio between microwave power (P) and the tire mass square (M2) was selected as a expressive factor since it gave a good and brief connection between experimental environments and outcomes of pyrolysis test. It is to be noticed that under these experimental circumstances a power connection among the P/M2 ratio and the tire mass (M) can be known ($R2 = 0.9532$)

$$P \quad 3.0242\ M - 2.045\ M2$$

In every test MW control was reserved steady over the time. Trials were ceased when gas development was not additionally recognized. Pyrolysis was thought to be finished if natural substance was absent in the buildup.

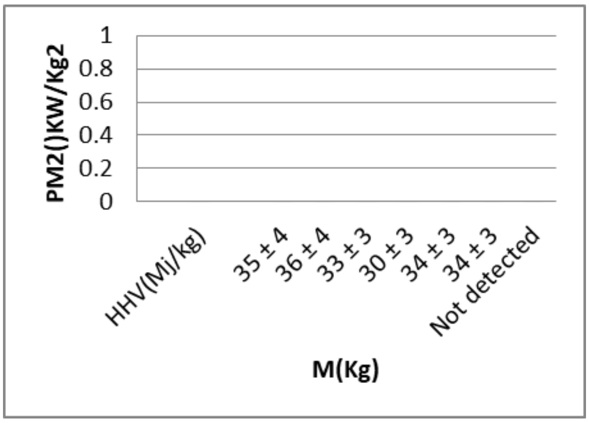

Figure 5. Relationship between P/M2 and M.

3) *Solid product*

The solid yields stood unscented black dusts, providing uncompleted pyrolyzed substance was not existing (entry 1–3, 6–7, Table III).

Table III Leading Assets of Solids

ENTRY	HHV(Mj/kg)	LHV(Mj/kg)		Definitive Analysis		
			C (wt %)	H(wt%)	N(wt%)	S(wt%)
1	36 ± 4	34 ± 3	89.34	0.37	0.16	2.4
2	36 ± 5	36 ± 5	87.98	0.57	0	1.8
3	34 ± 3	33 ± 3	81.32	0.84	0.48	2
4	30 ± 4	30 ± 4	85.71	3.22	0.34	1.4
5	33 ± 3	35 ± 3	84.91	1.62	0.41	1.5
6	34 ± 4	33 ± 3	86.64	0.31	0.79	1.6
7	Not detected	Not detected	92.03	0.53	0	Not detected

4) *Liquid products*

The investigation demonstrated no noteworthy contrasts among every pyrolysis tests. The fluids don't contain any huge oxygenated hydrocarbons. A portion of the liquid characteristics are accounted for in beneath table (coded "Ln" while "n" is the passage of pyrolysis.

CONCUSLION

Microwave pyrolysis of tires is appeared as a profitable method to change over an inconvenient waste into a sensible fuel or a wellspring of synthetic substances. To Explore 60,100 and 200 work tire powder under the heating rate of 10, 20 and 40°C/min the pyrolysis of tire was tried by TG/DTG. The investigation outcomes demonstrated that three phases that made up the tire pyrolysis procedure, containing the arrival of unstable and dampness at lesser temperature pursued by the warm deterioration of characteristic elastic and the disintegration of polybutadiene and polybutadiene-styrene elastic at higher temperature, separately. The utilization of a straightforward microwave mechanical assembly for an dynamic heat exchange has been portrayed. Pyrolysis of scrap tires was acknowledged in a brief span. The warming range had a more significant impact on the pyrolysis procedure than tire powder estimate. The procedure gave three distinct items (strong, fluid and gas) that were completely described. The initiation vitality and the recurrence factor were determined. The two system capacities for mass misfortune rate can depict tire pyrolysis well.

ACKNOWLEDGEMENTS

The authors would like to acknowledge the financial support from National Science Foundation of China (51706044), the Natural Science Foundation of the Jiangsu of China (BK20170666), and the Recruitment Program for Young Professionals in China.

REFERENCES

[1] Wang, H., et al., Characterization of Bitumen Modified with Pyrolytic Carbon Black from Scrap Tires. Sustainability, 2019. **11**(6): p. 1631.

[2] Alvarez, J., et al., Improving bio-oil properties through the fast co-pyrolysis of lignocellulosic biomass and waste tyres. Waste Management, 2019. **85**: p. 385-395.

[3] Zhang, X. and R.C. Brown, Introduction to Thermochemical Processing of Biomass into Fuels, Chemicals, and Power. Thermochemical Processing of Biomass: Conversion into Fuels, Chemicals and Power, 2019: p. 1-16.

[4] Kalogiannis, K.G., S.D. Stefanidis, and A.A. Lappas, Catalyst deactivation, ash accumulation and bio-oil deoxygenation during ex situ catalytic fast pyrolysis of biomass in a cascade thermal-catalytic reactor system. Fuel Processing Technology, 2019. **186**: p. 99-109.

[5] Haeldermans, T., et al., Microwave assisted and conventional pyrolysis of MDF–characterization of the produced biochars. Journal of Analytical and Applied Pyrolysis, 2019. **138**: p. 218-230.

[6] Martínez, J.D., et al., Waste tyre pyrolysis–A review. Renewable and Sustainable Energy Reviews, 2013. **23**: p. 179-213.

[7] van Geldern, R., et al., Stable carbon isotope analysis of dissolved inorganic carbon (DIC) and dissolved organic carbon (DOC) in natural waters–Results from a worldwide proficiency test. Rapid Communications in Mass Spectrometry, 2013. **27**(18): p. 2099-2107.

[8] Venderbosch, R.H., Fast pyrolysis. Thermochemical processing of biomass: conversion into fuels, chemicals and power, 2019: p. 175-206.

[9] Lin, C.J. and W.L. Hergenrother, Tire compositions comprising epoxidized natural rubber and a functionalized polyolefin. 2005, Google Patents.

[10] Kumarn, S., et al., Investigating the Mechanistic and Structural Role of Lipid Hydrolysis in the Stabilization of Ammonia-Preserved Hevea Rubber Latex. Langmuir, 2018. **34**(43): p. 12730-12738.

[11] Schürmann, O., Pneumatic Vehicle Tyres. 2018, Google Patents.

[12] Gauthier-Maradei, P., C.P.T. Ruiz, and M. Capron, Oil and Aromatic Yield Maximization During Pyrolysis of Scrap Tire Rubber. Waste and Biomass Valorization, 2019: p. 1-11.

[13] De Sciarra, F.M. and P. Russo, Experimental Characterization, Predictive Mechanical and Thermal Modeling of Nanostructures and Their Polymer Composites. 2018: William Andrew.

[14] Dimpe, K.M., A. Mpupa, and P.N. Nomngongo, Microwave assisted solid phase extraction for separation preconcentration sulfamethoxazole in wastewater using tyre based activated carbon as solid phase material prior to spectrophotometric determination. Spectrochimica Acta Part A: Molecular and Biomolecular Spectroscopy, 2018. **188**: p. 341-348.

Kaleemullah: The author was born in Pakistan in the year 1992. He holds a bachelors degree in Electrical Engineering from Quaid-e-Awam University of Engineering Science and Technology. He is a Master student at school of Energy and Environment, Southeast University, Nanjing China. His research interests include biomass pyrolysis and gasification and environmental engineering.

International Journal of Engineering Works
ISSN-p: 2521-2419
ISSN-e: 2409-2770
Vol. 6, Issue 06, PP. 208-211, June 2019
https://www.ijew.io/
https://doi.org/10.34259/ijew.19.606208211

Pyrolysis of Chickpeas Waste and Peanut Shells for the Production of Oil and its Analysis

Najam Iqbal[1], Ben Haoxi[2]*, Zhihong Wu[3]
[1,2,3]Key Laboratory of Energy Thermal Conversion and Control of Ministry of Education, School of Energy and Environment, Southeast University, Nanjing, China Nanjing, China.
najam1122@qq.com[1], benhaoxi@gmail.com[2], 18915408402@163.com[3]
corresponding author*: benhaoxi@gmail.com
Received: 28 April, Revised: 27 May, Accepted: 11 June

***Abstract*—** Pyrolysis is one of the widely used technique among the thermal conversion processes of biomass. Biomass in the form of agricultural residues is prevalent in new renewable energy sources, especially in view of its broad potential and rich use. In this paper, the pyrolysis of chickpeas and peanut shells in laboratory-scale tubular furnace reactors is studied, which is considered to be an effective method to utilize agricultural residues in China. The effects of raw material ratio and reaction temperature on the distribution of pyrolysis products are described quantitatively, as well as some characteristics of these products produced in the tubular furnace reactor system developed in this study. The main constituents of bio-oil are categorized into three kinds including aromatic compound, carbonyl compounds and carboxyl compounds that were analyzed with 1H NMR (nuclear magnetic resonance characterization). The maximum yield of bio-oil, about 44.80% from the peanut shell biomass, and 10.3% from the waste of chickpeas by weight was extracted, at a flow rate 10 L/min of N2 at a reaction temperature of 500°C was achieved.

***Keywords*—** Pyrolysis, Chickpeas, Peanut shells, Bio-oil analysis, tubular furnace reactor.

I. Introduction

In today's world, the extraction of second-generation fuels from biomass raw materials and waste feed is attracting large quantities of biofuels because of the negative impact of first-generation biofuels (fuels of sugar, starch, animal fats, and vegetable oils) on food resources. Fast pyrolysis is a thermochemical transformation process, described by fast heating of biomass raw materials to medium temperature levels without oxygen, and rapid extinguishing or quenching of volatile intermediary products in the absence of oxygen (O2), which is an attractive technology for the production of liquid biofuels [1-3]

Biomass is an economical substance and thought as a high energy renewable feed for the 2nd generation biofuel, which is reasonable to yield fuel oil and chemical substances of various platforms sustainably. Thus helps to overcome this very large dependency consumption of fossil fuels. Biomass fast pyrolysis yields a nominal quantity of bio oil, gaseous products, and solid bio char, so it's of particular interest [4-6]

Biomass residues produce a variety of energy through a variety of unique processes, such as mechanical, thermochemistry, and organic processes. Bio-treatment is highly selective, providing only a few unique products. Contrarily, in the majority of the thermochemical change process, pyrolysis is generally can create a wide scope of items in short response time, including bio-charcoal, bio-oil, and non-condensable gases [7, 8]

There have been considerable efforts on converting biomass to liquid bio-oil [12]. Fatimatul Zaharah Abbas [9] took a sample of oil palm fiber (OPF) and performed and performed pyrolysis, about 41.2 wt % of maximum yield of oil is obtained at the temperature of 500°C. Yunpu Wang [10] in his research work, co-pyrolysis of pretreated bamboo sawdust and soap stock was performed. After the pyrolysis experiment, the yield of (40.00 wt %) bio-oil was obtained at temperature of 200°C for 60.0 minutes with 0.50ml of hydrochloric acid.

Aziz et al. [11] in order to produce bio-oil using microwave power of 1kw over a temperature of 250-390°C in 2 to 10 minutes, microwave assisted pyrolysis on palm shells, sage and wood chips wastes was performed. Bio-oil yield of about 3.92 to 16.51 wt. % was reported according to the raw material and reaction conditions.

In China, Peanut shells and chickpeas waste are abundantly. They have good physical properties and a stable supply of peanut and chickpeas processing plants that is why considered as suitable raw material for bio oil production. For the pyrolysis of chickpeas and peanut shell a tubular furnace reactor was setup for bio-oil production in Southeast University. In this experimental work, fast pyrolysis of chickpeas and peanut shell was investigated with a maximal 10.32 and 52% yield of bio-oil in a tubular furnace reactor, and characterization of final product were also performed by spectroscopic technique which are 1H-NMR and elemental analysis.

II. EXPERIMENTAL

A. Materials

The peanut shells used as feedstock is obtained from a peanut-oil processing plant in Nanjing, Jiangsu Province and chickpeas from Youi foods in Suzhou. The chickpeas and peanut shells naturally dried in the sunlight for 5 days to remove surface water. And these raw materials were used without any pretreatment. Chickpeas was crushed and grounded to get a size fraction of 1–3 mm; peanut shells was grounded of size ~3 mm × 3 mm.

B. Pyrolysis procedure

A tubular furnace reactor is used to perform the pyrolysis of biomass mass samples (chickpeas and peanut shells) fig 1. It is made of stainless steel tubes with an inner diameter of 55mm and a length of 540 mm. Concisely, the reactor consisted of a cylindrical quartz glass tube heated by a stainless steel block furnace. To measure the temperature, inside the furnace an alumel/ chromel thermocouple was placed, fixed in the tube. A sample carrier boat made of porcelain in which samples was placed in the middle of the tube, and nitrogen as the carrier gas was supplied having a flow rate of 10L/min. At the beginning, the furnace is heated in an empty part of the tube, and the desired temperature is balanced between 300 and 600°C. When the desired temperature is reached, the biomass is moved into the furnace for pyrolysis. These operations are carried out at temperatures of 300 to 600°C under atmospheric pressure and under approximate isothermal conditions. The gases released during the pyrolysis leaved the furnace and passed through the condenser arrangement. The bio-oil portion was collected in a beaker placed in cold water. To achieve a fast condensation, gases were extracted by the vacuum pump and also cooled. The bio-oil was separated and weighed. The following conditions used during pyrolysis:

Heating rate: 15°C /min

Temperature: 350, 400, 450, 500, 550 and 600 °C

Cooling temperature set at = -10°C

TABLE I. DATA OF PROXIMATE AND ULTIMATE ANALYSES PERFORMED ON PEANUT SHELLS

Chemical properties	**As received Value**
Proximate analysis, (wt %)	
Ash	12.44
Volatile matter	72.47
Fixed carbon	15.75
Moisture	9.39
Elemental composition, wt%	
Oxygen [a]	36.12
Hydrogen	6.75
Nitrogen	0.8
Carbon	45.46

[a]by difference

TABLE II. DATA OF PROXIMATE AND ULTIMATE ANALYSES PERFORMED ON CHICKPEAS WASTE

Chemical properties	As received Value
Proximate analysis, wt%	
Fixed carbon	17.85
Volatile matter	79.27
Ash	11.24
Moisture	10.49
Elemental composition, wt%	
Oxygen [a]	32.87
Hydrogen	5.45
Nitrogen	0.4
Carbon	47.22

[a]by difference

Figure 1. tubular furnace reactor used in experiment

C. Analysis method

The ultimate analysis was conducted using elemental analyzers (Elementar Vario EL) for bio-oils extracted from the waste of chickpeas and peanut shells. . It was determined the hydrogen, nitrogen and carbon content of the bio-oil with chickpeas and peanut husk wastes. Oxygen content in this studies was calculated by difference. The oil analyzed in this section is obtained under experimental conditions, which give maximum oil yields.

The 1H NMR spectra of Bio-oil were obtained at 400M HZ frequency using the Bruker ARX 400 device. As an internal standard, anhydrous samples are dissolved in chloroform D containing the tetra methyl silane (TMS).

III. RESULTS AND DISCUSSION

A. Product yields

In the nitrogen atmosphere, the pyrolysis of chickpeas and peanut shell waste was carried out in 350, 400, 450 and 500°C , and the distribution of products was shown in table 3 and table 4. As can be seen from table 3, in the case of peanut shells, the yield of bio-oil increases with the increase of temperature, reaching a 500°C after that it goes reduces. Due to the increase of secondary cracking reactions at high temperatures, the yield of gas increases with the increase of temperature from 350 to 500°C. The output of bio-Char is the opposite of gas production, that is, the yield decreases with the increase of temperature.

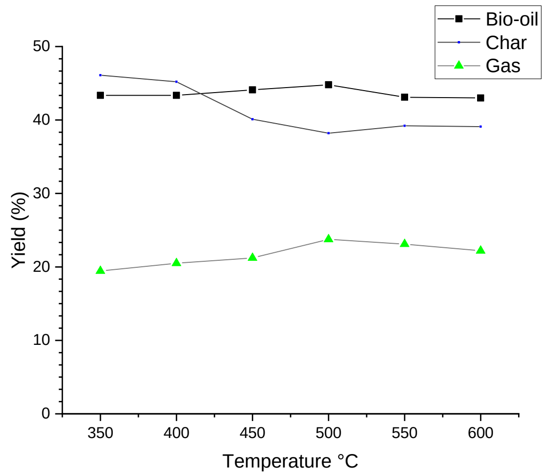

Figure 2. The graph shows the effect of temperature on yield when peanut shells used as biomass with heating rate 15◦C min-1

TABLE III. THE FINAL PRODUCT OF PYROLYSIS OF PEANUT SHELLS AT DESIRED TEMPERATURES.

Temperature, °C	Bio-oil, wt.%	Bio-char, wt.%	Gas, wt.%
350	43.35	46.10	19.41
400	43.35	45.20	20.50
450	44.10	40.10	21.21
500	44.80	38.20	23.70
550	43.10	39.22	23.12
600	43	39.11	22.20

It can be concluded from table 4 that biofuel yield of chickpeas as a biomass sample increases with the increase of temperature up to 500°C, after that it goes reduces. In case of chickpeas waste we get higher amount of the gas yield. So, in comparison with peanut shells sample we get less amount of bio-oil from chickpeas waste.

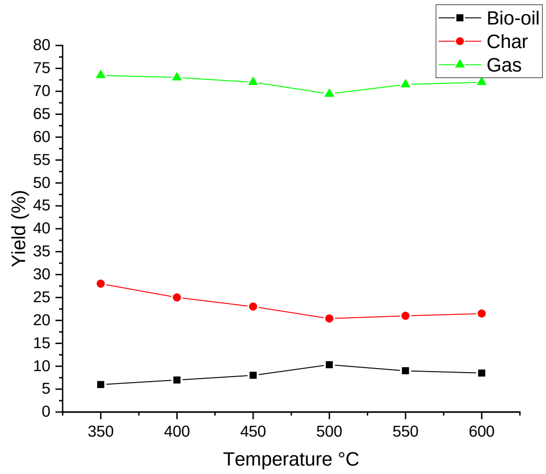

Figure 3. the graph shows the effect of temperature on yield when chickpeas waste used as biomass with heating rate 15◦C min-1

TABLE IV. THE FINAL PRODUCT OF PYROLYSIS OF CHICKPEAS AT DESIRED TEMPERATURES.

Temperature, °C	Bio-oil, wt.%	Bio-char,wt.%	Gas, wt.%
350	6	28	73.5
400	7	25	73
450	8	23	72
500	10.3	20.4	69.4
550	9	21	71.5
600	8.5	21.5	72

B. Bio oil chemical analysis

The 1H NMR spectra comprise of primarily two regions, namely aliphatic and aromatic and hydrogen resonances (Table 5). The aliphatic hydrogen resonances occurs in the 0.5–6.5 ppm range. In the range of 6.5-9.0 ppm the aromatic hydrogen resonances occurs. [12]

The molar percentages of the hydrogen types that were calculated on the basis of the chemical deviation values obtained from the 1H NMR spectra of oils extracted from both peanut shell and chickpeas samples are in Table 5 and 6. The 1HNMR spectra of bio-oil obtained from peanut shells shows that majority of the bio oil belongs to the aromatic region (CH_3, CH2, and CHα) having 39.45 mol percent. In case of chickpeas waste, 29.74 mol percent of bio-oil recorded in aromatic region (CH_3, CH2, and CHα).Hence, it is concluded that oil obtained from peanut shells having more aromatic compounds as compared to the bio-oil obtained from chickpeas waste.

TABLE V. EXTRACTED BIO-OIL FROM PEANUT SHELLS AND THEIR 1H NMR ANALYSIS RESULTS

Type of Hydrogen	Chemical Shift (ppm)	Bio-oil
$CH_{3}\gamma$	0.5–1.0	11.2

β-CH_3, CH2, and CHγ	1.0–1.6	6.54
CH_2 and CHβ	1.6–2.0	14.74
CH_3,CH_2, and CHα	2.0–3.3	39.45
Ring-join methylene(Ar-CH2-Ar)	3.3–5.0	19.43
Phenolic (OH) or olefinic proton	5.0–7.0	1.51
Aromatic	7.0–9.0	2.38

Table VI. Extracted bio-oil from chickpeas waste and their 1H NMR analysis results

Type of Hydrogen	Chemical Shift (ppm)	Bio-oil
CH3γ	0.5–1.0	13.87
β-CH3, CH2, and CHγ	1.0–1.6	9.78
CH2 and CHβ	1.6–2.0	13.54
CH3,CH2, and CHα	2.0–3.3	29.74
Ring-join methylene(Ar-CH2-Ar)	3.3–5.0	17.88
Phenolic (OH) or olefinic proton	5.0–7.0	3.55
Aromatic	7.0–9.0	4.88

ACKNOWLEDGEMENT

The authors would like to acknowledge the financial support from National Science Foundation of China (51706044), the Natural Science Foundation of the Jiangsu of China (BK20170666), and the Recruitment Program for Young Professionals in China.

CONCUSLION

Pyrolysis temperature have great effect on pyrolysis yield. The maximum yield of oil obtained in case of peanut shells as biomass sample was 44.80% at temperature of 500°C and in case of chickpeas waste it was only 10.30% and during the experiment the heating rate fixed around 15°C min-1. It was concluded that peanut shells waste gave more value aided bio-oil as compared to chickpeas waste biomass. The spectroscopic analysis results show that the bio-oil obtained from peanut shells waste have more aromatic compounds that is 39.45 mol percent as compared to the bio-oil 29.74 mol percent obtained from chickpeas.

REFERENCES

[1] Bridgwater, A. and G. Peacocke, Fast pyrolysis processes for biomass. Renewable and sustainable energy reviews, 2000. **4**(1): p. 1-73.

[2] Vamvuka, D., Bio- oil, solid and gaseous biofuels from biomass pyrolysis processes—an overview. International journal of energy research, 2011. **35**(10): p. 835-862.

[3] Vamvuka, D. and E. Kakaras, Ash properties and environmental impact of various biomass and coal fuels and their blends. Fuel Processing Technology, 2011. **92**(3): p. 570-581.

[4] Robinson, J., et al., Microwave pyrolysis of biomass: control of process parameters for high pyrolysis oil yields and enhanced oil quality. Energy & Fuels, 2015. **29**(3): p. 1701-1709.

[5] Beneroso, D., et al., Microwave pyrolysis of biomass for bio-oil production: Scalable processing concepts. Chemical Engineering Journal, 2017. **316**: p. 481-498.

[6] Wu, C., et al., Conventional and microwave-assisted pyrolysis of biomass under different heating rates. Journal of Analytical and Applied Pyrolysis, 2014. **107**: p. 276-283.

[7] Bridgwater, A.V., Review of fast pyrolysis of biomass and product upgrading. Biomass and bioenergy, 2012. **38**: p. 68-94.

[8] Bridgwater, A.V., Upgrading biomass fast pyrolysis liquids. Environmental Progress & Sustainable Energy, 2012. **31**(2): p. 261-268.

[9] Abas, F.Z., F.N. Ani, and Z.A. Zakaria, Microwave-assisted production of optimized pyrolysis liquid oil from oil palm fiber. Journal of Cleaner Production, 2018. **182**: p. 404-413.

[10] Wang, Y., et al., Production of bio-oil from agricultural waste by using a continuous fast microwave pyrolysis system. Bioresource technology, 2018. **269**: p. 162-168.

[11] Aziz, S.M.A., et al., Bio-oils from microwave pyrolysis of agricultural wastes. Fuel Processing Technology, 2013. **106**: p. 744-750.

[12] Sutcu, H., I. Toroglu, and S. Piskin, Structural characterization of oil component of high temperature pyrolysis tars. Energy sources, 2005. **27**(6): p. 521-534.

Najam Iqbal received degree of BSc. Mechatronics Engineering from University of Engineering and Technology (UET) Peshawar, Pakistan in 2017. He is currently pursuing Masters degree in Power and Thermal Engineering from Southeast University Nanjing , China. His area of specialization in the field of biomass conversion into renewable energy.

International Journal of Engineering Works
ISSN-p: 2521-2419
ISSN-e: 2409-2770
Vol. 6, Issue 06, PP. 212-216, June 2019
https://www.ijew.io/
https://doi.org/10.34259/ijew.19.606212216

Modeling and Simulation of a Novel Module for Thermoelectric Power Generation from Solar Photovoltaic Panels

Muhammad Suleman Malik[1], Muhammad Naeem Arbab[2], Bilal Mehmood[3],Haseeb Aman[4], Hayat[5], Pir Jalal[6]
[1,2,3,4,5,6] University of Engineering & Technology Peshawar (Pakistan).
suleman2113@gmail.com[1], mnarbab@yahoo.com[2], bilal1208@gmail.com[3], Haseebamaankhattak@gmail.com[4], hayat_ullah@hotmail.com[5], pirjalal11@gmail.com[6]
Received: 12 June, Revised: 19 June, Accepted: 21 June

***Abstract*—**Electricity is a basic need of humans in this modern era and plays a role of a backbone in our daily life as well as in the economic growth of a country. The efficiency of a power system is very important parameter which helps in analyzing its overall performance. So due to this reason effective and efficient utilization of solar energy is very important. Heat losses occurs in solar panels which reduces power output and hence overall efficiency is decreased. These heat losses can be utilized in such a way that works as waste heat recovery system. This system uses light and heat energy of the sun. When sunlight strikes the PN Junctions of solar PV panels, photovoltaic electricity is produced. Whereas, heat of sun and heat losses in the solar panels can be utilized and temperature difference is created by different means so as to generate electricity using thermoelectric cells (TEC) which works on the principle of Seebeck effect. Electricity generated from both sources can be common pooled and feed to the load either directly or it can be stored in batteries. This makes the system more effective and efficient.

***Keywords*—** Electricity, power generation, Seebeck effect, solar energy, solar panels.

I. Introduction

Electricity plays a major role in building the economy of a country. All the domestic, industrial, commercial and metropolitan areas need electricity for their daily operations. If the prices of electricity are low and it is available whole day without any interruption, then the products made by the industries or factories are large in quantity and cheap in price.

Pakistan is an under developed country, its economy is unstable and its energy sector is at continuous downfall. The resources available for electrical power generation are either not used properly or there is lack of facilities or there is absence of expertise to utilize it in an efficient and effective manner to generate electricity from it. Transmission losses in the existing outdated system, uncontrolled power theft, reduction of water available for hydroelectric power due to seasonal variations, increase in the prices of fuel has increased the difficulty in the system. There is a dip between the electricity generation and the demand so due to this reason we are facing electricity shortage. The electricity production in Pakistan from 2008 to 2018 is shown in Fig 1.

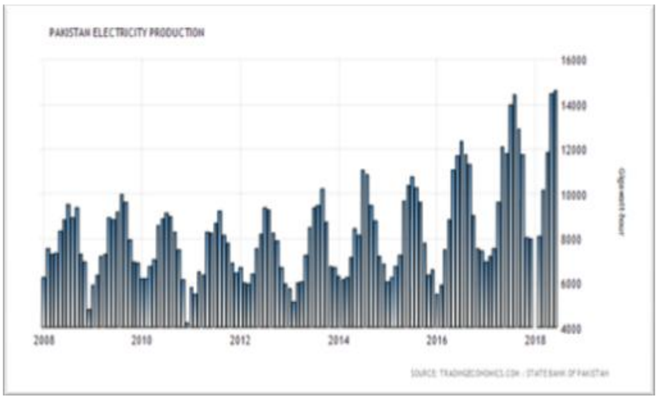

Figure 1. Electricity Generated during last 10 years in Pakistan [1]

During last five years, work has been done in the energy sector of Pakistan. From 2013 to 2018, 39 power projects were installed which added a capacity of 12,230 MW to the national grid [2]. The energy of the sun is due to continuously occurrence of nuclear fusion reactions. When hydrogen atoms specifically protium or deuterium or hydrogen and helium are forced to combine by some external agents (energy) it releases a tremendous amount of energy in a form of light, heat and sound along with hydrogen or helium as a byproduct. Individually, fusion produces less energy as compared to fission but due to the presence of abundant amount of hydrogen on the surface of sun. The overall energy produced due to fusion is more in the sun if compared with the fission reaction.

Ongrid system is directly connected to the regional or national grid to supply electricity generated by different sources locally through bi-directional meters. ON grid system doesn't possess battery backup system. When grid supply is properly working and is switched on, ON grid system will work but when the feeders in grid station are switched off, ON grid system willn't supply electricity to the national grid [3].

Off grid system generates electricity and supply it to its local load along with storage facility without connecting it to regional or national grid is called OFF grid system. OFF grid system is connected with the battery backup. It can be connected with renewable as well as non-renewable sources such as wind turbines, hydro-turbines and diesel generators etc. It can be used to generate as well as store electricity in case of emergency or in case of cloudy weather or at night [4].

Hybrid system, which has both features of ON Grid and battery backup is called hybrid system. This system is not only connected to the regional or national grid but also charges the battery at the same time. Electricity is fed to the grid through bi-directional meters [5].

There are different methods of generating electricity including electricity generation from fossil fuels [6], Solar thermal power generation using heliostates to through light on a receiver tank [7] or using Seebeck effect for electrical power generation [8].

Solar radiations consist of infrared, visible light and ultraviolet rays as shown in Fig 2.

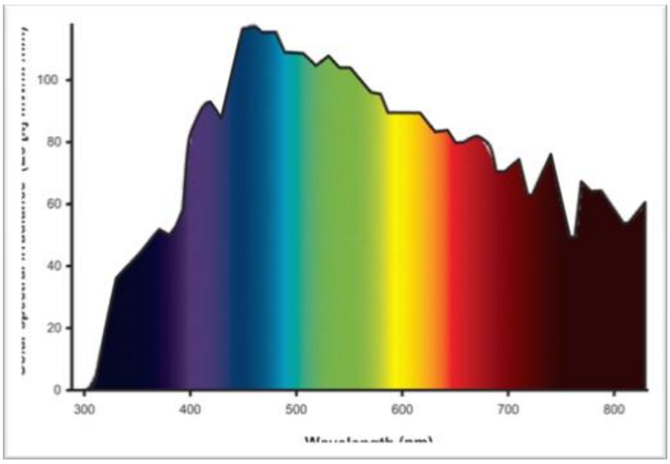

Figure 2. Spectral distribution of sun light [9]

II. MATERIALS

Thermoelectric cells are made up of semiconductor materials. These extrinsic semi-conductor materials consist of P-Type and N-Type Pallets. P-Type materials are made by doping group 3 elements of periodic table with silicon or arsenic and in doing so there is a deficiency of electrons i.e. a presence of hole so it is called P-Type semiconductor. Majority charge carriers are holes and minority charge carriers are electrons. Similarly, N-Type semiconductors are made by doping group 5 elements of periodic table with silicon or germanium and in doing so there is an excess of electron i.e presence of one extra electron so it is called N-Type semiconductor. Majority charge carriers are electrons and minority charge carriers [10-12]. The best thermoelectric materials for thermoelectric cells along with there figure of merit is shown in Fig 3.

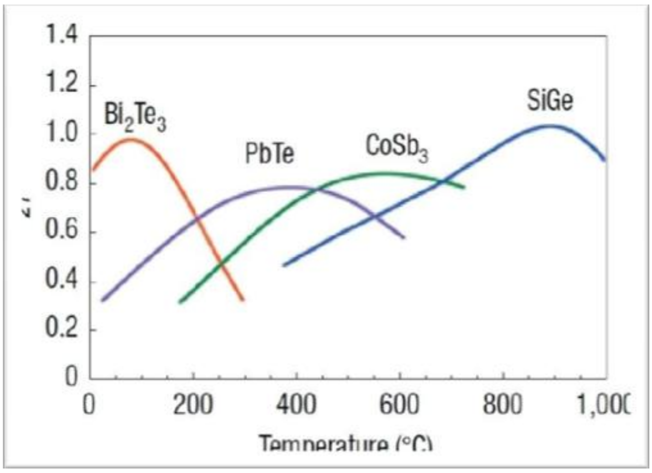

Figure 3. Figure of merit of different termoeletric materials at different temperatures [13].

Thermoelectric cells vary in size, depending upon power requirement [14]. The length and width of the cell is in range of 2.5 to 50 mm each and thickness is in range of 2.5 to 5 mm as shown in Fig 4.

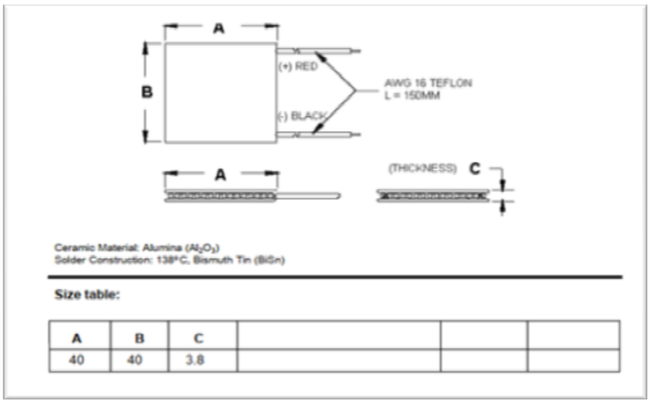

Figure 4. Dimensions of thermoelectric cell

When two thermoelectric cells are staked together with slight modifications in internal structure it is called two stage thermoelectric cell [15]. The efficiency of two stage thermoelectric cells is more than one stage thermoelectric cell [16]. Two stage thermoelectric cell is shown in Fig 5.

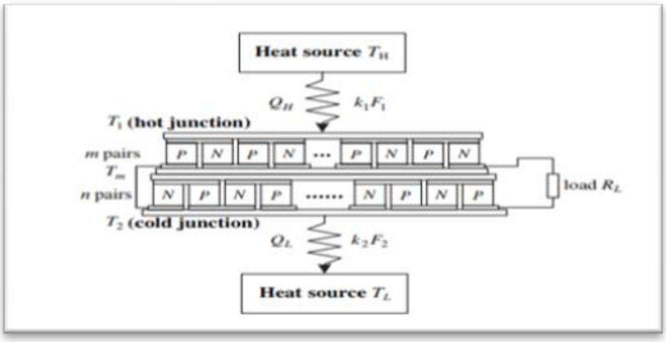

Figure 5. Two stage thermoelectric cell

III. METHODOLOGY

Thermoelectric cells and solar panels are modeled in Simulink and Autocad. Thermoelectric cells can be attached on the backside of solar panels. The dimensions of solar panels areshown in Fig 6.

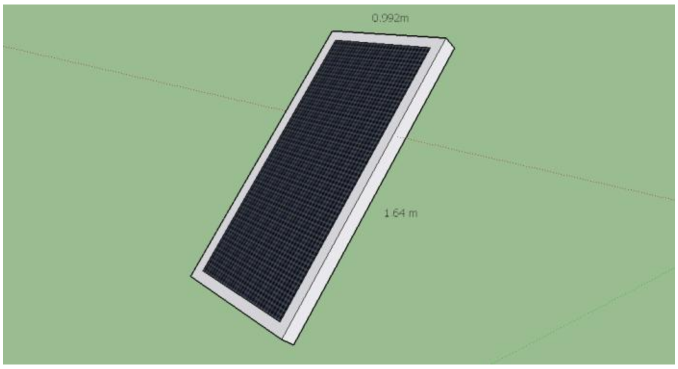

Figure 6. Dimensions of solar panel

Electrical power generated from thermoelectric cells mainly depends on Seebeck coefficient (S), Electrical resistance (R) and thermal conductance (K). So each parameter must be modeled separately in simulink.

Seebeck coefficient determines the voltage generated by thermoelectric cell. Simulink model of Seebeck coefficient of thermeoelectric cell is shown in Fig 7.

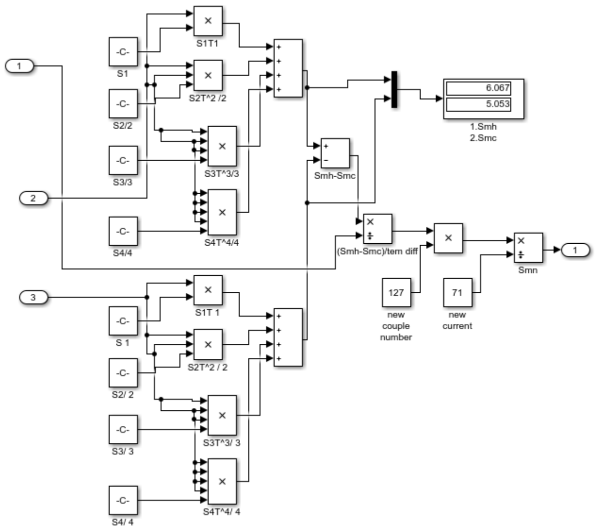

Figure 7. Simulink Model of Seebeck Coefficient

It determines the opposition faced by thermoelectric cell to the flow of electricity.Simulink model of electrical resistance of thermoelectric cell is shown in Fig 8.

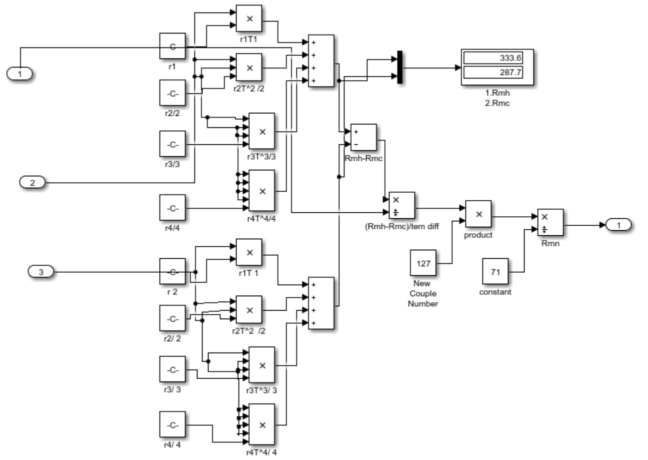

Figure 8. Simulink Model of Electrical Resistance

Thermal conductance determines the flow of heat with in a thermoelectric cell. Simulink model of thermal conductance of a thermoelectric cell is shown in Fig 9.

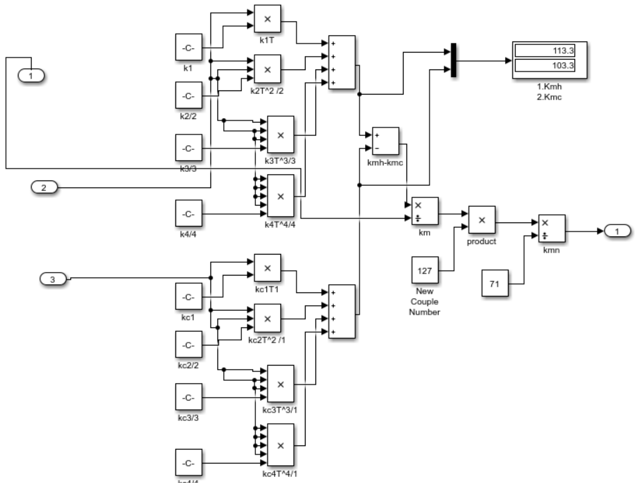

Figure 9. Simulink Model of Thermal conductance

The modeling of all the parameters of a commercially available thermoelectric cell is shown in Fig 10.

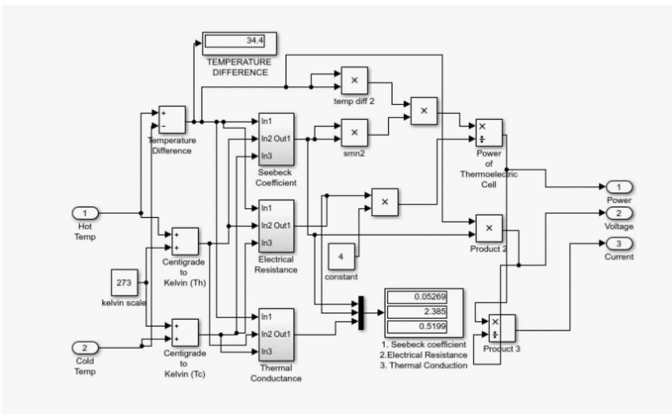

Figure 10. Simulink Model of commercially available thermoeletric cell

IV. Simulations and Results

All the parameters of thermoelectric cells are simulated in Simulink. The variation of the parameters of thermoelectric cell with the rise in the temperature difference is shown in Fig 11. It is clear that with the rise in temperature difference the value of Seebeck coefficient changes slightly, value of resistance increases linearly , value of thermal conductance also changes slighty whereas the value of power changes slightly in the start but rises ecponentially with the increase in temperature.

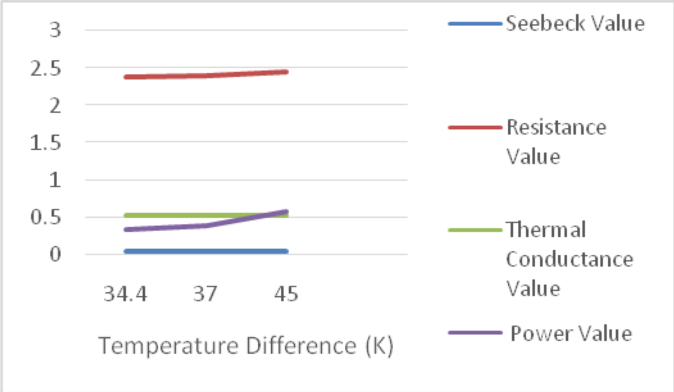

Figure 11. Variation of the parameters of thermoelectric cell with the rise in temperature.

If we integrate power of twenty solar panels with the power generated by thermieletric cell then the contribution of each sourves is shown in the form of a table 1.

TABLE I. POWER GENERATION BY EACH SOURCE

S.NO	ΔT(°C)	$E_{Solar\ per\ year}$	$E_{Tec\ per\ year}$	$E_{Total\ per\ year}$
1	34.4	9581.25	12636.3	22217.55
2	37		14490.5	24071.75
3	45		21341.55	30922.8

The share of electrical power by each source is shown in Fig 12. It is clear that power generation from thermoeletric system is more than that of solar panels system.

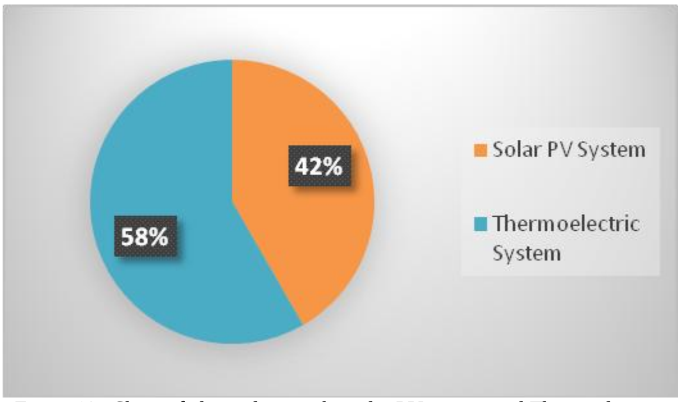

Figure 12. Share of eletrical power by solar PV system and Thermoelectric system.

Conflict of Interest

The authors declare no conflict of interest.

Concuslion

It is concluded that with the increase in the temperature of solar panels, electrical power is reduced . So utilizing this temperature for electrical power generation by means of thermoelectric cells, we can increase the overall electrical power , by integrating both solar panels and thermoelectric cells. The overall output power is increased by adopting this method of integration of solar panels with thermoeletric cells.

References

[1] Trading Economics, "Pakistan Electricity Production," Trading Economics, 2018. [Online]. Available: https://tradingeconomics.com/pakistan/electricity-production.

[2] Ministry of Finance, "Pakistan Economic Survey 2017-2018," Ministry of Finance, Islamabad, 2017-2018.

[3] N. M. Kumar, M. S. P. Subathra and J. E. Moses, "On-Grid Solar Photovoltaic System: Components,Design Considerations, and Case Study," in 4th International Conference on Electrical Energy Systems (ICEES), 2018.

[4] M. P. Monfort, S. L. Oña, D. Ribó-Pérez and S. Z. Djokic, "Modelling and Evaluating Performance of Large Off-Grid PV Systems for Water Pumping," in 2018 IEEE PES Innovative Smart Grid Technologies Conference Europe (ISGTEurope), Sarajevo, Bosnia-Herzegovina, 2018.

[5] K. Alluhaybi, X. Chen and I. Batarseh, "A Grid Connected Photovoltaic Microinverter with Integrated Battery," in IECON 2018 - 44th Annual Conference of the IEEE Industrial Electronics Society, Washington, DC, USA, 2018.

[6] D. A. Tillman, Coal-Fired Electricity and Emissions Control: Efficiency and Effectiveness, Butterworth-Heinemann, Elsevier, 2018.

[7] U. Pelay, L. Luo, Y. Fan, D. Stitou and MarkRood, "Thermal energy storage systems for concentrated solar power plants," Renewable and Sustainable Energy Reviews, vol. 79, pp. 82-100, 2017.

[8] S. Huang and X. Xu, "A regenerative concept for thermoelectric power generation," Applied Energy, vol. 185, pp. 119-125, 1 1 2017.

[9] M. Md. Kafiul Islam, "Performance assessment and degradation analysis of solar photovoltaic technologies: A review," Renewable and Sustainable Energy Reviews, vol. 78, pp. 554-587, 2017.

[10] M. Ibañez-Puy, J. Bermejo-Busto, C. Martín-Gómez, M. Vidaurre-Arbizu and J. Sacristán-Fernández, "Thermoelectric cooling heating unit performance under real conditions", *Applied Energy*, vol. 200, pp. 303-314, 2017. Available: 10.1016/j.apenergy.2017.05.020

[11] D. Zhao and G. Tan, "A review of thermoelectric cooling: Materials, modeling and applications", *Applied Thermal Engineering*, vol. 66, no. 1-2, pp. 15-24, 2014. Available: 10.1016/j.applthermaleng.2014.01.074.

[12] H. Zhang, W. Kong, F. Dong, H. Xu, B. Chen and M. Ni, "Application of cascading thermoelectric generator and cooler for waste heat recovery from solid oxide fuel cells", *Energy Conversion and Management*, vol. 148, pp. 1382-1390, 2017. Available: 10.1016/j.enconman.2017.06.089.

[13] "Thermoelectrics", *Thermoelectrics.matsci.northwestern.edu*,2019. [Online].Available: http://thermoelectrics.matsci.northwestern.edu/thermoelectrics/index.html. [Accessed: 20- Jun- 2019].

[14] D. Li, Y. Xuan, Q. Li and H. Hong, "Exergy and energy analysis of photovoltaic-thermoelectric hybrid systems", *Energy*, vol. 126, pp. 343-351, 2017. Available: 10.1016/j.energy.2017.03.042.

[15] H. Zhang, H. Xu, B. Chen, F. Dong and M. Ni, "Two-stage thermoelectric generators for waste heat recovery from solid oxide fuel cells", *Energy*, vol. 132, pp. 280-288, 2017. Available: 10.1016/j.energy.2017.05.005.

[16] K. Cheng, J. Qin, Y. Jiang, S. Zhang and W. Bao, "Performance comparison of single- and multi-stage onboard thermoelectric generators and stage number optimization at a large temperature difference", *Applied Thermal Engineering*, vol. 141, pp. 456-466, 2018. Available: 10.1016/j.applthermaleng.2018.05.127.

Muhammad Suleman Malik is a student of University of Engineering and Technology Peshawar.doing MS in Electrical engineering. He has written two research papers in international journals. His main research interest is electrical power generation.
Email: suleman2113@gmail.com

Muhammad Naeem Arbab is a professor at University of Engineering and Technology Peshawar. He got his Phd degree from University of Manchester , England. He has written 3 books in the field of electrical engineering o.e Electrical power generation, high voltage engineering and Control systems. He has published more than 25 research papers in local and international journals and conferences.
Email: mnarbab@yahoo.com

IJEW 国际工程期刊 International Journal of Engineering Works انجینرنگ کاموں کا بین الاقوامی جرنل

International Journal of Engineering Works
ISSN-p: 2521-2419
ISSN-e: 2409-2770
Vol. 6, Issue 07, PP. 217-220, July 2019
https://www.ijew.io/
https://doi.org/10.34259/ijew.19.607217220

Application of Polyvinyl Acetate (PVAc) in Dye Sensitized Solar Cells (DSSC) as Electrolyte in The Presence of Acetonitrile as Highly Soluble Organic Solvent and KI as Inorganic Redox Salt

Shafi ur Rehman[1]*, Hizb Ullah Khan[2], Muhammad Khitab Ahmed[3], Rizwan Kamal[4]
[1,4]US Pakistan Center For Advanced Studies in Energy, University of Engineering and Technology, Peshawar
[2]National Center of Excellence in Physical Chemistry University of Peshawar
[3]National University of Engineering & Technology (NUST), Islamabad, Pakistan
engr.shafi2962@gmail.com[1]*, hizbullah382@gmail.com[2], khitab.770@gmail.com[3], rkrizwan891@gmail.com[4]
Received: 22 June, Revised: 02 July, Accepted: 09 July

Abstract— The dye sensitized solar cells technology is one of the highly efficient, low cost and easily fabricated renewable energy technology. The highly soluble PVAc was prepared by solution polymerization. The PVAc was employed as an electrolyte in third generation, Dye sensitized solar cell (DSSC). The PVAc was characterized using SEM, XRD and conductivity measuring techniques. The prepared electrolyte behaved as gel electrolyte. SEM images shows the excellent dispersion PVAc in liquid electrolyte. The conversion efficiency achieved using gel electrolyte was 4.18%, which was comparable to liquid electrolyte with a value of 4.57%. This new technique reduces the degradation of DSCs rising from volatilization and leakage of the liquid electrolyte and endorses the commercialization process of DSSC.

Keywords— Polyvinyl acetate, Acetonitrile, Gel electrolyte, Dye sensitized solar cell.

I. Introduction

Solar cells are the renewable energy resources that pick up their energy from sun and supply this endless energy for human beings. It is one of the most hopeful energy resources due to its profusion, purity, safety and higher economic values that causes energy creation in distant rural areas [1]. The Solar energy can be used for three purposes: Photoelectric energy i.e. Solar PV, solar thermal energy and passive solar energy [2]. Technology of producing electricity directly from the solar energy was discovered by Alexander Edmond Becquerel, who was a French physicist at 1839 and that was the start of solar energy [3]. A solar cell is an electric device that directly convert incident light into electricity by photovoltaic effect [4].

The solar cell technology is grouped into three different generations, as shown in Fig.1. Illustration of solar cell technology, it is grouped into first, second, and third generations and These generations are additionally arranged into various kinds [5].

In 1991 the seminal work was initiated on DSSCs by O'Regan and Grätzel [6]. The DSSC is an emerging technology which is one of the third generation PV technology.

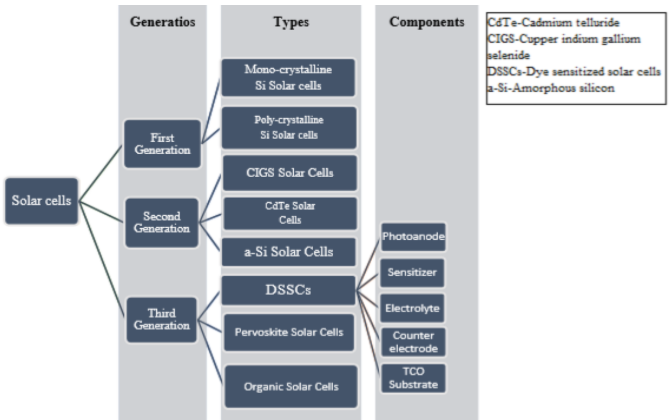

Figure 1. Illustration of solar cell technology, it is grouped into first, second, and third generations and These generations are additionally arranged into various kinds [5].

An extensive research has been made in this technology on its applications during the last two decades because of its cheaper and easier fabrication process [7]. This technology mimics the natural photosynthesis in the way of light absorption [8]. DSSCs work better than other PV devices in dark condition that is in cloudy climate or in sunset and in diffused light radiations which makes it outstanding choice for indoor applications like sunroof and windows [9]. So far, the efficiency achieved by DSSC is from ~7% to ~14% [10]. A DSSC basically comprises a semiconductor (e.g. ZnO, SnO2 and TiO2 etc.) of few microns thick film as working electrode that is coated on transparent conducting substrate, a dye i.e. Organic dye or inorganic metal complex dye, a counter electrode (e.g. carbon materials and Pt etc.) also coated on conductive glass substrate and an electrolyte (i.e. Co^{2+}/Co^{3+} and I_3^-/I^- etc. as a redox couples) inserted between counter electrode and dye, as shown in Fig.2 [11]. The light is absorbed

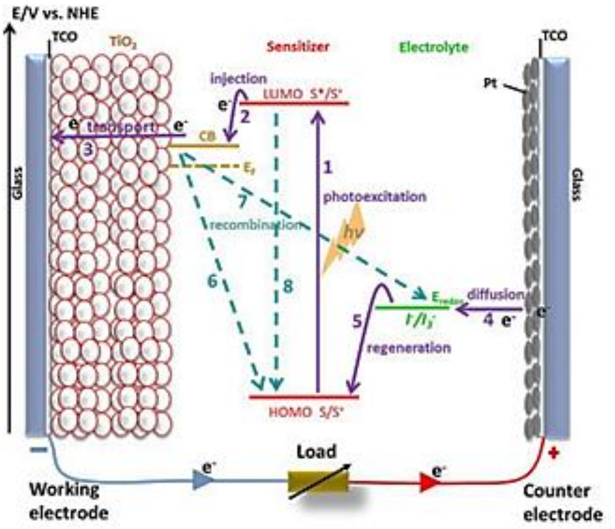

Figure 2. Working principle of TiO_2 based

by the dye molecules and electrons are injected into the conduction band of semiconductor. The electrolyte in contact with dye, provide electrons to the oxidized dye and restores it to its initial state. Then the oxidized electrolyte moves toward counter electrode and reduced to its neutral state [13].

The organic solvents have the volatility problem of its solvent caused by thermal stress and as a result cell deterioration is caused over long use. Consequently, ionic liquid solvents have been the promising electrolyte because of its good thermal and chemical stability, tuneable viscosity, high ionic conductivity and low volatility. Researchers are in interest to discover new liquid electrolyte, to increase the efficiency of DSSCs, such as 1,3-dialkylimidazolium etc. [14,15]. Low-viscosity ionic liquid is mixed with imidazolium iodide, to higher the efficiency [15].

Polymers has a unique network structure in gel electrolyte and shows, long term stability, higher electrical conductivity and good interfacial contact as compare to liquid electrolyte [16]. Polyvinyl acetate was discovered by Germany scientist Fritz Klatte in 1912. The manufactured polymer has the formula (C4H6O2)n and the general formula with the polyvinyl esters family is - [RCOOCHCH2] -. It is a kind of thermoplastic materials and its IUPAC name is poly (1-acetyloxiethene). Polyvinyl acetate is profoundly soluble polymer in organic solvents [17, 18].

This study, therefore demonstrate the application of polymer in DSSC's electrolyte in the presence of acetonitrile as solvent and KI (potassium iodide) as redox ion. The prepared Polymer was characterized through FTIR, XRD and the IV characteristics was done by solar simulator.

II. EXPERIMENTAL

A. Materials:

Vinyl acetate, sodium dodecyl sulphate, acetone and ethanol were purchased fromuni-chem Lab Ltd (india) whereas KI, iodine and acetonitrile from Schalab SL (Spain). The FTO glasses and N3 dye was obtained from Solaronics (Switzerland). All the chemicals purchased were in pure form.

B. Synthesis of PVAc

The Polyvinyl acetate was synthesized with the help of free radicle solution polymerization technique. Simply, 30 mL of monomer vinyl acetate was taken in flask and in a certain amount of water and 5 mL of methanol and 0.1 G of ammonium persulfate ((NH4)2S2O8) as an initiator were added. The reaction was refluxed at 70 °C for 2 hours. Once the mixture turned gelatinous 40 mL of methanol was mixed to the system and then stopped heating. The prepared polymer was dried in vacuum chamber for 24 hours at 40 °C. Then it is characterized for further applications.

C. Electrolyte preparation:

The prepared liquid electrolyte consisted of 0.4 M 1-methyl-3-propyl imidazoulium iodide, 0.2 M Kl, 0.3 M pyridine in acetonitrile as solvent. A 0.4 g of the PVAc was mixed with 1.5 g of liquid electrolyte and then mixer was stirred till complete dissolution of the polymer and then the electrolyte converted into quasi solid electrolyte and then employed both the electrolytes in DSSC separately. The prepared gel and Liquid electrolytes and DSSC module are shown in Fig.3.

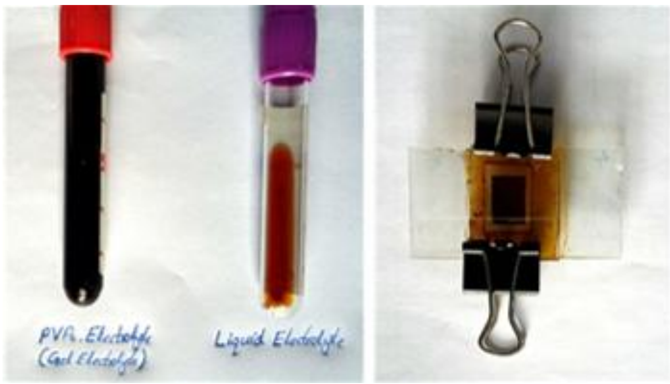

Figure 3. Liquid and Gel Electrolyte prepared in Lab

III. RESULTS AND DISCUSSION

A. SEM Micrographs:

The SEM micrograph of PVAc is shown in fig 4. The fig 4. (a) shows that PVAc has uniform, non-porous and amorphous structure while fig 4. (b) shows the scanning electron micrograph of the gel electrolyte on the TiO2 working electrode.

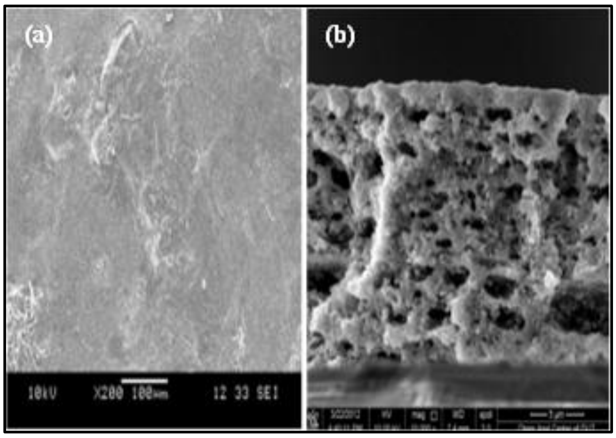

Figure 4. SEM image of (a) PVAc pure and (b) PVAc as gel electrolyte.

As shown in the figure, the TiO2 surfaces are completely covered by the gel electrolyte. The big holes show the spongy network of PVAc through which the liquid electrolyte can pass through it and retains the volatility of the organic solvent by making bond with acetonitrile as a result stability of DSSC is improved.

B. XRD Analysis:

As shown in Fig 5. native PVAc is amorphous as expected. The peaks at 15o, 22o represent PVAc. As the figure shows the almost zero peaks which shows that it has non-crystalline structure [20].

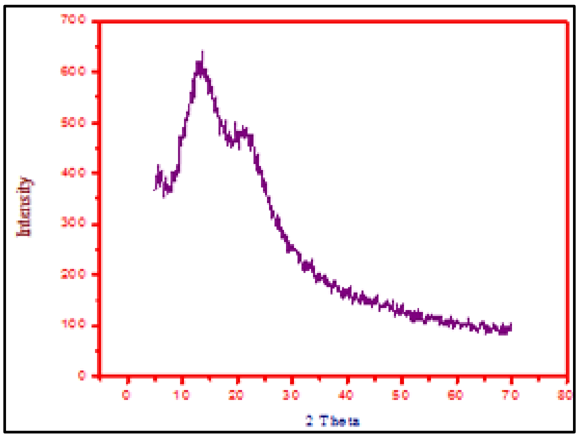

Figure 5. XRD Diffractogram of PVAc

C. Electrical Conductivity:

The fig 6 showed the conductivity of 2.3×10 -3 S/cm at high frequency of PVAc. The lower conductivity of the polymer is because of low level protonation of PVAc chain. The increase of the polymer conductivity with frequency is the radiation which cause splitting of the polymer chain. The conductivity is based upon electronic jumping which cause high energy free electrons, ions [19-22]. The fig 7 shows the conductivity of the gel electrolyte. This increase of the electrolyte conductivity is due to the free iodide ions present in the liquid electrolyte.

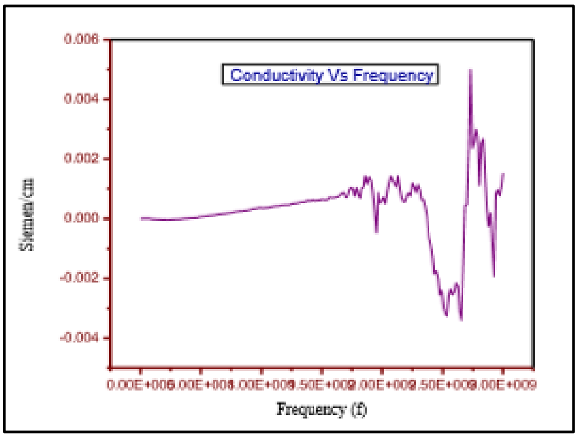

Figure 6. Conductivity of PVAc

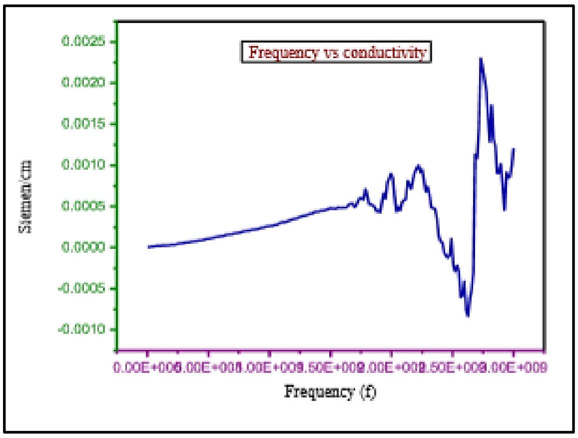

Figure 7. Conductivity of Gel Electrolyte

D. Performance Parameters:

The photovoltaic performance was done under illumination (AM 1.5G, 100 W cm−2) on DSSC employing gel electrolyte as shown in fig 7. The Voc, Jsc and FF of DSSC based on liquid and gel electrolyte are 0.712 V, 12.78 mAcm−2 and 57 %, respectively, yielding conversion efficiency of 4.18%. The values (Voc, Jsc, FF, and η) for the liquid electrolyte are 0 .686 V, 13.88 mA cm−2, 59%, and 4.57%, respectively. By comparing the data of the two electrolytes show that the increase of the Voc of liquid electrolyte is compensated by the slight decrease of FF of the gel electrolyte.

Conclusion

In summary, the highly soluble PVAc was prepared by solution polymerization. The PVAc was employed as an electrolyte in DSSC. The PVAc was characterized using SEM, XRD and conductivity measuring techniques. The prepared electrolyte behaved as gel electrolyte. SEM images shows the excellent dispersion PVAc in liquid electrolyte. The conversion efficiency achieved using gel electrolyte was 4.18%, which was comparable to liquid electrolyte with a value of 4.57%. the gel electrolyte has the advantage of high efficiency, cheap, easy fabrication, environmentally friendly and stable. As a result, the stability and efficiency of DSSC can be improved by improving the conductivity of the gel electrolyte in case of polymer nanocomposite.

ACKNOWLEDGMENT

We would like to acknowledge Assistant Professor Dr. Muhammad Noman for his valuable knowledge and experience which helped us in achieving this milestone. We are also thankful to our fellow students, faculty and all the staff members of United States Pakistan Center for Advanced Studies in Energy (US.PCAS-E) at UET Peshawar for their support in this work. We are also thankful to USAID for providing us financial support in our MS studies.

REFERENCES

[1] Su'ait, M. S., Rahman, M. Y. A., & Ahmad, A. (2015). Review on polymer electrolyte in dye-sensitized solar cells (DSSCs). Solar Energy, 115, 452-470.

[2] Mussard, M. (2017). Solar energy under cold climatic conditions: A review. Renewable and Sustainable Energy Reviews, 74, 733-745.

[3] Kibria, M. T., Ahammed, A., Sony, S. M., Hossain, F., & Islam, S. U. (2014). A Review: Comparative studies on different generation solar cells technology. In Proc. of 5th International Conference on Environmental Aspects of Bangladesh.

[4] Bagher, A. M., Vahid, M. M. A., & Mohsen, M. (2015). Types of solar cells and application. American Journal of Optics and Photonics, 3(5), 94-113.

[5] Kumar, S., Nehra, M., Deep, A., Kedia, D., Dilbaghi, N., & Kim, K. H. (2017). Quantum-sized nanomaterials for solar cell applications. Renewable and Sustainable Energy Reviews, 73, 821-839.

[6] Gong, J., Sumathy, K., Qiao, Q., & Zhou, Z. (2017). Review on dye-sensitized solar cells (DSSCs): Advanced techniques and research trends. Renewable and Sustainable Energy Reviews, 68, 234-246.

[7] Yun, S., Freitas, J. N., Nogueira, A. F., Wang, Y., Ahmad, S., & Wang, Z. S. (2016). Dye-sensitized solar cells employing polymers. Progress in Polymer Science, 59, 1-40.

[8] Bagher, A. M., Vahid, M. M. A., & Mohsen, M. (2015). Types of solar cells and application. American Journal of Optics and Photonics, 3(5), 94-113.

[9] Al-Alwani, M. A., Mohamad, A. B., Ludin, N. A., Kadhum, A. A. H., & Sopian, K. (2016). Dye-sensitised solar cells: Development, structure, operation principles, electron kinetics, characterisation, synthesis materials and natural photosensitisers. Renewable and Sustainable Energy Reviews, 65, 183-213.

[10] Lee, C. P., Li, C. T., & Ho, K. C. (2017). Use of organic materials in dye-sensitized solar cells. Materials Today.

[11] Ye, M., Wen, X., Wang, M., Iocozzia, J., Zhang, N., Lin, C., & Lin, Z. (2015). Recent advances in dye-sensitized solar cells: from photoanodes, sensitizers and electrolytes to counter electrodes. Materials Today, 18(3), 155-162.

[12] Kumara, N. T. R. N., Lim, A., Lim, C. M., Petra, M. I., & Ekanayake, P. (2017). Recent progress and utilization of natural pigments in dye sensitized solar cells: A review. Renewable and Sustainable Energy Reviews, 78, 301-317.

[13] Mehmood, U., Al-Ahmed, A., Al-Sulaiman, F. A., Malik, M. I., Shehzad, F., & Khan, A. U. H. (2017). Effect of temperature on the photovoltaic performance and stability of solid-state dye-sensitized solar cells: A review. Renewable and Sustainable Energy Reviews, 79, 946-959.

[14] Lee, C. P., Li, C. T., & Ho, K. C. (2017). Use of organic materials in dye-sensitized solar cells. Materials Today, 20(5), 267-283.

[15] Yusof, S. M. M., & Yahya, W. Z. N. (2016). Binary ionic liquid electrolyte for dye-sensitized solar cells. Procedia engineering, 148, 100-105.

[16] Mohamad, A. A. (2016). Absorbency and conductivity of quasi-solid-state polymer electrolytes for dye-sensitized solar cells: A characterization review. Journal of Power Sources, 329, 57-71.

[17] Mittal, G., Dhand, V., Rhee, K. Y., Park, S. J., & Lee, W. R. (2015). A review on carbon nanotubes and graphene as fillers in reinforced polymer nanocomposites. Journal of Industrial and Engineering Chemistry, 21, 11-25.

[18] https://en.wikipedia.org/wiki/Polyvinyl_acetate#cite_note-1. 23 sept. 2018.

[19] Fares, S. (2011). Frequency dependence of the electrical conductivity and dielectric constants of polycarbonate (Makrofol-E) film under the effects of [gamma]-radiation. Natural Science, 3(12), 1034.

[20] Yeum, J. H., Park, J. H., Choi, J. Y., Kim, J. W., Han, S. K., & Oh, W. Polymer/Montmorillonite/Silver Nanocomposite Micro-and Nanoparticles Prepared by In-Situ Polymerization and Electrospraying Technique.

[21] Safenaz, M. R., & Sheikha, M. (2012). Synthesis and electrical properties of polyaniline composite with silver nanoparticles. Advances in Materials Physics and Chemistry, 2012.

[22] Fares, S. (2011). Frequency dependence of the electrical conductivity and dielectric constants of polycarbonate (Makrofol-E) film under the effects of [gamma]-radiation. Natural Science, 3(12), 1034.

Shafi ur rehman has received B.Sc Mechanical Engineering degree from department of Mechanical Engineering University of Engineering and Technology Peshawar, Pakistan in 2014. He is currently pursuing M.Sc degree in Materials for energy storage and conversion from United States Pakistan Center for Advanced Studies in Energy (USPCAS-E) at University of Engineering and Technology Peshawar. He worked on Third generation solar cells that is Dye sensitized solar cells to improve its performance and stability.

International Journal of Engineering Works
ISSN-p: 2521-2419
ISSN-e: 2409-2770
Vol. 6, Issue 07, PP. 221-223, July 2019
https://www.ijew.io/
https://doi.org/10.34259/ijew.19.607221223

Insulated Concrete Blocks Using Plastic Waste and Steel Fibers

Umair Khan[1], Qazi Sami Ullah[2], M.Fawad Gul[3], Iftikhar Ahmad[4], Khawar Naveed Abbasi[5]
[1,3]Research Student, Center for Advance studies in Energy, University of Engineering and Technology, Peshawar, Pakistan
[2]Assistant professor, Dept. of Civil Engineering, University of Engineering and Technology, Pakistan.
[4]Assistant Professor, Dept of Energy Research Center, Comsates University Islamabad, Lahore Campus.
[5]Assistant professor, Dept. of Mechanical Engineering, Capital University of Science & Technology, Pakistan.
umair221143@gmail.com[1], Fawad9809701@gmail.com[2]
Received: 01 July, Revised: 07 July, Accepted: 09 July

***Abstract*—** Plastic is used in abundance due to its various beneficial properties. All forms of consumed plastic become waste and require large areas of land for storage. The low biodegradability of plastic and its presence in large quantity negatively affects the environment. Researchers have developed numerous techniques to recycle plastic. However, each technique has its own demerits. Such as use of solid plastic waste as aggregates in concrete, affects the concrete mechanical properties. Therefore, the objective of this research work is to regain concrete strength by using steel fibers in combination with PET plastic aggregates and investigate its effect on mechanical and thermal insulation properties of concrete. Different specimen were tested for compressive and tensile strength to find out the effect of plastic aggregates incorporation as fine aggregates replacement on strength of concrete. There was noticeable decrease in the compressive and split tensile strength of concrete at 20% replacement of sand by PET plastic aggregates. Steel fibers were also added to the concrete mixes which increase the strength of concrete mixes. After getting satisfactory results of mechanical properties, finally specimen were tested for thermal insulation properties. Results showed that thermal conductivity of samples decrease considerably with addition of plastic aggregates and it leads to good insulation properties of concrete.

Keywords--- Concrete, Plastic, Aggregates, Mechanical, Analysis.

I. INTRODUCTION

Plastics have become an inseparable and integral part of our lives. The amount of plastics consumed annually has been growing steadily. Its low density, strength, fabrication capabilities, long life, light weight, and low cost are the factors behind such phenomenal growth. Plastic waste has many harmful effects on environment and its proper disposal is essential. Landfilling is one approach for waste plastic disposal but it is dangerous due to its slow degradation rate. The waste mass may hinder the ground water flow and causes water contamination. Plastic waste also contains various toxic elements especially cadmium and lead, which can mix with rainwater and pollute soil and water. Due to high calorific value of plastic waste, incineration can also be used as a method of disposal. However, burning of plastic pollute the air by releasing numerous poisonous gases, including dioxins. Plastic can be recycled through different techniques but it is not an economically efficient process to recycle the plastic as it degrades in quality and needs some new plastic to produce the original product. Recycling of plastic waste to produce new materials, such as cement composites appears as one of the best solution for disposing of plastic waste due to its economic and ecological advantages.

Although these disposal methods are feasible, recycling of plastic waste to produce new materials, such as cement composites, appears a best solution due to its ecological and economic benefits. Extensive work in recycling is already done on the use of plastic waste as polyethylene terephthalate (PET) bottle [1,2], high density polyethylene (HDPE) [3], poly vinyl chloride (PVC) pipe [4], shredded and recycled plastic waste [5], glass reinforced plastics (GRP) [6], expanded polystyrene foam (EPS) [7], polycarbonate [8], polypropylene fiber [9], polyurethane foam [10,11], a fiber or filler in the making of concrete. This paper investigates the effect of PET plastic aggregates in combination with steel fibers on mechanical and thermal insulation properties of concrete. The use of PET waste aggregates in concrete will help in disposal of wastes and, will also reduce the environmental damages caused by the use of natural mineral aggregates resources.

II. EXPERIMENTAL

A. Materials

Materials use in this study are Type 1 Portland cement, river sand, ¾ inch coarse aggregates and water. ASTM C33 was used to examine gradation of fine and coarse aggregates. PET aggregates were obtained from PET bottles. [12] Hooked shape steel fibers with dimensions 65mm length and .5mm diameter were used. Mix design ratio of 1:2:4 was used with targeted strength of 20MPA.

B. Test Methods

Twenty four cylinders (r=3inch, h=12inch) and 12 rectangular samples (25*100*100)mm were prepared. All specimens cured in water for 28 days. Cylinders were tested for compression and splitting tensile strength and rectangular samples were tested for thermal conductivity. UTM machine was used to determine Compressive and Split tensile strength. Thermal conductivity was calculated by thermal conductivity of building apparatus. After calculation of heat flux and temperature difference, Fourier's law was used to determine thermal conductivity. ASTM C39 was used for compressive strength, ASTM C496 was used for split tensile strength and ASTM C518 was use for thermal conductivity measurement.

III. RESULTS AND DISCUSSION

A. Density

Density of concrete is an important property and it depends on the amount and density of aggregates added along with air content and water and cement ratio. Results in kg/m^3 are shown in figure 1. Plastic aggregates are lighter than sand that is why there is a decrease in density upon addition of plastic aggregates.

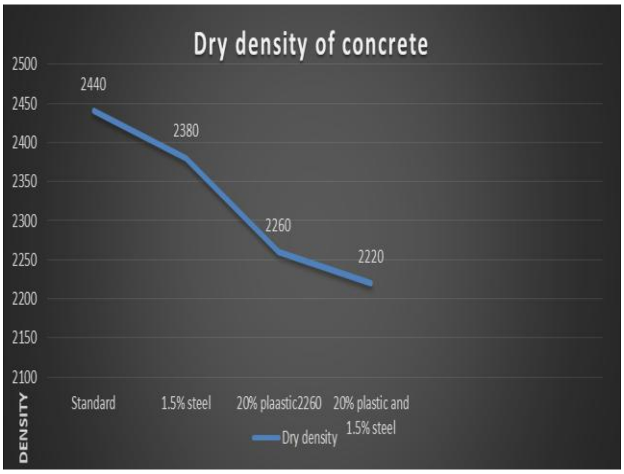

Figure 1 Density of different samples

B. Compressive strength

Compressive strength results at 28 days are shown in table I. Compressive strength decreases by 38% after replacing sand with 20% of plastic aggregates. This is attributed to the fact that adhesive forces are less between plastic surface and natural aggregates and lower strength of plastic aggregates.[13] Similarly after addition of 1.5% steel fibers there is 15% increase in compressive strength which can be attributed to good mechanical properties of steel.[14]

TABLE I. COMPRESSIVE STRENGTH RESULTS

Type of sample	Compressive Strength (MPA)	Percentage change
Standard	18.64	0%
20% plastic	11.71	-38%
1.5% Steel	21.91	15%
20% plastic + 1.5% Steel	15.1	-19%

C. Splitting Tensile Strength

Results of split tensile strength are given in table II. Split tensile strength decreases by

10% after replacing sand with 20% of plastic aggregates. Similarly after addition of 1.5% steel fibers there is 16% increase in split tensile strength which can be attributed to good mechanical properties of steel.

Final sample of concrete where both steel fibers and plastic aggregates are added show average strength of 6.75 MPA, with 4.4% decrease compared to control samples.

TABLE II. SPLITTING TENSILE STRENGTH RESULTS

Type of sample	Split Tensile Strength (MPA)	Percentage change
Stanadard	6.96	0%
20% plastic	6.27	-10%
1.5% Steel	8.27	16%
Final	6.75	-4.4%

D. Specific Heat

Results of specific heat are shown in table IV. Results indicate that with addition of 20% plastic aggregate there is 13% increase in specific heat value. Decrease in specific heat value is just 1% with addition of 1.5% steel fibres.

TABLE III. SPECIFIC HEAT RESULTS

S.No	Type of sample	C (J.Kg-1 .K-1)
1	Control samples	725
2	20% Plastic	828
3	1.5 % steel	731
4	20% Plastic+1.5 % steel	810

E. Thermal Conductivity

Results of thermal conductivity are shown in table III. Results show that with addition of plastic aggregates thermal conductivity decrease considerably. This can be attributed to the lower thermal conductivity and density of plastic aggregates as compared to natural sand. After the addition of 20% plastic aggregates, thermal conductivity decrease by 28%. Addition of steel fibers increase thermal conductivity by 7.5% but due to 28% decrease because of plastic aggregates, final specimen have 17% decrease in the value of thermal conductivity.

TABLE IV. THERMAL CONDUCTIVITY RESULTS

Type of sample	Thermal conductivity (Wm-1 K-1)	Percentage change
Stanadard	1.31	0%
20% plastic	.94	-28%
1.5% Steel	1.40	7.5%
20% plastic and 1.5% Steel	1.09	-17%

CONCLUSION

The following conclusion can be drawn from this research.

1. The dry density of concrete decreases with addition of plastic aggregates as replacement of sand, which means it can be used as light weight concrete.

2. The compressive strength decreases with incorporation of 20% plastic aggregates, but with addition of 1.5% steal fibers some lose in strength is recovered. Compressive strength decreases by 38% with incorporation of 20% plastic and increases by 15% with incorporation of 1.5% steel fibers.

3. The splitting tensile strength also decreases with plastic aggregates, but this decrease is much smaller compared to compressive strength. Splitting tensile strength decreases by 10% with incorporation of 20% plastic and increases by 16% with incorporation of 1.5% steel fibers.

4. Plastic has low thermal conductivity compared to concrete. Thermal conductivity of concrete will decreases with addition of plastic aggregates, which means it will provide better insulation in building compared to normal concrete. After the addition of 20% plastic aggregates, thermal conductivity decreased by 28%. There is a slight increase of 7.5% in thermal conductivity with incorporation of 1.5 % steel fibers. On the other hand specific heat increases with addition of plastic aggregates. Specific Heat Increases with Incorporation of plastic aggregates. Overall our final specimen shows much better insulation properties compared to standard concrete.

ACKNOWLEDGEMENT

I am very thankful to my supervisor Dr.Qazi Sami Ullah for his sincere counseling and guidance. I am also thankful to Dr.Khawar Naveed for allowing thermal testing on the apparatus available in CUST Islamabad. I would also like to thank Dr. Iftikhar Ahmed for his counseling.

REFERENCES

[1] Cordoba, L.A., Berrera, G.M., Diaz, C.B., Nunez, F.U., Yanez, A.L., 2013. Effects on mechanical properties of recycled PET in cement-based composites. Int. J. Polym. Sci. 2013, 1e6

[2] Araghi, H.J., Nikbin, I.M., Reskati, S.R., Rahmani, E., Allahyari, H., 2015. An experimental investigation on the erosion resistance of concrete containing various PET particles percentages against sulfuric acid attack. Constr. Build. Mater. 77, 461e471.

[3] Naik, T.R., Singh, S.S., Huber, C.O., Brodersen, B.S., 1996. Use of post-consumer waste plastic in cement-based composites. Cem. Concr. Res. 26, 1489e1492.

[4] Kou, S.C., Lee, G., Poon, C.S., Lai, W.L., 2009. Properties of lightweight aggregate concrete prepared with PVC granules derived from scraped PVC pipes. Waste Manag. 29, 621e628.

[5] Bhogayata, A., Shah, K.D., Arora, N.K., 2013. Strength properties of concrete containing post-consumer metalized plastic wastes. Int. J. Eng. Res. Technol. ISSN: 2278-0181 2 (3).

[6] Asokan P, Osmani M, Price ADF. Improvement of the mechanical properties of glass fibre reinforced plastic waste powder filled concrete. Constr Build Mater 2010;24:448–60

[7] Kan A, Demirbog˘a R. A novel material for lightweight concrete production. Cem Concr Compos 2009;31:489–95.

[8] Hannawi K, Kamali-Bernard S, Prince W. Physical and mechanical properties of mortars containing PET and PC waste aggregates. Waste Manage 2010;30:2312–20

[9] Bayasi Z, Zeng J. Properties of polypropylene fiber reinforced concrete. ACI Mater J 1993;90:605–10

[10] Fraj AB, Kismi M, Mounanga P. Valorization of coarse rigid polyurethane foam waste in lightweight aggregate concrete. Constr Build Mater 2010;24:1069–77

[11] Mounanga P, Gbongbon W, Poullain P, Turcry P. Proportioning and characterization of lightweight concrete mixtures made with rigid polyurethane foam wastes. Cem Concr Compos 2008;30:806-14

[12] Van Krevelen, D.W., 1990. Properties of Polymers, Elsevier, Amsterdam, The Netherlands, 1990.

[13] Al-Manaseer, A.A., Dalal, T.R., 1997. Concrete containing plastic aggregates. Concrete International 19 (8), 47–52.

[14] Klein, R. Laser Welding of Plastics, 1st ed.;Wiley-VCH: Hoboken, NJ, USA, 2011

Umair Khan who graduated from Ghulam Ishaq khan Institute of engineering sciences and technology in 2015. He holds B.S degree in Mechanical Engineering. He is currently postgraduate student in M.Sc Materials for Energy Storage and Conversion (MESC) at US Pakistan Center for Advanced Studies in Energy (USPCASE) UET Peshawar.

International Journal of Engineering Works
ISSN-p: 2521-2419
ISSN-e: 2409-2770
Vol. 6, Issue 07, PP. 224-227, July 2019
https://www.ijew.io/
https://doi.org/10.34259/ijew.19.607224227

Energy Efficient and CO2 Absorbing Concrete Material

M Fawad Gul[1], Qazi Sami Ullah[2], Umair Khan[3], Iftikhar Ahmed[4], Hayat Khan[5]
[1, 3] Research Student, Center for Advance studies in Energy, University of Engineering and Technology, Peshawar
[2]Assistant Professor, Dept. of Civil Engineering, University of Engineering and Technology, Peshawar.
[4]Assistant Professor, Dept. of Energy Research Center, Comsats University Islamabad, Lahore Campus.
[5]Lecturer, Dept. of Civil Engineering, University of Engineering and Technology, Peshawar.
fawad9809701@gmail.com[1],engrsami@gmail.com[2]
Received: 03 July, Revised: 09 July, Accepted: 12 July

Abstract— Concrete greater consumption in construction due to its high strength releases greenhouse gas emissions both directly and indirectly. In order to reduce the effects of global warming, this research work objective is to construct concrete that can absorb carbon dioxide without affecting strength and life span of concrete structures. Therefore to absorb CO_2, Zeolite is added to cement which would help CO_2 absorption from environment and hence decrease the overall CO_2 content. Moreover concrete has heavy weight and has higher thermal conductivity. Efforts are made in order to make concrete lighter and energy efficient. Introducing foam material in form of polystyrene beads can decrease its density as well as make it energy efficient as its insulation properties will be enhanced. The blocks will be tested for Tension, Compression, and Thermal Insulation as well for CO_2 absorption. Addition of zeolite for absorption of CO_2 and EPS beads for Insulation properties is an innovative approach and helps in a cleaner and healthier environment.

Keywords— Concrete, Zeolite, Eps beads, Compressive Strength, Insulation.

I. Introduction

Concrete is used in abundance on earth after water, however, it use causes greenhouse effect due to emission of gases both directly and indirectly [1].The direct emission of CO_2 occurs during process called calcination that occurs through chemical process in which $CaCO_3$ is converted into CaO and CO_2, however indirect emission is due to the burning of fuels to heat the kiln [2]. To reduce the atmospheric imbalance as well as global warming, we need to design blocks that can absorb CO_2[3]. Zeolite is a material, which absorb CO_2 after adding it to cement due to its sieve like structure and catalytic behaviour. This will help cement absorbing specific amount of CO_2 and thus it can minimize the amount of CO_2 in atmosphere [4,5]. Moreover Zeolite replaced in place of cement will help reduce CO_2 in process of calcination.The second major problem is greater thermal conductivity of concrete, which can be decreased by adding some insulating material like polystyrene beads. This arrangement decreases the concrete density, thus reduces the weight of structural members. Addition of polystyrene beads inturn increases sound proofing and insulation properties of these blocks as well as make them energy efficient as environment will have less impact on them [6].Emissions of CO_2 varies, and it depends on the production of cement, range may be from 0.73 to 0.99 per ton, where more than half of its total amount is released during its production. Many materials like supplementary cementitious material (SCM) or fly ash are substituted in concrete [7,8]. Probably the most common material used is zeolite. This decreases the consumption of cement in concrete which in turn reduces the CO_2 emissions in cement industries. Natural zeolite as volcano or volcanic sediment material having 3D frame has a structure divided into extremely small channels and pores, which can help in CO_2 absorption in the later stages due to its sieve like structure [9]. In this study, we will describe the feasibility of adding zeolite and polystyrene beads as partial replacement in concrete production, which will help us to generate ecofriendly material in building [10,11].

II. Experimental

A. Materials

Materials used in this study are Type 1 Portland cement, river sand, ¾ inch coarse aggregates and water. ASTM C33 was used to determine gradation of fine and coarse aggregates. Expanded polystyrene beads (EPS) of size 3 to 5mm were used with density of 18 kg/m^3. Zeolite with chemical formula of $NaAlSi_2O_6.H_2O$ was used and had a density of 1.04 g/mL at 25ºc. . Mix design ratio of 1:2:4 was used with targeted strength of 2500psi.

B. Test methods

Twenty four cylinders (radius=3inch, height=12inch), 12 rectangular specimen (25×100×100mm) and 6 rectangular specimens (50×100×100mm) were prepared of normal concrete and samples substituted with EPS beads and zeolite. EPS substitution was 15% in place of coarse aggregates and sand while zeolite was also substituted as 15% in place of cement and sand. The final specimens had both EPS beads and zeolite replacement for 30%. All specimens were compacted with a compacting rod and cured for 28 days in water. Cylinders were tested for compression and splitting tensile strength and rectangular samples were tested for thermal conductivity and CO_2 absorption test. Thermal conductivity was calculated by "Thermal conductivity of building material apparatus" by Guarded Heat Flow Meter Technique [12]. After calculation of heat flux and temperature difference across the specimens, Fourier's law was used to determine their thermal conductivities. CO_2 absorption was confirmed by weight analysis of rectangular specimens using weigh machine. ASTM C39 was used for compressive strength, ASTM C496 was used for splitting tensile strength and ASTM C518 was used for thermal conductivity measurement [13].

III. RESULTS AND DISCUSSION

A. Dry Density

Dry density of concrete depends on the amount and density of added aggregates along with air content and water to cement ratio. Zeolite has its physical properties close to that of cement and sand therefore it doesn't affect the density of concrete too much. EPS beads are very lighter than coarse aggregates and sand hence there is a greater decrease in density upon addition of EPS beads. The results are shown in fig.1 with concrete types on X-axis and their densities in Kg/m^3 on Y axis.

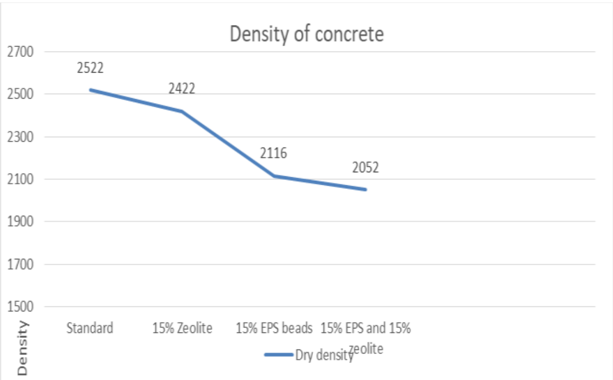

Figure 1 Dry Density of Concrete

B. Compressive strength

All the samples were tested in Universal Testing machine for compressive strength. The testing was done according to ASTM C39 standards. The following results were obtained in table I.

TABLE I. COMPRESSIVE STRENGTH RESULTS

Type of sample	Compressive Strength	Percentage change
Control	2751	0%
15% Eps Beads	2176	-20.1%
15% zeolite	2384	-13.1%
15% Eps Beads + 15% zeolite	2005	-27.01%

The results show that the strength of control samples is quite high and we achieved our targeted strength, but with the addition of 15% EPS beads the strength was reduced almost by 20.1%. Zeolite addition of 15% reduces strength by 13.1%. In our final samples containing both EPS beads and zeolite the strength is reduced by almost 27%. The strength achieved for our final samples is acceptable for concrete structures [14].

C. Splitting Tensile Strength

All the samples were tested in Universal Testing machine for split tensile strength. The testing was done according to ASTM C496 standards. The following results were obtained in table II.

TABLE II. SPLITTING TENSILE STRENGTH RESULTS

Type of sample	Split Tensile Strength	Percentage change
Control	1079	0%
15% Eps Beads	774	-28.1%
15% zeolite	861	-20.2%
15% Eps Beads + 15% zeolite	712	-34.01%

The results show that the strength of control samples is quite high and we achieved our targeted strength, but with the addition of 15% EPS beads the strength was reduced almost by 28.1%. Zeolite addition of 15% reduces strength by 20.2%. In our final samples containing both EPS beads and zeolite the strength is reduced by almost 34%. The strength achieved for our final samples is acceptable for building concrete structures.

D. Thermal Conductivity

Results of thermal conductivity are shown in table III. The aim was to check thermal conductivity value "k" of simple concrete and concrete having zeolite and EPS beads substitutions [15]. Results show that with addition of EPS beads the thermal conductivity decreases considerably. This can be attributed to the lower thermal conductivity and density of EPS beads as compared to coarse aggregates and natural sand. After the addition of 15% EPS beads, thermal conductivity decreases by almost 62.1%. Zeolite doesn't affect the thermal conductivity too much due to the similarity of its properties with sand and cement. Addition of 15% zeolite decreases the thermal conductivity by 8%.Hence, thermal conductivity in final samples is reduced by a total of 70% which is considerably quite high.

TABLE III. THERMAL CONDUCTIVITY RESULTS

Type of sample	Thermal Conductivity	Percentage change
Control	1.38	0%
15% Eps Beads	0.52	-62.1%
15% zeolite	1.27	-8.03%

15% Eps Beads + 15% zeolite	0.42	-70.01%

E. Test on Zeolite Block (CO_2 absorption test)

The aim was to check CO2 absorption by zeolite concrete blocks. The apparatus required was weighing balance, moulds of size 10×10×5 cm. The table IV as shown below.

TABLE IV. WEIGHT ANALYSIS TO CONFIRM CO2 ABSORBTION

	Block B1	Block B2	Block B3	Average of block B1, B2 and B3.	Block B4(Normal concrete block)
Weight of Block on 10th day(gm)	1226	1232	1227	1228	1269
Weight of Block on 14th day(gm)	1233	1240	1231	1234	1264
Weight of Block on 21st day(gm)	1249	1248	1239	1245	1261
Weight of Block on 28th day(gm)	1260	1256	1248	1254	1261

Calculations: Increase in weight of Zeolite block while weight of Normal block remained almost same.

Amount of CO2 absorbed by block: Final Weight – Initial weight/Molecular weight of CO2

Taking the average value of zeolite blocks B1, B2 and B3: 1254-1228/44=0.59 mole CO2 absorbed. Hence a block with 15% substitution of zeolite can absorb about 0.59 mole of CO2 in 28 days.

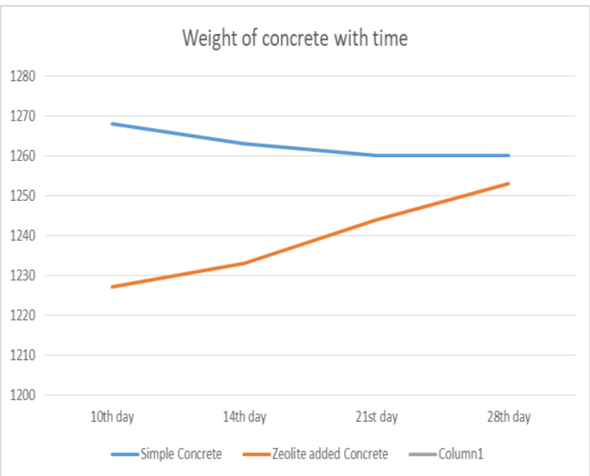

Figure 2 Weight of normal and Zeolite added concrete block with time

CONCUSLION

The following conclusions are drawn out from this research:

1. The dry density of concrete decreases with addition of EPS beads as replacement of Coarse aggregates and sand, which means it can be used as light weight concrete.

2. The compressive strength decreases with incorporation of both EPS beads and Zeolite, but the decrease with EPS beads is high due to very low density of EPS beads. Compressive strength decreases by 21% with incorporation of 15% EPS beads. Addition of 15% zeolite decreases compressive strength by 13%.

3. The splitting tensile strength also decreases with EPS beads and Zeolite addition. Splitting tensile strength decreases by 28% with incorporation of 15% EPS beads and 20% with addition of 15% zeolite.

4. Zeolite helps us in carbon capture in the later stages and substituting it in place of cement also helps to decrease CO2 release in the production stages during calcination hence decreasing the overall carbon signature. Zeolite can be substituted in place cement and sand.

5. The thermal conductivity of concrete decreases with addition of EPS beads, which means it can provide better insulation in building compared to normal concrete. After the addition of 15% EPS beads, thermal conductivity decrease by 62%. Eps beads can be substituted in place of coarse aggregates and sand. The decrease in thermal conductivity in case of zeolite is less as it has its physical properties close to that of sand.

REFERENCES

[1] Madeleine Rubenstein, Emissions from the cement Industry, News from the Earth Institute, May 9, 2012.

[2] Ernst Worrell,Lynn Price, Nathan Martin, Chris Hendriks, and Leticia Ozawa Meida, Carbon Dioxide Emissions from the Global Cement Industry, Annual Review of Energy and the Environment, Vol. 26, pp 303-329, 2001.

[3] Balraj More, Pradeep Jadhav, Vicky Jadhav, Giridhar Narule, Shahid Mulani, CO2 Absorbing Concrete Block, International Journal of technology enhancements and emerging engineering research, Volume 2, pp 2347-4289.

[4] Ranjani V, Siriwardane, Ming-Shing Shen, and Edward P. Fisher, Adsorption of $_2$ on Zeolites at Moderate Temperatures U.S. Department of Energy, Energy & Fuels, 19 (3), pp 1153-1159, 2005.

[5] Semsettin Kılıncarslan "The effect of zeolite amount on the physical and mechanical properties of concrete" International Journal of the Physical Sciences Vol. 6(13), pp. 3041-3046, 4 July, 2017.

[6] G. M. Parton and M. E. Shendy-EI-Barbaryt, Polystyrene-bead concrete properties and mix design, The International Journal of Cement Composites and Lightweight Concrete, Volume 4, pp 153-161, 1982.

[7] Eva Vejmelkova, Dana Konˇakova, Tereza Kulovana, Martin Keppert, Jaromir Z umar, Pavla Rovnanikova, Zbyne k Keršner, Martin Sedlmajer, Robert C erny "Engineering properties of concrete containing natural zeolite as supplementary cementitious material: Strength, toughness, durability, and hygrothermal performance" Cement & Concrete Composites Vol. 55, (2015) pp 259–267M.

[8] Meysam Najimi Meysam Najimi, Jafar Sobhani, Babak Ahmadi, Mohammad Shekarchi "An experimental study on durability properties of concrete containing zeolite as a highly reactive natural pozzolan" Construction and Building Materials Vol. 35, (2012) pp 1023–1033Marcelo Bertalmio, Luminita Vese, Guillermo Sapiro, Stanley Osher, "Simultaneous Structure and Texture Image Inpainting", IEEE Transactions On Image Processing, vol. 12, No. 8, 2003

[9] Fereshteh Alsadat Sabet, Nicolas Ali Libre, Mohammad Shekarchi "Mechanical and durability properties of self-consolidating high performance concrete incorporating natural zeolite, silica fume and fly ash" Construction and Building Materials Vol. 44 pp 175–184 (2013)

[10] J.M. Irwan, R.M. Asyraf, N. Othman, H.B. Koh, M.M.K. Annas and Faisal S.K,The Mechanical Properties of PET Fibre Reinforced Concrete from Recycled Bottle Wastes , Advanced Materials Research Vol. 795, pp 347-351, 2013.

[11] B.D. Ikotun, S. Ekolu "Strength and durability effect of modified zeolite additive on concrete properties" Construction and Building Materials Vol. 24, (2010) pp 749–757

[12] Md Azree Othuman Mydin "Effective thermal conductivity of foam concrete of different densities" School of Housing, Building and Planning, University Sains Malaysia, 11800, Penang, Malaysia.

[13] Bing Chena, Juanyu Liub "Properties of lightweight expanded polystyrene concrete reinforced with steel fiber" Cement and Concrete Research 34 (2004) 1259–1263.

[14] Mark G. Stewart, David V. Rosowsky, Time-dependent reliability of deteriorating reinforced concrete bridge decks, Structural Safety, Volume 20, pp 91-109, 1998.

[15] Aman Mulla, Amol Shelake "Lightweight Expanded Polystyrene Beads Concrete" International Journal of Research in Advent Technology (E-ISSN: 2321-9637) Special Issue National Conference "VishwaCon'16", 19 March 2016.

M. Fawad Gul who graduated from Ghulam Ishaq khan Institute of Science and Technology in 2015. He holds B.Sc degree in Material Engineering.He is currently postgraduate student in M.Sc Materials for Energy Storage and Conversion (MESC) at US Pakistan Center for Advanced Studies in Energy (USPCASE) UET Peshawar.

International Journal of Engineering Works
ISSN-p: 2521-2419
ISSN-e: 2409-2770
Vol. 6, Issue 07, PP. 228-234, July 2019
https://www.ijew.io/
https://doi.org/10.34259/ijew.19.607288234

A Survey Report on Multi Level-Inverter Topologies

Muhammad Ilyas[1], Tanvir Ahmad[2], Shifaat Ur Rehman[3]
[1,2,3]US Pakistan Center For Advanced Studies in Energy, University of Engineering and Technology, Peshawar, Pakistan
milyas0009@gmail.com[1], tanvir.ahmad@uetpeshawar.edu.pk[2], shifaatqurtuba@gmail.com[3]
Received: 12 July, Revised: 17 July, Accepted: 24 July

Abstract—Electricity demand is continuously increasing due to dependency of industrial, commercial and residential users on advance technology. To address this issue is the prime need of time. Modern trend is to harvest energy from renewable sources such as wind, PV etc, which is environmental friendly and economical comparatively. However, as Renewable-Energy- Sources (RES) are sprinkled in small scale by the nature, so usually it is difficult to get a scalable amount of energy. Furthermore, the power quality is much affected due to varying nature of these RES sources. To get maximum efficiency and reliable operation from RES, different inverter topologies are presented. This paper highlights four types of Multilevel-invertertopologies commonly used for smoother, reliable and efficient operation of renewable energy sources (RES) in medium and high power applications. These are Neutral Point-Clamped (NPC) or also called Diode-Clamped Multi Level-Inverter(DCMLI), Flying-Capacitor(FCMLI), Cascaded-Inverter (CMLI) and a Hybrid/ Mixed Multi Level-Inverter topology(HMLI/MMLI). Each topology when used with renewable energy sources has its own features with corresponding advantages and disadvantages. This review is based on controlling methodologies, Total-Harmonic-Distortion (THD), construction complexity and components need for the respective topology. Multi-level-inverter (MLI) has the advantage of extinguishing the need of passive filtering at the grid side, and hence efficiency of the grid and cost minimization can be achieved.

Keywords— Multi Level Inverter(MLI), Clamped-Inverter, Total-Hormonic Distortion(THD).

I. Introduction

Electrical energy in this modern era of technology acts like backbone in the economic development of state as well as to enhance the living standards of the mankind. With recent advancement in technology during last several decades, human dependency on electrical energy hiked up. Machinery becomes a part of our life. Electrical equipments are widely used in industrial sector, house holds and commercial building to accomplish different task. Furthermore, the rise in population and industries occurs at alarming rate, in such a case it is a huge challenge to meet the energy demand for country development and boosting-up economy [1] . Majority of the energy nowadays is produced from Non-Renewable-energy sources (NRES) including Gas, Petroleum, Coal etc. but after several hundred years it will enervates [1]. Also it has enormous environmental impacts on the environmental, as it yields responsible for the destruction of ozone layer, hence causing Green-House-effects and rise in temperature [1].

Over the last few decades, research interest is diverted to get energy fromRenewable-Energy-sources(RES) instead of conventional ways of harnessing energy from fuels, coals etc. due the environmental concerns and depleting fossil fuels to meet the increasing demand of the load [2]. By integrating RenewableeEnergy Sources(RES) with the traditional grids can help us in overcoming energy shortage issue. The power from renewable energy sources can not be used directly by load or fed into grid, so a power electronics converters are used for interfacing.

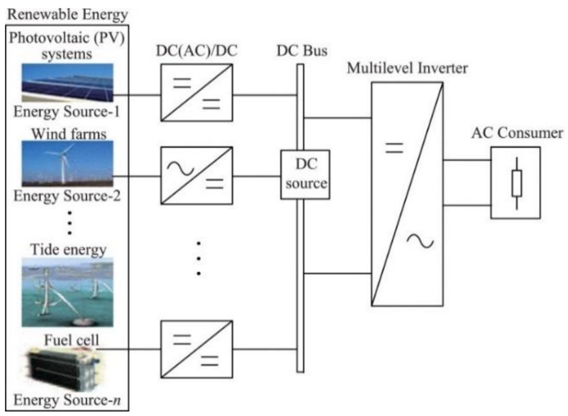

Figure 1: Illustration of Renewable-Energy-Integrated-System (REIS) [3].

As some of the Renewableeenergy sources (PV) like Fuel cell, Solar PV generate DC at it output while some produce AC, in such a case it is prerequisite to convert AC in-to DC for the purpose of storage in batteries. Whenever fault occur or power demand increases from the traditional-Grid, the stored energy is then converted back into AC from stored-DC with the help of Multi-level-Inverter(MLI) to bear the increased demand from load side. Figure 1 below shows an integrated solar PV, Wind,Tide, and so on.., connected to a DC-Bus by AC-DC/DC-DC converters which is then stored in capacitors or batteries [3, 4]. DC-Bus is then connected to a traditionallGRID with the help of Multi-Level-inverter(MLI) converting DC current either stored in batteries or directly from RES sources into AC [5].

Different types of Multi-Level-Inverter(MLI) topologies are recommended in last two decades for improving power quality, Total Harmonic Distortion [6], efficiency and is widely used nowadays for different application of renewable energy integration system (REIS) [5]. It is a well known fact, that Renewable-energy-sources (RES) efficiency is relatively less, if compared with other types of traditional fossil fuels, so it is needed to address this drawback and boost the system efficiency and power quality by harvesting the maximum possible energy from Renewable-Energy-Sources(RES). To maximize generation usually MPPT algorithm is applied at the source side while power quality can be increased and Total-Harmonic-Distortion(THD) can be condensed by increasing the Number of voltage-levels, and thus efficiency of Renewable-Energy-Sources(RES) enhances.

II. Literature Survey

Over the past two decades, Multi-level-inverter have been developed with having a medium and higher power ratings and is used for integration and interfacing of Renewable Energy Sources(RES) like wind, Solar Photo-Voltaic(PV) etc, to the grid [7]. Majority of the Renewable Energy-Sources(RES) produce DC, which can be converted into desired AC power level by the help of Multi-Level-Inverter(MLI). Multi-Level- Inverter(MLI) are best for medium and higher power application [8] and are more worthy for Renewable-Energy- Sources(RES), due to its reduced disturbances and operation at lower switching frequency [9]. It provide smoother output waveforms due to increased number of level and hence a considerable reduction in Total harmonic distortion(THD) [10, 11]. There is an inverse relation between Total harmonic distortion and number-of-levelsNL, if the number-of-levels are increased such that it reaches to infinity, the total harmonic distortion will be zero [12].

However it is not that much easy task to rise the No oflevels (NL), because increasing the No-of-levels(NL) requires additional components and similarly increases the control complexity and hence cost [9]. Therefore it is required to select the best suitable topology from the available topologies in order to overwhelm the mentioned complications. Multiple multi-level-inverter topologies are highlighted in the relevant works for this cause [13].

The principal Multi Level-Inverter topologies are:

A. Diode Clamped Multi Level-Inverter(DCMLI) [14–16].
B. Flying-Capacitor Multi Level-Inverter(FCMLI) [17, 18].
C. Cascaded Multi Level-Inverter(CMLI) [19, 20].
D. Hybrid Multi level-Inverter(HMLI) [20].

Each of the topology mentioned above has its own advantages and disadvantages which are highlighted in detail below. Research and efforts of the engineers are for topology that gives better control of both voltage and frequency, increase the number of AC level with minimized control complexity and there drive circuits, reduced Total harmonic distortion and use small number of components i.e. switches and capacitors e.t.c. This paper presents a comparison between several principal topologies, emphasizing their pros and cons, number of components used. The detail study is as under.

(A) Diode-Clamped Multi Level Inverter(DCMLI):

Diode-clamped Multi-Level-Inverter was presented for the first time by Nabae in 1981, which was consist of 3-levels [21]. Experimental outcomes for 4, 5 and 6-level inverter articles are published in 1990's, by many researchers [22, 23]. Diode- Clamped or also called Neutral-Point-Clamped Multi-level- Inverters(MLI) has diode for clamping the DC voltage of the source and hence a step waveform is formed at the output [24]. For achieving -levels in a Diode clamped MLI to achieve -levels the following components are required [24]:

- Diodes for clamping:
- Number of switches:
- Capacitors for DC Link:)

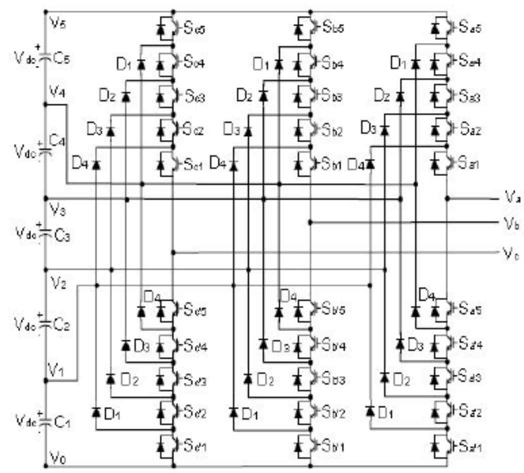

Figure 2: 6-level, 3-Phase Diode clamped MLI [25].

Figure 2, shows a sketch of -phase, -level Diode-clamped MultiiLevel-Inverter(MLI).Capacitor -to- are connected in series with each other, which are connected across the voltage source Vdc. The source voltage Vdc divides in capacitor -to- .The semi-conductor switches and , (where) are controlled by employing Pulse-Width-Modulation(PWM) approach. The function of switches is to allow the capacitor voltage to appear at the output. The Diode is used to block different level of voltages. Diode is used to block Four-Levels, and the process continues in such away that finally is used to block One-Level, respectively. By following this sequence, a step waveform is generated at the output of MLI.

Advantages

- Requires Less number of sources [24].
- Single source is shared by Cascaded Capacitors [25].
- THD decreases as the number of level increases, enhancing power quality [10].
- Gives Better Efficiency for switching at fundamental frequency [26].
- Capacitors can be Pre-Charged in the form of Group [25].
- Suitable for adjustable speed drive applications[27].

Disadvantages

- Over-charging and Dis-charging of inverter DC-Levels is hard to control and monitor [27].
- Real Power flow is affected [28].
- If Number-of-Levels are , Then Number of Clamping-Diodes are needed. Thus increasing complexity [27, 29, 30]

(B) Flying-Capacitor Multi-Level Inverter(MLI)

Flying-Capacitor Multi level-Inverter(FCMLI) or also called Capacitor-Clamped Multi Level-Inverter, is analogous in appearance to Diode-Clamped Multi-Level-inverter, but instead of diodes it uses balancing capacitor to keep voltages at the required value [1]. Figure 3, shows a schematics of Flying-Capacitor Multi Level-Inverter, in which charging and Dis-charging of the capacitors connected to neutral point determines the level of voltage [31, 32].When semi-conductor switches and is Switched-ON, Flying Capacitors in link start charging. When the same switches is switched-off, semiconductor switches and charges the flying capacitor link, while in switched-off condition of these switches, the same capacitors start dis-charging [31]. Multi-levels of voltage at the output of MLI is produced due to different time-constants of each Clamping-Capacitor. The number of Clamping-Capacitors required to obtain -levels is $((N_L - 1)$ [32]. Similarly the number of capacitors required is ( ) , as like for that of Diode Clamped MLI.

Advantages

- Active and reactive power flow is controllable [31].
- No need of T/F, to get the desired number-of voltage levels [31, 32].
- No need of Clamping-Diode [31].
- Single DC-Source is shared by balancing capacitors[18, 33].
- The inverter can withstand to voltage sags and to outages for short because of enormous number of capacitors [30].

Disadvantages

- Monitoring the voltage-levels is a tedious job in capacitors compared to diodes [34].
- Switching efficiency is lower in real power transmission scenarios[34].
- Difficult to determine the pre-charging time for all capacitors [18].
- Large number of capacitor increases weight and cost and thus complexity in packaging [29].
- Complex control strategy and high frequency, leading to high switching losses in real power transfer [35].

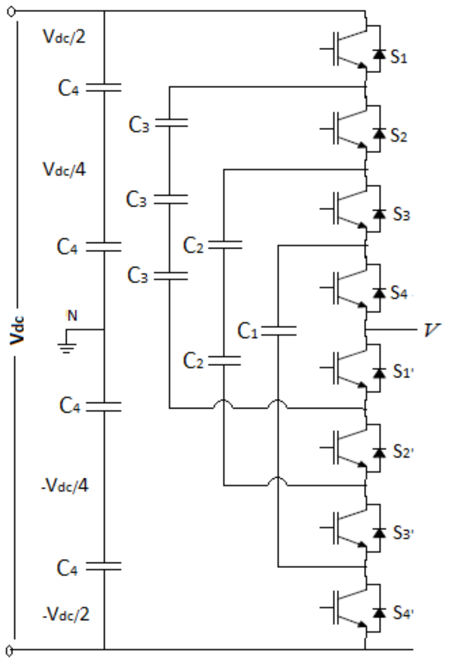

Figure 3: 5-level, 1-Phase Flying-Capacitor MLI [9].

(C) Cascaded Multi-Level-Inverter(CMLI)

Cascaded or H-Bridge Multi-Level-Inverter was invented by Jih-Sheng, in 1996 [36]. It is the simplest of all Multi-levelinverter topologies. Structurally Cascaded-MLI topology is different from Diode-Clamped MLI and Flying-Capacitor MLI topology. No-of-levels in the output waveform can be easily regulated by either joining or elimination of H-bridge. The number of sources required for -levels in cascaded MLI topology is . H-Bridge consist of 4 Semi-conductor switches and a separate supply source is connected to each Bridge [10]. In cascaded MLI topology, all the H-Bridges are attached to one another in cascade. Output is taken between the upper hand of initial bridge and lower hand of last-bridge as demonstrated in Figure 4.

If there are N-number of bridges, the output AC voltage produces will be of levels [37]. The output waveform is generated by individual bridge as, when First-Bridge is in the ON-State, Voltage-level at output is form due to Vdc of respective source connected to that bridge. If Second-Bridge is put into service at same time with first-bridge already in service, Now voltage level in the output waveform will be the sum of two sources connected to first and second bridge, respectively and so on. Finally, in case of N-bridges in the turn ON-state, the voltage-level in output waveform will be the sum of all the sources connected to each bridge, Thus maximum voltage at the output can be achieved. Increasing the number of H-bridges will increase the voltage-levels at the output, thus reducing Total Harmonic-Distortion(THD).

Advantages

- No need of Clamping-Diodes or Capacitors, So total number of components required is less if compared with other topologies [14].
- Possibility to implement soft switching [3].
- DC-Bus regulation is easy [20].
- Semi-conductor switching cycle control is simple with ease in construction [28].
- Packaging is simple and hence can be manufactured in low cost [28].

Disadvantages

- To get higher voltage-levels the number of DC sources required increases [38, 39].
- No common DC Bus [38].
- MLI control technique is implied for controlled operation of H-Bridges, thus output waveform is generated [34].
- Carrier and reference wave form should be synchronized for proper communication between H-Bridges[3].

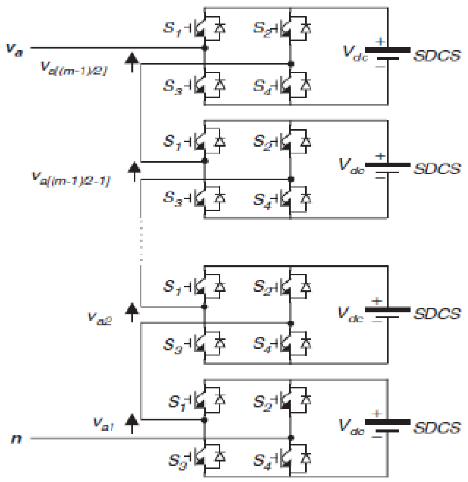

Figure 4: Cascade H-Bridge MLI with N-Bridges

(D) Cascaded Hybrid-Multi-Level-Inverter

Hybrid Multi Level-Inverter is the combination of two or more topologies discussed above in a single structure [20]. The aim of Hybrid Multi-Level inverter topology is to overcome the limitation of basic topologies by combining their benefits into single one and to minimize the number of DC sources connected individually in more power & high voltage applications. A simple Cascaded-Hybrid Inverter is shown in Fig. 5, in which 9-level cascaded inverter is integrated with a 3-level diode-clamped inverter.

In conventional Cascaded H-bridge Multi Level-Inverter(MLI), Single-phase MLI require four DC-sources, while Three-Phase MLI requires 12 DC-sources [40]. However, in this hybrid topology the number of DC sources needed is less comparatively. Also it can be noticed from Figure 5, that the semi-conductor switches required is less compared to other topologies thereby minimizing total number of components, which results in reduction in size,weight and cost [41].

Advantages

- Simple in construction with high reliability [9, 42].
- Less number of separated DC sources is required [9].
- Improved power quality and efficiency [39, 43].
- Lower Electromagnetic interference [42]
- Reduced Power losses and low cost [41, 43].

Disadvantages

- It's use is limited to specific application [34].
- Hybrid structure make its control complex[7, 36].

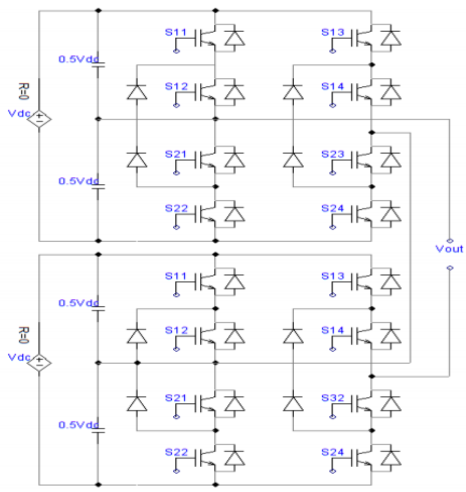

Figure 5: Cascaded Hybrid Multi-Level Inverter(MLI). [38]

III. Topology Comparison

This section gives a brief comparison between Capacitor-Clamped, Diode-Clamped and Cascaded H-Bridge Multi-Level-Inverter topologies. Comparison of components needed for different Multi-LevelInverter topologies are conveyed in Table I.

Figures 6 to 8 shows a general comparison of the components required for each topology, in which Cascade H-Bridge MLI requires the minimal number of elements comparatively.

TABLE I. COMPONENT REQUIRED FOR EACH TOPOLOGY

Basic Topology	Diode-Clamped MLI	Capacitor-Clamped MLI	Cascaded H-bridge MLI
Semi-conductor Switches	*2*(-1)*	*2*(-1)*	*2*(-1)*
Clampingdiodes/ phase	*(-1)*(-2)*	*None*	*None*
DC-Bus-Capacitor	*(-1)*	*(NL-1)*	*0.5*(-1)*
Balancing-Capacitors	*None*	*0.5*(-1) *(-2)*	*None*
Voltage-Unbalancing	*Moderate*	*Maximum*	*Minimum*
Applications	*Motor-drives application's*	*Motor-drives application's*	*Batteries,Wind, PV systems*

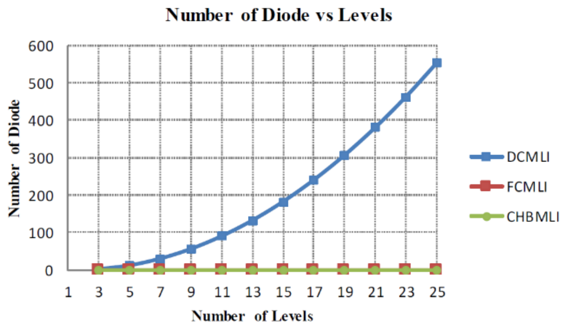

Figure 6: Clamping-Diodes required for MLI.

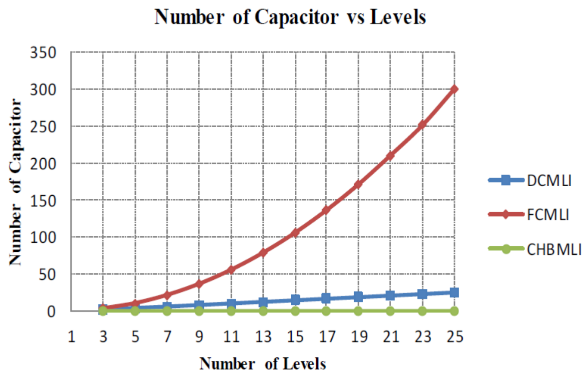

Figure 7: Balancing Capacitors required for MLI.

Figure 6, show that for Diode-clamped Multi-LevellInverter only clamping-diodes are required. Figure-7 is a graph between Number of level and capacitor required. It can be seen from the graph that diode-clamped and capacitor-clamped MLI requires balancing capacitor. Figure 8, shows the total number of components required for each topology. It can be observed, that cascaded H-bridge MLI topology entail minimum number of components and is therefore preferred in various application. like PV,high AC Power supplies etc.

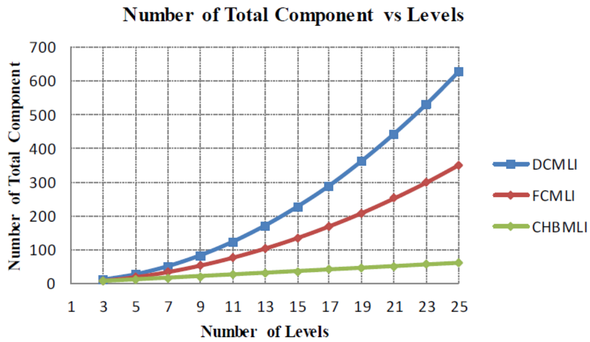

Figure 8: Total Components Required for each topology.

However, the number of sources needed in cascade H-Bridge MLI topology is high. Diode-Clamped and Capacitor-Clamped MLI inverter topologies share a common DC-bus, resulting in reduced number of supply sources [2, 39]. Taking into account the level of complexity, Diode-clamped MLI and Cascaded MLI can be easily controlled than Flying-Capacitor MLI, but construction wise it is a bit complex topology, as it is difficult to select clamping diodes [24]. On the other hand, in case of Flying-Capacitor it is difficult to determine capacitor Pre-charging and Dis-charging time. Detail analysis of all the topologies based on the components requirement and application, Cascaded H-Bridge MLI topology proves to be the best selection among other choices and is widely use in different applications.

CONCLUSION

In this paper a comprehensive discussion on basic multilevel inverter topologies are carried out and compared in different aspects. As each of the topology has its own strength and weaknesses, so the choice of each inverter can made depend upon it application. The most important benefit of Multilevel inverter is providing a solution to THD problem. For Renewable-energy-sources (RES) Cascaded H-Bridge MLI topology seems to be the best option.In Hybrid Renewable-Energy-system (HRES) there are multiple sources like Wind, PV etc. The use of Cascaded H-Bridge MLI topology gives flexibility to connects all the sources to a single inverter, as this topology need to be fed from different sources to get Multi-Level waveform at the output. Cascaded Multi-Level-Inverter(MLI) can be designed using less number of components compared to other MLI topologies. So less number of semi-conductor switches are used, due to which losses as well as total cost is reduced with increased efficiency. The complexity of the circuit also decreases with the decrease of semiconductor switches. Furthermore, the most important benefit is reduction in Total-Harmonic-Distortion as the number of level increases, thus improving power quality.

REFERENCES

[1] G. P. Adam et al. "New flying capacitor multilevel converter". In: 2011 IEEE International Symposium on Industrial Electronics. 2011, pp. 335–339. DOI: 10 . 1109/ISIE.2011.5984181.

[2] S. S. Priyan and K. Ramani. "Implementation of closed loop system for flying capacitor multilevel inverter with stand-alone Photovoltaic input".

In: 2013 International Conference on Power, Energy and Control (ICPEC). 2013, pp. 281–286. DOI: 10 . 1109 / ICPEC . 2013 .6527666.

[3] L. Wang, Q. H. Wu, and W. Tang. "Novel Cascaded Switched-Diode Multilevel Inverter for Renewable Energy Integration". In: IEEE Transactions on Energy Conversion 32.4 (2017), pp. 1574–1582. ISSN: 0885- 8969. DOI: 10.1109/TEC.2017.2710352.

[4] P. Sotoodeh and R. D. Miller. "Design and Implementation of an 11-Level Inverter With FACTS Capability for Distributed Energy Systems". In: IEEE Journal of Emerging and Selected Topics in Power Electronics 2.1 (2014), pp. 87–96. ISSN: 2168-6777. DOI: 10 . 1109 / JESTPE.2013.2293311.

[5] S Senthil and K Ravi. "A new compilation of renewable energy sources using multilevel inverter with space vector modulation techniques". In: Green Computing Communication and Electrical Engineering (ICGCCEE), 2014 International Conference on. IEEE. 2014, pp. 1–6.

[6] Amrita Tuteja, Amita Mahor, and Aarti Sirsat. "A review on mitigation of harmonics in cascaded H-bridge multilevel inverter using optimization techniques". In: International Journal of Emerging Technology and Advanced Engineering 3.2 (2013), pp. 30–34.

[7] J Rodiguez. "Multilevel inverter: a survey of topologies, controls, and application". In: IEEE Transaction on Industrial Electronics 49.4 (2002), pp. 724–738.

[8] Ashish Bendre and Giri Venkataramanan. "Neutral current ripple minimization in a three-level rectifier". In: IEEE transactions on industry applications 42.2 (2006), pp. 582–590.

[9] Derakhshanfar Mohammadreza. "Analysis of different topologies of multilevel inverters". In: (2010).

[10] Dogga Raveendhra, Pracheta Prakash, and Parvesh Saini. "Simulation based analysis of FPGA controlled Cascaded H-Bridge Multilevel inverter fed solar PV system". In: Energy Efficient Technologies for Sustainability (ICEETS), 2013 International Conference on. IEEE. 2013, pp. 568–572.

[11] Yugo Kashihara and Jum-ichi Itoh. "Power losses of multilevel converters in terms of the number of the output voltage levels". In: Power Electronics Conference (IPEC-Hiroshima 2014-ECCE-ASIA), 2014 International. IEEE. 2014, pp. 1943–1949.

[12] H Jabir et al. "Development of a transformer-based multilevel inverter topology for stand-alone photovoltaic system". In: Power Electronics and Applications (EPE),topology for stand-alone photovoltaicvsystem". In: Power Electronics and Applications (EPE), 2013 15th European Conference on. IEEE. 2013, pp. 1–10.

[13] S Boobalan and R Dhanasekaran. "Hybrid topology of asymmetric cascaded multilevel inverter with renewable energy sources". In: Advanced Communication Control and Computing Technologies (ICACCCT), 2014 International Conference on. IEEE. 2014, pp. 1046 1051.

[14] Md Rabiul Islam et al. "A 43-level 33 kV 3-phase modular multilevel cascaded converter for direct grid integration of renewable generation systems". In: Innovative Smart Grid Technologies-Asia (ISGT Asia), 2014 IEEE. IEEE. 2014, pp. 594–599.

[15] Edris Pouresmaeil, Daniel Montesinos-Miracle, and Oriol Gomis-Bellmunt. "Control scheme of three-level NPC inverter for integration of renewable energy resources into AC grid". In: IEEE systems journal 6.2 (2012), pp. 242–253.

[16] Miguel Chaves et al. "New approach in back-to-back mlevel diode-clamped multilevel converter modelling and direct current bus voltages balancing". In: IET Power Electronics 3.4 (2010), pp. 578–589.

[17] Xianglian Xu et al. "FPGA based multiplex PWM generator for diode-clamped cascaded inverter in the direct-driven wind power system". In: Power Electronics and Motion Control Conference (IPEMC), 2012 7th International. Vol. 2. IEEE. 2012, pp. 1268–1272.

[18] Sanghun Choi and Maryam Saeedifard. "Capacitor voltage balancing of flying capacitor multilevel converters by space vector PWM". In: IEEE Transactions on Power Delivery 27.3 (2012), pp. 1154–1161.

[19] Ahmad Alyan et al. "New topology three phase multilevel inverter for grid-connected photovoltaic system". In: Industrial Electronics (ISIE), 2014 IEEE 23rd International Symposium on. IEEE. 2014, pp. 592–599.

[20] Xiaonan Lu et al. "High performance hybrid cascaded inverter for renewable energy system". In: Applied Power Electronics Conference and Exposition (APEC), 2011 Twenty-Sixth Annual IEEE. IEEE. 2011, pp. 970– 975.

[21] Akira Nabae, Isao Takahashi, and Hirofumi Akagi. "A new neutral-point-clamped PWM inverter". In: IEEE Transactions on industry applications 5 (1981), pp. 518–523.

[22] Hee-Jung Kim, Hyeoun-Dong Lee, and Seung-Ki Sul. "A new PWM strategy for common-mode voltage reduction in neutral-point-clamped inverter-fed AC motor drives". In: IEEE Transactions on Industry Applications 37.6 (2001), pp. 1840–1845.

[23] Changliang Xia et al. "Discontinuous space vector PWM strategy of neutral-point-clamped three-level inverters for output current ripple reduction". In: IEEE Transactions on Power Electronics 32.7 (2017), pp. 5109–5121.

[24] Yong Wang et al. "Diode-free T-type three-level neutralpoint- clamped inverter for low-voltage renewable energy system". In: IEEE Transactions on Industrial Electronics 61.11 (2014), pp. 6168–6174.

[25] Muhammad H Rashid. Power electronics handbook. Butterworth-Heinemann, 2017.

[26] Engin Ozdemir, Sule Ozdemir, and Leon M Tolbert. "Fundamental-frequency-modulated six-level diodeclamped multilevel inverter for three-phase stand-alone photovoltaic system". In: IEEE Transactions on Industrial Electronics 56.11 (2009), pp. 4407–4415.

[27] Leon M Tolbert, Fang Zheng Peng, and Thomas G Habetler. "Multilevel converters for large electric drives". In: IEEE Transactions on Industry Applications 35.1 (1999), pp. 36–44.

[28] ID Pharne and YN Bhosale. "A review on multilevel inverter topology". In: Power, Energy and Control (ICPEC), 2013 International Conference on. IEEE. 2013, pp. 700–703.

[29] Sergio Daher. Analysis, design and implementation of a high efficiency multilevel converter for renewable energy systems. Kassel University Press, 2006.

[30] Ibrahim Haruna Shanono. Multilevel converters: the future of renewable energy: design, simulation and implementation of a multilevel converter. LAP LAMBERT Academic Publishing, ein Imprint der/a trademark of AV Akademieverlag GmbH & Company KG, 2012.

[31] Mohamad Agha Shafiyi et al. "A grid-connected PV power supply based on flying capacitor multicell converter with modified MPPT based control for active power filtering". In: Renewable Energy and Distributed Generation (ICREDG), 2012 Second Iranian Conference on. IEEE. 2012, pp. 141–146.

[32] Georgios Konstantinou et al. "The seven-level flying capacitor based ANPC converter for grid intergration of utility-scale PV systems". In: Power Electronics for Distributed Generation Systems (PEDG), 2012 3rd IEEE International Symposium on. IEEE. 2012, pp. 592–597.

[33] Mostafa Khazraei et al. "Active capacitor voltage balancing in single-phase flying-capacitor multilevel power converters". In: IEEE Transactions on Industrial Electronics 59.2 (2012), pp. 769–778.

[34] Ilhami Colak, Ersan Kabalci, and Ramazan Bayindir. "Review of multilevel voltage source inverter topologies and control schemes". In: Energy conversion and management 52.2 (2011), pp. 1114–1128.

[35] Moncef Ben Smida and Faouzi Ben Ammar. "Modeling and DBC-PSC-PWM control of a three-phase flying capacitor stacked multilevel voltage source inverter". In: IEEE Transactions on Industrial Electronics 57.7 (2010), pp. 2231–2239.

[36] Jih-Sheng Lai and Fang Zheng Peng. "Multilevel converters-a new breed of power converters". In: IEEE Transactions on industry applications 32.3 (1996), pp. 509–517.

[37] Muhammad Sadikin, Tomonobu Senjyu, and Atsushi Yona. "High-frequency link DC for power quality improvement of stand-alone PV system in cascaded multilevel inverter". In: Power Electronics and Drive Systems (PEDS), 2013 IEEE 10th International Conference on. IEEE. 2013, pp. 597–601.

[38] Surin Khomfoi and Leon M Tolbert. "Multilevel power converters". In: Power Electronics Handbook (Third Edition). Elsevier, 2011, pp. 455–486.

[39] M Charai et al. "Performance Evaluation for Different Levels Multilevel Inverters Application for Renewable Energy Resources". In: Journal of Engineering Technology (ISSN: 0747-9964) 6.1 (2017), pp. 90–96.

[40] WA Hill and CD Harbourt. "Performance of medium voltage multi-level inverters". In: Industry Applications Conference, 1999. Thirty-Fourth IAS Annual Meeting. Conference Record of the 1999 IEEE. Vol. 2. IEEE. 1999, pp. 1186–1192.

[41] Y. Suresh and Anup Kumar Panda. "Investigation on hybrid cascaded multilevel inverter with reduced dc sources". In: Renewable and Sustainable Energy Reviews 26 (2013), pp. 49 –59. ISSN: 1364-0321. DOI: https : / / doi . org / 10 . 1016 / j . rser . 2013 . 04 . 027. URL: http : / / www. sciencedirect . com / science / article / pii / S1364032113002797. [42] E. Najafi and A. H. M. Yatim. "Design and Implementation of a New Multilevel Inverter Topology". In: IEEE Transactions on Industrial Electronics 59.11 (2012), pp. 4148–4154. ISSN: 0278-0046. DOI: 10.1109/TIE. 2011.2176691.

[42] E. Najafi and A. H. M. Yatim. "Design and Implementation of a New Multilevel Inverter Topology". In: IEEE Transactions on Industrial Electronics 59.11 (2012), pp. 4148–4154. ISSN: 0278-0046. DOI: 10.1109/TIE. 2011.2176691.

[43] Sizhao Lu et al. "Modularized high frequency high power 3-level neutral point clamped PEBB cell for renewable energy system". In: Energy Conversion Congress and Exposition (ECCE), 2014 IEEE. IEEE. 2014, pp. 2594–2599.

Authors Details:

Engr. Muhammad Ilyas has received B.Sc Electrical Engineering degree from Department of Electrical Engineering, University of Engineering and Technology, Peshawar, Pakistan in 2015. He is currently pursuing MS in Electrical Energy Systems Engineering from United States Pakistan Center for Advanced Studies in Energy (USPCAS-E) at University of Engineering and Technology Peshawar. He worked on Efficiency Improvement of Small Scale and Micro Hydro Power Plants for the potential sites in KPK, Pakistan.

Dr. Tanvir Ahmad has received PhD degree with specialization in Wind Farm Coordinated Control and Optimization from School of Engineering and & Computing Science, Durham Universtiy, UK in 2017. He is currently working as a Assistant Professor at US-Pakistance Center for Advance Studies in Energy, University of Enegineering and Technology Peshawar, Pakistan. Tanvir's main research interests involve Smart Control of power system based on Artificial Intelligence (AI) and heuristic based optimization techniques, Energy Management Systems, Energy Auditing, Socio-Technical models for Energy Systems, Data Analytics for efficient utilization of Renewable Energy, Wake Flow Models and Wind Deficit Models.

Engr. Shifaat Ur Rehman has received BS degree in Electrical Engineering from University of Engineering & Technology Peshawar KP, Pakistan in 2014. Currently pursuing MS degree in Electrical Energy System Engineering from US Pakistan Center for Advanced Studies in Energy(USPCAS-E), University of Engineering & Technology Peshawar. He has availed exchange program to the partner university of USPCAS-E Arizona State University (ASU), USA in 2016, as a research scholar. He has good hands on experience in the field of renewable energies especially PV reliability.

国际工程期刊
International Journal of Engineering Works
International Journal of Engineering Works
ISSN-p: 2521-2419
ISSN-e: 2409-2770
Vol. 6, Issue 07, PP. 235-243, July 2019
https://www.ijew.io/
https://doi.org/10.34259/ijew.19.607235243

Minimization of Losses and Improving Stability of High Tension Network using Load Flow Analysis

Tariq Ahmad[1], Inzamam Ul Haq[2], Ahmad Amin[3], Abdul Basit[4]
[1,2,3]Research Assisstants, USPCAS-E, UET Peshawar, Pakistan
[4]Assistant Professor, USPCAS-E UET Peshawar, Pakistan
tariq.ahmad839@yahoo.com[1], inzee@live.com[2], ahmadamin019@gmail.com[3], abdul.basit@uetpeshawar.edu.pk[4]
Received: 07 July, Revised: 16 July, Accepted: 21 July

***Abstract*—** Accessibility of electric power has been the most dominant source for helping social, economic and industrial improvements of any state. From generation station to the feeders and consumers transmission lines are used to carry the power. Pakistan's current energy system is very weak and requires adequate attention, most of it requires upgrading of the transmission scheme. An real-time issue such as voltage degradation, severe outages and system stabilization of a distribution company's is evaluated here. Some of the serious points are evaluated and also the causes discovered for large losses. After analysis using ETAP simulation load flow analysis was carried out and different methodologies were proposed like addition of distributed generation (Micro hydro, PV, Wind etc.) at the load end to how economically we can mitigate these contingencies and make power system more safe and stable. We discovered the most possible, cost-effective alternatives for a certain serious area after full assessment..

***Keywords*—** Technical Losses, Energy, Power Losses, T&D Losses, NTDC, DISCOs, Advance Metering.

I. Introduction

An essential need for the industrial and economic improvement of any country is the electrical power. Electrical power can be classified in various types , yet the most significant sort is the electrical energy [1]. A contemporary and educated society is dependent on the utilization of electrical energy badly. Tasks, which relates with the generation of electricity, distribution to the stations, consumers and transmission of electricity must be dole out the most importance in the national arranging technique of any country due to the significance of electrical energy to the social and economic improvement of the community [2, 3]. Transmission line connects the generation of electrical energy with the substations in power network and is one of the important part of power system; The exploration, calculation and mitigation of transmission and distribution losses in these networks are of incredible worry to electrical engineers [4, 5]. PESCO is one of the important distribution company in total ten companies of Pakistan which has 34% losses [6], the second most in term of losses in all the ten distribution companies.

Electrical power is basically required for the development of any nation [7]. To keep up the generation of electric power at satisfactory dimension the power must be transmitted in appropriate structure and quality to the users. Pakistan's Power Sector is, and has been for a long time, looked by noteworthy difficulties [8]. These incorporate restricted accessibility of dependable and reasonable electric power, aging and insufficient distribution and transmission systems and utility strategies and practices that seriously fall behind those of present day utilities somewhere else on the planet. Besides a current-day, innovation foundation that can empower proficient, back-office activities, for example, dealing with client administration solicitations isn't in proof.

Hazara circle is the 2nd largest circle of PESCO. It contains 14 No of 132KV GSS, 3 No of 66KV GSS and 3 no of 33 KV GSS. After the complete analysis of Hazara network it is found that some of the week points need proper attention for that all the required data has been collected from different points and by using ETAP simulation load flow analysis is done which give a clear a contrast picture of the whole network. Some points were found in very stress and unstable conditions. After the whole analysis different methodology were proposed to take remedial action that how to avoid these stresses (over loading, losses, and force load shedding). After the load flow analysis (LFA) using ETAP many methods were proposed like Integration at load end of Micro Hydro, PV, Wind and Hydel generation that how to remove such type of contingencies from this system, and how to improve system stability. In last the most feasible and long term methods were also proposed, up gradation of 132KV GSS Mansehra to 220KV GSS, Double the Circuit, Renewable integration, bundling, and conductor replacement. But the most economical is the conductor replacement from LYNX to LION conductor.

Electrical energy distribution sector is considered as the poorest connection in the whole power system. Distribution losses are roughly 50 percent while Transmission losses are around 17 percent [9]. Distribution as well as Transmission losses are sorted into two kinds.

A. Technical Losses

Technical losses depends on network characteristics and also on operation mode, these losses are ordinarily 22.5 percent

[9]. Technical losses are further portioned into two sub categorize.

i. Fixed / Permanent Technical losses

- Corona losses
- Losses of continuous load measuring elements
- Leakage Current losses
- Losses of continuous load control elements
- Open-circuit losses
- Dielectric losses

ii. Variable Technical losses

Variable losses change with the distribution of electrical energy and are, all the more precisely, proportionate to the square of the current. so, a 1% change in current prompts a change over 1% [7].

- Between 0.66 and 0.75 of specialized (or physical) losses are variable Losses in a distribution systems.
- Losses of contact resistance.
- Joule losses at each voltage level.
- Cables and cross sectional area of transmission lines are inversely related to losses. This prompts direct exchange between capital expenses cost and expense of losses. It has been prescribed that best normal utilization rate on a distribution stations that considers the expense of losses in its structure could be as low as 30 percent.
- Impedance losses.

Pakistan has an extraordinary rate of electric distribution and transmission losses and is ranked in the top 14th among 131 countries [10]. In figure 1, the statistics of losses in transmission and distribution is shown from 1971 to 2010 according to World Bank analysis.

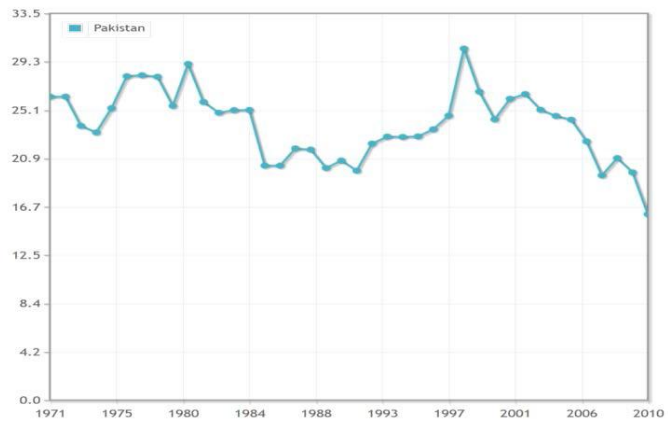

Figure 1. Statistics of losses in transmission and distribution from 1971-2010 [6].

8.8 is the world average, T&D losses in the range of 6 to 8 per centare considered normal in electrical world [11]. PESCO is one of the most important distribution company in total discos, while the losses in PESCO is too much high and it is on no 2nd in losses in total discos which is quite unsatisfactory and mostly affects the consumers as well as the company. These losses are technical and non-technical losses. Some of the places under PESCO need proper attention because the system is old and week.

Load shedding is nowadays a great problem because the deficiency of power in Pakistan is increasing from 1998 [12]. The present operating system is quite weak and unable to sustain more integration, some of the points in system are too weak and proper attention is required, load shedding is also increasing because the generation deficiency but there are also some places where unscheduled load shedding take place which is a big problem and this is due to the system old vintage equipment's so in this project we will find and show some severe places and then propose some methods on how to make those weak points to stable position.

II. Methodology

In this research analysis of a complete power circle and load flow analysis is done using ETAP simulation. It is easily found that some places in the whole network need proper planning and attention, the whole company comprises of many circles of network but Hazara circle is in more stress condition because of its outages and voltage un-stability. In Hazara circle 132KV lines are spread from Burhan (220KV) GSS to Haripur, Abbottabad, Mansehra and Balakot, from Burhan to Haripur and then Mansehra two circuits line are coming while from Abbottabad to Mansehra the line is single circuit, its conductor is LYNX and its current carrying capacity is 480A, The transmission line spread from Abbottabad to Mansehra and then leads to Muzafarabad.

Most of the time when the load increase from 480A or any contingencies occurs due to which system burden increase due to which the conductor starts heating. So to avoid such type of conditions the grid operator used only force load shedding(Outages) which is not the actual solution of this problem.

For vanishing this problem we take the ratting of whole the system and conductor specification, and by ETAP simulation we analyze it by doing its load flow analysis. After analysis it is fond that what was the actual cause of these problems and how we can erase these from over system. For this we proposed different models and methods which are given below:

- Renewable Integration
- Conventional plant integration
- Up-gradation of Mansehra 132KV GSS to 220KV GSS
- Doubling the circuit
- Bundling of transmission line
- Conductor Replacement

III. Modeling

The transmission lines are demonstrated by methods for the parameters such as capacitance, inductance, conductance and resistance. The impedance of the transmission lines are due to the inductance and resistance while the admittance are due to the parallel combination of conductance and capacitance. These four electrical elements play an important role in transmission and distribution system [13].

A. Resistance

The resistance of conductor are negligible[14]. Resistor play significant role in short distance lines. Line current and resistance losses are directly related a current increases the losses are also increases (I2R loss). At the point when the current surpass a specific threshold the heat created because of losses begins to liquefy the conductor and the conductor turns out to be longer that outcomes in more sag [13]. The current at which the state of conductor is irreversible is called thermal threshold of conductor. Short overhead lines ought to be worked well inside this point of confinement.

The value of the ohmic power loss, is given as

$$L_{ohmic} = I^2R \qquad KW / Km / Phase$$

Where

I Indicates current.

R Indicates resistance.

B. Inductance

The line inductance (reactance) is more overwhelming in long as well as in medium distance than resistance[15]. The estimation of current that conducts in a conductor is related with another parameter, inductance. The electrical symbol for inductor is L and its unit is Henry (H). The value of inductor is usually very small, milli Henry(mH). Companies often indicate the inductance per kilometer or mile of transmission lines and cables.

i. Inductance of a two-wire line

A single phase line consists of two conductors 'a' and 'b' (Phase & Neutral) having equal radius 'r' is considered. The conductors are situated at a distance 'D' meters. The diagram below shows the cross section of the conductors. The current flow in conductors is considered in opposte direction as the neutral conductor is return path for the other.

The flux linkages of conductor 'a' is given by the formula [11][13]

$$\lambda_a = 2 \times 10^{-7}\left[I_a In\frac{1}{D_{aa}} + I_b\frac{1}{D_{ab}}\right]$$

Where,

$$I_a = +I$$
$$I_b = -I$$
$$D_{aa} = r'$$
$$D_{ab} = D$$

Substituting these values in above equation

$$\lambda_a = 2 \times 10^{-7}\left[I_a In\frac{1}{r'} - I_b\frac{1}{D}\right]$$

$$= 2 \times 10^{-7} I\, In\frac{D}{r'}$$

Similarly, the flux linkage of conductor 'b' will be

$$\lambda_b = 2 \times 10^{-7} I\, In\frac{D}{r'}$$

The inductance of conductor 'a'

$$L_a = 2 \times 10^{-7} \ln\frac{D}{r'}\ H/m$$

Similarly, the inductance of conductor 'b'

$$L_b = 2 \times 10^{-7} In\,\frac{D}{r'} H/m$$

Inductance per conductor

$$L = L_a = L_b = 2 \times 10^{-7} In\frac{D}{r'} H/m$$

Inductance of both conductors is given by the formula

$$Loop\ inductance = L_a + L_b = 2 \times 2 \times 10^{-7} In\frac{D}{r'}\ H/m$$

$$= 4 \times 10^{-7} In\frac{D}{r'}\ H/m$$

The total inductance of a two-wire line is double the inductance of an individual conductor.

ii. Inductance of symmetrical three-phase line

In symmetrical three-phase line, all the conductors are placed at the corners of the equilateral triangle. This type of arrangement of conductors is also known as 'equilateral spacing', as shown in the diagram below.

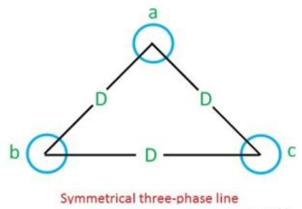

Consider 'D' is the spacing between the conductors and 'r' is the radius of each conductor. Then the equation of conductor 'a' flux linkages will be:

$$\lambda_a = 2 \times 10^{-7}\left(I_a In\frac{1}{D_{aa}} + I_b In\frac{1}{D_{ab}} + I_c In\frac{1}{D_{ac}}\right)$$

In this case

$$D_{ab} = D_{bc} = D_{ac} = D$$

$$D_{aa} = r'$$

$$\lambda_a = 2 \times 10^{-7}\left(I_a In\frac{I}{r'} + I_b In\frac{1}{D} + I_c\frac{1}{D}\right)$$

The algebraic sum of the currents in conductors of a three-wire system is zero.

$$I_a + I_b + I_c = 0$$

$$I_a = -I_b - I_c$$

$$I_a = -(I_b + I_c)$$

So the flux equation becomes

$$\lambda_a = 2 \times 10^{-7} \times \left(I_a In\frac{1}{r'} + (I_b + I_c) In\frac{I}{D}\right)$$

$$\lambda_a = 2 \times 10^{-7}\left(I_a In\frac{1}{r'} - I_a In\frac{1}{D}\right)$$

$$= 2 \times 10^{-7} \times I_a \left(In\frac{1}{r'} - In\frac{I}{D}\right)$$

Using the formula

$$\left(In\, m - In\, n = In\frac{m}{n}\right)$$

The inductance of conductor, 'a' is

$$\lambda_a = \frac{\lambda}{I_a} = 2 \times 10^{-7} In\frac{D}{r'} H/m$$

The inductance of conductor 'b' and 'c' will also be the same as that of 'a'. The inductance of the three-phase line is equal to the two-wire line.

iii. Inductance of unsymmetrical three-phase line

A Three-phase line is said to be unsymmetrical when its conductors are placed at different distances. Such arrangement of conductors is most common in practice because of their cheapness and convenience in design and construction. Consider a three-phase unsymmetrical line, having different spacing between their conductors where the radius of each conductor is r. It is shown in the diagram below [16].

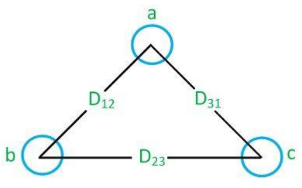

Unsymmetrical three-phase line

Flux linkage in 'a' is expressed by the formula

$$\lambda_{a1} = 2 \times 10^{-7}\left(I_a In\frac{1}{r'} + I_b In\frac{I}{D_{12}} + I_b In\frac{1}{D_{31}}\right)$$

Flux linkage in conductor 'a' due to 'b' is given by the formula

$$\lambda_{a2} = 2 \times 10^{-7}\left(I_a In\frac{1}{r'} + I_b In\frac{1}{D_{23}} + I_c\frac{1}{D_{12}}\right)$$

Flux linkage in conductor 'a' due to 'c' is given by

$$\lambda_{a3} = 2 \times 10^{-7}\left(I_a In\frac{1}{r'} + I_b In\frac{1}{D_{23}} + I_c In\frac{1}{D_{23}}\right)$$

The average value of flux linkages of 'a' is

$$\lambda_a = \frac{1}{3}(\lambda_{a1} + \lambda_{a2} + \lambda_c)$$

$$\lambda_a = \frac{2}{3} \times 10^{-7}\left[\left(I_a In\frac{1}{r'} + I_b In\frac{1}{D_{13}} + I_c\frac{1}{D_{31}}\right) + \left(I_a In\frac{1}{r'} + I_b In\frac{1}{D_{23}} + I_{12}\frac{1}{D_{12}}\right) + \left(I_a In\frac{1}{r'} + I_b In\frac{1}{D_{31}} + I_c In\frac{1}{D_{23}}\right)\right]$$

$$\lambda_a = \frac{2}{3} \times 10^{-7}\left[3I_a In\frac{I}{r'} + I_b In\frac{1}{D_{12}D_{23}D_{31}} + I_c In\frac{1}{D_{12}D_{23}D_{31}}\right]$$

$$\lambda_a = \frac{2}{3} \times 10^{-7}\left[3I_a In\frac{1}{r'} - I_a In\frac{1}{D_{12}D_{23}D_{31}}\right]$$

Since for balanced conditions

$$I_a + I_b + I_c = 0$$

$$I_b + I_c = -I_a$$

$$\lambda_a = 2 \times 10^{-7}\left[I_a In\frac{1}{r'} + \frac{1}{3} I_a In(D_{12}D_{23}D_{31})\right]$$

By using formula

$$\frac{1}{2} In\, m = In\, m^{\frac{1}{2}} \quad \lambda_a = 2 \times 10^{-7} \times I_a In\frac{(D_{12}D_{23}D_{31})^{\frac{1}{3}}}{r'}$$

The average inductance of phase a is

$$L_a = \frac{\lambda_a}{I_a} = 2 \times 10^{-7} \times In\frac{(D_{12}D_{23}D_{31})^{\frac{1}{3}}}{r'} H/m$$

Similarly,

$$L_b = L_c = 2 \times 10^{-7} \times In\frac{(D_{12}D_{23}D_{31})^{\frac{1}{3}}}{r'} H/m$$

Thus, it is found that the values of the inductance for the three phases are equalized by transpositions.

C. Capacitance of Transmission Line

Transmission line conductors creates a capacitor between them. The transmission line conductors act as a parallel plate of capacitor and the air act like a dielectric medium between them. The line capacitance give rise to the leading current between the conductors. It depends on the length of the conductor. Capacitance of two-wire line is given as

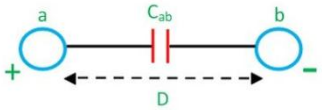

Line-to-line Capcitance

$$C_{ab} = \frac{q_a}{V_{ab}} = \frac{\pi\varepsilon}{In\frac{D}{r}} F/m$$

C_{ab} is referred as line-to-line-capacitance.

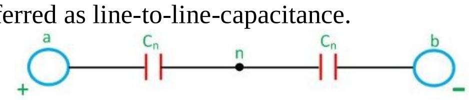

Line-to-neutral Capacitances

$$C_n = \frac{q_a}{\frac{1}{2}V_{ab}} = \frac{2\pi\varepsilon}{In\frac{D}{r}} F/m$$

Capacitance of the symmetrical three-phase line-to-neutral is,

$$C_n = \frac{q_n}{V_{an}} = \frac{2\pi\varepsilon_0}{\ln\frac{D}{r}} = \frac{1}{18\times10^9 \ln\frac{D}{r}} F/m$$

$$C_n = \frac{1}{18\ln\frac{D}{r}} \mu F/km \text{-----------} equ(9)$$

The symmetrical three-phase line capacitance is same as that of the two-wire line.

IV. SMULATION AND RESULTS

A. Present Condition

Figure 3 shows the Power Grid which supplies power to the 132 kV Haripur GSS (Black in colour). Then by double circuit lines it feed power to 132 KV Abbottabad GSS (Pink in colour) and then from 132KV Abbottabad single circuit line feed power to 132KV Mansehra GSS, Hazara network is spread from Burhan 220KV GSS to Muzaffarabad and up to Pattan.

Simulation through ETAP(Electrical transient analysis program) clearly shows that the present operating high tension network is overloaded due to which system bus voltages reduces to 119KV from nominal 132KV. Black colour of bus show Normal bus voltage and bus is in safe position, pink colour of bus shows less severe condition and the bus voltage is between 124KV to 128KV. The red colour show most severe condition whenever the system overloaded and the bus voltage less the 123KV.

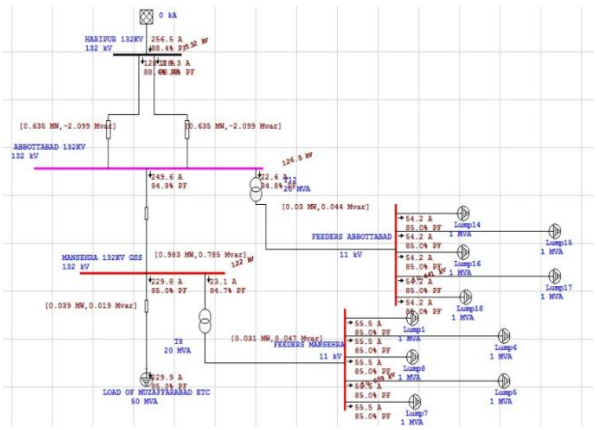

Figure 2. Simulation of present conditions of 132 KV GSS of Hazara Division.

TABLE I. ACTUAL CONDITION OF THE SYSTEM

Name of GSS	Voltage level	Color of Buses	Condition
Haripur(132KV)	132KV	Black	Healthy
Abbottabad (132KV)	128KV	Pink	Marginal/Under Voltage/Over load
Mansehra (132KV)	120KV	Red	Critical/Severe Under voltage/Overload
Abbottabd Feeders (11KV)	9.8 KV	Pink	Margnal/Under Voltage/Over load
Mansehra (11KV)	9.0 KV	Black	Severe Under voltage/Overload

From the figure we can easily see that the Haripur GSS is in normal operating position while the Abbottabad is in less severe state, while Mansehra 132KV GSS is in most severe state and proper attention required. This overload is due to some factors, which are, single circuit line from Abbottabad GSS to Mansehra GSS, old vintage system, not proper designing.

Now how to overcome this overloading and force load shedding problems we have proposed different methods and also by simulation we shows there actual results.

B. By Integration of Micro Generation

To overcome these effects the first method is by penetrating power from micro hydro generation. From the simulation in Figure 4 we can easily see that all the buses voltages come to its nominal position if we penetrate power using micro hydro at Mansehra 132KV GSS. All the buses in Fig 2 are in black colour and at nominal voltage level.

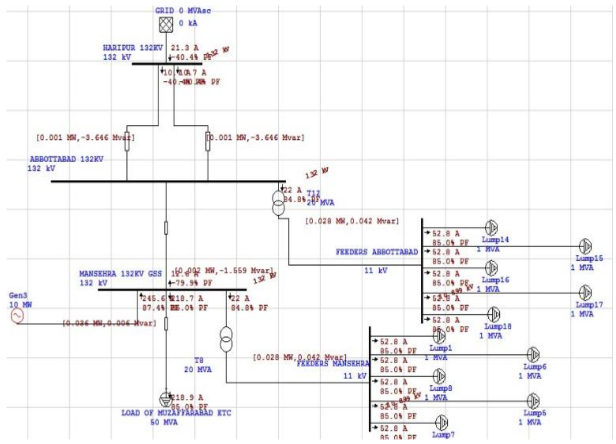

Figure 3. Integration of micro hydro to Mansehra 132 KV GSS.

TABLE II. RESULTS AFTER INTEGRATION OF MICRO HYDROS TO MANSEHRA GSS ESULTS

Name of GSS	Voltage level	Color of Buses	Condition
Haripur(132KV)	132KV	Black	Healthy
Abbottabad (132KV)	132KV	Black	Healthy
Mansehra (132KV)	132KV	Black	Healthy
Abbottabad Feeders (11KV)	11KV	Black	Healthy
Mansehra (11KV)	11KV	Black	Healthy

C. By Integration Of Renewable (PV)

The effect of overloading , force load shedding or any other contingencies from this system can also be reduce by renewable integration, in Figure 5, shows how these effects are reduce from system by integration of PV.

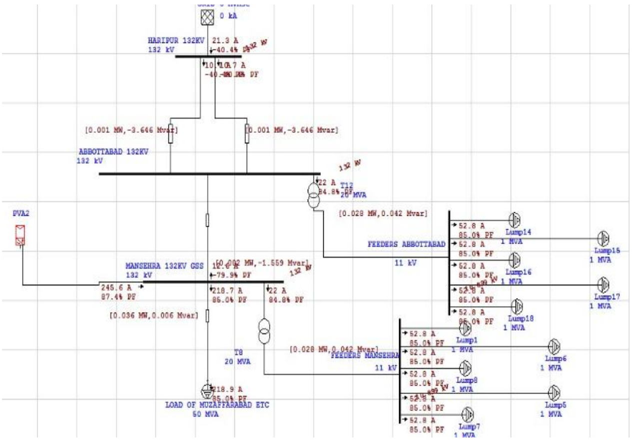

Figure 4. Integration of PV to Mansehra 132 KV GSS.

TABLE III. BY INTEGRATION OF RENEWABLES PVS

Name of GSS	Voltage level	Color of Buses	Condition
Haripur(132KV)	132KV	Black	Healthy
Abbottabad (132KV)	132KV	Black	Healthy
Mansehra (132KV)	132KV	Black	Healthy
Abbottabd Feeders (11KV)	11KV	Black	Healthy
Mansehra (11KV)	11KV	Black	Healthy

By integration of renewable PVs, from the simulation results it is cleared that the system become more stable as it is taking load from near by PVs generation and transmisiion losses minimized. All the voltages of GSS became stable.

D. By Integration Of Renewable (Wind Generation)

From figure 6, we can see that by integrating wind power with the present operating system we can erase all the contingencies.

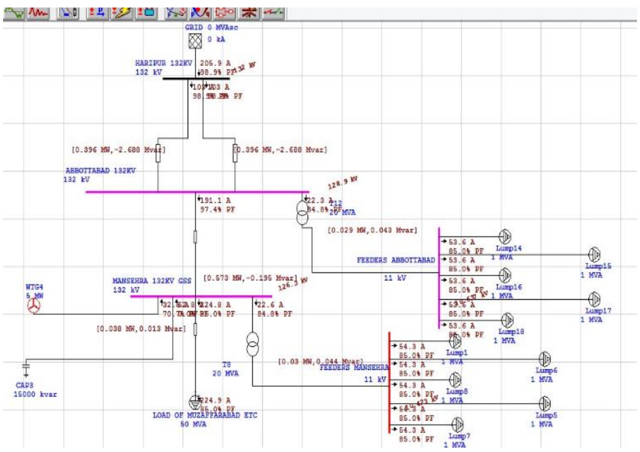

Figure 5. Integration of Wind energy to Mansehra 132 KV GSS.

TABLE IV. BY INTEGRATION WIND POWER PLANT

Name of GSS	Voltage level	Color of Buses	Condition
Haripur(132KV)	132 KV	Black	Healthy
Abbottabad (132KV)	130 KV	Black	Healthy
Mansehra (132KV)	127 KV	Pink	Under Voltage/ Over load
Abbottabd Feeders (11KV)	9.8 kV	Pink	Under Voltage/ Over load
Mansehra (11KV)	9.8 KV	Pink	Under Voltage/ Over load

From the results it is clearly seen thatwind Integration of wind generation the system voltage improves a little bit but not came under stable position because of low reliability of wind generation

E. By Doubling The Circuits

Figure 7 show that if we double the circuit so we can also reduce force load shedding because the load on single circuit is some time beyond the ratting of conductor due to which only one method is used force load shedding, so to vanish this effect we can double the circuit so the load will be divided in two different paths and the bus voltages will be near to nominal

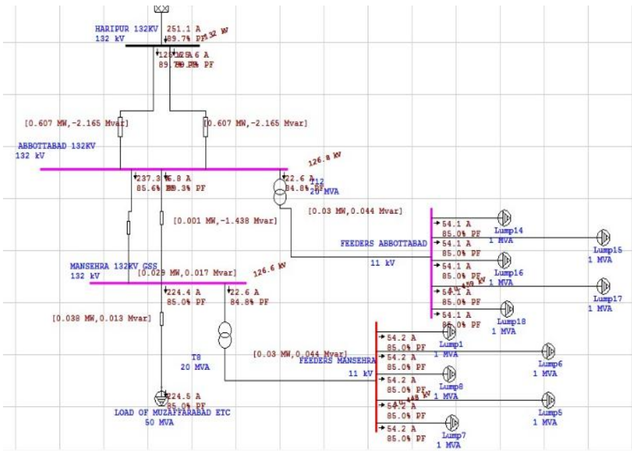

Figure 6. Effect of Circuit doubling

TABLE V. BY DOUBLING THE CIRCUIT

Name of GSS	Voltage level	Color of Buses	Condition
Haripur(132KV)	132KV	Black	Healthy
Abbottabad (132KV)	128.4 KV	Pink	Under Voltage/ Over load
Mansehra (132KV)	126.6 KV	Pink	Under Voltage/ Over load
Abbottabd Feeders (11KV)	10.5 KV	Pink	Under Voltage/ Over load
Mansehra (11KV)	10 KV	Pink	Under Voltage/ Over load

F. By Connecting 132kv Gss To Allai Khwar Power Plant(220kv)

Allay Khwar Hydropower Plant located in the Battagram District on the Allay Khwar River, is a run-of-the-river project having generation capacity of 121 MW. The head of the project is 687 meters. We can also integrate power from Allay khwar power plant to 132KV Mansehra so by this we can easily stabilize our system to nominal and avoid unnecessary load shedding. Allai khwar power plant generation is in 220 KV so we will use two approaches for this which is given in figure 8 and figure 9.

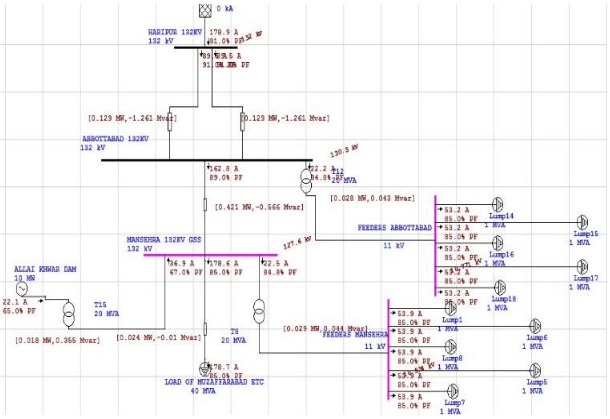

Figure 7. Integration of Mansehra 132 KV GSS to 220 kV Allai Khwar Power Plant (Approach 1).

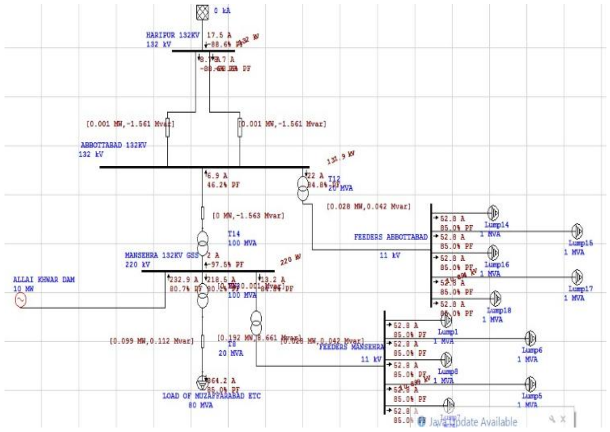

Figure 8. Integration of Mansehra 132 KV GSS to 220 kV Allai Khwar Power Plant (Approach 2).

TABLE VI. INTEGRATION OF HYDEL POWER POWER STATION

Name of GSS	**Voltage level**	**Color of Buses**	**Condition**
Haripur(132KV)	132KV	Black	Healthy
Abbottabad (132KV)	132KV	Black	Healthy
Mansehra (132KV)	132KV	Black	Healthy
Abbottabd Feeders (11KV)	11KV	Black	Healthy
Mansehra (11KV)	11KV	Black	Healthy

G. Conductor Replacement

The last method which we can use to vanish the effect of overloading and force load shedding is to replace the existing conductor LYNX to LION conductor, mostly time this single circuit from Abbottabad 132KV GSS to Mansehra 132KV GSS is in overloaded position which is responsible for force load shedding, the current carrying capacity of LYNX conductor is 480A while the lion conductor is 654A. The max current recorded in summer is 543A which is greater than the ratting if LYNX conductor and LION can easily sustain current up to 700A. Due to replacement of conductor the losses on conductor also reduce up to some extent and the system burden reduce quite well in figure 10 to figure 12 all the effect before and after conductor replacement are shown.

TABLE VII. DIFFERENTS CONSUCTORS EFFECTS UPON THE LOSSES

Code Name		**LYNX**	**PANTHER**	**LION**	**BEAR**
Al	No/mm	30/2.79	30/3.00	30/3.18	30/3.35
Steel NO/mm		7/2.79	7/3.00	7/3.18	7/3.35
Weight Kg/Km		842	1001	1093	1213
Overall Diameter	(mm)	19.53	21	22.26	23.45
Nominal Cross sectional Area	(mm2)	226.2	261.53	293.85	326.11
Calculated DC resistane Ώ/Km		0.158	0.1362	0.1171	0.1055
Inductive Reactance Ώ/Km		0.37658	0.372045	0.36835	0.36508
Current Rating (A)		488	606	654	700

TABLE VIII. DIFFERENTS CONSUCTORS EFFECTS UPON THE LOSSES

Code Name		**LYNX**	**PANTHER**	**LION**	**BEAR**
Voltage		132KV	132KV	132KV	132KV
DC Resistance Ώ/Km		0.158	0.1362	0.1171	0.10558
Inductive Reactance Ώ/Km		0.37658	0.37204	0.36835	0.36508
Losses in (%) Percent for load 450A	P=I2 Z	3.062	2.9714	2.898	2.85
Losses in (%) Percent for load 550A	P=I2 Z	3.74	3.6317	3.543	3.484
Losses in (%) Percent for load 650A	P=I2 Z	4.424	4.292	4.1872	4.117

TABLE IX. SIMULATION RESULTS BEFORE CONDUCTOR REPLACEMENT

Device ID	**Status**	**Type**	**Condition**	**Limit**	**Operating**	**% Operating**
Bus 4	Critical	Bus	Under voltage	132KV	120.95	91.6
Mansehra 132KV GSS	Critical	Bus	Under voltage	132 KV	117.8	89.2
Abbottabad 132 KV GSS	Critical	Bus	Under voltage	132 KV	121.20	90.9
Mansehra Feeder 11KV	Critical	Bus	Under voltage	11 KV	9.99	90.9
T/L ABN to Mansehra	Critical	Line	Over load	450A	563A	125.11

132 KV						
Abbottab ad Feeder 11KV	Margin al	BU S	Under voltage	11 KV	10.69	96.8

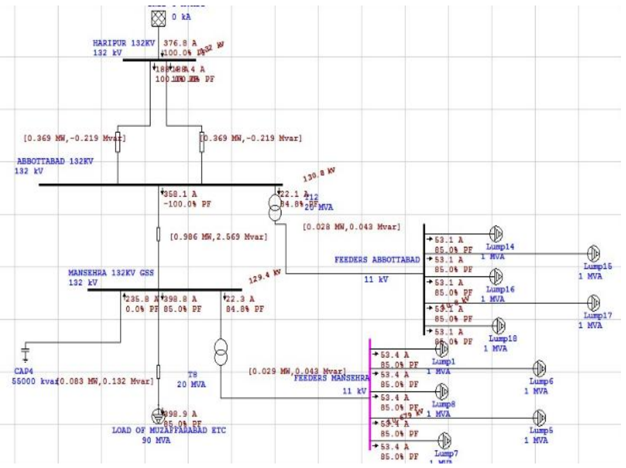

Figure 9. After Conductor Replacement approach

From Table 9 and 10 it is clear that befor conductor replacement the system in overloaded and in critical condition as most of the buses and feeders are working under voltage while after the replacement of conductor it is clearly seen from the simulation results in figure 9 and in table 10 that the system came out of critical position.

TABLE X. SIMULATION RESULTS AFTER CONDUCTOR REPLACEMENT APPROACH

Device ID	Status	Type	Conditi on	Limi t	Operati ng	%Ope rating
Bus 4	Marg inal	BUS	Under voltage	132 KV	129.132	97.8
Mansehr a Feeder	Marg inal	BUS	Under voltage	11 KV	10.579	96.11

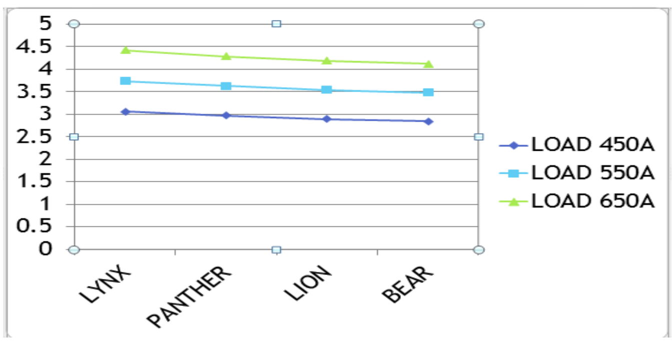

Figure 10. Differents consuctors effects upon the losses.

From figure 10 we can easily see that the GSS voltages of Mansehra and Abbottabad are in critical condition and less than 119 KV, and as we replace the conductor using simulation all the voltage of Bus Bars of GSS came to normal range.the losses of the transmision network decreases upto 4.1 % after the replacement of conductor and the load handling capability of the system increase from 465A to 700A.

CONCUSLION

From the whole simulation and results it is conclude that thier are various factors responsible for T & D losses which need to be eliminated. The approaches taken by government over the years in Pakistan has created an inefficient distribution system having very high T & D losses and poor quality and reliability of power supply to consumers. The whole power system network needs proper up-gradation and overhauling because this system is very weak and have a lot of severe places. PESCO is on second number in the whole ten no of discos whose losses is more the 34%. To reduce these losses the renewable integration, conductor replacement, increasing voltage level and replacement of these old vintage system is needed. The area which is anlyse in this research analysis has many potential regarding power generation and with each Integration of the generation we can solve the critical condition of power system. the most fesible and long term method is to penetrate power from Allai khwar power plant if not than conductor replacement is the most Economical method which can mitigate this issue for about 20 years of future demands.

ACKNOWLEDGMENT

The research has been carried out and supported by US-Pakistan Center for Advanced Studies in Energy, UET Peshawar . I am thankful to USAID and USPCASE UET Peshawar for the opportunity provided to complete my postgraduation. I am very nuch grateful to my supervisor Dr. Abdul Basit for his support throughout my research.

REFERENCES

[1] Bhatti, S.S., et al., Electric power transmission and distribution losses overview and minimization in Pakistan. International Journal of Scientific & Engineering Research, 2015. 6(4): p. 1108-1112.

[2] Kanagawa, M. and T. Nakata, Assessment of access to electricity and the socio-economic impacts in rural areas of developing countries. Energy policy, 2008. 36(6): p. 2016-2029.

[3] Lopes, J.P., et al., Integrating distributed generation into electric power systems: A review of drivers, challenges and opportunities. Electric power systems research, 2007. 77(9): p. 1189-1203.

[4] Nair, N.-K.C. and L. Zhang, SmartGrid: Future networks for New Zealand power systems incorporating distributed generation. Energy Policy, 2009. 37(9): p. 3418-3427.

[5] Quezada, V.M., J.R. Abbad, and T.G.S. Roman, Assessment of energy distribution losses for increasing penetration of distributed generation. IEEE Transactions on power systems, 2006. 21(2): p. 533-540.

[6] Haseeb, M. and S.A.R. Kashif. Transition to competitive power market framework—A case study of Pakistan. in 2018 International Conference on Computing, Mathematics and Engineering Technologies (iCoMET). 2018. IEEE.

[7] Xu, S. and W. Chen, The reform of electricity power sector in the PR of China. Energy Policy, 2006. 34(16): p. 2455-2465.

[8] Roberts, J.M. and H. Sattar, Pakistan's Economic Disarray and how to Fix it. 2015: Heritage Foundation.

[9] Parmar, J., Total losses in power distribution and transmission lines. Trans - mission and Distribution Electrical Engineering Portal (EEP), 2013.

[10] Blavette, A., et al. Analysis of the flicker level generated by the grid-connection of a fleet of electric vehicles. in 2016 IEEE PES Innovative Smart Grid Technologies Conference Europe (ISGT-Europe). 2016. IEEE.

[11] Chiradeja, P. Benefit of distributed generation: A line loss reduction analysis. in 2005 IEEE/PES Transmission & Distribution Conference & Exposition: Asia and Pacific. 2005. IEEE.

[12] Kessides, I.N., Chaos in power: Pakistan's electricity crisis. Energy policy, 2013. 55: p. 271-285.

[13] Eisenstadt, W.R. and Y. Eo, S-parameter-based IC interconnect transmission line characterization. IEEE transactions on components, hybrids, and manufacturing technology, 1992. 15(4): p. 483-490.

[14] Sheen, D.M., et al., Current distribution, resistance, and inductance for superconducting strip transmission lines. IEEE Transactions on Applied Superconductivity, 1991. 1(2): p. 108-115.

[15] Tsuk, M.J. and J.A. Kong, A hybrid method for the calculation of the resistance and inductance of transmission lines with arbitrary cross sections. IEEE Transactions on microwave Theory and Techniques, 1991. 39(8): p. 1338-1347.

[16] Chang, W., The inductance of a superconducting strip transmission line. Journal of Applied Physics, 1979. 50(12): p. 8129-8134.

Tariq Ahmad: The author was born in KPK province, District Buner, Pakistan in the year of 1991. He did his matriculation from “Falcon Public School”. Afterwards, He pursued his Higher secondary education in Pre-Engineering from “Quaid azam group of school and colledges swabi”, Pakistan. After that He did his Bachelors Degree in Electrical Power Engineering from “COMSATS” Abbottabad, Pakistan. Recently, He has completed his Master’s in Electrical Energy System Engineering from USPCAS-E UET Peshawar, Pakistan. Recently, the author started his professional career as Assistant Dirderctor(E)/Junior Engineer in a Public sector organistation WAPDA.

International Journal of Engineering Works
ISSN-p: 2521-2419
ISSN-e: 2409-2770
Vol. 6, Issue 08, PP. 244-248, August 2019
https://www.ijew.io/
https://doi.org/10.34259/ijew.19.608244248

Performance Study of Thermoelectric Generator Using Waste Heat

Said Ali[1], Naeem Arbab[2], Muhammad Bais[3], Nisar Ahmad[4], uzair Muhammad[5]
[1,2,3.4,5]Department of Electrical Energy Systems Engineering, US Pakistan Centre for Advanced Studies in Energy, University of Engineering and Technology Peshawar, Pakistan.
engr.saidali@live.com[1], mnarbab@nwfpuet.edu.pk[2], muhammadbais92@yahoo.com[4], nisarmarwat10@gmail.com[4], uzair.uetpeshawar@gmail.com[5]
Received: 25 July, Revised: 02 August, Accepted: 05 August

***Abstract*—**There is alot waste heat from power consuming companies. This waste heat is added to atmosphere, which is unusable and it adds to global warming. Most of energy sources are consumed by energy sectors. These sectors are energy spending sectors all over world. Consequently, they are answerable for the discharging huge quantity of heat to the atmosphere. This heat is called waste heat which is in form of hot exhaust gases or other hot discharges. Since high prices of sources and wastage of heat made us to think that to recover its energy. It will benefit us from two perspectives in which first one is decreasing carbon amount in discharges and second one is this energy is cheap. Moreover, decreasing the ecological impact. Heat recovery via thermoelectric modules enables us to recover the waste contents with energy. Thermoelectric generator (TEG) is a semiconductor device. TEG module is made which produce electrical voltages whenever thermal gradient is developed on its surfaces. The study of TEG performace is presented in this paper. Voltage, current and power produced are the performance charateristics of TEG. The increase and decrease of temperature difference on both the surfaces of TEG module will show the output results increasing and decreasing respectively [1].

***Keywords*—** Bi_2Te_3 TEG, waste heat recovery, thermoelectric system, thermoelectric modules.

I. INTRODUCTION

Out of 100% energy used in productions, 33% of it is discharges out which is named as waste heat [2]. Presently world is facing issues related to global warming, high prices of fossil fuels and its depletion. Therefore we must need to develop other methods to full fill our needs of energy. So we are moving towards clean and green energy technologies and also developing more efficient way for energy recovery of heat and heat transformation systems using the pumped out waste heat as source.

In process industry low grade heat energy is pumped out. This heat is considered useless because of low degree of temp. For generation of electrical power by old generation systems which uses rotating parts like turbines.. it is very hard to ger energy of this waste heat from waste heat of low temperature and low energy density. Some well know systems are available for the conversion of heat of low which are ORC (Organic Rankine Cycle). But we have some issue using this kind of system as they are costly and they have rotatory parts which will need maintenance periodically, which is not economical.

Conversion of heat of low temperature to energy of electricl form, we need to choose an economical method. We need similar method like solar cells which is economical and one time costed. Capital cost is less. Maintenance on periodic basis should be not included for which we need to ignore the rotatory parts. So we need a system which operate with out rotatory part and easy to handle. We have a method used for heat recovery called heat pipe. Which is the best method of all having more applications in this field [4]. There is another method called direct energy conversion from thermal form to electrical form by using a device or module called thermoelectric generator. This TEG system is having good performance of conversion thermal energy to electricl. The TEG is kept between two surfaces in which one is heat source and other is heat sink or heat exchanger based on the Seebeck effect [7]. TEG is best device for using on low temperature of pumped out heat. As this device is what we needed that don't have any movable part. So its maintenance cost is negligible. And its size is very small [8].

In current market, the efficiency of TEG is low which is lower than five percent, but still some people claimed that they are obtaining more than 20% efficiency. NASA lab of jets also discovered more than 20% efficiency of TEGs [2].

Researchs are in progress just for increasing the efficiency of TEGs, but still there is wastage of heat energy in three different forms. In which along with gases, solid and liquids are counted [11]. In france 75% of energy is used in process plants out of which 31% of heat is further wasted [12]. USA dischages 20-50% of the energy as heat [13]. Turkey cement plants losts 51% of the total heat energy used.[14]. We have so many other countries that pump out the waste heat to the outside world. Which is dangerous for the life on the earth for all animals and every kind of organisms.

It is considered that in near future power will be produced by TEG system which will utilize the waste heat efficiently.

II. LITERATURE REVIEW

A. *Waste Heat*

Waste heat refers to that energy which is considered useless. It is generated in process industries. Currently 20-50% of fuel energy is added to the environment by convection,conduction and radiation. Waste heat has three categories. Temperature above 600°C is considered high, below 230°C is considered low and in between is medium category. There are several advantages of waste heat. it is free source of energy. It reduces energy consumption in furnaces and boilers. it improves efficiency of plant more than 50%. It can be converted to other form of energy.

B. *Thermoelectricity:*

The phenomenon in which temperature difference generates electrical power and vice versa. The three effects, Seebeck effect, Peltiers and Thomson effect, plays very important role in thermoelectricity.

C. *Thermoelectric devices*

Thermoelectric (TE) devices are the centre of attention because of their role that they have ability to directly convert heat energy to electrical energy. It is prepared of semiconductors. Usually the shape of this device is a rectangular boxes in parralet as shown in figure 1. These units are combined in parallel or in series according to the need.

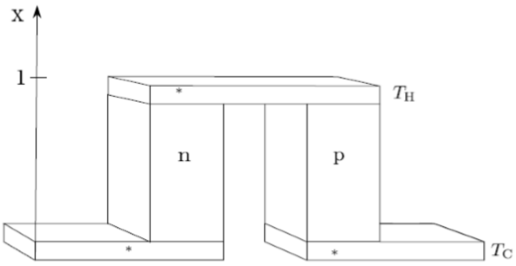

Figure 1.

D. *Thermoelectric devices and Thermoelectric effect:*

Thermo stand for heat energy and Elecric for electrical power. So it means conversion of heat energy to electrical directly. We will discus three effect here. Thomas Johan Seebeck for the first time in 1821 observed that if a circuit is made of two different metals. A measuring instrument needle is deflected when heat was applied to the metals. This effect was named as Seebeck effect and eq 1 is given below. The second one was named as Peltier effect which is opposite of Seebeck effect was observed by him. The current passed through two metal produced heat and equation 2 is given below. Thomson and joule effects are not discussed in detail as they are not used in this research.

$$I = \sigma E - \sigma\alpha \nabla T \left(\frac{A}{m^2}\right) \quad (1)$$

$$q = \pi I - k\nabla T \left(\frac{W}{m^2}\right) \quad (2)$$

Where, E is symbol of electric field, T is symbol for temp, α is symbol for Seebeck coefficient, π is symbol for Peltier Coefficient, and σ is symbol for electrical conductivity. Symbol k is for thermal conductivity. From eq 1 and 2 we can say that heat and electrical energy in transformable into one another.

The direct relation of Seebeck effect to the Seebeck coeficient is defined by:

$$\alpha = -\frac{\Delta V}{\Delta T} = -\frac{V\ hot - V\ cold}{T\ hot - T\ cold},\ \alpha\ [V/K] \quad (3)$$

The relation of Peltier effect to the peltier coefficient is defined by:

$$Q_P = \pi I = \alpha T_j I \ \text{ or } \ \pi(T) = \frac{Q}{I} \quad (4)$$

Both these relation in eq 3 and eq 4 were combined and experimentally by Lord Kelvin. The relation of α and π is given by:

$$\alpha(T) = \frac{\pi * (T)}{T} \text{Kelvin relation} \quad (5)$$

Showing that only Seebeck coefficient will do all to describe all the TE properties of TE material.

Semiconductors of N-type and P type have dissimilar properties. That why we get opposite signs of Seebbeck coefficients. TE modules are generally prepared from two semiconductors materials which are connected in series electrically. And in parallel thermally. See Figure 2.

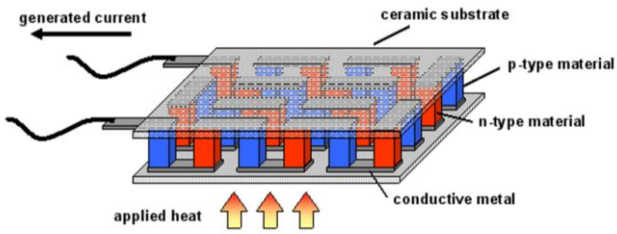

Figure 2.

The eq 5 is efficiency for TE module

$$\eta_{max} = \frac{T_H - T_L}{T_H} \frac{\sqrt{1+\frac{Z(T_H+T_L)}{2}} - 1}{\sqrt{1+\frac{Z(T_H+T_L)}{2}} - \frac{T_L}{T_H}} \quad (5)$$

Eq 6 is just like the efficiency of ideal Carnot engine and is multiplied by Z factor. Z is called figure of merit, given by:

$$Z = \frac{\alpha^2 \sigma}{k} \quad (6)$$

σ is symbol used for electrical conductivity.
Symbol k represents thermal conductivity.

V-I characteristics of TE modules are shown in figure 3. The power and voltage graph is here for commercial thermo electric module when 20watts of heat flux is applied to the sides.

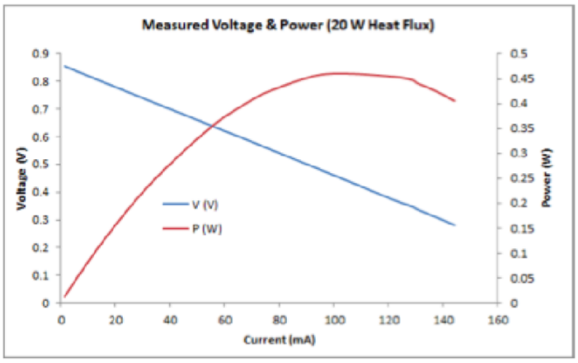

Figure 3.

The highest point for the max power is expressed by:

$$I_{Pmax} \approx \frac{\alpha\,(T_H - T_L)}{2R_e} \qquad (7)$$

Where R_e is the module electrical resisitance.

E. *Advantages of thermoelectric generators*

The advantages of TEGs are large in number but some are:

- Most reliable device which exceeds over 100,000hours of life.
- No moving part so don't produce any noise.
- Compact size and simplest construction design.
- Lowest weight and smalled in size.
- Work with high degree of temperature.
- Best option for distant places where there is no energy.
- Eco-friendly system.
- No problem of position placements.

F. *Applications of TEGs:*

For combustion engines it is best option to combine TEGs with them and recover the hot gases heat energy. With solar energy the solar panels get heated so that energy can be recovered by using TEGs with them and more energy can be utilized from the solar. The solar panels efficiency can be raised up by adding its power. Very light generating system enables us to use it everywhere in the world. Even on spaceships we can provide power to them by the heat recovery method using TEGs.

III. Working Principle of TEG

Working principle of TEG is based on the Seebeck effect which is described in detail. When two unlike materials are joined and they make two junctions and they both these metals are provided with different temperatures. On the output we will get generated voltage of micro volts per degree kelvin. The material we use for thermoelectric generation is called thermoelectric material. seebeck coefficient and properties like electrical and thermal were kept in consideration for selection of this material which is very important.

The generated power of TEG is dependent upon the applied temp difference to its opposite surfaces. The conduction of the heat from one surface to the other takes place and in this way the difference of temp is reduced. Hence a heat sink will be required on the second surface to maintain proper temperature difference between plate surfaces. our aim is to study the performance of TEG for vaious temp gradients.

IV. Methodology

We have numerious number of materials for preparing TEG modules. But we have choosen Bismuth Telluride because of better power ratings and easy availability in market. Therefore we preferred studying Bi_2Te_3 Module. Maintaining constant difference of temperature is very important so for that purpose a heat sink is designed for the faces of TEG. As heat sink we preferred to use Aluminum for its property of high thermal conductivity. The amount of heat required to be pumped and water flow rate are the two parameters needed to be considered. In heat sink a flow rate was kept constant. The TEG specs as given below.

- 230°C is limit of operating temp.
- OC voltage is 12.1v. (OC stands for open circuit)
- Dimensions are (40mm x 40mm x 3.4mm).
- Properties of Bi_2Te_3 are:
  - Condcuts heat of 2W/m-K.
  - Its density is 7790 Kg/m^3
  - Specific heat transfer is 250 J/Kg-K

Cover of 0.8mm made of porcelain is used on both sides of TEG. Thermal conductivity of porcelain is 30W/m-K. And 3300Kg/m^3 is the density of porcelain.

V. Experimental Setup

Figure 4 and 5 shows a custom made test bench is being used in this test. This apparatus is composed of electric heater with adjustment knows and TEG made of thermocouple modules. Heat exchanger or sinker is added on the second side of the modules. This sink helps in creating high temperature gradient which further helps in maximum power generation. A voltmeter and ammeter was used to for measuring voltage and current from modules connections.

A heater or heating plate in this setup is used to supply heat to bottom side of the module. From ammeter and voltmeter we noted the readings. The readings range was started from 35°C and we raised with steps of 10°C upwards until 145°C was reached.

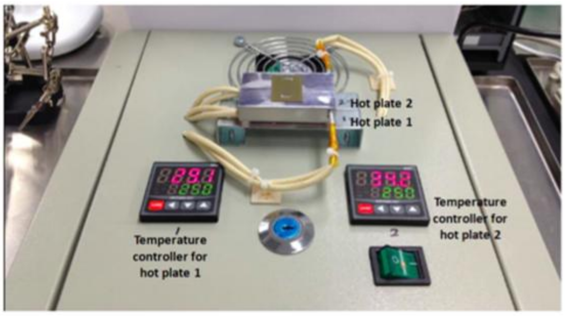

Figure 4.

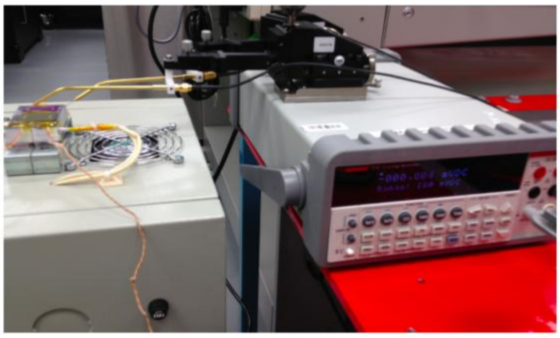

Figure 5.

TABLE I. SHOW THE TEMP VS VOLTAGE, CURRENT, AND POWER

Temp (°C)	Voltage (mV)	Current (mA)	Power (mW)
35	21.80	1.000	0.02180
45	443.0	1.900	0.84170
50	464.5	3.651	1.73305
60	497.0	9.201	4.61420
70	539.0	18.95	10.3985
80	607.5	30.45	18.7065
90	693.5	44.01	30.9020
100	795.0	64.40	51.8552
110	975.0	86.60	85.6897
120	1225	109.1	134.940
130	1513	144.8	222.775
140	1879	187.0	355.192
150	2184	218.5	478.388
155	2287	231.0	528.297

VI. RESULTS

The Reading were pen down from 35°C with 10 degrees steps increment upto 150°C. The temperature vs voltage graph is show in figure 6. Figure 7 shows the temperature vs current graph and figure 8 show the temperature vs power graph.

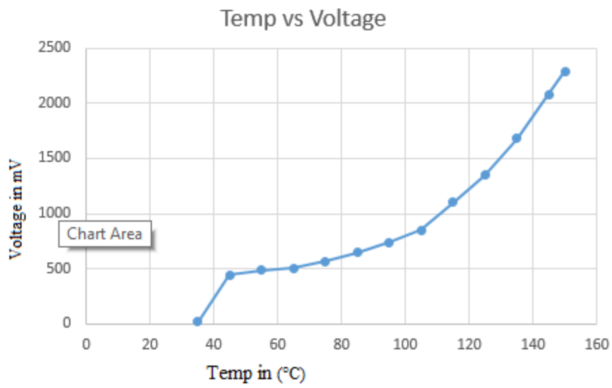

Figure 6.

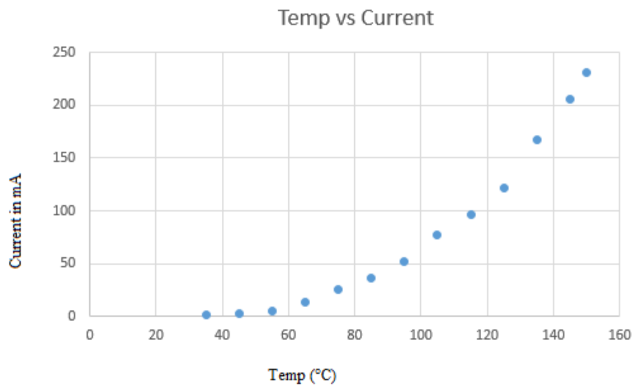

Figure 7.

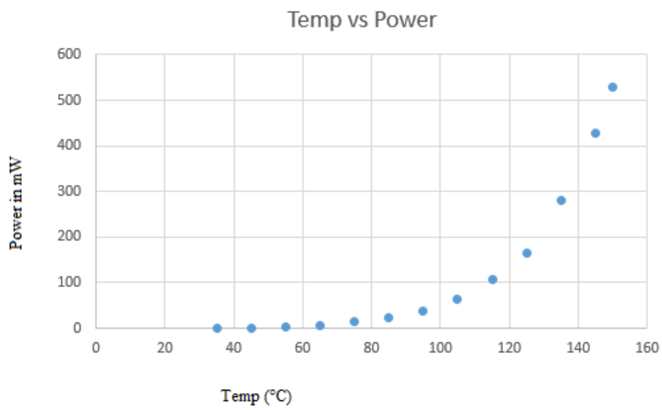

Figure 8.

CONCLUSION

The full pledge details about the study of Power generation by using thermoelectric generators were presented in this paper. the applications of TEG are also described as its is very efficient system from the heat recovery point. this study is very important to understand the use of Bismuth Telluride as thermoelectric generator when there is free of cost available waste heat like heat of engines, furnaces, or other processes industries. In this paper we can conclude that the electrical power produced is directly proportional to the heated surface provided. Maximum output power obtained was 528.297 mW. Further experiments are soon be conducted in order to improve the efficiency and performance of systems using heat recovery process.

REFERENCES

[1] BP. BP Statistical Review of World Energy 2014; Available from: http://www.bp.com/content/dam/bp/pdf/Energy-economics/statistical-review- 2014/BP- statistical-review-of-world-energy-2014-full-report.pdf

[2] Fleurial, J.-P., Thermoelectric power generation materials: Technology and application opportunities. JOM Journal of the Minerals, Metals and Materials Society, 2009. 61(4): p. 79- 85.

[3] Tchanche, B.F., et al., Low-grade heat conversion into power using organic Rankine cycles–A review of various applications. Renewable and Sustainable Energy Reviews, 2011. 15(8): p. 3963-3979.

[4] Hamid Elsheikh, M., et al., A review on thermoelectric renewable energy: Principle parameters that affect their performance. Renewable and Sustainable Energy Reviews, 2014. 30: p. 337-355.

[5] Ismail, B.I. and W.H. Ahmed, Thermoelectric Power Generation Using Waste- Heat Energy as an Alternative Green Technology. Recent Patents on Electrical Engineering, 2009. 2(1).

[6] Jiin-Yuh Jang, Ying-Chi Tsai, "Optimization of thermoelectric generator module spacing and spreader thickness used in a waste heat recovery system," Elsevier, no. 51, pp. 677-689, 2012.

[7] Laia Miró, Jaume Gasia, Luisa F. Cabeza, "Thermal energy storage (TES) for industrial waste heat (IWH) recovery:A review," Elsevier, p. 285, 2016.

[8] Tongcai Wang, Weiling Luan ⇑, Wei Wang, Shan-Tung Tu, "Waste heat recovery through plate heat exchanger based thermoelectric generator system," Elsevier, p. 860, 2014.

[9] Cynthia Haddad, Christelle Périlhon, Amélie Danlos, Maurice-Xavier François, Georges Descombes, "Some efficient solutions to recover low and medium waste heat: competitiveness of the thermoacoustic technology," in The International Conference on Technologies and Materials for Renewable Energy, Environment and Sustainability, TMREES14, Paris, 2014.

[10] S. Spoelstra, M.E.H. Tijani, Thermoacoustic heat pumps for energy savings," in Presented at the seminar "Boundary crossing acoustics" of the Acoustical Society of the Netherlands, Netherlands, 2005.

[11] Fitriani, R.Ovik , B.D.Long , M.C.Barma, M.Riaz , M.F.M.Sabri , S.M.Said ,, "A review on nano structures of high – temperature thermoelectric materials for waste heat recovery," Elsevier, p. 636, 2016.

[12] Law, R., A. Harvey, and D. Reay, Opportunities for low-grade heat recovery in the UK food processing industry. Applied thermal engineering, 2013. 53(2): p. 188-196.

[13] Jorge Vázquez, Miguel A. Sanz-Bobi, Rafael Palacios, Antonio Arenas "State of the Art of Thermoelectric Generators Based on Heat Recovered from the Exhaust Gases of Automobiles" .

International Journal of Engineering Works
ISSN-p: 2521-2419
ISSN-e: 2409-2770
Vol. 6, Issue 08, PP. 249-252, August 2019
https://www.ijew.io/
https://doi.org/10.34259/ijew.19.608249252

Power Loss Analysis of a Radial Distribution Feeder by using Distributed Generator

Mushtaq.A.K.Khattak[1] Amjadullah khattak[2], Mohammad Ismail[3],Waqar Hussain[4], Jahangir Bahadur[5], Najum saqib[6]
[1, 2,3,4,5,6]University of Engineering and Technology, Peshawar
M.A.K.Khattak@uetpeshawar.edu.pk[1]
Received: 30 July, Revised: 05 August, Accepted: 10 August

***Abstract*—** The desire and required place for providing electricity i.e. Homes, industries, markets, etc. are far away from the place where electricity is produced (power stations). It results in low efficiency and also increases the cost. It has so many dis-advantages. It may also have environmental and security issues as well.
The primary objective of this resaerch is to evaluate and reduces the percentage loss. The power loss is performed for different locations. The result shows the appropriation of distributed generator in to power system.

***Keywords*—** losses reduction, Distributed generator, Radila Feeder

I. Introduction

Nowadays the generation is producing new technologies. They aim are providing facilities to users. Which includes good quality and high power as well. They have promised to generate electricity with high efficiency and producing very low pollution. [1,3,6].

Distributed Generation is acknowledged through a number of names like On-Site generation, Dispersed Generation, Decentralized Generation, or Embedded Generation. It is a small scaleelectricity generating technology(typically in the range of 50kW up to a hundred MW) and used to supply anchoice to or enhancementof the historically current electric energy structures such as hydropower system, thermal power system, nuclear energydevice etc [1,5].

Distributedgeneration can be viewed as “taking energy to load”. Distributed generation guaranteesto generate electricity withhigh efficiency and lowpollution. Unlike massive central (conventional) massive energy plants, distributed generatorcan be established at or close to the load.Maintenance price for distributed generation such asfuel cells and photovoltaicdevice is pretty low due to thefact of the absence of transferring components [4,9].

Many of these technologies are at the stage of development including micro turbines, wind energy, gas turbines, fuel cell system and many more. This will make the users ease. These advantages include the line loss reduction, reduces the environmental impacts. It also increase the efficiency, power and voltage as well. [5,7].

II. Modeling of System

There are following two cases shown in fig 1 and fig 2.

a) System without the integration of Distributed generator
b) System with the addition of Distributed generator

These two systems have the concentrated0load. The length for these two system have to be assumed L (KM).

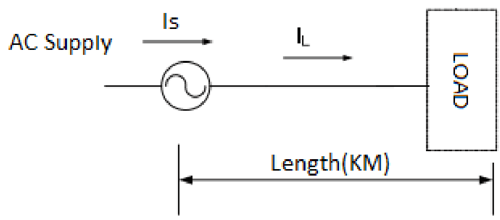

Figure 1. Radial System without integration of Distributed generator

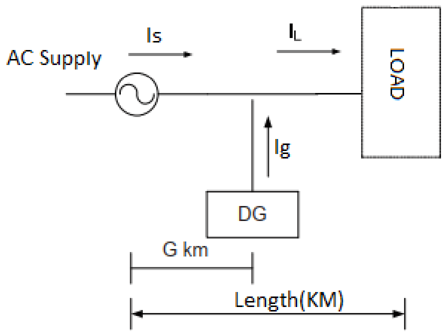

Figure 2. Radial system with the integration of distributed generator

Before analysis the following assumption to be taken:

1. Y-connected load i.e. the phase current(Ip) should be same to line current(IL):

$$I_{Phase} = I_{Line}$$

2. At specified power factor the load consume some real active power.

3. At lagging leading or unity factor the distribution generator produce real power.
4. V_P is the value of RMS voltage
5. V_P is the phasor reference voltage to be chosen

The complex load power is $S_L = P_L + JQ_L$ so
The load absorb the current

$$\boldsymbol{I}_L = (\boldsymbol{P}L - \boldsymbol{JQ}L)/3\boldsymbol{V}P \quad (1)$$

III. Analysis Loss Reduction

When current passes through transmission line the losses occur. The line loses depends on amount of current passes and line resistance.so the losses is to be minimize due to decreased the current or resistance0or the both. When DG is provided in to the load the losses may be reduced due to current passing to some of network part.

A. Analysis of line losses without the distribution generator

Diagram of the analysis for the system as shown in figure 1.in distribution system line losses is equal to the square times current and resistance.so for three phase system the equation foe line losses as:

$$L.LOSS_{BDG} = \frac{rL(P_L^2 + Q_L^2)}{3V_P^2} \quad (2)$$

B. Analysis of line losses with integration of distributed generator

Diagram for the system is shown in figure 2. Let assume that the line is to be short and across that line the voltage drop is neglected.
The DG delivered the complex power which is equal to the $S_{DG}=P_{DG}+JQ_{DG}$
So the output of DG will be given as;

$$I_{DG} = \frac{(P_{DG} - JQ_{DG})}{3V_P} \quad (3)$$

There are two main causes of line loss integrated with DG

1. Line from source to DG

Line losses for the several allocation of DG to their load Centre.

It is clear from figure 2

$$I_{Source} = I_{Line} - I_{DG} \quad (4)$$

So the line loss equation for the system from source to DG is expressed as

$$L.LOSS_{S-DG} = \frac{rG(P_L^2 + Q_L^2 + P_{DG}^2 + Q_{DG}^2 - 2P_{DG}P_L - 2Q_{DG}Q_L)}{3V_P^2} \quad (5)$$

2. Line losses from DG location to load Centre

When distributed generator is not allocated between the systems so the line current must be equal to load current, thus the equation for this system is given as:

$$L.LOSS_{DG-S} = \frac{r(L - DG)(P_L^2 + Q_L^2)}{3V_P^2} \quad (6)$$

3. Over all line losses in the system

Line losses in the system is given as in the following equation

$$L.LOSSES_T = L.LOSSES_{S-DG} + L.LOSSES_{DG-s}$$

By substituting the equation 5 and equation 6 in the above equation, the following equation gets.

$$L.LOSSES_T = \frac{RG}{3LV_P^2}[P_L^2 + Q_L^2 + (P_{DG}^2 + Q_{DG}^2 - 2P_{DG}P_L - 2Q_{DG}Q_L)] \quad (7)$$

C. Reduction of line loss due to integration of DG in the system

Reduction of line losses is equal to the difference between integration of DG before in the system and integrate DG in to the system is given in the following equation

$$L.Losses = L.Losses_{BDG} - L.Loss_{ADG} \quad (8)$$

By substituting the equations in the above equation (8). The following equation gets,

$$L.Loses = \frac{RG}{3LV_P^2}(2P_{DG}P_L + 2Q_{DG}Q_L - P_L^2 - Q_{DG}^2) \quad (9)$$

If the losses in the system is decreased then the L.Loss will indicate the positive sign due to connection of DG. And inversely when system has higher losses then L.Loss will show negative sign.

D. Per-unit reduction of line losses

Per-unit rduction of L.Losses is equal to reduction of L.Losses to the L.Losses without the integration of DG Therefore

$$PULLR = \frac{L.Losses}{L.Losses_{BDG}} \quad (10)$$

By putting the two equations line the above equation (10), gets

$$PULLR = \frac{G}{L(P_L^2+Q_L^2)}(2P_{DG}P_L + 2Q_{DG}Q_L - P_L^2 - Q_{DG}^2) \qquad (11)$$

So, percentage of line loss reductionis expressed as:
$\% \, L.Losses = PULLR \times 100$

E. Both the load and DG power factor at the time operating:

There are four different conditions which are given below.

Condition1: Load has leading and DG has lagging power factor.

Condition 2: Load has lagging and DG has leading power factor.

Condition 3: Load and DG having same leading power factor.

Condition 4: Load and DG having same lagging power factor

From above discussion it's expressedthat the condition 3 and 4 give the actualresult whereas the condition 1 and 4 gives the actual results.

The equation of PURLL is given below for two dissimilar conditions

For condition 3 and 4:

$$PULLR = \frac{ZG(P.F_L)^2}{L}\left[2 - \frac{Z}{(P.F_G)^2} - \frac{2\sqrt{1-(P.F_L)^2} \times \sqrt{1-(P.F_G)^2}}{(P.F_L)^2 \times (P.F_G)^2}\right] \qquad (12)$$

For condition 1 and 4:

$$PULLR = \frac{ZG(P.F_L)^2}{L}\left[2 - \frac{Z}{(P.F_G)^2} + \frac{2\sqrt{1-(P.F_L)^2} \times \sqrt{1-(P.F_G)^2}}{(P.F_L)^2 \times (P.F_G)^2}\right] \qquad (13)$$

IV. RESULTS AND DISCUSION

A. Reduction of line losses Analysis Conclusion

The impact of DG on line losses it assumed that DG should be kept at the Centre of feeder line that is DG=1 and take the length 2 km of system i.e. L=2km.the power factor of DG and load is too constant. The twenty five different values is taken and changing the output of DG and the load is constt at 2.3 pu. To use the equation 12 to find the different values of DG output power. It's shown in the figure3

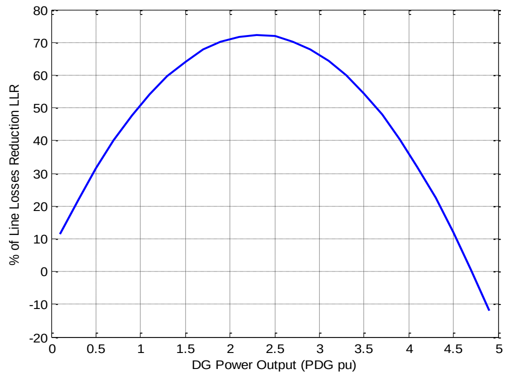

Figure 3. Reduction in system losses by varying DG output power

The above figure show that due DG in the system it reduce the losses. And DG delivers active and reactive power to the load Centre. And it is clearly that the reactive and active power is supply by DG to their load center.When the location of DG and their rating are not well matched then it's a high losses in the system.

A. Changing of DG position at different location

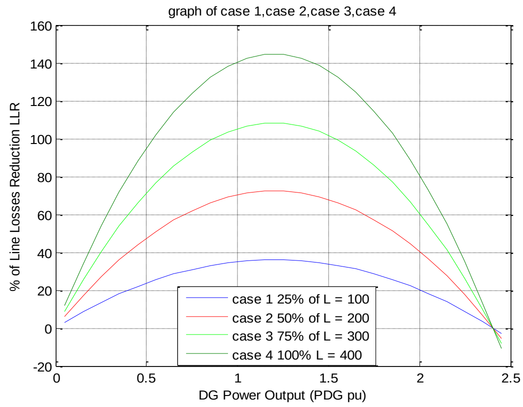

Figure 4. Line loss reduction by varying the location of DG and output power

The position of DG at four different location is to be consider.so it's assumed that DG is varying along the feeder line it would be taken four different location.

Location 1: fist DG keep at the 25% of total length

Location 2: second DG keeps at the 50% of total length

Location 3: third DG keeps at the 75% of total length

Location 4: at the end DG keep at 100% of total length

From above figure it is clearly shows that when DG near to the load the system losses is reduced .near the DG to load less will be the losses. This will only possible when the load and DG both are well matched. The total load can't consume the power which is given by DG. So at distance of DG from source there will be higher losses.

B. *At different power factor the system Analysis*

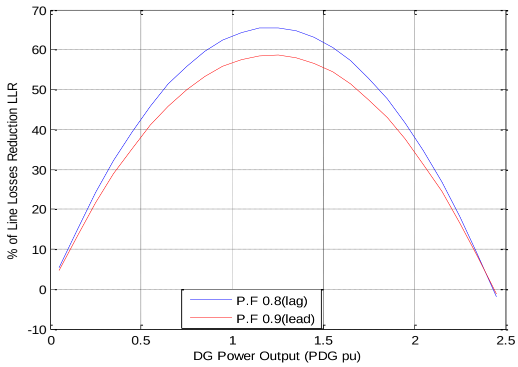

Figure 5. Line loss reduction by varying DG location and power factor

From above figure its show that when there is lagging power factor there is more reduction in the system and providing the DG reactive power to the load. DG power factor either lag or lead to calculate the reduces of line losses. Consider the two different values of DG power factor to analysis the reduction of loss.

CONCLUSION

This paper shows the reduction of line losses of radial distribution when DG is incorporate in the system. From result it clearly shows the line losses reduction. A simple distribution system is taken and incorporates the DG. The location, rating and power factor of DG is important to reduce the line losses.

Similarly, when DG is closer the load there is a reduction in line losses and at the distance from source to load be high losses in the system. This would be possible only when the load and DG both are well matched.

The purpose of this research is to integrate the one DG in a system to reduce line losses. Further if clearly result look then many DG incorporate in the distribution feeder will give better results.

REFERENCES

[1] K. Dang, J. Yu, T. Dang, and B. Han, “Benefit of distributed generation on line loss reduction,” in 2011 International Conference on Electrical and Control Engineering, 2011, pp. 2042-2045.

[2] A. Kumar and W. Gao, “Voltage profile improvement and line loss reduction with distributed generation in deregulated electricity markets,” TENCON 2008 - 2008 IEEE Region 10 Conference, pp. 1-6, Nov. 2008.

[3] P. Chiradeja, “Benefit of Distributed Generation: A Line Loss Reduction Analysis,” in 2005 IEEE/PES Transmission & Distribution Conference & Exposition: Asia and Pacific, pp. 1-5.

[4] Sonderegger, R. C., Henderson, D., Bubb, S., and Steury, J.,“Distributed Asset Insight,“ IEEE Power&Energy Magazine, pp. 32-39, May/June 2004.

[5] Puttgen, H. B., Macgregor, P. R., and Lambert F.C., “Distributed Generation: Semantic Hype or the Dawn of a New Era?,” IEEE Power&Energy Magazine, pp. 22-29, January/February 2003.

[6] A. D. T. Le, M. A. Kashem, S. Member, M. Negnevitsky, and G. Ledwich, “Optimal Distributed Generation Parameters for Reducing Losses with Economic Consideration,” pp. 1-8, 2007.

[7] P. Chiradeja, R. Ramakumar, and L. Fellow, “An Approach to Quantify the Technical Benefits of Distributed Generation,” vol. 19, no. 4, pp. 764-773, 2004.

[8] R. Abbasi, “Reduction of Transmission Line Losses Using VLSI Interconnect,” Procedia Engineering, vol. 30, no. 2011, pp. 10-19, Jan. 2012.

[9] T. Q. D. Khoa, P. t. t. Binh, and H. b. Tran, “Optimizing Location and Sizing of Distributed Generation in Distribution Systems,” in 2006 IEEE PES Power Systems Conference and Exposition, 2006, pp. 725-732.

[10] H. Iyer, S. Member, S. Ray, S. Member, R. Ramakumar, and L. Fellow, “Assessment of Distributed Generation Based on Voltage Profile Improvement and Line Loss Reduction,” pp. 1-6, 2010.

[11] P. A.-d-vimal Raj, S. Senthilkumar, J. Raja, S. Ravichandran, and T. G. Palanivelu, “Optimization of Distributed Generation Capacity for Line Loss Reduction and Voltage Profile Improvement Using PSO,” vol. 10, no. 2, pp. 41-48, 2008.

[12] W.-T. Huang and S.-T. Chen, “Line Loss Reduction by Distribution System Upgrading from Radial to Normally Closed-Loop Arrangement,” 2009 Ninth International Conference on Hybrid Intelligent Systems, pp. 334-339, 2009.

[13] H. B. Puttgen, P. R. Macgregor, and F. C. Lambert, 2003. Distributed generation: Semantic hype or the dawn of a new era?. vol. 1, p. 22-29. Power and Energy Magazine, IEEE.

[14] R. K. Rajput, 2005. Internal Combustion Engines: Laxmi Publications.

[15] D. M. Tagare, 2011. Electricity Power Generation. The Changing Dimensions: Wiley

Mushtaq Khattak who graduated from University of WAH in 2015. He holds B.Sc degree in Electrical Power Engineering.He is currently postgraduate student in M.Sc Electrical Power Engineering at UET Peshawar.

IJEW 国际工程期刊 International Journal of Engineering Works انجینئرنگ کاموں کا بین الاقوامی جرنل

International Journal of Engineering Works
ISSN-p: 2521-2419
ISSN-e: 2409-2770
Vol. 6, Issue 08, PP. 253-257, August 2019
https://www.ijew.io/
https://doi.org/10.34259/ijew.19.608253257

Rural Electrification through an Efficient Regulated System

Muhammad Safdar[1], Alamgir Ahmad Khattak[2], Asad Nawaz Khan[3], Abdul Basit[4]
[1,2,3,4] Department of Electrical Energy Systems Engineering, US Pakistan Centre for Advanced Studies in Energy, University of Engineering and technology Peshawar, Pakistan
salarsafdar@gmail.com[1], khattak.seecs@gmail.com[2], p096409@nu.edu.pk[3], abdul.basit@uetpeshawar.edu.pk[4]
Received: 07 August, Revised: 16 August, Accepted: 19 August

***Abstract*—**Due to the environmental concerns the focus is on clean energy generation globally. Hydrokinetic is one such emerging technology that is clean and abundantly available in Pakistan. Also we have energy crises so in areas where these resources are abundant if fed from locally generated electricity, the load on central grid can be reduced. This paper focuses on a battery-less system for hydrokinetics. PMSG is used and then a rectifier to convert its output to DC. This changing DC is then converted to a fixed 12 volts and regulated. Eliminating storage the output of this converter is fed to a UPS which changes it to alternating current of fixed voltage and frequency.

***Keywords*—** Buck converter, permanent magnet synchronous generator, hydrokinetic.

I. BACKGROUND

Pakistan has serious energy crises, this crises has affected every aspect of life from industry to household. Around 40,000 villages which comprises over 3 million households, do not have grid connectivity and depends on cell batteries, coal, kerosene oil, woods or petroleum etc. 7876 of the faraway villages cannot be connected to gird for another 20 years due to the distance from national grid, which leave these villages economically and technically unavailable [1].

On one side the crisis getting worse with each passing day on the other hand the current energy mix is majorly based on thermal sources. The fluctuating prices of oil in the international market affect its cost and supply, as these changes can never be forecasted therefore it's not a reliable source for generating electricity. Coal was considered as a best alternative due to its cheapness and wide availability but nowadays due to the environmental concerns it's also not much preferred [2-4]. Apart from the environmental concerns oil, gas and coal for generation purposes are imported mainly in Pakistan and if the current situation persists it will be a huge burden on the foreign exchange reserves of the country. The energy prices are continuously increasing and this results in the export surplus becoming more uncompetitive, local consumption goods are becoming costlier and some industries could face closure if this trend continues. All these factors pushing the country to a more economic stress. Therefore, there is an urgent need for quicker solutions to the energy crises, a switch over from the conventional to easily exploiting renewable energy resources which are sustainable and able to meet not only the current but also the projected energy demands of the country [5].

The need for clean and environment friendly techniques is obvious mainly due the environmental impacts of fossil fuels; the fear of depletion of these resources also gearing up this search for newer techniques of extracting clean energy. These resources other than the conventional are named as alternative. Alternative resources "are derived from natural replenish able resources that do not use up necessary resources or harm environment". Currently a lot of research work is going on in solar and wind energy conversion systems for improving its performance. Over the past few years the installation of solar and wind has boosted much.

The rural villages that are hard to reach for the national grid can be electrified by standalone RETs such as solar home systems (SHS) and wind home systems (WHS).

Wind and solar are dependent sources and to cope with its unreliable nature extra cost is put in the form of storage. We have rivers gushing from the Himalaya to the Arabian Sea and many hydro power projects are built on these rivers, tapping its potential energy for generating electricity.

The estimated theoretical potential of hydropower in Pakistan is 41.5GW, just 16% of this huge capacity is tapped so far. Micro hydro potential of the northern areas of Pakistan is estimated to be about 500MW [6-8]. Although having abundant resources there are many areas that either have no grid electricity or experience low voltages due to being faraway from grid. Implementing a local solution for electricity will help these communities flourish also the load on central grid can be reduced.

Hydropower is a cheap form of energy production due to very low running cost. But due to very high initial cost and other problems that the reservoirs pose, it has lost its charm. As an alternate we can go for hydrokinetic energy system that utilizes the kinetic energy of the flowing water and doesn't need much of the civil work that the conventional hydro generation systems demand.

This crises has affected not only the daily life standard but equally or more severely the industry. The inflation has increased over the years and the use of thermal resources for power generation is costing a lot to the nation. The already crippling industry is on the verge of death due to the persistent situation. Importing oil was never a viable option for us and the recent increase in the oil import has deteriorated the balance between imports and exports. Therefore the already available resources of Pakistan has to be exploited for electricity generation to lessen the import of oil for generation purposes. Other than the global trend towards clean energy resources, it is our necessity to exploit our indigenous resources for an overall balance [9]. In the past few years steps have been taken on the governmental level towards clean energy production.

II. INTRODUCTION

Simply stating hydrokinetic energy is the energy of moving water. Hydrokinetic turbines get its energy from the water current, it may be from waves, tidal currents or canals. This is the main difference between a hydropower and hydrokinetic production, hydropower uses the hydraulic head of water while hydrokinetic uses the kinetic energy of the running water for producing electricity. Hydrokinetic generation is similar to that of wind energy generation system. The difference to wind is the speed of water, which is quite lower than that of wind but the water density adds to the significance of hydrokinetics which is about 800 times more than that of air. Also it is more concentrated and reliable than wind.

Hydrokinetic technology is a promising clean energy source. And has distinct advantages over other existing resources. One of the capability of hydrokinetics is its adaptability. Hydrokinetic turbine can be placed in the already existing water channels thus the expense of infrastructure can be reduced. Other being the time of installation that is, a hydrokinetic system can be installed in much lesser time and it can start production quickly. Also the cost for setting up a hydrokinetic system is much lower than for the same amount of solar or wind production. Constructing a dam may render more power but the land and resources required are quite considerable and that part of land cannot be then used for any other purposes. A hydrokinetic system on the other hand require much less space and do not alter the flow direction.

Many rivers and canal structures are available for relatively easy and burden-free use by hydrokinetic turbines to produce clean energy. Land requirement and high cost for infrastructure are rarely obstacles for hydrokinetic energy.

One of the concern that hover over all of the renewable energy resources is the inconsistency of the output. Investors are generally reluctant to invest on dependent sources of renewable energy due to the fluctuating amounts of energy produced, that are difficult to

predict accurately. This fear slows down investment on new technologies and especially renewable sources that are dependent mainly. This risk is not involved in hydrokinetics, hydrokinetic turbines are installed in streamlines or man-made structures which have consistent water flows throughout the year. Some canals may have a lower flow or a drought period, usually the energy extracted from most of the canals can be predicted. This is a major advantage over other renewable energy resources, and makes hydrokinetic energy more appealing, proving its potential for substantial growth. Although these distinct advantages prove hydrokinetic at an edge from other clean energy sources; the shadow of hydropower has affected its growth. The clear difference between hydropower and hydrokinetic need to be put forward to enable its growth and general acceptance as a clean non-polluting source. Hydrokinetic systems for sure pose a worthwhile alternative to hydropower. It doesn’t pose any of hydropower’s problems to the environment (the environmental impact of hydrokinetic system is still not very much known). Despite the differences between a conventional hydropower and hydrokinetic systems, they can work very well together. Hydrokinetic can piggyback the traditional hydropower stations. The canals that emanates from the dams are most suitable for generating electricity through hydrokinetics. Studies and surveys are already completed for such sites and hydrokinetic can piggyback by using the already existing channels.

Hydrokinetic can be called a relatively new field in the domain of power generation. Researches all over the world is focusing mainly to achieve more efficient systems in terms of cost and power generation. Different types of turbine designs are in line for different applications. Areas with different speeds and other parameters are measured and the design of more efficient systems for power generation is acquired. In addition to harnessing the energy of the rivers there is a greater tendency towards the oceanic waves. Also making hybrid systems of more than one renewable resources like hybridizing wind and hydrokinetic system. A hydrokinetic system is usually for the local use therefore it works as an isolated system. Isolated systems are getting popular nowadays. Sites with less turbulence and flow continuous for whole year are best suited for hydrokinetics.

Since hydrokinetics system is designed for slow running volumes of water it can be applied to canal system and man-made streams. In Pakistan where the canal system is stretched over thousands of miles, deploying such systems will help in generating electricity for various purposes like for local needs, battery charging, and checking flow control for water levels in canals or for supplying energy for operate drip irrigation. Drip irrigation is efficient technique of farming, it saves water and is more efficient. In fast flowing rivers like river swat, extracting more power will help in meeting more purposes like heating water or pumping can be met through such system.

Standalone systems like wind and solar energy systems are implemented with batteries to deal with the problems of reliability. In the absence of sun light like at night the storage is used for supporting loads. In wind systems the storage helps in coping the problem of reliability and also at times when there is no load, the batteries act as load to the system because running a turbine system on no-load can torn out the blades quickly. On the other hand hydrokinetic systems are implemented for streams or currents that are exhibit known speeds and are steady throughout the year, a battery system is an extra burden both cost wise and maintenance wise in implementing a hydrokinetic system therefore avoided in this work.

III. DESIGN METHODOLOGY

A great deal of research is going on in the world on hydrokinetics. In this paper a topology is proposed for

obtaining fixed voltage equal to battery that is equal to 12 volts. Changing of water speeds affect the voltage and power significantly, during different seasons of the year the water speed vary much and this in turn effect the voltage generated.
In this paper we have come up with a solution to this problem. An AC generator is put in place, the output of this generator is rectified i-e changed to DC. This DC is then regulated and maintained at a fix level of 12V. We can then use this as power coming from a battery, as this is a constant 12V, or we can change this to a fixed AC by a home-inverter. Thus we can obtain a fixed AC from the changing water current with a simple technique and low cost.
Different components needed are; turbine for extracting energy, generator for converter that mechanical energy to electrical and then the control circuitry to regulate this voltage.

A. Mechanical design

Mechanical design comprises of turbine and generator section in this hydrokinetic system.

1) Turbine

Hydrokinetic turbines are mainly derived from its wind energy counter parts. They can be categorized into two categories of horizontal and vertical axis. On water flow basis they can be either vertical axis or horizontal axis turbines or they can be cross-flow [10]. Turbines are also classified as lift/drag nature, Equation for turbine power

$$P = C_p \frac{1}{2} \rho A v^3$$

A thorough detail of turbines is given in [11-14]. Turbine selection is not part of this study. The purpose of this study is to present an overall efficient system for generating hydro-power. A single turbine for different set of applications will affect the overall efficiency of the system. For different applications different turbine should be selected based on the requirement and condition of the water body. In the papers mentioned, different employability techniques are discussed and turbine selection will based on that research. Our aim in this paper is beyond turbine, the efficiency of the overall system by selecting proper generator and the control circuitry to achieve better power quality without interruptions and variations

2) Generator

Permanent magnet synchronous generator is a best choice due to its many benefits. PMSG has high efficiency and requires low maintenance as discussed in [15] and [16]. For this test therefore a permanent magnet generator was selected.

B. Electrical design

For the said application a converter was needed that has greater conversion ratio because the generator's output has to brought down to 12V also with less ripples so that the output is ripple free and a smooth inverter action takes place like that of a 12V battery to inverter. Bulky circuits are hard to mount therefore we needed a circuit that has lower switching losses so that if we increase the frequency for the purpose of minimizing the inductor and capacitor sizes, the losses do not go up. For large conversion ratios normally isolated DC-DC converters are preferred[17]. These converters are low cost and easy to make but they are more suitable for small power applications. For greater power their losses go up rapidly and the leakage losses also increases. Simple buck converter is also not suitable because as the conversion ratio becomes smaller the efficiency goes down with it. Efficiency is highly desirable in this application therefore a multi-phase buck converter is used in this application. Two phase buck converter is similar to a half bridge converter. The input voltage is split in the two phases by a series capacitor thus the duty ratio becomes half of the normal buck converter[18].
The circuit shown in figure 1 is a two-phase buck converter. A capacitor inserted between switch_1 and inductor L1, we call this additional capacitor as Ca. Switch 1 and 2 are operated with 1800 of phase shift and a duty cycle less than 0.5. The circuit has four states of operation.

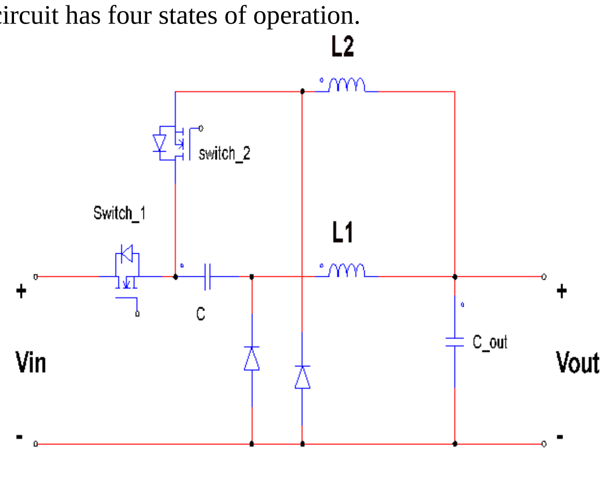

Figure 1. Circuit diagram of two-phase buck converter

In state 1, switch_1 is turned ON, inductor L1 is connected to the input and output capacitor and also to C_a in the first state. The input voltage to phase 1 is lower than the input voltage as it is source voltage E_i minus the voltage of the the additional capacitor, V_{Ca}. The stored energy in the inductor and its current rises as depicted by the equation,

$$\Delta i_{l1on} = \frac{(E_i - V_{Ca} - E_0)T_{ON}}{L1} \quad (1)$$

Switch 1 is then turned OFF and it remains OFF during states 2-4. Now inductor L1 get connected to the output capacitor and the inductor current falls continuously in a linear manner, given by the equation,

$$\Delta i_{l1OFF} = \frac{E_0 T_{OFF}}{L1} \quad (2)$$

The repetitions of this triangular waveform continues in cycles.

In state 3, second switch of the phase 2 is turned ON. L2 is connected with C_0 and C_a through switch_2 thus the input to this phase is now the voltage V_{Ca}. Change in current of L2 is as follows,

$$\Delta i_{L2on} = \frac{(V_{Ci} - E_0)T_{ON}}{L_2} \quad (3)$$

In states 1, 2 and 4, switch_2 is turned OFF. Inductor L2 is now in connection with the output capacitor and its current fall linearly as shown below,

$$\Delta i_{l2OFF} = \frac{E_0 T_{OFF}}{L2} \tag{4}$$

This waveform which is triangular in shape is recurrent with 180^0 phase shift; the inductor currents are both added up in the output capacitor.

$$(E_i - V_{Ca} - E_0)T_{ON} - E_0 T_{OFF} = 0 \tag{5}$$

Also (3) and (4)

$$(V_{Ci} - E_0)T_{ON} - E_0 T_{OFF} = 0 \tag{6}$$

From equation (5) and (6) the capacitor voltage V_{Ca} is,

$$V_{Ca} = \frac{E_i}{2} \tag{7}$$

From equation (7) it can be inferred that the voltage of the additional capacitor C_a becomes half of the input voltage, hence in state 1 where switch_1 is turned ON, the input voltage is shown as the input source voltage detriment the V_{ca}, in this manner input to the converter gets $E_i/2$, in state 3 the input voltage of phase 2 equals $V_{Ca} = \frac{E_i}{2}$, therefore in this manner the converter functions like a simple buck converter with an input halved i-e Ei/2.

The voltage conversion ratio is derived from (5) and (7) as,

$$\frac{E_0}{E_i} = \frac{1}{2}\frac{T_{ON}}{T_{ON}+T_{OFF}} = \frac{D}{2} \tag{8}$$

It is clear from this equation that the conversion ratio is halved as compared to that of a conventional buck. For a conversion ratio of D the duty cycle should be given twice. Current ripples are reduced.

In this converter the inductor currents are balanced automatically[19-20].

IV. EXPERIMENTAL SETUP AND RESULTS

Permanent magnet synchronous generator is used in this experiment for the testing of this circuit. Firstly the AC signal is rectified through a bridge rectifier to convert the incoming AC from the motor to a DC. A filtering capacitor is not incorporated to the output because the circuit that we designed was able to handle the ripples.

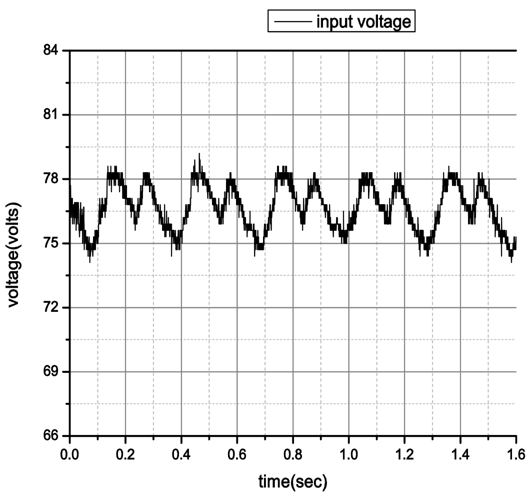

Figure 2. Output voltage waveform of the PMSG

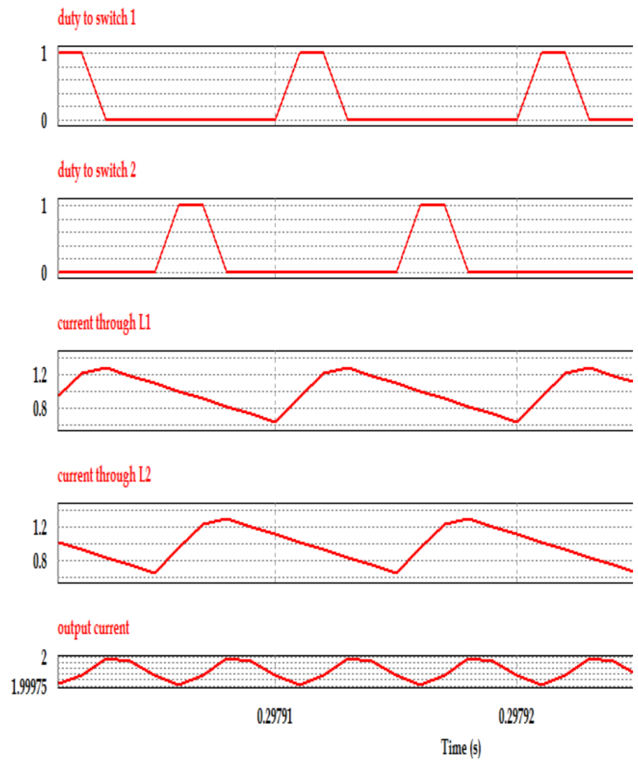

Figure 3. PSIM simulation results of the circuit

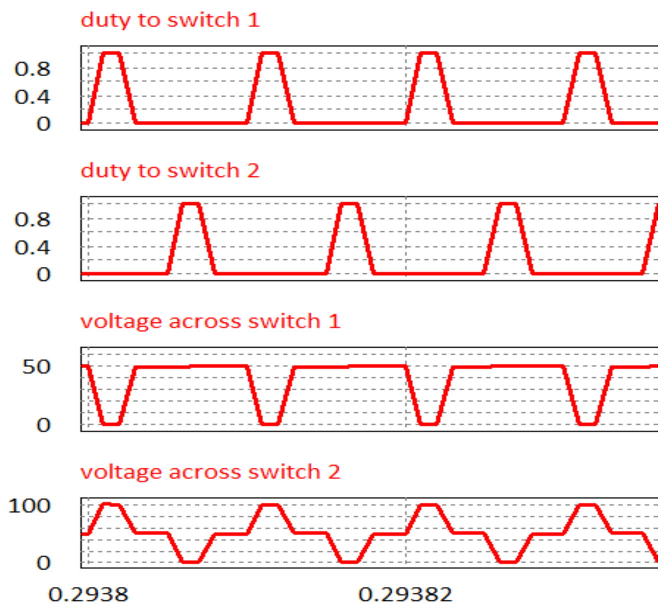

Figure 4. PSIM results for stress across switches

As evident from figure (3) and (4),

With this converter we were able to achieve;

(a) Conversion ratio of step down doubled (Eo/Ei = D/2).

(b) Reduction in losses of switching.

(c) Minimizing voltage stress across switching elements.

(d) Current ripple reduction.

(e) Balanced inductor currents.

(f) No need of current sensing part in the circuit.

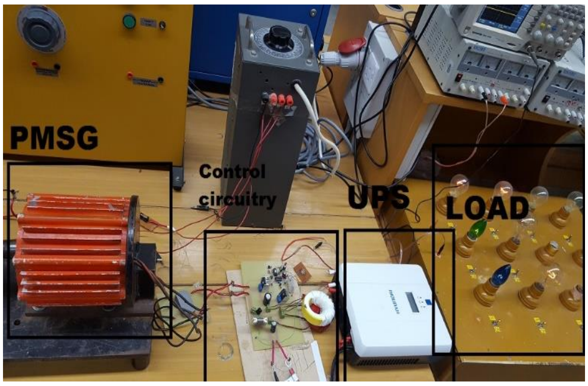

Figure 5. Experimental setup

CONCUSLION

From the above graphs it is evident that we have achieved our presented goals. The voltage stresses across the switches were low, the current was balanced and the output ripple free. The experimental setup is shown in the figure 5. All the results obtained in PSIM were verified in the experimental setup. A ripple free voltage was obtained through this circuit. Such type of systems can be implemented in the northern areas of Pakistan. In the northern areas there is tremendous resources that can be easily exploited through this technique. Most of the far northern areas are hard to reach for the national grid hence why some areas are even without electricity from the central grid and some, if have electricity from the grid, face severe low voltage problem. Through this technique these areas can be fed with electricity that would not fluctuate and hence beneficial for growth there. There is an option of scalability in this system also. If many such systems are installed over an area, we can arrange the overall output either in DC or AC microgrid or may be connected to the central grid, based upon the feasibility.

REFERENCES

[1] Dudley, Bob. "BP statistical review of world energy." London, UK (2012).

[2] Hartwick, John M. "Natural resources, national accounting and economic depreciation." Journal of public Economics 43.3 (1990): 291-304.

[3] Awan, Ahmad Bilal, and Zeeshan Ali Khan. "Recent progress in renewable energy–Remedy of energy crisis in Pakistan." Renewable and Sustainable Energy Reviews 33 (2014): 236-253.

[4] Khalil, Hafiz Bilal, and Syed Jawad Hussain Zaidi. "Energy crisis and potential of solar energy in Pakistan." Renewable and Sustainable Energy Reviews 31 (2014): 194-201.

[5] Asif, Muhammad. "Energy crisis in Pakistan: Origins, challenges, and sustainable solutions." OUP Catalogue (2012).

[6] Masood, Muhammad Tahir, and Fawad Shah. "Dilemma of third world countries-problems facing pakistan energy crisis a case-in-point." International Journal of Business and Management 7.5 (2012): 231.

[7] Yazhou, Lei. "Studies on wind farm integration into power system [J]." Automation of Electric Power Systems 27.8 (2003): 84-89.

[8] Bhutta, Muhammad Mahmood Aslam, et al. "Vertical axis wind turbine–A review of various configurations and design techniques." Renewable and Sustainable Energy Reviews 16.4 (2012): 1926-1939.

[9] Shakeel, Shah Rukh, Josu Takala, and Waqas Shakeel. "Renewable energy sources in power generation in Pakistan." Renewable and Sustainable Energy Reviews 64 (2016): 421-434.

[10] Rauf, Omer, et al. "An overview of energy status and development in Pakistan." Renewable and Sustainable Energy Reviews 48 (2015): 892-931.

[11] Kusakana, Kanzumba, and Herman Jacobus Vermaak. "Hydrokinetic power generation for rural electricity supply: Case of South Africa." Renewable energy 55 (2013): 467-473.

[12] Behrouzi, Fatemeh, et al. "Global renewable energy and its potential in Malaysia: A review of Hydrokinetic turbine technology." Renewable and Sustainable Energy Reviews 62 (2016): 1270-1281.

[13] Chica, E., et al. "Design of a hydrokinetic turbine." WIT Trans. Ecol. Environ 195 (2015): 137-148.

[14] Lago, L. I., F. L. Ponta, and L. Chen. "Advances and trends in hydrokinetic turbine systems." Energy for sustainable development 14.4 (2010): 287-296.

[15] De Battista, Hernan, Ricardo J. Mantz, and Carlos F. Christiansen. "Dynamical sliding mode power control of wind driven induction generators." IEEE Transactions on Energy Conversion 15.4 (2000): 451-457.

[16] Malinowski, Mariusz, Marian P. Kazmierkowski, and Andrzej M. Trzynadlowski. "A comparative study of control techniques for PWM rectifiers in AC adjustable speed drives." IEEE Transactions on power electronics 18.6 (2003): 1390-1396.

[17] Hansen, Anca D., and Gabriele Michalke. "Modelling and control of variable-speed multi-pole permanent magnet synchronous generator wind turbine." Wind Energy: An International Journal for Progress and Applications in Wind Power Conversion Technology 11.5 (2008): 537-554.

[18] Barnes, Arthur K., Juan C. Balda, and Corris M. Stewart. "Selection of converter topologies for distributed energy resources." 2012 Twenty-Seventh Annual IEEE Applied Power Electronics Conference and Exposition (APEC). IEEE, 2012.

[19] Nishijima, K & Harada, K & Nakano, T & Nabeshima, Toshitaka & Sato, T. (2005). Analysis of Double Step-Down Two-Phase Buck Converter for VRM. 497 - 502. 10.1109/INTLEC.2005.335149.

[20] Wu, Wenkai, Nai-Chi Lee, and George Schuellein. "Multi-phase buck converter design with two-phase coupled inductors." Twenty-First Annual IEEE Applied Power Electronics Conference and Exposition, 2006. APEC'06. IEEE, 2006.

Muhammad Safdar Buner Khyber Pakhtoonkhwa, March 30, 1992.
MSC Electrical Energy Systems Engineering, USPCAS-E Universityy of Engineering and Technology, Peshawar, Pakistan. 2019.
BSC Electrical Engineering, University of Engineering and Technology, Peshawar, Pakistan. 2015.

国际工程期刊
International Journal of Engineering Works
انجینرنگ کاموں کا بین الاقوامی جرنل

International Journal of Engineering Works
ISSN-p: 2521-2419
ISSN-e: 2409-2770
Vol. 6, Issue 08, PP. 258-268, August 2019
https://www.ijew.io/
https://doi.org/10.34259/ijew.19.608258268

Comparative Analysis of Linear and Nonlinear Control Strategies for Grid-tie Inverter in PV based Distributed Generation System

Rizwan Nadeem Shah[1*], Muhammad Jamil[2], Khuram Shahzad[3], Abdul Basit[4]
[1234]US Pakistan Center for Advance Studies in Energy, University of Engineering and Technology Peshawar
rshah27@asu.edu [1*], engrjamil.iub@gmail.com[2], kshahza1@asu.edu[3], abdul.basit@uetpeshawar.edu.pk[4]
Received: 14 August, Revised: 20 August, Accepted: 22 August

***Abstract*—**In this paper five different control strategies for grid-tie inverter in PV based DG systems have been implemented in MATLAB/Simulink for comparative analysis purpose to evaluate the performance. The control strategies are "Inner loop PI controller with outer loop PI controller in NRF", "Inner loop PI controller with outer loop PI controller in SRF", "Inner loop PR controller with outer loop PI controller", "Inner loop Hysteresis controller with outer loop PI controller", "Inner loop Repetitive controller with outer loop PI controller". The performance has been evaluated in both static and dynamic conditions and from the results it is evident that PI controller in SRF, PR controller and Repetitive controller perform best in both static conditions as well as in case of disturbances coming in either from PV side or grid side.

***Keywords*—**Proportional Integral Controller, Proportional Resonant Controller, Hysteresis Controller, Repetitive Controller, Single Stage PV System.

I. Introduction

As PV based DG system are becoming important part of today's electrical power system. The penetration of PV based DG system has increased tremendously. The total installed capacity of PV system has increased to 138GW globally [1]. To make the efficient use of this energy they must be brought on grid. Thus, PV based distributed generation system uses inverter interface extensively for grid integration. Power injection from PV systems into the main grid must be carried out in a controlled manner. But the penetration of PV system at high level has created grid instability issues. The main cause of these issues is the lack of proper control system for inverter. In literature many strategies have been presented for grid-tie inverter to control the output voltage, output current, output power (both active and reactive) and harmonics [2]. According to IEC 61727 2% change in frequency is allowed in 50 Hz system, while according to IEEE Std. 519-1990 total harmonic distortion should be less than 5%. Moreover, individual current harmonics are listed in table 1. IEC 61727 has also given voltage range for the operation of PV system connected to low voltage distribution network as given in table 2. The important parameters that need to be controlled are DC-link Voltage, otherwise will cause harmonic distortion and output current to inject the required amount of power into the grid.

TABLE 1: IEEE STD. 929-1992 INDIVIDUAL CURRENT HARMONICS

Odd Harmonics	Distortion limit
3^{rd} - 9^{th}	< 4%
11^{th} – 15^{th}	< 2%
17^{th} – 20^{th}	< 1.5%
23^{rd} – 33^{rd}	< 0.6%
Above the 33^{rd}	< 0.3%

TABLE 2: IEC 61627

Voltage Range	Disconnection time (cycles)
V < 50%	5
50% < V < 85%	100
85% < V < 110%	Normal Operation
110% < V < 135%	100
V > 135%	2.5

In [3][5] the control strategies presented in the literature have been reviewed based on design, implementation and performance. Depending upon the system types different types of control schemes have been implemented so far. the classical controllers like Proportional, Proportional-Integral, Proportional-Derivative, and Proportional-Integral-Derivative are the basic controller used in linear systems [3]. In [4] proportional resonant controller has been implemented; proportional resonant controller is the same as the proportional integral controller, but the only difference is the way through which integration takes place in both controllers. In Proportional Resonant controller the integrator integrates the frequencies closest the resonant frequency which exclude the steady state error or phase shift. Nonlinear controllers have shown remarkable operation as compare to conventional controllers, but they have complexity in implementation and design. In [6] slide mode controller has been used for grid tie inverter. It has been used to adjust the output voltage and to control the output current of the inverter. The good thing about this technique is the ruthless behavior to load disturbances and parameter variation [3]. Therefore, ideal case zero steady state error is achievable. But microprocessors used in the digital system have limited sampling rate which leads to other phenomena called chattering affect which degrades the performance and reduces the efficiency in power electronics interfaced system. In [7-11] current hysteresis control has been presented, this controller because of its accessibility and ease of implementation was popular for integrated DG systems. In this method the error signal is being kept within a band called “Hysteresis band”. Hysteresis controller causes greater harmonic distortion when the bandwidth of the hysteresis band is kept large, however switching losses gets reduced so trade off should be made while designing hysteresis band. Robust control technique is useful to be implemented when there is error in the system modelling. Controller is designed considering the system uncertainties to achieve vigorous and stable performance in the presence of limited errors in the system model. While designing robust controller, excellent benchmark, neat elucidation and limitations need to be defined clearly. Even if the number of variables needs to be controlled are more than one, guaranteed robust performance and stability in the close loop system can be achieved [12]. In [13,14] H infinity controller has been used as a current controller but it requires accurate system model and involve high level of computational complexity and unable to manage non-linear constraints. PC (Predictive controller) can be implemented when accurate model of the system is known for future prediction. It can handle nonlinearities but requires high level of computations to be done with fast digital system. In [15,16] deadbeat control theory has been presented, in this control scheme the differential equations that control the dynamics of the controlled system need to be derived first and discretized. Based on these dynamic equations, the sampling period of the control signal is first calculated in such a way that the state variables got matched with the reference value at the end of the sampling period. In [17,18,19] repetitive controller is used. The principle behind RC comes from the internal model principle. Which states that by entering the cause of a disturbance/reference in closed loop path, it is possible to obtain a good rejection / location. To deduce whether the error has been reduced or eliminated requires the storage of error signal for one period. Therefore, the RC has remained in for nonlinear periodic loads. By nature, RC lacks dynamic response in spite of showing excellent performance against non-linear periodic loads. However, this problem can be eliminated by combining conventional controller with desired transient response in parallel or cascading. Fuzzy control is a method has made it possible to put in use human knowledge and intelligence in an artificial way to control a system. In [20] Fuzzy controller works based on set of predefined rules but inherently lacks performance parameters. In [21] Autonomous controller has been presented; Autonomous systems are capable of performing complex tasks autonomously. The process of autonomy can be improved by applying human intelligence. This system needs further improvement as engineers are trying to apply human intelligence and knowledge directly with the aim of achieving high level of automation. In [22,23] Neural Network controller has been presented. Neural Network (NN) contains number of artificial neurons connected together which imitate a biological system of the brain. Neural Network is capable of estimating a map of elective characteristics and can achieve a higher defect endurance. NN can train both online and offline when used in a control system [24]. Adaptive control method has the regulation capability of control actions what so ever the operating conditions of the system are. The precise knowledge of system parameters for high performance of the system. Even though, the computational complexity of this control scheme is high [24,25, 26].

In literature the focus has been designing a controller however performance evaluation must be done against different types of disturbances either coming from grid side or PV side before implementing any control strategy. In this research, combination of different control strategies has been used to evaluate the performance against grid side and PV side disturbance to see which controller performs best in both static and dynamic conditions.

II. MODEL OF SINGLE STAGE PV SYSTEM

Single stage PV system as presented in figure 1 has been modelled in MATLAB/Simulink to evaluate the performance with different control strategies. It consists of 5kW PV array connected to a capacitor at the output which regulates the output voltage of PV array, grid-tie inverter with LCL filter connected to the grid and associated control and pulse generator to drive the switches. To inject high quality of power two parameter must be controlled which are the DC-link capacitor voltage and output current of the inverter. DC-link voltage controller regulates the input voltage by generating reference for the current controller. While current controller regulates the output current of the inverter by following the reference value.

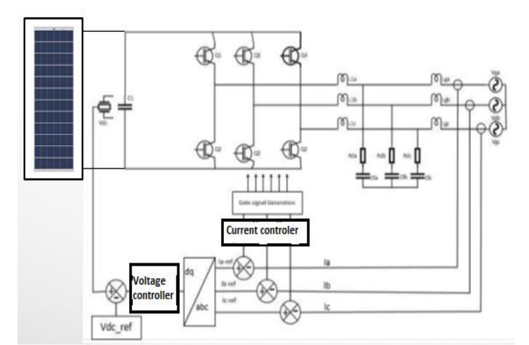

Figure 1: Single Stage PV System

A. Modelling of PV Array

PV (Photovoltaic) cell has been modelled as a current source in parallel with a resistor as in [33] represented in

Figure 2. Rc is the shunt resistor while Rs is the series resistor which represents the resistance of the wire.

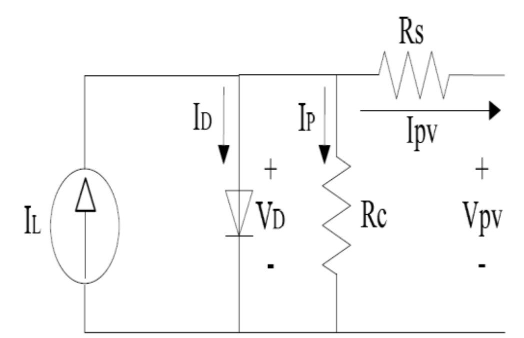

Figure 2: Photovoltaic cell model

5kW PV array has been designed in MATLAB/Simulink using "TRINA SOLAR TSM-250PA05.08" which consists of 60 cells per module. Each Module has 248.86 W at maximum power while there are 22 modules connected in series which generate 700V at the output with 8.06A current. The I-V and P-V curve of 5kW array is shown in Figure 3.

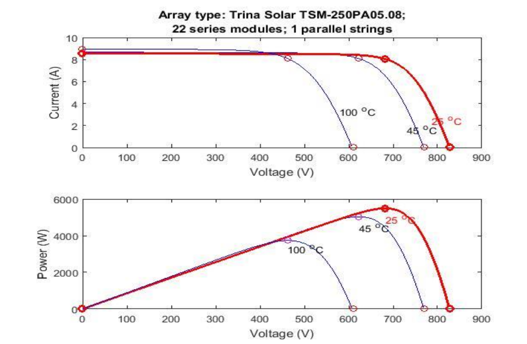

Figure 3: I-V and P-V cureve of 5kW PV Array

B. *Modelling of Grid-Tie inverter*

Grid tie inverter consist of switching part which is nonlinear and LCL filter which is linear as represented in Figure 4. the dynamic equation of the system can be obtained by applying KCL and KVL to the model. Before that switching function must be defined,

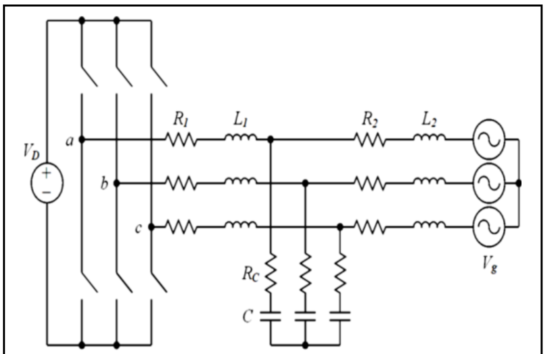

Figure 4: Grid-tie Inverter Model

$$S_i = \begin{matrix} 1\ (i_{th}\ switch\ on) \\ -1\ (i_{th}\ switch\ off) \end{matrix} \qquad i = 1,2 \ldots 6 \tag{1.1}$$

$$S_{ak} = \frac{1}{2} + \frac{1}{4}(S_1 - S_2) \tag{1.2}$$

$$S_{bk} = \frac{1}{2} + \frac{1}{4}(S_3 - S_4) \tag{1.3}$$

$$S_{ck} = \frac{1}{2} + \frac{1}{4}(S_5 - S_6) \tag{1.4}$$

Where k = 0,1….7.

The system state model can be obtained by applying KVL and KCL to the per phase model of the LCL filter as represented in Figure 5.

$$\frac{di_1}{dt} = -\left(\frac{R_C + R_1}{L_1}\right) i_1 + \left(\frac{Rc}{L_1}\right) i_2 - \left(\frac{1}{L_1}\right) v_C + \left(\frac{V_D}{2L_1}\right) S \tag{1.6}$$

$$\frac{di_2}{dt} = \left(\frac{R_C}{L_2}\right) i_1 - \left(\frac{R_C + R_2}{L_2}\right) i_2 + \left(\frac{1}{L_2}\right) v_C - \left(\frac{1}{L_2}\right) v_g \tag{1.7}$$

$$\frac{dv_c}{dt} = \left(\frac{1}{C}\right) i_1 - \left(\frac{1}{C}\right) i_2 \tag{1.8}$$

The state vector $x(t)$ contains inductor current $i_1(t)$ at the switching side, inductor current $i_2(t)$ at grid side and the filter capacitor voltage $v_C(t)$ as state variables in stationary reference frame. For per phase system the state vector $x(t)$ would become:

$$x(t) = [i_{1a}(t)\ \ i_{2a}(t)\ \ v_{Ca}(t)]^T \tag{1.9}$$

the continuous time state space model derived from the KVL equations in given below:

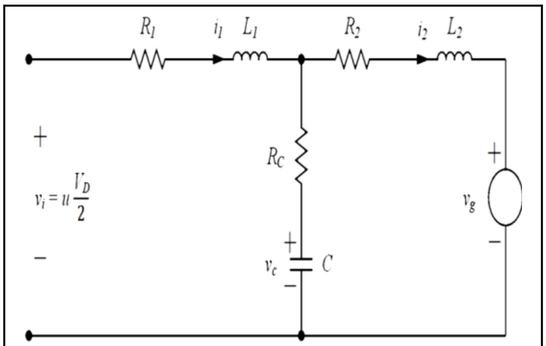

Figure 5: Per phase model of LCL filter

$$\frac{dx(t)}{dt} = Ax(t) + BU(t) + Pg(t) \tag{1.10}$$

$$y(t) = Cx(t) \tag{1.11}$$

Where,

$$A = \begin{bmatrix} \frac{R_C + R_1}{-L_1} & \frac{R_C}{L_1} & -\frac{1}{L_1} \\ \frac{R_C}{L_2} & \frac{R_C + R_2}{-L_2} & \frac{1}{L_2} \\ \frac{1}{C} & \frac{-1}{C} & 0 \end{bmatrix}, B = \begin{bmatrix} \frac{V_D}{2L_1} \\ 0 \\ 0 \end{bmatrix}, P = \begin{bmatrix} 0 \\ -\frac{1}{L_2} \\ 0 \end{bmatrix},$$

$$C = [0 \quad 1 \quad 0]$$

C. Design of LCL filter

LCL filter provides better harmonics attenuation as compared to simple L and LC filter however designing LCL filter is a complex task. The values of L and C must be chosen in such a way that the resonance frequency should be far away from the switching frequency as well as fundamental frequency $\omega_g \times 10 \leq \omega_{res} \leq 0.5 \times \omega_{sw}$ [27].

$$(\omega_{res})^2 = \frac{L_1 + L_2}{L_1 L_2 C} \tag{1.12}$$

While

$$CL_T = \frac{1}{(\omega_{res})^2 \left(\frac{r_1}{(r_1+1)^2}\right)} \tag{1.13}$$

Where $L_1 + L_2 = L_T$ and $r_1 = \frac{L_2}{L_1}$, thus $(\omega_{res})^2 = \frac{4}{CL_T}$. The values of capacitance can't be greater than $0.05(C_{base})$ By selecting $\omega_{res} = 2000\pi\ rad/sec$, $r_1 = 1$ and $C = 5\mu F$ the value of inductor can be found out $L_T = 5.1mH$. thus $L_1 = L_2 = 2.55mH$. The values of damping resistor can be found out from the following formula. $R_C = \frac{1}{3\omega_{res}C}$, Thus $R_C = 10.6\ \Omega$.

III. Control Strategies

In order to do performance evaluation five different control strategies have been implemented in MATLAB/Simulink each control strategy contains two controllers, voltage controller that control the voltage across DC-link capacitor and generates reference for current controller, while current controller regulates the grid injected current according the reference value. in each case proportional integral controller has been used as DC-link voltage controller while current controller varies. The implemented control strategies are given below:

A. PI DC-link voltage controller with PI current controller in NRF

In this control scheme proportional integral controller regulates the DC-link voltage according the reference value while proportional integral controller in the inner loop regulates the output current. Current controller is implemented in natural reference frame where the current vectors are rotating while reference frame is stationary. While reference current is being generated through Clark's and Park's transformation as given in [28] for current controller. The control block is represented in Figure 6. PI controller is tuned in MATLAB/SISO tool according the required performance parameter such as 20% overshoot, setlling time 20ms and zero steady state error.

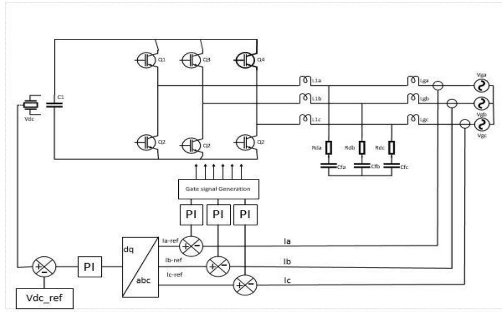

Figure 6: Control schems with PI controller in NRF

B. PI DC-link voltage controller with PI current controller in SRF

In this control strategy DC-link voltage controller is the same PI controller as implemented in A, while PI current controller is implemented in Synchronous reference frame by transforming three phase rotating current vectors into DC form while the reference frame rotates at synchronous speed as in Figure 7. PI controller is tuned by using MATLAB/SISO tool according to the required transient response and steady state error.

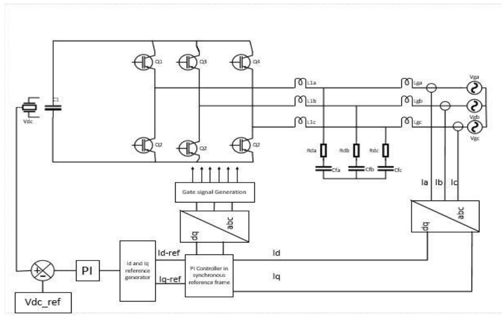

Figure 7: PI DC-link voltage controller with PI current controller in synchronous reference frame.

C. PI DC-link voltage controller with PR current controller in NRF

In this control strategy same PI controller has been adopted to control DC-link voltage while Proportional resonant controller controls the output current of the inverter. As the ideal PR controller is difficult to realize that's why improved version as mentioned in [29] has been used. In PR controller the proportional gain remains the same as in PI controller

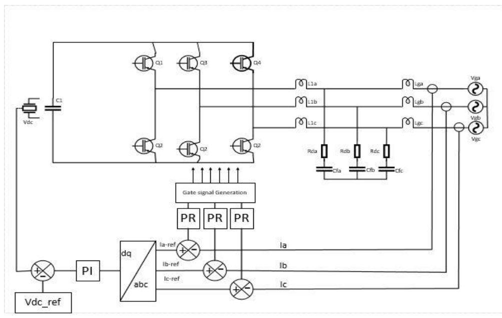

Figure 8: Proportional Resonant current controller with PI DC-link voltage controller

which forms the dynamics of the system according to the bandwidth (gain and phase margin). The values of integral and proportional gains are determined as mentioned in [38]. Figure 8 represents the controller scheme with PR current controller in NRF.

D. *PI DC-link voltage controller with Hysteresis current controller in NRF*

Hysteresis current controller is a non-linear controller and special case of slide mode controller where the error signal is kept within a band called hysteresis band. It inherently lacks transient response parameters. Hysteresis band defines the maximum switching frequency and output error with reference to the reference signal. Hysteresis current controller along with PI controller has been implemented as mentioned in [30] and represented in Figure 9. In this control strategy the transient response parameters are determined solely by PI DC-link voltage controller.

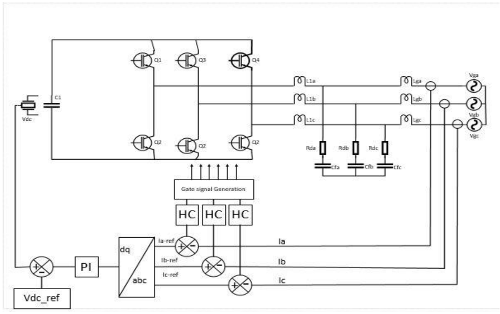

Figure 9: Hysteresis Current controller with PI DC-link voltage controller

E. *PI DC-link voltage controller with Repetitive current controller in NRF*

Repetitive controller has been used for the tracking of periodic signal which mainly works based on internal model principle. RC Controller as mentioned in [31] has been implemented along with Proportional integral DC-link voltage controller as presented in Figure 10. Just like Hysteresis current controller Repetitive current controller also inherently lacks transient response parameters, that's why conventional PI controller is used in cascade to stabilize the plant [32].

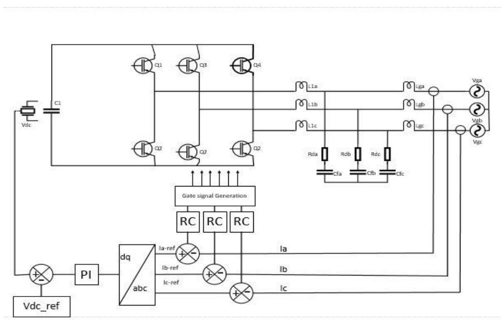

Figure 10: RC controller with PI DC-link voltage controller

IV. SIMULATION RESULTS

The Simulation results have been obtained for each control strategy in both static and dynamic conditions to evaluate the performance. In static conditions there is no change in parameters either on the grid side or PV side such that the system operates in ideal conditions. While in dynamic conditions the system performance has been evaluated against different types of disturbances coming either from the PV side or grid side. The possible disturbances on PV side can be the change in irradiance level or temperature which may vary the output power of PV system. While on grid side the disturbance can be in the form of short term voltage dip or voltage swell which can't be detected by the protection system and change in frequency in grid phase angle.

A. *Static conditions*

The response of each control strategy has been shown in this section. In static conditions there is no change of parameter either on grid side or PV side. DC link voltage and reference tracking of current controller in case of each control strategy has been presented in the Figure 11, Figure 12, Figure 13, Figure 14 and Figure 15 below.

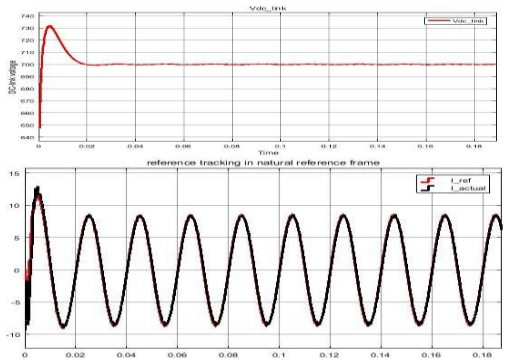

Figure 11. DC link voltage and reference tracking of PI controller in NRF

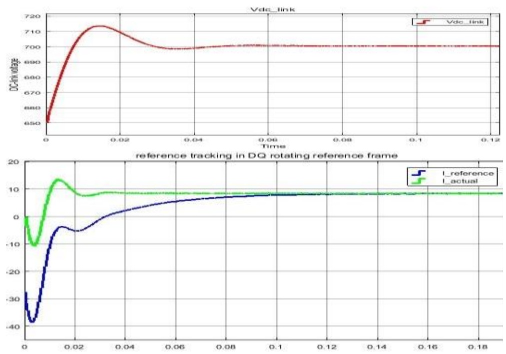

Figure 12: DC-link Voltage and current reference trakcing of PI controller in SRF

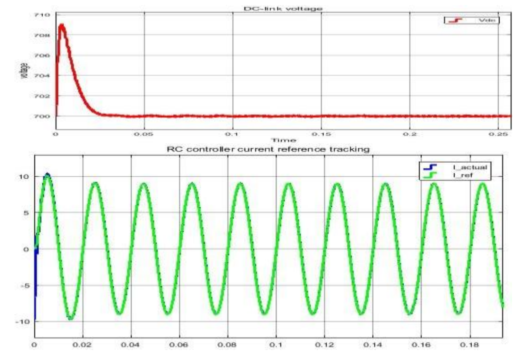

Figure 13: DC-link voltage and RC reference tracking

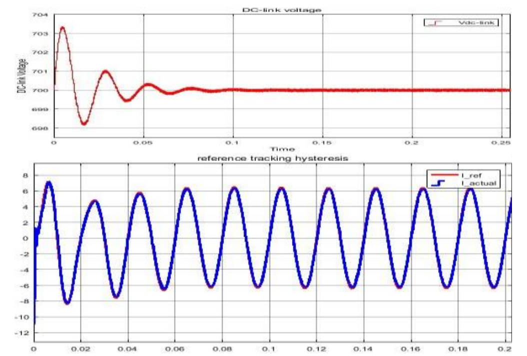

Figure 14: DC-link voltage and Hysteresis current controller reference tracking

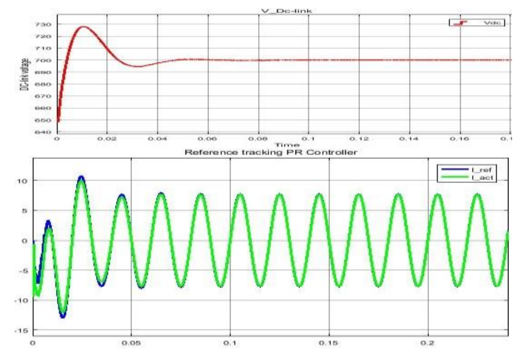

Figure 15: DC-link Voltage and current reference tracking of PR controller in NRF

In static conditions each control strategy perform well as expected. Each controller gets stable according to the preset transient parameters. As it can be seen in Figure 11 the inner loop gets stable first than the outer loop gets stable while the current loop tracks the reference value with zero steady state error. Another important parameter that should be monitored is the total harmonic distortion in the output current that should follow the ieee standards. Figure 16 to Figure 20 show the THD in the output current of each control strategy. As it is evident from Figure 20 Hysteresis controller results greater Harmonics as compare to any other control strategy while PR controller results in least Harmonics in the output current as it is depicting from Figure 19. total harmonic distortion in each case is less than 5%.

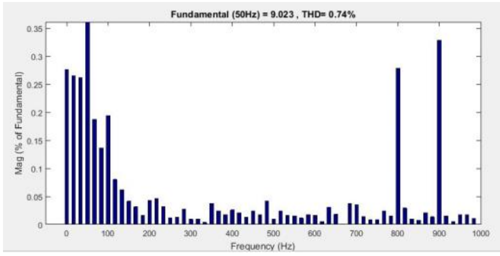

Figure 16: Current THD with RC controller in NRF

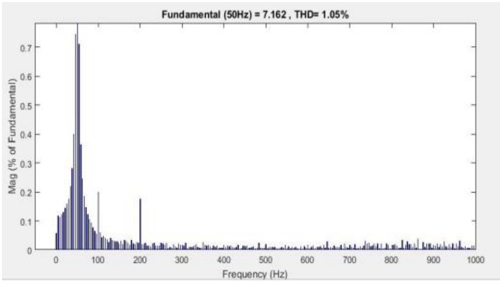

Figure 17: Current THD with PI controller in SRF

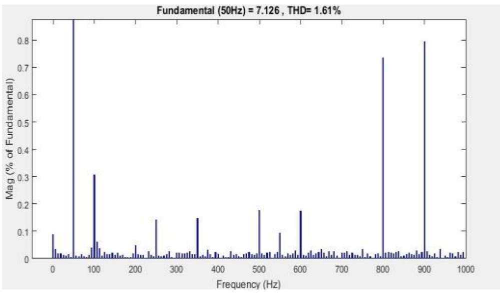

Figure 18: Current THD with PI controller in NRF

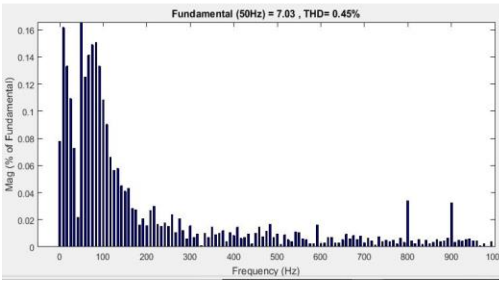

Figure 19: Current THD with PR controller

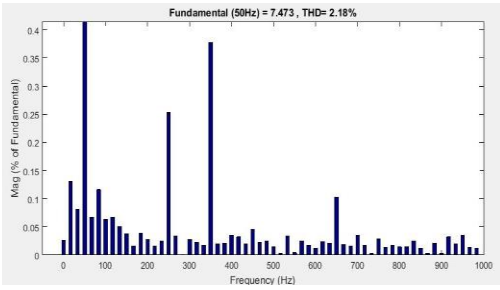

Figure 20: Current THD with Hysteresis controller

B. Dynamic Conditions

In dynamic conditions the performance has been evaluated against grid side disturbances as well as PV side disturbances. PV side disturbance could the change in PV output power while on grid side disturbances can in the form of voltage swell and voltage dip.

1) Reference tracking

To see the reference tracking ability of each control strategy the output power of PV has been changed in different time intervals in dynamic conditions, the results have been shown in Figure 21 to Figure 25.

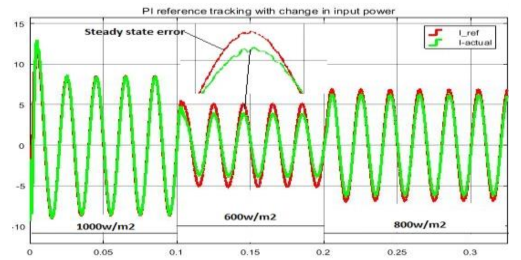

Figure 21: Reference tracking PI controller in NRF

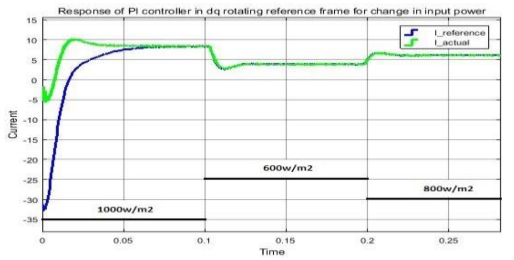

Figure 22: Reference tracking PI controller in SRF

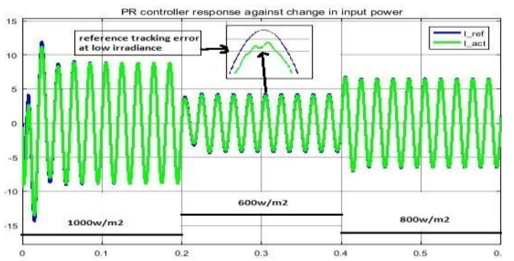

Figure 23: Reference tracking PR controller in NRF

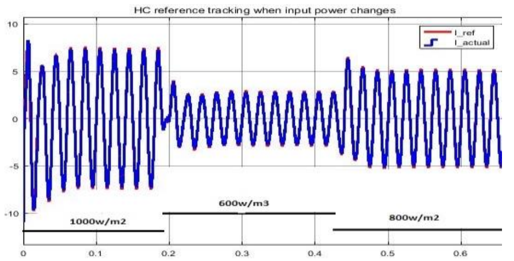

Figure 24: Reference tracking of Hysteresis controller

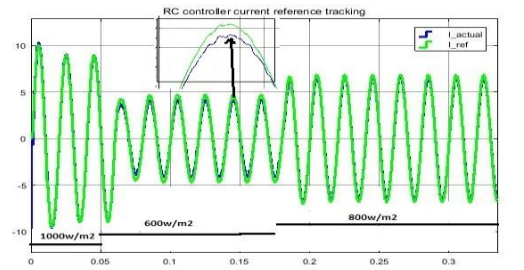

Figure 25: RC controller reference tracking

As it is evident from Figure 21 that PI controller in Natural reference frame is not good reference tracker as it causes steady state error at low irradiance level which about 25%. So efficiency of the system will drop at low irradiance level. While PI controller in SRF and Hysteresis controller are good reference trackers with zero steady error as in Figure 22 and 24. While PR controller and RC controller presents same steady state error at low irradiance level as can be seen in Figure 23 and 25.

C. Voltage Dip of 0.1pu

Voltage dip is common phenomena which can occur because of connection of large inductive load and ground faults, so controller should provide stable operation in case of short-term faults that can't be sensed by the protection system. Thus, the performance of the implemented control strategies is evaluated for voltage dip of 5ms. Figure 26 to Figure 30 show the response of each control strategy.

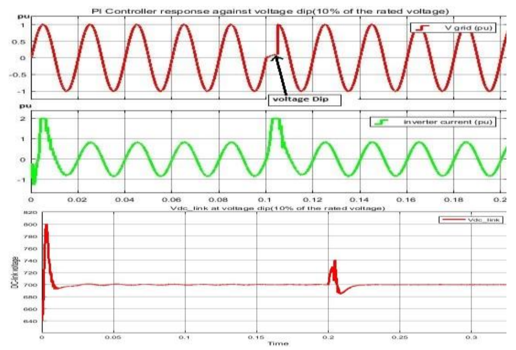

Figure 26: PI Controller in NRF at voltage dip

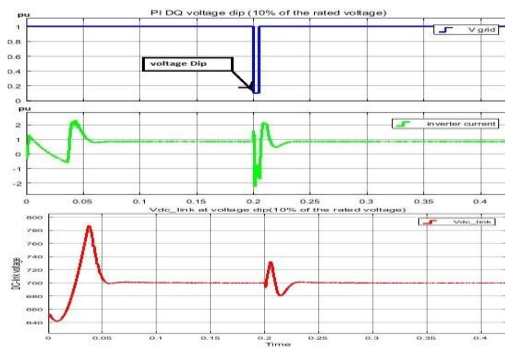

Figure 27: PI Controller in SRF at voltage dip

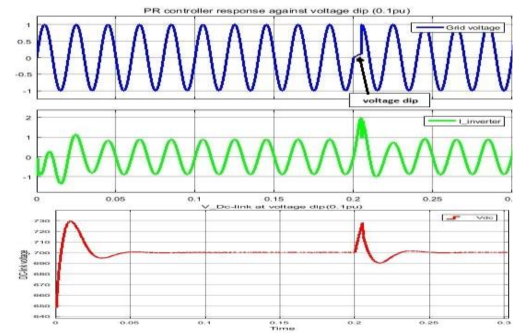

Figure 28: PR Controller at voltage dip

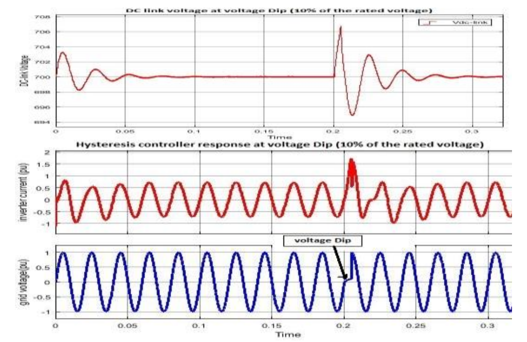

Figure 29: Hysteresis Controller at voltage dip

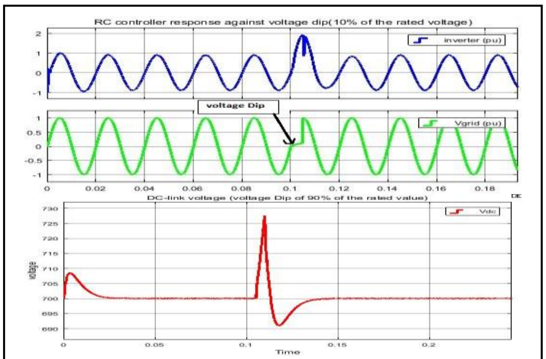

Figure 30: RC Controller at voltage dip

D. Voltage Swell 1.8 pu

Voltage swell is common phenomena which can occur as results of disconnection of large inductive load and in resistance grounded system when there is fault in any phase, voltage of the other healthy phases goes high. So controller should provide stable operation in case of short term faults that can't be sensed by the protection system. So, the performance of the implemented control strategies is evaluated for voltage swell of 5ms. Figure 31 to Figure 35 show the response of each control strategy.

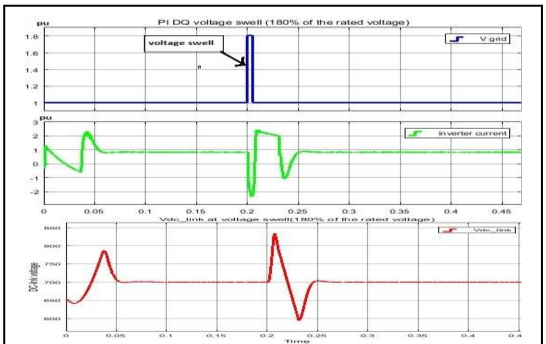

Figure 31: PI Controller in SRF at voltage swell

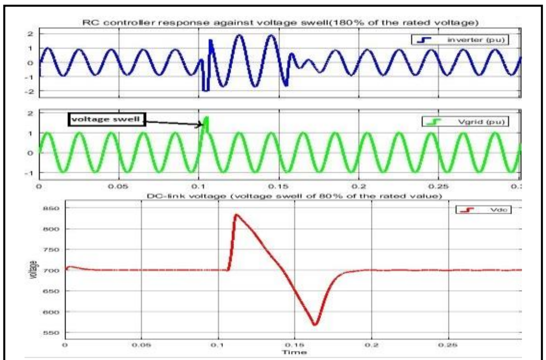

Figure 32: RC Controller at voltage swell

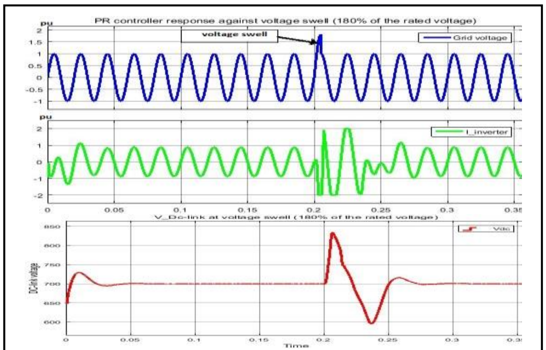

Figure 33: PR Controller at voltage swell

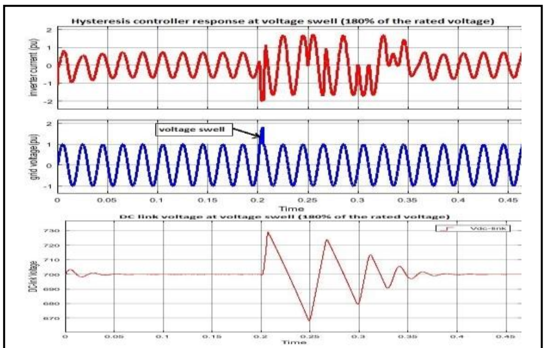

Figure 34: Hysteresis Controller at voltage swell

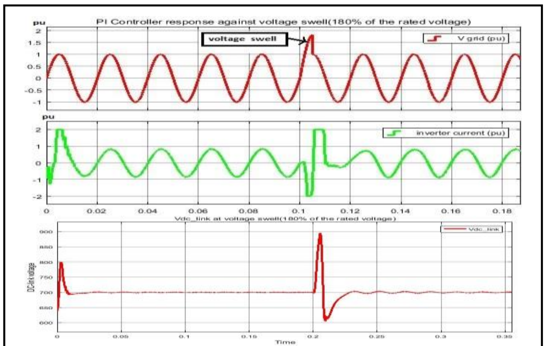

Figure 35: PI Controller in NRF at voltage swell

E. *Power Injection*

Single stage PV systems does not have MPPT controller, that's why it is important to evaluate the performance the system efficiency in terms of Power generated by PV system and power injected into the grid. Figure 36 to Figure 40 present the power injection of each control strategy.

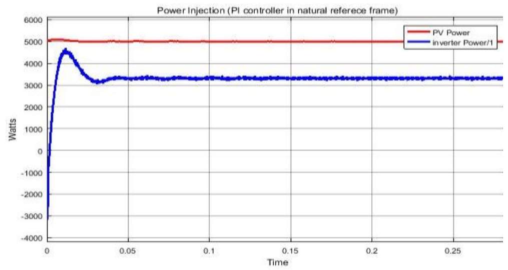

Figure 36: Injected Power PI controller in NRF

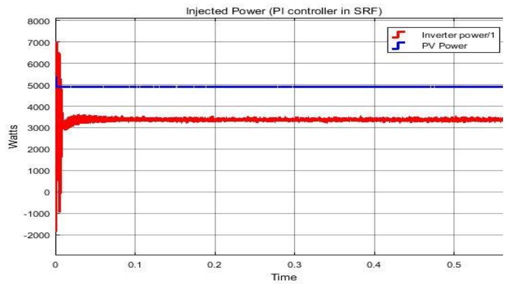

Figure 37: Injected Power PI controller in SRF

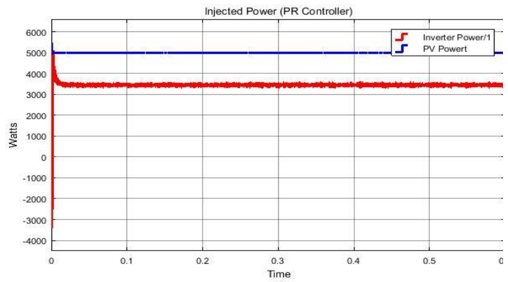

Figure 38: Injected Power PR controller

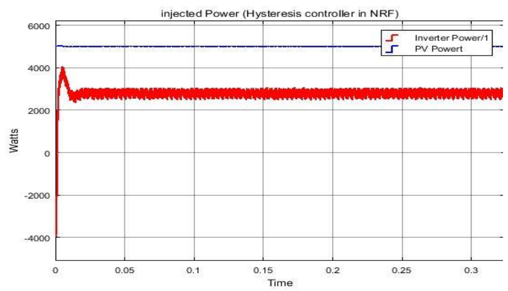

Figure 39: Injected Power Hysteresis controller

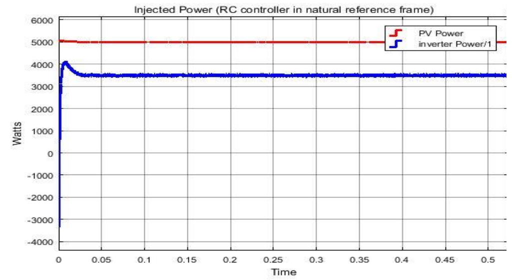

Figure 40: Injected Power RC controller

V. RESULTS OF THE CASE STUDIES

The results of the case studies run for performance evaluation have been summarized in the below tables to ease the understanding. Table 3 presents the Total Harmonic Distortion in the output current in case of each control strategy. Table 4 presents the time taken by each controller to get stable after the removal voltage dip while table 5 presents the time taken by each controller to get stability after the removal of voltage swell in terms of no of cycles, while table 6 presents the efficiency of the system with different control strategies. As it is evident from table 3 that PI control in natural reference frame offer the least harmonic distortion in the output current while hysteresis controller total harmonic distortion is maximum among all control strategies.

TABLE 3: TOTAL HARMONIC DISTORTION

S.No	Control Strategy	%THD
1	PI DC-link voltage controller, PI current controller in Natural reference frame	1.61
2	PI DC-link voltage controller PI current controller in Synchronous reference frame	1.05
3	PI DC-link voltage controller with Proportional resonant current controller	0.45
4	PI DC-link voltage controller with hysteresis current	2.18
5	PI DC-link voltage controller with repetitive current controller	0.74

TABLE 4: STABILITY TIME AFTER REMOVAL OF FAULT (VOLTAGE DIP)

S.No	Control Strategy	Time (no of cycles)
1	PI DC-link voltage controller, PI current controller in Natural reference frame	1
2	PI DC-link voltage controller with PI current controller in Synchronous reference frame	2
3	PI DC-link voltage controller Proportional resonant current controller	3
4	PI DC-link voltage controller with hysteresis current	5
5	PI DC-link voltage controller with repetitive current controller	1

TABLE 5: STABILITY TIME AFTER REMOVAL OF FAULT (VOLTAGE SWELL)

S.No	Control Strategy	Time (no of cycles)
1	PI DC-link voltage controller with PI current controller in Natural reference frame	1
2	PI DC-link voltage controller with PI current controller in Synchronous reference frame	2
3	PI DC-link voltage controller with proportional resonant current controller	3
4	PI DC-link voltage controller with hysteresis current	10
5	PI DC-link voltage controller with repetitive current controller	3

TABLE 6: EFFICIENCY OF PV SYSTEM WITH DIFFERENT CONTROL STRATEGIES

S.No	Control Strategy	Efficiency
1	PI DC-link voltage controller PI current controller in Natural reference frame	65.8%
2	PI DC-link voltage controller PI current controller in Synchronous reference frame	69.2%
3	PI DC-link voltage controller with proportional resonant current controller	76.8%
4	PI DC-link voltage controller with hysteresis current controller	55.8%
5	PI DC-link voltage controller with repetitive current controller	69.8%

CONCUSLION

In this paper five different control strategies have been implemented in MATLAB/Simulink for grid-tie inverter in PV based distributed generation system applications. The performance of each control strategy has been evaluated both in static and dynamic conditions to see which controller performs best. As it is evident from the results that PI controller in Synchronous reference frame, PR controller in natural reference frame and RC controller show better performance in terms of reference tracking, stability, THD and efficiency in both static and dynamic conditions, while PI controller natural reference frame causes steady state error at low irradiance level causing efficiency drop. Moreover, hysteresis controller results in high total harmonic distortion in the output current.

REFERENCES

[1] European Photovoltaic Industry Association, “Global market outlook– for photovoltaics 2014 2018,” EPIA, Tech. Rep., Jun. 2014, ISBN 9789082228403.

[2] Ned Mohan, Tore M. Undeland, and William P. Robbins, *Power Electronics*, 2nd ed., pp. 23, 241, and 726, John Wiley & Sons, Inc., New York, 1995.

[3] Athari, Hamed, Mehdi Niroomand, and Mohammad Ataei. "Review and classification of control systems in grid-tied inverters." *Renewable and Sustainable Energy Reviews* 72 (2017): 1167-1176

[4] Teodorescu R, Blaabjerg F, Liserre M, Loh PC. Proportional-resonant controllers and filters for grid-connected voltage-source converters. IEEE Proc Electr Power Appl 2006;153(5):750–62, [Sept.].

[5] Chatterjee, Aditi, and Kanungo Barada Mohanty. "Current control strategies for single phase grid integrated inverters for photovoltaic applications-a review." *Renewable and Sustainable Energy Reviews* 92 (2018): 554-569.

[6] Komurcugil H. Rotating-sliding-line-based sliding-mode control for single-phase UPS inverters. IEEE Trans Ind Electron 2012;59(10):3719–26, [Oct.].

[7] Krismadinata C, Rahim NA, Selvaraj J. Implementation of hysteresis current control for single-phase grid connected inverter. In: Proceedings 7th International Conference on Power Electronics and Drive Systems, Bangkok; 2007. p. 1097–1101.

[8] Dahono PA. New hysteresis current controller for single-phase full-bridge inverters. IET Power Electron 2009;2(5):585–94.

[9] Yao Z, Xiao L. Control of single-phase grid-connected inverters with nonlinear loads. IEEE Trans Ind Electron 2013;60(4):1384–9.

[10] Elsaharty MA, Hamad MS, H. A. Ashour HA. Digital hysteresis current control for grid-connected converters with LCL filter. In: - Proceedings 37th Annual Conference of the IEEE Industrial Electronics Society (IECON), Melbourne, VIZ; 2011. p. 4685–4690.

[11] Ichikawa R, Funato H, Nemoto K. Experimental verification of single-phase utility interface inverter based on digital hysteresis current controller. In: Proceedings International Conference on Electrical Machines and Systems.

[12] Damen A, Weiland S. Robust Control. Measurement and Control Group Department of Electrical Engineering Eindhoven University of Technology P.O. Box 513, Draft version, July 2002.

[13] Zames G. Feedback and optimal sensitivity: model reference transformations, multiplicative seminorms, and approximate inverses. IEEE Trans Autom Control 1981:301–20.

[14] Hornik T, Zhong Q Ch. A current-control strategy for voltage-source inverters in microgrids based on H∞ and repetitive control. IEEE Trans Power Electron 2011;26(3), [March].

[15] Abu-Rub H, Guzin´ski J, Krzeminski Z, Toliyat HA. Predictive current control of voltage-source inverters. IEEE Trans Ind Electron 2004;51(3), [Jun.].

[16] Moreno JC, Huerta JME, Gil RG, Gonzalez SA. A robust predictive current control for three phase grid-connected inverters. IEEE Trans Ind Electron 2009;56(6):1993–2004, [Jun.].

[17] Bojoi R, Limongi LR, Roiu D, Tenconi A. Enhanced power quality control strategy for single-phase inverters in distributed generation systems. IEEE Trans Power Electron 2011;26(3):798–806, [March].

[18] de Almeida PM, Duarte JL, Ribeiro PF, Barbosa PG. Repetitive controller for improving grid connected photovoltaic systems. IET Power Electron 2014;7(6):1466–74, [June].

[19] Ramos C, Martins A, Carvalho A. Complex state-space current controller for grid connected converters with an LCL filter. In: 35th Annual conference of IEEE industrial electronics, IECON '09. 2009. pp. 296–301.

[20] Passino KM. Intelligent control: anan overview of techniques. Department of Electrical Engineering, Ohio State University; 2015.

[21] Wang X, Blaabjerg F, Chen Z. Autonomous control of inverter-interfaced distributed generation units for harmonic current filtering and resonance damping in an islanded microgrid. IEEE Trans Ind Appl 2014;50(1):452–61, [Jan.- Feb.].

[22] Lin FJ, Ch. Lu K, Ke TH. Probabilistic Wavelet Fuzzy Neural Network based reactive power control for grid-connected three-phase PV system during grid faults. Renew Energy 2016;92:437 49, [July].

[23] Kyoungsoo R, Rahman S. Two-loop controller for maximizing performance of a grid-connected photovoltaic-fuel cell hybrid power plant. IEEE Trans Energy Convers 1998;13(3):276–81, [Sep].

[24] Niroomand M, Karshenas HR. Review and comparison of control methods for uninterruptible power supplies. In: 1st power electronic and drive systems and technologies conference, 2010.

[25] Eren S, Pahlevani M, Bakhshai A, Jain P. An adaptive droop DC-bus voltage controller for a grid-connected voltage source inverter with LCL filter. IEEE Trans Power Electron 2015;30(2):547–60, [Feb.].

[26] Zhong QC, Hornik T. Control of power inverters in renewable energy and smart grid integration. John Wiley & Sons; 2013.

[27] M. Liserre, F. Blaabjerg and S. Hansen. "Design and control of an LCL-filter based three-phase active rectifier. Industry Applications, IEEE Transactions vol. 41, no. 5, 1281-1291, 2005.

[28] Damen A, Weiland S. Robust Control. Measurement and Control Group Department of Electrical Engineering Eindhoven University of Technology P.O. Box 513, Draft version, July 2002.

[29] Zmood, D.N.; Holmes, D.G. Stationary frame current regulation of PWM inverters with zero steady-state error. *IEEE Trans. Power Electron.* **2003**, *18*, 814–822.

[30] Wei Gu and Issa Batarseh, "Interleaved synchronous buck regulator with hysteretic voltage control," *2001 IEEE 32 Annual Power Electronics Specialists Conference*,Vol. 3, pp. 1512–1516, 2001.

[31] Youqing Wang, Furong Gao, and Francis J. Doyle. Survey on iterative learning control, repetitive control, and run-to-run control. J. Process Control, 19(10):1589{1600, 2009.

[32] Yongheng Yang, Keliang Zhou, and Frede Blaabjerg. Harmonics suppression for single phase grid-connected PV systems in different operation modes. 2013 Twenty-Eighth Annu. IEEE Appl. Power Electron. Conf. Expo., pages 889{896, mar 2013.

[33] Youqing Wang, Furong Gao, and Francis J. Doyle. Survey on iterative learning control, repetitive control, and run-to-run control. J. Process Control, 19(10):1589{1600, 2009.

[34] X. Lu and J. Wang, "A Game Changer: Electrifying Remote Communities by Using Isolated Microgrids," *IEEE Electrif. Mag.*, vol. 5, no. 2, pp. 56–63, 2017.

Rizwan Nadeem Shah was born in Dictrict Chitral Khyber Pakhtunkwa Pakistan. on 3rd April 1990, He has got his bachelor's degree in electrical power engieering from COMSATS Institute of Information Technology Abbottabad Pakistan in 2015, currently he is getting his master's degree in electrical energy system Engineering from US Pakistan Center for Adavanced Studies in Energy, University of Engineering and Technology Peshawar Pakistan. His research interest includes distributed generation, microgird operation and control.

IJEW 国际工程期刊 International Journal of Engineering Works انجینرنگ کاموں کا بین الاقوامی جرنل

International Journal of Engineering Works
ISSN-p: 2521-2419
ISSN-e: 2409-2770
Vol. 6, Issue 09, PP. 269-274, September 2019
https://www.ijew.io/
https://doi.org/10.34259/ijew.19.609269274

Performance Analysis of Micro Strip Patch Antenna at 2.4 GHz using Metamaterial

Faizan Dad[1], M.Irshad Khan[2], Abdul Wajid[3]
[1,2,3]Department of Electrical Engineering, UET Peshawar
faizandadkhattak@gmail.com[1], irshadnawab@outlook.com[2], wajid_khalil040@yahoo.com[3]
Received: 20 August, Revised: 28 August, Accepted: 04 September

***Abstract*—** In this article, rectangular shape Micro strip Patch Antenna (MPA) with cut edges is proposed at 2.4 GHz for ISM and Wi-Fi application. The proposed antenna is designed on fr-4 material having standard thickness of (h=1.6mm), relative permittivity (εr= 4.3) and loss tangent 0.02. PEC is used as a conducting element for radiating patch and ground plane. The volume of proposed antenna is 58 x 58 x 1.6 mm3. The proposed antenna resonates at 2.4 GHz having return loss -21dB, gain 3.14dB and efficiency 41%. For achieving good performance of antenna 4 x 4 Electromagnetic Bandgap (EBG) structure is used. By utilizing EBG structure as a ground plane a discernible improvement occur in the performance of proposed antenna. Proposed antenna with EBG structure gives gain up to 68.14dB, return loss -32dB and efficiency 85%. The antenna and mushroom type EBG is designed and simulate in CST microwave studio.

***Keywords*—** Micro strip antenna, EBG (metamaterial), in-phase reflection, surface waves suppression.

I. Introduction

In the advancement of wireless communication, use of planer Micro strip patch antenna (MPA) in various wireless application become increases due to certain advantages like, low profile, low weight, less costly and easily integration with other devices and compact size. However, MPA has drawbacks like low radiation efficiency, limited bandwidth, less directive gain and unstable radiations. The use of metamaterial can lessen these drawbacks.

Metamaterials are firstly used by Bose [1] where he introduced the use of metamaterial with chiral structure. Afterwards, the use of metamaterial was put in practise in the field of radio frequency and system design.

According to Veselago [2], metamaterials are unnatural uniform material which doesn't exist in natural world. Mostly attributes of meta material are described by electric permittivity and magnetic permeability [3]. Air is the thinnest material in nature having permittivity εo and permeability μo. The relative permittivity and permeability is expressed as $\varepsilon r = \varepsilon / \varepsilon o$ and $\mu r = \mu / \mu o$ [35]. Naturally most of the materials have permittivity and permeability greater than εo. Although metamaterial exhibits either ε or μ or both of them negative [4].

Metamaterial structure acts as high-impedance surface (HIS) in specific frequency band and is known as band gap of the (HIS). Electromagnetic bandgap structure (EBG) has two characteristics which offer [5]. i) It suppresses the surface waves, minimize back radiations which results in improvement in gain and radiation efficiency. ii) It also gives in-phase reflection. These surfaces have also the property of protecting human body from intensive radiation and reduce the specific absorption rate (SAR) and reduction in impedance match when antenna operates nears the body for wearable applications [6].

In literature, dual band MPA is modelled using fr-4 substrate as a dielectric material which is applicable for WI-MAX, W-LAN and WIFI [7]. A wearable planer E-shaped single band antenna for rescue operations, while single band circular shape having T-shape slot operating at 2.45GHz are studied in [8-9]. In [10] metamaterials are utilized in the designing of low profile antenna for compact portable electronic devices. Slots are taken in Mushroom-type EBG increase capacitance thereby reducing in-phase frequency and size reduction [11].

In study, Metamaterial EBG structure is designed with no cylindrical vias; due to which surface wave propagate on the surface of EBG metamaterial [12]. Reduction in the length of antenna is achieved, by increasing the relative permittivity of dielectric material in [13]. By using EBG surface as ground improvement in the behaviour of antenna can be achieved [14]. Novel EBG is designed by creating slots in the conventional EBG to improve the return loss is studied in [15].

A single band Micro strip patch antenna having FR-4 substrate as a dielectric material, operating at 2.4GHz is presented in this paper. To enhance the performances of antenna i.e. (gain, directivity, efficiency, beamwidth) by employing the antenna with Mushroom-like EBG, which is created through taking small rectangular slots at the top and bottom of EBG unit cell to provide in-phase reflection at 2.4GHz. A good improvement occurs in gain and directivity by using EBG (metamaterial) surface as a ground plane. The optimization of EBG structure gives surface wave band gap at 2.4GHz, which suppress the surface waves providing the better gain and efficiency.

This article is organized as: Section II describes the antenna designing theory and results of proposed fracture antenna without metamaterial. The design of mushroom-like EBG to provide in-phase reflection and surface wave band gap is covered in Section III. while Section IV present the integration of proposed fracture antenna with mushroom-like EBG, and comparison of results with and without EBG. Conclusion is derived in Section V.

II. ANTENNA DESIGN THEORY AND RESULTS

A. *Antenna Designing theory:*

A single band micro strip patch fracture antenna operating at frequency 2.4 GHz is modelled in CST microwave studio. FR-4 material is used as substrate, having relative permittivity 4.3 and loss tangent 0.02 respectively. The thickness of the substrate is chosen as standard thickness which is (h=1.6mm). Total volume of proposed antenna is ls×ws×h (58×58×1.6mm3). Where ls is length of the substrate, Ws is width of substrate and h is the height of substrate.

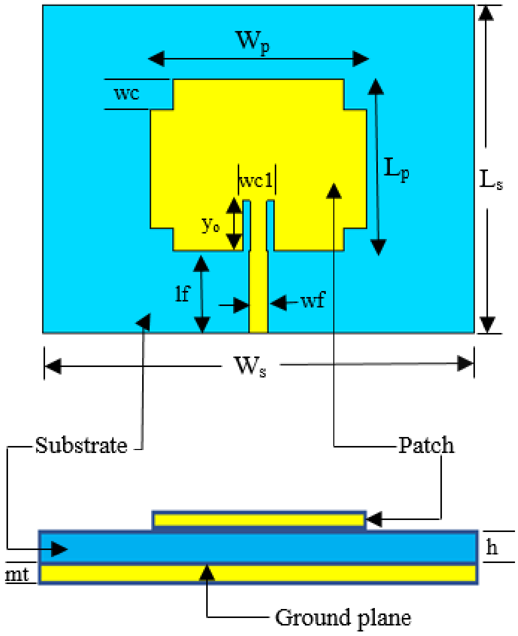

Fig.1. Proposed Antenna Geometry (top and side views) of patch antenna

PEC is used as conducting material for radiating patch and ground plane. Fig.1. shows the geometry of prosed fracture antenna. At all side of rectangular patch (wc=3×2mm) cuts are etched in the patch. The antenna is fed through 50 (ohm) micro strip feed line. The dimension of the proposed antenna is calculated form transmission line theory [16].

The width of the antenna (wp) is determined from the equation:

$$W=\frac{c}{fr}\sqrt{\frac{2}{\varepsilon_r+1}} \qquad (1)$$

Where ε_r is dielectric constant, c is the speed of light, f_r is resonating frequency.

The effective dielectric constant ε_r is determined from equation 2.

$$\varepsilon_{reff}=\frac{\varepsilon_r+1}{2}+\frac{\varepsilon_r-1}{2}\times\sqrt{(1+(\frac{12h}{w}))} \qquad (2)$$

H represents the thickness of dielectric material. Length (l_P) of the antenna is determined from equation 3.

$$L_{eff}=\frac{c}{2fr\sqrt{\varepsilon_{reff}}} \qquad (3)$$

Where ΔL represent difference between original and electrical lengths.

$$\Delta L=0.412\times h\times\frac{(\varepsilon_{reff}+0.3)(\frac{w}{h}+0.26)}{(\varepsilon_{reff}+0.253)(\frac{w}{h}+0.8)} \qquad (4)$$

Therefore, the effective resonant length of the radiating patch is:

$$L=L_{eff}-2\Delta L \qquad (5)$$

The optimized parameter of proposed antenna is given in table.1.

TABLE I. DIMENSIONS OF FRACTURE ANTENNA

parameters	Description	values(mm)
L_S	Substrate length	58
W_S	substrate width	58
L_P	patch length	30.4
W_P	patch width	38
W_F	Feed line width	3.2
L_F	Feed line length	14.5
Y_O	Feed cut	8.85
WC	Length and width of rectangular cut	3×2
WC1	width of feed cut	5.6
h	Substrate thickness	1.6
mt	Patch thickness	0.035

B. *Proposed Antenna: Results*

S_{11}, vswr, polar plots of (Gain and directivity) simple ground surface is given below.

a) *S_{11} (Reflection coefficient)*

S11 of proposed Micro strip antenna is -25dB at 2.4GHz, while 60MHz bandwidth is achieved at resonance frequency. S11 of investigated antenna with full ground plane is given in fig.2.

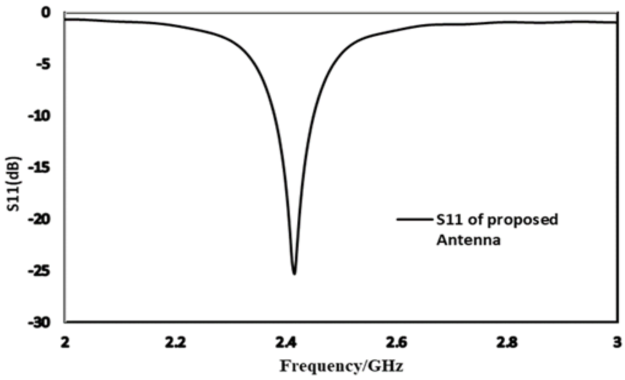

Figure.2. S_{11} of proposed antenna simple ground

b) VSWR (Voltage standing wave ratio)

For good matching the vswr should be nearly equal to one at the resonance frequency. The value of vswr at 2.4GHz is 1.3 respectively. Fig.3. shows good matching of proposed antenna.

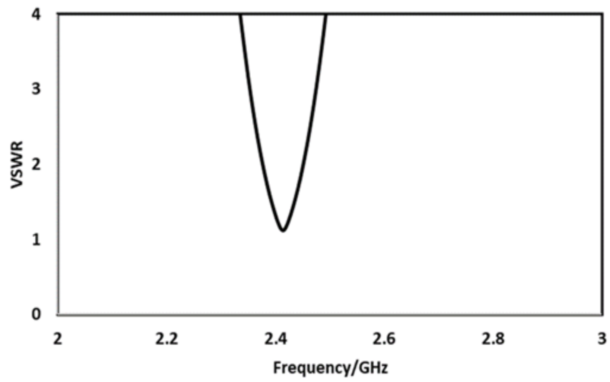

Figure.3. VSWR of proposed antenna without EBG

c) Radiation patterns

Directivity and Gain polar plots at 2.4GHz are presented in fig.4. E-plane is taken ta (yz plane at phi=900) while h-plane is taken at (xz plane at phi=00). From the figure.4 it is observed that proposed antenna is linearly vertical polarized.

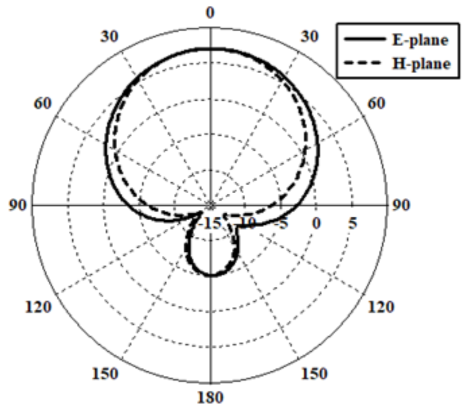

(a)

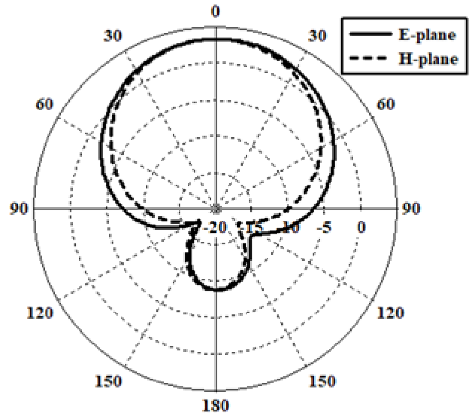

(b)

Figure.4. polar plots at 2.4GHz (a) Directivity (b) Gain

III. DESIGN OF MUSHROOM-TYPE EBG

This portion covers design and analysis of mushroom type EBG structure using cst micro wave studio.

a) Design of single band EBG unit cell

To layout Mushroom EBG structure which give in phase reflection and also have the attribute of suppression of the surface waves. These structures illustrate the property of high impedance surface (HIS) which provides the surface wave suppression in certain frequency band gap [17]. These surfaces are being employed in antennas to reduce backscatter radiation and to enhance the characteristics parameter like gain and radiation efficiency along the main lobe position.

The design consists of radiating patch, cylindrical via having radius 0.8mm in the middle of unit cell connecting patch and ground plane. Single band unit cell is design consist on fr-4 substrate having length and width L=W=32.6mm. The radius of the R is 0.8mm while the gap between the adjacent unit cell g=2.5mm respectively. A rectangular shape cuts are etched in the patch of the dimensions 2×4mm. fig.5(a) shows the proposed single band unit cell design.

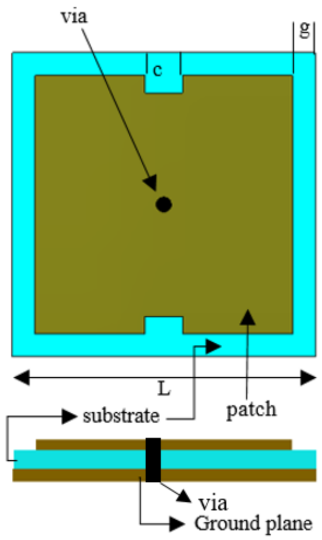

(a)

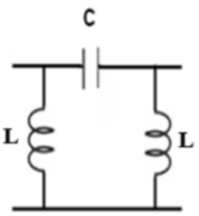

(b)

Figure.5. Geometry of unit cell (a) proposed Geometrical model (b) LC-resonant circuit.

The parameters of Mushroom type EBG unit cell are determined from the sieve piper's design equation [18].

The unit cell surface behaves like parallel LC-resonant circuit, where inductance and capacitance are the main elements of the circuit. The In-phase reflection and the resonance frequency depend upon inductance L where capacitance depends on dimensions and the geometry of EBG unit cell [19]. The resonance frequency of the unit cell is given by:

$$f_r = \frac{1}{2\pi\sqrt{lc}} \quad (6)$$

Where, C is the capacitance due to the surrounding effect of the neighbour cells, is given by:

$$C=\frac{w\varepsilon_o(1+\varepsilon_r)}{\pi} cosh^{-1}\left(\frac{w+g}{g}\right) \quad (7)$$

Where, ε_o is free space permittivity, w, is the width of unit cell and g is gap between the adjacent unit cell. The inductance L is dependent on thickness of substrate t or radius of metal cylindrical via.

$$L=\mu_o\mu_r t \quad (8)$$

The periodicity of unit cell a=L+g=32.5+2. 5=35mm.The optimized parameter of single band unit cell is listed in table 2.

TABLE 2. CHARACTERISTIC PARAMETER OF UNIT CELL

Parameter	Description	Value(mm)
L=W	Length and width of substrate	32.5
Lp=Wp	Length and width of patch	30
r	Radius of via	0.8
c	Length and width of cut in the patch	2×4
g	Gap between adjacent cells	2.5

b) Results of Mushroom-type EBG unit cell

1) In-phase reflection

The simulated scattering parameter and reflection phase of mushroom-type EBG is shown in fig.6. The EBG unit cell surface provides in-phase zero reflection at 2.4GHz and act like a perfect Magnetic Conductor (PMC) at the required frequency. The simulated reflection phase changes from +900 to -900 within the band from 2.3GHz to 2.45GHz and also in this band of frequency the surface act as an Artificial Magnetic Conductor (AMC). The behaviour of in-phase reflection is need full in the design of low profile and compact size antennas.

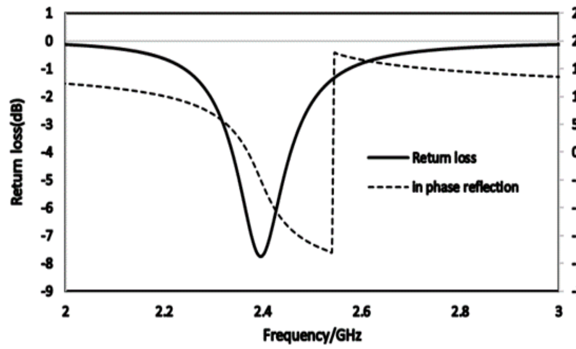

Figure.6. In-phase reflection of Mushroom-type EBG

2) Band Gap of EBG Structure

The Expanse of EBG unit cell is High Impedance Surface (HIS) which have the property of surface wave suppression and can be achieved by different means, i.e. by dispersion diagram or transmission line method. In this article, suspend transmission line method is used. In this procedure a conducting metal strip is mounted 3mm above the EBG surface and excited in a way that one port act as source and the other act as matched load. The setup for surface wave suppression is shown in Fig.7(a).

The simulated result shows that transmission coefficient (S21) is minimum (< -40dB) within the range of 2.38 to 2.6GHz. Within this specific band the transmission of surface wave is limited minimum low level. In this band the surface acts like high impedance surface to suppress the surface waves, is known as surface wave band gap of mushroom-type EBG. The Fig.7(b) shows the band gap of EBG.

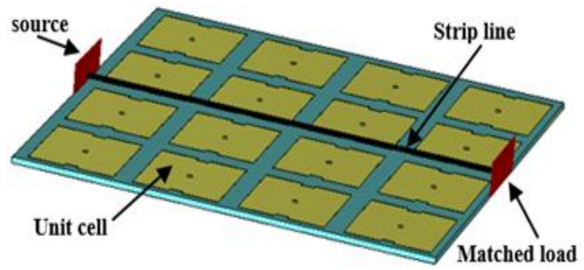

(a)

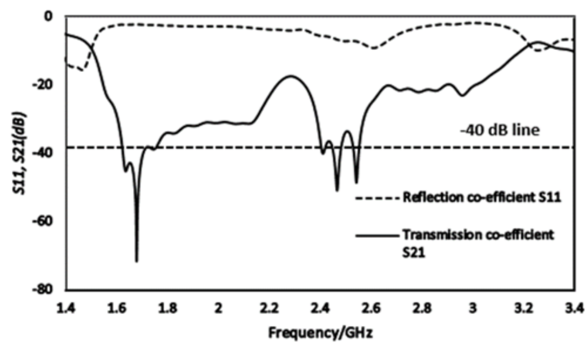

(b)

Figure.7. 4×4 EBG array (a) Suspend line model of EBG (b) Simulated (S11, S21) of EBG array

IV. Integration Of Proposed Antenna With EBG (Metamaterial Surface)

In this section, the proposed antenna has been integrated with 4×4 single band mushroom-like EBG as shown in Fig.8.

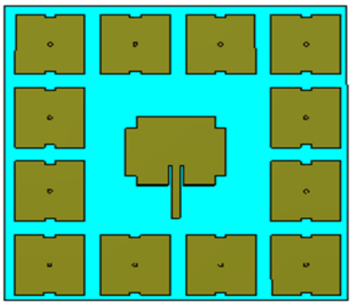

Figure.8. Antenna integration with 4*4 EBG

a) Return loss

Return loss of proposed antenna with and without Mushroom-like EBG is given below in Fig.9. A Good improvement occurs in the return loss up to -32dB when the antenna is employed with EBG.

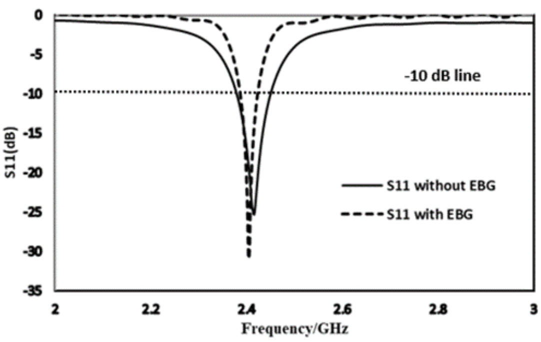

Figure.9. S_{11} comparison of proposed antenna with and without EBG

b) Voltage standing wave ratio (VSWR)

VSWR is given in Fig.10 also it is observed from the graph the vswr is nearly equal to 1 at 2.4GHZ with the value of 1.12.

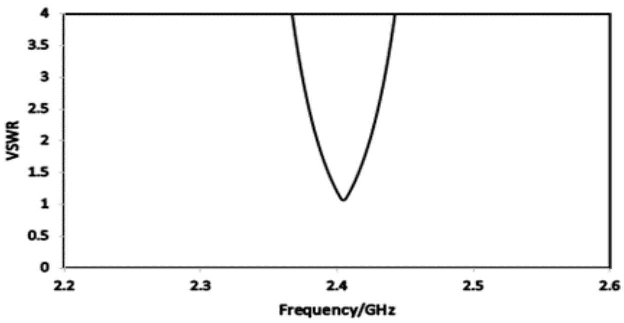

Figure.10. VSWR of Antenna with EBG

c) Surface currents

At 2.4GHz surface currents are dense and linearly distributed over rectangular patch which enhances the radiation at the resonance frequency.

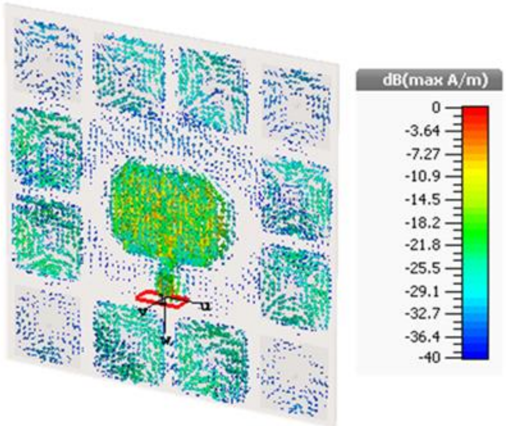

Figure.11. Surface currents of Antenna with EBG

d) Polar plots and 3D-Radiation pattern

Directivity and Gain polar plots are shown in Fig.12 (a,b). A major improvement occurs in the Beamwidth, Directivity and Gain.

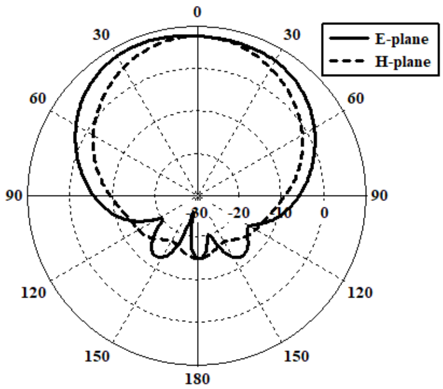

(a)

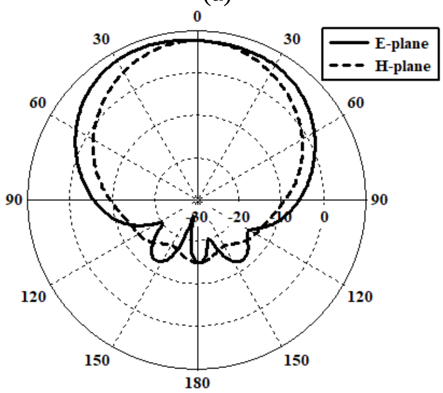

(b)

Figure.12.Polar plots at 2.4 GHz (a) Directivity (b) Gain

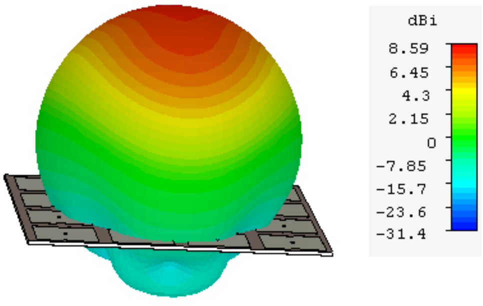

(a)

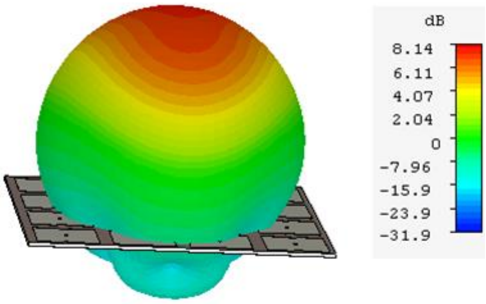

(b)

Figure.13. 3D-Radiation pattern of Antenna with EBG (a) Directivity (b) Gain.

TABLE 3. SUMMARY OF RESULTS WITH AND WITHOUT EBG

Parameters	Without EBG	With EBG
Frequency (GHz)	2.41	2.40
Return loss (dB)	-25	-32
Directivity (dBi)	6.97	8.59
Gain (dB)	3.42	8.14
Beam width (deg)	78.9	94
Efficiency (%)	50	85
VSWR	1.3	1.12

CONCLUSIONS

In this article, A single band patch antenna is modelled at 2.4GHz by using simple and EBG surface as a ground plane which is discussed and compared in (Table 3). The proposed fracture antenna is designed on FR-4 substrate. A ponderable enhancement occurs in gain, directivity and beam width. It is observed that Antenna with simple ground plane exhibits less efficiency (50%) and maximum efficiency (80%) when EBG surface is used as ground plane. In this work, the EBG ground plane lead to better enhancement in the performance of the proposed antenna. The EBG based antenna will be fabricated in future to valid the simulation results. The proposed antenna finds its applications in WIFI and ISM band.

REFERENCES

[1] Raval, Falguni, Y. P. Kosta, and Harshita Joshi. "Reduced size patch antenna using complementary split ring resonator as defected ground plane." AEU-International Journal of Electronics and Communications 69.8 (2015): 1126-1133.

[2] Veselago VG. The electrodynamics of substances with simultaneously negative values of and ε. Sov Phys Usp 1968;10:509–14

[3] Cui Tie Jun, Smith David, Liu Ruopeng. Metamaterials: theory, design, and applications. Springer Science & Business Media, Technology & Engineering; Oct,2009. p. 1–2.

[4] Marqués Ricardo, Martín Ferran, Sorolla Mario. Metamaterials with negative parameters: theory, design and microwave applications. John Wiley& Sons –Technology & Engineering; Sep, 2011

[5] A. Basir, S. Ullah, M. Zada, and S. Faisal. "Design of efficient and flexible patch antenna using an electromagnetic band gap (EBG) ground plane." . In IEEE International Conference on Open Source Systems and Technologies (ICOSST), 2014, pp. 1-5.

[6] Nacer Chahat, Maxim Zhadobov, Ronan Sauleau, and Kouroch Mahdjoubi. "Improvement of the on-body performance of a dual-band textile antenna using an EBG structure." In Antennas and Propagation Conference (LAPC), Loughborough, IEEE,pp. 465-468., 2010.

[7] MD. Ashikur Rahman, Moinul Hossain, Ibnul Sanjid Iqbal, and Syed Sobhan. "Design and performance analysis of a dual-band microstrip patch antenna for mobile WiMAX, WLAN, Wi-Fi and bluetooth applications." In Informatics, Electronics & Vision (ICIEV), International Conference on, IEEE ,pp. 1-6, 2014

[8] H.S. Zhang, K. Xiao, L. Qiu, and S. L. Chai. "Wide band e-shape wearable antenna for wireless body area network." In IEEE International Wireless Symposium (IWS), 2014, pp. 1-4

[9] Priyanarayan Misra, and Amaresh Tripathy. "Triple Band Planar Antenna for Wireless Communication." International Journal of Computer Applications 48, vol. 23, pp. 28-30, 2012

[10] R. Dewan M. K. A. Rahim M. R. Hamid H. A. Majid M. F. M. Yusoff M. E. Jalil "Reconfigurable antenna using capacitive loading to Artificial Magnetic Conductor (AMC)"Microwave and Optical Technology Letters, vol. 58 pp. 2422-2429 2016.

[11] A. B. Jagadeesan A. Alphones M. F. Karim L. C. Ong "Metamaterial based reconfigurable multiband antenna" 2015 IEEE International Symposium on Antennas and Propagation & USNC/URSI National Radio Science Meeting, pp. 2389-2390 2015.

[12] Behera, Bikash Ranjan and Priyadarshi Suraj. “Rectangular microstrip patch antenna for wireless fidelity application: Design of a Wi-Fi antenna using the concept of metamaterials.” *2016 IEEE International Conference on Recent Trends in Electronics, Information & Communication Technology (RTEICT)* (2016): 1933-1937.

[13] Ali, Usman & Ullah, Sadiq & , Haroon. (2016). Design and Analysis of a 2.4 GHz Antenna using Metamaterial Ground Planes for Body Worn Wireless Applications. Bahria University Journal of Information & Communication Technologies (BUJICT). 9.

[14] Smyth, Braden P. et al. “Dual-Band Microstrip Patch Antenna Using Integrated Uniplanar Metamaterial-Based EBGs.” *IEEE Transactions on Antennas and Propagation* 64 (2016): 5046-5053.

[15] Aravind, V.S. & Gupta, Shilpi. (2015). Compact EBG ground plane microstrip antenna for high gain applications. 10.1109/ET2ECN.2014.7044963.

[16] C.A.Balanis, antenna theory: Design and Analysis, Second edition, pages 722-736 to 869-870, John Wiley and Sons, 1997.

[17] Rahmat-Samii, Yahya, and H. Mosallaei. "Electromagnetic band-gap structures: classification, characterization, and applications." (2001): 560-564.pp

[18] Sievenpiper, Dan, et al. "High-impedance electromagnetic surfaces with a forbidden frequency band." IEEE Transactions on Microwave Theory and techniques 47.11 (1999): 2059-2074.

[19] Rahmat-Samii, Yahya, and H. Mosallaei. "Electromagnetic band-gap structures: classification, characterization, and applications." (2001): 560-564 DOI10.1049/ CP 20010350.

International Journal of Engineering Works
ISSN-p: 2521-2419
ISSN-e: 2409-2770
Vol. 6, Issue 09, PP. 280-287, September 2019
https://www.ijew.io/
https://doi.org/10.34259/ijew.19.609280287

Energy Efficient Routing Protocols and Introduction to Wireless Recharging of Sensor Nodes in Wireless Sensor Networks

Farman Ullah[1]
[1]Department of Electrical Engineering, University of Engineering and Technology, Peshawar, Pakistan
farmanfareed@gmail.com[1]
Received: 20 August, Revised: 26 August, Accepted: 05 September

***Abstract*—**This paper gives a brief review of the concept of sensor networks which has become feasible due to large scale development in micro electro-mechanical systems technology and wireless communications. First of all, sensor node deployment and sensor networks applications are presented, and then various issues regarding sensor node lifetime are discussed. Then, to solve sensor node issues, various energy conservation techniques, their advantages and limitations are discussed. The energy conservation techniques are compared using MATLAB and best routing protocol is shown. Lastly, wireless power transfer to replenish sensor node battery is discussed. A review of wireless power transfer history and various development in this technology is also given to solve the energy issue of sensor node. Research issues for efficiency improvement of wireless sensor network are also discussed.

***Keywords*—** Wireless sensor network (WSN), energy conservation, wireless energy transfer, Routing, energy harvesting.

I. Introduction

The recent development in wireless communication has enabled scientists to develop a low cost and multi-functional sensor node. These sensor nodes consist of various components and work in a combined manner to sense and forward data from surroundings [1]. These sensors can be deployed in the surrounding areas through various methods [1], [3]. A huge number of sensor nodes when joined together form a sensor network. After sensing data from physical environment, these sensors forward data to a sink node. The sensed data is converted into signals and forwarded to a processing unit to reveal the characteristics of the area surrounded by the WSN.

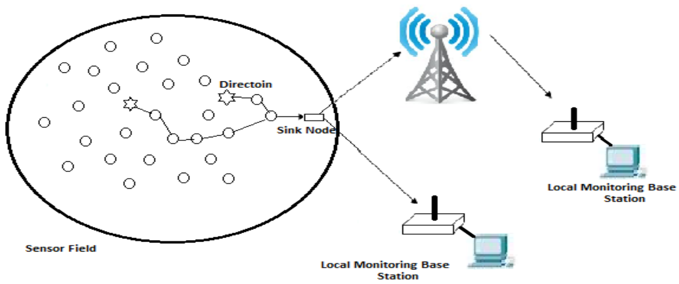

Figure 1: Deployment of sensor nodes in a sensor field

Figure 1, [1] shows deployment of nodes in a sensor field. Sensor nodes are generally deployed in remote areas. They must possess self-organizing technique and work in combine manner. In this way sensor differentiates the required data from surrounding noise and forwards it. Sensor networks have wide range of applications which include indoor, battlefield, underwater, e-health etc. [1], [3], [4]. To get a better understanding of these applications, we need to know about wireless ad-hoc networking. The various differences between sensor and ad-hoc networks are defined in [1], [3] as:

- Number of nodes in sensor network is greater than ad-hoc network.
- Sensor network is more stable than ad-hoc network.
- Broadcasting technique is used by sensor nodes while ad-hoc uses point-to-point communication.
- There is power constrain in case of sensor nodes.

Since sensor nodes are very large in number and placed closed to each other, multi-hop communication is considered better for data transmission [1]. Also, sensor nodes have limited battery life and generally placed in remote areas where manual battery replacement is impossible, so priority should be power conservation for sensor nodes.

A lot of papers have been proposed to tackle the issue and still a lot of research is being done on the problem. In this paper we have a look on various protocols which have been proposed for energy conservation. We also survey various techniques used for sensor battery recharging from outside. We try both of the techniques and try to figure out which one is better in all conditions. The rest of the paper is organized as follows: Section II shows the application of sensor nodes, section III shows energy conservation, section IV results, section V wireless recharging techniques while section VI concludes the paper.

II. APPLICATIONS OF SENSOR NODES:

Different types of sensors are described in [1] like thermal, infrared, seismic, acoustic, low sampling rate and visual which can monitor data in every type of harsh environments. These sensors can monitor various factors like motion of vehicles, smart grid, pressure, temperature, noise level, humidity etc. We can divide these applications into various categories like battle field, e-health, indoor, underwater and several other categories [1].

A. Battlefield Applications

WSN can be necessary part of military command and control, surveillance, computing, targeting systems, intelligence etc. To increase military capabilities, a large number of sensor data analyses can be connected. So WSN have become a vital part of military information system. Sensors are used for targeting, battlefield surveillance, damage estimation, checking opposite forces movement and monitoring friendly forces equipment [1].

B. Indoor Applications

Nowadays humans are depending upon sensors for indoor applications too. A wide range of sensors have been deployed inside smart home for various applications. Some of the major uses of sensors are to switch on or switch off the light or TV, boil water and eggs, open the door, prevent theft cases, heating, air conditioning and ventilation. They also take good care of elderly people who otherwise need care taker for their necessities. Sensor deployed in smart home can also detect smoke and alert passersby or call the fire department automatically [1].

C. E-health Applications

Health applications of sensor nodes includes helping the disabled patients, drug administration inside hospitals, locating the exact position of patients and hospital staff while on duty, monitoring and diagnostics of patients and tele-monitoring human psychological data [2].

D. Environmental Applications

Some of the environmental application of sensors includes detecting forest fire and flood, tracking the movement of migratory birds and small insects, Irrigation, Pollution study, chemical and biological detection and monitoring various conditions that effects crops and livestock [3].

E. Issues restricting WSNs

The main issue encountered by WSN is Routing. It is complicated in WSN because of limited battery lifetime, no conventional addressing scheme, self-organization and limited transmission range, dynamic nature of nodes and computational overhead. A sensor generally has limited lifetime and cannot be easily replaced due to remoteness of deployed area. The initial capacity of battery plays a vital role in lifetime of sensor node. Routing, power issues, security and random topology are the main limitations faced by WSN [1].

III. ENERGY CONSERVATION OF WSNS

As we all know that routing is the main issue faced by WSN due to several factors [2]. The factors include limited power supply, non-applicability of IP to WSNs, limited resources, abundance of data collected by WSN, data collection must be in form of multiple inputs to single output and finally data must be collected in specific time. According to [2], energy conservation has more priority over quality of service as it is related to network lifetime. Routing can be flat or hierarchical with flat having nodes performing same tasks and hierarchical having nodes performing different tasks. We are more focused on hierarchical in which cluster are generally formed for data transmission and energy conservation. A brief survey of cluster-based routing protocol is presented in [2],[5],[6],[7],[8] which describes two steps in cluster formation. The cluster head selection and data transmission. Routing through cluster formation has several advantages like less energy consumption, scalability, data aggregation, less load and more robustness, fault tolerance, guarantee of connectivity, Avoidance of energy hole and quality of service. The cluster head can be predetermined and fixed or can be selected randomly. Similarly, the cluster head may be stationary or mobile. The clustering scheme may be homogeneous or heterogeneous based on energy of the sensor nodes. Also, the clustering may be centralized, distributed or hybrid based on control manners. Similarly, the clustering may be proactive, reactive or hybrid depending on the proactivity of clustering routing [2]. We are going to explain different cluster-based routing protocols with their advantages and deficiencies in order to have a better understanding of the concept. A brief explanation of those cluster-based protocols is stated in the following portion.

A) Low Energy Adaptive Clustering Hierarchy (LEACH);

The pioneer in clustering routing protocols for WSNs is LEACH [2], [5], [6], [7], [8], [9]. Its main advantage is load balancing which is achieved by cluster formation. One node act as the head of the cluster which is responsible for collecting data and transmitting it to the base station. Usually the node with maximum energy left acts as cluster head for one round and then each node in the cluster takes its turn to become cluster head. The cluster head fuses data of its own and other nodes and sends a single fused data to the base station [9]. For cluster head selection, certain probability is seen. The communication energy should be minimum between participating nodes and the cluster head. Data transmission within a cluster is done through a fixed schedule and the nodes should be in sleep condition for the remaining time to save the battery power.

When clustering starts, a node selects a random number between 0 and 1. If the number is less than a fixed threshold T (n), node will be cluster head for the current round which is then broadcasted within the cluster. The threshold is determined as:

$$\mathrm{T\,(n)} = \begin{cases} \dfrac{p}{1-p*(r\,mod\frac{1}{p})} & if n \in G \\ 0 & otherwise \end{cases}$$

G represents nodes which were not cluster head in last rounds, p is percentages of cluster head and r is current round.

The advantage [2] of LEACH is that it is fully distributive and do not requires information about global network, node serves as CH once in a round, unnecessary collisions are prevented and excessive dissipation of energy is prevented. Some of the deficiencies of LEACH are given single hop communication, lack of real load balancing and extra overhead due to dynamic clustering.

B) Distributed Energy Efficient Cluster Formation Protocol (DEEC):

In DEEC [10], the energy is distributed without having known the entire network. The network lifetime has an ideal value which gives us the amount of energy for each node to use in a single round. The cluster head selection again depends upon probability which is ratio of energy of the whole cluster to the energy of a single node. So, nodes with more energy left, become cluster head. It works better in an environment having different energy levels. The initial energy of the network is described by following equation:

$$E_{total} = \sum_{i=1}^{N} E_o(1+a_i) = E_o\left(N + \sum_{i=1}^{N} a_i\right)$$

For cluster head selection, let n_i is the number of rounds for becoming cluster head for the node s_i . For heterogeneous environment, the node having higher energy left has more probability p_i . The threshold for cluster head selection is given as:

$$T(s_i) = \begin{cases} \dfrac{p_i}{1 - p_i(r mod \frac{1}{p_i})} & if s_i \in G \\ 0 & otherwise \end{cases}$$

G is number eligible nodes to become cluster head. S_i will be part of G if it was not a cluster head in recent rounds. A random number is again chosen for the range of 0 to 1 which should be less than threshold T (s_i) for a node to become cluster head.

C) Stable Election Protocol (SEP):

Stable Election Protocol (SEP) [11] increases the duration between start of operation and the point at which the first node is drained completely of energy. This protocol has knowledge of the different energy nodes in the network. Certain fixed probability is assigned to every node in the network to become cluster head. This probability depends upon energy level left in a single node to that of the whole network [11]. As the energy of nodes is not same, so n represents the network and m is its part. Let suppose two types of nodes are there in the network, one having more energy and the other having less energy. Advance nodes are the one having high energy and the remaining nodes are normal nodes. If normal nodes have energy E_o , the energy of advance nodes is little higher by a factor of (1+ a)E_o . The total energy of the system having different energies is represented by the equation:

$$n.(1-m).E_o + n.m.E_o.(1+a) = n.E_o.(1+a.m)$$

The decision for each node to become a cluster head depends upon its remaining energy. Based on this energy, a probability is given to advance and normal nodes which is given as:

$$p_{nrm} = \frac{p_{opt}}{1+a.m}$$

$$p_{adv} = \frac{p_{opt}}{1+a.m} * (1+a)$$

Also, the threshold for the advance and normal nodes is given by following equations:

$$T(S_{nrm}) = \begin{cases} \dfrac{p_{nrm}}{1 - p_{nrm}\left(r * mod\left({}^{1}/_{p_{nrm}}\right)\right)} & if S_{nrm} \in \acute{G} \\ 0 & otherwise \end{cases}$$

$$T(S_{adv}) = \begin{cases} \dfrac{P_{adv}}{1 - P_{adv}(r * mod({}^{1}/_{P_{adv}}))} & if S_{adv} \in \ddot{G} \\ 0 & otherwise \end{cases}$$

So, by the concept of weighted probability, SEP increases the time duration before the first node is drained off energy completely. This region is called stable region which is very much greater than previous routing techniques used for the task.

D) Threshold sensitive Energy Efficient sensor Network protocol (TEEN):

In TEEN [2], [12], nodes form cluster by passing through different hierarchies. The formation is cluster head is same as explained in previous routing schemes. The main difference between TEEN and other routing techniques is that in TEEN manual setting of values for the cluster head is needed. That is why it is called reactive protocol. These values of cluster head are of two types, one is soft and the other is hard threshold. When the cluster head receives both these values manually, it sends them to all nodes. The member node regularly collect data but send it to cluster head only if it becomes greater than the value of hard threshold. So, setting hard threshold, unnecessary transmission between member node and cluster head is prevented. The cluster head stores values of the member node in a variable naming “sensed value.” This sensed value is the soft threshold value and the member nodes transmit data only when their sensed data become greater than this value. The values of soft and hard threshold are changed manually when a new cluster is forming. Because of large value of high threshold, cluster head will have no information about death of member nodes in the cluster.

A few advantages of TEEN are presented in [2] which say that the transmission energy can be decreased by taking advantage of two thresholds. TEEN is more suitable for reactive and time critical applications. Some disadvantages of TEEN according to [2] include its non-efficiency for periodic reports, wasted time-slots and chance of data loss.

E) Tree Based Routing Protocol (TRP):

This routing protocol [13] constructs the best route between a sensor node and a base station. In TRP, a node selects another nearby node as its parent calculating the amount of energy required for communication, the distance from the neighboring nodes to the BS, and the amount of energy left in the neighboring nodes.

Tree based routing protocol works better for a phenomenon in which sensor nodes want to transmit data to BS in every round of data transmission. TRP takes advantage of data aggregation techniques in order to increase the lifetime of the network by reducing the dissipated energy during the communication process.

a) Network Model:

Generally, sensor nodes are dispersed randomly, BS is stationary, sensor nodes have same initial energy and location unaware, each sensor node has limited amount of energy but BS has infinite, sensor nodes can perform data fusion and can find the distance between nodes through received signal strength indication (RSSI).

b) Tree Formation:

Each node choses nearby node as parent node on the basis of given criteria:

1: The parent node must have shorter distance to base station than the child node.

2: The child node must have less communication and residual energy than its parent node.

If more than two nearby nodes have same distance or number of hops to the base station, the node with the best link quality is selected as its parent. When every participating node finds its parent node, a tree rooted at the base station is formed. In tree-based topology, a node at certain level L, selects a node at the immediate lower level (L-1) as its parent. In this way the sensed data is sent to the base station.

F) Chain Based Routing Protocol:

Power-Efficient Gathering in Sensor Information Systems (PEGASIS) [14] is a protocol which follows chain-based technique. In PEGASIS each node collects data and transmits it to the nearby node and waits for its turn to forward the data to the base station. In PEGASIS a chain is formed among sensor nodes and each receives and transmits data to its closest node. The data gets fused and moves from one node to another until a designated node sends the data directly to the BS. In order to reduce the energy spent during transmission, all the nodes take turn to communicate with the BS. Multi-hop transmission is utilized when nodes are far away from each other's transmission range. Chain based protocol will not be affected because of communication between neighbor nodes only and multi-hop transmission can be adjusted in transmission to the BS. In case of heterogeneous environment, the remaining energy of each node is considered along with the transmission energy cost. The BS generally determines each node's location however through received signal strength nodes can determine it too.

The equations for transmission and reception of k-bit message at distance d are given as [14]:

$$E_{Tx}\,(\mathrm{k, d}) = E_{Tx}\text{ - }elec\;(\mathrm{k}) + E_{Tx}\text{ - }amp\;(\mathrm{k, d})$$

$$E_{Rx}\,(\mathrm{k}) = E_{Rx}\text{ - }elec\;(\mathrm{k})$$

The number of transmissions should be less as it also costs highly. Compared to LEACH [9], PEGASIS saves energy by minimizing the transmission, reception and the distance d. Furthermore, in LEACH more nodes become CH in every round and transmit fused data to BS. To save maximum energy, only one node should send data to CH and the remaining sends it to their immediate neighbors [14]. PEGASIS works on the idea that to transmit and receive data each node has to contact its immediate neighbor and has to wait for its turn to connect directly with the BS. As a result, the energy load is uniformly distributed among all the nodes. The random distributed nodes form a chain according to greedy algorithm [15]. This chain is recognized by the BS and is broadcasted over the whole network. When a node is run out of battery, it is bypassed and another chain is formed in the same manner. Leader of the chain can be at any random position. Every node fuses data of its own and its neighbor to form a single packet of data except the last one of the chains. Thus, only one packet is sent by each node in every round. It is possible that some nodes have large distance from their neighbor nodes. Such nodes cannot become leader as they dissipate more energy. To prevent this, a threshold is set on neighbor node distance. In PEGASIS the transmission distance is less than LEACH, amount of data received by leader is less and only single node transmits to the BS. In PEGASIS energy load is uniformly distributed among all nodes which increase the lifetime and quality of network. The results are better for a large network.

IV. Simulations and Results

The Hierarchical based routing protocols are compared using MATLAB simulator. 100 nodes are distributed equally in a network area of 100m * 100. The system is compared for a total of 4000 rounds. Various networks parameters are represented using following table.1.

Table 1: Network Parameters

Parameters	**Values**
Network Size	100m * 100m
Initial Energy (Eo)	0.5 J
Total number of nodes (n)	100
Data Aggregation Energy (EDA)	50 pJ/bit J
Data Transmitting Energy (ETX)	50 pJ/bit J
Data Receiving Energy (ERX)	50 pJ/bit J
Distance (do)	87.7058 m

Number of rounds (r)	4000
Probability (p)	0.1
Amplification Energy (Emp) when (d>do)	0.0013 pJ/bit J
Amplification Energy (Efs) when (d<do)	10 pJ/bit J

A. Dead Nodes Comparison

The dead nodes can be compared with the help of following MATLAB figure. From the figure, it is clear that DEEC outperforms all hierarchical based routing protocols because it is heterogeneous aware while others have certain limitations.

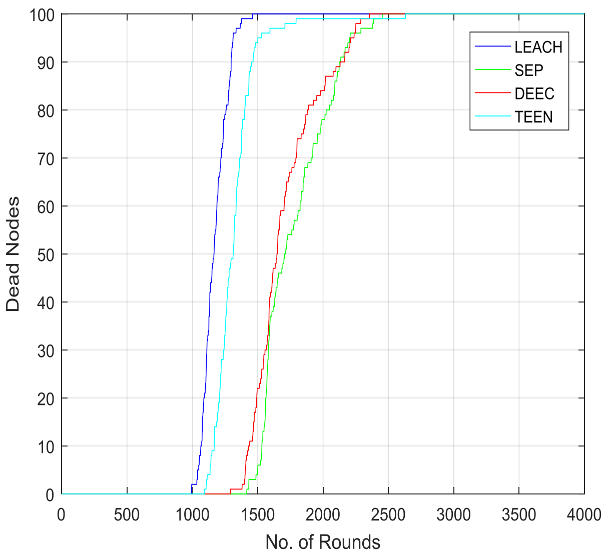

Figure 2: Comparison of dead nodes

The above figure shows the comparison of energy efficient routing protocols for dead nodes.

B. Data Packets Comparison

The total amount of data packets sent to base station can be compared using the following figure. DEEC again outperforms all the hierarchical routing protocols since it is more heterogeneous aware.

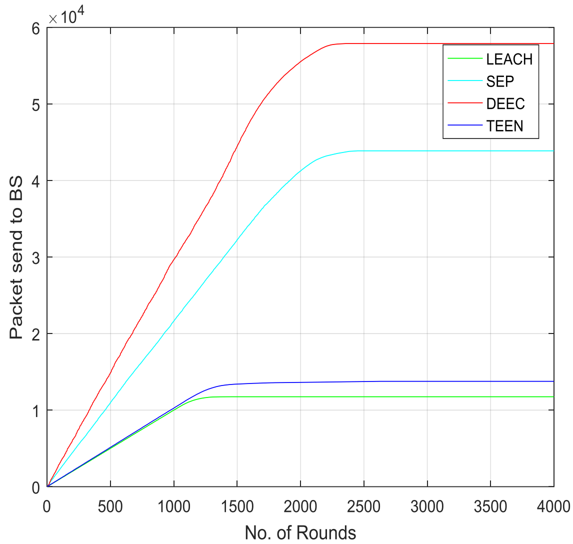

Figure 3: Total Data Packets Comparison

The total amount of data packets has been compared in the above figure.

C. Data Packets per Round Comparison

The amount of data packets sent to base station per round can be compared in the following figure. DEEC again outperforms all routing protocols.

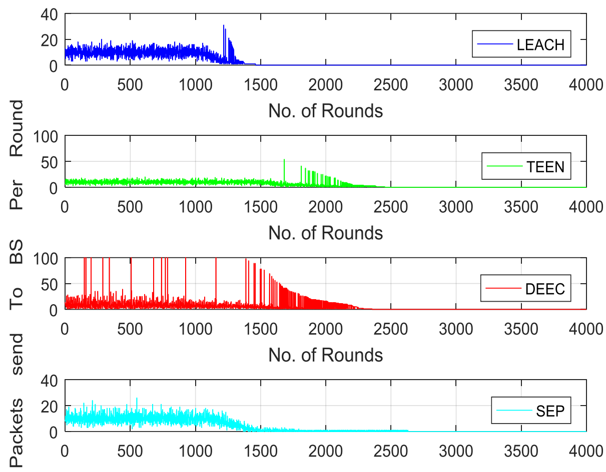

Figure 4: Data Packets sent per Round Comparison

The above figure shows the number of data packets sent per round.

V. WIRELESS RECHARGING OF SENSOR NETWORK:

Sensor nodes consist of batteries which do not last long. Several energy conservation techniques [9-14] have been proposed which are thoroughly discussed in the upper portion. However, these energy conservation techniques only slow down the energy usage process and cannot be considered as life-long processes. To tackle this issue, several energy harvesting techniques like wind [26], solar [25] and vibration energy [27] have been proposed. These techniques have numerous advantages but they are uncontrolled and not applicable to certain harsh environments like underground vault or power line sensing, underwater monitoring and certain other environments where these energy harvesting techniques have their bottleneck. A more robust and reasonable technique is wireless recharging of these sensors manually or through robots [15], [16], [18], [19], [21]. The pioneer in wireless charging techniques is presented in [28] which have opened new ways of wireless energy transfer. The overview of wireless charging is presented by the following figure [15].

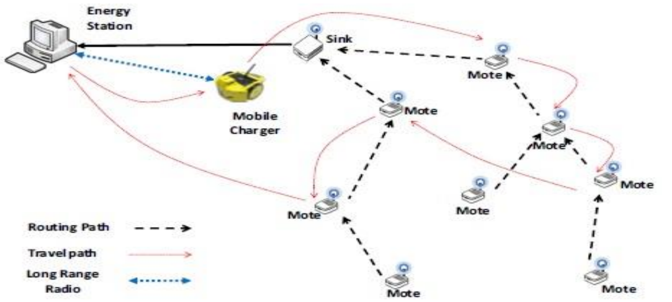

Figure 5: Overview of wireless energy transfer

The history of wireless power transfer dates back to Tesla, who tried to transmit signal and electricity wirelessly. Due to certain circumstances, Tesla's idea was not put to practical use until the use of electronic devices became popular in the 20th century. Various power transfer techniques have been proposed which will be discussed in detail in the following part.

I. *Inductive Coupling:*

The basic principle for inductive coupling [19] is magnetic field induction. An alternating current in the primary coil (source) produces changing magnetic field due to which a voltage is induced across secondary coil's terminals (receiver). Due to safety and simplicity, it is a good choice for wireless power transfer. Cell phone's charging pad and electric tooth-brush works on inductive coupling. Although inductive coupling is pioneer technology in wireless power transfer but there are certain issues which limits its performance. It works well when the power source and destination are in close contact and aligned. Due to this limitation it does not work well in the case of wireless sensor network.

II. *Magnetic Resonance Coupling:*

The magnetic resonance coupling [28], [19] is based on resonant coupling principle which states that "by having magnetic resonant coils operate at the same resonance frequency so that they are strongly coupled via irradiative magnetic resonance induction" [19]. The magnetic and mechanical resonance can be considered same by giving example of a string, tuned to specific tune and can be vibrated by a sound source at a distance only if their resonance frequencies match. The energy transfer between source and receiver coil in case of resonant coupling is much efficient. An experiment was conducted to light a 60 W bulb at a distance of 2 meter in [28] was not achieve able through inductive coupling. It can be considered as enhanced form of inductive coupling that is more transfer efficient and has high range. Magnetic resonant has some limitation like maximum distance can only be achieved if source and receiver are placed along a common axis and careful tuning is needed to prevent interference. It is more efficient, less harmful and do not requires line of line of sight between sender and receiver.

Following figure [19] shows a wireless charger vehicle which travels inside a network and wirelessly charging each sensor node based on magnetic coupling. Upon charging the whole network, the vehicle returns to its station, fills its battery and becomes ready for the next trip. The concept of renewable energy concept described fully in [19] to recharge sensor nodes in time. The magnetic resonant coupling, if rightly designed can provide life-long energy to sensor nodes. But through this technology only one sensor is charged at a time. When the network size increases, this technology becomes non-scalable.

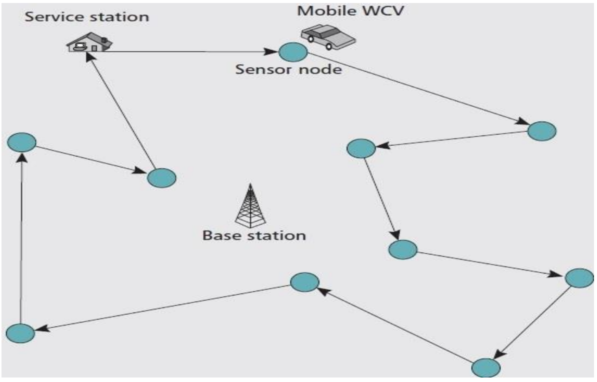

Figure 6: A mobile charge carrying vehicle charging sensor nodes

III. *Electromagnetic Radiation:*

Energy is transmitted between source and receiver antenna through electromagnetic waves. This type of radiation can be unidirectional or omni-directional. For omni-directional transmission a frequency range of 902 to 928 MHz is used for transmission in omni-direction while tuning the receiver to a similar frequency range. But omni-directional transmission suffers greatly with transmission distance and harmful to humans. So, it is only useful for very low power sensor nodes (up to 10mW). The unidirectional transmission is more efficient if a clear line of sight exists between transmitter and receiver. The maximum value of power for RF energy harvesting is 7 µW and 1 µW for a frequency range of 900 MHz to 2.4 GHz for a distance of 40m [24]. The summary of all these techniques is presented in following table [20].

Table 2: Summary of wireless recharging techniques

Wireless energy transfer technique	Field region	Propagation	Effective distance	Efficiency	Applications
RF energy transfer	Far-field	Radioactive	Depends on distance, frequency and sensitivity of energy	0.4, 18.2 and 50% at -40 dBm,20 dBm,-5	Wireless sensor and body networks
Resonance inductive coupling	Near-field	Non-radioactive	From a few millimeters to a few centimeters	From 5.81% to 57.2% when frequency varies from 16.2	Passive RF identification tags, contactless smart cards,cell
Magnetic resonance coupling	Near-field	Non-radioactive	From a few centimeters to a few meters	From above 90% to above 30% when distance varies from 0.75m to 2.25m	PHEV charging, cell phone charging

A more inside of radio frequency RF energy harvesting is presented in [20], [21] and [24]. The wireless sensor network application to monitor chronic disease patients is presented in [23] and smart grid monitoring is presented in [21], [22]. In [21] sustainable wireless rechargeable sensor network (SuReSense) is presented which makes use of mobile wireless rechargeable robots (MICROs) to recharge the batteries of sensor nodes. Two steps are involved during operation of MICROs, one step being minimum number of landmark selections on the basis of energy requirement and location. This step is done with the help of integer linear programming. In the second step a cluster is formed from these landmarks, each being taken care of by a single MICRO. The MICRO follows shortest Hamiltonian path to serve each landmark in its cluster and transmits power wirelessly to the sensor nodes. In this way the traversed path is further reduced which enables the MICRO to pass more time at the energy source to refill its own battery. The waiting time of sensor nodes is also reduced in this manner.

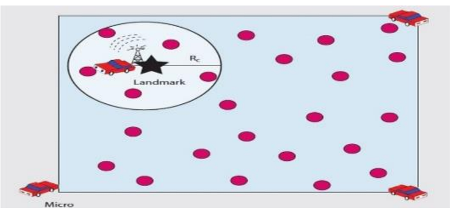

Figure 7: Cluster, Landmark and SenCar during Operation of SuReSense

The mobile charger shown in the above figure [21] is called SenCar and it consists of high capacity battery, a DC/AC converter and a resonant coil. It goes to the nodes which are deprived of battery power while collecting data in the meantime. Another RF energy harvesting technique for mobile sensor nodes is presented in [24], which makes use of Schottky diodes to implement energy harvesting. This technique is very much helpful in charging a low battery mobile device by placing it near a fully charged mobile device and draining energy to recharge it.

Conclusion

Wireless communication has become vital part of our life nowadays, playing a role in almost every field. As the sensor network is dependent on small sensors, which have limited battery life and will be of no use if the battery charge is drained. To enhance the battery life, various energy efficient protocols are proposed. But these protocols only decrease the energy expenditure by various techniques and do not last long. To have a better solution, wireless recharging of the sensor nodes is proposed. Through wireless charging, the life of sensor nodes last life-long. Three different techniques of wireless charging were proposed, the best of which was electromagnetic radiation (RF) technique. A lot of work has been done in this field but for future research combining energy efficient techniques with wireless charging of sensor nodes can increase the efficiency further. Also, wireless data gathering along with recharging can be done to improve performance i.e. the phenomenon of LEACH [9] can be combined with wireless energy transfer process. The sensor nodes chose their cluster head and only this cluster head communicates with the mobile charger. It takes charge from the mobile charger and distributes this charge among members of its cluster. In return it transmits the collected data to the mobile charger and this process goes on.

References

[1] I.F. Akyildiz, W. Su, Y. Sankarasubramaniam, E. Cayirci, "Wireless sensor networks: a survey," Computer Networks 38 (2002) 393–422.

[2] Xuxun Liu, "A Survey on Clustering Routing Protocols in Wireless Sensor Networks," Vol.12, 2012, pp. 11113-11153.

[3] Ian F. Akyildiz, Weilian Su, Yogesh Sankarasubramaniam, and Erdal Cayirci, "A Survey on Sensor Networks," IEEE Communications Magazine • August 2002.

[4] David Culler, Deborah Estrin, Mani Srivastava,"Overview of Sensor Networks,"Published by the IEEE Computer Society August 2004.

[5] Nikolaos A. Pantazis, Stefanos A. Nikolidakis and Dimitrios D. Vergados, "Energy-Efficient Routing Protocols in Wireless Sensor Networks: A Survey," IEEE Communications Surveys and Tutorials.

[6] Chunjuan Wei, Junjie Yang, Yanjie Gao, Zhimei Zhang, "Cluster-based Routing Protocols in Wireless Sensor Networks: A Survey," 2011 International Conference on Computer Science and Network Technology.

[7] Ahmed Badi, Imad Mahgoub, Fadi Sibai, "Impact of Transmission-related Parameters on the Energy Performance of Cluster-based Routing Protocols for Wireless Sensor Networks," 2011 International Conference on Innovations in Information Technology.

[8] Guangyan Huang, Xiaowei Li, Jing He, "Energy-Efficiency Analysis of Cluster-Based Routing Protocols in Wireless Sensor Networks," IEEEAC paper #1088, Version 6, Updated Nov. 21, 2005.

[9] W. Heinzelman, A. Chandrakasan, and H. Balakrishnan, "Energy-Efficient Communication Protocol forWireless Microsensor Networks," Proceedings of the 33rd Hawaii International Conference on System Sciences – 2000.

[10] Li Qing , Qingxin Zhu, Mingwen Wang, "Design of a distributed energy-efficient clustering algorithm for heterogeneous wireless sensor networks," Computer Communications 29 (2006) 2230–2237.

[11] G. Smaragdakis, I. Matta, A. Bestavros, "SEP: A Stable Election Protocol for clustered Heterogeneous wireless sensor networks," Proceedings of 2nd International Workshop on Sensor and Actor Network Protocol and Applications (SANPA), Boston, U.S.A, 2004, pp. 1-11.

[12] Manjeshwar, E.; Agrawal, D.P., "TEEN: A Routing Protocol for Enhance Efficiency in Wireless Sensor Networks," In Proceedings of the 15th International Parallel and Distributed Processing Symposium (IPDPS), San Francisco, CA, USA, 23–27 April 2001; pp. 2009–2015.

[13] Bencan Gong Tingyao Jiang, "A Tree-Based Routing Protocol in Wireless Sensor Networks," 978-1-4244-8165-1/11/$26.00 ©2011 IEEE.

[14] S. Lindsey and C. Raghavendra: PEGASIS: Power- Efficient Gathering in Sensor Information Systems. IEEE Aerospace Conference Proceedings (2002) 1125-1130.

[15] Yang Peng, Zi Li, Wensheng Zhang, and Daji Qiao, "Prolonging Sensor Network Lifetime through Wireless Charging," 2010 31st IEEE Real-Time Systems Symposium.

[16] Liguang Xie, Yi Shi, Y. Thomas Hou and Hanif D. Sherali, "Making Sensor Networks Immortal: An Energy-Renewal Approach With Wireless Power Transfer," IEEE/ACM Transactions on Networking, Vol. 20, No. 6, December 2012.

[17] Yinggang Bu, Masahiro Nishiyama, Takuto Ueda, Yoshimi Tashima, and Tsutomu Mizuno, "Examination of Wireless Power Transfer Combined With the Utilization of Distance Detection," IEEE Transactions on Magnetics, Vol. 50, No. 11, November 2014.

[18] Liguang Xie, Yi Shi, Y. Thomas Hou, Wenjing Lou, Hanif D. Sherali, and Scott F. Midkiff, "Multi-Node Wireless Energy Charging in Sensor Networks," IEEE/ACM Transactions on Networking, Vol. 23, No. 2, April 2015.

[19] Liguang Xie, Yi Shi, Y. Thomas Hou, Andwenjing Lou, "Wireless Power Transfer and Applications to Sensor Networks," IEEE Wireless Communications • August 2013.

[20] Xiao Lu, Ping Wang, Dusit Niyato, Dong In Kim, and Zhu Han, "Wireless Networks with RF Energy Harvesting: A Contemporary Survey," arXiv:1406.6470v6 [cs.NI] 5 Sep 2014.

[21] Melike Erol-Kantarci and Hussein T. Mouftah, University of Ottawa "SuReSense: Sustainable Wireless Rechargeable Sensor Networks for the Smart Grid," IEEE Wireless Communications • June 2012.

[22] Vehbi C. Gungor, Bin Lu and Gerhard P. Hancke, "Opportunities and Challenges of Wireless Sensor Networks in Smart Grid," IEEE Transactions on Industrial Electronics, Vol. 57, No. 10, October 2010.

[23] Silvia Jimenez-Fernandez, Paula de Toledo and Francisco del Pozo,"Usability and Interoperability in Wireless Sensor Networks for Patient Tele-monitoring in Chronic Disease Management," IEEE Transactions on Biomedical Engineering, Vol. 60, No. 12, December 2013.

[24] Hamid Jabbar, Young. S. Song, Taikyeong Ted. Jeong, "RF Energy Harvesting System□and Circuits for Charging of Mobile Devices," IEEE Transactions on Consumer Electronics, Vol. 56, No. 1, February 2010.

[25] A. Kansal, D. Potter, and M. B. Srivastava, "Performance aware tasking for environmentally powered sensor networks," SIGMETRICS Perform. Eval. Rev., 32(1):223–234, 2004.

[26] C. Park and P. Chou, "Ambimax: Autonomous energy harvesting platform for multi-supply wireless sensor nodes," In SECON '06, pages 168–177, Sept. 2006.

[27] S. M. Jose, J. O. Mur-mir, R. Amirtharajah, A. P. Ch, and J. H. Lang, "Vibration-to-electric energy conversion. IEEE Transactions on Very Large-scale Integration (VLSI) Systems," 9(1):64–76, Feb 2001.

[28] A. Kurs, A. Karalis, R. Moffatt, J. D. Joannopoulos, P. Fisher, and M. Soljacic, "Wireless power transfer via strongly coupled magnetic resonances," Science, vol. 317, no. 5834, pp. 83–86, 2007.

Farman Ullah, is currently doing his MSc in Electrical Engineering at University of Engineering and Technology, Peshawar, Pakistan and is working as Junior Transmission Engineer in a public organization.

International Journal of Engineering Works
ISSN-p: 2521-2419
ISSN-e: 2409-2770
Vol. 6, Issue 09, PP. 275-279, September 2019
https://www.ijew.io/
https://doi.org/10.34259/ijew.19.609275279

Mitigating Low Frequency Oscillations in Interconnected Power System

Juveria Anwar[1], Asfand Yar Ali[2], Dr.Tanvir Ahmad[3]
[1,2,3] US-Pak Center of Advanced Studies Energy (USPCASE)
University of Engineering and Technology(UET), Peshawar KPK, Pakistan
Received: 20 August, Revised: 26 August, Accepted: 05 September

***Abstract*—** Low frequency oscillations are one of the major causes which reduce the capabilities of power system. Low frequency oscillations (LFO) have taken the attention of engineers therefore different techniques are introduced. This paper will help out to damp low frequency oscillations using one of the best and effective technique i.e. Power system stabilizer (PSS). Since among various techniques power system stabilizer has taken the attention by working effectively to damp low frequency harmonics. The model will is implemented using Simulink and the graphical results are analyzed and compared. The system efficiency is improved up to 82%, by employing power system stabilizer.

***Keywords*—** LFO, PSS, Harmonics, AVR.

I. INTRODUCTION

Interconnected arrangement is used for power systems which make it complicated and complex. Due to interconnection systems constantly variations are experienced in generation, transmission and distribution of electric power. The main problem of interconnected power system stability is low frequency oscillations. As stability is the prime goal in electric power system [1]. Constantly complications occurring in power system have initiate curiosity for developing best and effective solution for PSS to damp out LFO. Largely interconnected power system causes the system spontaneously affected by very low frequencies. In oscillatory mode electromechanical oscillations are called as weak damping, ranging 0.2-0.3Hz, and if once they started, they continue for long time period. In some cases they leave a severe effect on system, like they continue to grow which cause system separation and limits the power transfer if bold steps are not followed to damp LFO or small signal stability.

The tendency of synchronous machine of interconnected power system to remain run & step and synchronized with each other after being perturbed by small disturbance is known as small signal stability. This stability depends on the skill of maintaining equilibrium between electromechanical and mechanical torques connected to power systems [2]. The perturbation followed by change in electromechanical torque of synchronous machine can be resolved by two components "synchronizing torque component in phase with rotor angle deviation" and "a damping torque component in phase with speed deviation". LFOs are generator rotor angle oscillations having frequency 0.2-0.3 Hz or 0.1- 2.0 Hz (generally) and they are classified according to their source of oscillations. In earliest age of power system development the oscillations were almost zero (non-observable) this was due to close connection of generators and loads. But now days due to increase demand, electric power systems are installed farthest from load. Due to which power is transmitted through long transmission line which increase the power oscillations [3][4]..The basic cause of oscillations is the difference between the demand and generation. Therefore to maintain power system stability, PSS are used.

Power system stability [5] is the ability of an electric power system, for a given initial operating condition, to regain astate of operating equilibrium after being subjected to a physical disturbance, with most system variables bounded so that practically the entire system remains intact. PSS [6,7] is a controller device which is installed in synchronous machine to damp LFO. The working principle of PSS [8, 9] is to add damping to generator rotor oscillations by controlling its excitation by using auxiliary stabilizing signals or it can explain as PSS [10] is aid for damping oscillations via modulations of excitation system of generators. For damping purpose stabilizer produces electrical torque on rotor which is in phase with speed variations. This control is beneficial for large power transfers [11,12]. However, in certain conditions when the negative damping effects of PSS on rotor occur then the power system instabilities arises. The reason behind negative damping effects is that PSS [13,14] is tuned around steady- state operating point. And at this operating point the damping effect is only valid for small excursions. At severe disturbances this may happen that PSS cause the generator under its control to lose synchronism in an attempt to control its excitation field [15].

Thus, the aim of this paper is to damp the unrequired low frequency oscillations. Since LFOs are harmful for power system stability. Therefore the latest and updated technique is used i.e. power system stabilizer. There are many phases from which the signals are passed and due to which LFOs are extracted from the power system.

II. PROBLEM STATMENT

Power production with good quality is the main objective of every power utility company so that their generation, transmission, distribution of electrical power is efficient and the consumers are satisfied. Most of the power systems suffers from various unwanted internal generators effects such as production of low frequency oscillations and harmonics. This is due the difference between the rotor angle and the pole. To overcome this hazardous problem, we proposed a solution to which is a control system that will sense the synchronous generator transient response and will provide feedback signal to reduce the low frequency oscillations and make the system stable. By employing this method, the overshoot will be reduced and the response will be approximately smooth.

III. METHODOLGY

The block diagram of PSS is shown in Figure 1. to understanding the structure. It contains washout

filter, gain block, phase compensator block and input signal.

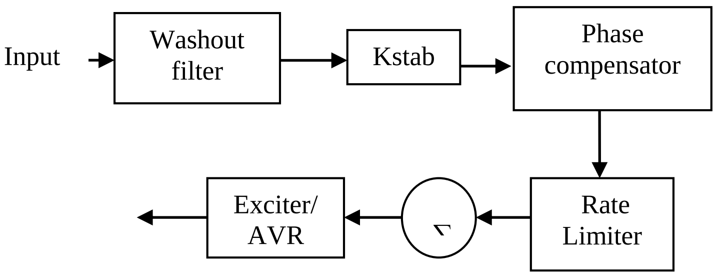

Figure 1: Block Diagram of PSS

A. *Washout filter:*

Washout filter works as high pass filter, with time constant Tw, which is high enough and allow signal to pass unchanged which are associated with oscillations in wr. It is important because without it steady variations in speed would modify the terminal voltage. It allows PSS to react only to make changes in speed. According to washout function, the Tw value isn’t critical and it may ranges from 1 to 20 seconds. It diminishes dc component present in input signal.

B.Gain block:

The stabilizer gain finds the amount of damping introduced by PSS. The value of gain should be set according to maximum damping (ideally) but it is often limited by other considerations. Generally its value is set between 2 to 10.

C. *Phase compensator block:*

Phase compensation provides appropriate phase-lead characteristics to compensate the phase-lag between the exciter input and generator torque.

D. *Input signal:*

Input signals that have been identified as valuable include deviations in rotor speed ($\Delta\omega$), the frequency (Δf), the electrical power (ΔPe) and the accelerating power (ΔPa). Since main function of PSS is to control rotor oscillations. In this paper speed signal is used as input signal.

E.Exciter /AVR:

Automatic voltage regulator (AVR) is connected PSS and it inject signal at summing junction. AVR with PSS is connected to generator to control its terminal voltage by adjusting excitation voltage at rotor side of it. To evaluate performance of PSS SMIB is used (single machine infinite bus), which will explain later. Generator connected with AVR and PSS is connected to infinite bus by transmission line and some disturbances are produced to create oscillations in power system.

F. *Rate limiter:*

PSS output requires limits in order to prevent conflicts with AVR actions during load rejection. The AVR acts to reduce the terminal voltage while it increases the rotor speed and bus frequency. Thus, PSS is compelled to counteract and produce more positive output .the negative and positive limit should be around the AVR set point to avoid any counteraction. The positive limit of PSS output voltage contributes to improve transient stability in first swing during fault. The negative limit appears to be very important during the backswing of rotor.

The system is designed and simulated using Simulink and the analysis is performed. The Power System Stabilizer is incorporated with the synchronous generator as feedback element. The rest of power system comprised of three phase Transmission lines, RLC Loads, Transformers, SPDT Switches and Scopes. The results of the system response is observed with and without power system stabilizer. Both results are compared graphically and the conclusion is obtained by analyzing those figures. The algorithm of the project is illustrated below which indicate the step by step sequence of the power system stabilizer operation during transient state.

IV. FLOW CHART

The algorithm for power system stabilization is depicted in the flow chart as shown in fig. 2. First the system is run and then the synchronous generator response is determined. This response is compared with ideal variables and when the system response is unstable then the PSS feedback run and optimizes the parameters. After the response gets smooth and stable, the whole results are displayed on scope windows.

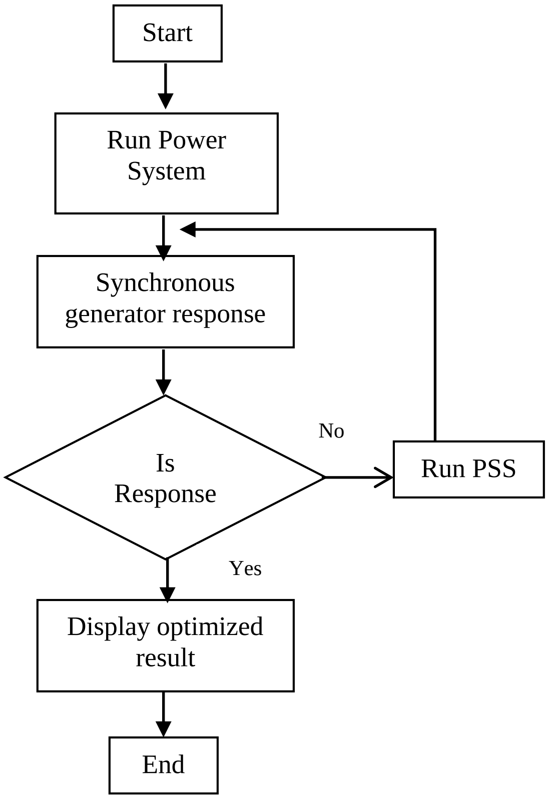

Figure 2 Flow chart of the PSS

V. Results

Following are results of models and their results without PSS and with PSS. Figure: 3 shows the synchronous generator response is obtained without using the PSS Controller. It can be clearly seen in the above Simulink model that the switch is open which is installed between synchronous generator and PSS. The results are obtained on scope windows.

Figure: 4 scope windows show the rotor deviation angle, output active power, output reactive power and stable voltage level from Excitation system. The results show that the rotor deviation angle increases from zero which is undesired. The output active power is variable and is not smooth. Same is the case for the reactive power and stable voltage level

Figure:5 shows switch is now closed which connects the synchronous generator and feedback system. The results are depicted on the scope which shows much improvement all the parameters.

Figure: 6 describes that the rotor deviation angle is near to zero which is desired. The output active power is also smooth which is suitable for loads. Same is the case for reactive power and stable voltage levels. From these graphical results it is clear that by using PSS, the performance of power system and its efficiency improves to the required level.

Conclusion

This paper is proposed for the development of a model to overcome the unstable behavior during transient state. The PSS compensator filter out all the unnecessary effects and the improved response is obtained. The results comparison shows that the synchronous generator response oscillatory and increases with time which moves into unstable region of operation. The rotor deviation angle increases from zero to onward which produces the harmonics. Also the output active power is variable which is not desired to the end loads. Similarly, the reactive power shows variable and not constant. On the other hand, by employing Power system stabilizer in feedback with the generator, the system responses show a better and stable behavior. The rotor deviation angle is almost zero as well as the active and reactive power values. Therefore, it is concluded that PSS play an important role for improving power system stability.

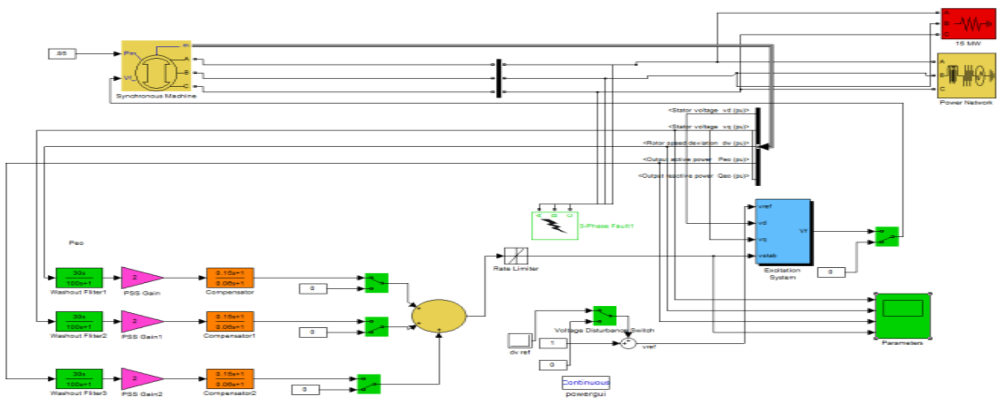

Figure: 3 Simulink Model without Power System Stabilizer Feedback

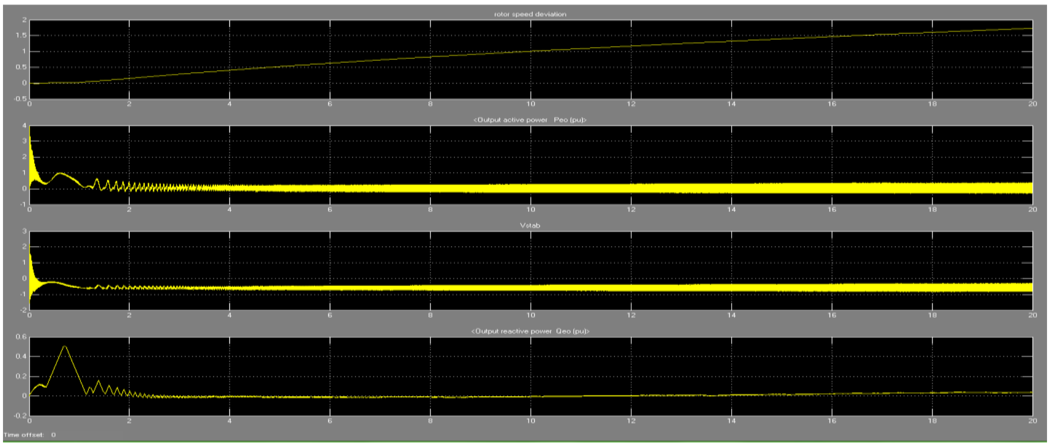

Figure: 4 Simulink Model without Power System Stabilizer Feedback Result

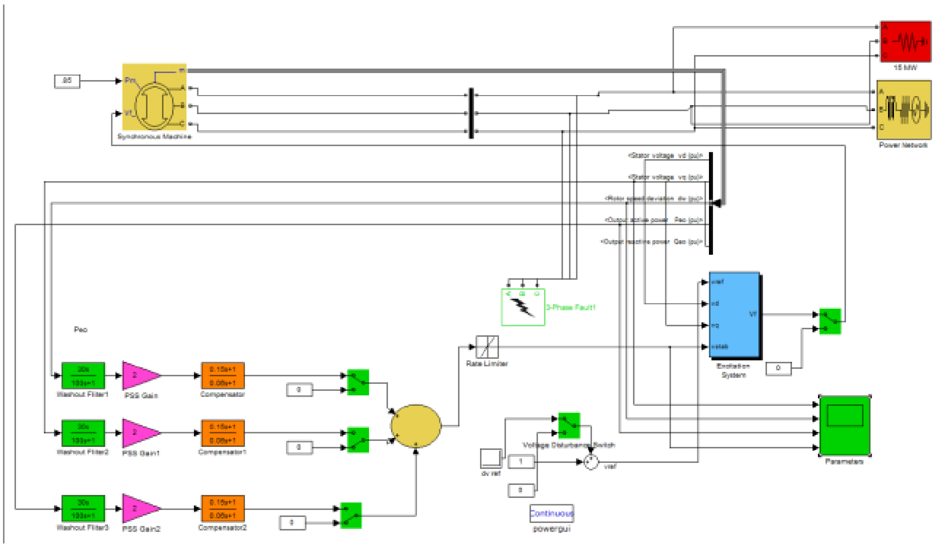

Figure: 5 Simulink Model with Power System Stabilizer

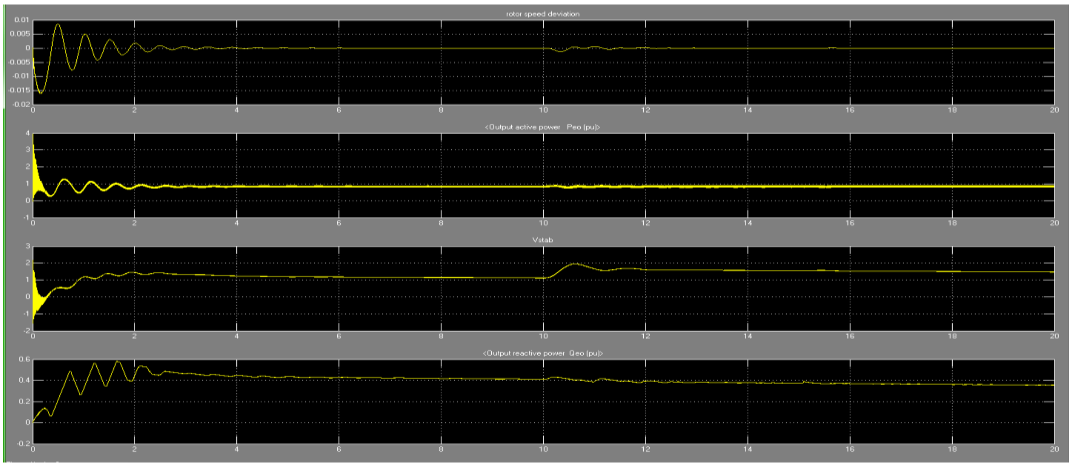

Figure: 6 Simulink Model with Power System Stabilizer

REFERENCES

[1] F. Maury, Summary of the answers to the questionnaire on the dynamic performances of future power system, *CIGRE, Electra*, pp. 87-100, 1975

[2] J. H. Chow and J. J. Sanchez-Gasca, Pole-Placement Designs of Power System Stabilizers, *IEEE Transactions on Power Systems*, Vol. 4, No. 1, February 1989.

[3] M. A. Abido and Y. L. Abdel-Magid, Robust design of electrical power-based stabilizers using Tabu search, *Power Engineering Society Summer Meeting,* Vol. 3, pp. 1573-1578, 2001.

[4] P. Kundur, *Power System Stability and Control*. New York: McGraw-Hill, 1994.

[5] K. T. Law et. al, Robust Co-ordinated AVR-PSS Design, *IEEE Transactions on Power Systems*, Vol. 9, No. 3, August 1994

[6] P. S. hamsollahi, *Neural Adaptive Power System Stabilizer,* Thesis at University of CALGARY, CALGARY, ALBERTA, July, 1997

[7] G. Rogers, *Power System Oscillations*. Boston, MA: Kluwer, 2000.

[8] K.. Hongesombut, and Y. Mitani: Implementation of Advanced Genetic Algorithm to Modern Power System Stabilization Control, *Power Systems Conference and Exposition*, pp. 1050-1055 vol.2, 2004 .

[9] G. R. Bérubé, L. M. Hajagos, and R. Beaulieu, "Practical utility experience in application of power system stabilizers," in *Proc. IEEE PESSummer Meeting*, vol. 1, Jul. 1999, pp. 104–109.

[10] C. W. Taylor, "Improving the grid behavior," *IEEE Spectrum*, vol. 36, no. 6, Jun. 1999.

[11] C. W. Taylor, C. Erickson, K. E. Martin, R. E. Wilson, and V. Venkatasubramanian, "WACS-wide-area stability and voltage control system: R&D and on-line demonstration," *Proc. IEEE*, submitted for publication.

[12] N. Martins, A. A. Barbosa, J. C. R. Ferraz, M. G. dos Santos, A. L. B. Bergamo, C. S. Yung, V. R. Oliveira, and N. J. P. Macedo, "Retuning stabilizers for the North-South Brazilian interconnection," in *Proc. IEEEPES Summer Meeting*, vol. 1, Jul. 1999, pp. 58–67.

[13] A. Fischer and I. Erlich, "Impact of long-distance power transits on the dynamic security of large interconnected power systems," *Proc. 2001IEEE Power Tech. Conf.*, vol. 2, p. 6, Sep. 2001.

[14] L. Gérin-Lajoie, D. Lefebvre, M. Racine, L. Soulières, and I. Kamwa, "Hydro-Québec experience with PSS tuning," panel on system reliability as affected by power system stabilizers," in *Proc. IEEE PESSummer Meeting*, vol. 1, Jul. 1999, pp. 88–95.

[15] D. M. L. Crenshaw, C. J. Bridenbauch, A. Murdoch, R. A Lawson, and M. J. D'Antonio, "Microprocessor-based power system stabilizer anddisturbance recorder," *presented at the IEEE Joint Power Generation Conference,* Chicago, IL, Mar. 1991.

International Journal of Engineering Works
ISSN-p: 2521-2419
ISSN-e: 2409-2770
Vol. 6, Issue 09, PP. 288-291, September 2019
https://www.ijew.io/
https://doi.org/10.34259/ijew.19.609288291

Comparison of Satellite and Ground based Solar Data for Peshawar, Pakistan

Adnan Ayaz[1], Mohammad Abdul Aziz Irfan[2], Muhammad Noman[3]
[1,3]Department of Renewable Energy Engineering, U.S.-Pakistan Center for Advanced Studies in Energy, University of Engineering and Technology Peshawar, Pakistan,
[2]Mechanical Engineering Department, University of Engineering and Technology Peshawr, Pakistan
[1]adnanayaz@uetpeshawar.edu.pk, [2]mairfan@uetpeshawar.edu.pk, [3]muhammad.noman@uetpeshawar.edu.pk
Received: 04 September, Revised: 08 September, Accepted: 13 September

***Abstract*—**This study presents one of the first analyses carried out on solar energy resource measurement using meteorological station established at University of Engineering and Technology (UET) Peshawar by World Bank under Energy Sector Management Assistance Program (ESMAP). Ground based direct normal irradiance (DNI) and global horizontal irradiance (GHI) were measured and analyzed for year 2017 and then compared with the data of satellite based solar model called SUNY. Ground based data was measured with the help of Kipp & Zonen CMP10 Pyranometer and Twin sensor Rotating Shadowband Irradiometer (RSI). Data of satellite based solar model (SUNY) was based on daily total monthly mean averaged over 15 years, starting from 2000 till 2014. The maximum value of ground based GHI was found for the month of June which was 6,415 Wh/m^2 and minimum GHI was found for the month of December which was 1,605 Wh/m^2. On the other hand, highest DNI was recorded in the month of April which was 5,884 Wh/m^2 and lowest DNI was recorded in the month of January which was 1,718 Wh/m^2. Comparison of the data showed higher values of GHI and DNI for satellite based model (SUNY) in most of the months. In February, March and April, ground based GHI and DNI were overestimated compared to satellite based model. Maximum difference of 1,346 Wh/m^2 in GHI was noticed in November and minimum difference of -181 Wh/m^2 was recorded in the month of March. On the other hand, maximum difference of 2,348 Wh/m^2 in DNI was observed in the month of November and a minimum difference of -140 Wh/m^2 was seen in March. This study will be helpful in further assessment of solar energy resource at any location in Pakistan as it will provide help for base-line studies. Moreover, it will also help in establishing any solar energy program particularly concentrating solar power (CSP) in Pakistan.

***Keywords*—** GHI, DNI, UET Peshawar, satellite data, ground data

I. Introduction

Establishment of any solar energy program needs accurate solar energy resource measurement. Solar energy resource assessment is one of the important phases for development of any solar energy program to properly estimate the available solar energy received on earth. Solar energy resource can be estimated from satellite based models or real time ground based measurements. For any investor, to invest in any solar energy program, accurate ground based solar energy needs to be measured. There are various satellite based solar energy resource estimation models available worldwide; each has its own significance and estimation approach. These models can only provide data based on estimated value of solar energy. Satellite based solar energy resource and ground based measured solar resource need to be compared to each other in order to find correlation between them.

Various research studies have been carried out in different regions of the world to assess solar energy resource. One such study was done in Saudi Arabia which showed that DNI in the country ranged from 9,000 Wh/m^2/day in the summer to 5,000 Wh/m^2/day in the winter season. Same study showed that GHI in many regions of the country was as high as 8,300 Wh/m^2/day. DNI was locally measured at Qassim University which ranged from a maximum value of 8,367 Wh/m^2/day in July to a minimum value of 4,702 Wh/m^2/day in January [1].

Another study was done which investigated performance of photovoltaic systems at 32 different sites of Saudi Arabia on the basis of real time solar radiation data. In this research, grid connected photovoltaic system was used for study whose maximum output was 100,000 W. The performance of the system at 32 sites was measured through RETScreen program on the basis of collected data through RRMM (Renewable Resource Monitoring and Mapping) program for 2 years. This research showed that highest energy was produced in Najran site which was 218.5 MWh for fixed photovoltaic systems [2].

A study was done in Saudia Arabia which concluded that, for 30 stations, the annual average daily GHI was in range of 5,700 Wh/m^2 to 6,700 Wh/m^2. This study also stated the higher values of GHI for inland while lower values of GHI for coastal areas [3].

One of the studies in Chile shows very good agreement between ground based and satellite based irradiance, showing an rRMSE (relative root mean square error) of 8.9% only. They also found that for radiation values less than 3,000 Wh/m^2/day, satellite based data overestimated the actual radiation received on earth [4].

A satellite based model was developed by using climatic conditions of Thailand. The model was used to analyze the data of 25 ground based measurement stations having pyranometers. They found that monthly average hourly global radiation agreed very well with ground based data having root mean square difference of only 10% from the mean value [5].

Peshawar is located at 34.01^o N latitude and 71.58^o E longitude in Khyber Pakhtunkhwa province of Pakistan [6]. Currently, country is suffering from severe shortfall of energy. In order to mitigate power crises, different energy programs are employed in the country. In connection to that, World Bank in collaboration with Alternative Energy Development Board (AEDB) Pakistan has established meteorological station at University of Engineering and Technology (UET) Peshawar. The purpose of this station is to record ground based solar radiation which will be used for assessment and generation of solar energy maps. Ground based data used in this study has been taken from station established at UET Peshawar.

A. Definitions

1) Direct Normal Irradiance (DNI)

The direct irradiance received on a plane normal to the sun is called direct normal irradiance [7]. The device which measures DNI is known as pyrheliometer. DNI is usually measured in Wh/m^2/day. DNI is very handy for concentrating solar technologies.

2) Global Horizontal Irradiance (GHI)

The maximum solar radiation at a specific time and place on the earth's surface when no cloud is present is called global horizontal irradiance [8]. GHI is measured in Wh/m^2/day. GHI is useful for flat plate solar collectors.

II. METHODOLOGY

Study presented in this paper has been done using World Bank's Energy Sector Management Assistance Program (ESMAP). This program focuses to monitor and map various parameters out of which wind and solar energy is of prime importance. Under this program, ESMAP tier 2 meteorological station has been installed at roof top of Mechanical Engineering Department, University of Engineering and Technology (UET) Peshawar on April 10, 2015. Other stations installed through this program at various locations of Pakistan are listed in Table 1.

Meteorological tier 2 station at UET Peshawar consists of various instruments to measure different parameters. It is equipped with Concentrated Solar Power Services (CSPS) Twin sensor Rotating Shadowband Irradiometer (RSI) and Kipp & Zonen CMP10 Pyranometer. They are used to direct normal irradiance (DNI), global horizontal irradiance (GHI) and diffuse horizontal irradiance (DHI) received at this station. It is also equipped with CS215 Temperature and Relative Humidity probe which measures temperature and relative humidity of the ambient air. This station also has CS100 barometric pressure sensor which measures barometric pressure. NRG #40C Anemometer and NRG #200P wind direction sensor are also part of the station which are fixed on a wind mast at 10 m height above the surface of roof top. Data logger used in this station is Campbell Scientific CR1000. All these sensors have been integrated into the same meteorological tier 2 station data acquisition system. All the components are being powered by a battery connected to solar panel which is fixed in the station. Figure 1 shows portion of meteorological station established at UET Peshawar.

Table 1: Meteorological Stations installed at different location by World Bank in collaboration with AEDB Pakistan [9]

S. No.	Location
1	Quaid e Azam Solar Park, Bahawalpur
2	National University of Science and Technology (NUST), Islamabad
3	Kala Shah Kaku (KSK) Campus of UET Lahore, KSK
4	MNS Campus of UET Lahore, Multan
5	NED University, Karachi
6	Mehran University, Jamshoro
7	Balochistan University of Information Technology (BUITEMS), Quetta
8	Balochistan Univeristy of Engineering and Technology (BUET), Khuzdar


Figure 1: Portion of meteorological station at UET Peshawar

Data chosen for this research was taken from the tier 2 meteorological station established at UET Peshawar. Ground based measured data used in this study is for year 2017. Satellite based data has been taken from National Renewable Energy Laboratory NREL's National Solar Radiation Database (NSRDB). NRSDB provides solar resource data based on different models for different regions of the world. For South

Asia which includes Pakistan, NRSDB has developed a satellite based model, which it has named SUNY. SUNY has temporal resolution of 1 hour and spatial resolution of 10 x 10 km. SUNY provides data for Peshawar region from year 2000 to 2014.

In this study, data received for both GHI and DNI at the established station were analyzed for the year 2017. Satellite based DNI and GHI were taken from SUNY. For Peshawar, data of SUNY was downloaded from NREL's website [10]. These satellite based GHI and DNI were analyzed on the basis of monthly mean daily total averaged over 15 years (2000 to 2014). All values reported are in Wh/m2. A comparison between ground based and satellite based measurements for both GHI and DNI was made by plotting data against each month.

III. Results and Discussion

A. Analysis of ground based data

All values of DNI and GHI reported here are based on monthly mean daily total. Ground based measured data chosen for analysis is for year 2017. It can be seen from Figure 2 that maximum GHI is reported for the month of June which is 6,415 Wh/m^2. Similarly, Figure 2 shows minimum GHI for the month of December which is 1,605 Wh/m^2. On the other hand, Figure 3 shows maximum DNI recorded in the month of April which is 5,884 Wh/m^2 and lowest DNI noted in the month of January which is 1,718 Wh/m^2.

B. Comparison of ground based measurements with satellite based model SUNY

As discussed above, values reported here for ground based DNI and GHI are based on monthly mean daily total for year 2017. For SUNY model, values of DNI and GHI are based on monthly mean daily total averaged over 15 years period starting from 2000 and ending on 2014.

Figure 2 shows that for most of the months satellite based averaged GHI is greater compared to ground based measured GHI except for the months of February, March and April where GHI measured at UET Peshawar Station is more compared to Satellite based model SUNY. In February, March and April, ground based measurements report values 277 Wh/m2, 181 Wh/m2 and 366 Wh/m2 respectively higher than that of satellite based model SUNY.

Figure 3 shows the same trend for DNI. For most of the months, satellite based averaged DNI is higher compared to ground based measurements except for the month of February, March and April. In February, SUNY reports a value 794 Wh/m2 less than that of ground based measurements while for the months of March and April, SUNY shows values 140 Wh/m2 and 641 Wh/m2 lower than that of ground based measurements respectively.

In most of the months ground based DNI is underestimated compared to satellite based models. This could be due to varying aerosol optical depth (AOD) as aerosols are considered to be one of the main reasons for attenuation of solar irradiance through atmosphere. Optical properties of aerosols highly vary with time and space and may be the prime cause for extinction of DNI in our study.

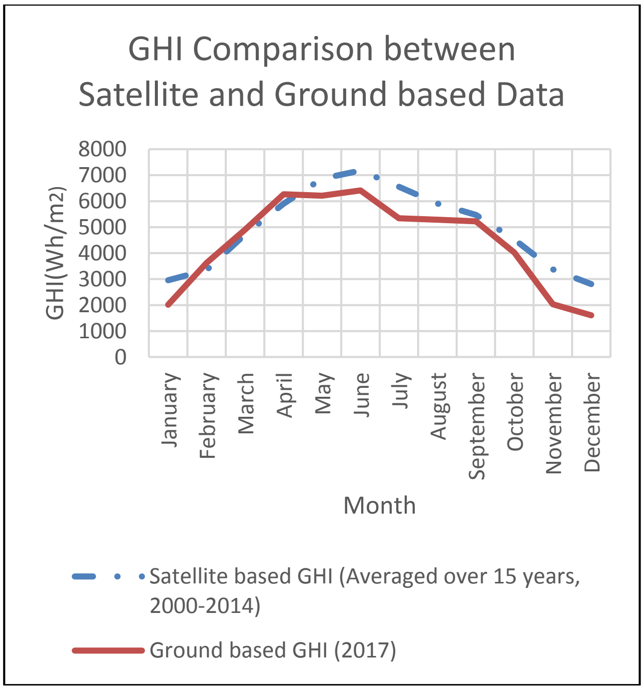

Figure 2: GHI Comparison

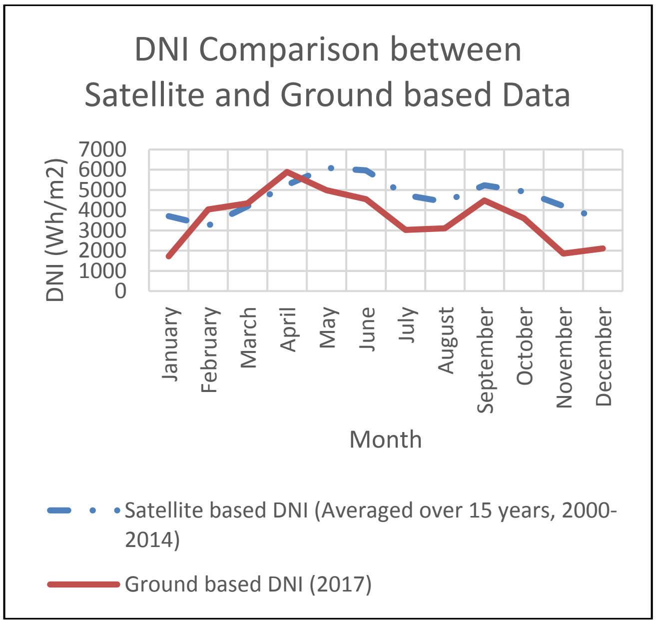

Figure 3: DNI Comparison

IV. Conclusion

This paper presents one of the first studies done on meteorological station of UET Peshawar. Station at UET Peshawar is fully functional and currently recording all weather parameters for which it was desired and established. Solar resource data collection is one of the core objectives of this station. In connection to that, this paper analyses DNI and GHI for year 2017. Highest GHI received at this station is 6,415 Wh/m2 which has been recorded in the month of June. Lowest

GHI recorded at this station is 1,605 Wh/m2 which has been reported for the month of December. Similarly, highest DNI recorded at this station is 5,884 Wh/m2 for the month of April while lowest DNI recorded is 1,718 Wh/m2 for the month of January. It can be easily concluded that maximum global irradiance received at this station is in month of June which is summer time in Peshawar. Minimum global irradiance received at this station is in month of December which is winter time in Peshawar.

Data comparison in the study is based on 15 years average estimated data of SUNY satellite based model (averaged data between year 2000 and 2014) and ground based measurements recorded in 2017 at meteorological station of UET Peshawar. The comparison of the data showed higher values of GHI and DNI for satellite based model SUNY when compared to ground based measurements except for the months of February, March and April where ground based measured values of GHI and DNI are higher compared to satellite based values of model SUNY. Maximum difference of 1,346 Wh/m2 in GHI is recorded in November and minimum difference of -181 Wh/m2 is noted in the month of March. Average difference of 556 Wh/m2 in GHI is observed between ground based measurements and satellite based model SUNY. On the other hand, maximum difference of 2,348 Wh/m2 is observed in November and a minimum difference of -140 Wh/m2 is seen in March. Average difference noted in DNI between ground based data and satellite based data is 983 Wh/m2.

It is perceived that results presented in this study will be fruitful for establishing any solar energy program, particularly establishing solar power plants in Peshawar. Ground based measurements will act as evidence for actual assessment of any solar energy program to carry out feasibility studies.

In future, same study can be done for other eight stations installed by World Bank and Alternative Energy Development Board (AEDB) Pakistan at different locations of Pakistan. This sort of study at other locations of Pakistan will provide ground based data which will be really helpful for feasibility studies to establish solar power plants in those locations.

ACKNOWLEDGMENT

The authors acknowledge Mr. Muhammad Qadeer and Mr. Fahim Ahmed from Alternative Energy Development Board (AEDB) Pakistan whose on time support and guidance made this study possible.

REFERENCES

[1] S. AlYahya and M. A. Irfan, "Analysis from the new solar radiation Atlas for Saudi Arabia," Solar Energy, vol. 130, pp. 116-127, 2016.

[2] A. F. Almarshoud, "Performance of solar resources in Saudi Arabia," Renewable and Sustainable Energy Reviews, vol. 66, pp. 694-701, 2016.

[3] S. G. Erica Zell, Stephen Wilcox, Suzan Katamoura, Thomas Stoffel, Husain Shibli, Jill Engel-Cox, Madi Al Subie, "Assessment of solar radiation resources in Saudia Arabia," Solar Energy, vol. 119, pp. 422-438, 2015.

[4] C. C. Rodrigo A.Escobar, Alan Pino, Enio Bueno Pereira, Fernando Ramos Martins, José Miguel Cardemil, "Solar energy resource assessment in Chile: Satellite estimation and ground station measurements," Renewable Energy, vol. 71, pp. 324-332, 2014.

[5] P. P. S. Janjai, J. Laksanaboonsong, "A model for calculating hourly global solar radiation from satellite data in the tropics," Applied Energy, vol. 86, pp. 1450-1457, 2009.

[6] (May 15). Where is Peshawar, Pakistan? Available: https://www.worldatlas.com/as/pk/kp/where-is-peshawar.html

[7] B. E. P. Blanc, N. Geuder, C. Gueymard, R. Meyerd, R. Pitz-Paal, B. Reinhardt, D. Renné, M. Sengupta, L. Wald, S. Wilbert, "Direct normal irradiance related definitions and applications: The circumsolar issue," Solar Energy, vol. 110, pp. 561-577, 2014.

[8] P. J. Yang Dazhi, Wilfred M.Walsh, "The Estimation of Clear Sky Global Horizontal Irradiance at the Equator," in Energy Procedia, 2012, pp. 141-148.

[9] (May 24). Solar Resource Mapping. Available: https://www.aedb.org/ae-technologies/solar-power/solar-resources

[10] (May 21). International Data. Available: https://nsrdb.nrel.gov/international-datasets

International Journal of Engineering Works
ISSN-p: 2521-2419
ISSN-e: 2409-2770
Vol. 6, Issue 09, PP. 292-299, September 2019
https://www.ijew.io/
https://doi.org/10.34259/ijew.19.609292299

Analysis of Heat Generation, Hardness Distribution and Tensile Strength of Friction Plug Welding

Preetam[1] & Yan Chongjing[2*]
[1,2] College of Mechanical and Electrical Engineering, Nanjing University of Aeronautics and Astronautics, Nanjing, China
preetamdhanja@gmail.com[1], yancj@nuaa.edu.cn[2]
Received: 17 August, Revised: 06 September, Accepted: 11 September

Abstract**—**The Friction plug welding (FPW), is a kind of process to join the two dissimilar/similar materials and no external heat is applied or no molten state involved. As no melting occurs, friction welding is not a kind of fusion welding process, but more than a counterfeit welding technique. The joint efficiency may be increased by interpolating heat source or pre-heating at the workpiece surface. The generation of heat flux at the mean surface is calculated by friction during the materials to consider the friction co-efficient. By changing the diameter of the plug, the land width can be changed to get an impact on the temperature profile. Mathematical and Analytical modeling has computed the impact of pre-heating. The temperature distribution values during the workpiece were computed for various plug diameters with various pre-heating temperature values from 250ºC-550ºC.

Keywords**—** Friction plug welding, Heat, Friction, Temperature.

I. Introduction

Friction welding is one of such machining processes where heat generation due to friction between the two parts which are being welded. This process is now being used throughout the world as a reliable and automated welding [1] process in industries.

Friction welding is a kind of joining process that generates adjustment of materials under compressive force contact of workpieces, which is rotating relative to each other to generate heat and plastically displace material from rubbing down surfaces do not melt. [2] Filter metal and flux are not needed with this procedure.

Friction Stir Welding, a solid-state procedure is being applied to weld aluminum alloys of a different kind that were arduous to weld. Because of re-solidification and non-melting of metal, distortion is less and welding is porousness free. A non-damperable, rotating tool is kept into the surface with the plates to be welded.[3] Tool movement in direction of welding surface [9], heat is generated and less than the solidus temperature; the welding joints are built up. When shoulder comes into contact with the surface of plates, the temperature increases due to the heat produced and the pin of the shoulder stirs in the joining surface allowing the flowing of the material backside of the pin. As the tool passes the metal cools and a processed zone is produced. A tool made of a harder material than the plates to be joined is used. Presently use of FSW process is used to join materials with high temperatures, as the harder tools are being developed.

The process of Friction plug welding (FWP), is a kind of welding in which initially faulty weld stuff is changed by the plug, that is friction welding into its original place. The basic principle is illustrated in figure 1.

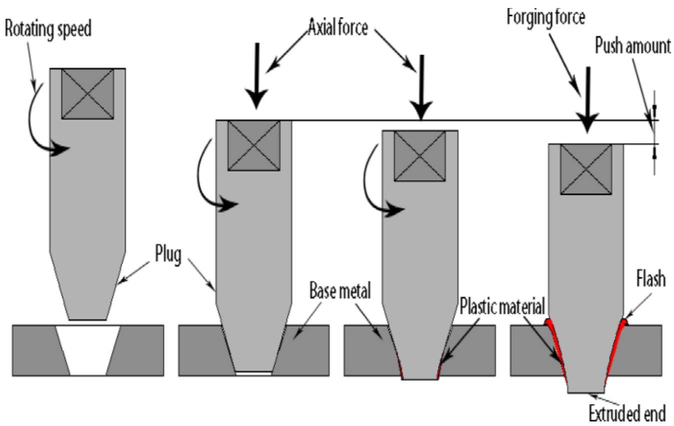

Figure 1: Schematic diagram of the FPW process

The FPW key process is as follows: first of all, a hole is produced into desired geometry parameters at the stand whence interested. Second, an expeditiously rotating plug is exerted into the hole underneath the action of axial force and interface between the hole and plug quick frictional heating and defacement, that is probably called the welding phase. Forthcoming, the plug rotation is suddenly stopped and a molding force is applied on weld surface when the hole is stuffy, hence create FPW weld. In the end, extract the plug and quern surface plain.

The FPW is used for repairing weld defects under the background of friction stir welding (FSW). As compared to other welding technologies, the FPW exhibits better performance to weld aluminum alloys. The defect can be repaired with better joint strength, low stress and smaller distortion. Friction plug welding (FPW) is a solid-state welding procedure by which a rounded plug is spinning, with a force applied, to fill the hole.

The use of a friction plug welding process is one of the proposed methods used to repair the defects that might occur during the friction stir welding process. Figure 2 shows a schematic view of the friction plug weld process.

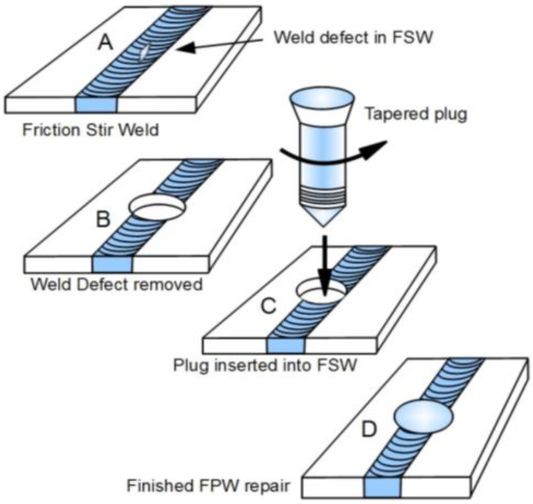

Figure 2: Friction plug weld process

The joining process begins when the moving part produces frictional heat at the bottom portion of the hole to permit plasticization. The 3-D finite element analysis was executed to perusal heat transfer and thermal phenomena of FSW of aluminum. Two welds, with very short pin and with long pin were checked out. The boundary condition for FSW is fixed and heat flux is calculated.[17]

Here in this work friction plug welding of aluminum alloy is pondered for mathematical modeling. on the basis of frictional heat, the generation of heat flux is calculated. The material pre-heating is changed in various ranges for getting the impact on temperature profile in the workpiece. Temperature distribution with various plug diameter is calculated using one-dimensional heat conduction.[18]

II. Literature Review

Friction stir welding (FSW) is a newly introduced process which provides better quality joints and also low cost. For any type of research work in this area, the most important phase is to get knowledge of already available literature.

Yong-Jai Kwon et al. [4] presented the friction stir welding among 5052 aluminum plates, having a thickness of 2 mm. The rotation speed of tool ranging from 500 to 3000 rpm with a constant stride speed of 100 mm/min. The tool rotation speed for Welded joints was 1000 to 3000 rpm. Onion ring structure was observed in the friction-stir-welded zone (SZ) At [500,1000,2000] rpm. On onion rings, the effect of tool rotation speed(TRS) was noticed. The grain size in the SZ is smaller than in base metal and is reduced with a decrease of the TRS. Observation showed that tensile strength, the strength of the joint is more than the parent metal. Observation also proved that the joint is not more ductile than the base alloy.

A study directed by G. CAO and S.KOU [5] was purposed at observing whether the boundary temperature in the workpiece can trigger liquation during friction stir welding (FSW) of Al alloys and limit lower bound of the melting temperature range which was seen in some computer simulations. AA 2219, an Aluminium-copper alloy was the workpiece material because of its certain lower bound of the melting temperature array whose eutectic temperature is 548°C. Besides friction stir welding (FSW), gas metal arc welding (GMAW) of Alloy 2219 was also introduced to give a stratum for checking liquation in FSW of Alloy 2219. Study under both scanning electron microscopy and optical shown and found that in GMAW of Alloy 2219, q (Al2Cu) particles featured as in-situ microsensors, which shows liquation due to reaction between Al and Cu forms eutectic particles when reaches eutectic temperature. No evidence of q-induced liquation was found in FSW suggesting that the eutectic temperature was not achieved.

J. Adamowski et al. [6] examined microstructural variations and mechanical properties in FSW in the AA 6082-T6 with changing process parameters. The tensile test of the welds was completed and the relationships among the process parameters were checked. Optical microscope observed the microstructure of the weld interface. Microhardness of resulting joint was also measured. Hardness reduction was observed in weld nugget and heat-affected zone (HAZ), test welds show resistance on the increment of welding speed in observation. Reason for this phenomenon was thermal asymmetry and kinetic of the friction stir welding process. At TMAZ and interface of weld nugget, the initial stage of the longitudinal, volumetric defect was found. Hardness was less to that of fusion welding (FW). In the nugget zone, wormhole (tunnel) defects were found.

H.J.LIU et al. [7] observed the friction welding characteristics of AA 2017-T351 sheet in which they have studied the microstructure of the weld joints and found that the relation between the parameters. The graphs were plotted between revolutionary strength and pitch, Vickers Hardness and distance from weld center, fracture location at the joints and revolutionary pitch. From tension tests and the hardness tests, it was deducted that FSW also decreases the tensile strength of the material and makes the material soft. The microscopic analysis indorses generations of fractures in joint at the interface between the thermodynamically affected zone and weld nugget.

M.Vural et al. [8] researched the FSW competency of EN AW 2024-0 and EN AW 5754-H22 Aluminium alloys. These Aluminium alloys are widely used in the industry. The experiment showed that the hardness value of EN AW 2024-0 at the weld area is increased about 10to40 Hv. This can be the outcome of compact grain structure formation and recrystallization. But the hardness of EN AW 5754-H22 decreased due to loose grain structure formation and recrystallization. Welding performance of EN AW 5754-H22 is 57% and for EN AW 2024-0 is 96.6. Welding performance of different Al alloys EN AW 2024-0 and EN AW 5754-H22 is reached to 66.39%. Scanning electron microscope showed no change in the microstructure in the welding zone in the analysis of the welding zone. At the weld zones, hardness distribution didn't show any relevant change in hardness.

III. Mathematical Modeling

FPW modeling can be done in many steps. The friction pressure and heat generation across the interface are considered uniform. [12]-[15] Some assumptions are incorporated in the model:

- The coefficient of friction is constant and heat is generated only by friction.
- The behavior of workpieces material has assumed perfect elastic-plastic.
- The heat loss due to radiation has been ignored, as plasticity was assumed.

A. Temperature distribution

Generation of Heat

The thermal modeling equation for friction welding procedure is mentioned as eq. (1)

$$K\left[\frac{\partial^2 T}{\partial x^2}+\frac{\partial^2 T}{\partial y^2}+\frac{\partial^2 T}{\partial z^2}\right]+G=\rho c\frac{\partial T}{\partial t} \qquad (1)$$

ρ, c, K is temperature-dependent, Friction welding process contains the heat generation by friction between two workpieces qf, and heating from irreversible plastic deformation of both workpieces qp.

Heat generation rate G is given as,

$$G = q_f + q_p \qquad (2)$$

In this study, it has been assumed that Friction law of Coulomb is followed for friction between workpieces; Generation of heat due to plastic deformation (qp) and due to friction (qf) and can be determined by equations 3 & 4,

$$q_f = 2\pi RN\mu F_n \qquad (3)$$

$$\eta\sigma\varepsilon \qquad (4)$$

For heat flux generation, the correlation between torque and heat energy is to be made. Heat production and the change of heat may be calculated by dimensions of parts and operating characteristics. By using machine torque, heat generation of friction can be calculated as below,

$$\tau$$

$$qf = \left(\frac{2\pi N\zeta}{60A}\right) * \eta \qquad (5)$$

Heat generation can also be determined using equation no 6,

$$q = U*A*\Delta T = U*A*(Tin-Tamp) \qquad (6)$$

Distance from the contact surface (T_L) is calculated by

$$\frac{TL-T\alpha}{Tb-T\alpha} = 1/\cosh(mL) \qquad (7)$$

Where At the nominal distance the temperature is T_L, T is denoted as ambient temperature and Tb is the temperature of the base plate. Tb can be determined by,

$$T_b = T_p + T_f \qquad (8)$$

Where Tp is defined as the Pre-heat temperature and Tf is temperature due to friction, produced by the generation of heat

$$m = \sqrt{\frac{hp}{KA}} \qquad (9)$$

The temperature at a distant place from the contact surface is determined,

$$\frac{T-T_a}{T_b-T_a} = e^{-mx} \qquad (10)$$

Where,
T is denoted as temperature distribution,
$T\alpha$ = ambient temperature,
T_b = baseplate temperature,
x = distance of contact surface.

On the basis of heat conduction (HC) equations, as explained above, heat flux can be determined. The variation of temperature distribution can be studied by varying the temperature, preheating, and distance of workpiece and contact area. The plug diameter depends upon land width.

B. Hardness distribution

With the Hardness tests, the measurement of resistance of the material to indentation is done. Strength of the material is indicated by its hardness. In the test, indenter made of a harder material than test material is pressed with force on the surface of the tested material. After that, the indentation is determined. The hardness of the material is inversely proportional to the indentation area. There are different-different types of hardness tests in which Rockwell, Brinell, and Vickers are the common tests. Vickers tests were used to study the hardness of both the welds and base material in the course of this work. A diamond pyramid indenter is used by Vickers hardness test, which produces a pyramidal indentation.

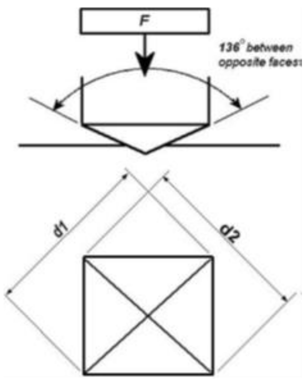

Figure 3: Vickers Hardness Test

The hardness is determined after the measurement of indentation:

$$VHN = 1.72 * \frac{F}{d1*d2} \quad (11)$$

Where 'VHN' is denoted as Vickers Hardness Number, 'F' is the force of indentation and d1, d2 is the distances of opposite corners of the indentation.

In Vickers hardness test method indenter is of the diamond which indents the test material, in the form of a right pyramid with the angle of 136 degrees between two opposite face subordinated a load of 1- 100 kg and a square base. For 10-15 seconds, full load is normally applied. The two diagonals of the indentation remained in the surface of the material on the removal of the load are measured using a microscope and they're average determined. The sloping surface area of the indentation is calculated. Vickers hardness is the quotient found after the division of the kgf load by the square mm area of indentation. From the calculation of force-area ratio using the area of diamond indents in the base material, the hardness number is determined. Three surfaces were tested for every material; the longitudinal surface, the transversal surface, and the top surface. Clamping area of conventional bus bar ends is thinner and flattened than extruded part of the bus bar. So, both the flattened and the extruded parts had their hardness investigated. A number of tests can be made for every sample and the indentations made so that they form a square as given in figure 3.

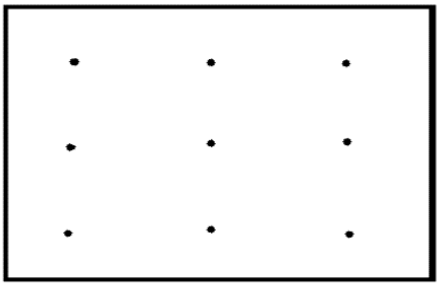

Figure 4: Hardness indentations for base materials

The hardness profile of FPW joint can be measured in three layers i.e. lower layer, the upper layer, and middle layer. The shape of the hardness profile would be in W-shape and the hardness of FPW joint depends upon microstructure and phases in different zones.

The hardness distribution on aluminum joints (AA5A06) is varied slightly for all the welding parameters. The maximum hardness appeared near the NZ and TMAZ. The reason for this AA5A06 joints is a non-heat treatable alloy, and therefore the temperature variation does not significantly affect the hardness. Near the NZ and TMAZ, the hardness was partially improved due to the refinement of the grains as a result of stirring action.

C. Tensile properties

The ability of a material to bear the loads tend to elongate is known as Tensile strength. Tensile strength(TS) resists tension(being pulled apart), while compressive strength resists compression(being pushed together). The ultimate tensile strength(UTS) is measured by the maximum stress that a material can undergo while being stretched or pulled before breaking. Some materials break very quickly, without the plastic deformation, which is defined as a brittle failure. Other materials, which are very ductile, including most of the metals, show some plastic deformation and possibly necking before the fracture.UTS is generally found by performing a tensile test and recording the engineering stress versus strain(S-S). UTS is the maximum point of the stress-strain(S-S)curve. This property is called intensive property; therefore the value of UTS does not depend on the size of the test specimen. It depends on other factors, such as preparation of the specimen the temperature of the test environment and material and the presence or otherwise of surface defects. Tensile strengths(TS) are generally not used in the design of ductile member but have importance in brittle members. It is known as stress, which is defined as force per unit area. Many materials shows linear elastic behavior, defined by a linear stress-strain relationship as in figure 4.Elastic nature of materials generally extends into non-linear region, represented up to which deformations are perfectly recoverable on removing the load; means, in tension a specimen loaded elastically will elongate, but it will return to its original shape and size when it is unloaded. Above this elastic region, for ductile materials, such as steel, deformations are totally plastic. While a plastically deformed specimen does not perfectly regain its original size and shape when it is unloaded.

Ductile metals pass a period of strain hardening after yield, in which value of stress increases again with an increase of the strain, and begin to neck, as the cross-sectional area of the specimen decreases due to plastic flow. In the sufficiently ductile material, if necking gets substantial, causes a reversal of the engineering stress-strain(S-S) curve (figure 5); this is due to the engineering stress is determined to take the original cross-sectional area before necking. Reversal point is the maximum stress on the engineering S-S curve, and the engineering stress coordinate of this point is the ultimate tensile strength(UTS), shown by point 1.

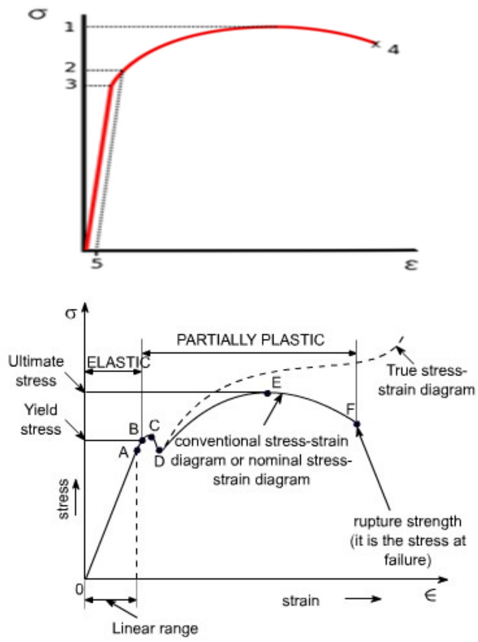

Figure 5: (a) & (b): Stress-Strain Curve

The points details of the curve are given below,

1 → Indicate the Ultimate Tensile Strength (UTS)
2 →Yield Strength
3 →Proportional Limit Stress
4 →Fracture
5 →Offset Strain

Yield strength(σy) is the point where plastic deformation gets a start. It is hard to specify correctly. But conventionally it is denoted as the intersection of the curve with a parallel straight line to elastic part of the curve offset 0.2% on x-axis. The yield strength is also defined as the stress needed to deform material by 0.2% permanently Slope of elastic part of the curve is known as modulus of elasticity, E. Tensile strength(TS) or Ultimate tensile strength(UTS), is the maximum stress achieved during a test. When the material starts to reach that point, the fractured cross-sectional area experiences reduction. This is the reason why the original area of the sample can't be used to model the true stress(σT) given below

$$\sigma T = \frac{P}{A\ actual} \qquad (11)$$

For most of the metals approximation of the true stress is possible - true strain (ϵT) curve between yield stress(YS) and ultimate tensile stress(UTS) by the equations shown below,

$$\sigma T = K * \in_T^n \qquad (12)$$

Where n and K are constant whose value change for every material.

From the tensile test, ending value acquired is the toughness of the material. Toughness represents ductility and combination of strength and is the ability of a material to bear mechanical energy up to failure point. Its value is equal to the area contained under the stress-strain curve and numerically given as,

$$U_T = \int_0^{\in f} \sigma * d \in \qquad (13)$$

Where ϵf strain upon failure and U_T is toughness.

Tensile testing is used to calculate the maximum load (tensile strength), the material can withstand without failure. The load value or elongation value is the basis of the tensile test.

The stress-strain graph and fracture position of FPW sample welded at different conditions can be determined. The maximum ultimate tensile strength (UTS) [15] is contained by FPW joint and elongation of its value equivalent to that of base metal. There are many regions to find the minimum hardness and maximum hardness. The loss for welded joint ultimate tensile strength and elongation is considered as the disintegration of precipitates and distribution of ingredient particles.

Developing Mathematical Model

The response function tensile strength (TS) of the joints is a function of tool profile (P), rotational speed (N), welding speed (S) and axial force (F), and it can be expressed as,

$$TS = \oint(P, N, S, F) \qquad (14)$$

The second-order polynomial (regression) equation used to represent the response surface 'Y' is given by,

$$Y = b_0 + \sum b_i x_i + \sum b_{ii} x_i^2 + \sum b_{ij} x_i x_j \qquad (15)$$

and for four factors, the selected polynomial could be expressed as

$$TS = b_0 + b_1(P) + b_2(N) + b_3(S) + b_4(F) + b_{11}(P^2) + b_{22}(N^2) + b_{33}(S^2) + b_{44}(F^2) + b_{12}(PN) + b_{13}(PS) + b_{14}(PF) + b_{23}(NS) + b_{24}(NF) + b_{34}(SF) \qquad (16)$$

Where b_0 is the average of all responses and $b_1, b_2, \ldots b_{23}$ are coefficients which depend on interaction effects and respective main of the parameters. Values of the coefficients have been determined using the given below expressions (rf13)

$$b_0 = 0.142857 * \left(\sum Y\right) - 0.035714 * \sum\sum X_{ii} Y$$

$$b_i = 0.041667 * \left(\sum X_i Y\right)$$

$$b_{ii} = 0.03125 * \left(\sum X_{ii} Y\right) + 0{:}00372 * \sum\sum X_{ii} Y - 0.035714 * \left(\sum Y\right)$$

$$b_{ij} = 0.0625 * \left(\sum X_{ij} Y\right)$$

Every coefficient was tested at 95% confidence level (CL) [16] for their significance by applying students t-test with the use of statistical software package (SPSS). After calculating the significant coefficients, the relations were formed only using these coefficients. To predict the tensile strength of FPW joints the last mathematical relationship is formed between the FPW variables, developed by statistical design of experiments procedure are given below:

$$TS = \{240.86 + 6.71(P) + 4.38(N) + 9.29(S) + 5.96(F)$$
$$-14.66(P^2) - 8.17(N^2) - 10.54(S^2) - 13.79(F^2)$$
$$-1.68(PS) - 1.44(PF) - 2.19(SF)\} \ MPa$$

<u>Advantages:</u>-

- Strength is high
- Having good mechanical properties
- Heat input is low
- Quick process time
- Low cast

IV. SIMULATION RESULTS

The work is based on the study, analysis, and simulation. I will purchase the MATLAB software to install in my system. After studying many research articles about friction plug welding, I will implement the complete system in MATLAB software. I will develop a MATLAB model for heat generation analysis, Hardness distribution, and Tensile strength. The different types of simulation results will be analyzed to test the FPW.

A. *Temperature distribution*

For analysis of temperature distribution, parameters like contact area, preheating temperature, and distance from workpiece are changed.

By changing the plug diameter, the land width is changed. The various graphs are displayed for temperature and workpiece distance. It can be seen that temperature is linearly decreasing, on decreasing land width.

As shown in figure 6, 7, 8 and 9, various pre-heating temperature values like 300ºC, 400ºC, 500ºC, and 600ºC are displayed.

In figure 10 and 11, Temperature distribution vs displacement from contact surface with 16.0 mm and 4.0 mm land width is shown. It has been observed that temperature distribution is gradually decreasing with respect to the workpiece through its center point.

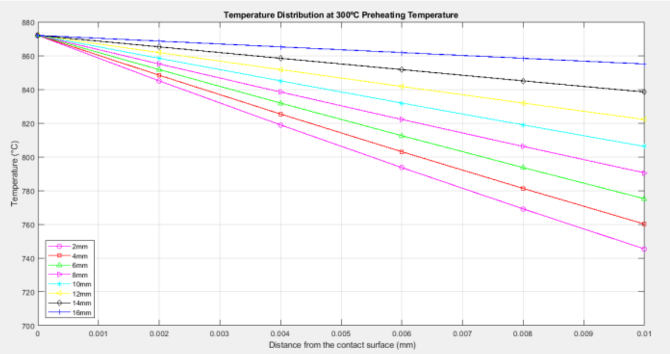

Figure 6: Temperature distribution at 300˚C preheating temperature

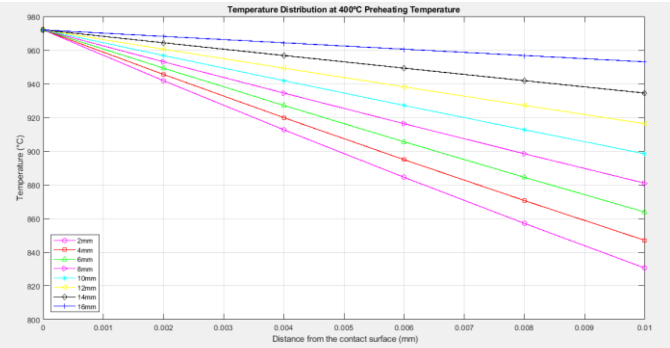

Figure 7: Temperature distribution at 400˚C preheating temperature

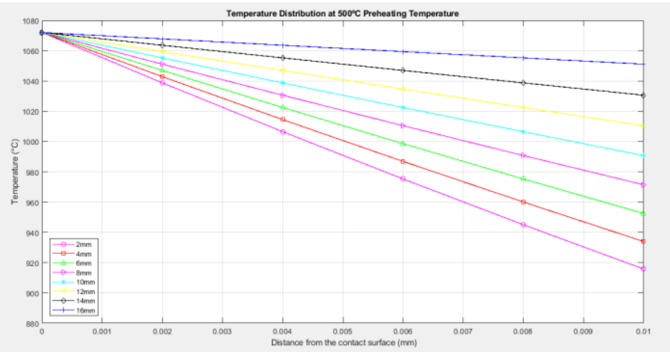

Figure 8: Temperature distribution at 500˚C preheating temperature

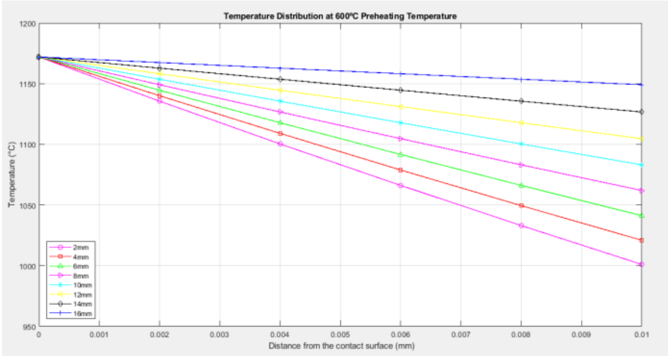

Figure 9: Temperature distribution at 600˚C preheating temperature

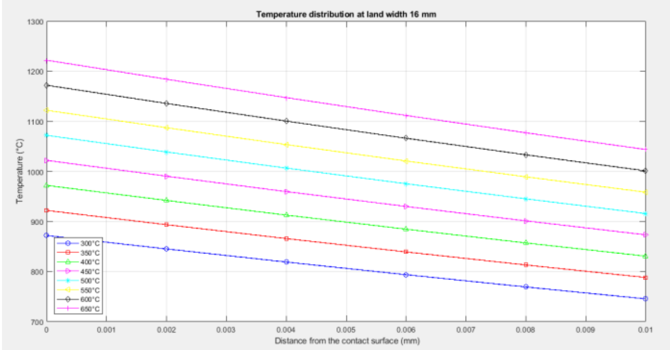

Figure 10: Temperature distribution at land width 16.0 mm

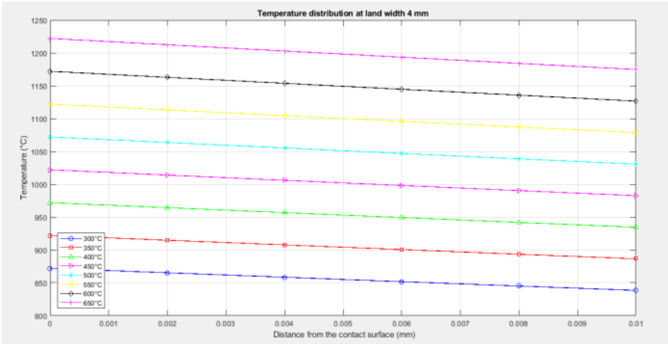

Figure 11: Temperature distribution at land width 4.0 mm

B. Hardness Distribution analysis

As shown in figure 6, the Vicker's hardness profile of the welding process is presented. The hardness of the TMAZ, HAZ, and HZ parent material region was computed. The hardness of the central zone was gradually less than the peripheral zone, and the hardness of the parent material was the lowest. The maximum value of hardness is at the central zone, shown in the TMAZ.

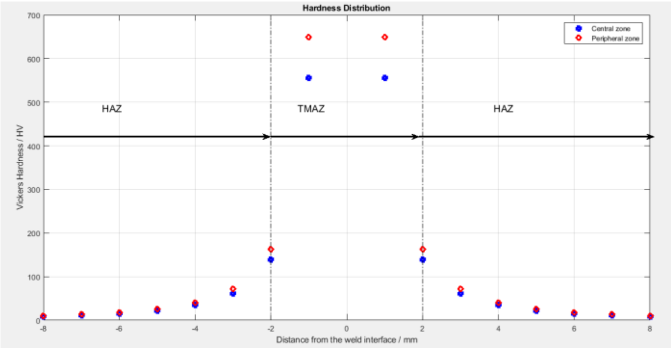

Figure 12: Hardness Distribution

C. Ultimate Tensile Strength (UTS) of Friction Plug Welding

As shown in figure 13, 14 and 15 graphs, used to understand the impact of FPW parameters on tensile strength like tool rotational speed, axial force, and welding speed.

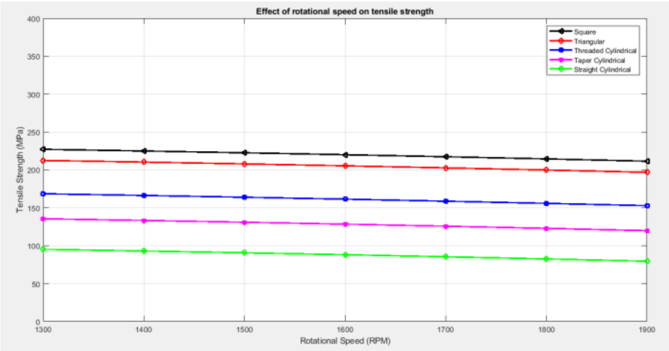

Figure 13: Effect of rotational speed on tensile strength

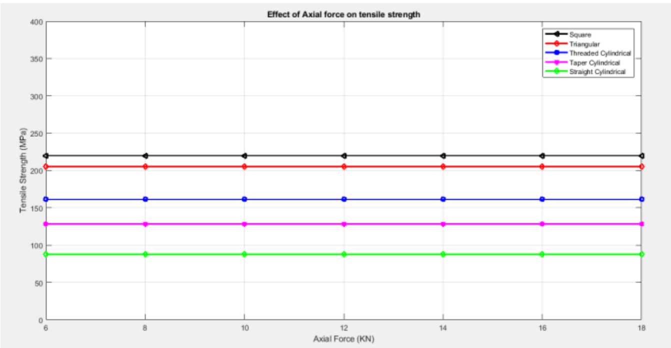

Figure 14: Effect of Axial force on tensile strength

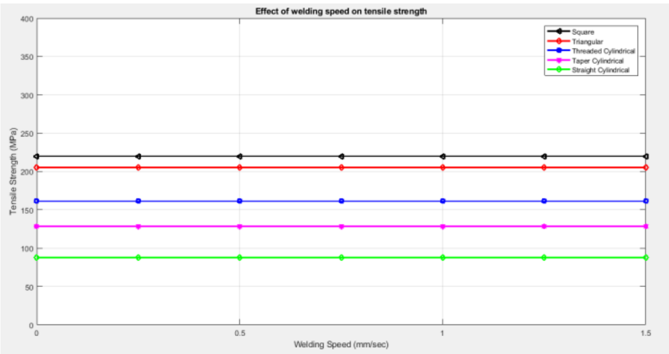

Figure 15: Effect of Welding Speed on tensile strength

CONCLUSION

A mathematical relation is formulated to get the tensile strength of friction stir welding joints by being inclusive welding parameters as well as tool profiles with the use of statistic tools like regression and experiments design. The heat flux is calculated because of friction during the materials for considering the coefficient of friction. Analytical model computed the impact of pre-heating. The temperature distribution in workpiece was computed for various plug diameters with various values of pre-heating temperature ranging 250ºC-550ºC.

REFERENCES

[1] Yong-Jai Kwon, Seong-Beom Shim, Dong-Hwan Park, Friction stir welding of 5052 aluminum alloy plates, Trans. Nonferrous Met. Soc. China 19(2009) s23−s27.

[2] G.Cao, S.Kou, friction stir welding of 2219 aluminum: the behavior of theta (Al2Cu) particles, The Welding Journal, January 2005.

[3] J. Adamowski , C. Gambaro, E. Lertora, M. Ponte, M. Szkodo, analysis of FSW welds made of Aluminium alloy AW 6082-T6, Archives of Materials Science and Engineering, Volume 28,Issue 8,August 2007.

[4] H. J. LIU, H. FUJII, K. NOGI, Friction stir welding characteristics of 2017-T351 aluminum alloy sheet, JOURNAL OF MATERIALS SCIENCE 40 (2005) 3297 – 3299.

[5] M. Vural, A. Ogur, G. Cam, C. Ozarpa, On the friction stir welding of Aluminium alloys EN AW 2024-0 and EN AW 5754-H22, Archives of Materials Science and Engineering, Volume 28,Issue 1,January 2007.

[6] R. Nandan,T. DebRoy,H.K.D.H.Bhadeshia;Recent Advances in Friction Stir Welding – Process, Weldment Structure and Properties, Progress in Materials Science 53 (2008) 980-1023.

[7] D. M. Rodrigues, C. Leita˜o, R. Louro, H. Gouveia and A. Loureiro, High speed friction stir welding of Aluminium alloys, Science and Technology of Welding and Joining, 2010.

[8] Adler, Yu, P, Markov, E & Granovsky, YV 1975, The Design of Experiments to Find Optimal Conditions, 1st edition. Moscow, Mir publishers.

[9] Hattingh D, Doubell P, Newby M, Wedderburn I, Steuwer A and James M (2009) Friction taper stud welding of creep resistant 10CrMo910 steel, TMS, Annual Meeting & Exhibition; Friction Stir Welding and Processing-V, San Francisco, California, pp 75-84.

[10] P. Hartley, Friction plug weld repair for the space shuttle external tank, NASA document ID 20000093962, Johnson Space Center, Marshall Space Flight Center, 2000.

[11] Xuefeng Lei, Ying Deng, Zhimin Yin, nd Guofu Xu.Tungsten inert gas and friction stir welding characteristics of 4-mm-Thick 2219-T87 plates at room temperature and −196 °C 23, ASM International (2014), pp. 2149-2158.

[12] Dongun Kim, Harsha Badarinarayan, Ill Ryu1, Ji Hoon Kim, Chongmin Kim, Kazutaka Okamoto, R. H. Wagoner, Kwansoo Chung(2009), Numerical simulation of friction stir welding process, Int J Mater Form, Vol.2, pp 383-386

[13] Rosenthal, D. (1941), Mathematical theory of heat distribution during welding and cut-ting, Welding Journal20 (5), pp. 220-234.

[14] Riki Takeshita, Terry L., Kenner, Friction Plug Welding. United States Patent, Patent No:US6213379 BI, April 10, 2001.

[15] Yuh J. Chao, Shu Liu and Chi-Hui Chien (2008) friction stir welding of al 6061-t6 thick plates: part ii – numerical modeling of the thermal and heat transfer phenomena Journal of the Chinese Institute of Engineers., Vol 31, pp 769-779

[16] N. Rajesh Jesudoss Hynes, P. Nagaraj and J. Angela Jennifa Sujana, Investigation on Joining of Aluminum and Mild Steel by Friction Stud Welding, Materials and Manufacturing Processes. 27 (2012) 1409-1413.

[17] N. Rajesh Jesudoss Hynes, P. Nagaraj, R. Palanichamy, C. A. K. Arumugham and J. Angela Jennifa Sujana, Numerical Simulation of Heat

Flow in Friction Stud Welding of Dissimilar Metals, Arabian Journal for Science and Engineering, DOI 10.1007/s13369-013-0932-3.

[18] N. Rajesh Jesudoss Hynes, P. Nagaraj and J. Angela Jennifa Sujana, Mechanical Evaluation and Microstructure of Friction Stud Welded Aluminium–Mild steel Joints, Arabian Journal for Science and Engineering, DOI 10.1007/s13369-014-1082-y.

[19] N. Rajesh Jesudoss Hynes, P. Nagaraj and R. Meby Selvaraj, Finite element based thermal modelling of friction welding of dissimilar materials, International Journal of Modern Physics. 22 (2013) 196–202.

[20] N. Rajesh Jesudoss Hynes, P. Nagaraj and S. Joshua Basil, Numerical simulation on joining of ceramics with metal by friction welding technique, International Journal of Modern Physics. 22 (2013) 190–195.

国际工程期刊
International Journal of Engineering Works
انجینئرنگ کاموں کا بین الاقوامی جرنل

International Journal of Engineering Works
ISSN-p: 2521-2419
ISSN-e: 2409-2770
Vol. 6, Issue 09, PP. 300-304, September 2019
https://www.ijew.io/
https://doi.org/10.34259/ijew.19.609300304

Evaluating the Effect of Different Burning Techniques on the Chemical Composition of RHA from Different Region of Pakistan

Muhammad Fahad Ullah[1], Sheraz Abbas[2], Faizullah Jan[3], Zeeshan Khan[4], Muhammad Khubaib[5]
[1,3]Department of Civil Engineering, University of Engineering and Technology, Peshawar, Pakistan
[2,4,5]Civil Engineering Department, City University of Science and Information Technology, Peshawar, Pakistan
engr.fuzi@gmail.com[1]
Received: 31 August, Revised: 11 September, Accepted: 13 September

Abstract— After maize and sugar cane, rice was ranked as third position as a horticultural commodity. At global level, majority of Asian countries produce and consume the rice. Disposing of rice husk is a big problem and needs attention. In the present study, three different techniques were compared for converting rice husk (RH) into rice husk ash (RHA). The RHA obtained by combustion in drum for 24 hours yielded maximum quantity 97.703 % of SiO2. Therefore, this method was adopted for further studies on samples collected from different regions (Charsada, Swat and Buner) of Province of Khyber Pakhtunkhwa (KPK), Pakistan. By comparing the contents of SiO2 obtained from combustion technique, the Charsada sample containing 97.073% of SiO2 was found best.

Keywords— Rice husk ash, Silica, Waste, SCM, XRF.

I. Introduction

Rice is cultivated in all countries covering about 1% of the world and provides primary food item for world population. It achieves 2nd position regarding its production as well as covering the area [1]. The rice husk (RH), an agro-waste material and having low nutrients, when burnt under controlled temperature, produces amorphous silica content and particles of large surface areas. The use of rice husk ash (RHA) as a supplementary cementitious material has gained significance in construction industry especially in the countries of high rice production like Pakistan [2].

Pakistan is one of the largest agricultural production countries. Rice is considered as one of the major Kharif crops of Pakistan. Further, it is one of the significant export items of the country, sharing 1.40% in Gross Domestic Product (GDP) in the Pakistan National Economy. In Pakistan rice is cultivated on 2.883 million hectors area and annual production of rice is 6.883 million tones [3]. Rice is mainly considered as one of the cash crops of Pakistan. Each year, Pakistan yields about 1.2 million tons of rice husk [4]. Pakistan is ranked 4th largest at international level and contributes about 30% of world rice production.

The annual production of rice in the province of Khyber Pakhtunkhwa (KPK) province is about 125,000 tons and rice husk of approximately 25 thousand tons attained normally [5]. Rice husk production in KPK and selected locations is given in Table 1.

TABLE 1: RICE HUSK PRODUCTION IN KPK FOR (2015-2016)

Year	2015-2016				
Location	Area (Hectare)	Production (Tonnes)	Area (Hectare)	Production (Tonnes)	Production of Rice Husk in Tonnes
KPK	44442	95948	53932	125312	2324
Buner	214	503	346	686	1983
Charsada	114	273	121	276	2281

Large quantity of RHA is obtained after burning process on RH, which is just used as a fertilizer in limited range so disposing of it is additionally a big problem and needs attention. As from the literature survey it is cleared that after burning of Rice Husk in controlled temperature yields Rice husk Ash having pozzolanic property. After further chemical procedure Silica fume can be extracted from RHA and used as a partial replacement of cement and enhances its properties as well as bring reduction in emission of CO2 caused due to manufacturing of cement. Combustion of Rich husk followed by chemical procedure obtaining Silica Fume and its replacement with cement will enhance the quality of cement.

Rice Husk (RH) is an agro-waste obtained in a rice milling process. Rice husk ash (RHA) is long been famous to have pozzolanic property. Most of the agricultural and rice importing countries produce rice husk as waste in large quantity that makes rice husk ash the most deserving candidate to be used as supplementary cementing materials (SCM) [6]. The annual production of rice was recorded about 6 million tons [4]. Based on research, it was concluded that approximately 20 percent of rice paddy was husk, it indicates that Pakistan has produced 1.2 million RHA. Rice yields large amount of agro wastes. Rice husk (RH) are agro wastes produced from rice mills [7]. RHA was produced from RH if burnt under controlled temperature. Researchers claimed that RHA contains majorly high silica content in its composition approximately 80-90% and construction industry used it as a replacement of cementitious materials to enhance mechanical properties. RHA composed of silica and carbon in addition some other constituents also present in small quantity [7-8]. RHA was used as a pozzolanas which when react with Ca (OH) 2 in the existence of water form materials having cementitious properties and use of RHA as a pozzolanas which reduce the cost and make environment friendly [9].

RHA has three types amorphous, partially crystalline and crystalline, however from the research it was concluded that the pozzolanic activity, mechanical properties and durability of amorphous RHA were superior to partially crystalline and crystalline RHA [10]. The RH was used as a fuel for drying of rice. The burning of RH in air formed rice husk ash containing silica and carbon with inorganic impurities [11]. The uncontrolled combustion lead to the formation of crystalline RHA which processes low pozzolanic characteristics. The commercially available RHA contain 3 % of carbon and restrict their use in architectural purposes due to dark pigmentation. [12]. RHA if burnt under control temperature will yield maximum silicon dioxide SiO2 that can be used as replacement of cement giving more compressive strength [6]. The occurrence of un-burnt carbon in RHA has negative effect on pozzolanic reactivity. The burnt temperature, incineration, ample oxygen was important parameter regarding influencing the reactivity of RHA [9]. 95% silica content powder can be obtained through incineration with heat at 700 oC for 6 hours [11]. After treatment with different temperatures ranging from 300 oC to 1000 oC, the best result in terms of silica is 750 0C which enhances compressive strength compared to others [6].

The requirement of minimizing the content of carbon evolved during the cement manufacture attracts the researchers to work on the usage of industrial by-products to be utilized as a SCM. During the manufacturing of cement one ton net production of cement yields normally about one ton of CO2. Research on the use of RHA as agro waste RHA was conducted earlier. At a temperature of 500–600 oC incineration of RH yields amorphous SiO2. While, at a temperature of 800 oC, Cristobalite was observed in the ash at increase temperature of 1150 0C, tridymite as well as huge amount of cristobalite was also seen in the ash [2].

Approximately 90 percent of the rice is formed and consumed by Western and Eastern Asia. Amongst them, Pakistan is also a part of them and is sharing maximum proportion of the rice. In 2009, Pakistan annually produced 9.5 million tons of RHA out of which 0.53 million tons of paddy was produced [13]. So, if that is effectively utilized cement industry will get rid of CO2 by decreasing its outflow. On other hand it would play important and vital role in reducing the environmental in addition to land pollution. Accordingly, using RHA as a replacement of cement in making of concrete will mark an agro-waste one of the valuable materials. Evaluating RHA cementitious property and its utilization in the low budget housing structures by Ordinary Portland Cement (OPC) replacement by some proportions in concrete one would take good advantage of RHA, disposed off, as an agro waste. By this means enhancing rural economy in addition to it also increases chances of employment [14].

Keeping in view the burning of issue of agro-waste ad importance of RHA in the cement industry, the present research was conducted.

II. METHODOLOGY

The different stages involved in the research methodology are outlined below:

2.1. Rice husk (RH) samples collection

This research was focused on the classification and assessment of RHA collected from different sources i.e. Charsada, Buner and Swat areas of Province of Khyber Pakhtunkhwa. Collection of RH samples is shown in Figure 1.

Figure 1. Rice husk (RH) collection from different location of KPK

2.2. Facilities for Tests

Experimental work was conducted at Pakistan Council of Scientific and Industrial Research (PCSIR), Laboratories Complex, Jamrud Road, Peshawar, Pakistan while analyses and various tests were performed at Central Resource Labs (CRL), Department of Physics, University of Peshawar, Pakistan.

2.3. Conversion of RH into RHA

Rice husk ash (RHA) was generated using three different methods to evaluate maximum SiO2 at Pakistan Council of Scientific and Industrial Research, Peshawar. RHA specimens were then analyzed for chemical composition by applying X-Ray Fluorescence (XRF) at Central Resource Laboratories, Department of Physics, University of Peshawar.

It was found that the chemical profile of the rice husk ash was varying which was highly depended on the geographical as well as climatic conditions of the rice crop, therefore, specimens of RH (rice husk) from Province of Khyber Pakhtunkhwa (KPK) in the areas of Charsada, Buner and swat were collected as shown in Figure 1.

The rice husk obtained from Khyber Pakhtunkhwa (KPK) Province was firstly burnt under controlled condition. The process of burning was conducted in the PCSIR Complex Labs, Peshawar using the blast furnace. Upon burning, as the changes in the chemical composition of the RHA depends at the degree of applied temperature and different time duration, therefore, following three different methods for burning were used to check the impact of mentioned factors in addition to the geographical as well as climatic conditions:

(a) Method A: Burning of rice husk at 700 oC for 5 hours (sample kept in furnace from the start 0 oC).

(b) Method B: Burning of rice husk at 700 oC for 5 hours (sample kept in furnace when temperature reaches 700 oC).

(c) Method C: Burning of rice husk by combustion process for 24 hours in control environment.

RH samples were kept in the blast furnace made of refractory bricks. Incineration technique adopted for method (A) Sample was kept in the blast furnace made of refractory bricks from the start and temperature was raised to 700oC was fixed and kept this temperature for 5 hours, Though in the 2nd method (B), Sample was kept after temperature reached to 700 oC and was maintained for 5 hours, in the method (C) Sample was kept in Ferro-cement furnace for 24 hours Figure 3 2. After the incineration was completed, the ash was turned cool gradually and the ash was left in furnace. After burning of rice husk, approximately 22% of the ash was collected as ash. When RHA was cooled, then the sample was packed in the polythene bags for further investigations. Methods are shown in Figure 2.

(a)

(b)

(c)

Figure 2. Burning of RH to RHA by (a) Method A (b) Method B (c) Method C

2.4. X-ray Florescence (XRF) Analysis

The ash obtained were analyzed for SiO_2 contents using XRF, installed in Central Resource Labs (CRL), University of Peshawar. After the incineration process the RHA Samples were present in fine powder form. Each sample with a mass of 10-15 g was placed in polythene packets for analysis.

III. Results and discussion

Tremendous quantity of rice husk ash (RHA) has been obtained after incineration process that is just used as a fertilizer in limited range so disposing of it is additionally a big problem and needs attention.

This section explains the results of all performed laboratory test including XRF analyses of the collected rice husk (RH) samples of different sites locations of the Pakistan's Province of Khyber Pakhtunkhwa (KP) and obtained from three selected methods of incineration.

A. XRF results

The XRF (X-ray Fluorescence spectroscopy) test was performed on Rice Husk Ash samples obtained from various sites of Charsada, Bunair and Swat Khyber Pakhtunkhwa (KP) province of Pakistan for determining the oxide profile in the CRL (Centralized Resource Laboratories) situated in the University of Peshawar. The analyses were conducted using TEM Model (JEM2100), Oxford Instruments, United Kingdom, for obtaining the composition of all the major desired oxides in the RHA sample. The finding was applied for the samples obtained from three methods of burning i.e. (A) Burning of RH at temperature, 700oC for 5 hrs (sample kept in furnace from the start 0oC (B) Burning of RH at 700oC for 5 hrs (sample kept in furnace when temperature reaches 700oC) (C) Burning of Rice Husk (RH) by Combustion process for 24 hrs in control environment. It is observed that contents of SiO_2 was recorded in the range of 95.40 to 97.073. It was found that RHA obtained from method C yields maximum amount of SiO_2.Tables 2 shows RHA major oxides content produced by Methods A, B and C respectively for the same sample by using different processes.

TABLE 2: OXIDE COMPOSITION OF RHA USING DIFFERENT COMBUSTION METHODS

Oxide Composition	Method A	Method B	Method C
SiO2	95.400	96.530	97.073
CaO	2.202	1.305	1.033
K2O	1.350	1.245	1.159
Fe2O3	0.589	0.439	0.399
SO3	0.237	0.327	0.206
MnO	0.071	0.067	0.061
TiO2	0.069	0.040	0.032
CuO	0.034	0.020	0.0013
ZnO	0.019	0.015	0.011
SrO	0.011	0.007	0.006
Rb2O	0.003	0.003	0.003
ZrO2	0.002	0.001	0.001

Method C was then further used for combustion of RHA obtained from different regions (Charsada, Swat and Buner) of Khyber Pakhtunkhwa, Pakistan. Table 3 shows the XRF results of the samples and it was clearly indicating that Sample obtained from Charsada yields maximum amount of SiO2.

TABLE 3: THE RHA PERCENTAGE COMPOSITION FROM CHARSADDA, BUNER AND SWAT USING METHOD C.

Oxide Composition	Charsadda	Buner	Swat
SiO2	97.073	95.400	95.018
CaO	1.033	2.202	1.666
K2O	1.159	1.350	1.554
Fe2O3	0.399	0.589	1.262
SO3	0.206	0.237	0.323
MnO	0.061	0.071	0.072
TiO2	0.032	0.069	0.061
CuO	0.0013	0.034	0.014
ZnO	0.011	0.019	0.016
SrO	0.006	0.011	0.007
Rb2O	0.003	0.003	0.003
ZrO2	0.001	0.002	0.002

CONCLUSIONS

The main conclusions drawn from the present experimental work include

(a) Based on categorization and evaluation of RHA and comparing the contents of SiO2 from different areas i.e. Charsada, Buner and swat of KPK, the Charsada sample was found best

(b) By applying three different methods for incineration of Rice Husk to RHA to evaluate maximum SiO2, combustion process for 24 hours in control environment (Method C) gave maximum yield of silica.

RECOMMENDATIONS

Based on experimental work following recommendations were drawn for industry:

- In order to get ash of best quality, advanced furnaces and incinerators are required for burning as well as grinding of rice husk.
- Pilot and commercial scale facilities may be established to burn RH into RHA in bulk amount.
- Awareness campaign are required so that Federal and Provincial Ministries for Commerce and Industries should adopt the findings of present studies on large scale in structural materials for socio-economic benefits.

According to the experimental work following recommendations has been suggested for Future Research work:

- A detailed survey of the country is required to investigate the best RH to be utilized in future.
- Further work is suggested to fix exact temperature and time of combustion to obtain a good content of ash.

ACKNOWLEDGMENT

Supervision and guidance of Prof. Dr. Khan Shahzada and Engr. Kafayatullah Khan for conducting research work are highly acknowledged. The authors are thankful to Engr. Waheed ur Rahman and Mr. Sohail Noor for helping in preparing the samples at Pakistan Council of Scientific and Industrial Research (PCSIR) Labs, Peshawar. The authors are also grateful to Mr. Ihsan ul Haq and Mr. Khan Malook for analyzing the samples for silica contents at Central Resource Labs, University of Peshawar.

REFERENCES

[1] Food and Agriculture Organization (FAO), the United Nations, Statistical Database, 2002.http://apps.fao.org.

[2] W. Khan, K. Shehzada, T. Bibi, S.U. Islam, S.W. Khan, Performance evaluation of Khyber Pakhtunkhwa Rice Husk Ash (RHA) in improving mechanical behavior of cement, Construction and Building Materials 176 (2018) 89–102.

[3] Economic Survey of Pakistan, Ministry of Planning and Development, Islamabad, 2009-2010.

[4] S.A. Memon, M.A. Shaikh, H. Akbar, Production of low cost self-compacting concrete using rice husk ash. In First International Conference on Construction in Developing Countries (ICCIDC-l), Advancing and Integrating Construction Education, Research & Practice, Karachi, Pakistan, 260-269 (2008).

[5] Development of Statistics of Khyber Pakhtunkhwa, Bureau of Statistics Planning & Development Department Government of Khyber Pakhtunkhwa, Pakistan (2017). www.kpbos.gov.pk.

[6] S. Wansom, S., Janjapuraphan, S. Sinthupinyo, Characterizing pozzolanic activity of rice husk ash by impedance spectroscopy, Cement and Concrete Research, 40 (2010) 1714-1722.

[7] C.B. Majumder, M. Sharma, G. Soni, A simple non-conventional method to extract amorphous silica from rice husk. Bioresource Technology, accepted 28 April (2014).

[8] I.J. Fernandes, D. Calheiro, F.A.L. Sánchezb, A.L.D. Camacho, Characterization of Silica Produced from Rice Husk Ash: Comparison of Purification and Processing Methods, Materials Research. 20(Suppl. 2) (2017) 512-518.

[9] D.G. Nair, K.S. Jagadish, A. Fraaij, Reactive pozzolanas from rice husk ash : An alternative to cement for rural housing, 36 (2006) 1062–1071. https://doi.org/10.1016/j.cemconres.2006.03.012.

[10] L.A. Bui, C. Chen, C. Hwang, W. Wu, Effect of silica forms in rice husk ash on the properties of concrete. International Journal of Minerals, Metallurgy and Materials 19(3) (2012) 252–258. https://doi.org/10.1007/s12613-012-0547-9.

[11] V.P. Della, I. Ku¨hn, D. Hotza, Rice husk ash as an alternate source for active silica production, Materials Letters 57 (2002) 818–821.

[12] R.M. Ferraro, A. Nanni, A. (2012). Effect of off-white rice husk ash on strength, porosity, conductivity and corrosion resistance of white concrete, Construction and Building Materials 31 (2012) 220–225.

[13] Muthadhi, S. Kothandaraman, Optimum production conditions for reactive rice husk ash, Materials and Structures 43(9) (2010) 1303–1315.

[14] R. Khan, A. Jabbar, I. Ahmad, W. Khan, A.N. Khan, J. Mirza, Reduction in environmental problems using rice-husk ash in concrete, Construction and Building Materials 30 (2012) 360-365.

IJEW 国际工程期刊 International Journal of Engineering Works انجینئرنگ کاموں کا بین الاقوامی جرنل

International Journal of Engineering Works
ISSN-p: 2521-2419
ISSN-e: 2409-2770
Vol. 6, Issue 09, PP. 305-309, September 2019
https://www.ijew.io/
https://doi.org/10.34259/ijew.19.609305309

Synthesis of Non Precious Metals (NPM) Electrocatalysts for Higher ORR Efficiency in Fuel Cell Applications

Afaf Ali[1], Ihtesham Ahmed[2], Dr.Saim Saher[3]
[1'2] Research Scholars,[3]Assistant Professor
[1,3] US-Pakistan Centre for Advanced Studies in Energy, University of Engineering and Technology, Peshawar,Pakistan.
[2]Department of Energy Systems Engineering, US-Pakistan Centre for Advanced Studies in Energy, National University of Science and Technology, Islamabad, Pakistan.
aali42@asu.edu / afaf.ali13@gmail.com[1], ahmad.ihtesham58@gmail.com[2], s.saher@uetpeshawar.edu.pk[3]
Received: 06 September, Revised: 11 September, Accepted: 14 September

***Abstract*—** Pt-less electrocatalysts for the assistance in Oxygen Reduction Reaction, elucidating at the cathode of PEMFC have been widely researched. To be considered as an alternative this research work focuses two different classes of Non-Precious Group Metals (Non-PGM),carbon base supports and Metal Organic Frameworks have been synthesized and tested for ORR characteristics i.e Cobalt doped Graphitic Carbon Nitrides (Co-C3N4) and Zeolitic Imidazole Framework with iron as a dopant i.e Fe+2. Potentiodynamic steady state convectively diffusing the reacting material within the electrolyte is employed at varying rpm to attain Linear Sweep Voltammograms at 20 mV.s-1 in 0.1M KOH and 0.1 HCLO4 electrolytes are obtained at 400, 800,1200 and 1600 rpm. Charge transfer number is obtained, showing the rate determining step of the reaction kinetics of transport of ionic species in the Oxygen reduction.

***Keywords*—** Electrocatalysts , Proton Exchange Membrane Fuel Cells (PEMFCs) , Zeolitic Immidizole Frameworks (ZIF), Graphitic Carbon Nitrides, Hydrodynamic methods.

I. Introduction

Green Energy alternatives have been explored widely pertaining to mass increase in global warming, to provide secure energy shift we have various technologies available at commercial and lab scale. Fuel cell among the sustainabale solution behave like a charge generator, an electro-chemical cell, provided with two electrodes.i.e Anode and Cathode.Among various fuel cell classes, Proton exchange Membrane Fuel Cells (PEMFCs) are widely encouraged. Oxygen-Reduction Reaction (ORR) happening at cathode of low temperature Proton Exchange Membrane Fuel Cells occurs at very slow kinetics[1] than Hydrogen Reduction Reaction (HOR) at anode of the PEMFC.[2] To catalyze the ORR process Pt-based catalysts are utilized.[1,2] ORR process occurs either in a 2e- or 4e- pathway,[2,3] resulting in an undesirable intermediate peroxide in the rate determining step.4e- transfer is much desirable comparably shown by Pt/C supports.[3] Pt-based catalysts are formed by Pt-nanoparticles deposition on carbon black (Vulcan X-72) substrate commercially, known as Pt/C where Pt concentration varies while material is sintered at slow rate to fix Pt-particles on organic substrate.[4] Pt-particle inclusion as a catalyst increases capital cost by 56%, hindering commercialization economically.[5] Downsizing Pt-nanoparticles to atomic level still renders Pt-based catalyst as the best choice, reducing its capital cost.[6] Non- Precious group metals (non-PGM) used as catalytic materials to eradicate the need of platinum electrocatalysts have been reported, Transition metal doped nitrogen carbon composites (T-NC) showed promising results.[7] Pyrolyzed transition metal group, acting as ligand precursors (Fe+2 or Co+2) on the carbonic substrate have been researched widely, higher catalytic activity can be achieved in condition while these materials exhibit efficient onset potentials in basic medium.[8]Corrosion of carbon supports suggests them to be more synthetically developed into nano porous particles. A controlled synthesis of nano-porous particles doped with mesoporous silica, aluminosilicate and crystallized particles of colloidal crystals have been considered lately for ORR applications.[9]

A new class of self-supported materials have been reported in literature, showing greater electrolytic activity for ORR applications, surface porosity, current density, stability and electron transfer efficiency.[10] Metal Organic Frameworks (MOF) represents a large variety of novel material where organic linkers are doped with metal ions, providing a flexible structure and effective substrate base template for porous carbon composites. MOF's have been widely used in catalyst applications, energy storage systems and sensors.[11] The morphology and composition greatly affects the efficiency of a catalyst material [10,11], Zeolitic imidazole Frameworks (ZIF), a subclass of MOF materials first synthesized at Argonne National Laboratory in 1950's with Co+2 doping act to various functional precursors based on carbon.[12]Zhang et al, stated the addition of ZIF-67 precursor attaining higher porosity of composite structure followed by pyrolyzing after adding thioacetamide. An equilibrium was achieved between dopant concentrations while maintaining impedance at minimum.[13] Papuans et. Al reported synthesizing novel materials based on ZIF including II valency ligands for ORR applications, through calcination of materials in nitrogen environment at higher temperatures. The actives sites detected by qualitative analysis showed the bonding Fe+2 within the ligand (nitrogen). Rotating disk analysis stated that charge transfer of 4e- in alkaline medium.[14]

Zhao et al, stated a state of art method for synthesizing ZIF electrocatalyst in all solid-state mixing. Iron acted as a dopant in addition to ZnO and imidazole (Im) at 200°C in a single step reaction.[15] Xia et al, reported the synthesis and thermal activation of ZIF-67, which showed increased surface area and ORR activity in HClO4.[16] ZIF precursors have been utilized to tailor nitrogen doped carbon nanotubes N-CNT's.[17] Shui et al, developed materials based acrylates doped with Fe, methyl ZIF and ZIF-8.The pyrolysis was carried out for 1hr in Argon gas at 1000°C.Ammonia was supplied at 900°C.The N-coordinated Fe+2 acted as an active site in porous channel of ligand.[18]

Carbon support based, transition metal complexes are considered Non-precious materials for ORR activity i.e, CNT's and g-C3N4 structures,[19] where N doping has been widely reported providing structural stability.[20] g-C3N4 refers to a class of structural misnomers having different chemical compositions, but the same structural linkage of the bonding atoms are known as Graphitic Carbon Nitrides. A graphitic carbon layered planar sheet structure providing greater surface porosity is formed, when N-doping occurs at higher temperatures. [20,21] N-doped precursors are pyrolyzed with carbonaceous materials developing g-C3N4 structure. A 2e-pathway is followed in these carbon support structures producing peroxide.[22] Higher electronic coupling between graphitic linkages in both acidic and basic mediums provide greater ORR abilities to carbon support catalysts. [23] Increased chemical activity dependent on transition metal doping in nano-porous structure with reasonable ORR catalytic abilities were observed.[24]

The physiochemical behavior of components forming a catalyst,formation of dense active sites along with reasonable porosity to surface area ratio determines the characteristics of the ORR catalytic behavior after pyrolysis, providing enhanced limiting currents and onset potentials. [12-24] This research explored the controlled synthesis and electrochemical activity for ORR process within the scope of Non-precious materials group, having no trace of Pt particles for Low temperature PEMFC's application.

II. MATERIAL AND METHODS

A. *Synthesizing ORR-Catalysts*

A ligand is formed in autoclave, Zn(Fe) ZIF was synthesized by one-pot hydrothermal treatment of Zinc Nitrate Hexahydrate Zn(NO3)2.6H2O(Sigma-Aldrich), FeSO4.7H2O

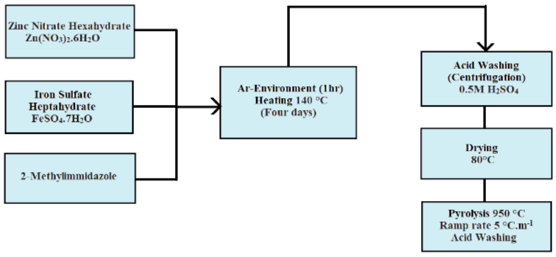

Figure 1. Flowsheet for preparing ZIF based catalyst

(Sigma-Aldrich) and 2-Methylimidazole 1hr purging in Ar-environment followed by 4 days continuous drying at 140°C.Acid washing was done in 0.5M H2SO4 by centrifugation and catalyst is dried at 80°C.

At ramp of 5°C/min for 1hr, carbonization in tubular furnace is done at 950 °C. The ZIF is washed to exfoliate unreacted metallic content with Sulfuric acid and dried at 80°C. Graphitic carbon nitride having g-C3N4 stoichiometry was synthesized by thermal treatment at of 1,3,5-trichloromelamine(C3N3Cl3), sodium amide (NaNH2) with induction of benzene at 220°C.While keeping 1/6 Co: N ratio, 1g of g-C3N4,0.5 g FeSO4.7H2O (Sigma-Aldrich), and 0.52g of Cobalt Chloride (Sigma-Aldrich) were added and dried at 450°C for 1 day. A brief pyrolysis was done at 600°C ,1 hr in tubular furnace at 5°C/min ramp. Washing was done by 0.5 M H2SO4 followed by drying at 80°C for 24 hrs.

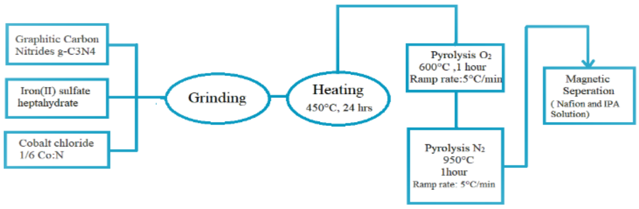

Figure 2. Preparation methodology of Graphitic carbon nitrides

B. *Material testing*

Hydrodynamic Rotating Disk Electrode technique is used to analyze the electrochemical reduction of oxygen at cathode. A 3-electrode system, providing a steady-state diffusion through rotating disk at varying rotation per minute. A dispersant formed by 24ml IPA, 5 % wt Nafion (1100 EW, Sigma-Aldrich) and DI water ((Thermo Scientific Barnstead MicroPure) was used 1ml and 4mg/ml of solid catalyst material was added to formulate ink slurry for testing. To homogenize the slurry, agitation was done followed by acoustic exposure/sonication for 30 min. Alumina polish and DI water cleaning of electrode (Dia=5mm) to render electrode surface dust free. The ink layer is dropped (~ 48µl) on Glassy carbon (GC) electrode, the hydrophilic region of electrode. A uniform layer is obtained by air-heater drying at 700 rpm. Nitrogen (99.9% pure) purging is done and Cyclic voltammograms are obtained at 400 rpm to activate the catalytic activity. CV scan was done at 50 mV.s-1 for 50 cycles, higher scan rates are used because unreacted impurities hinders the catalytic ORR activity of the material. Linear Sweep Voltammetry (LSV) scans determine reactive capacity of oxygen reduction. Electrode potential varied in electrolytic mediums, (0.9 to –1.0) vs SCE for 0.1M HCLO4 and (0.2 to-1.0) vs SCE for 0.1M KOH. A constant scan rate of 20 mV.s-1 ,while succeeding rpm to induce convective-diffusion at 400,800,1200 and 1600 rpm was maintained.

III. Results and Discussion

ORR elucidates at the onset potentials, for this higher value of Onset potential are required. A reversible electrochemical equilibrium is achieved at exchange current density i.e backward and forward reaction at same potential level.[25] This parameter defines the reaction rate, depending on the active surface area of electrode. To validate the ORR, Nitrogen current values are deducted from the oxygen current value due to presence of capacitive current.[24]

Table 1, indicates the values obtained through experimentation on three electrode system, reference electrode being Calomel Electrode (Koslow Scientific) while the electrolytic medium was basic (0.1 M KOH). The efficient values of limiting current are shown by Graphitic carbon nitrides at the same conditions, while Fe-ZIF restrains from showing better performances on both onset potentials and limiting current. A reason could be the hindered active sites, not definite reactive surface area available, since morphology is yet unknown. Linear Sweep voltammograms obtain at varying torque increase in reactivity at higher rotation rates represents the convective diffusion.

Table 1.ORR defining parameters at room temperature 25°C

Electrocatalyst material	Onset potential (V)	Limiting current ($mA.cm^{-2}$)
Pt/C (20% wt pt)	0.89- ~0.90	5.3
Zn(Fe)ZIF	0.65	2.7
Co-C3N4	0.74	4.5

A chemical gradient referring to the transfers of ion from active surface area towards electrolyte. Fig 3, presents LSV scan in perchloric acid, slower scan rates dissolves material in electrolyte instead of testing it gives the ORR pattern for Pt/C in acidic media, while other scans are in basic electrolyte.

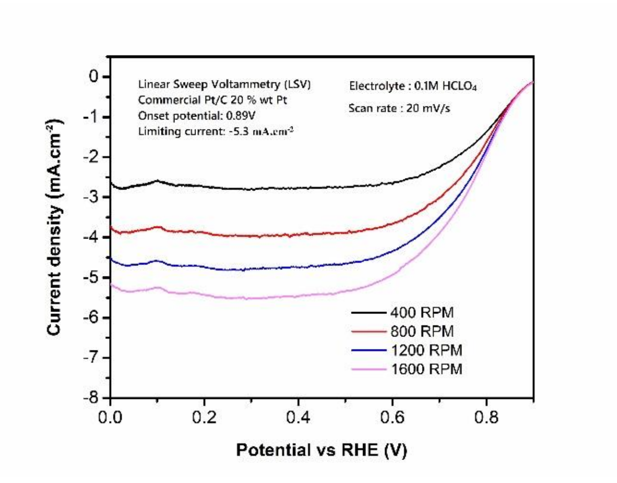

Figure 3. LSV scan (20 mv.s-1) 20% Pt on carbon black

The electrochemical analysis of Graphitic Carbon Nitrides provide an acceptable limiting current and onset potential, result showed in Fig-4 provided their layered planar structure expose active areas for reaction. A comparison analysis of Non-PGM catalyst is done in Fig.6 where Graphitic carbon nitrides show promising aspects as compared to Pt/C. Charge transfer of ionic species with respect to electrode potentials is governed by Nernst Equation,[26] when reacting species are brought to reactive surface of electrode. Where the net charge transfer is given by eq (1), ***i*** is the exchange current density ($mA.cm^{-2}$) and $F=96485\ C.mol^{-1}$ (Faraday's constant).

$$V_{net} = \frac{i}{nF} \qquad \text{eq.(1)}$$

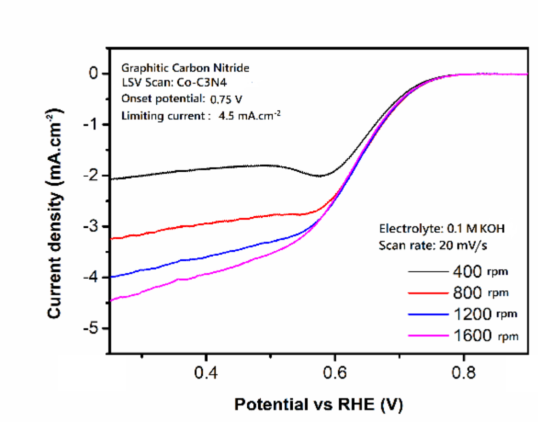

Figure 4. Linear sweep voltammogram for CoC3N4

Iron dopant ZIF catalyst shows low onset potentials ,relative to the acceptable limiting current as non precious metal catalyst. A fact to that is presence of tetrahedral structure of metal organic framework,placing one atom with thin crystalline morphology of four atoms.Fig-5 refers to LSV analysis of ZIF based catalyst formed by one pot method. Fig-6

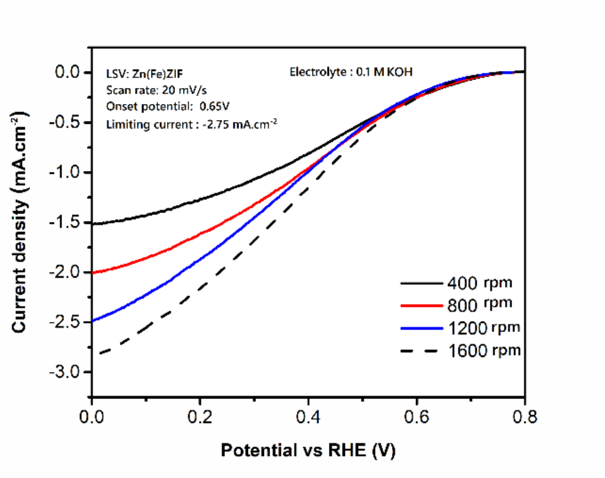

Figure 5. Linear sweep voltametery of iron doped ZIF

Higher onset potentials defines a sharp initiation of reaction, whereas there are some applications requiring lower onsets. Open circuit voltages and half wave potentials are also looked upon for characterization in potentiodynamic techniques.

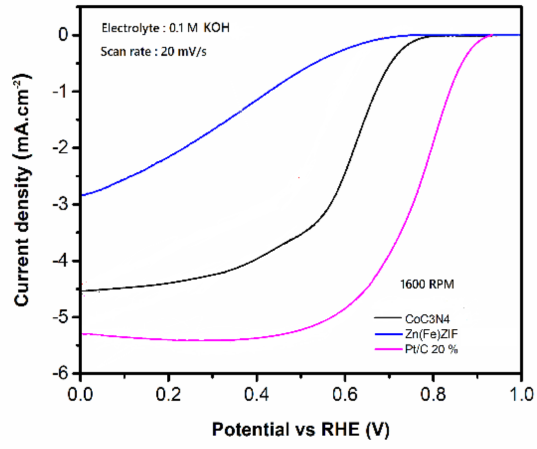

Figure 6. Performance comparison of LSV scans at 1600 RPM

Charge transportation is either by reaction taking a 2e- or a 4e- transfer, depends upon the reactivity of electrode surface. Cell potentials are higher at 2e- reaction process, but deteriorating towards membrane, on the other hand a 4e-pathway is much favorable shown by Pt/C in Figure 2 ,the Non-PGM catalysts following a 2e- transfer. Graphitic Carbon Nitrides are close to attaining a four-electron transfer, while a hindered reactivity due to unavailability of the active sites [27] can be seen in Fig-7. This parameter greatly effects the selectivity of catalyst for ORR applications as it defines the path of electrochemical kinetics highlighting the intermediate reaction that is responsible for rate. Electrolytic material in which diffusion occurs also plays a vital role in the ORR and durability of catalyst reactivity.

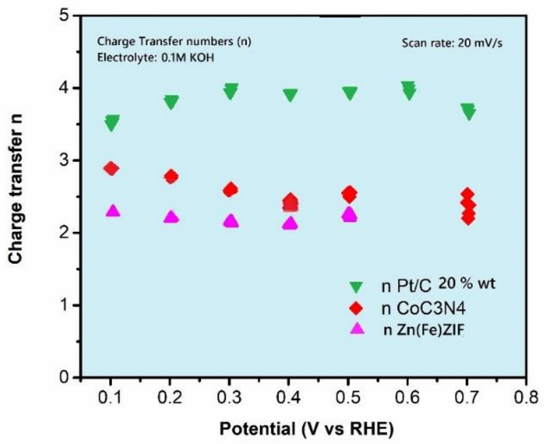

Figure 7. Charge number comparison for brtter ORR efficiencies

CONCUSLION

The research work discussed in this paper, identifies potential candidates for Oxygen-reduction reaction elucidating at the cathode of Low Temperature Proton Exchange Membrane Fuel Cells. Non-PGM catalysts provide a variety of electrocatalysts for ORR application, among them two entire different classes of Non precious metals have been synthesized in this work namely Graphitic Carbon Nitrides and Iron Zinc ZIF material. Co-C3N4 offer acceptable values of electrocatalytic limiting current due to presence of layered planar structure exposing more surface activity while showing low onset potentials. Iron Zinc ZIF shows less performance then the former catalyst, in terms of composite formation having reduced probable sites for oxygen reduction. Moreover, pyrolyzing environment contributes a lot to the morphology, there trying different gases can be beneficial to have better ORR characteristics of electrocatalysts.

ACKNOWLEDGEMENT

The research scholars are highly obliged to USAID for providing funding opportunity pertaining to Research collaboration between Arizona State University,USA and US-Pakistan Center for Advanced Studies in Energy, Pakistan. Also the highly regard research supervisor Dr.Saim Saher for his kind guidance.

REFERENCES

[1] Tabbi et al, Fuel cells in stationary and portable fuel cell applications. International journal of hydrogen energy.41 (2016)

[2] Wroblowa H et al, Adsorption and kinetics at platinum electrodes in the presence of oxygen at zero net current. J Electroanal Chem 1967; 15: 139–50.

[3] Wang Junye. Barriers of scaling-up fuel cells: cost, durability and reliability. Energy 2015;80:509e21

[4] Jiujun Zhang et al.PEM Fuel Cell Electrocatalysts and Catalyst Layers: fundamentals and applications. Springer,2008.

[5] Raza R et al, 2005.Kordesch K, Simader G. Fuel cells and their applications VCH; 1996.

[6] Parthasarathy A et al, J Electrochem Soc 1992; 139: 2530–7.

[7] Fuel Cell Technical Team Roadmap, US drive road map, http://www1.eere.energy.gov/vehiclesandfuels/pdf, 2013

[8] R. Borup, et al., Scientific Aspects of Polymer Electrolyte Fuel Cell Durability and Degradation Chem. Rev.,107, 3904-3951, 2007.

[9] Raza R et al, Fuel cell technology for sustainable development in Pakistan – An over-view. Renewable and Sustainable Energy Reviews 53 (2016) 450–461.

[10] Damjanovic A, Bockris JO'M. The rate constants for oxygen dissolution on bare and oxide-covered platinum. Electrochim Acta 1966; 11: 376–7.

[11] Yao Nie, Li Li and Zidong Wei. Recent Advancements of Pt and Pt-free Catalysts for Oxygen Reduction Reaction. Chemical Society Reviews. DOI: 10.1039/x0xx00000x

[12] Kim TK1 et al .Nanoporous metal oxides with tunable and nanocrystalline frameworks via conversion of metal-organic frameworks. J Am Chem Soc. 2013 Jun19;135(24):8940-6. doi: 10.1021/ja401869h.

[13] H. T. Chung et al, Polymer Electrolyte Fuel Cells. Electrochem. Commun., 2010, 12,1792–1795.

[14] L. Chong et al, Investigation of Oxygen Reduction Activity of Catalysts Derived from Co and Co/Zn Methyl‐Imidazolate Frameworks in Proton Exchange Membrane Fuel Cells .Chem Electro Chem, 2016, 3, 1541‐1545.

[15] P. Gai et al., Efficient and selective aerobic oxidation of alcohols catalysed by MOF-derived Co catalysts. Mater. Chem. B, 1, 2742-2749, 2013.

[16] S.Phapan et al, Nitrogen-doped carbon nanotubes derived from Zn–Fe-ZIF nanospheres and their application as efficient oxygen reduction electrocatalysts with in situ generated iron species. Chem. Sci., 4, 2941, 2013

[17] B. Chen et al, Cobalt sulfide/N,S codoped porous carbon core–shell nanocomposites as superior bifunctional electrocatalysts for oxygen reduction and evolution reactions.Nanoscale, 2015, 7, 20674–20684.

[18] J. shui et al, Highly efficient nonprecious metal catalyst prepared with metal–organic framework in a continuous carbon nanofibrous network. 10.1073/pnas.1507159112, 2015.

[19] Chang H et al, Proceedings of the Symposium on Materials for Advanced Batteries and Fuel Cells. Solid State Ionics 2002; 148: 601–6

[20] Kim et al, Novel ordered nanoporous graphitic C3N4 as a support for Pt–Ru anode catalyst in direct methanol fuel cell.J. Mater. Chem. 17 (2007) 1656–1659.

[21] M.J. Bojdys et al, Ionothermal synthesis of crystalline, condensed, graphitic carbon nitride.Chem. Eur. J. 14 (2008) 8177–8182

[22] W. Zhang et al, Palladium nanoparticles supported on graphitic carbon nitride-modified reduced graphene oxide as highly efficient catalysts for formic acid and methanol electrooxidation, J. Mater. Chem. A 2 (2014) 19084–19094.

[23] Chan SH et al, A mathematical model of polymer electrolyte fuel cell with anode CO kinetics. Electrochim Acta 2003;48:1905–19.

[24] Kazuma Shinozaki et al, Oxygen Reduction Reaction Measurements on Platinum Electrocatalysts Utilizing Rotating Disk Electrode Technique. II. Influence of Ink Formulation, Catalyst Layer Uniformity and Thickness. Journal of The Electrochemical Society, 162 (12) F1384-F1396 (2015)

[25] Thacker R, Hoare JP. Sorption of oxygen from solution by noble metals: I. Bright platinum. J Electroanalysis Chem 1971; 30:1–14

[26] Yeager E. Dioxygen electrocatalysis: mechanisms in relation to catalyst structure. J Mol Catalyst 1986;38(1 2):5–25.

[27] Jiujun Zhang et al. PEM Fuel Cell Electrocatalysts and Catalyst Layers: fundamentals and applications. Springer,2008.

IJEW 国际工程期刊 International Journal of Engineering Works انجینیرنگ کاموں کا بین الاقوامی جرنل

International Journal of Engineering Works
ISSN-p: 2521-2419
ISSN-e: 2409-2770
Vol. 6, Issue 09, PP. 310-313, September 2019
https://www.ijew.io/
https://doi.org/10.34259/ijew.19.609310313

Projecting Future Temperature using CMIP5 GCMs over Transboundary Gomal River Basin

Amjad Khan[1*], M. Shahzad Khattak[2], Mahmood Alam Khan[3], Saadia Rehman[4]
[1,2,3,4] Department of Agricultural Engineering, Univeristy of Engineering & Technology Peshawwar
amjad_uet91@yahoo.com[1], shahzadkk2004@gmail.com[2], mahmmod_marwat@yahoo.com[3], saadiarehman93@yahoo.com[4]
[*]corresponding author
Received: 29 August, Revised: 10 September, Accepted: 13 Septemebr

***Abstract*—** Temperature is a key driving force in hydrological cycle, defining the extent of climate change. It causes the alteration in hydrological cycle process, limiting and intensifying the rainfall, increasing the rate of evapotranspiration and changes the crop pattern and duration over a region. Its future analysis is utmost to cope with negative effects of climate change over a specified region. This study also investigates, the future temperature pattern over Gomal River Basin (GRB). To undertake the study, downscaled daily temperature data of four General Circulation Models (GCMS) namely; bcc_csm1_1_m, mpi_esm_mr, ncar_ccsm4 and ncc_noresm1_m and their ensemble mean were first compared and validated with observed data for the period of 1980-2005. After that, temperature was projected for the mid-century (2020-2060) for the Representative Concentration Pathways (RCPs) 4.5. The analysis were carried out based on the four seasons; winter (December-February), spring (March-May), summer (June-August) and autumn (September-November). The results indicate that, the basin temperature was accurately predicted by the ensemble mean of the four GCMs with R^2 value of 0.9. All the GCMs projected a warming in future in all seasons. Winter warming is more compared to other seasons. Proper adaptation strategies are needed to cope with the adverse impacts of global warming in the basin.

Keywords— Temperature, Climate Change, CMIP5, GCMs, GRB

I. Introduction

Mean surface air temperature is an important meteorological parameter which influences hydrological cycle causing evaporation from water bodies and occurrence of precipitation. It plays an important role in the germination and growth of the crops. It cause droungts and floods by altering precipitation patterns [1]. Higher temperature over a region is the feature of global warming. The global average temperature has increased by an average of 0.85 °C during 1800–2012 relative to 1961–1990 [2] and 0.74 °C (1906.-.2005) [3]. Over Southeast Asia, the mean annual temperature would rise by about 3.2 °C under RCP 8.5 [4] while over East Asia it is projected to likely increase by 0.98 °C and 4.06 °C for low and high emission scenarios respectively. Also, an increase of 10-15 % in summer precipitation was projected. at the end of 21st century in the East Asia [5]. Across South Asia region, the daily mean temperature would rise by 2.9 °C in 2046-2075 comparative to 1976-2005 [6]. In Pakistan, the 21st century temperature would increase by around 6.7 °C under RCP 8.5 [7]. This increase is higher in the northern parts and smaller in the southern parts. This increase in the temperature has caused the change in the bowing and sowing seasons of crops, movements of the inhabitants.

General Circulation Models (GCMs) included in the Coupled Model Inter-comparison project, Phase 5 (CMIP5) are the most advance tools to analyze future global warming and its effects on different socio-economic sectors such as agriculture, industries, tourism and hydropower generation ([8], [9], [10], [11]). Due to this reason different researches across the world are using the output of these GCMs in climate change impacts studies. Detailed information on the experimental design of GCMs included in the CMIP5 are given by [12]. In this study four GCMs namely; bcc_csm1_1_m, mpi_esm_mr, ncar_ccsm4 and ncc_noresm1_m and their ensemble were used to project temperature in the mid-21st century (2020-2060) using RCP 4.5 for the transboundary GRB.

II. Data and Methodology

A. Study Area

The GRB is a transboundary river basin shared between Pakistan (76%) and Afghanistan (24%) (Figure 1). The basin area is 34167 km2 and the runoff generated from the basin contributes to the Gomal Zam Dam constructed on the Gomal River at Khajuri Katch in Pakistan. The average annual temperature over the basin is 12.7 °C and average annual precipitation is 228 mm. There are two major rivers in the basin, namely; Gomal River and Zhob River. These both rivers drain the basin into Gomal Zam Dam, which is a sole sources of water supply to the lands and community living downstream in the command area. The rise in temperature will affect the precipitation pattern and hence the water availability to the Dam affecting the socio-economic wellbeing of the community. Hence its future quantification is necessary to mitigate and adopt to the impacts of climate change.

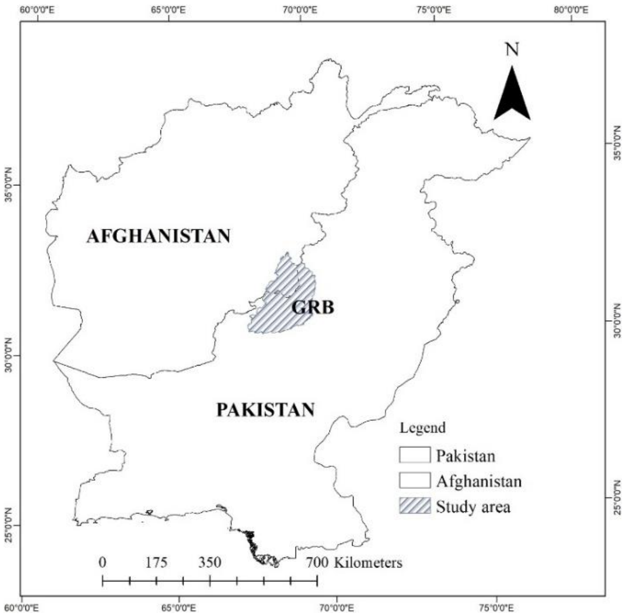

Figure 1. Location Map of Gomal River Basin (GRB)

B. *Temperature Data*

In this study, four GCMs from 5th Couple Model Inter-comparison Project (CMIP5) of the Intergovernmental Panel on Climate Change (IPCC) was used. Downscaled data of the four GCMs (Table 1) and its ensemble mean were downloaded from http://ccafs-climate.org/ at the four stations covering the basin. Observed data for the period of 1980-2005 at Dera Ismail Khan station was obtained from Pakistan Meteorological Department. To select best GCM, the GCMs historical data was compared with the observed data. For future analysis, the daily data of the GCMs were transformed into four seasons, namely winter, spring, summer and autumn.

TABLE 1. DETAILS OF GCMS USED IN THIS STUDY

GCM	Organization/Institute	Model ID	Resolution (Lat x Long) °
bcc_csm1_1_m	Beijing Climate Center (Climate System Model)	BCC	2.7906 x 2.8125
mpi_esm_mr	Max Planck Institute of Meteorology	MPI-ESM	1.8653 x 1.875
ncar_ccsm4	National Center for Atmospheric Research, USA	NCAR	0.9424 x 1.25
ncc_noresm1_m	Norwegian Climate Centre, Norway	NCC	1.8947 x 2.5

C. *Methodology*

The methodology consists of comparing and validating the GCMs data by comparing the data with the observed data. For this purpose, the GCMs data were compared at four stations (S1, S2, S3 and S4) (Table 2) using Pearson Correlation Coefficient (r) (Equation 1) and Root Mean Square Error (RMSE) (Equation 2). Then descriptive statistic (Equation 3-4) was applied to quantify the future temperature in the Mid of 21st Century (2020-2060).

TABLE 2. LOCATION OF STATIONS USED TO PROJECT FUTURE TEMPERATURE OVER THE GRB

S.No.	Station	Coordinates (Lat x Long)°
1	S1	32.40 x 68.97
2	S2	31.53 x 69.19
3	S3	31.53 x 68.38
4	S4	30.84 x 68.25

1. Pearson Correlation Coefficient (r)

$$r = \frac{\sum_{i=1}^{n}\left(O_i - \bar{O}\right)\left(P_i - \bar{P}\right)}{\sqrt{\sum_{i=1}^{n}(O_i - \bar{O})^2}\sqrt{\sum_{i=1}^{n}(P_i - \bar{P})^2}} \qquad (\text{II}.1)$$

Where "O" is the observed and "P" is the GCM data

2. Root Mean Square Error (RMSE)

$$RMSE = \sqrt{\frac{\sum_{i=1}^{n}(O_i - P_i)^2}{n}} \qquad (\text{II}.2)$$

3. Statistical Mean ($\bar{X}$)

$$\bar{X} = \frac{\sum_{i=1}^{N} X_i}{N} \qquad (\text{II}.3)$$

where, X is the data point and N is the total number of data points.

4. Standard Deviation (σ)

$$\sigma = \frac{\sqrt{\sum(X - \overline{\overline{X}})}}{n} \qquad (\text{II}.4)$$

where, $\bar{X}$ is the mean of the data set and n is the number of data points.

III. RESULTS AND DISCUSSIONS

A. *Validation of GCMs*

The results of the statistical test applied for the validation of GCMs with the observed data are presented in the Table and Figure. All the four GCMs have good correlation with observed data. The correlation coefficient (r) value ranges from a minimum of 0.90 to a maximum of 0.95 for station S1 while it ranges from 0.89 to 0.95 for station S2. The GCM ncc_noresm1_m has higher value of "r" while bcc_csm1_1_m has lower value of "r" compared to other GCMs at all the four stations. The RMSE value ranges from a minimum of 15.66 to a maximum of 21.65. On average, the minimum values of RMSE were observed for ncar_ccsm4 while the maximum values of RMSE were observed for mpi_esm_mr. Compared to the individual GCM, the ensemble means of all the GCMs indicate a strong correlation with the observed data. Also, the RMSE showed lowest values for the ensemble mean at all stations. Hence, the ensemble mean is the most suitable for future analysis as it predicts the basin accurate climate in terms of temperature.

B. *Projections of Fuutre Temperature*

1) *Winter Temperature*

The results of winter temperatures projected in the 2020-2060s are presented in the Table 4. The results were compared with the observed historical temperature for the period of 1980-2005. The average mean observed temperature over the basin is 1.0 °C in winter. The results indicate that the mean temperature over the basin will increase in future. At S4, highest warming was observed compared to other stations. For bcc_csm1_1_m, the mean temperature is projected to increase by 4 °C at S1 and 8.26 °C at S4. Least warming were projected by the GCM mpi_esm_mr which is 3.62 °C at S1 and 7.85 °C at S4 compared to the historical observations. The ensemble means also show warming in winter temperature which is highest at S4.

TABLE 3. STATISTICAL RESULTS OF THE VALIDATION OF THE GCMS WITH THE OBSERVED DATA

Station	bcc_csm1_1_m		mpi_esm_mr		ncar_ccsm4		ncc_noresm1_m		Ensemble Mean	
	r	RMSE	r	RMSE	r	RMSE	r	RMSE	r	RMSE
S1	0.90	18.7	0.91	19.20	0.90	16.70	0.92	19.35	0.95	18.31
S2	0.89	20.3	0.91	21.65	0.91	17.10	0.92	21.53	0.95	19.97
S3	0.90	15.6	0.91	17.13	0.90	15.87	0.92	16.65	0.96	16.11
S4	0.89	20.3	0.91	21.65	0.91	16.60	0.92	18.35	0.95	18.33

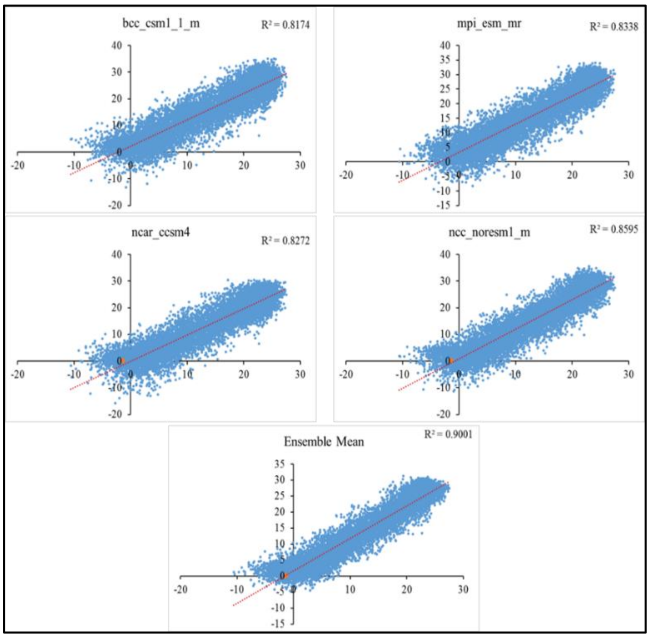

Figure 2. Comparison of GCMs and its ensemble mean with the observed data for the period of 1985-2005

TABLE 4. PROJECTIONS OF WINTER TEMPERATURE IN THE MID-21ST CENTURY OVER THE GRB

Station	Observed	bcc_csm1_1_m	mpi_esm_mr	ncar_ccsm4	ncc_noresm1_m	Ensemble Mean
S1	1.0	5.37	4.62	4.85	5.38	5.89
S2	1.0	5.56	4.89	4.98	5.25	5.96
S3	1.0	6.20	5.60	5.72	5.88	6.64
S4	1.0	9.26	8.59	8.85	9.66	8.88

2) Spring Temperature

Spring temperatures also show warming in the future (Table 5). The mean historical temperature over the basin is 12.4 °C. compared to the historical, the bcc_csm1_1_m shows an increase of 1.37 °C at S1 while 8.04 °C at S4. The least projected increase were observed for ncar_ccsm4 which is 1.19 °C at S1 and 7.91 °C at S4. The results of the ensemble means of the GCM also show warming in the basin in spring season.

TABLE 5. PROJECTIONS OF SPRING TEMPERATURE IN THE MID-21ST CENTURY OVER THE GRB

Station	Observed	bcc_csm1_1_m	mpi_esm_mr	ncar_ccsm4	ncc_noresm1_m	Ensemble Mean
S1	12.4	13.77	13.70	13.59	13.68	14.46
S2	12.4	16.96	17.05	16.79	16.90	17.71
S3	12.4	17.47	17.74	17.35	17.44	18.31
S4	12.4	20.44	20.65	20.31	21.22	20.36

3) Summer Temperature

The results of the historical and projected summer temperature are presented in the Table 6. The mean summer temperature over the basin is 22.9 °C. in future the highest warming were projected by the mpi_esm_mr while the lowest warming were projected by ncar_ccsm4. The bcc_csm1_1_m GCM results indicate that temperature will increase by 0.81 °C at S1 while .10 °C at S4. The ensemble mean of the four GCMs used also indicate warming in summer season. This warming is highest at S4 which is 6.30 °C.

TABLE 6. PROJECTIONS OF SUMMER TEMPERATURE IN THE MID-21ST CENTURY OVER THE GRB

Station	Observed	bcc_csm1_1_m	mpi_esm_mr	ncar_ccsm4	ncc_noresm1_m	Ensemble Mean
S1	22.9	23.71	24.14	23.53	23.83	24.46
S2	22.9	25.73	26.36	25.58	25.83	26.47
S3	22.9	26.95	27.71	26.74	27.18	27.88
S4	22.9	29.00	29.71	28.75	29.85	29.20

4) Autumn Temperature

The results of the autumn temperature is shown in the Table 7. The mean observed temperature is 13.4 °C. results indicate a warming in future in autumn season. The projected increase at S1 for bcc_csm1_1_m, mpi_esm_mr, ncar_ccsm4 and ncc_noresm1_m is 1.32 °C, 1.49 °C, 1.38 °C and 1.44 °C respectively. The results of the ensemble mean indicate that temperature will increase by 1.85 °C at S1 and 6.54 °C at S4 in the mid-21st century.

TABLE 7. PROJECTIONS OF AUTUMN TEMPERATURE IN THE MID-21ST CENTURY OVER THE GRB

Station	Observed	bcc_csm1_1_m	mpi_esm_mr	ncar_ccsm4	ncc_noresm1_m	Ensemble Mean
S1	13.4	14.72	14.89	14.78	14.84	15.25
S2	13.4	16.61	16.82	16.61	16.71	17.13
S3	13.4	17.38	17.60	17.41	17.58	17.97
S4	13.4	19.80	19.95	19.81	20.35	19.94

CONCLUSIONS

The main objective of this study was to project temperature in the mid-21st century (2020-2060) over the transboundary Gomal river basin using CMIP5 GCMs for the RCP 4.5. GCMs were first validated with the observed data for the period of 1980-2005. It was found that ensemble mean of the four GCMs used performed well with "r" value of 0.95. Projected results of all the GCMs used indicate a warming in future in all seasons. The winter warming is more compared to other seasons. The ensemble means of the GCMs indicate that on average the winter, summer, spring and autumn temperatures will increase by 7.5 °C, 7.9 °C, 6.0 °C and 6.5 °C respectively. this rise in temperature will significantly affect precipitation patterns with increase rate of evapotranspiration in the basin. Hence, planner and managers are required to adopt strategies to minimize the adverse impacts of global warming and climate change on agriculture and socio-economic activities of the communities in the basin.

REFERENCES

[1] M.S. Khattak, A. Khan, M.A. Khan, W. Ahmad, S. Rehman, M. Sharif, and S. Ahmad, "Investigation of characteristics of hydrological droughts in Indus basin,". Sarhad Journal of Agricultural, vol, 35(1), pp. 48-56, 2019. DOI:http://dx.doi.org/10.17582/journal.sja/2019/35.1.48.56

[2] IPCC, "Climate Change: The Physical Science Basis; Contribution of Working Group I to the Fifth Assessment Report of the Intergovern-mental Panel on Climate Change, " Cambridge University Press: Cambridge, UK; New York, NY, USA,p. 1535, 2013.

[3] IPCC, "Climate change 2007: the Physical Science Basis. Contribution of Working Group I to the 4th Assessment Report of the Intergovernmental Panel on the climate change". Cambridge and New York: Cambridge University Press, 2007. 996, 2007.

[4] S. Dhar, and A. Mazumdar, "Impacts of climate change under the threat of global Warming for an agricultural watershed of the Kangsabati River," International Journal of Agricultural and Biosystems Engineering, vol. 3 (3), 2019.

[5] X. Xin, L. Zhang, J. Zhang, T. Wu, and Y. Fang, "Climate change projections over East Asia with BCC_CSM1.1 Climate Model under RCP Scenarios," Journal of the Meteorological Society of Japan, vol. 91 (4), pp. 413-429, 2013. DOI:10.2151/jmsj.2013-401.

[6] H.X. Zheng, F.H. Chiew, S. Charles, and G. Podger, "Future climate and runoff projections across South Asia from CMIP5 global climate models and hydrological modelling. Journal of Hydrology," Regional Studies, vol. 18, pp. 92-109, 2018.

[7] N. Rehman, M. Adnan, and S. Ali, "Assessment of CMIP5 climate models over South Asia and climate change projections over Pakistan under representative concentration pathways," International Journal of Global Warming, vol. 16 (4), pp. 381–415, 2018.

[8] T.J. Zhou, and R.C. Yu, "Twentieth-century surface air temperature over China and the globe simulated by coupled climate models," Journal of Climate. Vol. 19: pp. 5843-5858, 2006.

[9] Z.H. Jiang, J. Song, and L. Li, W. Chen, Z. Wang, and J. Wang, "Extreme climate events in China: IPCC-AR4 model evaluation and projection," Climatic Change, vol. 110, pp. 385-401, 2012.

[10] V.N. Dike, M.H. Shimizu, M. Diallo, Z. Lin, O.K. Nwofor, and T.C. Chineke, "Modelling present and future African climate using CMIP5 scenarios in HadGEM2-ES" International Journal of Climatology, vol. 35 (8), pp. 1784-1799, 2014; DOI: 10.1002/joc.408.

[11] N. Khan, S. Shahid, K. Ahmed, T. Ismail, N. Nawaz, and M. Son, "Performance assessment of General Circulation Model in simulating daily precipitation and temperature using multiple gridded datasets" Water, vol. 10, pp. 1793, 2018. DOI: 10.3390/w10121793.

[12] K.E. Taylor, R.J. Stouffer, and G.A. Meehl, "An overview of CMIP5 and the experiment design" Bulletin of the American Meteorological Society, vol. 93: pp. 485-498, 2012; DOI:10.1175/BAMS-D-11-00094.1.

Amjad Khan was born in district Lakki Marwat, Khyber Pakhtunkhwa, Pakistan on 11th April 1991. He has got his bachelor degree in Agricultural Engineering from University of Engineering & Technology (UET), Peshawar-Pakistan in 2015. Currently he is enrolled in Masters in Soil and Water Engineering in UET Peshawar. His Research interests includes climate change, hydrological modeling and watershed management.

国际工程期刊
International Journal of Engineering Works
انجینرنگ کاموں کا بین الاقوامی جرنل

International Journal of Engineering Works
ISSN-p: 2521-2419
ISSN-e: 2409-2770
Vol. 6, Issue 09, PP. 314-323, September 2019
https://www.ijew.io/
https://doi.org/10.34259/ijew.19.609314323

Analysis of Biogas Technology Adoption at Household Level and its Impact on Sustainable Livelihoods

Muhammad Haseeb[1], Saddam Ali[2], Saim Saher[3]
[1,2,3] United States Pakistan Center for Advanced Studies in Energy UET Peshawar, Pakistan
Received: 06 September, Revised: 15 September, Accepted: 17 September

***Abstract*—**The incessant depletion of world energy resources and the global environmental deterioration are a good indicator of banishing the conventional energy extraction technologies in favor of renewable and sustainable options. Pakistan being an agrarian society is home to one of the largest proportion of population dependent on agricultural products and livestock to make ends meet. Fortuitously this also provides an abundant resource for biomass which can be utilized for generating biogas energy. In the era of renewable energy boom, the resource has poignantly not been fully utilized. Whatever portion of the biogas energy has been tapped is not proliferating across the country owing to the lack of knowledge about the impacts of this precious resource. This research endeavor attempted to investigate the impact the biogas technology is imposing on the households that have adopted it. A total of 162 households composed of both adopters and non adopters of the technology were surveyed in the Dera Ismail Khan District of Pakistan in addition to the meetings and discussions with the relevant stakeholders. Resultantly the factors vastly impacting the adoption of the biogas technology were uncovered. Accordingly the apprehensions and misconceptions of the households not employing the technology despite possessing the resources necessary also came to surface. It was found out that the technology had profound impacts on the environment, education, and the health of the adopting families. However the age, education level, and gender of the target population did not bear any correlation with the decision to adopt the technology itself. The major barrier to the adoption of the technology in the target area was the high upfront costs of the technology, and low awareness about the technology's installation, and maintenance.

***Keywords*—** Biogas, Social impact, Livelihoods, rural development, Environment

I. INTRODUCTION

Global fossil fuel deposits are depleting at an alarming pace and slated to run out somewhere in the late third quarter of the ongoing century. Contrarily the energy demand, and consequently the fossil fuel prices, is increasing the world over. The most plausible way the staggering demand could be satiated is to augment the conventional energy resources with the alternative sources. This will have the added benefit of tackling the soaring pollution and the resultant global warming. Besides following Kyoto protocol there is a growing consensus among the world leader that the energy demands be met mostly by alternative resources and the dependence on the conventional resources should be mitigated. The energy demand in the developing countries of Asia and Africa is slated to surpass the energy demand in the developed countries for the first time in 2020 [1].

Renewable energy has witnessed the most remarkable proliferation into the energy arena in the last decade, leading to an increased competitiveness with the fossil fuels in terms of marketability and annual deployment. According to International Energy Agency (IEA) Renewable Energy Report for the year 2017 renewable energy makes the lion's share of new energy projects with 167 GW of new additions compared to 57 GW from coal and 29 GW from gas. The same report posits a forecasted renewable deplo0yment of another 920 GW by 2022, as shown in the figure 1, which is an upward adjustment in the previous year's forecast, enabling renewables to make up 30% of total energy resources around the world. All this points to a bright future for the renewable energy [2].

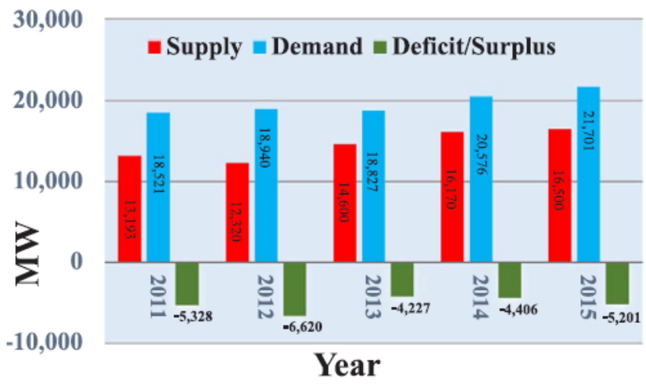

Figure.1 Electricity shortage in Pakistan [5]

Unfortunately the renewable energy potential has not been tapped mostly due to the high capex and technology. Pakistan is an agrarian country with more than 60% of the country's population dependent on agricultural income directly or indirectly [16].

This provides an opportunity in the form of abundance of biomass in the form of crop residue, forest residue, and more importantly the animal waste. Capitalizing on this opportunity and extracting a portion of the available resources could provide clean energy for rural community as well as industries where organic waste is generated. Even the sugar mills in the country produce biomass sufficient for a potential energy generation of 3000 MW. Only 4 sugar industries are currently generating 145.1 MW electricity from the bagasse, that is a byproduct of sugar cane [18, 19]. In addition to these operational projects another 9 projects are in various developmental stages and are estimated to produce a total of 297 MW electricity upon completion [18, 19] as shown in the table 1.

TABLE 1 SUGAR MILLS IN VARIOUS STAGES OF BIOGASS PLANT DEVELOPMENT [18,19]

Sr. no.	Company	Capacity(MW)
1	RYK Energy	36
2	Alliance Sugar Mills Ltd.	19
3	Layyah Sugar Mills Ltd.	41
4	Safina Sugar Mills	20
5	Chanar Energy Ltd	22
6	Etihad Power Generation Ltd.	67
7	Shahtaj Sugar Mills Ltd.	32
8	Almoiz Industries Ltd.	45
9	Hamza Sugar Mill Ltd.	15
	Total	297

Social value of energy is defined as the cumulative sum of the benefits derived by person or society from energy including the obvious economic gains, the concomitant development and prosperity minus any adverse impacts the energy generation may carry in the form of health impacts, environmental impact or any other negative outcome [24]. The challenge of energy poverty has thus far been tackled by access to basic level of energy provision [25-27].

Certain drawbacks are part and parcel of this approach including its inability to convert the energy access in to durable value for the communities leading to poverty alleviation [28,29]. Here social value consideration in the designing and implementation of energy projects is of key importance. In economically destitute societies energy resources are usually scarce, and thus the electrification projects relatively non-economical [30].

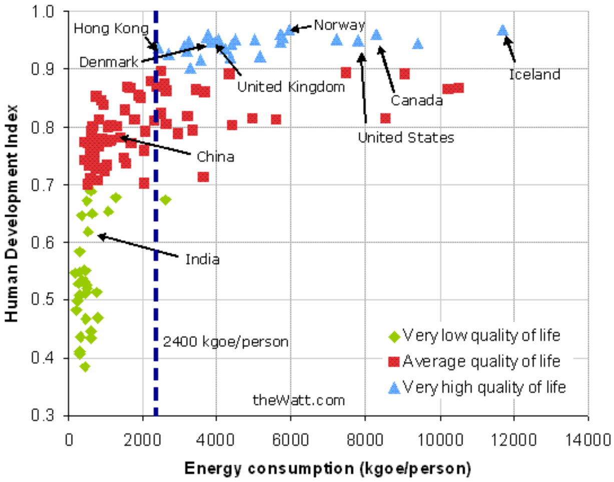

Figure 2 HDI-Energy correlation [23]

Usually the concept of social value is incorporated into the project by the measure of HDI index as function of energy consumption per capita as witnessed in the figure 4 as well [33]. However it is also evident from the figure that some countries achieve a much higher HDI for similar levels of energy consumption per capita. For instance Denmark while having similar levels of HDI as Canada consumes less than half the energy per capita. Same is the scenario for China and Costa Rica. Thus the ratio of energy consumption per capita to the HDI could point to the ability of the country to derive social value from the energy as shown in the table 2.

This discussion is at the heart of the second objective of this thesis; to gauge the social value produced by the biogas plants installed in Khyber Pakhtunkhwa province of Pakistan. The social value here is measured in terms of the satisfaction of the adopters and the health, education, and other benefits they derive from the energy produced by the biogas plants installed at domestic level

Studies related to adoption and socioeconomic impacts of biogas have been done but there are very few studies that analyze adoption and socioeconomic impact collectively. This study uses integrated approach to identify barriers to adoption and the various benefits in terms of socioeconomic impacts that can be enjoyed with the adoption of biogas technology. This study will be based on the detailed survey of biogas plants . The study aims to assess the role of biogas technology in saving wood, mitigating green-house gases emissions, improving livelihoods and impacting the households socially and economically. The current study will also investigate the various social and economic factors effecting the adoption of biogas plants. For this purpose both adopters and non-adopters of biogas will be interviewed and the adoption will be analyzed. Impact of biogas on the livelihoods of the households will be assessed by using DFID (1999) framework on sustainable livelihoods [34]. Carbon emission reduction will be calculated from fuel consumption reduction with biogas use, and will be presented in CO2 equivalent.

TABLE 2 RATIO OF ENERGY CONSUMPTION TO THE HDI_ INDICATOR OF SOCIAL VALUE [24]

Country	Human development index (HDI)	Percapita electricity consumption (kWh	Ratio
India	0.58	700	1
Denmark	0.9	6100	0.17
Canada	0.9	16500	0.06
China	0.71	3300	0.25
Costa Rica	0.76	1800	0.48

There are two types of Biogas plants currently prevalent in the market.

1. Floating Gas Holder Biogas Plant [44]
2. Fixed Dome Biogas Plant [45]
3. Expansion Chamber with Fixed Dome Biogas Plant [46]

A. Biogas Resources of Pakistan

Paksitan is regarded as an agrarian society with close to 60% of its population directly or indirectly dependent on agriculture or livestock for their subsistence [5]. The crop residue and cattle waste are an ideal resource for biogas generation. In addition poultry farms are also a useful biomass resource capable of being used in biogas generation. The poultry population in the country is 319 million generating revenue of 750 billion annual revenue [47]. Resultantly billions of kilograms of biomass is produced in the country which can be used as biomass.

Sugar cane is an important cash crop in Pakistan. Paksitan is the world's 5th largest producer of sugarcane with its annual sugar cane production averaging 50 million tons, resulting in by product of 10 million tons of bagasse [48]. The 84 odd sugar mills in the country have an estimated potential of 3 GW of electricity generation from biogas resource. Unfortunately the current tapped potential is only 700 MW [48].

Similarly livestock sector of Pakistan is well equipped for biogas electricity generation. The 159 million cattle population in the country has the ability to produce manure for electricity generation as well as environmental impacts are extraordinary [49].Even half the available potential, if tapped, would produce 8.1 million m3 per day biogas [50].

Biogas technology has been prevalent in Pakistan for quite a while dating back to 1959 when the first use of this technology was made in construction of a farm manure plant in Sindh for biogas generation, used mostly in cooking [51]. Government of Pakistan, in 1974, made its first major step in the mainstreaming of the biogas technology through a project of 4137 biogas units; first stage with government funding, second stage with shared funding, and last stage with technical assistance only. Albeit the project was ambitious hardly any further progress was made. Another resurgence of the program occurred in 1990 when 1700 new plants were installed all over the country [52]. Similarly, in 2000 Biogas Support Programme (BSP) helped set up 1200 new digestors, amounting to 27% of domestic biogas capacity.

II. METHODOLOGY

The study was carried out in the Dera Ismail Khan District of Khyber Pakhtunkhwa province of Pakistan. The district shown in the figure 3.1 is the most populated district in the southern half of the province. Located on the west bank of River Indus, it is located at a distance of approximately 300 km from the provincial capital. The population of Dera Ismail Khan according to the 2017 census is 1,627,132, and ranks 37th in population across country. The climate of Dera Ismail Khan is hot desert like with extreme hot weather in summers and mildly cold in winters.

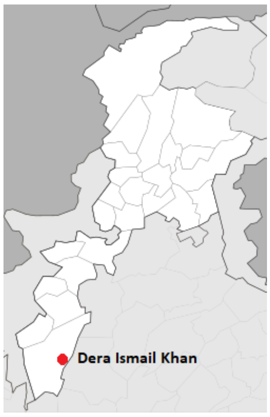

Figure 3. Geographic location of Dera Ismail Khan

The geographical spread of Dera Ismail Khan is 9,334 km2. The main crop of Dera Ismail khan is Wheat and sugar cane. It is home to three sugar mills. The educational situation is extremely bleak with only 47% literacy among the male and 21% literacy rate among the female population.

1) 3.2 Methods and Approach

a) Data collection

Primary data for DI Khan District was collected through questionnaires and sureveys conducted on ground. Secondary data was collected through internet research and consultation with relevant stakeholders such as Pakhtunkhwa Energy Development Organisation (PEDO), Provincial Energy Ministry, Municipal Corporation of DI Khan, and local elected bodies of each village visited. The surveys were targeting data relating to:

1. Socio economic spectrum of the respondents
2. Age of the respondents
3. Education level of the respondents
4. Questions relating to the satisfaction level of the households
5. Reasons for adopting biogas technology
6. Reasons for not adopting biogas technology
7. Financial details of the biogas installation and the cost benefits

b) Sampling procedures

Purposive Stratified Sampling Protocol (PSSP) was incorporated in the selection of the households for sampling of data and the sampling size and various dimensions in itself. Adopters and non adopters were selected from various villages and union councils of DI Khan District. The sample of household was geographically spread as much as possible to capture the whole strata of economic, social and educational variations. A total of 100 households were surveyed for the purpose of this research from 10 villages of DI Khan split among adopters and non adopters in 70 ratio 30.

c) Data Analysis

Following the collection and sorting of primary and secondary data in MS Excel, Statistical Package for Social Science (SPSS) and Statistical Analysis Systems (SAS) software were used for getting insights in to the raw data.

SPSS and SAS software have provision for performing various tests on social sector data for instance t-tests, chi-square test for determining significance of the data to end outcome, while logistic regression tests have the capacity to establish correlation among various variables in the data. Here we determined the impact of biogas technology on different socio economic variables and also the impact of socioeconomic and educational factors on the adoption of technology. A major question of the research: impact of biogas technology on livelihoods, was determined using DFID (1999) framework for sustainable livelihoods.

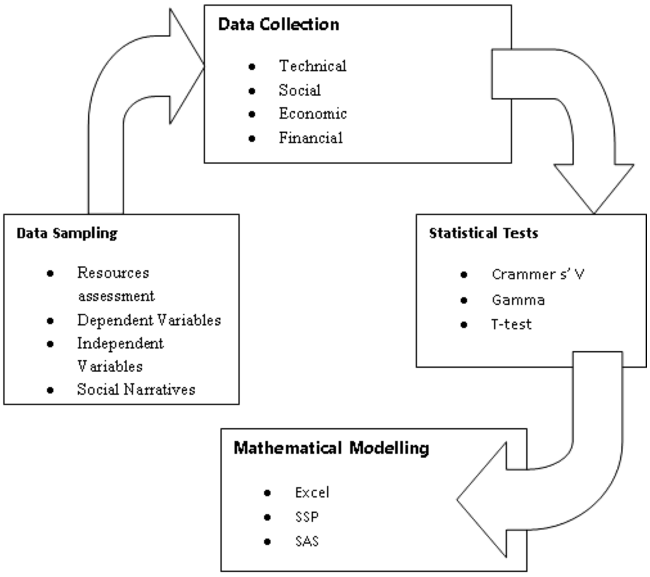

Figure 4 Concept of the research subject

d) Other analysis

In addition to the direct impact of the biogas technology on livelihoods and socioeconomic impacts, additional analyses were carried out as a part of the research. These analyses included:

1. Fuel and wood savings resulting from the use of biogas technology
2. Motivation of adopters for adopting the technology and barriers to non adopters in adopting the technology
3. Comparison of fuel usage and the concomitant savings for adopters of biogas technology
4. Time and workload reduction in fire wood collection
5. Impact of the technology on improving health of the adopters against the non adopters

A schematic of the research methodology from the data sampling techniques to the end impact assessment of the technology through SPSS, SAS software is given in the schematic below.

III. RESULTS AND DISCUSSIONS

This chapter deals with the various correlations and statistical analysis of the adopter and non adopters of the biogas technology. The analyses presented in the form of the tables and figures in the following sections are based in the first sections on establishing the significance of the various parameters to the end output i.e. the decision to adopt or not to adopt the biogas technology, while in the later sections the impact is quantified in form of the savings for adopters or environmental impact or the health benefits of the technology.

1) Socioeconomic demographic characteristics of the subjects

The research was based on 100 household surveys conducted in the district of DI Khan, among which 70 had biogas plants installed on their farms or households, while 30 did not have the technology. In the coming sections of this chapters the factors that the respondent perciece to be a deciding factor in their installing or not installing the technology is also delineated. A household, for the purpose of this study, was said to be adopter of the technology if the biogas plant installed on their premises was operational at the time of the survey or was operational for a considerable amount of time, say more than 6 months, to give them a better idea of the perks and benefits of the technology.

2) Size of the household

Here the role of size of the family is vetted in the adoption of biogas technology. It observed that size of the family for a major chunk of the respondents, 61.9% for adopters and 66.7% for non adopters, ranged from 2-5 persons. A few households, however, had members greater than ten. Chi-square test suggests that the very little significance is imparted to size of family in the determination of them being adopters or non adopters of the technology, $\chi 2$ was 0.811with df=2, and P=0.667 as shown in the table 3.

TABLE 3 SIZE OF THE HOUSEHOLD

Household size	Adopters Stats	Non-Adopters Stats	Total Dist.	Chi square $\chi 2$	P value

	N	%	N	%	0.811 (ns)	0.667
2 to 5	60	61.9	42	63.8		
6 to 9	33	34	19	32.5		
10 to 13	4	4.1	2	3.8		

The average family size for the 162 households was 5.3 and 4.9 for the biogas adopters and non adopters respectively. The T-test did not point to any significance for family size as influencer in the adoption of the technology as well, as shown in the table 4.

TABLE 4 IMPACT OF VARIOUS DEMOGRAPHICHS OF THE HOUSEHOLDS ON ADOPTION

Variable	Adopters stats			Non adopters stats		
	Mean	Std. Dev.	Std. Mean Error	Mean	Std. Dev.	Std. Mean Error
Family size	5.30	1.98	0.14	4.98	1.75	0.16
Farm Size	2.24	1.88	0.15	1.78	1.65	0.16
Age of Household Head (Yrs)	53.4	10.7	0.79	47.1	11.5	1.04
Children below 5 years	1.60	1.37	0.20	1.43	0.68	0.11
Number of People Living in the Household	1.60	1.37	0.20	1.43	0.68	0.11
Number of Cattle	9.20	7.40	0.52	5.19	4.34	0.42

3) Impact of farm size on adoption of biogas technology

The results for the chi square test for the adopters and non adopters of biogas technology among the 162 respondents are given in the table 3 below. The results show that the land size on average among the adopters is 2.24 while among the non adopters it is 1.78 acres. The land size in majority of the cases was between 0.1 and 1 acre as shown in table 5, in 78.2% among non adopters and 68.3 % among adopters. Farm size was found to be a significant influencing factor in the decision to adopt biogas technology as the chi squared value of 2.08 suggests. This could be because a larger land could mean greater wealth and resultantly no impact on other expenditures from diverting funds to installation of the plant. Also it could be because of the greater number of cattle or livestock on large farm and hence more feed for the plant.

4) Impact of Age, Education, and Gender of respondents on satisfaction

In the majority of the cases a single person in the household was responsible for the financial decision making in the family as is required when deciding to install a biogas plant. This head of household was usually the respondent in our survey. The gender of the household in most cases was male owing to the culture of DI Khan district. Gender of the head of household was not found in any considerable conformation with the adoption of the technology; a fact also supported by literature [90].

Furthermore the middle age group of 41 to 60 years was most recurrent when the respondents were asked about their ages. The age of the respondent, or age in general, was significant in the adoption of the technology as shown in the table 6 with Chi square value of 18.41 and P value of 0.001.

Surprisingly the education level of the adopters and non-adopters of the biogas technology did not indicate any statistically significant correlation with the decision to adopt the technology as shown in the table 3with a Chi square value of 2.12 and P value of 0.331.

TABLE 5 IMPACT OF FARM SIZE ON ADOPTION OF BIOGAS TECHNOLOGY

Farm parameters	Adopters Details		Non-Adopters Details		Total distribution		Chi Square	P value
	N	%	N	%	N	%		
Farm Size in Acre								
0.1-1.0	56	68.3	43	78.2	99	68.3	2.08 (s)	0.038
2.1-3	12	14	7	12.7	19	14		
3.1-4.0	9	11	2	4.5	11	11		
4.1-12	5	6.7	3	4.5	8	6.7		
Construction material in the households								
Mud and stone	19	0	35	62.2	22	1	63.36	<=0.001
Wood	0	19.6	3	2.7	58	35.1		
Cement, bricks	78	80.4	20	35.1	98	63.9		
Roof Type in the households								
Cement	59	47	59	93	105	80.8	18.87 (s)	P<= .001
Steel Sheets	5	7	5	7	32	19.2		

TABLE 6 IMPACT OF AGE, EDUCATION, AND GENDER OF RESPONDENTS ON SATISFACTION

Demographics	Adopters		Non-adopters		Total		Chi Square	P Value
	Number	Percent	Number	Percent	Number	Percent		
				Age Demographics				
21-40	12	13.3	20	32	32	20.8	18.41 (s)	≤0.001
41-60	57	63	35	57.4	92	60.7		
61-80	21	23.8	6	10.7	27	18.5		
				Gender Demographics				
Male	78	87.7	53	83.5	132	85.9	1.11 (ns)	0.292
Female	11	12.3	11	16.5	22	14.1		

				Education Demographics				
Primary	24	29.1	17	33	41	30.6	2.12 (ns)	0.331
Secondary	33	40	24	44.3	57	41.7		
Tertiary	26	30.9	12	22.6	38	27.7		

5) Livestock type and abundance: Impact on biogas adoption

Since the country as a whole and DI Khan specifically is an agricultural country, the elevated levels of cattle and livestock ownership is not surprising. The variety and abundance of the livestock is shown in the table 7. Interestingly the non-adopters also owned livestock in significant numbers, hence the availability of animal waste or biomass, or lack thereof, could not be deemed a significant factor in the adoption of the technology.

TABLE 7 LIVESTOCK TYPE AND ABUNDANCE

Type of Livestock	Adopters				Non-adopters			
	N	Mean	Std Deviation	Std. Error of Mean	N	Mean	Std Deviation	Std. Error of Mean
Cattle	98	4.11	7.44	0.29	55	2.6	2.11	0.21
Poultry	47	69.4	190.4	19.54	35	18.3	38.5	4.68
Sheep	15	2.25	1.94	0.384	9	3.74	4.93	1.33

6) Why do the adopters prefer biogas technology

When asked about the reasons why they preferred biogas technology to the conventional technologies, the respondents gave a variety of reasons. In most cases the biogas technology being clean energy technology and its fuel cost saving potential is considered the most convincing reason for the technology adoption among other reasons as shown in the table 8.

7) Information access about biogas technology

The first step in the adoption of the biogas technology, or any technology for that matter, is knowledge about its existence and its installation procedures along with the benefits it offers. Our survey of the adopters and non adopters of the biogas technology suggests that they came to know about the technology from varying sources. The majority of cases of awareness of the technology was brought about by word of mouth with 75% in adopters and 54% in non adopters. The government and NGOs have a lot of work to improve their share in the awareness creation about this useful technology with their 18 % influence rate through aggressive campaigns as shown in the table 9.

TABLE 8 WHY DO THE ADOPTERS PREFER BIOGAS TECHNOLOGY

Motivation	Responses		
	N	%	Rank
Cooking time	77	77	1
Fuel savings	76	77	2
Economical	73	73	3
Environmentally beneficial	63	62.5	4
Smoke eradication	61	61	5
Health	36	36	6
Affordable cost	27	27.5	7

Subsidy from govt.	26	15.5	8
Social benefits/ status symbol	17	16.5	9
Avenue of use for farm wastes	11	11	10
Durability	9	9.5	11
Neighbors inspired	7	7.5	12
Service provider motivated	4	3.5	13
High cost of other fuels	2	1.5	14
Other motivators	3	1.5	15

TABLE 9 SOURCES OF INFORMATION ABOUT BIOGAS TECHNOLOGY

Source of information	**Adopters**		**Non Adopters**		
	N	**%**	**Non Adopters**	**%**	**rank**
Word of Mouth	79	75	43	54	1
Government or NGO	18	18	14	17.4	2
TV or Radio	14	14	13	16.8	3
Exhibitions and Promotional events	9	9	7	9.7	4
Relatives	4	3.5	-	-	5
Shops	0	0	1	0.6	6

The abovementioned analyses have given us a first of its kind insight into the hurdles and supporting factors in the progression of biogas plant installations in the Khyber Pakhtunkhwa Province of Pakistan.

The recommendations based on these findings in the next chapter will be extremely helpful in making biogas plants common in the rural areas of the province. Furthermore the lessons learnt will be instrumental in devising the strategies and policies in future by the energy department and NGOs to best tackle the issue.

CONFLICT OF INTEREST

The author declares no conflict of interest.

CONCUSLION

Biogas provides energy in the adopting households essential to the life of the adopters. Primarily installed as a cheap cooking resource, the technology is a groundbreaking addition to the rural electrification cause. Despite all the benefits of the technology the adoption rate is extremely low for which this research was successful in investigating the root causes.

At first a variety of independent variables for instance size of the farm, Education level of the households in general and the decision makers in particular, type and abundance of cattle owned by the households, and the age and gender of the decision makers in the households was compared with the adoption to investigate the existence of any correlation, however these factors were all found to have low significance in the adoption of the technology.

In addition the surveys uncovered the most important reasons the adopters of the technology gave for their installation of the technology. The major awareness factor about the technology for adopters was through the word of mouth. On the contrary the chief hampering agent in the adoption of the technology among the non adopting families was found to be the high upfront installation costs of the technology.

Furthermore the health benefits of the biogas technology adoption were beyond the initial expectation accrued mainly from the reduction of hazardous wood smoke that the family members are subjected to during conventional cooking techniques of directly burning the wood under the food. This indirectly leads to ease of work for the female population of the adopting household, giving them extra time for doing progressive skill acquisition practices and enhanced child care.

The technology was found to give a more efficient mechanism for burning biomass than the conventional techniques. The costs thus saved on conventional fuel procurement by the economically disadvantaged population of DI Khan are very desirable for the social and economic upliftment of the area. The technology could be emulated in other regions of the province and country to extend these social and livelihood enhancement.

The environmental benefits of the technology are another desirable factor which could be used to advocate the technology to funding and governmental agencies. On average a single biogas plant installed in the DI Khan District was found to be mitigating approximately 2.2 tones of CO2 from being released in to the atmosphere on account of the conventional fuel avoided, and efficient burning of the fuel.

The type of the digester being used by the locals did not seem to influence the adoption rate of the technology. This could be because of the small impact the type of digester has on the performance of the plant.

REFERENCES

[1] J. C. L. Liu Yang, Haiyan Yan, "Thermal comfort and building energy consumption implications- A review," Appl. Energy, vol. 115, pp. 164–173, 2014.

[2] World Energy Outlook 2017. OECD, 2017.

[3] H. Zhao and F. Magoulès, "A review on the prediction of building energy consumption," Renew. Sustain. Energy Rev., vol. 16, no. 6, pp. 3586–3592, Aug. 2012.

[4] I. Economic Adviser's Wing, Finance Division, Government of Pakistan, "Economic Adviser's Wing, Wing Finance Division, Government of Pakistan, Islamabad www.finance.gov.pk," 2018.

[5] M. ud D. Q. Ahmed Sohail, "Energy-Efficient Buildings in Pakistan," A Sci. J. COMSATS – Sci. Vis. Vol.16 Vol. 17, vol. 16, no. December, pp. 27–38, 2011.

[6] A. Masood, "SAARC Energy Centre," 2010.

[7] K. Ahmad, A. F. Rafique, and S. Badshah, "Energy Efficient Residential Buildings in Pakistan," Energy Environ., vol. 25, no. 5, pp. 991–1002, 2014.

[8] ASHRAE, Handbook Heating, Ventilating, and Air-Conditioning system and equipement. Atlanta: The American Society of Heating, Refrigerating and Air Conditioning Engineers, Inc., 2012.

[9] B. A. Holm, L. Blodgett, D. Jennejohn, and K. Gawell, "Geothermal Energy : International Market Update Geothermal Energy Association," no. May, 2010.

[10] U. Younas et al., "Pakistan geothermal renewable energy potential for electric power generation: A survey," Renew. Sustain. Energy Rev., vol. 63, pp. 398–413, 2016.

[11] H. Zaisheng, "Geothermal Heat Pumps in China – Present Status and Future Development," pp. 31–33, 2008.

[12] G. Florides and S. Kalogirou, "Ground heat exchangers-A review of systems, models and applications," Renewable Energy. 2007.

[13] L. Ozgener, "A review on the experimental and analytical analysis of earth to air heat exchanger (EAHE) systems in Turkey," Renew. Sustain. Energy Rev., vol. 15, no. 9, pp. 4483–4490, 2011.

[14] E. Mands, M. Sauer, E. Grundmann, B. Sanner, and U. Gbr, "Shallow geothermal energy use in industry in Germany," Eur. Geotherm. Congr. 2016, vol. 2010, no. 2013, pp. 19–24, 2016.

[15] A. Chel and G.N.Tiwari, "Performance evaluation and life cycle cost analysis of earth to air heat exchanger integrated with adobe building for New Delhi composite climate," Energy Build., vol. 41, no. 1, pp. 56–66, Jan. 2009.

[16] R. Kumar, S. C. Kaushik, and S. N. Garg, "Heating and cooling potential of an earth-to-air heat exchanger using artificial neural network," Renew. Energy, vol. 31, no. 8, pp. 1139–1155, 2006.

[17] G. Mihalakakou, "On estimating soil surface temperature profiles," Energy Build., vol. 34, pp. 251–259, 2002.

[18] K. Labs, "Ground cooling, in: J. Cook (Ed.), Passive Cooling." MIT Press, Cambridge, 1992.

[19] G. Florides and S. Kalogirou, "Ground heat exchangers-A review of systems, models and applications," Renew. Energy, vol. 32, no. 15, pp. 2461–2478, 2007.

[20] B. B. Popiel, C., J. Wojtkowiak, "Measurements of temperature distribution in ground," Exp. Therm. Fluid Sci., vol. 25, pp. 301–309, 2001.

[21] A. O. Ogunlela, "Modelling Soil Temperature Variations," J. Agric. Resour. Dev., pp. 100–109, 2003.

[22] H. Ben Jmaa Derbel and O. Kanoun, "Investigation of the ground thermal potential in tunisia focused towards heating and cooling applications," Appl. Therm. Eng., vol. 30, no. 10, pp. 1091–1100, 2010.

[23] F. Al-Ajmi, D. L. Loveday, and V. I. Hanby, "The cooling potential of earth-air heat exchangers for domestic buildings in a desert climate," Build. Environ., vol. 41, no. 3, pp. 235–244, 2006.

[24] R. J. Sharan, G., "Soil temperature regime at Ahmedabad," J. Agric. Eng., vol. 39, no. 1, 2002.

[25] A. G. Kanaris, A. A. Mouza, and S. V. Paras, "Flow and Heat Transfer Prediction in a Corrugated Plate Heat Exchanger using a CFD Code," Chem. Eng. Technol., vol. 29, no. 8, pp. 923–930, 2006.

[26] V. P. Kabashnikov, L. N. Danilevskii, V. P. Nekrasov, and I. P. Vityaz, "Analytical and numerical investigation of the characteristics of a soil heat exchanger for ventilation systems," Int. J. Heat Mass Transf., vol. 45, no. 11, pp. 2407–2418, 2002.

[27] M. Santamouris, G. Mihalakakou, A. Argiriou, and D. N. Asimakopoulos, "ON THE PERFORMANCE OF BUILDINGS COUPLED EARTH TO AIR HEAT EXCHANGERS WITH If a balance temperature , Tb is used where :," Sol. Energy, vol. 54, no. 6, pp. 375–380, 1995.

[28] G. Mihalakakou, M. Santamouris, J. O. Lewis, and D. N. Asimakopoulos, "On the application of the energy balance equation to predict ground temperature profiles," Sol. Energy, vol. 60, no. 3–4, pp. 181–190, 1997.

[29] O. Ozgener, L. Ozgener, and J. W. Tester, "A practical approach to predict soil temperature variations for geothermal (ground) heat exchangers applications," Int. J. Heat Mass Transf., vol. 62, no. 1, pp. 473–480, 2013.

[30] H. Su, X. Liu, L. Ji, and J. Mu, "A numerical model of a deeply buried air – earth – tunnel heat exchanger," Energy Build., vol. 48, pp. 233–239, 2012.

[31] A. Sehli, A. Hasni, and M. Tamali, "The potential of earth-air heat exchangers for low energy cooling of buildings in South Algeria," Energy Procedia, vol. 18, pp. 496–506, 2012.

[32] M. De Paepe and A. Janssens, "Thermo-hydraulic design of earth-air heat exchangers," Energy Build., vol. 35, no. 4, pp. 389–397, 2003.

[33] J. Pfafferott, "Evaluation of earth-to-air heat exchangers with a standardised method to calculate energy efficiency," Energy Build., vol. 35, no. 10, pp. 971–983, 2003.

[34] A. De Jesus Freire, J. L. Coelho Alexandre, V. Bruno Silva, N. Dinis Couto, and A. Rouboa, "Compact buried pipes system analysis for indoor air conditioning," Appl. Therm. Eng., vol. 51, no. 1–2, pp. 1124–1134, 2013.

[35] K. H. Lee and R. K. Strand, "The cooling and heating potential of an earth tube system in buildings," Energy Build., vol. 40, no. 4, pp. 486–494, 2008.

[36] P. Hollmuller, "Analytical characterisation of amplitude-dampening and phase-shifting in air/soil heat-exchangers," Int. J. Heat Mass Transf., vol. 46, no. 22, pp. 4303–4317, 2003.

[37] M. Cucumo, S. Cucumo, L. Montoro, and A. Vulcano, "A one-dimensional transient analytical model for earth-to-air heat exchangers, taking into account condensation phenomena and thermal perturbation from the upper free surface as well as around the buried pipes," Int. J. Heat Mass Transf., vol. 51, no. 3–4, pp. 506–516, 2008.

[38] V. Badescu, "Simple and accurate model for the ground heat exchanger of a passive house," Renew. Energy, vol. 32, no. 5, pp. 845–855, 2007.

[39] X. Li, J. Zhao, and Q. Zhou, "Inner heat source model with heat and moisture transfer in soil around the underground heat exchanger," Appl. Therm. Engiineering, vol. 25, no. 10, pp. 1565–1577, 2005.

[40] J. Zhao, H. Wang, X. Li, and C. Dai, "Experimental investigation and theoretical model of heat transfer of saturated soil around coaxial ground

coupled heat exchanger," Appl. Therm. Engiineering, vol. 28, no. 2–3, pp. 116–125, 2008.

[41] T. S. Bisoniya, A. Kumar, and P. Baredar, "Study on Calculation Models of Earth-Air Heat Exchanger Systems," J. Energy, vol. 2014, pp. 1–15, 2014.

[42] V. Bansal, R. Misra, G. Das Agrawal, and J. Mathur, "Performance analysis of earth – pipe – air heat exchanger for winter heating," Energy Build., vol. 41, no. 11,05, pp. 1151–1154, 2009.

[43] K. W. A.Flaga-Maryanczyka, J. Schnotale, J. Radon, "Experimental measurements and CFD simulation of a ground source heat exchanger operating at a cold climate for a passive house ventilation system.pdf," Energy Build., vol. 68, pp. 562–570, 2014.

[44] L. Ramírez-Dávila, J. Xamán, J. Arce, G. Álvarez, and I. Hernández-Pérez, "Numerical study of earth-to-air heat exchanger for three different climates," Energy Build., vol. 76, pp. 238–248, Jun. 2014.

[45] R. Kumar, A. R. Sinha, B. K. Singh, and U. Modhukalya, "A design optimization tool of earth-to-air heat exchanger using a genetic algorithm," Renew. Energy, vol. 33, no. 10, pp. 2282–2288, Oct. 2008.

[46] F. Ascione, L. Bellia, and F. Minichiello, "Earth-to-air heat exchangers for Italian climates," Renew. Energy, vol. 36, no. 8, pp. 2177–2188, 2011.

[47] A. N. Z. Sanusi, L. Shao, and N. Ibrahim, "Passive ground cooling system for low energy buildings in Malaysia (hot and humid climates)," Renew. Energy, vol. 49, pp. 193–196, Jan. 2013.

[48] N. Aziah, M. Ariffin, A. Nur, Z. Sanusi, and A. M. Noor, "Materials for the Earth Air Pipe Exchanger (EAPHE) system as a passive ground cooling for hot-umid climate," 2nd Int. Conf. Emerg. Trends Sci. Res. 2014, no. November, 2014.

[49] S. Jakhar, R. Misra, M. S. Soni, and N. Gakkhar, "Parametric simulation and experimental analysis of earth air heat exchanger with solar air heating duct," Eng. Sci. Technol. an Int. J., vol. 19, no. 2, pp. 1059–1066, 2016.

[50] M. K. Ghosal, G. N. Tiwari, D. K. Das, and K. P. Pandey, "Modeling and comparative thermal performance of ground air collector and earth air heat exchanger for heating of greenhouse," Energy Build., vol. 37, no. 6, pp. 613–621, Jun. 2005.

[51] A. H. Poshtiri and N. Gilani, "Feasibility study on using solar chimney and earth-to-air heat exchanger for natural heating of buildings," World Renew. Congr., pp. 1773–1780, 2011.

[52] S. F. Ahmed, M. M. K. Khan, M. G. Rasul, M. T. O. Amanullah, and N. M. S. Hassan, "Comparison of earth pipe cooling performance between two different piping systems," Energy Procedia, vol. 61, pp. 1897–1901, 2014.

[53] M. S. Kristen, "Final report laboratory research for the determination of the thermal properties of soils," 1949.

[54] K. H. Lee and R. K. Strand, "The cooling and heating potential of an earth tube system in buildings," Energy Build., vol. 40, no. 4, pp. 486–494, 2008.

[55] F. Ascione, L. Bellia, and F. Minichiello, "Earth-to-air heat exchangers for Italian climates," Renew. Energy, vol. 36, no. 8, pp. 2177–2188, 2011.

[56] A. P. H. Maerefat, "Passive cooling of buildings by using integrated earth to air heat exchanger and solar chimney," Renew. Energy, vol. 35, no. 10, pp. 2316–2324, 2010.

[57] Incropera, Introduction to Heat transfer. 1996.

[58] "Engineering Toolbox," 2009. [Online]. Available: https://www.engineeringtoolbox.com/prandtl-number-d_1068.html 9.

Muhammad Haseeb is a postgraduate researcher at United States Pakistan Center for Advanced Studies in Energy at University of Engineering and Technology Peshawar, Pakistan. He is studying Materials for Energy Storage and Conversion at MS level after doing his undergraduate degree in Mechanical Engineering. His research interest include finding ways to maximize the social and economic benefits of the distributed energy systems with an end goal of poverty alleviation through sociotechnical models. This paper is a part of his Masters degree research studies.

International Journal of Engineering Works
ISSN-p: 2521-2419
ISSN-e: 2409-2770
Vol. 6, Issue 10, PP. 324-332, October 2019
https://www.ijew.io/
https://doi.org/10.34259/ijew.19.610324332

Analysis of Electricity from Municiple Solid Waste of Peshawar City by Utilized plasma Arc Gasification Technique

Wajid Ali[1], Muhammad Asif[2]
[1,2]Department of Electrical Engineering, University of Engineering & Technology Peshawar, Pakistan
Received: 15 September, Revised: 30 September, Accepted: 02 October

***Abstract*—**The utilization of the waste to energy technology was studied for Peshawar city, the data was compiled from the authentic data base of Municipal Corporation Peshawar. It includes the data from twelve different regions of Peshawar city. It is estimated that the flammable share of MSW of Peshawar city in tons will be 544.38 tons. Hence a power of 18.5 MW can be generated from MSW of Peshawar City by utilization of Plasma Arc Gasification Technique. It's suggested that 18.5MW Power Plant will generate electricity @ 9 ₵/ KWh which is less as compare to current national average rate.

***Keywords*—** Municipal Solid waste Fueled Power Plant, Pakistan Power Crises, Waste to Energy, Electric Power Generation.

I. Introduction

Imagine a process in which we convert the inorganic components of the municipal solid waste in architectural tiles and construction bricks, at the same time we convert all the organic contents of the waste into synthesis gas, that is actually a mixture of hydrogen and carbon mono oxide (h2 + co), almost a green fuel and in addition we generate electrical power. furthermore, Showing Power generation (Energy mix) of Pakistan in year 2014[3] in summer minimum 3340 and max 6902 ,could we have a system that doesn't generate ashes, and doesn't pollute the air, the water nor the soil, as incineration does? The answer is yes. The first wind turbine was designed and built in 1888 by Charles brush generated a peak power of 12 KW [11] but so it is not beter.

The plasma torches that operate at very high temperatures (between 5,000ºC and 100,000ºC) can process all kinds of waste: municipal solid, toxic, medical, biohazard, industrial and nuclear waste at atmospheric pressure. The inorganic waste is vitrified effectively, in solid-like glass materials that are used to manufacture aggregates for the construction industry (Magmavication process) and the organic materials that includes plastics, paper, oil, bio-materials, etc. are converted into Syngas with caloric value, fuel that is used on the Heavy-duty advanced gas turbines for the generation of electrical power (Gasification process). No ashes are produced because at more than 5,000ºC, all the Organic Molecules Are Disintegrated And Only The Mix Of H2 + Co Remains At High Temperature The per capita electricity availability is 43W, which is 1/7th of the world average [6].This Paper Is Going To Describe The Emerging Waste-To-Energy (Wtssse) Technology, Called Plasma Gasification. The Technology Will Be Described And Compared To Incineration And Gasification. A Model Will Be Employed To Compare The Energy Content Of The Resulting Gas Products From The Plasma Gasification Process For Various Types Of Waste Feedstock. Plasma Gasification Has Many Advantages And Some Disadvantages Compared To Other Wte Methods Which Will Be Described. Depending On The Objective Of Developing A Particular Wte Plant, The Plasma Gasification Technology Advantages Could Outweigh The Disadvantages The burden on the economy of Pakistan due to heavy oil imports can be revealed from the fact that 40% of the total imports in 2011 were consist of oil with overall trade deficit of 14% [6].

A. *Contents of Municipal Waste*

Municipal Solid Waste (MSW) is garbage or trash waste which consists of day to day used or discarded item by the public. The main composite of MSW includes our daily life refuses house holes such as fruits refuses, vegetable refuses, remaining of tree trimming. The major types of MSW are Recyclable waste, inert waste and Bio degradable waste. Recyclable waste contain cloths, paper, pin cans, glass bottles and certain plastic etc. Inert waste is type of waste which consists of demolition sites, dirt, rocks, and debris from construction. Bio degradable generally includes the waste of kitchen (vegetable and fruits). The main things among all the conversion technologies are the burring of MSW to generate steam or heat which is then converted to generate power.

B. *Technologies used to process Wastes*

The four common techniques used for MSW are Pyrolysis, Conventional gasification,

II. Plasma gasification and Incineration or Conventional Mass-burn incineration

A. *Pyrolysis*

This process involves thermal decomposition of organic substances in the absence of atmosphere or oxygen. This technique is an endothermic process. The organic wastes are placed in sealed air tight drums known as pyrolysis chamber. If one tone of MSW is used by this process, an average of 571KWH power can be generated.

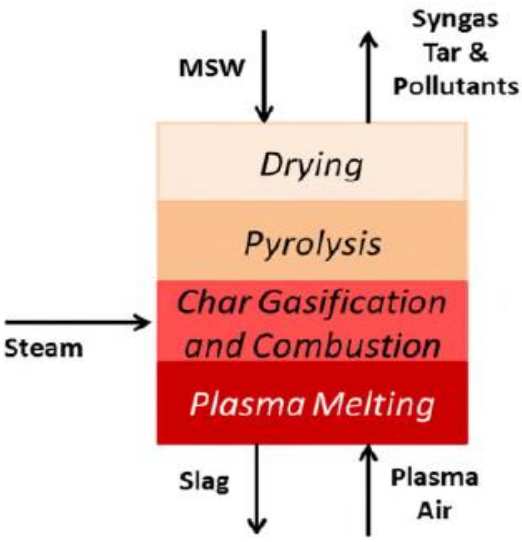

Figure.1

III. INCINERATION OR CONVENTIONAL MASS-BURN INCINERATION

Incineration or mass burn is a technique of the burning of municipal solid waste in the presence of oxygen or air, the technique is known as Incineration. The average power generation in incineration conversion technique is 544KWHper ton ,The end products from the process of conventional methane CH4 and predominantly gases Hydrogen H2 and CO[1] Municipal solid waste in limited availability of oxygen or air. In conventional gasification process one ton of municipal solid waste can produce an average of 685KWh of power.

Plasma gasification: Plasma arc gasification is a conversion technology. It produces electricity from organic compound in which hot ionized gas is used to decompose the organic compound. The main advantage of this technology is to decrease the harmful effects of ash from the incinerator. In this technique the amount of power generated is 816KWH per ton which is the highest among all conversion technologies of MSW. Slag is produce as by-product and can be used in construction of road or other material like flower tiles, roof tiles and insulating material.

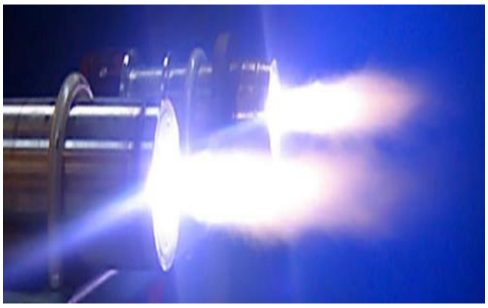

Fig No 2: Plasma arc gasification.

B. Municipal Solid Waste Collection in Peshawar

The waste collected by Municipal Corporation can be estimated by the schedule of MSW collection facility computation and capability. The waste collection from Peshawar city is collected by municipal corporation Peshawar. The waste is mainly collected from the old city area of Peshawar. The Cantt board of Peshawar collected MSW from cantonment region. MSW amount is approximately 1331 tons per day. MSW generated by each person can be calculated as

$$MSW = \frac{1331 tons}{3.5 millions} = \frac{0.38 Kg}{person\ per\ day}$$

Pakistan is 6th most populated country in the world, with population of around 190 million and is 2.56 % of world total population. However, our energy consumption standing is 37th in the world which is about 0.37 % of worlds total energy consumption. Energy available to per person is 43 watt that is 0.14 times the average utilization of per person in the world.[6] The sun radiates light energy like photons which rush toward the earth with a speed of 670 million miles per hour and reaches to the earth in approximately eight minutes [14]. Photovoltaic material such as silicon absorbs light photons and increases the kinetic energy of the electrons of its own and transfers them into higher energy levels within the material and some of them to conduction band to produce electricity. According to Pakistan Electric Power Company PEPCO, in April 2011, the shortfall in power generation across the country reached up to 5000MW, with demand standing at 14,475MW and supply at 9465 MW[7] In order to increase the portion of hydel energy in energy mix of Pakistan some of medium and small hydel power projects are under construction amongst which the most effective will be Neelam Jehlum Hydro power plant having a capacity of 969 MW and will be available in system till 2016 [13].

Methodology:

Pyrolysis and conventional gasification are less effective than mass burn is low generation. Plasma Arc Gasification is a conversion technology to produce electricity from organic compound in which hot ionized gas is used to decompose the organic compound to generate power. The main advantage of this technology is to decrease the harmful effects of ash from the incinerator. In this process the temperature of the air is kept up to7000F. The heat is provided using AC or DC electric discharge in Plasma Arc gasification chamber Waste incineration to generate power[19] and new technologies such as Plasma Arc Gasification [5]. Generation of electricity from Waste. The inorganic material is converted into melted form and is later on converted into glassy material which is non-harmful by cooling process. Conventional Gasification and pyrolysis has less efficiency then other two conversion techniques [5] due to slow and sensitive conversion process and hence not desirable. In Arc Plasma gasification technique air is controlled in the chamber. It has better results as compared to conventional mass burn that is 816 KWh/ton with the cost of approximately 9 to 10 ₵/ KWh which is comparatively less than our national average cost of 14 cents per KWh. Slag produce from Plasma Arc gasification technique is much less harmful as compare to others. It can be used as insulating material, road construction and making of industry tiles and has almost costs 15$/ ton [1, 2]. The operational complexities and high capital cost are the hurdles to this technique but with the ongoing research in this field is overcoming these complexities. The cost of power generation through direct incinerations is approximately 5₵/ KWh [15] which is comparatively less than other conversion techniques but the main dis advantage of this conversion technique is the harmful effectives of hazardous gases produce through this process, less power generation and less power generation per unite mass of MSW as 544KWH. While in plasma arc gasification process less harmful gases produce and the unite power generation through this process is much greater than other conversion technique which is 816KWH/ton and its cost is 9 - 10 ₵/ KWh which is comparatively less than our national average cost of electricity 14₵/ KWh[8]. As there is electricity crises in Pakistan that's why plasma Arc Gasification technique is most suitable due to its high power generation in future for Peshawar city . Diagram Plasma arc gasification process.

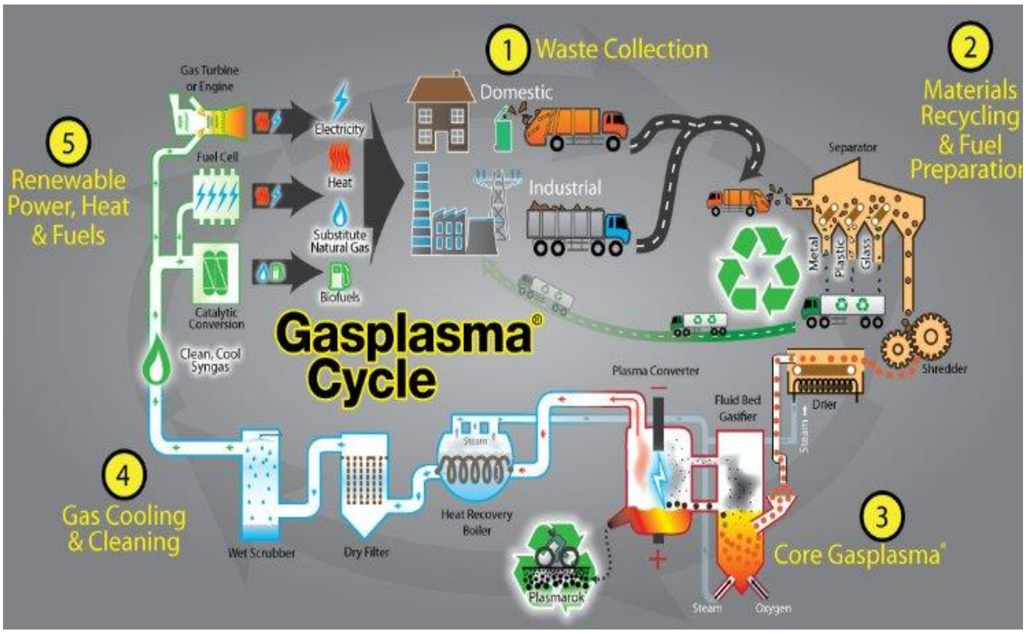

Fig no5:Gas Plasma Cycle

Average msw collected by city Municipal Corporation per day:

TABLE NO1: TOTAL MSW OF PESHAWAR CITY/DAY

vehicle	Number of vehicles	no of trips	waste carrying capacity of each in ton	total in ton
container	130	1	5	650
trucks	24	2	4	192
tructor trolly	30	3	3.5	315
mini tractor trolly	15	3	2	90
pick ups	28	3	1	84
total				1331

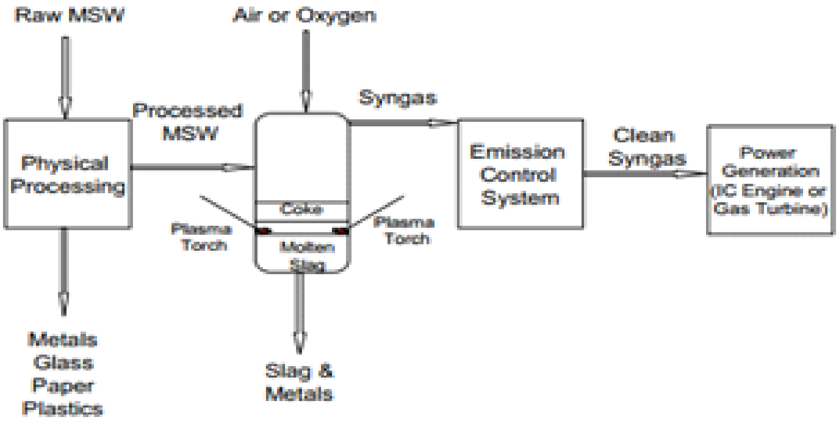

Fig: No3Plasma Arc gasification chamber

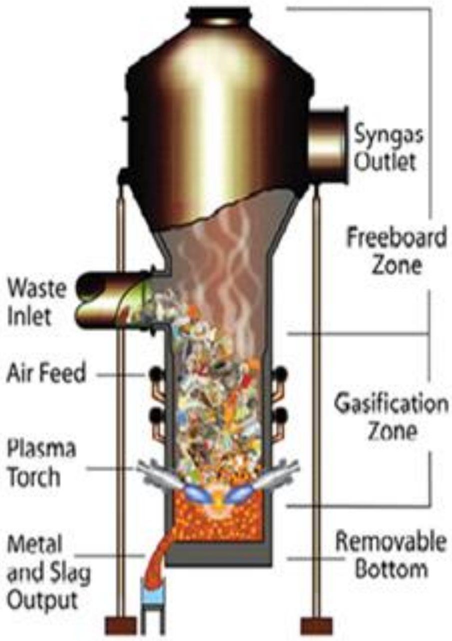

Fig no4:The inside 3D view of Plasma Arc gasification chamber

The Composition of MSW of Peshawar City.

MSW is combination of paper products, textiles products, plastics, cardboard materials wood fragments and Food wastes such as vegetables and fruits. Paper products and plastics can be recycled to manufacture new products but all of them cannot be separated from one another. The percentage arrangement MSW is described in the figure.

The below figures present the percentage composition of MSW of Peshawar city :

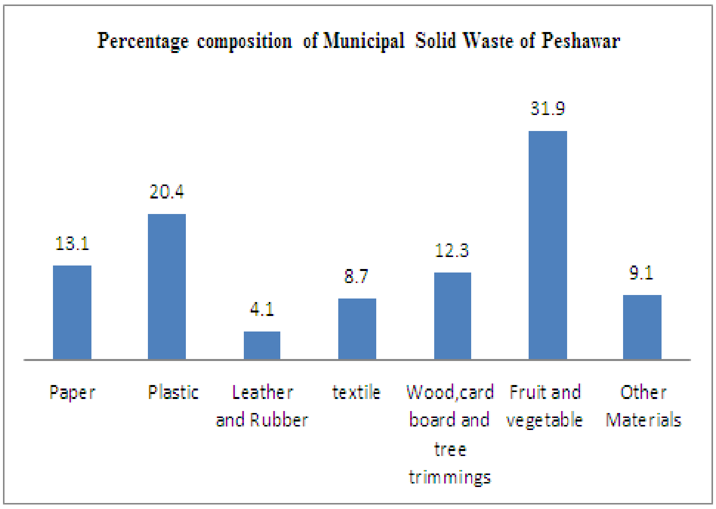

Fig no5 : Percentage Composition Of Municipal Solid waste

The The analyses of composition of the waste sample are collected from 12 different locations of Peshawar city and the composition in percentage is shown above. The result

Shows that main components of MSW are vegetable and fruit wastes which share about 31.9% of total waste. The second component of MSW is plastic which about 20.4% of the total waste is,. The third component of MSW is paper product which has calorific value of 1677.6KJ/kg. The other component of MSW are dry grass, card board, tree trimming and practical of wood which has calorific value of 19305.8KJ/kg which consist 12.3%of the waste of Peshawar city. The non-flammable materials of MSW are metal, clay and ceramics which is 9.1% of the total waste of Peshawar. The below figures present the percentage composition of MSW of Peshawar city. Power generation capacity of different MSW Conversion Technologies [4] Mass burn (Incineration) 544 kWh/ton MSW, Pyrolysis 571 kWh/ton MSW, Conventional Gasification685 kWh/ton MSW, Plasma Arc Gasification 816 kWh/ton MSW the some different other source is also used for power generation tidal energy .

Turbines are used in water passages to convert the potential energy of difference in water levels into the kinetic energy and then to rotational energy to generate power. The openings are designed with specific gates which allow large flow of water with modest differential head [16] Bio-energy is a form of renewable energy derived from materials of biological sources Since 1990 world energy supplies growth is recorded as 1.4 % and the growing contribution of renewable sources is 1.7%. 10.4 % of world total energy is contributed by Bio mass and new renewable sources such as Wind, Solar and tidal contributes only 1 % of total energies. In Sweden biomass provides 16% of total energy produced, in Brazil 27% and in Finland 19% [17]. Bio energy sources are made up of mainly forests, agricultural, and wastes A 23 MW of Tracy in California a plant uses wood straws as a fuel and generated 138,139 MWh in 2010 only by running at an average capacity of 69MW[18].

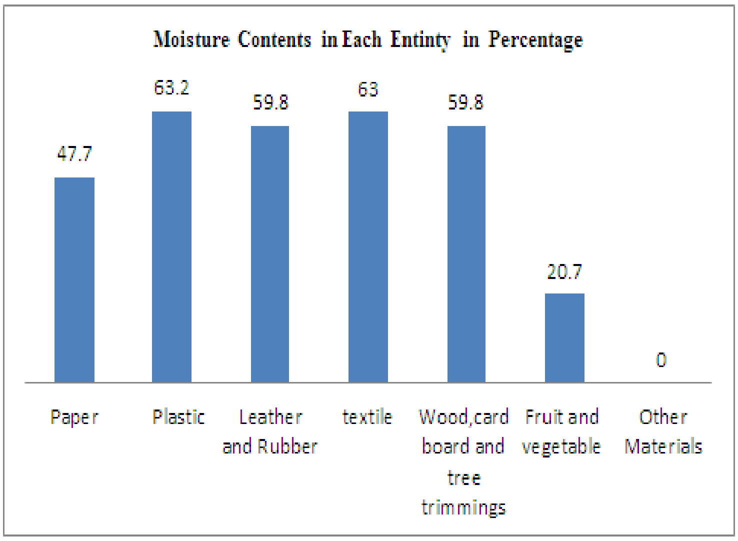

Fig no6: Moisture Contents in Each Entinty in Percentage

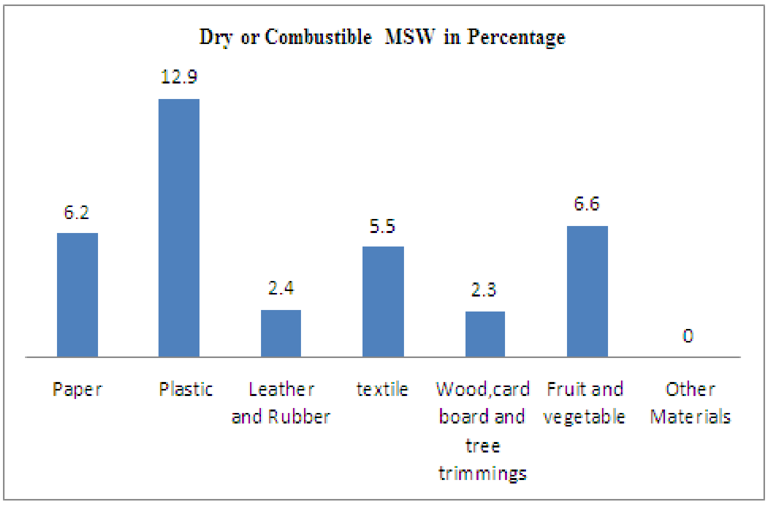

Fig no 7: Dry or Combustible MSW in Percentage

The Heat Generating Estimation: Each component is have a heating value, the below table is showing the heating value of different compound of MSW in BTU/Lb and KJ/Kg [20]. Each component of municipal solid waste have a specific value of water contents. The demographics condition and climate have a deep effect on the moisture intensity in waste. The analysis of MSW shows that dry waste is 40.9% [20] of the total MSW.

The capacity of MSW power plant and its estimation:

The combustible or dry part of Municipal Solid Waste in percent is given as 40.9 % In above Fig

The combustible share of MSW of Peshawar city in tons will be = = 544.38 tons

The share of combustible MSW of Peshawar city in tons will be = 544.38 Tons

Converting the value of 9841.1KJ/Kg into MJ/ton

9841.1 MJ/ton

And also 1 joule = 0.000277 Wh So 9841.1MJ/ton can produce 2.7336 MWh/ton

Considering 20 % thermal efficiency [19], the energy generated in KJ per ton will be

2.7336*0.2 MWh = 544 KWh

The equation in fig shows the results much closer to the standard values as mentioned in the above fig Now by taking the value of combustible MSW of Peshawar city as 544.38 and the standard value of 816 KWh/ton through Plasma arc gasification.

816 KWh/ton * 544.38 tons = 444214 KWh/ day
So =[444214 KWH/24 =18508.9 KW]=18.5 MW

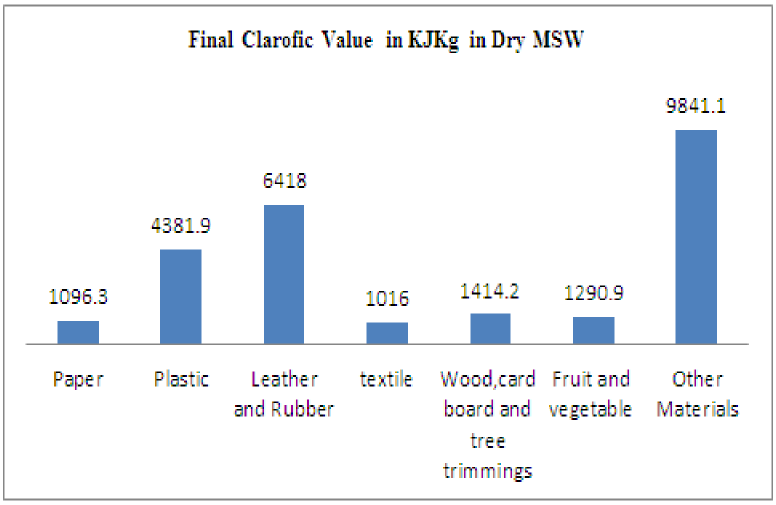

Fig no 8: Final Clarofic Value in KJKg in Dry MSW

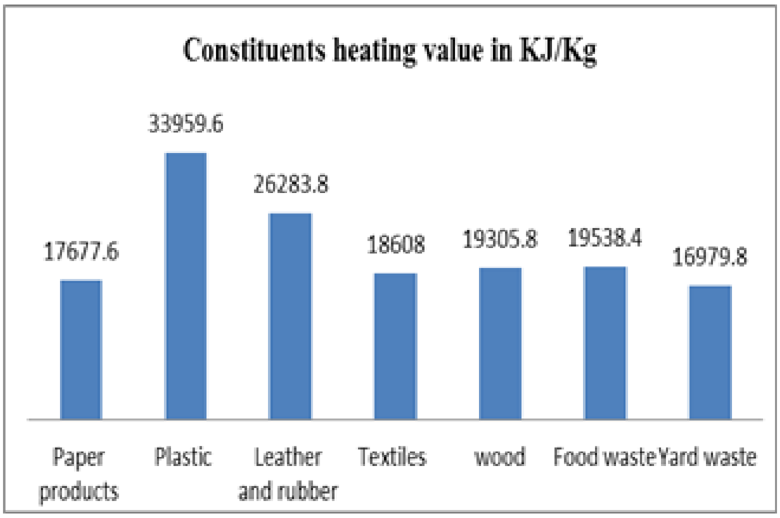

Fig no 9:costantan heating value:

Cost Estimation of Proposed MSW Thermal power plant:

From literature survey cost of the proposed scheme is calculated, which is expected to effected as per change in era.

TABLE NO2 : COST ESTIMATION OF PROPOSED MSW THERMAL POWER PLANT

S.No.	Equipment	Cost (Rs)	References
1	Steam boiler	76,132,335.1	[37]
2	Steam turbine and generator	3,501,170.7	
3	Feed pumps	35,000.0	
4	Cond. extraction pump	9000.0	
5	Condenser	17,306,123.8	
6	Civil works	57,418,809.8	
7	Electrical works	59,663,488.1	
	Total Cost	**214,065,927.50**	

FUTURE WORK:

The proposed scheme may be extended to get further improvements. Some of the changes are suggested as follow

1.Liquid Waste Utilization in the proposed scheme.

2. Analysis of environmental effect of this plant.

3. How to Improve Power Generation of this scheme.

Other Techniques in addition to the existing with plasma Arctechnique.

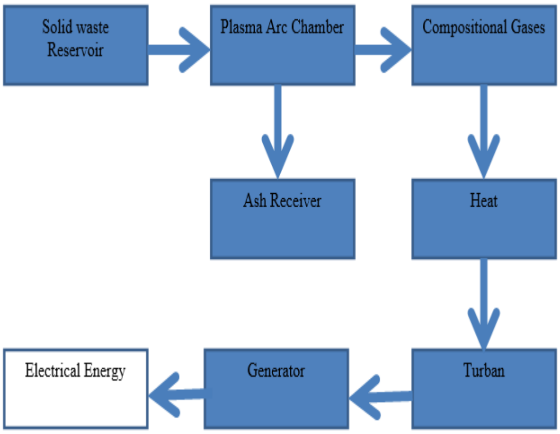

Fig no. 10 Block Diagram of Generalized power plant is suggested for the [1] proposed scheme, which is Shown in the following figure

THE" LOCATION" OF POWER PLANT

The location for power plant mainly defends upon certain constants such as supply of MSW, distance from power station, Fuel supply of Municipal Solid Waste etc. in below drawing location of power plant selected near Badaber because of fast dumping point in which is 7KM away. Second dumping point is shown 06 kilometer away from power plant. The second dumping points 6KM away from the power hub of the city. The site of plant is 15KMaway from the center of city. Currently Two locations have design by MCP, Which have a vast land and can be used as dumping station of MSW. The first dumping point is shown in fig 1 and the waste of whole city to and its surrounding areas can use it for dumping. The first dumping point is marked On ring road abrader Kalley .The second dumping point is marked on ring road near Shahid Abad shown in fig 4.1. Sheikh Mohammad grid station of 500KV is power control transmission of Peshawar city and its surrounding, which is 20KM away from city center. The collecting and delivering the waste to the site of power plant [9]by optimal rotating technique can be useful and effective by using real genetic algorithm.

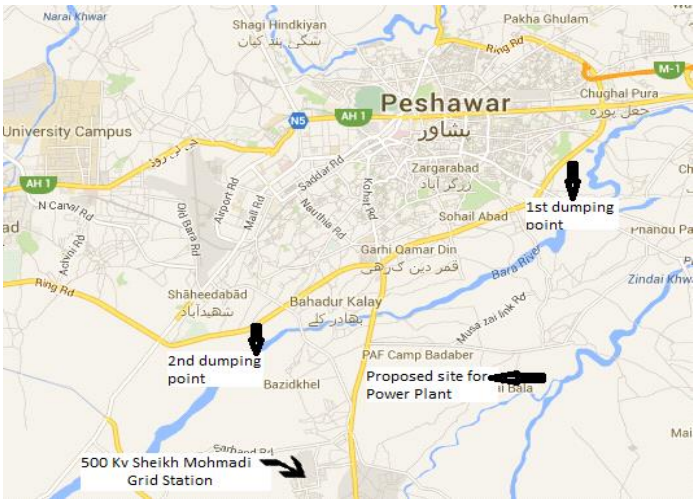

Fig No 10 (Map of Peshawar city showing proposed site of power plant, existing first dumping point, second dumping point and 500 KV Grid Station) [10]

CONCULSION

In this research work the feasibility analysis of Municipal Solid Waste fueled power plant has been carried out. The estimation of MSW of Peshawar city has caring the analysis; the ability of generation of power plant is 18.5MW. The powers dilemma of our country is higher cost of per unit of electricity due to more dependence on oil based power plants. Plasma Arc Gasification is having better results as compared to conventional mass burn i.e. 816 KWh/ton with the cost of approximately 9 - 10 ₵/ KWh which is comparatively less than our national average cost of 14 cents per KWh. Slag produce from Plasma arc gasification technique is much less harmful as compare to others, it can be used insulating material, road construction and making of industry tiles and has almost costs 15$/ ton. The operational complexities and high capital cost are the hurdles to this technique but with the ongoing research in this field is overcoming these complexities.

REFERENCES

[1] Los Angeles County Solid Waste Management Committee, "Conversion Technology Evaluation Report" 2005.

[2] G. C. Young, Municipal Solid Waste to Energy Conversion Processes: Economic, Technical, and Renewable Comparisons: Wiley, 2010.

[3] Water and Power Development Authority (WAPDA) Pakistan. (11/12/2014). Existing Generating Capacity. Available: http://www.wapda.gov.pk/htmls/power-index.html

[4] S. Saini, P. Rao, and Y. Patil, "City based analysis of MSW to energy generation in India, calculation of state-wise potential and tariff comparison with EU" Procedia-Social and Behavioral Sciences, vol. 37, pp. 407-416, 2012.

[5] R. R. Baidoo, F. Yeboah, and H. Singh, "Energy and economic analysis of closed-loop plasma waste-to-power generation model and in comparison with Incineration and Micro-Turbine Models,"Electrical Power & Energy Conference (EPEC), 2009 IEEE, 2009, pp. 1-7.

[6] S. Z. Farooqui, "Prospects of renewables penetration in the energy mix of Pakistan," Renewable and Sustainable Energy Reviews, vol. 29, pp. 693-700, 2014.

[7] I. N. Kessides, "Chaos in power: Pakistan's electricity crisis," Energy Policy, vol. 55, pp. 271-285, 2013.

[8] National Electric Power Regulatory Authority (NEPRA). (06/11/2014). Tariff. Available: http://www.nepra.org.pk/tariff.htm

[9] Macrotrends. (06/11/2014). Oil Prices History Chart. Available: http://www.macrotrends.net/

[10] V. C. Nelson, Introduction to Renewable Energy: Taylor & Francis, 2011.

[11] W. Tong, Wind Power Generation and Wind Turbine Design: WIT Press, 2010.

[12] Pakistan Meteorological Department. (06/11/2014). Wind Power Potential of Pakistan. Available: http://www.pmd.gov.pk/wind/Wind_Project_files/Page694.html

[13] C. Palanichamy, N. S. Babu, and C. Nadarajan, "Municipal solid waste fueled power generation for India," Energy Conversion, IEEE Transactions on, vol. 17, pp. 556-563, 2002.

[14] S. A. Kalogirou, Solar Energy Engineering: Processes and Systems: Elsevier Science, 2013.

[15] EduPic Graphical Resource. (06/11/2014). Energy Resources. Available: http://www.edupic.net/energy.htm

[16] A. C. Baker, Tidal Power: P. Peregrinus, 1991.

[17] S. Silveira, Bioenergy - Realizing the Potential: Elsevier Science, 2005.

[18] California Biomass Energy Alliance. (06/11/2014). Tracy Biomass Plant. Available: http://www.calbiomass.org/facilities/tracy-biomass-plant/

[19] P. S. Khan and M. Hoque, "Installation of a Solid-Waste fuelled Power Plant in Chittagong, Bangladesh: A feasibility study," in Strategic Technology (IFOST), 2010 International Forum on, 2010, pp. 208-212.

[20] World Bank, "Municipal Solid Waste Incineration," 1999.

Wajid Ali: Research Scholar in Department of Electrical Engineering, University of Engineering & Technology Peshawar, Pakistan.

Muhammad Asif: Assistant Professor in Department of computing and Engineering Abasyn University Peshawar Pakistan

International Journal of Engineering Works
ISSN-p: 2521-2419
ISSN-e: 2409-2770
Vol. 6, Issue 10, PP. 333-338, October 2019
https://www.ijew.io/
https://doi.org/10.34259/ijew.19.610333338

Analysis Stduy of Different Control Schemes used for the Improvement of Transient Stability: A Review

Naveed Ullah[1], Muhammad Naeem Arbab[2], Uzair Muhammad[3], Tanvir Ahmed[4], Nisar Ahmed[5]
[1,2,3,4,5]US Pakistan Center for Advance studies in Energy, University of Engineering and Technology, Peshawar, Pakistan
naveedullah491@gmail.com[1], mnarbab@nwfpuet.edu.pk[2], uzairmuhammad416@gmail.com , tanvir.ahmad@uetpeshawar.edu.pk[4], nisarmarwat10@gmail.com[5]
Received: 10 September, Revised: 18 September, Accepted: 22 September

***Abstract*—** In this paper various control schemes used for the enhancement of tranisent have been studied. There are two main control schemes used for transient stability enhancement: Prevntive controle scheme and Emergency control scheme. In this paper the main focus is on emergency control scheme. Further various emergency schemes have been presented in this paper like fast valving, braking resistors, fast valving in coordination with braking resistor, HVDC link for the improvement of transient stability. At the end of this paper a new control scheme has also been proposed in which PMU's are used in coordination with HVDC link for the improvement of transient stability. PMU's are used for the continuous monitoring of the system parameters.

***Keywords*—** HVDC link, Emergency control scheme, PMU, MPC, SIME.

I. Introduction

Transient stability shows the system ability to maintain synchronism when the sytem is in normal operating condition and regain the state of synchronism when a severe disturbance occurs in the system. The severe disturbance may occurs as a result of three phase fault on the transimission line, failure of generating unts, or disconnection of major portion of load. Due to these disturbances the sytem may loss synchronism because of the increase in rotor angle [1,2]. Due to the loss of synchronism a blackout occurs if there is a cascading tripping of the generating units [3]. Therefore to avoid the cascaded tripping of generatings various control schemes have been proposed. These control schemes are classified into two major categories: Preventive control and Emergency control scheme.

In preventive control scheme the system is prepared for any future severe contingency to be withstanded by changing the operating conditions that result the system to become unstable. Many researchers have worked on emergency control scheme for the system transient stability improvement. In reference [4] an another control scheme has been presented which wotk on the dynamic characteristics of the system limits of stability.. Reference [5] proposes an emergency control scheme for shedding of generator using PMU. Reference [6] proposes an open loop control scheme for the tripping and rescheduling of generator. In [7] and [8] closed loop emergency control scheme has been designed for transient stability. There are other control schemes which are used as an emergency control schemes such as braking resistors are used in coordination wit fast valving for the improvement of transient stability [9]. Excitation system may also be utilized for the enhancement of transient stability [10]. Tie-line reactance is also used for transient stability enhancement[11].

Many other control schemes have been proposed for the improvement of transient stability like Model Pridictive Control scheme (MPC). MPC is widely used for the applications of power system. In reference [12] MPC is used for electomechenical oscillation damoing where variable reactance is used, in reference [13] MPC technique is proposed for voltage control, in [14] MPC has been proposed to reduce thermal overload. In reference [15] MPC technique has been proposed for the control of Flexible Alternating Current Transmission System (FACTS) making the system more stable during transient. MPC collects real time information through Wide Area Monitoring System (WAMS). It calculate the control actions for maximizing transient stability at various discrete time intervals and uses these control actions to modulate power flow through the HVDC line [16].

II. Emergency Control Scheme

It is one of the effective control scheme used for the improvement of transient stability [17]. As many of the old controls are off-line. They have the disadvantages of large computation time, therefore the system response to any change is slow and poor. This was the reason that researchers worked to design an on-line emergency control scheme for the transient stability and therefore an on-line scheme was introduced [18]. There are two types of emergency control scheme: Open loop control scheme and Closed loop control scheme [19], [20].

Open loop emergency control (OLEC) [21]:

OLEC uses the following method for the improvement of the stability:

1. the negative margine of the system going to instability is calculated and on the basis of this negavtive margine the critical machines are determined.
2. Once the critical machines are determined, The number of machines are found to be tripped which are connected with emergency control scheme.
3. The Single Machine Equivilant (SIME) is run, and it is run from the start and it has been running upto the tripping delay of the generator and the machines selected in step 2 are tripped out. The simulation is continued till the system becomes stable [22].
4. The simulation is run again and again until the negative margin become that changes the machines from noncritical to critical machines. An extra task may be done, If Optimum Power Flow (OPF) is also used [23].

Closed loop emergency control scheme:

As in open loop emergency control scheme, the power system actions are controlled in off-line mode based on simulation and it can not be readjusted when the system is in on-line mode. Therefore, the best alterntive for the control of power system operation is the Close Loop. In Closed loop emergency control scheme it is first checked that the fault that is occurred will make the system unstable and if the system becomes unstable due the fault, the control actions are triggered appropriately so as to make the system stable [8].

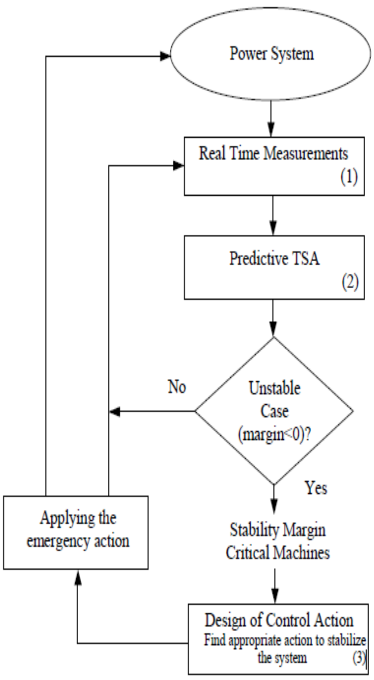

Figure-1 general algorithm for closed loop control [28].

Closed Loop Emergency Control is also called Emergency-SIME is proposed in [24], [25], [26]. The whole process includes the determination of the system stability, the size of the instability, control actions designing, and triggering of the system [27]. Figure-1 is the general algorithm for design Close Loop Emergency Control Scheme.

Although the Close Loop is more effective than Open Loop however the wole process in Closed Loop takes a lot of time and the controller is slower as compared to Open Loop. In such situations Open Loop is sbetter than Close Loop [6].

concept of SIME

SIME is a simulation method used for the enhancement of transient stability which replace the whole system by a Single Machine Equivalent (SIME). SIME combines the Equal Area Criteria and Time Domain analysis. The Equal Area Criteria is used for emergency control and the Time Domain Analysis for preventive method. However both have the same basic principles. The characteristics of the whole system are replaced by One Machine Infinite Bus (OMIB) and more accurate informations are obtained [29].

Emergency-SIME (E-SIME):

Once the fault is cleared after the occurance of fault, the transient stability margin is checked by E-SIME. If the system has the possibility of loss of synchronism, the control actions are selected and triggered to avoid the system from any loss of synchronism . The selected control actions are continuously monitored whether they are enough to avoid the loss of synchronism or should be readjusted. The informations obtained from E-SIME are measured in real time [30]. After occurance of the faut, the machines are divided into critical machines and non-critical machines.

Critical machines are close to the stability limits and may cause the system to loss synchronism. Non-critical machines are strong enough to remain stable even if the synchronism has been lost [32, 33]. Figure-2 represnets three machine system which are subjected to a disturbance. Machine 2 and 3 are divided into Critical machines and machine 1 is divided into Non-critical machine [34].

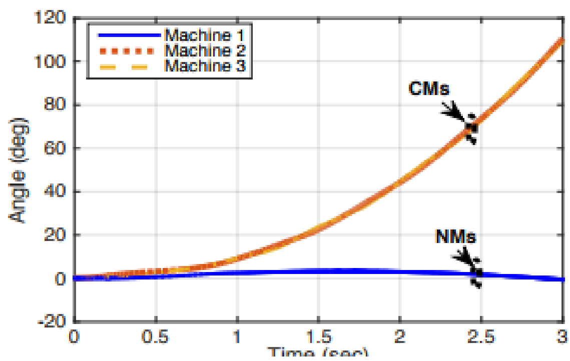

Figure-2: critical and non-critical machines [34].

FACTS devices are also used for the enhancement of the system stability. These devices are used as emergency control devices for the stability of the system. For instance tie line reactacne controller, fast valving and braking resistors, excitation system etc. [29].

Fast valving and braking resistors:

Fast valving and Braking Resistors belong to the family of Discrite Suplementary Controllers (DISCOS). These two members of DISCOS are the supplementary controllers which only active during the faulty conditions and they do not work when the system is in normal operating condition [35]. Speed governor and excitation system are the primary controllers used only for small variation and these controllers may not work during transient faults [36]. The use of DISCOS as an alternative of primary controller is necessary. The cost of theses controllers are less even for the construction of new transmission line. [37].

Braking resistors:

Braking resistor may be installed at any location in the system however the preferred location for installation of braking resistor is that bus where weakest generators are connected. Weakest generators are those that are operating close to the stability limits. Many researchers have worked to sort out the suitable switching strategy for the Braking resistors [38]. Reference [39] shows three strategies in which resistors resistor reactor, and reisistor capacitor are used for the enhancement of transient stability. Reference [40] proposes two new strategies in which in one thyristor rectifier has been used and the in the second diode rectifier and chopper have been used. In [41], [42] control strategies for single insertion and multiple insertion brakes of braking resistors heve been presented of braking resistors

Fast valving:

Fast valving are the most effective means for transient stability improvement which were used before 1929 but this technique was largely used in the period 1970s and 1980s. There are two ways of applying fast valving; Sustained Fast Valving (SFV) and Momentary Fast Valving (MFV). In MFV the valve is closed for a very short movement after the occurrence of fault and reopens and restores the driving power of the turbine while in SFV the steam is passed through the bypass system[43]. For small variation the governor control is enough however in case of large variation the governor control is not sufficient to adjust the variation. In such situation the system may loss synchronism. If the system loss synchronism, the power will reduce almost to zero. In scuh case fast valving is one the effective solution to avoid the loss of synchronism [44].

In case of fault the valve of the turbine is closed and kept close for a while to check the increase in mechanical torque in the form of acceleration of the rotor. The circuit breaker takes a time to remove the faulted area from the rest of the system [9]. For the improvement of the system transient stability using fast valving, many control schemes have been designed. For instance [26] proposes a control scheme which basis on the tracking of active power and rotor angle. In [27] the turbine power is controlled depending upon the fault severity.

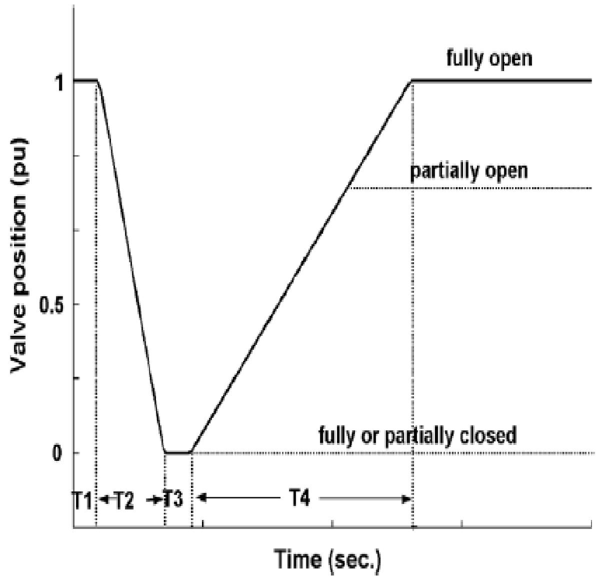

Figure-3 shows fast valving scheme [9]

High Voltage Direct Current (HVDC):

In beginning of 1880, for the transmission of electric power DC was used. The transmission of low voltage DC power over long distance was difficult [45, 46]. Also wth the arrival of induction motor, transoformer, synchronous motor, electronics converters AC replaced the DC. It became easy to transmit AC at High, Extra high voltage over long distances. DC power has the advantage of controllability over AC power. It is easy to control the DC power as compared to AC power [45]. DC power has other advantages such as interconnection of power system which may be operating in different mode of operation [47, 48]. In 1903 when the mercury arc was first introduced, the growth of HVDC was started. The first contract of 60 Mw power transmission over a distance of 115 km but unfortunately this project never become operational due to world war 2. The first DC system of 20 MW in 1954 was commissioned. The transmission voltage used by this system was of 115 kv. However with the arrival of thyrister valves, the HVDC system got more attention [49].

HVDC main components:

Figure-4 represents the genral arrangement of HVDC . conversion from AC into DC and back to AC from DC is the main pupose of HVDC system. Conversion from AC into DC takes place at the sending end and from DC into AC at receiving end.

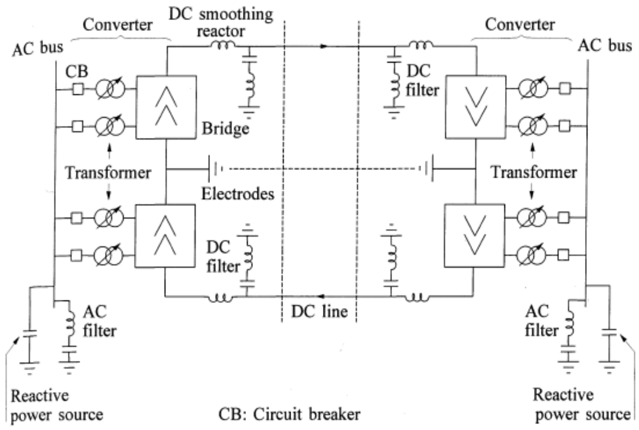

Figure-4 General components of HVDC [47]

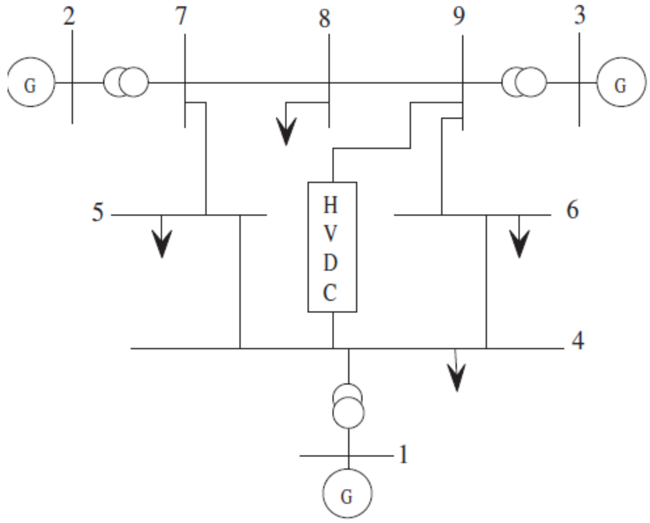

Figure-5 IEEE 9 bus system with HVDC link

III. Transient stability through HVDC

Researchers have worked to propose various control scheme for the enhancement of tranisent stability by modulating power flow through the HVDC line. In reference [52] a control scheme has been proposed in which VSC-HVDC is utilized for the improvement of the system stability. VSC-HVDC has the ability to control both the active and reactive powers independently. That is the size of equipments used in VSC-HVDC is small as compared conventional HVDC system [53]. Model Predictive Control (MPC) has been also for transient stability improvement [54]. In reference [55] for the improvement of the system stability Voltage Source Converter-HVDC is used, which uses the active power control through the HVDC line. In [56] a control strategy has been proposed modulating HVDC power flow using the same transmission line of AC.

Model Predictive Control HVDC Scheme:

MPC collects real time information through Wide Area Monitoring System (WAMS). It calculate the control actions for maximizing transient stability at various discrete time intervals and uses these control actions to modulate power flow through the HVDC line. Figure-5 shows a 9-bus system incorporated with a single HVDC line, in which the concept of MPC is utilized [57].

Figure-6 shows a 24-bus system incorporated with two HVDC links. This system was alos simulated for the improvement of transient [].

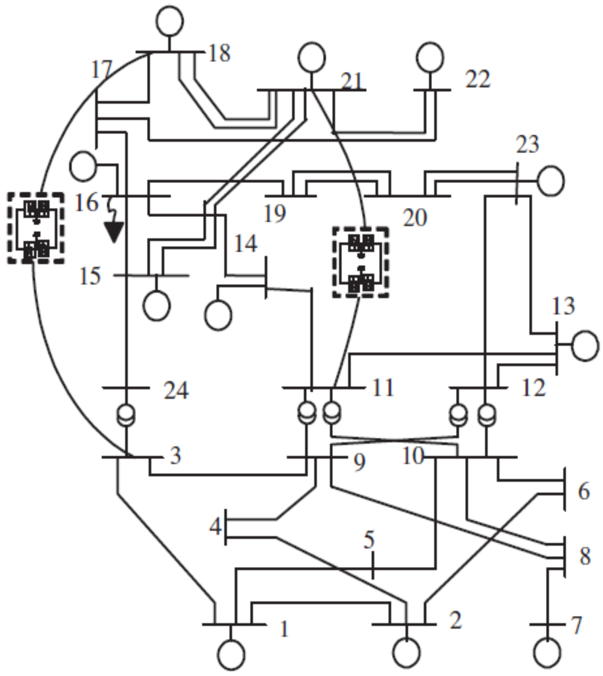

Figure-6 IEEE 24 bus system with two HVDC links

Control Mode of VSC-HVDC:

Pulse width modulation technique is used in VSC-HVDC , in which the magnitude and phase angle of VSC may be controlled separately. Each VSC in normal operation is independent of the other VSC, therefore the reactive power through each VSC can be controlled independently. However the injection of active power into the DC system must be equal the power coming out from the system. The active power can be kept balance when one of the VSCs utilize DC voltage for the control of power and the othe VSC control its power [58].

NEW PROPOSED CONTROL SCHEME

A new scheme is proposed in which Phasor Measurement Units (PMUs) are used in coordination with HVDC link for the enhancement of the stability. This new proposed scheme uses PMUs for the continuous monitoring of the system parameters where HVDC link is used for the modulation of powere flow through it. The advantage of using PMU for measuring the system parameters is that PMU measure the parameters in real time. Therefore it is easy to monitor the system parameters in real time using PMUs [59].

CONCLUSION

In this paper the detailed study of the control schemes used for the improvement of the transient stability have been carried out. The two main schemes preventive and emergency control schemes have been discussed; however the main focus in this paper was given on emergency control scheme. Furthermore, each emergency control shceme such as braking resistor, tie-line reactacne, fast valving, HVDC link has been discussed. At the end of this paper a new control scheme is proposed in which the combination of PMU and HVDC link is used for the enhancement of the system stability. All the schemes discussed in this paper are only for the three phase sysmmetrical faults. A more advance control scheme may be designed which can be used for all types (symmetrical and non-symmetrical) of faults.

REFERENCES

[1] P. Kundur, "Power System Stability and Control". McGraw-Hill, 1994.

[2] M. Pavella, D. Ernst, and D. Ruiz- Vega, "Transient Stability of power systems". Kluwer Academic, 2000.

[3] P.Gomes, "New strategy to improve bulk power system security : lesson learned from large blackout,"

[4] Y. Min, K. Hou, R. Zhang, and Q. Tu, ÒA, "new method for generation shedding and load shedding in power system emergency control". Ó in Proc. IEEE International Conference on Electric Utility Deregulation, Restructuring and Power Technologies, vol. 1, April 2004, pp. 210-214.

[5] Chunyan. Li, Changhong. Deng, Y. Sun, and X. Chen, Ò "An on-line transient stability emergency control strategy based on PMU forecasted trajectory", in Proc. International Power Engineering Conference, Dec 2007, pp. 807-812.

[6] D. Ruiz-Vega and M. Pavella, ÒA comprehensive approach to transient stability control. II. Open loop emergency control, Ó IEEE Trans Power System, vol. 18, no. 4, pp. 1454-1460, Nov 2003.

[7] D. Ernst and M. Pavella, "Closed-loop transient stability emergency control". in Proc. IEEE Power Engineering Society Winter Meeting, vol. 1, 2000, pp. 58-62

[8] M. Glavic, D. Ernst, D. Ruiz-Vega, L. Wehenkel, and M. Pavella, "E-SIME - a method for transient stability closed-loop emergency control: achievements and prospects," in Proc. iREP Symposium- Bulk Power System Dynamics and Control - VII, Revitalizing Operational Reliability, Aug 2007, pp. 1-10.

[9] R. Patel, T. S. Bhatti, and D. P. Kothari, "A modified approach to transient stability enhancement with fast valving and braking resistor applications", in J Electrical Power & Energy Systems, vol. 28, no. 10, 729-738, Dec 2006.

[10] N.fermendopulle and R.Ramshaw"Domain of stability of synchronous machine with excitation control-a cell mapping approach, Electric Power Systems Research, vol. 27, no. 3, pp. 173-181, Aug 1993.

[11] D. K. Reitan and N. Ramarao, "A method of improving transient stability by bang-bang control of tie-line reactance", IEEE Trans Power Apparatus and Systems, vol. PAS-93, no. 1, pp. 303-311, Jan 1974.

[12] D. Ernst, M. Glavic, F. Capitanescu, and L. Wehenkel, "Reinforcement learning versus model predictive control: a comparison on a power system problem," IEEE Transactions on Systems, Man, and Cybernetics - Part B: Cybernetics, vol. 39, pp. 517–529, April 2009.

[13] M. Larsson, D. Hill, and G. Olsson, "Emergency voltage control using search and predictive control," International Journal of Power and Energy Systems, vol. 24, no. 2, pp. 121–130, 2002.

[14] B. Otomega, A. Marinakis, M. Glavic, and T. Van Cutsem, "Model predictive control to alleviate thermal overloads," IEEE Transactions on Power Systems, vol. 22, pp. 1384–1385, August 2007.

[15] J. Ford, G. Ledwich, and Z. Dong, "Efficient and robust model predictive control for first swing transient stability of power systems using flexible ac transmission systems devices," IET Proceedings on Generation, Transmission, and Distribution, vol. 2, no. 5, pp. 731–742, 2008.

[16] Y.Phulpin, J.Hazra, D.Ernst, "Model predictive control of HVDC power flow to improve transient stability in power system", Smart grid communications, 2011

[17] C. Li, C. Deng, Y. Sun, and X. Chen, Ò "An on-line transient stability emergency control strategy based on PMU forecasted trajectory", in Proc. International Power Engineering Conference, Dec 2007, pp. 807-812.

[18] Y.Xue, "practically negative effects of emergency controls", in proc.1997 IFAC/CIGRE symposium on control of power system and power plants, p.134-138.

[19] M. Pavella, D. Ernst, and D. Ruiz-Vega, Transient Stability of Power Systems: A Unified Approach to Assessment and Control. Norwell, MA: Kluwer, 2000.

[20] L. Wehenkel, "Emergency control and its strategies," in Proc. Power Syst. Comput. Conf., vol. 1, Trondheim, Norway, June 28–July 2, 1999, pp. 35–48

[21] Daniel Ruiz-Vega, Mania Pavella, "A Comprehensive Approach to Transient Stability Control: Part II—Open Loop Emergency Control", IEEE TRANSACTIONS ON POWER SYSTEMS, VOL. 18, NO. 4, NOVEMBER 2003.

[22] D. Ruiz-Vega and M. Pavella, "A comprehensive approach to transient stability control—Part 1: near-optimal preventive control," IEEE Trans. Power Syst., vol. 18, pp. 1446–1453, Nov. 2003.

[23] D. Ruiz-Vega, "Dynamic Security Assessment and Control: Transient and Small Signal Stability," Ph.D. dissertation, Univ. Liege, Liege, Belgium, 2002.

[24] Y, Zhang, L. Wehenkel and M. Pavella. .A Method for Real-Time Transient Stability Emergency Control, Proc. of CPSP97, I FAC/CIGRE Symp. On Control of Power Systems and Power Plants, August 1997, Beijing, China, pp. 673-678.

[25] D. Ernst, A. Bettiol, Y. Zhang, L. Wehenkel and M. Pavella. .Real Time Transient Stability Emergency Control of the South- Southeast Brazilian System., SEPOPE, Salvador, Brazil, May 1998, (Invited paper, IP044).

[26] D. Ernst, M. Pavella, .Closed-Loop Transient Stability Emergency Control, Proc. of IEEE/PES Winter Meeting, Singapore, 2000.

[27] Duniel Ruiz- Vega, Mevludin Glavic, Damien Ernst "transient stability emergency control combining open loop and closed loop techniques",

[28] J.Hazra, Y.Phulpin, D.Ernst, "HVDC control strategies to improve transient stability in interconnected power system", Power Tech, IEEE Busharest pp.1-6 oct. 2009.

[29] Duniel Ruiz-Vega, Louis Wehenkel, Damien Ernst, Alejandro Pizano-Martinez and Claudio R. Fuerte-Esquivel, "Power system transient stability preventive and emergency control, chapter 5".

[30] Duniel Ruiz- Vega, Mevludin Glavic, Damien Ernst "transient stability emergency control combining open loop and closed loop techniques",

[31] Pavella M, Ruiz-Vega D, and al. SIME: A Comprehensive Approach to Transient Stability. Real-Time Stability Assessment in Modern Power System Control Centers, John Wiley & Sons, Inc 2008; 353-400.

[32] Pavella, M., D. Ernst, and al. Transient Stability of Power Systems: A Unified Approach to Assessment and Control, Kluwer Academic Publishers 2000.

[33] Youcef Oubbati, Salem Arif, “Securing transient stability Assessment Using Single Machine Equivalent Method”, Electrical Engineering (ICEE), pp. 1-4, Dec 2015

[34] Durrant CW. Boiler response to partial load rejection resulting from System upsets. IEEE Trans 1982; PAS-10(8):2630–9.

[35] IEEE Working Group on Special Stability Controls Power System Engineering Committee. Bibliography on the application of discrete Supplementary controls to improve power system stability. IEEE Trans ‘1987; PWRS-2(2):474–85.

[36] Ramnarayan Patel, T.S.Bhati, D.P.Kothari, “A modified approach to transient stability enhancement with fast valving and braking resistor applications”, electric power and Energy system, p.729-738, 2006

[37] Patel Ramnarayan, Bhatti TS, Kothari DP. Dynamic braking control strategies: a comparative analysis. In: Proceedings international conference on energy automation and information technology 2001

[38] A.H.M.A. Rahim, A.I.J. Al-Sammak, “Optimal switching of dynamic Braking resistor, reactor or capacitor for transient stability of power system”, IEE Proceedings C-Generation, Transmission and distribution, pp. 89-93 vol 138 Jan 1991.

[39] Riya Saluja, Mohd. Hasan Ali, “Novel Braking resistor models for transient stability enhancement in power grid system”, Innovative Smart Grid Technologies (ISGT), April 2013

[40] Al-Azzawi FJ, Omar F. Dynamic brake switching time in multimachine Power system during emergency: Proceeding of the 24th University power engineering conference, Belfast, Britain, September 1989. p. 101–6.

[41] Al-Azzawi FJ, Al-Wafi NM, Jassim AK, Omar F. Braking resistorsize, switching instants and assessment of power system transient stability by direct methods. J Inst Engrs (India) 1995;76-175–80.

[42] Patel, Ram Narayan. Bhatti, T.S. Kothari, D.P. “Improvement of Power System Transient Stability using Fast Valvings: A Review”, Electric Power Components and Systems, P-927-938, Nov 30, 2010

[43] A.H.M.A. Rahim, A.I.J. Al-Sammak, “Optimal switching of dynamics braking resistor, reactor, or capacitor for transient stability of power system”, IEE proceeding C-Generation, Transmission and Distribution, vol 138, no.1, pp-89-93, 1991

[44] G.G.Karady, M.A.Mohammad, “improving transient stability using fast valving base on tracking rotor angle and active power”, power engineering society meeting summer, 2002.

[45] K.Koyanagi, T.Komukai, “a study of fast valving as an aid to power system transient stability part1. Some considerations of control methods for fast valving”, p.1-5, 1977

[46] Shri Bhagwan, “A Review: High Voltage Transmission System”, International Journal on Recent Technologies in Mechanical and Electrical Engineering (IJRMEE) pp. 1-4, vol 02.

[47] Vijay. K. sood, “High Voltage Direct Current And FACTS controller”, USA Kluwer Academic Publisher 2004.

[48] N. Flourentzou, V. G. Agelidis, and G. D. Demetriades, “VSC based HVDC power transmission system: an overview”, IEEE transaction on power electronics, vol. 24, pp. 593-602, March 2009.

[49] Chan-ki Kkim, Vijay K. Sood. Gil-Sood Jang, Seong-Joo Lim, and Seok-Jin Lee, “High Voltage Direct Current transmission” chapter 01 Development of HVDC Technology,

[50] P. Kundur, “Power system Stability and Control”, McGraw-Hill, 1994.

[51] “Compendium of HVDC schemes throughout the world”, International conference on Large High Voltage Electric systems, CIGRE WG 04 of SC 14. 1987.

[52] Brahim. Bekki, Mohamed Moujahid, Mouhamed. Boudiaf, “Transmission System Transient stability enhancement based on VSC-HVDC”, Journal of Electrical Engineering, pp. 1-6

[53] Schetter F, Huang H, Christl N, "HVDC transmission systems using voltage source converter-design and applications" IEEE Power Engineering Society Summer Meeting, July 2000.

[54] Y.Phulpin, J.Hazra, D.Ernst, “Model predictive control of HVDC power flow to improve transient stability in power system”, Smart grid communications, 2011

[55] Javier Renedo, Aurelio Garci’ a-Cerrada, Luis Rouco, “Active power control strategies for transient stability enhancement of AC/DC grids with VSC-HVDC multi-terminal systems”, IEEE transaction on Power system, pp.4595-4604, vol 31, November 2016.

[56] K. P. Basu, “Stability enhancement of power system by controlling HVDC power flow through the same AC transmission line”, Industrial Electronics and Application, pp. 1-6 Oct 2009

[57] Y.Phulpin, J.Hazra, D.Ernst, “Model predictive control of HVDC power flow to improve transient stability in power system”, Smart grid communications, 2011

[58] J.Hazra, Y.Phulpin, D.Ernst, “HVDC control strategies to improve transient stability in interconnected power system”, Power Tech, IEEE Busharest pp.1-6 oct. 2009.

[59] Daniel Dotta, Joe H. Chow, Luigi Vanfretti, Muhammad S. Almas, & N. Gostini, “A MATLAB-based PMU Simulator”, IEEE.

International Journal of Engineering Works
ISSN-p: 2521-2419
ISSN-e: 2409-2770
Vol. 6, Issue 10, PP. 339-346, October 2019
https://www.ijew.io/
https://doi.org/10.34259/ijew.19.610339346

Extensive Performance Evaluation of a 75Kg Solar-Biomass Hybrid Tunnel Dryer with Several Types of Agricultural Products

Sahibzada Imad ud din[1], Asif Ali[2], Suhail Zaki Farooqui[3]
[1,2,3] Department of Renewable Energy Engineering, U.S.-Pakistan Center for Advanced Studies in Energy, University of Engineering and Technology Peshawar, Pakistan
immiedwardian@gmail.com[1], chemasif85@gmail.com[2], suhail.zaki@uetpeshawar.edu.pk[3]
Received: 26 September, Revised: 01 October, Accepted: 03 October

***Abstract*—**Solar-biomass hybrid tunnel dryer has been designed to dry different kinds of agricultural products.The dryer is comprised of three major parts, solar collector(inside the drying chamber), backup heating stove and an additional collector connected to the drying chamber through PVC pipes. This study presents the performance evaluation of the dryer. Collector average efficiency was found to be 29.7% and the drying efficiency for the system was 22.8%. The tunnel dryer was run on solar energy and solar-biomass energy for different set of tests. Different types of vegetables and fruits were dried in the tunnel dryer. A total of 7 solar-biomass hybrid tunnel dryer were constructed out of which 6 were installed in Swat KP Pakistan (Regions: Chikrae, Tal sar, Badalae, Jarro, Charbagh and Khwazakhela). Swat being the most effective area in respect of producing fruits. The post harvest losses are high. The total capacity of the dryer was found to be 75Kg.

***Keywords*—** Solar drying, Solar-biomass dryer, Hybrid Drying, Temperature, Relative Humidity

I. INTRODUCTION

Solar drying is one of the cheapest method to preserve food. Solar drying systems are reliable and environment friendly [1]. Drying cost of solar dryers are very low compared to other drying techniques [2]. Additionally, drying of food through solar drying systems require generally little space and brief amount of time to dry the food material [3]. Moreover, solar drying is one of the most efficient drying method used worldwide. It is far more advantageous than Open Sun Drying (OSD). In OSD the food is spreaded on the sheets placed on the grounds. Microbacterial and other enivironmental friendly insects can easily attack the food material in OSD [4,5]. The food in OSD needs an intensive labor, because one has to cover the food during night time or rainy days. Quality deterioration occurs when direct UV rays falls on the food material.

Solar dryers are one of the most used food drying systems in 21st century. Food material is well protected inside the drying chamber. Temperature inside the drying chambers are high, so no microorganism can grow on the surface of food material. The moisture inside the drying chamber is carried by the hot air. This moisture is thrown into atmosphere through a chimney or an exhaust fans depending upon the type of the dryer. The optimum temperature for drying is in the range of 40-60 ^{0}C. Solar dryers encourages farmers to overcome the post harvest losses. Because post harvest losses are one of the major issue rural areas farmers are facing [6].

Persimmons, locally known as Amluk, are cultivated in northern areas of KP Pakistan on large scale. According to Small and Medium Enterprises Development Authority (SMEDA) 71,265 tons of Persimmons are produced annually in Swat; 28,000 tons of which are wasted [7]. In Swat KP Pakistan mostly persimmon are dried on customarily methods. The short usability time after harvesting of persimmons makes it a challenge for farmers to reduce the post harvest losses. For this purpose 6 commercial scale 75Kg solar-biomass tunnel dryer was designed, fabricated and installed in Swat.

This paper presents the extensive performance evaluation of the solar-biomass hybrid tunnel dryer. Different tests were performed to find the extensive paramteres of the dryer. A 50Kg of batch of tomatoes, as well as different fruits and vegetables were dried.

II. MATERIALS AND METHODS

A. Description of the Dryer

Solar-biomass hybrid tunnel dryer was designed and fabricated shown in Figure 1. It is composed of three major parts; GI stove, Drying Chamber(contains a solar collector and a heat exchanger) and an additional solar collector. The GI stove is fabricated with a height of 0.72m and width of 0.57m. Drying chamber is supported by a mild steel frame. The height of the drying chamber from the ground is 1.6m. The length and width of the chamber is 2.4m and 1.2m respectively. The additional solar collector is connected to the drying chamber. This collector is fabricated with the length, width and height of 2.4m, 2.4m and 0.2m respectively.

Figure 1: Design of the tunnel dryer

Four DC exhaust fans are installed on the drying the chamber (2 at each opposite ends). These exhaust fans are run a solar PV system shown in Figure 2. Furthermore two blowers are run by the battery. The blowers are connected to GI stove and additional solar collector for different set of experiments.

Figure 2: Solar PV system (Dryer installed in SWAT)

B. *Performance Evaluation of the Dryer*

Performance of the dryer was categorized based on the following sections.

1) *Temperature Measurement*

A digital thermometer logger(Tm-947SD) was used to determine temperature at different points in the dryer. Temperature readings were taken at the top,middle and bottom trays. The ambient temperature readings were also logged.

2) *Humidity Measurement*

A digital hygrometer (Elitech RC-61) was used to measure relative humidity inside and outside of the dryer.

3) *Solar Radiation Intensity*

Solar radiation intensity readings were taken from the meteorological station installed at UET Peshawar Pakistan.

4) *Collector Unit Efficiency*

Collector unit efficiency for the dryer was calculated by using the formula:

$$\eta_c = \frac{\dot{m} C_p (T_c - T_{am})}{I_s}$$

$\dot{m}$; Mass Flow Rate
C_p ; Specific Heat Capacity of Air
T_c ; Collector Temperature
T_{am} ; Ambient Temperature
I_s ; Solar Radiation

5) *Drying Efficiency*

The drying efficiency for the dryer was calculated using the formula:

$$\eta_{\text{drying}} = \frac{W \ L_v}{I_{st} A_e}$$

η_{drying} ; Drying Efficiency
W ; Total Weight Loss
L_v ; Latent heat of vaporization of water
I_{st} ; Total Solar Radiation
A_e ; Effective area of collector receiving I_s

6) *Drying Rate*

Drying rate of the dryer was found using the equation:

$$DR = \frac{W_i - W_f}{t}$$

DR ; Drying Rate
W_i ; initial weight of the sample
W_f ; final weight of the sample
t ; Total Drying Period

III. Results and Discussions

This solar-biomass hybrid tunnel dryer can be operated in four different modes.

- Solar Energy Drying
- Solar Drying with Additional Solar Collector
- Solar-biomass Drying
- Biomass Drying

A. *Solar Energy Drying*

A batch of 50Kg tomotoe was dried using the solar energy. Temperature on top, middle and bottom trays, and solar radiation intensity was recorded throughout the experiment, shown in figure 3. It is noticed that the temperature at the top trays are high, it is because the top trays get both direct and indirect solar radiations. It took only four days to dry the whole batch of tomatoes. Total weight of the tomatoes were reduced to 3.1Kg. The dried tomatoes were kept into closed containers after the drying. Relative humidity was also recorded inside and outside of the drying chamber, shown in figure 4. We observe that relative humidity inside the dryer is very small as compared to outside relative humidity, which makes it easier inside the dryer to capture more and more water molecules from the food product.

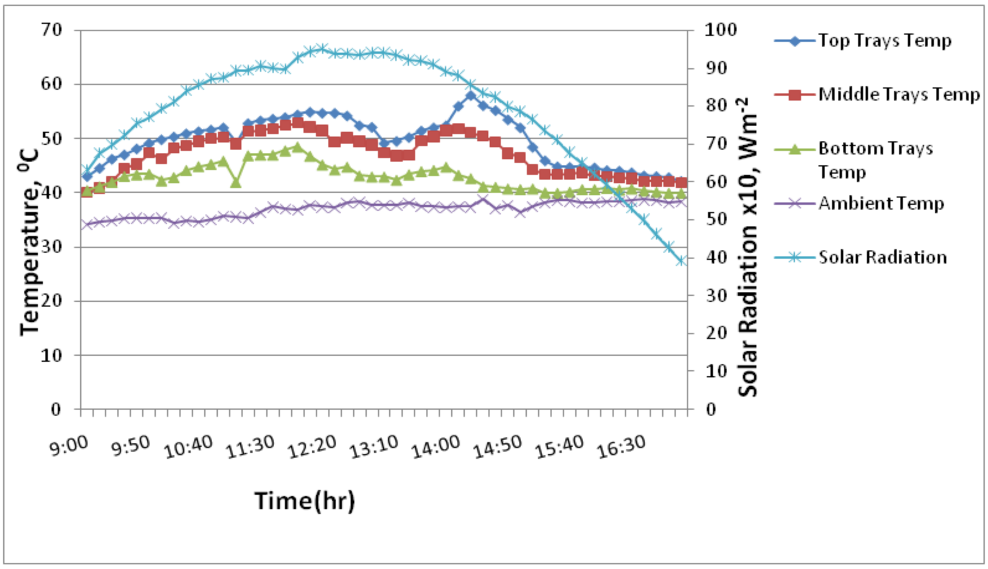

Figure 3: 13th June,2019 Temperature Inside Drying Chamber

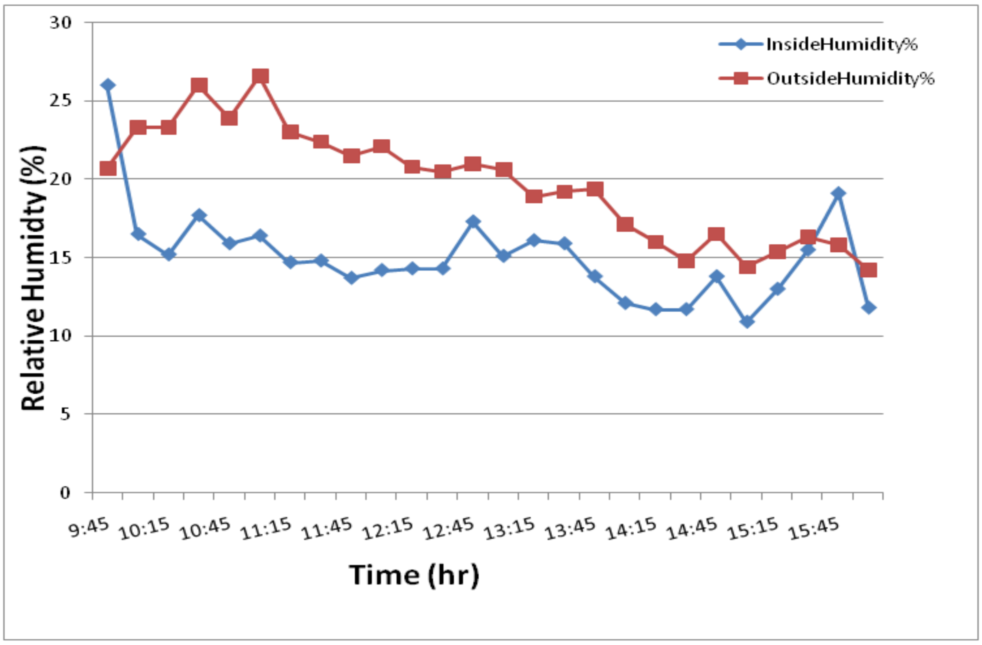

Figure 4: 13th June, 2019 Relative Humidities

B. Solar-Biomass Hybrid Drying

Different types of fruits and vegetatables were dried using solar-biomass drying. Similarly for this drying the temperature and humidity data was logged for three days, shown in figure 5 and 6. The data was logged for continously 24 hours. It is noticed that the drying temperature was controlled for 5 hours after the sunset using the charcoal as a fuel. Total of 5Kg charcoal was burnt in the stove for five hours. It took three days to completely dry the sample of mangoes ,melon, green chilli, bitter gourd and eggplant.

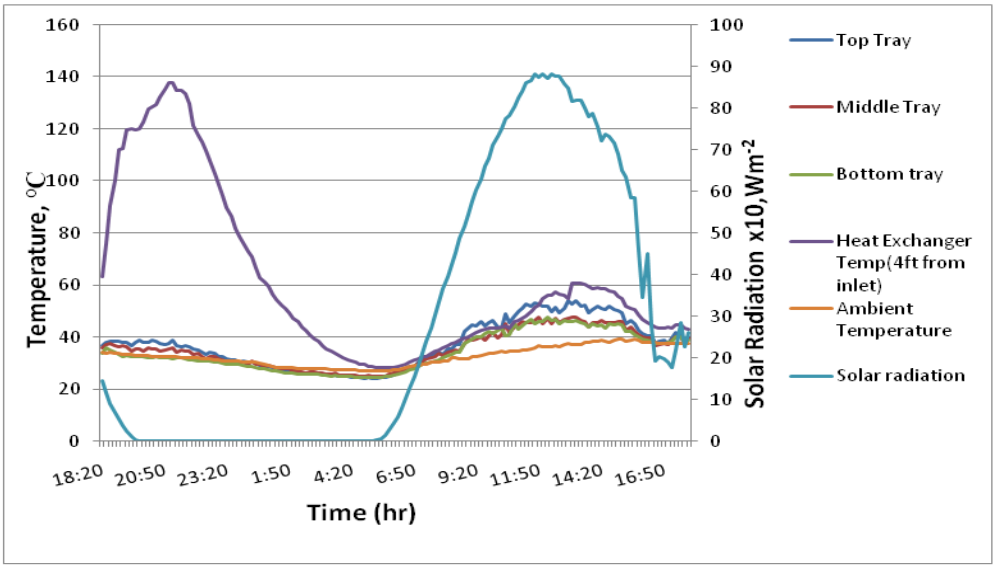

Figure 5: Hybrid Drying 24 hours (18-19June, 2019)

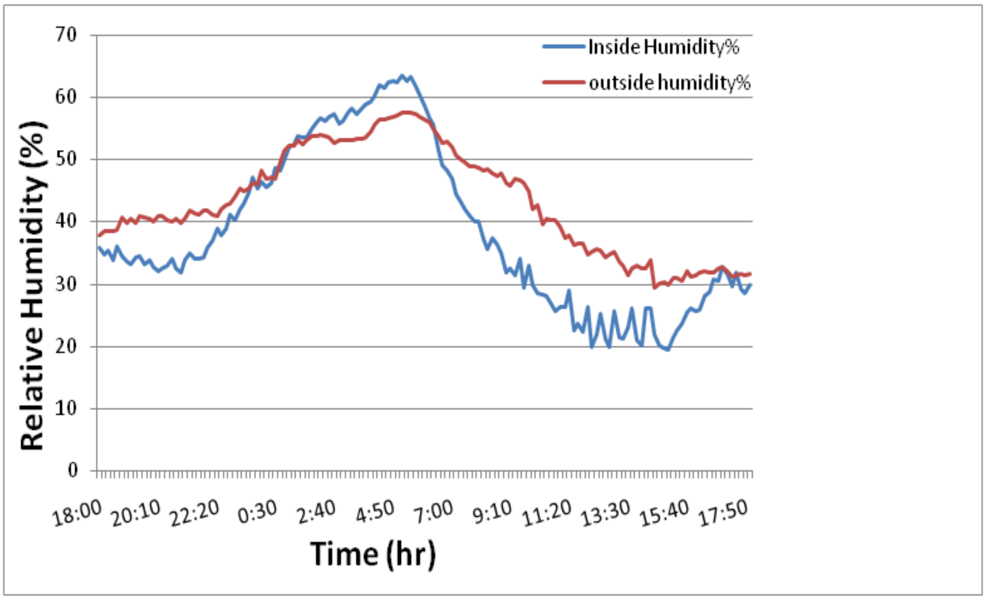

Figure 6: Hybrid Drying Relative Humidity (18-19June,2019)

C. *No-Load Biomass Test*

This test was performed to find out the temperature gradient of the heat exchanger. Charcoal was burnt in the GI stove. Hot gases were pushed into heat exchanger through a DC blower connected to the bottom of the stove. The temperature readings were recorded on various points throughout the length of the plate surface. We can see from figure 7,8 and 9 the different temperature values at different points of the plate. Figure 10 shows the peak temperatures on different points, while figure 11 shows the temperature gradient of the plate.

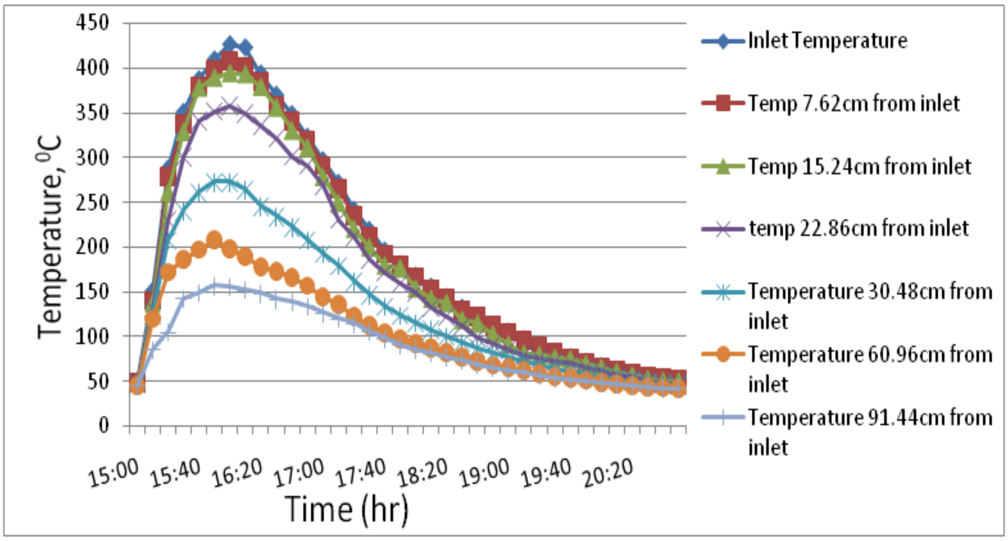

Figure 7: Plate Temperature (0-91.4Cm)

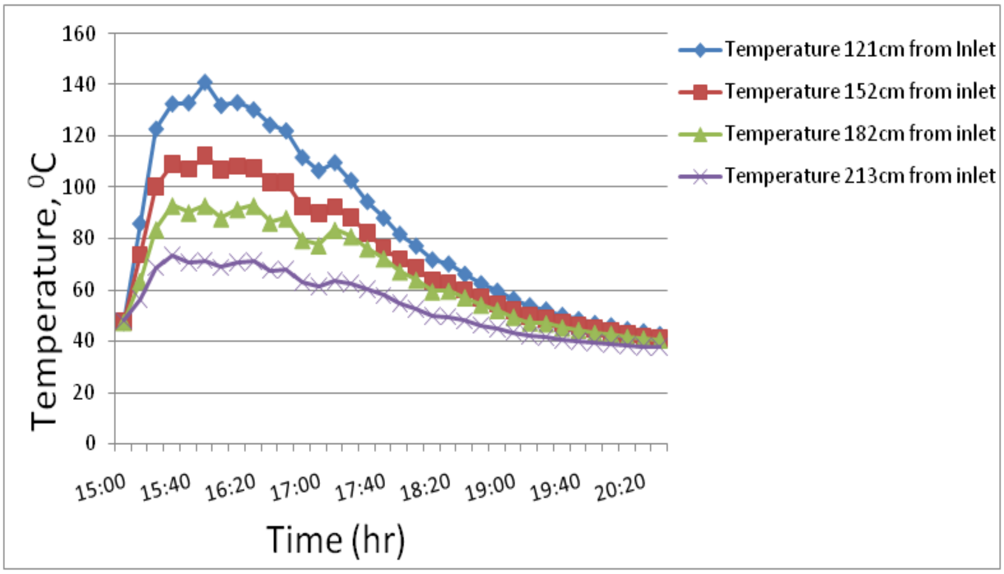

Figure 8: Plate Temperature (121-213Cm)

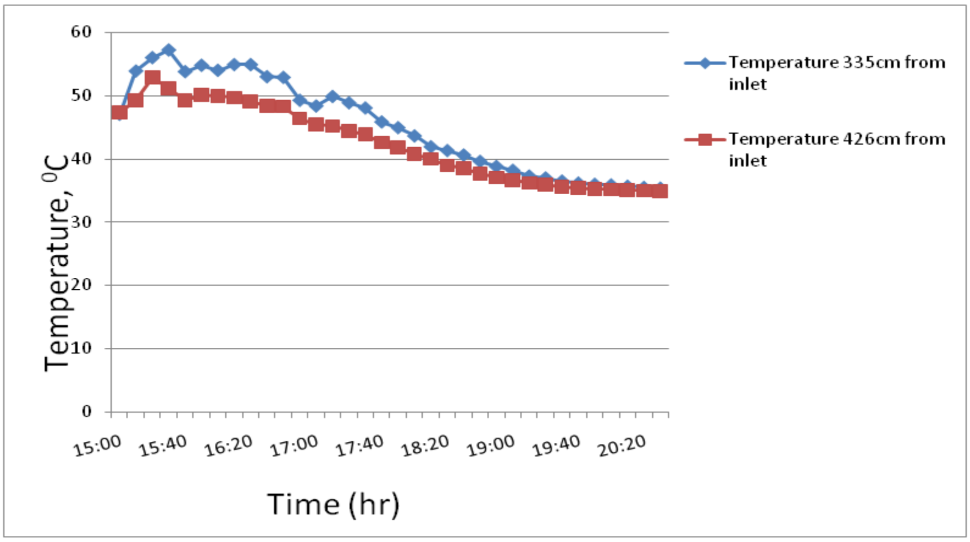

Figure 9: Plate Temperature on 335Cm and 426Cm

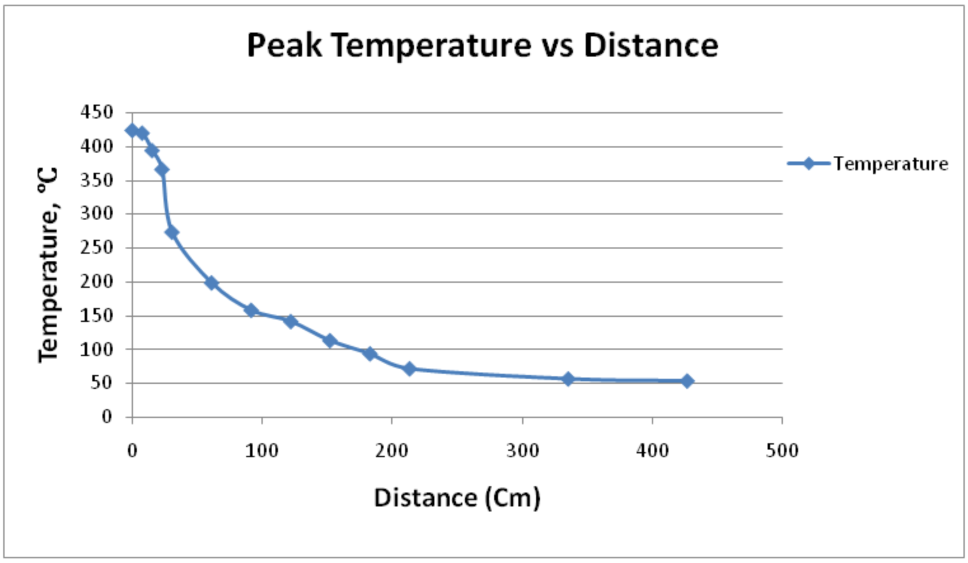

Figure 10: Peak Temperature on Different Points

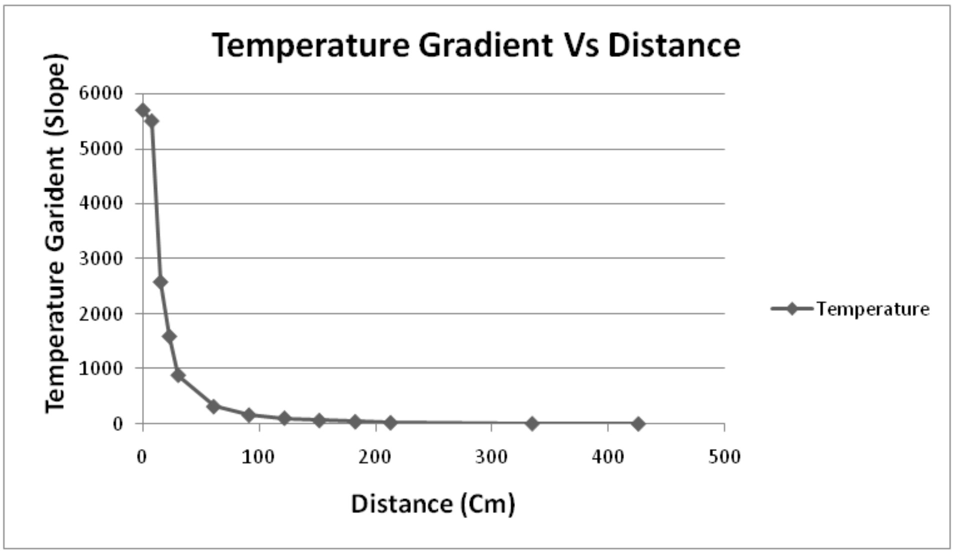

Figure 11: Tempearature Gradient

D. Dryer Performance Evaluation

Collector unit efficiency was calculated on 20th June 2019. From figure 12 we can see that the collector efficiency varies from 8% to 46% throught out the day. Hence the average efficiency of the collector was found to be 29.7%. The drying efficiency for the system was found to be 22.8%. These efficiencies can vary depending on the solar radiation intensity of that area. These experiments were conducted in Peshawar, Pakistan. The drying rate for the 50 Kg batch of tomatoes was found to be 1.48Kg/h. The volumetric flow rate of air going out of the chambers was $0.11m^3/s$.

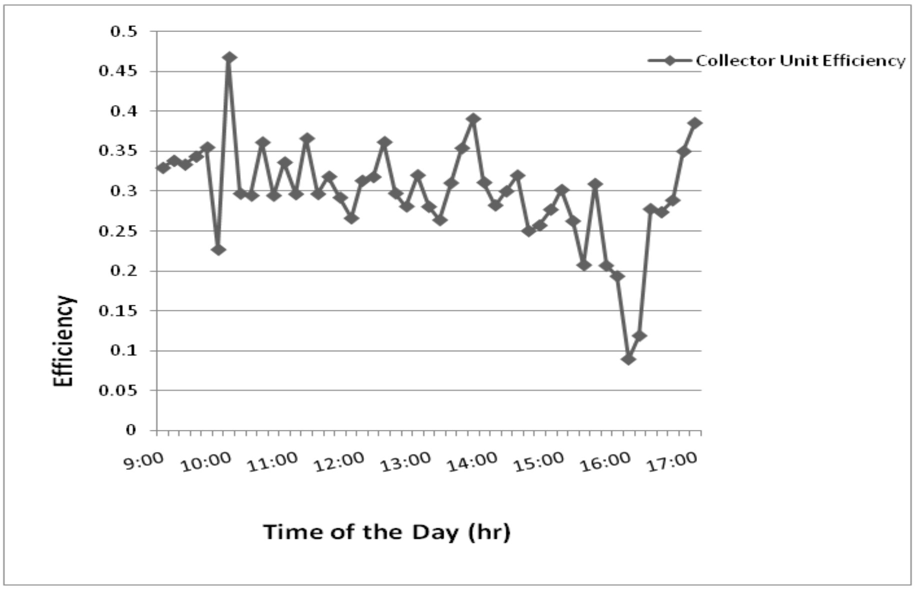

Figure 12: Collector Unit Efficiency

CONCLUSION

A mixed mode solar-biomass tunnel dryer was constructed from the locally available material in market. The maximum temperature attained inside the dryer was 59.2 ℃. The biomas backup heating system ensures the drying of food products on rainy days or night time. Tomato batch of 50Kg was reduced to 3.1KKg during 32 drying hours. Food inside the dryer is safe from the environmental contaminations. The moisture content is continuously removed by the exhaust fans installed on the drying chamber. Swat being the most productive in respect of fruits; post harvest losses are high. This solar-biomass hybrid tunnel is expected to provide a way for preserving the food for longer periods of time.

REFERENCES

[1] A, Sharma et. al (2009) Solar-energy drying systems: a review, Renewable and sustainable energy review, 13(67): 1185-1210.

[2] GuttiBabagana, Silas, K and Mustafa, B.G., Design and construction of forced/natural convection solar vegetable dryer with heat storage, ARPN journal of engineering and applied science, 7(10), (2012) 72-77.

[3] Mujumdar, Arun and DevahastinSakamon, Mujumdars practical guide to industrial drying, Montreal: Exergex corporation, (2000).

[4] Joshi, Pallavi and Mehata, Dipika, Effect of drying on the nutritive value of drumstick leaves, *Journal of Metabolomics and Systems Biology*,1(1), **(**2010**)** 5-9

[5] Joshi, Pallavi and Mehata, Dipika, Effect of drying on the nutritive value of drumstick leaves, *Journal of Metabolomics and Systems Biology*,1(1), **(**2010**)** 5-9

[6] Blair R. et. al (2007) Design of a solar-powered fruit and vegetables dryers

[7] SMEDA to establish fruit dehydration unit in swat https://fp.brecorder.com/2017/06/20170623191996/

.

International Journal of Engineering Works
ISSN-p: 2521-2419
ISSN-e: 2409-2770
Vol. 6, Issue 10, PP. 347-353, October 2019
https://www.ijew.io/
https://doi.org/10.34259/ijew.19.610347353

Improved Steiner Tree Scheme Applied to Wireless Sensor Networks for Path and Energy Optimization

Muhammad Zahoor
Department of Computer Systems Engineering, University of Engineering and Technology, Peshawar Pakistan
mzahoor757@gmail.com
Received: 23 September, Revised: 29 September, Accepted: 02 October

***Abstract*—**This research work presents two optimization algorithms to optimize the path and energy in the wireless sensor network. Minimum Spanning Tree (MST) and Particle Swarm Optimization (PSO) algorithms both are utilized to optimize the path and energy of a system, which is connected on a fifty nodes network deployed randomly on 100x100 meters region. The proposed scheme is for the constrained improvement problem, or more explicitly, a weighted spanning tree problem and its appliance to Wireless Sensor Network (WSN) is examined here where definite exploratory discoveries on the energy improvement of the network have been exhibited.

***Keywords*—** Minimum Spanning Tree, Optimization, Particle Swarm, Shortest Path Tree, Wireless Sensor Networks.

I. Introduction

Energy optimization in a Wireless Sensor Network (WSN) has been one of the most researched topics in the field of wireless communication. Numerous recent journals has pointed out to it in the current year, such as [1], which has worked on Ant Colony Algorithm for the optimization of the energy consumption in a WSN. The reason behind using the sensors is to extend the capacities of an individual. For example in the distant magma-based regions, for the search of natural resources and other earth components [2]. Addition to the system some uncommon incentive in a WSN, dormancy, decency just as the nature of administration of the system are of most extreme significance. In a down to earth situation, the parameters of the framework counteract one another and consequently, they become balanced.

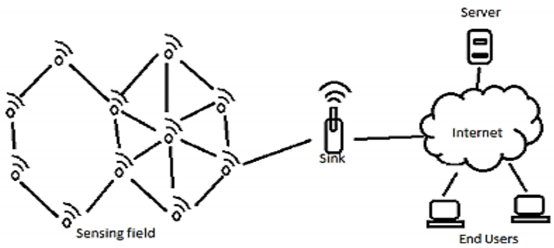

Figure 1. A Wireless Sensor Network

By counterbalancing, it is implied that these measurements are orchestrated in the system so that if we upgrade one parameter it will outcomes in the squalor of some other essential parameters. In this way, finding a parity of the considerable number of measurements of a WSN isn't just significant, yet in addition inescapable.

Effective correspondence system and calculations are eminent with an end goal to diminish the vitality utilization, amplify the lifetime, and improve the working of the system in general [3].

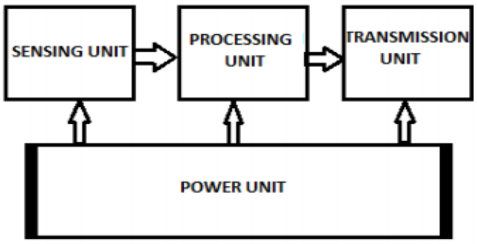

Figure 2. Architecture of a wireless sensor node

MOO calculations can take care of an issue with different parameters compelled by equity or disparity limitations so that the arrangement of the qualities for the parameters of the issue can't be called definitive and completed. It is difficult to observe the answer that is exact fit to the parameters of the issue, this type of the solution is known as Pareto-Optimal (PO) arrangement. The metaheuristic algorithms are normally used to tackle the MOPs. The most generally examined algorithm from the metaheuristic's sub-class Non-Dominated Sorting Genetic Algorithm (NSGA-II) because of their productivity in discovering Pareto-arrangements.

So as to diminish vitality utilization, correspondence plans or conventions have been created in the course of recent decades that have filled the need. The examination field is as yet crude and more issues in WSNs are rising as it grows imaginatively.

The Wireless Sensors Network can be enhanced through various ways for the energy and path optimization, the improvement can be made with in a multi-bounce, staggered, various leveled WSN, regardless of whether it is an incorporated or a decentralized system with both of sound information hubs or the opposite, is one technique [4]. Different techniques are connected with the examination points of nodal situation issue, inclusion issue, sending approach type, adaptation to non-critical failure and traffic mindfulness, among numerous different measurements.

The most significant of the measurements in an improvement-based research with respect to a remote sensor arrange are Latency, Throughput, Energy utilization, Lifetime, Death and future, detecting capacities, organize overhead, etc[5].

A. To Find the Shortest Communication Path

Proficient information trade with minimal measure of energy loss is a significant prerequisite in the present territory of WSN technology [5][6]. A few advancements, that merit referencing. Djikstra's most brief way calculation has been the base of different late investigations in these research areas [7][8]. For example, in research [9], the algorithm estimates the base number of nodes between the source and goal node that could be utilized in the calculation of the path.

The work in [10] proposed a new method for the separation of the adjacent nodes in a system. The proposed work presents that if the two nodes in the network has same signal properties they will be terms as same nodes. In the brought together sort of systems, the plan for estimations of separations for the non-neighboring sensors must be unique in relation to the previously mentioned one. A few analysts are referenced in [11],[12],[13] and [14].

Amid the estimation of a separation between two hubs, if nature is loud, it takes various jumps for a similar data to reach with a specific precision to have the option to effectively help out there figuring [15]. Therefore, in specific situations, the mistake in counts about the separation increments relatively with the measure of engendering of blunders in estimations over the system. This makes its very own issue in a similarly disseminated WSN, which is intensified if the kind of system conveyance is non-reasonable for example at the point when the hubs are put arbitrarily [16][17].

B. WSN Energy Optimization

Various well- known journal publications are available that covered different networking setup and approaches for handling the energy streamlining issue in the Wireless Sensor Networks. It will be difficult here mentioning all the survey regarding the problems of the networks, but some of the issues that has to be explored in the survey are as followed through leading journal publications.

In the research work [18] a short diagram of the different sorts of sensors, internal design, kinds of working frameworks ready and distinctive correspondence related issues and difficulties. In this audit, in any case, the vitality issue has been talked about all around quickly.

The research study in [19] presents a top-down rundown of vitality streamlining calculations has been reviewed, in which the focal point of center has been the information total in WSNs. A few analysts reviewed vitality reaping systems for WSNs, that could demonstrate to be a superior answer for the sensors in [20] [21] [22].

C. The research problem

In the below shown WSN, let us characterize quantity of sensors introduced in a given region. Expect that every sensor can compute the separation to some other sensor utilizing the RSS or some other technique [23] [24]. In the event that there is a staggered, coherent progressive system with grouping and a conceivable multi-sink situation, in that case the standard parameters that will help in the streamlining of the sensor organize is the most limited way finding for the system. This ensures the sensor sending the information to a hub is utilizing as meager vitality as could reasonably be expected and that the information it means to deliver to the sink is achieving it in as meager jumps of sensors as could be allowed. Consequently, requiring the shortening of way for correspondence.

Another issue that emerges when getting ready for the way of correspondence is the measure of vitality accessibility. The accessible vitality may be displayed as a factor of nodes weight produced during networking of the hubs. Accordingly, when the ways are proposed to be made by the system, the heaviness of the sensor hub as a proportion of the accessible vitality in the hub is to be mulled over too. This makes the issue a blend of voyaging sales rep issue (SRI) and a specific improvement calculation. TSP guarantees that a determination of hubs from the system adds to the production of way to the sink. The determination of hubs in the WSN is made so that the contribution of the hubs in the way doesn’t make them bite the dust very soon.

Steiner Tree is a seeking calculation in chart hypothesis, that are been utilized as of late in an application to WSNs for discovering the most limited conceivable way that a lot of hubs can be canvassed with so as to transmit information from a detecting hub to the sink. It has certain restriction of its own, for example it can't be connected to under three hubs at any given moment and this makes it in fact hard to apply to remote sensor hubs for most brief conceivable way creation. The Steiner calculation makes a virtual hub in the middle of the three hubs so that the way from any of the three hubs to some other hub is the briefest conceivable. Subsequently, the all-out separation between each pair of hubs in the set is by normal, the least conceivable.

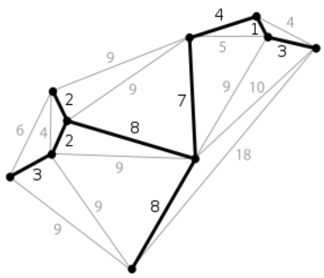

Figure 3. Minimum Spanning Tree

II. MATERIALS AND METHOD

A. Graphs and Trees

A scientific set that contains collection of edges and vertices is known as Graph. For example, in a real time environment, a lot of towns go about as hubs and the streets joining them go about as edges. Correspondingly, a system with sensor hubs and the interfacing pathways go about as hubs and edges separately. As per directionality, charts are defined in two types, coordinated and undirected diagrams. The coordinated diagrams have additional element to bear reliance for the ways, for example certain ways are enabled uniquely from one course to the next, and not a different way. A run of the mill diagram comprising of eight edges and six vertices is demonstrated as follows:

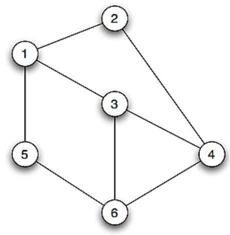

Figure 4. A simple undirected graph example

Definition: The graph is shown as a couple of (V, E), where V is a limited arrangement of qualities representing the chart's edges, while E has a lot of limited edges. E is encompassed in VxV and G denotes the diagram. G is a coordinated diagram if E has a lot of requested combines and is undirected if the arrangement of edges is unordered sets.

The Vertices, V= {1,2,3,4,5,6} and the Edges, E= {(1,2), (1,3), (1,5), (2,4), (3,4), (3,6), (4,6), (5,6)}

Definition: A way is along these lines, characterized in a graph as a succession of vertices associated by the edges, in which the vertices don't happen on numerous occasions. This is represented by P. For example, for the precedent diagram appeared, the path is like {6, 5, 1, 2}.

In light of the paths and their availability, there are two kinds of charts, one is the connected and the other one is non-connected. In the connected graph each pair of vertices is associated, for example there is a way for each pair of particular vertices. In the detached or non-connected graph there is in any event one sets of detached vertices, between which, a way can't exist.

Definition: A cycle is an exceptional way in which the start and end vertices are equivalent.

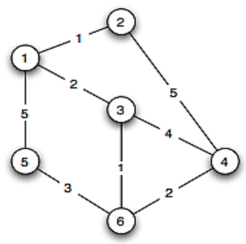

Figure 5. Example of a Weighted Graph

B. Dijkstra's algorithm

Djikstra's - a Dutch researcher, who introduced an instinctive method to discover the briefest route in a chart between the two vertices of any associated chart. In a given chart G= (V,E,w) with identified loads w, where w is a capacity that maps positive whole numbers to the area of the edges, for each edge in the diagram spoken to by an arranged pair of c and y organizes for example e=(x,y) ϵ E, the load is then denoted by w(e) and w(x,y) denotes the separation in between the vertices of the system. Thus, w shows the system's nodes separation, for example the chart's vertices.

The path is shown mathematically as $\pi = v_1 v_2 v_3 \dots v_n$ with n vertices. v_1 to vertex v_n can be denoted arithmetically by $w(\pi) = w(v_1, v_2) + w(v_2, v_3) + \cdots w(v_{n-1}, v_n)$.

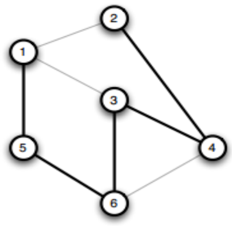

Figure 6. A spanning tree of graph in figure.[4]

On the off chance that for a similar chart or system, no other path with w(π) not as much as this esteem exists, at that point the path is considered shortest between vertex v_1 and v_n. Give us a chance to signify the separation between two vertices of chart by d(a,b), at that point if the hubs are associated, this separation d is limited, and vast generally.

Problem: The issue is characterized in scientific terms as pursues. Given a weighted diagram with associated vertices, represented by G=(V,E,w), as clarified in advance of, and an essential vertex s and auxiliary vertices v, it is wanted to locate the briefest route from the source vertex s to every one of the vertices v. Dijkstra's calculation discovers the briefest route issue's answer by utilizing an insatiable way to deal with the inquiry of the paths.

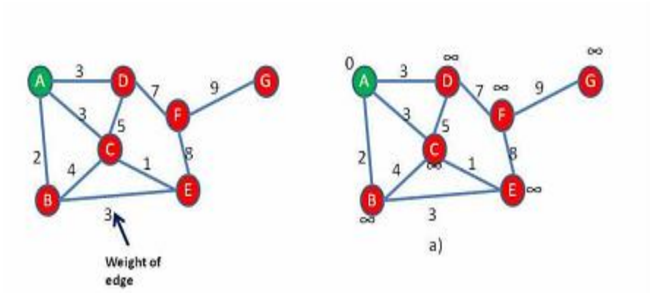

Figure 7. Dijkstra algorithm greedy method described with a graph

It begins off by discovering every conceivable route from a solitary vertex to other vertex by picking just vertices those are nearest to the past vertex. It basically implies the tree that is made by the Dijikstra's calculation is the base weighted tree.

This tree is called as the shortest path tree (SPT). Most significant point to be recollected here is that the SPT shouldn't be an extraordinary arrangement of the chart. There can be numerous SPT in a solitary chart, and this is entirely distinctive from the minimum tree spanning (MST) as follow.

Minimum Spanning Tree

In an allied chart G with E edges, w loads and V vertices G=(V,E,w), a Minimum Spanning Tree (MST) is can be defined as an intersecting tree for the said diagram to such a degree that the comprehensive load of the tree is least.

It infers that of the different possible results of the SPT, just a single hopefully fits for the MST of the chart. For our model network, the example of SPT and MST are ensued as:

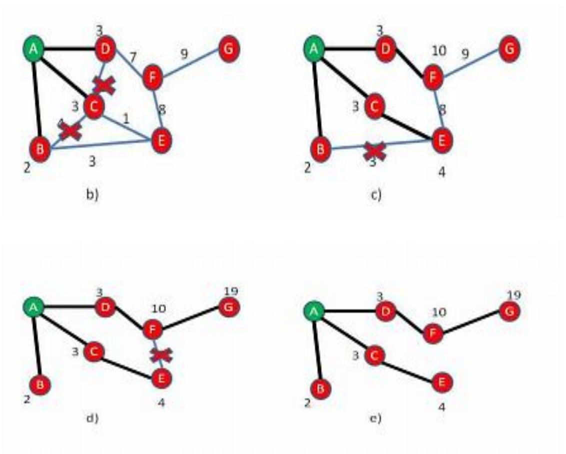

Figure 8. Dijkstra's algorithm explained graphically

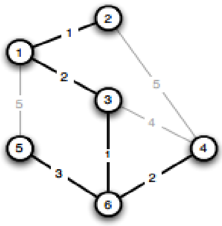

Figure 9. MST of the example graph

- *SPT and MST appliance to WSNs*

While the appliance and preparation of these SPT and MST calculations to the WSN situation, the weighted diagram idea need to be slightly elucidated. The loads in the chart proposes as referenced before signifies the parting of the hubs from one another, yet it may communicate to some other model parameter of WSN. Give us an option to indicate the weight "w" as the separation between any two sensors of the system.

- *The issue in MST*

The concern in the minimum spanning tree associated with wireless sensor systems is that the disconnections between the sensors isn't the main standards that can handle the issue of energy prolific information transmission in WSN. Be that as it may, there is likewise another parameter of the system, specifically, the rest of the energy in the node of the system.

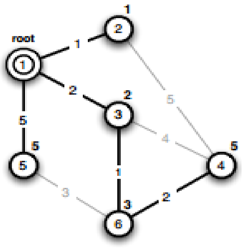

Figure 1. SPT of the graph with root vertex 1

The rest of the energy perhaps won't be enough in a state that may necessitate minor separation to transmit information efficiently, yet because of the insignificant amount of residual energy in a sensor, the assignment probably won't be accessible. From a node that is left with an insignificant measure of vitality may prompt its initial failure during transmission of information and may break the MST path generated to transmit the data.

III. Simulation And results

The simulations start by mounting fifty sensors in a 100×100 meters region. The total 1225 possible routes developed in between fifty sensors are stated by blend calculation without redundancy. All routes are properly examined for the loads categorized by separation and remaining vitality. The loads represent a plotted arithmetical incentive for the separation between two sensors just as the vitality utilized while their talking with the route.

In each cycle of the process, the system is counted to have transmitted and received fifty signals, every last one of the sensors has used a portion of their energy and in this manner, and the estimation of remaining vitality has reduced. The fundamental phase of the system can appear with every single probable route in between nodes.

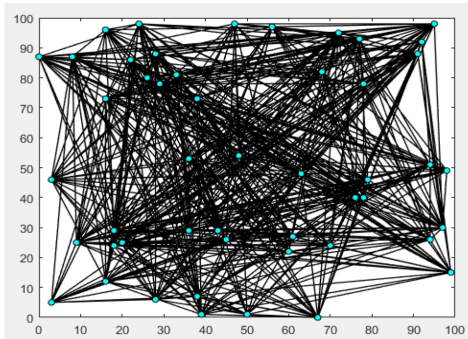

Figure 11. Initialization of the network

After executing the algorithm, when it kept running for 1000 cycles, the energy and the path that optimized can be viewed distinctly. The results of the work have shown in the associated images. The following chart has the minimum spanning tree of the system came about and improved by PSO computation.

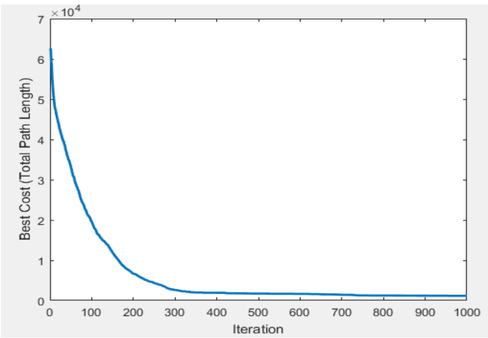

Figure 12. Progression, Minimalization of each sensor's cost

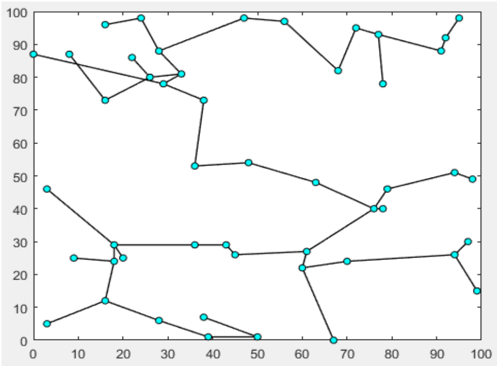

Figure13. MST of the particular network

The X and Y directions of the existent testing system's conveyed sensors are listed in table III given below. The total energy usage of the system in one cycle is 2.91172E-05. In the event that the total energy of the system is counted as 250J, at that point the system will survive about 9 Million cycles taking into consideration the largest quantity of energy per cycle as 5.24023E-07J. Suppose each sensor takes 1ms to receive, process, decide and then transmit data in an information flooding scenario, and that RF waves travel at 87% of speed of light in air, the trip time of a sensor at the far end of a network from where data will reach the other far end in a 100m distance in 0.00707 seconds or 7.0 ms.

Thus, the latency of a single transmission reception data exchange will be 14ms. For 9 million iteration life time, the real life of the network becomes 9000000*14ms= 33 to 35 Hours (2.91E-05 to 5.2E-07 energy usage per iteration) of Peak Connectivity Lifetime with no delays, no sleep state, no data retransmissions, and no idle state of the sensor. These values are exaggerated. The actual life time will account to many days depending on sensors type and usage frequency. As conferred previously, the sleep mode is 1/10th in energy consumption than the active state, so a normal working of the sensors would be 350 Hours, or at least 14.5 days, which is a substantial enhancement.

TABLE I. WIRELESS SENSOR NETWORK PARAMETERS

Parameter Name	**Value / Property**
Total Nodes	50
Area Dimensions	100x100 meters
Initial Energy of sensor	Considered any large value
Data aggregation energy	05 nJ
Maximum Cycles	1000
Free Space Loss Energy	10 pJ
Multipath Loss	1.2 Fj
Transmit Amplifier	50 nJ
Receive Amplifier	50 nJ

TABLE II. ALGORITHM RELATED PARAMETERS

Name of parameter	**Value/Property**
Maximum coding iterations $iter$	1000
Population of particles n	250
Weight constant of inertia, ω	0.2
Inertia weight damping ratio w	1-yes
Learning Coefficients for w_{damp}	0.2
Personal Learning Coefficient c_1	0.7
Global Learning Coefficient c_2	1.0

TABLE III. DISTANCE AND ENERGY UTILIZATION

From	To	Distance (m)	Energy (J)	From	To	Distance (m)	Energy (J)
7	1	79.1	3.96E-07	27	26	5.1	2.55E-08
7	2	79.1	3.96E-07	50	26	83.7	4.18E-07
38	2	75.7	3.78E-07	26	27	5.1	2.55E-08
32	3	23.3	1.16E-07	42	27	63.5	3.18E-07
19	4	25.5	1.27E-07	45	28	71.6	3.58E-07
29	4	35.7	1.79E-07	4	29	35.7	1.79E-07
43	4	89.7	4.49E-07	12	29	71.6	3.58E-07
49	4	96.2	4.81E-07	21	30	42.8	2.14E-07
18	5	73.6	3.68E-07	35	31	87	4.35E-07
9	6	58.1	2.90E-07	38	31	49.3	2.46E-07
1	7	79.1	3.96E-07	3	32	23.3	1.16E-07
2	7	79.1	3.96E-07	44	32	83.2	4.16E-07
18	8	80.5	4.02E-07	11	33	34	1.70E-07
6	9	58.1	2.90E-07	14	33	104.7	5.24E-07
23	9	58.1	2.90E-07	20	33	39.6	1.98E-07
34	9	24.1	1.20E-07	9	34	24.1	1.20E-07
17	10	48.4	2.42E-07	40	34	55.3	2.77E-07
47	10	27.7	1.38E-07	31	35	87	4.35E-07
15	11	72.4	3.62E-07	39	35	67	3.35E-07
33	11	34	1.70E-07	38	36	90.6	4.53E-07
38	11	80.1	4.01E-07	16	37	67.4	3.37E-07
15	12	57.8	2.89E-07	22	37	15.5	7.76E-08

From	To	Distance (m)	Energy (J)	From	To	Distance (m)	Energy (J)
29	12	71.6	3.58E-07	48	37	73	3.65E-07
39	13	104.8	**5.24E-07**	2	38	75.7	3.78E-07
45	13	100.4	5.02E-07	11	38	80.1	4.01E-07
33	14	104.7	5.24E-07	31	38	49.3	2.46E-07
11	15	72.4	3.62E-07	36	38	90.6	4.53E-07
12	15	57.8	2.89E-07	13	39	104.8	5.24E-07
37	16	67.4	3.37E-07	35	39	67	3.35E-07
10	17	48.4	2.42E-07	34	40	55.3	2.77E-07
42	17	48.4	2.42E-07	48	41	99.5	4.98E-07
5	18	73.6	3.68E-07	17	42	48.4	2.42E-07
8	18	80.5	4.02E-07	25	42	3.6	1.80E-08
20	18	75.1	3.76E-07	27	42	63.5	3.18E-07
4	19	25.5	1.27E-07	4	43	89.7	4.49E-07
18	20	75.1	3.76E-07	48	43	49.3	2.46E-07
33	20	39.6	1.98E-07	22	44	54.4	2.72E-07
24	21	42.1	2.10E-07	32	44	83.2	4.16E-07
30	21	42.8	2.14E-07	13	45	100.4	5.02E-07
37	22	15.5	7.76E-08	23	45	70	3.50E-07
44	22	54.4	2.72E-07	28	45	71.6	3.58E-07
9	23	58.1	2.90E-07	24	46	28.2	1.41E-07
24	23	24	0.00000012	47	46	22	**1.10E-07**
45	23	70	3.50E-07	10	47	27.7	1.38E-07
21	24	42.1	2.10E-07	46	47	22	1.10E-07
23	24	24	0.00000012	37	48	73	3.65E-07
46	24	28.2	1.41E-07	41	48	99.5	4.98E-07
42	25	3.6	1.80E-08	43	48	49.3	2.46E-07
26	50	83.7	4.18E-07	4	49	96.2	4.81E-07
26	50	83.7	4.18E-07	4	49	96.2	4.81E-07

The coordinates of the nodes in the network are shown below:

TABLE IV. COORDINATES OF THE NODES OF THE NETWORK

Node	X Coord	Y Coord	Node	X Coord	Y Coord
1	98	49	26	92	92
2	79	46	27	91	88
3	38	7	28	0	87
4	18	29	29	36	29
5	97	30	30	16	96
6	22	86	31	63	48
7	94	51	32	50	1
8	99	15	33	60	22
9	26	80	34	16	73
10	68	82	35	48	54
11	61	27	36	78	40
12	43	29	37	16	12
13	38	73	38	76	40
14	67	0	39	36	53
15	45	26	40	8	87
16	3	5	41	9	25
17	72	95	42	77	93
18	94	26	43	18	29
19	3	46	44	39	1
20	70	24	45	29	78
21	24	98	46	47	98
22	28	6	47	56	97
23	33	81	48	18	24
24	28	88	49	20	25
25	78	78	50	95	98

The average separation of these inter-nodal paths is 59.422 meters.

CONCLUSIONS

This research is a combination of MST and PSO algorithms exercised together to optimize the path and energy of fifty nodes network distributed casually on a 100x100 meters region. This study is a complete demonstration of the sensor network to the particular coordinates so that a scholar in coming time may enhance and refer to it. However, the unavailability of existing researches published codes form and comprehensive facts, have hindered to perform the comparison course of this work.

REFERENCES

[1] S. Bouarafa, R. Saadane, and M. Rahmani, "Inspired from Ants Colony: Smart Routing Algorithm of Wireless Sensor Network," Information, vol. 9, no. 1, p. 23, 2018.

[2] A. Khan et al., "A localization-free interference and energy holes minimization routing for underwater wireless sensor networks," Sensors (Switzerland), vol. 18, no. 1, pp. 1–17, 2018.

[3] A. Ali, Y. Ming, T. Si, S. Iram, and S. Chakraborty, "Enhancement of RWSN lifetime via firework clustering algorithm validated by ANN," Inf., vol. 9, no. 3, pp. 1–13, 2018.

[4] A. Darwish and A. E. Hassanien, "Wearable and implantable wireless sensor network solutions for healthcare monitoring," Sensors, vol. 11, no. 6, pp. 5561–5595, 2011.

[5] S. Tomic and I. Mezei, "Improvements of DV-Hop localization algorithm for wireless sensor networks," Telecommun. Syst., vol. 61, no. 1, pp. 93–106, 2015.

[6] M. S. Elgamel and A. Dandoush, "A modified Manhattan distance with application for localization algorithms in ad-hoc WSNs," Ad Hoc Networks, vol. 33, pp. 168–189, 2015.

[7] R. Lachowski, M. Pellenz, M. Penna, E. Jamhour, and R. Souza, "An Efficient Distributed Algorithm for Constructing Spanning Trees in Wireless Sensor Networks," Sensors, vol. 15, no. 12, pp. 1518–1536, 2015.

[8] A. G. Bakirtzis, P. N. Biskas, C. E. Zoumas, and V. Petridis, "Optimal power flow by enhanced genetic algorithm," IEEE Trans. Power Syst., vol. 17, no. 2, pp. 229–236, 2002.

[9] B. Risteska Stojkoska, "Nodes Localization in 3D Wireless Sensor Networks Based on Multidimensional Scaling Algorithm," Int. Sch. Res. Not., vol. 2014, pp. 1–10, 2014.

[10] I. Banerjee, I. Roy, A. R. Choudhury, B. D. Sharma, and T. Samanta, "Shortest path based geographical routing algorithm in wireless sensor network," Commun. Devices Intell. Syst. (CODIS), 2012 Int. Conf., pp. 262–265, 2012.

[11] P. Chen, H. Ma, S. Gao, and Y. Huang, "SSL: Signal similarity-based localization for ocean sensor networks," Sensors (Switzerland), vol. 15, no. 11, pp. 29702–29720, 2015.

[12] J. Cota-Ruiz, J.-G. Rosiles, P. Rivas-Perea, and E. Sifuentes, "A Distributed Localization Algorithm for Wireless Sensor Networks Based on the Solutions of Spatially-Constrained Local Problems," IEEE Sens. J., vol. 13, no. 6, p. 11, 2013.

[13] Y. Shang, W. Ruml, Y. Zhang, and M. P. J. Fromherz, "Localization from mere connectivity," Proc. 4th ACM Int. Symp. Mob. ad hoc Netw. Comput. - MobiHoc '03, p. 201, 2003.

[14] A. a Kannan, G. Mao, and B. Vucetic, "Simulated Annealing based Wireless Sensor Network Localization with Flip Ambiguity Mitigation," Most, vol. 00, no. c, 2006.

[15] [C. Alippi and G. Vanini, "A {RSSI}-Based and Calibrated Centralized Llocalization Technique for Wireless Sensor Networks," Proc. IEEE Int. Conf. Pervasive Comput. Commun. Work., 2006.

[16] [B. Huang, C. Yu, and B. D. O. Anderson, "Analyzing Error Propagation in Range-based Multihop Sensor Localization," Proc. IEEE Conf. Decis. Control, pp. 865–870, 2009.

[17] G. Anastasi, M. Conti, M. Di Francesco, and A. Passarella, "Energy conservation in wireless sensor networks: A survey," Ad Hoc Networks, vol. 7, no. 3, pp. 537–568, 2009.

[18] R. Rajagopalan and P. Varshney, "Data aggregation techniques in sensor networks: A survey," pp. 48–63, 2006.

[19] K. Akkaya and M. Younis, "A survey on routing protocols for wireless sensor networks," Ad Hoc Networks, vol. 3, no. 3, pp. 325–349, 2005.

[20] S. Sudevalayam and P. Kulkarni, "Energy harvesting sensor nodes: Survey and implications," IEEE Commun. Surv. Tutorials, vol. 13, no. 3, pp. 443–461, 2011.

[21] I. Dietrich and F. Dressler, "On the lifetime of wireless sensor networks," ACM Trans. Sens. Networks, vol. 5, no. 1, pp. 1–39, 2009.

[22] C. E. Jones, K. M. Sivalingam, P. Agrawal, and J. C. Chen, "A survey of energy efficient network protocols for wireless networks," Wirel. Networks, vol. 7, no. 4, pp. 343–358, 2001.

[23] J. N. Al-Karaki and A. E. Kamal, "Routing techniques in wireless sensor networks: A survey," IEEE Wirel. Commun., vol. 11, no. 6, pp. 6–27, 2004.

[24] A. A. Abbasi and M. Younis, "A survey on clustering algorithms for wireless sensor networks," Comput. Commun., vol. 30, no. 14–15, pp. 2826–2841, 2007.

Muhammad Zahoor is currently student of Msc in Computer Systems Engineering at Department of Computer systems Engineering, University of Engineering & Technology, Peshawar, Pakistan. His research interests include control systems and wireless sensors networks He can be reached via email mzahoor757@gmail.com.

International Journal of Engineering Works
ISSN-p: 2521-2419
ISSN-e: 2409-2770
Vol. 6, Issue 10, PP. 354-359, October 2019
https://www.ijew.io/
https://doi.org/10.34259/ijew.19.610354359

Modelling and Optimization of Small Scale Solar Organic Rankine Cycle for Islamabad, Pakistan

Marva Hadia[1], Tariq Talha[2]
[1,2] NUST, ISB, Pakistan
marva.hadia@gmail.com[1], tariqtalha@gmail.com[2]

Received: 22 September, Revised: 29 September, Accepted: 02 October

***Abstract*—**In recent decades, energy demand has grown exponentially. Fossil fuels, which today meet the bulk of global energy demand, can be gradually replaced by renewable energies, thus limiting its dangerous consequences such as climate change, environmental pollution, depletion of natural resources, etc. Solar energy can play an important role in the satisfaction of energy demand, especially in a heavily sun-ridden country. The current study focuses on the modelling and optimization of Organic Rankine Cycle (ORC) based on different organic fluids operating in a temperature range below 50-100 °C. The ORCs are a good choice to produce small-scale energy due to the lower temperature range of 50 to 99 °C. They are therefore simple and inexpensive. Flat plate (FPC) or evacuated tube solar collectors (ETC) can also provide the desired energy. In this work, two system configurations are analyzed. In configuration-I (C-I), the water from the collector outlet moves to the hot water storage tank (HWST) connected in series, while in configuration-II (C-II), HWST is not used. Therefore, the hot water from the solar collector outlet enters directly into the auxiliary heater (which will be lit if necessary, otherwise) and the water return from the heat exchanger will become the input of the solar collector. Working fluids suitable for a solar-powered ORC at a temperature of 100 °C or lower are selected using predefined criteria such as higher fluid densities, maximum cycle efficiency, safety and environmental data, a moderate temperature and inexpensive and uncomplicated equipment. The R125 and R245ca were found to be good fluids due to the minimum collector area for the desired yield and maximum efficiency, respectively. For the R125, the minimum required collector area is estimated to be 50 m² for the ETC and 68.14 m² for the FPC. For these areas, the optimized size of the HWST is estimated at 1350 L. System configurations are modelled and simulated in TRNSYS for the entire year, from January 1st to December 31st, to investigate optimal collector tilt, the smallest collector area for maximum solar fraction, and solar collector thermal efficiency. Monthly solar collector efficiency is calculated for both configurations. The results of the simulation showed that C-II gives a comparatively higher solar collector thermal efficiency and solar fraction. For both collectors, the maximum seasonal solar fraction is obtained at an inclination of approximately 14°. A thermal efficiency of evacuated tube solar collector is comparatively higher for C-II than that of C-I and one observes the same trend for FPC. In addition, the thermal efficiency of the ETC at 50 m² is higher than that of the FPC at an area of 68.14 m².exhibited.

***Keywords*—** Organic rankine cycle, Trnsys, flat plate collector; evacuated tube collector, solar fraction, tilt angle.

I. Introduction

OSSIL fuels fulfilled the energy demand throughout the entire modern era. Coal, oil and natural gas remained in use for ages. However, accelerated human development threatened the sustainability of these energy sources. The persistent and widespread reliance on fossil fuel resources so far led to their depletion. It also challenged environment by an increase in air pollution and global warming. This caused a search for renewable sources of energy that ensure a sustainable future for the humanity. For production and industrial processes global economy revolves around energy. The efficient energy production and its use have a significant consequence on our society and environment as well. As per International Energy Agency (IEA), the current trend for energy consumption and efficiency increases energy requirement by 70% and 60% and emissions respectively by 2050 in comparison to 2011. The global average temperature by associated emissions will increase by 6 °C by 2050, which might result in massive adverse impact i.e. climate change, energy security and unendurable future [1].

The fossil fuel burning generates nearly 21300 million tons of toxic carbon dioxide (CO2) every year. As per reports it is claimed that natural processes absorb only about half of this amount thus there is net increase of 1065 million tons of atmospheric CO2 every year. [2] Renewable energy sources are an alternative to conventional fossil fuels which are available in various forms and their energy can be harnessed through various means. There is no region in the world that lacks one form of renewable energy source or another but their abundance might vary. Getting energy from renewable sources like solar, wind, hydro, biomass, geothermal and industrial waste heat is becoming attractive to conventional sources. Research into efficient, effective and energy harnessing techniques from renewable sources is trending worldwide. In 2016, clean energy installations of 160 GW introduced globally. This shows an increase of 10% compared to 2015, but their cost is reduced almost a quarter. Furthermore, solar power provided the biggest boost and consisted of half of all new capacity. 2016 was the first year in history that introduced solar capacity that surpassed all other electricity-producing technologies. [3].

Many techniques generate electricity from low temperature thermal energy for the reduction of environmental pollutants and ORC is amongst them. The Rankine cycle technology, one of the incipient energy conversion techniques, harnesses energy from renewable sources efficiently and effectively. Compression of wet vapors in Carnot cycle became a problem so ORCs stepped in as an advancement. Rankine cycle comprises four main thermodynamic processes namely compression, evaporation, expansion and condensation. Four main components of the cycle namely the pump, boiler/ evaporator, turbine/expander, and condenser perform these processes. The technology of ORCs is applicable in various applications such as geothermal, hydropower, wind, solar, biomass and industrial waste heat recovery etc. High, medium and low-grade heat sources are defined by their temperature facilitate such applications. Medium to high thermal sources provide high efficiency of an ideal Rankine Cycle (RC) system with temperatures above 370 °C. The ORC operates on the same principle as that of an ideal RC with the exception of using organic fluid as working fluid. The effective utilization of low-grade energy resources gives ORC a great advantage. The additional features of the organic Rankine technology such as dry expansion process, low adverse environmental impact, high thermal efficiency, simple expander design make it a valuable technology. For many years, the research trend shifted towards power generation from sustainable and clean resources. Industrialization, socio-economic and environmental factors mainly contribute to this trend.

Small-scale Solar Organic Rankine cycles are best suitable for off-grid remote areas. In comparison to the PV collectors, solar ORCs usually have local manufacturing. They also show much more flexibility that allows the hot water production as a byproduct for domestic or industrial use with a low appropriate investment cost. For medium and large scale, the technology is much developed but only a few solutions are available for small size systems in the low kW power range. The evolution of small organic Rankine power systems is due to lack of efficient components for decades.

Pakistan faced severe energy crisis since the last two decades. The region shows sufficient solar radiation but lacks solar assisted ORC on small scale. This opens a doorway to research that determines the potential of solar energy to fulfil energy demand in remote areas on domestic level in Pakistan. Results from this research work address some of the fundamental issues linked with the conventional way of energy generation from fossil fuel, moreover, present the benefits of renewable energy production. This research aims to:

- Conduct a comprehensive literature review of the renewable energy resources and the technologies being used to capture them.
- Develop and optimize a suitable model for ORC that works in low temperature range.
- Present the output of ORC system in terms of generated power and efficiency.
- Show the effects of variation in input parameters i.e. pressure, heat source temperature and refrigerant flow rates, for the model developed and on the solar ORC performance thus determining optimum performance conditions.

The current research presents the power production potential available in renewable energy sources with low to medium temperature range. Factors which influence the selection of working fluid for the ORC technology are discussed in detail and selection of appropriate refrigerants is made. In the standard formulation of this research work, the law of conservation of energy has been carefully examined.

The cost analysis and evaluation of the materials used for the current study were not taken into account.

A. *Algorithm*

The algorithm for the modelling and optimization of small scale solar Organic Rankine Cycle is given in figure 1.

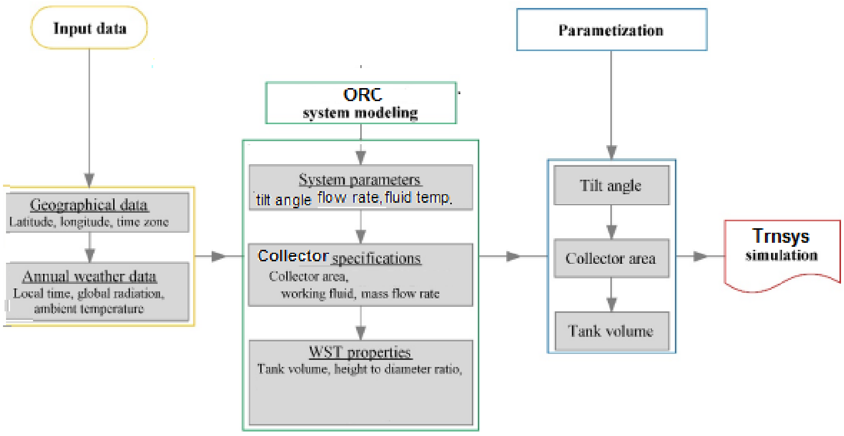

Figure 1: Algorithm for Modelling and Optimization in Trnsy

II. METHODOLOGY

The system consists of two circuits: the primary and the secondary circuit. The working fluid expands in the turbine in the primary circuit from where it goes into a condenser where it is condensed. In the secondary circuit, the pump circulates the hot water of the solar collector (Type 1b or 71) in the hot water tank (Type 4a). And two possibilities are discussed: solar collectors without solar thermal energy storage tank (CI) and solar collectors connected to a solar thermal energy storage tank (C-II). Solar collector thermal efficiency is calculated by:

$$\eta = a_0 - a_1 \frac{\Delta T}{I_T} - a_2 \frac{\Delta T^2}{I_T} \quad (1)$$

where:

$\Delta = (Tin{-}Tamb)$

In this study values of ao, a1 ($W/m^2.K$) and a2 ($W/m^2.K^2$) are taken as 0.845, 1.47 and 0.01 for ETC and 0.749, 2.770 and 0.023 for FPC, respectively. These values are taken from a manufacturer "Apricus" collector's catalogue. a0, a1 and a2 define the thermal efficiency. [4] The equations 1 and 2 calculate the capacity of each side of the heat exchanger [5].

$$C_c = m_c C_{pc} \quad (2)$$

$$C_h = m_h C_{ph} \quad (3)$$

Equation (4) is used to calculate the heat exchanger effectiveness at each time step which depends upon heat exchanger's configuration.

$$\varepsilon = \left[\left(\frac{1-\varepsilon_1 \frac{C_{\min}}{C_{\max}}}{1-\varepsilon_1} \right)^N - 1 \right] \left[\left(\frac{1-\varepsilon_1 \frac{C_{\min}}{C_{\max}}}{1-\varepsilon_1} \right)^N - \frac{C_{\min}}{C_{\max}} \right]^{-1} \quad (4)$$

The amount of energy that is needed to raise the inlet water temperature to the required temperature (provided that control signal to the boiler is ON and there is a flow through the boiler) is calculated by using:

$$\dot{Q}need = \dot{m}fluidCpfluid\,(Tst - Tin) \quad (5)$$

If control signal is ON and set temperature is less than inlet temperature, heater will not find negative value of $Qneed$. The energy required is limited by capacity of the boiler. Equation used to determine the amount of fuel utilized by the boiler after calculating the required energy is given as: [3]

$$Qfuel = Qneed/\eta boiler \quad (7)$$

System Performance Indicators

Following performance indicators, based on integrated values of various energies over the whole, optimize the system:

Solar Fraction

$$SF = \frac{\int Q_u}{\int Q_u + \int Q_{aux}} \quad (8)$$

Equation (8) is used to calculate the solar fraction on each collector.

Collector Efficiency

Solar collector efficiency is calculated by:

$$\eta = \frac{\int Q_u dt}{A \int G\, dt} \quad (9)$$

Model Validation

The present model is applied in Trnsys and results are compared with the available experimental and numerical data. It is observed that results of present model are in a good agreement with the past research presented in [4], [6], [7], [8]. The comparison of collector efficiency for both configurations for ETC and FPC was done with [4]. Similarly simulation results of [6], [7] showed that optimum angle is 12° for maximum solar heat gain for the location under consideration and simulation results of [8] for optimal study of a solar air heating system with pebble bed energy storage verify the trend for solar collector area vs solar fraction.

III. RESULTS AND DISCUSSIONS

Simulations were performed in TRNSYS from 0 hour i.e. 1st hour of 1st January till 8760 hr. i.e. last hour of 31st December and Simulation time step is 0.125 hr.

A. *Variation of Solar Fraction with Collector Area and Collector Tilt*

Fig. 2 exhibits the effect of varying ETC area and tilt angle on SF. Maximum value of SF is achieved at 14° tilt angle for each value of solar collector area. Increasing tilt angle further causes SF to decrease. As collector area increases SF increases. Maximum value of SF is achieved at 14° tilt angle for each value of solar collector area. Increasing tilt angle further causes SF to decrease.

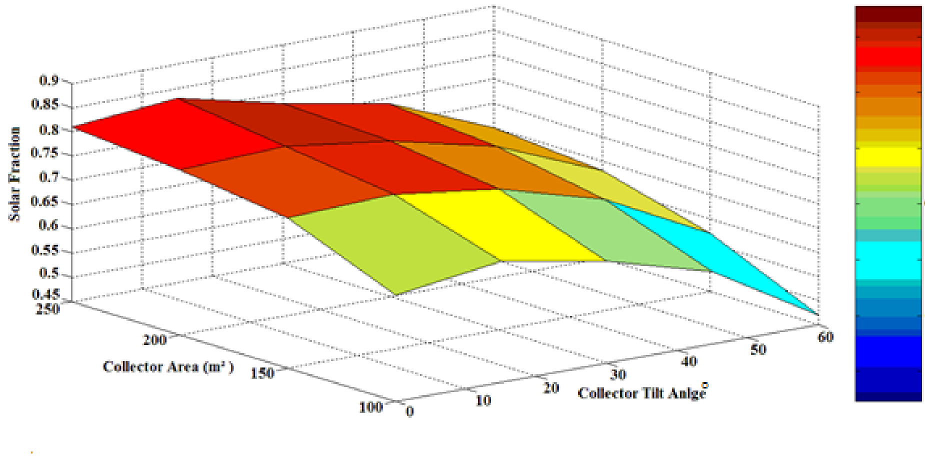

Figure 2: slope, Area vs solar fraction

B. Collector Efficiency

Figure 3 presents monthly thermal efficiency of FPC and ETC for both configurations corresponding to FPC and ETC areas of 68.14 m² and 50 m² respectively. It is evident that ETC yields higher monthly efficiency than FPC, however the effect of system configuration (C-I or C-II) on collector efficiency is marginal. It is also observed that for fixed collector areas of 68.14 m² and 50 m², system without HWST has higher values of collector thermal efficiency. It is because that temperature of the water entering the array of solar collector in a system without HWST is comparatively lower as water entering in the solar collector from HWST.

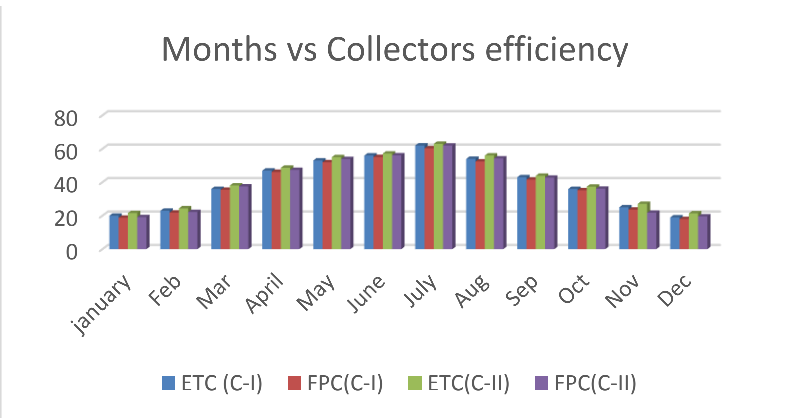

Figure 3: Months vs Collector's efficiency

C. Variation of solar Fraction with respect to Storage Tank size

Figure 4 and 5 shows variation of with respect to specific storage volume for both configurations corresponding to ETC areas of 50 m², 70 m² and 100 m². C-II has higher SF than C-I. Moreover, for any solar collector Area, solar fraction increases as storage tank size increases up to 30 L/m². By further increasing size of storage tank, solar fraction decreases by increasing solar collector area. This is also valid for FPC.

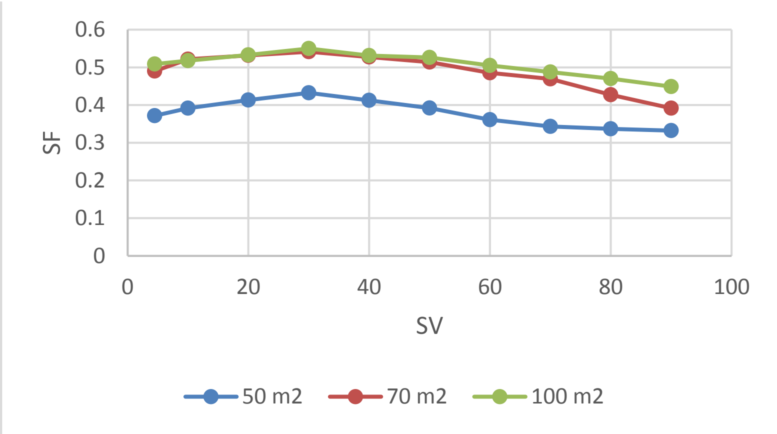

Figure 4: Variation of solar Fraction with respect to Storage Tank size for C-I

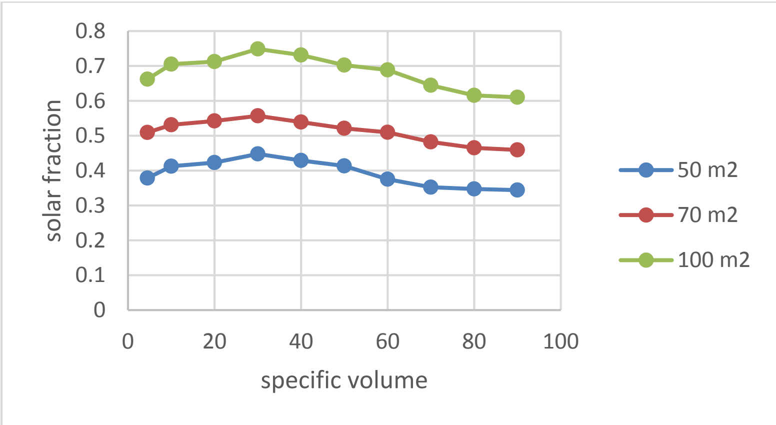

Figure 5: Variation of solar Fraction with respect to Storage Tank size for C-II

D. Most suitable Organic fluid for targeted output:

The table 1 shows that the organic fluid R125 is the best option amongst all as it requires least collector area i.e. 50 m² to obtain the targeted output i.e. 1KW.It is also suitable option if we consider the quality of steam at turbine outlet as Tout for R125 which is higher. This shows that it is comparatively drier and is least damaging to turbine blades. Moreover, it requires minimum optimum storage. Lastly, R245ca has maximum efficiency amongst all.

TABLE 1: PERFORMANCE COMPARISONS OF DIFFERENT ORGANIC FLUIDS

Substance (Fluid)	Tout (°C)	ηth (%)	Ac (m²) for ETC	Ac (m²) for FPC	Storage Tank size (liters)	Substance (Fluid)
R125	89.45	3.36	50	68.14	1350	R125
R218	81.78	7.5	58.24	83.17	1570	R218
R236ea	55	12.83	63	87.4	1700	R236ea
R245ca	51.54	12.83	68.12	92.3	1832	R245ca

CONCLUSIONS

This paper presents the modelling and optimization of two system configurations of solar assisted ORC system for Islamabad (33.71° N, 73.06° E). Simulations of the system are done in TRNSYS for the whole year to investigate the possibilities of driving ORC with low grade heat, i.e. from an evacuated tube or flat plate solar collector. Results of the analysis showed that for the given collector area, highest solar fraction is achieved at collector tilt of 14°.Simulation results showed that C-II gives comparatively higher collector thermal efficiency and same trend was observed for FPC. Moreover, efficiency of ETC is higher than FPC. R125 and R245ca emerged as good fluids owing to the least collector area (50 m² for ETC and 68.14 m² for FPC) for desired output i.e. 1KW and maximum fluid efficiency i.e. 12.8 3% respectively. Corresponding to these areas optimized size of HWST is estimated to be 1350 litters. The thermal efficiency for ETC at 50m² is higher as compared to FPC at an area of 68.14 m². Increasing the collector area improves the solar fraction remarkably but its rise decreases gradually after 70 m².R125 requires least storage tank size i.e. 1350 L for desired output. Increasing the specific storage volume above 30 L/m² has no significant effect on solar fraction rather the solar fraction is adversely affected, particularly after 90 L/m² due to heat dissipation of the storage tank. It is also concluded that if system has to be installed without HWST then solar collector area must be increased for the purpose of achieving SF similar to that of system with HWST. The optimum ratio between storage volume and collector area increases as the collector area increases. Therefore, a trade-off between heat collection and heat loss has to be made while attempting to increase solar fraction by improving collector area.

REFERENCES

[1] Kiyarash Rahbar, Saad Mahmoud, Raya K Al Dadah, Nima Moazami, Seyed A. Mirhadizadeh. (2017). Review of organic Rankine cycle for small scale applications Energy Conversion and Management 134, 135-155.

[2] N. Abas, A. Kalair, N. Khan'Review of fossil fuels and future energy technologies' Futures 69 (2015) 31–49

[3] Dolf Gielen, Francissco Boshell 'The role of renewable energy in the global energy transformation' Energy Strategy Reviews volume 24 p38-50

[4] M. Wajahat, M. Shoaib, A. Waheed 'Modeling and Analysis of Solar Assisted Adsorption Cooling System Using TRNSYS' World Academy of Science, Engineering and Technology International Journal of Energy and Power Engineering Vol:9, No:7, 2015

[5] TRNSYS 17 A Transient System Simulation Program Mathematical Reference 4th Vol, 486p

[6] Jakob, Uli, and Walter Mittelbach. "Development and investigation of a compact silica gel/water adsorption chiller integrated in solar cooling systems." In VII Minsk international seminar "Heat pipes, heat pumps, refrigerators, power sources", Minsk, Belarus, pp. 8-11. 2008.

[7] Aldubyan, M., and A. Chiasson. "Thermal Study of Hybrid Photovoltaic-Thermal (PVT) Solar Collectors Combined with Borehole Thermal Energy Storage Systems." Energy Procedia141 (2017): 102-108.

[8] Zhao, D. L., Y. Li, Y. J. Dai, and R. Z. Wang."Optimal study of a solar air heating system with pebble bed energy storage." Energy conversion and management 52, no. 6 (2011): 2392-2400.

International Journal of Engineering Works
ISSN-p: 2521-2419
ISSN-e: 2409-2770
Vol. 6, Issue 10, PP. 360-364, October 2019
https://www.ijew.io/
https://doi.org/10.34259/ijew.19.610360364

Renewable Energy Potential in Khyber Pakhtunkhwa

Asif Ijaz[1], Suhail Zaki Farooqui[2]
[1, 2] USPCAS-E, University of Engineering & Technology, Peshawar, Pakistan
asifarab@hotmail.com[1]

Received: 26 September, Revised: 30 September, Accepted: 02 October

***Abstract*—** Energy is a prerequisite for sustainable development in todays world. Pakistan is a developing country in the South East Asia with a population of more than 210 million. Pakistan is highly dependent on imported oil and gas since a long time. The share of installed renewable energy capacity uptil now is 6%. Khyber Pakhtunkhwa (KP) is one of the four provinces of Pakistan. KP is blessed with a significant amount of renewable energy potential which includes hydroelectric, solar, wind and biomass. This paper starts with Pakistan's energy scenario including the current energy supply and demand gap. It is then followed by a discussion on the renewable energy potential across KP. Hydropower alone has a total potential of around 25000 MW. Average daily solar radiation for KP is found to be 4.99kWh/m^2/day It was found that daily solar radiation remains high in the summer season from April-July and then falls in the winter season. In KP, Mardan receives the highest daily solar radiation in June and Chitral receives the lowest daily solar radiation in December. The province is also blessed with biomass. KP has total livestock population of 43 million including cows, buffaloes, sheep and goats. Waste from animals can be converted into biogas which can be used for cooking and heating purposes. Some parts of the province like Malakand, Buner, Haripur have also some wind potential which is enough to provide electricity to the nearby villages and communites. The paper then discusses reasons for energy shortfall followed by short term and long term measures that can be adopted by KP government to tackle energy crisis.

***Keywords*—** renewable energy, hydroelectric, solar energy, wind energy, biomass, Khyber Pakhtunkhwa

I. INTRODUCTION

Energy security has strong correlation with the socioeconomic development of any country. Due to rapid growth in population, industrialization and urbanization Pakistan is facing great energy challenges [1][2]. Pakistan has a population of more than 220 million and is the sixth most populous nation in the world. Pakistan used to be a nation with agrarian economy, but with passage of time, services and industry sector are dominating to the GDP [3]. Pakistan is one of the developing countries in Asia whose energy demand is rising day by day due to increasing population. Pakistan, like many other countries, is oil dependent to meet its energy demand.

In 2015, the two major sources of energy were oil and natural gas. Oil accounted for 36% share and Natural Gas accounted for 43% share in total primary energy supply [4]. Figure 1 below shows total primary energy supply for Pakistan until 2015. From 2006-2015, the production and supply of natural gas did not change and was constant because of no increase in inhouse gas production. But still, natural ga is playing vital role in meeting energy demand of nation. On the other hand, the share of oil in last ten years (2006-2015) has increased with an average of 4.5% per year.

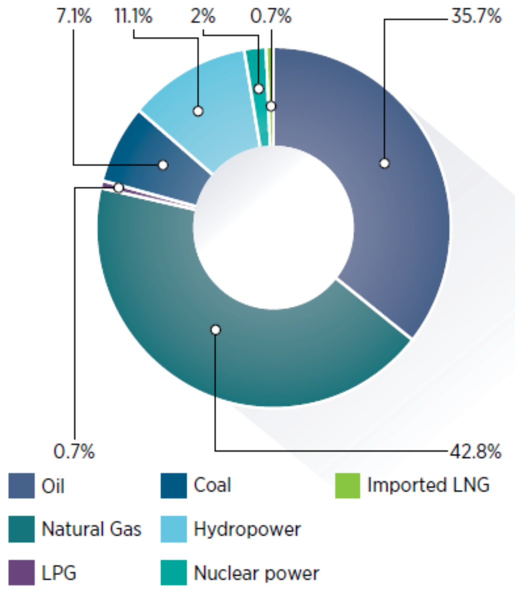

Figure 1 Total primary energy supply by source, 2015 [4]

During last ten years (2006-2015), the population has been increasing at a higher rate as compare to increase in demand. Pakistan electrification rate also increased in that period which resulted in a gap between supply and demand. The electricity defecit started in 2005 with 55MW and is still increasing.
Energy shortfall indicates that current energy resources are unable to meet the electricity demand of Pakistan. The solution to this problem is to harness energy using renewable energy resources which includes solar, hydroelectric, wind energy and biomass. Currently the share of installed renewable energy is 4% [5]. However, the government has plans to increase the share of renewable energy in the total power generation by 30%

[5]. Different form of renewable energy resources are being utilized in other developing countries to increase the share of power generation from renewable energy resources, referring to solar energy, hydroelectric, wind energy, biomass, geothermal and tidal energy.

II. Literature Review

Pakistan is blessed with tremendous amount of renewable energy resources which is a source of power generation. Pakistan has four major renewable energy resources found in excess and this includes solar, hydroelectric, wind and biomass. Small potential of geothermal and tidal energy are also found in the country. Proper utilization of these renewable energy sources can play significant role in overcoming energy crisis.

A. Hydropower

Hydropower is the cheapest source for power generation. This source of renewable energy is available with great potential in country especially in Khyber Pakhtunkhwa. As of 2015, Pakistan was generating 7116 MW of electricity by hydroelectric, most of which is operated by WAPDA [6]. Pakistan has total identified hydro power potential of around 60GW. The province of Khyber Pakhtunkhwa and Gilgit Baltistan have 45GW of the identified potential. Other than large hydropower, Pakistan also has significant potential for development of small scale (1-50MW) and mini/micro (1-1000 kW) Hydel power plants (MMHPP's) [7]. In KP, 142 sites have been identified with a generating capacity of around 25000 MW. In the Punjab province, 296 potential sites have been identified on barrages and canals with a total generation capacity of 7291. In the Sindh province, eighteen hydropower sites have been identified with a total capacity of 193 MW. In Balochistan, there is water scarcity and hardly any hydropower site is identified. Currently, there is no operational project in Baluchistan

B. Solar Energy

Pakistan lies in a geographic region which receives about 2500 hours of sunshine annually. Sheikh [8] in his research concluded that 100 km^2 of area can generate 30 million tons of oil equivalent in Pakistan. Adnan [9] used Hargreave and Agnstrom equation to calculate monthly solar enegy potential using different parameter including sunshine hours, maximum and minimum temperature.

C. Wind Energy

Wind Energy is another useful renewable energy resource which has huge potential in coastal areas of Pakistan including Sindh and Balochistan province. Pakistan has total potential of around 345 GW out of which just 120 GW can be technically extracted as studied by Baloch [10] and Farooqui [11]. Like China and India, Pakistan cal also harness wind energy and tackle energy crisis problem.

D. Biomass

Livestock is building block of Pakistan's economy and contributes significantly to the agriculture sector of the country. Pakistans livestock increases at an annual rate of 4% [12] and 70 million animals (cows and buffaloes) [13] can produce 1140 million tons of dung. Livestock is growing business in developing country where animals are found in great amount as in Pakistan. Livestock can play a vital role in reducing poverty and increase power generation. Iqbal et al [9][14] in his study concluded that by products of livestock business can help in increasing foreign exchange of the nation. Uddin [13] in his paper states that 35.625 million kWh can be generated from biomass on daily use. A complete process for bioenergy has been studied in [15].

III. Renewable Energy Potential In Khyber Pakhtunkhwa

A. Hydropower

Water is the major constituent of our life and is also used as a source for power generation. There are two types of hydropower referred as Small Hydro Power Plants (SHPP's) and Large Hydro Power Plants. The forme has lower generation capacity and the latter has higher generation capacity.

Khyber Pakhtnkhwa (KP) has boundary touching with Gilgit Baltistan and Azad and Jammu Kashmir in its northern side, Afghanistan on its west side, and Punjab and Balochistan on Southern side. The main river that flows in KP are Kunhar, Swar, Indus, Kabul, Kohat, Kurram, Panjkoora, Ushu, Gabral, Tochi and Chital [6].

In KP, there are two major entities working on hydro sector on large scale. Both of them are government entites. The first one is WAPDA and the other one is PEDO. WAPDA is managed by federal government where PEDO is managed by provincial government. There is another department under the ministry of Science & Technology known as Pakistan Council for Renewanle Energy Technology (PCRET). Other than these tow government entities, there are some Non-Government Organizations like Sarhad Rural Support Program (SRSP), Agha Khan Rural Support Program. Table 1 below shows the project that are in operation by WAPDA.

Table 1 Detail of the projects that are in operation by WAPDA [6]

S. No	Project Name	Location	Operated By	Capacity (MW)
A. WAPDA				
1	Tarbela	Tarbela (Reservoir)	WAPDA	3478.00
2	Warsak	Warsak (Reservoir)	WAPDA	240.00
3	Jaban (Malakand-I)	Swat Canal	WAPDA	20.00
4	Dargai (Malakand-II)	Swat Canal	WAPDA	20.00
5	Kurram Garhi	Kurram Garhi (canal)	WAPDA	4.00
			Sub Total	3762

Table 2 below shows list of hydro project executed by PEDO

TABLE 2 LIST OF COMPLETED PROJECTS EXECUTED BY PEDO

Sr. No	Project Name	Location	Capacity (MW)	Status
1	Malakand III Hydro Power Project (HPP)	Dargai	81	Completed
2	Daral Khwar HPP	Bahrain	36.6	
3	Pehur HPP	Swabi	18	
4	Ranolia HPP	Kohistan	17	
5	Machai HPP	Mardan	2.6	
6	Shishi HPP	Chitral	1.875	
TOTAL (MW)			**157.075**	

Other and WAPDA and PEDO, PCRET has also installed 553 Mini Micro Hydro Power Projects across KP with a total generation capacity of 8 MW. SRSP has also installed MMHPP's with generation capacity of 28 MW. AKRSP has installed 147 MMHPP's with a total generation capacity of 13.5 MW.

B. Solar Energy

Solar Energy is the energy received through the solar radiation. This energy can be converted either into heat or electricity depending on the need. The two common methods of generating electricity are solar photovoltaic and solar thermal conversions. Pakistan has a solar PV potential of 2.9 million MW, with annual average temperature of 26-28 degree Celsius [9].

RETScreen software was used to calculate daily solar radiation for 9 cities of Khyber Pakhtunkhwa. Table 16 below shows the data for 9 cities of KP for 12 months. For all the cities, the daily solar radiation increases from January to June. The values are maximum for all the cities in the month of June and July and then start decreasing from June to December.

TABLE 3 DAILY SOLAR RADIATION- HORIZONTAL (KWH/M2/D) FOR 9 CITIES OF KHYBER PAKHTUNKHWA

	Daily Solar Radiation-Horizontal (kWh/m²/d) for 9 Cities of Khyber Pakhtunkhwa												
Cities/Month	Jan	Feb	Mar	Apr	May	Jun	Jul	Aug	Sep	Oct	Nov	Dec	Average of 12 months
Peshawar	3.08	4.03	4.99	6.11	7.15	7.24	6.55	5.98	5.43	4.55	3.73	3.02	5.16
Mardan	3.08	3.77	4.76	6.18	7.31	7.88	6.96	6.21	5.87	5.02	3.76	2.86	5.31
Kohat	3.18	3.89	4.74	5.92	6.86	6.96	6.12	5.64	5.33	4.86	3.79	2.98	5.02
Doaba	3.24	3.96	4.84	5.85	6.87	7.19	6.55	5.97	5.53	4.89	3.85	3.04	5.15
Dir	2.39	2.9	3.81	4.73	5.93	7.05	7	6.39	5.62	4.27	3.07	2.29	4.62
Abbottabad	2.95	3.57	4.55	5.88	6.99	7.46	6.6	5.94	5.7	4.89	3.69	2.79	5.08
Bannu	3.34	4.09	4.89	6.04	6.46	6.72	5.8	5.51	5.15	4.67	3.81	3.15	4.97
Chitral	2.49	3.2	4.07	4.99	6	7.1	7.39	7.03	6.11	4.38	3.03	2.28	4.84
Tal	2.58	3.13	4.05	5.13	6.23	7.08	6.96	6.23	5.56	4.41	3.27	2.44	4.76
											Annual Average		4.99

Table 3 above shows 9 different cities of Khyber Pakhtunkhwa (KP) for daily solar radiation-horizontal is calculated. It can be clearly seen that solar radiation remains high in summer season from April-July and are lower in other months. In KP, Chitral receives lowest intensity (2.28 kWh/m^2/d) in December whereas Mardan records highest daily solar radiation (7.88 kW/m^2/d) in June.

For all the cities, the solar radiation increases from January to June. The values are maximum for all the cities in the month of June or July and then start decreasing from July to December. As compared to other cities, Chitral experiences less radiation throughout the year.

C. Wind Energy

Wind Energy remained the world's fastest growing energy source until 2016. It is clean, green and renewable source of energy. Pakistan has significant potential for wind energy. As the paper is specific to Khyber Pakhtunkhwa, only wind energy potential in Khyber Pakhtunkhwa will be discussed.

Pakistan Meteorological Department (PMD), a national entity, in coloration of Ministry of Science & Technology (MoST) has completed two wind mapping projects referred to as Phase 1 and Phase 2. The former project is 'Wind Power Potential Survey of Coastal Areas of Pakistan (Phase-I)' completed in June 2005. The latter project is 'Wind Mapping of Northern Areas of Pakistan (Phase II)' and is still an on-going project since June 2010. A wind resource map of Pakistan developed by NREL and USAID is shown in the Figure 3 below.

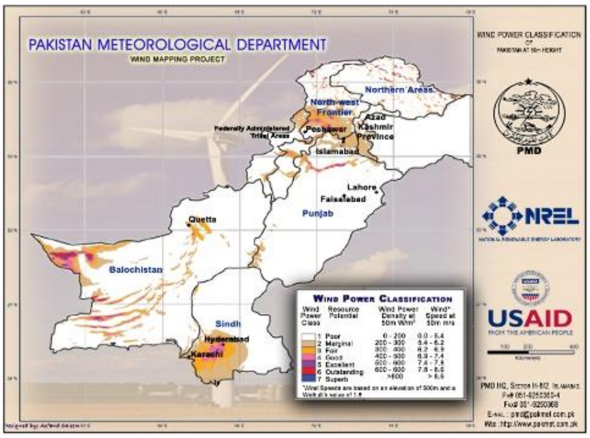

Figure 2 Wind Resource Map for Pakistan [16]

In Figure 3, it can be seen that there exists some areas in Khyber Pakhtunkhwa which have wind energy potential. The violet color areas in the picture are identified as the areas having good wind speed. These violet colour areas are identified as Mardan, Malakand, Buner, Shangla, Swabi and Haripur. These areas in KP are identified to have wind potential that can run small wind turbines to generate electricity for communities.

D. Biogas

Gas produced by decomposition of organic matter in the absence of oxygen is called as biogas. The process of producing biogasis also referred as anaerobic digestion of biodegradable material. 20 kg of animal waste is used to produce 1m^3 of biogas [8] and 2.5 kWh of electricity is generated from 1m^3 [13]. Biogas can be produced from biomass by three techniques:

- Floating Gas Holder Type Plants [17]
- Fixed Dome Type Biogas plant [18]
- Fixed Dome with Expansion Chamber type Biogas Plant [19]

Table 3 below shows livestock population of Khyber Pakhtunkhwa (KP). There were 49.32 million animals in 2006 in the rural areas of KP. As per 2006 livestock census, goats are found in maximum number, followed by goats, cows, sheep and then buffaloes accounting for 9.59 M, 5.98 M, 3.36 M 1.928 million respectively. This data was extrapolated till year 2019 and it was found that number of animals have increased significantly. The total number of cow, buffaloes, sheep and goat were found to be 10, 4, 20 and 10 million respectively. Energy generated from animal waste is not only environment friendly but also highly sustainable and economically viable.

TABLE 4 LIVESTOCK POPULATION OF KHYBER PAKHTUNKHWA FROM 1960 TO 2006 [14]

						(000 Heads)
Khyber Pakhtunkhwa	1960	1972	1976	1986	1996	2006
Cows	3206	2962	3000	3285	4237	5968
Buffaloes	651	791	762	1271	1395	1928
Sheep	2432	2455	3675	1599	2821	3363
Goats	3035	3737	4686	2899	6764	9599
Camels	76	101	95	70	65	64
Horses	23	31	29	34	47	76
Asses	306	408	381	446	534	560
Mules	19	32	28	23	60	67
Poultry	4190	4939	9708	17203	22501	27695

About 70% of KP population lives in rural areas. Most of the people living in rural areas have at least two or more cows or buffaloes. The waste of these animals can be mixed with equal proportion of water to produce biogas. This gas can be further used for cooking purposes or other ways to generate electricity. It is estimated that 11.6 GWhr/day of electricity can be generated from 14 million animals including cows and buffaloes.

IV. ORIGIN OF ENERGY CRISIS

1. Poor Management: Pakistan had a population of 210 million [11] in 2017.Energy crisis in Pakistan started in 2000 and got worse in 2006. As top management of the country did not forecast the future of the energy, the country started facing electricity shortfall. Poor planning by the top management of the nation lead to all time worst energy crisis.
2. Policy Problems: Since 1947, policy makers are unable to provide attractive incentives to investors. Other than foreign investors, locals investors are not even satisfied. Pakistan lacks policy makers.
3. Distribution & Transmission Capacity: In spite of the fact that additional transmission and distribution lines would be needed with increase in time, the federal government have remained failed to lay down these lines on proper time.
4. Power Theft: Power theft results when unit price of electricity goes high. Consumers are unable to pay high electricity bills and are forced to steal electricity.
5. Financial Problems: Pakistan is a poor nation. Pakistan takes loan in the form of of aid from other countries and donor agencies to start new power projects. The dependence on foreign investment has damaged our economic system.

Figure 3 Major reasons for energy crisis in Pakistan

V. SOLUTIONS TO TACKLE ENERGY CRISIS

1. The provincial Government of Khyber Pakhtunkhwa (GoKP) should start solar and mini hydro hydro electric projects across the province. Large hydro electric power palnts and solar parks can be taken into consideration. Where possible, small scale wind turbines should be installed.
2. GoKP should work on weak transmission and distribution network. The network of lines should be strengthened to sustain the electricity generation and transmission needs of the future.

3. All the previous power plants installed in the province should be monitored by GoKP for
4. increasing efficiency. This includes large hydro dams.
5. High wattage electrical appliances should be replaced with energy efficient appliances immediately at every cost. High wattage appliances consumes a lot of electricity. Power theft should be minimised across the province.
6. There should be awareness campaigns in the province to educate the people of Khyber Pakhtunkhwa about renewable energy.

CONCLUSION

Khyber Pakhtunkhwa (KP) is blessed with a significant amount of renewable energy resource. This includes hydroelectric power, solar energy, biomass and wind energy. To conclude; In the hydroelectric sector there is a total potential of around 25,000 MW out of which only about 4,000 MW of potential is tapped. The amount of solar energy that can be harnessed in Khyber Pakhtunkhwa is $2*10^7$ MWh/m^2 where only around 2 MW of electricity is being generated by solar currently. Similarly in biomass there is a total potential of 3 million biogas plants in the province but only 2000 biogas have been installed so far.

REFERENCE

[1] F. Fatai, K and Oxley, Les and Scrimgeour, "Modelling the causal relationship between energy consumption and GDP in New Zealand, Australia, India, Indonesia, The Philippines and Thailand," Math. Comput. Simul., vol. 64, pp. 431–445, 2004.

[2] M. A. T. Muneer, S. Maubleu, "Prospects of solar water heating for textile industry in Pakistan.," Renew. Sustain. Energy Rev., vol. 10, no. 1, pp. 1–23, 2006.

[3] "Pakistan: rapid assessment and gap analysis. [UNDP] - United Nations Development Programme. Sustainable energy for all (SE4ALL) http://www.se4all.org/sites/default/files/Pakistan_RAGA_EN_Released.pdf," 2014.

[4] "Hydrocarbon Development Institute of Pakistan," 2016. [Online]. Available: https://www.hdip.com.pk/. [Accessed: 05-Mar-2019].

[5] "Pakistan to set 30% plus 30% renewable energy target by 2030." [Online]. Available: https://wwindea.org/blog/2019/04/02/pakistan-to-set-30-plus-30-renewable-energy-target-by-2030/. [Accessed: 02-Feb-2019].

[6] "Hydro power Resources of Pakistan," 2011. [Online]. Available: http://www.ppib.gov.pk/HYDRO.pdf. [Accessed: 05-Jan-2019].

[7] "IRENA Renewables Readiness Assesment Pakistan," 2018. [Online]. Available: https://www.irena.org/publications/2018/Apr/Renewa

[8] M. A. Sheikh, "Renewable energy resource potential in Pakistan," Renew Sust Energy Rev, vol. 13, pp. 2696–702, 2009.

[9] M. R. Adnan S, Khan AH, Haider S, "Solar Energy Potential in Pakistan," J. Renew. Sustain. Energy, vol. 4, 2012.

[10] M. Z. Baloch MH, Kaloi GS, "Current scenario of the wind energy in Pakistan challenges and future perspectives: a case study.," Energy Rep, vol. 2, pp. 201–10, 2016.

[11] Farooqui SZ., "Prospects of renewables penetration in the energy mix of Pakistan.," Renew Sustain Energy Rev, vol. 29, pp. 693–700, 2014.

[12] "Pakistan economic survey 2009-10. Ministry of Finance, Government of Pakistan." [Online]. Available: http://www.finance.gov.pk/survey_0910.html. [Accessed: 02-Feb-2019].

[13] M. M. Uddin W, Khan B, Shaukat N, "Biogas potential for electric power generation in Pakistan: a survey.," Renew Sustain Energy Rev, vol. 54, pp. 25–33, 2016.

[14] "Livestock Consensus of Khyber Pakhtunkhwa." [Online]. Available: http://www.pbs.gov.pk/content/livestock-population. [Accessed: 02-Feb-2019].

[15] M. T. Mirza UK, Ahmad N, "An overview of biomass energy utilization in Pakistan.," Renew Sustain Energy Rev, vol. 12, no. 7, pp. 1988–96, 2008.

[16] "Wind Resource Map for Pakistan." [Online]. Available: http://www.pmd.gov.pk/wind/Wind_Project_files/Page694.html. [Accessed: 04-May-2019].

[17] M. Realff, "Bio Renewable Resources," J. Ind. Ecol. IND ECOL, vol. 7, pp. 227–228, 2004.

[18] Donald L Klass, "Biomass for Renewable energy, Fuels and Chemicals," 2006. [Online]. Available: https://www.sciencedirect.com/book/9780124109506/biomass-for-renewable-energy-fuels-and-chemicals. [Accessed: 25-Dec-2018].

[19] G N Tiwari and M K Ghosal, Renewable Energy Resources: Basic Principles and Applications. Alpha Science International, 2005.

IJEW 国际工程期刊 International Journal of Engineering Works انجینئرنگ کاموں کا بین الاقوامی جرنل

International Journal of Engineering Works
ISSN-p: 2521-2419
ISSN-e: 2409-2770
Vol. 6, Issue 10, PP. 365-373, October 2019
https://www.ijew.io/
https://doi.org/10.34259/ijew.19.610365373

Energy Audit In Boys Hostel (Case Study Ali Hall)

Madiha Chaudhary[1], Muhammad Imran Akbar[2], Rida Rasheed[3], Engr. Tauheed ur Rehman[4]
[1,2,3,4] Electrical Engineering Department, University College of Engineering and Technology, Bahauddin Zakariya University
Multan, Pakistan
madihachaudhary26@gmail.com[1], imran.akbar2011@gmail.com[2], ridarasheed797@gmail.com[3], trehmank@yahoo.com[4]

Received: 22 September, Revised: 29 September, Accepted: 07 October

***Abstract*—** Conservation and management of energy and power in any sector especially in large institutes, is of much significance. Energy efficient electrical systems lead to energy efficient delivering systems by keeping the power losses minimum. Energy audit is the best solution for the energy conservation where the system is verified and observed to reduce energy consumption without any negative effect on the system. It is an energy audit of a given case study of an accommodation area, a Boys Hostel (ALI Hall) of Bahauddin Zakariya University, Multan Pakistan. It is the comprehensive energy audit of hostel with tariff C-2b (29) T and 11.21 rupees per unit. Hostel is estimated as consuming 44836.42 units and cost of 502616 rupees. This survey and analysis suggests certain recommendations for energy savings and to reduce unit consumption up to 20098.572 and cost of 225305 rupees.

***Keywords*—**Energy Audit, Consumption, Capital Cost, Payback Period, Savings

I. INTRODUCTION

The energy use in the world is growing rapidly and this is causing supply deficiencies and heavy environmental disorders [1]. The issue of energy consumption and deficiency of energy is also increasing day by day in Pakistan. Pakistan is facing many energy problems. Generation of electricity is less as compare to the energy consumption. This is the cause of load shedding due to which our most of the sectors and industries are facing issues [2]. So, the need of today is to save and conserve energy. To achieve this public should be aware of energy audit and management system in order to save power. The most detailed method to analyze the energy usage and its wastage in an area or building is "ENERGY AUDIT" [3]. Energy audit is verification and analysis of use of energy including submission of a technical and official report containing recommendations for improving the efficiency of energy system with cost benefit analysis and the plan to decrease energy consumption. As Pakistan is facing energy crisis so energy audit is a fundamental way by which the system can be supervised and improved. To stimulate energy consumption is a little bit tough job as it varies with the consumer's goods and their operating duration. In this sense, there are some research techniques and approaches with some tools to estimate the energy performance of building. Energy management strategy and specially energy reduction can be done with energy [4-6]. Goals for energy management provide well organized strategies for calculated energy management [7].

II. ENERGY AUDIT

An energy audit is an investigation, survey and analysis of energy flow for energy preservation or conservation in an industry or any other area of consideration and a mechanism to reduce amount of energy input to the system without any negative effect on output. Energy audit is analysis of how consumers use the energy [8, 9].

A. Steps of Energy Audit

Audit consists of following steps:

- Identification of whole energy system
- Analysis of the system (Electrically & Mechanically)
- Collection, observation, organization and analysis of the data
- Determination of cost reducing alternatives
- Analyzing the system on those alternatives
- Establishment of cost saving projects and their implementation
- Analysis of the findings and calculations and issue a report that outlines energy consumption and system improvement recommendations [10] [11].

According to the results of many surveys and researches it is concluded that a bulk of energy can be saved by energy audit.

III. TYPES OF ENERGY AUDIT

There are three types of Energy Audit:

- Walk through Energy Audit
- Mini Energy Audit
- Comprehensive Energy Audit [4]

A. *Walk through Energy Audit*

This is also called preliminary or common Energy Audit. It is simplest type which is carried out in limited time with limited efforts. Its major focus is on the energy supply its demand and the user methods of conservation [12]. It includes activities related to collection, classification, calculation and analysis of available data for the establishment of energy consumption [13].

B. *Mini Energy Audit*

Mini energy audit is also called site energy audit. It actually expands the walk-through energy audit by collecting more information about facilities and performing a detail evaluation and calculation of energy consumption. Metering of a specific energy consumption sector is often a performed postscript of utility data.

C. *Comprehensive Energy Audit*

This is also called detailed energy audit. It is expansion of mini energy audit. It includes estimation of energy input for different sectors, collection of previous data on production level and specific energy consumption. This audit is a comprehensive account of energy use, including a quantitative and qualitative study of the implementation with detailed investments, functional and maintenance costs and an analysis. Not only the simple payback period is concerned but the life cycle cost parameters as interest rate, tax rate are also determined [10].

IV. CASE STUDY

The case study considered here is the audit of Ali hall boy’s hostel of Bahauddin Zakariya University. As university consists of thousands of consumers and appliances so it was provided with a bulk power or with 11KV feeder from WAPDA. University has its own distribution system for different departments, institutes, colleges, cafe, banks and hostels. The power cables and transformers are under the university not WAPDA. There are different tariffs of WAPDA for electricity distribution system. University has tariff C-2b (29) T. Ali hall is the boy’s hostel in the university. It accommodates almost 510 students. Total 255 rooms are available in which 13 are for official use and rest of the rooms are for the students. The structure of hostel is described in the TABLE I.

TABLE I. THE STRUCTURE OF ALI HALL

Sr. N	**Name of locat**	**Number of locations**
01	Student room	242
02	Washrooms	08
03	Wings	16
04	Crush hall	02
05	Computer lat	01
06	TV hall	01
07	Mess hall	01
08	Official room	13

V. METHODOLOGY

Energy management can be defined in terms of energy audit methodology as it is the strategy being used to adjust and optimize energy by using the methods and procedures to minimize energy requirements per unit of output. So, energy auditing is an effective tool to manage energy consumption in a given area. The methodology used in this case study is actually based on total energy consumption per month [14, 15].

The case study consists of three phases

Phase I - Pre-Audit Phase

Phase II - Audit Phase

Phase III - Post Audit Phase

VI. POWER CONSUMPTION IN THE HOSTEL

Evaluation of data is also based on the participation of consumers towards the audit program. Lack of knowledge causes the consumers to respond them to high energy consumption and prices by taking involuntary cutbacks in their lifestyles [16, 17]. Most of energy is wasted at different levels. Wastage of energy is maximum in case of hostel due to lack of awareness and use of appliances that consume more power. In order to calculate total power consumption, a study of total running appliances and their power consumption is tabulated individually.

TABLE II. ENERGY BILL OF EXISTING ELECTRIC SYSTEM IN ALI HALL

Sr. No#	Name of appliances	Power ratings (W)	Usage time (Hours)	Power consumed pe day (KW)	Power consumed per month (KW)	Power consumed pe year (KW)
01	Tube light	40	12	0.48	14.4	175.2
02	CCTV camera	15.4	24	0.36	10.8	131.4
03	Air conditioner	3500	06	24	720	8760
04	Ceiling fan	75	15	1.125	33.75	410.625
05	Electric kettle	3000	01	03	90	1095
06	Oven	2150	03	6.45	193.5	2354.25
07	Deep freezer	500	16	08	240	2920
08	LCD (55 inch)	150	03	0.45	13.5	160.25
09	Laptop charger	50-100	04	0.28	8.4	102.2
10	Search light	500	10	05	150	1825
		400	10	04	120	1460
		100	10	01	30	365
		50	10	0.5	15	82.5
11	Computer	30	03	0.06	1.8	21.9
12	Iron	1000	01	01	30	365
13	Electric cooler	70-100	24	2.4	72	876
14	Internet router	5-15	24	0.36	10.8	131.4
15	Air cooler	150	10	1.5	45	547.5

The cost per unit of electric power is Rs 11.21

TABLE III. ENERGY BILL OF ELECTRICITY SYSTEM IN ALI HALL

Sr. No#	Equipment	Energy consu by an equipment (watts)	Energy consumed b an equipment (unit)	Total energy of an equipment per month (rupees)	Number of equipment	Total energy cost month (rupees)
01	Tube light	14400	14.4	161.4	720	116225.28
02	CCTV camera	11088	11.08	124.207	19	2359.929
03	Air conditioner	720000	720	8071.2	01	8071.2
04	Ceiling fan	33750	33.75	378.34	278	105178.52
05	Electric kettle	90000	90	1008.9	50	50445
06	Oven	193500	193.5	2169	01	2169
07	Deep freezer	240000	240	2690.4	02	5380.8
08	LCD (55 inch)	13500	13.5	151.3	01	151.3
09	Laptop charger	8400	8.4	94.16	150	14124

10	Search light	150000	150	1681.5	14	23541
		120000	120	1345.2	7	9416.4
		30000	30	336.3	4	1345.2
		15000	15	168.15	1	168.15
11	Computer	1800	1.8	20.2	07	141.4
12	Iron	30000	30	336.3	100	33630
13	Electric cooler	72000	72	807.12	09	7264.08
14	Internet router	10800	10.8	121.068	16	1937
15	Air Cooler	45000	45	504.45	240	121068

Total cost per month = Rs. 502616

A. *QUANTIFICATION OF END USE*

The loads were sequester based on the end use as lights and fans, air conditioners, computer/printers, hostel mess cooking loads, electrical kettles and irons. Quantification and necessary measurements were carried out [18]. The details are given here [19]

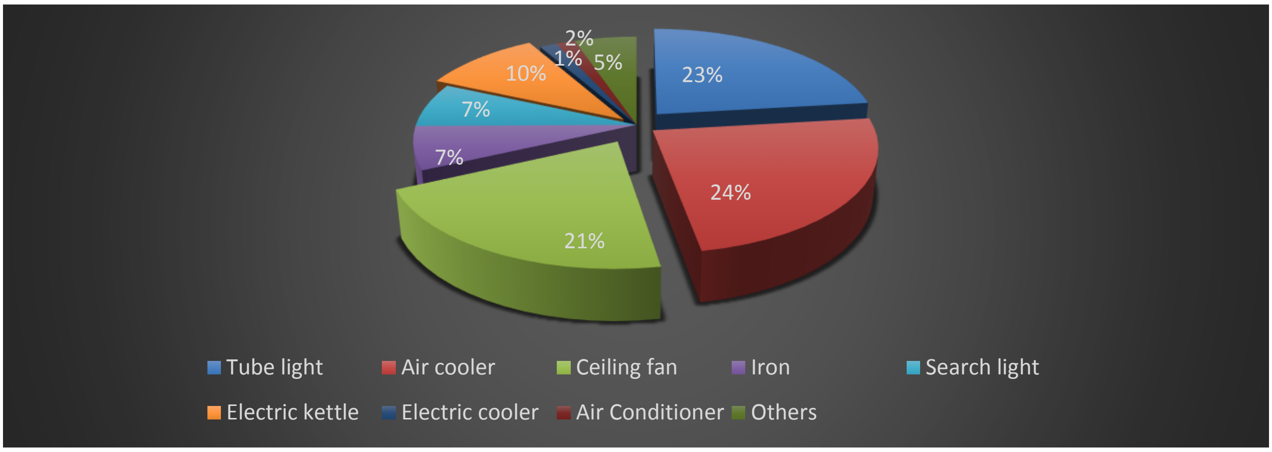

Figure 1. Quantification graph

VII. Energy Audit Recommedndation

Energy management is a technique of fulfilling all the required energy demands. By using energy saving systems and optimizing strategies, energy consumption can be conserved to minimize the energy utilization per unit and its cost [20, 21]. Energy enhancing measures should not have only impact on energy consumption but also on all other such measures because in some cases they can conflict each other resulting an increment in energy consumption [22]. Energy Conservation Opportunities (ECOs) usually originate from energy providers or sources for example fossil fuels, electricity or alternating energy sources. For every end use equipment (transformers, geezers, fans, blowers, tube lights etc.) there exists an energy conservation opportunity.

ECOs give the potential trades off between initial costs, operating costs and life cycle of those equipment [23]. To invest in new energy saving mechanism is a risky task that it is uncertain about the long-term capital cost savings. Respondents across energy audit show some measures to reduce initial costs and for lower energy bills in a few years [17, 24]. Imperfect information like search or transaction cost is a barrier towards proper energy audit [25]. So, Energy Audit Recommendation is provided on the basis of capital cost and their payback periods. Detailed analysis of all the recommendations for reducing power consumption in hostel after assuming its capital cost is recommended here [26].

TABLE IV. RECOMMENDED POWER EQUIPMENT AND ENERGY BILL

Sr. No#	Name of applianc	Recommended Appliances	Power rati (Watt)	Usage time (Hour)	Power consumed pe month (Watt)	Energy consumed by a equipment (unit)	Total energy cost of an equipment per month (rupees)	Number of equipment	Price
01	Tube light	LED tube light	18	12	6480	6.48	72.64	720	52300.8
02	CCTV camera	-	15.4	24	11088	11.088	124.296	19	2361.624
03	Air conditioner	DC converter	1470	6	264600	264.6	2966.17	01	2966.17
04	Ceiling fan	Energy saver ceil fan	50	15	22500	22.5	252.225	278	70118.55
05	Electric kettle	Energy efficient kettle	1200	1	36000	36	403.56	50	20178
06	Oven	-	2150	3	193500	193.5	2169.135	01	2169.135
07	Deep freezer	Stand-alone dee freezer	200	16	96000	96	1076.16	02	2152.32
08	LCD (55 inch)	-	150	3	13500	13.5	151.335	01	151.335
09	Laptop charger	-	50-100	4	8400	8.4	94.164	150	14124.6
10	Search light	LED Flood Ligl	100	10	30000	30	336.3	14	4708.2
		LED Flood Ligl	50	10	15000	15	168.15	7	1177.05
		LED Flood Ligl	10	10	3000	3	33.63	4	134.52
		LED Flood Ligl	10	10	3000	3	33.63	1	33.63
11	Computer	-	30	3	2700	2.7	30.267	07	211.869
12	Iron	-	1000	1	30000	30	336.3	100	33630
13	Electric cooler	-	70-100	24	72000	72	807.12	09	7264.08
14	Internet router	-	5-15	24	10800	10.8	121.068	16	1937.08
15	Air Cooler	DC air cooler	12	10	3600	3.6	40.356	240	9685.44

Total: Rs. 225305

VIII. RECOMMENDATIONS FOR ENERGY CONSUMPTION OF ALI HALL

Energy management is an important tool to meet all the energy demands for the short-term survival and its long-term success [27]. Energy consumption is increasing day by day due to the expansion in built areas and its concerned energy needs. To control energy, some recommendations are provided to conserve energy by reducing energy consumption [1].

A. *Replacing all Fluorescent Lights by LED Tube Lights*

1) *Reasons for Replacement*

Fluorescent tube light is used in observation area (Ali hall) having electromagnetic ballast. The components of electromagnetic ballasts are usually a magnetic choke, a starter and a capacitor for power factor correction. Iron and copper losses in magnetic choke of ballast causes higher power losses and poor power regulation. In short, fluorescent tube lights are not power saving equipment especially when it is working for 12 hours per day.

2) *Recommendation*

In our existing system, LED lights are recommended for fluorescent tube lights. In these LEDs, electromagnetic ballast is replaced by electronic ballast. These are more energy efficient (usually 10%-15%) than electromagnetic ballasts. So now it will not cause such amount of power losses as in the case of electromagnetic ballasts. It permits to deliver constant supply of power to load during its entire useful life. These LEDs work on 18 Watt dissimilar to Tube lights which were consuming 40 Watt [4]. Energy can be saved in Lighting system by reducing their illumination levels, changing its operating hours, improving their efficiency and taking the benefit of day light.

Table V. COMPARISON

EXISTING SYSTEM		RECOMMENDED SYSTEM	
Total number of rooms	= 255	Total number of rooms	= 255
Total number of tube lights in rooms	= 720	Total number of tube lights in rooms	= 720
Total watts consumed	=720*40	Total watts consumed	=720*18
	=28800W		=12960W
Total usage time/day	=12 hours	Total usage time/day	=12 hours
Total usage time in a year	=12*365	Total usage time in a year	=12*365
	=4380 hours		=4380 hours
Total watts in a year	=28800*12*365	Total watts in a year	=12960*12*365
	=126144000		=56764800
Total units in a year	=126144	Total units in a year	=56764.8
Cost of 1 unit	=RS 11.21	Cost of 1 unit	=RS 11.21
Total cost in a year	=126144*11.21	Total cost in a year	=56764.8*11.21
	=Rs 1414074.24		=Rs 636333.4
Total Savings			
Saved unit of power	= 126144-56764.8		
	= 69379.2 units		
Saved money	= 1414074.24-636333.4		
	= RS 777740.8		
Total investment	=720*550		
	=RS 396000		
	= (396000/777740.8) *12		
	6 months		
We can regain the led tube light cost within 6 months			

There are some steps should be taken to conserve energy from lighting system:

Use of natural day light should be maximum Compact fluorescent lights should be used instead of incandescent fluorescent light. The circuits controlling the lighting should be separate from other circuits [28].

B. Replacing All Fans by Energy Saving Ceiling Fan (Royal Company)

1) Reasons for Replacement

A fan is one of the major contributions in energy consumption in house hold as well as in hostels. The fans used in our existing systems are AC induction motor fans which approximately rate from 60-75 Watt. These motors are less efficient and are heavier providing maximum efficiency of 50%. All the motors should be energy efficient [29]. Normally power rating of ceiling fan at different regulations is given as [4]

Speed	1	2	3	4	5
Wattage	14 W	26 W	39 W	48 W	76 W

2) Recommendation

To save energy, ceiling fans are recommended to replace the present ones by Royal Fans which

consumes 50 watts not 75 watts. Re lubricate all the grease fitting and belt driven units of wheel shaft bearings after each three year. Every three to five (3-5) years, lubrication of pre-lubricated motors is needed. Belt tension should be checked every 6 months. Out of balance running of motor

can be caused by blade damage or due to blower blades. So, check all these on regular basis [23].

TABLE VI. COMPARISON

EXISTING SYSTEM		RECOMMENDED SYSTEM	
Total number of rooms	= 255	Total number of rooms	= 255
Total number of fans in rooms	= 278	Total number of fans in rooms	= 278
Total watts consumed	=278*75	Total watts consumed	=278*50
	=20850W		=13900W
Total usage time/day	=15 hours	Total usage time/day	=15 hours
Total usage time in a year	=15*365	Total usage time in a year	=15*365
	=5475 hours		=5475 hours
Total watts in a year	=20850*15*365	Total watts in a year	=13900*15*365
	=114153750		=76102500
Total units in a year	=114153.75	Total units in a year	=76102.5
Cost of 1 unit	=RS 11.21	Cost of 1 unit	=RS 11.21
Total cost in a year	=114153.75*11.21	Total cost in a year	=76102.5*11.21
	=RS 1279663.5		=RS853109
Total saving			
Saved unit of power	= 114153.75-76102.5		
	=38051.25 units		
Saved money	=1279663.5-853109		
	= RS426554.5		
Total investment	= 278*2900		
	= RS 806200		
	= (806200/426554.5) *12		
	= 23 months		
We can regain the ceiling fan cost within 23months			

TABLE VII. REPLACING AC AIR COOLER BY DC AIR COOLER (USING CONVERTER)

EXISTING SYSTEM		RECOMMENDED SYSTEM	
Total number of Air coolers	= 240	Total number of Air coolers	= 240
Total watts consumed	= 240*150	Total watts consumed	= 240*12
	= 36000W		= 2880W
Total usage timing/day	= 10 hours	Total usage timing/day	= 10 hours
Total usage time annually	= 10*365	Total usage time annually	= 10*365
	= 3650 hours		= 3650 hours
Total watts annually	= 36000*10*365	Total watts annually	= 2880*3650
	= 131400000		= 10512000
Total units annually	= 131400	Total units annually	= 10512
Cost of 1 unit	=RS 11.21	Cost of 1 unit	= RS 11.21
Total cost annually	= 131400*11.21	Total cost annually	= 10512*11.21

= RS 1472994	= RS 117840
Total Saving	
Saved unit of power	= 131400-10512
	= 120888
Saved money	= 1472994-117840
	= RS 1355154
Total Investment	= 240*5000
	= RS 1200000
	= (1200000/1355154) *12 = 10 months
We can regain the cost within 10 months	

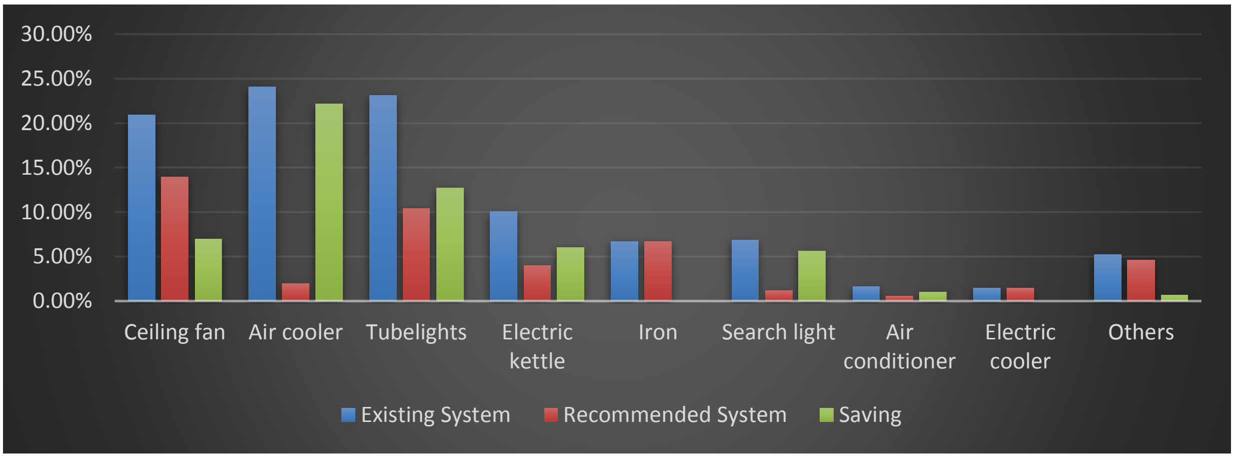

Figure 2. Comparison chart

CONCLUSION

By the procedure of energy audit, total 24737.848 units are saved. The energy cost is reduced from 502616 rupees to 225305 rupees per month. Energy audit is a powerful technique to examine and solve the energy deficiency and consumption problems. On monthly basis, energy can be conserved annually by ding the more power consuming equipment due to their poor efficiency. By recommending efficient and less power consuming devices, energy cost can be reduced. This way is counted as the proper authentic way to reduce energy losses. If such audit is conducted for the whole institute i.e. Bahauddin Zakariya Univeristy, then more energy can be conserved.

REFERENCE

[1] Pérez-Lombard, L., J. Ortiz, and C. Pout, A review on buildings energy consumption information. Energy and buildings, 2008. 40(3): p. 394-398.

[2] McIntosh, M., Report: Iowa has 24,000 bridges, 5,000 structurally deficient. KCCI News, 2013. 20.

[3] Wong, H. and C.K. Lee. Application of energy audit in buildings and a case study. in 1993 2nd International Conference on Advances in Power System Control, Operation and Management, APSCOM-93. 1993. IET.

[4] Ahila, C. and W.J. Femi. Energy audit in ladies hostel. in TENCON 2015-2015 IEEE Region 10 Conference. 2015. IEEE.

[5] Fischer, C., Feedback on household electricity consumption: a tool for saving energy? Energy efficiency, 2008. 1(1): p. 79-104.

[6] Fumo, N., A review on the basics of building energy estimation. Renewable and Sustainable Energy Reviews, 2014. 31: p. 53-60.

[7] Chiu, T.-Y., S.-L. Lo, and Y.-Y. Tsai, Establishing an integration-energy-practice model for improving energy performance indicators in ISO 50001 energy management systems. Energies, 2012. 5(12): p. 5324-5339.

[8] Goyal, P., B.S. Kumar, and K. Sudhakar. Energy audit: A case study of energy centre and Hostel of MANIT, Bhopal. in 2013 International Conference on Green Computing, Communication and Conservation of Energy (ICGCE). 2013. IEEE.

[9] Zhang, J., et al. How to reduce energy consumption by energy audits and energy management: The case of province Jilin in China. in 2011 Proceedings of PICMET'11: Technology Management in the Energy Smart World (PICMET). 2011. IEEE.

[10] Krarti, M., Energy audit of building systems: an engineering approach. 2016: CRC press.

[11] Gordić, D., et al., Development of energy management system–Case study of Serbian car manufacturer. Energy Conversion and Management, 2010. 51(12): p. 2783-2790.

[12] Baechler, M., C. Strecker, and J. Shafer, A Guide to Energy Audits. PNNL-20956. Pacific Northwest National Laboratory, Richland, WA. Prepared for US Department of Energy under Contract DEAC05-76RL01830, 2011.

[13] Manjunatha, P., et al., Energy audit, conservation and power factor improvement for BMSIT campus. International Journal of Research in Engineering and Technology, 2013. 2(11): p. 354-359.

[14] Unachukwu, G.O., Energy savings opportunities at the University of Nigeria, Nsukka. Journal of Energy in Southern Africa, 2010. 21(1): p. 2-10.

[15] Kamalapur, G. and R. Udaykumar. Electrical energy conservation in India-Challenges and achievements. in 2009 International Conference on Control, Automation, Communication and Energy Conservation. 2009. IEEE.

[16] Dillman, D.A., E.A. Rosa, and J.J. Dillman, Lifestyle and home energy conservation in the United States: the poor accept lifestyle cutbacks while the wealthy invest in conservation. Journal of Economic Psychology, 1983. 3(3-4): p. 299-315.

[17] Hirst, E., L. Berry, and J. Soderstrom, Review of utility home energy audit programs. Energy, 1981. 6(7): p. 621-630.

[18] Abraham, C., et al., Energy Audit Of IIT-Bombay Campus. Draft Final Report, Indian Institute of Technology-Bombay, 2008.

[19] Ng, T.F., et al., Energy Consumption in Student Hostels of Universiti Sains Malaysia: Energy Audit and Energy Efficiency Awareness, in Handbook of Theory and Practice of Sustainable Development in Higher Education. 2017, Springer. p. 191-207.

[20] Abdelaziz, E., R. Saidur, and S. Mekhilef, A review on energy saving strategies in industrial sector. Renewable and sustainable energy reviews, 2011. 15(1): p. 150-168.

[21] Mehta, V. and R. Mehta, Principles of power system. S. Chand, New Delhi, 2004.

[22] Radhi, H., A systematic methodology for optimising the energy performance of buildings in Bahrain. Energy and buildings, 2008. 40(7): p. 1297-1303.

[23] Thumann, A. and W.J. Younger, Handbook of energy audits. 2003: Fairmont Press.

[24] Hirst, E. and M. Brown, Closing the efficiency gap: barriers to the efficient use of energy. Resources, Conservation and Recycling, 1990. 3(4): p. 267-281.

[25] Fleiter, T., J. Schleich, and P. Ravivanpong, Adoption of energy-efficiency measures in SMEs—An empirical analysis based on energy audit data from Germany. Energy Policy, 2012. 51: p. 863-875.

[26] Sameeullah, M., et al., Energy Audit: A Case Study of Hostel Building. International Journal of Research in Management, Science & Technology, 2014. 2(2).

[27] Doty, S. and W.C. Turner, Energy management handbook. 2004: Crc Press.

[28] Ibrik, I.H. and M.M. Mahmoud, Energy efficiency improvement procedures and audit results of electrical, thermal and solar applications in Palestine. Energy Policy, 2005. 33(5): p. 651-658.

[29] Ramya, L. and M. Femina, Energy auditing a walk-through survey. International Journal of Advanced Research in Electrical, Electronics and Instrumentation Engineering, 2014. 3(2): p. 2320-3765

MADIHA CHAUDHARY

FIRST AUTHOR: The author was born in Chishtian, District Bahawalnagar, Punjab Province, Pakistan. She did her Bachelors Degree in Electrical Power Engineering from University College of Engineering and Technology, Bahauddin Zakariya University, Multan.
The author has experience in renewable energy efficiency and conservation methods. She has also served as a junior engineer in KICS&PEECA for doing Energy Audit of Bahauddin Zakariya University Multan. In addition to this, she has participated in different energy auditing and conservation conferences and workshops.

IJEW 国际工程期刊 International Journal of Engineering Works انجینئرنگ کاموں کا بین الاقوامی جرنل

International Journal of Engineering Works
ISSN-p: 2521-2419
ISSN-e: 2409-2770
Vol. 6, Issue 10, PP. 374-378, October 2019
https://www.ijew.io/
https://doi.org/10.34259/ijew.19.610374378

Design and Analysis of Neutral Grounding Transformer for Hydro Alternators

Muhammad Bais[1], Abdul Basit[2], Said Ali[3], Muhammad Sadiq[4], Israr Ahmad[5]
[1,2,3] Department of Electrical Energy System Engineering, U.S.-Pakistan Center for Advanced Studies in Energy University of Engineering and Technology Peshawar, Pakistan
[4,5] Khyber Pakhtunkhwa Technical Education and Vocational Training Authority Peshawar, Pakistan
muhammadbais92@yahoo.com[1], abdul.basit@uetpeshawar.edu.pk[2], engr.saidali@live.com[3], sadiqorakzai@hotmail.com[4], israr9975@yahoo.com[5]
Received: 16 Septemeber, Revised: 03 October, Accepted: 07 October

***Abstract*—** Power Generators of high KVA rating especially that of hydropower plant are very much prone to the ground faults. Stator ground faults are the most common winding failure in generators. During stator ground faults, short circuit currents flow from the damaged phase to ground through the stator core. Experience has shown that stator ground fault damages are proportional to phase-to-ground fault current as well as fault duration.

For that reason, Generator Neutral Grounding must be applied in order to;

I. Limit phase-to-ground fault current.
II. Provide a means of stator ground fault detection.

There are various generator grounding classes and types available. In this paper, high-resistance grounding has been chosen. High-resistance generator neutral grounding scheme based on a grounding transformer with a secondary resistor

The advantage of the distribution transformer resistor combination is that the resistor used in the secondary is of comparatively low ohmic value and of rugged construction as compared to obtaining the same result by installing a high-ohmic, low-current resistor directly in the generator neutral.

This research introduces some important and applicable practices which came from few years of practical as well as theoretical studies and discussions with some national and international power system experts. The research was made on the hydro power plants installed at Tarbela generating unit. The important parameters concerning the high impedance grounding of the generator were calculated. These results will be a kind of ready references for neutral grounding transformer design calculations and analysis.

***Keywords*—** NGT (Neutral Grounding Transformer), KVA Rating (Kilo Volt Amperes), Secondary Resistor, Tarbela Generating Unit.

I. Introduction

One of the important parts of the power system is generators. They are basically the in charge of the uninterrupted power supply to the consumers hence it's very crucial that it works in its normal conditions. The compromise on their reliability can possibly result in the blackouts and affects not only the power system but also the customers. Usually, if the generators get damage then they are returned to the manufacturer to rewind or re-stack them because utility normally is incapable to rewind the damaged generator. This fixing cost is normally very high hence it is also very important to protect the generator against abnormal situations and the faults [1].

Currently, in the modern era, the rate of overall failure of the generators and other machines is very low as compared to the past 10-20 years. The main reason is because of the improved materials and the design practices that effectively reduces the faults. Unfortunately, the rate of failure is never zero but is reduced because of improvements made in the design and technology. It is important to recognize the faults and effectively isolate it, thus allowing minimum damage to occur. The abnormal conditions include overload, over speed, winding faults, loss of excitation, out of step condition, excitation loss, sub-synchronous oscillations, and un-balance current conditions. These all conditions do not require that generator will be tripped, in many conditions, the tripping is not necessary. For every hazard, the operating conditions, cost of maintenance and extent of protection must be weighed against the associated risks for no protection. The degree to which protection should be applied depends upon the importance and size of generator [1-2].

The protection system for the generator should be robust and reliable. It should not interrupt the while power system for the non-serious or minor faults and those schemes, on the other hand, should be capable to protect the generator against all types of faults in the windings of the generator thus providing a high degree of the seriousness. If the generator protection is sensitive and robust, the generator will not shut down the whole system for minor fault and prevent the generator from the damages against the faults [2, 3]. The generator needs to be protected against internal and external faults. Generators are being protected against the faults (external) by means of the circuit breakers which interrupt and switch off against the faults in the network (lines, buses, and transformer, etc.)

One of the internal faults of the generator is the stator ground fault. The faults of the stator ground are generally caused by the degradation of the insulation as well as influences of the environment such as oil or moisture in combination with the dirt that usually is present on the surface of the coil outside the slots of the stator. This can eventually result in discharges of the electrical tracking in the end winding that punctures the ground well [1, 3].

II. Literature Review

A. *Differential Protection*

For the systems which are grounded by low impedance or ungrounded, the short circuit currents are typically of very large value ranging from 400 A to 1200 A of the primary current. It is very high value which can damage the equipment as previously mentioned. This fault can also be detected by the differential protection scheme which depends on the phase current on the neutral and terminal side of the machine. As the level of the fault current is very high, the secondary amperes can be much higher than the relay trip settings. For example, in case of the 6kV 10 MVA current transformer, the value of the phase-to-ground current is limited in range of the 2 to 6 A, the protection should detect the difference in the value of the current.

B. *Machine Connection*

Many machines typically generators have y-connected winding. The 3 relays which are coupled to they-connected CT gives the phase and in few of the cases (depending on the system grounding and the neutral) ground fault protection. Figure 2.5 gives the protection system for the delta generators. In this system, the winding of delta should be brought out such that CTs can be inserted inside the delta [4, 6].

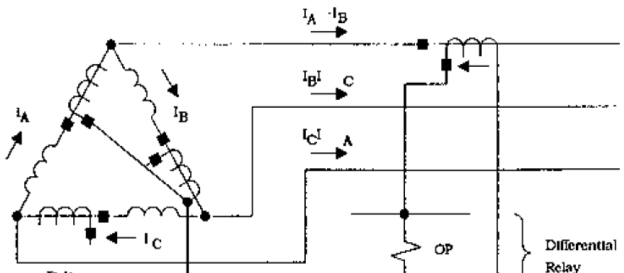

Figure 2. 1: Differential relay schematic for the delta connected machine

C. *Split Phase*

The generators having the winding of the split phase can be possibly be protected by using the differential relay sets as depicted in figure 2.4 and 2.6. This sort of configuration prevents against the fault types which exits internally typically including the open circuited or short-circuited. This arrangement can further be extended for accommodating the other types of winding arrangements that particularly involve the more than 2 equal winding per phase. The arrangement of figure 2.6 should be equipped with the auxiliary transformers for providing the balance in the normal working [7-8].

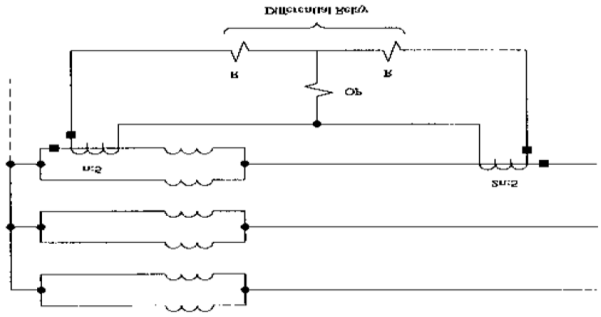

Figure 2. 2: Configuration for single phase with split phase winding

D. *87N3(Neutral to Ground Protection of Fault)*

Figure 2.8 depicts the phenomena for detecting the neutral to ground fault in machine. This fault is not hazardous. The occurrence of the second fault of the ground at the machine, eventually causes the phase to ground fault which is not limited to the neutral impedance. This magnitude of the fault current will increase from the value for which it is designed causing the destruction. The figure 2.7, compare the 3rd voltage of harmonic present between the ground and the machine neutral at the line terminals [9-10].

E. *Toroidal Transformer along with Differential Relay*

When the generator ratings are not too high, then some scientists have presented a solution based upon the 3-phase current and the neutral lead coupled with the toroidal transformer as depicted in the figure 2.9. Such scheme generates magnitude of the current of the secondary winding of the transformer similar to the internal fault of generator, and false trip of the relay is thus avoided when external fault occurs.

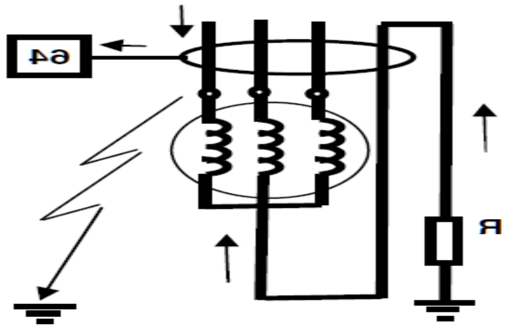

Figure 2. 3: Differential Over-current relay along with toroidal transformer

It has some limitations as it is only applicable for the generators having smaller ratings and leads of the cable on the terminal and the small section to be cabled via window of the toroidal transformer.

There are many issues of the relay settings as it should be adjusted according to the unbalance current that is calculated on the secondary winding of the toroidal transformer. The average tripping time which is present in literature for this relay is 300 ms to 1 second, particularly 500ms for avoiding occurrence of any external faults

III. WORKING PRINCIPLE OF NGT

The basic method for detecting the ground faults is to couple the over-voltage relay for monitoring the voltage impressed across the resistor as depicted in figure 2.17. It is observed that the high value of the harmonics is generated by the generator. Such an element should be made for measuring the fundamental component of the voltage and to filter or attenuate the harmonics [1, 5].

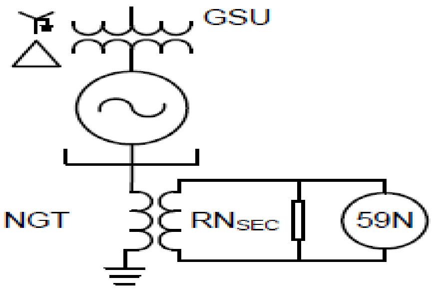

Figure 2. 4: Generator having the fundamental neutral over-voltage (59N)

The high value of the impedance grounded generators is coupled to the power system through the delta connected GSU. It is observed that under the operating conditions, no basic current flow through NGT and fundamental across the 59N and the grounding resistor is zero. During the stator ground faults, the fault current of the ground flowing through the NGT thus causes the voltage which is impressed by the grounding resistor. The over-voltage function relay is for measuring the magnitude of the fundamental voltage and hence detect the faults of the ground in the winding of the stator [11-12].

IV. METHODOLOGY

The calculations of the obtained data are shown in this chapter. The rating of the generator is depicted in table 4.1 and table 4.2 depicts the data of the GSU transformer, whereas that of 4.3 represents the capacitance values of the Generator;

TABLE 4. 1: GENERATOR RATED VALUE

Generator type	Abbreviations	Synchronous generator with salient poles
Rated power output	SGen	522 MVA
Rated stator voltage	UGen	18 kV
Operating range of stator voltage		+/- 5 %
Ext. operating range of stator voltage		+/- 10 %
Rated current	IGen	16743 A
Rated Frequency	F	50 Hz
Stator winding capacitance	CGen	2.46 µF

GSU Transformer:

TABLE 4. 2: GSU TRANSFORMER RATED VALUE

Rated power output	SGSU	3 x 174 MVA
Rated Voltage primary	UGSU,prim	500 kV
Rated Voltage secondary	UGSU,sec	18 kV
Capacitance HV-LV	CGSU, HV-LV	2.248 nF
Capacitance HV-E	CGSU, HV-E	3.983 nF
Capacitance LV-E	CGSU, LV-E	35.320 nF

The sum 1ph-to-ground capacitance is calculated according to following table. The main values are the capacitance of the generator winding and of the protection capacitors.

TABLE 4. 3: SINGLE PHASE TO GROUND VALUES ARE CALCULATED ACCORDING TO THE FOLLOWING TABLE

Equipment	Phase Capacitance to Ground (C0)	Remark
Generator	CGen = 2460.000 nF	
Capacitor, Main Transformer side	CCap = 100.000 nF	
Capacitor, Generator side	CCap = 50.000 nF	acc. to arrangement
Main IPB 65 m 100 kA IPB @ 114.7 pF/m	CIPB = 7.456 nF	
Main transformer LV/Earth	CGSU, LV-E = 35.320 nF	
Main Transformer Delta IPB 12.5 m 100 kA IPB @ 76.32 pF/m	CGSU,Delta = 0.954 nF	acc. to arrangement draw
Sum 1ph-to-ground capacitance	C0 = 2653.74 nF	

V. CALCULATIONS

Impedance criteria:

$$\acute{R} \leq \frac{1}{3\omega C_0} \quad \text{(Equation 4-1)}$$

$$= \frac{1}{3.2.pi.50.2.65e-6}$$

$$= \mathbf{400.4\ ohm}$$

Current criteria:

Resistive current component will be:

$$I_R \leq \frac{U_{norm}}{\sqrt{3}.\acute{R}} \quad \text{(Equation 4- 1)}$$

$$= \frac{19.10^3 V}{\sqrt{3}.400.4}$$

$$= \mathbf{25.95A}$$

Capacitive current component will be:

$$I_C = \frac{U_{nom}}{\sqrt{3}.\frac{1}{3\omega C_0}} \quad \text{(Equation 4- 2)}$$

$$= \frac{18e3\ V}{\sqrt{3}.\frac{1}{3.2.pi.50.2.65e-6}}$$

$$= \mathbf{25.95\ A}$$

Short circuit current will be:

$$I_{SC} = \sqrt{I_R^2 + I_C^2} \quad \text{(Equation 4- 3)}$$

$$= \sqrt{25.95^2 + 25.95^2}$$

$$= \mathbf{36.70\ A}$$

Grounding Transformer Design Ratio:

$$\mathrm{N_{GT}} = \frac{\mathrm{U_{GT,prim}}}{\mathrm{U_{GT,sec}}} \quad \text{(Equation 4- 4)}$$

$$= \frac{18\ \mathrm{kV}}{\sqrt{3}} \mathrm{VA}$$

$$= \mathbf{381.4\ kVA}$$

Transformer Data:

18kV /V3 /500V; 381.4 kVA

Secondary Resistor Design

$$\mathrm{R} = \frac{\acute{\mathrm{R}}}{\mathrm{N^2}_{\mathrm{GT}}} \quad \text{(Equation 4- 5)}$$

$$= \frac{400.4}{20.78^2}$$

$$= \mathbf{927\ m\Omega}$$

Resistor Data:

R=927 mΩ; V= 500V

Impedance criteria:

$$\mathrm{X_{C0}} = \frac{1}{\omega \mathrm{C_0}} \quad \text{(Equation 4- 6)}$$

$$= \frac{1}{2.\mathrm{pi}.50.2.65\mathrm{e}-6}$$
$$= 1201.2\Omega$$

$$\mathrm{X_{cg}} = \frac{\mathrm{X_{C0}}}{3} \text{(Equation 4- 7)}$$

$$= \frac{1201.2}{3}$$
$$= 400.4\ \Omega$$

$$\boldsymbol{\grave{R} = X_{cg} = 400.4}\Omega$$

Current criteria Short circuit current will be;

$$I_{SC} = I_R + jI_{Xcg} \quad \text{(Equation 4- 8)}$$

$$\acute{R} = X_{cg}$$
$$I_{SC} = I_R.(1 + J + 1)$$
$$= I_R.\sqrt{2} = \frac{\frac{U_{Gen}}{\sqrt{3}}}{\acute{R}}.\sqrt{2}$$
$$= 36.71\ A \ \rightarrow > 20\ A$$

Secondary Resistor Design:

$$\mathrm{R} = \frac{\acute{\mathrm{R}}}{\mathrm{N^2}_{\mathrm{GT}}} \quad \text{(Equation 4- 9)}$$

$$= \frac{\acute{R}}{\left(\frac{18.e3}{\sqrt{3}.500}\right)^2}$$

$$= 927\ m\Omega$$

$$\mathrm{I_{sec\ max}} = \frac{\mathrm{U_{sec\ max}}}{\mathrm{R}} \quad \text{(Equation 4- 10)}$$

$$= \frac{\frac{\mathrm{U_{Gen}}}{\sqrt{3}}.\frac{\mathrm{U_{GT,sec}}}{\mathrm{U_{GT,sec}}}}{\mathrm{R}}$$

$$= \mathbf{539.4A}$$

$$P = I_{sec\ max}^2.R \quad \text{(Equation 4- 11)}$$

$$= \boldsymbol{269.7\ kW}$$

Resistor Data:

R=927 mΩ, 269 kW, V=500V

Grounding Transformer Design:

$$\mathrm{N_{GT}} = \frac{\mathrm{U_{GT,prim}}}{\mathrm{U_{GT,sec}}} \quad \text{(Equation 4- 12)}$$

$$= \frac{18\ \mathrm{kV}}{\sqrt{3}}.\frac{1}{500V}$$
$$= 20.78$$

$$\mathrm{S} = \mathrm{U_{GT,sec}}.\mathrm{I_{sec,max}} \quad \text{(Equation 4- 13)}$$

$$= \mathbf{500V.539.4A = 269.7\ kVA}$$

CONCLUSION

In this thesis, the technique of neutral grounding transformer for the hydro-generators was analyzed. It was observed that grounding is very important for saving the generators from the stator to ground faults. These types of faults severely damage the generator stator's winding thus generator is prone to permanent damage.

The challenges which are faced during the no grounding, low resistance grounding and high resistance grounding are briefly discussed in the thesis. There are certain advantages and disadvantages of every technique. Moreover, the problems which are faced during the 3rd harmonic injection are also discussed. The ground coupling capacitance was observed to be had a major effect on the stator to ground faults. The capacitance value thus controls the capacitive current that is flowing from the winding to the ground.

The study includes the case study of the Tarbela Hydro Power Plants. The grounding techniques of the generators were observed, and certain values were calculated which were depicted in the chapter 4. In literature there are few standards that should be adopted while designing the grounding transformer. The design made by opting the standards provide the optimum results. It is recommended that to use modern techniques for sensing the stator to ground faults. From the literature study it is obvious that various intelligent deep learning and machine learning techniques can effectively detect the faults and provide the better results than the traditional techniques.

REFERENCES

[1] M. Gilany, O. Malik and A. Megahed, "Generator stator winding protection with 100% enhanced sensitivity", International Journal of Electrical Power & Energy Systems, vol. 24, no. 2, pp. 167-172, 2002. Available: 10.1016/s0142-0615(01)00018-7.

[2] B. Ravindranath and M. Chander, Power system protection and switchgear. New Delhi: New Age International, 2011.

[3] D. Reimert, Protective relaying for power generation systems. 2017.

[4] Y. Hase and Y. Hase, Handbook of power systems engineering with power electronics applications. Hoboken, NJ: John Wiley, 2013.

[5] The 10th IET International Conference on Development in Power Systems Protection (DPSP 2010). [Stevenage, Hertfordshire]: Institution of Engineering and Technology, 2010.

[6] L. Hewitson, M. Brown and B. Ramesh, Practical power systems protection. Amsterdam: Elsevier, 2008.

[7] S. Horowitz and A. Phadke, Power system relaying. Chichester, England: Wiley/Research Studies Press, 2008.

[8] M. Kezunovic, J. Ren and S. Lotfifard, Design, modeling and evaluation of protective relays for power systems. 2015.

[9] J. Martínez-Velasco, Transient analysis of power systems. Chichester: Wiley, 2015.

[10] Y. Paithankar, Fundamentals of power system protection. Delhi: PHI Learning Private Limited, 2014.

[11] W. Rebizant, J. Szafran and A. Wiszniewski, Digital signal processing in power system protection and control. London: Springer, 2011.

[12] L. Singh, Advanced power system analysis and dynamics. New Dehli: New Age International (P) Ltd., 2007.

International Journal of Engineering Works
ISSN-p: 2521-2419
ISSN-e: 2409-2770
Vol. 6, Issue 10, PP. 379-386, October 2019
https://www.ijew.io/
https://doi.org/10.34259/ijew.19.610379386

Potential Assessment of Biogas and its Social Values in Khyber Pakhtunkhwa

Abd-Ur-Rehman[1], Zohaib Ur Rehman[2]
[1, 2] U.S.-Pakistan Centre for Advanced Studies in Energy, University of Engineering & Technology, Peshawar, Pakistan
rehman.inayat12@gmail.com[1]
Received: 04 October, Revised: 08 October, Accepted: 10 October

***Abstract*—** Khyber Pakhtunkhwa is considered to be one of the greenest province of Pakistan. But the province is in a great threat of deforestation as majority of the population are cutting trees rapidly in order to meet their need of cooking fuel. Majority of the rural population are using firewood as their cooking fuel as they have no access to national gas transmission line and cannot afford the LPG cylinders. Installation of domestic biogas plant is one of the alternative green solutions to this problem. This research is conducted to evaluate the overall potential of biogas from cattle manure in KPK and to carry out the multi prospect assessment of current biogas plants in KPK. Potential of biogas from cattle manure was calculated from statistical data of KPK and literature review. Questionnaires were designed to conduct survey of 15 installed biogas plants in different districts of KPK. The total potential of biogas from cattle manure in KPK was found to be 532.9 million cubic meter per year. The equivalent potential of electricity generation from biogas is 1,344200 GWh per year. FATA regions have the highest potential of biogas which is 22 percent of the total whereas district D.I. Khan has a potential of 8 percent of the total. From the results of multi prospect assessment of current biogas plants it was found that 26.67 percent of the total plants were dismantled. 60 percent of the plants were fixed dome type while 40 percent were floating type. 40 percent of the plants were funded by the government, 33.33 percent by the NGOs and 26.67 percent were constructed by user on their own finance. 100% of the user agreed that biogas helps in firewood reduction. 92.86 percent of the users complaint about the maintenance of plant as a major challenge. 64.29 percent of the users wanted storage of biogas facility in the plant. On average, Rs. 2130 per month per household were saved in energy expenditure of cooking fuel with the help of biogas. 40 percent of plants users were satisfied, 33.33 percent were highly satisfied and only 26.67 percent responded as not satisfied.

***Keywords*—** Biogas, Sustainable Energy, Social Values, SPSS

I. Introduction

Energy is thought to be the backbone of any economy and most important measure of socioeconomic development of a country. In Pakistan the current situation of energy and human development process is at susceptible and the power outage and energy crisis is affecting each and every sector of the economy and ultimately the human development. Although Pakistan has abundant natural resources and there is huge potential of investment in the renewable and green energy resources [1]. Pakistan has always been facing severe crisis of energy since decades and currently facing an electricity outage of almost 8-12 hours in urban areas while 18 hours in rural areas. These energy crisis has directly or indirectly affected all sectors of the economy of the country [2]. The installed capacity of electricity generation in year 2017-2018 was 33,433 MW which has now recorded as 34,242 MW in July 2019. Similarly the generation in 2017-2018 was recorded as 82,011 GWh which has now increased to 84,680 GWh. The percentage increase in capacity counts 2.5% and in generation 2.1% [2] Due to increasing population, the demand of energy in Pakistan is increasing day by day. Like many other developing nations of Asia, Pakistan is dependent on import oil and LNG.

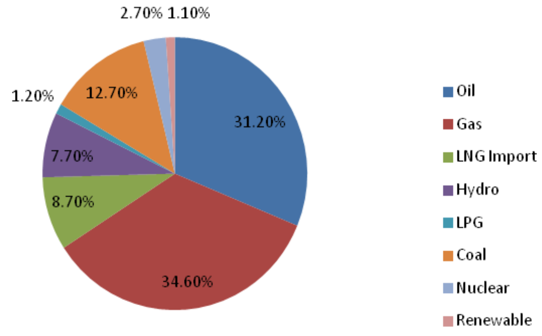

Figure I Energy Supply Mix of Pakistan [3]

Since the renewable sources of energy are gained of natural process, they are more reliable, always available and cost effective in some cases. They have widespread benefits to meet the energy crisis. Renewable energy resources are clean, green and free of carbon dioxide. The contribution of renewable energy in Pakistan energy supply was 0.3% in 2015. This contribution has steadily increased to 1.1% in the year 2018.

The total install capacity of renewable energy in Pakistan is 1,637 MW, while the generation is 3857 GWh [3].

TABLE 1: ELECTRICITY FROM RENEWABLE ENERGY SOURCES [3]

Technology	Capacity(MW)	Genration (GWh)
Solar Energy	430	768
Wind Energy	1006	2101
Bagass	201	988
Total	1637	3857

Per capita consumption of energy of a country is directly proportional to its economic growth. In Pakistan period of a high GDP growth rates were found because of high per capita consumption of energy and vice versa. However, the growth rate of energy consumption per capita as a whole is very discouraging. Pakistan is ranked as 164th in world based energy per capita consumption that is 449kWh. Comparison of Pakistan with other developed nations is given in the figure below [4].

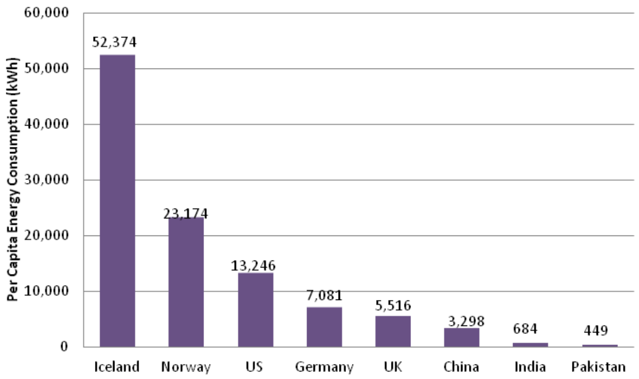

Figure I-1: Per Capita Energy Consumptions in 2013 (kWh) [4]

A. Domestic Fuel used in Pakistan

As per Household Survey of Pakistan (2015-16) the table below shows the average monthly expenditure on energy (cooking fuel and lightning) of Pakistan rural and urban areas at the household level. The total expenditures on energy, at the domestic level is about Rs. 2622.92 in Pakistan.

TABLE 2: HOUSEHOLD AVERAGE EXPENDITURE ON ENERGY IN PAKISTAN[5]

Energy Type	Pakistan	Rural Area	Urban Areas
Average Exp. in Rs. Per month	2622.92	2520.52	2800.36
PercentExpenditure	100.00	100.00	100.00
Fire Wood	20.70	30.80	4.94
Kerosene Oil	0.61	0.95	0.08
Charcoal	0.44	0.66	0.10
Coal	0.08	0.12	0.01
Dung Cakes	5.00	7.78	0.65
Gas(Piped/LPG)	13.07	8.78	19.76
Electricity	50.64	38.61	69.40
Generator	2.59	1.48	4.34
Cotton Sticks	3.44	5.40	0.40
Other	3.43	5.42	0.32

The highest single expenditure on energy in rural and urban areas of Pakistan is electricity. Similarly the second highest expenditure is natural gas in the urban area and firewood in the rural area of Pakistan. It is clear from the table that the rural areas consume more of their expenditure on the fuels for cooking puposes. 50.18% of their energy expenditure, is on biomass fuels (wood, agricultural wastes, coal, and dung) [5].

B. Rural Area Dependency on Biomass

Rural households in Pakistan are mostly dependent on biomass (Firewood, shrubs, Dung Cakes, Agri. Wastes) for their cooking needs. About 29% of biomass consumers residing in rural areas have reported that they buy wood for the cooking needs. In this about 84% of biomass consumers buying firewood in urban areas and the remaining are collecting it. Another major source of fuel for cooking needs in rural areas is dried animal dung cakes. About 70% of the Pakistani population lives in rural areas. Collecting of firewood and shrubs and manual formation of dung cakes is mainly done by women and children in rural areas of Pakistan [6].

C. Biogas as an Alternative

The energy crises can be very efficiently solved with the help of biofuels with advanced energy technologies. Like other renewable sources of energy, biogas (methane rich) that is obtained through the process of anaerobic digestion (AD) is thought to be an important source of energy. The development of this technology is very high in Europe due to their supportive renewable energy policies. For example the highest rate of biogas technology adoption is in Germany where 8700 large scale biogas plants are operating for the generation of heat and electricity. In Germany 137 biogas plants supply gas to the transport sector [4–6] Similarly this technology is also advanced in China. They are using densified biofuels at small as well as large scale. These densified fuels are very popular due to high energy density [7,8]. In developing nations however this technology is used only as a fuel for cooking and lighting at the domestic level. In order to overcome the current energy crses of Pakistan, initiatives are required to harness other sources like hydel, biogas energy, nuclear energy, micro hydel and biodiesel energy [12].

D. Potential of Biogas in Pakistan

Mostly people in the rural area of Pakistan, are self employed and have adopted livestock animal for their source of income. Almost 30 million to 35 million of people, get their 30 percent to 40 percent of income, from livestock animals [13]. By 2017-18 economic survey of Pakistan the total population of livestock is about 196.5 million that produce total manure of 744 million of Kg per day, that can be use for the generation of biogas with the help of anaerobic digestion. As 1 m^3 of biogas can be produced from 6 kg of animal manure. So the total potential of biogas from animal manure in Pakistan is 124 million m^3 [14].

E. Benefits of Biogas

The aim of a biogas plants technology is to utilize the organic wastes like animal manure and produce two worthy products, which are biogas and the digested slurry which is also called the digestate. The first one is a source of renewable energy, that could be further use for the purpose of green electricity generation, cooking, heat, and as a transport fuel etc. The digestate can be utilized as an organic fertilizer or can be processed to a refine fertilizer product [15]. According to a research, a family sized biogas plant replaces 316 L of kerosene, 5,535 Kg of firewood, and 4,400 Kg of cattle dung cake per year. Which means that a family sized biogas plant can reduce NOx of 16.4 KG, SO_2 of 11.3 KG and CO of 987 Kg where as volatile organic compounds of 69.7 KG per year [16]. In most of the developing countries diseases of respiratory infections, pneumonia of younger childrens, pulmonary diseases, asthma, cataracts, tuberculosis, hypertention and lung cancer have been reported, which are associated with the indoor smoke of biomass fuel burning [17]. Use of biogas technology for the rural household can help to relief from the abdominal pains associated to the reduced workload on the women and children which are collecting and carrying the fuelwood over a long distance and making of the dung cakes from the animal manure [18]. The use of the digestate from biogas plant as biofertilizer is an efficient way, to maintain nutrients in society. By adopting it, it will be possible to regain the broken cycle of nutrient between the consuming people of the cities nowadays and the productive soils of the countryside, which could help to reduce the use of synthetic fertilizers [19].

II. METHODOLOGY

The research methodology for this study consists of Literature Review, Data Collection, Questionnaire Survey and Data Analysis. First of all in order to evaluate the total potential of biogas plants in KPK, data of livestock in KPK was collected through different organization. Using literature review and that data of livestock the total potential of biogas plants in KPK was calculated. In the second phase a questionnaire was designed for a survey based on different questions to investigate different biogas plants that are installed in KPK. The socio-economics of those plants were investigated along with sustainability and challenges related to biogas plants. SPSS software was used to analyze this survey data. In the third phase a survey was conducted of the househods who are not using biogas. Data was collected through questionnaire about their cooking expenditure, biogas potential, livestock existence, health concerns etc.

In order to evaluate the social and economic values, sustainability, impacts on society, health and environment of biogas plants, 15 biogas plants that are installed in KPK were visited. These plants were selected from different districts of KPK Dir, Swat, Mardan, Malakand, Nowshehra, Pesawar and Kohat. Both self installed, government installed and NGO installed plants were assessed. 100 households randomly were interviewed from different rural areas of KPK.

Since the objectives of this research is completely based on the qualitative analysis. So, the methodology approach for the qualitative analysis of current biogas plants installed in KPK was the use of SPSS software. Different parameters about the biogas plants were entered into this software and complete analysis were performed with the help of it.

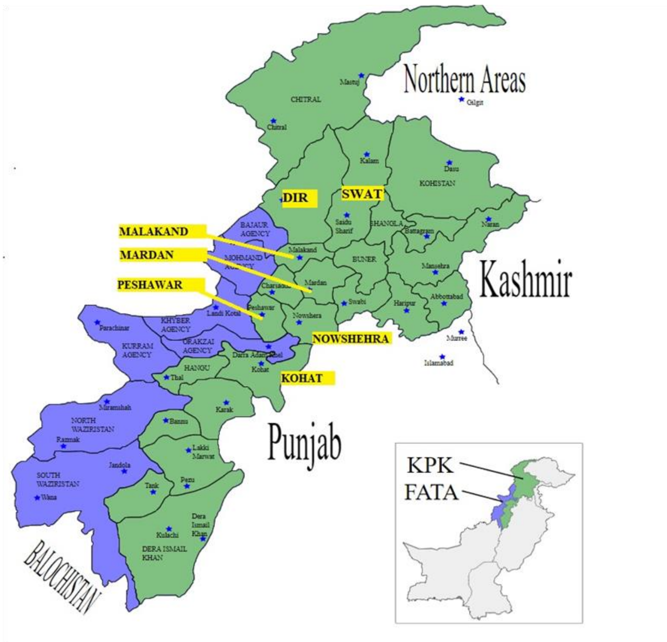

Figure II-1: Location of Biogas Plants Survey

A. Calculations for Total Biogas Potential

For the assessment of total potential of biogas in KPK, statistical data of livestock has been used from the KPK Bureau of Statistics. The data which is used for the determination of biogas potential in KPK is only for the dairy cattle and buffaloes. Because the attainability of manure from the cattle is maximum. The following formulae will be used to calculate the overall potential of biogas in KPK from manure of cattle. These formulas will be applied over the manure obtained from cattle each district wise.

The fresh manure obtained in tons per day is given by the following formula.

$$M_F = \frac{N_A \cdot M_{PPA}}{1000}$$

Where M_F is fresh manure obtained in tons per day (t/d), N_A is total number of animals, M_{PPA} is Manure production per animal in Kg. In Pakistan, the average manure production per animal(cattle/buffalo) per day is 15Kg [13].

Now, the total solid manure obtained in tons per day is calculated as follow:

$$M_S = M_F \cdot M_{SR}$$

Where M_F is Fresh Manure in tons per day and M_{SR} is Solid manure ratio and is equal to 12.5% for fresh manure [20].

The main factor required for the total potential of biogas annually is called annual total usable soild manure and is calculated in tons per year by the following relation.

$$M_{T\cup S} = M_S \cdot M_A \cdot 365$$

Where M_{TUS} annual total usable solid manure in tons per year, M_S is solid manure in tons per day and M_A is attainability of manure in percentage. We will take the attainability of animal manure as 50%.

After calculating the total annual usable solid manure the relation for total biogas amount in cubic meter per year is as follow:

$$BG_T = M_{T\cup S} \cdot BG_{Conv}$$

Where BG_T is the total biogas amount in cubic meter per year and BG_{Conv} is the amount of biogas obtained in cubic meter from 1 ton of solid manure. This value is 200m^3/t and is assumed to be constant [21].

B. Calculations for Total Electricity Generation from Biogas

Once, the total biogas production from the animal manure is obtained in cubic meter per year. The next important stage is to determine the total potential of electricity from biogas. For that the heating value of biogas will be important to calculate. If a gas engine is used for the electric generation from biogas, we must first find out the total heating value of biogas from the following equation:

$$H_{VT} = BG_T \cdot H_V$$

Where H_{VT} is the total heating value in MJ of the total biogas BG_T. Whereas, H_V is the heating value of unit cubic meter of biogas. It is important to note that the H_V of one cubic meter of biogas is known to be 22.7MJ/m^3 [21].

Now the final equation for the potential of electricity generation from biogas of animal manure will become as follows:

$$E_{BG} = \frac{H_{VT} \cdot \eta_{BG}}{3 \cdot 6}$$

Where, E_{BG} is the total electricity potential from biogas in MWh per year. If a gas engine is used for the electricity generation. Then using biogas as fuel its efficiency is η_{BG} which is 40% [j].

C. Population of Livestock in KPK

Since the last census of livestock has been carried out in 2006 and there is no latest data available in Pakistan Bureau of Statistics. So, our results will be based on data of census 2006. In this research our target is to calculate the potential of biogas from manure of cattle and buffaloes. The total population of cattle and buffaloes in KPK according to the census 2006 is given in table below [22].

TABLE 3: POPULATION OF LIVESTOCK IN KPK [22]

District	Cattle	Buffaloes	Total Heads
Peshawar	223,150	143,481	366,631
Nowsheha	190,669	106,892	297,561
Charsadda	239,899	110,697	350,596
Mardan	247,445	115,841	363,286
Swabi	203,076	103,566	306,642
Kohat	174,299	27,277	201,576
Hangu	70,451	9,521	79,972
Karak	212,496	2,054	214,550
D.I. Khan	411,432	205,634	617,066
Tank	67,104	17,975	85,079
Bannu	168,927	56,181	225,108
Laki Marwat	98,550	3,827	102,377
Abbottabad	111,415	104,582	215,997
Haripur	130,215	106,911	237,126
Mansehra	181,973	191,064	373,037
Battagram	119,699	78,233	197,932
Kohistan	250,910	51,163	302,073
Swat	253,790	117,101	370,891
Shangla	204,946	129,041	333,987
Buner	131,985	79,644	211,629
Chitral	174,842	296	175,138
Upper Dir	232,013	4,964	236,977
Lower Dir	249,007	16,258	265,265
FATA Regions	1,619,593	145,292	1,764,885
Total in KPK	5,967,886	1,927,495	7,895,381

III. RESULTS AND IMPACTS

A. Total Potential of Biogas in KPK

According to the calculation as discussed in the methodology chapter, the results of total biogas potential were generated using excel sheet. The attainability of manure M_A was assumed as 50%. The formulae were putted in excel sheet and after putting value of different constants against every district of KPK the potential was calculated. According to these calculations, the overall potential of biogas in KPK is 532.9 million cubic meter per year. Similarly the total potential of equivalent electricity from biogas is calculated as 1,344200 GWh per year. The results of biogas potential and electricity potential from animal manures district wise in KPK are shown in the excel sheet below:

TABLE 4: BIOGAS POTENTIAL RESULTS

District	N_A	$M_F = N_A.M_{PPA}/1000$ (t/d)	$M_S=M_F.M_{SR}$ (t/d)	$M_{TUS} = M_S.M_A.360$ (t/y) (1000)	$BG_T = M_{TUS}.BG_{Conv}$ (m^3/y) (million)	$H_{VT} = BG_T.H_V$ (GJ/y) (1000)	$E_{BG} = H_{VT}.\eta_{BG}/3.6$ (GWh/y) (1000)	Percentage%
Peshawar	366,631	5,499.5	687.4	123.7	24.7	561.8	62.4	4.6%
Nowsheha	297,561	4,463.4	557.9	100.4	20.1	455.9	50.7	3.8%
Charsadda	350,596	5,258.9	657.4	118.3	23.7	537.2	59.7	4.4%
Mardan	363,286	5,449.3	681.2	122.6	24.5	556.6	61.8	4.6%
Swabi	306,642	4,599.6	575.0	103.5	20.7	469.9	52.2	3.9%
Kohat	201,576	3,023.6	378.0	68.0	13.6	308.9	34.3	2.6%
Hangu	79,972	1,199.6	149.9	27.0	5.4	122.5	13.6	1.0%
Karak	214,550	3,218.3	402.3	72.4	14.5	328.7	36.5	2.7%
D.I. Khan	617,066	9,256.0	1,157.0	208.3	41.7	945.5	105.1	7.8%
Tank	85,079	1,276.2	159.5	28.7	5.7	130.4	14.5	1.1%
Bannu	225,108	3,376.6	422.1	76.0	15.2	344.9	38.3	2.9%
Laki Marwat	102,377	1,535.7	192.0	34.6	6.9	156.9	17.4	1.3%
Abbottabad	215,997	3,240.0	405.0	72.9	14.6	331.0	36.8	2.7%
Haripur	237,126	3,556.9	444.6	80.0	16.0	363.3	40.4	3.0%
Mansehra	373,037	5,595.6	699.4	125.9	25.2	571.6	63.5	4.7%
Battagram	197,932	2,969.0	371.1	66.8	13.4	303.3	33.7	2.5%
Kohistan	302,073	4,531.1	566.4	101.9	20.4	462.9	51.4	3.8%
Swat	370,891	5,563.4	695.4	125.2	25.0	568.3	63.1	4.7%
Shangla	333,987	5,009.8	626.2	112.7	22.5	511.8	56.9	4.2%
Buner	211,629	3,174.4	396.8	71.4	14.3	324.3	36.0	2.7%
Chitral	175,138	2,627.1	328.4	59.1	11.8	268.4	29.8	2.2%
Upper Dir	236,977	3,554.7	444.3	80.0	16.0	363.1	40.3	3.0%
Lower Dir	265,265	3,979.0	497.4	89.5	17.9	406.5	45.2	3.4%
FATA Regions	1,764,885	26,473.3	3,309.2	595.6	119.1	2,704.2	300.5	22.4%
Total in KPK	7,895,381	118,430.7	14,803.8	2,664.7	532.9	12,097.7	1,344.2	100.0%

The district wise potential of biogas is shown in the figure below. According to this figure the highest potential area is FATA, which is almost 120 million cubic meter per year. District D.I.Khan has the second highest potential of biogas which is about 41.7 million cubic meter. Similarly, Peshawar, Charsadda, Mardan, Nowshehra, Mansehra, Swat, Shangla and

Kohistan are the high potential areas having potential more than 20 million cubic meter per year each. The low potential Districts are, Hangu, Kohat, Bannu, Laki Marwat, Tank, Lower Dir, Upper Dir, Chitral, Battagram, Buner, Haripur, Abbotabad, and Karak which have potential of less than 20 million cubic meter per year each.

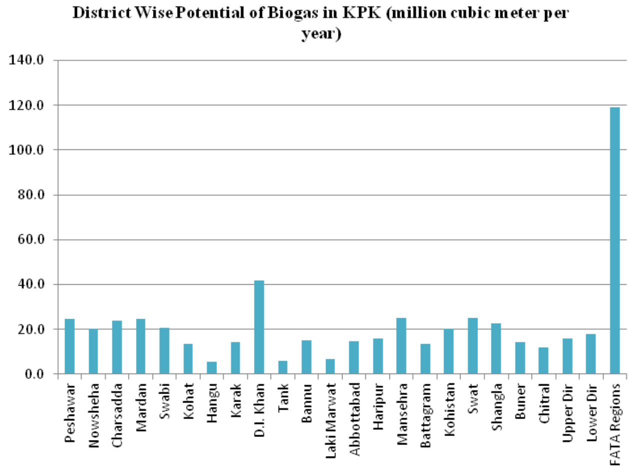

Figure III-1: District Wise Potential of Biogas in KPK

B. *Analysis of Biogas Plantsin KPK*

In order to understand the current situation of biogas plants in KPK, 15 biogas plants were visited in different districts of KPK. Different aspects of the plants were observed on the household. Like its social impact, social value, environmental benefits, impact on energy expenditures, and challenges related to the plants.

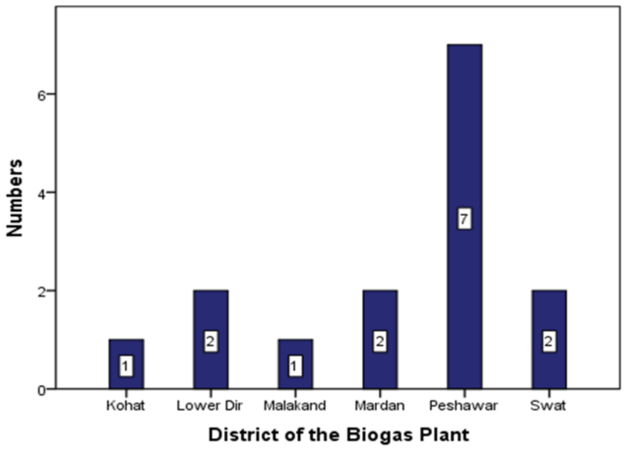

Figure III-2: Plants Visited Each District

Out of the total 15 plants, 4 plants were found non operation and were dismantled. Only 11 plants, which become 73.3% of the total were in operational conditions.

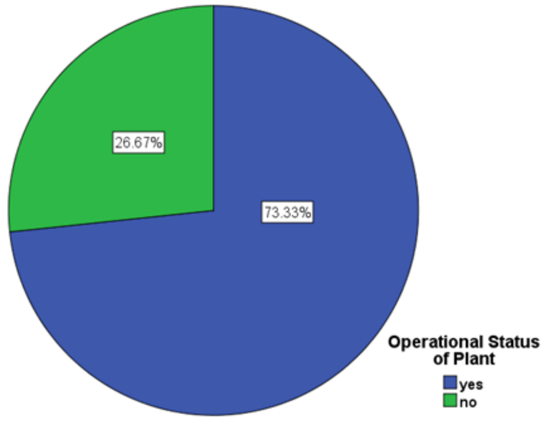

Figure III-3: Operational Status of Plants

The main reason of the dismantled plants was maintenance. The plants constructed with government subsidy were dismantled. It was observed during the visit that there were only two types of the plants installed in KPK. In which 60% of the plants were fixed dome plants. While 40% of the plants were floating type. It is worth noting that the plants installed by PCRET with the government subsidies were floating type.

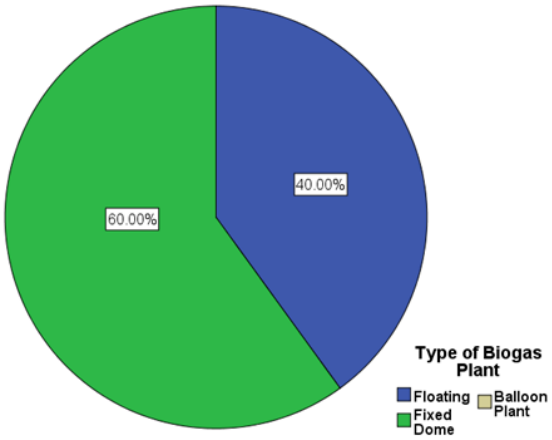

Figure III-4: Types of the Plants

40% of the plants were funded by government, 33.3% were sponsored by NGOs while only 26.6% of the plants were constructed by owners on self financed basis. This means, that adoptability of the plants with self finance is very less in KPK and people cannot afford to construct the plants on their own

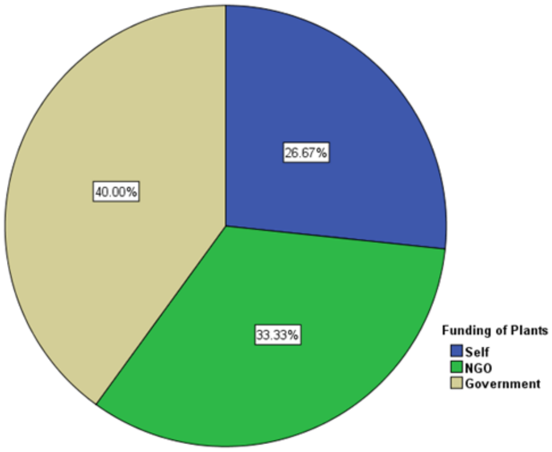

Figure III-5: Funding of the Plants

The biogas plant owners were asked about the benefits of it through structured questionnaire. Out of the 11 operational plants, 100% agreed that using biogas helps to reduce the use of firewood. 36.3% agreed upon reduction in electricity bills. 72.3% of the owners said that biogas is always available. 45.5% agreed with health benefits of using biogas.

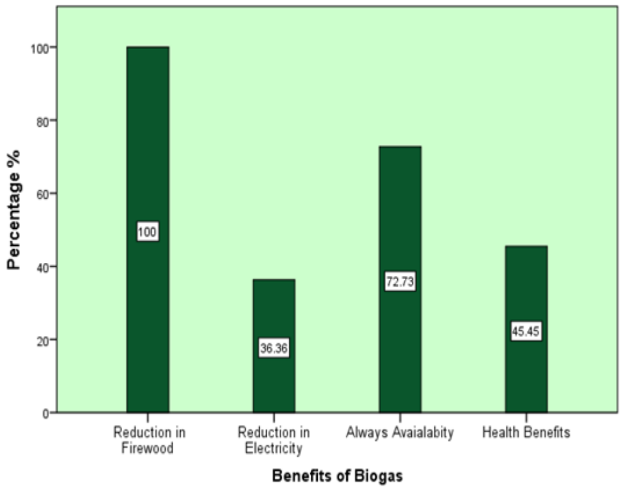

Figure III-6: Benefits of Biogas Plants

92.86% users complaint about the maintenance of the digester. The next important challenge to the biogas owner was the storage of biogas. 64.29% of the respondents said that they want to store the gas in cylinders. 42.86% of the users said that they face difficulties in operation of the plants. 28.57% of the users said that they face difficulties in providing animal manure to the plant, since they have less quantity of cattle.

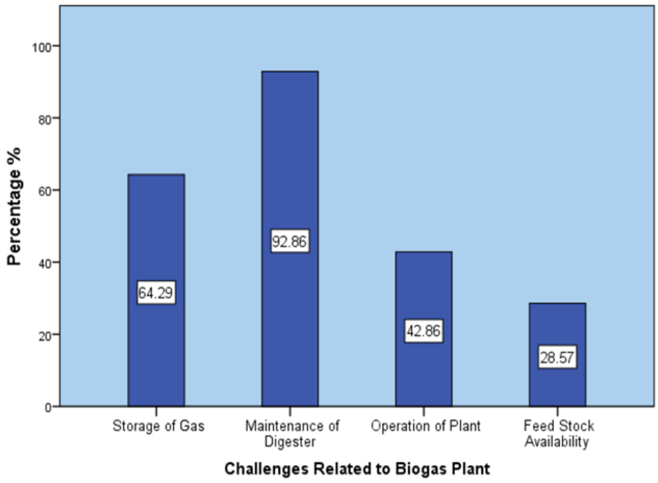

Figure III-7: Challenges Related to Biogas Plants

Considerable amount of reduction have been reported by the biogas plants owners in their household cooking fuel's expenditures. 1 of the 11 plants was installed by a restaurant owner and according to that owner the total saving of cooking fuel bill was recorded as Rs. 2000-3000 per day. 4 of the households have reported reduction in cooking fuel expenditure by Rs. 2000-3000 per month. Similarly, 3 households recorded reduction by Rs. 1000-15000 per month, while the other 3 households said that their energy expenditure on cooking fuel has been reduced by Rs. 1500-2000 per month. On average Rs. 2130 per month can be saved by each household with the help of biogas.

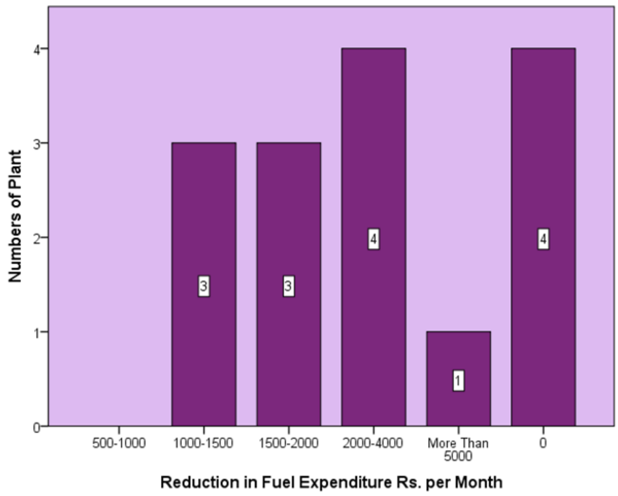

Figure III-8: Reduction in Fuel Expenditure (Rs. Per Month)

The satisfaction level of the biogas plants user was quite satisfactory as 5 numbers of the users responded to the question as highly satisfied. While, 6 numbers of users responded as satisfied. 4 numbers of the users were those whose plants were dismantled so they responded as not satisfied to the question.

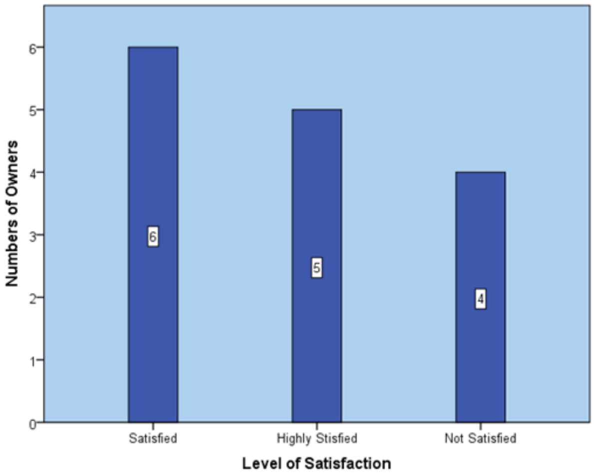

Figure III-9: Leverl of Satisfaction of Households Using Biogas

In Khyber Pakhtunkhwa the average energy expenditure on cooking and lighting fuel was recorded as Rs. 3364.28 per month per household. In which the major share was recorded of firewood which was 35.81% of the total expenditure.

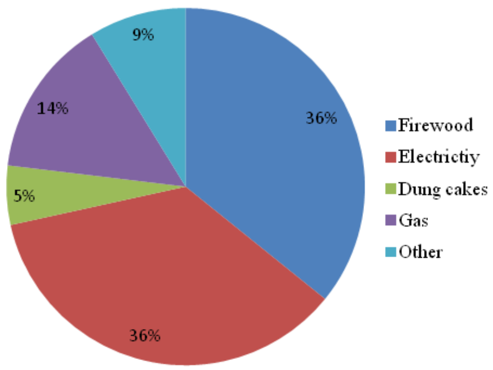

Figure III-10: Expenditures on fuels for cooking and lighting in KPK

The next major share was of electricity which was 35.78% of the total expenditure. Other than that, SNGPL gas expenditures were 14.33%, and dung cakes were as much as 5.34% of the total expenditure.

Conclusion

From the literature review it is concluded that biogas has plenty of benefits towards the sustainable development of communities. With increasing population, the need of cooking fuel is increasing as well. The need of the time is to go towards the alternative energy solutions that should be sustainable, affordable as well as eco friendly. Biogas is one of the energy alternative options that cover these three important aspects. Majority of the population in KPK is depending on agriculture and livestock as their source of economy. Having a huge population of 7.89 millions of cattle, KPK has potential of 532 million cubic meter of biogas production per year in KPK and has a potential of equivalent electricity generation of 1,344200 GWh per year. The highest potential district of KPK is D.I.Khan, which has 8 percent of total potential. FATA regions have collectively 22 percent of the total potential. It is concluded from the structured questionnaires designed for the analysis of current biogas plants at KPK, that 26.67 percent of the plants in KPK has been dismantled while 73.33 percent of the plants are in perational conditions. 40 percent of the users were satisfied with the biogas technology, 33.3 percent of the respondents were highly satisfied, while only 26.67 percent of the respondents were not satisfied. The average expenditure on cooking fuel in KPK is Rs. 3364.28 per month per household Whereas, the average reduction by biogas in cooking fuel expenditure per household per month was found to be Rs. 2130. 100 percent of the plants installed in KPK are for cooking purpose, while 26.67 percent of the plants were also running generators through biogas. 100 percent of the respondents were facing challenges in the maintenance of the plants. It was also found through the study that most of the plants user wanted gas storage facility so that they can have gas for any emergency use. It is worth noting that, 100 percent of the plant owners said that the biogas plant helps in firewood reduction and during survey it was noted that those household who has biogas plants installed have no use of firewood for the cooking purpose, which means that deforestation issue can be solved by developing the biogas technology in the rural communities of KPK. The bio slurry of the plant was used as a bio fertilizer for the agricultural activities by 73.3 percent of the users and they were very satisfied with the yield of crops and other agricultural products.

Refrences

[1] F. Fatai, K and Oxley, Les and Scrimgeour, “Modelling the causal relationship between energy consumption and GDP in New Zealand, Australia, India, Indonesia, The Philippines and Thailand,” Math. Comput. Simul., vol. 64, pp. 431–445, 2004.

[2] GOP, “Pakistan Economic Survey 2018-19. Ministry of Finance, Government of Pakistan, Islamabad.,” 2019.

[3] M. of Energy, Pakistan Energy Year Book 2018, no. 2018. 2018.

[4] I. Jan and W. Akram, “Willingness of rural communities to adopt biogas systems in Pakistan: Critical factors and policy implications,” Renew. Sustain. Energy Rev., vol. 81, no. June, pp. 3178–3185, 2018.

[5] Pakistan Bureau of Statistics, “Household Integrated Economic Survey,” p. 2017, 2015.

[6] B. Pandey and S. Bajgain, “Feasibility Study of Domestic Biogas in Pakistan,” Rspn, no. July, pp. 1–38, 2007.

[7] J. Daniel-Gromke et al., “Current Developments in Production and Utilization of Biogas and Biomethane in Germany,” Chemie-Ingenieur-Technik. 2018.

[8] H. Oechsner, S. K. Khanal, and M. Taherzadeh, “Advances in Biogas Research and Application,” Bioresour. Technol., 2015.

[9] C. Sawatdeenarunat et al., “Anaerobic biorefinery: Current status, challenges, and opportunities,” Bioresource Technology. 2016.

[10] Y. Zhou et al., “A comprehensive review on densified solid biofuel industry in China,” Renewable and Sustainable Energy Reviews. 2016.

[11] M. Shan, D. Li, Y. Jiang, and X. Yang, “Re-thinking china’s densified biomass fuel policies: Large or small scale?,” Energy Policy, 2016.

[12] M. A. Sanz-Bobi, F. De Cuadra, and C. Batlle, “A review of key points of an industrial biogas plant. A European perspective,” in 2012 International Conference on Renewable Energy Research and Applications, ICRERA 2012, 2012.

[13] W. Uddin et al., “Biogas potential for electric power generation in Pakistan: A survey,” Renew. Sustain. Energy Rev., vol. 54, pp. 25–33, 2016.

[14] GOP, "Pakistan Economic Survey 2017-18. Ministry of Finance, Government of Pakistan, Islamabad.," p. P: 13-32, 2018.

[15] J. B. Holm-Nielsen, T. Al Seadi, and P. Oleskowicz-Popiel, "The future of anaerobic digestion and biogas utilization," Bioresour. Technol., vol. 100, no. 22, pp. 5478–5484, Nov. 2009.

[16] H. Pathak, N. Jain, A. Bhatia, S. Mohanty, and N. Gupta, "Global warming mitigation potential of biogas plants in India.," Environ. Monit. Assess., vol. 157, no. 1–4, pp. 407–18, Oct. 2009.

[17] K. C. Surendra, D. Takara, A. G. Hashimoto, and S. K. Khanal, "Biogas as a sustainable energy source for developing countries: Opportunities and challenges," Renewable and Sustainable Energy Reviews, vol. 31. Elsevier Ltd, pp. 846–859, 2014.

[18] B. Amigun, W. Parawira, J. K., A. O., and A. S., "Anaerobic Biogas Generation for Rural Area Energy Provision in Africa," in Biogas, InTech, 2012.

[19] M. Lantz, M. Svensson, L. Björnsson, and P. Börjesson, "The prospects for an expansion of biogas systems in Sweden - Incentives, barriers and potentials," Energy Policy, vol. 35, no. 3, pp. 1819–1829, 2007.

[20] J. Lorimor, W. Powers, and A. Sutton, "Manure Characteristics - Manure Management Systems Series," p. 24, 2018.

[21] C. Karaca, "Determination of biogas production potential from animal manure and GHG emission abatement in Turkey," Int. J. Agric. Biol. Eng., vol. 11, no. 3, pp. 205–210, 2018.

[22] Govt of Pakistan Statistics Division, "PAKISTAN LIVESTOCK CENSUS 2006," 2006.

IJEW 国际工程期刊 International Journal of Engineering Works انجینرنگ کاموں کا بین الاقوامی جرنل

International Journal of Engineering Works
ISSN-p: 2521-2419
ISSN-e: 2409-2770
Vol. 6, Issue 10, PP. 387-391, October 2019
https://www.ijew.io/
https://doi.org/10.34259/ijew.19.610387391

Review of Remote Acting Fire Valve (RAF) Calibration and Rework Problems in Tesla Technology Private Limited Pakistan

Wiqas Alam[1] Zafar Ahmad[2]
NWFP, University of Engineering and Technology, Peshawar
wiqassuit17@gmail.com, engrzafar90@outlook.com
Received: 03 October, Revised: 08 October, Accepted: 11 October

Abstract— The need for safety devices is increasing day by day in a fast-growing technology era. Many heating appliances involve oil fuel or liquefied petroleum gas burning in furnaces providing heat to the working facilities and our homes with controlled fires and careful management. The risk of blazing fire escaping from furnaces will cause potential harm and hazardous to our lives and damages to our houses. Remote acting fire valve (RAF) safeguard against the fuel being fed into the fire and prevent the total destruction by fire. The automated fire safety valve utilizes the temperature control sensor governed to minimize the risk of fire. The RAF with cut off temperature 66 ℃ or 90 ℃ depends on the model, the flow rate of 395 liters/hour with 2m head approved by BS5410. This paper demonstrates the operation, calibration, function, and Reworks of Remote Acting Fire valve (RAF), manufactured and assembled in Tesla Technologies Private limited Pakistan. RAF is a safety device designated to cut off fuels supply to heating appliances that may have malfunctioned. Failure and Reworks of RAF are the problems need to be resolved. The proposed solution to the rework problems at Tesla Private limited would be beneficial to the company and customers.

Keywords— RAF, Calibration, Reworks, Aluminum die

I. Introduction

RAF is a fire-actuated device mounted on oil boiler providing safety against overheating, which may cause extreme harm to the oil boiler. The valve activate as the temperature exceeds the safe operating heating limit and allow the device to cool down to predetermined limit. Tesla Technology is Pakistan's largest manufacturing of CNG equipment's, RAF, electrical control devices. RAF composed of body, cover, bellow pipe, and brass rod, copper capillary, and rubber rings. The latch, adjuster, and knob are assembled with the body. A remote acting fire valve is a safety device designated to shut down the supply of oil fuel to heating appliances involving oil fuel burning or liquefied petroleum gas inside furnaces. The purpose of heating appliances to provide heat to working facilities and homes. The heat provided on the basis of controlled fire and careful management. The failure of the valve against explosions of the tanks of oil-filled boiler have been found to be the sensor's fault to compensate for the temperature and to follow constant Boyle's Law. The risk of blazing fire at our home can be potentially harmful and hazardous to our lives. Also, the failure of preventing fire escaped from furnaces cause damages to our house. Remote Acting Fire valve avoids such failure by providing a safe cut off from furnace supply to heating appliances. Unique mechanism followed by RAF to prevent fires from blazing above certain temperature range through temperature sensors.

The capillary sensors are exposed to the excessive heating, the firing valve closed tightly, preventing the main tank from fueling the fire. The temperature of the bulb increases, transmits heat through copper made capillary (excellent heat conductor), heat energy is sent to the bellow through the cap inside the bellow pipe. The bellow expands due to excessive heating and pushing the latch through the large gap for the rod to pass through. At first, the rod is fixed in the small gap of the latch shows the normal temperature and knob extended outwards. Knob extension is the 'ON' position and the latch has been pushed to allow the rod to pass through a large gap and moving the knob inwardly (the OFF position). The on and off position shows the normal and extreme temperature state inside the heating appliances. The capillary sensors are exposed to the excessive heating, the firing valve closes tightly, preventing the main tank from fueling the fire.

The sensor is mounted inside the insulating casing of boiler or furnace connected through capillary tube, a thin tube, to remotely fire valve. The valve installed in the fuel line supplies to the furnace. The liquid present inside the capillary tube expands as the heat exceed the expected level for the furnace. The expanded liquid cause the shutdown of the valve that turn off the fuel supply to the furnace. As a precaution once the valve close, it will not reopen unless manually reset standard set. The RAF is assembled, calibrated, and carefully tested in the facilities. Defects like crack, deformation and problems in the design are immediately rejected and placed in the specific component bin for correction and rework. The assembled remote acting fire valve is shown in Figure. 1

Figure 1. Remote Acting Fire Valve

II. Literature Review

A fire valve having a cooperating seat and shift able valve half. The valve half is carried by a floating valve stem. The primary valve includes a piston and cylinder combination that is operatively related to the valve stem and that causes the valve half to be by selection spaced from the valve seat in response to fluid pressure within the valve. A furnace destruction device at some point of which fireplace craving material was contained inside an exceeding reservoir, the reservoir having an outlet and inlet system containing number of nozzles that delivered fuels for fireplace to practical area. The device combines a valve between the reservoir outlet and the nozzle valve collectively with a movable valve. The valve member is movable from a closed function with relevance the valve seat stopping the exchange between the reservoir and nozzle to an open role permitting the flow of the fuels from the reservoir to the nozzle. The mechanism maintains a fluid pressured to closed position and is operable to vent the fluid to lower the strain inside the valve, so allowing the valve member to open. A coupling association joins the reservoir outlet to the valve stressed is carried out from the reservoir through the coupling member. This check valve prevents result the coupling device in an exceedingly reverse direction towards the mechanism proposed by Thompson et al.1977, Northill et al. 1993 [1, 2].

An activating device operated by a pressure medium, like compressed gas, acting at intervals will be secured to a valve by a mounting member hooked up to the valve. The activating device includes a primary piston radio-controlled during a cylinder half positioned on one surface of the valve and a toothed rack hooked up to the primary piston and meshed engagement with a pinion shaft. The pinion shaft is connected by a coupling half to the valve shaft, an equivalent activating device will be used for a bigger valve by putting a second piston in another cylinder half on the alternative facet of the primary piston with a toothed rack hooked up to the second piston and in meshed engagement with the pinion shaft. The primary and second pistons act in opposite directions and double the force working on the pinion shaft as compared to the force delivered by the primary piston observed by Hilpert and Hunziker et al. 1987 [3].

A method and system studied by Kelada et al. 2000 [4] for mechanically validate the pressure relief based operation valves for thee aggressive storage tanks, which may be remotely operated to protect discharge once disasters occur, permits the on-line substantiation of the escape practicality and correct operation. A method of activating a valve mechanism comprise injecting controlled fluid from a fluid reservoir of the valve mechanism system into a primary chamber of the valve mechanism, discharged controlled fluid from a second chamber into the fluid reservoir, and activating the valve mechanism from a primary position to a second position concluded by Lymberopoulos 2015 [5].

The fast-acting valve testing designed for blast generators (Blast/Thermal machine (LB/TS) by Eaton Consolidated Controls to be used in driver tubes, simulate decaying nuclear explosion's blast waves. The Eaton Throat Valve component (ETVE) was tested at the Idaho National Engineering Laboratory (INEL) to judge its performance against the planning criteria set by Stacey et al. 1992 [6].

A protection system for oil furnace consists of a pump that drives cylinder component with a double-acting piston movable through a rod to a suction piston component in the course of a suction element of the pump cylinder. The oil furnace is supplied with oil from a route having a shutoff valve or valves vicinity unit linked via a suction line to the suction phase of the piston. The suction component is linked through a check valve to the pressure cylinder that manage the motion of the power piston so it moves when the burner is turned off to displace the suction piston to impact a suction on the provision line to the oil of the burner consequently withdrawing the oil observed by Oppenberg et al. 1981 [7].

Morse et al. 1936 [8] worked on Safety valves; Equalizing valves, e.g. pressure relief valves motivated in consequence of extraneous circumstances, e.g. shock, modification of excessive temperature in the valve comprising liquefied, softening or soluble components, e.g. used as link, block part, seal, closure plug. Actuating devices; operative means; releasing devices motivated by fluid performing on a piston observed by Phillips et al. 1930 [9]. Systems for dominant combustion exploitation devices tuned in to thermal changes or to thermal growth of a medium studied by Smith et al. 1926 [10].. Burners within which liquid fuel evaporates within the combustion area, with or without chemical conversion of gaseous fuel examined by Grant et al. 1931[11].

Buchanan and Buchanan et al. 1992 [12] study on an accelerated mixture steam and heating oil provide and purge valve characteristic a steam valve and mechanism member that presents a closed position, a purge operation mounted between steam discharges lines ensuing in a furnace. In its closed position the oil provide to the recirculation valve member between the oil itinerary and a recirculation line that redirects oil to a tank or sort for reheating and for protection of the favored physique at some point of burner termination.

Kagi et al. 2006 [13] Presented invention related typical devices designed for the combustion of liquid fuels specifically to an improved methodology and equipment for burning high-viscosity and waste oil. The topic invention utilizes fuel transported from a distant supply fed oil regulator in conjunction with magnet valve set on the external burner assembly. The oil yield preheating chamber contained at intervals a pre heater block. A constituent within the oil preheating chamber is dormant till the burner requires heat. Controlled air from a distant supply enters the burner assembly through regulator and air magnet valve then yield into a additive air tank. The controlled air is step by step free from the air preheating chamber at intervals the pre heater block, possessing a separate air constituent.

III. CALIBERATION OF REMOTE ACTING FIRE VALVE

RAF have to be calibrated before they can be used to provide safety to the oil boilers. The calibration of an instrument refers to the manner of marking-up a scale on the instrument to be used as intended function. Proper tag on threaded portion of the cover body is placed such that facing upward seen openly. RAF type depends upon the operating temperature, capillary length and the date (three digits signifying the year like 2019 as "9" and the two extreme digits for the week of the year e.g. "29"). According to the Table 1, tag would be assign accordingly to RAF.

Table 1. Remote Acting Fire Valve Tag codes at Tesla Private Limited.

Sr. No.	Tag Codes	Remote Acting Fire Valve
1	TVF66015	66 Degree × 1.5 m
2	TVF66030	66 Degree × 3 m
3	TVF66060	66 Degree × 6 m
4	TVF66090	66 Degree × 9 m
5	TVF66150	66 Degree × 15 m
6	TVF90015	90 Degree × 1.5 m
7	TVF90030	90 Degree × 3 m
8	TVF90060	90 Degree × 6 m
9	TVF90090	90 Degree × 9 m
10	TVF90150	90 Degree × 15 m

The following procedure to be followed to perform the calibration of RAF. Tank temperature adjustment depends on ambient temperature. Thermometer vertically hanging measure the room temperature. The RAF valve mostly fail due to the ambient conditions and incorrect reading of the temperature taken for calibrations. The calibration chart shown in table 2 give the required temperature depending on type and size of the RAF.

Table 2. Calibration Chart for RAF at Tesla Private Limited

Ambient temp℃> 5 10 15 20 25 30 35 40

Model	**Size**								
66	**1.5**	77	72	68	63	58	54	49	45
	3	79	74	68	63	58	52	45	45
	6	78	73	68	63	58	53	48	45
	9	77	72	68	63	58	54	49	45
	15	82	76	69	63	57	50	45	45
90	**1.5**	95	94	92	90	87	84	81	79
	3	95	94	92	90	87	84	81	78
	6	95	94	92	90	86	83	79	75
	9	95	94	92	90	86	82	79	75

Tank temperature is set to the reading obtained from the calibration chart. But the reading must be 10℃ lower than the calibrated chart reading. The temperature reading attained for the calibration chart must be decodes into temperature range. Reaching the required value of temperature, bulb is placed inside the tank for 10 minutes and note the time using stop watch. After that, the adjuster nut rotated and adjusted at the point where the piece automatically turns to "off" position. Mark that point and lock threads there. Make sure that bulb is inside the oil tanker and motor works properly. Placing the RAF in the test bench properly and setting the temperature for specific type of RAF. The heat must evenly circulate by turning on the heater and fan. Temperature need to rise to the required set values. As the temperature reached, start stop watch and wait for an hour. Afterwards, the RAF in the "ON" position pass whereas the "OFF" RAF's are sent back for rework.

IV. REWORK OF REMOTE ACTING FIRE VALVE

The bellow pipe inserted inside the cover body with a spring attached to latch cover. A key inserted beneath the knob to allow slow and upwards push to the ON position while doing so latch is pushed with greater force inside the cover body. Make sure that knob is at OFF position. A problem at that phase lead to spring or latch changes. The failed pieces of RAF are sent back for reworks. Reworking include disassembles of remote acting fir valve, which is the real issue in Tesla Technology private limited. The workers in the RAF department use the heat gun to reopen or disassemble the RAF valve by hot air blow directly into the pieces. The remote acting fire valve capillary damages with excessive heating and cannot be rework. This issue damages the RAF capillary permanently, causing economic and customer losses.

Heat gun comprises a heating element and emits hot air stream at the temperature range between 100 C and 550 C. Variety of heat guns available depending on the temperature range and type of applications. Shrink heat, shrink tubing and shrink packing are the various application of heat guns. Hot air guns also known as hot air stations are used in rework mounted circuit board and De soldering of electronic circuits. The bellow pipes shown in Figure 2 tightly closed with capillary tubes of the remote acting fire valve.

Figure 2. The remote acting fire valve assemblies and bellow pipe.

The tightly fixed bellow pipe with brass body and capillary tubes make the rework difficult to proceed further. The heat gun with high temperature air blower damage the remote acting fire valve pieces. The U bend shape die is designed to hold the bellow pipes such that slow and steady heating of the pipe make the disassembly of RAF easy without damaging the piece. The proposed die made of Aluminum model and drawing is shown in Figure 3.

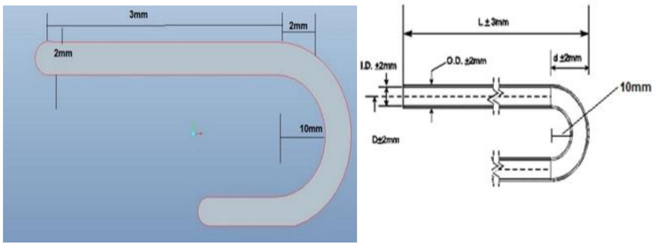

Figure. 3 The Pro e model and drawing of the aluminum made die for rework of RAF.

V. Performance Comparison

The remote acting fire valve rework performance comparison were made based on the average monthly production and theirs rework. The rework with heat gun for the disassembly of the valve has been investigate. The comparison were made for both cases shown in Figure 4. In the first case, the remote acting fire value reopened with direct blow of hot air stream blowing from heat gun and mostly the piece get damaged. The high heat directly flowing toward the capillary tubes bend the capillary permanently and the mobile oil filled within the capillary wasted. The damage pieces cannot be processed further. On the other hand the die made of aluminum in contact with bellow pipe and fitted in heat gun blower increase the temperature of aluminum die first and transmit heat to the bellow pipe steadily. The conduction mode of heat transfer safely open the RAF valve without damages. The monthly rework pieces damaged by heat gun with or without die were compared in order to compare the performance shown in Figure 4. The result clearly show the few pieces damaged with aluminum compared to the direct heating.

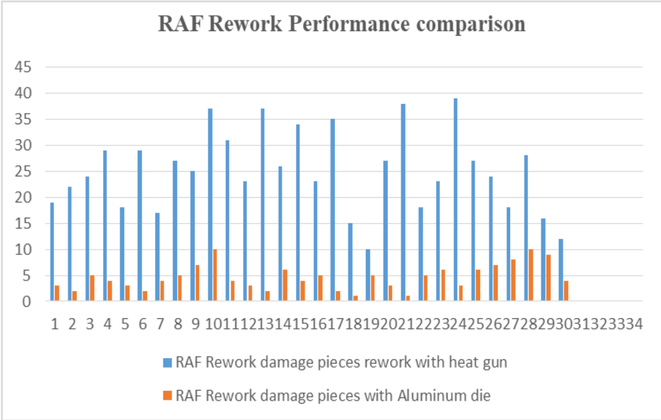

Figure 4. RAF rework performance comparison for both heat gun without die and with aluminum die.

Discussion

Tesla Technology private limited utilize heat gun for reopening of the failed pieces of RAF. The reopening involves the disassembly of the capillary tube, bellow pipes and other assembled parts. The continuous heat flowing through capillary, permanently damage the part. Die made of excellent thermal conductor materials grasp the tightly fitted bellow pipe and capillary. Turning on the heat gun and blowing the hot air through the die will slowly heat up the bellow pipe and capillary. Continuously checking with a key along with heating will make it easier for the bellow pipes to open without damaging the capillary. The accurate reading of ambient temperature at RAF small room inside the Tesla Technologies will prevent the valve's failure. Environmental changes greatly affect the temperature inside the company rooms and also, the calibration chart changes with it. The RAF limits changed during calibration which lead to the failure of the most valves. Isolating the calibration room from external environment will give positive impact on RAF valves. The valve opening for reworks comparison between direct heat gun without die and with the die were done. The aluminum give satisfactory result for the opening valve of the remote acting fire valve.

Conclusions

Tesla Technologies private limited company formed in 1992 providing services of design and produce hi-tech refined and reliable equipment, control and safety instruments for local and engineering uses at reasonable costs. Remote acting fire vale being exported generate a substantial amount of foreign exchange. The two main issue regarding RAF assemblies, calibration and reworks arises are the poor performance due to inaccurate measurement of ambient temperature and disassembly of the RAF. Excellent thermal conductive material die could resolve the issue without damaging the remote acting fire valve. The bellow pipe and capillary separation can be easily done with the help of continuously slow heating the die, otherwise, consequences are that more than half work pieces of remote acting fire valve would fail. The aluminum die gives satisfactory result regarding the opening of the failed pieces for rework. Tesla Technologies need to gear up the productivity by resolving such critical problems.

REFERENCES

[1] Thompson, W. S. (1977). Pressure reducing fire valve, Google Patents.

[2] Northill, B. W. (1993). Fire suppression systems, Google Patents.

[3] Hilpert, B. and B. Hunziker (1987). Remote control actuating device for a valve, Google Patents.

[4] Kelada, M. I. (2000). Remote function verification of low pressure and vacuum relief devices, Google Patents.

[5] Lymberopoulos, D. (2015). Valve actuator control system and method of use, Google Patents.

[6] Stacey, M. R. (1992). Performance Tests of a Fast-acting Valve for the Driver Tubes of a Large Blast/Thermal Simulator, EG AND G IDAHO INC IDAHO FALLS.

[7] Oppenberg, R. (1981). Safety device for an oil burner, Google Patents

[8] Morse, L. H. (1936). Valve, Google Patents.

[9] Phillips, S. C. (1930). Steam-operated emergency valve for oil and gas wells, Google Patents.

[10] Smith, I. E. (1926). Oil-burner-control system, Google Patents.

[11] Grant, W. S. (1931). Oil burner, Google Patents.

[12] Buchanan, B. F. and J. R. Buchanan (1992). Combination steam and fuel oil supply and purge valve with recirculation feature, Google Patents.

[13] Kagi, T. (2006). Waste oil multi-fuel fired burner, Google Patents.

Engr. Wiqas Alam
DOB: 1st, Sept, 1990, Karak, KPK
Master in Material Engineering, University of Engineering and Technology, Peshawar.

IJEW 国际工程期刊 International Journal of Engineering Works انجینرنگ کاموں کا بین الاقوامی جرنل

International Journal of Engineering Works
ISSN-p: 2521-2419
ISSN-e: 2409-2770
Vol. 6, Issue 11, PP. 392-398, November 2019
https://www.ijew.io/
https://doi.org/10.34259/ijew.19.611392398

Control and Modelling of Rotor and Grid Side Converters Control of Doubly Fed Induction Generator for the Application in Micro Hydro

Mohsin hamid[1], Dr Abdul Basit[1], Muhammad Ilyas[1], Fazl-e-Hilal[1], Imran Haseeb[1]
[1] US Pakistan Center for Advanced Studies in Energy, UET Peshawar
Received: 08 October, Revised: 15 October, Accepted: 25 October

***Abstract*—** Micro hydro power is considered as one of the lucrative options for electricity generation, it can work both autonomously and in Grid connected mode.Most of the MHP's are built on obsolete technology due to which only a portion of flow is utilized for power generation. In micro hydro power plant Voltage and frequency of induction generator are not constant due to change in discharge of water.To overcome these issues technology is moving from fixed speed operation (FSO) to variable speed operations (VSO). Doubly Fed Induction Generator (DFIG) is the most suitable option for variable speed operation .In this research paper working and operation of DFIG in MHP system in Grid connected mode is observed which allow to compensate the variations in acceptable proportion while guaranteeing a good quality of electrical outputs.A control algorithm is developed which enable the stator voltage and frequency of DFIG to a constant value in spite of speed variation in driving shaft and load changes. A vector control technique is adopted for the regulation of rotor side converter (RSC) and grid side converter(GSC) to keep the voltages and frequency with in limits and also ensure the reactive power exchange with the grid according to the reference value.Operation of the established model is tested by different operating conditions in Simulink MATLAB.

***Keywords*—** Doubly Fed Induction generator (DFIG),variable speed operation (VSO), micro hydro power (MHP),Rotor side converter (RSC),Grid side converter (GSC).

I. Introduction

The demand in electrical energy is increasing day by day across the globe to fulfil this demand electrical power is generated from various natural resources.In which some methods are non environmental friendly like by using fossil fuels which results in carbon emission.To overcome this issue and to produce clean and green energy the world is moving toward renewable energy generation.solar,hydro,wind,biomass are the major resources from which power can be generated.

Hydro power play a vital role in fulfilling the gap between supply and demand of electric power.hydro power has the maximum potential to harvest energy from water and is most abundantly available in nature.By the end of year 2014, in the total electricity production hydro estimated share is 16.6% while the percentage share of hydro electricity generated from renewable resources is 72.8% [1].hydro power is generated on many levels from Mega watt to few kilo watt.the initial cost of giant hydro power is very high and require huge civil work on the other hand micro hydro power is the most lucrative option for small scale power generation and can be distributed easily without any complexities. In Europe the total installed capacity of micro hydro power is about 11500MW sharing 1.79% of electricity generation and 9.5% of total hydroelectricity[2].For countries where the gap between supply and demand of electric power is vast micro hydro provide the best solution for distributed generation.it can work both autonomously and in grid connected mode.Mostly two types of generators are run by hydro turbine synchronous generator and Induction generator Both generators operate at constant rotor speed. Normally the generated power is controlled by varying the degree of flow gate, these configurations are not well suited, too expensive, and having maximum mechanical stress.To utilize the maximum potential of micro hydro power plant a control scheme should be developed which will be able to operate in a varying angular speed without a mechanical gate control. With advancement in power electronics converters, in order to harvest maximum power from the source, technology is moving toward the variable speed operations [3] For this purpose, a variable speed operation is used as alternative solution for Micro-hydro power plant.

Variable speed operation can be obtain by various techniques.one is direct drive system with no gear box with bulky generator having many number of poles due to slow speed of hydro turbine,with full rated power electronic converters due to which the cost of system is high.Another method is gear drive train using gear boxes to attain variable speed operation.the size of generator along with size of power electronic converter is reduced resulting decrease in cost.the most suitable example for this method is best implemented in Doubly Fed Induction Generator (DFIG) which is very successfully implemented in wind power generation for variable speed operation.in this paper we will coupled hydro turbine with DFIG and will check its result while changing different parameters like head,discharge or reactive power exchange with the grid.

II. Related Work

To harvest maximum energy from water many researcher's focus on redesigning of generators while many worked to improve the control strategy for voltage and frequency regulation.the aim is to develop a more efficient model for hydro generation with maximum efficiency and less losses.to get a more efficient model technology is shifting from fixed speed operation to variable speed operation in order to generate more power from the available resources. For variable speed operation DFIG is the most feasible option for micro hydro power generation.DFIG give a constant output at varying flow rate and speed with in acceptable proportions.some researcher develop a model for VSO in micro hydro in which DFIG is autonomously [4] and in some cases it is taken in Grid connected mode connected with the utility Grid[5] while in [6] the DFIG is working hybridly with solar PV system.

The work done by sirodez [7]is that generator speed is kept constant to its nominal speed by using a governor system by regulating water flow. The governor is controlled by using a microcontroller device to accelerate the response due to load variation and act as a monitoring device. The generator speed is maintained to a constant value by regulating the wicket gate opening through microcontroller. The response time of the governor is 20 secs to return the generator speed to its nominal speed, with load variation given to generator is every 20%.

Another method for regulating the voltage and frequency is proposed by C.P.Ion [8] based on impedance controller also known as dump Load (DL). The regulation of electrical parameters is ensured by using VSI in combination with DL. Results of the simulation shows that when a load of 900W is connected at 2.1 sec and disconnected at 5.4 sec, after load is connected the generator voltage drop to 370 v from rated voltage 400v for 0.2 sec in around 1 sec the voltage is return to its nominal value by the diminishing the power through DL.

The main goal is to maintain voltage and frequency in pre defined values despite of change in site parameters like load,flow head etc.Tradionally there are two ways to achieve this goal one is to regulate the flow that run the turbine by using speed regulator and another is by using electronically controlled addional load[7,8].The draw back to these system are that we have maximum mechanical stress and only a portion of water is utilized for power generation and high cost. DFIG provide the most appropriate solution for voltage regulation in variable speed operation.This method is based on generator control which is robust and more efficient then other.

III. DOUBLY FED INDUCTION GENERATOR

A. *DFIG in Grid Connected Mode*

Doubly fed induction generator is basically a wound rotor induction machine (WRIM) which can run both as a generator and motor.DFIG can be operated in sub-synchrounous, synchrounous and super-synchrounous mode.DFIG supply power at constant voltage and frequency with rotor rotating at variable speed[4].It can work both in Grid connected mode and in islanded mode specially in remote areas.DFIG has both stator winding and rotor winding.In grid connected mode the stator windings are directly connected with the grid for bidirectional power flow and magnetization of the machine,while Rotor winding is coupled with Grid through back to back bidirectional PWM power electronic converters as shown in fig (1).These converters are two level voltage source converter (VSC) namely as rotor side converter (RSC) and grid side converter (GSC) with a DC link between them.By adopting vector control strategy the bidirectional VSC assure the generation at standard Grid voltage and frequency regardless of variation in rotor speed.the main purpose of converters is to neutralize the difference between the rotor speed and the reference synchronous speed.

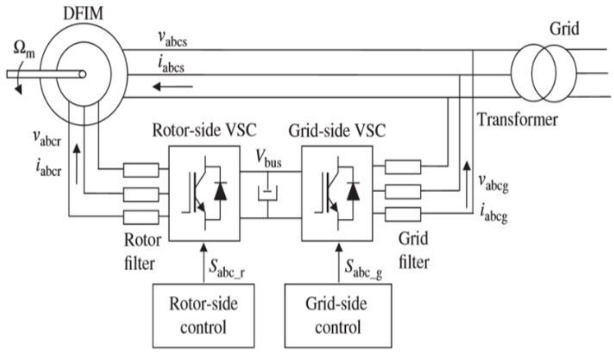

Figure 1. DFIG in Grid Connected Mode

B. *Bidirectional back to back PWM Converters*

The converters used in in this topology are two 3 phase back to back bidirectional PWM converter which are coupled through DC link as shown in Fig (2).controlled exchange of active and reactive power between rotor side and grid side occur through these converters and in addition these converters ensures control output voltage,frequency and phase for Rotor circuit.For fast switching modern power electronic converters uses IGBT's along with free wheeling diode for bidirectional power flow.In this simulation ideal two level VSC is considered.the converters linked with DFIG and utility grid is rotor side converter(RSC) and Grid side converter (RSC).RSC is responsible for controlling the generated torque and imaginary power exchange between the stator of DFIG and Grid by generating three phase voltages with variable frequency and magnitude.while GSC maintain fixed value of DC link Voltage.

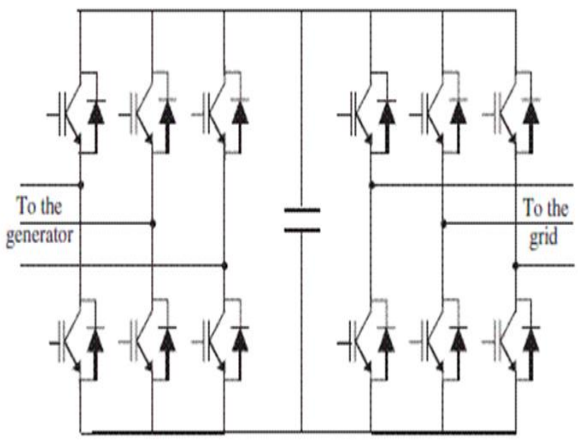

Figure 2. Bidirectional PWM converter

C. Hydro Turbine Model

In hydro generation the running water hit the turbine which in result convert the rotational mechanical energy into electrical energy.Turbines are categorized into different types based on their operational values of head and flow rate.the best turbine which will coupled with DFIG will be the Kaplan turbine which is a reaction turbine.from fig (3) it is clear that kaplan turbine have maximum operational area,it best work for low head and high flow rate and its efficiency remains constant for wide ranges[9].

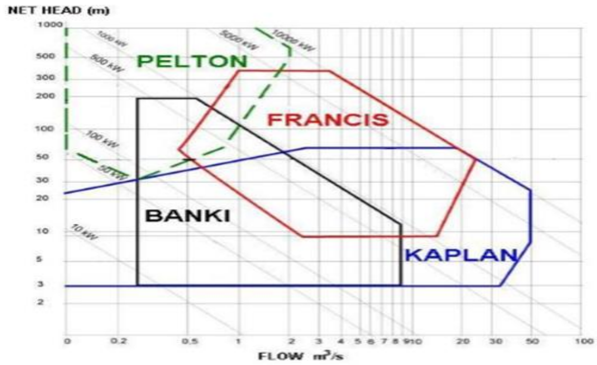

Figure 3. Conditions for hydro turbine selection

In kaplan turbine water flow is adjusted through wicket gates and propeller (runner gate).water is directly in contact with wicket gate which then fall on runner blades resulting in rotation of turbine.the wicket gate angle changes according to the desired flow of water as shown in fig (4).the pressure at the outside is decreased by installing a nozzle at the outlet which results in increase in pressure due to difference between inlet and outlet enabling the turbine to harvest more energy from water.Mathematically Power from a hydro Turbine can be derived as

$$P_{hydro} = \rho * Q * g * H \tag{1}$$

Where ρ is the density of water,Q is discharge of water,g is acceleration due to gravity and H is head.The efficiency can be calculated as

$$\eta = \frac{P_{turbine}}{P_{hydro}} \tag{2}$$

Efficiency of most of Kaplan turbine is 0.85 or more [10]. $P_{turbine}$ can be calculated as

$$P_{turbine} = T * \omega \tag{3}$$

Where T is the torque of the turbine and ω is the rotational speed of the turbine.modelling of Kaplan turbine which include penstock,wicket gate,hydraulics and mechanical modelling is done in [9].As in this paper our more focus is on control side so we consider a simple model of Kaplan turbine which is run by water flow.

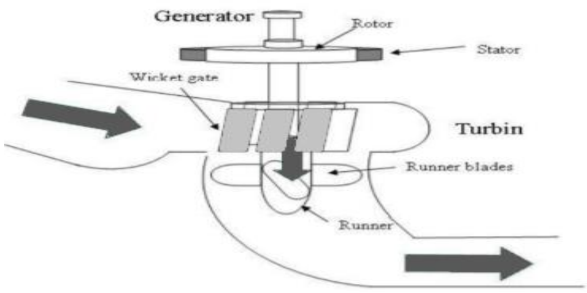

Figure 4. Working of Kaplan Turbine

IV. VECTOR CONTROL OF DFIG

DFIG control is more complicated and complex as compared to other induction generator.for variable speed operation of DFIG the control strategy needs to be more accurate and reliable.Researchers have developed many control strategies for DFIG control [11][12][13].the control strategy adopted in this research is Vector control method which is also known as field oriented control (FOC).Fast and dynamic response of generator is achieved through vector control.In vector control the three phase of generator is transformed into two synchrounously rotating reference frame d-q reference frame (parks and clarks transformation). The d-q circuits are decoupled like DC machine due to which machine response is linear faster and dynamic.By adjusting the voltage extend and phase angle of d-q axis the torque and machine flux is controlled independently.

A. Control of Rotor side Converter

The d-q axis current of rotor circuit is adjusted by rotor side converter (RSC) in which d axis is aligned with stator space vector.Based on this arrangement the d component of synchronously rotating d-q axis is in direct relation with stator reactive power and the q component of rotor current is responsible for controlling stator active power or torque. Rotor voltage is obtained from rotor current and stator flux as

$$\boldsymbol{v_{dr} = R_r i_{dr} + \sigma L_r \frac{d}{dt} i_{dr} - \omega_r \sigma L_r i_{qr} + \frac{L_m}{L_s} \frac{d}{dt} \psi_s} \tag{4}$$

$$\boldsymbol{v_{qr} = R_r i_{qr} + \sigma L_r \frac{d}{dt} i_{qr} - \omega_r \sigma L_r i_{dr} + \omega_r \frac{L_m}{L_s} \psi_s} \tag{5}$$

From the above equations d-q current control strategy for rotor currents is developed.The values of rotor current from DFIG is converted into stator reference frame which is then compared with the reference values of d-q currents as shown in Fig (5).the error from reference value and measured valued is the input to the PI regulator.The output from PI regulator and with cross coupling term gives the desire voltage values.the resulted voltage values are again transformed into three phase quantities before applying it to the converter or generator.

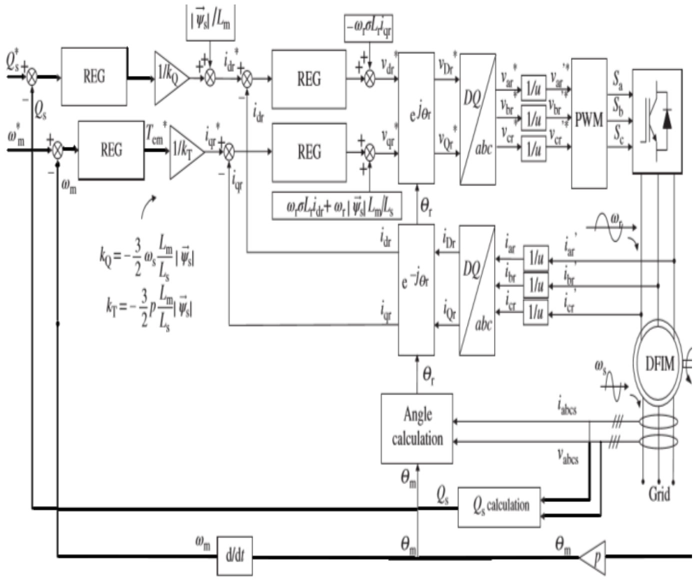

Figure 5. Rotor side converter control

For reference frame transformation, rotor angle θ_r must be estimated.a simple Phase lock loop (PLL) can be used for this purpose.In d-q reference frame the equation for toque is

$$\boldsymbol{T_{em} = -\frac{3}{2} p \frac{L_m}{L_s} \psi_s i_{qr}} \quad \rightrightarrows \quad \boldsymbol{T_{em} = K_T i_{qr}} \tag{6}$$

It is clear the $\boldsymbol{i_{qr}}$ component is responsible for speed and torque control.the equation for reactive power is expressed as

$$\boldsymbol{Q_s = -\frac{3}{2} \omega_s \frac{L_m}{L_s} \psi_s \left(i_{dr} - \frac{\psi_s}{L_m} \right) \rightrightarrows Q_s = K_Q \left(i_{dr} - \frac{\psi_s}{L_m} \right)} \tag{7}$$

It is conculded from the above equation that Reactive power of stator circuit is controlled by $\boldsymbol{i_{dr}}$ component.

B. Grid Side converter Control

Grid side converter is responsible for maintaining constant DC voltage across the bus and to ensure bidirectional power flow between RSC and GSC with controlled imaginary power.the derived equations for voltages from dynamic model of GSC is expressed below

$$\boldsymbol{v_{df} = i_{dg} R_f + \frac{di_{dg}}{dt} L_f - \omega_s L_f i_{qg} + v_{dg}} \tag{8}$$

$$\boldsymbol{v_{qf} = i_{qg} R_f + \frac{di_{qg}}{dt} L_f - \omega_s L_f i_{dg}} \tag{9}$$

Grid voltage oriented vector control (GVOVC) strategy is adopted in this work.the equations for real and reactive power of grid terminal is derived as

$$\boldsymbol{P_g = \frac{3}{2} v_{dg} i_{dg} = \frac{3}{2} v_g i_{dg}} \tag{10}$$

$$\boldsymbol{Q_g = -\frac{3}{2} v_{dg} i_{qg} = -\frac{3}{2} v_g i_{qg}} \tag{11}$$

The three phase current Ia,Ib,Ic is transformed into synchronously rotating d-q coordinate which is the input to the regulator as shown in block diagram Fig 6.then dq reference voltage $(v*_{df}, v*_{qf})$ is generated from dq current controller $(i*_{dg}, i*_{qg})$ .abc reference voltages are generated from dq reference voltages through transformation which is then used to generate reference pulses for Grid side converter.For current and voltage transformation the angle θ_g of grid voltage is estimated by using phase lock loop (PLL).

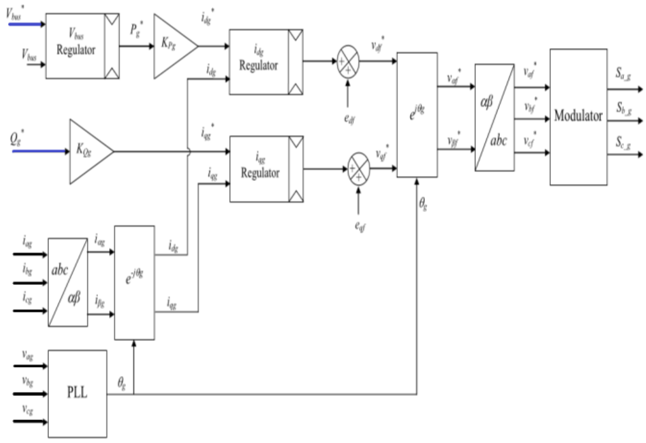

Figure 6. GVOVC of GSC

V. SIMULATION

A control model for DFIG driven by hydro turbine is developed in matlab Simulink,a control model for rotor side converter and grid side converter is developed separately and then coupled with generator and Grid.the variable speed operation of DFIG run by hydro source is analyzed by varying different site parameter like discharge,head with in acceptable limits.

A. Discharge of water

The main purpose of this work is to implement variable speed operation in micro hydro operations.for this purpose a simple turbine model is considered which is running on variable flow.the flow rate changes after every 2.5 sec.

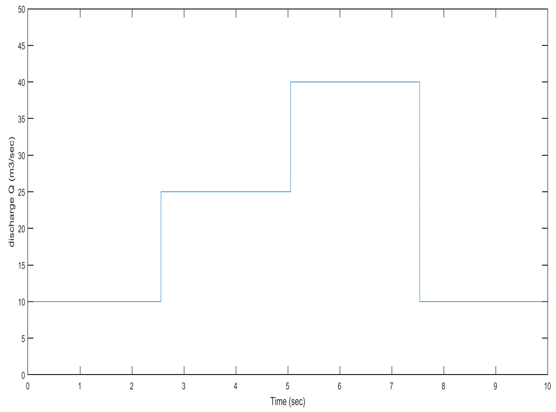

Figure 7. Discharge of water

B. Speed control of DFIG

We obtained a constant speed operation despite of the change in flow after every 2.5 sec as shown in simulation result Fig 8.the initial perturbation for 1.7 sec is due to the direct start up of the generator from the grid.the speed is maintained to a constant value of 189 m/sec with change in flow after 2.5 sec.

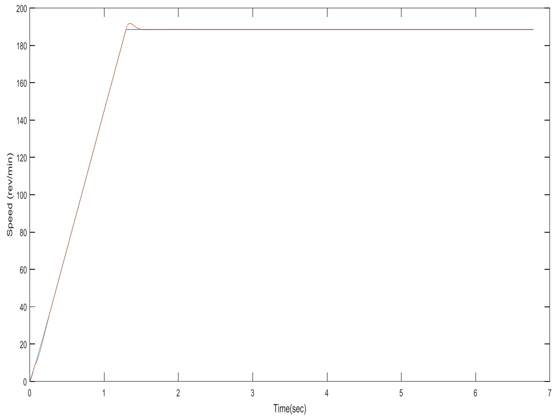

Figure 8. Speed control of DFIG

C. *Torque control of DFIG*

The torque of the machine changes according to the change in flow rate.In order to maintain constant speed operation and constant output voltage the torque increases with increase in flow rate as shown in simulation result

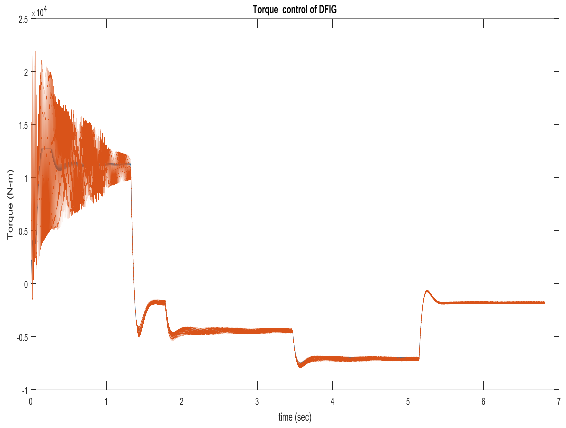

Figure 9. Torque of DFIG

D. *Three phase stator voltage*

The three phase stator voltage is maintained to a constant value of 320v despite of changes in flow rate.

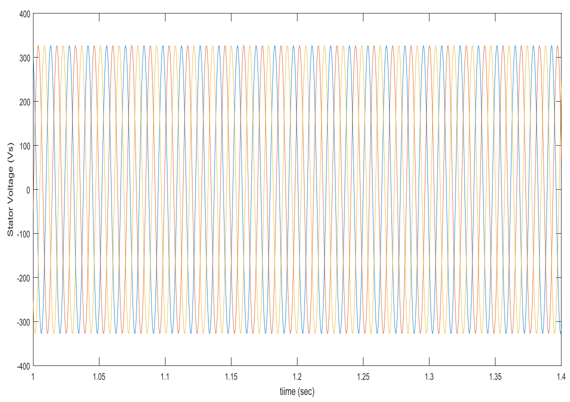

Figure 10. Three phase stator voltage

E. *DC Bus voltage*

Grid side converter is responsible for maintaining constant DC bus voltage between rotor side converter and grid side converter.it maintain a fixed voltage across the terminal by storing or releasing energy from the capacitor.1150v fixed dc value is maintained after initial perturbation in this work.

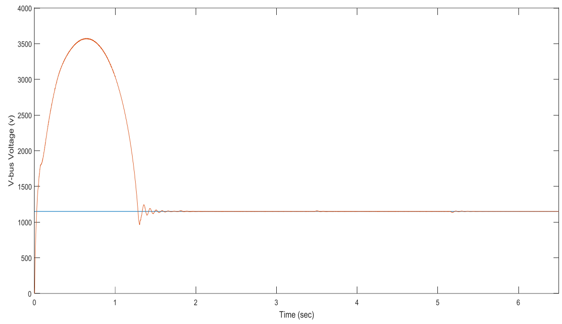

Figure 11. DC bus voltage

F. *Three phase rotor and Grid Current*

The values of grid and rotor currents are in direct proportion with the change in flow rate.both values increases with increase in flow and vice versa in order to maintain constant amplitude of voltage at the output.

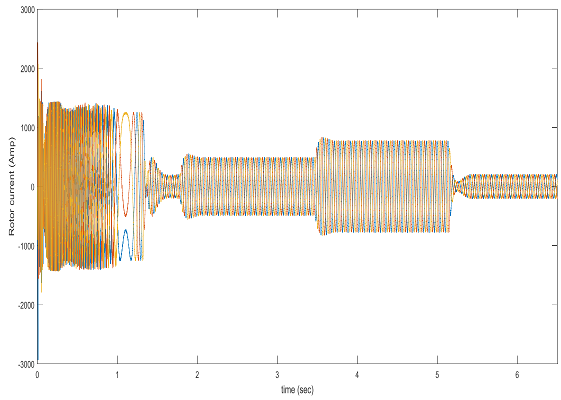

Figure 12. Three phase rotor current

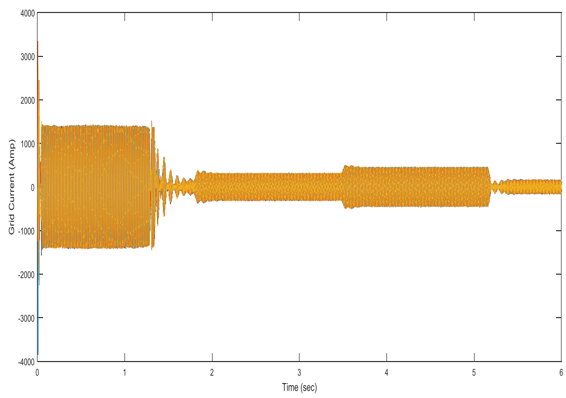

Figure 13. Three phase grid current

G. Reactive power Reference

reactive power exchange between grid and DFIG is zero by setting the reference value of reactive power exchange to zero.but it can be change according to grid code and demand.

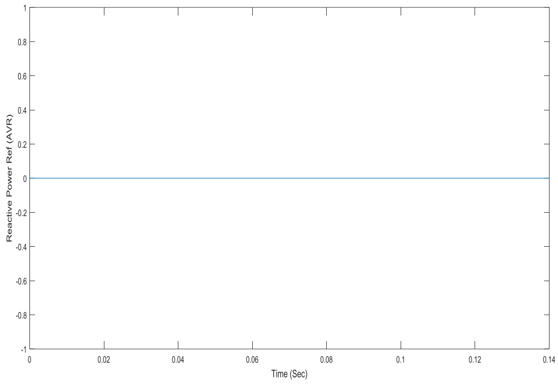

Figure 14. Change in reactive power Reference value

TABLE I. SYSTEM PARAMETERS OF DFIG

Frequency	50 Hz
Rated stator voltage	400v
Rated Power	2 MW
Rated rotational speed	1500 rpm
Pole pair	2
Stator and Rotor turns Ratio	1.0/3.0
Bus voltage (DC)	1150.0 V
Inertia	127 j
Switching frequency	4 kHz
Grid side filter resistance	20 micro ohm
Grid side inductive filter	400 micro ohm

CONCUSLION

In this work a control logic is developed for a variable speed operation for a limited speed range as an alternative solution for micro hydro operation.the variable speed operation can be used in both Grid connected mode or in isolated mode.A better quality of power is generated by DFIG with back to back power electronic converter connected to the machine and grid.the simulation results shows that proposed model is a valid solution for variable speed operation of micro hydro power generation.

REFERENCES

[1] R. Adib, R. Coordinator, and C. Webinar, "Renewables 2015 Global Status Report Distrbuted Renewable Energy for Energy Access," no. September, 2015.

[2] S. Breban, M. M. Radulescu, and B. Robyns, "Direct active and reactive power control of variable-speed doubly-fed induction generator on micro-hydro energy conversion system," 19th Int. Conf. Electr. Mach. ICEM 2010, pp. 0–5, 2010.

[3] C. Mi, M. Filippa, J. Shen, and N. Natarajan, "Modeling and control of a variable-speed constant-frequency synchronous generator with brushless exciter," IEEE Trans. Ind. Appl., vol. 40, no. 2, pp. 565–573, 2004.

[4] A. Ansel and B. Robyns, "Modelling and simulation of an autonomous variable speed micro hydropower station," Math. Comput. Simul., vol. 71, no. 4–6, pp. 320–332, 2006.

[5] S. Breban, M. Nasser, A. Ansel, C. Saudemont, B. Robyns, and M. Radulescu, "Variable Speed Small Hydro Power Plant Connected to AC Grid or Isolated Loads," *EPE J.*, vol. 17, no. 4, pp. 29–36, 2008.

[6] M. B. Camara, B. Dakyo, C. Nichita, and G. Barakat, "Simulation of a doubly-fed induction generator with hydro turbine for electrical energy production," *2009 8th Int. Symp. Adv. Electromechanical Motion Syst. Electr. Drives Jt. Symp. ELECTROMOTION 2009*, no. July, pp. 1–3, 2009.

[7] S. Mpn, P. Ts, A. Hermanto, and B. Ian, "Innovative Energy & Research Electric Speed Governor for 1kw Microhydro Generator," vol. 6, no. 2, pp. 6–9, 2017.

[8] C. P. Ion and C. Marinescu, "Autonomous micro hydro power plant with induction generator," *Renew. Energy*, vol. 36, no. 8, pp. 2259–2267, 2011. IEE Proc. - Electr. Power Appl., vol. 143, no. 5, p. 380, 1996.

[9] A. L. U. Quilisch, "Object Oriented Modelling and Simulation of Kaplan Turbines," no. February, 2008.

[10] Z. Husain, Basic Fluid Mechanics and . Hydraulic Machines.

[11] D. Zhi and L. Xu, "Direct power control of DFIG with constant switching frequency and improved transient performance," *IEEE Trans. Energy Convers.*, vol. 22, no. 1, pp. 110–118, 2007.

[12] A. D. Hansen, "Overall control strategy of variable speed doubly-fed induction generator wind turbine," *Grid Integr. Electr. Syst. Wind Turbines Wind Farms*, 2004.

[13] M. I. Martinez, G. Tapia, A. Susperregui, and H. Camblong, "Sliding-mode control for DFIG rotor- and grid-side converters under unbalanced and harmonically distorted grid voltage," *IEEE Trans. Energy Convers.*, vol. 27, no. 2, pp. 328–339, 2012.

Mohsin Hamid Received his B.E degree in Electrical Power engineering from Comsats institute of technology(Ciit) Abbottabad in Electrical power engineering in 2015.He did Ms in electrical energy system engineeing from US-PAKISTAN CENTER FOR ADVANCE STUDIES IN ENERGY UET Peshawar Pakistan.His research interest includes Control of micro hydro Power generation and integeration of renewable resources with grid.

IJEW 国际工程期刊 International Journal of Engineering Works انجینئرنگ کاموں کا بین الاقوامی جرنل

International Journal of Engineering Works
ISSN-p: 2521-2419
ISSN-e: 2409-2770
Vol. 6, Issue 11, PP. 399-405, November 2019
https://www.ijew.io/
https://doi.org/10.34259/ijew.19.611399405

Numerical Analysis of Flow through High Pressure Ratio Centrifugal Compressor Impeller and Effect of varying Diffuser Exit Width on Performance

Amjid Khan[1], Tariq Ullah[2]
[1,2] Centre for Advanced Studies in Energy, NUST, ISB, Pakistan
17teeamjid@uspcase.nust.edu.pk, 17teetariq@uspcase.nust.edu.pk
Received: 07 October, Revised: 15 October, Accepted: 20 October

***Abstract*—**This paper carries out a comprehensive numerical investigation of turbocharger high-pressure ratio centrifugal compressor impeller. The aim is to study the effect of varying mass flow rate on the pressure ratio and efficiency from stall to choke using (3D) numerical simulations. The transonic SRV2 compressor developed by DLR (German Aerospace Center) has been used as the test case in this study. Numerical simulations have been performed using Reynolds Averaged Navier-Stokes (RANS) based k-ε model to predict turbulence. Y-plus is kept 35 for the structured mesh near the boundaries. In first part, calculations were carried out for design speed of 50,000 1/min to study the suitability of ANSYS CFX in the design procedure and compared the results with experimental data and four other (3D) solvers. The numerical simulations showed that ANSYS CFX over predicts the experimental data by 9% in this compressor.

The second part describes the effect of vaneless diffuser exit width on performance parameters of centrifugal compressor at design high rotational speed, which shows that decreasing vaneless diffuser exit width increases pressure ratio, isentropic efficiency and operating range from stall to choke.

***Keywords*—** Centrifugal compressor, Diffuser Exit width, Numerical simulations, Entropy generation, Transonic, Pressure, Efficiency, Performance, Pressure ratio

I. INTRODUCTION

In this age of renewable energy, energy efficiency is the most important thing to make contribution toward power consumption and power generation. The aim of this research paper is to improve the performance of centrifugal compressor in order to reduce power consumption. The extremely huge use of high-pressure centrifugal compressors in automotive turbochargers and micro-gas turbines make it necessary to improve its performance by increasing operating range and reducing losses. For these applications, usually unshrouded impellers with splitter blades are used. To circumvent huge stresses with rise in weight unshrouded compressors are used [1].

In this case, vaneless diffuser compressor (SRV2-O) designed and fabricated by German Aerospace center (DLR) is used to achieve the goal of high operating range using numerical simulations. Using conventional techniques and laser velocimetry at DLR test rig, this compressor was investigated experimentally at design speed (50,000 1/min) and design mass flow rate (2.55 kg/s). The total pressure ratio at these design conditions is 5.65:1 and performance map is shown in Fig. 1 [2].

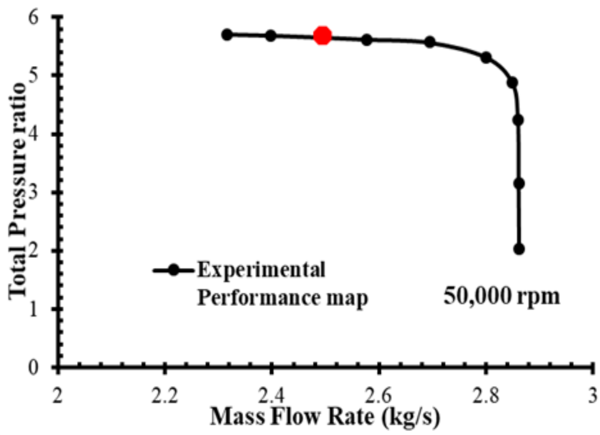

Figure 1: Experimental Performance Map

Over the last few decades, many 3D solvers have been developed and made commercially available. The computing power have been increased so many times, which made it possible to use it for industrial purposes for fluid dynamics analysis and reduce the experimental prices by designing the most optimized model using numerical simulations. Many 3D solvers like VISIUN, STAGE3D, TASCFlow and FLOWSIM have been used to predict the performance of centrifugal compressor and all of them have given quite reasonable results [3]. The first purpose of this paper is the applicability and suitability of commercial ANSYS-CFX mostly used nowadays to validate the experimental results and compare these results with other computational fluid dynamics commercial solvers mentioned above. It is worth mentioning that ANSYS-CFX and ANSYS-FLUENT gives almost similar results.

The second part of this paper is variation in the diffuser exit width and its effect on the performance of transonic centrifugal compressor. Diffuser exit width can be varied in two ways; first by reducing diffuser exit width from shroud side and second by decreasing diffuser exit width from hub side. From literature it has been clarified that decreasing exit width from hub side has too minor effect on the performance of centrifugal compressor, while reducing exit width from shroud side can increase pressure ratio, efficiency and operating range [4]. The aim of this research is working on variation of diffuser exit width from shroud side and studying its effect on pressure ratio, efficiency and operating range. This phenomena of variation in diffuser exit width is called pinching.

It has been studied that as diffuser-exit width has been reduced, it results increase in efficiency and pressure ratio at low rotational speed. At high rotational speed, the result was different as it given us high efficiency but lower pressure ratio [5]. The other advantange of reduced diffuser-exit width is that it reduce secondary flow losses caused by tip-leakage flow. At reduced diffuser exit width, shroud forces the flow towards centre, accelerate it and decrease losses in diffuser section, which results in high pressure ratio of the stage. When the diffuser-exit width is reduced it decreases stall phenomena chances as it provide greater margin to critical flow angle at impeller exit. It also make it possible to increase the pressure ratio by increasing the diffuser length [4].

The numerical simulated results showed valuable increase in the isentropic efficiency then the original standard compressor as diffuser exit width is reduced 20% and 25%, while in case of 10% and 15% reduction in diffuser exit width has lower isentropic efficiency then experimental test case compressor [6]. The wake fluid area has also been reduced on the blade suction-side as the diffuser exit is reduced. In case of vaned diffuser performance of centrifugal compressor has improved significantly as diffuser exit width is reduced to optimized level [7].

Numerical simulations have been performed by reducing the blade exit width by 5% and 10% and results pronounced great increment in isentropic efficiency and static pressure rise with reduced losses in diffuser [5].

A. Specifications of Simulated Case

A centrifugal compressor test case has been studied to understand effect of diffuser exit width, having high pressure ratio, mass flow coefficient and specific speed. The test case was designed and built by DLR (German Aerospace Center). As shown in the Fig. 2, impeller with 13 full and 13 splitter blades. Splitter blades leading edges is at 26% of full blade chord. The exit diameter of test case compressor is 112mm and nominal tip speed is 586m/s at 50000 1/min. A vaneless diffuser is connected after the impeller as depicted in Fig. 2 [3].
The compressor (SRV2-O) test case data is shown in table:

Table 1: Specifications of SRV2-O compressor [3]

Parameter	**Value**	**Unit**
Inlet ambient pressure, P_{t1}	101325	[Pa]
Inlet ambient temperature, T_{t1}	288.15	[K]
Design Shaft speed, n	50000	[1/min]
Design mass flow rate, m	2.55	[kg/s]
Number of full/splitter blades	13/13	-
Tip speed of Impeller	586	[m/s]
Pressure ratio of Impeller	6.1	-
Impeller efficiency	84%	-

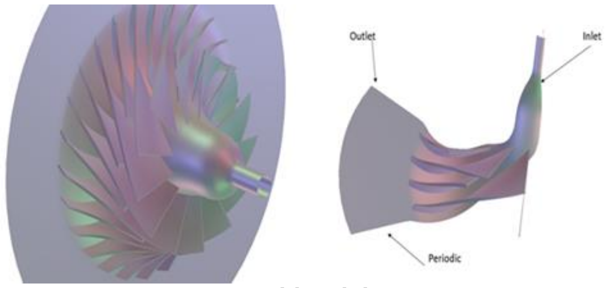

Figure 2: Model in BladeGen

II. NUMERICAL SETUP

A. Turbulence Model

The first step is to model 3D geometry for compressor. Based on available test case data, 2D blade shape has been modified to 3D model using Commercial modeler ANSYS BladeGen. Only single passage of impeller having single pair of blades (full and splitter) has been modeled to reduce computational time for simulation due to smaller number of mesh elements as illustrated in Fig. 4. For CFD simulations ANSYS CFX 15.0 is used to model flow field for test case (SRV2-O) compressor under steady state conditions. K-epsilon model used as turbulence model as it gives better results for planar shear layer and recirculating flows as is the case of centrifugal compressor. According to the K-epsilon turbulence model criteria, the value of Y-plus is set to 35.

B. Grid Generation (Turbogrid)

After modelling centrifugal compressor in BladeGen, an H-grid mesh topology was created in ANSYS TurboGrid module. TurboGrid is a meshing scheme for turbomachinery configurations, it selects automatic and refined mesh quality for most complex geometries creating structured mesh. For the better mesh quality, compressor computational domain is divided to H-grid topology with splitter blades arrangement. Design tip clearance for this case is variable tip clearance of 0.5,0.3mm and diffuser exit width of 7.06mm. Mesh is generated using H-grid with 25 number of elements at the inlet and outlet each. A grid independency test executed using 3 distinct grid sizes for complete compressor. The grid with total number of mesh elements 560788 and total number of nodes 504345, has been found adequate as alteration in pressure ratio and isentropic efficiency was negligible in this range of elements as depicted in Fig. 3.

C. Computational Solver

In order to study inlet, impeller and diffuser, boundary conditions were specified in CFD model and stage mixing approach is used. First order finite volume discretization is used for turbulence numerics and high resolution as advection scheme. The simulations of compressor were performed using commercial ANSYS CFX flow solver. The time scale factor 1 is used for calculations over 1000 iterations for steady state 3D centrifugal compressor analysis.

To analyse diffuser exit width effect, numerical simulations using Reynolds Averaged Navier-Stokes (RANS) based K-ε Model for turbulence modelling.

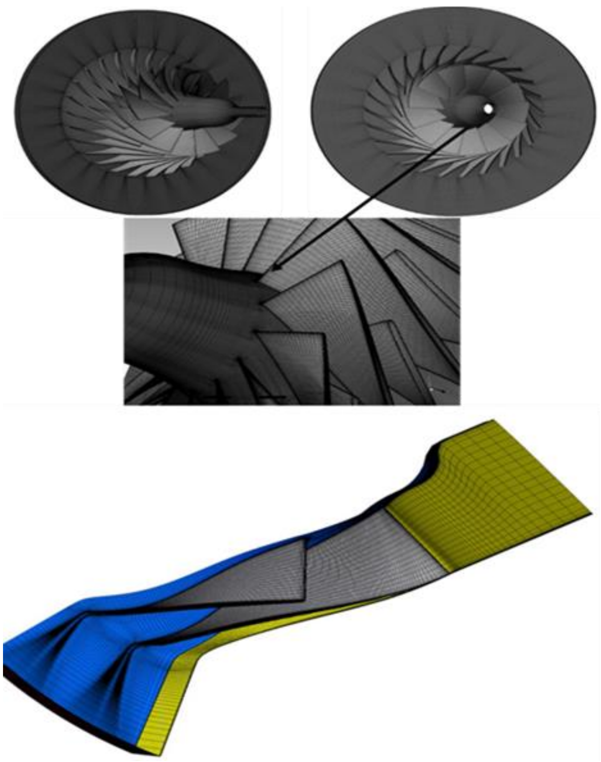

Figure 3: Computational Mesh (TurboGrid)

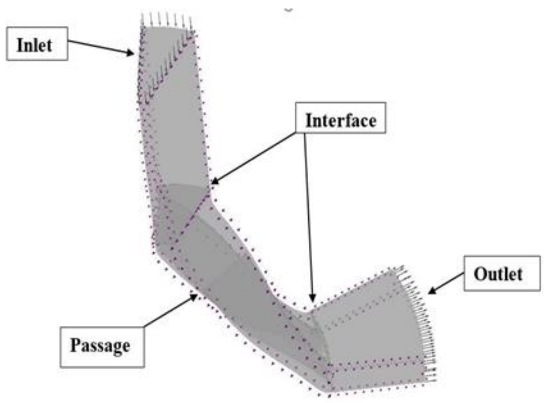

Figure 4: Computational Domain

D. Boundary conditions:

The compressor inlet conditions for all simulated cases; total inlet pressure of 101.325 kPa and total inlet temperature is 288.15 K respectively with 5% medium turbulence intensity, according to standard ambient conditions used by DLR (German Aerospace Center) for turbocharger configuration. The convergence criterion is set to 1x10-5 for all residuals while for monitoring convergence, mass flow rate and isentropic efficiency has been recorded for choke margin. As at choke point minor variation in mass flow rate cause substantial variation in performance, so to check choke limit, static pressure is defined at outlet while mass flow rate is monitored, and choke point is found by slightly reducing static pressure at outlet. The stage or mixing plane interfaces have been defined between diffuser, impeller and inlet. The rotational periodicity has been defined at boundaries of single passage assuming flow symmetry in all passages [2]. The total number of flow passages are 13 and each passage consist of 1 main and 1 splitter blade as shown in Fig. 4.

III. RESULTS AND DISCUSSIONS

A. Validation results:

For numerical simulations following agreements were made similar for all Computational fluid dynamics solvers and codes, which are given below:

- Compressor stage geometry is same for all (3D) solvers
- Turbulence model is K- ε model
- Design mass flow rate 2.55kg/s
- Design speed of 50,000 1/min

Numerical calculations for performance map of compressor stage are carried out on VISIUN and ANSYS-CFX at design conditions and the total pressure ratio data extracted from stall to choke is validated with experimental data, which shows suitability of these solvers compared to experimental data as shown in Fig. 5. The impeller total pressure ratio has been calculated for all solvers including ANSYS-CFX and compared it with experimental data calculated by DLR [3] as depicted in Fig. 6.

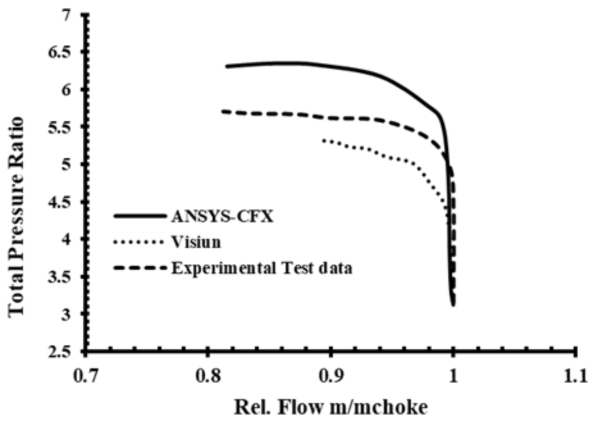

Figure 5: Compressor Stage Validation

The validation results of compressor stage show that ANSYS-CFX over predicts total pressure ratio by 9% while VISIUN shows lower pressure ratio value than experimental measured values. It depends on the compatibility of software which shows different results, but both the solvers showed almost similar results close to experimental test total pressure ratio.

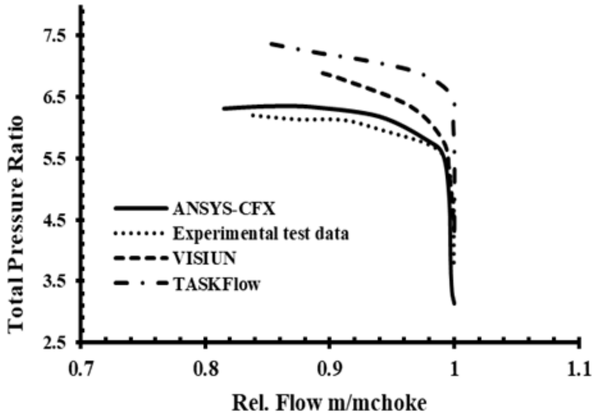

Figure 6:Validation of SRV2-O validation

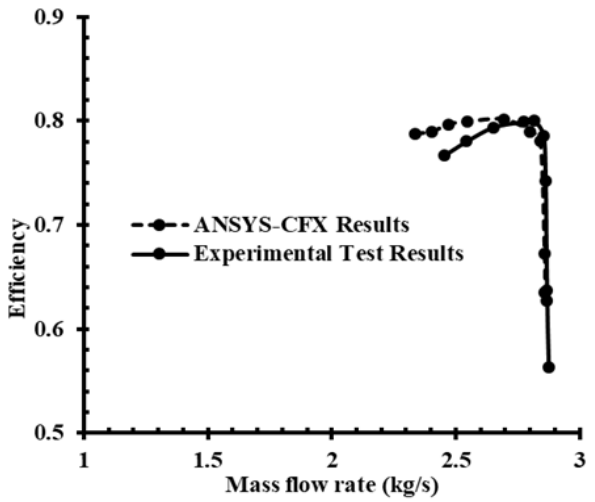

Figure 7: Efficiency Validation

Then the validation of impeller is executed using numerical simulations on ANSYS-CFX. The total pressure ratio and mass flow rate were extracted from results as depicted from Fig. 6. The prediction of total pressure ratio of ANSYS-CFX is appropriate compared to the design of DLR.

The data for efficiency has been extracted from ANSYS-CFX and compared it with experimental test results as illustrated in Fig. As the efficiency data from other solvers is not available, so the experimental data is only validated using ANSYS-CFX data. Which shows pretty similar results with test case data as shown in Fig. 7.

It is thus concluded from the current analysis that the computation results and simulations are capable of predicting the realistic results for the performance parameters i.e, pressure ratio and isentropic efficiency of centrifugal compressor, despite of the fact that at low mass flow rate it shows some deviation from experimental results. This deviation from experimental data can be allocated to the limitations of turbulence model and stage mixing frame approach applied at the interfaces.

Effect of Diffuser exit width on Performance

The performance of centrifugal compressor has been studied and evaluated by extracting data for total pressure ratio and total to total isentropic efficiency. The study of flow field has been carried out using ANSYS-CFX for numerical simulations. Performance and flow field analysis is given below:

B. Overall Performance:

The performance curves shown in Fig. 8 as centrifugal compressor has been analyzed for design conditions; mass flow rate of 2.55 kg/s, rotational speed of 50,000 1/min and design exit width of 7.06 mm. The numerical simulations predicted the total pressure ratio and isentropic efficiency very close to design experimental test statistics. Now, off design conditions are applied. By increasing diffuser exit width, isentropic efficiency reduces, which results in flow separation and flow obstruction (due to change in incidence angle to impeller inlet). The performance of centrifugal compressor has been analyzed as the diffuser exit width is raised to 8mm, 9mm and 10mm.
At each diffuser exit width performance map has been drawn and compared it with design performance map for both total pressure ratio and isentropic efficiency as shown in Fig. 8 and 9. It has been observed that total pressure ratio for all the cases is lower than design pressure ratio and efficiency is also reduced for each increment in diffuser exit width. The reduction in the performance parameters is because of secondary flow losses at impeller exit. Operating range is reduced in each case of incremented diffuser exit width as depicted in Fig. 8.

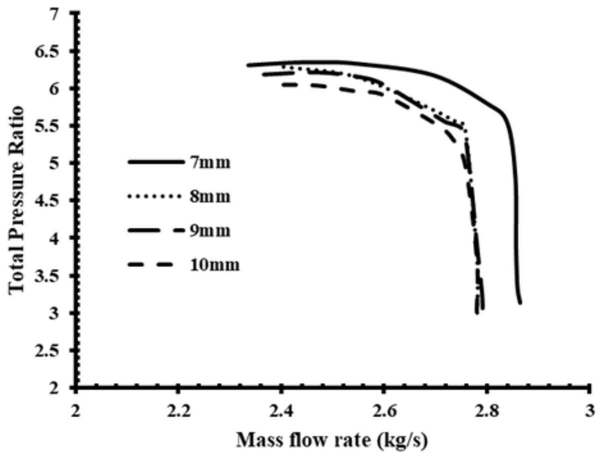

Figure 8:Performance Map for Total Pressure Ratio at Different Diffuser Exit Width

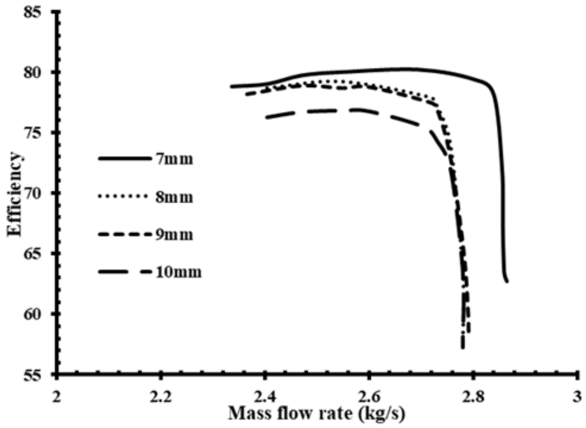

Figure 9: Performance Map for Efficiency at Different Diffuser Exit Width

A. Flow Field analysis:

To find out energy losses in flow circulation path, flow field analysis has been performed. The main reason behind flow losses are flow mixing, flow separation, flow-leakage and flow obstruction. Due to centrifugal and Coriolis forces, secondary flow vortex is formed by flow separation boundary layer and tip-leakage flow as mostly flow in centrifugal impeller is three dimensional. This secondary flow mixes with primary flow at impeller exit and diffuser inlet, which cause diffuser to stall phenomena and key contributor towards stall phenomena is flow separation near hub of diffuser. This flow separation results in entropy generation at impeller exit. secondary flow pass through the high entropy regions, which results in compressor losses as depicted in Fig. 10. The flow field analysis for the test case compressor has been performed near choke and stall conditions and both points showed energy losses due to high-negative or high-positive incidences respectively. Drop in static pressure occurs at impeller inlet at choke mass flow rate, as the relative Mach number is too high due to high-negative incidence at impeller inlet shown in Fig. 11. The performance map obtained from ANSYS-CFX were analyzed for stall, choke and design point mass flow rate for various diffuser exit widths as shown in Fig. 9.

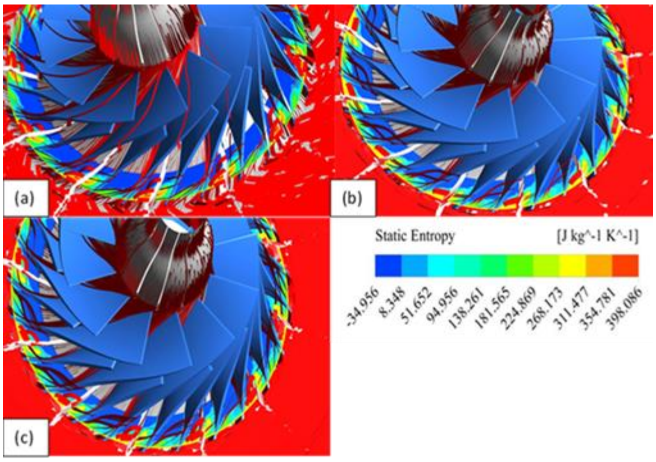

Figure 10: Secondary Flow Field at diffuser exit width (a)7mm (b)9mm (c)10mm

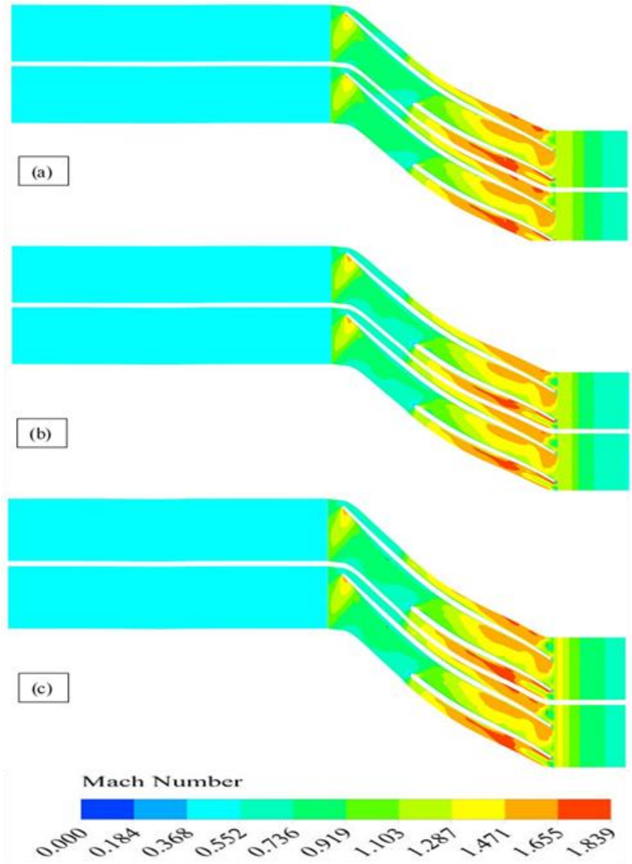

Figure 11: Mach Number for Different Diffuser Exit Widths (a)7.06mm (b)9mm (c)10mm

A. Relative Mach number:

As relative Mach number is too high near choke mass flow rate, so blade to blade analysis has been carried out near choke point for all values of diffuser exit width (7.06mm, 9mm and 10mm). As shown in Fig. 11 as the diffuser exit width increases, it increases Mach number at the suction-side of splitter and main blade. It can be observed from the Fig. 11 that wake area increases as the diffuser exit width increases and hence, variation in wake structure at impeller exit is detected.

B. Entropy Generation:

The main reason behind entropy generation is the secondary flow vortices and flow separation at the shroud of diffuser. The streamwise location of high entropy is impeller exit and diffuser inlet. Different contours have been drawn to analyze the effect of entropy for all values of diffuser exit width and results showed that entropy generation increases as the diffuser exit width increases as shown in Fig. 12 and 13.

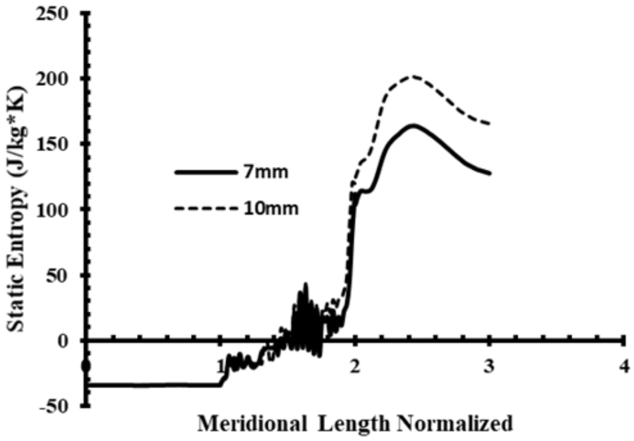

Figure 12: Static Entropy along Meridional Length for different diffuser Exit width

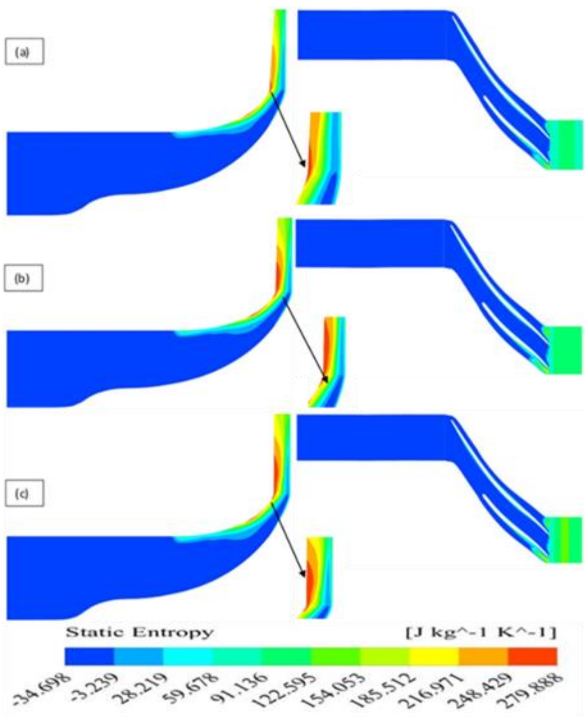

Figure 13: Static Entropy contours at meridional length of impeller at diffuser exit width of (a) 7mm (b) 9mm (c) 10mm

A. Static Pressure Variation along meridional length:

Static pressure rise has been investigated along meridional length normalized from inlet to outlet for test case compressor from stall to choke and then static pressure rise has been examined at design mass flow rate for 7 mm and 10 mm diffuser exit width. As it can be evaluated from the Fig. 14 that static pressure appears to decrease at choke point as the flow usually accelerate at that point due to negative flow incidence. Static pressure rise along meridional length from inlet to outlet for all diffuser exit widths investigated is shown in Fig. 15. It has been observed that at different diffuser exit widths, static pressure rise at choke point does not change along meridional length.

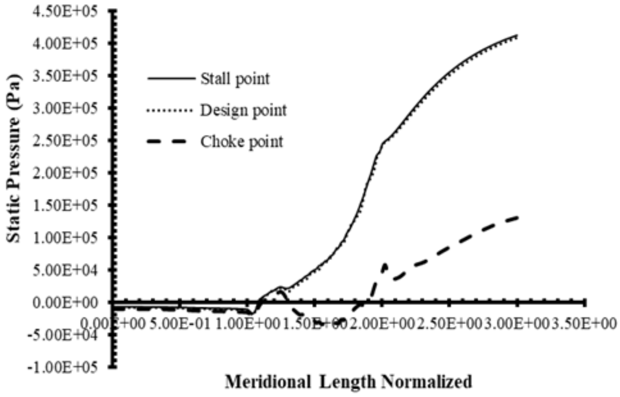

Figure 14: Static Pressure Rise for Stall, Design and Choke point

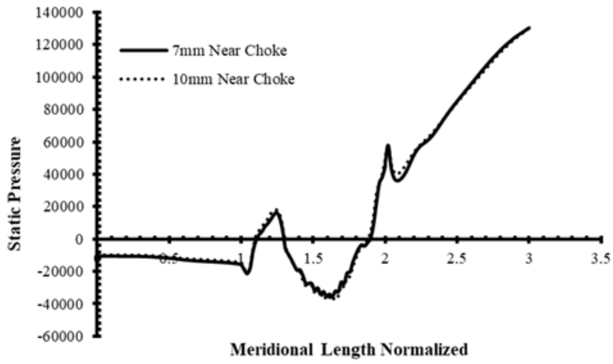

Figure 15: Static Pressure Rise for diffuser exit width of 7mm and 10mm at Choke point

CONCLUSIONS

Numerical simulations have been performed on the test case compressor (SRV2-O) and validated the experimental test results and then the effect of variation of diffuser exit width on the performance and flow pattern has been simulated. The following evaluations have been drawn from results:

- The test case compressor has been validated using ANSYS-CFX and evaluation showed quite similar results to design experimental data as it overpredicts the experimental data by only 9%
- As diffuser exit width has been increased, it decreases the performance parameters (Isentropic efficiency and pressure ratio)
- Entropy generation in a compressor showed that entropy increases as diffuser exit width increases, which results in drop in efficiency and pressure ratio
- Peak pressure ratio and peak efficiency at off design condition is lower than the experimental test case
- Static pressure at choke condition for all diffuser exit widths has no significant change

ACKNOWLEDGMENT

The authors wish to express their gratitude to U.S-Pakistan Center for Advance Studies in Energy (USPCAS-E), National University of Sciences and Technology (NUST) and the United States Agency for International Development (USAID).

REFERENCE

[1] S. N. Danish, Chaochen Ma, and Y. Ce, "The influence of tip clearance on centrifugal compressor stage of a turbocharger," Proc. 4th WSEAS Int. Conf. Fluid Mech. Aerodyn. Elounda, Greece, vol. 2006, pp. 6–11, 2006.

[2] G. Eisenlohr et al., "Gt-2002-30394 Investigations of the Flow Through a High," pp. 1–9, 2002.

[3] G. Eisenlohr, P. Dalbert, H. Krain, H. Pröll, F.-A. Richter, and K.-H. Rohne, "Analysis of the Transonic Flow at the Inlet of a High Pressure Ratio Centrifugal Impeller," p. V001T01A007, 2014.

[4] A. Jaatinen-Värri, P. Röyttä, T. Turunen-Saaresti, and A. Grönman, "Experimental study of centrifugal compressor vaneless diffuser width," J. Mech. Sci. Technol., vol. 27, no. 4, pp. 1011–1020, 2013.

[5] A. S. Rathore and K. B. Ravichandrakumar, "International Journal of Aerospace and Mechanical Engineering PARAMETRIC STUDY ON IMPELLER EXIT BLADE WIDTH VARIATION ON CENTRIFUGAL COMPRESSOR International Journal of Aerospace and Mechanical Engineering," vol. 4, no. 3, pp. 16–22, 2017.

[6] Q. H. Nagpurwala, "Numerical Investigation of the Effect of Exit Width Trim on the Performance of a Centrifugal Compressor Impeller Numerical Investigation of the Effect of Exit Width Trim on the Performance of a Centrifugal Compressor Impeller," no. January 2010, 2018.

[7] T. C. Siva Reddy, G. V. Ramana Murty, M. V. S. S. S. M. Prasad, and D. N. Reddy, "Experimental studies on the effect of impeller width on centrifugal compressor stage performance with low solidity vaned diffusers," Proc. Inst. Mech. Eng. Part A J. Power Energy, vol. 221, no. 4, pp. 519–533, 2007.

IJEW 国际工程期刊 International Journal of Engineering Works انجینئرنگ کاموں کا بین الاقوامی جرنل

International Journal of Engineering Works
ISSN-p: 2521-2419
ISSN-e: 2409-2770
Vol. 6, Issue 11, PP. 406-413, November 2019
https://www.ijew.io/
https://doi.org/10.34259/ijew.19.611406413

Material Selection for Micro Channel Heat Exchangers for Industrial Waste Heat Recovery

Wiqas Alam
Mechanical Department, NWFP, University of Engineering and Technology, Peshawar
wiqassuit17@gmail.com

Received: 07 October, Revised: 18 October, Accepted: 22 October

***Abstract*—** The aim of this paper is to provide the software-based materials selection approach for the micro channel heat exchanger for high-temperature industrial waste heat recovery. Industrial heat processing and heat recovery places increasing demand for material performance in extreme conditions. These extreme conditions accelerate the material's degradation in turn leading to performance and efficiency reduction. Therefore the development of new compatible materials demand material qualification for the miniaturized technology to function over a long period of time with full efficiency. This paper proposes methodology for the material identification and selecting appropriate material for the micro channel heat exchanger to recover high-temperature (>500 ℃) industrial waste heat. Thermally stable materials such as aluminum nitride, silicon carbide, alumina, tungsten carbide, tungsten alloys, and nickel and TZM alloys were observed to perform exceptionally well in extreme condition. Thus silicon carbide, aluminum nitride and molybdenum TZM alloys were selected as the most promising materials for micro channel heat exchanger recover high-temperature (500-750 ℃) waste heat from different industries.

***Keywords*—** Cambridge Engineering Selector, Micro channel heat exchanger, Materials selection

Abbreviations and Nomenclatures

MCHE	Micro Channel Heat Exchanger
CES	Cambridge Engineering Selector
WHR	Waste Heat Recovery
TZM	Molybdenum Titanium Zirconium
Nu	Nusselt number
h_c	Convection heat coefficient
D_h	Hydraulic diameter (mm)
q	Heat transfer rate
ΔT	Temperature difference
α	Coefficient of expansion
k	Thermal conductivity
Sy	Yield Strength

I. INTRODUCTION

Micro channel heat exchanger is an advanced field full of challenges. The compact design, higher heat transfer capabilities, lower weight, and cost expand MCHE applications in heating, ventilation, and air conditioning, petroleum, and chemical processing engineering, automotive, electronic equipment and waste heat recovery from various heat processing industries. Micro channel heat exchanger recovers waste heat from various industries including furnace heat and exhaust from steam boiler, gas turbine, and heat treatment furnaces. The exhaust temperature varies from a lower heat source such as gas-fired boiler exhaust to high nickel refining furnace. The MCHE material’s exposure to high temperature (>500℃) exhaust/ waste heat imposes a challenge of thermal degradation. The degradation might be caused by corrosion and erosion due to metal oxides and impure particle reacts with material in a high-temperature harsh environment. Based on functional and design requirements, possible candidates will be evaluated for overall performance and cost of MCHE applications. Given the growing number of materials available today, finding suitable material is a time-consuming process. The selection of low cost and high-performance materials for MCHE is vital to achieving optimum waste heat recovery. The essential criteria for suitable materials involve higher heat transfer, lower thermal expansion, and thermal stability at harsh environments. The high heat transfer coefficient and greater cross-sectional area to volume ratio are the key advantages of MCHE over conventional heat exchanger. The heat transfer flowing through working fluid inside the micro channel diameter (< 1mm) can be described by the MCHE basic equation as follows.

$$hc = Nu\ k/Dh \tag{1}$$

Tuckerman and Pease et al. 1981 [1] Presented the idea of heat exchange in micro channel by receiving the bloodstream flow concept in human supply routes. The increase in convection heat transfer results from the decrease in channel dimension shown in equation 1. The limited space heat dissipation problems were given a boost in the electronics industry by the introduction of micro channel’s concept. This revolutionary concept explored different perspective for researchers. Dixit and Ghosh et al. 2015 [2] Reviewed the micro channel's fabrication hurdle with conventional technology led to the development of non-conventional techniques. Micro channels currently used for high heat processing industry instead of removal of dissipated heat. The main hurdle for commercialization of micro channels is the higher fabrication cost and non-conventional methods. The laminar flow conventional theory validation about constant Nusselt number was proved by Tuckerman and Pease et al. 1981 [1]. The silicon-based micro channel was tested with distilled water as a working fluid and showed high heat dissipation about 790 W/cm2. The hydraulic diameter reduction significantly improves the convection heat transfer for a specific fluid. The design parameters play key role in heat transfer optimization apart from dimensional parameters. Knight, Hall et al. 1992 [3], Lee, Kim et al. 2005 [4], and Riera, Barrau et al. 2015 [5] studied the importance of design constraint in micro channel's performance optimization. Harms, Kazmierczak et al. 1999 [6] Proposed the macro scale law for micro channels and suggested the single and multiple channels can be related by classical correlation but failed in the experimental investigation due to Nusselt number deviation for the lower value of Reynolds number.

Mohammed, Bhaskaran et al. 2011 [7] Studied correlation of Reynolds number in micro channels with Nusselt number for accuracy and the proposed threshold value (1.2 mm) of hydraulic diameter. Segre and Silberberg et al. 1962 [8] studied and determined the constant value of Poiseuille number for laminar flow within stainless steel and fused silica micro channels with water, methanol, and isopropanol as a working fluid. Khan and Fartaj et al. 2011 [9] published their detail on micro channel heat exchanger and was potentially introduced by Peng and Peterson et al. 1996 [10]. The author proposed the Joule Thomson effect applications inside the channels. Review work on cross-flow micro channel heat exchanger's fabrication and fluid dynamics were done by many researchers such as Wu and Cheng et al. 2003 [11], Harms, Kazmierczak et al. 1999 [6] and Jiang, Fan et al. 2001 [12].

A. Applications

Westphalen and Koszalinski et al. 1999 [13] and Kandlikar et al. 2005 [14] illustrated the micro channel heat exchanger's application in HVAC systems as energy saver defined by less refrigerant consumption and deliver higher overall efficiency. Apart from the higher fabrication's cost, MCHE gained importance in various refrigeration applications. The MCHE applications in air conditioning field, heat pump, and vapor compression refrigeration's system proposed and investigated by Pettersen, Hafner et al. 1998 [15], Han, Liu et al. 2012 [16] and Leland and Ponnappan et al. 2001 [17]. The smaller size and lower weight along with micro channel heat exchanger's improvement in heat transfer performance have made compulsory choice in space applications studied by Harris, Despa et al. 2000 [18], gas turbines Min, Jeong et al. 2009 [19] and waste heat recovery Sommers, Wang et al. 2010 [20], Meng, Wang et al. 2016 [21]. The other applications involve gas liquefaction plant Baek, Kim et al. 2010 [22] and heat processing industries Thonon and Breuil 2001 [23]. Micro channel heat exchangers became an integral part of electronic circuits and devices cooling Kandlikar, Garimella et al. 2005 [24], Walpole and Missaggia 1992 [25]. MCHE have been employed to fuel and solar cell systems Reuse, Renken et al. 2004 [26], Li, Flamant et al. 2011 [27] and for biomedical applications by Silvestri and Schena et al. 2012 [28].

B. Material

Materials play an important role in mechanical design. Numerous research has been done on design, fabrication, applications and heat transfer characterization through the micro channels. The aforementioned literature on different materials for MCHE has been summarized in the material section. Although, Silicon and Copper are the two common materials for MCHE. Subsequently, the researcher investigated the fluid flow through single-phase and two-phase micro channels. This paper explores the methodology of identifying materials for micro channel heat exchangers. The mathematical model developed validate the experimentally measured value of temperature distribution and pressure drops within the aluminum-based micro channel heat exchanger. The experimental procedure was arranged for copper-based MCHE by Dixit and Ghosh et al. 2015 [2]. The manufacturing of copper MCHE and investigations conducted on varying heat flux value by Qu and Mudawar et al. 2002 [29] concluded the temperature profile correlation for non-uniform heat flux. Liu, Xiao et al. 2016 [30] Concluded that decrease in saturation temperature and rise in vapor eminence and bulk flux significantly increase the heat transfer coefficient and pressure drop inside the square shape copper mini channels. Del Col, Bortolin et al. 2011 [31] Did a similar study on square shape micro channels but observed no significant improvement in heat transfer coefficient regardless of similar test conditions. Brandner, Anurjew et al. 2006 [32] Analyzed the various parameters to enhance the heat transfer coefficient of copper made micro channel heat exchangers. The author concluded the shortest distance between the heat source and sink, the decrease in dimensional characterization (<100 µm) and changing the laminar flow regime to three-dimensional array increase the heat transfer coefficient. David, Miler et al. 2011 [33] Designed and conducted an experimental investigation on copper made parallel flow two-vapor phase MCHE. The two-phase vapor included a non-venting heat exchanger and vapor-separation version reduced the pressure drop for lower substrate temperature.

Bronze made MCHE were investigated by Kan, Ipek et al. 2015 [34] for varying heat flux and channel angles in order to enhance the heat transfer coefficient. The study concluded the channel angle 30o and with two-phase fluid input temperature, 60 ℃ for hot and 15 ℃ for cold give maximum heat transfer. Lee, Kim et al. 2005 [35], Shen, Xu et al. 2006 [36] and Park, Peng and Punch et al. 1995, 1996 [37. 38] studied silicon MCHE experimentally for pressure drop and convection mode of heat transfer and observed the laminar Nusselt number direct relation with lesser Reynolds number. The geometric parameter and surface structure altered for higher Reynolds numbers. Plexiglass and glasses micro channel heat exchangers were investigated by Pramod Chamarthy et al. 2010 [39] and developed a laser-induced method for temperature measurements. T-junction between hot and cold fluid mixing demonstrated based on both temperature-dependent and independent dies made of Rhodamine (RhB, 10). Peiyi Wu, Little et al. 1984 [40] measured gas flow through silicon and glass micro channel heat sink for refrigeration purpose and concluded the effective heat transfer due to the asymmetrical roughness and variation in wall temperature.

C. 1.3 CES Based Material Selection

Sameer et al. 2012 [41] used CES software approach for selecting the phase changing materials for high temperature applications. The optimization of thermal energy storage with multi-objective to identify phase changing materials for thermal energy storage. The phase changing materials considered for high-temperature (400-750℃) steam investigation were metal and their eutectics such as 60Al-34Mg-6Zn and 88Al-22Si. Thermal conductivity, environmental performance, and heat of fusion were the few attributes upon which selection of phase changing material was made. 88Al-22Si was selected as a most promising material for latent heat energy storages compared to the traditional molten salt. Camila et al. 2015 [42] generated phase changing material database for the selection of PCM at phase temperature ranges from -50℃ to 150℃ using CES selector. The investigation led to the classification of PCM including commercial and non- commercial list.

Shanian et al. 2004 [43] utilized the CES software approached to select material on the basis of multiple decision making attributes. The cost of production along with other attributes for engineering applications were considered for the ranking of the materials from the best to worst one. The case study done on non-heat treatable cylinder materials for covering worked under static load and carried efficiency closer to the room temperature. Materials were ranked based on both cost inclusion and exclusion.

II. Material Selection Methodology

Granta Design Selector (CES) package by MA. Ashby et al. 2009 [44] is used for the selection of suitable materials for MCHE. The CES selector considers various inputs for design methodology such as thermal, mechanical and chemical stability, costing and optimization of the most suitable outcome. The MCHE material can be exposed to the passive atmosphere for a prolonged period without substantial problems, such as thermal degradation due to corrosion and erosion, phase and chemical changes, loss of strength and other assets for which material propose to custom. The highest temperature in the inert atmosphere to which material is exposed is referred to service temperature. The necessary attributes of materials for high-temperature waste heat recovery MCHE applications are given in Table 1.

Table 1. Desirable Properties for MCHE Materials

Attributes	Desirable characteristics
Thermal properties	Extensive thermal stability (T> 500 ℃), High heat capacities, high thermal conductivity
Organic properties	Long term chemical stability, high corrosion resistance, non-toxic and no chemical decompositions.
Mechanical properties	Low thermal expansion coefficient, high fracture toughness and mechanical stability
Economic and Environmental propertied	Cheaper and low cost of fabrication, lower energy requirement and CO_2 footprint

For heat processing Industries, within the operating temperature, the thermal properties of the designated materials are important comprises thermal conductivity, thermal stability, heat capacities, thermal expansion, and corrosion resistance. CES classified the material's universe into six basics categories as polymers, ceramics, elastomers, glasses, metals and composites/hybrids. Thermal and chemical stability along with high service temperature was considered as the primary requirement. Based on the specification and desirable properties (Table 1), primary selection identified ceramics and metals as promising materials for micro channel heat exchangers. The CES generated material's properties chart in Figure 1 shows a variation of service temperature with melting points of ceramics and metals/alloys families. Only common materials are named for the clear presentation in Fig. 1. For MCHE applications in industrial waste heat recovery considered here, the materials should have higher service temperature (> 500 ℃) and not undergo any thermal failure that might involve phase and chemical changes, corrosion, etc. Materials like concrete, aluminum, magnesium, and titanium alloys can decompose or spall below 450 ℃ and hence cannot be used for MCHE waste heat recovery applications. Alumina, silicon and tungsten carbide, tungsten alloys, and aluminum nitrides are, however, proper candidates for high-hotness above 500 ℃ MCHE uses shown in Figure 1. Material like Molybdenum, titanium, zirconium (TZM) alloy is also a candidate for high-temperature applications.

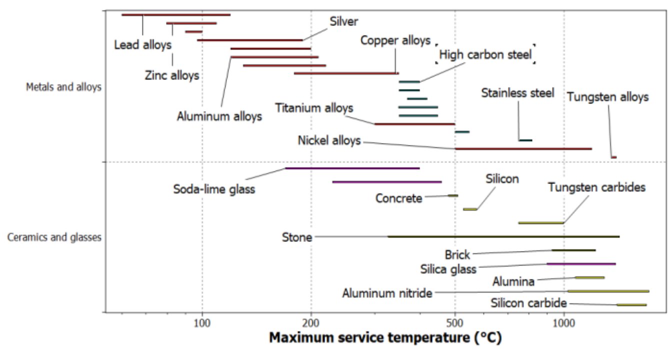

Figure 1. Illustrates the variation of ceramics and metal alloys plotted on ordinate against the maximum service temperature (℃) on abscissa.

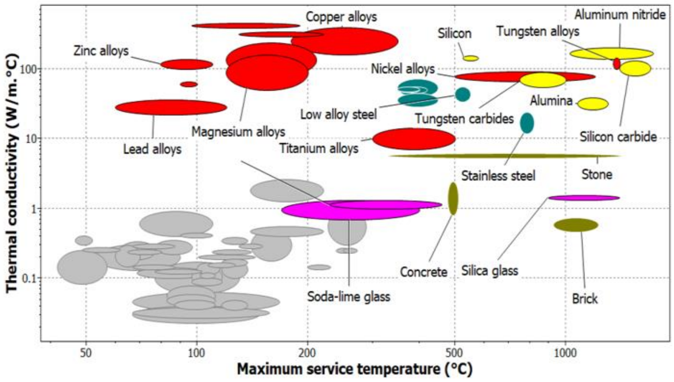

Figure 2. Illustrates the effect of maximum service temperature (℃) plotted on ordinate against the different material's thermal conductivity (W/m. ℃) on abscissa.

The material's ability to conduct heat per unit time per unit area through solid material per degree rise in temperature is plotted on the horizontal axis against the maximum service temperature in Fig. 2. Ceramics such as silicon carbide, aluminum nitride, tungsten carbide and alumina on the top right shows higher thermal conductivity above 500 ℃. Nickel alloys and stainless steel shows greater compatibility compared to other metals and alloys.

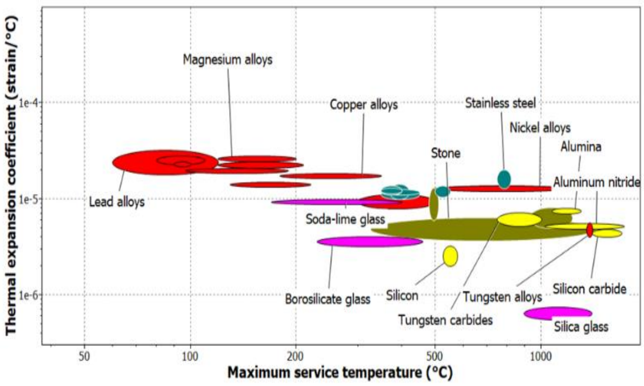

Figure 3. The effect of maximum service temperature (℃) plotted on the ordinate against the thermal expansion coefficient (starin/℃) of different available materials on abscissa.

The material's expansion per degree rise in temperature plotted on the horizontal axis against the maximum service temperature on the vertical axis illustrated in Fig. 3. The ceramic materials like silicon and tungsten carbide, alumina, aluminum nitride and metal's alloy such as nickel and tungsten alloys shown on the top left in Fig.3.are the compatible candidates for above 500 ℃ temperature applications with lower thermal expansion coefficient.

Figure 4 compares the fracture toughness (resistance to crack propagation) of materials on vertical axis against maximum service temperature on horizontal axis. The higher fracture toughness of ceramics and metals alloys such as alumina, aluminum nitride, silicon carbide, tungsten carbide, tungsten and nickel alloy shown on the right side of the chart describes the compatibility of these materials. The inverse plot of fracture toughness represents that materials at the lower right bottom had the highest fracture toughness. Other materials (upper left-hand side of Figure 4) might be prone to failure due to repeated thermal cycle.

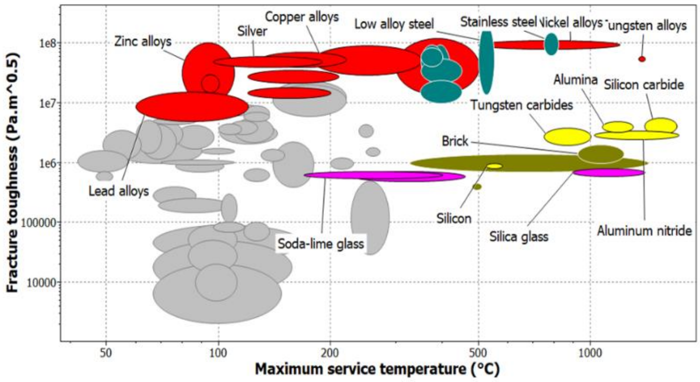

Figure 4. The effect of maximum service temperature (℃) on fracture toughness of various materials.

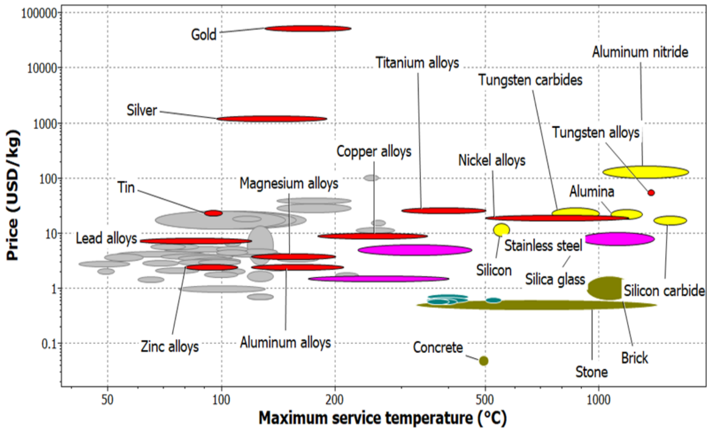

Figure 5. Illustrates the maximum service temperature (℃) materials such as ceramics and metals plotted on ordinate against the Price (USD/kg) on abscissa.

The maximum service temperature plotted against the cost of the materials shown in Fig.5. The CES graph shows the bulk materials price per unit mass. The silicon carbide and alumina are the cheapest ceramics compared to tungsten carbide and aluminum nitride, however, metal alloys such as tungsten alloy are much costlier than nickel and copper alloys. The overall analysis is done so far concluded that the ceramics such as aluminum nitride, silicon carbide, alumina and tungsten carbide and metal alloys such as tungsten, nickel and molybdenum zirconium and titanium alloy are the acceptable combination of materials for micro channel heat exchanger high-temperature waste heat recovery applications.

III. Performance Matrices

The performance equation contains material properties known as material indices. The material indices is a mathematical expression which relates performance with various material's properties. Micro channel heat exchanger served maximizing heat transmission to the working fluid (maximize heat flux) by reducing the hydraulic diameter of the channels given as follows.

$$hc = Nu\ K / Dh \quad (1)$$

According to the Fourier's law, heat transfer (Conduction) can be expressed as

$$q. = -k\ A\ \Delta T/\Delta t \quad (2)$$

The stresses due to internal pressure drop inside the channel can be expressed as follows.

$$\sigma = pi.r/\ t \quad (3)$$

The material indices for MCHE derived from above equations can be written as follows

$M1 = k\ \sigma$,

The thermal deformation that results from thermal stresses due to the exposure to high-temperature must be resisted by the materials. The thermal deformation occurs due to the temperature difference can be expressed as:

$$\partial = \alpha l \Delta T \quad (4)$$

$$\varepsilon = \alpha \Delta T \quad (5)$$

According to Hooks law of deformation

$$\varepsilon = \sigma/E \quad (6)$$

Comparing equation (5) and equation (6)

$$\sigma/E = \alpha \Delta T$$

$$\Delta T = \sigma/\alpha E \quad (7)$$

The material index is $M2 = \sigma/\ \alpha\ E$

The performance matrices given in Table 2 were calculated based on various scales set for material's properties. Each property was assigned a particular value based on the application's requirements. The materials shown in table 2 were shortlisted after screening and ranking from materials universe. The combination of various properties such as high heat transfer, lower thermal expansion, thermal and chemical stability in an inert atmosphere, thermal conductivity and fabrication cost finalized the top three materials for MCHE shown in Table 3.

Table 2. Summary of material's performance for high-temperature MCHE applications

Material	High temperature performance T(K) and corrosion resistance	Thermal Conductivity K (W/m K)	Specific Heat C_p (J/Kg K)	Thermal Expansion α (µ.m/m. K)	Elastic Limit E (MPa)	Price (USD/kg)	Hardness H (MPa)	Density ρ (Mg/m³)	Total Performance ∑R	Performance ratio ∑R/∑r
Silicon Carbide	Resist at <1300 ℃ (S)	10*9=90	7*10=70	3*5=15	8*7=56	5*7=35	4*7=28	2*7=14	308	7.89
Aluminum Nitride	Satisfied	10*10=100	7*10=70	3*9=27	8*5=40	5*7=35	4*2=8	2*9=18	298	7.64

Tungsten Carbide	Satisfied	10*5=50	7*5=35	3*10=30	8*7=56	5*5=25	4*2=8	2*2=4	208	5.33
Tungsten	Satisfied	10*10=100	7*2=14	3*7=21	8*5=40	5*5=25	4*5=20	2*2=4	224	5.74
Tungsten ASTM class 1 W 90%	Satisfied	10*7=70	7*2=14	3*7=21	8*9=72	5*5=25	4*10=40	2*9=18	260	6.76
Tungsten ASTM class 4 W97%	Satisfied	10*9=90	7*2=14	3*7=21	8*9=72	5*2=10	4*10=40	2*9=18	265	6.80
Elkonite 10 Cu Tungsten alloy	Satisfied	10*5=50	7*2=14	3*9=27	8*9=72	5*7=35	4*9=36	2*9=18	252	6.46
Alumina	Satisfied	10*2=20	7*10=70	3*10=30	8*7=56	5*9=45	4*2=8	2*9=18	247	6.33
Nickel Alloy	Satisfied	10*2=20	7*7=77	3*10=30	8*7=56	5*7=35	4*9=36	2*5=10	264	6.85
TZM alloy	Satisfied	10*9=90	7*5=35	3*9=27	8*9=72	5*7=35	4*9=36	2*9=18	313	7.02

Table 3. Materials properties of performance based selected materials.

S. No.	Material	Thermal conductivity (W/m.℃)	Heat Capacity (J/kg. ℃)	Thermal expansion coefficient (10^{-6} /K)	Density (kg/m^3)
2	Silicon Carbide	80-130	663-800	4-4.8	3210
2	TZM (Mo 99.40%, Ti 0.5%, Zr 0.08%, and C 0.02%)	200	305	4.5	10241
3	Aluminum Nitride	140-200	780-820	4.9-5.5	3260

CONCLUSION

The micro channel heat exchanger’s compactness, reduction in weight and size along with heat transfer enhancement has showcased their promising and preferable choice in waste heat recovery and other applications. However, higher manufacturing cost and material’s degradation in the harsh environment has limited MCHE commercialized applications. CES software package identified some common materials for high-temperature MCHE applications. Thermal properties considered, included maximum service temperature, long term chemical stability, thermal conductivity, corrosion resistance, heat capacity, thermal expansion coefficient and cost of the materials. Suitable materials included metal alloys such as tungsten and nickel alloy, TZM alloy and ceramics such as alumina, aluminum nitride, silicon carbide, and tungsten carbide. Metal alloys such as aluminum are used commercially in low-temperature micro channel heat exchanger’s applications but are unsuitable for high-temperature above 500 ℃ applications. The economical assessment was made on the basis of the market price in (USD/kg). Silicon carbide and alumina were found to be the cheaper materials than tungsten carbide and aluminum nitride. The high-temperature ceramics such as silicon carbide, aluminum nitride and molybdenum alloy (TZM) were identified as promising materials for MCHE waste heat recovery. Their thermal and chemical stability for the extended period made them the best suited materials for high-temperature applications.

REFERENCES

[1] Tuckerman, D. B. and R. F. W. Pease (1981). "High-performance heat sinking for VLSI." IEEE Electron device letters 2(5): 126-129.

[2] Dixit, T. and I. Ghosh (2015). "Review of micro-and mini-channel heat sinks and heat exchangers for single phase fluids." Renewable and Sustainable Energy Reviews 41: 1298-1311.

[3] Knight, R. W., et al. (1992). "Heat sink optimization with application to microchannels." IEEE Transactions on Components, Hybrids, and Manufacturing Technology 15(5): 832-842.

[4] Lee, J., et al. (2005). "Optimum design of cold-formed steel channel beams using micro Genetic Algorithm." Engineering Structures 27(1): 17-24.

[5] Riera, S., et al. (2015). "Stepwise varying width microchannel cooling device for uniform wall temperature: Experimental and numerical study." Applied Thermal Engineering 78: 30-38.

[6] Harms, T. M., et al. (1999). "Developing convective heat transfer in deep rectangular microchannels." International Journal of Heat and Fluid Flow 20(2): 149-157.

[7] Mohammed, H., et al. (2011). "Heat transfer and fluid flow characteristics in microchannels heat exchanger using nanofluids: a review." Renewable and Sustainable Energy Reviews 15(3): 1502-1512.

[8] Segre, G. and A. Silberberg (1962). "Behaviour of macroscopic rigid spheres in Poiseuille flow Part 2. Experimental results and interpretation." Journal of fluid mechanics 14(1): 136-157.

[9] Kan, M., et al. (2015). "Plate heat exchangers as a compact design and optimization of different channel angles." Acta Physica Polonica A 12: 49-52.

[10] Peng, X. and G. Peterson (1996). "Convective heat transfer and flow friction for water flow in microchannel structures." International journal of heat and mass transfer 39(12): 2599-2608

[11] Wu, H. and P. Cheng (2003). "An experimental study of convective heat transfer in silicon microchannels with different surface conditions." International journal of heat and mass transfer 46(14): 2547-2556.

[12] Jiang, P.-X., et al. (2001). "Thermal–hydraulic performance of small scale micro-channel and porous-media heat-exchangers." International journal of heat and mass transfer 44(5): 1039-1051.

[13] Westphalen, D. and S. Koszalinski (1999). "Energy consumption characteristics of commercial building HVAC systems. Volume II: Thermal Distribution, auxiliary equipment, and ventilation." Arthur D. Little Inc (ADLI) 20(October): 33745-33700.

[14] Kandlikar, S., et al. (2005). Heat transfer and fluid flow in minichannels and microchannels, elsevier.

[15] Pettersen, J., et al. (1998). "Development of compact heat exchangers for CO2 air-conditioning systems." International journal of refrigeration 21(3): 180-193.

[16] Han, Y., et al. (2012). "A review of development of micro-channel heat exchanger applied in air-conditioning system." Energy Procedia 14: 148-153.

[17] Leland, J. E. and R. Ponnappan (2001). Method of making micro channel heat pipe having corrugated fin elements, Google Patents.

[18] [18] Harris, C., et al. (2000). "Design and fabrication of a cross flow micro heat exchanger." Journal of Microelectromechanical Systems 9(4): 502-508.

[19] Min, J. K., et al. (2009). "High temperature heat exchanger studies for applications to gas turbines." Heat and mass transfer 46(2): 175.

[20] Sommers, A., et al. (2010). "Ceramics and ceramic matrix composites for heat exchangers in advanced thermal systems—a review." Applied Thermal Engineering 30(11-12): 1277-1291.

[21] Meng, J.-H., et al. (2016). "Performance investigation and design optimization of a thermoelectric generator applied in automobile exhaust waste heat recovery." Energy Conversion and Management 120: 71-80.

[22] Baek, S., et al. (2010). Micro channel heat exchanger for LNG-FPSO application. The Ninth ISOPE Pacific/Asia Offshore Mechanics Symposium, International Society of Offshore and Polar Engineers.

[23] Thonon, B. and E. Breuil (2001). Compact heat exchanger technologies for the HTRs recuperator application.

[24] Kandlikar, S. G. (2005). "High flux heat removal with microchannels—a roadmap of challenges and opportunities." Heat transfer engineering 26(8): 5-14.

[25] Walpole, J. N. and L. J. Missaggia (1992). Microchannel heat sink with alternating flow directions, Google Patents.

[26] Reuse, P., et al. (2004). "Hydrogen production for fuel cell application in an autothermal micro-channel reactor." Chemical Engineering Journal 101(1-3): 133-141.

[27] Li, Q., et al. (2011). "Compact heat exchangers: A review and future applications for a new generation of high temperature solar receivers." Renewable and Sustainable Energy Reviews 15(9): 4855-4875.

[28] Silvestri, S. and E. Schena (2012). "Micromachined flow sensors in biomedical applications." Micromachines 3(2): 225-243.

[29] Qu, W. and I. Mudawar (2002). "Experimental and numerical study of pressure drop and heat transfer in a single-phase micro-channel heat sink." International journal of heat and mass transfer 45(12): 2549-2565.

[30] Liu, X. and J. Yu (2016). "Numerical study on performances of mini-channel heat sinks with non-uniform inlets." Applied Thermal Engineering 93: 856-864.

[31] Del Col, D., et al. (2011). "Effect of cross sectional shape during condensation in a single square minichannel." International journal of heat and mass transfer 54(17-18): 3909-3920.

[32] Brandner, J., et al. (2006). "Concepts and realization of microstructure heat exchangers for enhanced heat transfer." Experimental thermal and fluid science 30(8): 801-809.

[33] [33] David, M. P., et al. (2011). "Hydraulic and thermal characteristics of a vapor venting two-phase microchannel heat exchanger." International journal of heat and mass transfer 54(25-26): 5504-5516.

[34] M Kan, O Ipek, B et al. (2015) "Plate heat exchangers as a compact design and optimization of different channel angles" GurelActa Physica Polonica A 12, 49-52

[35] Liu, N., et al. (2016). "Experimental investigation of condensation heat transfer and pressure drop of propane, R1234ze (E) and R22 in minichannels." Applied Thermal Engineering 102: 63

[36] Shen, S., et al. (2006). "Flow and heat transfer in microchannels with rough wall surface." Energy Conversion and Management 47(11-12): 1311-1325.

[37] Peng XF, Peterson GP. The effect of thermo fluid and geometrical parameters on convection of liquids through rectangular micro channels. Int J Heat Mass Transfer 1995; 38: 755–8.

[38] Peng XF, Peterson GP. Convective heat transfer and flow friction for water flow in micro channel structures. Int J Heat Mass Transfer 1996; 39: 2599–608

[39] P Chamarthy, SV Garimella, ST Wereley - Measurement of the temperature non-uniformity in a micro channel heat sink using micro-scale laser-induced fluorescence of Heat and Mass Transfer, 2010.

[40] P Wu, WA Little - Measurement of the heat transfer characteristics of gas flow in fine channel heat exchangers used for micro miniature refrigerators Cryogenics, 1984.

[41] Khare, S., Dell'Amico, M., Knight, C., & McGarry, S. (2013). Selection of materials for high temperature sensible energy storage. Solar Energy Materials and Solar Cells, 115, 114–122. doi:10.1016/j.solmat.2013.03.009.

[42] Barreneche, C., Navarro, M. E., Cabeza, L. F., & Fernández, A. I. (2015). New database to select phase change materials: Chemical nature, properties, and applications. Journal of Energy Storage, 3, 18–24. doi:10.1016/j.est.2015.08.003.

[43] Shanian, A., & Savadogo, O. (2006). A material selection model based on the concept of multiple attribute decision making. Materials & Design, 27(4), 329–337.

[44] MF Ashby, A Miller, F Rutter, C Seymour, UGK Wegst the CES Eco Selector – Background Reading – 2009[42] MF Ashby, A Miller, F

Rutter, C Seymour, UGK Wegst the CES Eco Selector – Background Reading – 2009.

Engr. Wiqas Alam is a postgraduate researcher in Mechanical Department at Uinversity of Engineering and Technology, Peshawar, Pakistan. He is working on Micro Channel Heat Exchanger for Industrial Waste Heat Recovery in his Master in Material Engineering as a research project. This paper is a part of his Master degree research study.

International Journal of Engineering Works
ISSN-p: 2521-2419
ISSN-e: 2409-2770
Vol. 6, Issue 11, PP. 420-430, November 2019
https://www.ijew.io/
https://doi.org/10.34259/ijew.19.611420430

Economic Impact Assessment of Mini Micro Hydel Power Projects in Khyber Pakhtunkhwa

Ijaz ur Rahman[1], Maoz[1], Tanvir Ahmad[1]
[1]United States Pakistan Center for Advanced Studies in Energy UET Peshawar, Pakistan
Received: 17 October, Revised: 25 October, Accepted: 31 October

***Abstract*—** The exhaustion of the fossil fuel supply of the world is an understood eventuality, considering the pace at which these resources are being exploited the world over. More so when the global energy requirements are increasing without much interruption; suffice to say the current state of operations in the energy arena is not going to last long. Alternative energy resources, in this worldview, provide an auspicious avenue of fulfilling the burgeoning human thirst for energy. The impact of these alternative energy resources utilization will be twofold: the satiation of the energy demand, and the culmination of the global warming resulting from the incessant use of the fossil fuels. The urge for alternative resources of energy is key to survival and demand of future. In comparison to all the alternative resources of energy, Hydro power present better results in terms of efficiency and long term viability.The viability of Hydro Power is subject to its high initial cost and major construction with no return in the initial phase of construction. This work is aimed at presenting the technical and financial aspects of Micro-Hydro power. The financial assessment is based on the Net Present Value (NPV), Internal Rate of Return and Benefit to Cost Ratio (B/C). Apart from the social benefits to the residents and improving the quality of life, the financial feasibility is tested on the basis the above parameters and results shows the micro hydro are feasible in the lights of mentioned parameters. The proposition is tested and implemented on three different case studies, i.e. Ajmera Hydro power plant, Bersa Payen and Sheri Dumrai HPP. The data shows successful results in the all the mentioned cases.

***Keywords*—** Biogas, Social impact, Livelihoods, rural development, Environment

I. INTRODUCTION

The exhaustion of the fossil fuel supply of the world is an understood eventuality, considering the pace at which these resources are being exploited the world over. More so when the global energy requirements are increasing without much interruption; suffice to say the current state of operations in the energy arena is not going to last long. Alternative energy resources, in this worldview, provide an auspicious avenue of fulfilling the burgeoning human thirst for energy. The impact of these alternative energy resources utilization will be twofold: the satiation of the energy demand, and the culmination of the global warming resulting from the incessant use of the fossil fuels. The global consensus on keeping the world temperature hike post industrialization below 2 degrees is ushering in a new era of increasing dependency on renewable energy harvesting techniques at the expanse of shunning away the centuries long use of conventional fuels. Resultantly a drop in the installation of power generating facilities operating on the conventional fuels can be seen from reports delineating the energy outlook of the yesteryears [1]. Another trend noticeable in the recent years is the shifting of global energy usage patterns where the developing countries of Asia and Africa are increasingly using more and more energy and slated to leave the developed western economies for the first time in 2020 in terms of energy usage [2].

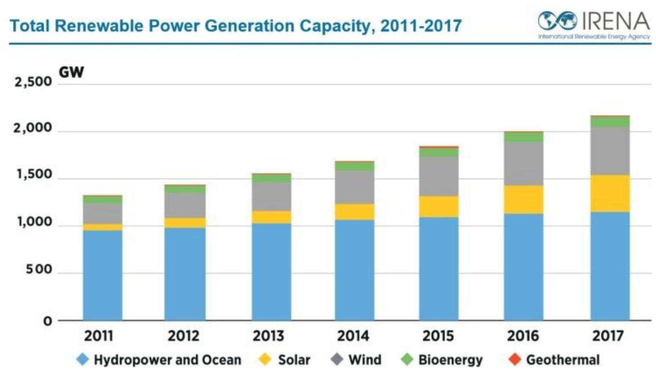

Figure 1. World renewable energy capacity addition by resource since 2011 [1]

Renewable energy installation as evident from the graph above has been at the forefront of energy growth endeavors for the past decade. The increased demand has inevitably lead to slashing of prices as per Swanson's law which predicts decrease of 20% in a technology's price for every doubling of demand[3]. International Energy Agency report for the outlook of world energy installation puts renewable growth at a higher pace than the conventional energy resources with 167 GW of new installation against a 57 GW coal power plants installations and a 29 GW gas power plants. Furthermore, the forecasts paint an even greener picture prognosticating upwards of 920 GW installations of renewable energy extraction facilities by 2022 as shown in the figure. This, fortuitously, has been an improvement on the previous forecasts and if true will put renewable energy at 30% of world energy applications by 2022 as shown in figure 1[1].

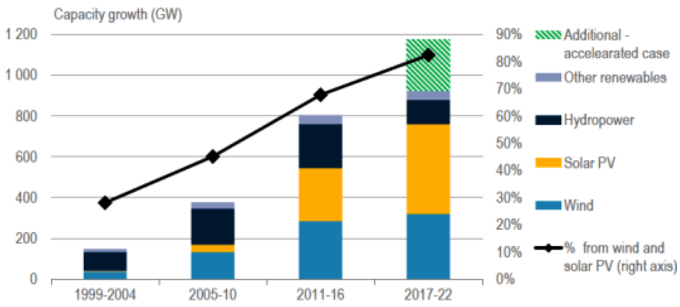

Figure 2. Figure 1 Renewable energy Past and Future [2]

In Pakistan the electricity mix is heavily tilted towards non-renewable thermal power plants making up 35.2% of total energy pie. Renewable energy, albeit a less time consuming and cleaner option, is not prevalent in the country[4]. The country has been able to achieve 80% electrification for the last twenty years and the energy consumption in TOE has reached 79 million in comparison to the 34 million TOE in 1994-95 but the overall makeup of the energy mix and the non-availability of much of the generation potential has pushed the country towards the incessant load shedding which severely disrupts the everyday lives and economic activities of the country[5]. Moreover the abundance of renewable energy potential in the country also make it an obvious low cost tool for handling the energy shortage and price hike[6]. The potential of the country as shown in the table below gives ample opportunity for cheap energy generation at the doorsteps of the consumers to bypass the transmission and distribution charges over larger distances[7]. Only one resource coastal wind power has the potential to generate 50000 MW electricity, with northern areas also have some wind potential and so does the Sindh Gharo sector[8]. The renewable past and future shown in figure 2.

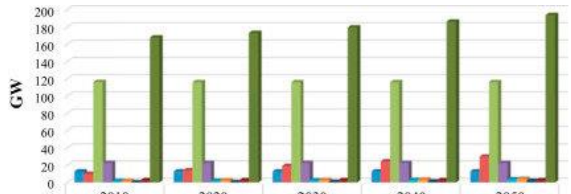

	2010	2020	2030	2040	2050
Wind (grid connected)	12.8	12.8	12.8	12.8	12.8
Solar PV (DCNT)	9.9	14.1	19.1	24.5	29.9
Solar PV (CNT)	116.2	116.2	116.2	116.2	116.2
Solar thermal (CNT)	22.6	22.6	22.6	22.6	22.6
Biomass (field residues)	1.7	2	2.5	3	3.7
Biomass (animal waste)	1.6	2.3	2.8	3.4	4.1
Biomass (MSW)	0.2	0.4	0.7	1.1	1.9
Small Hydro	2.7	2.7	2.7	2.7	2.7
Total	167.7	173	179.3	186.1	193.9

Figure 3. Pakistan renewable energy generation projections 2010-2050

The energy demands have remained elusive from the capacity growth for the past decade in the country with the demand growing at an astounding rate of 8% compared to economy growth, on average, of 3-4%[6]. The contemporary power generation scenario is heavily dependent on imported fuels, 36%, and indigenous depleting natural gas resources, 27% [9] as shown in the Figure 4. Albeit the energy crisis has to some extent been curtailed, the cost on economy of the imported hydrocarbons is telling and diminishing the growth rate[9].

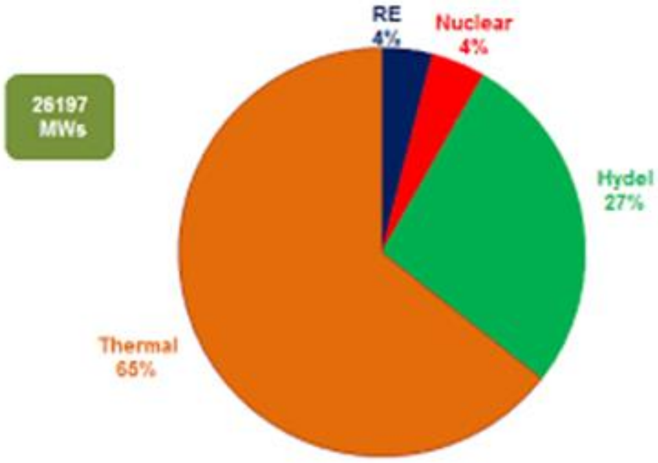

Figure 4. Figure 2 Pakistan's Energy mix 2017

Sooner than later the policy formulators would have to start thinking on the lines of sustainable renewable energy options for a self-reliant durable economic growth[10].In addition to the expensive kWh produced using imported fuels another big concern for Pakistan's power sector is the remote unelectrified communities which stands over 25% of the population[11]. Owing to the remote and diasporic nature of this disenfranchised population the gird access would be too costly to be worth the economic output promised[6]. Renewable energy technologies owing to their prevalence and ease of adoption are a ray of hope for these communities [12]. The Figure 3 is shwon Pakistan renewable energy generation projections 2010-2050.

Foremost among the renewable energy technologies and the most mainstreamed is the hydropower responsible for 19% of worldwide electricity generation[13]. The distinction of Large, small, and mini, micro hydropower makes the technology most suitable for vast outreach and application. Small hydro with its run of the river power generation also alleviates the environmental concerns concomitant with the large hydro dams, in addition to the low cost of electricity generation [14]. A further division of the hydro power generation technologies has been made into mini/micro hydropower which encapsulates the hydropower projects of less than 1 MW capacity. Recent estimates put mini/micro hydropower potential in the northern districts at 1200 MW[15]. Unfortunately, only close to 5% of this potential has yet been realized[16]. Furthermore an additional potential of 300 MW and 400 MW exists in the northern areas of Pakistan for installing 100 kW and 500 kW power projects respectively and The figure 4 is shown Pakistan energy mix 2017 [5].

The province of Khyber Pakhtunkhwa has vast resources of Hydropower generation and the provincial government has been leaving no stones unturned for tapping its potential through its mini/micro hydropower projects, first step towards which was the provincial power policy of 2016, the first of its kind after the 18th amendment[17].

Energy and Power Department of the province of Khyber Pakhtunkhwa and Pakhtunkhwa Energy Development Organization (PEDO) has initiated various projects of off grid electrification of remote communities of the province. In this initiative the pilot project consisted of 356 MHPP projects in the province through various non-government al organizations[18]. The project has recently been extended to second phase where 1200 MHPP projects have been planned for installation in the province[19].

The project aims to provide electricity access to 240000 households[19] across the province in remote areas by 2021[16][5 prop]. The details of the project are given in the table 1 and 2 below.

TABLE 1 BREAKDOWN OF THE 356 MHPP PROJECTS BY GOVERNMENT OF KHYBER PAKHTUNKHWA (PHASE 1)

S. No.	No. of MHPs	Capacity (MW)	Stream	Estimated No of House holds	Start	Planned Completion
1.	310	29.04	Stream	104,000	20-2-2015	2018
2.	46	5.67	Stream		1-2-2017	
Total	356	34.69				

TABLE 2 MHPP PROJECTS PHASE II BY KP GOVERNMENT

Sr. No.	No. of MHPPs	Capacity (MW)	Stream/Canal	Estimated No of House holds	Planned Completion
1.	512	37.41	Stream	159,000	2021-22
2.	160	15.72	Canal		2021-22
Total	672	53.13			
Total	1028	87.82			

The 356 MHPPs are distributed among various districts of KP with an estimated cost of PKR. 5501.66 million PKR detailed in the table 3.

The projects, albeit a commendable initiative, would require a thorough consideration to the impact aspect of the project for achieving far reaching impact[12]. Energy in itself is not a goal but rather an alleyway to the fulfillment of national prosperity objectives. That is why the socioeconomic, specifically economic, impact of electrification is a key focus in modern power projects. The figure 5 below gives ample evidence to support this claim where the energy usage per capita of a number of countries around the world are plotted against their human development index (HDI)[11].

TABLE 3 SCOPE AND LOCATIONS OF THE 356 MHPP PROJECTS

Name of Scheme	Districts	Capacity (MW)	Cost (M.Rs)
Construction of 356 Mini/Micro Hydropower projects in Khyber Pakhtunkhwa	Swat, Buner, Shangla, Lower Dir, Upper Dir, Chitral, Mansehra, Abbottabad, Batagram, Torghar & Kohistan	35.6	5501.66

It is obvious that the provision of energy in sufficient amounts is directly correlated to the national prosperity[20]. That however is not the full picture as some countries, as seen from the figure, have achieved more human development for relatively same per capita energy consumption. This puts the need of energy projects' economic impact study into perspective [21]. As can be seen Pakistan has a mild energy consumption of around 450 kWh per person yearly and that directly translates in to a meager HDI of 0.52 and allots it rank 150 among the 189 countries listed [19].

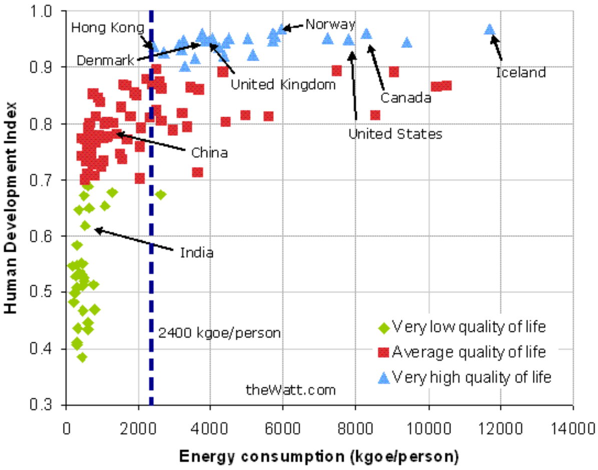

Figure 5. HDI-Energy Nexus[10]

In the contemporary world struggle with poverty alleviation, energy access projects need to take in to account the social and economic impact that stem from these projects. Countries world overachieve disproportionate social and economic development from similar energy consumption per capita[22]. From the figure 5, Denmark for instance, achieves similar HDI from half the energy consumption as Canada [19].

In this context the MHPP projects attain even more importance as they are targeted at the remote, economically and socially disadvantaged communities of the world and in Pakistan[23]. These projects provide a golden opportunity for leapfrogging these disadvantaged communities out of their economic destitution. The objectives of this thesis, given in the next section, are a first of its kind endeavor in Pakistan for successfully evaluating the economic progress that the installed MHP projects have brought about in the lives of the benefiting communities[24]. This thesis will provide basic primary knowledge of the ways in which the economic impact can be furthered and will prove a precious resource for the energy policy and power projects implementing agencies to better plan these projects for elevated benefit to the society[25].

II. METHODOLOGY

The study was carried out in the Battagram District of Khyber Pakhtunkhwa province of Pakistan. The district shown in the figure 6 lies mostly in the northern mountaineous region. Three MHPPs were chosen for the study from within the district's premises. There are tens of MHPPs installed but these three were chosen because of their easier accessibility and data availability. The three MHPPs are listed in the following.

1. Ajmera Hydro power plant
2. Bersa Payen
3. Sheri Dumrai HPP

The main point of this analysis was presenting the technical and financial aspects of Micro-Hydro power. The financial assessment is based on the Net Present Value (NPV), Internal Rate of Return and Benefit to Cost Ratio (B/C). Apart from the social benefits to the residents and improving the quality of life, the financial feasibility is tested on the basis the above parameters and results. The technical work is based on evaluating the soundness of the civil works, equipment, and distribution network designs and the ensuing implementation on ground.

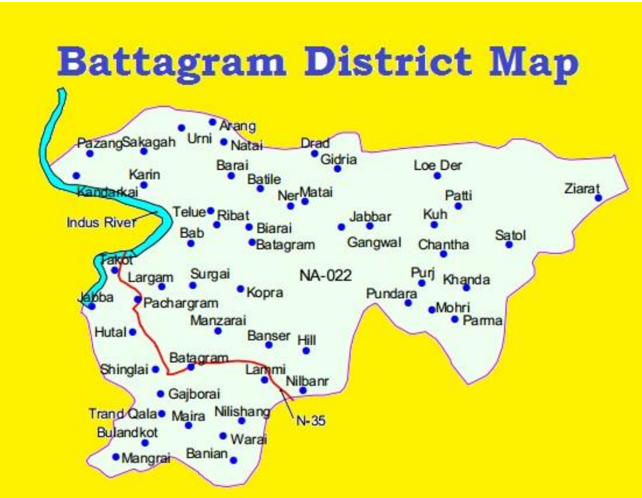

Figure 6. Geographical map of District Battagram

Technical terms and parameters

CapitalCost

Capital cost of any small hydro project entails the following

Direct cost

Which includes the following

Civil works

Electromechanical equipment

Other direct cost, like laborer etc.

Indirect Cost

Indirect cost includes

(i) Land establishment
(ii) Financing cost
(iii) Local area development charges
(iv) Interest during construction for commissioning the project
(v) It also contains initial capitalized spares

III. RESULTS AND DISCUSSIONS

1) Techno-Economic Impact Analysis of Ajmera Micro Hydro Power Station

a) Stream Hydrology

The Ajmera power project is located on the right bank of Ajmera Stream which is one of the two main source streams of the Nandihar Khowar. Discharge of the stream has been calculated on four years hydrological data by using catchment area method. For this purpose, daily discharge data of four years recorded at the Batli Ajmera Gauge station has been used of the Pakistan. As the Hydrological study and analysis given below shows that for three months (November, December and January) discharge in the Khowar have chances to be reduced below the design discharge. Hence, imported Francis Turbine of 400 kW is proposed to be installed at Ajmera MHP. So, the unit will remain operational throughout the year in case of low discharge without any remarkable decrease in power generation.

This Power Project (Ajmera) is located on the bank of Ajmera Khwarr and an important of the two stream in Batagram. The optimum flow rate of the stream is calculated on the basis of five years of hydrological data by deploying catchment area technique. The data is constantly collected and monitored through gauge station at Batli Ajmera. The hydrological data suggest variation in flow rate from the months November, December to January. The flow data from the tables below shows that the flow falls below designed flow in some months. The head vs flow rate suggests the installation of Francis turbine as shown in the figure 7 below.

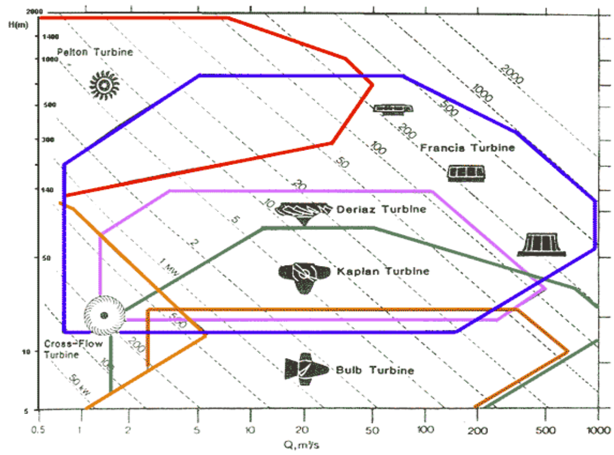

Figure 7. Turbine selection chart

b) Design Flow by Catchment Area Method

The design flow is calculated from the gauge station data installed at Ajmera. The daily discharge values are computed in the hydrograph to find the optimal flow as shown in figure 8.

The catchment area is found from the high points of the contour map. The area of 442 km2 is selected for this purpose.

The catchment area is shown in the diagram below.

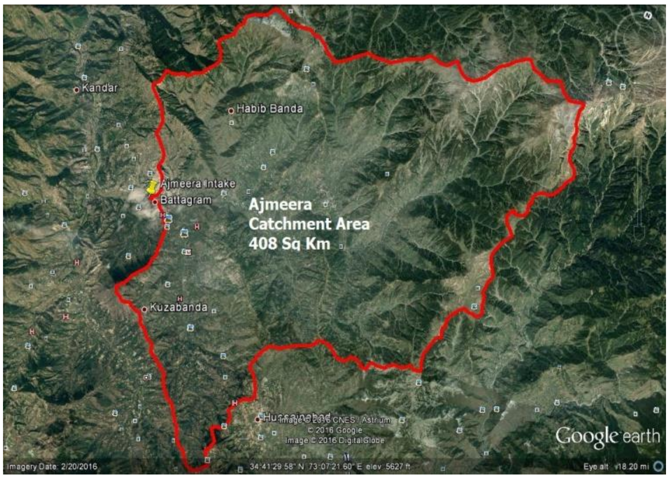

Figure 8. Catchment area at Nandihar Khwarr

The design discharge is found from the above data as shown in the Hydro-graph in figure 19, 20.

The design flow rate for this project is thus comes out to be 159 cusecs.

c) Power Calculation (Energy Production)

The power potential of a scheme is theoretically calculated by the following given formula shown in equation (A). The design flow calculation in figure 9 and flow duration curve for Ajmeera shown in figure 10.

The energy (kW) is calculated using the famous equation;

$$\mathbf{P = \eta * g * Q * H} ----------\text{III-1}$$

Years	Annual Mean Discharge (Guage Station) CMS	Annual Mean Discharge (Design Station) CMS Qd= Ad/Ag x Qg	
2010	8.03	7.396	Qd= Design station Discharge
2011	8.1	7.460	Qg= Gauge station Discharge
2012	6.76	6.226	Ad= Catchment Area of Design Station
2013	9.14	8.418	Ag= Catchment Area of Gauge station

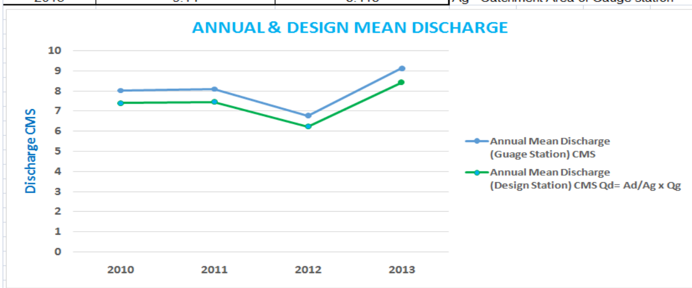

Figure 9. Design Flow Calculation

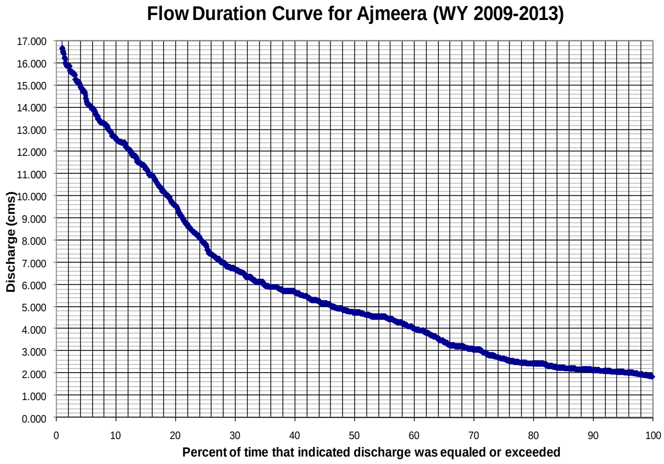

Figure 10. Flow Variation, Curtesy, PEDO

Where

η	=	Overall efficiency coefficient
P	=	Power in (kW)
H	=	Net head (m)
Q	=	Design discharge (m3/sec)
g	=	Acceleration due to gravity

d) Energy Calculation

The energy generated by HPP station in each year depends strictly on the flow rate, which fluctuates round the year. The energy calculated by using the above equation gives only the theoretical value for better understanding. The daily production is given by

$$ED = pa \times h$$

Where

Pa	=	Average power daily (MW)
ED	=	Energy output, Daily (MWh)
h	=	Hours in a day

the annual energy production is

$$EA = ED \times d$$

Where as

ED	=	Daily average output (MWh)
EA	=	Annual Daily energy output (MWh)
d	=	Nos. of days in a year

e) Number of Units

On the basis of average daily production and maximum flow availability a total of 500 kW is calculated for Ajmera power station.

f) Efficiency of Electromechanical Equipment

As per design Francis Turbine (Imported) is suited for this site. Normal efficiency of the turbines is 86% and based on the site parameters the peak efficiency may reach 92% (Highest). Therefore, the overall efficiency of the scheme for the Ajmera site is approximately 80%. Efficiencies of major electromechanical equipment are given in the following table 4 and 5.

Francis turbine is proposed for the Ajmera site based on the turbine selection chart. The efficiencies are high for Francis unit and vary between 85-93%. The generator have has comparative efficiency, thus the overall efficiency of the station is about 80%.

TABLE 4 EFFICIENCIES OF E & M EQUIPMENT

S.no	Component (Type)	Efficiency (%)
1	Turbine (Francis)	90
2	Generator (Brushless)	91

g) Energy Production and Installed Capacity

As the Hydrological study and analysis given above shows that for three months (November, December and January) discharge in the Stream (Khwar) have chances to be reduced below the designed discharge. Hence, imported Francis Turbine of 500kW capacity is proposed to be installed at Ajmera MHP. So, the unit will remain operational throughout the year and no remarkable decrease in power generation can be observed for the said three months in case of low discharge. Direct coupled single unit of 500kW power plant is proposed to be installed at Ajmera Power Plant. Power plant shall remain operational throughout the year at full capacity except for the months of November, December and January. The selected turbine is necessary to address the electricity requirement of the area. Annual energy from the plant will be 2625.00 MWh as per given formula.

The hydrological data shows drastic changes in the flow, especially reduction in flow is seen in the months of November, December and January; wherein the flow falls below the design conditions. The energy production is seen to be lesser than theoretical value. The Francis unit will be operational round the year and 500 kW production rate could be considered for calculations. The turbine serves to provide energy for the local community. The annual energy production is calculated as while, installed capacity is 500kW.

$$\frac{\text{Energy production}}{\text{year}} = \text{Plant capacity} * \text{Plant factor} * \text{hours in a year}$$

TABLE 5. COMPONENT DETAILS

S. N	Component Details	Rs. Mn.
1.	Vertical axis Francis unit with wicket gates assembly adjusting to optimal flow to avoid fluctuation in power output	30
2.	Brushless electric generator for converting rotational mechanical energy to electrical energy	20
3.	Miscellaneous power plant equipment	10
4.	Electrical transmission line costs	10
	Total	70
	Insurance at 3%	6
	Total	76
	Erection and commissioning @ 10%	16
	Total	82
	Unforeseen & contingencies L.S.	10
	Grand Total	92

$$\frac{Energy production}{year} = 500kW * 0.75 * 8750$$

$$= 3282.30\ MWh$$

This amount of energy could be extracted in one year, considering the condition that plant is in running condition and there are no emergency shutdowns for prolonged period of time.

2) TECHNO-ECONOMIC IMPACT ANALYSIS OF BURSA PAYEEN MICRO HYDRO POWER STATION

a) Hydrology

Bersa Payen Khwarr is one of the important streams in Rashang UC (Union Council), Tehsil Allai, District Batagram. This is a perennial stream, meaning its water rising from rain fed springs. The flow pattern at Bersa Payeen Khwarr is a function of winter and summer precipitation. The details are given in Table 6.

b) Environmental Impacts

This project is an ideal ecofriendly scheme and commissioning of the project cast no harmful impact on the environment, habitat, flora and fauna. Some of the features and presented below.

TABLE 6: FEATURES OF BARSA PAYEN

Village:	Bersa Payeen
Union Council:	Rashang
District:	Batagram
Length of power Channel (Rft):	115 Round ft
Households:	38 Nos.
Distance from Batagram:	58 Km
Plant factor:	75 percent

Total Capacity :	15 kW
No of Units:	01
Size of Power Channel:	2.00 x 1.75 Ft
Generator (brushless):	15 kW
Design Discharge:	8.5 cusecs
Diameter and thickness of penstock	14 inches, 4 mm
Annual Mean Discharge:	cusecs
Minimum Discharge	10 cusecs
Gross Head:	32 Ft
Net Head :	30.6 Ft
Crossflow Turbine :	15 kW
Total Annual Energy Production:	**88.80 MWh**

c) Project Location

The location of the proposed project is 34°48'38.11"N & 73°06'57.10"E. The proposed project is located at 58 km via main Allai road, from Batagram town. This site a very suitable choice for the installation of Hydro Power scheme. The water enters the headrace tunnel to the forebay on the bank of Nulla/ Stream. The water at tail race discharges directly into open atmosphere into the Bersa Khwarr/ Stream.

d) Hydro Power Potential

Hydro-Power potential is calculated by considering maximum flow availability in the stream throughout the year. This energy produced from the project is utilized by mostly households and some commercial uses. The energy from the project is a step for better prospects of the community. The site is capable of producing 15 kW power (theoretical basis). The available head for energy production is 33 feet, while the design discharge is 9.5 cusecs. The project suitability can also be confirmed from the fact that this area has no grid connectivity and the demand for electricity is maximum for the community. The supply demand balance suggests that the project should be installed on priority basis.

e) Stream Hydrology

The project is located on the right bank of the mainstream (Bersa stream) and is one the important tributary stream of Allai Khwarr. Flow rate (Discharge) is calculated on the basis of 6 years hydrological data using the famous catchment area technique. The gauge station for data collection used was Banna Allai installed on the stream of Barsa Payeen. The unit is operational round the year with no significant decrease in power generation.

f) Flow rate using Catchment Area Method

The annual flow pattern at Barsa Payen, recorded at Banna gauge station is used for the design of electromechanical equipment. The flow rate could also be determined using the float method.

The total catchment area at the gauge station at Allai Khwarr was 280 km2. The map presented below taken from google map and the red circle shows the bounds of the catchment area. It is about 10 % of the total catchment area.

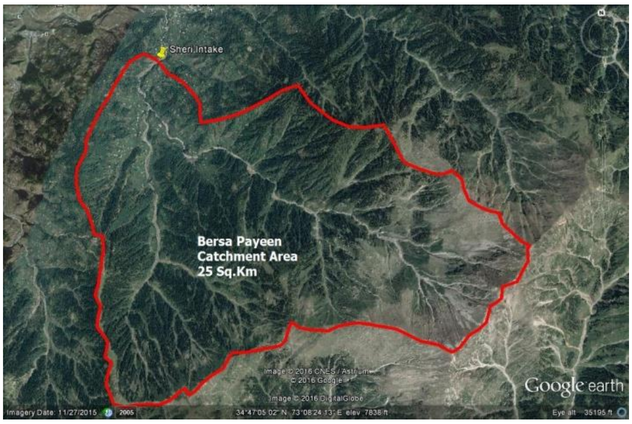

Figure 11. Catchment Area at Allai Khwarr Gauge Station

Years	Annual Mean Discharge (Guage Station) CMS	Annual Mean Discharge (Design Station) CMS Qd= Ad/Ag x Qg
2003	4.975	0.444
2004	4.131	0.369
2005	5.197	0.464
2006	5.304	0.474
2007	5.442	0.486
2008	5.264	0.470

Figure 12. Design Discharge calculated from the Gauge station data

The comparative discharge graphs and that of Bersa Payeen Intake with Flow Duration Curve are given below:

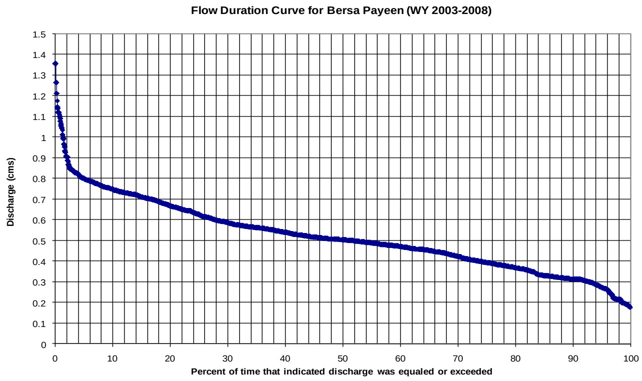

Figure 13. Flow pattern of discharge as seen from the 6 years of data

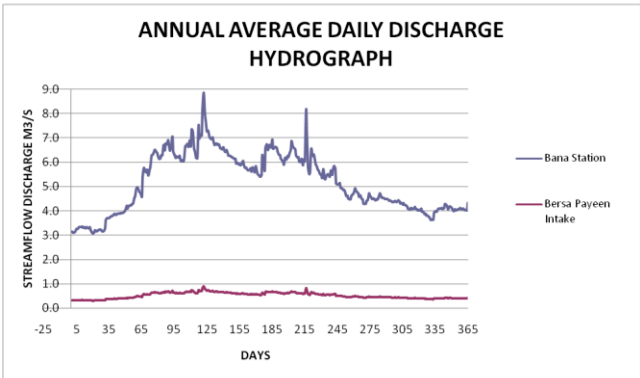

Figure 14. Discharge variation in year

The design discharge is thus 20.11 Cusecs for the proposed project at Bersa Payeen

Cross Flow turbine is proposed for the Bursa Payeen site based on the turbine selection chart. The efficiencies are high for Francis unit and vary between 85-93%. The generator has comparative efficiency;thus, the overall efficiency of the station is about 80% as shown in table 7 and table 8.

TABLE 7. EFFICIENCIES OF E & M EQUIPMENT

S.no	Component (Type)	Efficiency (%)
1	Turbine (Single unit Cross flow)	88
2	Generator (Brushless)	91

g) Pre-Feasibility Economic Analysis:

TABLE 8. DETAILS OF BERSA PAYEEN HPP

Head	**32 feet**	**Penstock Length**	**50 feet**
Overall Efficency	80%	Economic life	25 Years
Yearly geneation	88.08 Mh	Selling Price	9/unit
Capacity	15 kW		

TABLE 9. COST BREAKDOWN OF AJMERA HPP

Investment Cost Turbine, Generator and Civil Additional Station, Equipment (Multi-unit)	**Price in Million PKR**
Penstock	0.4
Transmission Line	0.7
Others (access, miscellaneous site construction)	1.6
Contingencies at 11% - 20%	2
Indirect at 20%	2
Cross Flow Turbine	0.6
Generator (Brushless)	0.7
Total Investment Cost (IC)	6.9

3) TECHNO-ECONOMIC IMPACT ANALYSIS OF SHERI DUMRAI HYDROPOWER

Sheri Dumrai is located on the bank of Allai Khwarr in Union Council Bateela, Tehsil Allai, Batagram. The flow is perennial, i.e. arising from spring (rain fed). The flow variation is observed in summer in winter due to pattern of precipitation.

Some of the salient features of this projected are presented in table 10 below.

TABLE 10. SOME FEATURES OF SHERI DUMRAI HP

Village:	Sheri Dumrai
Union Council:	Bateela
District:	Batagram
Cropping Zone:	Kharif & Rabbi Crops
Distance from Batagram:	54 Km
Households:	20 Nos.
Total Capacity :	15 kW
No of Units:	01
Plant factor:	75 percent
Lengthof power Channel (Rft):	20 Round feet
Size of Power Channel:	2.33 x 2.00 Ft
Length of Penstock Pipe (Rft):	28 Ft
Annual Mean Discharge:	30 cusecs
Minimum Discharge:	20 cusecs
Design Discharge:	15.5 cusecs
Gross Head:	17 Ft
Net Head :	16.1 Ft
Diameter and thickness of penstock:	20 inches, 4 mm
Crossflow Turbine :	15 kW
Generator (brushless):	15 kW
Total Annual Energy Production:	87.60 MWh

a) Environmental Impacts

The project is much suited one opt to its environmental friendliness and posing no harm to natural habitat and horticulture, flora and fauna. Deforestation is avoided to major extent in pulling out this project.

The economy of Batagram depends on natural resources and agricultural subsistence to a major extent. Despite this fact, no proper irrigation system is developed in this area. The forest also is hub to medicinal plants. Livestock; goat, cattle, sheep and poultry contribute to the livelihood of community. Literacy rate is poor and cheap labor also contribute to the livelihood of community.

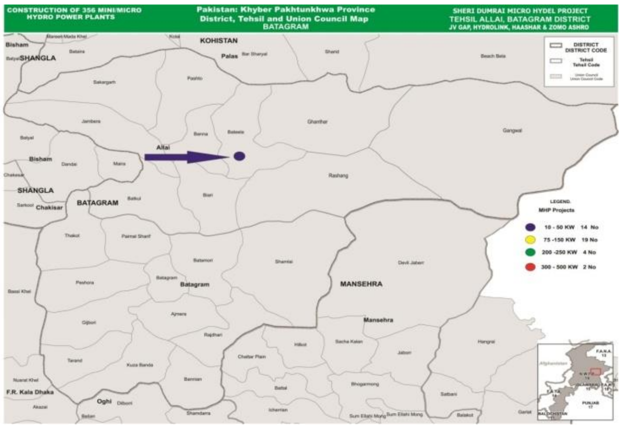

Figure 15. ap of Batagram, Proposed project location, Courtesy PEDO

b) Hydro Power Potential

Hydropower potential and tapping the energy from this resource can studied in an area on the basis of maximum availability water and head for major portion of the year. Batagram has both, and the energy obtained from hydro would serve two purposes; electrifying the village and encouraging small startup and established businesses. The data collected from the Sheri Dumrai site suggests a hydropower potential of 15 Kilowatt. The available head is 17 feet, while the optimum flow rate is 15.5 cusecs. The important factor for electrifying this area is, most of the area has no or poor grid connectivity and the community faces long hours of load shedding, thus there is a demanded need of hydropower in this area.

Design Flow by Catchment Area Method

The design flow is calculated from the gauge station data installed at Sheri Dumrai . The daily discharge values are computed in the hydrograph to find the optimal flow.

The catchment area is found from the high points of the contour map. The area of 442 km2 is selected for this purpose.The catchment area is shown in the diagram below.

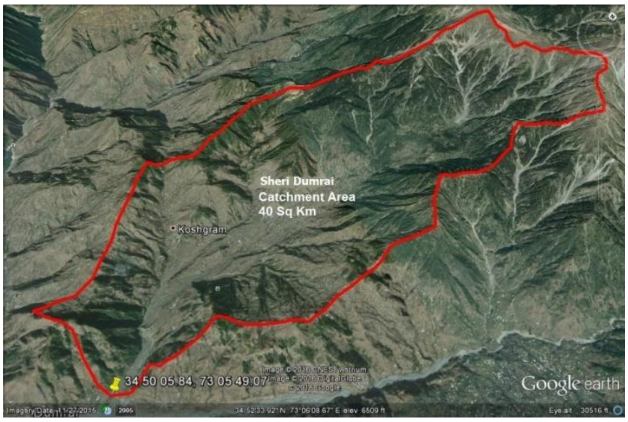

Figure 16. Catchment area at Nandihar Khwarr

Annual Mean Discharge Table

Years	Annual Mean Discharge (Guage Station) CMS	Annual Mean Discharge (Design Station) CMS Qd= Ad/Ag x Qg
2003	4.975	0.711
2004	4.131	0.590
2005	5.197	0.742
2006	5.304	0.758
2007	5.442	0.777
2008	5.264	0.752

Qd= Design station Discharge
Qg= Gauge station Discharge
Ad= Catchment Area of Design
Ag= Catchment Area of Gauge

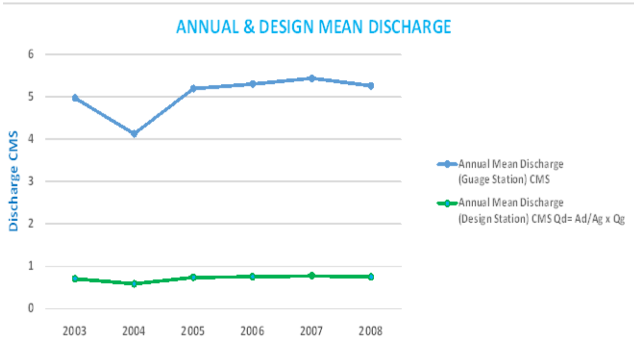

Figure 17. Design Flow Calculation

The design discharge is found from the above data as shown in the Hydro-graph above: Flow Variation is presented here in Figure 18. And annual average daily discharge hydrograph shown in figure 19 and figure 20.

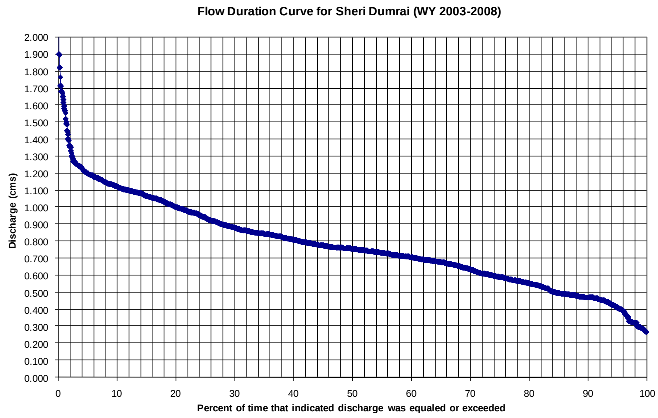

Figure 18. Flow Variation, Courtesy, PEDO

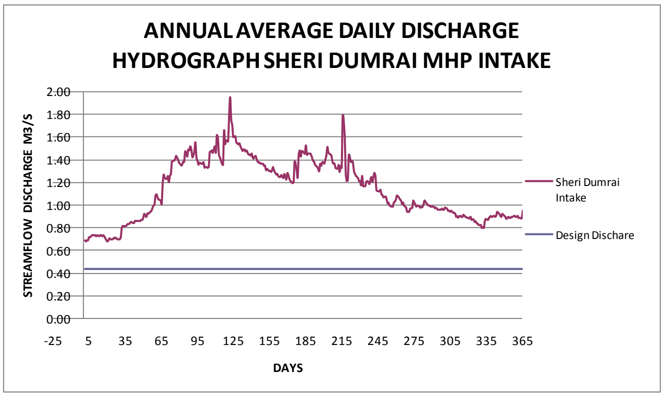

Figure 19. Figure Annual Average Daily Discharge Hydrograph Sheri Dumari MHP Intake

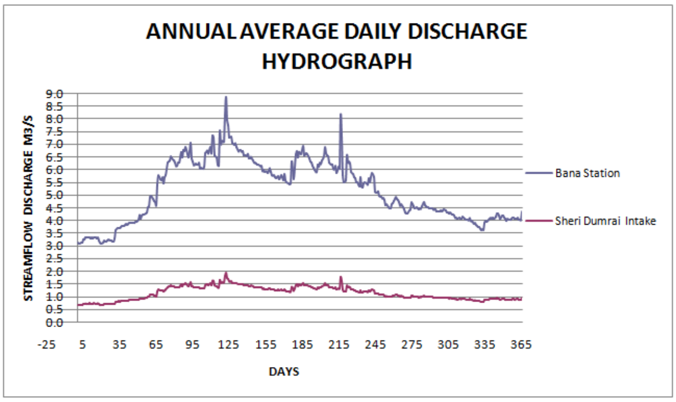

Figure 20. Figure Annual Average Daily Discharge Hydrograph

c) *Determining Economic Feasibility*

A project is said to be economically viable when the benefits streams exceeds the costs streams. The Internal Rate of Return (IRR) method is also a reasonable approach, and it is the discount rate at which the costs and benefits becomes equal. IRR compares the return rate from the project with the opportunity cost of alternatives. If the IRR is greater than the interest rate/ opportunity rate, the project is economically viable. The Ajmera project analysis is performed the all the installed capacities under study.

d) *Pre-Feasibility Economic Analysis:*

The detail of Ajmera micro hydro project and its cost breakdown is given in table 11 and table 12.

TABLE 11. DETAILS OF AJMERA MICRO HYDRO PROJECT

Head	**32 feet**	**Penstock Length**	**50 feet**
Overall Efficiency	80%	Economic life	25 Years
Yearly generation	87.60 MWh	Selling Price	5/unit

TABLE 12. COST BREAKDOWN OF AJMERA MICRO HYDRO PROJECT

Investment Cost Turbine, Generator and Civil Additional Station, Equipment (Multi-unit)	**Price in Million PKR**
Penstock	0.4
Transmission Line	0.7
Others (access, miscellaneous site construction)	1.6
Contingencies at 11% - 20%	3
Indirect at 20%	2
Cross Flow Turbine	0.65
Generator (Brushless)	0.7
Total Investment Cost (IC)	7.95

CONCLUSION

The exhaustion of the fossil fuel supply of the world is an understood eventuality, considering the pace at which these resources are being exploited the world over. More so when the global energy requirements are increasing without much interruption; suffice to say the current state of operations in the energy arena is not going to last long. Alternative energy resources, in this worldview, provide an auspicious avenue of fulfilling the burgeoning human thirst for energy. The impact of these alternative energy resources utilization will be twofold: the satiation of the energy demand, and the culmination of the global warming resulting from the incessant use of the fossil fuels. The urge for alternative resources of energy is key to survival and demand of future. In comparison to all the alternative resources of energy, Hydro power present better results in terms of efficiency and long term viability.The viability of Hydro Power is subject to its high initial cost and major construction with no return in the initial phase of construction. This work is aimed at presenting the technical and financial aspects of Micro-Hydro power. The financial assessment is based on the Net Present Value (NPV), Internal Rate of Return and Benefit to Cost Ratio (B/C). Apart from the social benefits to the residents and improving the quality of life, the financial feasibility is tested on the basis the above parameters and results shows the micro hydro are feasible in the lights of mentioned parameters. The proposition is tested and implemented on three different case studies, i.e. Ajmera Hydro power plant, Bersa Payen and Sheri Dumrai HPP. The data shows successful results in the all the mentioned cases.

Firstly, a broad and comprehensive study of the technical and economic aspects of hydropower, installed in the north part of Khyber Pakhtunkhwa e.g. Bersa Payen, Sheri Dumrai etc.

District Batagram. The key technical aspects are presented, like the flow pattern from catchment area and the anticipated hydropower that could be tapped from the HPP. The next phase is the proper selection of hydropower unit, in this case was cross flow unit. The cost of all the major units including construction and repair and maintenance is introduced in the thesis. After commissioning the power production and the revenue streams generated thus have been computed. The future streams of benefits against all the cost have been taken in the calculation to find out the key parameters for financial viability of the project, such as; Benefit to Cost Ratio, Internal Rate of Return, Net Present Value etc. The results depict a clear and vivid picture of financial viability in terms of all the parameters mentioned above.

The case studies of Bersa Payen and Sheri Dumrai have also been assessed in the similar fashion; showing successful results in terms of the parameters defined to assess financial viability. The implementation of HPP apart from its successful viability, also draws impeccable impact on the wellbeing of society and uplifting the social status of community

CONFLICT OF INTEREST

The author declares that there is no conflict of interest in the execution and publication of this research.

REFERENCES

[1] N. E. F. Bloomberg, "New energy outlook 2018," ed: Informs BNEF). Disponible en: http://about. bnef. com/content/uploads/sites …, 2016.

[2] L. Yang, H. Yan, and J. C. Lam, "Thermal comfort and building energy consumption implications–a review," Applied energy, vol. 115, pp. 164-173, 2014.

[3] A. Amin, N. Muhammad, S. A. Maoz, A. Basit, and T. Ahmad, "A Socio-Technical Survey of Micro Hydro Power Projects in District Shangla, Pakistan," 2018.

[4] N. Qureshi, "Exploring the energy consumption environmental impacts and economic consequences of," 2018.

[5] M. A. Sheikh, "Energy and renewable energy scenario of Pakistan," Renewable and Sustainable Energy Reviews, vol. 14, pp. 354-363, 2010.

[6] A. Raheem, S. A. Abbasi, A. Memon, S. R. Samo, Y. Taufiq-Yap, M. K. Danquah, et al., "Renewable energy deployment to combat energy crisis in Pakistan," Energy, Sustainability and Society, vol. 6, p. 16, 2016.

[7] M. K. Farooq and S. Kumar, "An assessment of renewable energy potential for electricity generation in Pakistan," Renewable and Sustainable Energy Reviews, vol. 20, pp. 240-254, 2013.

[8] M. Shahbaz, N. Loganathan, M. Zeeshan, and K. Zaman, "Does renewable energy consumption add in economic growth? An application of auto-regressive distributed lag model in Pakistan," Renewable and Sustainable Energy Reviews, vol. 44, pp. 576-585, 2015

[9] S. Z. Farooqui, "Prospects of renewables penetration in the energy mix of Pakistan," Renewable and Sustainable Energy Reviews, vol. 29, pp. 693-700, 2014.

[10] F. Wagner, "The complex story of energy transition—an introduction," in EPJ Web of Conferences, 2018, p. 00002.

[11] W. Uddin, S. Hussain, K. Zeb, M. A. Dildar, Z. Ullah, . U. Khalil, et al., "Energy Scenario and Potential of Hydroelectric Power in Pakistan," in 2018 International Conference on Power Generation Systems and Renewable Energy Technologies (PGSRET), 2018, pp. 1-6.

[12] S. Stiebert, "Pakistan Low Carbon Scenario Analysis," 2016.

[13] A. Hussain and Z. Gillani, "Fulfilling environment related international commitments through implementation of multilateral environmental agreements (meas) in pakistan," A scientific journal of COMSATS–Science Vision, vol. 18, pp. 1-2, 2014.

[14] O. Paish, "Small hydro power: technology and current status," Renewable and sustainable energy reviews, vol. 6, pp. 537-556, 2002.

[15] M. S. Rahman, I. M. Nabil, and M. M. Alam, "Global analysis of a renewable micro hydro power generation plant," in AIP Conference Proceedings, 2017, p. 020014.

[16] M. Bilal, R. Ullah, A. Ali, M. H. Khan, and Z. Ullah, "Wheeling hybrid energy system for industries," in 2016 International Conference on Computing, Electronic and Electrical Engineering (ICE Cube), 2016, pp. 169-174.

[17] M. H. Baloch, S. T. Chauhdary, D. Ishak, G. S. Kaloi, M. H. Nadeem, W. A. Wattoo, et al., "Hybrid energy sources status of Pakistan: An optimal technical proposal to solve the power crises issues," Energy Strategy Reviews, vol. 24, pp. 132-153, 2019.

[18] H. A. Sher, A. F. Murtaza, K. E. Addoweesh, and M. Chiaberge, "Pakistan's progress in solar PV based energy generation," Renewable and Sustainable Energy Reviews, vol. 47, pp. 213-217, 2015.

[19] B. K. Sovacool, "The political economy of energy poverty: A review of key challenges," Energy for Sustainable Development, vol. 16, pp. 272-282, 2012.

[20] W. Uddin, K. Zeb, A. Haider, B. Khan, S. ul Islam, M. Ishfaq, et al., "Current and future prospects of small hydro power in Pakistan: A survey," Energy Strategy Reviews, vol. 24, pp. 166-177, 2019.

[21] M. Umar and A. Hussain, "Micro hydro power: a source of sustainable energy in rural communities: economic and environmental perspectives," The Pakistan Development Review, pp. 487-504, 2015.

[22] A. Hussain, G. K. Sarangi, A. Pandit, S. Ishaq, N. Mamnun, B. Ahmad, et al., "Hydropower development in the Hindu Kush Himalayan region: Issues, policies and opportunities," Renewable and Sustainable Energy Reviews, vol. 107, pp. 446-461, 2019.

[23] M. A. Khan, "Policy review and recommendations on the promotion of renewable energy and energy efficiency," 2016.

[24] D. Moulick, B. Chowardhara, and S. K. Panda, "Agroecotoxicological Aspect of Arsenic (As) and Cadmium (Cd) on Field Crops and its Mitigation: Current Status and Future Prospect," in Plant-Metal Interactions, ed: Springer, 2019, pp. 217-246.

[25] P. Purohit, "Small hydro power projects under clean development mechanism in India: A preliminary assessment," Energy Policy, vol. 36, pp. 2000-2015, 2008

Ijaz ur Rahman is a postgraduate researcher at United States Pakistan Center for Advanced Studies in Energy at University of Engineering and Technology Peshawar, Pakistan. He is studying Energy Management and Sustainability at MS level after doing his undergraduate degree in Mechanical Engineering. His research interest include finding ways to maximize the social and economic benefits of the distributed energy systems with an end goal of poverty alleviation through sociotechnical models. This paper is a part of his Masters degree research studies.

International Journal of Engineering Works
ISSN-p: 2521-2419
ISSN-e: 2409-2770
Vol. 6, Issue 11, PP. 414-419, November 2019
https://www.ijew.io/
https://doi.org/10.34259/ijew.19.611414419

Feasibility Analysis of Green Technologies For Residential Buildings

Tayyaba Sony[1], Muhammad Jamal Farooq[2], Adan Zahid[3], Uzair Muhammad[4], Haseenullah[5]
[1,2,,3,4,5] Department of Electrical Energy System Engineering, US-Pak Center for Advanced Studies in Energy (USPCAS-E), UET, Peshawar, Pakistan
Tayyaba_sony@yahoo.com[1], engr.jamal.farooq@gmail.com[2]
Received: 17 October, Revised: 25 October, Accepted: 29 October

***Abstract*—** Pakistan is suffering from acute energy crisis since last decades. There is a big gap between power supply and demand and the shortfall is about 5000 MW per day. This shortfall is badly affecting all sectors which consumes electricity like residential, commercial, industrial and agriculture etc. Among the total energy about 43 % is consumed by the residential buildings. This high consumption needs to be minimized so finding desirable and effective ways to minimize the energy consumption of existing residential buildings and to propose strategies that are energy efficient is the aim of this research work. Each household has its own energy consumption pattern which is affected by the socio-economic conditions, number of occupants, the age group and gender. Thus, figuring out a generalized procedure for the transformation of residential buildings into the energy efficient building becomes very challenging. The proposed methodology aims at optimizing the energy consumption of residential buildings and finding a generalized procedure that can be adopted to transform any residential building into a low energy building. The test site selected for the proposed work is situated at canal town Peshawar which is a residential building. To lower down the electricity consumption of the selected building different insulation materials and energy efficient equipment's along with different retrofitting strategies are analyzed in this research work. The financial analysis is also carried out based on the KWH savings, with an improvement in energy consumption up to 30%.

***Keywords*—** LEB, Retrofitting, Energy Efficiency, Green technologies.

I. Introduction

Energy is essential to any society because of its critical role for social and economic development besides the improved standards of living in the world [1]. Due to increasing population of the world the global demand of energy is rapidly increasing as the time is passing. Pakistan is also facing the severe energy crisis since last decade. This energy crisis has seriously hampered the economic growth and development progress.

In Pakistan there is shortfall of electricity, there exists big gap between supply and demand that has caused load shedding in rural and urban areas. There is a need of total of 20,223 MW of electricity per day in the country while the supply is less than the demand which is 15,700 MW per day, hence the country is facing a shortfall of approximately 5000 MW per day due to inadequate supply [2]. Due to this shortfall the electricity load shedding occurs for about 8-10 hours in urban areas and 15 hours in rural areas, which is badly affecting all spheres of life [3]. To overcome this shortfall we need to both increase the generation of energy as well as optimize the energy consumption. Every year the national demand for the electricity increases and hence the associated cost also increases, there is a need to minimize the existing energy consumption in an efficient way, so that the end consumer will fulfill their energy requirements at minimum price.

In Pakistan, electricity is consumed by various sectors as shown in fig 1. As it is can be seen from the figure that most of the energy is consumed by building sectors, which is about 43%. This high consumption of electricity needs to be minimized. There are different building types in Pakistan i.e. industrial, commercial and residential etc [3]. In this propose research work, the aim is to analyze the energy consumption of existing residential buildings and to propose strategies that are energy efficient so that the energy consumption is minimized. In residential buildings the average annual energy consumption is approximately 150-230kwh/sq.-m [4]. There is no standard characterization of Residential buildings with respect to energy ratings in Pakistan. National energy efficiency and conservation authority (NEECA) and Pakistan Engineering council (PEC) has devised codes for commercial buildings not for Residential buildings.

Most of the Residential buildings are built based on poor energy conservation based on space heating requirement. There is a need for an investigation, which can provide some mechanism to characterize the energy profile of residential buildings w.r.t space heating requirements and a mechanism to somehow generalize it based on some pre-defined parameters.

The cost of Retrofitting of a Residential building to transform it to energy efficient building is very high, so the proposed strategy aims to reduce the annual space-heating requirement based on energy efficient technologies and also calculating the payback period of the project. In the proposed study, I have considered the analysis of a residential house of covered area of 138sq-m consisting of two bedrooms, two washrooms, kitchen and six occupants. The house on average requires the annual electricity consumption of 2548Kwh units (data collected from actual utility bills).

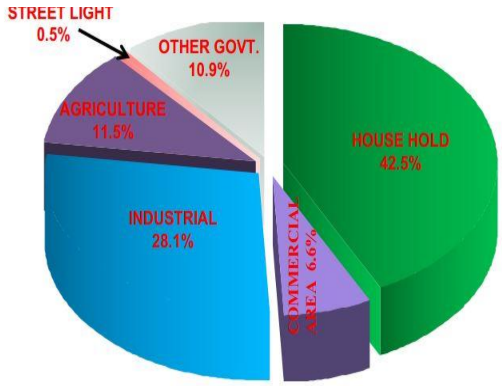

Figure 1 Consumption of electricity in various sectors of Pakistan [3]

II. Energy Efficient Buildings

Energy Efficient buildings are those buildings that consumes considerably less energy than normal buildings. Energy efficient buildings are mostly based on passive techniques such as building site selection, orientation, windows number and position, material used in façade of the building, skylights, green roofing, shading devices [5]. To remodel or reconstruct an existing building into an energy efficient building is called retrofitting. Retrofitting of an existing building costs more than building a new one. A fundamental goal of retrofitting is to reduce the energy requirement for space heating without effecting ambience requirements to achieve human comfort[6]

III. Net Zero Energy Buildings

A net zero energy building is a building that has zero energy consumption and carbon dioxide annually [6]. Residential or commercial building may fall under net zero energy buildings if they have significantly minimized their energy requirements by adopting energy efficient technologies or through renewable energy technologies.

IV. eQuest Software

The eQuest software is an open source software. It calculates the buildings total energy consumption on hourly, monthly and annual basis.

V. System Components

A. Insulation Material

Insulation of the building has significant potential to minimize the consumption of electricity. In first step the building was analyzed for two different insulation types i.e. polystyrene and polyurethane the results were in favor of polystyrene as described below. Thermally insulated model consists of polystyrene foam with different arrangements that has applied to the rooms. There are basic three models designed with polystyrene, which can be incorporated in the analysis phase so that the results from the analyses can be different from one another. These three models have insulations with on different locations, i.e. insulation on the outer face of the wall which is termed as external insulation, insulation on the inner face of the wall which is termed as internal insulation and the combination of the internal and external insulation which is termed as mixed insulation.

B. Energy Efficient Appliances

By incorporating the energy efficient appliances, the energy consumption can be definitely low down as compared to the conventional appliances, so in this model the energy efficient appliances were considered and reduction in the energy consumption was noticed.
In this model the tube lights are to be replaced with energy saver bulbs or LED, conventional AC with inverter type etc.

C. Combination of Insulation Material And Energy Efficient Appliances

In this technique as the name suggests combination of insulation that is polystyrene and energy efficient appliances was proposed. A significant reduction in consumption of electricity was observed.

VI. System Configurations

The residential building was analyzed for different energy efficient strategies in the form of different scenarios. All these scenarios are discussed below.

A. Scenario-I Insulation Using Polystyrene

In this model polystyrene is used against the 8-inch brick having 0.25 inch mortar on both sides. This insulation arrangement is same both for wall and roof. Arrangement is given below in table 1.

Table 1 Wall material using Polystyrene

1	Cement mortar 0.25 inch
2	Common brick 8 inch
3	Polystyrene 3 inch
4	Cement mortar

B. Using Energy Efficient Appliances

As the conventional electric appliances consumes a significant amount of electricity so it is better to use energy efficient appliances as these appliances definitely reduce the consumption of electricity. The tube lights which are in use in the house to be modeled is of 60 watts that can be replaced by energy saver that consumes only 25 watts, similarly Air condition which is in operation in the house is conventional AC that is to be replaced with inverter type AC to reduce consumption of electricity. All other conventional appliances can also be replaced with energy efficient appliances. The e quest software manipulates all these information of energy efficient appliances in the form of W/sq. ft., which is reduced in case of using energy efficient appliances.

C. *Scenario-III Insulation using 1-inch Internal Polystyrene with EEA*

In this model internal insulation of polystyrene that is 1 inch is applied on the wall and roof and also using energy efficient appliances. The arrangement of insulation for wall is given below in table 2.

TABLE 2 WALL MATERIAL USING INTERNAL 1-INCH POLYSTYRENE

1	Cement mortar 0.25 inch
2	Common brick 8 inch
3	Polystyrene 1 inch
4	Cement mortar 0.25 inch

D. *Scenario-IV Insulation using 1.5 inch internal polystyrene with EEA*

In this model one and half inch polystyrene is applied internally on the wall and roof of the building and also using energy efficient appliances. The composition of the wall is given in the table 3 below.

TABLE 3 WALL MATERIAL USING 1.5-INCH POLYSTYRENE INTERNALLY

1	Cement mortar 0.25 inch
2	Common brick 8 inch
3	Polystyrene 1.50 inch
4	Cement mortar 0.25 inch

E. *Scenario-V Insulation using 3 inch internal polystyrene with EEA*

In this model 3-inch polystyrene is applied internally to the wall and roof and also considering energy efficient appliances in the rooms. The composition of the wall is shown in the table 4 below.

TABLE 4 WALL MATERIAL USING INTERNAL 3-INCH POLYSTYRENE

1	Cement mortar 0.25 inch
2	Common brick 8 inch
3	Polystyrene 3 inch

F. *Scenario-VI Insulation using 3 inch polystyrene external with EEA*

In this model three-inch insulation is applied externally and also using energy efficient appliances. In external insulation polystyrene is applied before brick. The composition of wall is shown in table 5 below.

TABLE 5 WALL MATERIAL USING EXTERNAL 3-INCH POLYSTYRENE

1	Cement mortar 0.25 inch
2	polystyrene 3 inch
3	Common Brick 8 inch
4	Cement mortar 0.25 inch

G. *Scenario-VII Mixed Insulation with EEA*

In this model both internal and external insulation is applied which is termed as mixed insulation. In this type of insulation polystyrene is applied on both sides of the brick and then covered by cement mortar. Also energy efficient appliances are used along with mixed insulation. The wall composition is as shown in table 6 below.

TABLE 6 WALL MATERIAL USING MIXED INSULATION

1	Cement mortar 0.25 inch
2	polystyrene 3 inch
3	Common Brick 8 inch
4	polystyrene 3 inch
5	Cement mortar 0.25 inch

VII. RESULTS

This section deals with results obtained as simulations and analysis were done for seven different scenarios. All these results are briefly described below in the form of different scenarios.

A. *Scenario-I Insulation using polystyrene*

When polystyrene is applied on the walls and roof of the rooms the total annual energy consumption reduced to 1965 kWh. The simulation results shows almost 23% decrease in total energy consumption per year. The following figure 2 shows the comparison between baseline case and scenario-I.

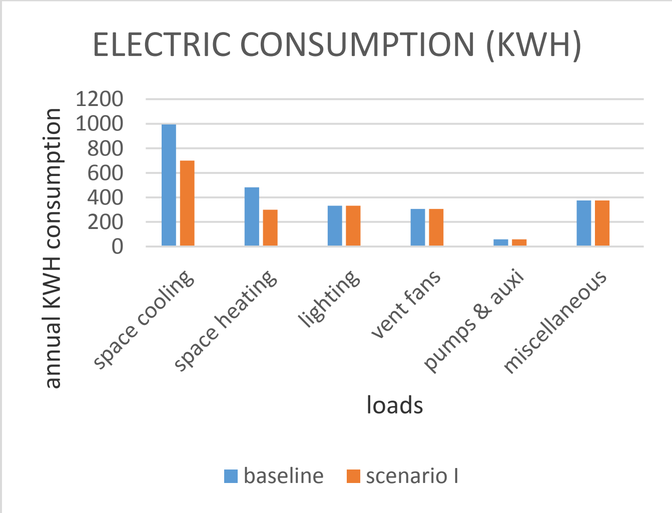

Figure 2 Comparison between Baseline and Scenario-I

B. *Using Energy Efficient Appliances(EEA)*

When Energy Efficient Appliances (EEA) were proposed, the total annual energy consumption reduced. The consumption of energy reduced to 1971 kWh units. The following figure 3 shows the comparison between baseline case and scenario-II.

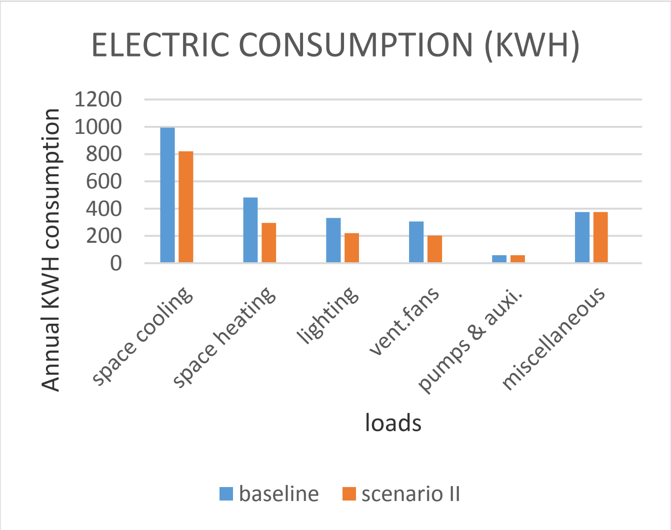

Figure 3 Comparison between Baseline and Scenario-II

C. Scenario-III Insulation using 1-inch internal polystyrene with EEA

When one inch expanded type of polystyrene was applied internally and also proposing EEA
The total consumption of electricity reduced to 1789 Kwh units. The following figure 4 shows the comparison between baseline case and scenario III.

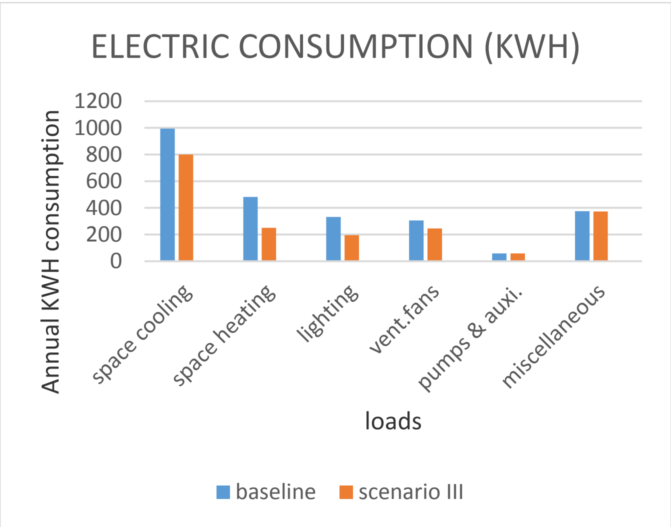

Figure 2 Comparison between Baseline and Scenario-III

D. Scenario-IV Insulation using 1.5 inch internal polystyrene with EEA

In this model when one and half inch expanded type of polystyrene was applied along with considering EEA the total consumption of electricity reduced to 1724 kWh units. The following figure 5 shows the comparison between baseline case and scenario IV.

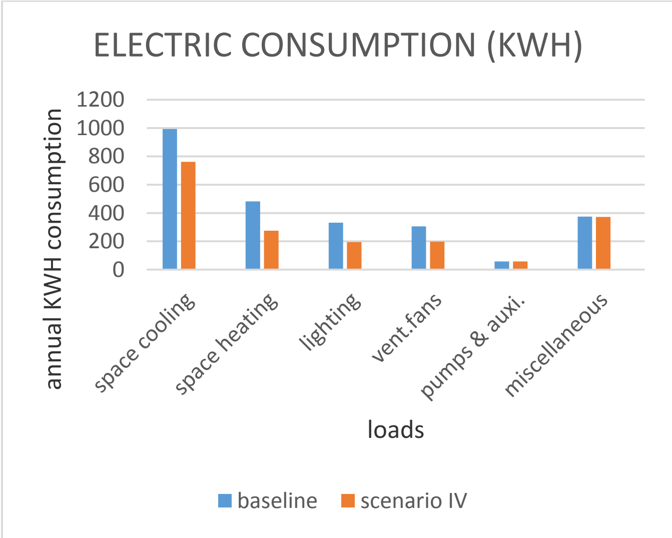

Figure 5 Comparison between Baseline and Scenario-IV

E. Scenario-V Insulation using 3 inch internal polystyrene with EEA

When three inch expanded type of polystyrene was applied along with considering EEA, the consumption of electricity reduced to 1681 kWh units per year. The energy consumption decreases as the thickness of the insulating material increases. The following figure 6 shows the comparison between baseline case and scenario -V.

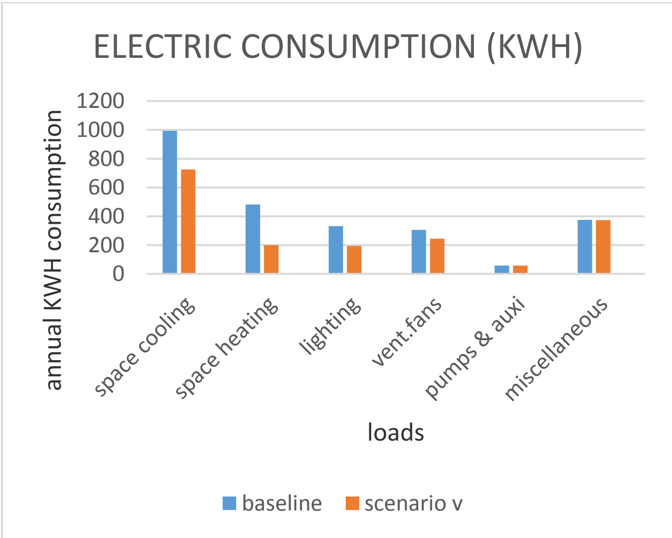

Figure 6 Comparison between Baseline and Scenario-V

F. Scenario-VI Insulation using 3 inch polystyrene external with EEA

As the 3-inch polystyrene gives the best results among all other, so in this model external insulation is done for 3 inch of expanded type of polystyrene which gives the best result. The energy consumption is the lowered to 1600 kWh units in this scenario. In this case about 34% energy saving is achieved. The following figure 7 shows the comparison between baseline case and scenario-VI.

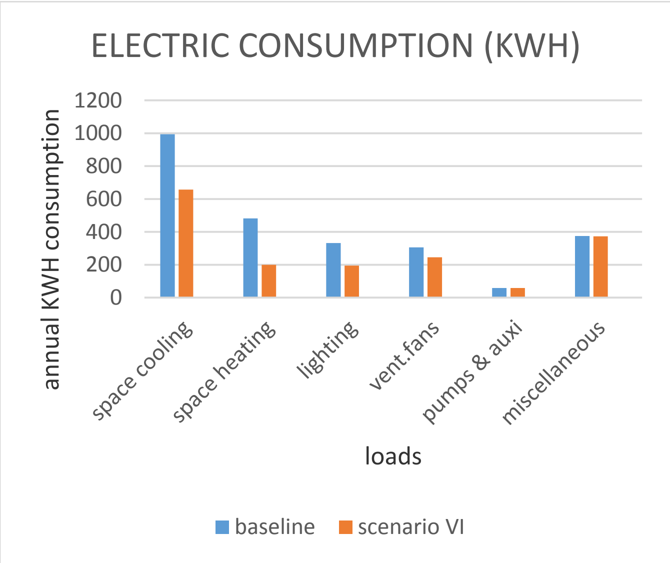

Figure 7 Comparison between Baseline and Scenario-VI

G. Scenario-VII Mixed Insulation with EEA

The total electricity consumption per year has been reduced to 1588 kWh units. This model gives outstanding results but it costs too much. The following figure 8 shows the comparison between baseline case and scenario-VII.

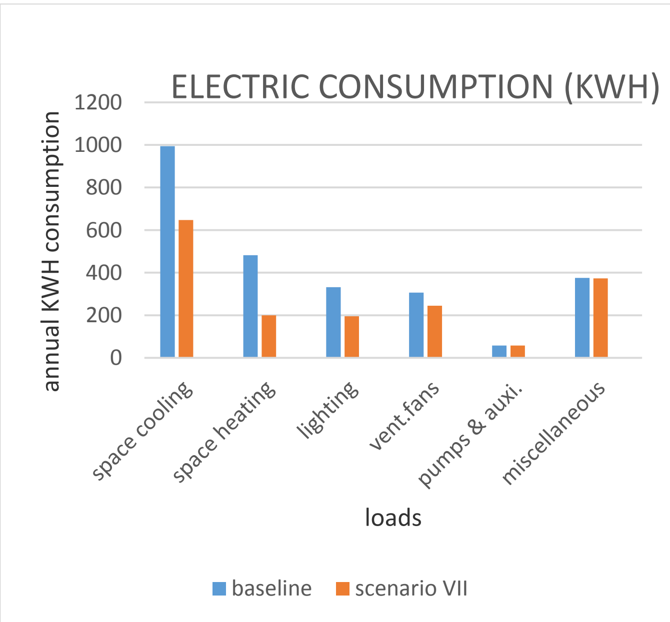

Figure 8 Comparison between Baseline and Scenario-VII

VIII. Comparison

In this section the results of the seven different scenarios with baseline are compared. The comparative graph of all the scenarios with baseline is shown below in figure 11 in the form of line graph. The Y-axis shows the total annual KWH consumption of electricity while X-axis shows various scenarios and the baseline case. A gradual reduction in consumption of electricity can be seen from the graph at each scenario.

IX. Financial Analysis

As the comparative graph showed that scenario seven has the most least electricity consumption. The graph did not provide about the viability and cost of the different scenarios, so detailed financial analysis was conducted to see which scenario is feasible and viable under a 20 years project life. The following table 7 shows the total annual units saved and the payback period of each scenario.

TABLE 7 PAYBACK PERIOD OF DIFFERENT ENERGY EFFICIENT STRATEGIES

S.no	Energy Efficient Strategies	Total cost (PKR)	Units Saved (KWH)	Payback Period (years)
1	Polystyrene (3-inch)	109200	583	14
2	Energy Efficient Appliances	100000	577	13
3	Internal (1-inch) polystyrene + EEA	138220	759	14
4	Internal (1.5-inch) polystyrene +EEA	154600	824	14
5	Internal (3-inch) polystyrene + EEA	209200	867	19
6	External (3-inch) polystyrene + EEA	151000	948	12
7	Mixed polystyrene + EEA	360200	960	31

Conclusion

To overcome energy crisis of Pakistan either the generation of electricity needs to be increased or to adopt building design which consumes less amount of energy. First type of solution requires more resources while the second type needs public awareness to design buildings in such a way that it reduces the total consumption of electricity. This research work provided different optimization techniques to lower down the total electricity consumption of a residential building. Seven different scenario analysis is done in this work. Different optimization techniques discussed in this work were, insulation of polystyrene, use of Energy Efficient Appliances and then Energy Efficient Appliances were considered in combination with different thickness of polystyrene. Polystyrene was taken in different arrangements and in different thickness. Among all the scenarios the sixth scenario i.e. polystyrene (3-inch) external + EEA showed the best results in terms of energy savings as well as it was cost effective. Other models reduced the total consumption up to some extent, the mixed insulation model along with energy efficient appliances lowered down the amount of electricity consumption the most as compared to other models but the drawback in this model is that it costs too much, it is expensive so it is not recommended instead external insulation along with energy efficient appliances i.e. sixth scenario provided the best results, the consumption of electricity reduced to about 37% in this case and also the payback period is less as compared to other scenarios.

REFERENCES

[1] Rashid, Tanzeel-ur. *Energy Modeling and Policy Analysis of Pakistan's Residential Energy System*. Diss. University of Engineering and Technology, Taxila, 2016.

[2] K. kiani, DAWN NEWS, May 2017.

[3] Valasai, Gordhan Das, et al. "Overcoming electricity crisis in Pakistan: A review of sustainable electricity options." *Renewable and Sustainable Energy Reviews* 72 (2017): 734-745.

[4] Balaras, Constantinos A., et al. "Heating energy consumption and resulting environmental impact of European apartment buildings." *Energy and buildings* 37.5 (2005): 429-442.C. Balaras,

[5] Asimakopoulos, D. A., et al. "Modelling the energy demand projection of the building sector in Greece in the 21st century." *Energy and Buildings* 49 (2012): 488-498.

[6] Zhang, Tao, Peer-Olaf Siebers, and Uwe Aickelin. "Modelling electricity consumption in office buildings: An agent based approach." *Energy and Buildings* 43.10 (2011): 2882-2892.

International Journal of Engineering Works
ISSN-p: 2521-2419
ISSN-e: 2409-2770
Vol. 6, Issue 12, PP. 439-444, December 2019
https://www.ijew.io/
https://doi.org/10.34259/ijew.19.612439444

Analysis of Vehicle Accidents using Spatio-Temporal Tools in ArcGIS; A Case Study of Hayatabad, Peshawar

Muhammad Babar Ali Rabbani[1], Prof. Dr. Sher Afzal Khan[2], Dr. Qaiser Iqbal[3], Engineer Qamar Zaman[4]
[1,2,3,4] Sarhad University of Science & Information Technology, Peshawar
babaralirabbani@yahoo.com[1], hod.civil@suit.edu.pk[2], qi.civil@suit.edu.pk[3], qamar.civil@suit.edu.pk[4]
Received: 23 October, Revised: 11 Novemeber, Accepted: 20 November

Abstract— Identification of traffic accident spots play a pivotal role in planning of roads and application of effective strategies in order to minimize the traffic accidents. This study puts into use the spatial distribution of the traffic accidents scattered throughout the area using spatial analysis and statistical approaches. The purpose of this research study is to analyze the traffic accidents occurring in the Hayatabad area of Peshawar. The fundamental objective of this study is to detect accidents hotspot in an observed area by a complex statistical algorithm. A methodology was developed in ArcGIS 10.2 to analyze the spatial patterns of traffic accidents and to identify hotspots. This study has conducted NNHA spatial clustering method in CrimeSTAT for the identification of hotspot clusters for accidents points in ArcGIS. Moreover, based on the detected hotspots, spatio-temporal tool like Kernel Density Estimation (KDE) analysis was performed in Crime STAT to create a temporal map of RTAs hotspots in ArcGIS. A geostatistical method known as Kriging Interpolation method (KI) was also used to assess the results computed by KDE. The results indicated that the roundabouts located in this area are the major hotspot of accidents, which includes Bagh-e-Naran roundabout, Phase-6 roundabout, Tatara Park roundabout and Jamrud road. Comparison of KDE and KI was performed and it was found that KI outperforms KDE in identifying hotspots. It has been concluded that these hotspots lacked the basic traffic controlling devices, which are necessary for controlling the speed and converging or merging of vehicles at these locations.

Keywords— Accident hotspots, spatial analysis, clustering, kernel density estimation, kriging interpolation.

I. Introduction

Nowadays, accident is one of the essential leading causes of deaths worldwide. It is estimated that the Road Traffic Accidents (RTAs) is the 8th major cause of deaths worldwide in 2016 and is even surging to the top despite of modern use of preventive measures. Most accidents conclude in fatalities and severe injuries, which results in financial burden like medical costs, car damage and the injured are often left with permanent defects. Above 90% accidents take place in middle income or low-income countries [11]

According to a report published by [12] about 27,081 deaths occurred in Pakistan in 2017 due to RTAs, hence pushing Pakistan up to the rank of 104th country in the list of highest number of deaths due to the RTAs happen in any country. This constitutes of the total 15 deaths daily in Pakistan. It was also reported that the lives lost in RTAs exceeds than the lives lost due to terrorism in the same country. This abhorrent situation leads to the urgent need for awareness in public about the compliance of traffic rules. One of those safety provisions to be provided is to pinpoint the hotspots of RTAs. This can only be achieved by congregating the RTAs data of a certain area. About, 7000 RTAs takes place yearly in Pakistan reported to the Police stations in 2006, which has become an epidemic in the country [1]. Pakistan has seen a significant rise in accidents for the past 15 years, therefore, its evaluation has become an integral issue that is vital to be addressed [13]. According to the Global Status report on Health Safety by [12], Pakistan is regarded as a middle-income country with the majority of people are unable to afford the advanced pre-crash vehicle accident system, which includes anti-lock braking system and electronic stability control. Even Pakistan has no strict law for vehicles seat belt and there is an absence of statistics about the person's seat belt wearing ratio. Meanwhile, only 10% of the bike riders throughout the country uses helmet as a safety precaution. As an example, Karachi RTAs crash damage was assessed in terms of money damage. In collecting the data, most of the companies rejected to share their details of accidents, which puts a negative impact on the conclusions [7]. Crime STAT was put into application in order to pinpoint the highest crime happening spots. Similarly, Crime STAT can be efficiently used to detect other hotspot provided that the data is spatially located [8]. A study was conducted to assess the conventional analysis and statistical analysis called as Kernel Density Estimation, in which it was proven that results were identical [9]. A plethora of programmable applications are available for spatial analysis, which can be used for statistical analysis because they utilize specific algorithms irrespective of coding language hence visualizing akin results when plotted in ArcGIS [10]. It was found that ordinary KDE performs its analysis on counting the naturally occurring clusters, which is more efficient than the conventional tally count method. The majority of the clusters were found near a residential area, entertainment area, hotels and hospital area. It was also stressed that the implementation of spatial analysis for improving traffic safety is in its development stages. This industry needs new implementing methods, precise data collection using the modern intelligent transportation system to prevent the loss of valuable data, which can ensure precise results [18]. A research study was conducted in Manhattan Area in New York State using shapefile provided by New York GIS office, which successfully pointed out the point of clustered accidents using spatial and temporal tools available in 3rd party GIS-linked software. They proposed that spatio-temporal nature of accidents can efficiently be analyzed by the method of KDE [19]. KDE helps in estimating the traffic accident hotspots due to its ability to assess the land usage of an area as well as its ability to evaluate the current road system in real time [2]. In Western Australia, a spatial analysis was performed to detect heavy vehicle crashes. The analysis was performed using KDE method. It was expected that the clusters would be near to the Perth metropolitan area and the results also generated the same model, which proved the consistency in the results [4]. Kriging method is seldomly used as an evaluating technique but the Kriging method was found more superior and promising as compared to Kernel Estimation because the nature of autocorrelation in its algorithms. Another positive outcome that can be obtained using Kriging method is that instead of using the Personality Assessment Inventory (PAI) as a severity measure of the accident, Kriging method can be incorporated into the analysis and it can also produce akin results as of conventional method approach [16].

According to Pakistan Bureau of Statistics in 2018, accidents became a major nuisance in Pakistan. In 2018, the number of accidents taking place was the highest ever recorded, escalating to 11121 accidents. The trends of accidents became more dominant in the year 2014-2015 and has ever been on rise shown in Fig 1.

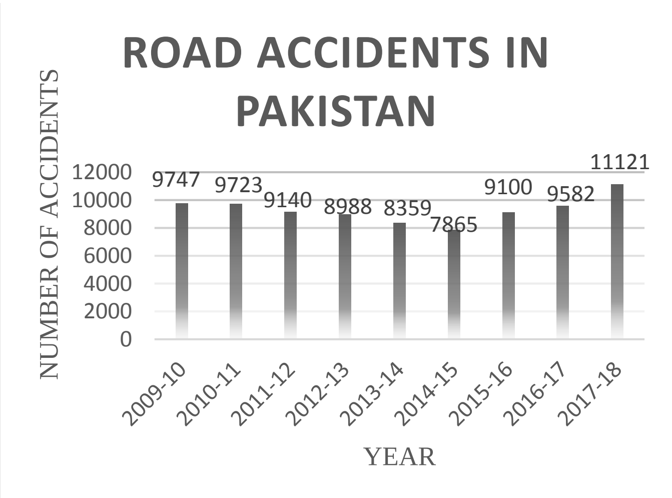

Fig 1: Roads Accidents counts in Pakistan by Pakistan Bureau of Statistics

The objectives of this study are:

1) To convert the raw textual data into numerical values in order to identify the highest frequency accident spots in Hayatabad area.

2) To analyze the accidents points and produce the most clustered accident areas.

3) To compare Kernel Density and Kriging results regarding accident hotspots.

II. MEHODOLOGY

ArcGIS operates using maps, which can easily be downloaded via its native option called Open Street Maps (OSM). Afterwards, hotspot analysis is performed to locate the different spots by various methods based on its diverse algorithms. Spatio-temporal tools like KDE method of analysis and KI algorithm is performed to identify accident hotspots.

A. Accident data collection:

Hayatabad area is situated in the North West of Peshawar, which is the capital of the Khyber Pakhtunkhwa province of Pakistan. Traffic accident analysis and its staggering results depend on the correct input of accidents location and the accident coordinates. In order to achieve the reliable results, it is necessary to collect the data from authentic accident data collecting agency, which is maintained by the area's traffic police department and the local police stations.

Fig 2 data indicates the number of accidents with respect to the accident type. These graphs signify the numbers of accidents leading to death, accidents resulted in injuries and non-fatal accidents. The data collected is of the past 10 years, that is, from 2009 to 2018.

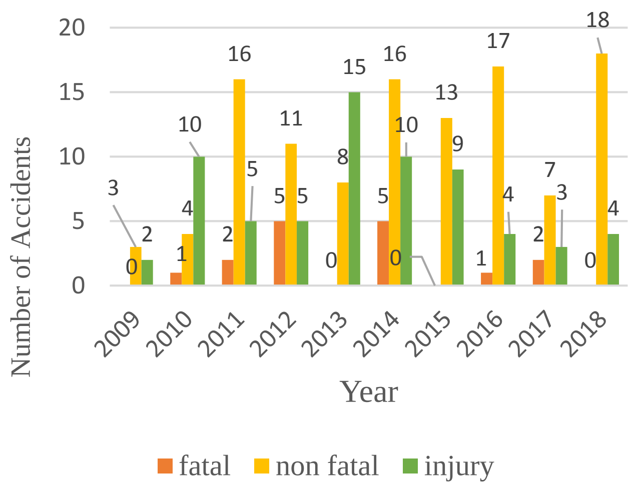

Fig 2: Overall accidents taking place in past 10 years

B. Accident data analysis approach:

Hotspot analysis:

Nearest Neighbor Hierarchical Analysis (NNHA) for spatial clustering estimation is a method used conveniently for analyzing the spatially distributed data. It determines the cluster of accidents on the bases of any two nearest distance accidents taking place in the studied phenomenon. The user must identify a value for a fixed distance, which can marginally affect the outcomes of the result because it becomes more of a subjective rather than objective oriented. The unique advantage of NNHA is that if the weight density and the intensity of the traffic accident is known, the risk analysis of nearby traffic accident spots can also be assessed and it can detect risky areas, which is called as risk adjusted NNHA. This method can also be performed using SANET and other spatial analyst tools [15].

Kernel Density Estimation:

This method is used to detect accidents points and then it calculates the density using numerical statistical algorithms, hence the riskiest areas are detected in an area under consideration. In other words, this method underlying principle is that it defines the density of the nearest neighboring accident points by creating density and then calculating the distance of another accident from the initial reference accident point. Finally, combining the values from highest frequency to lowest of each point to that reference point. The KDE algorithm is shown below using (1), which was formulated by [14]:

$$f(x, y) = \frac{1}{nh^2}\sum_{i=1}^{n} K \ \binom{di}{h} \ldots . (1)$$

Where K is the kernel constant and di is distance among the accident points from the *i*th point of any under the observation point of accident, n is a number of points and h is kernel width. There are two methods to determine the density, one is conventional and the other is a kernel. The former creates a large number of arbitrary mesh cells and perform its analysis while the later one creates a bandwidth of a user defined value then a circular area of known magnitude from highest to lowest frequency is encircled and finally a numerical analysis is performed [20].

Kriging Interpolation Method:

Kriging is also used for spatial interpolation. Kriging method is sometimes called as a smoothening technique. The underlying concept behind the kriging method is that the outputs are the weighted mean of the data instead of density in KDE. The weighted pattern is predicted in such a way that the weighted average is different to every point and a lag distance is predicted between the known point and predict point. It can account for the missing points that KDE might have left due to the overlapping of some points. Kriging is useful because it discourages the repetition of the points if they have similar coordinates. The mathematical form, given by [5] of kriging model is stated below in (2).

$$\mathrm{Z}(x) = m\ (x) + \sum_{i=1}^{n} \lambda\mathrm{i}\ [\mathrm{Z}(x_i) - m(x_i)\ ] \ldots\ldots . (2)$$

Where,

λi is a Kriging weight allocated to $\mathrm{Z}(x_i)$ for prediction of accidents frequency at a location where $\mathrm{m}(x)$ and $\mathrm{m}(x_i)$ are the predicted values of the variables $\mathrm{Z}(x)$ and $\mathrm{Z}(x_i)$, at any location x.

III. Results and Discussion

A. Hotspot Analysis:

Nearest Neighbor Hierarchical Analysis (NNHA) performance is based on the number of simulations and minimum clusters to be needed in the output. NNHA determined the risky areas for the accidents using the police provided data record of accidents.

NNHA is executed using the radius as Nearest Neighbor distance, keeping the search radius in the middle. Minimum cluster points were selected as 10 and the units of those clusters were selected in Miles as shown in Table 1. Simulations runs were selected as 30. Higher the simulation runs, higher will be the accuracy of the results. Cluster identification output file are saved in convex hull shapes and ellipses.

Table 1: Risk adjusted Nearest Neighbor Hierarchical

Risk adjusted NNHA		
Name	***Risk adjusted NNHA***	***Fixed distance NNHA***
Search Radius	Medium	10
Minimum points per cluster	10	10
Units	Miles	Miles
Simulation runs	30	40
Number of Accident points	196	196

NNHA is vital for further analysis due to the fact that this step of analysis indicates the riskiest roads in an area, thereby, enabling the researchers to know about the hotspots in further steps of this analysis. In other words, this step is also a check for statistical analysis if the hotspot were not clustered at these riskiest roads.

The riskiest areas in Hayatabad are identified at different locations by blue ellipses as shown in Fig 3. The riskiest area is Bagh-e-Naran round about, second risky area is Jamrud Road and Hayatabad entrance road came third riskiest area in this method for accidents to happen, Fig 3

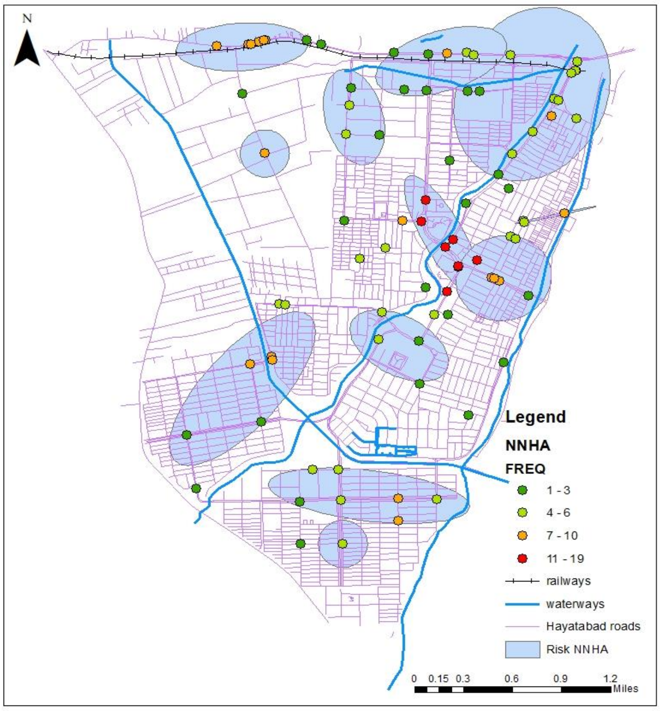

Fig 3: Hotspot identification by NNHA

B. *Kernel Density Estimation:*

The KDE spatial analyst tool is a powerful tool when density estimation is required. KDE has shown Bagh-e-Naran roundabout as a potential risk for accidents. Bagh-e-Naran roundabout and Tatara Park roundabout are near, it they both were regarded as a major hotspot. Here Phase-6 round about is regarded as a cold spot with 95% confidence results and standard deviation range of 9.5-12.7 shown in Fig 4. Jamrud road linking to the Industrial Estate road is also a major hotspot as shown by spatial analyst tool of KDE. Table 2 shows the parameters selected for analysis in CrimeSTAT and its visualization in ArcGIS.

Table 2: KDE parameters selected for analysis

Kernel Density Estimation in Crime STAT & ArcGIS	
Name	***Kernel Parameters selected***
Kernel Estimate method	single
Interpolation method	normal
Bandwidth type	adaptive
Minimum sample size	100
Area (units)	square miles
Output Density	absolute densities
Output cell size	15.386
Search Radius	50

Figure 4 indicates the hotspot with red color. The road accidents are more clustered towards the roundabout roads of the area.

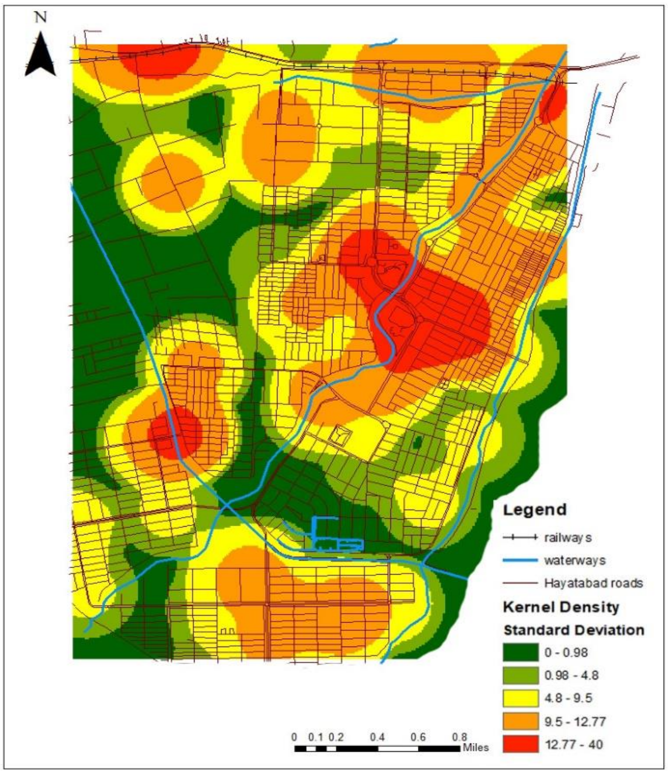

Fig 4: Kernel Density Estimation of accident hotspots

C. *Kriging Interpolation Method:*

The estimation of output of Kriging is more visually user friendly and easy to interpret. Besides Bagh-e-Naran round about an essential hotspot, Kriging has combined Tatara Park round about as one body and identified these locations as one body of the hotspot. The results predicted by the KDE and KI methods are marginally different from each other, therefore, indicating the need for a more accurate method to be implemented for traffic accidents hotspot identification. This result difference does not indicate the discrepancy in any other method but this difference has its own place in the analysis due to the reason that each method is correct on its statistical algorithmic computation. Table 3 shows the parameters for Kriging Interpolation

Table 3: Kriging parameters for analysis

Kriging Interpolation in CrimeSTAT & ArcGIS	
Name	***Kriging Parameters selected***
Number of points in radius	12
Kriging model	Universal
Search radius	Variable

Jamrud Road was detected as second hotspot but its standard deviation was marginally less than the Bagh-e-Naran round about hotspot and Tatara Park round about. Phase-6 round about was regarded as a cold spot by Kernel density because of the repetition of same coordinates, which Kriging treats as one point as seen in below Fig 5

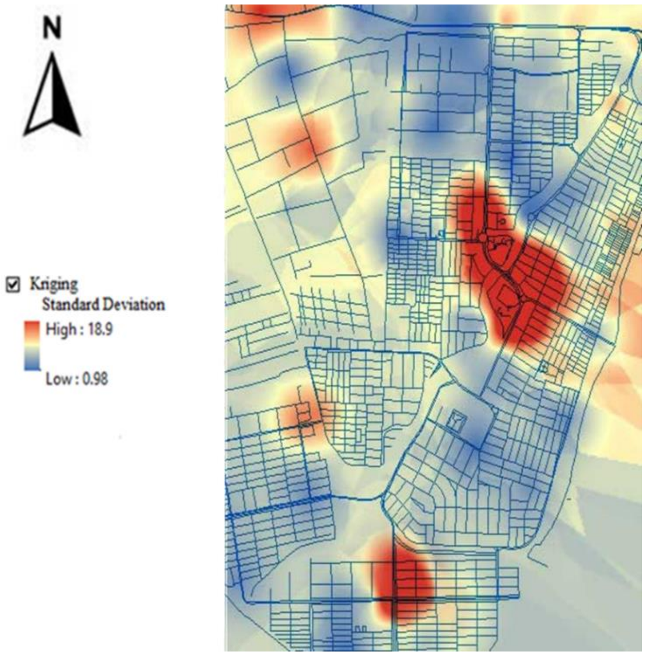

Fig 5: Kriging Interpolation output of accident hotspots

D. Comparison of Kernel Density and Kriging Interpolation:

These two methods are different in analysis techniques, difference in algorithm and produced marginally different results in hotspot detection. Therefore, the comparison of these two methods is essential. The mathematical comparison is performed using an equation known as Prediction Accuracy Index (PAI) used initially by [3]. This equation is the ratio of percentage of crashes occurring inside any hotspot to the percentage of length covered. This (3) was previously used in crime investigation mapping to identify the hotspots by [17], [16] and [6].

$$PAI = \frac{\frac{n}{N} * 100}{\frac{m}{M} * 100} \; .... \; (3)$$

Where,

n is the number of accidents in a hotspot, N is the total number of accidents, m is defined as the length of road inside a hotspot and M is the overall length of roads in area consideration. The numerator is regarded as the Hit rate and denominator as the Length covered.

The higher value of PAI shows the power of a certain method to identify riskiest accident's location in a proportionally smaller area, which can help the traffic agencies to introduce economical accident prevention resources. Evident from the Table 4, KI method outperforms the KDE for hotspot detection. Kriging method is often neglected for analysis purposes; however, it can be used as a promising alternative to the Kernel method.

Table 4: PAI comparison of KDE and Kriging Method

Kernel Density versus Kriging					
Kernel Density Estimation					
Accident inside hotspot	Total Accidents	Length of Road (km)	Length of hotspot (km)	Area (km^2)	PAI
15	196	312	20	24	1.19
Kriging Interpolation					
43	196	312	50	24	1.36

CONFLICT OF INTEREST

The contents of this study are free from plagiarism and therefore the study is original and is not copied from anywhere. Previous work of original authors has also been referenced.

CONCLUSION

This study has concluded that:

- Hotspots are mostly clustered at roundabouts in Hayatabad area.
- Accidents at these hotspots happen due to illegal parking at roundabouts, failure to observe traffic laws, illegal immediate turn instead of going around the roundabout in order to change the direction of the vehicle, point of converging and diverging at roundabout.
- Tatara park roundabout accidents happen due to the traffic generated by a park nearby, whose condition worsens in public holidays and two lanes of road is reduced to one lane.
- Bagh-e-Naran roundabout is a major hotspot, which is due to the merging and diverging of vehicles at roundabout and absence of traffic controlling devices.
- Jamrud road is also identified as a major hotspot due to the absence of observing traffic rules, improper road width decreased due to encroachment, poor road maintenance and unchecked operations of cargo and freight vehicle movement at this spot.
- The comparison of Kernel Density Estimation method and Kriging interpolation shows that the latter outweighs the former in the hotspot detection. Kriging interpolation, which is often ignored in the analysis, is capable of producing promising results.

Future work:

The future work should be focused on KDE of network street distance of the Hayatabad City instead of Euclidean distance and its results must be compared with Moran's I statistics. In order to assess the degree of correctness of both the implemented methods, regression models and Empirical Bayes model followed by Monte Carlo Simulation should be implemented.

RECOMMENDATIONS

It is recommended through this study that the Jamrud road carries freight transportation, therefore the its route should be changed to avoid it mixing with residential traffic. Tatara roundabout creates a lot of traffic congestion due to the presence of park near the roundabout, therefore, a dedicated road should be constructed that enters inside the park, which will avoid the vehicles to stop near the roundabout and therefore, the traffic lane would not be reduced. The presence of service road in the Phase-6 roundabout creates havoc during rush hour. As the service road opens in roundabout, this opening should be closed and the opening must be shifted at a considerable distance from the roundabout to deter road users to take opposite turns in the roundabout. Bagh-e-Naran roundabout needs to be installed tire busters' spikes to stop users to park their vehicles in the roundabout. Most accidents occur at this spot is due to the merging and diverging of vehicles, therefore, keeping in view the traffic volume at this roundabout, traffic controlling devices like traffic signals should be installed.

ACKNOWLEDGEMENT

The author is thankful for the police department Hayatabad and Traffic police department Peshawar headquarters for providing the accident data for the Hayatabad area. Author is thankful to his supervisors for their consistent help throughout this study.

REFERENCES

[1] Ahmed, Aizaza. "Road safety in Pakistan." National Road Safety Secretariat, Islamabad, 142, 2007.

[2] Chen, Yen-Chi. "A tutorial on kernel density estimation and recent advances." Biostatistics & Epidemiology 1.1, 161-187, 2017.

[3] Chainey, Spencer, and Jerry Ratcliffe. GIS and crime mapping. John Wiley & Sons, 2013

[4] Gudes, Ori, and Richard Varhol. "Using a spatial analysis approach to investigate Articulated Heavy Vehicle." Journal of Transport Geography 31, 64-71. 2015

[5] Goovaerts, Pierre. Geostatistics for natural resources evaluation. Oxford University Press on Demand, 1997.

[6] Hart, Timothy C., and Paul A. Zandbergen. "Effects of data quality on predictive hotspot mapping." Final report submitted to the National Institute of Justice 1, 2012.

[7] Kazmi, Jamil H., and Salman Zubair. "Estimation of vehicle damage cost involved in road traffic accidents in Karachi, Pakistan: a geospatial perspective." Procedia engineering 77, 70-78, 2014

[8] McCullagh, Michael J. "Detecting hotspots in time and space." ISG06 349 : 1-17, 2006

[9] Nakaya, Tomoki, and Keiji Yano. "Visualising crime clusters in a space‐time cube: An exploratory data‐analysis approach using space‐time kernel density estimation and scan statistics." Transactions in GIS 14.3: 223-239, 2010

[10] Prasannakumar, V., et al. "Spatio-temporal clustering of road accidents: GIS based analysis and assessment." Procedia-Social and Behavioral Sciences 21, 317-325, 2011

[11] World Health Organization. Global status report on road safety 2015. World Health Organization, 2015.

[12] World Health Organization. Global status report on road safety 2018. World Health Organization, 2018.

[13] Razzak, Junaid Abdul, et al. "A successful model of road traffic injury surveillance in a developing country: process and lessons learnt." BMC public health 12.1, 357.2012

[14] Rosenblatt, Murray. "Remarks on some nonparametric estimates of a density function." The Annals of Mathematical Statistics 832-837, 1956

[15] Shafabakhsh, Gholam Ali, Afshin Famili, and Mohammad Sadegh Bahadori. "GIS-based spatial analysis of urban traffic accidents: Case study in Mashhad, Iran." Journal of traffic and transportation engineering (English edition) 4.3, 290-299, 2017

[16] Thakali, Lalita, Tae J. Kwon, and Liping Fu. "Identification of crash hotspots using kernel density estimation and kriging methods: a comparison." Journal of Modern Transportation23.2, 93-106, 2015

[17] Van Patten, Isaac T., Jennifer McKeldin-Coner, and Deana Cox. "A microspatial analysis of robbery: Prospective hot spotting in a small city." Crime Mapping: A journal of research and practice 1.1, 7-32., 2009

[18] Jia, Ruo, Anish Khadka, and Inhi Kim. "Traffic crash analysis with point-of-interest spatial clustering." Accident Analysis & Prevention 121, 223-230, 2018

[19] Romano, Benjamin, and Zhe Jiang. "Visualizing traffic accident hotspots based on spatial-temporal network kernel density estimation." Proceedings of the 25th ACM SIGSPATIAL International Conference on Advances in Geographic Information Systems. ACM, 2017.

[20] Rushton, G., and C. Tiwari. "Spatial filtering/kernel density estimation.", 359-364. 2009

Muhammad Babar Ali Rabbani, the author, is resident of Peshawar. He completed in bachelor degree of Civil Engineering from University of Engineering & Technology, Peshawar in 2013. The author is pursuing his master's degree in Transportation Engineering from Sarhad University of Science & Information Technology, Peshawar. This paper is his research study for the master's degree.

国际工程期刊
International Journal of Engineering Works
انجینیرنگ کاموں کا بین الاقوامی جرنل

International Journal of Engineering Works
ISSN-p: 2521-2419
ISSN-e: 2409-2770
Vol. 6, Issue 12, PP. 445-447, December 2019
https://www.ijew.io/
https://doi.org/10.34259/ijew.19.612445447

Comparative Review of the Factors Affecting the Performance of Solar Photovolatic System

Uzair Muhammad[1], Naveedullah[2], Haseenullah[3], Said Ali[4], Tayyaba Sony[5]
[1,2,3,4,5] USPCAS E UET PESHAWAR
uzair.uetpeshawar@gmail.com[1], naveedullah491@gmail.com[2]
Received: 26 October, Revised: 12 Novemeber, Accepted: 20 November

***Abstract*—**The increasing trend in the photvoltaic technology ask not only for efficient photvoltaic technology but also requires the best utilization of the solar power. As many factor effecting the performance of photvoltaic system such as Temperature, Dust depositon, Humidity, Tilt angle, wind speed. So a qualitative study is carried out to summarize the effect of these factors. Among all these temperature is the main culprit in degrading the performance of the Photovoltaic System. Due to dust deposition slightly reduce the open circuit voltage of the system while it significantly reduce the short circuit current and hence affecting the performance. Humidity has also negative impact on the performace of the PV system. Similar with increase in tilt angle the ability of the system to receive maximum irradiance decrease but it has the advantage of reducing the dust deposited on the photvolataic panel. Among all the parameters wind speed has positive impact on the performance of the system as it reduce temperature, dust deposition, humidity and hence improve the performance of the system

***Keywords*—** Photovoltaic System (PV), Temperature, Dust, Humidity, Tilt angle, Wind Speed

I. INTRODUCTION

The world is striving to look for energy resources which are environmental friendly, sustainable, efficient and reliable . Renewable energy is an option but its environmental dependency and low efficiency is one of the dishearting factor in using it. Among all Renewable Energy Resources, it has been seen that people have increased interest in solar energy due to their abundance and availability everywhere.In addition to the abundance and availability, it is also neeccessory to unitlize the solar energy efficiently which not only required the efficient photvolataic technology but also requires to take into account the factor which degrade the performance of solar photovoaltaic system.As photovoltaic system is exposed to many environmental paranmeter such as hot weather coniditon, dusty environment, humid weather condition, windy condition. The study of the these factor is essential to utilize the solar energy efficiently and increase the life of photvolatic system. In this paper a qualitative study is carried out to analys and study the effect of these parameter and give the users a qualitative knowledge of these parameter to use their photovoltaic system efficiently.

II. BACKGROUND

Photo voltaic technology is based on the conversion of light energy of sun to electrical energy. Its working principle is based on the famous Einstein's Photoelectric effect. Material mostly used in the Photovoltaic Technology is Silicon. The improvement in the conversion efficiency of silicon is noted up to 23% [1], which has result in the reduction of the solar photovoltaic technology cost and size; the material required for the 100-watt panel is less than that of the low efficiency, is one of the main reason of the increasing interest in PV technology along with other important reasons [2]. The output of the PV technology is not only based on the material conversion efficiency but also depends on the incident radiation, Temperature, Humidity, accumulated dust and the wind speed surrounding the PV panel [3].

The output generated by the PV panel is directly dependent on the solar irradiance absorbed by the PV panel in addition several other environmental parameter besides the internal conversion parameters [4]. As the PV plant is long run system and exposed to changing environmental conditions and different factors which influence the solar PV output and performance directly or indirectly and the life of the PV plant. The most important factors are temperature, humidity, amount of dust deposited on PV panel, and air speed surrounding the PV plant [5].

III. FACTOR AFFECTING THE PERFORMANCE OF THE PV SYSTEM

A. Temperature

The most important factor affecting the performance and life of the PV plant is temperature. The power output of the PV plant is reduced with the rise in temperature and it contribute more to the degradation of the PV plant than any other parameter and hence is the main cause of the reduced life of the PV plant [6]. With the increase in temperature the current of the PV plant increases along with the increase in voltage drop. The increase in voltage drop is more than the increase in current and hence the power, which is the product of current and voltage, get reduced and hence decreasing the efficiency of the PV panel. In [7] a relationship between the PV panel efficiency and temperature is given as:

$$\eta = -0.05Tm + 12.75 \qquad (1)$$

Where

$$Tm = Tamb + (NOCT - 20)E / 800 \qquad (1.1)$$

Tm= module temperature, NOCT= normal cell operating temperature; can be calculated according to the IEC standard method from equation (1) Based on the equation (1.1) characteristic of an arbitrary PV module is given in the figure. Which shows the variation of efficiency of pv module with the increase in temperature.

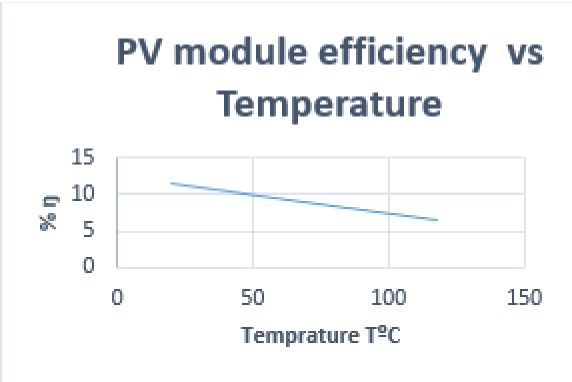

Figure III-1 Photovoltaic efficiency vs temperature

It was calculated that for every degree rise in temperature the efficiency of PV module will decreased by 0.006%. which is also an indicator of the degradation of the pv module.

In addition to this, with the rise in temperature there may be uneven distribution of temperature which may create hot spots in the PV panel and destroy some cells which enormously effect the panel and sometime the panel needs to be replaced and hence one can say the main culprit behind the degradation of the PV panel is temperature [8].

B. Humidity

The effect of humidity on the performance of PV panels in [9] by considering two cases: one is the effect of water vapors on the irradiance level and second is the ingression of humidity into the solar cell enclosure. The light may reflect, refract or diffract when it hit the water droplet due to which reduction in the direct component of solar irradiance may occur. The irradiance level is changed non linearly due to humidity. open circuit voltage (V_{oc}) of the panel is slightly affected by the irradiance level but significantly affect the short circuit current $I_{sc.}$ Due to humidity the power output of the PV plant and hence the efficiency drops [9]. In fig.1 and 2 the effect of humidity on irradiance and of the irradiance on the V_{oc} and I_{sc} is elaborated which is based on the case study carried out in Nigerian tropical climate.

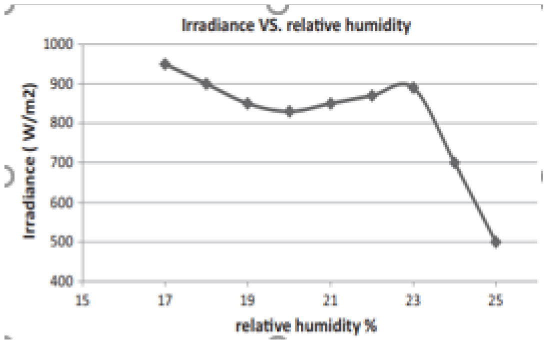

Figure III-2 Irradiance absorpotion vs relative humidity

In second case the water molecule may ingress into the cover of the pv panel and may not let the escaping out of the heat or reflect radiation in addition to the reduction in the irradiance level which increases the temperature and hence degrading the power output and efficiency of the panel [10].

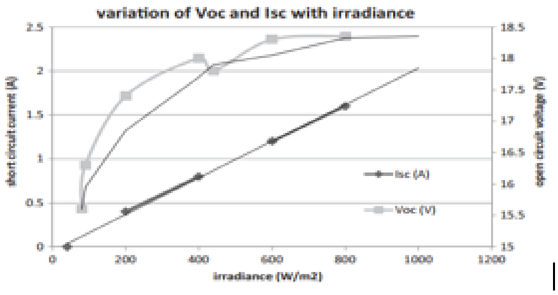

Figure III-3 variotion of Voc and Isc vs irradiance

C. Dust Depostion on Photovoltaic Panel

The amount of dust deposited on the PV panel significantly reduces the panel output power. The power loss is different for different amount of dust, different dust particle composition, dust particle optical properties, and uniformity and non-uniformity of the accumulated dust [11]. Non uniform dust deposition is more dangerous than the uniform dust deposition as it introduces the partial shading which adversely affect the PV performance [12].

In [13] it is observed that the transmittance of the PV panel cover is affected by dust deposition and transmission loss of around 0.05% was observed for every increase of $1g/m^2$ dust deposited, resulting in optical power loss and hence reduction in output current of the panel; as current is directly related to the received radiation, and hence the output power is reduced.

D. Tilt Angle

In [14] the effect of different tilt angle of the PV panel on dust deposition on the pv panel was investigated. It was noted that with the increase in tilt angle the amount of dust deposited reduces due to the gravity pull on the dust particle and hence reduction in the power loss due to reduction in dust deposition was noted but increasing tilt angle can reduce the irradiance absorption area of the panel which again lead to reduction in power of the panel. Therefore, the panels should be so placed that the dust accumulation is reduced and the irradiance absorption is not affected.

It is followed from the above discussion that the dust deposition has adverse effect on the PV performance. However, the only aiding effect of the dust deposited on the panel can be seen if the dust is uniformly deposited and composed of a material which absorb Infra-red radiation and heat, which could happen very rarely [15]. Therefor dust particle composition and their thermal and optical properties needs to be considered while studying the effect of dust deposition on the pv panels performance.

The reduction in output is also observed with the increase in tilt angle of the photovoltaic panel as it reduces the absorption of the irradiance, therefore it is necessary to find the best optimum tilt angle for the PV system. Increase in tilt angle have the advantage of reducing the soiling on the surface of panels.

E. Air Speed (Wind Speed)

In [16] the effects of air speed surrounding the PV plant has been studied. It was observed that The increase in wind speed within limit have a positive impact on the performance of the PV panel and counteract some of the harmful effects of the above discussed parameters such as temperature, humidity and dust deposition. As the humidity is inversely related to the wind speed so the humidity in the surroundings reduces and hence minimizing its adverse effect on the performance of PV panel. It is also observed that with the increase in air speed the dust deposition is also reduced and the rate of heat evacuation is also increased; reducing temperature of the pv panel and hence increasing the efficiency and output of the panel.

CONCUSLION

It is found that temperature greatly degrade the performance of PV plant by lowering the voltage and increasing the current, but the increase in current is less than the decrease in voltage so result in reduction of the output. It was also found that efficiency of the Photovoltaic plant doesn’t remain constant but greatly depended on environmental factors and greatly reduced due to temperature.

It was found that dust deposition also lowers the output of the panel by lowering the voltage up to 5% and greatly reduce the panel current. 20 to 30% reduction is noted in the current depending on the amount of dust deposited on the panel.

Humidity also affects the performance of the panel and reducing the photovoltaic plant output by reducing the absorption of solar irradiance by the solar panel and if ingress into the panel may result in increase in temperature which again reducing the output of the PV.

The reduction in output is also observed with the increase in tilt angle of the photovoltaic panel as it reduces the absorption of the irradiance, therefore it is necessary to find the best optimum tilt angle for the PV system. Increase in tilt angle have the advantage of reducing the soiling on the surface of panels.

REFERENCES

[1] Shariff, Farihah, Nasrudin Abd Rahim, and Hew Wooi Ping. "Photovoltaic remote monitoring system based on GSM." *2013 IEEE Conference on Clean Energy and Technology (CEAT)*. IEEE, 2013.

[2] Goswami, D. Yogi, et al. "New and emerging developments in solar energy." *Solar energy* 76.1-3 (2004): 33-43

[3] Singh, Girish Kumar. "Solar power generation by PV (photovoltaic) technology: A review." *Energy* 53 (2013): 1-13.

[4] Jordan, Dirk C., and Sarah R. Kurtz. "Photovoltaic degradation rates—an analytical review." *Progress in photovoltaics: Research and Applications* 21.1 (2013): 12-29

[5] Meral, Mehmet Emin, and Furkan Dincer. "A review of the factors affecting operation and efficiency of photovoltaic based electricity generation systems." *Renewable and Sustainable Energy Reviews* 15.5 (2011): 2176-2184.

[6] Bhalchandra, V. Chikate, and Y. A. Sadawarte. "The factors affecting the performance of solar cell." *International Journal of Computer Applications, International Conference on Quality Up-gradation in Engineering, Science and Technology*. 2015.bstrate interface,”

[7] Skoplaki , Elisa, and John A. Palyvos. "On the temperature dependence of photovoltaic module electrical performance: A review of efficiency/power correlations." *Solar energy* 83.5 (2009): 614-624

[8] Gwandu, B. A. L., and D. J. Creasey. "Humidity: a factor in the appropriate positioning of a photovoltaic power station." *Renewable Energy* 6.3 (1995): 313-316.

[9] Hussein, H. M. S., G. E. Ahmad, and H. H. El-Ghetany. "Performance evaluation of photovoltaic modules at different tilt angles and orientations." *Energy conversion and management* 45.15-16 (2004): 2441-2452.

[10] Kacira, Murat, et al. "Determining optimum tilt angles and orientations of photovoltaic panels in Sanliurfa, Turkey." *Renewable energy* 29.8 (2004): 1265-1275.

[11] Kaldellis, J. K., and M. Kapsali. "Simulating the dust effect on the energy performance of photovoltaic generators based on experimental measurements." *Energy* 36.8 (2011): 5154-5161

[12] Meral, Mehmet Emin, and Furkan Dincer. "A review of the factors affecting operation and efficiency of photovoltaic based electricity generation systems." *Renewable and Sustainable Energy Reviews* 15.5 (2011): 2176-2184.

[13] Tin Tai. "A review on photovoltaic/thermal hybrid solar technology." *Applied energy* 87.2 (2010): 365-379.

[14] Dirk C., and Sarah R. Kurtz. "Photovoltaic degradation rates—an analytical review." *Progress in photovoltaics: Research and Applications* 21.1 (2013): 12-29.

[15] Lineykin, Simon, Moshe Averbukh, and Alon Kuperman. "An improved approach to extract the single-diode equivalent circuit parameters of a photovoltaic cell/panel." *Renewable and Sustainable Energy Reviews* 30 (2014): 282-289.

[16] Sera, Dezso, Remus Teodorescu, and Pedro Rodriguez. "PV panel model based on datasheet values." *2007 IEEE international symposium on industrial electronics*. IEEE, 2007.

[17] Gökmen, Nuri, et al. "Investigation of wind speed cooling effect on PV panels in windy locations." *Renewable Energy* 90 (2016): 283-290.

IJEW 国际工程期刊 International Journal of Engineering Works انجینرنگ کاموں کا بین الاقوامی جرنل

International Journal of Engineering Works
ISSN-p: 2521-2419
ISSN-e: 2409-2770
Vol. 6, Issue 12, PP. 448-452, December 2019
https://www.ijew.io/
https://doi.org/10.34259/ijew.19.612448452

Analysis and Monitoring of 500 KV Grid; Innovation in Power, Control, and Optimization, using ETAP Software

Roman Fazal
Department of Electrical Engineering
University of Engineering and Technology, Peshawar
Received: 06 November, Revised: 17 Novemeber, Accepted: 20 November

***Abstract*—**In this research work, we have modeled and analyzed an existing 500 KV power station located at Shiekh Muhammadi, Peshawar in ETAP, using the actual real time data taken carefully for simulation in order to improve the voltage profile of the system using different techniques. It was revealed that voltage profiles of most of the buses are far below the nominal values with high losses causing considerable voltage drop at the bus. The optimization was very carefully performed by analyzing each simulation results in light of classical Newton Raphson technique in order to get the best possible optimized value without going through tedious iterations. Reactive power compensation using Static Capacitor Banks was used for voltage profile improvement of the power system. After performing optimization through above techniques, the voltages of all the buses including those with previously critical under voltage conditions, experienced boost in voltage to the nominal value with increased in real power supplied, thus improving the overall efficiency of the system.

***Keywords*—**Newton Raphson Technique, Voltage Profile, ETAP-Electrical Transient and Analyzer Program, Static Capacitor Banks, Distributed Generator.

I. Introduction

Energy plays vital role in economics development of a country. Though energy may be required in different forms but amongst all, electrical energy has dominance mainly due to ease in its conversion into any form of energy. Besides, it can be easily regulated, has superior flexibility, cleanliness and high transmission efficiency. These characteristics of electrical energy make it essential for the overall advancement and prosperity of the modern world [1].

The aim of this project is to derive a mechanism to analyze a complex power grid using Electrical transient analyzer program (ETAP). Power system analysis is the process of assessing the magnitude of line current and voltages during different types of disturbances. The magnitude of these parameters mainly depends on the internal impedances of generators and intervening circuits. The magnitude of fault current which are usually to the tune of tens of thousands of Amperes, must be precisely calculated in order to estimate the impact of mechanical and thermal stresses on operational equipments. These estimations are also helpful while selecting appropriate protective equipments i.e. circuit breakers, relays and isolators etc. and other allied devices of switchgears.

The process of determining the line voltages and currents in case of fault conditions is a tedious task; requires multifaceted mathematical calculations. These calculations get more and more complex as the number of busses in a grid increases. Thus mathematical calculations are only possible for simpler power system with lesser number of busses. However, dealing with large number of busses requires programming software to perform complex calculations.

It has always been a challenge for electrical engineers to first generate electrical energy and then transport it to the end users without compromising the efficiency, reliability and safety. Modern age electrical power system consist of complex integrated network where electrical energy is collected from generating units mostly located at remote areas and then transported through transmission and distribution system for ultimate utilization by consumers. The power demand of these consumers varies with time so as the load on power station thus the different parameters i.e. voltage and currents of different segments do not remain constant, rather varies from time to time[2].

Power system in its normal operating condition is analyzed and investigated by load flow studies. A typical electric power grid has a large number of buses and that can only be analyzed with computational tools. A variety of computational tools are available for load flow analysis.

In recent past, Pakistan Electric Power Company (PEPCO) has gone through frequent black outs in different part of the country due to power shortages. One of the reasons of these energy crises is the lack of technological capabilities in the field of power system analysis and monitoring as the existing power distribution system is mainly analyzed by FDR-ANA(Feeder Analysis) software [3].

Whereas, ETAP (Electrical Transient Analyzer Program) offers a state of the art Electrical Engineering programming arrangements with the help of which offline monitoring i.e. current flowing in every branch, power factor, active and reactive power flow of a power system, voltage drops, can be effective performed.

ETAP can also be handful in performing monitoring and real time simulation for energy management system. ETAP is fully equipped with the software solutions; required in an electrical system i.e. load flow, transient stability, relay coordination, open circuit and short circuit analysis, arc flash, conductor and cable ampacity and many more, by simply creating and editing one line diagram.

The above characteristics of ETAP make it suitable for any electrical power company [4,11,12].

II. Problem Statement

The power system selected for this study is 500 KV grid station located at Shiekh Muhammadi, Peshawar. It is being feed from Terbella through 500 KV transmission line. It consists of 9 Nos. of power transformers, 11 feeders, 22 circuit breakers, 26 current transformers, 12 potential transformers and total 16 Nos. of buses. The total load connected to all the 11 kV feeders is 21.614 MVA.

If a power system comprises of N Nos. of buses and R Nos. of Generators, than the total Nos. of unknown variables during power system analysis are $2\ (N-1)-(R-1)$ which requires $2(N-1)-(R-1)$ Nos. of equations to be calculated [5].

Keeping in view the foregoing, the unknown variables in case of power system under study are 30 Nos. which requires 30 Nos. of equations to be solved simultaneously, in order to calculate all the elements for analysis.

III. Newton Raphson Method

Newton Raphson method is one of the famous tools that can be used to solve these non linear equations. However, Newton Raphson method involved series of iterations starting with a suitable guess of unknown variables i.e. voltage magnitude, angle, active and reactive power etc. and then the process is again repeated by taking the most recent values found. The process of iteration continues until the values converge on a stopping limit [6].

After reviewing the literature, it has been revealed that carefully guessing the initial value and then properly analyzing the results can ease the process of iteration. It has been noted that a multiplying factor can also be used to speed up the process.

The above technique of analyzing the results and suggesting the new input value has been used in this research for optimization.

IV. Methods of Voltage Profile Improvement

Load flow study provides different elements of power system but the most important of all is the voltage profile i.e. the voltage value of each bus. If the voltage profile of the system varies greatly, it will results in undue reactive power, causing real power losses to increase and in most of the cases there is an excessive voltage drop leading to the under-voltage condition [6].

Literature review indicates that different methods have been devised to improve the voltage profile of the system each having its own benefit and constrains. The method adopted in this research work is static capacitor.

V. Static Capacitor Placement

The power system under study is in readial scheme. In such scheme, all the load are connected to single feeding unit mainly due to simplicity and low cost [7,9,10,13]. But the major drawback in this type of scheme is the fluctuation in system voltage that cause huge disturbance in voltage profile. As most of the load in distribution system are inductive in nature, thus causing deficiency of reactive power available to the load locally. Resultantly, the flow of current increases in distribution lines which reduces the voltage.

Capacitor on other hand is a reactive device with theoretically no power loss. Placing capacitor in the system balances the reactive power requirement causing reduction in reactive power supplied by the system which in turn reduces the current and ultimately improve the voltage profile of the system. It is important to place the capacitor at right location and to identify the optimum size of the capacitor.

VI. Problem Methadology

The power system under case study is 500kV Sheikh Muhammadi Grid station, which is located at Indus Highway near Badhaber, Peshawar. It consists of 9 Nos. of power transformers, 11 feeders, 22 circuit breakers, 26 current transformers, 12 potential transformers and 500kV incoming Transmission line from Tarbella power station. The total load connected to all the 11 kV feeders is 21.614 MVA. ETAP has been used for simulation purpose in this research work.

The SLD using actual real time data of 500kV Shiekh Muhammadi grid station constructed in ETAP for our research work is shown in figure 1.

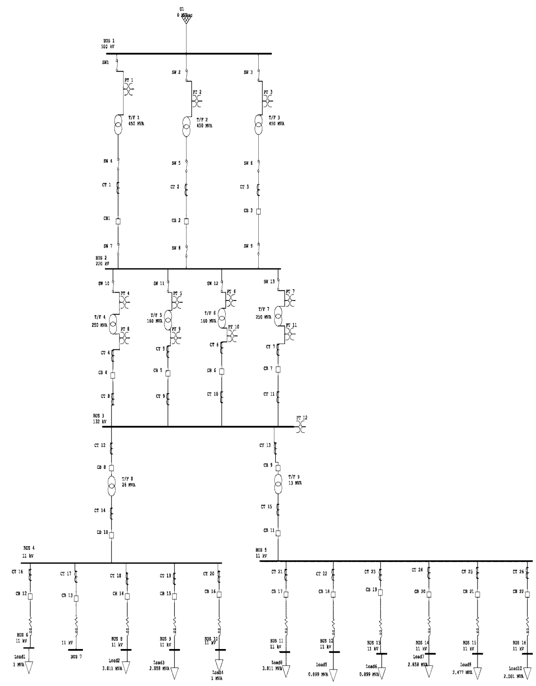

Figure 1: Single Line Diagram of Power System

VII. Simulation Results

The simulation results reveal that some of the load buses are in under voltage condition as depicted in Table 1. The under voltage condition is defined as "a condition in which an electrical equipment is receiving less than the required voltages". The under voltage condition occurs when the voltage level goes 90% of the nominal voltage.

TABLE 1: BUS VOLTAGE CONDITIONS

BUS ID	Nominal Kv	Type	Voltage kV	Under Voltage Condition
BUS 1	500	SWING	500	Not
BUS 2	220	Load	219.932	Not
BUS 3	132	Load	131.892	Not
BUS 4	11	Load	10.905	Not
BUS 5	11	Load	10.767	Marginal
BUS 6	11	Load	10.593	Marginal
BUS 7	11	Load	10.909	Not
BUS 8	11	Load	9.738	Critical
BUS 9	11	Load	8.751	Critical
BUS 10	11	Load	10.302	Critical
BUS 11	11	Load	9.933	Critical
BUS 12	11	Load	10.619	Marginal
BUS 13	11	Load	10.619	Marginal
BUS 14	11	Load	10.183	Critical
BUS 15	11	Load	10.277	Critical
BUS 16	11	Load	10.389	Critical

A. Load Flow Report

The power flows in different buses are given in Table 2.

TABLE 2: POWER FLOW STUDY OF EXISTING POWER SYSTEM

Bus ID	Voltage	kW Loading	kvar Loading	Amp Loading
BUS 1	500	18754	5015	22.42
BUS 2	219.232	18754	4993	50.95
BUS 3	131.892	18753	4958	84.91
BUS 4	10.905	7115	1861	389.4
BUS 5	10.767	11588	1919	629.8
BUS 6	10.593	927	0	50.54
BUS 7	10.909	0	0	0
BUS 8	9.738	2987	0	177.1
BUS 9	8.751	1664	709	119.3
BUS 10	10.302	877	0	49.16
BUS 11	9.933	3107	0	180.6
BUS 12	10.619	838	0	45.55
BUS 13	10.619	838	0	45.55
BUS 14	10.183	2449	0	138.9
BUS 15	10.277	2162	0	121.5
BUS 16	10.389	1785	0	99.19

B. Voltage Profile

Voltage profile is the graph showing the buses and its voltage levels. As discussed earlier in Table:1, the BUS 1, BUS 2, BUS 3 are not in under voltage condition therefore the graph of voltage profile consists of only BUS 4 to BUS 16 as shown in Figure 2.

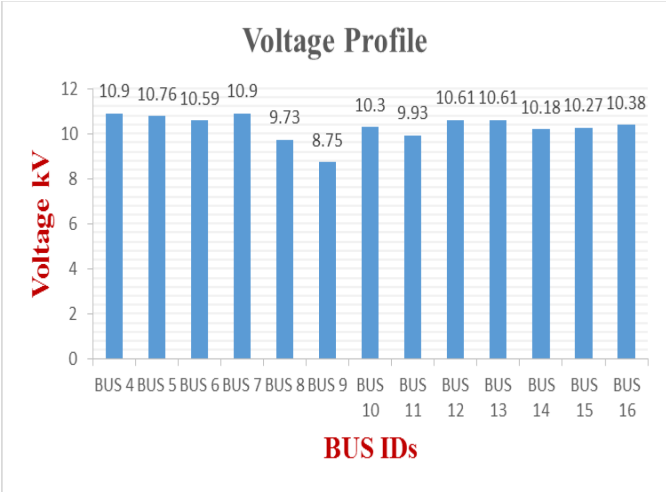

Figure 2: Voltage Profile of Existing Power System

C. Optimal Capacitor Placement

The main process involved in achieving the desired voltage level at all the buses without compromising the power delivered, is the determination of optimum size of the capacitor and location [8,14,15,16]. Using the ETAP optimal capacitor placement (OCP) tool, the optimal size and place of the capacitor bank is selected as shown in Table 3.

TABLE 3: POSITION AND SIZE OF CAPACITOR BANKS

BUS IDs	Capacitor IDs	No of Banks	kVAR	kVAR/Bank
BUS 5	CAP 1	4	1200	300
BUS 6	CAP 2	2	600	300
BUS 7	Spare	Spare	Spare	Spare
BUS 8	CAP 3	8	2400	300
BUS 9	CAP 4	11	3300	300
BUS 10	CAP 5	2	600	300
BUS 11	CAP 6	4	1200	300
BUS 12	CAP 7	1	300	300
BUS 13	CAP 8	1	300	300
BUS 14	CAP 9	2	600	300
BUS 15	CAP 10	2	600	300
BUS 16	CAP 11	2	600	300

D. Voltage Profile of the System After Capacitor Placement

Table 4 clearly illustrates that the under voltage conditions of all the buses have been improved after placement of capacitors and so does the voltage profile as shown in Figure 3.

TABLE 4: BUS VOLTAGES AFTER CAPACITOR PLACEMENT

BUS ID	Nominal kV	Voltage kV	Under Voltage Condition
BUS 5	11	11.09	Improved
BUS 6	11	11.17	Improved
BUS 7	11	11.12	Improved
BUS 8	11	11.07	Improved
BUS 9	11	10.83	Improved
BUS 10	11	10.97	Improved
BUS 11	11	10.98	Improved
BUS 12	11	11.16	Improved
BUS 13	11	11.13	Improved
BUS 14	11	10.88	Improved
BUS 15	11	10.99	Improved
BUS 16	11	11.12	Improved

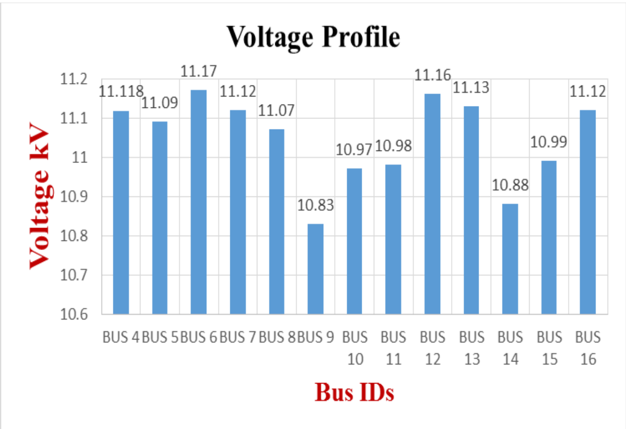

Figure 3: Voltage Profile After Capacitor Bank Placement

E. Comparison of Active Power Delivered

The comparison of active power delivered by the system before and after placement of capacitor banks is shown in Table 5. It is evident from the results that placing of capacitor banks on more than one buses simultaneously is not only helpful in improving the voltage profile of the system but the overall active power delivered by the system will also be increased, thus improving the overall efficiency of the power system.

TABLE 5: COMPARISON OF ACTIVE POWER DELIVERED BEFORE AND AFTER CAPACITOR PLACEMENT

Bus ID	Active Power KW Without Capacitor Banks	Active Power KW With Capacitor Banks
BUS 1	18754	23297
BUS 2	18754	23297
BUS 3	18753	23296
BUS 4	7115	9731
BUS 5	11588	13496
BUS 6	927	1032
BUS 7	0	0
BUS 8	2987	3865
BUS 9	1664	2553
BUS 10	877	995
BUS 11	3107	3803
BUS 12	838	926
BUS 13	838	926
BUS 14	2449	2800
BUS 15	2162	2475
BUS 16	1785	2047
Total	**92598**	**114539**
Average	**5787**	**7159**

CONCLUSION

In this research work, ETAP software was used to analyze the 500 KV, Shiekh Muhammadi grid station for voltage profile improvement. It was observed that using capacitor banks on more than one bus simultaneously in a power system, has eased the process of optimization in order to achieving the desired voltage profile and to increase the overall active power delivered by the system. The following conclusions have been drawn from this research:

- The reactive power plays important part in system reliability as it directly affects the voltage that has to be controlled.
- Under voltage condition can be improved by absorbing or injecting the reactive power to the system, depending upon the nature of the load.
- Using capacitor bank on more than one bus simultaneously has improved the voltage profile in addition to the increase in total active power delivered by the system, thus improving the overall efficiency of the power system.
- In order to get accurate and absolute results, the optimal value and best location for the capacitors to

be placed, can be easy find from ETAP software simulation.

References

[1] L. Grigsby Leonard. Power System. New York: CRC Press, 2006

[2] J.GRAINGER and D.STEVENSON. Power System Analysis. London: McGraw-Hill, 1994.

[3] Rohit Kapahi "Load Flow Analysis of 132 kV substation using ETAP Software" International Journal of Scientific & Engineering Research Volume 4, Issue 2, February-2013 ISSN 2229-5518.

[4] Rana Abdul Jabbar Khan, Muhammad Junaid, Muhammad Mansoor Asgher "Analyses and Monitoring of 132 kV Grid using ETAP Software" 2009 - ieeexplore.ieee.org.

[5] Vivek Raveendran, Sumit Tomar "Modeling, Simulation, Analysis and Optimisation of a Power System Network- Case Study" International Journal of Scientific & Engineering Research Volume 3, Issue 6, June-2012.

[6] Folorunso O.1, Osuji C.C.1, Ighodalo O.S.2 "Enhancement of Power System Voltage Stability with the Aid of Reactive/Capacitive Power Switching Mechanism (A Case Study of Oweeri Transmission Company of Nigeria)" Received: September 4, 2014, Accepted: October 8, 2014, Published: October 8, 2014.

[7] Pravin Chopade1 and Dr.Marwan Bikdash "Minimizing Cost and Power lossby Optimal Placement of Capacitor using ETAP" 978-1-4244-9593-1/11/$26.00 ©2011 IEEE.

[8] S Yunus, Y I Rahmi, R Nazir, Aulia, and U G S Dinata "Static VAR compensator for improving voltage profiles and transmission losses: Case study in Batam", Conference on Innovation in Technology and Engineering Science, 2019.

[9] D.Mc.Donald. Electric Power Substations Engineering. New York: CRC Press, 2006.

[10] V.K Mehta and Rohit Mehta. Principals of Electric Power Systems. Delhi: Revised Edition2008.

[11] Kiran Natkar, Naveen Kumar "Design Analysis of 220/132 KV Substation Using ETAP" IRJET Volume: 02 Issue: 03 | June-2015

[12] C. J. Soni, P. R. Gandhi, S.M.Takalkar "Design and analysis of 11 KV Distribution System using ETAP Software" 2015 INTERNATIONAL CONFERENCE ON COMPUTATION OF POWER, ENERGY, INFORMATION AND COMMUNICATION.

[13] J. A. Michline Rupa, S. Ganesh "Power Flow Analysis for Radial Distribution" World Academy of Science, Engineering and Technology International Journal of Electrical, Computer, Energetic, Electronic and Communication Engineering Vol: 8, No: 10, 2014.

[14] Guneet Kour1, G. S. Brar1, Jaswanti Dhiman2, "Improvement by Voltage Profile by Static Var Compensators in Distribution Substation", International Journal of Instrumentation Science 2012, 1(2): 21-24 DOI: 10.5923/j.instrument.20120102.03.

[15] Divesh Kumar1*, Amritpal Singh1 and Satish Kansal2, "To Improve the Voltage Profile of Distribution System with the Optimal Placement of Capacitor", Indian Journal of Science and Technology, Vol 10(31), DOI: 10.17485/ijst/2017/v10i31/113897, August 2017.

[16] L.Ramesh, S.P.Chowdhury, S.Chowdhury, A.A.Natarajan, C.T.Gaunt, "Minimization of Power Loss in Distribution Networks by Different Techniques", World Academy of Science, Engineering and Technology International Journal of Electrical, Computer, Energetic, Electronic and Communication Engineering Vol:3, No:4, 2009.

Author of this paper is the student of MS Electrical Power Engineering at Department of Electrical Engineering, University of Engineering and Technology, Peshawar.

International Journal of Engineering Works
ISSN-p: 2521-2419
ISSN-e: 2409-2770
Vol. 6, Issue 12, PP. 453-458, December 2019
https://www.ijew.io/
https://doi.org/10.34259/ijew.19.612453458

Assesment of Renewable Energy Sector in Pakistan

Adan Zahid[1], Tayyaba Sony[2], Shehla Noor[13]
[1,2,3] USPCAS E UET Peshawar
azahid2@asu.edu[1]
Received: 06 November, Revised: 17 Novemeber, Accepted: 20 November

Abstract— With the increasing technological advances, the global energy needs are increasing exponentially. The ever increasing demand of electricity has compelled generation sector to highly depend on fossil based fuel but the irony is that the fossil fuel is not only costly but also pose hazard to environment. Therefore, shift towards Renewable Energy (RE) is vital for every country. Currently, RE sector in Pakistan is underdeveloped though some projects have been initiated in Pakistan to decrease reliance on fossil fuel and to lessen the energy shortage in Pakistan. Globally, many countries like Germany and China are heavily investing in renewable energy. Hence, it is important to know the status of renewable energy project growth in Pakistan in comparison to other countries. The proposed methodology aims to find the growth of RE in Pakistan energy mix in comparison to bench mark country as China, Germany, India and Saudi Arabia. This is done to understand the current progress of Pakistan in expanding RE projects, against certain developed and under developed counties. For this study, solar, wind and small micro hydro sectors of Pakistan has been considered. After analysis, the challenges and way forward for successful integration of RE in Pakistan is put forth by this study.. The results of this study will help the policy makers of Pakistan in choosing the right energy resource which is not only cost effective but also environmental friendly. This will help Pakistan in ensuring economic energy projects along with mitigation of greenhouse emissions.

Keywords— Renewable Energy, LEAP

I. Introduction

With the dawn of new millennium, the Renewable resources (RE) has captured the attention of policy makers and researchers due to exponential rise of energy demand and loaming threats of global warming. In case of Pakistan, the gap between electricity demand and supply plummeted to 5201 MW which resulted in load shedding of 14–18 h daily [1]. During ,1980 , in Pakistan the total share of hydro power in energy mix was almost 70% [1]. According to the same study, due to political instability of 1990's, every elected government adhered to short term electricity projects that relied on extravagant oil import which resulted in reduction of the hydropower share to 31%. In recent years, the public and government sensitivities towards environmental issues has resulted in incorporation of RE into Pakistan energy mix. But the total exploitable RE potential of Pakistan is greater than the total percentage of RE in energy mix. On the contrary, many countries around the globe has made significant success in terms of augmenting share of RE in energy mix one such as Germany and China. Therefore, it is important to make an analysis of growth trend of RE in Pakistan against certain bench mark countries. This thesis deals in comparing the growth of RE in Pakistan against Developed and Developing countries. For this scenario, Germany is taken as a case study from developed nation whereas China and India cases have been taken from category of developing nation. Moreover, one OPEC country i.e. Saudi Arabia will be also taken into consideration in order to compare the status of renewable in Saudi Arabia vs. Pakistan.

Furthermore, to enhance the share of RE in Pakistan energy mix and to know its impact on economy and environment; it is essential to model the current energy generation sector of Pakistan. Most of developed countries rely heavily on results of energy models for their future energy policies. Hence the need of the hour is that the policy makers of Pakistan should take into account the results of energy models for formulating future energy policy. The result of energy models predicts cost effective and environmental friendly resources for Pakistan's energy mix.

II. Background

Energy related challenges are among the greatest world has to endure in the coming years. This and with an ever increasing population of over 200 millions), the shift to renewable energy becomes even more important. Moreover, a growing gap between energy demands and supply in Pakistan, has is because economic competitiveness of emerging economies is highly dependent on reliable energy resource availability. If proper support is provided, renewable energy technologies can satisfactorily meet much of the growing demand at prices less than those usually forecasted for conventional energy [1,2]. Therefore, for countries like Pakistan (blessed with natural resources further increased threat to our long-term survivability and existence as a just nation. Although many renewable energy projects have been initiated by Pakistan over past decade especially in micro hydel, wind and solar sector yet the growth of renewable sector is not heartening if we compare growth trend of renewable with other countries. There is a need to analyze previous installed projects in order to assess their efficiency and growth. Moreover, to calculate the impact of RE integration in Pakistan energy mix a full-fledged energy modeling is necessary. The result of such a simulation can help policy maker to put forward a future energy policy.

A. Conventional Energy Resources in Pakistan

1. Oil

Pakistan utilizes 25% of its total oil import in energy sector, during 1990’s and by 2015, 45% of oil import is consumed by electricity sector [4]. According to the study mentioned, when oil price surged from 25$/barrel to 50$/barrel from 2001 to 2005; government decided to diversify its energy mix. Hence, shift to other resources was made.

1.1.1.1 Hydroelectric power

The Two break through projects that gave impetus to hydroelectric power in Pakistan energy mix are: Mangla dam and Tarbela. These were completed between 1967 and 1976, respectively, after Pakistan became signatory of Indus water Treaty [3]. Today, the net installed capacity of hydroelectric power in Pakistan is approximately 7116 MW, which accounts for 17% of total hydroelectric potential which stands at 41,700 MW[3].

1.1.1.2 Coal

According to several surveys, the total coal reserves of Pakistan are approximately 186 billion tones [2]. Despite of such a huge reserves the share of coal in energy mix is meager. It remained at less than 1% in the power sector during 2014 [2].

1.1.1.3 Natural gas

The total resource potential of natural gas in Pakistan is approximately 282 trillion cubic feet [2]. According to same study the country produces approximately 4 billion cubic feet per day which places Pakistan among large consumers of the natural gas.

1.1.1.4 Nuclear energy:

Pakistan Atomic Energy Commission (PAEC) is the government institution which is primarily assigned with the task of planning and management of national nuclear plants. Currently , the nuclear power plants in Pakistan account for 5% of total electricity generation in Pakistan [2] . According to study [2] Pakistan Atomic Energy Commission (PAEC) is now aiming for the installation of over 8000 MW nuclear power capacities by the year 2030. Apart from conventional energy resources, Pakistan is striving to make renewable apart of its energy mix.

The government of Pakistan has strived to avail the Solar, Micro Hydro and Nuclear Energy Resources:Since, this study will compare the growth of renewable sector of Pakistan against China, India, Germany and Saudi Arabia; it is essential to have a look at the status of renewable in these countries. Renewable energy status in Pakistan:

B. Renewable Energy Status In Pakistan

Pakistan is among SAARC nations, located in South Asia. It is energy deficient since it lacks hydro carbons and hence it has to make its need by importing hydrocarbons [4]. The import of hydrocarbons makes up 20% of entire annual import bill [5]. According to study [6] Pakistan has the potential to generate at least 167.7 GW. The terrain of Pakistan receives approximately 15.5x1,014 kWh solar radiation [7]. This shows Pakistan has high potential to exploit solar energy to make electricity since in most part of the country the effective sun shines hours are approximately eight to nine hours/day [7] . Recently, Pakistan seems keen is utilizing more of solar energy. For instance, Pakistan engineering council (PEC) commissioned first on grid power plant in 2010 [7]. The power plant has facility of net metering to IESCO. Moreover, The Parliament of Pakistan has been fully powered with solar energy. The success of these projects encouraged other investors to extend investment in renewable energy sector. These solar based renewable energy projects are in different developmental stages. Further, 7 IPPs have obtained letter of support from AEDP for a total of 72.23 MW [8]. As per study [9] poor policy and lack of technology is a constraint that solar industry faces in Pakistan

Government of Pakistan has also made some progress in harvesting potential of wind energy. Pakistan meteorological department has conducted a thorough survey about Pakistan’s wind potential. The study shows Sindh has more potential in terms of wind energy than coastal areas. Almost 9700 sq.km has potential to make electricity from wind. If area’s utilization constraints are kept in view, still 43000 MW appears to be gross power potential whereas studies show that almost 11000MW, can be exploited from this coastal belt [10]. Similarly , the survey from meteorological department has depicted low wind potential in Northern area of Pakistan [11]. The first wind project was installed by renowned Fauji Fertilizer in early 2013 with total installed capacity of 50 MW [11]. Later on 6 more such a projects have been initiated in coastal areas of Sindh [11].

A far as small micro hydro is concerned; Pakistan has good potential in micro hydro in Northern areas. Government hands also taken initiative to exploit hydel potential. different micro hydro projects are under developmental stages whose aggregate capacity is 2638 MW [12].

1.2 Status of renewable energy in China

China has heavy demand of energy for its expanding economy. but the lack of hydro carbons has pushed China to explore renewable energy resources. The government China has set a target of increasing share of renewables in its energy mix and reach milestone of 15.4% by 2010 [13]. In 2010 China excelled USA in wind energy production by 2010 [14]. Since 2000, the installed capacity of wind energy in Chinese energy mix has augmented exponentially, from 300MW to 42,287 MW [14]. Among total wind energy of the world which is 194,390 MW, China makes 21.8 % [14].As far as wind sector in China is concerned, stress on wind energy started in 1994, when government enunciated regulations to encourage wind energy exploration. These regulations resulted in production of 224 MW in late 1998 [15]. The study [16] has concluded that by 2007 the net installed capacity of wind in China crossed 5900 MW. This drastic increase was made possible by the high wind potential onshore regions of China. The offshore Chinese regions displayed comparatively low progress. According to the aforementioned study china is aiming to have an installed capacity of 30 GW by 2020 [16] .

The Chinese land stretches a good 9.6 Mn km-sq land. It is also included among solar belt countries [14]. The study [17] gives an overview of growth of solar energy in China in past years. As per CSP, a region with DNI level above 1800 KWh produces economic energy. According to aforementioned study, the northern and western terrain of PRC meets this criterion. The installed solar energy capacity in China in 2004 was approximately 0.06 MW. As per the same study, the government is aiming to achieve a milestone of 1.8 GW in solar energy.

1.3 Status of Renewable Energy in India

India is industrializing at a rapid pace. Like china, India is also deficient in hydrocarbons. India is blessed with a geography and climate weather that enables it to exploit wind energy. In India, the summer and winter monsoons ensure effective wind speed to run turbine and generate wind energy [13]. As per The Indian Renewable Energy Development Agency (IREDA), the wind potential of India is approximately 45,195 MW. But due to certain constraints, 12000MW can be utilized. The study (Sharma et al, 2012) reveals that over the time, wind generation has grown and the cost has been brought down. The cost per kW t ranges from $1413.8/kW to $1908.6/kW (Sharma et al, 2012). This growth in wind energy can be attributed to Government policy which ensures incentive, income tax holidays and other subsidies to those investors who are investing in this sector [36]. India has a good potential to explore solar energy since it has good DNI [18]. According to study aforementioned study, the 5000 trillion kWh per year is the estimated potential for solar energy. During 2014, the installed solar capacity in India is estimated to be 2.2 GW according to the same study. The solar energy couldn't grow the way wind energy was integrated in India. Several reasons have been enlisted by the aforementioned study such lack of availability of reliable data, lack of technology and proper infrastructure. According to the Institute of Energy Economics and Financial Analysis Wholesale price of small micro hydro, wind and solar INR/KWh is 3.5 ,4.5 and 5.6 respectively [18] which are higher than price of domestic coal and nuclear power plant. According to study [19], the installed capacity of small micro hydro in India by 2006 was 1800 MW. The growth rate according to same study for small micro hydro over year 2000 to 2006 is approximately 6 % which is pretty small than that of wind is 40 %.

1.4 Status of Renewable Energy in Saudi Arabia

Saudi Arabia is rich in hydrocarbons but constant use of fossil based fuel Saudi Arabia in late 20th century has led to depletion of the hydro carbons. Saudi Arabia is equally blessed with a terrain that receive an average 2200 kWh/m2 of solar radiation annually [8]. But less importance has been given to renewable energy in Saudi's energy policy due to a prevailing perception that solar energy has negligible importance in industrial development of the country. According to the same study, the first use of solar energy application commenced in 1960's. Later on, in 1980's; Saudi kingdom collaborated with Germany. In 2010, the Saudi Aramco took the project of constructing 10 MW solar power plant [8].

1.5 Status of Renewable Energy in Germany

Efforts are being made globally to explore renewable energy resources to limit the increasing carbon dioxide content in atmosphere and to minimize the increasing cost of fossil based fuels around globe, especially after the oil crisis of 1979. For electricity generation, wind energy is considered one of the best choices in world. Several researches have been undertaken to make wind energy cost effective and efficient energy resource. Different studies have been conducted in past to know the wind energy potential across the Europe. Hence, a total of 56 GW wind potential has been achieved in Europe. Over the past few years, Germany has increased seen major growth in share of renewable energy in its energy mix. Renewable energy increase in 2009 is almost triple the value of 1998. In 1998, the share of renewable energy was mere 3.6, which reached to a high value of 8.4%[20]. According to the same study, the highest growth was seen in wind energy sector. During 2009 the According to the study the success of renewable energy in Germany can be attributed to legislative measures by the government. In 2008, the new initiated setups were using renewable (8.5 GW) [20].

C. Comparative analysis of growth of RE across the World

The purpose of this study is making a comparative analysis of the growth trend of renewable in Pakistan against certain bench mark countries. For this reason, let's have a look at different comparative analysis of renewable growth performed by various researchers.

The study [21] has made a comparative analysis of shift towards renewable energy in developed and under developing countries. For this reason, data is collected from various data banks such as World Bank, Factbook etc. For case study of developed country, USA is considered whereas Kenya and Morocco has been assumed from category of developing nation. The current growth and future trend has been discussed by making projection till 2040. Based on energy demand till 2040, a blueprint for 100 % integration of renewable energy as a case study has been produced. Though, an ideal situation of 100% renewable energy integration has been produced by study [21], it provides useful information in step wise phasing out dependence of a country on non-renewable energy resources.

Another study [22] has solely stressed on comparative analysis of determinants that are responsible for renewable energy sector of China and India. The basis for this study was that similar challenges faced by two countries in term of population, greenhouse emissions (GHE's), greater energy needs for expanding economies. The researchers; to find linkages between renewable energy growths, carbon dioxide emission, have used the multivariate vector error correction model (VECM). The causality found between outputs in case of China is one-directional but bidirectional in case of India. This result points towards inherent interdependency of GHE's, growth and energy production.

Similarly, another comparative analysis of renewable sector of across Europe is undertaken by study [23]. This time causal relationship between economic growth and renewable has been taken under consideration. The researcher has used data for 27 countries, comprising of real GDP of people, percentage of RE in energy consumption and GHE emission. Various component models are used to analyze the data. This study reveals a weak relation between economic growth and renewable energy consumption. Researcher through neutrality principle explains this result.

In another paper [24], a brief review on the supporting policies adopted for Renewable energy resources in Europe has been conducted. For this purpose, a case study of four countries: France, Germany, Italy and Spain is considered. The purpose of this study is to highlight the main differences in the support policies adopted for Photovoltaic (PV) and Wind systems. The supporting policies assumed in this study are: Green tags (GT), Net-metering and Feed-in tariff (FIT).

The aim of paper [25] is to analyze the development status of PV system of some European Union (EU) countries. These countries include France, Germany, Greece, Italy and the U.K. The convenience of several support policies for PV has been evaluated by keeping in view the specific situation of these five member states. The net present value (NPV) and the internal rate of return (IRR) have been chosen in this comparative study as economic indexes. This study is particularly helpful in assessing the impacts of energy policy in selected E.U. members, in what manner PV market will grow in near future and which policy is beneficial for future PV sector of these countries.

III. COMPARATIVE ANALYSIS

A. Case Study of Pakistan vs Developing Cuntries with similar Geagraphic and Econmic Condition

The figure 6 depicts share of renewable energy in Pakistan and India energy mix. The portion of renewable energy in India is far greater than that of Pakistan but this can be attributed to the 6th times more population and hence greater energy needs of India. But figure 20 shows the percentage increase of renewable energy in Pakistan occurred at faster pace than India. If we break down different sectors of renewable energy in India and Pakistan and further compare their performance; observe that the wind sector of India is doing better than that of Pakistan. This can be attributed to the fact that India enjoy comparatively more coastal belt, almost 7,516.6 km compare to Pakistan which has 1050 km of coastline. Similarly, India has shown remarkable progress in PV solar energy after 2016.

In case of small micro hydro, Pakistan's generation capacity is almost similar to that of India. Keeping in view the 6 times more population of India, these results depicts Pakistan is doing well in micro hydro.

To conclude, Pakistan can look up to the PV and wind sector of India for improvement in its renewable energy in total energy mix. This is because India and Pakistan lies is South Asia, both are neighbors and listed among developing nations. Hence it will be easy for Pakistan to look up to PV and wind sector of India and implement it in Pakistan.

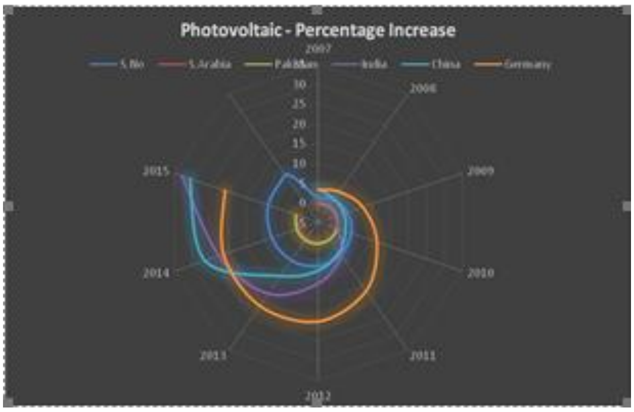

Figure III-1 Caparison of Solar Energy Resource of Pakistan vs other Countries

B. Case study of Pakistan vs. Developed nation (China)

The figure III-I depicts share of renewable energy in Pakistan and China energy mix. The portion of renewable energy in China is greater than that of Pakistan. This can be attributed to the fact that China is 7 times more populous than Pakistan and is going through industrialization. Hence energy needs of China are greater. But figure III-2 shows the percentage increase of renewable energy in Pakistan occurred at faster pace than China. If we break down different sectors of renewable energy further in China and Pakistan, we observe that the growth sector of wind sector in China and Pakistan is almost same in 2009. But by 2019 the growth rate of China is better than Pakistan.

Similarly, China has excelled Pakistan in solar and micro hydro sector as well. This fact can be attributed to the fact that China enjoys superior technological advancement accompanied by trained work force as compare to Pakistan.

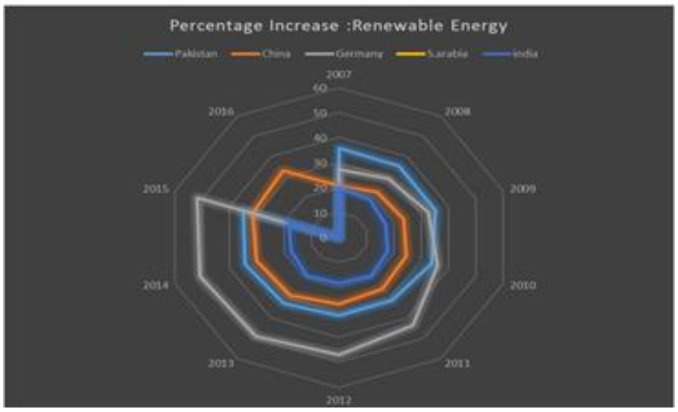

Figure III-2 Percentage Increase in Renewable Energy

C. Case study of Pakistan vs. Developed nation (Germany)

Germany is a developed nation like China. The comparison of renewable energy sector of Germany in contrast to Pakistan is almost similar to that of China. This can be attributed to the availability of state of art technology of renewable resources exploitation in Germany. Moreover, the RE friendly national policies adopted in Germany has also helped in vigorous developed RE sector of Germany.

Last but not the least, the energy demand of Pakistan will soar in upcoming years hence it is necessary to implement an effective RE policy based on above recommendations and simulation.

The preferred spelling of the word "acknowledgment" in America is without an "e" after the "g". Avoid the stilted expression, "One of us (R. B. G.) thanks . . ." Instead, try "R. B. G. thanks".

CONCUSLION

Countries all over the globe are making shift to renewable energy due to limited hydro carbon. Though many RE projects are installed in Pakistan, it is important to know the growth RE in Pakistan energy mix with respect to other countries. This will help Policy makers of Pakistan to implement identify any loopholes and make amendments in future energy policy for successful integration of RE in Pakistan energy mix. Pakistan RE sector development pace is relatively slow as compare to the bench mark countries. This study also reveal that huge potential exist in Pakistan to make RE projects sustainable. In this milieu, the Indian RE sector can be looked up by the policy makers of Pakistan due the fact that India is Pakistan's neighbor and both countries has similar social, economic and technologically advanced. Moreover, the both countries have almost similar terrain condition. Another prospect for Pakistan energy sector is that China is investing in energy projects under CPEC. Pakistan can immensely benefit from Chinese technology, since China is leading in Renewable resources in world. Chinese cooperation can enable Pakistan to produce RE equipment indigenously. Furthermore, the simulation results show that solar and coal energy of Pakistan should be utilized since both ensure comparatively cheaper electricity. On the other hand, wind energy proves to be more expensive option in terms of RE utilization since it has high investment cost. This is evident from the result of cost of production and Investment cost results. If we analyze the result of carbon emission, the Coal and biomass scenario gives more carbon emissions as compare to wind and solar. Hence, it can be concluded that if tradeoff between Cost and Carbon emission has to be made than Biomass Scenario suits Pakistan. This will help Pakistan in mitigating the loaming environmental challenges along. Similarly, solar can ensure comparatively cheaper energy which can be translated into economic boom for Pakistan since the end product of any industry depends on the cost of energy.

REFERENCES

[1] M. Kamran, "Current status and future success of renewable energy in Pakistan," *Renewable and Sustainable Energy Reviews*, vol. 82. Elsevier Ltd, pp. 609–617, 2018

[2] G. Das, M. Aslam, H. Rahman, R. Samoo, N. Hussain, and K. Harijan, "Overcoming electricity crisis in Pakistan : A review of sustainable electricity options," *Renew. Sustain. Energy Rev.*, vol. 72, no. January, pp. 734–745, 2017.

[3] O. Rauf, S. Wang, P. Yuan, and J. Tan, "An overview of energy status and development in Pakistan," *Renewable and Sustainable Energy Reviews*. 2015.

[4] S. A. Ur Rehman, Y. Cai, N. H. Mirjat, G. Das Walasai, I. A. Shah, and S. Ali, "The future of sustainable energy production in Pakistan: A system dynamics-based approach for estimating hubbert peaks," *Energies*, vol. 10, no. 11, 2017.

[5] M. Ragazzi, M. Maniscalco, V. Torretta, N. Ferronato, and E. C. Rada, "Anaerobic digestion as sustainable source of energy: A dynamic approach for improving the recovery of organic waste," *Energy Procedia*, vol. 119, pp. 602–614, 2017.

[6] M. K. Farooq and S. Kumar, "An assessment of renewable energy potential for electricity generation in Pakistan," *Renew. Sustain. Energy Rev.*, vol. 20, pp. 240–254, 2013.

[7] M. S. Malkani, A review of coal and water resources of Pakistan, vol. 31. 2012.

[8] A. Hepbasli and Z. Alsuhaibani, "A key review on present status and future directions of solar energy studies and applications in Saudi Arabia," *Renew. Sustain. Energy Rev.*, vol. 15, no. 9, pp. 5021–5050, 2011.

[9] U. K. Mirza, M. Mercedes Maroto-Valer, and N. Ahmad, "Status and outlook of solar energy use in Pakistan," *Renew. Sustain. Energy Rev.*, vol. 7, no. 6, pp. 501–514, 2003.

[10] J. C. Godenzzi, "No 主観的健康感を中心とした在宅高齢者における健康関連指標に関する共分散構造分析 Title," vol. XX, no. 1990, pp. 317–331, 1996.

[11] "Pakistan Meteorological department." [Online]. Available: http://www.pmd.gov.pk/wind/Wind_Project_files/Page767.html.

[12] M. Kamran, "Current status and future success of renewable energy in Pakistan," *Renew. Sustain. Energy Rev.*, vol. 82, no. September 2017, pp. 609–617, 2018.

[13] M. Carolin Mabel and E. Fernandez, "Growth and future trends of wind energy in India," *Renew. Sustain. Energy Rev.*, vol. 12, no. 6, pp. 1745–1757, 2008.

[14] X. Changliang and S. Zhanfeng, "Wind energy in China: Current scenario and future perspectives," *Renew. Sustain. Energy Rev.*, vol. 13, no. 8, pp. 1966–1974, 2009.

[15] C. W. E. Association., "Status and development of China wind industry," 2006. [Online]. Available: http://www.crein.org.cn.

[16] David K., "A method for developing geographic–economic wind supply curves: China case study." 2008.

[17] Q. Hang, Z. Jun, Y. Xiao, and C. Junkui, "Prospect of concentrating solar power in China — the sustainable future," 2008.

[18] K. Kapoor, K. K. Pandey, A. K. Jain, and A. Nandan, "Evolution of solar energy in India: A review," *Renew. Sustain. Energy Rev.*, vol. 40, pp. 475–487, 2014.

[19] I. R. Pillai and R. Banerjee, "Renewable energy in India: Status and potential," *Energy*, vol. 34, no. 8, pp. 970–980, 2009.

[20] R. Hinrichs-Rahlwes, "Renewable energy: Paving the way towards sustainable energy security. Lessons learnt from Germany," *Renew. Energy*, vol. 49, pp. 10–14, 2013.

[21] N. Vandaele and W. Porter, "Renewable Energy in Developing and Developed Nations : Outlooks to 2040," vol. 15, no. 3, pp. 1–7, 2015.

[22] S. Rafiq, H. Bloch, and R. Salim, "Determinants of renewable energy adoption in China and India : a comparative analysis Determinants of renewable energy adoption in China and India : a comparative analysis," no. July, pp. 37–41, 2014.

[23] A. N. Menegaki, "Growth and renewable energy in Europe : A random effect model with evidence for neutrality hypothesis," *Energy Econ.*, vol. 33, no. 2, pp. 257–263, 2011.

[24] N. Park, S. Yun, and E. Jeon, "An analysis of long-term scenarios for the transition to renewable energy in the Korean electricity sector," *Energy Policy*, vol. 52, pp. 288–296, 2013.

[25] L. Dusonchet and E. Telaretti, "Comparative economic analysis of support policies for solar PV in the most representative EU countries," *Renew. Sustain. Energy Rev.*, vol. 42, pp. 986–998, 2015.

International Journal of Engineering Works
ISSN-p: 2521-2419
ISSN-e: 2409-2770
Vol. 6, Issue 12, PP. 459-465, December 2019
https://www.ijew.io/
https://doi.org/10.34259/ijew.19.612459465

Improvement of Dynamic Performance using the Grid-Tied Photovoltaic (PV) System with Nonlinear Controller

Amir Nangyal[1], Dr. Abdul Basit[2], M. Asif Khan[3] Zeeshan Ullah[4]
anangyal@asu.edu[1], abdul.basit@uetpeshawar.edu.pk[2], zeeshan.ullah@asu.edu[4]
[1,2,3,4] US Pakistan Center for Advance Studies in Energy (USPCAS-E) UET Peshawar
Received: 07 November, Revised: 18 Novemeber, Accepted: 21 November

***Abstract*—** Grid connected Photovoltaic (PV) system installations are rapidly growing around the globe to meet the increasing demand of electricity, this results in a high penetration to the electrical grid. A great deal of effort should be made to ensure the functionality of the PV system at the optimal level. Due to its non-linear nature, PV system can't handle electrical faults, which may lead to voltage sag at DC side while simultaneously generating dynamics at AC side. This work offers techniques for improving the dynamic performance of the PV system by controlling voltage sag through the application of fuzzy logic (FLC) based maximum power point techniques (MPPT) at DC-DC boost converter and the regulation of dynamics at inverter by using positive and negative sequence current controlling techniques at the time of grid faults. In the event a fault occurs, fuzzy logic based MPPT controller will be activated, instead of the simple MPPT techniques to maintain constant DC voltages. Such methods are applied by designing a MATLAB / SIMULINK 1-MW PV system and validating the tests by adding faults in the system.

***Keywords*—** Fuzzy logic based MPPT, positive and negative current controlling techniques, voltage sag, boost converter, point of common coupling.

I. Introduction

In the domain of electricity generation, the share of renewable energy and that of grid connected PV system are increasing day by day, and as a result, winning major part in fulfilling the growing electricity demand. Some new complications seem to have arisen in grid connected PV systems, which must be encountered for secure and reliable system operation. The PV panel has an optimum operational point at which maximum power can be delivered to the load by PV panel [9]. Such operating point is generally called the maximum power point (MPP). Due to the non-linearity of the voltage-current behavior of the solar panel, the maximum operating voltage due to variance in response to variation in solar irradiance and cell temperature is difficult to assess accurately. Maximum power point (MPP) monitoring shall be carried out to recognize the maximum power point of operation; the solar panel shall be adjusted accordingly to operate at that operating voltage for the acquisition of maximum power. The PV system efficiency can be improved by extracting maximum power from the PV module while adjusting the voltage of the PV module. The MPPT controller is therefore expected to control the new adjusted maximum power point (MPP) if temperature and/or irradiance changes occur. Most monitoring methods for MPPT have been developed for this function in the last years [15-16]. Photovoltaic (PV) panel has an optimum voltage where it can produce maximum power at that particular point. As PV modules have non-linear characteristic due to changes in temperature and solar irradiance, it is difficult to determine the point where maximum power can be extracted [7]. Genetic algorithms-based optimized fuzzy logic controller has been used for maximum power-point-tracking in PV system and compared with perturbation and observation techniques, showing better performance [8]. Fuzzy logic-based MPPT has been designed to improve the performance of the PV system. It has been examined under varied irradiances at different temperatures and has been observed to produce more stable power as compared to common MPPT techniques. Hard effort should be made to operate PV system optimally [12] due to which different techniques and methodologies have been suggested for extracting maximum power from the PV modules, with each technique having its own pros and cons and limitations. During the grid fault, the main goal is to keep the DC voltages of boost converter constant at the inverter. In this work, fuzzy logic based MPPT control scheme is presented to adjust the duty cycle and produce regulated DC voltages. Fuzzy design is simple and as such, does not require knowledge of the precise model. The aim of fuzzy is to assist the MPPT to minimalize voltage variations during grid fault. By gaining information about the variation of power Δp and the variation of power due to variation in voltages $\Delta p/\Delta v$, the fuzzy can control the appropriate magnitude of the perturbed voltages to P&O MPPT for more iterations. P&O MPPT [14] will decide, and accordingly place an increment or decrement of voltage to the existing PV operational voltage and will continue to provide pathway to the MPP. There are components of positive and negative sequence during grid fault, resulting in ripples twice the grid frequency if proper control schemes are not introduced for controlling the negative and positive sequence of the grid current; as a result, the AC power vaccinated to the grid will not be constant. This will in turn result in ripples in the DC bus voltage, which may produce some serious issues for the grid connected PV system. Several techniques are implemented for the improvement of the dynamic behavior of the PV system during grid fault; feed-forward current-control loop (FFCL) improves the dynamic performance of the PV system when the irradiance of the PV system is changing suddenly and continuously [1], resulting in fluctuations in the DC-bus voltages. FFCL turns to hasten the response of inverter current references, resulting in dynamic response improvement of the injected current. A new control strategy has been used [2], by proposing uncertainty and distribution estimator (UDE) based current controller; the DC bus voltage of DC/DC converter controller is regulated in a way so as to build the relation between the MPPT function and the power flow control. By proposing bounded voltage power flow control strategy, AC voltage regulation through UDE has been improved. Since the voltage sag period is short, the soft behavior of the controller, along with a fast-dynamic performance, is the utmost significant issue in the low voltage ride through (LVRT) duration. Recently, some techniques have been introduced, such as Proportional Resonant (PR) controllers, to control single-phase PV systems in LVRT mode [3]. However, these techniques were uncertain as to their involvement in the LVRT mode. In PR controllers, a fast-dynamic response can be achieved by tuning the gains of high bandwidth PR controllers, but typically the phase margin is reduced. The design of PR controllers, therefore, requires a trade-off between dynamic response and stability. In order to make the development of grid-connected PV systems a successful business opportunity, it is necessary to improve the cost, efficiency and life expectancy of the power digital interface [4].

Whenever there is a fault on the grid side, the DC voltages at inverter change abruptly; consequently, traditional MPPT techniques can't handle the sudden change in voltage, resulting in voltage sag [10] at the inverter and the production of harmonic at the AC side. Based on the symmetrical components, a protection scheme is implemented [11] to deal with the LVRT problem but has the failure of the high current pressure on the low grid and unbalanced voltage. The current-source-inverter (CSI) provides benefits over voltage-source-inverter (VSI) in terms of intrinsic boosting and short-circuit protection capability, direct current output regulation and simplified ac-side filter design. Distributed generation (DG) systems are usually based on power electronic converters that produce harmonics, and by using passive filtering switching harmonics need to be minimized by using LCL filter [5-13]. Model-Predictive Control (MPC) for single-phase PV inverters has been proposed for the LVRT operation. Proportional-integral controller designed using Whale-Optimization-Algorithm (WOA) techniques has been used to control DC chopper and grid inverter for achieving maximum power point and improving dynamic voltage performance of the Photo-voltaic system [6]. Based on the aforementioned discussion, no controlling techniques have been applied for constant DC link voltages and stability of the system during unbalanced condition. Some of the challenges, which have not been addressed here, shall be dealt with in the coming paragraphs.

This focus of this paper is on controlling DC link voltages and maintaining system stability by applying a negative and positive sequence current regulator to provide appropriate voltage references to the grid-connected inverter and a fuzzy logic based MPPT controller to extract maximum power in order to sustain DC link voltages at a constant level. Voltage/current loop restriction-based controller, while selecting the PI controller, was used to control positive and negative current sequences produced during the unbalanced state, keeping in mind the delay produced by the filtering technique while extracting the current and voltage sequences.

II. DESIGN OF CASE SYSTEM

The PV farm used in this paper is designed in MATLAB-SIMULINK, a three-phase (3- Ø) grid connected PV system (GCPS) with generation capacity of 1MW at standard test conditions (STC), connected to fuzzy logic based MPPT DC-DC converter. The input of 1.1 MVA inverter is connected to the output of DC-DC converter, low voltage side (415V/20KV) of 1.2 MVA transformer is connected to the output of the inverter through a filter having L=100µH/phase and R=1mΩ/phase, the magnitude of instantaneous voltage is represented by e_{abc}. Fault is introduced at low voltage (LV) side of transformer for system analysis and tests. System design is shown in Figure. 1.

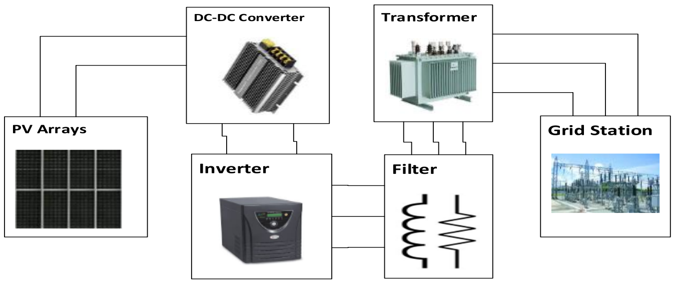

Figure 1. Design of case system

A. *Design of Fuzzy Logic Controler (FLC)*

During the occurrence of a grid fault, while sensing the change in voltages at point of common coupling a fuzzy logic controller has been designed, because, it has the capacity to deal with imprecision and uncertainty and can be used to make the most of the opportunity to design control rules. An FLC competes with human decision-making and has the capability to perform approximate data, resulting in the determination of accurate solutions. FLC is effective when mathematical modeling is difficult to implement and FLC is designed by using If/Then rules. It is used to operate a closed or controlled loop system with a range of rules. Below is the rule table for fuzzy controller:

Table 1. Fuzzy logic rules

C-E / **E**	N-B	N-S	Z-O	P-S	P-B
N-B	Z-O	Z-O	N-B	N-B	N-B
N-S	Z-O	Z-O	N-S	N-S	N-S
Z-O	N-S	Z-O	Z-O	Z-O	P-S
P-S	P-S	P-S	P-S	Z-O	Z-O
P-B	P-B	P-B	P-B	Z-O	Z-O

Using FLC, the regulated DC link voltages are plotted in the Figure. 2 below:

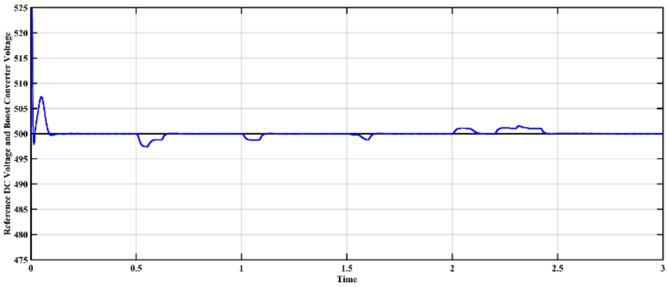

Figure 2. Reference voltages Vs regulated DC Link voltages

B. Phase Lock Loop (PLL) System

Eventually, due to the presence of low-frequency ripples in the detected voltage angle, SRF-PLL does not perform properly during the grid fault. Therefore, a more intelligent PLL should be selected to detect positive sequencing voltage during the unbalanced condition. The alternative PLL technology on the basis of moving-average filters (MAFs) has been used in this paper.

III. SYSTEM DESCRIPTION AND EQUATION

If only the positive sequence component for a grid-connected VSI is controlled, the active reference current value is obtained from the DC connection voltage and the reactive reference current is obtained through the droop control. However, the application of DC link voltage cannot be regulated by the positive sequence of active current, but also affects the negative and positive sequence of reactive and active current references when dealing with the negative and positive sequence. The instantaneous reactive and active power is given below equation (1):

$$\begin{aligned} p &= P_o + P_{c2}cos(2\omega t) + P_{s2}sin(2\omega t) \\ q &= Q_o + Q_{c2}cos(2\omega t) + Q_{s2}sin(2\omega t) \end{aligned} \qquad (1)$$

Where,

P_o represents average instantaneous value of active power
Q_o represents reactive power
P_{c2}, Q_{c2}, P_{s2} and Q_{s2} represents second order harmonics

To measure and solve the terms of power, stating relative current and voltages in a (dq) synchronous reference frame obtaining the below equations (2), shows second order hormonics.

$$\begin{aligned} P_O &= e_d^+ i_d^+ + e_q^+ i_q^+ + e_d^- i_d^- + e_q^- i_q^- \\ P_{c2} &= e_d^- i_d^+ + e_q^- i_q^+ + e_d^+ i_d^- + e_q^+ i_q^- \\ P_{s2} &= e_q^- i_d^+ - e_d^- i_q^+ - e_q^+ i_d^- + e_d^+ i_q^- \\ Q_O &= e_q^+ i_d^+ - e_d^+ i_q^+ + e_q^- i_d^- - e_d^- i_q^- \\ Q_{c2} &= e_q^- i_d^+ - e_d^- i_q^+ + e_q^+ i_d^- - e_d^+ i_q^- \\ Q_{s2} &= -e_d^- i_d^+ - e_q^- i_q^+ + e_d^+ i_d^- + e_q^+ i_q^- \end{aligned} \qquad (2)$$

On consideration of the (dq) transformation the above equation is based. The above equation can be changed into irreversible 6x4 matrix. Power ripples are produced by P_{s2} and P_{c2}. Therefore, the only terms to be controlled are the first four terms. The current reference obtained from the above equation (2) is given below as equation (3)

$$\begin{bmatrix} i_d^{+*} \\ i_q^{+*} \\ i_d^{-*} \\ i_q^{-*} \end{bmatrix} = \begin{bmatrix} e_d^+ & e_q^+ & e_d^- & e_q^- \\ e_d^- & e_q^- & e_d^+ & e_q^+ \\ e_q^- & -e_q^- & -e_q^+ & e_d^+ \\ e_q^+ & -e_d^+ & e_q^- & -e_d^- \end{bmatrix} \begin{bmatrix} P_o^* \\ P_{2c}^* \\ P_{2s}^* \\ Q_o^* \end{bmatrix} \qquad (3)$$

The main objective of the design controller is to deliver constant power during fault and voltage sag. Therefore, P_{s2} and P_{c2} should be kept to zero.

When dealing only with positive sequences, the angle extracted from the PLL can control it, but when the goal is to send constant power to the grid during the fault, both sequences should be encountered and controlled. Therefore, the current should first be calculated and then converted into a synchronous dq frame that rotates in the opposite direction and creates 100HZ ripples by communicating with each other. Filtering methods should be used to track ripples. Figure.3 denotes the extraction of current sequences and filtering techniques.

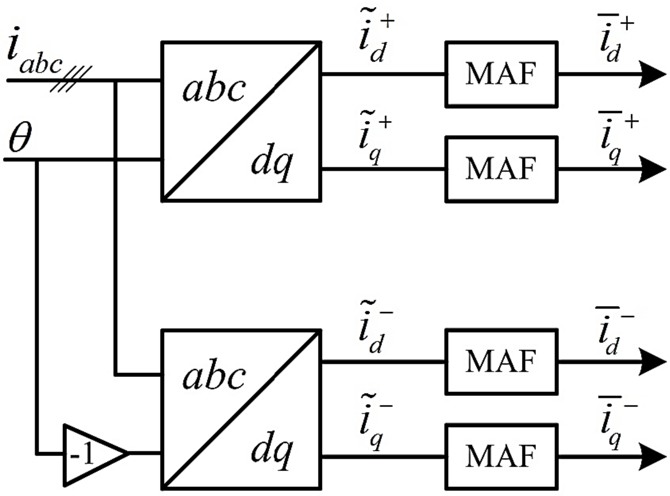

Figure. 3. Extraction of current sequences using MAF

The MAF equation (4) is as follows:

$$\bar{x}(t) = \frac{1}{Tw}\int_{t-Tw}^{t} x(t)dt \qquad (4)$$

The current control loop consists of two parallel loops, one for negative sequence control and the other for positive sequence control. There is a PI operator, decoupling terms, and dq transformed grid voltages feed forward terms in each circuit. Same technique is used for current control but with reverse direction of *w*L for negative sequence due to the reverse direction of the negative sequence rotation vector. Reference voltages will eventually be given by summing up the negative sequence and the positive sequence of voltage components to the inverter.

As shown in figure.4 i_q^{+-} and i_d^{+-} e_q^{+-} and e_d^{+-} are the positive sequence extracted currents and voltages. v_q^{+*} and v_d^{+*} are the reference positive sequence voltages. The filtered components are the grid voltage components which is used to obtain the current references. i.e., e_q^{-+}, e_d^{-+}, e_d^{--} and e_q^{--}.

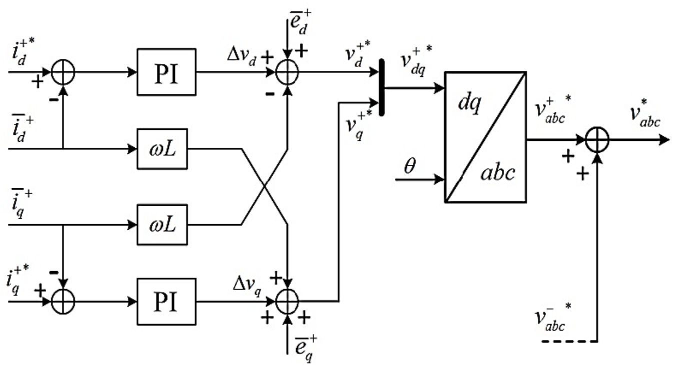

Figure. 4. Current-Control Loop (CCL)

IV. ANALYSIS OF THE SYSTEM WITH CONSTANT DC VOLTAGE SOURCE

The system's behavior and performance are evaluated firstly by keeping the dc-link constant through a dc voltage source. For steady-state analysis the power reference Q_0 is set to zero and P_0 is set to 1MW. However, during the voltage sag process Q_0 is kept 0.8 MVar and P_0 is set to zero for addressing the requirements of fault ride- through (FRT).

A. Analysis for Stability of the System

The stability of current-control-loop (CCL) is analyzed before evaluating the performance of the system during voltage sags while applying the MAFs. The MAFs introduces the delay to the current control loops which weakens the fast dynamics and may be the cause of instability.

Two independent blocks are used while considering the CCL average model for compensation of the coupling terms. The same loops are used for negative CCL.

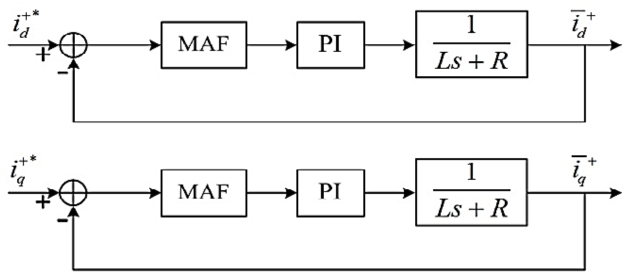

Figure. 5. Compensated average CCL for coupling terms

Converting the figure to s-domain. Equation (5) shows average model of CCL

$$\bar{X}(s) = \frac{1}{T}[1-e^{-Tw\,s}]X(s) \qquad (5)$$

To obtain the PI controller's stability region parameter, linearization of MAF is done primarily by the ' padeapproximation ' (MATLAB toolbox) process. The stable region for PI controller parameters is the small green area shown in Figure.6, considering the MAFs a 5th order approximation and filtering parameters about the other filtering procedures, i.e. a quarter (T/4) of the period of grid voltage, involving the golden and green areas in Figure. 6. Therefore, with a delay half (T/2) of the MAF is utilized in this work, the stable region is noticeably greater, lesser delays leads to have broader stable area for the parameters of the PI controllers' in the CCL.

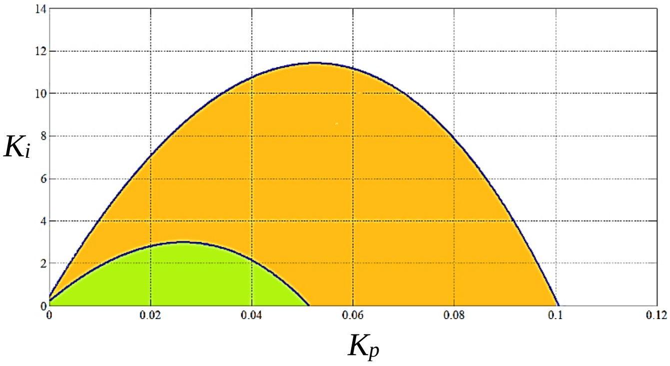

Figure. 6. Stable area for PI current controller parameters when considering MAFs in extracting the grid currents ' positive and negative sequences.

V. SIMULATIONS

Looking into the parameters defined for PI controller in Figure. 6, two regions (green and golden) defines the values for the PI parameters. The green region of Figure. 6 explains small values for the parameter of PI controller *(K_p, K_i)*. Therefore, it is known from the values that the controller's dynamic output will be slow. After some tests step responses is plotted, the values accepted for the parameters of PI *(K_p, K_i)* are (0.0015, 0.15). While using the accepted PI parameters for the test system, the fault time and steady-state response is shown in Figure. 7 and Figure. 8. Looking into figure, after fault removal and during the process of voltage sag, the dynamics are relatively slow for the PI controllers. However, the system continuous to stable in both fault and steady-state conditions. Using MAFs for filtering the grid currents has a significant impact on the dynamics of CCL. Besides, the grid voltages measured are also filtered as shown in Figure. 4, for using as feed-forward terms.

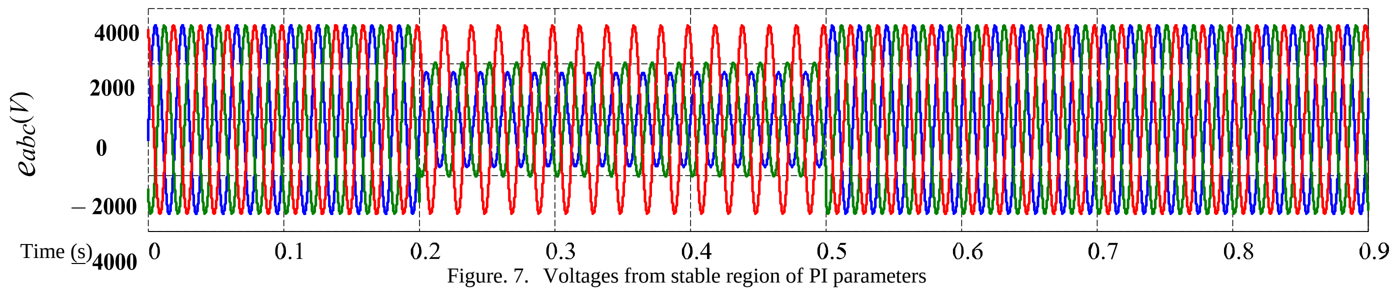

Figure. 7. Voltages from stable region of PI parameters

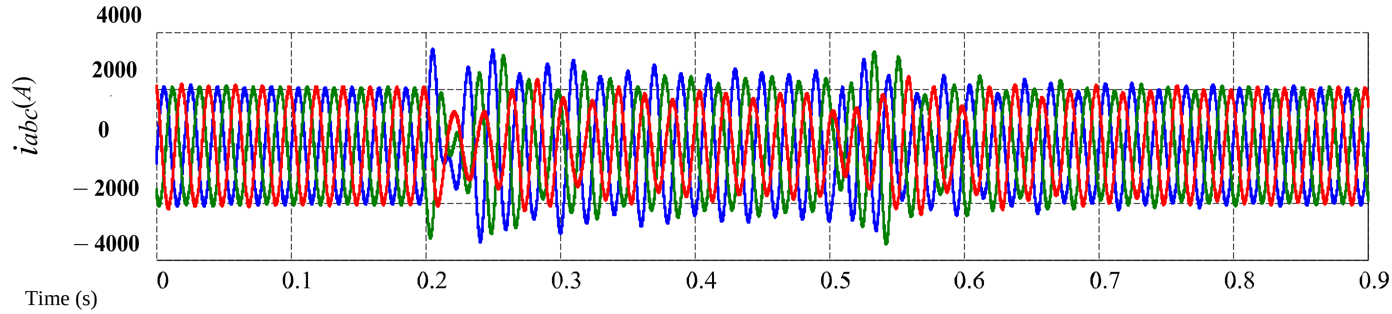

Figure. 8. Current from stable region of PI parameters

Again, the voltage filtering procedure generates some delays that weakens the system dynamic. A solution is proposed for the development of the dynamics of the current loops (CL) is to include the e_{abc} grid voltages as feed-forward terms applied after the inverter's positive and negative voltage comparisons have been summed up. The terms of the feed-forward voltage must therefore not be filtered, and the inverter voltage comparisons more easily obey the changes in the grid voltages.

The enhanced currents with the same PI controller parameters are shown in Figure. 9, and the active and reactive power generated are shown in Figure. 10. It should be noted that the system analyzation is done with a constant dc source.
However, dc-link voltages for a real PV system the should be regulated and for this purpose fuzzy logic based MPPT techniques has been used.

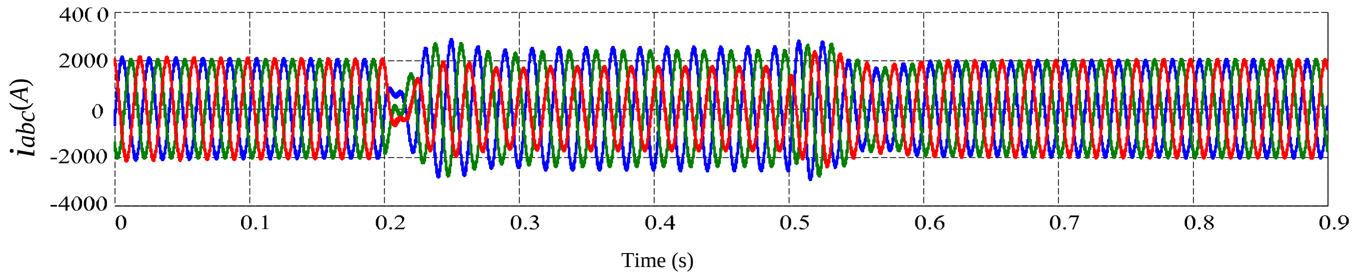

Figure. 9. Output currents improved when the grid voltage is applied as feed-forward-terms at the end of the CCL

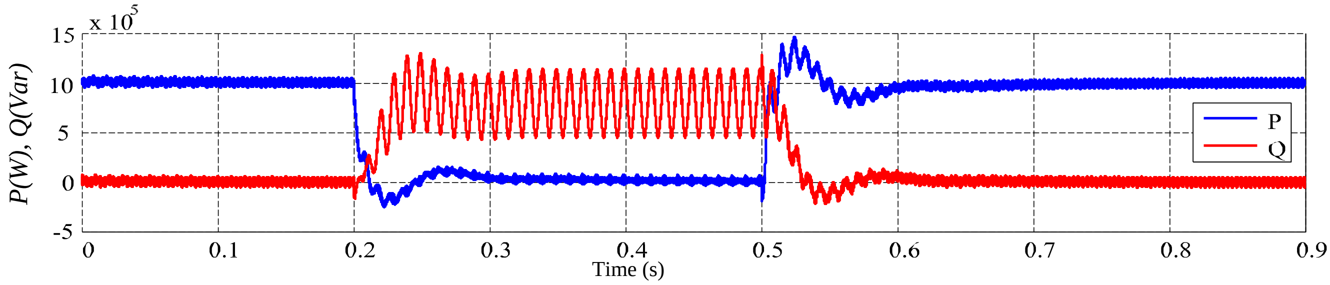

Figure. 10. Active and reactive power

A. Analysis of the Voltage Regulation with DC-Link

The system performance is evaluated in this section under regulating the dc-link voltages. The dc-link voltage is regulated at the time of the steady-state condition for obtaining P_o while it is set to zero during the voltage sag. The reactive power relationship is the same as in the previous section. However, as the aim is to provide the grid with constant power during the voltage drop there will be power fluctuations in the grid filter due to unbalanced grid currents that enable the dc-link voltage to fluctuate. A MAF is therefore used to remove these ripples for the measurement of the dc-link voltage. The system response is calculated when the dc-link voltage control loop is tested with an MAF as well as the internal current control loops. The results with the same parameters which are used in the previous section for the current control loop PI controllers with settling time t_s= 41ms and (7.65, 489) for the dc-link PI controller t_s= 78ms are shown in Figure.11. The oscillatory currents can make the inverter to disconnect due to the slow dynamics of CCL and the interaction between the MAFs and the external loop (DC link voltage loop). The CCL dynamics should be five time faster than external loop dynamics for separate analyzation. However, the structure of the external and internal loops is almost identical to that of the MAFs in the control loops. The one solution for improving the system's performance is to slow down the dynamics of the external loop; however, it will influence the dynamics of the entire system which is not really desirable. The new parameters tested for the voltage loop PI controller are (2.16, 39), which produces t_s= 176ms the settling time. The currents of the grid are shown in Figure. 12 and the active and reactive power generated are shown in Figure. 13. However, the dynamics are comparatively slow, but the system is stable.

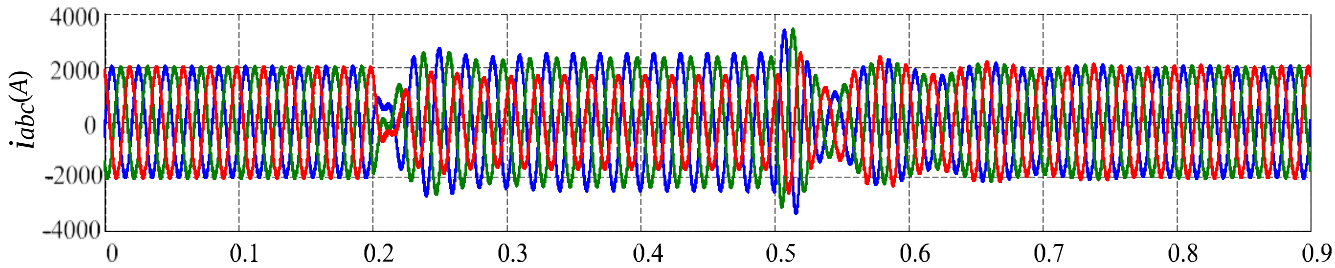

Time (s)
Figure. 12. Waveform of the grid current

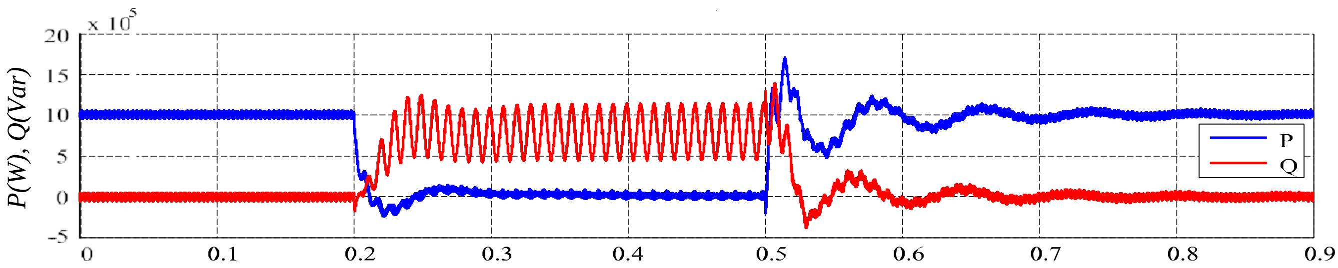

Time (s)
Figure. 13. Waveform of the active power and reactive power generated

CONCUSLION

The GCPS response is studied in this work on both positive and negative sequences under unbalanced voltage conditions. For current loops using PI controllers, it is required to implement a filtering technique for extraction of dq components from currents and voltages. All the filtering procedures, however, introduce certain delays and slow the controller dynamics. As a result, these filtering methodologies constrain the stable region parameters of the PI controller. In addition, low values must be selected for the parameters of the PI. Therefore, if the dc-link voltage is governed by an external loop, the dynamics of the controller must be relatively slow to the current control loops in order to achieve stable system performance. The overall dynamic performance is therefore substantially degraded. Using proportional-resonant controllers would be an alternative to using PI controllers. Since there would be no need for the positive and negative sequences of grid currents in the control loops, it is predicted that faster dynamics will be achieved. The future research can be done on using PR controllers.

REFERENCES

[1] Bacon, A. A. (2016). Dynamic Performace Improvement of Grid connected PV system using a Feed Forward Control Acting on the NPC Inverter Currents. IEEE TRANSACTIONS ON INDUSTRIAL ELECTRONICS, 10.

[2] Yeqin Wang, B. R. (2017). Fault Ride-Through Enhancement for Grid-tied PV Systems with Robust Control. IEEE TRANSACTIONS ON INDUSTRIAL ELECTRONICS, 11.

[3] Esmaeil Zangeneh Bighash, S. M. (Nov 2017). Improving performance of LVRT capability in single-phase grid-tied PV inverters by a model-predictive controller. ScienceDirect,Electrical Power and Energy Systems, Elsevier Ltd., 13.

[4] C. Larbes, S. A. (2009). Genetic algorithms optimized fuzzy logic control for the maximum power point tracking in photovoltaic system. ELSEVIER, 8.

[5] Camilo C. Gomes, A. F. (2018). Damping techniques for grid-connected voltage source converters based on LCL filter: An overview. ELSEVIER, 20.

[6] Hasanien, H. M. (Dec 2017). Performance improvement of photovoltaic power systems using anoptimal control strategy based on whale optimization algorithm. ELSEVIER Electric Power Systems Research, 9.

[7] Chin, C. S. (2011). Fuzzy Logic Based MPPT for Photovoltaic Modules Influenced by Solar Irradiation and Cell Temperature. 13th International Conference on Modelling and Simulation, (p. 6). UKSim .

[8] Prajna Paramita Dash, M. K. (2011). Dynamic Modeling and Performance Analysis of a Grid-Connected Current-Source Inverter-Based Photovoltaic System. IEEE TRANSACTIONS ON SUSTAINABLE ENERGY, 9.

[9] M. K. Hossain and M.H. Ali, “Overview on Maximum Power Point Tracking (MPPT) Techniques for Photovoltaic Power Systems,” Int. Rev. Electr. Eng., vol. 8, no. 4, pp. 1363–1378, 2013.

[10] W. Kou, D. Wei, P. Zhang, and W. Xiao, “A Direct Phase-coordinates Approach to Fault Ride Through of Unbalanced Faults in Large-scale Photovoltaic Power Systems,” Electr. Power Components Syst., vol. 43, no. 8–10, pp. 902–913, 2015.

[11] C. T. Lee, C. W. Hsu, and P. T. Cheng, “A low-voltage ride-through technique for grid-connected converters of distributed energy resources,” IEEE Trans. Ind. Appl., vol. 47, no. 4, pp. 1821–1832, 2011.

[12] Patsalides-M, Stavrou A, Efthymiou V, Georghiou GE. Towards the establishment of maximum PV generation limits due to power quality constraints. Electr Power Energy Syst 2012; 42:285 98.

[13] Pena -Alzola R, Liserre-M, Blaabjerg F,-Sebastian R, Dannehl J, Fuchs FW. Analysis of the passive damping losses in lcl-filter-based grid converters. IEEE Trans Power Electron 2013; 28:2642–6.

[14] M.S.-At Cheikh, C. Larbes, G. F. “Maximum-power point-tracking using a fuzzy logic-control scheme”, Revue des energies-Renouvelables, Vol. 10, 2007, pp. 387-395.

[15] Salas-V, Olıas E,-Barrado A, Lazaro A. Review of the maximum power point tracking algorithms for stand-alone photovoltaic systems. Solar Energy Materials & Solar Cells 2006; 90:1555–78.

[16] EsramT,-Chapman PL. Comparison-of photo-voltaic array maximum-power point tracking methods-IEEE Transactions on Energy Conversion June 2007;22(2).

IJEW 国际工程期刊 International Journal of Engineering Works انجینئرنگ کاموں کا بین الاقوامی جرنل

International Journal of Engineering Works
ISSN-p: 2521-2419
ISSN-e: 2409-2770
Vol. 6, Issue 12, PP. 466-470, December 2019
https://www.ijew.io/
https://doi.org/10.34259/ijew.19.612466470

Advance Energy Meter With Tariff Indication, Theft Detection and Prepaid System using GSM

Amir Nangyal[1], Dr. Abdul Basit[2], Zeeshan Ullah[3], Samra Kanwal[4]
anangyal@asu.edu[1], abdul.basit@uetpeshawar.edu.pk[2], zeeshan.ullah@asu.edu[3], skanwal_26@yahoo.com[4]
[1,2,3] US Pakistan center for advance studies in Energy (USPCAS-E) UET Peshawar
[4]Electrical Engineering Department, Wah Engineering College University of Wah, Wah Cantt
Received: 07 November, Revised: 17 Novemeber, Accepted: 21 November

***Abstract*—** Due to electricity stealing, electricity providers in divergent territories particularly inside progressing ones are experiencing from massive losses. This work focuses on electricity energy metering technique which is prepaid with an additional function of theft detection and changing tariff time to peak time and off-peak time. The suggested system has two parts. First part is service main side which will be installed on pole and is connected to distribution lines through service line while second part is main meter which will be installed at consumer side on service main wire. The suggested meter is equipped with transmitter/receiver used for theft detection and GSM module which open the door for bidirectional communication between service provider, users, and main meter getting advantage of the pre-installed GSM framework. Electricity meter can be recharged by customers, simply scratching card and sending hidden code with the help of SMS utilizing GSM module. This work presents new techniques to cover meter tampering and bypassing. In case of theft detection, it will cut off supply, inform the service provider and will show the exact location of theft using GSM. The tariff time will be changed by service provider using SMS with the help of GSM module to meter. The bidirectional GSM communication using SMS is very helpful for user as well as service providers. In case of low balance and if remaining balance become zero, it will cut off supply and inform user as well as service provider.

***Keywords*—** Prepaid energy meter; theft detection; transmitter/receiver; Global System for Mobile (GSM); Short Message Service (SMS); bypassing.

I. Introduction

In power sectors electricity stealing is a serious problem particularly in the succeeding countries. Due to electricity theft an enormous amount of collection is lost. This is so serious problem in some countries that governments faced losses instead of income. Government pays in some cases to energy sector to sustain a negotiable rate of electricity. Existing power capacity is not expanding due to financial losses and governments are becoming unsuccessful to fulfill the growing demand of energy. Power stealing is a serious problem in systematic energy system like USA and methodical organization like Malaysia [1]. Regardless, in under developed and progressing nations the enactment of electricity stealing is very usual that it is frequently condemn of conversation. Electricity stealing exhibits a low meter reading, stealing power by circumventing a meter, overdue bills and billing indentation. Billing deformity is caused by office employees in trade of illegitimate remittances from the costumers and meter reader recording wrong readings. Distinct technical and nontechnical techniques were suggested in[15] the former to identify energy plunder. An impractical methods approach is observation of consumers with hooks and doubtful load profile [2,11]. While recurrent investigation is helpful and appreciably diminishes theft, but this method demands immense manpower and enormous labor. But this kind of attempt also let down in many instances because of the duplicity of the employees. Some practical ways like use of principal onlooker meter at the low voltage side of residential transformer to detect thievery, genetic brace vector machines, harmonic generator, supreme learning machine, and power line impedance procedure [3, 4, 5, 6, and 7]. However, these practical methods can be efficiently executed only if genuine communication is fortified between the suitable test points and centralized station. Currently, GSM based prepaid energy meters has been suggested [8, 9]. These meters are helpful to provide solution for prepaid energy metering system and can control load consumers load locally. The pre-installed metering system and prepaid system [12] can be made more advanced for the use of electricity thievery. This project presents a suggested metering system which will be prepaid and will be pedestaled on GSM which incorporate different angles of electricity thievery like meter bypassing, meter tampering and prevents deformity of billing, disinclination of customers to reimburse bills in time and electricity theft from lines.

II. Suggested Energy Metering System

The suggested system has two parts. One is main meter which is installed on consumer unit and second part is service main side which will be installed on pole or may be in center of service main line. Service main side will communicate with main meter to avoid meter bypassing. An energy meter is allotted to individual consumer and power utility preserves a server. The energy meter and server will utilize GSM module and modem consequently to liaise with each other with the help of GSM network. The sketch of suggested energy metering techniques is shown in Fig.1 and simplified block diagram of the suggested system is shown in Fig. 2.

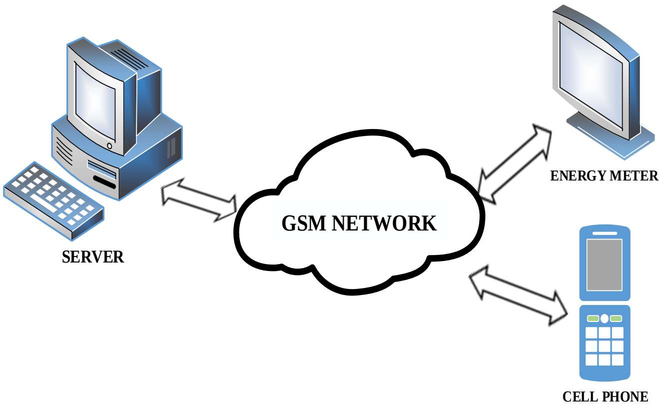

Figure 1. Sketch of the suggested advance energy metering system.

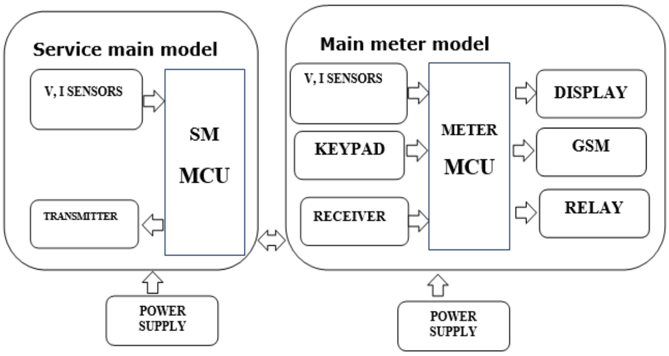

Figure 2. Block diagram of the advance energy meter.

A. Main Meter Part

The whole block diagram of the main meter is shown in Fig. 3a. This model calculates consumed units and remaining units on the basis of V, I parameters[13]. The main meter communicates with service main part through receiver and with sever through GSM. All data to user and service provider regarding balance recharging, low balance, changing tariff time or theft detection is uploaded and controlled by the main meter. The recharging method is similar to the existing recharging techniques of mobile phones. Simply, costumers have to buy a scratch card and send the hidden code for the corresponding units. Suppose, a user wants 100 units so he will buy scratch card for 100 units and will send the hidden code if the code was registered and correct for 100 units then it will recharge the electricity meter and will inform the user with the help of SMS about the recharge of corresponding units. The recharging process can also be done by using server. As customers are consuming energy, so consumed units will be deducted from the total units earned by customers, information about consumed units and total units will also be displayed on LCD. When remaining units reach to certain limit (20) it will send a message to user and will inform him to recharge again while if the consumer did not recharge the energy meter and consume all the units, the energy meter will disconnects the load automatically with the help of relay and will send message to inform the user about finished units and as well as service providers. The consumer has to charge again to use electricity. So, this kind of system is helpful in deformity of billing system, bribed meter readers and employees.

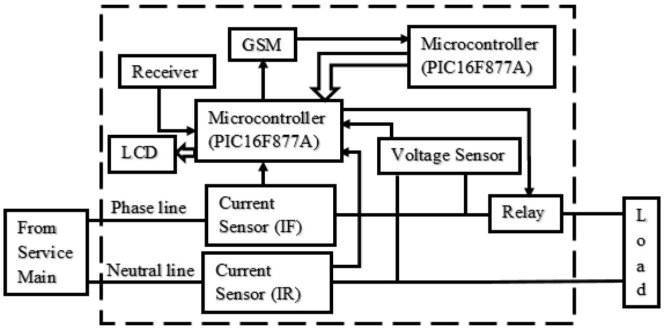

Figure 3a. Block diagram of the suggested advance energy meter. (Main meter model)

B. Service Main Part

Service main part has transmitter which communicate with the main meter for theft detection. When load is sensed by current sensor, transmitter will be activated by microcontroller and will continuously transmit the signal which will be received by receiver of main meter part. Main meter part compares the data received from transmitter [14] with load data sensed by sensors installed at main meter. Theft is detected if this difference exceeds the threshold limit. It will be installed on pole or on service wire. The complete block diagram of the service main is shown in Fig 3b.

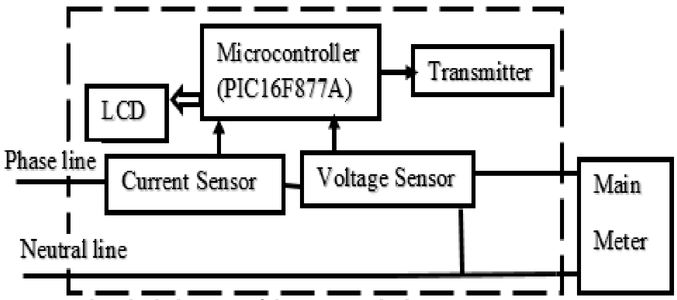

Figure 3b. Block diagram of the suggested advance energy meter. (Service main model)

III. SIMULATION MODELS FOR CONNTROLLING ELECTRICITY THEFT

The software's for simulation is Proteus and Proton IDE compiler.

A. Protection Against Shorting the Phase or Neutral Wire

Fig.4 shows bypassing the phase wire which is a favored technique of circumventing normal electricity meter. If one current sensor is installed in energy meter on phase wire so it will record zero energy consumption. Similarly, another technique of circumventing is detaching of the neutral wire which is illustrated by Fig.5. In this scenario zero energy consumption will be recorded because the consumption observed will be zero by the step-down transformer. To protect this kind of thievery, in our suggested system two separately current sensors are used in the phase and neutral wire. Both sensors are connected on ADC pin of microcontroller. If any of the wire, phase or neutral is disconnected then it will record difference among the out of both sensors. The output of both current sensors will be compared in microcontroller and if there is significant difference, it will disconnect the load immediately with the help of relay and inform the service providers about corresponding bypassing. In such cases the service providers will block the electricity meter and will take legal action against the costumers. The simulation result is shown in figure 6.

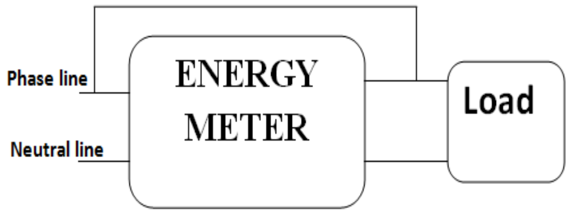

Figure 4. Shorting the phase line.

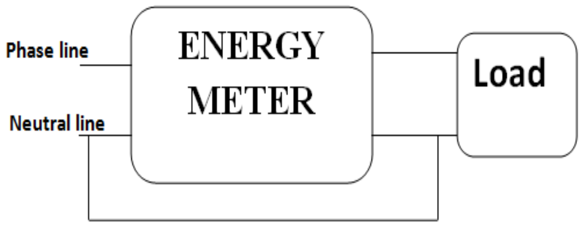

Figure 5. Shorting the neutral line.

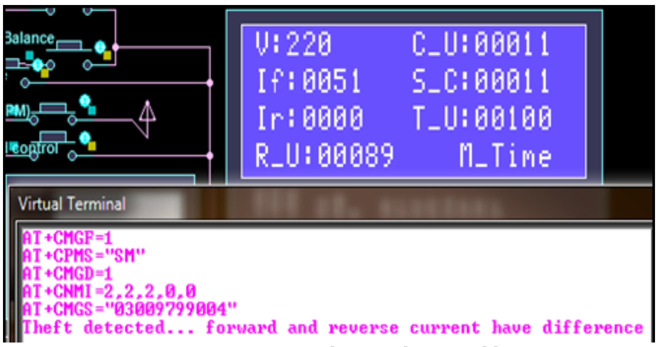

Figure 6. Shorting the neutral line.

B. Protection Agianst Whole Meter Bypassing

In utmost cases the consumers disconnect both the neutral and phase wire from meter, shown in Fig. 7. In such scenario zero energy consumption the meter will be recording. To avert such kind of thievery, we have divided our suggested energy meter into two parts one is service main part and other is main meter part. The service main side have transmitter and main meter have receiver. If no load is connected, then the transmitter will not transmit signal. If load is connected so service side sense the load and continue transmission while on the receiver side the receiver, receives signal and give to microcontroller so there is counter for the service main side in the main meter. The counter increases its value as the consumer units consumed means at the same time the service main units also change as the consumer unit's count by the main meter. If the whole meter is bypassed then the consumed unit will stop and the service counter will increase its value because load is sensed by service main part so it will continuously transmit signal which will be received by receiver and continues counting in main meter part and if the difference between consumed units and service count increase than threshold valve, it detaches the load instantly with the help of relay and the electricity meter alerts the service providers about bypassing through SMS. The simulation result is shown in figure 8.

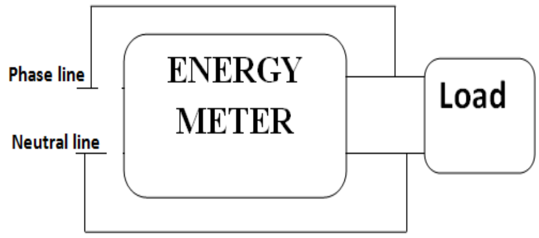

Figure.7. Whole meter bypassing.

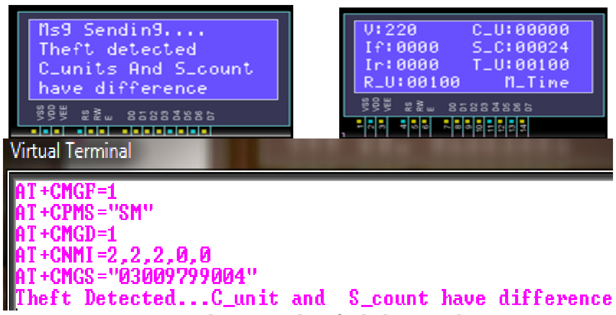

Figure 8. Simulation results of whole meter bypassing.

C. Protection in Case of Tampering

Some consumers are proficient, may attempt to unbolt the electricity meter and dabble it to show zero energy consumptions or manifest. To relive such case, push buttons are installed at each side of the suggested energy meter which is normally closed. So, these buttons are opened by pushing with the sides of electricity meter. One end of every button is given to the pin of microcontroller and second end is given to 5Vdc power supply. If a customer attempts to unbolt the meter the push button will be closed and 5V will appear at input pin of microcontroller. In such case, the microcontroller promptly informs the service providers and detaches electricity from the load. Result is shown in figure 9.

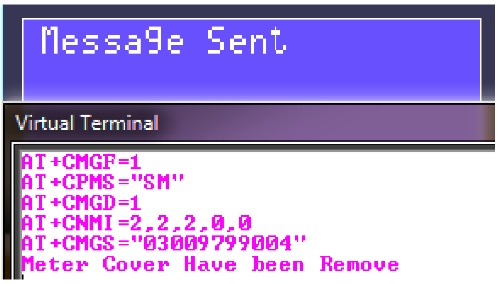

Figure 9. Protection against tampering

D. *Changing Tariff Time*

The tariff time is controlled by server because tariff time change with respect to weather or months. The tariff will change when the server sends a specific code to meter. When it is received by GSM module it will be recognized by microcontroller and will change the tariff time with respect to code received. These are shown in figure 10.

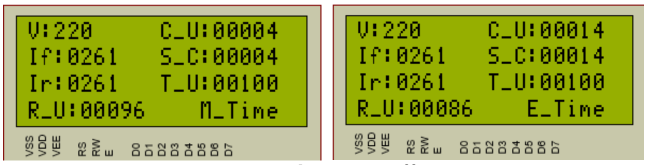

Figure 10. Changing tariff time

IV. EXPERIMENTAL SETUP

The laboratory prototype of suggested model is shown in figure 11.The service main model contain one microcontroller (PIC16F877A), voltage and current sensor and transmitter TX2B. Transmitter is activated when load is sensed by microcontroller using output of current sensor.

The main meter part consists of two parallel connected microcontrollers (PIC16F877A). One controller is used as energy measuring chip having receiver RX2B which communicate with service main part. GSM module (Sim900d in our work) is connected serially to energy measuring chip while RX output is given to energy measuring chip. Current sensors, step down transformers, LCD and a relay are also connected to energy measuring chip. The energy metering chip calculates the energy consumption on basis of the outputs of current and voltage sensors and display V, I parameters on LCD. The microcontroller is in continuous communication with GSM module. To record data of consumed, remaining and total units and detect thievery a battery backup is also installed.

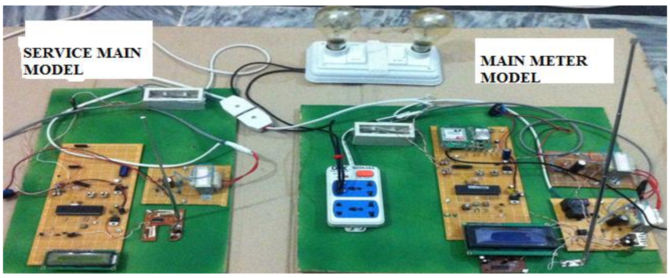

Figure 11. Prototype of the suggested advance energy meter.

V. EXPERIMENTAL SETUP

The experimental results are shown below.

A. *Result of Shorting the Phase or Neutral Wire*

Threshold is defined between forward and reverse current forward current is measured on phase line while reverse current is measure on neutral line. If any one bypass neutral or phase line so the differnece of forward and reverse curent will exced throshold hence theft will be detcted and a message will be sent to inform utility (service providers) against theft. The results are shown in figure 12.

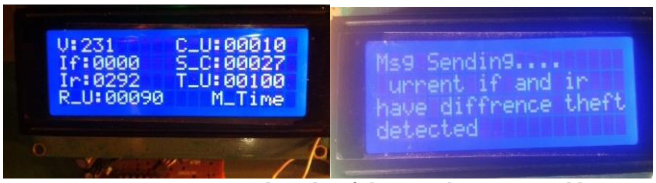

Figure 12 Experimental results of shorting phase or neutral line.

B. *Result of Whole Meter Bypassing*

If phase and neutral lines are bypassed so current sensed by both current sensors will be zero and no unit will be consumed. To detect this kind of theft transmitter and receiver are used. When load is connected and meter is bypassed the load will be sensed by the current sensor of service main model and continuously transmit signal to main meter, service unit will count when exceed threshold value it will inform utility (service providers) against this theft by sending message. The results are shown in figure 13.

Figure 13 Experimental results of whole meter bypassing.

C. *Card Recharging*

The user have send the hidden code A1 from the scratch card to meter. When card recharge the user will be informed accordig to the card he have rechaged by sending messge to user and server. The results are shown in figure 14.

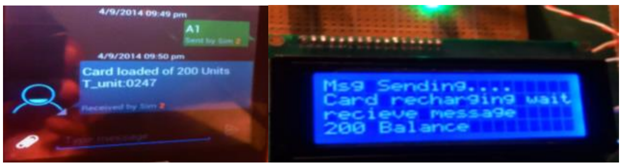

Figure 14 Experimental results of card recharging process.

VI. CONTROLING THEFT OF ELECTRICITY FROM POWER LINES USING SPECTATOR METER

Electricity steal may happen from power lines if someone is using hooks on power lines or illegal load which is shown in Fig. 15. Power theft from power line can be controlled by using transceivers DRF7020D13 instead of transmitter and receiver. The DRF7020D13 can be used point to point or point to multi point applications. User need to set one module as host and other as client module. Each module must have unique ID. The client module should be present in meter which will send the consumed units to host or observing meter. The host is located in observer meter which is installed on power line. The observer meter will calculate all the power consumed on power line and will compare with the received power from all clients of the hosting meters or observer meter if any significant difference is found, it warns the service providers of the corresponding illegal load through SMS.

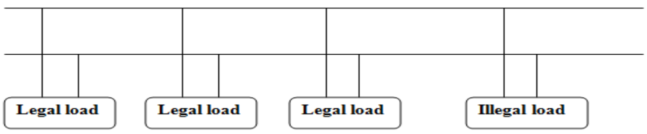

Figure 15 Illegal load

CONCUSLION

In this work, we have suggested advanced electricity metering techniques which utilizes the advantage of existing GSM infrastructure which has implicit approach to every customer house and covering disparate nations. The installation of GSM module not only covers the idea of making electricity meter prepaid but also play role in detecting electricity thievery. Information of the electricity theft is reported instantaneously to service providers with the help of GSM module and it will show the exact location of thievery whether it is done by consumer or in the form illegal load from power lines. So, it will be easy find such thievery for service providers and can take legal action immediately, hence suggested system is very helpful for service providers to diminish electricity plunder and ensuring revenue collection.

REFERENCES

[1] T. B. Smith, “Electricity theft: a comparative analysis,” Elsevier Journal Energy Policy, vol. 32, no. 18, pp. 2067-2076, Dec. 2004.

[2] Prepaid Energy Meter with GSM Technology Jubi.K, Mareena John Department of Instrumentation and Control Engineering PSG College of Technology Peelamedu, Coimbatore, India.

[3] Karan Gandhi and Hari Om Bansal, “Smart Metering in Electric Power Distribution System”, IEEE International Conference on Control, Automation, Robotics and embedded system (ICARE),2013.

[4] Rezaei, N., & Haghifam, M. R. (2008). Protection scheme for a distribution system with distributed generation using neural networks. International Journal of Electrical Power & Energy Systems, 30(4), 235-241.

[5] Bar-Ilan, A., Sacerdote, B., 2004. The response of criminals and non-criminals to fines. Journal of law and Economics, 47, 1-17. Nagi, K.S. Yap, S.K. Tiong, S.K. Ahmed, and A.M. Mohammad, “Detection of abnormalities and electricity theft using genetic Support Vector Machines,” in proceedings of IEEE Region 10 Conference, pp. 1-6, Nov. 2008.

[6] A.H. Nizar and Z.Y. Dong, “Identification and detection of electricity customer behavior irregularities,” in proceedings of IEEE Power Systems Conference and Exposition, pp. 1-10, Mar. 2009.

[7] An Advanced Smart Energy Metering System for Developing Countries Sai Kiran Ellenki 1 , Srikanth Reddy G 2 Srikanth Ch. 2 1.BITS – Dubai, 2. SLC’s Institute of Engineering and Technology-Hyderabad, India.

[8] Eduardo Werley S.dos Angelos,Osvaldo R.Saavedra, Member IEEE,Omar A.Carmona Cortes,and Andre nunes de Souza,”Detection and Identification of Abnormalities in coustmer Consumptions in Power Distribution Systems”,IEEE 2011,0885-8977

[9] A. Barua, N. Mohammad, M. A. Arafat, K. Khan, A. I. Abbas, and R.Chaudhary “Threephase SMS prepaid digital energy meter,”International Conference on Electrical and Computer Engineering, Dec.2012, in press.

[10] S.S.S.R. Depuru, L. Wang, V. Devabhaktuni, and N. Gudi, “Measures and setbacks for controlling electricity theft,” in proceedings of North American Power Symposium, pp. 1-8, Sept. 2010.

[11] S. H. Ahmad Usman "Evolution of Communicaton Technologies for Smart Grid Application " 2013.

[12] Q. Z. Weiqing Tao1, Beijing Cui 1, "The design of Energy Management Terminal Unit based on double MSP430 MCU," pp. 1-4, 2008.

[13] T.Instruments, "Analysis of Sallen-Key Architecture," p. 1, July 1999 – Revised September 2002.

[14] S. Limited, "TCPIP Application Note," vol. 3, vol. 1, p. 7, pp. 1-10, 20.01.2010 2010.with 2.1 kVRMS Isolation and a Low-Resistance Current Conductor," pp. 1-3.

[15] D. S. Naidu, "The Hybrid Meter Reading System " International Conference on Electrical and Computer Engineering 2012.

IJEW 国际工程期刊 International Journal of Engineering Works انجینئرنگ کاموں کا بین الاقوامی جرنل

International Journal of Engineering Works
ISSN-p: 2521-2419
ISSN-e: 2409-2770
Vol. 6, Issue 12, PP. 471-478, December 2019
https://www.ijew.io/
https://doi.org/10.34259/ijew.19.612471478

Performance Evaluation of Reclaimed Asphalt Pavements

Asif Nawaz[1], Fazle Karim[2], Khalid Mahmood[3], Sher Afzal Khan[4]
[1,2,3,4] Sarhad University of Science & Information Technology, Peshawar
asifnawaz739@gmail.com[1], engr_fazli@yahoo.com[2], khalid.civil@suit.edu.pk[3], hod.civil@suit.edu.pk[4]
Received: 15 November, Revised: 20 November, Accepted: 22 November

***Abstract*—** The extensive use of organic and virgin aggregates contributes to their resource exploitation. High priority must be given to the partial substitution of conventional aggregates with recyclable construction material, which must be environmentally responsible and should function equally too as the conventional material. Reclaimed Asphalt Pavements (RAP) is a great choice for the asphaltic wearing and asphaltic base courses of road pavements. In this research, the properties were determined for various combinations and proportions of virgin and aged asphalts.

In this study, six blends which were the mixtures of virgin materials and RAP, were analyzed. The blends were designed with a wide variety of RAP blends from 0 to 100 percent by Marshall Method of design. The rutting performance of the blends was also determined in-order to check the deformation. The RAP content was combined with virgin aggregates in such a way that all the test samples had about the same gradation. RAP-containing mixtures showed significant variation and the properties indicated improvement with the increase in RAP material. The results show that up to 40 percent of RAP material can be used efficiently in the construction of wearing courses.

***Keywords*—** RAP, Hot Mix Asphalt, Marshal Mix Design, Rutting performance, Recycling.

Abbreviations:

RAP------------Reclaimed Asphalt Pavement

HMA----------Hot Mix Asphalt

OBC-----------Optimim Binder Content

NHA-----------National Highway Authority

Va--------------Air voids

VMA----------Voids in mineral aggregates

VFA-----------Voids filled with aggregates

NMAS--------Nominal Maximum Aggregate Size

I. Introduction

A. General:

Expansion, rehabilitation, and maintenance of any transportation system depend on fiscal resources to finance the system; the technology to plan, design, construct, and maintain the facility in an economic manner; supplies of aggregate and binder; and equipment and manpower resources with which to construct and maintain the facilities. Transportation facilities controlled by federal, state, and local agencies are faced with several problems, including:

- Decrease in assets that are available for transportation potentials, has given rise due to these circumstances has resulted in a decrease in assessment base, inflation, a decrease in revenue from fuel costs and also in monetary demands for further projects.
- Resource supply issues arising from the use of sources close to the purpose of utilization; increased separate pull and associated transport costs; strictures forced by zoning laws; strong ecological codes restricting the production in specific regions and requiring substantial uses for the protection of pit and quarry reconstruction, for the quality of air and water, and for the reduction of noise; and the use of asphalt materials for different purposes.
- Issues of accessibility that regards with the equipments coming about as a result of diminished budgets, various components and the new gear's high cost.
- Work related issues arise due to because of financial wage constraints on wages that often contributes to the absence of prepared equipment administrators and eligible building-focused officials; work organization problems; & the need to extend the value of efficient operation.
- Vitality issues related to the availability of fuel, as well as the cost and urgent need to reduce the use of fuel.

Because of the problems discussed above, there is a pressing need to improve the use of binders, aggregates, manpower, equipment and energy, funds from planning, design, construction, rehabilitation, and maintenance standpoints.

Asphalt:

Asphalt is not only a strong, climate-resistant, chemical-resistant and flexible binding material but it also adapts to a number of uses, most commonly for the purpose of binding crushed stone with aggregate in to a hard, tough surface for roads, streets and airport taxiways or runways.

Within the processing method of crude oil, the primary supplies of asphalt can be found. The ever-changing characteristics (physical and chemical) are primarily due to the natural changes in crude oil sources or refining practices, thereby affecting residual asphalt quality on the road.

Hot asphalt concrete mixture (HMAC) consists of:

- Aggregates
- Asphalt binder
- Mineral Filler

Reclaimed Asphalt Pavement:

Milled materials are still importance, even if hot mix asphalt (HMA) reaches the end of its useful life. These Milled Materials can be reused and lessen the quantity of new material if combined with virgin HMA which furthermore degrades the new bitumen's quantity required in the production of Hot Mix Asphalt (HMA) and thereby the cost decreases and preserve natural resources [1].

B. Historical Background:

During the last several years in United States, hot mix asphalt processing has been used comprehensively. As Reclaimed Asphalt Pavements (RAP) typically have performed the same or better than the new HMA pavements, it is no longer considered as an experimental program. Consequently, much less research programs are assessing the relative performance of reclaimed and virgin hot mix asphalt pavements.

In Florida, recycled HMA is being used since 1978. Reports shows that pavements constructed by milling or replacement by reclaimed HMA performs better than those constructed of virgin overlay and wearing courses. By full-depth milling of cracked layers, various reflective cracks have been removed successfully. Compared to virgin HMA, the laboratory and in-place analysis of reclaimed HMA showed similar or better results [4].

In an evaluation study in Georgia comprised of the performance of evaluation of reused & conventional hot mix asphalt surface layers in five projects. The content of 'Reclaimed Asphalt Pavements' (RAP) in these mixtures was from 10% to 40%. The results of both conventional & the reclaimed portions were described to be conducting acceptably having no notable rutting, weathering and raveling, and fatigue crackings. The average rut depth of the reclaimed sections was 2mm (0.08 in.), with no fatigue cracking or raveling, and a very less longitudinal and transverse cracking. A quantitative analysis found no noticeable difference in in-service HMA mix and reclaimed asphalt cement properties and quality of recycled and virgin HMA test portions in these 5 projects [2].

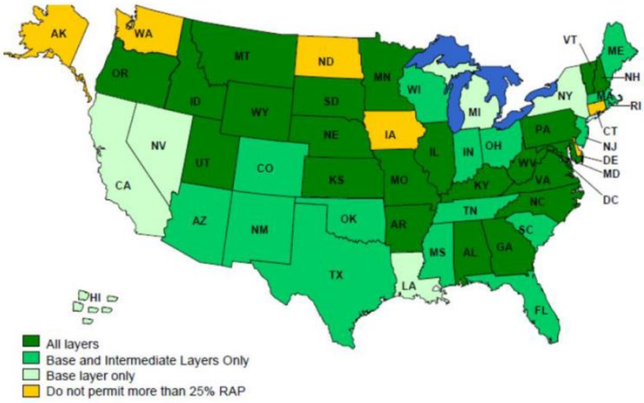

Fig 1: The states that use various %ages of rap in HMA mixtures [1]

From 1987 to 1992, eight warm in-place recycled programs were accomplished in New York. All these projects were satisfactorily accomplished in 1992. Of the eight projects, six had average daily traffic volumes ranging from 9000 to 62000 vehicles on interstates [5].

The objectives of this study are:

1) To find out the best compatible amount of RAP with new pavement materials to withstand the traffic and climate loads in Pakistan.
2) To minimize the cost of new materials required for construction of pavement.

II. Methodology

The methodology acquired to attain the objectives of this research that includes collection of materials, testing of materials, sample's preparation and different tests on specimens. The study was carried out under controlled conditions. The determination of OBC was determined at varying percentages of asphalt (3% to 5%) using Marshal Mix Design. Based on the OBC results, performance testing was done. Performance testing includes Marshal Mix design and Rutting performance test at various percentages of reclaimed asphalt pavements (RAP).

A. Material Collection

For this research new aggregates were obtained from Margalla hills crush plant site which is observed to be the vast live aggregate quarry in Pakistan and bitumen binder of penetration grade 60/70 that is usually being used in many of the highway projects was collected from Attock Refinery Limited.

The RAP material was collected in the form of pieces from Naguman located on main charsadda road leading to Peshawar. To meet the specified grading needs, the RAP pieces were crushed & broken to various sizes. Prior to bitumen extraction, the particles of size 25mm were eliminated as the standard NMAS was 19mm.

B. GRADATION SELECTION

"Gradation is perhaps the aggregate's most important property. It affects nearly all of the major properties of HMA which includes permeability, stability, stiffness, workability, durability, frictional resistance, fatigue resistance and moisture resistance." [3]. In this research, NHA Class A wearing course and gradation was used, which is further discussed in this chapter. Wearing course samples is of 4-inch diameter, for the Marshall method were prepared.

Table 1: NHA Class 'A' Wearing Course Aggregate Gradation

Sieve Size		**% Commulative Passing**	**% Passing (AVG)**
(mm)	**(inch)**		
25	1	100	100
19	3/4	90-100	95
9.5	3/8	50-70	63
4.75	#4	35-50	42.5
2.38	#8	23-35	29
1.18	#16	5-12	8.5
0.075	#200	2-8	5
Pan			

The extraction of Asphalt test was performed using AASTHO T 164, "the quantitative extraction of bitumen out of paving mixtures", to determine the % of asphalt binder in RAP material. The gradation of RAP source and the binder content of the source after extraction and are listed in (Table 3.2). All these tests were performed in duplicate & the values that are mentioned are the average values.

Virgin and RAP source was used in various proportions (0, 20%, 40%, 60%, 80%, and 100% RAP). For this work, laboratory testing was restricted to 19 mm nominal total aggregate size (NMAS). The Marshall Mix design technique was adopted for the design of wearing section mixture and further rutting test was performed in order to check the deformation.

Table 2: Gradation of RAP Source

Bitumen Content (%)		3.3
Sieve Size		**% Passing (Avg)**
(mm)	**(inch)**	
25	1	100
19	3/4	93
9.5	3/8	66
4.75	#4	40
2.38	#8	32
1.18	#16	9
0.075	#200	6
pan		

According to AASHTO T 166, water absorption and bulk specific gravity of the Marshall mixes were calculated. The flow and stability tests were performed in conjunction with AASHTO T 245 after assessing the bulk specific gravity of the test samples. For both marshal testing and rutting performance testing based on 4 percent air void, the optimum asphalt content was 4.2 percent for control mix. The maximum amount of asphalt in the mixture was estimated to be equal to the mixtures of 100 percent virgin wearing course mixtures.

C. Calculation of Percentage of New Bitumen Required:

The new bitumen binder percentage was determined using the equation shown below for the 10 to 80 percent RAP mixtures. The 100 percent RAP mixture samples were compacted without the addition of new binder as the RAP binder then exceeds the optimum asphalt content.

% New Asphalt, $= Pnb = \{(100^2 - rPsb)Pb/100(100 - Psb)\} - \{(100 - r)Psb/(100 - Psb)\} - - - - - - - - - - - - - (Asphalt\ Institute, 1986)$

Where,

Pb = Asphalt content of recycled mix, %

Pnb = Amount of additional asphalt &/or recycling agent in reclaimed mix, percent

R = Percent New asphalt &/or recycling agent in recycled mix to total asphalt

D. Marshal Stability and Flow Test:

The Marshall flow & stability test for the Marshall mix design method provides the performance prediction determination. The test's stability section measures the specimen's maximum load at a loading rate of 50.8 mm / min (2 in/min). Primarily, the load is increased up to it reaches a peak, then the load is stopped and the maximum load is recorded when the load just starts to decrease.

As a result of the loading, a dial gauge attached tests the plastic flow of the sample. The flow value is measured increments of 0.25 mm (0.01 in) concurrently with the measurement of the maximum load.

Table 3: Typical Marshal Mix Design Stability and Flow criteria

Mix Criteria	**Light Traffic (less than 104ESALs)**		**Medium Traffic (104 – 106ESALs)**		**Heavy Traffic (greater than 106ESALs)**	
	Min.	**Max.**	**Min.**	**Max.**	**Min.**	**Max.**
Compaction (number of blows on each end of the sample)	35		50		75	
Stability (minimum)	2224 N (500 lbs.)		3336 N (750 lbs.)		6672 N (1500 lbs.)	
Flow (0.25 mm (0.01 inch))	8		20		8	
Percent Air Voids	3		5		3	

III. RESULTS AND DISCUSSIONS

The Marshall Mix design of conventional mix i-e (virgin aggregates from Margalla Hills and Attock Refinery bitumen of penetration grade 60/70) and of RAP source with Margalla aggregates are summarized in Table 4 and 5 as shown. All the mixtures containing RAP, satisfy the minimum stability criteria of 6 KN for heavy traffic and also fulfill the VMA and VFA specifications, but the flow values of the last three samples of RAP, two of which (80% & 100% RAP) failed to meet the maximum specification criteria i.e. 16 (0.25mm (0.01in)) and the samples containing 60% RAP nearly satisfies the maximum flow criteria. The rutting performance of the mixtures (shown in Table 6) also satisfied the rut depth specifications criteria up to 40% of RAP, the mixtures containing amount of RAP above 40% failed to satisfy the maximum rut depth criteria. Generally the properties of the mixtures improve with the By RAP material; the properties of the mixtures generally improve which shows that recycling is a viable option for HMA design. The variability in the properties of the mixtures is due to the variability of the RAP material that generally increases with the increase in percentages of RAP.

Table 4: Marshal Parameters Determined For Conventional Mix

Bitumen %	Va (%)	VMA (%)	VFA (%)	Gmb	Gmm	Stability (KN)	Flow (0.25 mm (0.01in))
3.5	5.54	14.12	53.65	2.334	2.500	10.12	12
4	4.25	13.69	63.82	2.361	2.484	11.50	11.87
4.5	3.35	13.45	72.85	2.378	2.468	12.87	11.53
5	3.00	14.02	78.15	2.375	2.451	11.95	11.7
5.5	2.82	14.56	80.26	2.372	2.443	10.56	11.9

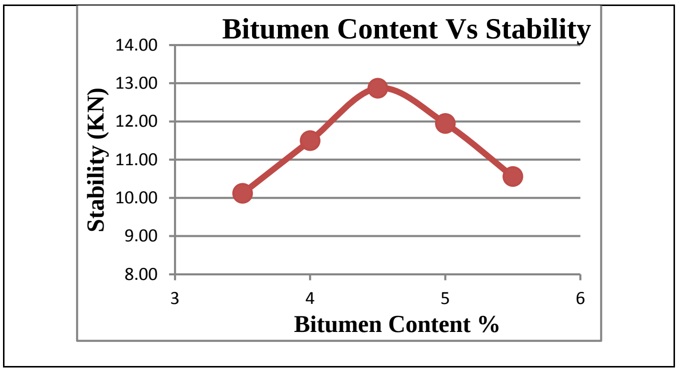

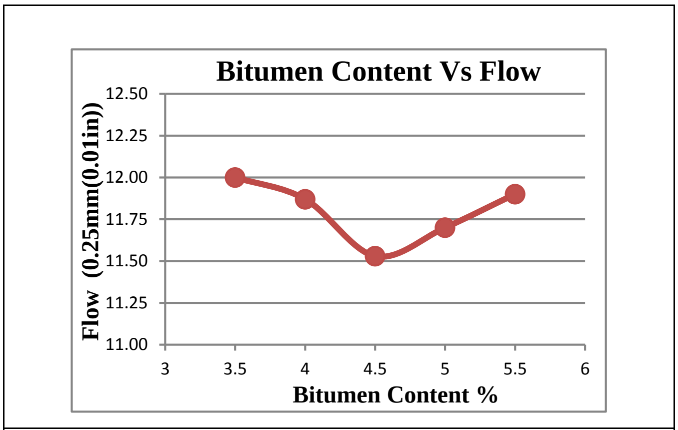

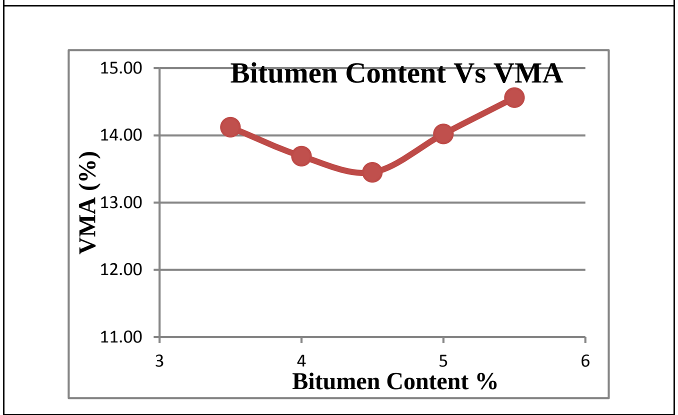

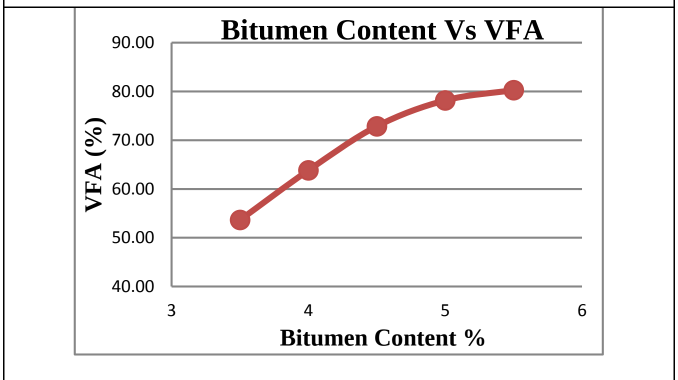

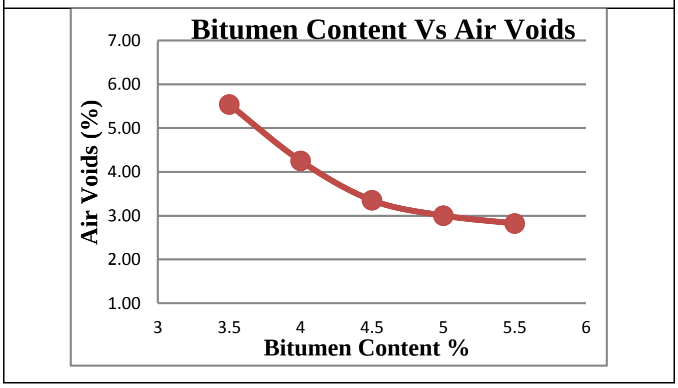

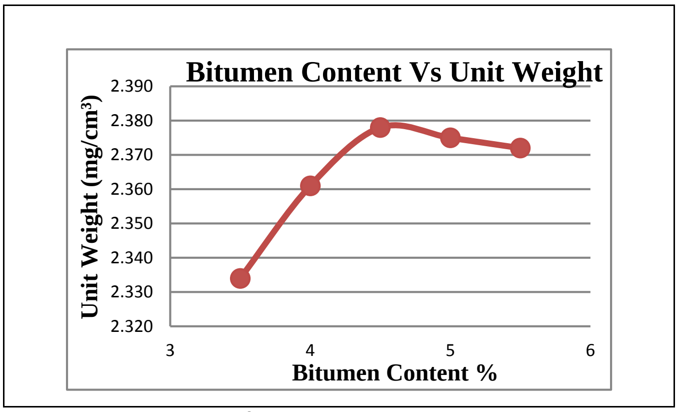

Figure 2: Plots of Bitumen Content Vs Volumetrics

Table 5: Marshal Parameters Determined for RAP Mix

RAP %	Va %	VMA %	VFA %	Gmm	Gmb	Stability (KN)	Flow(0.25mm (0.01in))
0%	4.0	13.25	70.50	2.365	2.530	11.50	11.50
20%	3.87	13.95	74.56	2.379	2.470	10.50	10.50
40%	3.80	14.00	77.97	2.391	2.410	09.77	09.77
60%	3.00	12.80	82.21	2.387	2.360	12.97	12.97
80%	2.69	12.25	84.51	2.384	2.280	16.11	16.11
100 %	2.42	11.55	86.55	2.380	2.200	17.12	17.12

The plots below indicates that using RAP content up to 40 percent is acceptable as the stability increases because of the mixture containing aggregates from two sources(i.e virgin and RAP source) and also the RAP material comprises of the thin bitumen film coating which makes the mix more stable but above 40 percent the flow is exceeding the maximum flow requirement of Marshal Mix Design, as the amount of bitumen increases so as the flow also increases which makes the mix susceptible to rutting.

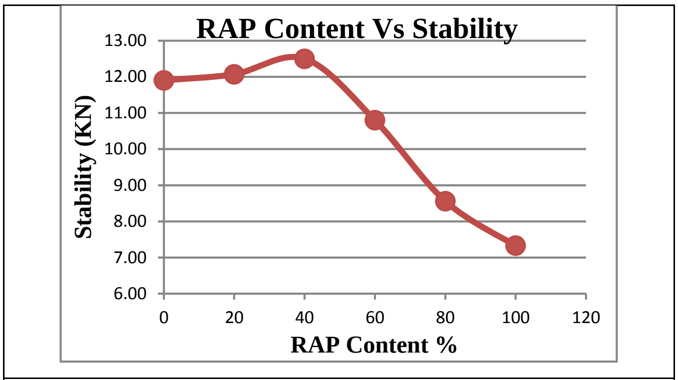

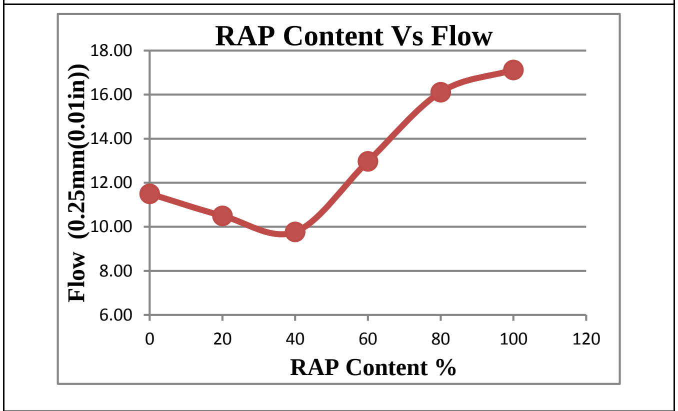

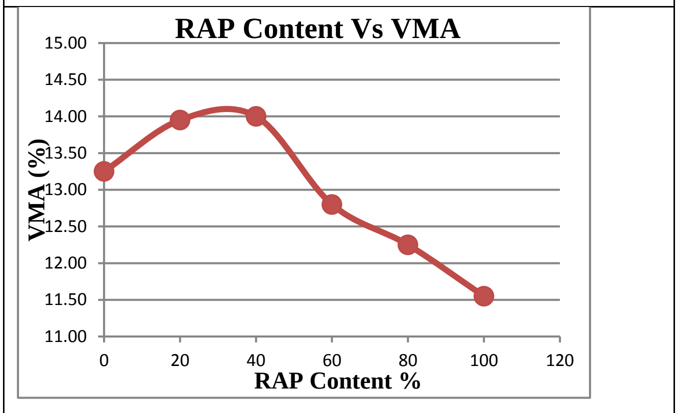

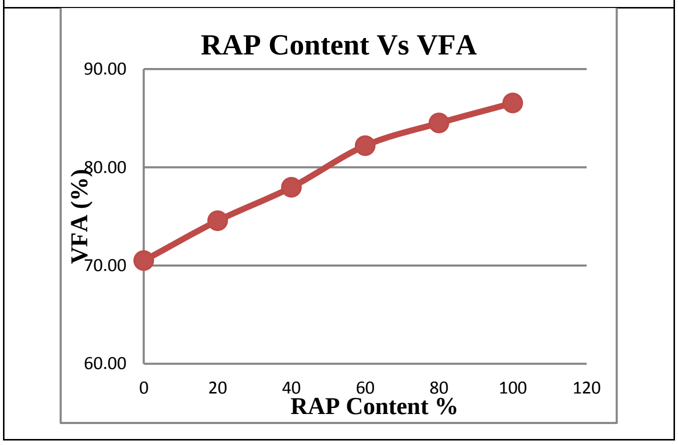

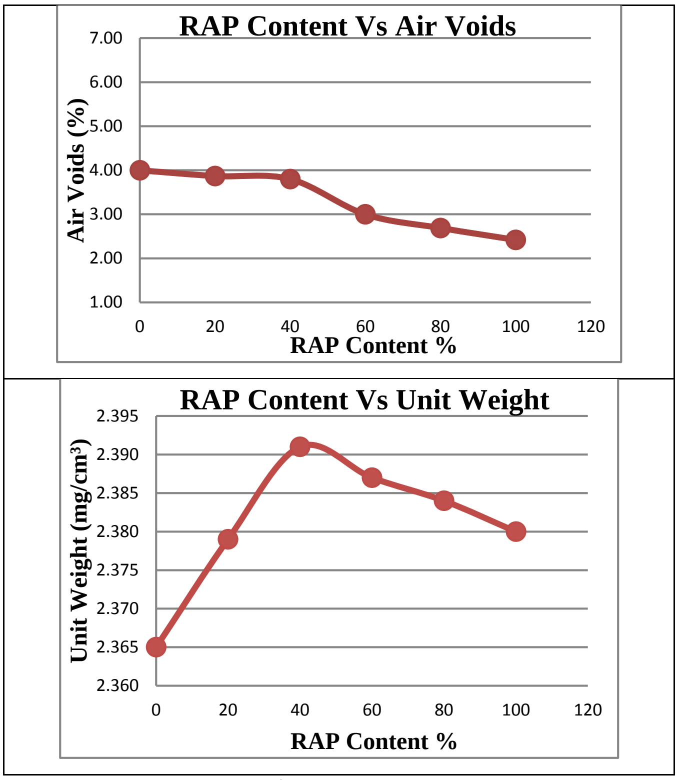

Figure 3: Plots of RAP Contents VS Volumetrics

Table 6: Summary of Rutting Performance of Mixtures

Pass Criteria: Maximum 12mm Rutting depth at 10000 Passes	
RAP%	**Rut Depth(mm)**
0%	8.51
20%	7.61
40%	4.18
60%	11.97
80%	13.21
100%	15.21

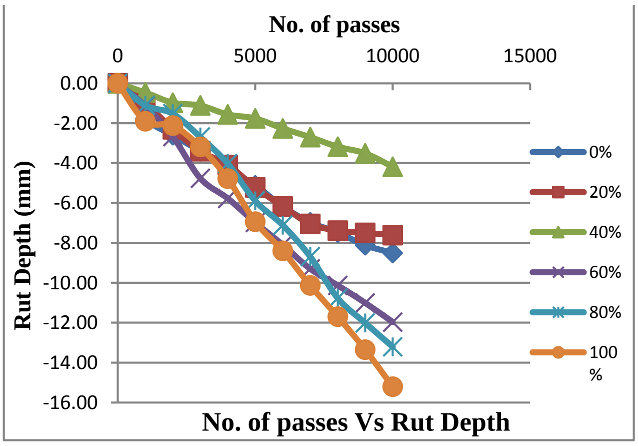

Figure 4: Rutting Performance of the Mixes

Conflict of Interest

The contents of this study are free from plagiarism and therefore the study is original and is not copied from anywhere. Previous work of original authors has also been referenced.

Conclusion

This study concludes that:

- RAP mixtures designed in laboratory using Marshall Method perform the same or even better than the conventional mixture but up to some limit.
- Generally the Marshall stability generally increases linearly as RAP content increases up to 40 percent. The stability of the 40 percent RAP mixtures is even more than that of the stability of conventional mixture.
- Using percentage of RAP above 40%, most of the mixtures did not meet the maximum flow requirements suggesting that the aged bitumen did not participate well and that the mixtures were stressed during loading.
- The use of RAP in design up to 40% would help to preserve natural resources, reduce price of HMA and improve the performance.
- Also the results of rutting performance shows that RAP contents performs better than the conventional mix but up-to a certain limit i.e 40% RAP content.
- The rut depth of the mixture containing 20% and 40% RAP shows rut depth less than that of a virgin mixture which concludes that RAP contents up-to 40% can perform better than virgin mixture.
- But exceeding RAP content higher than 40% fails to reach the maximum rut depth of 12 mm at 10000 passes as per standard which shows the failure of the mixtures containing RAP contents higher than 40%.

Recommendations

Based on the conclusions of the research the following recommendations are to be considered appropriate.

- It is recommended to construction of a trial section using virgin and RAP blends is suggested to verify the suitability of RAP mixtures to climate conditions and traffic loadings in the country.
- It is recommended for future study, it is recommended that modified binder and 25 mm NMAS be used to see the performance of the RAP mixtures as the base course material.

Acknowledgement

Author is thankful to his supervisors for their consistent help throughout this study. The author is thankful to the Department of Civil Engineering, Sarhad University for providing Lab equipments.

References

[1] Copeland, Audrey. Reclaimed asphalt pavement in asphalt mixtures: State of the practice. No. FHWA-HRT-11-021. 2011.

[2] Kandhal, Prithvi S., Shridhar S. Rao, and Brad Young. Performance of recycled mixtures in state of Georgia. No. FHWA-GA-94-9209. Georgia. Dept. of Transportation, 1994.

[3] Roberts, Freddy L., et al. "Hot mix asphalt materials, mixture design and construction." (1991).

[4] Sullivan, John. Pavement recycling executive summary and report. Federal Highway Administration, 1996.

[5] Thomas E. Wohlscheid, In-Place Pavement Recycling in New York State, Paper Prepared for the 19th Annual Meeting of the Asphalt Emulsion Manufacturers Association and the 16th Annual Meeting of the Asphalt Recycling & Reclaiming Association,1992.

Asif Nawaz, the auther, is resident of Charsadda. He completed his bachelor degree of Civil Engineering from Sarhad University of Science & Informtaion Technology, Peshawar in 2016. The auther is pursuing his master’s degree in Highway & Transportaion Enginnering from Sarhad University of Science & Information Technology, Peshawar. This paper is his research study for the mster’s degree.

International Journal of Engineering Works
ISSN-p: 2521-2419
ISSN-e: 2409-2770
Vol. 6, Issue 12, PP. 479-489, December 2019
https://www.ijew.io/
https://doi.org/10.34259/ijew.19.612479489

A Comparative Study of Power Factor Improvement in Pakistani Industry Using Different Strategies; A Case Study

Muhammad Bilal [1], Abdul Basit [2], Shifaat Ur Rehman [3], Kamil Shaheed [4], Niaz Ali[5]
[1,2,3,5] US-Pakistan Center for Advance Studies in Energy (USPCASE) University of Engineering and Technology Peshawar, Pakistan
[4] International Islamic University Islamabad, Pakiatan
engr.bilal92@gmail.com[1], abdul.basit@uetpeshawar.edu.pk[2], shifaatqurtuba@gmail.com[3], kamil.bsme102@iiu.edu.pk[4], engr.niazi91@gmail.com[5]
Received: 08 November, Revised: 17 November, Accepted: 19 November

***Abstract*—**Most of the industrial machines have reactive power during operation due to which these machines are facing low power factor. One of the important existing public sector industries (where heavy mechanical products are manufactured) of Pakistan is under study, which has a very low power factor i.e. in the range of 0.60 to 0.75. This low power factor not only increase the cost (when there is extra bill and power factor penalty in the rate clause) but also decrease electrical capacity of power distribution system. In the public sector organization, there are five loads in the public sector industry i.e. machine shop load, heat treatment shop load, non-ferrous shop load, gal/forge shop load and fabrication shop.

In the proposed thesis, we have utilized capacitor bank in the existing distribution network .We investigated the shunt capacitor banks for Power Factor Correction (PFC). After analysis of the proposed distribution network in Matlab/Simulink software, it was found that using shunt capacitor bank in parallel with load, the power factor increased to 0.95, due to which proposed system and devices efficiency increased. The power losses decreased tremendously. Voltage drop has been reduced. Reduction in size of a conductor and cable reduced cost of the copper. Three different strategies (Central PFC, Regional PFC, Local PFC) are followed in this power factor improvement study and each one is then compared with the previous system.

***Keywords*—** Machines, Capacitor bank, Transformer, bus bar, distribution parameters, Power Factor Correction (PFC).

I. Introduction

The power that runs in the power systems is a combination of active and reactive power. As an example, for the proper functioning of a motor in a fan, a specific amount of active power P and reactive power Q are to be supplied to the fan. The process of rotation of fan requires the magnetization of the winding and the rotation of the fan. The former is achieved through the reactive power and the latter is accomplished through the active power. One of the problems that normally take place in such scenarios is that the load takes up a lot more of the reactive power as compared to the normal conditions or rated values. Majority of the load at the consumer end is inductive load.

The voltage slumps at the load whenever the demand for the reactive power increases. This scenario is always catered for by introducing the capacitive components in the circuit like a capacitor bank or a FACTs device. A black out is always on the cards if the reactive power compensation is not provided immediately within a fraction of seconds.

Motors are undoubtedly the most commonly and massively existing and installed inductive load in the industry globally. Their inductive nature causes the phase between current and angle to shift such that current lags and voltage leads as shown in Figure 1.

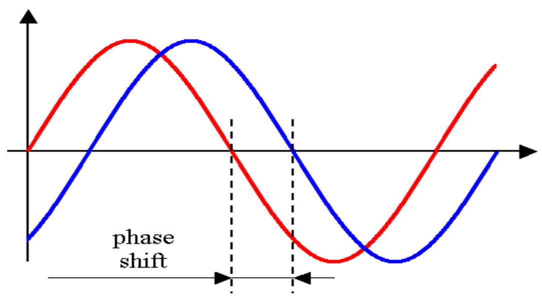

Figure 1. Phase shift

Current is said to be in an advanced state and voltage in a delayed state if it leads, mainly in a capacitive load. On the other hand voltage is said to be in an advanced state and current in a delayed state if it is an inductive load. The change in this difference of the angles of current and voltage result as a decreased value of the usable power or the real power P, as compared to the supplied power that is kVA or MVA.

Representing those powers by vectors, the "power triangle" may be as shown in figure. 2.

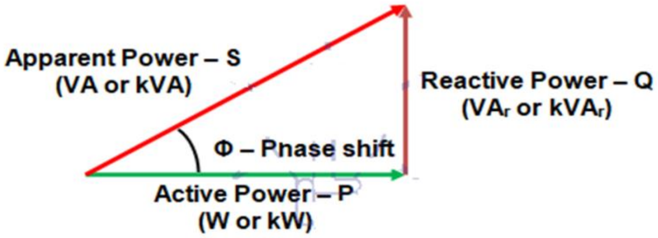

Figure 2. Power triangle

The trigonometric ratio cosine, when applied to the difference of the angles of current and voltage, denoted by Φ, gives the power factor.

$P = S * \cos \Phi$

$Q = S * \sin \Phi$

If the power factor is low then the following unwanted phenomena can take place such as:

a) Massive drops in voltages.
b) Massive current flow in the lines.
c) Higher losses by Joule effect in the conductors.

Majority of the countries follow a strict rule that does not permit power factor to drop short of 0.9 Else, many penalties and fines are imposed for the violation. The process of power factor correction, at the clients' end, involves the reduction in the apparent power by shrinking the power demand at the substation when operating at the peak hours where load is at its maximum. It is at this stage where the vacated capacity of the system is employed for delivering more power to the load. This inherently improves the system by increasing its efficiency. The improvement of power factor also comes with many advantages such as savings in terms of money because the wire can now be used of a smaller cross sectional area.

Capacitors are commonly found in distribution circuits. By freeing up some space for capacity, reducing the end losses and by making up for the loss of the voltage, the capacitors, as a result, amplify the performance of a distribution system. Mainly they are employed for power factor correction, voltage regulation and reduce the losses. Just like dams store water, capacitors store reactive power, which is readily supplied to the reactive load in case of need. Distribution capacitors are generally pad mounted and pole mounted but mostly the pole mounted is followed. A switch ON and OFF mechanism is usually followed to initiate and terminate respectively the charging process of a capacitor. The capacitors which do not have such a switch are always ON or OFF.

Capacitors bank provide benefits to the distribution system, it can devise a condition in which a best location and sizing of the capacitor is achieved i.e.

1- Power Factor Correction.
2- Increase the voltage of the load bus.
3- Reduce transmission losses ($I^2 R$).
4- Improve bus-voltage stabilization /regulation.
5- Release of system capacity.
6- Reduce the lagging component of the circuit current.
7 - Efficient power utilization.
8- Reduce electricity billing cost based on kVA demand.

Although capacitors provide benefits to distribution systems, when not properly employed they can create losses and over voltages. The scenario when a capacitor is completely or nearly completely charge, the closing of the capacitor results in the form of generation of transient inrush current. A transient response gets introduced in the circuit whenever a sudden change is encountered such as that of switching ON or OFF.

As stated above, Capacitor Bank can be fixed or controllable nature. Fixed Capacitor Banks are typically only switched on or off a few times during their useful lifespan, leading to few transients. In contrast, switched capacitor banks offer a greater threat of generating transients in distribution circuits since these banks may switch on and off several times during the day, each time generating a transient. In this study we are installing fixed capacitor banks.

The points that need to be taken care of while performing the installation of capacitor banks are as under:

a) Careful selection of the control mechanism to be employed in the system.
b) Cautiously determining the location to install the capacitor bank.
c) Calculation of the bank size (the size of a capacitor bank in kVAR)

A special type of relay is also used in capacitor bank for the protection and supervision of capacitor banks. The one shown in diagram is "ABB" made "REV615". They are responsible for monitoring the safety levels and in response perform the switching operation in the network in real time as quickly as possible which is shown in Figure 3.

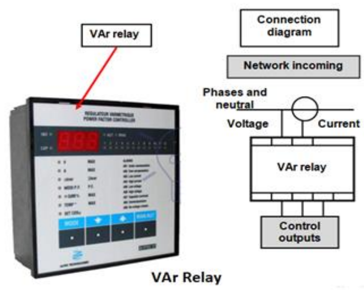

Figure 3. VAR relay

The equation below helps calculate the size of the required capacitor for compensation.

$Q\,[kVAR] = P\,[kW] \times (\tan \Phi 1 - \tan \Phi 2)$

Here P refers to the real component of the power at the installation node. Φ1 and Φ2 represent the phase shifts of voltage and current at the installation and the desired one respectively. In order to characterize the location of installation of the capacitor bank, there are three schemes that are dominantly in use. Which technique to be used depends upon the location where the load is inductive and the real power that is to be sent.

A. Centralized correction

In this scheme there is only one capacitor bank which is installed close to the main incoming switchboard as shown in figure 4.

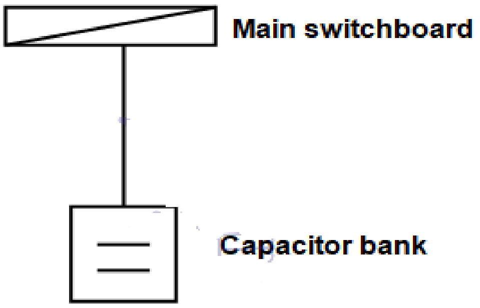

Figure 4. Centralized Power Factor (P.f) correction

B. Regional correction*:*

This scheme proposes the installation of capacitor banks in proximity of the distribution switchboards. These are responsible for furnishing the required energy to the most important consumers that cause the degradation of the power factor as shown in figure 5.

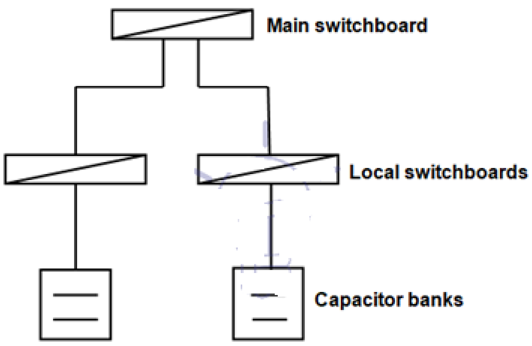

Figure 5. Regional Power Factor correction

C. Local correction

Suggests that capacitor banks be installed in the neighborhood of the individual consumers as shown in Figure 6.

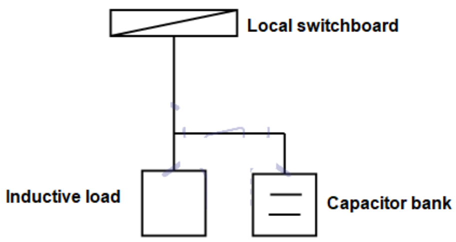

Figure 6. Local correction

II. Literature overview

Power factor is actually cosine of the angle between voltage and current phase shift. It ranges between 0 and 1. If the load is purely resistive (ideal), the angle between voltage and current becomes zero, therefore the cosine of this zero, which is the power factor, becomes 1 [1,2]. It is an ideal condition. In case, if the load is not resistive, then it is either capacitive or inductive, broadly classified as reactive. In such case the angle difference between the voltage and current is 90O, therefore the power factor, cosine of 90O becomes equal to zero thus rendering the worst possible value of the power factor. Power factor is leading in capacitive load and lagging in inductive load. Where the power factor is leading, it implies that the load is generating the reactive power. If the power factor is lagging then it means that VARs are being consumed by the load. [3]. The value of Power factor cannot be zero or unity and will always be higher than zero or less than one [4].

When an increase in reactive power happens, the value of the voltage in the line drops meanwhile increase in the current is observed. In order to get rid of such a situation, it is inherently important that power factor be maintained in the range of 0.8 to a maximum value of 1 at all times. If not, the equipment at the user end might go out of order causing millions in losses [5]. Harmonics generated in the system distort the voltage and current waveform and consequently distort the power factor. The power factor distortion can be obtained by considering the total harmonic distortion of the voltage and current [6]. The root mean square of voltage or current harmonics over the fundamental voltage or current computes the total harmonic distortion. The extent of disfigurement caused to the power factor can be found out by finding the ratio of the fundamental voltage and current to the total values of voltage and current. [6,7]

A large phase shift and harmonics create low power factor displacement and distortion. A capacitor is useful to correct the power factor displacement in linear loads. But when dealing with the loads that are non-linear, harmonic filter is widely preferred since power resonance generates mighty values of the higher order harmonics [8]. While talking about industries, almost half of the load is of Induction Motors [9]. Mechanical resistance and magnetization reactance are in direct proportion in an induction motor. Even a slight change in the values of the above mentioned two considerations, mechanical resistance and magnetization reactance, results as a huge variation in the value of the power factor.[10][12]. In an industry load as well as power factor is changing at every instant hence requires immediate and sharp catering for. To solve this problem, reactive power compensation is required by the user. A capacitors bank is a substantial solution to generate reactive power [13, 14, 15].

To find out the value of the reactive power needed for the motor, research works have depicted that the reactive component of the no load current is always equals to the nine tenth of the current in the no load case. However, if full load current is available, the no-load current can be predicted as 30% of the full-load current. Then, 90% of the full-load current provides the required reactive power in VAR [16]. However, this method is not sufficient to determine the proper size of capacitor because it only provides an approximation, in particular at fixed load. Therefore, this empirical technique may create under- or over-correction at operating time, where under-correction causes a penalty charge for the user while overcorrection produces self-excitation, which is harmful for the induction motor winding [17].

The study found that the power factor correction equation is a suitable technique to calculate the exact amount of reactive power required at any loading point in individual or group induction motors, or even at a point of common coupling. This method took three factors into consideration which were the power factor before any device, the power factor to reach and the power at the input.[18][19]. One method to find the exact value of capacitor is also carried out in MATLAB/Simulink. It renders a value of kVAr which is the required capacitor value for compensation. [13]. Another methodology comes with the installation of a device that is called a power analyzer. It is responsible for the measurement and saving of the parameters which are power factors, current, voltage and power.[14][20][21]

The method known as Measured Current and Manufacturer's Data (MCMD) has been used for the calculation of power factor of an induction motor with rated power of 2200 W. It is calculated at many loads. It takes into account a mathematical equation for the sake of providing an optimal, feasible and practical solution [14]. In this approach, the measured current method is used to obtain the load. The results of the proposed method are compared with the instantaneous power method and zero crossing method, and show errors of + 0.04 at the full-load condition and -0.18 at the no-load condition [14]. Kriging and regression are also techniques for estimation of power factor mostly for the residential houses. In the regression method, a locally weighted regression technique with an exponential function has been used. The Kriging method with a semivariogram model is considered.[24,25]. In case of small induction motor (mostly under 250 W) A zero crossing method and instantaneous power method are presented to determine the power factor from no-load to full-load conditions. Also, using equivalent circuit parameters in the induction motor can be a great way to determine the power factor because the total resistances over impedance obtain the power factor [11][23]. The Kriging method is also applied in this induction motor to estimate the power factor. For the motor ,mentioned above, results showed that the zero crossing and instantaneous method produced errors of 22% and 35%. However, the Kriging method created an average error of 14% [22]. In this induction motor, MCMD and Kriging are also applied to estimate the power factor from no-load to full-load conditions [26]. However, the Kriging and regression methods were not able to estimate the power factor from full-load to over-load conditions because both methods are interpolation techniques and cannot extrapolate unseen points.

ANN is an intelligent technique used to estimate the power factor in distribution systems by analyzing the real parameters of the power system. In a research made by power distribution company in Victoria (Australia), the results showed that the ANN is able to estimate the power factor at unseen points with an accuracy of 93% [27].

We can have some economic benefits by improving power factors.

- Benefits due to increase in generation capacity of the system
- Benefits due to energy conservation or reduction of energy losses
- Benefits due to increase in the capacity of distribution substation
- Benefits due to reduction of system voltage drops (or we can say voltage improvement)
- Benefits due to increase in the capacity of feeder
- Benefits due to increase in the transmission capacity of the system

The total benefits we can avail due to installation of shunt capacitor banks can be summarized as shown in Eq. (1).

$$\sum \Delta\$ = \Delta\$_G + \Delta\$_T + \Delta\$_S + \Delta\$_F + \Delta\$_{ACE} + \Delta\$_{GBCE} \quad \text{--------(1)}$$

Where:
$\Delta\$_G$ = Annual benefits due to increase in generation capacity \$/yr
$\Delta\$_S$ = **A**nnual benefits due to increase in substation capacity, \$/yr
$\Delta\$_F$ = Annual benefits because of increasing feeder capacity, \$/yr
$\Delta\$_{ACE}$ = **A**nnual benefits due to conservation of energy, \$/yr
$\Delta\$_{GBCE}$ = **A**dditional annual revenue due to increase in the consumption of kWh energy, \$/yr
$\Delta\$_T$ = **A**nnual benefits because of increasing transmission capacity, \$/yr [28]

We can calculate the approximate value of the percent voltage rise (%VR) along the line can be calculated as given in equation (2):

$$\%VR = \frac{Q_{C,3\phi} \times l}{10 \times V_{L-L}^2} \quad (2)$$

By putting the values in the above equation we can easily calculate the percent voltage rise along the line [28].

Capacitor Bank

A capacitor, also known as "condenser" is an electrical element with two electrical conductors separated by an insulator material (dielectric), as shown in Figure 7.

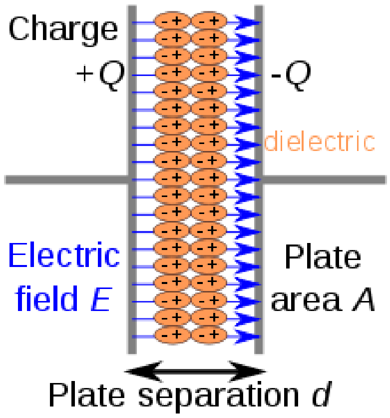

Figure 7. Simplified scheme of a capacitor

The multipurpose device known as the capacitors that fall under the requirements of the IEEE standards which are namely 60871 60143, standard 824 are in use for the research purpose [1]. The primary applications and advantages of capacitors are:

a) Power factor correction and reactive power compensation requirements which arise due to MV and LV consumers.
b) The induction effect of transmission lines which are either overhead or underground.
c) Achieving voltage regulation in HV transmission lines. [3]
d) Starting the 1φ motor (Squirrel Cage-Low Voltage).

The capacitors are amassed either in a series or a parallel combination. Capacitors are either connected in a delta formation or a Y formation depending upon the nature of the distribution network. An MV distribution network is equipped with a delta formation of capacitors, so does the LV network.

Figure. 8 shows casing of above mentioned capacitors.

When capacitors remain in use for a longer period of time, then being a charge storage device, they preserve the charge in them. This turns the capacitors into a two way sword which can even cause the connected devices to get a sudden and unexpected charge resulting in them burning out and requiring an immediate maintenance or often replacement. Sometimes capacitors come with internally integrated resistors to discharge the stored charges and causing the other devices to remain safe [4].

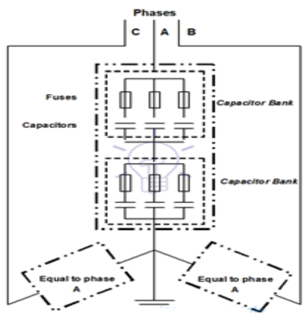

Figure 8. Schematic diagram of a capacitor bank

III. METHODOLOGY

Simulation is done with Matlab/Simulink of the existing power system of the case industry and the existing parameters and other relevant data(current, voltage, power, power factor etc) are in study. Three different strategies of capacitor bank installation for the purpose of power factor correction are under study.

1) Centralized correction(strategy 01)
2) Regional correction (strategy 02)
3) Local correction (strategy 03)

Each sytem involving the above mentioned strategy is then simulated in Matlab/Simulink. All the relevant output data and power parameters of these strategies are compared with the data of the system without capacitor bank. Also the output data and power parameters of each strategy are also compared among each other in the end.

Methods used for power factor correction:

Method1:

$\theta 1 = \text{Cos}^{-1}(0.XX)$; Tan θ1

$\theta 2 = \text{Cos}^{-1}(0.95)$; Tan θ2

So the Required Capacitor kVAR to improve P.F from 0.XX to 0.95

Required Capacitor kVAR = Q (Tan θ1 – Tan θ2)

Method 2:

Multiplier to improve PF from 0.XX to 0.95 and load rated power will result the desired Capacitor kVAR to improve power factor to 0.95

Required Capacitor KVAR = P(w) x Multiplier of 0.XX and 0.95 as shown in Table I.

Where Multiplier = crossing point to existing and desired P.F.

TABLE I. KVAR MULTIPLYING FACTOR OF 0.XX AND 0.95

Multiplying factor for KVAR

cosφ		0.93	0.94	0.95
	tg φ	0.40	0.36	0.33
0.40	2.29	1.896	1.924	1.959
0.41	2.22	1.831	1.840	1.896
0.42	2.16	1.771	1.800	1.836
0.43	2.10	1.713	1.742	1.778
0.44	2.04	1.647	1.677	1.712
0.45	1.98	1.592	1.626	1.659
0.46	1.93	1.533	1.567	1.600
0.47	1.88	1.485	1.519	1.532
0.48	1.83	1.430	1.464	1.467
0.49	1.78	1.386	1.420	1.453
0.50	1.73	1.337	1.369	1.403
0.51	1.69	1.291	1.323	1.357
0.52	1.64	1.249	1.281	1.315
0.53	1.60	1.206	1.237	1.271
0.54	1.56	1.164	1.196	1.230
0.55	1.52	1.124	1.156	1.190
0.56	1.48	1.085	1.117	1.151
0.57	1.44	1.047	1.079	1.113
0.58	1.40	1.010	1.042	1.073
0.59	1.37	0.973	1.005	1.039
0.60	1.33	0.939	0.971	1.005
0.61	1.30	0.904	0.936	0.970
0.62	1.27	0.870	0.902	0.936
0.63	1.23	0.838	0.870	0.904
0.64	1.20	0.805	0.837	0.871
0.65	1.17	0.774	0.806	0.840
0.66	1.14	0.743	0.775	0.809
0.67	1.11	0.713	0.745	0.779
0.68	1.08	0.684	0.716	0.750
0.69	1.05	0.654	0.686	0.720
0.70	1.02	0.625	0.657	0.691
0.71	0.99	0.597	0.629	0.663
0.72	0.96	0.568	0.600	0.634
0.73	0.94	0.541	0.573	0.607
0.74	0.91	0.514	0.546	0.580
0.75	0.88	0.487	0.519	0.553
0.76	0.86	0.460	0.492	0.526
0.77	0.83	0.434	0.466	0.500
0.78	0.80	0.408	0.440	0.474
0.79	0.78	0.381	0.413	0.447
0.80	0.75	0.355	0.387	0.421

Method 3:

Required KVAR = S x (sin (cos (θv – θI))

Where S is the induction motor apparent power and θv – θI is the angle difference between voltage and current.

B. Existing Distribution Network

The three phase source was being used to provide 11kv/50Hz generation to consumers via transformer and distribution line. The transformer is being used to step down the 11kv voltage to 440v at the distribution side to provide consumer's appliances. In existing factory, large motors have been used to manufacture products but as we know that the induction motors power factor were lagging and draws high current so that reactance factor has been increased.

Here in this public sector organization which is under study, there is load of five workshops:

i) Machine shop
ii) Heat treatment shop
iii) Non-Ferrous shop
iv) Gal/Forge shop
v) Fabrication shop

The data of the existing system is given in Table II.

TABLE II. DATA SHEET OF ALL SHOPS WITHOUT CAPACITOR BANK

Machine/ Shop No.	P.F	KW	KVAR	KVA	I(LV)	I(HV)(Line	I(HV)(Phase)
MACHINE SHOP	0.71	4035	4002	5683	8202	516.64	298.2822
FAB SHOP	0.69	4207	4408	6097	8800.4	554.282	320.0149
HEAT TREATMENT	0.7	2200	2244.3	3142.8	4536	285.71	164.9547
NON FERROUS	0.74	405	368.114	547.3	789.95	49.7543	28.72566
GAL/FORGE	0.75	1464	1291	1952	2817.47	177.455	102.4534

IV. SIMULATION AND RESULTS

This existing system is implemented in MATLAB/Simulink. We have seen that without capacitor bank, there is a large gap between voltages and current angle so due to which if we take power factor into account; the cosine angle between voltage and current is power factor. If the voltage and current cosine angle difference will be large so power factor will lag. So in the existing system, the system power factor is lagging nearly 0.7 due to which system draws large current from the source via three phase transformer. In addition, Power losses have been increased. The simulations and its results are shown in Table III and Table IV.

TABLE III. SIMULATION RESULTS FOR POWER SYSTEM OF THE CASE INDUSTRY

	SHOPS	Vph (volts) RMS	VL (volts) RMS	Iph/IL (Amps) RMS	S (VA)	Total GEN (VA)	Q (VAR)	Total Q (VAR)
WITHOUT CAPACITOR BANK	NFS	232.85	403.308	796.36	556297.278	17380250.63	373831.771	12279613.59
	M/S	230.21	398.7354	8176.91	5647219.35		3975642.42	
	H/T	231.53	401.0217	4546.46	3157925.65		2254758.92	
	G/F	232.08	401.9744	2831.29	1971257.35		1303001.11	
	F/B	230.07	398.4929	8761.9	6047551		4372379.37	

TABLE IV. SIMULATION RESULTS FOR POWER SYSTEM OF THE CASE INDUSTRY

	SHOPS	P.F	P with respective P.F (Watts)	P with unity P.F (Watts)	P Loss (Watts)	Total Loss (Watts)
WITHOUT CAPACITOR BANK	NFS	0.74	411659.9857	556297.278	144637.2923	5097263.747
	M/S	0.71	4009525.741	5647219.353	1637693.612	
	H/T	0.7	2210547.956	3157925.651	947377.6954	
	G/F	0.75	1478443.012	1971257.35	492814.3374	
	F/B	0.69	4172810.189	6047550.999	1874740.81	

PROPOSED DISTRIBUTION NETWORK

To improve the power factor we are using static capacitor banks in parallel with each load. A capacitor bank is a grouping of several identical capacitors interconnected in parallel or in series with one another. These groups of capacitors are typically used to correct or counteract undesirable characteristics, such as power factor lag or phase shifts inherent in Alternating Current (AC) electrical power supplies. Capacitor banks may also be used in Direct Current (DC) power supplies to increase stored energy and improve the ripple current capacity of the power supply. We have used different strategies of placing capacitor at the system to check the behavior of power factor and reactive power.

Strategy 1 (One Capacitor bank with combined Load or Centralized Correction):

In this type, single capacitor bank is connected to the bus bars of the main LV distribution board for the installation, and remains in service during the period of normal load.

For this scenario the value of capacitor bank required is calculated to achieve power factor of 0.95. The data is shown in Table V.

TABLE V. EXISTING OVERALL LOAD VALUES AND REQUIRED CAPACITOR BANK FOR 0.95 PF

OVERALL SHOPS						
S/NO	LOAD NO	KWA	P.F	KVA	KVAR	REQ CAP
1	L_M1	12331	0.72	17126.39	11885.27	7830.185

Simulation and Results

We have combined all of the loads and installed one capacitor bank to analyze the behavior of the proposed distribution network system, as suggested in strategy 01. It is implemented in the MATLAB/Simulink. The generating source is providing 11kv .The three phase transformer steps down the 11kv to 440kv which is useful for the industry induction motors. The main purpose of providing capacitor bank in case of power system is to supply reactive power to the system and they are installed at the receiver end, this is also called as VAR Compensation. Figure 9 below shows the system designed in Matlab/Simulink for centralized compensation. The capacitor banks here used are Static VAR Compensator. The result shown in table below shows that the power factor has been increased from 0.7 to 0.95.

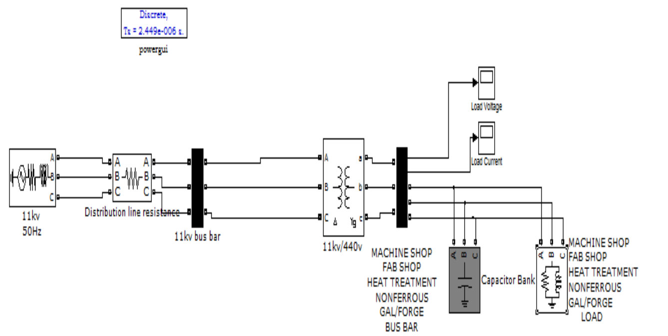

Figure 9. Strategy 1 (One Capacitor bank with overall Load)

TABLE VI. STRATEGY 1 (ONE CAPACITOR BANK WITH OVERALL LOAD)

	SHOPS	RMS Vph (volts)	RMS VL (volts)	RMS Iph/IL (Amps)	S (VA)	Total GEN (VA)	Q (VAR)	Total Q (VAR)
STRATEGY 1	Overall	231.34	400.6926	18736.32	13003380.8	13003380.81	4060304.36	4060304.355

TABLE VII. STRATEGY 1 (ONE CAPACITOR BANK WITH OVERALL LOAD)

	SHOPS	P.F	P with respective P.F (Watts)	P with unity P.F (Watts)	P Loss (Watts)	Total Loss (Watts)
STRATEGY 1	Overall	0.95	12353211.77	13003380.81	650169.0403	650169.0403

Strategy 2 (De-Centralized or Regional Correction):

In this strategy, Capacitor banks are connected to bus bars of each Regional distribution board of each workshop discussed lately. In this system a significant part of the system take benefits from this arrangement, mainly the feeder cables from the main distribution board to each of the regional distribution boards at which the power factor compensation is required.

For this scenario the value of capacitor bank required is calculated to achieve power factor of 0.95. The data is shown in Table VIII.

TABLE VIII. EXISTING REGIONAL LOAD AND REQUIRED CAPACITOR BANK TO ACHIEVE 0.95 PF

PARAMETERS WITH DESIRED POWER FACTORS								
Machine/ Shop No.	P.F	KW	KVAR	KVA	I(LV)	I(HV)(Line	(HV)(Phas	Required KVAR
MACHINE SHOP	0.95	4035	1326.03	4247.37	6130.55	386.124	222.929	2675
FAB SHOP	0.95	4207	1382.55	4428.42	6391.88	402.584	232.432	3029
HEAT TREATMENT	0.95	2200	722.989	2315.79	3342.55	210.526	121.547	1520
NON FERROUS	0.95	405	133.096	426.316	615.334	38.756	22.3758	235
GAL/FORGE	0.95	1464	481.117	1541.05	2224.32	140.096	80.8843	810

Simulation and Results

In strategy 2, we have isolated all loads (each shop is isolated) and installed capacitor bank with individual load(workshop) to analyze the behavior of the proposed distribution network. We have investigated that the power factor has been increased smoothly to 0.95. Moreover, the power loss has been reduced from 5MW to 0.66 MW. Figure 10 shows the system designed in Matlab/Simulink for de-centralized or regional compensation. The capacitor banks here used are Static VAR Compensator. The design is shown in figure 10 and the resultant data after simulation is also shown in the Table IX and Table X.

TABLE IX. STRATEGY 2 (FIVE CAPACITOR BANKS WITH SEPARATE LOAD)

	SHOPS	RMS Vph (volts)	RMS VL (volts)	RMS Iph/IL (Amps)	S (VA)	Total GEN (VA)	Q (VAR)	Total Q (VAR)
STRATEGY 2	NFS	234.93	406.9107	625.9	441128.061	13180429.66	137631.955	4112294.055
	M/S	232.44	402.5979	6170.8	4303022.26		1342542.94	
	H/T	233.69	404.763	3382.33	2371250.09		739830.029	
	G/F	234.2	405.6463	2255.59	1584777.53		494450.591	
	F/B	232.33	402.4074	6428	4480251.72		1397838.54	

TABLE X. STRATEGY 2 (FIVE CAPACITOR BANKS WITH SEPARATE LOAD)

	SHOPS	P.F	P with respective P.F (Watts)	P with unity P.F (Watts)	P Loss (Watts)	Total Loss (Watts)
STRATEGY 2	NFS	0.95	419071.658	441128.061	22056.40305	659021.4832
	M/S	0.95	4087871.143	4303022.256	215151.1128	
	H/T	0.95	2252687.588	2371250.093	118562.5047	
	G/F	0.95	1505538.657	1584777.534	79238.8767	
	F/B	0.95	4256239.134	4480251.72	224012.586	

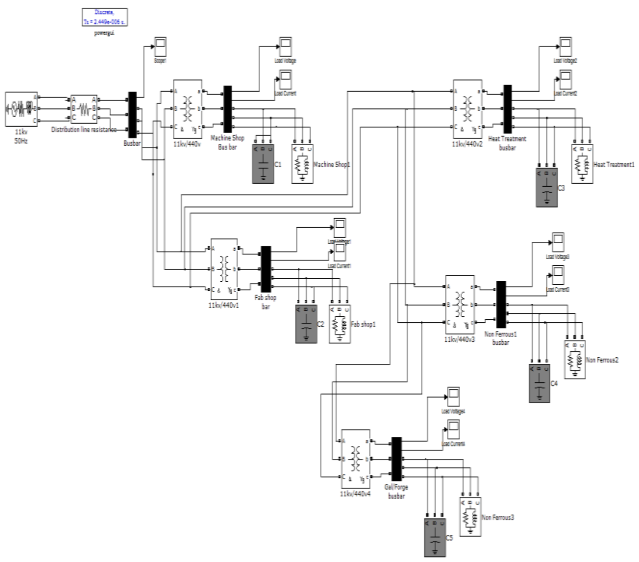

Figure 10. Strategy 2 (Regional correction)

Strategy 3 (Capacitor banks with Individual Load or Local Correction):

In this strategy, Capacitor banks are directly connected to the terminals of each inductive load(or small group of loads).

As in this public sector organization, there are five shops (regional loads) i.e. machine shop load, heat treatment shop load, nonferrous shop load, gal/forge shop load and Fabrication shop. Here in this strategy we install the capacitor banks to each load of every shop. Table XI shows the existing system and the proposed capacitor banks values, after calculation, for separate loads of each shop(one shop is mentioned)to achieve the power factor of 0.95. Table XII and XIII shows the simulation results after capacitror bank installation.

TABLE XI. EXISTING DATA OF H/T SHOP AND REQUIRED CAPACITOR BANK FOR 0.95 PF

HEAT TRT						
S.No	Load	KW	P.F	KVA	KVAR	REQ CAP KVAR
1	L_HT1	200	0.71	281.6901	198.3667	132.6
2	L_HT2	186	0.72	258.3333	179.2766	118.11
3	L_HT3	224	0.7	320	228.5257	154.784
4	L_HT4	250	0.74	337.8378	227.2321	145
5	L_HT5	160	0.68	235.2941	172.5205	127.04
6	L_HT6	240	0.72	333.3333	231.3247	152.4
7	L_HT7	250	0.66	378.7879	284.5703	202.25
8	L_HT8	90	0.68	132.3529	97.04278	71.46
9	L_HT9	160	0.69	231.8841	167.8399	115.2
10	L_HT10	140	0.65	215.3846	163.6781	117.6
11	L_HT11	190	0.73	260.274	177.8835	115.33
12	L_HT12	110	0.7	157.1429	112.2224	76.01

Simulation and Results

In Strategy 3, the case is slightly different. We isolated following loads in each shop and installed capacitor bank with individual load in order to analyze the behavior of the proposed distribution network for strategy 03. We have investigated that the power factor has increased rapidly to 0.95.

The design is shown in figure 11 and results in Table XII and Table XIII.

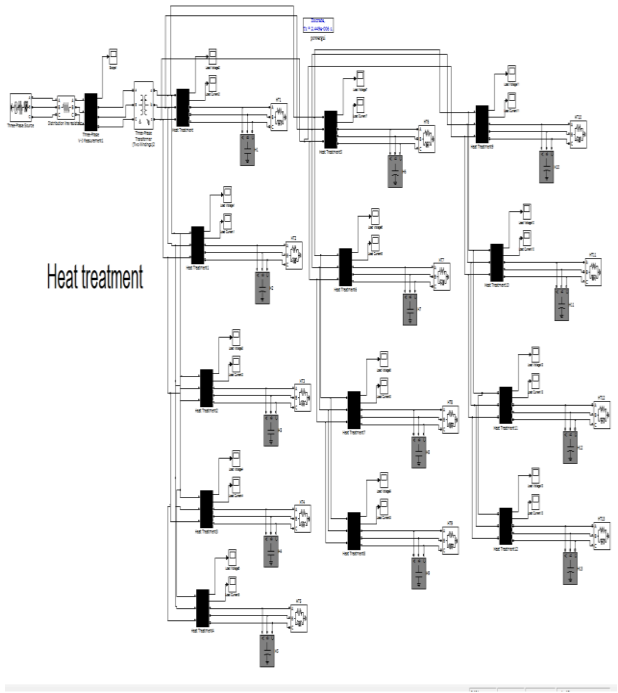

Figure 11. Strategy 3 (Capacitor bank for H/T shop Local Correction

TABLE XII. STRATEGY 3 (CAPACITOR BANKS WITH INDIVIDUAL LOAD)

		RMS						
	SHOPS	Vph (volts)	VL (volts)	Iph/IL (Amps)	S (VA)	Total GEN (VA)	Q (VAR)	Total Q (VAR)
STRATEGY 3	NFS	234.8	406.6855	626.65	441412.26	14901259.53	140369.099	4666137.631
	M/S	232.66	402.9789	7022	4901215.56		1558586.55	
	H/T	233.68	404.7456	3767	2640817.68		839780.022	
	G/F	234.37	405.9407	2501	1758478.11		548645.17	
	F/B	232.78	403.1868	7388	5159335.92		1578756.79	

TABLE XIII. STRATEGY 3 (CAPACITOR BANKS WITH INDIVIDUAL LOAD)

	SHOPS	P.F	P with respective P.F (Watts)	P with unity P.F (Watts)	P Loss (Watts)	Total Loss (Watts)
STRATEGY 3	NFS	0.948	418458.8225	441412.26	22953.43752	750711.1957
	M/S	0.948	4646352.351	4901215.56	254863.2091	
	H/T	0.948	2503495.161	2640817.68	137322.5194	
	G/F	0.95	1670554.205	1758478.11	87923.9055	
	F/B	0.952	4911687.796	5159335.92	247648.1242	

A. Comparison between Existing and Proposed Distribution Network

If we summarize all the strategies, we know that in our daily use electrical systems we use lot of devices (actuators) most of which run by the help of motors. All the rotating devices are based upon coil that and their working and proper functioning is always governed by the Principle of Electromagnetic Induction. The impedance component of an inductor is always taken as a positive value whenever solving the circuit and the impedance component of the capacitive element is taken with a negative sign. Addition of extra inductive devices or components results as an enlarged reactive power in the circuit.

Hence the circuit faces a huge drop in the power factor because the value obtained as a result of the division of real power P by apparent power S. this in turn causes an increase in the value of the apparent power because the latter is a complex sum of P and Q. But the power factor of a system should always and essentially be high. This is advisable for the reason that it will end up maintaining the efficiency of the system. The incorporation of the capacitive element causes a decline in the Q which in turn makes S to drop also. Concomitantly the power factor rises. This new value of the power factor is then maintained at the acceptable value. Hence it can be extracted from the above few lines that the capacitor bank responsibly performs the reactive power compensation.

The Table XIV and Table XV clearly show us that without capacitor, the system efficiency will reduce, draws large current and lagged the power factor. We investigated that the static capacitor bank achieved our goal to increase power factor to 0.95 .Furthermore, increasing in power factor nearly unity have reduced the power losses.

As shown in Table XV , the power losses have been reduced from 5MW to .65MW in strategy 1 strategy 2 and 0.75 MW in strategy 3.Slightly higher value of power loss in strategy 3 is because of not exact values of capacitor banks (as we are using standards). A high value of the power factor means that there will be a very small requirement of the amount of reactive power compensation. This will mean that a very minute amount of current will be obtained from the supply. In this case the copper loss that is the I2R loss will decline. The losses also fade when the power factor is high owing to the less values of the reactive devices.

Furthermore, the reactive power has been reduced from 12MVAR to 4MVAR.Power that is used up by the load is referred to as true, real or active power. Active or real power is denoted by P, the power that is reflected, because load is reactive, back into the system is known as reactive power. The sum of P and Q is the apparent power denoted by the letter S. In an analogy of a triangle, if theta is the angle between P and Q, where neither P nor Q is the hypotenuse, S will be the hypotenuse of the triangle.

The apparent power is also reduced from 17MVA to 13 MVA. When capacitive and inductive components are attached in a parallel assembly, the resultant current is zero. That is to say that the amount of current that flows through the inductor flows in a direction opposite to that of the one flowing through the capacitor. Hence the cancellation results as zero current. The reactive devices capacitors and inductors, when placed in a circuit, generate and consume the reactive power respectively. The theory of power factor control orbits around this mechanism. In practical observation and usage, the load always has active, capacitive and inductive elements. Hence the power S that flows to the load also carries active and reactive components to deliver to the loads.

Multiplication of voltage and the conjugate of electric current render the reactive power Q. A major use of apparent power is that it can generate a very close estimate of the size of the electric equipment. A proper and accurate value of the sum of S component of several loads can only be made if the value of angle leading or that of angle lagging between voltage and current is the same or to say that they both have the same power factors.

TABLE XIV. COMPARISON BETWEEEN EXISTING AND PROPOSED SYSTEM

	SHOPS	RMS Vph (volts)	RMS VL (volts)	RMS Iph/IL (Amps)	S (VA)	Total GEN (VA)	Q (VAR)	Total Q (VAR)
WITHOUT CAPACITOR BANK	NFS	232.85	403.308	796.36	556297.278		373831.771	
	M/S	230.21	398.7354	8176.91	5647219.35		3975642.42	
	H/T	231.53	401.0217	4546.46	3157925.65	17380250.63	2254758.92	12279613.59
	G/F	232.08	401.9744	2831.29	1971257.35		1303001.11	
	F/B	230.07	398.4929	8761.9	6047551		4372379.37	
STRATEGY 1	Overall	231.34	400.6926	18736.32	13003380.8	13003380.81	4060304.36	4060304.355
STRATEGY 2	NFS	234.93	406.9107	625.9	441128.061		137631.955	
	M/S	232.44	402.5979	6170.8	4303022.26		1342542.94	
	H/T	233.69	404.763	3382.33	2371250.09	13180429.66	739830.029	4112294.055
	G/F	234.2	405.6463	2255.59	1584777.53		494450.591	
	F/B	232.33	402.4074	6428	4480251.72		1397838.54	
STRATEGY 3	NFS	234.8	406.6855	626.65	441412.26		140369.099	
	M/S	232.66	402.9789	7022	4901215.56		1558586.55	
	H/T	233.68	404.7456	3767	2640817.68	14901259.53	839780.022	4666137.631
	G/F	234.37	405.9407	2501	1758478.11		548645.17	
	F/B	232.78	403.1868	7388	5159335.92		1578756.79	

TABLE XV. COMPARISON BETWEEEN EXISTING AND PROPOSED SYSTEM

	P.F	P with respective P.F (Watts)	P with unity P.F (Watts)	P Loss (Watts)	Total Loss (Watts)
WITHOUT CAPACITOR BANK	0.74	411659.9857	556297.278	144637.2923	
	0.71	4009525.741	5647219.353	1637693.612	
	0.7	2210547.956	3157925.651	947377.6954	5097263.747
	0.75	1478443.012	1971257.35	492814.3374	
	0.69	4172810.189	6047550.999	1874740.81	
STRATEGY 1	0.95	12353211.77	13003380.81	650169.0403	650169.0403
STRATEGY 2	0.95	419071.658	441128.061	22056.40305	
	0.95	4087871.143	4303022.256	215151.1128	
	0.95	2252687.588	2371250.093	118562.5047	659021.4832
	0.95	1505538.657	1584777.534	79238.8767	
	0.95	4256239.134	4480251.72	224012.586	
STRATEGY 3	0.948	418458.8225	441412.26	22953.43752	
	0.948	4646352.351	4901215.56	254863.2091	
	0.948	2503495.161	2640817.68	137322.5194	750711.1957
	0.95	1670554.205	1758478.11	87923.9055	
	0.952	4911687.796	5159335.92	247648.1242	

CONCUSLION

Capacitor banks are good devices for improving the network and are already used in the industries. In this thesis a solution to the Optimal Capacitor Problem (OCP) applied to a particular distribution network. The reactive power compensation plays very important role, especially for the industry. Nowadays, there are many power electronic devices that are used such as converters, inverters, UPS systems etc. They all generate distortions to the supplying voltage and current waveforms. In order to avoid poor power quality, it is necessary to apply reactive power compensating device minimizing reactive power consumption.

In the proposed thesis, we have utilized capacitor bank in the existing distribution network where power factor was tremendously on the lower side .We have investigated using static shunt capacitor banks for Power Factor Correction (PFC). A comparative analysis of the strategy 1(Centralized Correction), Strategy 2(De-Centralized Correction or Regional Correction) and Strategy 3 (Local Correction) have been carried out to focus the aforementioned research problem and then each of one is compared with the previous system. Good and Bad things of every system is discussed. Any industrialist in Pakistan can have benefit from this research and can opt a better strategy after studying this study keeping in view the nature of his installed industry, power system setup and his economic status.

Furthermore, after analysis of the proposed distribution network in Matlab/Simulink software, it was found that using shunt capacitor bank in parallel with load, the power factor increased to 0.95 due to which proposed system and devices efficiency increased as current requirement reduced. Active power (P),Reactive Power (Q), Current and Voltage at LV side of each shop was simulated and results was displayed in the form of tables and graphs which clearly shows the increase in the efficiency in the power system of each shop. The power losses reduced from 5MW to the range of 0.65MW. Voltage drop also reduced. Reduction in size of a conductor and cable reduced the cost of the whole system. After PFC, system becomes able to manage more loads with the same capacity.Moreover in future, the proposed system can be automated the capacitor banks using switching devices, for betterment of the power system performance. Instead of static capacitor banks, simulations can be done for automatic capacitor banks. Also other power factor improvement devices like synchronous condenser, phase advancers (individually or in mixed form) can be used and results can be simulated for these devices respectively. Simulations can be done for PFC at the HV side of the transformer and the result can be compiled. PID, Fuzzy Logic and SMC controllers can be used to get optimal values so that we can prevent our system from any unpredictable bad event.

REFERENCES

[1] L. Saribulut, “Electrical Power and Energy Systems,” Electrical Power and EnergySystems, vol. 62, no. 5, pp. 66-71, 2014.

[2] A. Feher, “Definitions and Measurment of Power Factor,” 8th InternationalSymposium of Hungarian Research on Computational Intelligence and Informatics,Hungary, 2001.

[3] F. Marafao, “Power Factor Analysis Under Nonsinusoidal Systems and UnblancedSystems,” Conference on Harmonics and Quality of Power, vol, no, pp.1-8, Oct 2003.

[4] C. Sankaran, Power Quality, CRC Press, 2002, p. 202M. Abdel Aziz, “Power Factor and your Electrical Utility Bill in Egypt,” Transactions on Power Delivery , vol. 18, no. 4, pp. 1567 - 1568, 10 Oct 2003.

[5] L. Cividino, “Power Factor, Harmonic Distortion; Causes, Effects and Considerations,”14th International Telecommunications Energy Conference, vol, no, pp. 1-7, Oct 1992.

[6] E. F. Fuchs, Power Quality in Power Systems and Electrical Machines, AcademicPress, 2008, p. 664.

[7] A. Zobaa, “Comparing Power Factor and Displacement Factor Corrections Based onIEEE Std. 18-2002,” 11th International Conference on Harmonics and Quality of Power, vol, no, pp. 1-5 Sep 2004.

[8] J. Bednarczyk, “Induction Motor Theory,” PDH, 2012, p. 52P. Bimbhra, Electrical Machinery, Khanna, 1997, p. 420.

[9] S. J. Chapman, Electric Machinery Fundamentals, McGraw Hill, 2012, p. 680.J. Siar, “Power Factor of Motors and Generators,” ABB Company, 2014, p. 68.

[10] Neagle NM, Samson DR. Loss reduction from capacitors installed on primary feeders. Power Apparatus Syst Part III Trans Am InstElectrEng 1956;75:950–9.

[11] Kasztenny B, Schaefer J, Clark E. Fundamentals of adaptive protection of large capacitor banks. Power Systems Conference: Advanced Metering, Protection, Control, Communication, and Distributed Resources; 2007 PSC 2007: IEEE; 2007. p. 154–86.

[12] Segura S, Romero R, Rider MJ. Efficient heuristic algorithm used for optimal capacitor placement in distribution systems. Int J Electr Power Energy Syst 2010;32:71–8.

[13] Lidula NWA, Rajapakse AD. Microgrids research: a review of experimental microgrids and test systems. Renewable Sustainable Energy Rev 2011;15:186–202.

[14] Eltawil MA, Zhao Z. Grid-connected photovoltaic power systems: technical and potential problems— a review. Renewable Sustainable Energy Rev 2010;14:112–29.

[15] Taylor CW. Shunt compensation for voltage stability. Power plants and power systems control 2003.In: A proceedings volume from the fifth IFAC symposium, Seoul, South Korea; 15–19 September 2003: Gulf Professional Publishing; 2004. p. 43.

[16] ENERGI. Guidelines to install, operate and maintain ht capacitors & it's associated equipment⟨http://www.energegroup.com/CapacitorManual.pdf⟩

[17] Singh H, Hao S, Papalexopoulos A. Transmission congestion management in competitive electricity markets. IEEE Trans Power Syst 1998;13:672–80.

[18] Hemmati R, Hooshmand R-A, Khodabakhshian A. State-of-the-art of transmission expansion planning: comprehensive review. Renewable Sustainable Energy Rev 2013;23:312–9.

[19] Rao RS, Narasimham S, Ramalingaraju M. Optimal capacitor placement in a radial distribution system using plant growth simulation algorithm. Int J Electr Power Energy Syst 2011;33:1133–9.

[20] Mekhamer SF, Soliman SA, Moustafa MA, El-Hawary ME. Load flow solution of radial distribution feeders: a new contribution. Int J Electr Power Energy Syst 2002;24:701–7.

[21] https://www.electricaltechnology.org/2013/11/How-to-Calculate-Suitable-Capacitor-Size-for-Power-factor-Improvement.html

[22] M. Khodapanah, A. F. Zobaa and M. Abbod, “Monitoring of Power Factor for Induction Machine Using Estimation Technique,” 50th International Universities Power Engineering Conference,(UPEC), vol, no, pp. 1-5, Sep 2015.

[23] M. Khodapanah, A. Zobaa and M. Abbod, “Estimating Power Factor of Induction Motors at any Loading Conditions using Support Vector Regression,” Journal of Electrical engineering, pp. 1-8, Submitted Oct 2017.

[24] R. Guntaka, “Regression and Kriging Analysis for Grid Power Factor Estimation,” Journal of Electrical Systems and Information Technology, pp. 223-233, 2014.

[25] R. Gunaka, Regression and Kriging Analysis for Grid Power Factor Estimation, Lamer university, 2013, p. 98.

[26] M. Khodapanah, A. Zobaa and M. Abbod, “Estimating Power Factor of Induction Motors Using Regression Technique,” International Conference on Harmonics and Quality of Power (ICHQP), vol, no, pp. 1-5 Oct 2016.

[27] Z. J. Paracha, “Estimation of Power Factor by the Analysis of Power Quality Data for Voltage Unbalance Zahir,” Third International Conference on Electrical Engineering, vol, no, pp. 1-6, Sep 2009.

[28] Neelima, S & Subramanyam, Pisupati & A, Srinivasula. (2010). Capacitor Placement in a Distribution System for Power Factor Correction: An Optimization Approach.

Muhammad Bilal has Received his Master's in Electrical Energy System Engineering from USPCAS-E UET Peshawar, Pakistan in 2019. He worked as a research scholar at Power system Lab of Arizona state university U.S.A in 2016. Currently he is working as Assistant Manager in an R & D Department of a public sector industry. he is doing a project on Grid connected 5MW Solar project for that industry with increased efficiency. His major research is in smart Micro-grid architecture, control and economic dispatch problems.

Abdul Basit has received his PhD from the Department of Wind Energy of the Technical University of Denmark (DTU) in 2015. His PhD research on 'Wind Power Plant System Services' has developed and analysed the control strategies which can increase the WPPs capability to provide system services, such as active power balancing control, in a modern power system with large scale integration wind power. He is currently employed as an Assistant professor at the Pakistan Centre for Advanced Studies in Energy (PCASE-E) of the University of Engineering & Technology (UET) Peshawar.

Kamil Shaheed has received BS mechanical engineering from international islamic university. Ms mechanical engineering from international islamic university. Currently working at heavy mechanical complex as assistant manager at R&D department.

Shifaat Ur Rehman has received MS degree in Electrical Energy System Engineering from US Pakistan Center for Advanced Studies in Energy(USPCAS-E), University of Engineering & Technology Peshawar. He has availed exchange program to the partner university of USPCAS-E Arizona State University (ASU), USA in 2016, as a research scholar. He has good hands on experience in the field of renewable energies especially PV reliability. He has worked on "Optimization of Off grid Solar-Gas genrator hybrid power system for rural areas of Karak, Pakistan ".

Niaz Ali has received his Bachelor Degree in Electrical Engineering from University of Engineering and Technology, UET, Peshawar in 2014. Currently he persuing his Masters from US Pakistan Center for Advanced Studies in Energy(USPCAS-E), University of Engineering & Technology Peshawar in the field of Electrical Energy System Engineering. His major research interests include Solar Photovoltaic (PV), MPPT Techniques for Solar PV, DC-DC converters, Active Power Filters (APFs) and Unified Power Conditioners(UPQCs).

IJEW 国际工程期刊 International Journal of Engineering Works انجینئرنگ کاموں کا بین الاقوامی جرنل

International Journal of Engineering Works
ISSN-p: 2521-2419
ISSN-e: 2409-2770
Vol. 6, Issue 12, PP. 490-495, December 2019
https://www.ijew.io/
https://doi.org/10.34259/ijew.19.612490495

Using Fly Ash and Rice Husk Ash as Soil Improving Materials along with its Cost Effectiveness in Flexible Pavement Construction

Afaq Ali[1], Prof. Dr. Sher Afzal Khan[2], Engr Fazle Karim[3]
[1 2 3]Sarhad University of Science & Information Technology, Peshawar
afaqali369@gmail.com[1], hod.civil@suit.edu.pk[2], engr_fazli@yahoo.com[3]
Received: 15 November, Revised: 25 November, Accepted: 26 November

Abstract— Unstable soil has always been a hurdle in swift construction projects, which can only be eradicated by soil stabilization. Soil stabilization is used for a plethora of projects; however, it is more common in pavement construction, where the purpose is to enhance the strength of soil and to minimize the expenses by providing indigenous available materials. Thus the use of alternative materials like coal combustion product (fly ash) and agriculture waste (Rice husk ash) will certainly lower the cost of construction and therefore reducing the environmental hazards. Hydrometer analysis, Atterberg limits, modified proctor test and California Bearing Ratio (CBR) tests were carried out on the natural soil. Next three different percentages of fly ash (5%, 10% and 15%) were mixed with soil for the CBR test. In this study, the Rice Husk Ash (RHA) was also used for soil stabilization same as the percentages (5%, 10% and 15%) we selected in stabilization for fly ash. After finding CBR, the pavement was designed for natural soil and stabilized soil. The detail cost estimation was performed for 1km long and 7.62m wide road construction with specific thicknesses of designing road on natural soil and stabilized soil. In conclusion, the fly ash and RHA resulted in less thickness of road layers as compared to road design on natural soil. Furthermore, it was also concluded that the road construction cost using the fly ash and RHA is significantly less than the natural soil.

Keywords— Stabilization, Fly ash, Rice Husk Ash, Hydrometer analysis, California Bearing Ratio.

I. INTRODUCTION

Civil engineering infrastructure projects located in areas with soft or clay soils need to be improved for the construction purposes. Different methods are used to improve the soil properties, i.e. chemical, mechanical or by adding modifiers to soil such as fly ash, cement, lime, RHA etc. The chemical and mechanical process of stabilization is quite expensive; therefore, economical stabilizers are used for soil stabilization. For different engineering works, soil stabilization is being used, but it is mostly carried out in the pavement construction. The purpose of stabilization is to enhance the strength of soil and to minimize the expenses by providing locally available materials. Usually cement and lime were being used for stabilization, but these materials expenses have surged with the passage of time. Thus the use of coal combustion product (fly ash) and agriculture waste (RHA) will certainly lower the cost of construction as well as reducing the environmental hazards they causes. Fly ash is a fine particle obtained from the combustion of pulverized coal and RHA is obtained from the milling of rice. In retrospect, when fly ash and RHA were not introduced to construction projects, they were simply disposed off, which is not environment friendly and cause many diseases. With the application of these kinds of waste materials, there will be no need of materials to buy like cement, lime (which is expensive) and will help the environment clean. Fly ash is a pozzolanic material; pozzolan has siliceous and aluminous properties [14].

This study shows the optimum amount of fly ash and rice husk ash for subgrade purposes through the effect of fly ash and RHA on subgrade California bearing ratio, optimum moisture content (OMC) and maximum dry density (MDD) test were carried out. Road design is carried out on natural soil, soil with fly ash mix (at 10% fly ash) and soil with RHA mix (at 10% RHA). After designing, the detail cost estimation is done for natural soil, soil with fly ash and soil with RHA.

A study was done in the improvement of the expansive soil by adding a different percentage of fly ash with soil. The MDD and workability is observed at 25% fly ash with soil [3]. A class F fly ash was used to improve the expansive soil of south Texas. The soil sample is prepared with 20% fly ash in it and for comparison, the 6% lime and 10% Portland cement was also selected. From results, these three materials improve the soil properties like plasticity and unified compressive strength of soil [7]. A Study was carried out on the effect of self-cementing (class C) fly ash on soil stabilization for a wide range of construction applications. Moisture control, compaction and rate of ash hydration affect the procedure of soil stabilization [8]. Fly ash was used to stabilize the organic soil and then the strength tests were performed on it. Untreated soil specimen and fly ash with organic soil, the unconfined compressive strength (UCS) and resilient modulus test were performed. The UCS and resilient modulus of the organic soil improves by adding fly ash, but it depends on the soil and fly ash properties [12]. A study was carried out on the stabilization of soft grained soil with self-cementing fly ash. At different percentage, specimens were prepared, resilient modulus, CBR and UCS test were performed on the sample. At 18% of fly ash, the best improvement in the CBR was noticed [1]. An investigation was carried out on geotechnical properties of expansive soil by using fly ash and lime. From the results, fly ash and lime increases the MDD, free swell decreases and OMC and CBR increases [6]. Similarly, freeze-thaw durability, enhance with the use of fly ash in soil improvement [10].

The laboratory tests like CBR and UCS were performed by using RHA as a soil stabilizer. By adding RHA content to soil, the OMC increases and MDD decreases and CBR and UCS improved [2]. A study carried about the improvement of different types of soil by using RHA. The results show that liquid limits was decreased by (11-18%) at 9% RHA and plasticity index decreased by (32-80%). RHA shows a general increase in the OMC and decrease in MDD at 9%. At (6-8%), addition of RHA content, the UCS was also increased [5]. An investigation of the effect of RHA on soil engineering properties for stabilization was studied. By addition of RHA to clayey soil, the soaked CBR improves from 2.4% to 4.4% [11]. The laboratory tests like Atterberg limits, CBR and UCS were carried out by using fly ash and RHA in black cotton soil. At 12% fly ash and 9% RHA content, the maximum improvements were noticed in CBR and UCS [13]. A wetting and drying phenomena of expansive soil cause a lot of problems in swift construction projects of civil engineering like highways. Fly ash in an industrial waste, results better in term of expenses and also utilization of fly ash in such projects can reduce many environmental hazards they cause. In this study fly ash and lime-fly ash mix was used in expansive soil to study its effectiveness and potential [15]. A study was evaluated on the soil of Indiana to check the engineering properties of soil with utilization of class C fly ash and loess (loess-fly ash mix). It was concluded that the optimum fly ash content used in a loess soil in wet condition avoid delay in the construction of road [16]. An experimental study was conducted on the stabilization of expansive soil by using the fly ash and cement to enhance the geotechnical properties of soil. For this study, various percentages of fly ash (0, 5, 10, 15 and 20%) with 5% cement were taken to evaluate its effectiveness on soil stabilization. It was also concluded that, cement-fly ash mix was recommended to use in the subgrades where clayey, soft grained and expansive soil were found [17].

The objectives of the study are:

- Using RHA and fly ash for stabilization purposes
- To design the pavement thickness before and after using the soil stabilizers
- To assess the use of fly ash and RHA cost effectiveness as soil stabilizers.

II. Methodology

The soil sample for this study was collected from local area at Pabbi near the GT road, Nowshera Khyber Pakhtunkhwa, Pakistan. The laboratory test (hydrometer analysis and atterberg limits) shows that the collected soil is clay soil (A6) with low plasticity (CL).

The fly ash was collected from Tradeworth international fly ash, upper Gizri, Karachi. The fly ash used for this study is class C fly ash, which has SiO2+Al2O3+F2O3 greater than 50%. Fly ash is a pozzolanic material having siliceous and aluminous properties [4].

RHA was collected from local area Bannu rice mill and passed through sieve number 200 before use. RHA is highly pozzolanic material depends on the firing temperature and retention period. 60% to 90% silica is present in the RHA, which is highly reactive [9]

A. *Conventional tests*

The laboratory tests carried out on natural soil, including wet sieving, atterberg limits, modified proctor test and CBR. The term OMC is used for preparing the samples for CBR test.

B. *CBR tests*

Three various percentages of fly ash (5%, 10% and 15%) are mixed with soil for the CBR test. In CBR, three samples on 5% fly ash with virgin soil are prepared on three different blows (10, 30, and 65) and these samples were placed into water for 96hours. After 96hours, the samples were subjected to CBR machine. The same method was used for remaining 10% and 15% fly ash mixes with natural soil. After fly ash, the RHA was used for soil improvement same as the percentages (5%, 10% and 15%) we opted in stabilization in fly ash.

C. *Road design and Cost estimation*

After soil stabilization, the traffic volume survey was conducted on the GT road Nowshera N5 to find out the equivalent single axle load (ESAL) for road designing. The pavement was designed using the natural soil as subgrade against ESAL. In comparison, the pavement was also designed for treated soil for both fly ash and RHA. The pavement was designed for 1km long and 7.62m wide.

Similarly, detail cost estimation was done for 1km long and 7.62m wide road construction with specific thicknesses of designing road on natural soil and treated soil.

III. Results and discussion

A. *Hydrometer analysis/ Wet sieving*

The soil is passed through sieve no 200 by water, to separate the sand particles from the soil. The sand particles which retained on sieve 200, passed through sieve analysis and on the soil hydrometer analysis test were performed. In the grain size distribution curve the blue line indicates the sieve analysis (sand particles) and the red line is a hydrometer analysis (silt and clay) shown in fig 1.

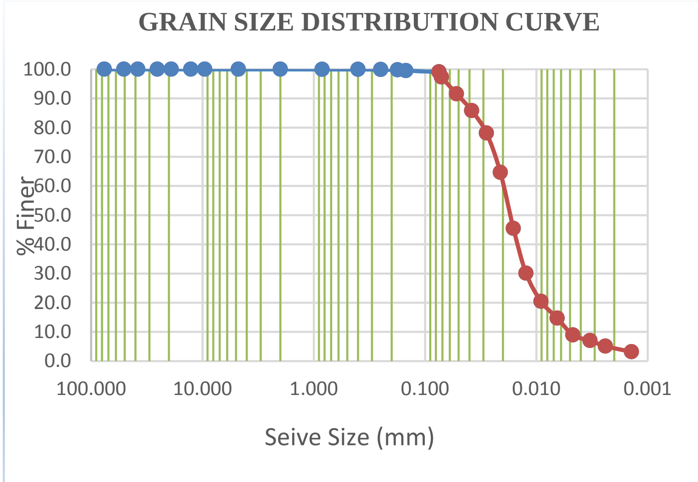

Fig 1: A grain size distribution curve of soil

B. *Atterberg limits*

To find out the plasticity index of the soil, Atterberg limits test was performed. In fig 2, the blue dot indicates that the soil is low plastic clay (CL).

TABLE 1: Atterberg Limits

Atterberg limits		
Liquid limit %	***Plastic limit %***	***Plasticity index %***
34.1	14	20.1

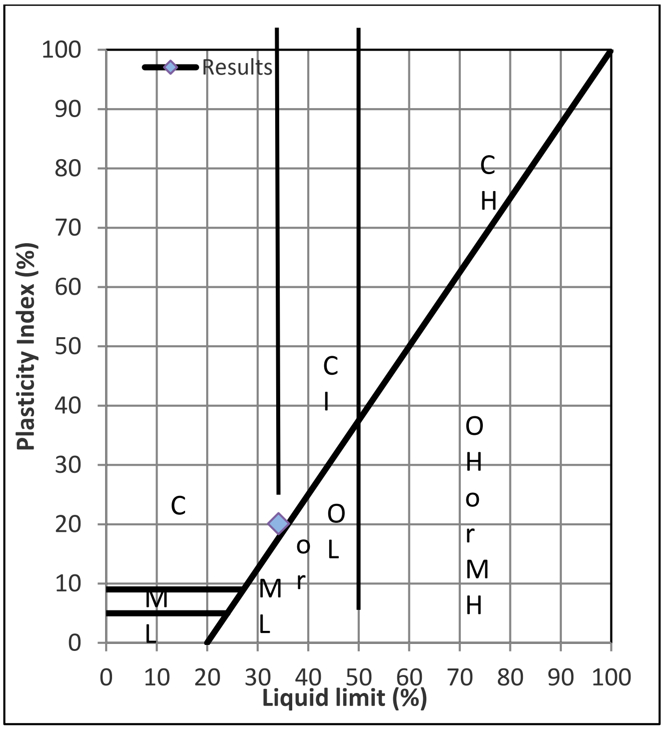

Fig 2: graph of liquid limit and plasticity index

C. *Modified proctor test*

This test is done to fine out the OMC and MDD of soil. These OMC is used for sample preparation for CBR.

Table 2: Modified proctor test on Fly ash

Modified proctor test on soil alone + % of fly ashes		
Description	***OMC %***	***MDD g/cc***
Soil alone	8.3	1.96
Soil + 5% fly ash	8.5	2.02
Soil + 10% fly ash	8.7	2.06
Soil + 15% fly ash	9.0	2.02

As the fly ash percentage increasing, the OMC is also increasing as shown in fig 3.

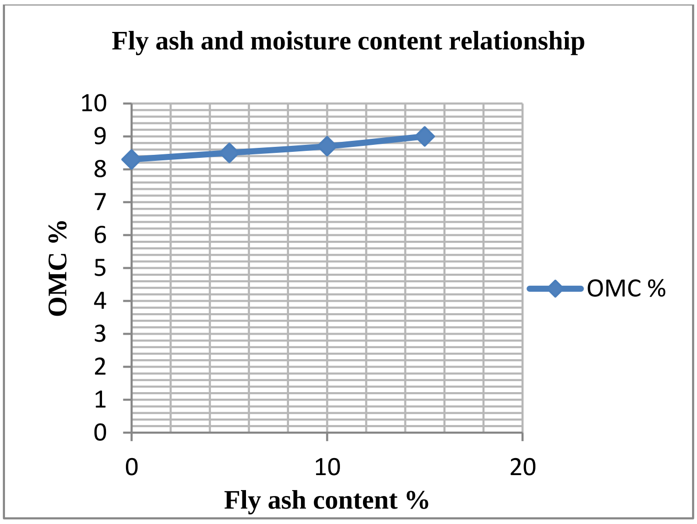

Fig 3: Fly ash content and OMC graph

Fig 4 shows that the MDD is high on 10% fly ash in the soil and after 10% fly ash the MDD starts decreasing.

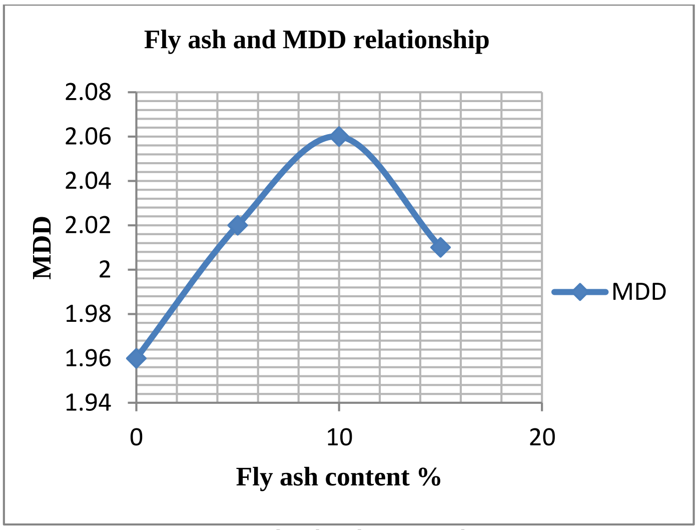

Fig 4: Fly ash and MDD graph

Table 3: Modified proctor test on RHA

Modified proctor test on soil alone + % of Rice husk ash (RHA)		
Description	***OMC %***	***MDD g/cc***
Soil alone	8.3	1.96
Soil + 5% RHA	8.6	1.98
Soil + 10% RHA	9.2	2.01
Soil + 15% RHA	9.7	1.99

Same as the fly ash, when RHA content increasing the OMC also increasing shown in fig 5. The peak MDD is obtained at 10% RHA content with soil shown in fig 6.

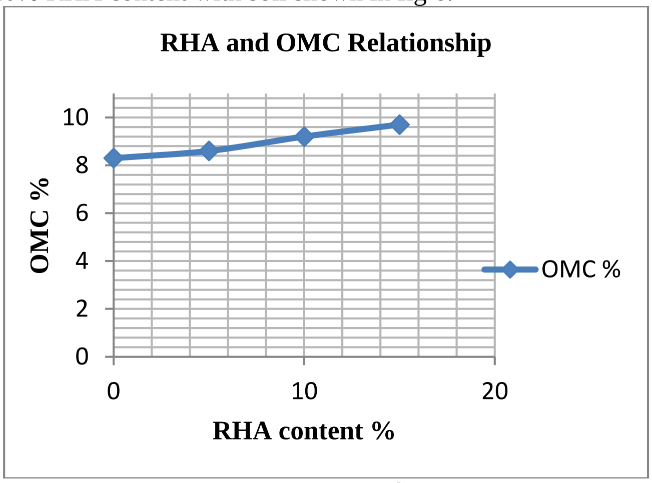

Fig 5: RHA content and OMC

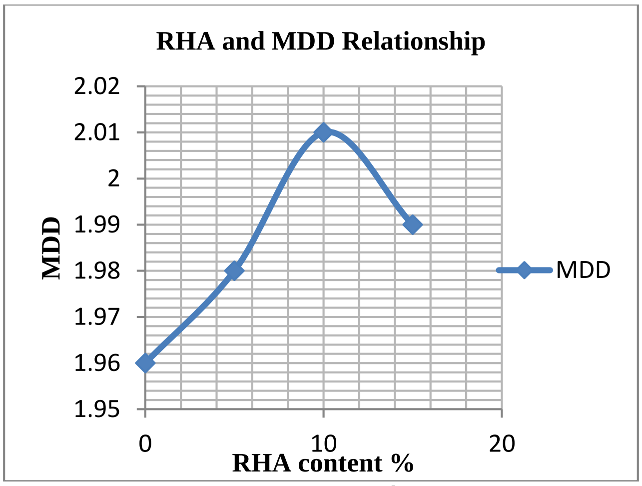

Fig 6: RHA content and MDD

D. California bearing ratio (soaked)

A 4.3% CBR was achieved for natural soil. Further, various percentages of fly ash (5%, 10% & 15%) were added to soil and samples were prepared, the results are shown in table 4. Fig 7 shows that the maximum CBR are achieved at 10% fly ash in soil.

Table 4: CBR test on fly ash

Description	***Soaked CBR %***
Soil alone	4.3
Soil + 5% fly ash	7.9
Soil + 10% fly ash	11
Soil + 15% fly ash	9.2

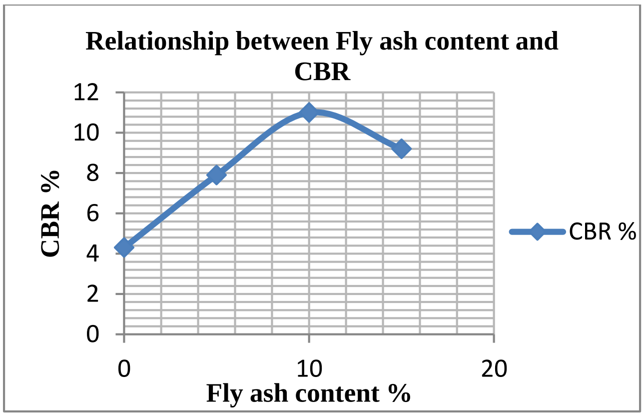

Fig 7: CBR of soil alone and fly ash with soil

Table 5 shows that the percentages of RHA (5%, 10% & 15%) mix with the soil and the CBR is obtained for these percentages. The peaked soaked CBR for RHA was obtained at 10% RHA content in soil shown in fig 8.

Table 5: CBR test on RHA

Description	***Soaked CBR %***
Soil alone	4.3
Soil + 5% RHA	6.1
Soil + 10% RHA	9.5
Soil + 15% RHA	8.9

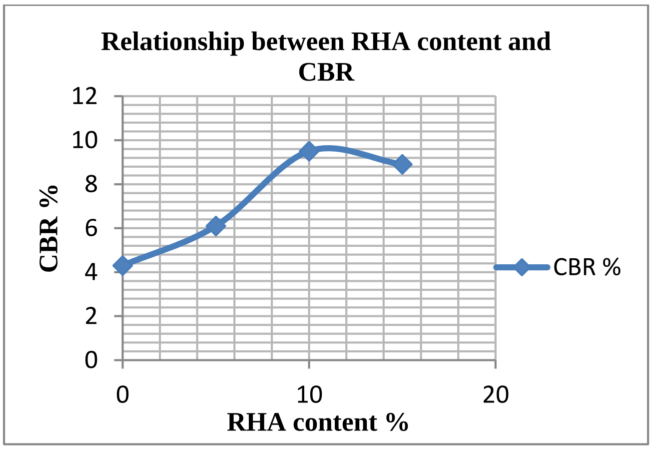

Fig 8: CBR of soil alone and RHA with soil

E. Road design

Table 6 and fig 9 shows the thickness of the various layers of road, which is designed for natural soil as a subgrade. The road was designed by nomograph method.

Table 6: Road design on natural soil as subgrade

Layers	*Thickness inches*
HMA	7.5
Base coarse	6.0
Sub base	8.0

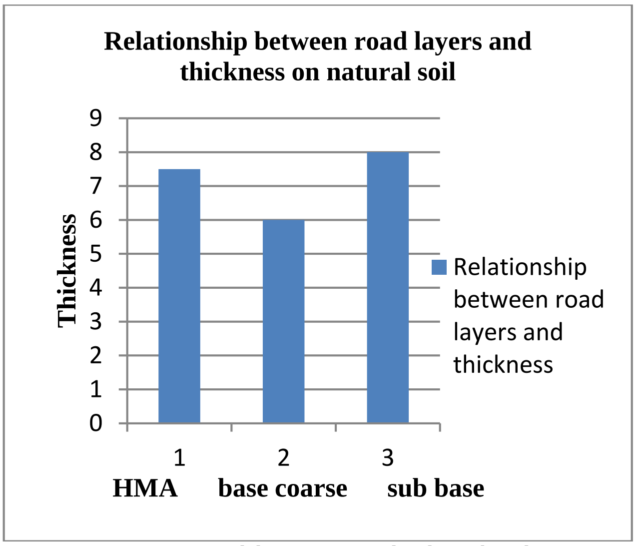

Fig 9: Road design on natural soil as subgrade

Table 7: Road design on 10% Fly ash in soil

Layers	*Thickness inches*
HMA	7
Base coarse	6
Sub base	5

Fig 10 shows the thickness of road layers designed on fly ash with natural soil. As from results, the CBR improved with fly ash so the thickness of the road layer in this case is less compared to design of road on natural soil.

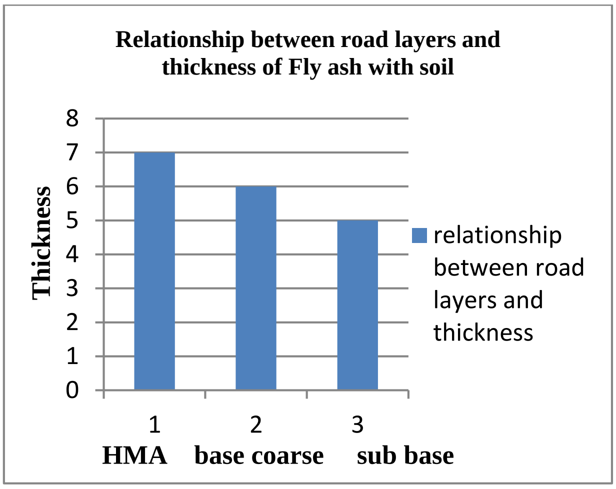

Fig 10: Road designs on 10% fly ash in soil as a subgrade

Table 8: Road design on 10% RHA in soil

Layers	*Thickness inches*
HMA	7
Base coarse	6
Sub base	5

RHA also resulted in less thickness as compared to thickness of road design on natural soil.

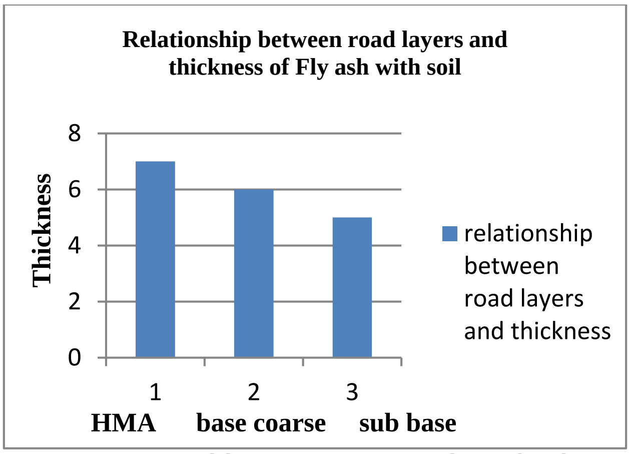

Fig 11: Road design on 10% RHA in soil as a subgrade

F. Cost estimation

Table 9: Cost estimation

Description	*Cost in millions*
Natural soil	41.82
Soil + 10% Fly ash	39.10
Soil + 10% RHA	39.16

Fig 12 shows the detail cost estimation of 1km long and 7.62m wide road construction on natural soil, fly ash with the soil and RHA with soil. The graph shows fly ash and RHA reduced the cost of construction as compared to cost on natural soil.

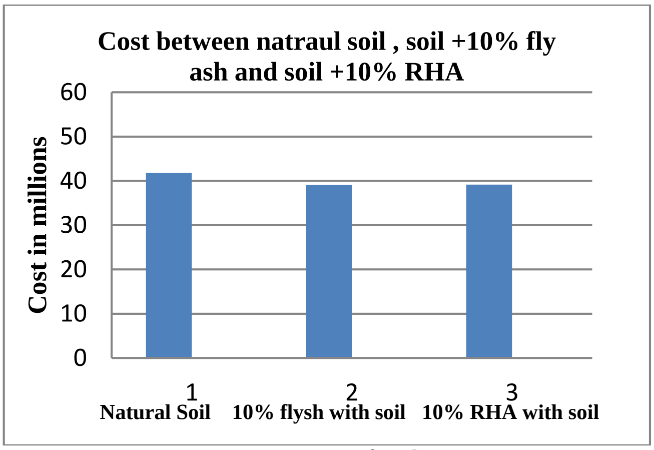

Fig 12: Cost estimation of road construction

Conflict of Interest

The content of this paper is original, not copied from anywhere and free of plagiarism. The previous work is referenced below.

Conclusion

- Soil with different percentages of fly ash gives a peak value of CBR at 10% fly ash. It increases from 4.3% to 11%. After 10% addition of fly ash, the strength of subgrade starts decreasing.
- Same as the fly ash, RHA also improves the soil CBR at 10% RHA content in soil. CBR increases from 4.3% to 8.9%. After 10%, adding of RHA the CBR of subgrade starts decreasing.
- From the results it is evident that fly ash improves the soil CBR significantly as compared to RHA.
- In road designing, fly ash and RHA resulted in less thickness of road layers as compared to road design on natural soil.
- The detailed cost estimation of road construction shows the fly ash and RHA cost is comparatively less than the natural soil.

Acknowledgement

The author is thankful to the Pakhtunkhwa Highways Authority (PKHA) department in order to perform tests in their laboratory. Author is also thankful to his supervisors for their continuous support throughout the study.

References

[1] Acosta, H. A., T. B. Edil, and C. H. Benson. "Soil stabilization and drying using fly ash." Geo Engineering Rep 3 (2003).

[2] Alhassan, Musa. "Potentials of rice husk ash for soil stabilization." Assumption university journal of technology 11.4: 246-250 2008.

[3] Bhuvaneshwari, S., R. G. Robinson, and S. R. Gandhi. "Stabilization of expansive soils using fly ash." Fly Ash India 8: 1-10 2005.

[4] Brooks, Robert M. "Soil stabilization with fly ash and rice husk ash." International Journal of Research and Reviews in Applied Sciences 1.3: 209-217 2009.

[5] Fattah, Mohammed Y., Falah H. Rahil, and Kawther YH Al-Soudany. "Improvement of clayey soil characteristics using rice husk ash." Journal of Civil Engineering and Urbanism 3.1: 12-18 2013.

[6] Ji-ru, Zhang, and Cao Xing. "Stabilization of expansive soil by lime and fly ash." Journal of Wuhan University of Technology-Mater. Sci. Ed. 17.4: 73-77 2002.

[7] Keshawarz, M. Saleh, and Utpal Dutta. "Stabilization of south Texas soils with fly ash." Fly ash for soil improvement. ASCE Geotechnical special publication No.36 1993.

[8] Mackiewicz, Scott M., and E. Glen Ferguson. "Stabilization of soil with self-cementing coal ashes." World of Coal Ash (WOCA): 1-7 2005.

[9] Prakash, J., K. Kumari, and V. Kunar. "Stabilization of Soil using Rice Husk Ash." International Journal of Innovative Research in Science, Engineering and Technology 6.7: 12997-13003 2017.

[10] Ramaji, Amin Esmaeil. "A review on the soil stabilization using low-cost methods." Journal of Applied Sciences Research 8.4: 2193-2196 2012.

[11] Rathan Raj, R., S. Banupriya, and R. Dharani. "Stabilization of soil using rice husk ash." International Journal of Computational Engineering Research (IJCER), ISSN (e): 2250-3005 2016.

[12] Tastan, Erdem O., et al. "Stabilization of organic soils with fly ash." Journal of geotechnical and Geo environmental Engineering 137.9: 819-833 2011.

[13] Yadu, Laxmikant, Rajesh Kumar Tripathi, and Dharamveer Singh. "Comparison of fly ash and rice husk ash stabilized black cotton soil." International Journal of Earth Sciences and Engineering 4.06 (2011): 42-45.

[14] https://www.fhwa.dot.gov/pavement/recycling/fach01.cfm

[15] Zha, Fusheng, et al. "Behavior of expansive soils stabilized with fly ash." Natural hazards 47.3 (2008): 509-523.

[16] Zia, Nayyar, and Patrick J. Fox. "Engineering properties of loess-fly ash mixtures for roadbase construction." Transportation Research Record 1714.1 (2000): 49-56.

[17] Zumrawi, Magdi ME. "Stabilization of pavement subgrade by using fly ash activated by cement." American journal of civil engineering and architecture 3.6 (2015): 218-224.

Afaq Ali, the author, belongs to Pabbi, Nowshera, Pakistan. He did a Bachelor of Civil Engineering from Sarhad University of Science & Information Technology Peshawar in 2016. The author is continuing his master's degree in Transportation Engineering from Sarhad University of Science & Information Technology, Peshawar. This study is his research work for the master's degree.

International Journal of Engineering Works
ISSN-p: 2521-2419
ISSN-e: 2409-2770
Vol. 6, Issue 12, PP. 431-438, December 2019
https://www.ijew.io/
https://doi.org/10.34259/ijew.19.612431438

A Framework for Sustainable Energy Policies: A Case of Pakistan

Maham Mujahid[1], Tanvir Ahmed[2]
[1,2]Pakistan Center for Advanced Studies in Energy, University of Engineering and Technology, Peshawar
mahammujahid1@gmail.com[1]
Received: 08 September, Revised: 28 September, Accepted: 15 October

Abstract— In this paper the energy crisis of Pakistan is discussed with comparative analysis due to a continuous and wide gap among available system producing capacity and demand. The deteriorating of shortages (power) has become a main problem in the view of politics, showing the difficulties for persons and companies. It looms to weaken the reliability and legality of government and to additional pressure the societal fabric of the nation. The energy crisis did not arise suddenly. It is the straight consequence of impulsive and irresponsible energy policies over the last three years. These energy policies have obstructed the growth of low and plentiful domestic energy resources. They have also caused in very incompetent fuel mix selections, lack of energy and security of the economics. The country's energy insolvency is eventually due to huge official and failure of the governance. This paper analyzes the issues confronting Pakistan's energy sector and classifies the key elements of a hidden policy reply to address the nation's tough energy crisis. In order to assess these diverse renewable energy alternatives a comparative analysis of SAARC countries is performed using a standard criteria framework that are likely to be decisive in the making of decisions. The assessment shows that completely the renewable energy system conformations are not economically viable in the country while the renewable energy local resources could bring down the price of energy. An improved understanding of the whole processes by which innovation occurs is important, both theoretically and to inform the policy makers to support innovation to attain more sustainable technologies.

Keywords— Energy policy, sustainability, sustainable development, framework

I. Introduction

There is a dire requirement for an inclusive responsiveness and levitation of programs on renewable resource energy with distribution of satisfactory economical and other renewable resources that would make the overall public to grow, admit, and assist the extensive implementation of renewable resource energy and include the industries and other investors more extremely in gaining renewable resource energy. To improve access to data, the nationwide centers of information such as one stop shops on renewable resource energy should be recognized. These must be effortlessly accessible and extensively exposed by governments to deliver easy approach to fulfill the information on renewable energy scenarios, economical incentives, and needs and to deliver guidance to customers, investorss, and the public at huge. Besides energy policy, the technology, and structure development, the expansion of renewable resource energy includes sociopolitical and marketplaces and needs a systematic access covering entire issues. The governments should thus draw up inclusive schemes for generating a renewable resource energy industry and marketplaces involving the technology with the help of R&D, demo projects, and commercialization, assisting infrastructure, economical mechanisms, and the utilization of instruments that are based on market such as the renewable resource portfolio standards, green costs, the design of feed-in tariffs, system of net metering, along with renewable energy certificates that are tradable [1].

II. Literature Review

The showing up of the security of energy supply is determined by keeping in opinion some facts which comprises of dependence on imports, reliance on imports of solid fuels, dependability on imports of oil, dependence on natural gas imports, variation of primary fuel, diversity of fuel of electrical energy generation, reliance of energy fuel and planned supplies of oil. The goal of energy supply security should be to restrict the threats involved in relying of imports or exterior sources supply [1].

The development of renewable energy resources in the SAARC countries is incomplete due to many problems which comprises economic difficulties in which the renewable technology is expensive than the traditional ones. Likewise, the ambiguity in policies and procedures including the slow procedures of approval by managers, financial, dearth of skills and awareness are few other problems in the way of progress of renewables in SAARC states. These can be fixed with the seriousness of the local markets and with the sale economies which will drive to the lesser rate of renewable resources. The FIT i.e. feed in-tariff and the renewable support mechanism are the two for aid of renewables should be applied with other policies to provide it with best consequences [2].

Nigeria is a country which has plentiful reserves of renewables, but they are fronting the wasteful use of energy for which their policy is to support the evolvement of an energy combination that will point out the safeguarding of petroleum reserves in such a way that will allow their sustained exportation for foreign incomes for as many months as probable. The numerous areas where conservation in energy can be done should be recognized to safe energy. As observed in quite a number of wealthy countries supporting renewable energy resources such as Japan, Denmark and Germany a durable and enduring commitment from the government is vital in applying any type of policies which will lead to the development of renewable resources, in specific, and a sustainable change, in wide term [3].

The ideologies that offer significant guidelines to the development of energy security strategy are "Cost allocation" denotes to the detail that to confirm risk minimization all recipients require to share the total security charges justly. This involves illustrating who will get what assistances. "Lessing the cost" refers to escaping of over-obliging to any one track or protection policy and that risk reduction should not put an extreme burden on civilization. "Varied-dimensionality or multi-aims" refers to the statistic that risk reduction should be considered to deal with many kinds of risks, not only one or two. "Suppleness or to switch" refers to the necessity for any strong security strategy to adjust to exterior deviations. Lastly, "expectancy of non-reoccurrence" mentions to the detail that though security prices may not produce any visible coming back, the insurance providing is vital [4].

In evolving countries, high-tech jumping to the use of very competent applications, equipment, procedures, automobiles, and transportation systems proposes substantial potential for energy effectiveness enhancements. To ease the energy poverty in emerging countries there should be creativities taken to advance health and intensify productivity by providing worldwide access to suitable energy facilities especially for illumination, transport and cookery through inexpensive, high-superiority, harmless, and environmentally suitable energy haulers and end-use strategies. The commercial energy should be made accessible to upsurge income-producing chances [5].

III. RESEARCH METHODOLOGY

TABLE.1

Criteria Points	Explanation
Renewable energy development	A renewable portfolio standard is a special tool for policy making [6]. The leaders in the alteration of the energy system is Germany [7].
Specific design of Feed in tariff	Feed-in tariffs system approach is more effective than a system of bidding [8]. Germany, in specific, have shown that feed-in tariffs can be utilized as a powerful tool of policy to drive renewable resource energy deployment [9].
Localization of resources	Diversification and localization of energy resources would also offer a security for the energy demand and supply along with distribution as well for the energy customers [10]. In the energy sector, renewable resources mainly lessen the need of gas or coal importation as oil use is restricted in this area [11].
Diversifying resources	If the government is not to weaken the importance it has conventionally attached to electricity supply variety, it seems from this exercise that it should readjust intervention to the assistance of renewables rather than nuclear energy [12]. Investments in renewable energy resources also outgrowth innovation and job development [13].
Government economic framework (affordable price of energy)	The recognized objective of the energy shift is to lessen Germany's greenhouse gas emissions by eighty to above ninety percent from 1990 levels by 2050 without depending on the power of nuclear energy and while keeping secure and affordable energy approach [14]. The pricing policies such as carbon tax and cash allowances for renewable resource investments may not yield the desired consequences, and a high level of carbon tax may lessen the renewable energy resource investments, and cash allowances to renewable resources

	may rise emissions of carbon [15].
Reduction of fossil fuels	Renewable resource energy aids contribute to substitute the small-carbon transition but can suggest distributive properties, conditional on the way in which they are applied [16]. Generally, enforced early departures of fossil fuel resource generation in deep decarbonization situations bring a multitude of complications globally and provincially [17]. The future energy system of Denmark is putting stress on energy efficiency, reduction of carbon dioxide, and industrial expansion [18].
Fostering innovation	Presenting green energy market will make it likely for the new renewable energy technologies to be partially economically rewarded for the ecological profits, which they make compared to traditional energy production [19]. The discoveries of Bergek and Jacobsson's analysis of German, Swedish and Dutch wind turbine industries that policy makers requires to be mindful of the complication of innovation structures and the range of works that these systems offer, in order to progress the design of the mix of policy tools needed to encourage fruitful innovation system [20].
Energy security	A lot of nations have adopted to diversify energy supply policy in

	their energy security plan to control the import risk and price of energy to make sure that sufficient energy can be gained at reasonable cost level [21]. Energy is unavoidable for human lifespan and a safe and reachable supply of energy is vital for the sustainability of modern civilizations. Renewable resource energy sector, presently meeting 13.5% of the worldwide energy demand, is now rising faster than the development in overall market of energy [22].
Establishment of wind energy resources	The demand side strategies are required to encourage not only dissemination of wind resource energy, but novelty in the technology expertise itself [23]. Nowadays, about 50 percent of both the Danish electricity and heat demand are fashioned in combined heat and power production and more than 15 percent of the energy demand is produced by wind turbines. Equally both technologies are important for the implementation of Danish climate change response aims [24].
Broadening industrial capabilities	The transfer towards a fine fusion policy, intelligible with the goals of energy policy too and allowing more vision to energy economics, remains highly needed [25]. Energy is a key contribution in the industrialization method of any country. The example from such

	practices is that effective industrial policies need to be attended by consistent energy policies. Effective industrial policies require to be accompanied by consistent energy policies, specially in a country like Tanzania which is amongst the slightest electrified nations in the globe [26].

IV. Results

Based on the above points importance and their weightages, here the SAARC countries will be given weightage. If the SAARC country energy policies comply with the above points then it will be given higher weightage and if not then lesser. Each country points regarding their energy policy will be defined (reasoning) and then weightage will be given on it.

A. Validation

The following case validates the standard sustainable framework described above and discusses about the important parameters that needs to be present in a sustainable energy policy.

B. Denmark's Case

The resource of wind energy was considered as an opportunity to work towards an enhanced combination of sustainable fuels for the production of energy specifically by reducing the utilization of coal resource to support in progress of a developing industry. The buying needs premium fixed cost policies indulge values to allow straight forward approach to the grid for renewable energy manufacturers with a vibrant and financially reasonable systems of charging for grid access [27]. The aim was to device the energy act strategies that initiated from the year 1980 in line with the management's overall emission of carbon dioxide reducing targets. In the first step to entirely throw out the reserves of fossil fuels the government aims the drop in the utilization of gas, coal and oil reserves by around 33 percent between the year 2009-2020. The foremost aim of the Danish 2050 Energy plan is to gain 100% independence from fossil fuel resource in the country's energy mix by 2050 year. The target of RES is 30 percent in gross final energy consumption from 2010 to 2020 with feed- in tariff as a main aid strategy. The RE progress remained 17% of renewable energy share in the year 2005 and 22.2% in the year 2010. The green development agreement is between political parties founding a sustainable strategy for ecological policy in the industry of agriculture. This plan aims to lessen the greenhouse gas emissions from farming by 800000t yearly. The feed-in law scheme for wind energy resource was lately restructured in 2009. In the year 2012 new regulations about net metering were issued. They contributed to completely or partially exempt the paying tariffs and duties for the amount of energy exported to the grid [28].

C. Bangladesh

According to the renewable resource policy, the government intends to produce 800 megawatt of energy from renewable energy by 2015 year. To motivate people to utilize renewable resource energy, the IDCOL i.e. infrastructure development company limited has installed a full of 0.2 million SHS i.e. solar home systems since May, in the year 2013. As a consequence, around 0.8 million folks in the rural areas are now having access to solar energy resource [29]. The sustainable energy development agency will assist demonstration of the latest technologies and upcoming business models for renewable resource energy and other technologies including the clean energy ones [30]. However it may require time to familiarize fuel resources other than gas for energy generation, the diversification of the fuel mix in energy sector is a serious need for elongated energy security in the country of Bangladesh [31].

D. Bhutan

The renewable energy resources lead the present energy supply in Bhutan. The fuel such as firewood is the main source of initial energy resource and it signifies the major share of utilization of energy resource. Another resource which is hydropower is the largest renewable energy resource in the country Bhutan and is the source for 99 percent of the country's energy production today [32]. Renewable energy feed-in tariffs for the mini, micro and small hydropower plants to be linked to grid, the Bhutan electricity authority shall establish feed-in-tariff to allow the injection of energy to the grid with guaranteed inducement [33]. The initial mandate of the energy policy should focus to deliver affordable, ecological friendly, safe and efficient energy to increase the living level of the folks. While the growth of solar resource energy is hindered due to finances, high costs and lack of suitable financing [34].

The above comparative review of Bhutan showed that it needs to improve the localization and diversification along with fostering innovation.

E. India

India is splendidly endowed with the wind and solar resource technology and can harness them in an advanced way to meet energy needs at decentralized positions. In the fresh auctions, wind and solar energy resource prices have atatined bus bar grid equivalence at the generation end [35]. However, the system of feed-in tariff is not novel to wind energy projects in India, big-scale solar energy resource has been mainly procured through an opposite auction procedure since the beginning of the national solar mission. Since the Gujarat trial, no government agencies in the country India have tried to utilize the feed-in tariff procedure to procure solar resource [36]. By the time of March 2007, the renewable resource energy, except hydro above 25 megawatts installed capacity, has taken part in 10,243 megawatts representing 7.7 percent of total energy installed capacity. There has been remarkable progress in wind energy and, with an installed capacity of over 8757 megawatts, India inhabits the fifth place worldwide [37].

The above comparative review of India showed that it needs to improve the diversification and broadening of industries.

F. Nepal

The mini hydro resource and solar photovoltaic are the most extensively used resource of renewable energy technologies in the rural electrification of the country Nepal and these were also the dual attentive technologies. The examination shows that here is a growing trend in the community participations in the mini hydro resource projects which can be observed as an indication that the rural electrification is going towards the business of sustainability [38]. The rising dependence to import the fuels of petroleum coupled with growing fuel cost in the globe's market is harshly impacting the already delicate economy of the nation [39]. The solar photovoltaic delivers a feasible option to meet electrical energy demand in the non-electrified rural locations in country as well as completing the rising city energy demand. The renewable technology has been risingly implemented since the fitting of the first photovoltaic module in the year 1963 at the location of Bhadrapur Airport for the purpose of navigation [40].

The above comparative review of Nepal showed that it needs to improve the localization and reduction of fossil fuel resources.

G. Maldives

The resource of renewable energy does confronts some challenges such as absence of capabilities for design, development, implementation and management deficiency of economics available for the renewable resource energy uses and renewable resource based maintenance projects and also the deficiency of information on the choices available in renewable resource technology, statistics involved in renewable resource energy and in research [41]. The financial profits from the renewable resource energy system will originate from the scheme of feed in tariff mechanism for the renewable resource energy applied by the government of Ministry of environment and energy by the year 2013 of the expanse of feed in tariff grant delivered by the country Maldives is varied according to the kind of energy supply and the area [42]. To enhance the energy info net system there is a necessity of firming the existing systems of information and creating awareness of renewable resources; funding mechanisms for renewable resource projects, involving the regional structures of loan and technical aid to banks; policy assistances to operate the regulatory outlines that make renewable energy progress; and creating technical ability amongst players in the renewable resource field [43].

The above comparative review of Maldives showed that it needs to improve the localization and the Government economic framework.

H. Pakistan

An energy policy for progress of renewable resource was outlined in the year 2006 which was focused to deliver the sustainable energy to all customers involving those domestics which have not been delivered electricity and the resource of natural gas in remote and rural areas. The energy policy was prolonged for operation in the year 2011 and is still in usage. The Pakistan government framed a policy named as Renewable Energy for power generation in the year 2006 which was focused on to be improved and is till now the initial planning framework in the matter. Currently, the nation's energy sector is fronting poorest ever lack of its history and the folks of the nation bear elongated term energy outages in twisting heat of seasonal variations and natural gas resource shortage in the cold season of winter [44]. In evolving latest energy generation projects, a priority shall be made to enhance and specific design of feed in tariff which shall establish the higher ceiling. Furtherly, the good bidding may be utilized to lower the price of production [45]. The additional resources of renewables involve solar resource power, wind resource energy, biomass energy, geothermal and waste to energy and their combined role in the mix of energy is not more than 5 percent understanding the reality that the resources of renewables are very costly at this level for nation such as Pakistan and the fundamental aim of the proposed plan is to develop the energy available at maximum rate to every customer [46].

The above comparative review of Pakistan showed that it needs to improve the economic framework and indigenization of multiple renewable resources along with fossil resource reduction.

I. Sri Lanka

It was discovered that absence of economic tools, high early price and deficit of resource supply certainty or accessibility are the major blockages for the resource of renewable energy technologies [47]. In the year 2010, the country Sri Lanka established a scheme of feed in tariff and has few of the maximum tariffs in the emerging globe now. The subsequent energy technologies are suitable up to a range of 10 watt. The resources of hydro energy, wind resource energy, biomass resource technology and the mini micro hydro resources involves that the tariffs are based on prices and specific to the technology, and the inventers have the choice of choosing either a three-level tariff or a plane tariff [48]. A suitable cost policy for the sector will be followed focusing on vital factors including price reflectivity, demand for aimed subsidies, and competition between locally generated services/ goods in the local and global markets [49].

The above comparative review of Sri Lanka showed that it needs to improve the economic framework and indigenization of multiple renewable resources along with fossil resource reduction.

CONCUSLION

In this paper the comparative analysis of countries such as Germany and Denmark is considered as a progressive example in terms of attaining a sustainable energy policy. The country Pakistan has no prominent role from the renewable energy resources at nation wide stage but instead a main share of electricity is received from the fossil fuels reserves such as oil and gas. On the perkier side though, it may be considered that the nation makes wide use of river resources to produce the hydel resource power and compared to other nations it utilizes almost no coal resource for energy production in spite of around 175 billion tonnes resources being exposed in the southernmost domain. Between the reasons for absence of coal resource utilization in production are party-political issues and lack of investors for the purpose of deep mining that is needed. The resource of coal is also much in sulphur quantity, and the theme being discovered by the country scientists is gasification of coal resource as a replacement for of direct burning of it. The share of the renewable's resources needs to be amplified. A sequence of actions at both energy policy, societal and methodological levels are needed if the nation is to go into a sustainability situation by the end of 21st century. As discussed above, it is attainable and economiclly feasible, to diversify the energy resources of country by keeping it away from the fossil reserves based on to green path. The major emphasis of the energy policy should aim to deliver sufficient capacity for energy generation at the less cost, and to avoid shortfalls by fulfilling the demand/supply gap. To boost up and make sure the utilization of indigenous natural resources of energy, which involves renewable resources, mankind power, contribution of local manufacturing and engineering competences and also to make sure that all shareholders are observed after in the procedure that is a win-win state for all. There should be a focus on to safeguard the environment. Also, to raise the deployment of renewable resource technologies in the country. To deliver further power supplies to assist in fulfilling the increasing country demand. To present the investment friendly inducements and enable renewable resource markets to entice private interest in renewable projects. There should be a proper policy to devise measures to assist the private sector in mobilizing, supporting and enabling the investment (public sector) in renewable resource projects.

References

[1] Patlitzianas, K.D., et al., Sustainable energy policy indicators: Review and recommendations. Renewable Energy, 2008. 33(5): p. 966-973. & Promotion of Renewable Energy. 20-24 June, 2011.

[2] Javed, A., Study to assess renewable energy development in South Asia ; Achievements and the way forward in the perspective of policies aand investment opportunities SAARC Energy Centre, Islamabad, December 2015.

[3] Oyedepo, S.O., Energy and sustainable development in Nigeria: the way forward. Energy, Sustainability and Society, 2012. 2(1): p. 15.

[4] Von Hippel, D., et al., Energy security and sustainability in Northeast Asia. Energy Policy, 2011. 39(11): p. 6719-6730.

[5] Khatib, H.e.a., World Energy Assessment - Energy and the Challenge of Sustainability (UNDESA - UNDP - WEA - WEC). Energy Security, 2000. Chapter 4 of J. Goldemberg et al(United Nations Development Programme, New York).

[6] Berry, T. and M. Jaccard, The renewable portfolio standard:: design considerations and an implementation survey. Energy Policy, 2001. 29(4): p. 263-277.

[7] Jacobsson, S. and V. Lauber, The politics and policy of energy system transformation—explaining the German diffusion of renewable energy technology. Energy policy, 2006. 34(3): p. 256-276.

[8] Menanteau, P., D. Finon, and M.-L. Lamy, Prices versus quantities: choosing policies for promoting the development of renewable energy. Energy policy, 2003. 31(8): p. 799-812.

[9] Couture, T.D., et al., Policymaker's guide to feed-in tariff policy design. 2010, National Renewable Energy Lab.(NREL), Golden, CO (United States).

[10] Li, X., Diversification and localization of energy systems for sustainable development and energy security. Energy policy, 2005. 33(17): p. 2237-2243.

[11] Ozturk, I., Energy dependency and security The role of effciency and renewable energy sources. april, 2014.

[12] Stirling, A., Diversity and ignorance in electricity supply investment: addressing the solution rather than the problem. Energy Policy, 1994. 22(3): p. 195-216.

[13] Ream, M.K., When it comes to energy, countries should mix it up. May 6, 2015.

[14] Sturm, C., Inside the Energiewende: Policy and Complexity in the German Utility Industry. Issues in Science and Technology, Winter 2017. 2(33).

[15] A. Gürhan Kök, K.S., Şafak Yücel, Impact of electricity pricing policies on renewable energy investments and carbon emissions. December 2, 2016.

[16] Monasterolo, I. and M. Raberto, The impact of phasing out fossil fuel subsidies on the low-carbon transition. Energy Policy, 2019. 124: p. 355-370.

[17] Kefford, B.M., et al., The early retirement challenge for fossil fuel power plants in deep decarbonisation scenarios. Energy policy, 2018. 119: p. 294-306.

[18] Lund, H. and B.V. Mathiesen, Energy system analysis of 100% renewable energy systems—The case of Denmark in years 2030 and 2050. Energy, 2009. 34(5): p. 524-531.

[19] Morthorst, P.E., The development of a green certificate market. Energy policy, 2000. 28(15): p. 1085-1094.

[20] Foxon, T.J., et al., UK innovation systems for new and renewable energy technologies: drivers, barriers and systems failures. Energy policy, 2005. 33(16): p. 2123-2137.

[21] Chuang, M.C. and H.W. Ma, Energy security and improvements in the function of diversity indices—Taiwan energy supply structure case study. Renewable and Sustainable Energy Reviews, 2013. 24: p. 9-20.

[22] Asif, M. and T. Muneer, Energy supply, its demand and security issues for developed and emerging economies. Renewable and Sustainable Energy Reviews, 2007. 11(7): p. 1388-1413.

[23] Loiter, J.M. and V. Norberg-Bohm, Technology policy and renewable energy: public roles in the development of new energy technologies. Energy Policy, 1999. 27(2): p. 85-97.

[24] Lund, H. and W.W. Clark, Management of fluctuations in wind power and CHP comparing two possible Danish strategies. Energy, 2002. 27(5): p. 471-483.

[25] Verde, S., Everybody merges with somebody—The wave of M&As in the energy industry and the EU merger policy. Energy policy, 2008. 36(3): p. 1125-1133.

[26] Gussai Sheikheldin, B.D., Hezron Makundi, Energy policy for industrialization: Tanzania's big development challenge. Dec, 2018.

[27] Mourelatou, A., B.E. Research, and C. Limited, Renewable energies: success stories. 2001: Office for official publications of the european communities.

[28] Abdmouleh, Z., R.A. Alammari, and A. Gastli, Review of policies encouraging renewable energy integration & best practices. Renewable and Sustainable Energy Reviews, 2015. 45: p. 249-262.

[29] Mustafa K. Mujeri, T.T.C.a.S.S., Energy Sector in Bangladesh: An agenda for reforms The International Institute for Sustainable Development March 2014.

[30] POWER DIVISION MINISTRY OF POWER, E.A.M.R.G.O.T.P.S.R.O.B., , and Renewable Energy Policy Of Bangladesh. DECEMBER, 18 2008

[31] Roland-Holst, H.G.a.D., Energy Policy Options for Sustainable Development in Bangladesh ADB Economics Working Paper Series, November, 2013.

[32] Policy and regulatory overviews Bhutan 2012. REEEP Policy Database (contributed by SERN for REEEP), 2012.

[33] Bhutan Renewable Energy Policy, 2011

[34] Department of Energy Ministery of Economic Affairs, R.G.o.B., Overview Of Energy Policies Of Bhutan. May, 2009.

[35] NITI Aayog, G.o.I., Draft National Energy Policy June 27, 2017

[36] Prateek, S., Feed-In Tariffs to Make a Comeback in India for Small Solar and Wind Projects. Feb 03, 2018.

[37] REN21, Renewables 2009 global status report.

[38] Mainali, B. and S. Silveira, Financing off-grid rural electrification: country case Nepal. Energy, 2011. 36(4): p. 2194-2201.

[39] Reegle, Policy and regulatoy overviews- Nepal 2012.

[40] Nepal, R., Roles and potentials of renewable energy in less-developed economies: The case of Nepal. Renewable and Sustainable Energy Reviews, 2012. 16(4): p. 2200-2206.

[41] Promote renewable energy technologies (Policy no. 5, Maldives National Energy Policy and Strategy). 2010.

[42] Jung, T.Y., Y.T. Kim, and J.H. Hyun, An Economic Analysis of a Hybrid Solar PV-Diesel-ESS System for Kumundhoo, Maldives. Korea and the World Economy, 2017. 18(S1): p. 109-134.

[43] Timilsina, G.R. and K.U. Shah, Filling the gaps: Policy supports and interventions for scaling up renewable energy development in Small Island Developing States. Energy Policy, 2016. 98: p. 653-662.

[44] Aized, T., et al., Energy security and renewable energy policy analysis of Pakistan. Renewable and Sustainable Energy Reviews, 2018. 84: p. 155-169.

[45] Pakistan, G.o., National Power Policy. 2013.

[46] Engr. Arshad h Abbasi, F.M., Amna Baig, Maha Kamal, Sdpi Pakistan Energy Vision 2035. 2014.

[47] Wijayatunga, P.D., et al., Strategies to overcome barriers for cleaner generation technologies in small developing power systems: Sri Lanka case study. Energy conversion and management, 2006. 47(9-10): p. 1179-1191.

[48] Reegle, Policy and regulatory overviews Sri Lanka 2012.

[49] Energy, M.O.P., The Gazette of the Democratic Socialist Republic of Sri Lanka. 11th May, 2008.

Maham Mujahid was born in Dictrict Peshawar, Khyber Pakhtunkwa, Pakistan on 5 January 1996, She has got her bachelor's degree in Biotechnology from University of Peshawar, Pakistan in 2017, currently she is getting her master's degree in Energy management and sustainability from US Pakistan Center for Adavnced Studies in Energy, University of Engineering and Technology Peshawar, Pakistan. Her research interest includes energy policies and comparative analysis of Saarc countries energy policies.

IJEW 国际工程期刊 International Journal of Engineering Works انجینئرنگ کاموں کا بین الاقوامی جرنل

International Journal of Engineering Works
ISSN-p: 2521-2419
ISSN-e: 2409-2770
Vol. 6, Issue 12, PP. 496-506, December 2019
https://www.ijew.io/
https://doi.org/10.34259/ijew.19.612496506

Extensive Performance Evaluation of Dual Booster Mirror Solar Cooker under Tracking Free Conditions

Muhammd Irfan[1], Suhail Zaki Farooqui[2], Asadullah khan[3]
[1,2,3]Department of Renewable Energy Engineering, U.S.-Pakistan Center for Advance Studies in Energy, University of Engineering and Technology Peshawar, Pakistan
irfankhan9732@gmail.com[1], suhail.zaki@uetpeshawar.edu.pk[2], asadullah8080@gmail.com[3]
Received: 05 October, Revised:10 November, Accepted: 06 December

Abbreviations and Acronyms

SBC	Solar Box Cooker
DBM	Dual Booster Mirrors
BM	Booster Mirror
FOM	Figure Of Merit
FFOM	First Figure Of Merit
SFOM	Second Figure OF Merit
α	Solar altitude Angle
б	Solar Declination Angle
ω	Hour Angle
φ	Latitude of the location
t_s	Solar Time
SR	Solar Radiation
OTA	Optimal Tilt Angle

***Abstract*—**The aim of this research work is to conduct an extensive performance evaluation of a box type dual Booster Mirror solar cooker under tracking free conditions. To cope up with the need for continuous adjustment of the cooker during the cooking operation the optimal tilt angles of the Booster Mirrors have been calculated through numerical calculations for the location of 34^0 latitude. To evaluate the Performance parameters of the cooker, tests under tracking free conditions have been carried out and parameters such as, First and Second Figure of Merit, Cooking power, exergy efficiency and the Quality Factor, are evaluated for the BSC. Moreover, the cooker is tested on-field and different types of food items are cooked. The results indicate that orienting the Booster Mirrors at their respective optimal angles provides a viable and convenient alternative to the need for continuous tracking of the sun during cooking hours. With this technique the said cooker can be used for cooking 6.4 kg of 6 different dishes in a single day i-e. from 9:00 Am to 3:00 Pm in two batches.

***Keywords*—** Optimal tilt angles, Box Type Solar Cooker, Tracking free conditions

I. Introduction

Cooking counts as one of the major fuel consuming activity in the world. Conventional cooking poses a major threat to the forests since, approximately two-third of the developing country's population depends on firewood for their daily cooking and heating needs [1]. Solar cooking is a renewable activity that utilizes solar radiation to cook food. Solar cooking is a cost free, environment friendly, and convenient replacement for conventional cooking practices. Among all the types of solar cookers, box type solar cookers are the most preferred ones because of their lower cost and simple design. SBC utilizes the greenhouse effect to cook the food. Typically, a SBC has two transparent plan mirrors that act as the lid of the cooker box. Food is placed in the cooker box and the lid is closed under airtight conditions. The temperature of the air inside the cooker box is increased because of the greenohouse effect and thus the food inside the box starts cooking.The two BMs having the same size as the aperture of the SBC are mounted on both the edges of the SBC. These BMs direct the solar radiation onto the aperture of the SBC, thus making extra radiation fall on the aperture and thus speeding up the cooking process. The main disadvantage in SBC is the need for adjustment after every 15-30 minutes during the cooking operation due to change in the solar azimuth angle. The need for the solar tracking, makes the cooking process more hectic especially when the cooker is loaded, and is a major hurdle in the mass adoption of the SBC for cooking purposes [2].

A. The Dual Booster Mirror Solar Cooker

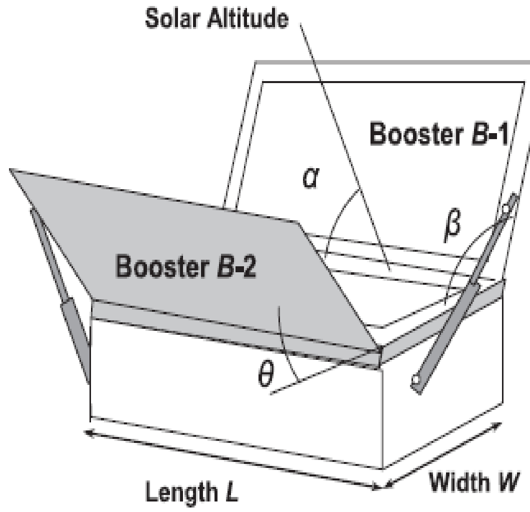

Figure.1 The DBM solar cooker with length L and width W and the BMs inclined at their respective angles with the horizon., α reprsent altiitude angle

The DBM Solar Cooker has two booster mirrors attached to the edges of the cooker box. The direct solar radiation fall on the aperture of the cooker directly where as the diffused radiation are reflected by the BMs onto the aperture of the cooker. The dimensions of the BMs are the same as that of the solar cooker's base. The BM B-1 and B-2 are inclined at an angle of β and θ with the horizon respectively as shown in Fig.1.

In order to make more and more diffused solar radiation fall on the solar cooker, The inclination of both the BMs should be varied every 15-30 minutes. To make the cooking process free of the need for solar tracking the optimal tilt angles of both the BMs are found through numerical calculations.This section covers the analysis of the solar radiation harnessed by both the BMs for 3 hours before and 3 hours after the solar noon I-e from 9:00 am to 3:00 pm , which is considered to be the most optimal time for solar cooking. The solar altitude angle at an instant is given by

$$\alpha = sin^{-1}[sin\delta sin\emptyset + cos\sigma cos\omega cos\varphi] \text{ degrees} \quad (1)$$

Where as the hour angle ω is shown by

$$\omega = 15(t_s - 12) \text{ degrees} \quad (2)$$

The solar declination angle is given by

$$\delta = sin^{-1}[0.39795 \cos[.98563(N - 173)] \text{ degrees} \quad (3)$$

The value of N in equation (3) varies form 1-365 based on the number of the day of the year. As fig.2. shows, the BMs B-1 and B-2 are inclined at angle β and θ respectively with the horizon.W is the width of the BMs. As the Fig.2 shows, I is the solar radiation intensity on a horizontal surface at time t then the solar radiation intensity on a surface held normal to the Sun I'will given by

$$I' = \frac{I}{sin\alpha} \quad (4)$$

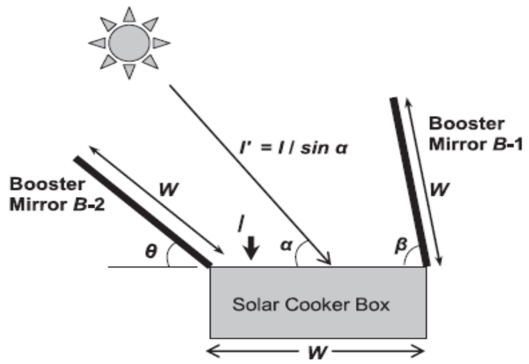

Figure.2 The Booster Mirrors inclined at their respective angles. W represents the width of the BMs

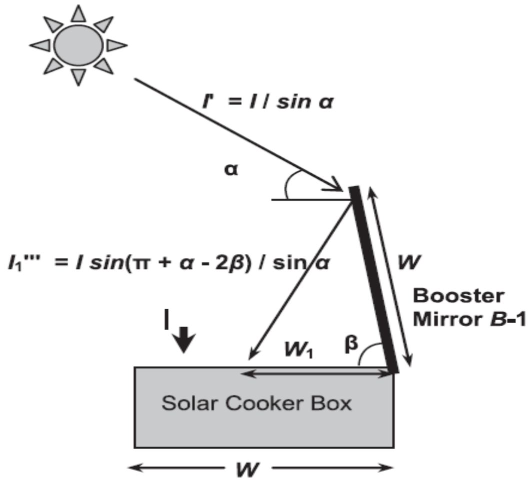

Figure.3 Solar radiation intensity on the top glazing after being reflected by the BM B-1

The solar radiation intensity normal to the surface of B-1 which is represented by I_1'' as shown in fig.3. is given by

$$I_1'' = I' \sin(\pi + \alpha - \beta) \quad (6)$$

If 'W' represents the width of the solar cooker and W_1 represent the projection length of the reflected light on the horizontal surface then the solar irradiance attenuated by the horizontal surface equals to the power per unit length reflected by the mirror. This statement is given by

$$I_1'''W_1 = I_1''W \quad (7)$$

I_1''' represents the solar irradiance reflected by the B-1 onto the top surface of the cooker. As clear the incident radiation is making an angle (β-α) with the mirror, this implies that the angle made by the reflected radiation with the horizontal surface of the top glazing will be (π+α-2β). Thus by the law of sines

$$\frac{W}{\sin(\pi+\alpha-2\beta)} = \frac{W_1}{\sin(\pi+\alpha-2\beta)} \quad (8)$$

By comparing equation 7 and 8 we get

$$I_1''' = I.sin(\pi + \alpha - 2\beta)/\sin\alpha \quad (9)$$

If the same analysis is carried out for BM B-2 it will give the results as

$$I_2'' = I' \sin(\alpha - \theta) \quad (10)$$

$$I_2''' = \frac{I_2'' \sin(2\theta - \alpha)}{\sin(\alpha - \theta)} = \frac{I\sin(2\theta-\alpha)}{\sin\alpha} \quad (11)$$

$$W_2 = \frac{W\sin(\alpha-\theta)}{\sin(2\theta-\alpha)} \quad (12)$$

Integrating $(I.W + I_1'''.W_1 + I_2'''.W_2)$ for 9:00 Am to 12:00 Pm for the ramge of values of α between α_{min} i-e at 9:00 Am and α_{max} i-e at 12:00 Pm for the fixed values of θ and β, gives the total energy per unit length received by the solar cooker box. The values of W_1 and W_2 are calculated using equation (9) and (12). Thus the total solar energy attained by the SBC is gives as

$$E = \int_{t_1}^{t_2} (I.W + I_1'''.W_1 + I_2'''.W_2)dt \;\; joules \quad (13)$$

B. Calculation of the Optimal tilt Angles for Booster Mirrors

The optimal tilt angles of the BMs are the angles at which, if the BMs are tilted, will give the maximum energy output for a specific day of the year. Since the extra terrestrial radiation intensity I_0 on a surface held normal to the sun on a specific day of the year is given as

$$I_o = I_{sc}[1 + 0.034412cos\left\{\frac{2\pi(N-3)}{365.35}\right\} \quad (14)$$

I_{sc} ; $1367\ W/m^2$

N ; Day of the year

The extra terrestrial solar radiation on a horizontal surface I_{oh} is given as

$$I_{oh} = I_o Cos\theta_z \quad (15)$$

θ_z ; Zenith Angle

θ_z, In terms of the solar altitude angle α is given as

$$\theta_z = 90 - \alpha \quad (16)$$

The extra terrestrial solar radiation when reach the earth atmosphere is reduced to

$$I = I_{oh} \,.\, 0.7^{AM^{.678}} \quad (17)$$

The Air Mass A.M is given as

$$A.M = [cos\theta_z + 0.50572(96.07995 - \theta_z)^{-1.6364}]^{-1} \quad (18)$$

Using the SR intensities, as deduced by the equations

(14)-(18) and (8)-(12), for a given location i.e. Latitude Angle, the last two components of Eq.(13) may be integrated between the minimum and maximum value of altitude angle i.e. the altitude angle at 9:00 am and at 12:00 PM respectively for specific value of θ and β to calculate the total energy contributed by each of the two BMs. The most optimal values of θ and β are achieved by repeating the integration for all possible values of θ between 0° and 60° and for the value of β between 40° and 110° for which the total energy received by the cooker is maximum[2].

B. Experimental Results

The fore-mentioned calculations are carried out for location of 34° Latitude i-e Peshawar Pakistan for the DBM solar cooker and the values of the OTAs for a 34° Latitude location, if plotted against the days of the year will give the result as shown in Fig.4. The BMs B-1 and B-2, with a length of 1.0 m and width 0.5 m if inclined at their calculated optimal tilt angles will contribute to the energy gained by the cooker as shown in Fig.5. Fig.6 is the depiction of energy contributed to the BSC by both the BMs and the top glazing. Fig.7 shows the dual BM Solar cooker with its primary Booster Mirror B-1 facing South.The dimensions of the SBC used for the evaluation of the dual BM solar cooker are given in Table.1. The optimal values of the tilt angles for both the booster mirrors calculated through numerical calculations for the location of 34° Latitude are given in Table.1 and Table.2

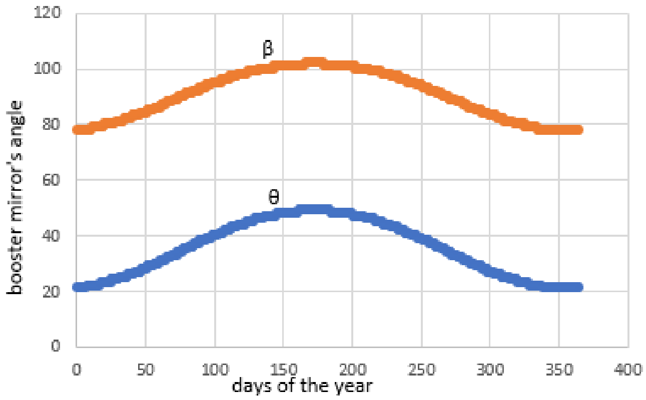

Figure.4 Plot of the optimal tilt angles of BMs Vs days of the year

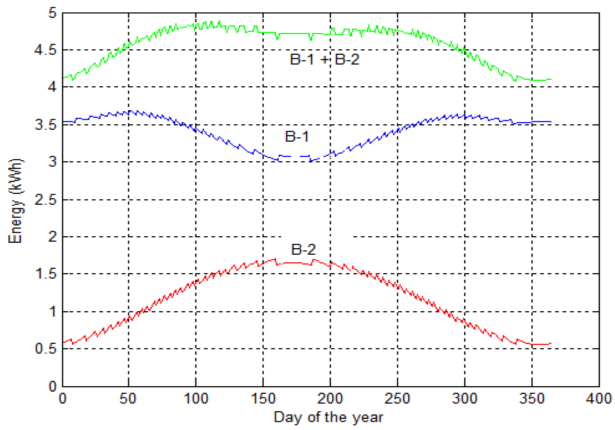

Figure.5 Collective as well as individual energy contribution by both BMs to the SBC

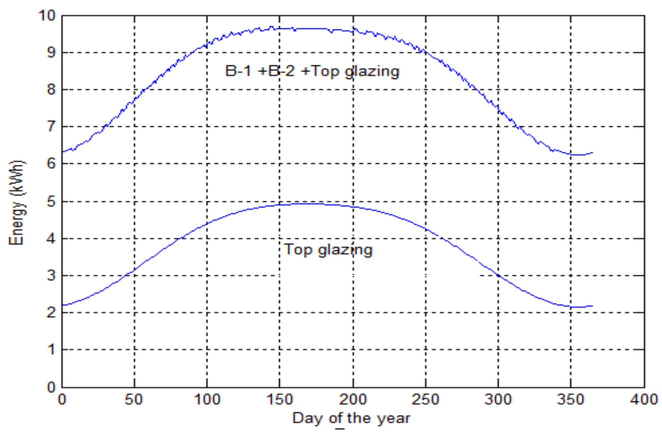

Figure.6 energy contributed by both the booster mirrors and top glazing

TABLE.1 OPTIMAL TILT ANGLES OF THE BOOSTER MIRROR B-1 AND THEIR CORRESPONDING DAYS FOR 34^0 LATTUDE LOCATION

N	β_{opt}	N	β_{opt}	N	β_{opt}	N	β_{opt}	N	β_{opt}	N	β_{opt}
1	78	**56**	85	**97**	94	**143**	100	**237**	96	**271**	89
12	79	**61**	86	**102**	95	**202**	101	**245**	95	**280**	88
24	80	**66**	88	**108**	96	**214**	99	**251**	94	**282**	87
33	81	**72**	89	**116**	97	**223**	98	**255**	93	**299**	84
46	83	**77**	90	**126**	99	**229**	97	**258**	92	**310**	82
51	84	**84**	91	**130**	99	**236**	96	**263**	91	**361**	78

TABLE.2 OPTIMAL TILT ANGLES OF THE BOOSTER MIRROR B-2 AND THEIR CORRESPONDING DAYS FOR 34^0 LATTUDE LOCATION

N	θ_{opt}	N	θ_{opt}	N	θ_{opt}	N	θ_{opt}	N	θ_{opt}	N	θ_{opt}
1	21	**39**	26	**71**	33	**113**	43	**180**	49	**255**	38
7	21	**44**	27	**79**	35	**116**	43	**201**	47	**263**	36
13	22	**50**	28	**84**	36	**123**	44	**211**	46	**272**	34
19	23	**56**	29	**89**	37	**129**	45	**223**	44	**305**	26
26	24	**58**	30	**103**	40	**137**	47	**236**	42	**319**	24
32	25	**65**	31	**108**	42	**159**	48	**240**	41	**365**	21

The dimensions of the SBC used for the analysis are given in Table.3. Fig.7 shows the actual dual BM Solar cooker, with it's primary BM facing South is shown in Fig.7.

TABLE.3 DIMENSION OF THE SBC

Height (cm)	**Width (cm)**	**Length (cm)**	**Aspect ratio (length/width)**
33	45	120	2.66

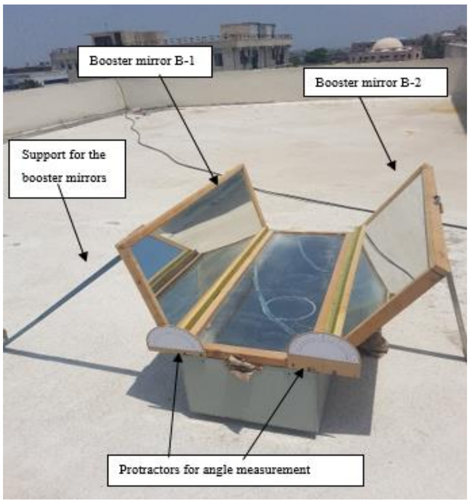

Figure.7 The dual BM solar cooker with the primary BM facing south

For conducting the extensive performance parameters of the dual BM solar cooker, four tests were conducted. The first test was conducted on 7th May, 2019 under unloaded conditions. And the rest of the three tests were conducted on 14th, 20th, and 21st May respectively under fully loaded conditions. The capacity of the cooker based on the aperture area was 3200 g . The exact same amount of Water was used for standard testing of the cooker. the load was evenly distributed in three containers of the same size. For the unloaded conditions the base temperature is noted until the point when there was no more rise in the base temperature. For the loaded conditions, along with the cooker base temperature, the food vessel's temperature was also noted down. The loaded tests were kept going on until the water inside the vessels reached its boiling point. For all the experiments the ambient temperature and solar irradinace was also measured. The readings were measured after every 5 minutes. The irradiance meter used for measuring the soalr irradiance was METEON 2.0 irradiance meter. The ambient temperature was measured with UNIT-T UT33D Multimeter. the results of the unloaded test are plotted in Fig.8. The data of all the three loaded tests are plotted in Fig.9-Fig.11. since there were three containers used, the cooking vessel's temperature at every instant is the average of the temperature of the three vessels. The solar irradiance measured for all the tests, if plotted against the solar time, will give the results as show in Fig.12

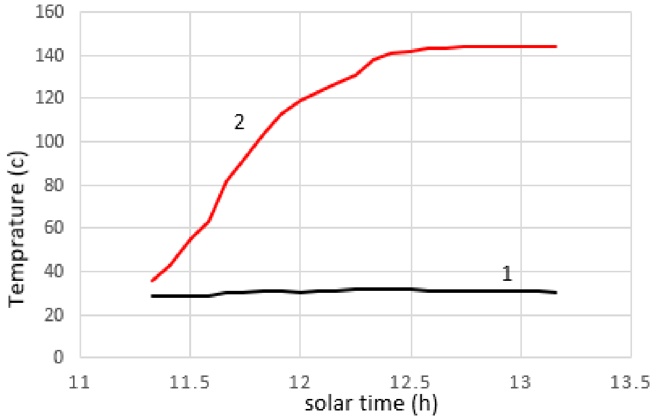

Figure.8 Temperature Vs time Plot for the unloaded conditions with curve 2 showing the cooker base temperature and curve 1 showing the ambient temperature

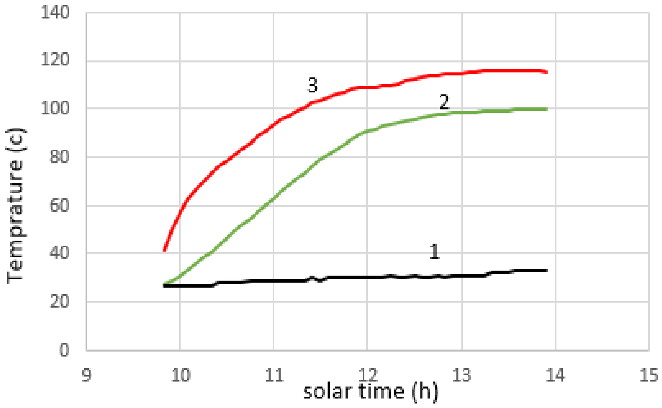

Figure.9 Temperature Vs Solar Time plot for first test under loaded conditions. curve 1 shows ambient temperature, curve 2 shows the average temperature of the water in the containers and curve 3 shows the base temperature

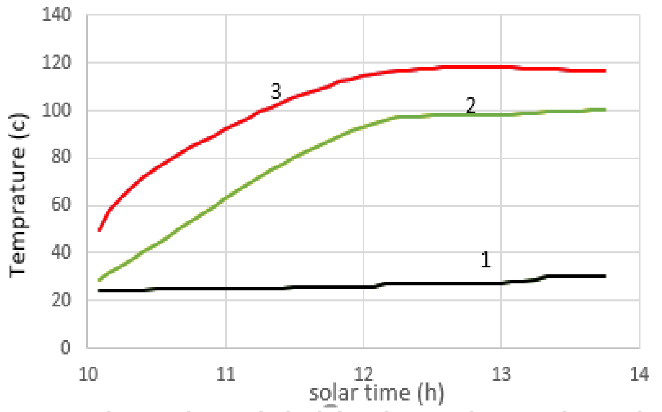

Figure.10 the second test under loaded conditions with curve 1 showing the ambient temperature, curve 2 showing the average temperature of the water in the containers and curve 3 showing the base temperature

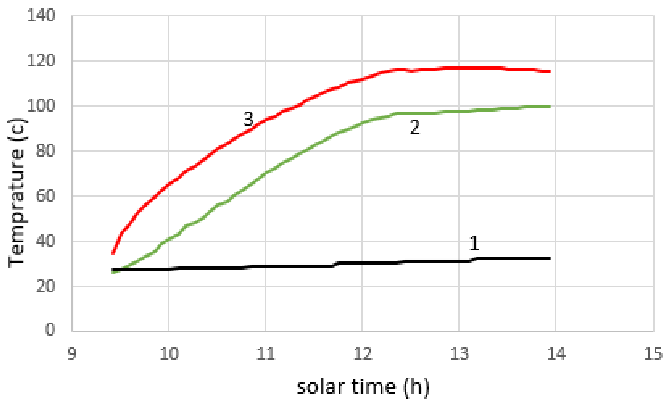

Figure.11 Temperature Vs ST plot for the third test under loaded conditions with curve 1 showing the ambient temperature, curve 2 showing the average temperature of the water in the containers and curve 3 showing the base temperature

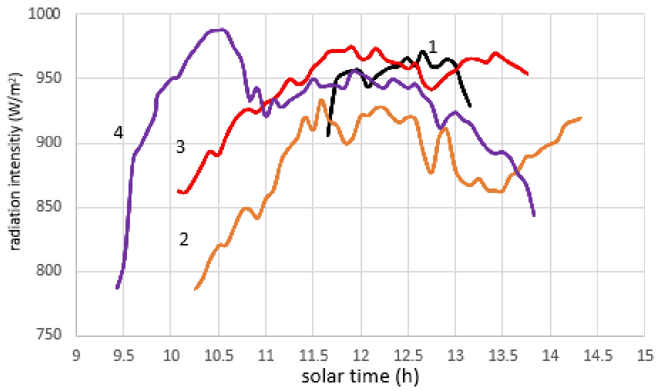

Figure.12 Plot of the solar irradiance Vs Solar time for all the four tests conducted under unloaded and loaded conditions

2. *First and Second Figures of Merit (F_1 and F_2)*

The first and second FOM are the thermal performance indicators of solar cookers. The first FOM is represented by F_1 and is the ratio of the optical efficiency to the heat loss factor.The first FOM is evaluated for the unloaded test and is given by

$$F_1 = \frac{T_b - T_{amb}}{H_s} \quad (13)$$

Tb ; solar cooker base temperature

Tamb ; ambient temperature

Hs ; average Solar insolation (W/m2)

The second FOM F_2 is evaluated for the solar cooker under loaded conditions. For the purpose of finding F_2 the water is heated sensibly up to 100 °C.The second figure of merit is the measure of heat transferred from the absorbing plate to the water that is being heated inside the solar cooker. F_2 is given by

$$F_2 = \frac{F_1(MC)}{A.t}\ln\frac{[1-\frac{(T_{wi}-T_{av})}{F_1.H_{av}}]}{[1-\frac{(T_{wf}-T_{av})}{F_1.H_{av}}]} \quad (14)$$

MC ; product of mass and specific heat of Water

A ; solar cooker aperture area

t ; time taken by the water to boil

T_{av} ; average ambient temperature

T_{wi} ; water temperature

T_{wf} ; final water temperature

H_{av} ; average solar insolation

The first FOM F_1 is given in Table.4

TABLE.4 CALCULATION OF THE FIRST FIGURE OF MERIT

T_b (°C)	T_{amb} (°C)	H_s (W/m²)	F_1
144	30	929	0.122

The cooking power of a solar cooker is an indication of the rate at which heat energy is supplied to a specific mass of the food inside the solar cooker. The cooking power is given by

$$\dot{Q} = \frac{M_w C_w (T_f - T_i)}{t} \quad (15)$$

M_w ; mass of water

C_w ; specific heat of water

T_i ; initial temperature of water

T_f ; final temperature of water

t ; time taken

The cooking Power and F_2 is calculated in Table.5. Since three loaded experiments are conducted, the value of F_2 and the cooking power for the solar cooker is the average of the values calculated for all the three experiments.

3. *Exergy Efficiency and Quality factor*

The exergy of a device is the measure of its potential to derive heat from the surrounding [3]. The exergy efficiency is the ratio of the exergy input to the system to the exergy output of the system. The exergy input to the solar cooker is the exergy of solar radiation flux which is given by equation

$$E_{xi} = I°A\Delta t[1 + \left(\frac{T_a}{T_s}\right)^4\left(\frac{1}{3}\right) - \left(\frac{4}{3}\right)\left(\frac{T_a}{T_s}\right)] \quad (16)$$

Where $I°$ is the instantaneous solar insolation, T_a is the ambient temperature, T_s is the temperature of the surface of the Sun, and A is the aperture area of the SC. The exergy out is given by

$$E_{xo} = MC_w[(T_f - T_i) - T_a \ln(T_f/T_i)] \quad (17)$$

Ta ; ambient temperature

The second term in equation (17) represents the exergy loss from the system. Exergy efficiency is calculated by diving equation (17) by (16) Thus exergy efficiency is given by

$$\varphi = \frac{\left[\frac{(MC)_w[(T_{wf}-T_{wi})-T_a\ln(T_{wf}/T_{wi})]}{t}\right]}{I°A\Delta t[1+\left(\frac{T_a}{T_s}\right)^4\left(\frac{1}{3}\right)-\left(\frac{4}{3}\right)\left(\frac{T_a}{T_s}\right)]} \quad (18)$$

The exergy input to the system as given by equation(16) is calculated and the result for all the three sets of experiment is plotted in Fig.13. similarly the exergy output calculated for all the three sets of the loaded experiments is plotted in Fig.14. The plots of the exergy efficiency for all the three loaded experiments is given in Fig.15.

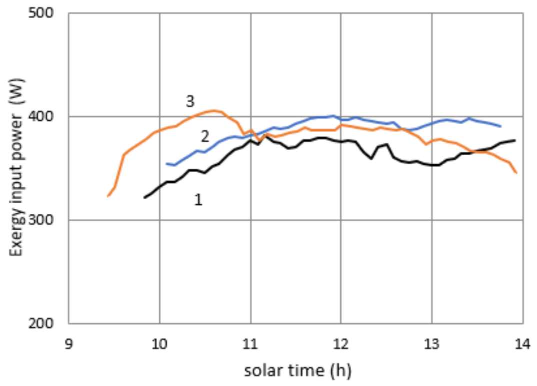

Figure.13 Plot of the Exergy input vs solar time for all the three experiments conducted under loaded conditions. Curves are labeled according to the experiments

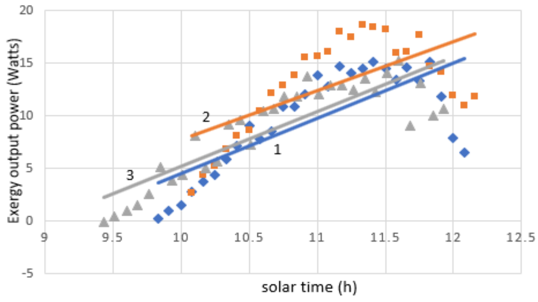

Figure.14 Exergy utput power Vs solar time plot for the three tests conducted under loaded conditions. the trendlines are numbered according to the experiments number

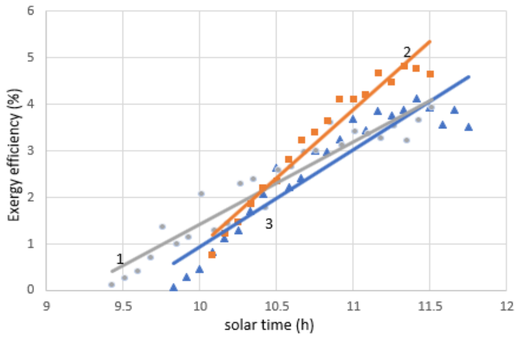

Figure.15 plot of the Exergy efficiency vs solar time. The curves are labelled according to the experimen

TABLE.5 CALCULATIONS OF THE SECOND FIGURE OF MERIT AND COOKING POWER

Exp no	Aperture Area (m^2)	T_{wi} (°C)	T_{wf} (°C)	T_{av} (°C)	H_{av} (W/m^2)	Duration (seconds)	(M.C) (j/k)	F_2	Cooking Power P(W)
1	0.44	27	100	29.8	884	16200	13440	0.25	60.5
2	0.44	28.4	100	26.44	943	13200	13440	0.278	72.9
3	0.44	25.6	100	29.5	928	16200	13440	0.233	61.7
						Average		0.254	65

TABLE.6 CALCULATION OF THE OVERALL HEAT LOSS COEFFICIENT

Exp No	Length of cooker L(m)	Width of the cooker W(m)	Gross aperture area A(m2)	Slope of the Exergy loss curve (W/K)	Heat loss coefficient (W/Km2)
1	1.2	0.45	0.54	0.416	0.832
2	//	//	//	0.648	1.2
3	//	//	//	0.2082	0.385
				Average	0.78

TABLE.7 CALCULATIONS OF THE QUALITY FACTOR FOR ALL THE THREE EXPERIMENTS CONDUCTED UNDER LOADED CONDITIONS

Experiment No	Peak Exergy gain EX_O (W)	Temperature difference ΔT	Exergy loss EX_L (W) at ΔT	Quality facorEx_o/Ex_L
1	14.17	37.05	350.3	0.04
2	18.22	39.901	370	0.049
3	12.654	37.109	375.9	0.033
			Average	0.04

The exergy analysis of the cooker is considered to be a more complete synthesis technique because of the fact that it considers the quality as well as quantity of energy transferred from the solar cooker and vice versa. As proposed by (Kumar et al.) a graph of exergy output and temperature difference is plotted and the data points are fitted to a second order polynomial. The fitting of the data points to a second order polynomial makes it easy to obtain the peak value of exergy which is in a close proximity with the actual value of the peak exergy[4]. The exergy output data is plotted against the temperature difference and the data is fitted to the second order polynomial for all the three loaded experiments. To give a clear view of the plot the results are plotted separately for all the three experiments as shown in Fig.16-Fig.18. From the fitted curves, the temperature difference gap is obtained which is the value of the x-axis (Twater -Tamb) corresponding to the half exergy point of the curve. The exergy output curves are plotted separately for all the three loaded experiments.The exergy loss data (Exi-Exout) is plotted againts the difference of the water and ambient temperature for all the three loaded experiments. The plots are given in Fig.19-Fig.21. The slope of exergy loss curve divided by the gross aperture area gives the overall heat loss coefficient of the solar cooker in (W/K.m2) . The overall heat loss coefficient of the cooker is the average of the overall heat loss coefficient for all the three experiments. The heat loss coefficient is calculated in Table.6.

TABLES.8 DATA OF THE ON-FIELD TESTS OF THE SOLAR COOKER

DATE: JUNE 18TH, 2019

container	food items	starting time	Irradiance (w/m^2)	T_{ave} (°C)	Time taken	comments
1	350g split green gram+700g water				2.1 hours	Properly cooked
2	350g Split Red Lentil+700g water	10:10 am	848	30	2.1 hours	Slightly overcooked
3	350g split black gram +700 g water				2.1 hours	Properly Cooked

DATE: JUNE 24 TH, 2019

container	food items	starting time	Irradiance (w/m^2)	T_{ave} (°C)	Time taken	comments
1	350g chickpeas+700g water				2.5 hours	Properly cooked

2	350g black chickpeas +700g water	10:20 am	856	31	2.5 hours	Properlycooked
3	350g split chickpeas +700 g water				2.5 hours	Properly Cooked

DATE: JUNE 26TH, 2019

container	food items	starting time	Irradiance (w/m^2)	T$_{ave}$ (^{o}C)	Time taken	comments
1	1kg chicken +250g yogurt paste				3 hours	Properly cooked
2	350g veal+600g water	10:20 am	821	31	3 hours	Properly oooked
3	300g rice + 200g Pea beans + 700 g water				3 hours	Properly Cooked

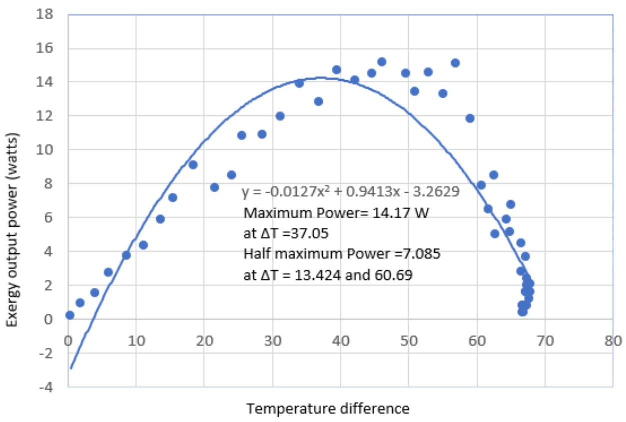

Figure.16 Second order polynomial fit to the Exergy output data for experiment No1 conducted on 14th May

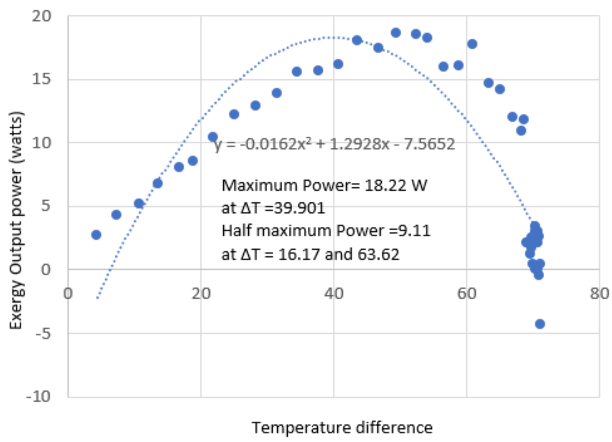

Figure.17 second degree polynomial fit to the Exergy output data for experiment No2 conducted on May 20th

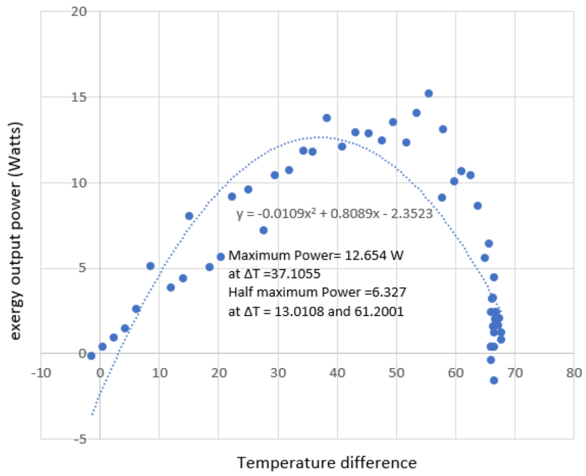

Figure.18 second degree polynomial fit to the Exergy output data for the 3rd experiment conducted on May 21st

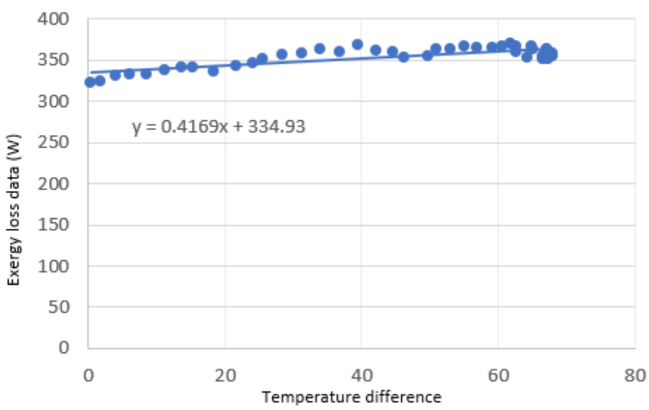

Figure.19 Least square fit to the Exergy loss data for experiment # 1

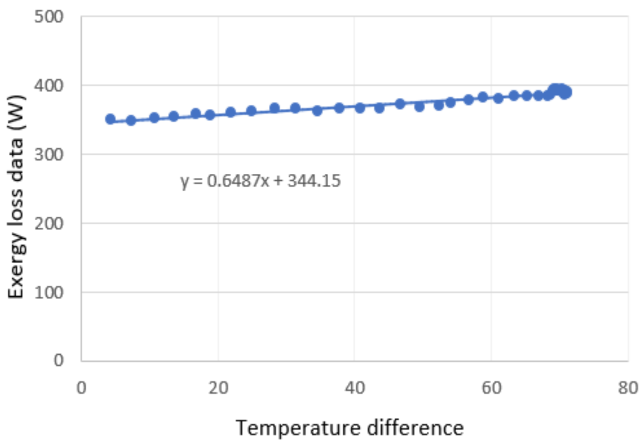

Figure.16: Least square fit to the Exergy loss data for experiment # 2

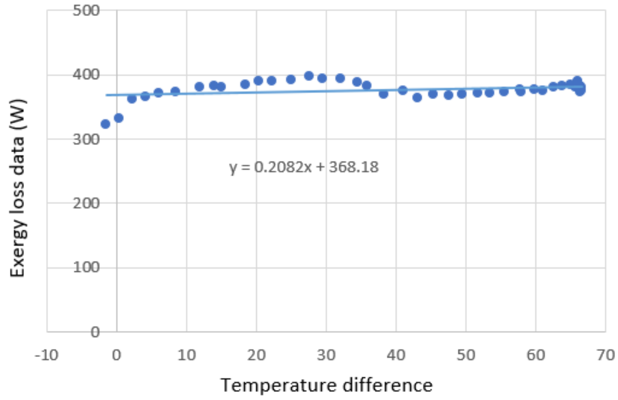

Fig.I-17: Least square fit to the Exergy loss data for experiment # 3

The Quality facor of the cooker is obtained by dividing the peak exergy value at that specific difference of temperature.The average Quality factor for all the three experiments is shown in Table.7.

C. *On-field testing of the solar cooker*

The cooker was also used for cooking different types of food items. During cooking, the full load of the food items was kept 3200 gm. Three containers were used to cook three different dishes in the cooker in one go. The start and end times of the cooking were noted down. The data of the on-field testing of the cooker is given in Tables.8-11.

CONCLUSIONS

The performance parameters of the dual BM BSC evaluated under tracking free conditions are satisfactory and suggest that the angular optimization technique is an excellent replacement for the labor involved in adjusting the solar cooker after every 15-30 minutes. The maximum time required to cook a dish is 3 hours, which implies that the same cooker can be used for cooking twice a day, making it possible to cook 6.4 kg of six different dishes in one day with no need for continuous attention thus making the cooking activity easy and less time consuming.Purohit and Purohit suggested that the value of F_1 should not be less than 0.11 [4]. The value of F_1 calculated for the box type dual BM SC is in the range of the optimal values for F_1 and the cooker is a "Grade-A SBC" based on its calculated value of F_1. The value of F_2 is found to be 0.254. The overall heat loss co-efficient is the average of the heat loss co-efficient for all the three experiments conducted under fully loaded conditions. The overall heat loss co-efficient for the cooker is 0.78 W/K.m2. The quality factor is the average of the quality factor for all the three loaded experiments which is found to be 0.04. The peak exergy power of the cooker is found to be 15.01 watts. All the values of the performance parameters are in a proximity with the suggested values of these performance indicators. It is concluded that under the tracking free conditions the performance of the dual BM BSC with the aspect ratio of 2.66 and optimal tilt angles become optimized and it becomes a viable option for the household water-based cooking.

REFERENCES

[1] Miller, K., Tangley, L., 1991. Trees of Life: Saving Tropical Forests and Their Biological Wealth. Beacon Press, Boston

[2] Farooqui, Suhail Zaki. "Angular Optimization of Dual BM SCs – Tracking Free Experiments with Three Different Aspect Ratios." *SE*, vol. 114, Apr. 2015, pp. 337–348.

[3] Kumar, Naveen, et al. "An Exergy Based Unified Test Protocol for SCs of Different Geometries." RE, vol. 44, Aug. 2012, pp. 457–462, 10.1016/j.renene.2012.01.085. Accessed 27 July 2019

[4] Purohit, I., and P. Purohit. "Effect of Instrumentation Error on the First and Seco F1nd Figures of Merit ($F_1$and F_2) of a Box-Type SC." International Journal of Ambient Energy, vol. 29, no. 2, Apr. 2008, pp. 83–92, 10.1080/01430750.2008.9675061. Accessed 6 Aug. 2019

International Journal of Engineering Works
ISSN-p: 2521-2419
ISSN-e: 2409-2770
Vol. 6, Issue 12, PP. 507-513, December 2019
https://www.ijew.io/
https://doi.org/10.34259/ijew.19.612507513

Effects of Aging on the Performance of Aggregates in Reclaimed Asphalt Pavement

Aftab Akbar[1], Dr.Qaiser Iqbal[2], Engr.Fazli-Karim[3], Engr.Kashif Akbar[4],
[1,2,3,4]Sarhad University of Science & Information Technology, Peshawar
engraftab123@gmail.com[1], qi.civil@suit,edu.pk[2], engr_fazli@yahoo.com[3], engrkashif0@hmail.com[4]
Received: 02 December, Revised: 12 December, Accepted: 18 December

***Abstract*—** Maintenance and Overlay resolve medium distress, but reconstruction can be feasible and cost-effective because asphalt pavement deteriorated drastically with time and traffic. Therefore, pavements are required to be reconstructed or rehabilitated. Reuse of such construction waste is gaining popularity with the passage of time due to its benefits. The cost and shortage of virgin aggregate have encouraged the use of reclaimed asphalt pavement, and involved in regular practice in various countries around the world. Asphalt is 100% recyclable product in some states of US, but RAP usage has not yet been established in Pakistan. Therefore, in this research different percentages of aged aggregates are used in conjunction with virgin aggregates in asphalt mixtures. The virgin and RAP asphalt samples were then compared in terms of Marshall Stability, Rut resistance and indirect tensile strength (IDT). 22 samples including conventional and different RAP percentages were prepared for Marshall Stability, 10 samples for Rutting and 12 samples for IDT. It has concluded that the 60 percent RAP aggregate when used in conjunction with virgin aggregate in asphalt mixture gives improved Marshall Stability as compared to virgin aggregates when used in asphalt mixture, also the flow values of the 60 percent aged aggregate sample is neither open to rut of fatigue as compared to asphalt mixture prepared with virgin aggregate, and the indirect tensile strength of RAP mixture with 60% aged aggregate is high as compared to the asphalt mixture prepared with 100 percent virgin aggregates.

***Keywords*—** Overlay,deteriorated,Asphalt pavement, stability, characterization, aggregate

I. Introduction

Composite materials such as concrete and asphalt concrete are components of aggregates; the aggregate serves as reinforcement to add strength to the overall composite material. Preferred bituminous aggregate sizes for road construction are given in (European Standard) EN 13043, EN 13242 for base layers of road construction and EN 13450 for railway ballast. By volume, aggregate generally accounts for 92 to 96 percent of Bituminous concrete and about 70 to 80 percent of Portland cement concrete. Aggregate is also used for both elastic and rigid pavements. Aggregates can be naturally produced or manufactured. Extracted rock is typically reduced by mechanical crushing to accessible sizes. The aggregate are the central load bearing asphalt segment. Aggregates have different properties that are individually tested for the pavement construction with various types of tests.

Fig:1 Margalla Aggregate

Classification by Shape of Aggregate
Rounded aggregates
Irregular/Partially rounded aggregates
Elongated aggregates
Angular aggregates
Flaky aggregates
Flaky and elongated aggregates

Classification by Size
1. Fine aggregate
2. Coarse aggregate

Fig:2 Fine and Coarse aggregate

Desirable Properties of Road Aggregates

1. Strength
2. Durability
3. Toughness
4. Hardness
5. Shape of aggregates
6. Adhesion with bitumen
7. Shape of aggregates
8. Freedom from deleterious particle

Strength

The aggregates used in the construction of roads, the aggregates used in the wearing of the pavement should be particularly strong/ resistant enough to crushing to withstand the high stresses induced due to heavy traffic wheel loads.

Hardness

Due to moving traffic, the aggregates used in the surface are subject to constant rubbing or abrasion. Due to the presence of abrasive material such as sand, the abrasive action increasing between the tyres of vehicle and the aggregates exposed to the top surface. Thus, they should be stiff enough to resist the wear due to abrasive action of traffic.

Toughness

Aggregates in the pavement are also influenced by shifting loads of the wheel. The magnitude of impact increase with roughness of road and speed of vehicle. Severe impact is common when heavily loaded steel tired vehicles move on WBM. Another attractive feature of aggregates is the resistance to impact or hardness.

Durability

The aggregates are exposed to rains and ground water physical and chemical behavior, the impurities in them and that of atmosphere. It is therefore, desirable that the road stones used in the construction should sufficiently strong enough to withstand the weathering action. Soundness can be called as the property of aggregate to withstand the adverse weather behavior.

Shape of Aggregate

Aggregates can be rounded, flaky, angular, or elongated. Flaky and elongated particles have less strength than rounded and cubical particles. Thus, too flaky and too much elongated particles should be avoided.

Adhesion with bitumen

The aggregates in bituminous pavements should be less water-related relative to bitumen; otherwise in presence of water, the bituminous coating on the aggregates will be striped.

Freedom from deleterious particle

Aggregates requirements used in bituminous mixtures usually require clean aggregates, tough and durable in nature and free from excess amount of flat or elongated pieces, dust, clay balls and other objectionable material.

Aggregate Characterization
Aggregate Physical Properties

1. Maximum Aggregate Size
2. Gradation
3. Crushing
4. Abrasion
5. Toughness and Abrasion Resistance
6. Specific Gravity
7. Particle Shape and Surface Texture
8. Durability and Soundness
9. Cleanliness and Deleterious Materials

A. *Reclaimed Asphalt*

Large quantities of Reclaimed asphalt pavement (RAP) materials are produced during highway maintenance and construction. A part of this can be used in new hot mix asphalt concrete and rest is available for other uses. If these materials can be reused in the base and sub-base of the roads, the environmental impact will be minimized reduce and also transportation costs connected with road maintenance and construction activities. The properties of RAP materials can be improved by blending of aggregates and by addition of chemical stabilizers. In recent years there was a gradual increase in construction and demolition wastes. It has resulted in waste disposal problem due to shortage of available landfills. Reuse of these materials after proper recycling can be the right solution for the same. There will be a reduction in cost about 25 to 30% by reusing the recycled road aggregate generated at same site. Before using such materials the mechanical properties must be tested and suitable blending is done if required. Reclaimed asphalt pavement (RAP) materials and recycled concrete aggregate (RCA) are the most common recycled materials. The generation of RAP and RCA result in an aggregate of high quality and grading. Due to coating of asphalt on the aggregate of RAP it reduces the water absorption in aggregates.

Fig: 3 Reclaimed Asphalt (GT Road site)

B. *Aging of Aggregates*

Asphalt binder properties change due to different factors. Asphalt binder aging is among the factors that caused shorter pavement service life. Aging adversely affects asphalt binder rheological properties causing deterioration in mixture performance. In the last decades, many tests were performed to evaluate the effects of aging on asphalt binder properties and asphalt mixtures. Also, many samples of the virgin, artificially aged and extracted asphalt binder were tested and comparative study between laboratory and field aging conditions were carried out. [1].

Asphalt aggregates are defined as the cumulative products o f breaking and sieving of asphalt (bituminous bound layers) fro m roads.Using these aggregates in new asphalt is a new way of saving economy and environment.But there are few points to consider before using these aggregates.
The repeated traffic on the road that can cause the properties of these aggregates to change.including changes in surface textur e, aggregate form and breakage due to heavy loads.The salt wat er under the soil also has an impact on the aggregates by enteri ng aggregates.Continuous freezing and thawing, causing aggregate cracks and unstable road conditions.

In Hot Mixed Asphalt pavements, RAP was used in different percentages, often reaching upto 80 percent, and typically from 20-50% [2] In this study sample of Reclaimed asphalt pavement (RAP) aggregate materials were collected and analyzed for suitability of their usage in flexible pavements. Their characteristics including gradation, California Bearing Ratio (C.B.R).Aggregate Impact value, Aggregate Crushing value, Specific gravity, Flakiness & Elongation Index, Loss Angles Abrasion value, Water absorption and soundness were determined and compared to the MORTH specifications [3].

Bitumen is a very high viscosity liquid or solid consisting mainly of mineral oil (containing a set of high molecular weigh t hydrocarbons asphaltic in nature and very no oxygen, sulphur and nitrogen. Hydrocarbon derivatives (such as Asphaltenes, M altenes) soluble in carbon disulphide and are nonvolatile and m ollify continuously when warming up.It depends on the derivati ve mode; it is either brown or black in colour, has waterproofin g and sticking properties and has uneven hardness and instabilit y.Asphaltenes play a vital role in the hydrocarbon's normal elastic nature, which is primarily responsible for elasticity and rigidity. [4]

Temperature with more effect on Flexible pavement softens the road when the temperature is high and when the temperatu re is low appears to crack.In addition, heavy traffic and high lo ading vehicles preregularly deflect roads and cause repair and maintenance costs.Therefore, to obtain these characteristics, it i s important to boost the standard asphalt by the product that ca n play the role as binder.[5]

Asphalt binder properties change due to different factors. Asphalt binder aging is among the factors that caused shorter pavement service life. Aging adversely affects asphalt binder rheological properties causing deterioration in mixture performance. In the last decades, many tests were performed to evaluate the effects of aging on asphalt binder properties and asphalt mixtures. Currently, due to the end up of its design life and traffic loads, asphalt pavements may badly deteriorate. The reconstruction of the pavement may become an economical and feasible solution. Reconstruction of a pavement requires removal of pavement surfaces. Waste asphalt removed from a failed pavement surface is a mixture of aggregate coated with bitumen and is collected from failed asphalt pavement surfaces and has been used as flexible layer construction material for more than 30 years. The use of reclaimed material considerably saves material, money and energy, without compromising the strength. Its importance rises in the light of increasing cost of bitumen, scarcity of good quality aggregate and priority towards the preservation of environment. Recycled aggregates are the materials of future. This sustainable practice is an effective means of pavement rehabilitation as the materials which have reached the end of their service life are still made valuable. In Europe and US, studies have concluded that 80% of the recycled material is used in construction of roads. However, the quality of the pavement constructed depends on the origin, variability, stocking and production conditions of the reclaimed material. The strength of the reclaimed material can be improved through the use of rejuvenators. Considering the material and construction cost alone it is estimated that using recycled materials, saving ranging from 14%- 34% can be achieved. Hence bituminous pavements using reclaimed aggregates can evolve into a regular practice for sustainable construction.

Sources of Reclaimed Aggregates

The use of reclaimed materials enables to improve the quality of infrastructure in sustainableways. This includes reclaiming aggregates and rejuvenating their component parts for use in new pavements. The two major sources to obtain them are *1*-Construction & Demolition waste (CDW) and *2*-Reclaimed Asphalt from old pavements (RAP).

The strength of concrete is dependent on size, shape, grading, surface texture mineralogy of the aggregate, strength, stiffness [6] suggested that the effect of aggregate strength on the compressive strength of concrete is not considered in the case of normal-strength concrete, as it is much stronger than the transition zone and cement paste matrix. [6] also explained that the transition zone and the cement paste matrix would fail before the aggregate and thus nullify the effect of the strength of aggregate. The aggregate strength is usually not a factor in normal strength concrete as the failure is generally determined by the cement paste- aggregate bond. Much research has linked the bonding of the aggregate to the strength of concrete [7].

Greater aggregate surface areas result in better bonding between the aggregate and the cement paste. They also observed that rough aggregates tend to exhibit better binding than smooth aggregates. [8]

They also noticed that rough aggregates appeared to be more binding than smooth aggregates. [9] made similar observations as [10] but linked the surface properties to the cracking stress suggesting rough aggregates would crack at a higher stress compared to smooth aggregates, compressive strength can be seen to decreases with an increase in maximum coarse aggregate size particularly for concretes with low water-cement ratios.

The Federal Highway Administration estimated that in US, 73 of the 91 million metric tons of asphalt pavements were removed every year during resurfacing and widening projects and are reused as part of new roads, roadbeds, shoulders and embankments. [11]. The use of Reclaimed asphalt also minimizes the cost of transportation. (Dr. Soosan et al.2016). Some technical operations are somehow required when reclaimed aggregates are used in asphalt mixtures. Some environmental, energy and cost benefits are considered to be achieved, as well as the mechanical performance. [12]

The utility of the road is impaired by the pathologies generated by the aging process, various research studies should be carried out with the idea of decreasing the effects of this phenomena, in order to have a greater sense of comfort and security when using this infrastructure. [13]. The usual statement damage caused by moisture is consistent loss of adherence and loss of cohesion in the mixture between the aggregate and bitumen and loss of adherence to the aggregate-asphalt or cohesion within the bulk mastic [14].

The Marshall approach was used to test the performance evaluation of asphalt mixtures with various Reclaimed asphalt pavement ratios. The wearing course mixtures with 20, 40, 60, 80 and 100% RAP content were made and then compare it with the control design (No RAP content). The Research purpose is to design good wearing surface with high RAP content without sacrificing quality. [15].

Objectives:

1. To check the performance of RAP aggregates in reclaimed asphalt pavement and compare it with the performance of Virgin aggregates used in conventional asphalt mixture.
2. To suggest the procedure to reuse the Recycle aggregates by suggesting the percentage addition of Fresh aggregates in order to restore its design properties.

II. METHODOLOGY

A. Materials

The bitumen used in this test was of penetration grade 60/70 brought from Attock Refinery. The course aggregate used in preparation of samples are 3/4” (inch) downgraded and were brought from Margalla. Sieve analysis was done in university.The RAP is collected from site of G.T road. Benzene or CTC is used for Extraction Purpose.

Fig: 4 Showing Asphalt, RAP, Aggregates, Benzene

B. Tests performed

1) Sieve Analysis (Gradation):

A sieve analysis (gradation test) is a common practice or technique in civil engineering for testing particle size distribution (also called gradation) of a granular material.

2) LOS Angeles Abrasion Test

The Los Angeles test is a measure of degradation of mineral aggregates of standard grading’s resulting from a combination of actions including abrasion or attrition, impact, and grinding in a rotating steel drum containing a specified number of steel spheres. The Los Angeles abrasion test is a common test method used to indicate aggregate toughness and abrasion characteristics

Fig: 5 Los Angeles Abrasion Testing

3) Water Absorption Test

Water absorption gives an idea of strength of aggregate. Aggregates having more Water absorption are more porous in nature and generally considered unsuitable unless they are found to be acceptable based on strength impact and hardness test.

Fig:6 Water Absorption Test

4) Crushing test

Aggregate crushing test on coarse aggregates offers a relative measure of aggregate crushing resistance under a progressive compressive load. Coarse aggregate crushing value is the percentage by weight of the crushed material obtained when test aggregates are subjected to a specified load under standardized conditions

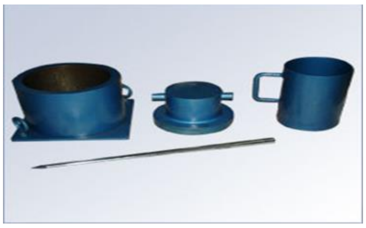

Fig: 7 Crushing Test Apparatus

5) Impact test

The aggregate impact test is conducted out to determine the resistance to impact of aggregates

Fig:8 Performing Impact test

6) Soundness test

Soundness test is intended to study the resistance of aggregates to weathering action, by conducting accelerated weathering test cycle

7) Shape tests

The particle shape of the aggregate mass is determined by the percentage of flaky and elongated particles in it.

Fig:9 Shape Testing for pavement works

III. RESULTS AND EXPERIMENTAL WORK

Table:1 Laboratory Results on Aggregate

TEST NAME	Fresh Aggregate	Rap Agg	Range	Standard
LOS Angeles abrasion test	11.2 %	18%	Max permissible Value =30%	ASTM C-131
Water absorption test	0.88 %	1.24%	Ranges from 0.1 to 2.0%	D-570-98
Impact test	5.105 %	6.715	10-20%= Strong 20-30%= Satisfactory	ASTM E-2248-18
Crushing test	17.5 %	20.2%	For Bituminous Surface dressing= 30	ASTM C-39
Soundness test	18	12	Should not be more than 25% with Na2s04(Sodium Sulphate)	ASTM C-88
Flakines, Elongation	22.5 %	26.8	Flakiness & Elongation test are not applicable to Aggregate sizes smaller than 6.33mm	ASTM-D 7491
Specific Gravity	2.89	2.62	Ranges from 2.5 to 3.0	ASTM C-127

Table:2 Marshall Parameter for Conventional Mix

Bitumen	VA%	VMA %	VFA %	Gmb	Gmm	Stability KN	Flow(mm)
3.5	6.42	13.95	52.55	2.32	2.56	14.1	9.08
4	5.10	13.10	61.12	2.34	2.76	14.4	8.89
4.5	4.12	12.95	68.20	2.36	2.39	14.4	8.87
5	3.12	13.8	72.12	2.38	2.46	13.7	9.31
5.5	2.81	14.25	76.80	2.34	2.49	12.9	9.79

Following graphs is based on Conventional data of the above table.

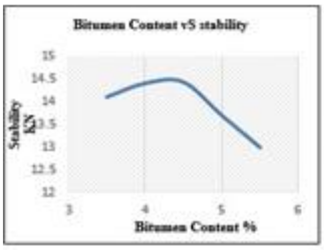

Fig 10: B.C Vs Stability

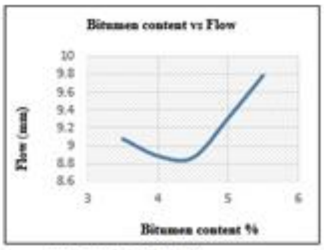

Fig 11: B.C Vs Flow

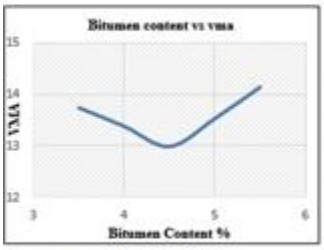

Fig 12: B.C Vs VMA

Fig 13: B.C Vs VFA

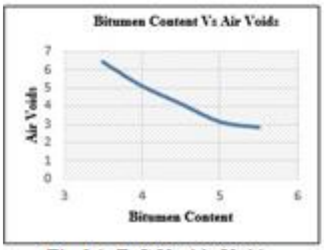

Fig 14: B.C Vs Air Voids

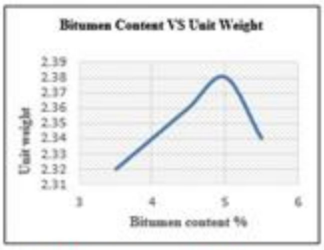

Fig 15: B.C Vs Unit Wt.

The optimum binder content for the following specimens are O.B.C=4.4, Samples with percentage of RAP Aggregate Mixed

Table:3 Results of Different % of RAP used in Samples

RAP %	VA %	VFA %	VMA %	Gmm	Gmb	Stability KN	Flow (0.25mm)
0	3.80	69.50	12.99	2.42	2.39	15.9	10.95
20	3.66	74.37	14.29	2.33	2.42	13.9	12.35
40	5.47	66.72	16.45	2.28	2.41	14.1	12.15
60	4.01	77.01	18.78	2.23	2.36	15.5	10.91
80	2.86	77.18	12.53	2.41	2.48	10.4	14.49
100	2.55	80.35	13.31	2.40	2.47	9.15	16.31

Following Graphs are based on Different % RAP Agg Data in the above table.

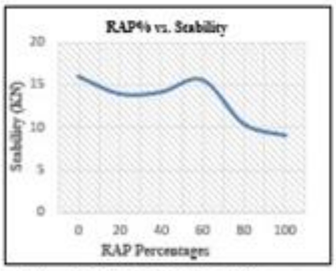

Fig 16: RAP % Vs Stability

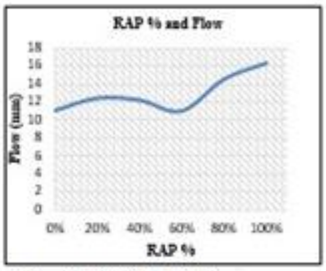

Fig 17: RAP % Vs Flow

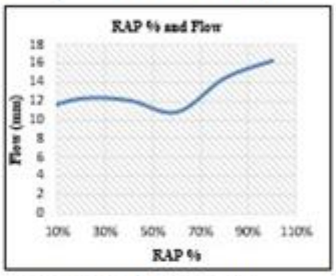

Fig 18: RAP % Vs VMA

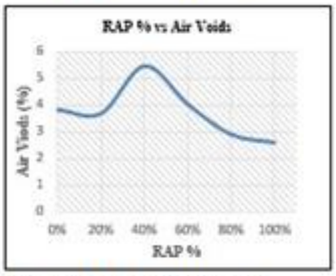

Fig 19: RAP % Vs Air Voids

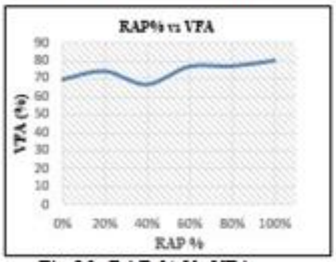

Fig 20: RAP % Vs VFA

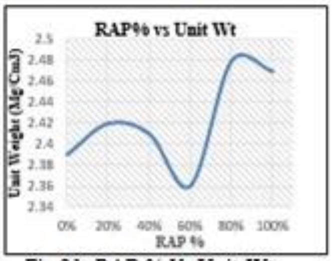

Fig 21: RAP % Vs Unit Wt.

C. Rutting test

This table and graph shows shows No. of passes Vs rutting, and as highlited in different colors.

Table:4 Showing No. of Passes Vs Rut Depth

No. of Passes	Rut depth 0 %	Rut depth 20 %	Rut depth 40 %	Rut deph 60 %	Rut depth 80 %	Rut depth 100 %
1000	-0.62	-1.01	-0.69	-0.97	-1.1	-1.9
2000	-1.26	-2.3	-1.9	-1.25	-2.45	-3.19
3000	-1.99	-3.4	-2.68	-1.99	-3.21	-4.95
4000	-2.62	-4.09	-3.66	-2.65	-4.4	-6.59
5000	-2.99	-5.22	-4.29	-2.98	-5.52	-7.95
6000	-3.45	-6.17	-4.82	-3.10	-6.89	-8.86
7000	-3.86	-7.05	-5.65	-3.42	-8.2	-9.99
8000	-4.25	-7.81	-5.99	-3.66	-8.56	-10.56
9000	-4.62	-8.97	-6.45	-3.72	-8.85	-10.75
10000	-4.82	-8.97	-6.59	-3.73	-8.86	-10.74

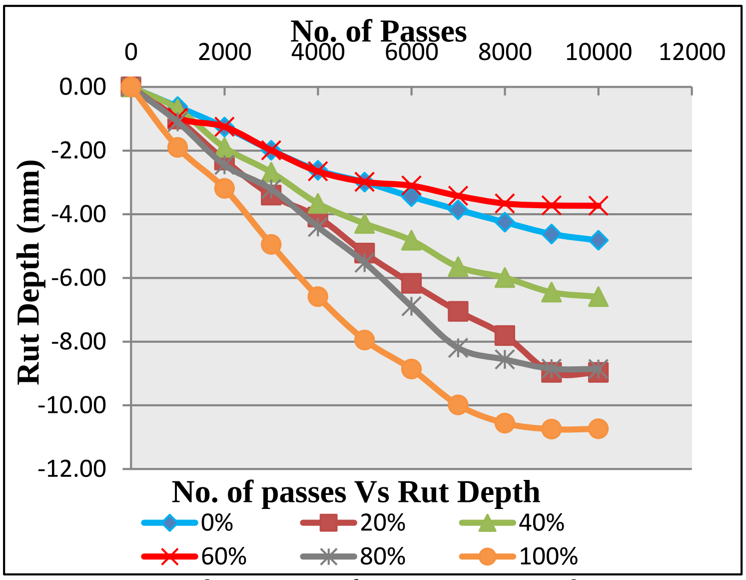

Fig 22: Showing No. of Passes Vs Rut Depth

Result of Indirect Tensile Strength

The values of IDT strength may be used to evaluate the relative quality of asphalt mixtures in conjunction with laboratory mix design testing and for estimating the potential for rutting or cracking. The results can also be used to determine the potential for field pavement moisture damage when results are obtained on both moisture-conditioned and unconditioned specimens.

Table: 5 Indirect Tensile Strength

S.No	Mixture Type (MPa)	IDT Strength (MPa) $\delta t = \frac{2p}{\lambda t D}$	
	Percentages	Before Freezing	After freezing
1	0	516	370
2	20	465.60	305.10
3	40	431.84	245.40
4	60	501.92	358.25
5	80	382.88	252.78
6	100	261.14	172.61

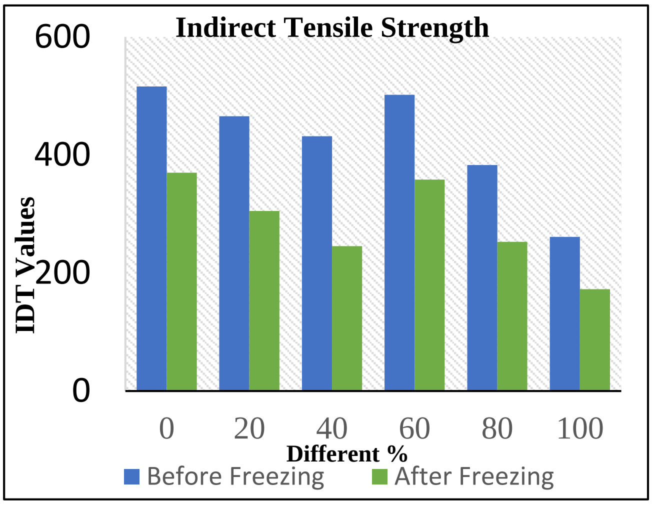

Fig 23: Different % of RAP Vs. IDT Values

CONFLICT OF INTEREST

I declare that there is no conflict of interest and the previous work of the original author has been properly cited.

CONCUSLION

In this research, different percentages of aged aggregates were used in combination with virgin aggregates in asphalt mixtures. The virgin and reclaimed asphalt pavement (RAP) samples were then compared in terms of Marshall Stability, Rut resistance and indirect tensile strength (IDT) of asphalt. Twenty two (22) samples prepared for Marshall Stability, Ten samples for rut resistance and twelve samples were prepared for indirect tensile strength.

1. The 60% RAP aggregates when used in conjunction with virgin aggregates it was established that the stability values were higher for mixtures made with aged asphalts as compared to virgin aggregates when used in asphalt mixture.
2. The flow values of the RAP prepared with 60 % shows that aged aggregate is neither open to rut nor fatigue as compared to asphalt mixture prepared with virgin aggregate.
3. The Rut resistance of the 60% RAP is maximum at 10,000 passes as compared to the virgin and other percentages of RAP aggregates when used in asphalt mixtures.
4. The indirect tensile strength of RAP mixture with 60% aged aggregate is high as compared to the asphalt mixture prepared with 100 percent virgin aggregates.

RECOMMENDATIONS

1. On the basis of the results given above, it is recommended that using 60% of RAP aggregates in new asphalt pavement can give better result.
2. Road pavement will get more strengthen when RAP aggregates is used in 60% ratio.
3. It will be more stable and will neither open to rut nor fatigue & will give better result than new pavement.
4. It can also minimize the construction cost and keep the environment clean.

REFERENCES

[1] Kheiralipour, Kamran, and Soraya Hoseinpour. "Determining and Modeling Shearing Properties of Peppermint Stem." Caspian Journal of Applied Sciences Research 5.3 (2016).

[2] Hussain, Arshad, and Qiu Yanjun. "Evaluation of asphalt mixes containing reclaimed asphalt pavement for wearing courses." Proceedings. International Conference on Traffic and Transportation Engineering, School of Civil Engineering, Southwest Jiaotong University, Chengdu, China, IPCSIT. Vol. 26. 2012.

[3] Mishra, Brajesh. "A Study on Characteristics of Subgrade Soil by Use of Foundry Sand and Iron Turnings."

[4] McDaniel, R.S., Soleymani, H., and Slah, A. (2002). Use of Reclaimed Asphalt (RAP) under Superpave Specifications, Report No. FHWA/IN/JTRP-2002/6, North Central Superpave Center, West Lafayette, IN, USA.

[5] McDaniel, R.S., Soleymani, H., Anderson, R.M., Turner, P., and Peterson, R. (2000). Incorporation of Reclaimed Asphalt Pavement in the Superpave System, NCHRP 9-12, National Cooperative Highway Research Program, Transportation Research Board.

[6] Nilsen, A. Ulrik, and Paulo JM Monteiro. "Concrete: a three phase material." Cement and Concrete Research 23.1 (1993): 147-151.

[7] Kosmatka, Steven H., Beatrix Kerkhoff, and William C. Panarese. Design and control of concrete mixtures. Vol. 5420. Skokie, IL: Portland Cement Association, 2002.

[8] Neville, Adam M., and Jeffrey John Brooks. Concrete technology. England: Longman Scientific & Technical, 1987.

[9] Jones, R., and MFi Kaplan. "The effect of coarse aggregate on the mode of failure of concrete in compression and flexure." Magazine of Concrete Research 9.26 (1957): 89-94.

[10] Neville, Adam M., and Jeffrey John Brooks. Concrete technology. England: Longman Scientific & Technical, 1987.

[11] Abdelhak, Bordjiba, et al. "Effect of recycled asphalt aggregates on the rutting of bituminous concrete in the presence of additive." Arabian Journal for Science and Engineering 41.10 (2016): 4139-4145.

[12] Handbook, Median. "Florida Department of Transportation." Tallahassee, FL (1997).

[13] Higuera Sandoval, Carlos Hernando, Xiomara Vanessa Camargo Amaya, and Edwin Alexander Suárez Molano. "Effect of Aging on the Properties of Asphalt and Asphalt Mixtures." Ingeniería y Universidad 19.2 (2015): 335-349.

[14] Caro, Silvia, et al. "Moisture susceptibility of asphalt mixtures, Part 1: mechanisms." International Journal of Pavement Engineering 9.2 (2008): 81-98.

[15] Hussain, Arshad, and Qiu Yanjun. "Evaluation of asphalt mixes containing reclaimed asphalt pavement for wearing courses." Proceedings. International Conference on Traffic and Transportation Engineering, School of Civil Engineering, Southwest Jiaotong University, Chengdu, China, IPCSIT. Vol. 26. 2012.

[16] Mehta, P. Kumar, and P. J. M. Monteiro. "Durability." P. K. Mehta.--Concrete, microstructure, properties and materials.--Westerville: JP Skalny (Ed) (1993): 113-155

Aftab Akbar is the resident of Khyber Pakhtunkhwa,Peshawar-Pakistan, He did his bachelors in civil engineering from Sarhad university of science and technology Peshawar and persuing Master in Transportation Engg from the same Institution (SUIT). The paper is the Resarch project for Master's Degree.

.

International Journal of Engineering Works
ISSN-p: 2521-2419
ISSN-e: 2409-2770
Vol. 6, Issue 12, PP. 514-520, December 2019
https://www.ijew.io/
https://doi.org/10.34259/ijew.19.612514520

Smart Triage System towards Crisis and Resuciation

Mohsin Raza[1], Farhan Ahmad[2], Kashif Hussain[3], Abdul Wahab[4], Ali Raza Barket[5]
[1]College of Internet of Things Engineering, Hohai University, Changzhou 213022, China
[2,3,4] School of Microelectronics and Communication Engineering, Chongqing University, China
[5] Beijing Key Laboratory of Millimeter Wave and THz Technology, School of Electronics Science and Technology, Beijing Institute of Technology, Beijing, China
mohsinrazabarket@yahoo.com[1], farhanahmad.re@yahoo.com[2], kashifhussain180@yahoo.com[3], wahab.engr55@yahoo.com[4], alirazabarket@yahoo.com[5]
Received: 17 November, Revised: 20 December, Accepted: 23 December

***Abstract*—** Disaster is a sudden accident or a catastrophic calamity that causes incredible damage or loss of life. Disaster has different types like Tornadoes, Floods, Wildfires, and Earthquakes. When a disaster occurs, many people get injured and many people die due to delay in timely treatment. But in a traditional rescue system, rescue workers are unaware of suitable and nearest health centers (hospitals) per patient condition. Rescue teams need to be updated about the capacity of the hospital and to know the shortest route to bring disaster patients to the most suitable hospital in minimum possible time. If resources are not available or occupied once they have arrived, retransfer from one hospital to another will be required which takes longer time and in severe condition, the patient could die. Smart Resource Allocation and Information System increases the chances of life in disaster by providing timely treatment. With the help of Smart Resource Allocation and Information System, the rescue teams will be aware of the shortest path, availability of specialist per patient condition and capacity of the hospital where disaster patient is to be assigned. So, the application allows timely treatment and better resuscitation services for catastrophic victims. Our designed system provides the solution for patient load balancing and patient load migration, better utilization of available resources, especially in resource constraint scenarios.

***Keywords*—** Automation, emergency rescue system, load balancing, cloud database; Information sharing; mass disaster

I. Introduction

Disaster is a sudden accident or a natural catastrophe that causes large destruction or loss of life. Disasters are of two types, natural and man-made. Natural hazards are naturally happening like earthquakes, tornadoes, landslides, wildfires, and floods. Man-made hazards are proceedings that are caused by humans like emergencies, conflicts, industrial accidents, transportation accidents, and terrorist attacks. Many countries have experienced a significant number of catastrophic disasters during the past 20 years which cause global effects on nature and societies [1] [2], as is shown in Table 1.

For reducing mortality during earthquakes well-planned disaster response is required. When a disaster occurs, some people die on spot but a large number of people die due to late treatment. Disaster patients require fast treatment that a traditional rescue system does not provide. In 2014, three hundred and twenty - four natural disasters occurred which caused the death of more than 7,823 individuals, 140.7 million people got injured, and 99.2 billion dollars' financial damages [3]. Asia has experienced the highest number of disasters (44.4%) with the highest number of victims (69.5%) [4]. The studies show that if first aid had been available immediately after disaster attack then around 25% to 50% of people who got injured could have been saved [5]. But they died slowly due to delay in timely treatment [6]. Figure I-1 shows that the chances of survival of victims decrease with time.

Table 1. Disaster Deaths

Date	Disaster Deaths	
	Location	***Deaths***
Dec 28,1974	Hunza earthquake, Pakistan	5,300
Oct 8, 2005	Muzaffarabad Earthquake, Pakistan	78,000
Aug 3, 2014	Ludian County, Yunnan Province, China	617
April 25	Nepal Earthquake	8,964

In such situations, triage is performed by the rescue team to

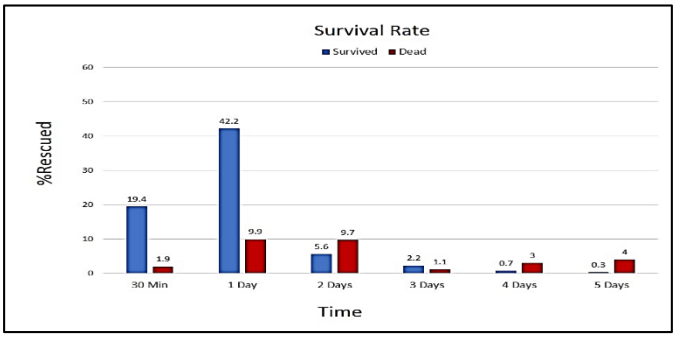

Figure 1. Survival Rate with the Passage of Time

prioritize the treatment of victims depending upon injury severity and treatment urgency. Management performance is affected by the increase in patient density [7]. Walking wounded are identified first and the remaining casualties will be divided into three categories: patient with immediate care requirement, patients whose treatment can be delayed and dead. They will be prioritized and treated further based on this triage. More lives can be saved by using limited medical resources efficiently based on this triage. The rescue teams provide help after reaching the disaster location. The basic task of rescue teams is to shift the patient to a hospital with the required resources and facilities. In this context, lack of proper infrastructure encompassing facility limits of hospitals, availability of specialists therein, hospital database as well as nearby hospitals makes it a tough target for rescue workers to help the victims in the best possible way. In emergency situations and unfamiliar environments, such information is very important. The type of injuries, the patients can have in a disaster are very similar and they need almost the same type of specialists and medicines. The scenarios during a disaster situation can be as follows:

- Numerous injuries may require highly qualified treatment (e.g. surgery) in urgent. An unsuitable circumstance which may confront restricted limits in nearby hospitals is in the form of equipment and specialists etc.
- The number of patients can significantly increase and will require additional hospital units and facilities.
- The rise of mobility problems, since many ambulances should shift the patients to more than one hospital.

So, there is a requirement of much better communication at different levels. Apart from unwavering and strong cooperation between all the acting bodies to handle the arisen situation of a catastrophic disaster, the cooperation between hospitals and other responsible organizations should be improved, hospitals also need a better organization for deployment of specialists, equipment, facilities, and medicines. The sharing of information between the hospitals and ambulances is another aspect to be improved.

The severity of the patient's condition is indicated by the assigned bands which points out whether the patient can be shifted to a different hospital or not. During a crisis workload balancing among available hospitals guarantees efficient distribution of workload. A load-balancing scheme is proposed which aims to prevent the hospitals from becoming overloaded. For bringing the hospital load in the acceptable limit a framework is outlined.

In this underlying work, a system that makes this rescue faster and efficient is proposed. It mainly focuses on the proper assignment of patients to hospitals and available facilities therein to patients, and communication between hospitals and ambulances. It provides information about patients to hospitals prior to their transportation to hospitals. It is developed to increase the chances of life in disasters by speeding up the working of rescue teams. The system allocates the resources automatically in a careful and efficient manner to escape more time so that precious lives can be saved.

This paper is organized as follows. Section II gives what has been done in the past relating to our work. Proposed scheme; Smart Resource Allocation and Information System for Victims of Catastrophic Disasters is discussed in detail in section III. Section IV presents the Implementation of our proposed scheme followed by results and conclusion in the succeeding sections.

II. Related Work

For emergency services, there are different meanings of tracking a casualty. One of the concepts refers to the tracking of the physical location of the patient and others. It shows the progress in the treatment of the patient. [8] Tracking the injured patient in disasters refers to recognizing and enlisting names of the injured, recording their data and condition, organizing plans for their evacuation from scenes as per the color of bands and positioning them to hospitals.

In the Katrina disaster in the USA, tracking of victims was inefficient and later it was recognized as a weakness in planning preparedness for handling the event [9]. In the Bam earthquake, the information of patients was insufficient and due to this inefficiency difficulties had to be confronted in management and effective assessment of their condition [10]. Marres stated that there is a need for coordination of different organizations when facing catastrophic disasters but the establishment of coordination among organizations in different locations is a complex process [11]. In such a condition, one of the biggest challenges is patient tracking. Mostly, there is no information about a number of patients, their condition and their transfer [12].

In an earthquake scenario, many victims dead or injured are at the sight. Such a large number of victims are beyond the capacity of the emergency system. Information is not provided to hospitals about the number of patients that they are about to admit. Supervisors or rescue teams do not have proper information such as how many patients are transported to hospitals. They are not updated with information about the hospital whether it has the capacity to admit patients or not. The hospitals which admit the patients are overcrowded due to this lack of communication and coordination among hospitals and rescue teams [13]. The patient doesn't have time to be retransferred from one hospital to another. So, it's necessary to transfer disaster patients directly to a suitable hospital that has the required facilities and specialists for treatment. The plans for disaster response should move toward comprehensive coordination between hospitals and rescue teams that can track not only the patients but the resources as well [14].

Although, many solutions aim to position the patients and track their medical conditions, yet there is a need to address the issue of selecting a suitable hospital for patients in accordance with their injuries that have necessary resources so that retransfer is not required. Rescue teams need to choose a hospital with the capacity to admit new patients, that are not overcrowded [15].

III. SMART RESOURCE ALLOCATION AND INFORMATION SYSTEM FOR VICTOMS OF CATASTROFIC DISASTERS

The effectiveness of disaster response depends upon specific disaster plans and efficient emergency coordination between hospitals and rescue teams. Currently, communication between hospitals and rescue teams is traditional. The communication available between hospitals and ambulances is via phone calls. The patients are then sent to hospitals without informing the hospital about any detail of the patient. Without the digital map, the rescue workers are not aware of the shortest distance hospital from the disaster location and they may not know the capacity or facilities availability with hospitals. With these limitations, there are chances that the patient is transported to a hospital where the required resources are not available. The resources are calculated in terms of facilities and capacity of each hospital and type of specialist there. In such a situation, the patient should be retransferred to another hospital which is a time taking the process and this may also lead to the death of the patient.

The proposed system allocates the resources automatically in a careful and efficient manner so that precious lives can be saved. Rescue workers can select injury types of patients and find suitable hospitals with sufficient required facilities. The information of resources i.e. capacity of a hospital, available facilities, equipment and specialists that a hospital can provide will be in a database in the cloud and this information will be updated time by time. With pre-information about resources in hospitals and their limits, there is no need to retransfer the patient to another hospital. It gives more time to patients and increases the chances of their survival, especially in the resource constraint scenario.

When a disaster occurs rescue workers at the disaster location using this application can search this location and find nearby hospitals in 50 km area. This hospital list becomes the source and all the resources are searched and assigned from this list. An alert about disaster location will be sent to these hospitals for preparing resources and making them available for disaster response. The rescue workers triage the patients and assign color bands. According to the condition of injuries, the victims are classified into four groups

- RED: a patient with major injuries and need immediate medical treatment
- BLACK: a casualty is deceased
- GREEN: a patient with minor injuries
- YELLOW: a patient with significant injuries but treatment can be delayed

The patients are prioritized in accordance with the color of their bands and they are dispatched to the hospital accordingly. According to injuries or casualties like maxilla, neck, femur, spinal injuries, the application suggests hospital with required resources and sends an alert to the hospital with patient condition, attributes and facilities required for treatment as well as band assigned. The hospital will be able to prepare the equipment, facilities, and specialists for the patient before their arrival. Thus, giving treatment to casualties will be well in time. The application also shows the track from disaster location to the nearest hospital assigned to the patient. This proposed system enables us to perform the following functions: extract location of nearest hospitals within 50 km driving distance of closest hospitals, send the information to rescue teams, people with severe injuries will be shifted to hospitals with required facilities. People whose care can be delayed will be shifted to any nearest hospital. Infected people are assigned to a hospital per number of doctors available and the capacity of hospitals.

The main modules of smart resource allocation and information system for victims of catastrophic disasters are:

1. *Find nearby hospitals* – It finds hospitals in a range of 50 km around the disaster place.
2. *Check availability of suitable resources* - Resources available in hospitals and specialists are checked
3. *Assign patients to doctors with facilities* - Triage categorizes the patients with different injury types and assigns to suitable doctors.
4. *Show the shortest path towards the assigned hospital*
5. *Send alert to the related hospital about patient's condition*

IV. IMPLIMENTATION

An android-based mobile application is developed to classify casualties into four triage categories. This mobile application can transfer the patient priority data to hospital via available cellular interface such as GSM [16]. The application allows a rescue worker to input the patient's condition and assign a color band. It also sends an alert message to that hospital that was assigned.

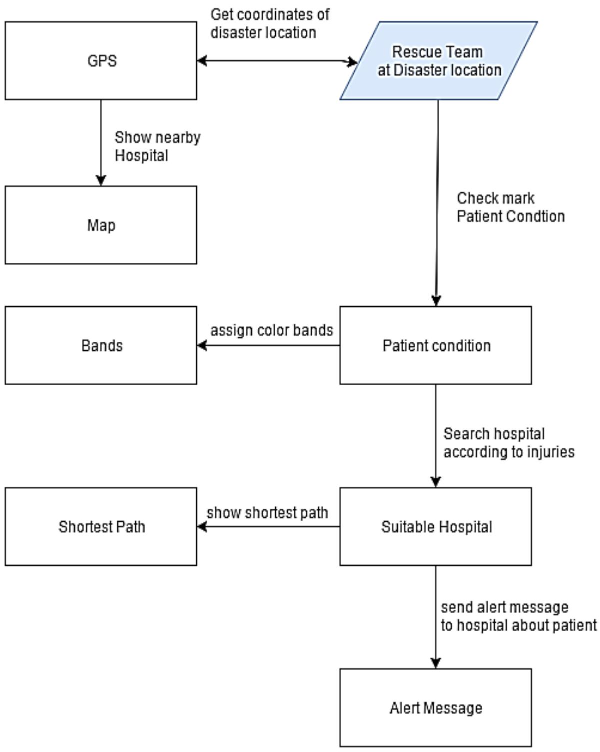

Figure 2. Work flow chart

Figure 3. Smart Resource Allocation Architecture

For positioning, the ambulance uses GPS inside a smartphone and using Google Maps API it finds current location i.e. disaster location as well as the location of hospitals in 50 km area. The application assigns a hospital with the shortest distance having treatment resources to a patient. Alert about the patient's condition is sent to the hospital so that resources are prepared pre-arrival of the patient. Figure 2 shows the flow of the rescue system and Figure 3 shows the architecture of the system. It also tracks effect time that is very important in such situations when resources are limited and need to be tracked when they will be free again. For example, a doctor checks five patients in 25 minutes, rescue workers can send five more patients after 25 minutes when the doctor is free again [17].

- ***Android Based Mobile Application***

The android-base mobile application is helpful for a rescue team in the fast selection of suitable and nearest hospitals. Figure 4 shows six application user interfaces describing the steps of finding a suitable hospital for patient treatment. The map provides the current location of rescue team by using Google Maps API and GPS services and show nearby hospital in the surrounding area on the map by using coordinates of the current location and store nearby hospital list in Cloud database. It sends an alert message about the location of disaster or damage to nearby hospitals to prepare for the response. This list searches resources from these hospitals and helps in searching and assign suitable hospitals to patients.

The application allows a user to select patient conditions from available possible injury conditions. Based on this condition application shows a list of hospitals that are suitable for this patient, have resources and are near to the location. Rescue workers can select a hospital that is more suitable and nearest to the current location. After the selection application shows the shortest path to the hospital and draws the track line which helps rescue the team in transporting the patient to the hospital. In this way, an alert about the patient's condition is sent to the hospital. This allows hospitals to prepare the required resources for the patients prior to their arrival and gives timely treatment to disaster patients. A database of hospitals that include the type of facilities available, number of medical officers, type of surgeon and capacity of hospitals is stored on the cloud. This database about the resources at the hospital is updated frequently. The updated information is helpful for rescue teams to track the resources in different hospitals.

V. Results

We assumed that an imaginary 25 storey building exists in a city. Such a building is supposed to have almost 10 apartments on each floor. Several hundred people present in the building will be affected if a disaster occurs in the form of an earthquake.

The system records the condition for all the patients. The application allocates victims to hospitals by assigning a suitable hospital to each patient. For this example, three hospitals were selected as the shortest distance hospitals within the radius of 50km of the disaster location. The main parameters of these hospitals labeled as H1, H2, and H3 for the selection of suitable hospital with appropriate resources are shown in Table 2. In Figure 5 the results of patient assignment to these three hospitals at the shortest distance are shown. For

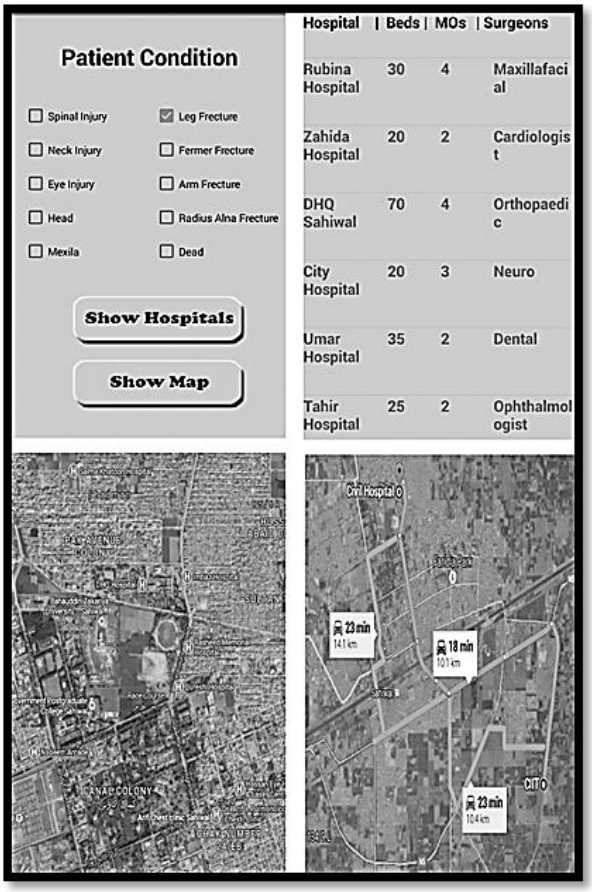

Figure 4. Smart Resource Allocation Application Screen Shots

this example, we varied the total number of patients from 300 to 500. The load did not reach the threshold value of 200 and 250 patients for all the hospitals. As the results for 200 and 250 do not cause any migrations of patients so these results are not presented. The hospitals were slightly overloaded when the number of patients reached 300. The algorithm for patient migration now executes reducing the load on these hospitals. When the number of patients increased to a total of 500, migration was required so a few patients were shifted from H1 to H2, balancing the load on hospitals. When all the hospitals are overloaded or lightly loaded, no transfer of the patient is required. No action is needed to balance the load when the hospitals are lightly loaded. However, in the case of overloading in all the hospitals, the research can be expanded and the algorithm for Extended Distance can be used to find additional hospitals in nearby areas. The results show that transfer of patients from one hospital to another hospital is not required when the traffic is balanced in all hospitals. This saves time for patient and delay in treatment is reduced.

The hospital H1 is located at 23.9 km and H3 is located at 15.2 km. If it takes 18 minutes to travel form disaster location to hospital H1 and 10 minutes to H3. In a disaster, mostly the nearest hospital is chosen by traditional systems for faster transportation and treatment but the suitability of hospital for victim per injuries is neglected. Some victims may require a treatment that is not available at the chosen hospital. These victims then require a retransfer to another hospital. Now, as H3 is at the shortest distance. In a traditional system, for a victim transferred to this hospital, the required treatment may not be available and retransfer will be required. This consumes 10 minutes for traveling to H3 and an extra 18 minutes for traveling to H1. This is a time taking process and may also lead to the death of the patient. The proposed system selects the hospital with capacity and resources. A hospital is allocated to a victim if it has the required treatment facility per patient condition. It selects H1 for the victim as required treatment is available here and the time will be reduced from 28 minutes to 18 minutes. There are more chances that treatment will save the victim’s life.

The patients are transferred to hospitals via an optimized route. The route is chosen based on distance. Hospital with the shortest distance having required facilities for the patient is allocated to the victim. All the possible routes from the disaster location to the assigned hospital are searched and distance is calculated by executing the algorithm. The route which takes less time for traveling to the hospital is chosen for shifting the patient. The possible paths are shown to rescue workers who can choose a path for delivering the patient to the hospital. In severe cases like internal injuries or bleeding surgical intervention is required. If such a patient is not managed properly complications may occur. So, transportation of patients suffering from severe injuries as fast as possible becomes a priority. As some injuries can cause patients to weaken very rapidly so keeping the time between injury and treatment to a bare minimum is ideal. The survival rate for traumatic patients decreases dramatically after primary hours. The chances of survival increase if patients get treatment on time. If the shortest path is followed there is a greater possibility that a patient will get treatment in a golden hour during which it is highly possible that given medical treatment will prevent death.

Thus, the victims of disaster get timely treatment and more time is available for survival with “smart resource allocation and information system for victims of catastrophic disasters”.

Table 2: Health Center Ranking

Health Centre	Distance	Treatment Rank
H1	23.9 Km	3
H2	28.3 Km	1
H3	15.2 Km	5

CONCLUSION

The main issue in a disaster situation is that rescue teams do not have updated information about nearby hospitals and resources available there. In this paper, we have developed an android application for disaster casualties. This application aims to quickly transport disaster patients to the hospitals having facilities required for disaster patients and have the shortest distance from disaster location. The application tracks the resources of the hospital in terms of capacity limit, facilities, specialists, equipment and rooms at hospitals. Information about casualty condition is relayed to the hospital prior to transportation so that the hospital can prepare resources for the coming patients. This way patients will get timely treatment and retransfer of patients from one hospital to others will not be required as the patient is transported after checking that hospital is not overcrowded and facilities and specialists

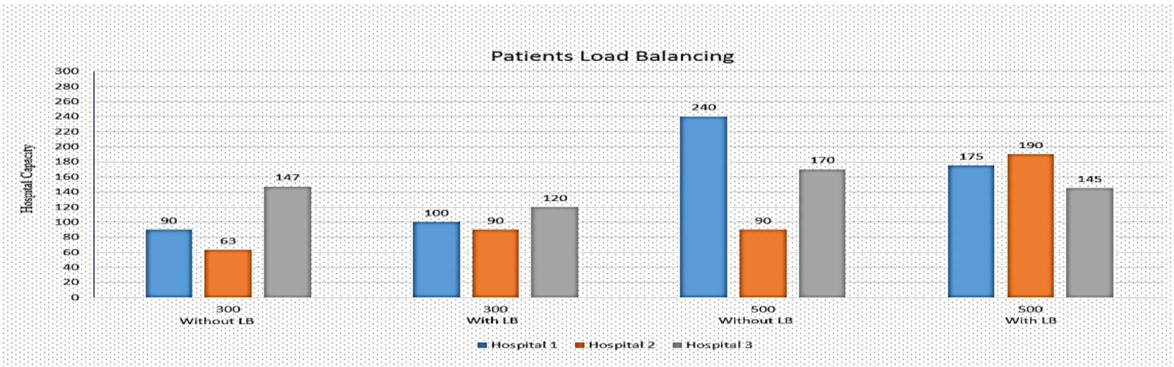

Figure 5: Patient load balancing

are available there. So, the application allows timely treatment and better resuscitation services for catastrophic victims who can't wait to be examined and provides a solution for patient load balancing and patient load migration, better utilization of available resources, especially in resource constraint scenarios. Additional hospitals can be found by an algorithm of extended distance if the number of patients in a disaster exceeds the early estimate. The patient with less critical injuries can be shifted to these additional hospitals. So, the application allows timely treatment and better resuscitation services for catastrophic victims who can't wait to be examined and provides the solution for patient load balancing and patient load migration. It allows for better utilization of available resources, especially in resource constraint scenarios.

REFERENCES

[1]. Dobson, Doan and Hung, "A systematic review of patient tracking systems," Journal of Emergency Medicine, p. 242-248, 2013.

[2]. J. Marshall and S. Mathews, "Disaster preparedness for the elderly: An analysis," J Aging Emerg Econ, vol. 2, p. 79-92, 2010.

[3]. Tavakoli, Nahid, Y. mohammadian, M. H. S. Reza and K. Mahmoud, "Health sector readiness for patient tracking in disaster: A literature reviewon concepts and patterns," International Journal of Health System and Disaster Management, vol. 4, no. 3, pp. 75-81, 2016.

[4]. D. Guha-Sapir, P. Hoyois and B. Below, "Annual Disaster Statistical Review 2014 – The Numbers and Trends," 2014.

[5]. Schultz, Carlh, Koenig, Kristil, Noji And Anderick, "A Medical Disaster Response To Reduce Immediate Mortality After An Earthquake," The New England Journal Of Medicine, Vols. 438-448, 1996.

[6]. C. Yu-Feng, K. Alagappan, G. Arpita, D. Colleen, T. Malti and Z. S. B, "Disaster management following the Chi-Chi earthquake in Taiwan," Prehospital and disaster medicine, vol. 21, pp. 196-202, 2006.

[7]. Sahar and Z. J. Ahmed, "Load Balancing for Disaster Recovery and Management," Wireless Personal Communications, vol. 90, no. 1, p. 369–379, 2016.

[8]. Ardalan, H. Mowafi, H. M. Ardakani, F.Abolhasanai, A. Zanganeh and H. Safizadeh, "Effectiveness of a primary health care program on Urban and Rural Community Disaster Preparedness,Islamic Republic of Iran: A Community Intervention Trial," Disaster Medicine and Public Health Preparedness, vol. 7, pp. 481-90, 2013.

[9]. D. Cook and S. Das, "How smart are our environments? An updated look at the state of the art," Pervasive and Mobile Computing, vol. 3, pp. 53-73, 2007.

[10]. Rathore, A. Farooq, G. J. E., G. R. Raissi and L. Jianan, "Experience and Preparedness of Major Incidents in Developing Countries," Disaster Medicine and Public Health Preparedness, vol. 7, pp. 127-8, 2013.

[11]. K. Murad, D. Sadia, J. Sohail, M. Gohar, G. Hemant and S. C. Mukhopadhyaye, "Context-aware low power intelligent SmartHome based on the Internet of things," Computers & Electrical Engineering, vol. 52, p. 208–222, 2016.

[12]. G. Marres, M. Bemelman, J. v. der and L. Leenen, "Development of a Permanent Facility for Management of Incident Casualties," Eur J Trauma Emerg Surg, vol. 35, pp. 203-11, 2009.

[13]. Paul, A. Ahmad, M. M. Rathore and S. Jabbar, "Smartbuddy: defining human behaviors using big data analytics in social internet of things," IEEE Wireless Communications, vol. 23, no. 05, pp. 68 - 74, 2016.

[14]. M. Carlton, "Surge capacity management and patient identification in," Elsevier Health Sciences, 2006.

[15]. T. Rich, P. Biddinger, R. Zane, A. Hassol, L. Savitz and M. Warren, "Recommendations for a National Mass Patient and Evacuee Movement," Agency for Healthcare Research and Quality, 2009.

[16]. Rehman, A.U., Asif, R.M., Tariq, R., Javed, A.: GSM based solar automatic irrigation system using moisture, temperature and humidity sensors. In: International Conference on Engineering Technology and Technopreneurship (ICE2T), Kuala Lumpur, pp. 1–4 (2017).

[17]. U. Christophe, U. F. Van, D. Emilie and D. Michel, "Pre-Hospital Simulation Model For Medical Disaster Management," in IEEE Proceedings of the 2013 Winter Simulation Conference, Neder-Over-Heembeek, 2013.

Mohsin Raza was born in Pakpattan, Punjab, Pakistan, in 1994. He received his BS Degree in Telecommunication and Networks from COMSATS University, Sahiwal Pakistan, in 2017 and Currently, he is pursuing MS degree in the College of Internet of Things (IoT) Engineering, Hohai University (HHU), Changzhou Campus, China. His research interests include Mobile crowdsensing network, Wireless Sensor Network(WSN) , Internet of Things (IoTs), Social Internet of Things (SIoTs) and Big Data.

Farhan Ahmad is currently doing his Masters in Electronics and Communication Engineering from Chongqing University, China. In 2018, he completed his BS Degree in Telecommunication and Networks from COMSATS University, Sahiwal Pakistan, His research interest includes energy harvesting, 5G, energy harvesting wireless communications, IOT. He is currently doing his research on narrow band internet of things.

Kashif Hussain is currently doing his Masters in Electronics and Communication Engineering from Chongqing University, China. In 2018, he completed his Bachelor's degree in Electrical Engineering (Telecommunications) from Government College University Faisalabad, Pakistan. His research interest includes Industrial networks, smart grid networking and 5G techniques. He is currently doing his research on Substation Protocols and Communications.

Abdul Wahab was born in Mardan KPK Pakistan.He received his bachelor degree in Electrical (Telecommunications) Engineering from University of Science and Technology,Bannu kpk Pakistan in 2018.he is Currently enrolled at Chongqing university for master degree in Electronics and Communications Engineering at Department of Microelectronics and Communications Engineering his research interst include Signal and processing ,IOTs,MIMO Radars ,SAR radars and remote sensing.

Ali Raza Barket born in Pakpattan, Punjab, Pakistan. He received his Bachelor's degree in Electrical Engineering from Sukkur IBA University, Sukkur, Pakistan in 2014 and his Master's degree from Beijing Institute of Technology in Electronics Science and Technology, Beijing, China. He is currently enrolled at the Beijing Institute of Technology for the PhD degree in Electronics Science and Technology at Beijing Key Laboratory of Millimeter-Wave and Terahertz Technology. His research interest includes THz Imaging, Radars, Security System, Control Systems, Signal and processing, IOTs and Remote sensing.

IJEW 国际工程期刊 International Journal of Engineering Works انجینئرنگ کاموں کا بین الاقوامی جرنل

International Journal of Engineering Works
ISSN-p: 2521-2419
ISSN-e: 2409-2770
Vol. 6, Issue 12, PP. 521-524, December 2019
https://www.ijew.io/
https://doi.org/10.34259/ijew.19.612521524

Active Power Control in Modern Power System through Demand Side Response

Syed Afzal Shah[1], Zafar Ahmad[2], Israr Uddin[3], Muhammad Nazeer[4]
[1,2,3,4] Department of Electrical Energy System Engineering, US-Pakistan Center for Advanced Studies in Energy (US-PCASE), UET Peshawar
afxalshaw@gmail.com[1], zafar.ahmad619@gmail.com[2], israreng93@gmail.com[3], muhammadnaxeer@gmail.com[4]
Received: 09 December, Revised: 19 December, Accepted: 25 December

***Abstract*—** Integration of renewable energy sources in power system has increased rapidly in recent years due to environmental effects such as climate change and global warming. Renewable sources provide clean and sustainable energy but it has some negative effects on power system. Renewable sources are mostly inertia-less sources and they increase instability in system. Frequency deviations are main indicator of their fluctuation because of their variable energy nature. To stabilize frequency, spinning reserves are there. Most of generators providing spinning reserves are fossil fuel generators, their operation is costly and not environment friendly. To minimize dependence on spinning reserves, demand side response is a method, which can provide frequency reserves cheaply and have a fast response. Demand side response is to shift loads of end users from peak hours to off-peak hours in response to frequency deviations or any contingency in power system with agreement with end users. This paper proposes the use of demand response through load management. Direct control method is used to control loads of end users. In response to frequency deviations, loads are ON/OFF to stabilize the frequency. For that purpose, a simple microgrid is designed in MATLAB/SIMULINK comprises of Solar PV and diesel generation sources. Loads are controlled through simple controller, which monitor frequency and act accordingly. Different scenarios are simulated, with demand side response and without demand side response. The results showed that with demand side response, frequency can be stabilizing quickly and system can be prevented from instability.

***Keywords*—** DSR, Frequency Reserves, Demand Response

I. Introduction

Stability and security of electrical power system is main concern of present as the population expanding rapidly so the demand of electricity as well. To contain the situation, new power generation sources are increasing in numbers. Mostly traditional generation sources are based on fossil fuels which are non-environmental friendly. Scarce of fossil fuels and growing concern of global warming and climate change the world is focusing on environmental friendly generation sources to tackle the problem of increasing demand. Apart from positive aspect of renewable sources, there are negative aspects which affect stability and security of power system. Since most of renewable sources are variable in nature and have less moving parts, their integration in power system affect frequency of the system. Fluctuation in system frequency occurs more regularly. These fluctuations in frequency often leads to instability of the system. Change in frequency is main indicator of temporary changes in supply and demand of power system [1]. Frequency rises when supply exceeds demand and it falls when demand exceeds supply. To control frequency of power system, there are spinning reserves which are used in case of contingencies. These spinning reserves are primary, secondary and tertiary reserves based on their time of response [2]. Spinning reserves are generating unit which are up and running but only contribute in case of contingency. So the operation cost of spinning reserves are high and these spinning reserves units are mostly fossil fuel based and are non-environmental friendly. Apart from these reserves, Demand side response (DSR) is an alternate way to control frequency of the grid and it is also cost effective.

Demand side response (DSR) is a response from loads to control any contingency related to frequency. Demand side response is to shift demand of end user to another time by agreement with the end user. End user can shift their loads from peak hours to off peak hours in case of under frequency. There is also economic benefit to it as tariff in off peak hours is less as compared to peak hours. Due to technological advancement world is shifting from traditional grid system to smart grids and demand side response is main feature of smart grids. Direct and indirect demand side response are main strategies based on its response type. In indirect strategy, the utility has no control over devices at end user side. It is generally based on tariffs and incentives. Utility forecast tariffs for day ahead to encourage end users to shift their loads according to these tariffs best suited to end users. Incentive based DSR is to encourage consumers to shed their loads in case of contingency in exchange for rewards in term of economics.

In this paper Direct demand side response strategy is considered. In direct DSR, utility has complete control over end user's devices. Utility can on/off devices according to its requirement. When there is peak time and generation is unable to handle the demand, the frequency of the system begins to fall, then to control frequency deviation utility can off some non-critical loads at consumer side to bring frequency back to its nominal value. A centralized controller is used, which generates signal according to frequency deviations and then send a signal to the devices at end user side, which have preset values. It can turn on/off the load according to preset value. In this method reserves can be provided by load management quickly and at low cost than spinning reserves and dependence on spinning reserves can minimized. In recent years, demand side response has gain a lot of interest due to its technical and economic benefits.

II. Related Work

The following scientific research proposes different strategies based on load management to better understand the concept and usage of demand side response. In [3], various strategies are considered for air conditions and refrigeration system and their contribution in demand side response. Incentive based and Time of use (TOU) based DSR are discussed and their reliability and implementation of demand response strategy is discussed. Assessment of DR and its application in china for the future is taken under study. Different strategies for the usage of air conditions and refrigeration system in DR are provided which can be used separately or in combination with one another.

In [4], contribution and effectiveness of DSR on residential load in Switzerland is discussed. Apart from industrial and commercial loads, participation of residential loads in demand response program is proposed. The survey is carried out on 30 utilities in Switzerland for data collection. DSM opportunities within residential load are identified. The impact of DSM on economic cost reduction per customer is obtained. The author discussed that residential load have very small effect in DSM but large number of residential customers can have major impact in Demand response program.

In [5], DSM opportunity in Refrigeration system in Turkey is discussed. The economic impact on customers by using refrigerators in DR program is analysed. The working of refrigerator model and its consumption throughout a week is explained. Direct load control method for refrigeration system is used. By changing working time of refrigerator from high demand period to low demand period, cost optimization is carried out and are compared in multiple and single pricing tariffs.

In [6], load control method for renewable energy resources is discussed. Load control method is used on basis of frequency and voltage sensors. Microcontroller is used to monitor the frequency and voltage deviation and take decision on basis of those measurements to connect or disconnect the loads. Software is designed for voltage and frequency monitoring and tested on 18 KW, single phase micro hydro system. For load switching fuzzy logic control system is developed which uses the input from algorithm which monitors voltage and frequency.

In [7], the impact of flexible load and wind power integration on power system imbalance is discussed. Cold storage rooms are considered as flexible loads as they can provide demand response. The author proposed that cold storage rooms as flexible loads can provide reserves of 90 MW through automatic governor control (AGC) in Danish power system. The cold storage room is designed in this study. AGC is used to monitor the frequency deviations. The reserves provided by Cold storage rooms can reduce dependency on spinning reserves generators and can provide stability to power system.

In [8], a stochastic programming model is developed for optimal performance of smart microgrid to reduce the operation cost and reduce the emission by usage of renewable energy sources. To resolve uncertainties from renewable sources, DR program is used in which industrial, commercial and residential consumers participate. Incentive based DR program is used. Multi-objective purpose particle swarm optimization (MOPSO) based on fuzzy logics is used in the study. The study shows that using Demand response program the operating cost and pollution is reduced by considerable amount.

In [9], a method to reduce the peak load of residential community by use of HAN system is proposed. The HAN devices are installed at end user. The main component of HAN system is HAN controller which analysis signal both utility and end user. The device uses two-way communication and the utility gets inform of actual load reduction at end user by HAN controller. The algorithm is developed by using UML (unified modelling language) and implemented in HAN controller in form of filed programming gate array (FPGA) device. The study shows that participation of large number of residential consumers in DR event can significantly reduce peak load and can support grid in case of instability such as under frequency situation.

The scientific research in [10] [11] [12] [13] also proposes different strategies for load control and contribution of responsive loads and their impact in power system. Strategies are proposed to provide primary frequency reserves in power system through smart load management.

III. Methodology

In this paper, model of microgrid is considered which uses Distributed energy resources Solar PV and diesel generator is also used for reliability of the system. Microgrid has been modelled in MATLAB/Simulink and it includes a 300 KW of Solar PV plant and 1 MW Diesel generator in generation side along with its required converters and transformers.

A. *Diesel Generator Model*

The generator modelled in microgrid is three phase synchronous machine which generates rated power of 1 MW at 60 Hz frequency. The generator increases or decrease output according to demand and supply. The diesel generator is directly connected to main transmission line.

B. *Loads and Controller Model*

In Simulink model, loads with different consumptions are used. Initially the load on the system is 1200 KW but later the load is increased to 1400 KW to create peak scenario. Three phase circuit breakers are used for switching purpose for loads. Signal for breaker is received from controller to whether open the switch or closed it. The controller is basically designed for frequency control. Grid frequency is taken as input signal to controller. Set points for frequency are defined in controller, when frequency exceeds from these points, the controller generates signal for breakers to operate. The controller is designed for under frequency and over frequency situation. It is designed to give support to the system through load management in case of under and over frequency.

IV. Simulation and Results

The model comprises of Solar PV and Diesel generator along with resistive load and a controller. Working of these components and results are explained. Solar PV and diesel generator have rated power of 300 KW and 1 MW respectively. Total resistive load is 1200 KW initially. A controller is designed for frequency monitoring and stabilizing the frequency. The frequency for the system in this model is 60 Hz. The threshold for frequency control is set at 59 Hz and 61 Hz for lower and higher limit respectively. The main purpose of controller is peak shaving in under frequency situation. When the load is increased, and peak occurs. The frequency begins to drop. When frequency crosses lower limit at 59 Hz. The controller cut off supply to some loads to contain frequency at 59 Hz. In this way the momentary deviation of frequency due to peak demand is contained.

Peak shaving through load management is part of demand response program. The study proposes active power control through demand side response. To show the effect of demand response by peak shaving of load to stabilize the frequency, different scenarios are considered in the simulations.

A. *Frequency response without Demand response*

In this scenario, the controller will keep the circuit breaker closed in order to observe the response of frequency of the system. Loads will not be cut off in this scenario. Initially the load on the system is 1200 KW. When frequency stabilizes after transient state, the load is increased at 20th second of simulation time to generate peak demand situation. Frequency of the system begins to drop as the demand is increased. At 22 second the frequency crossed the threshold point of frequency. Without frequency reserves and Demand response the frequency continues to drop and the system goes to instability as shown in figure 1.

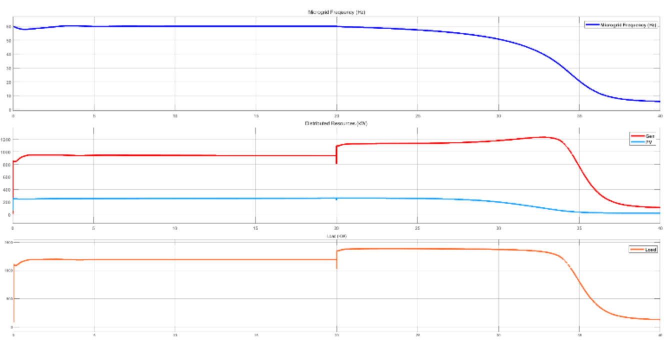

Figure 1. Frequency response without Demand response

B. *Frequency response with Demand response*

In this scenario, the simulation is carried out with using of demand response program. Direct control method is used to ON/OFF the load by using simple controller. The initial load on the system is 1200 KW, out of which 1000 KW is constant load and other two loads of 100 KW each are connected to controller. These two loads will participate in DR program of peak shaving. Initially when simulations run, the system is in transient state because of diesel generators starting cycle. The steady state is achieved, and frequency stabilizes at 60 Hz at 9th second. At 20 second the load is increased to 1400 KW to generate peak situation for simulations. The frequency begins to drop and crossed the threshold at of 59 Hz at 22 second. When the frequency drops from 59 Hz, the controller operates the circuit breakers at 22 second as shown in figure 2. The controller cut off the supply to two 100 KW loads. The frequency is contained at 59 Hz and frequency begins to rise at 23 second of simulation time. The momentary deviation of frequency is contained at 59 Hz and stabilizes the frequency back to 60 Hz at 29th second of simulation time.

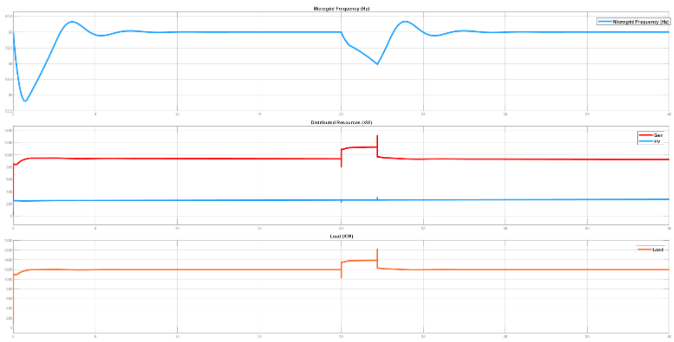

Figure 2. Frequency response with demand response

C. *Frequency response after generation loss*

In this scenario, the Solar PV is turned off to generate a situation of generation loss to observe characteristics of frequency. Initially generation of Solar PV is 300 KW and Diesel generator generates 1 MW power. The load connected to the lines are 1.2 MW. At time 20 of simulation time, Solar PV is cut off from generation side. Now the demand exceed generation. Demand is still 1.2 MW and generation is 1 MW. So the frequency begins to drop and without reserves and proper demand response, the frequency continues to drop until system goes into instability in matter of seconds as shown in figure 3.

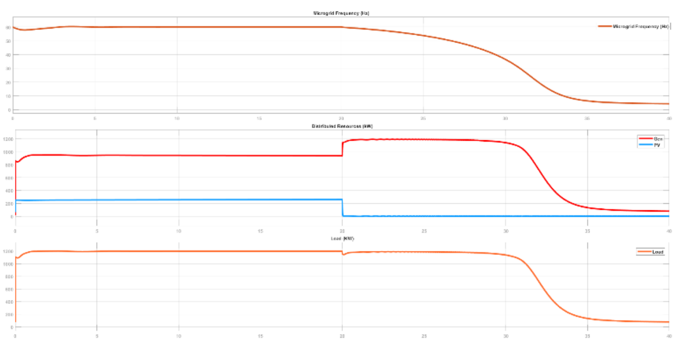

Figure 3. Frequency response after generation loss

D. Generation loss and Demand response

In this scenario, Solar PV is cut off to generate a generation loss situation and to observe frequency response with the use of demand response. Initially load on the system is 1.2 MW and generation of diesel generator and Solar PV is 1 MW and 300 KW respectively. At time 20 of simulation time, Solar PV is cut off. Now the demand is more the generation and the frequency begins to drop. As the frequency approaches the threshold point of 59 Hz, the controllable load of 200KW is turned off. Now the load is within limit of generation capacity and the frequency begins to rise at time 22 second. And the frequency stabilizes back to 60 Hz at 26th second as shown in figure 4.

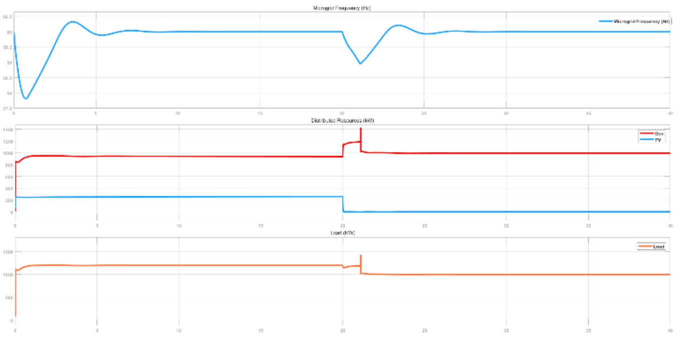

Figure 4. Frequency response after generation loss with demand response

As the results, shows in figure 2 and figure 4 that with use of demand side response the frequency stabilizes back to its normal value by switching OFF two loads of 100 KW. Peak is handled by switching these loads to stabilize the system. While in figure 1, when the peak occurred the frequency begins to drop and without demand side response, the frequency continues to drop and system goes into instability. In figure 3, when generation loss occurs the frequency begins to drop because of mismatch of generation and demand. Without demand response and reserves and frequency continues to drop until the system becomes unstable. While in figure 5.4, the frequency is contained at 59 Hz by switching off the controllable load to stabilize the system and the results shows that with use of demand response the system can be stabilized in case of contingencies. We can estimate the amount of reserves demand side provide by calculating the size of loads contributing in demand response. In this case controllable load in the system is 200 KW. So the reserves demand side offers in this case can be estimated at 200 KW.

CONCUSLION

Modern power system has an increased penetration of renewable energy sources, because of its environment friendly benefits. Distributed generation is also increased due to conventional grid difficulties of electrification of rural areas. Renewables are mostly used as D.Gs. Due to increased penetration of these DERs, stability and security of the power system is affected because of its variable nature. Renewable sources are mostly inertia less systems, chances of frequency and voltage fluctuation are great as compared to conventional generators. Frequency instability is most common contingency of increasing penetration of renewable sources. To stabilize frequency there are frequency response reserves, those generators are up and running but they are only connected in case of contingency. So cost of these conventional spinning reserves is high. Demand response can give those frequency reserves at economical cost and without polluting environment. Load can act as frequency reserves at time of contingency. Non sensitive loads can be cut-off in case of emergency to support frequency. Loads can be made sensitive to frequency deviation as frequency deviates from its set points and continues for some time, non-sensitive loads can be shed for some time to restore system frequency. This will help to minimize the amount of spinning reserves and will have economic benefits on economy.

REFERENCES

[1] U. N. Grid, "Frequency response National Grid," 2015.

[2] M. Aunedi, P. Aristidis Kountouriotis, J. E. Ortega Calderon, D. Angeli, and G. Strbac, "Economic and environmental benefits of dynamic demand in providing frequency regulation," *IEEE Trans. Smart Grid*, vol. 4, no. 4, pp. 2036–2048, 2013

[3] J. Han and M. A. Piette, "Solutions for Summer Electric Power Shortages : Demand Response and its Applications in Air Conditioning and Refrigerating Systems," *Refrig. Air Cond. Electr. Power Mach.*, vol. 29, no. 1, pp. 1–4, 2008.

[4] N. Boogen, S. Datta, and M. Filippini, "Demand-side management by electric utilities in Switzerland: Analyzing its impact on residential electricity demand," *Energy Econ.*, vol. 64, pp. 402–414, 2017.

[5] M. A. Zehir and M. Bagriyanik, "Demand Side Management by controlling refrigerators and its effects on consumers," *Energy Convers. Manag.*, vol. 64, pp. 238–244, 2012.

[6] K. Pandiaraj, P. Taylor, N. Jenkins, and C. Robb, "Distributed load control of autonomous renewable energy systems," *IEEE Trans. Energy Convers.*, vol. 16, no. 1, pp. 14–19, 2001.

[7] A. Basit, T. Ahmad, A. Y. Ali, K. Ullah, G. Mufti, and A. D. Hansen, "Flexible modern power system: Real-time power balancing through load and wind power," *Energies*, vol. 12, no. 9, pp. 1–15, 2019.

[8] G. R. Aghajani, H. A. Shayanfar, and H. Shayeghi, "Demand side management in a smart micro-grid in the presence of renewable generation and demand response," *Energy*, vol. 126, pp. 622–637, 2017.

[9] G. Bazydło and S. Wermiński, "Demand side management through home area network systems," *Int. J. Electr. Power Energy Syst.*, vol. 97, no. August 2017, pp. 174–185, 2018.

[10] J. A. Short, D. G. Infield, and L. L. Freris, "Stabilization of grid frequency through dynamic demand control," *IEEE Trans. Power Syst.*, vol. 22, no. 3, pp. 1284–1293, Aug. 2007.

[11] F. Baccino, F. Conte, S. Grillo, S. Massucco and F. Silvestro, "Frequency Regulation by Management of Building Cooling Systems through Model Predictive Control", In: *Power Systems Computation Conference*, Wroclaw, Poland, Aug. 2014

[12] A. Molina-García, F. Bouffard, and D. Kirschen, "Decentralized demand-side contribution to primary frequency control," *IEEE Trans. Pow. Syst.*, vol. 26, no. 1, pp. 411–419, 2011

[13] Z. Xu, J. Østergaard, and M. Togeby, "Demand as Frequency Controlled Reserve," *IEEE Trans. Pow. Syst.*, vol. 26, no. 3, pp. 1062–1071, Nov. 2011

International Journal of Engineering Works
ISSN-p: 2521-2419
ISSN-e: 2409-2770
Vol. 6, Issue 12, PP. 525-528, December 2019
https://www.ijew.io/
https://doi.org/10.34259/ijew.19.612525528

Optimization of a Hybrid System Connected with Utility Grid using Homer Software

Israr Uddin[1], Dr. Adnan Daud khan[2], Zafar Ahmad[3], Syed Afzal Shah[4]
[1,2,3,4] Department of Electrical Energy System Engineering, US-Pakistan Center for Advanced Studies in energy (USPCAS-E), UET Peshawar
israreneg93@gmail.com[1], adnan.daud@uetpeshawar.edu.pk[2], zafar.ahmad619@gmail.com[3], afxalshaw@gmail.com[4]
Received: 09 December, Revised: 19 December, Accepted: 25 December

***Abstract*—** A microgrid is a combination of distributed energy sources to generate power to the consumer or exchange electrical energy to the grid or working in a standalone system. The microgrid may be on-grid or off-grid. Distributed Generators (DG, s) are more reliable on-site selection. Therefore, a hybrid energy system came into existence. Like to combine solar PV, wind, small Hydro, and diesel generator and fuels cells. Solar PV, wind and diesel generator hybrid system are more analyzed previously in the research study. In this research PV, Batteries and diesel Gen are combined to make a hybrid system connected to the utility grid, which is economical and reliable. The potential resource data were downloaded from NASA through the homer tool. Homer software is used for the simulation to simulate and analyze the hybrid system.
***Keywords*—** DG,s, NASA, IEA, HRES, LOCE, NPC,AC, DC

I. Introduction

As the energy demand is increasing steadily due to industrialization, commercialization needs electricity. The increased demand illustration is one of the problems facing many communities in the world. Also in the coming era, the fossil fuel reserves will also reduce due to which high-cost factor is an issue for the world. International energy agency (IEA) predicted that nearly 1.6 billion billion persons of the world still having no access to power (electricity), also the energy demand will increase 53% by 2035 [1]. To fulfill the energy demand alternative energy resources are needed to utilize. Also, fossil fuels have many issues related to the environment, economic and lifestyle of a human being. The currently conventional energy sources used for the generation of electrical power are oil, coal and natural gas worldwide. These conventional energy sources have impacts on the environment as well as on human health due to the greenhouse effect are the major disadvantages [2][3].

The global institute researchers and scientists are working to find alternatives to replace conventional sources with renewable energy sources [4]. Since, in the past few years the interest has increased in renewable energy sources like solar PV, wind, micro-hydro, and biogas. These sources have many advantages envirementy as well as on human life [5]. Therefore, to make a system that combines renewable and non-renewable energy sources. Hybrid renewable energy system (HRES) is basically a combination of one or more sources to generate the electrical power either autonomously or connected to grid [6]. Solar and wind system either working autonomously or grid-connected mode however, the efficiency of these sources are less due to unpredictable nature. The hybrid system overcomes this problem to integrate renewables with grid mode to sustain energy [7]. In case of any lack of electrical power in a situation when there is not enough power generated from renewable energy sources diesel generator or battery storage are used for backup [8][9].

Hybrid renewable energy system (HRES) optimization and simulation can be carried out through many software nowadays, such as Homer, Hoga, and hybrid2 with various backgrounds and simulations. HOMER used an algorithm for the optimization and sensitivity analysis to assess the best feasible system configuration. Homer evaluate both types of system off-grid and grid-connected mode for different application. For a designer, it benefits to find out the optimum system of PV, wind, hydro, batteries, biogas and diesel generator by entering various inputs to the software. It calculates and offers the best optimum system based on feasibility and evaluating life cycle cost which permits the user to find the best system with net present cost to make their own power system. Homer removes a system that is incompetent to fulfill the load demand which is not suitable. Homer also simulates the sensitivity analysis to determine different constraint effects on the power system [10].

The most important benefit of the grid connection is that any sort of uncertainty from renewable will fulfill the Grid. Many researchers have worked on a grid-connected hybrid system. From previous research related work different researcher worked on the HOMER optimization tool for different areas to get the best-optimized configuration. In this paper [11] presented the techno-economic analysis to design a hybrid system composed of PV/wind with a grid connected for an average load demand 15000kwh/day and the maximum demand is 2395 kW for Riyadh city in Saudi Arabia. In [12] stated the cost analysis of different hybrid energy systems composed of solar PV, wind and diesel Generator with grid-connected, for an average energy demand of 35kwh/day and maximum load is 4.1kw in hilly area of Bangladesh. Most research has installed solar PV and wind in the hybrid system.

In this research, we selected the sources for our interest is solar PV, Diesel Generator and Batteries with grid-connected mode. To obtain different hybrid configuration from Homer optimization, and to obtain the optimized and economical hybrid system.

II. Methodology

For the hybrid energy system combination, we considered sources like solar PV, Diesel generator and storage batteries with utility grid. As the demand is AC so we need a converter to convert DC from PV and batteries to AC. The generator is connected to the AC side. For backup generator and storage batteries are used in case of any shortage of power or in peak hours.

A. Load data

The selected site for the study is Electrical Engineering Department University of Engineering and Technology Peshawar, Khyber Pakhtunkhwa, Pakistan located with latitude 34.01510 N and longitude 71.52490 E. The department consists of classroom, laborites, library and staff offices. HVAC system was installed in all building and lightning of different ranges. The department is open on weekdays from 9.00 am to 5.00 pm and it seems the load is high in these hours, because of the department schedule. The average daily load demand is 574.6(kwh/day) and maximum deand is 99.66 KW. The load demand of daily profile is shown in fig-1.

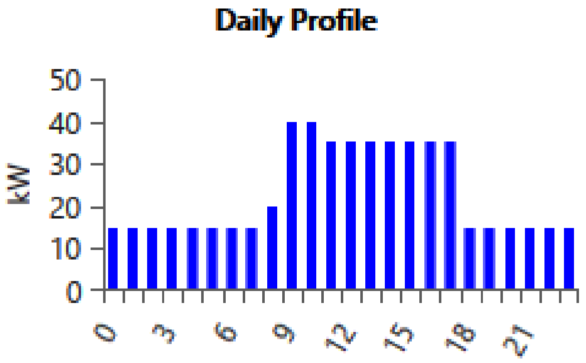

Figure 1. Daily profile of load demand

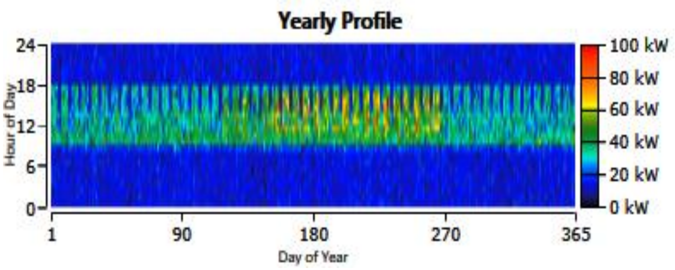

Figure 2. Yearly profile of load demand

The selected site is in the area which is very hot in summer and very cold in the winter period. However, the demand is high in summer because of the HVAC system which combines in summer periods. The yearly load profile is shown in figure-2.

B. Resource potential

Peshawar is located in the region where solar potential is remarkable. The resource potential is shown in fig-3. The resource potential is downloaded from NASA online through Homer software. The highest solar radiation is in June and the lowest is in December. While the average is 5.02 kWh/m2.

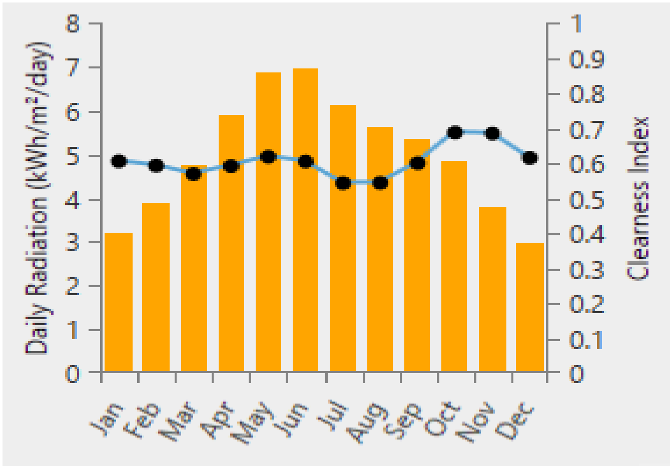

Figure 3. Daily solar insolation -(GHI)

C. System Modeling

In this hybrid system we have PV, Diesel Generator, and storage batteries connected to utility grid. The Gerator and Grid is linked to the main AC bus, while the Batteries and PV is linked to DC bus. As the load demand is AC so a converter is required to change DC from batteries and PV to AC. The schematic diagram of our proposed model is given in fig-4.

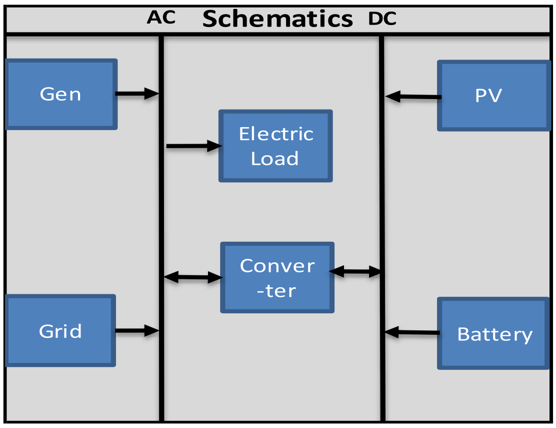

Figure 4. Proposed Model of HRES Schematic

III. Results and Discusion

After the putting all the inputs for the homer simulation we get the results as shown in fig-5 . The homer give the optimized configuration of different combination but we will select the HRES Configuration with lowest cost of energy (LOCE) and net present cost (NPC) .

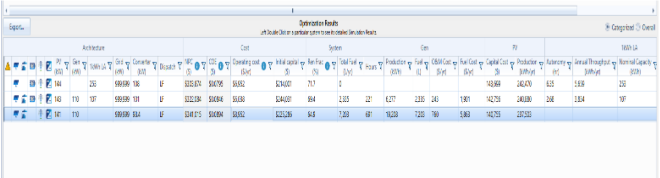

Figure 5. Simulated Results of different HRES

From the simulation the best optimized configuration is the 1st on which is the combination of PV, Battery and Grid. PV and Grid are the main sources which fulfill the primary load demand, while the Battery is used for backup in case when there is load not meet up. The electrical generation throughout the year of PV and grid is given in fig-6 .

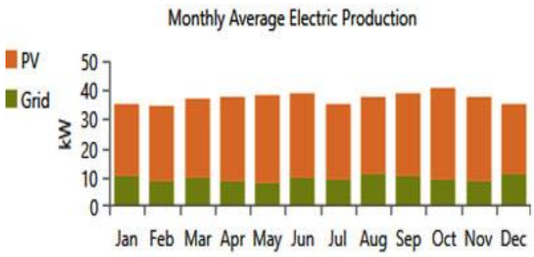

Production	kWh/yr	%
Generic flat plate PV	242,470	74.3
Grid Purchases	83,784	25.7
Total	326,254	100

Figure 6. MonthlyAverage Electrical generated (PV, Grid)

Electrical production from the battery energy storage is shown in figure-7.

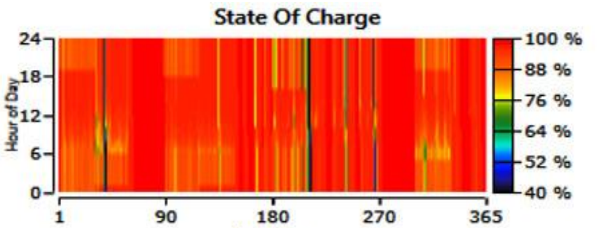

Quantity	Value	Units
Batteries	253	qty.
String Size	1.00	batteries
Strings in Parallel	253	strings
Bus Voltage	12.0	V

Quantity	Value	Uni
Autonomy	6.35	hr
Storage Wear Cost	0.210	$/
Nominal Capacity	253	kW
Usable Nominal Capacity	152	kW
Lifetime Throughput	56,594	kW
Expected Life	10.0	yr

Quantity	Value	Units
Average Energy Cost	0	$/kWh
Energy In	6,327	kWh/yr
Energy Out	5,062	kWh/yr
Storage Depletion	0	kWh/yr
Losses	1,265	kWh/yr
Annual Throughput	5,659	kWh/yr

Figure 7. Electrical eenrgy generated from Battery

The system total net present cost , operation & maintenance cost salvage and replacement cost is shown in figure-8.

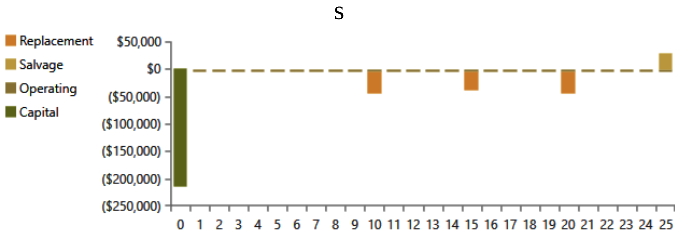

Figure 8. Cash Flow of HRES

From the above results, we select the first hybrid renewable energy system (HRES) because the net present cost (NPC) of the system and lowest cost of energy (LOCE) is low as compared to other HRES system configuration.

CONCLUSION

The researchers has a great intention towards to the increased interest in renewable day by day. Many organization are working to penetrate the renewable energy in the current power system in many countries, to meet their load demand. In this research study we have to find the best optimized hybrid renewable energy system (HRES) to fulfill the required load with lowest cost of energy (LOCE). From the results it is evaluated that the best optimized system is Solar PV, batteries and connected with Grid based on lowest cost of energy and net present cost.

REFERENCES

[1] M. pd. Zerta, P. R. Schmidt, C. Stiller, and H. Landinger, "Alternative World Energy Outlook (AWEO) and the role of hydrogen in a changing energy landscape," Int. J. Hydrogen Energy, vol. 33, no. 12, pp. 3021–3025, 2008.

[2] M. D. A. Al-falahi, S. D. G. Jayasinghe, and H. Enshaei, "A review on recent size optimization methodologies for standalone solar and wind hybrid renewable energy system," Energy Convers. Manag., vol. 143, pp. 252–274, 2017.

[3] Y. Z. Alharthi, M. K. Siddiki, and G. M. Chaudhry, "The New Vision and the Contribution of Solar Power in the Kingdom of Saudi Arabia Electricity Production," IEEE Green Technol. Conf., pp. 83–88, 2017.

[4] K. Y. Lau, M. F. M. Yousof, S. N. M. Arshad, M. Anwari, and A. H. M. Yatim, "Performance analysis of hybrid photovoltaic/diesel energy system under Malaysian conditions," Energy, vol. 35, no. 8, pp. 3245–3255, 2010.

[5] M. B. M. Rozlan, A. F. Zobaa, and S. H. E. A. Aleem, "The Optimisation of Stand-Alone Hybrid Renewable Energy Systems Using Integration of Stand Alone Hybrid Renewable Energy Systems Optimisation using HOMER," no. July, 2011.

[6] S. N. Kane, A. Mishra, and A. K. Dutta, "Preface: International Conference on Recent Trends in Physics (ICRTP 2016)," J. Phys. Conf. Ser., vol. 755, no. 1, 2016.

[7] V. Khare, S. Nema, and P. Baredar, "Solar – wind hybrid renewable energy system : A review," Renew. Sustain. Energy Rev., vol. 58, pp. 23–33, 2016.

[8] B. S. Borowy and Z. M. Salameh, "Methodology for optimally sizing the combination of a battery bank and PV array in a Wind/PV hybrid system," IEEE Trans. Energy Convers., vol. 11, no. 2, pp. 367–373, 1996.

[9] J. L. Bernal-Agustín and R. Dufo-López, "Simulation and optimization of stand-alone hybrid renewable energy systems," Renew. Sustain. Energy Rev., vol. 13, no. 8, pp. 2111–2118, 2009.

[10] T. Lambert, P. Gilman, and P. Lilienthal, "Micropower System Modeling with Homer," Integr. Altern. Sources Energy, pp. 379–418, 2006.

[11] Y. Z. Alharthi, M. K. Siddiki, and G. M. Chaudhry, “Techno-economic analysis of hybrid PV/Wind system connected to utility grid,” 2019 IEEE Texas Power Energy Conf. TPEC 2019, pp. 1–6, 2019.

[12] M. Moniruzzaman and S. Hasan, “Cost analysis of PV/wind/diesel/grid connected hybrid systems,” 2012 Int. Conf. Informatics, Electron. Vision, ICIEV 2012, pp. 727–730, 2012.

Israr Uddin is a postgraduate researcher at United States Pakistan Center for Advanced Studies in Energy at University of Engineering and Technology Peshawar, Pakistan. He is studying Electrical Energy System Engineering at MS level after doing his undergraduate degree in Electrical (power) Engineering. His research interest include finding the best optimized configuration of hybrid energy system with grid connected using HOMER. This paper is a part of his Master degree research studies.

International Journal of Engineering Works
ISSN-p: 2521-2419
ISSN-e: 2409-2770
Vol. 6, Issue 12, PP. 529-533, December 2019
https://www.ijew.io/
https://doi.org/10.34259/ijew.19.612529533

Operating Reserves Adequacy in Future Pakistan Power System

Zafar Ahmad[1], Syed Afzal Shah[2], Israr Uddin[3]
[1,2,3]Department of Electrical Energy System Engineering, US-Pakistan Center for Advanced Studies in Energy (USPCAS-E), UET, Peshawar, Pakistan
zafar.ahmad619@gmail.com[1], afxalshaw@gmail.com[2], israreng93@gmail.com[3]
Received: 09 December, Revised: 19 December, Accepted: 25 December

***Abstract*—**In this paper estimation of PFC (Primary frequency control) reserves and their adequacy has been investigated. Since Pakistan is aiming to add more renewable generation to its power system to reduce their dependency on fossil fuels and because of their concern about the environmental polution. And this renewable penetration adds variability and complexity to the power grid and doesn't add inertia to the system. So therefore overall inertia of the system decreases in result of addition of renewables. When the inertia of the system decreases, frequency deviations increases because of the renewable forecast error and other contingencies in the grid. To study thiese frequency deviations expected scenario for Pakistan power system are created for current and future Pakistan power system. From these studies, estimation of PFC reserves are made in this paper for future Pakistan power system. This paper also explain the frequency instability arises due to high renewable integration in power system and their feasible solutions for future Pakistan power system.

***Keywords*—** PFC reserves, Renewable penetration, frequency deviations, inertia, power system

I. Introduction

Reliability and security of a power system depends on the stability of frequency of the whole system. For frequency to be stable within range of 50 Hz ± 0.1% [1], load and generation of a power system must be balanced. Any mismatches between load and generation cause deviation in frequency. Now a days Pakistan is also trying to increase renewable penetration in its power system. Since renewable generation is variable in nature and it adds variability and uncertainty to the power system and in turn cause frequency deviation in the system and system becomes weak and more vulnerable to contingencies and these uncertainities arises due to renewable forcast error like wind forecast error and solar forecast error which we need hour ahead or more than one hour forecast data. To cope with these uncertainties, we need operating reserves in the power system, both manual and automatic reserves.

Operating reserves are of several types, in UCTE (Union for Co-ordination of Transmission of Electricity) [2], several reserves were named as (PFCR) primary frequency control reserves, (SFCR) secondary frequency control reserves and tertiary reserves.

Primary reserves are also called as FCR (Frequency containment reserves), secondary reserves are called as FRR (Frequency Restoration reserves) and tertiary reserves are called as RR replacement reserves according to their functions [3]. These operating reserves are called upon by different names in different countries according to their functions. Operating reserves and their different types are given in details in figure 1.

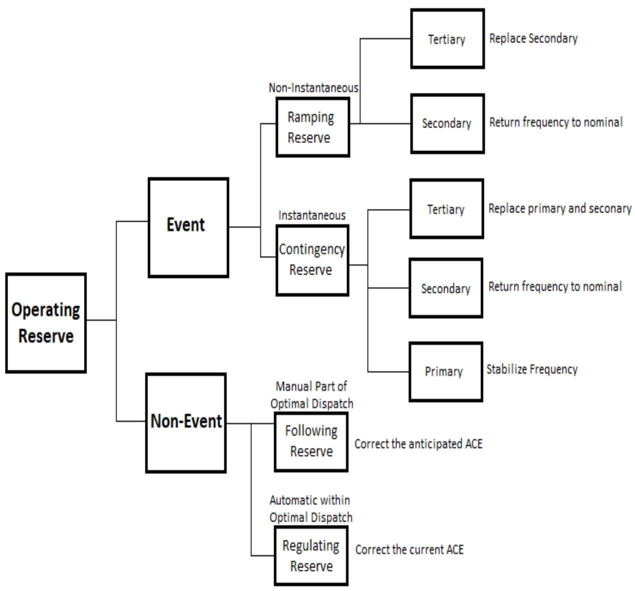

Figure 1. Classification of operating reserves

First of all, when any contingency appear on the system primary reserves are activated automatically to catch frequency deviation as fast as possible and keep it stable at some point below its reference value. Then secondary control reserves are activated to bring back frequency to its nominal value and tertiary reserves are activated to replace secondary reserves and to stabilize the power system. Activation manner of operating reserves are presented in figure 2.

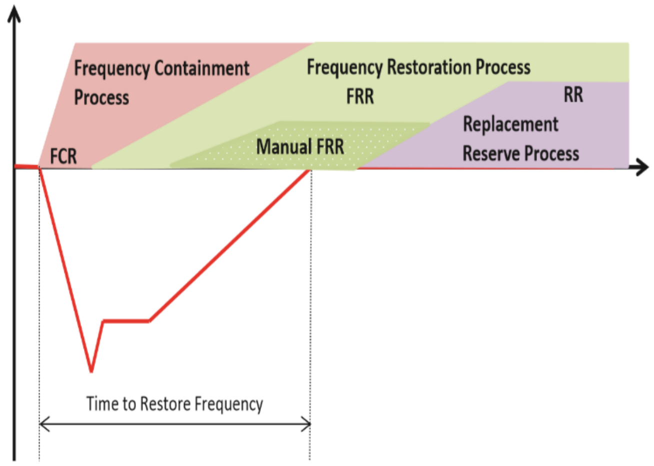

Figure 2. Operating reserves activation order

II. Related Work

In [4] author's have explained about different types of operating reserves and their need in power system as renewable integration increases day by day. Author's have explained how these reserves control the disturbances in the power system arises due to sudden generation loss, sudden load loss and renewable forecast error. They have also discussed how in future these reserves can be used in a power system due to increase penetration of renewables. It also explains how much reserves are required for the power system after a detail study of that system and to allocate the suitable amount of reserves for that power system. They have also classified these reserves according to their functions.

In [5] this paper author has presented different power scenarios for European power system and author has also recorded the forecasted values of wind for different times. But the main objective of this paper is to observe the primary reserve adequacy along with secondary reserves in Europe future power scenarios. this research also explains the difficulties arises due to renewable forecast error and present possible solution to these challenges.

In [6] author have presented a study of high wind power penetrated system and replacement of conventional generation by renewable power generation and its impact on inertia of the system. And impact on frequency of the power system due to decrease in inertia of the system. This research also discusses the ability of wind turbines to deliver backing during contingencies to avoid any unwanted situations. It also explains wind power penetration to its maximum possible level without causing any instability to the system.

III. Frequency Response to Assess PFC Reserves

Since renewable penetration is variable in nature and adds variability to the power system, therefore it has a huge impact on operating reserves. As renewable penetration increases in a power system, demand for operating reserves increases to cater with frequency deviation arises due to variability of renewable generation. Now if after a sudden contingency on a power system the availability of the power to customers in not interrupted, then we can say the primary reserves are enough. For this to evaluate either reserves are enough or not in the system we have responses of frequency, one is frequency nadir and PFC [7].

A. Inertia of System

Inertia of a system can be defined as the opposition to frequency deviation provided by the rotating mass of the system. Inertia of a system can be represented as

$$M = \frac{2HS}{f} \approx \frac{2HS}{f_0} = \frac{2H_{eq}P_{Generation,}}{f_0} \tag{1}$$

Where P_Generation is power of the system, S is apparent power, H is inertia constant, fo is reference frequency and f is frequency of the system. Inertia constant are different for different kind of generating units, it may be different for hydro generating unit and may be different for steam generating unit. Renewable generation doesn't add inertia to the system. Figure 3 below shows different generating units and its constant of inertia H [8].

Type of generation unit	H
Thermal unit	
(a) 3600[4] r/min (2 pole)	2.5 to 6.0
(b) 1800[5] r/min (4 pole)	4.0 to 10.0
Hydraulic unit	2.0 to 4.0

Figure 3. Inertia Constant values of generating units [1]

H for a single generating unit is given by

$$H = \frac{1}{2}\frac{J\omega_n^{\,2}}{S_n}\ [\mathrm{s}] \tag{2}$$

Where J is moment of inertia, where w_n represents angular mechanical velocity and S_n is apparent power. Now to calculate the inertia of the whole system, rated power and constant of inertia is used. Constant of inertia of the whole system is given by

$$\mathrm{H_{sys}} = \frac{\sum_{i=1}^{N} \mathrm{S_{ni}H_i}}{\mathrm{S_{n,sys}}} \tag{3}$$

Inertia of a whole grid can be calculated in form of kinetic energy stored in rotating machines. And its equation is given below:

$$E_{k,sys} = S_{n,sys} H_{sys} = \sum_{i=1}^{N} S_{ni} H_i \ [MW.s] \quad (4)$$

1) Synthetic Inertia

Synthetic inertia is explained by [9] which is given below:
Synthetic inertia: It is the inertia that is controllable with the help of electrical torque from a machine that is proportional to the RoCoF at the terminals of the generating unit.
Constant of synthetic inertia:

$$\Delta P_{e,i} = -2H_{syn,i}\frac{d\omega_t}{dt}\omega_t \quad (5)$$

To give an inertia response the torque must be proportional to RoCoF.

IV. Simulation and Results

In this research we will consider two cases for primary control reserve studies to study the behavior of the frequency after a sudden contingency on the power system. First case is high reserve case in which their will be sufficient reserves present in the system to cater any sudden contingency like load increase or sudden generation loss. Second case is low reserve case in which the amount of reserve present in the system is less than the amount required for frequency stabilization. These cases are discussed separately containing two scenarios separately in each of the case along with simulation results showing frequency deviations for different renewable penetration levels in the system.

A. Case 1

In this case primary reserves present in the system will be of amount of 2500 MW to withstand a sudden generation loss of 2000 MW in the system, it may be forecast error or load increase on the system. Contingency may be in form of sudden generation loss, load increase and forecast error of renewable generation. There are four renewable penetration level considered in this simulation, which are 0%, 10%, 20% and 30%. At these renewable penetration levels frequency behavior is checked. Also in this case FCR deployment rate considered are 20 seconds for first scenario and 10 seconds for second scenario.

1) First Scenario

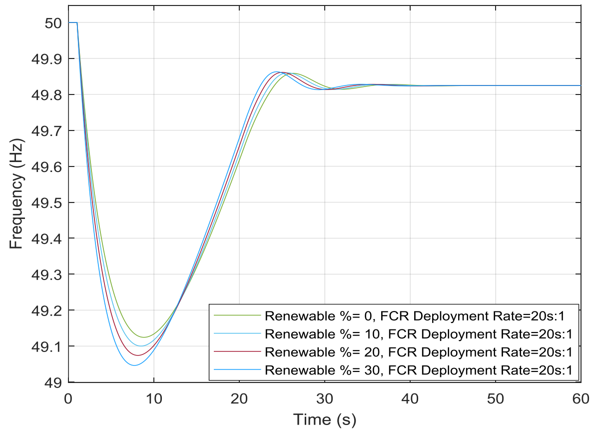

Figure 4. Simulation Result of Case 1, Scenario 1

Our main focus is renewable penetration, that is how it affect frequency of the power system. In the above figure 4 we can see that after a contingency, there is a deviation in the frequency of the system but primary reserve in the system catch the frequency and stabilize it at some point below its reference value 50 Hz. In Pakistan power act 2005 [10] the UFLS (Under frequency load shedding) is set to be 49 Hz, after this point load has to be shed to prevent system collapse and unstability. In this scenario FCR deployment is 20 seconds, mean all the reserve will be available within 20 seconds to cater any sudden contingency in the system. In this scenario all the renewable penetration levels frequency remains in UFLS point and the system doesn't goes into to load-shedding mode because all the frequency deviation curves shows that frequency is caught before 49 Hz, that is before UFLS point.

2) Second Scenario

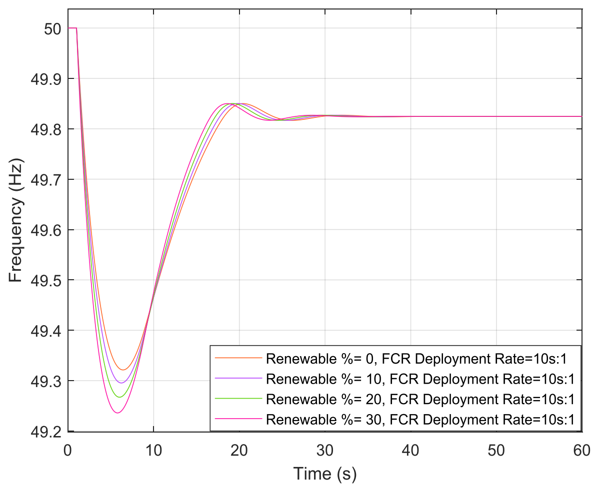

Figure 5. Simulation Result of Case 1, Scenario 2

In this simulation result FCR deployment rate is considered as 10 seconds to deploy primary reserves. Frequency deviation curves in this scenario are caught before 49.2 Hz so it is obvious that frequency deviation is caught before UFLS point and their will be no need of load shedding. So the primary reserves present are enough to stabilize the frequency to some point below its referency value 50 Hz. For frequency to get back to its nominal value secondary reserves will be activated.

In this case two scenarios are discussed and after the comparison of these scenarios we can say that when FCR deployment rate is increased, frequency deviations are arrested earlier than the previous one. In this case FCR deployment rate considered for first scenario is 20 seconds and for second scenario is 10 seconds. In fisrt scenario the lowest possible deviation of frequency cure is approximately 49.05 Hz and in second scenario the lowest possible frequency curve is 49.24 Hz. So from the above cases we can say that as the renewable penetration in a power system increases, system inertia decreases respectively and frequency deviation increases as inertia decreases. So from this we concluded that renewable penetration have a inverse impact on inertia of the system, as renewable penetration increases inertia of the system decreases and when renewable penetration decreases inertia of the system decreases respectively.

B. *Case 2*

In this case primary reserves present in the system will be less that the contingency appear in the system. Primary reserves available in the system will be 1800 MW, and the contingency appear in the system will be 2000 MW. In this case the system frequency deviate towards 48.5 Hz approximately which is too far below the UFLS point and the system will goes into load shedding. In this case frequency deployment rates will also be taken as 20 seconds and 10 seconds to deploy primary frequency control reserves. Inertia constant values in this case are also the same as previous case, so inertia of the system will also be the same in these scenarios as compared to the previous scenarios. Frequency deviation values in this case are higher as compared to the previous case.

1) *First Scenario*

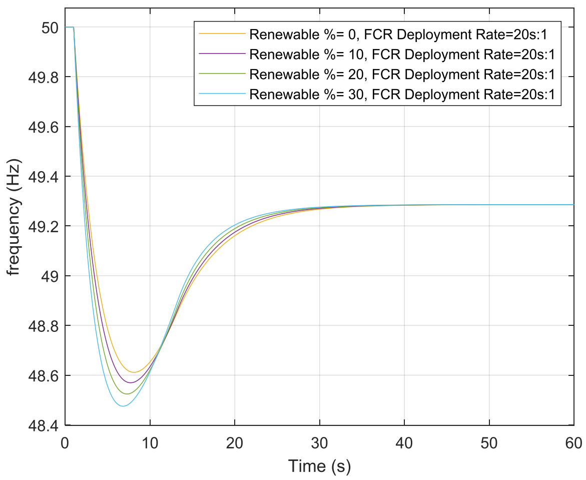

Figure 6. Simulation Result of Case 2, Scenario 1

In this scenario primary reserves are less than the contingency appeared in the system as compared to the previous case, therefore frequency. After the contingency system frequency starts to deviate from its nominal value, but the primary reserves available are not enough to catch frequency before ULFS point so the system will goes into load shedding to stabilize the frequency and frequency will be caught at approximately 48.48 Hz and will stabilize frequency at approximately 49.3 Hz. And for frequency to get back to its nominal value secondary reserves will be activated. In this scenario frequency control reserves deployment rates is 20 seconds. In this scenario renewable energy penetration levels are also same as the previous scenarios like 0%, 10%, 20% and 30% renewable generation penetration in the Pakistan power system. For renewable penetration of 30% the frequency deviation is 48.48 Hz and for 20% penetration frequency deviation is 48.52 Hz and for 10 % and 0% penetration frequency deviations are 48.57 Hz and 48.61 Hz respectively.

2) *Second Scenario*

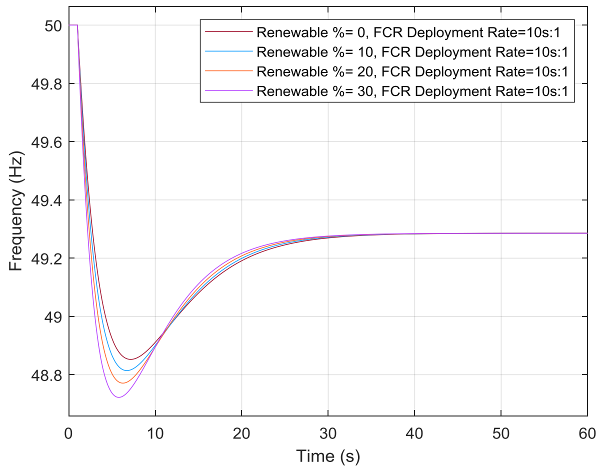

Figure 7. Simulation Result of Case 2, Scenario 2

In this scenario frequency deployment rate is 10 seconds, so frequency deviation is caught early in this scenario as compared to the scenario 1 in this case. For renewable penetration of 0% the frequency deviation value recorded is 48.85 Hz, and for renewable penetration of 10% frequency deviation value recorded is 48.81 Hz. For renewable penetration levels of 20% and 30% frequency deviation values recorded are 48.77 Hz and 48.72 Hz respectively. From the above both scenarios we concluded that as fast as the reserves deployment rate is, frequency of the power system is caught and stabilized fast. Also frequency dip in first scenario is large as compared to the second scenario because frequency control reserves deployment rate in first scenario is 10 seconds more and its response is late as compared to the second scenario which is 10 seconds. So in second scenario frequency is caught earlier than the first scenario in which frequency dip is larger.

C. FCR Deployment in both cases

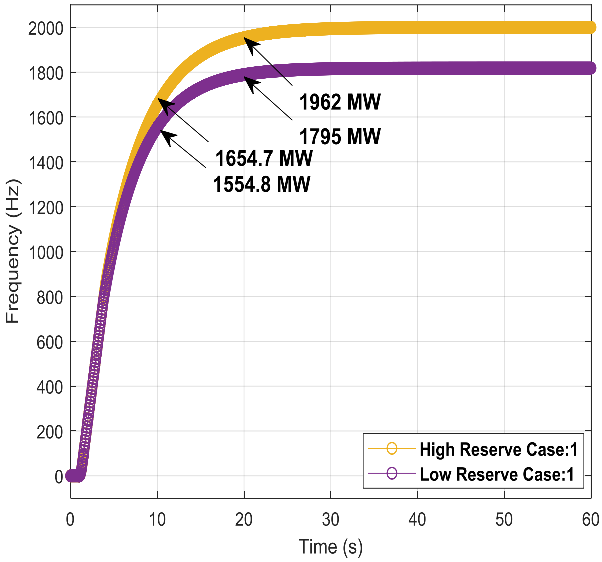

Figure 8. FCR Deployment in case 1 and 2

The above figure 8 shows frequency control reserves deployment in bothe cases in the simulations. In case 1 when primary reserves are deployed than the reserve power available to the power system at 10 seconds is 1654.7 MW and at 20 seconds reserve power available to the power system is 1962 MW. And in case 2 when primary reserves are deployed then the reserve power available at 10 seconds to the power system is 1554.8 MW and at 20 seconds reserve power available to the power system is 1795 MW.

CONCUSLION

As we know that addition of renewable generation to a power system creates variability and complexity and therefore all these problems are met with operating reserves to prevent large deviation in grid frequency. In Pakistan renewable penetration in national grid is also going to increase as compared to current situation. So, it was a need for frequency control studies in future Pakistan power scenarios. Focus of this research is the impact of renewable penetration on frequency of the grid and PFC reserves estimation in Pakistan national grid. Reserves deployment and its requirement in future Pakistan power scenarios are proposed. In high reserves case, when a sudden loss of generation occurs frequency starts to deviate from its nominal value. But due to high PFC reserves present in the system frequency deviation is arrested earlier and stabilized at a point lower than the reference value and in all the scenarios in first case not a single frequency curve passes the UFLS set point. In low reserves case, when we checked all the four scenarios for frequency deviations after a sudden contingency in the system. All the four frequency curves for different levels of renewable penetration, passes the UFLS set point and the system must shed some load to prevent any unwanted situation to appear in the system. In this case reserves were not enough to arrest frequency deviations before they pass the UFLS point but still frequency is stabilized at a point much lower than the reference value.

REFERENCES

[1] Hassan. Bevrani, Robust Power System Frequency Control, Second. Springer Cham Heidelberg New York Dordrecht London, 2009.

[2] European Network of Transmission System Operators (ENTSO-E), "ENTSO-E Operation Handbook (Policy 1)," no. Cc, p. 63, 2009.

[3] A. F. Guidelines, "Network Code on Load-Frequency Control and Reserves in line with the ACER Framework Guidelines on Electricity System Operation," vol. 6, no. February 2012, 2013.

[4] E. Ela, M. Milligan, and B. Kirby, "Operating Reserves and Variable Generation: A comprehensive review of current strategies, studies, and fundamental research on the impact that increased penetration of variable renewable generation has on power system operating reserves," no. August, pp. 1–103, 2011.

[5] K. Das, M. Litong-palima, P. Maule, and P. E. Sørensen, "Adequacy of Operating Reserves for Power Systems in Future European Wind Power Scenarios," 2015.

[6] K. Das, M. Altin, A. D. Hansen, P. E. Sorensen, and H. Abildgaard, "Primary reserve studies for high wind power penetrated systems," 2015 IEEE Eindhoven PowerTech, PowerTech 2015, 2015.

[7] N.2009c, "Procedure for Determining Interconnection Frequency Limits.," 2003.

[8] P. KUNDUR, "Power System Stability and Control." .

[9] R. Eriksson, N. Modig, and K. Elkington, "Synthetic inertia versus fast frequency response : a definition," vol. 12, pp. 507–514, 2018.

[10] E. P. Act, "Performance Standards (Distribution) Rules 2005 of Pakistan," vol. 1997, no. January, pp. 1–26, 2005.

IJEW 国际工程期刊 International Journal of Engineering Works انجینئرنگ کاموں کا بین الاقوامی جرنل

International Journal of Engineering Works
ISSN-p: 2521-2419
ISSN-e: 2409-2770
Vol. 6, Issue 12, PP. 543-546, December 2019
https://www.ijew.io/
https://doi.org/10.34259/ijew.19.612543546

Partial Replacement of Cement by Industrial Fly Ash as Binding Agent

Muhammad Moeen [1], Qi Tian [2]*, Muhammad Yaseen [3], Abdul Nasir [4], Zawar Hussain [5], Mudassir Habib [6]
[1,2,5,6] College of Environmental Science and Engineering, Taiyuan University of Technology, Taiyuan 030024, China
[1,2,] School of Civil Engineering, Taiyuan University of Technology, Taiyuan 030024, China
[1,3] Institute of Soil and Environmental Sciences, University of Agriculture, Faisalabad, 38000, Pakistan
[4] Department of Structure and Environmental Engineering, University of Agriculture, Faisalabad, 38000, Pakistan
moeenejaz79@gamil.com[1], 412559908@qq.com[2], dr.yaseen@gmail.com[3], anawan@uaf.edu.pk[4],
hussain.zawar1292@hotmail.com[5], mudassirhabib62@yahoo.com[6]
Received: 16 December, Revised: 26 December, Accepted: 28 December

***Abstract*—** Concrete is the key component that is usually used in construction as in the world containing 70-75 percent of natural rocks, sand and 10-15 percent of Ordinary Portland Cement (OPC). Concerns about global sustainability of construction technology and the efficient use of structural aggregates in concrete will help minimize construction problems. Because of the high cost of cement, construction has become more costly and due to CO_2 pollution and other harmful heavy metals during the cement production process, it becomes environmentally dangerous, so we can partly replace the portend cement with fly ash created as solid waste by different industries and power generation plants. At dumping sites, this fly ash is dumped locally, causing air pollution. Because of its binding behavior, we use fly ash as a binding constituent. The purpose behind this research work was to evaluate the tensile and compressive strength of specimens while using different fly ashes in favor of environmentally friendly technique and to perform the properties of workout strength and the variation pattern with mixing in different proportions of different tests such as tensile and compressive strength after 7, 14, 21 and 28 days of healing. Cement was replaced by various types of ashes including coal ash, *Vachellia nilotica* (Kikar) ash, *Dalbergia sisso* (shisham) with different concentration of 10, 20, 30, 40 and 50 % of each. Results showed that when 10% of coal ash, *Vachellia nilotica* (kikar) ash, *Dalbergia sisso* (shisham) was used, concrete and mortar tensile and compressive strength increased with the increase in healing time. While the decrease in intensity was observed in samples with proportions of 20, 30, 40 and 50% with the same healing time. In addition the samples with coal, *Vachellia nilotica* (Kikar) ash, *Dalbergia sissoo* (shisham) ash, a decreasing trend in strength along with weight decrease was observed. By using coal ash upto 10% can reduce the 13.5% construction cost without losing strength properties in concrete. Such building materials can be used in lightweight buildings such as farm buildings for poultry and dairy farm buildings.

***Keywords*—** Fly Ash, Incubation Time, Tensile Strength, Compressive Strength.

I. Introduction

The use of concrete is a construction constituent and one of the oldest methods used in a modern world. Concrete is largest natural resources consuming, and is durable, strengthen and easily available. So the largest number of natural resources is being consumed by concrete industry. 10-15% of the cement based adhesives and 15% of water is included in the 70-75% 0f total concrete, while it is estimated that annual production of concrete is 37-41.14 million tons in Pakistan. The production of portland concrete is very time consuming and energy consuming process [9].

'Calcinations' is a process in which clay and limestone are heated at 1450°C, and cement is a mixture of limestone and clay produces after the process of calcinations and is a powdery material in nature. Concrete is a mixture of cement, gravel, sand and water and cement is the main component of concrete and is used as binding agent. Concrete is durable, cheap and easily available in market, this is the reason that it is used as construction material in worldwide [14].Cement industry consumes 10-15% cement based adhesive material, 70-75% natural rocks and 15% water, that is why this industry is the biggest industry for consuming the natural resources. Cement production causes noise pollution by operating machinery, by emitting the airborne particles and greenhouse gases, it cause the air pollution and many other environmental pollutions at the stages of its manufacturing. Cement industry emits 5% anthropogenic CO2, among that 40% is emitted during fossil fuels use, and during the chemical process 50% is emitted [2].

During the cement production, many toxic heavy metals like thallium, cadmium and mercury are produced, and except this, during the production of 1000kg of cement, 900kg of CO2 is emitted. As a result of increasing the human population, there is a need of more construction for living, ultimately increase the environmental pollution and other health hazards [7]. In different industries, during the burning process of coal and wood, Ash is left as residue. The electricity power generation houses in Pakistan, which use coal as a fuel, ash is highly obtained from these power houses. In sugar mills, where the sugar fibers are burnt for the electricity power generation, million tons of the fly ash is produced from these mills. Annually Pakistan produced the 6102000 tons of coal ash while 25000 tons of wood [8].

Because of the pozzolanic behavior of ash, it is used in concrete production, for producing the low cost and light weight concrete. Ash can also be produced with the help of rubber, wood saw, wood, coal burning and brick kilns etc. Fly ash causes many health hazards issues by flying in the air, causing the air pollution, causing the environmental pollution [4]. For the production of concrete, fly ash can be used as cost effective and environmental friendly technique. To enhance the binding properties for the production of concrete, we can replace the cement with fly ash, because ash compounds have the binding properties, and also the ash particles are round and very similar in size with cement particles. Simply we can save the industrial waste, sand and cement by using the fly-ash [5].

Light weight aggregate concrete offers the environmental advantages, because it is versatile and an imperative material, and it is expected, this concrete can further help in twisting up the over-aching material for coming decades. The light weight concrete has various applications in floors, window decoration dividers, given way plates, ranges, shell house-tops, in extensive variety of precast elements and also in multi-story building houses. To reduce the dead weight of structure, light weight aggregate concrete is used [13]. The buildings which are being destroyed by the earthquakes, which have ultimately negative impact on civil engineering structures, this concrete can help to reduce the earthquake destroying risks. Higher quality/weight extent, better moldable strain limit, lower coefficient of warm augmentation and unrivaled warmth and sound partition properties because of air voids of the light weight sums are central purposes of helper lightweight aggregate bond [1]. So in this study we produce low cost and environment friendly mortar by adding coal, Vachellia nilotica (kikar) and Dalbergia sissoo (shisham) ash.

II. MATERIAL AND METHODS

Following materials were used during this research work for experimental purpose.

A. *Materials*

Ordinary Portland cement (OPC) was used for experimental purpose due to locally available in Pakistan. OPC is commonly used in concrete for construction purposes. Cement used for experiment purpose was bought from market. Before using in experiment sieve analysis of cement was conducted to find out the size of cement. Fine aggregate also known as sand which usually occurred in river, lake, sea and those areas where flood had happened. It is easily available in all countries like Pakistan. For manufacturing of concrete standard ratio was used as 1:2:3. In which 2 part of total weight sand was used. In concrete strength sand play important role to fill the pores in concrete. Almost 30% volume of concrete consists on sand [12].

Gravels also known as coarse aggregate used in concrete and play an important role to enhance the strength of concrete for construction purpose [10]. For manufacturing of concrete standard ratio was used as 1:2:3, in which 4 part of total weight of gravel was used. For experimental purpose different ashes were taken from different industries in Faisalabad (Toseef Housery, Rasheed Textile Mills Ltd, and some local Sizing Mills) which includes coal, Vachellia nilotica (kikar) and Dalbergia sissoo (shisham) ash.

B. *Samples prepartaion and Curing*

Multi stage random sampling technique was used for sampling. Fly ash was added in the samples with the proportion of 10, 20, 30, 40 and 50%. All the samples were cured in a water tank for four different time periods including 7, 14, 21 and 28 days [6]. Different samples of concrete were prepared with ratio 1: 2: 3 in which 1 part of gravel, 2 parts of cement and 3 parts of sand were used. So we prepare the samples according to shape and size of die [16]. For preparing sample tiles die was used for compressive strength and according the shape and size of machine the die was prepared and samples of almost 1000g weight were prepared.

C. *Testing*

For measuring tensile strength of the samples Tensile testing machine was used and for measuring the compressive strength concrete testing machine was used [11]. Before testing all the samples were taken out from water tank 3 hours before testing procedure and all the testing were done at room temperature.

III. RESULTS AND DISCUSSION

A. *Tensile Strength*

Total 216 briquettes samples were prepared to measure the tensile strength of samples. Briquettes tensile strength was measured using a cement testing machine with different percentages of Coal Ash, Vachellia nilotica (kikar) ash, Dalbergia sissoo (shisham) ash as a partial cement replacement are listed below.

1) *Tensile Strength of Briquettes Containing Coal Ash*

Fig.1 defines the average values of briquettes tensile strength containing different proportions of coal ash as a partial replacement of cement. Total 24 specimens of three replicates were tested as a partial substitution of cement for the tensile strength test with different proportions of coal ash 0, 10, 20, 30, 40 and 50%. According to the findings during 7, 14, 21 and 28 days of curing, the 10% coal ash replacement showed better results than all other treatments at 28 days 2.72 MPa. While the samples with 20, 30, 40 and 50% coal ash begin to decrease with respect to the 28-day curing treatment. Whereas the samples amended with coal ash of 20% ratio has strength closest to 10% replacement 2.51 MPa , similarly 30, 40 and 50% showed less tensile strength than 20% amendment and minimum tensile strength (1.98 MPa) as achieved by replacing coal ash up to 50% with 28 days curing. As the % of amendment was increased above 10 percent, there was significant reduction in tensile strength of samples as shown in figure 1. The findings were the same as the results of [18].

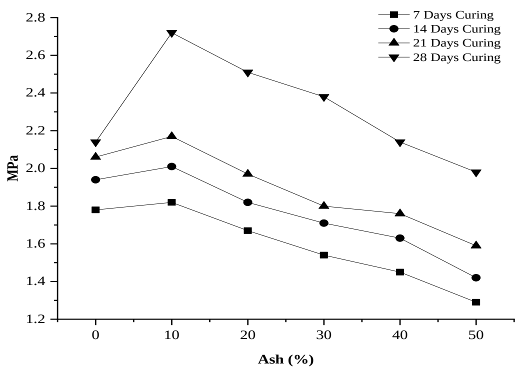

Fig.1: Tensile strength of briquettes Containing Coal Ash in MPa.

2) Tensile Strength of Briquettes Containing Vachellia nilotica (Kikar) Ash

Fig.2 represent the mean values of briquettes tensile strength containing different percentages of Vachellia nilotica (Kikar) ash as a partial cement substitute. Total 24 samples of three concrete replicates were tested as a partial substitution of cement for the tensile strength with different proportions of vachellia nilotica (Kikar) ash 0, 10, 20, 30, 40, and 50% cured for 7, 14, 21 and 28 days, according to the results the amendment of 10 % cured for 28 days showed the significant results of 2.49 MPa. When using the vachellia nilotica (kikar) ash the tensile strength of the 20, 30, 40, and 50% ratio begins to decrease with respect to the 28 days curing. While the 20% ash showed (2.03 MPa) tensile strength which was lesser than of 10% amendment similarly 30% showed a lower tensile strength than the 20% and 50% replacement showed the minimum tensile strength of (1.88 MPa). The results we obtained were identical to findings of [3].

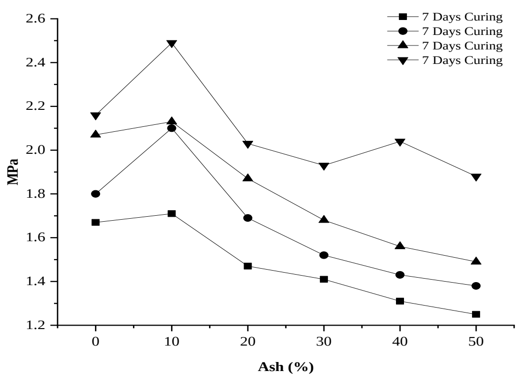

Fig. 2: Tensile Strength of Briquettes Containing Vachellia nilotica (Kikar) Ash

3) Tensile Strength of Briquettes Containing Dalbergia sissoo (shisham) Ash

Fig.3 defines the mean values of briquettes tensile strength containing the different percentage of dalbergia sissoo (shisham) ash as a partially replaced by ordinary Portland cement. Total 24 samples with three replications were analyzed as a partially replaced of cement for the tensile strength test with different proportions of Dalbergia sissoo (shisham) ash 0, 10, 20, 30, 40 and 50% with different curing of 7, 14, 21 and 28 days. Amendments showed better results than the controlled treatment and according to the results samples partially replaced by 10% Dalbergia sissoo (shisham) ash has the significant result of 2.12 MPa cured for 28 days. When dalbergia sissoo (shisham) ash concentration was increased to 20, 30, 40 and 50% the tensile strength of briquettes started decreasing with regard to 28 days curing time. 30% showed the lower tensile strength than the 20% ratio, this indicate that as the percentage of dalbergia sissoo (shisham) ash increases above 10%, the tensile strength of the briquettes decreases and the lower tensile strength and it was found by 50% replacement of dalbergia sissoo (shisham) ash the minimum tensile strength (1.58 MPa) was obtained which was the least value as compared to all other treatments. The results we obtained were similar to the finding of [15]

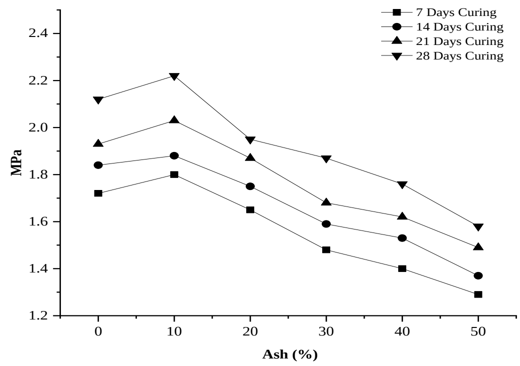

Fig.3 Tensile Strength of Briquettes Containing *Dalbergia sissoo* (shisham) Ash

B. Compressive Strength

Taking into account the above findings of the tensile strength of Coal, vachellia nilotica (Kikar) and dalbergia sissoo (Shisham) ash, we obtain the significant tensile strength by using coal ash, so to proceed further we partially substitute the cement only with coal ash for evaluating the compressive strength of concrete.

Fig.4 describes the mean values of compressive strength of tiles containing the different percentages of coal ash as a partial replacement of (OPC) cement. Total 24 specimens of three replicates were tested as a partial substitution of cement for the compressive strength with different proportions of amendment 0, 10, 20, 30, 40 and 50. According to the results the control procedure showed the best results in 7, 14, 21 and 28 days of curing compared to all other amendments (38.75 MPa). The samples having 10% coal ash showed the best performance of (40.83 MPa) compressive strength cured for 28 days. While the results of 20% coal ash replacement was close to the control treatment (35.37 MPa). 30% amendment showed a lower compressive strength than 20%, likewise 40% and 50% both showed a lower tensile strength than 30% and the least compressive strength (22.59 MPa) was noticed when the amount of amendment was increased to 50% cured for 28 days . As the percentage age of coal ash rises above 10%, it indicates that the compressive strength of the tiles begins to decline. The similar results were obtained in the study by [17].

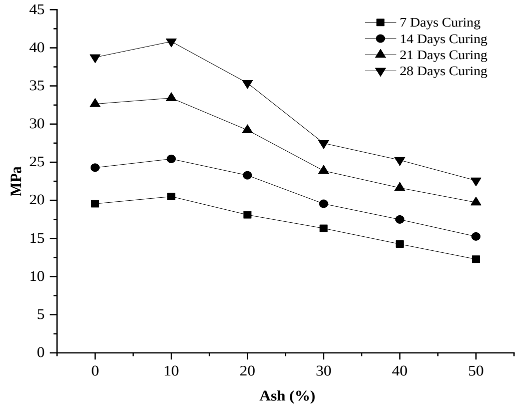

Fig.4 Compressive Strength of Tiles Containing Coal Ash

CONCUSLION

Based on the results of tensile and compressive strength of this experimental study, it was concluded that Fly ash could be used for the production of light weight concrete and the use of fly ash in concrete can reduce the environmental pollution. The coal ash can make the concrete of (40.83 MPa) strength which is light weight strengthened. Finally this technique is an environmental friendly and it can reduce the risk of earth quick damage in the locality.

ACKNOWLEDGMENT

The author wish to express the gratitude to his supervisors for their continuous support throughout the study and National Highways Authority (NHA), Faislaabad, Pakistan for helping to perform tests in their laboratory.

REFERENCES

[1] Aragão, F. (2007). Effects of aggregates on properties and performance of mastics and superpave hot mix asphalt mixtures.J. Clerk Maxwell, A Treatise on Electricity and Magnetism, 3rd ed., vol. 2. Oxford: Clarendon, 1892, pp.68–73.

[2] Benhelal, E., Zahedi, G., Shamsaei, E., & Bahadori, A. (2013). Global strategies and potentials to curb CO2 emissions in cement industry. Journal of cleaner production, 51, 142-161.

[3] Cheah, C. B., & Ramli, M. (2011). The implementation of wood waste ash as a partial cement replacement material in the production of structural grade concrete and mortar: An overview. Resources, Conservation and Recycling, 55(7), 669-685.

[4] Dmitrienko, M. A., & Strizhak, P. A. (2018). Coal-water slurries containing petrochemicals to solve problems of air pollution by coal thermal power stations and boiler plants: An introductory review. Science of the Total Environment, 613, 1117-1129.

[5] Drochytka, R., Zach, J., Korjenic, A., & Hroudová, J. (2013). Improving the energy efficiency in buildings while reducing the waste using autoclaved aerated concrete made from power industry waste. Energy and Buildings, 58, 319-323.

[6] Formosa, L. M., Mallia, B., Bull, T., & Camilleri, J. (2012). The microstructure and surface morphology of radiopaque tricalcium silicate cement exposed to different curing conditions. Dental Materials, 28(5), 584-595.

[7] Kampa, M., & Castanas, E. (2008). Human health effects of air pollution. Environmental pollution, 151(2), 362-367.

[8] Kazmi, Syed MS, Safeer Abbas, Muhammad A. Saleem, Muhammad J. Munir, and Anwar Khitab. "Manufacturing of sustainable clay bricks: Utilization of waste sugarcane bagasse and rice husk ashes." Construction and building materials 120 (2016): 29-41.

[9] Madlool, N. A., Saidur, R., Hossain, M. S., & Rahim, N. A. (2011). A critical review on energy use and savings in the cement industries. Renewable and Sustainable Energy Reviews, 15(4), 2042-2060.

[10] Meddah, M. S., Zitouni, S., & Belâabes, S. (2010). Effect of content and particle size distribution of coarse aggregate on the compressive strength of concrete. Construction and Building Materials, 24(4), 505-512.

[11] Pascale, G., Di Leo, A., & Bonora, V. (2003). Nondestructive assessment of the actual compressive strength of high-strength concrete. Journal of Materials in Civil Engineering, 15(5), 452-459.

[12] Qian, Z., Garboczi, E. J., Ye, G., & Schlangen, E. (2016). Anm: a geometrical model for the composite structure of mortar and concrete using real-shape particles. Materials and Structures, 49(1-2), 149-158.

[13] Sajedi, F., & Shafigh, P. (2012). High-strength lightweight concrete using leca, silica fume, and limestone. Arabian journal for Science and engineering, 37(7), 1885-1893.

[14] Schneider, M., Romer, M., Tschudin, M., & Bolio, H. (2011). Sustainable cement production—present and future. Cement and concrete research, 41(7), 642-650.

[15] Siddique, R. (2012). Utilization of wood ash in concrete manufacturing. Resources, conservation and Recycling, 67, 27-33.

[16] Wang, H. T., and L. C. Wang. "Experimental study on static and dynamic mechanical properties of steel fiber reinforced lightweight aggregate concrete." Construction and Building Materials 38 (2013): 1146-1151.

[17] Wongkeo, W., & Chaipanich, A. (2010). Compressive strength, microstructure and thermal analysis of autoclaved and air cured structural lightweight concrete made with coal bottom ash and silica fume. Materials Science and Engineering: A, 527(16-17), 3676-3684.

[18] Yasar, E., Atis, C. D., Kilic, A., & Gulsen, H. (2003). Strength properties of lightweight concrete made with basaltic pumice and fly ash. Materials Letters, 57(15), 2267-2270.

International Journal of Engineering Works
ISSN-p: 2521-2419
ISSN-e: 2409-2770
Vol. 6, Issue 12, PP. 556-563, December 2019
https://www.ijew.io/
https://doi.org/10.34259/ijew.19.612556563

Methodology to Find and Mitigate Transient Recovery Voltages (T.R.V) Considering Various Abnormal Scenarios: A Case Study of IEEE-39 Bus System

Rahman Ullah Khan[1], Dr. Abdul Basit[2]
[1,2] US-Pakistan Center for Advanced Studies in-Energy (USPCAS-E), University of Engineering & Technology (UET) Peshawar, Pakistan.
engr.rk@live.com[1], abdul.basit@uetpeshawar.edu.pk[2]
Received: 18 December, Revised: 26 December, Accepted: 27 December

***Abstract*—** Abnormal switching transients are those transients that arise during unbalanced faults interruption e.g., single-line-to-ground (S.L.G) fault, double-line-to-ground (D.L.G) fault, or three-phase fault. Circuit-breaker is the first line of defense to face these abnormal transients. Whenever a circuit-breaker encounters these abnormal transients, it changes its state from close to open by moving away its closed contacts. Circuit-breaker try to block large amount of fault-current from flowing, and these transients appear in the form of multitude-voltage around circuit-breaker' open contacts. This large amount of voltage is known as transient recovery voltage (T.R.V). This T.R.V is normally three to five-times of the rated operating voltage. Circuit-breaker failure/damage occurs only when it is unable to withstand this T.R.V for which it is designed. In this research, methodology is developed to correctly find the value of T.R.V by taking care of various abnormal and worst-case switching scenarios. T.R.V curtailment is a serious challenge for the power system experts. This study is a competent effort to address this challenge. Electromagnetic-Alternative Transient Program (EM-A.T.P) software is used for simulation of the test network IEEE-39 bus system.

***Keywords*—** Abnormal Switching; S.L.G; D.L.G; Circuit-breaker; T.R.V; EM-A.T.P software; IEEE-39 bus system.

I. Introduction

Whenever a circuit changes its operating-state, it generates transients. These transients produce high voltage around the contacts of a circuit-breaker known as transient recovery voltage (T.R.V). T.R.V depends upon circuit-parameters and conditions. T.R.V has a very important role in circuit-breaker, that's why it is very important to carry-out T.V.R study for circuit-breakers. [1]

Normally, circuit-breaker's selection is based upon its short-circuit withstand capability in a circuit. When a fault occurs, circuit-breaker interrupts that fault-current. This interruption of fault-current give rise to T.R.V, which produce maligning impacts on circuit-breaker. Different circuits have different T.R.V values due to different circuit parameters. It has multitude voltage and frequency. T.R.V is graphically represented in figure 1.

"T.R.V is each-step voltage-difference of current-entering and leaving points of a circuit-breaker. In a fault event, incoming-side of circuit-breaker try to maintain nominal voltage and frequency, while outgoing-side faces high voltage and frequency. This voltage difference is called T.R.V."

Whenever there is circuit-breaker operation, there will be T.R.V. But the worst-case T.R.V is produced when circuit-breaker faces fault-current. Hence, circuit-breaker selection must be based upon severity of T.R.V. [1]

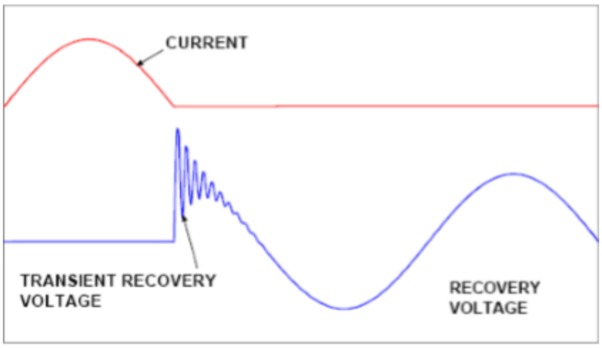

Figure 1: T.R.V

(1) T.R.V impacts on circuit breaker:
   i. Insulation- breakdown
   ii. Air-breakdown
   iii. Arcing-Medium-breakdown
   iv. Arc-Restriking Occurrence

(2) Impacting factors of T.R.V:
   i. System's load-characteristics.
   ii. Fault study information of a system.
   iii. Circuit-breaker' characteristics.
   iv. Transmission-lines characteristics.

v. Internal-characteristics of C.B.
vi. Grounding effect.
vii. T.R.V types and its wave-shapes [1] [2]

(3) Simulation Software:

Electromagnetic-Alternative Transient Program (E.M-A.T.P):

This software uses time-domain contingency variables. It collects the data of every circuit-component and converts this data into circuit-equations (differential-equations). The it solves these circuit-equations using integration-laws (Trapezium-rule) and Laplace-transforms. To produce the output in real-world time-domain, it uses inverse-Laplace transforms. [3] [4]

In this software model, electrical network is graphically represented. It is an easy drop-down software environment. It has the ability of multi-tasking, running multiple simulations at a time. All the circuits available in A.T.PDRAW are editable. [3] [4]

(4) Test Network:

New-England IEEE based 39-bus network:

IEEE based 39-bus test-network is a ten machines power system. Considered as widely used test network for research in power systems, it is mostly used in power system stability studies and other power system problems. There are many reasons for using this network as a simulation model instead of using a pragmatic network model, such as: [5]

i. Pragmatic model credentials are comparatively private.
ii. Pragmatic model outcomes are mainly nonspecific and particularly, fewer in number.
iii. Arithmetic scheming is tough since its data is in huge amount.
iv. Software abilities constraints is another drawback of a practical model, hence making it hard to handle huge amount of data.
v. System' data, static as well as dynamic data, is very hard to maintain. [5]

II. Literature review

Transient Recovery Voltage (T.R.V) depends on two categories of factors i.e. internal factors and external factors. These factors are categorized with reference to a circuit breaker of consideration. Internal factors are meant for internal characteristics of a circuit breaker e.g. arc characteristics (arching time, arc voltage, arc current etc.), arc quenching mechanism, and insulation level of circuit breaker. While external factors include type of fault, type of load connected, location of fault, length of transmission line, type of grounding, and surge capacitors. Some past work regarding T.R.V issue is briefed below.

A. Arc designing to cop up with T.R.V issue

Existence of a fault nearby to a circuit-breaker on the transmission-line is considered as the T.R.V from the transmission-line side. Short length of the transmission-line amid the circuit-breaker and fault-location produced this T.R.V. In the intermediate period of starting-T.R.V on transmission-line side, lasting for comparatively large time-span of some microseconds, SF6 circuit-breaker has the possibility of prevalence of thermal-breakdown. The way for determining T.R.V on the short transmission-line side subject to short-line fault scenario, is done by I.E.C-standards. [6]

T.R.V data that a circuit-breaker possibly to face during service is highly important in its designing and operation. sawtooth wave-shaped T.R.Vs are related to short line fault conditions. The sawtooth-shaped T.R.V's rising rate (ROR) is usually higher than that of encountered with oscillatory-T.R.V & it is a function of the line's characteristic-impedance. Peak value of T.R.V is normally lesser, due to distributed nature of parameters of transmission-line. Due to these parameters effect, travelling wave-shaped oscillation is observed in transmission-line voltage having positive and negative reflections at the location of fault & open-contacts of circuit-breaker, respectively. During the.starting portion of the T.R.V only triangular-shaped line side.T.R.V is significant. Fault current is high when fault is in the vicinity of a circuit-breaker, higher will be the initial rising-rate of the T.R.V. As the returning time required.for reflected-wave smaller, the peak of this wave drops. For short-line faults, T.R.V measurement are carried out using only single-phase faults for initial time span of fault. Assuming changes in source voltage is slight . [6]

EM-A.T.P software is used for T.R.V calculations and results comparison is done through I.E.C-standards. arc resistance modelling for SF-6 circuit-breaker is very important as it plays its role in initial-T.R.V. [6]

B. T.R.V's role investigation in circuit breaker failure analysis

T.R.V investigation studies are required to find out whether the circuit-breaker failure is linked with a T.R.V issue. T.R.V analysis is used to verify whether the circuit-breaker' rating can withstand these T.R.V's. [7]

When connected power system have fault scenarios of T.R.V-characteristics exceeding the rating of circuit-breaker, there is possibility of failing of C.B to interrupt fault-current. After the extinguishing of arc, the voltage producing around the C.B contacts called transient-recovery voltage (T.R.V). Inductive and capacitive parameters connected to the bus determine the behavior and shape of transients. [7]

For successful fault disruption, the fault-interrupting medium voltage known as break-down voltage, must always be higher than the T.R.V. If breaker rating is less than peak value of T.R.V, the increased value of T.R.V around the contact-gap will eventually breakdown the fault intruding medium. In other conditions, if the T.R.V-peak is within safe operating limits of the breaker, there is greater possibility of current re-ignition occurrence as initial micro-seconds just after current disruption the interrupting medium is still conducting and not become an insulator; it may have high conductivity and results in conduction. [7]

In starting few micro-seconds if T.R.V rate is high-rising, it may conjoin a current flow sufficient for arc-heating and reestablish the current-conduction. The T.R.V modification can be done by modifying the design of circuit-breaker or by means of added components. The best ever accepted methods are:

1. When the T.R.V is larger than circuit-breaker capacity, interchanging the existing C.B by one of greater voltage category, greater disrupting capacity, or together. As an substitute Zinc. Oxide -devices can also be used to decrease T.R.V. [7]

2. To modify the loading impedance of the circuit with the addition of capacitors, when the rising rate of T.R.V surpasses the definite value. [7]

In past, the focus was mainly upon internal factors of circuit breaker whenever there is need of addressing this issue of Transient Recovery Voltages (T.R.V). In recent developments, it is concluded that internal factors of circuit breaker play very little or no role in T.R.V. Therefore, in this research, my focus is only upon external factors. All of the external factors, upon which T.R.V depend, are designed to measure and preview the value of T.R.V. A bigger test network i.e. IEEE-39 bus system, is selected for simulation of different cases of T.R.V. This research is unique in its nature, as not only T.R.V measurement is presented, but also the mitigation of theses T.R.Vs is also presented.

III. METHODOLOGY

Methodology was developed in the following steps:

A. ATP simulation model development of IEEE-39 bus system

First of all, IEEE-39 bus system' components are modeled to get actual values as ATP software works on actual values rather than per unit values. It includes generator modeling, transmission line modeling, and load modeling.

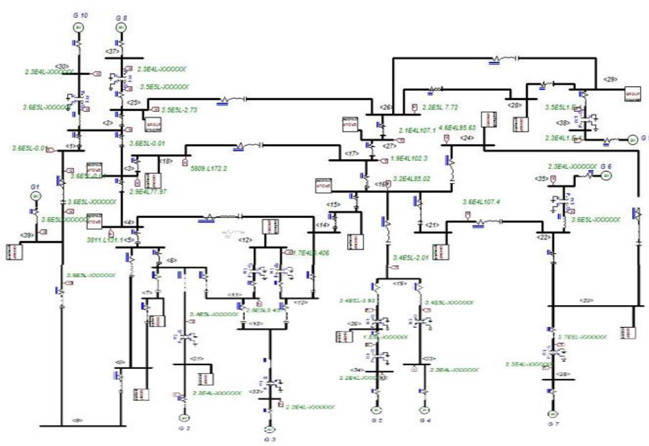

Figure 2: A.T.P Model of 39-bus network

B. Transient equations' derivation using network analysis

Mathematical representations and circuit analysis techniques are used for different networks to find out their transient equations. RL, RC, and LC networks are analyzed. LC network voltage equation is the actual mathematical representation of T.R.V.

RL circuit analysis:

$$I(t) = \frac{Vm}{\sqrt{R^2 + L^2\,\omega^2}}\left[\mathrm{Sin}\,(\omega t + \theta - \phi) - \mathrm{Sin}\,(\theta - \phi)e^{-\alpha t}\right]$$

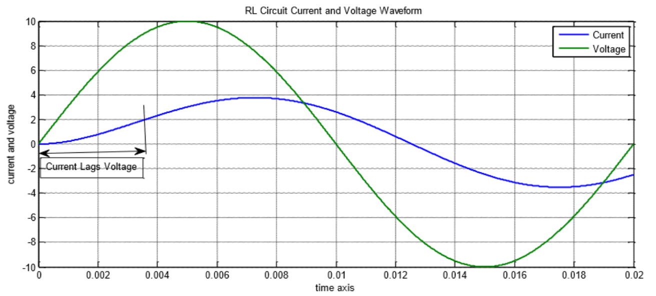

Figure 3: RL circuit waveform

RC circuit analysis:

$$V_c(t) = V_A\left[\mathrm{Sin}\,(\omega t + \theta - \phi) - \mathrm{Sin}\,(\theta - \phi)e^{-\alpha t}\right]$$

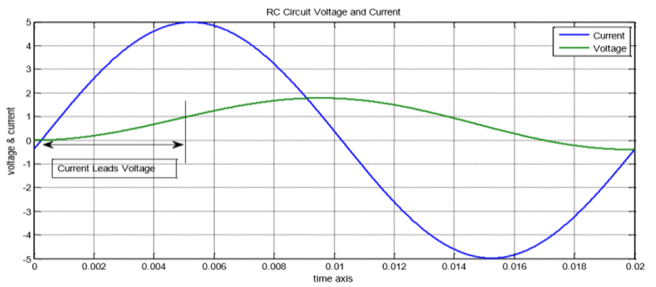

Figure 4: RC circuit waveform

LC circuit analysis:

$$Vc(t) = Vm\,(1 - \mathrm{Cos}\,\omega_o t)$$

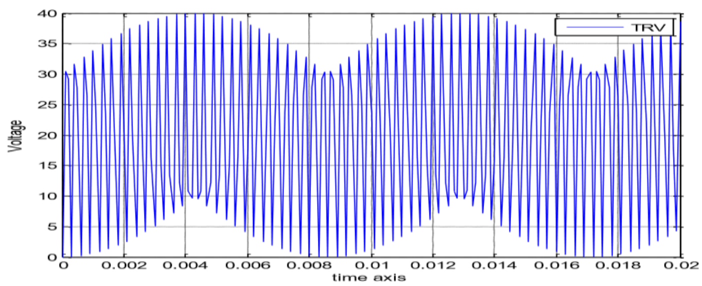

Figure 5: LC circuit waveform

C. Simulation of external factors affecting T.R.V in ATP

External factors include nature of fault, load-characteristics, transmission-line length, characteristic-impedance, fault-location, and grounding effect. [8] [9]

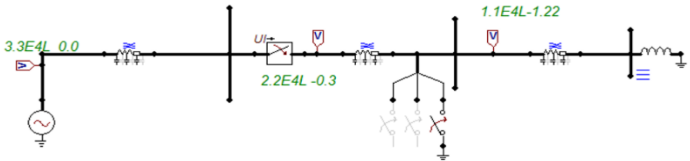

Figure 6: Test Network

1. Load Characteristics' Impact on T.R.V

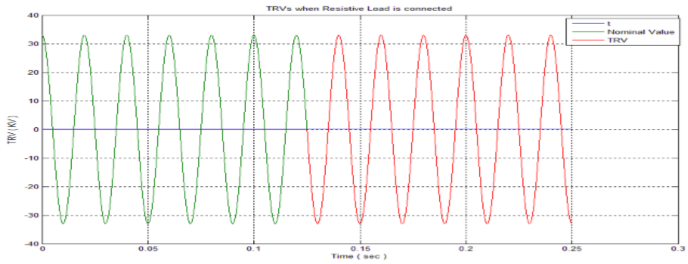

Figure 7: Resistive Load

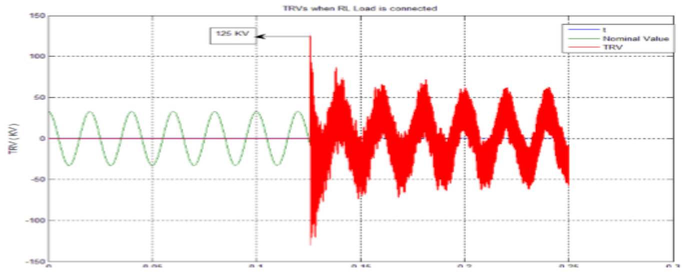

Figure 8: RL Load

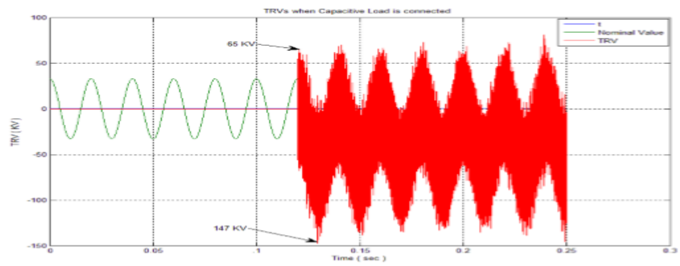

Figure 9: Capacitive Load

2. Transmission-line length [9]

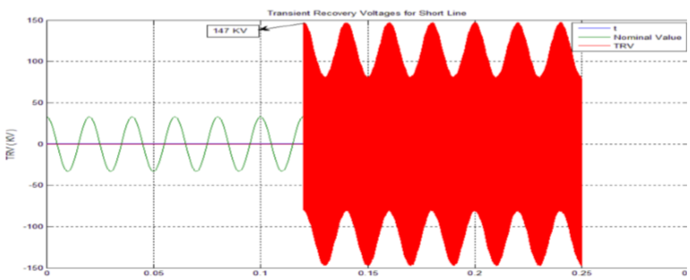

Figure 10: Short Line (80 kM)

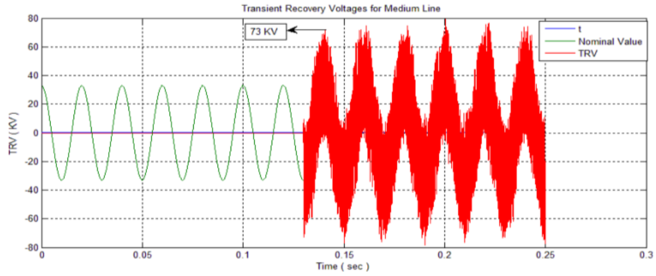

Figure 11: Medium Line (250 kM)

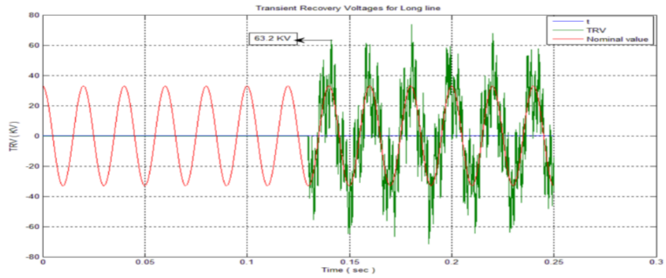

Figure 12: Long Line (>250 kM)

3. Fault location

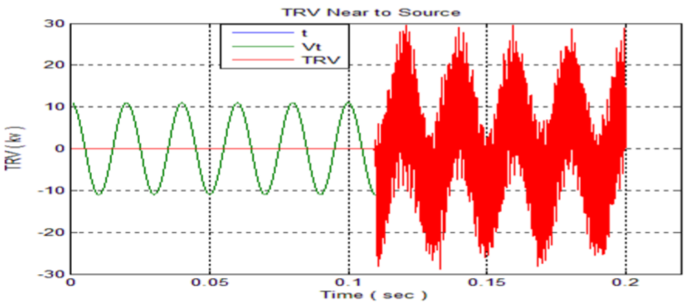

Figure 13: Fault near to source

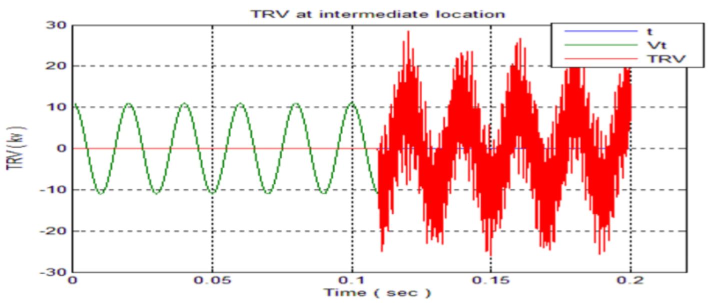

Figure 14: Fault at intermediate location

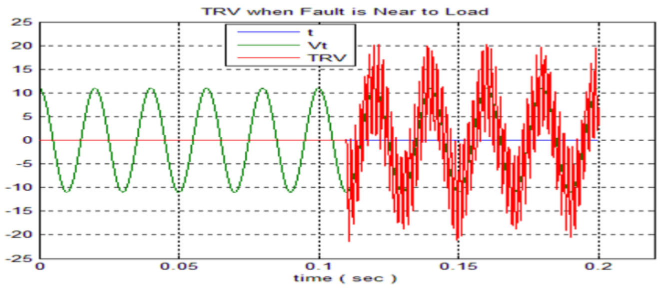

Figure 15: Fault near to load

4. Type of Grounding

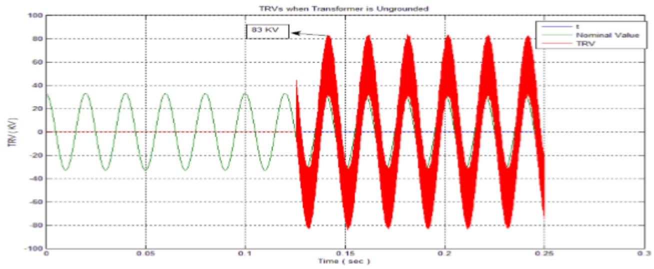

Figure 16: Ungrounded System

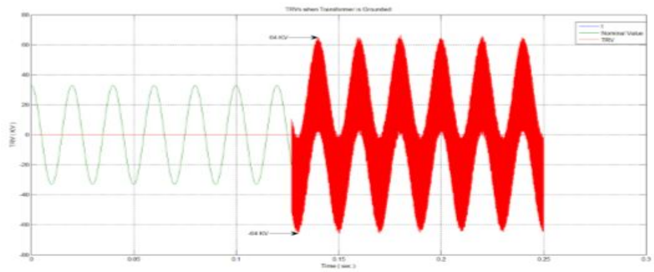

Figure 17: Grounded System

5. Characteristic Impedance

Zo = sqrt(L/C)

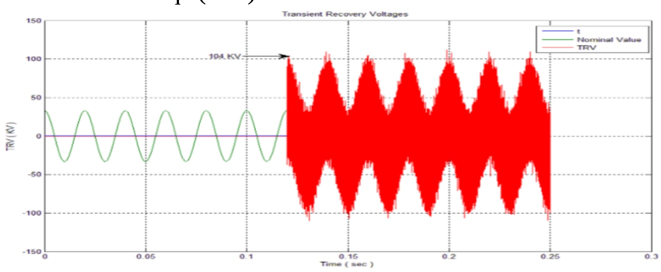

Figure 18: Case#1: L = 1.5mH , C = 0.1uF

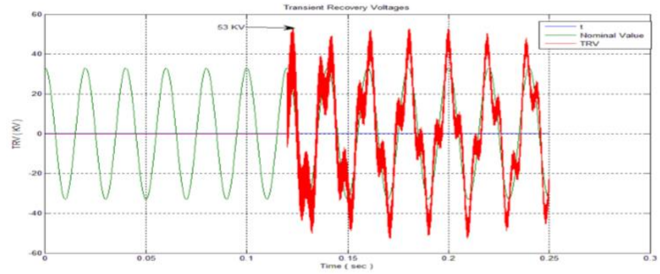

Figure 19: Case#2: L = 15mH , C = 10uF

Table 1: A.T.P Simulation Results of External Factors

External Factors	**Operating Voltage**	**Measured T.R.V**
Load-Characteristics	33-kV	33-kV (R) 104-kV (L) 105-kV (C) 125-kV (R.L)
Transmission-line length	33-kV	147-kV (Short) 73-kV (Medium) 63-kV (Long)
Characteristic-impedance	33-kV	106-kV (L=1.5 mH, C=0.1 µF) 53-kV (L =15 mH, C=10 µF)
Fault-location	11-kV	32-kV (Source Side) 26-kV (Midway) 22-kV (Load Side)
Grounding effect	33-kV	82-kV (Un-grounded N/W) 61-kV (Grounded N/W)

D. T.R.V Reduction Techniques

T.R.V is a quick and multitude phenomenon. Its implications to the power-system and its components are very severe. Following are some of the reasons explaining why this notorious phenomenon must be controlled.

Insulation- breakdown: Circuit-breaker' insulation is under so much stress due to this T.R.V, which causes Insulation-breakdown.

Air-breakdown: T.R.V puts huge stress on the air present in the space surrounding circuit-breaker, in close-proximity of fault-interrupting circuitry. And ultimately results in air-breakdown.

Arcing-Medium-breakdown: whenever there is a fault, circuit-breaker operates by switching its contacts from close to open state. During this contacts-switching process, arc is produced in the fault-interrupting medium due to fault-interruption. Fault will be successfully interrupted if this arc-medium sustains large value T.R.V. If arc-medium fails to sustain T.R.V, arc-medium collapses. As a result, current passes continuously through the circuit-breaker even if its contacts are opened. Eventually, circuit-breaker burns-down.

Taking in consideration the above mentioned reasons about severity of T.R.V, it is inevitable to devise techniques for curtailment of T.R.V. [2] [10]

1. Switching-Resistance technique

T.R.V can be controlled by correctly managing the arc-resistance. In this technique, rather than allowing the current to pass through the imaginary-resistance of the arc established, a physical by-pass resistor is employed around the contacts. So, current flow is divided between these two resistances. As a result, current flowing through arc decreases and deionization process of arc speeds-up. This speeding-up of the deionization process quickly quenches the arc. Now, the resistance of the arc is increased. Lesser the current in the arc-path, quickly the arc will die-out. When the arc fully dies-out, circuit-breaker is successful in interrupting the fault.

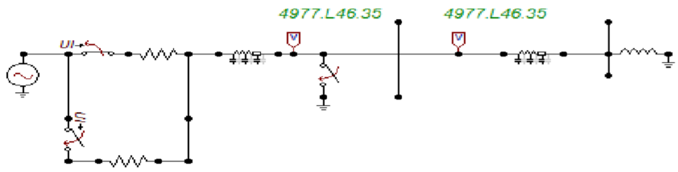

Figure 20: Switching-Resistance circuit

For 11-kV test network, switching-resistance technique result given below:

Measured T.R.V (without curtailment)= 21.5-kV

T.R.V reduction (after curtailment) =11.5-kV

Following are the A.T.P simulation results of above mentioned circuit.

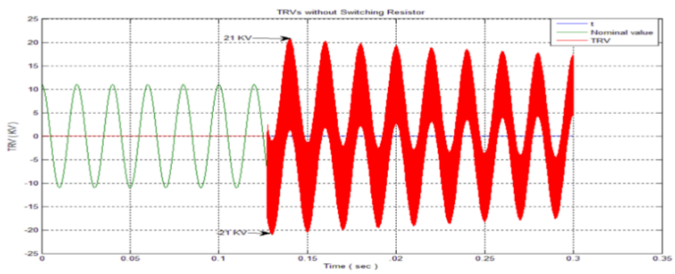

Figure 21: T.R.V without switching resistor

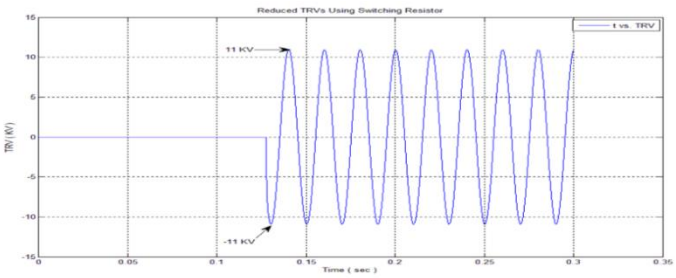

Figure 22: T.R.V with switching resistor

It is concluded that T.R.V can be significantly reduced (about 45%) by using switching-resistor.

2. Surge-absorbing Capacitor Switching

In this technique, voltage-surge absorber is used, which is basically a capacitor. This capacitor offers impedance to the fault-current.

$$X_C = \frac{1}{j\,\omega\,C}$$

This capacitor absorbs surges accompanying with voltage. A small-value capacitor is used to offer large impedance to the fault-current. Surges are termed as high-voltage and high-frequency transients. As frequency is very large, its capacitive-impedance (X_C) becomes very small. And high-frequency voltage surges are diverted to ground-path. In this way, our circuitry is protected from high-voltage surges. Fault-current absorption by this capacitor depends upon its size.

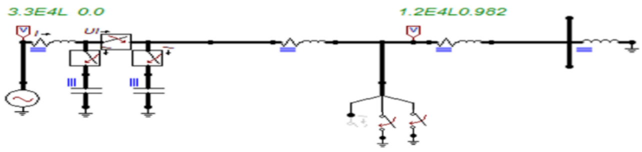

Figure 23: Surge-absorbing capacitor circuit

For 33-kV test network, switching-capacitance technique result given below:

Measured T.R.V (without curtailment) = 68.6-kV

T.R.V reduction (after curtailment)= 48-kV

Following are the A.T.P simulation results of above mentioned circuit.

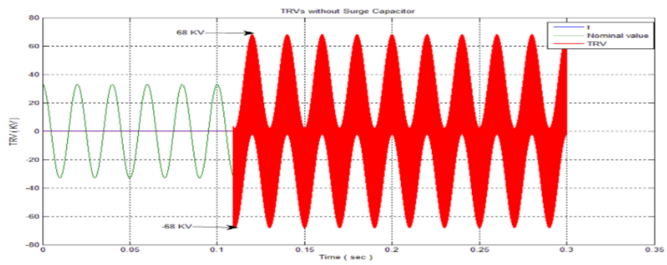

Figure 24: T.R.V without surge-absorbing capacitor

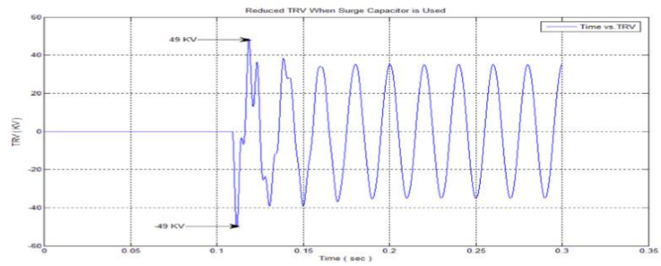

Figure 25: T.R.V with surge-absorbing capacitor

It is concluded that T.R.V can be significantly reduced (about 35%) by using surge-absorbing capacitor.

IV. Results & Discussions

A. *T.R.V Simulations of IEEE-39 bus system*

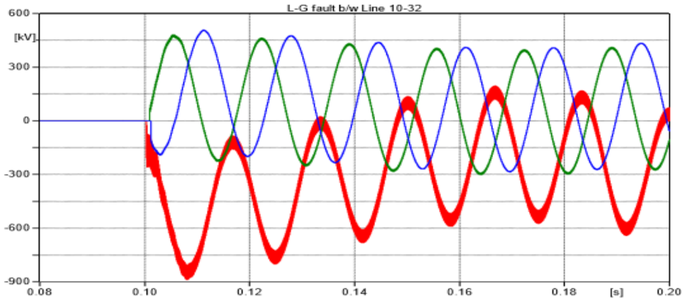

Figure 26: T.R.V for S-L-G fault at buses 10 & 32

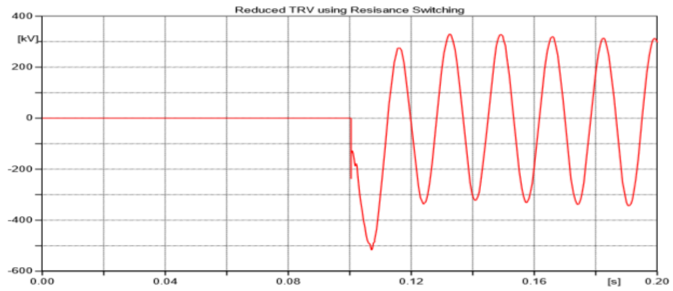

Figure 27: Reduced T.R.V for S-L-G fault at buses 10 & 32

Operating Voltage = 345-kV

Measured T.R.V = 880-kV

Measured T.R.V in an S.L.G-fault case is 2.8-times of operating voltage.

T.R.V-Reduction (switching-resistance technique)= 510 kV

In this case, we find 43% ($\frac{900-510}{900} \times 100$) reduction in T.R.V.

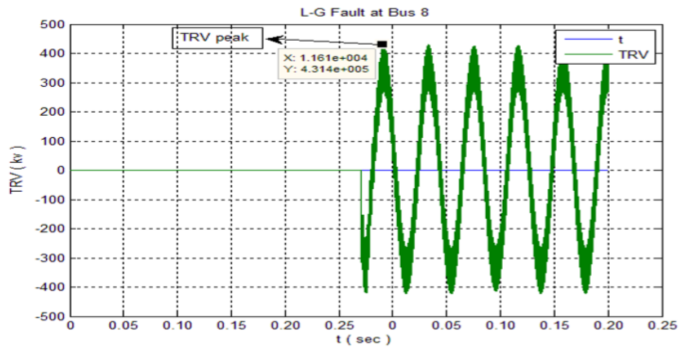

Figure 28: T.R.V for S-L-G fault at buse 8

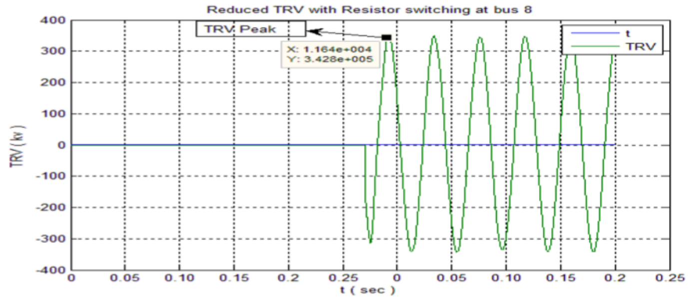

Figure 29: Reduced T.R.V for S-L-G fault at buse 8

Operating Voltage = 345-kV

Measured T.R.V for Case-1 = 452-kV

T.R.V-Reduction (switching-resistance technique)= 357kV

In this case, we achieved 21% ($\frac{452-357}{452} \times 100$) reduction in T.R.V.

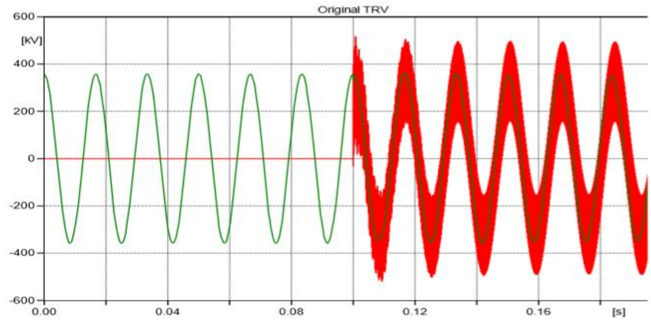

Figure 30: T.R.V for S-L-G fault at buses 6-31

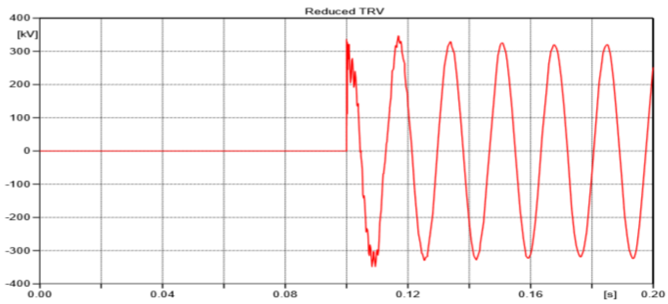

Figure 31: Reduced T.R.V for S-L-G fault at buse 6-31

Operating Voltage = 345-kV

Measured T.R.V for Case-1 = 570-kV

T.R.V-Reduction (switching-resistance technique) = 360kV

In this case, we achieved 37% ($\frac{570-360}{570} \times 100$) reduction in T.R.V.

Conclusion

Transient Recovery Voltages (T.R.V) depends on two types of factors i.e. internal factors and external factors. Internal factors include arc characteristics, arc quenching mechanism, and insulation level of circuit breaker. While external factors include fault type, type of load connected, location of fault, transmission-line length, grounding type, and surge capacitors. In this research, T.R.V is measured and previewed using external factors of circuit breaker. It was observed that T.R.V is highest for R.L load, short transmission line, ungrounded network, large surge impedance, and fault location near source side. Two techniques are used to mitigate these multitude T.R.V that is switching resistance technique and switching capacitance technique. Both of these techniques work in support of reducing fault-current, which ultimately reduces the T.R.V. Switching resistance technique achieved 45% reduction in T.R.V while switching capacitance technique achieved 35% reduction in T.R.V. This reduction in T.R.V is fair enough for circuit breaker to operate within limits and prevent the circuit breaker from failing due to large value T.R.V. In the last phase of this research, T.R.V measurements of IEEE-39 bus test network were performed using different external factors that affect T.R.V. These measurements were then cross-checked for validation using formulas for T.R.V. and reduction of the same measurements was performed by using resistance switching and capacitance switching technique. T.R.V was significantly reduced for about 35%.

REFERENCES

[1] D. Dufournet and .. Alexander, "Transient Recovery (TRV) for High Voltage Circuit Breakers".

[2] IEC , "High-voltage switchgear and controlgear", High-voltage alternating-current circuit-breakers,," in *IEC 62271-100:* , 2003.

[3] "https://www.atpdraw.net," [Online].

[4] "www.ece.mtu.edu>atp," [Online].

[5] "http://psdyn.ece.wisc.edu/IEEE_benchmarks," [Online].

[6] A. Greenwood, "Electrical Transients in Power Systems,," Wiley, 1991.

[7] P. W. J. Z. D. M. D. K. K.-W. L. Xuegong Wang, "Transient Recovery Voltage Investigation in the Application of 15 kV Circuit Breaker Failure," Vols. Paper No. IPST05 – 224, IPST’05.

[8] A. A. B. S. S. Chandankar, "Review: To Investigate Impacts of Various Factors on the Characteristics of Transient Recovery Voltage.,," *International Journal of Advanced Research in Electrical, Electronics and Instrumentation Engineering,* vol. 5.

[9] I. U. D. F.-G. Božidar Filipoviü-Grþiü, "Analysis of Transient Recovery Voltage in 400 kV SF6 Circuit Breaker Due to Transmission Line Faults," Vols. Vol. 6, N. 5, September-October 2011.

[10] R. Colclaser, "The Transient Recovery Voltage Application of Power Circuit Breakers," *IEEE Transactions on Power Apparatus and Systems,* Vols. PAS-91, no. 5, pp.1941-1947,, Sept. 1972.

Rahman Ullah Khan

The author has received BE degree in Electrical Engineering from NED University of Engineering & Technology, Karachi in 2014. He has one year industry experience of Fauji Fertilizer Bin-Qasim Limited (FFBL) from 2014 to 2015. Currently, he is doing MS in Electrical Energy Systems Engineering (EESE) from U.S.-Pakistan Center for Advanced Studies in-Energy (USPCAS-E), University of Engineering & Technology, Peshawar. He has availed exchange program to the partner university of USPCAS-E Arizona State University (ASU), USA in 2017, as a research scholar. He has good hands on experience in the field of electrical power and renewable energies especially PV reliability.

International Journal of Engineering Works
ISSN-p: 2521-2419
ISSN-e: 2409-2770
Vol. 6, Issue 12, PP. 547-555, December 2019
https://www.ijew.io/
https://doi.org/10.34259/ijew.19.612547555

Utilization of Unidirectional Links in AD-HOC Networks

Naeem khan[1], Dr. Majid Ashraf[2]
[1,2]UET Peshawar
eee103096@gmail.com[1]

Received: 16 December, Revised: 26 December, Accepted: 28 December

Abstract— In ad hoc network the unidirectional links and hidden node appear very frequently. There are few techniques that are used to avoid both unidirectional links and hidden nodes. Request to send/Clear to send (RTS/CTS) technique is used to avoid hidden link scenario and hello, blacklisting and reverse path search are used to avoid unidirectional links. In our research we opted for Dynamic source routing (DSR) which basically considers every route to be bidirectional, but as nodes moves frequently in ad hoc network these two problems occur. In the first part of the paper, we have implemented (RTS/CTS) and blacklisting techniques to avoid hidden links and unidirectional links to look into the improvement in the Dynamic source routing (DSR) by calculating certain parameters such as, Throughput (packet delivery at sink), End-to-End Delay, Network load and Packet delivery ratio. Furthermore our thesis also look into the link failure recovery, as nodes are continuously moving while data transferring as well so the node can move away from each other in these cases so the link broke down between the source and destination nodes so to avoid this scenario We implemented a mechanism of route recovery to efficiently tackle this problem. The result shows that the improved Dynamic source routing (Improved DSR) has shown more stability and performs very good overall in every performance parameter.

Keywords— Unidirectional links, hidden links, RTS/CTS, hello, blacklisting, reverse path search, Dynamic source routing (DSR).

I. INTRODUCTION

A network that does not have any base stations or centralized established infrastructure, a few nodes combines together to Form a network which is temporary pass information to each other for a specific purpose and they may be inter connected to each other through Wi-Fi links is called adhoc network. The links between the nodes are by default considered as bidirectional but due to certain reasons like nodes transceiver power difference, hurdles in signal propagation and sometime noise in the environment exists and these phenomena's creates unidirectional links between these nodes as shown in "fig.1".

These links can create problems in communication between the nodes if it is not tackled. Asymmetric (unidirectional) links are the main area of our research. Different researchers have different approaches to handle the unidirectional link [1] [2] [3] [4] [5] [6] [7] [8]. Using the unidirectional links is not so good, as it gives a high-overhead in the network [1]. So the question arises here to use unidirectional links or not. This is questionable and can vary from researcher to researcher. There is another problem to handle in ad hoc networks i.e. hidden link between nodes. The figure 2 shows hidden link scenario, due to hidden links the nodes cannot hear each other properly and this entirely jeopardizes the network. In the later part of our work we will look into the link failures while data transferring. As we know these all nodes are mobile in nature they frequently changes there position so it can move away from each other so that they lost their connection and the link in broken. This issue can also be detected due to interference in the environment.

Our research work is to efficiently look into the unidirectional links; avoid Hidden node cases and looking into link failure issues, thus ensuring the transfer of data packets over the network to avoid networks jeopardizing in DSR protocol.

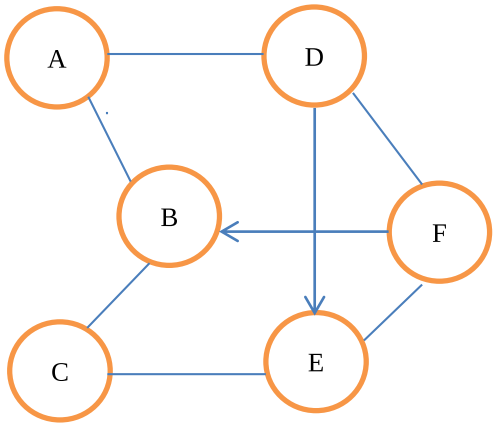

Figure 1. Bi-directional Adhoc network

II. DSR PROTOCOL

The Dynamic source Routing (DSR) is a special protocol that uses it resources when the route is needed for communication. A node is DSR sustain route in its caches memory or routing table of the other nodes. The cache tables of these nodes are updated when a node gets information about new routes of its neighbor. The protocol has two phase's i.e.

- Discovery of its routes
- Maintenance of the routes it has already found

When there is a desire of a single node that he wants to send some information to a node, it will look into its routing table that if he had its address or not, if he had an address of a route to this specific node it will connect to this node by send RREQ directly through that route and when he gets RREP from that node it will start sending information. But if there he found no route in its memory it will start a mechanism by flooding the RREQ to its neighbors and if there is no destination node in the neighbor, they will send it to their neighbors and this process is continued until the destination node is found. When a node want to send data, first it sends RREQ packet in which it adds the address of the node and its own address for RREP and it also adds a very unique number through which all the nodes can identify that this packet has been sent by source which source node. When any of the nodes receives this packet it looks into its own table that if he knows the path, if he do not he floods the RREQ packet [9][12]. RREQ is received by a node; the address it holds of a destination is its own or of other node but it knows its route so this node will generate a RREP packet. The node will append its own information and the information from the RREQ packet into this and will send it through a route on which it has received the RREQ packet as shown in "fig. 4" DSR protocol uses two methods to maintain its route i.e.

- Route error packet
- Acknowledgement

When node finds error in its transmission it generates the Route error packet (RERR) and sends it to other nodes. When the other nodes receive this specific packet it initiates a process and removes the route of the node from its route cache. The acknowledgment packet is used in DSR to find that the Packet has been successfully received at the specific node or neighbor. There is also a passive acknowledgment by which the node knows that the Packet has been forwarded to other nodes.

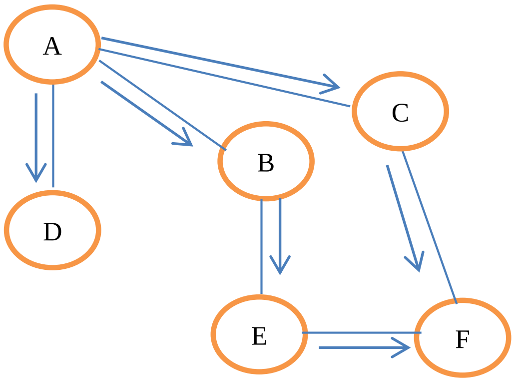

Figure 2: RREQ packet sent from A to F

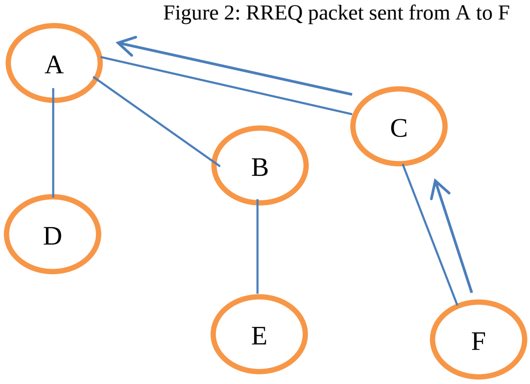

Figure 3: RREP packet sent from F to C to A

III. TECHNIQUE FOR HANDLING UNIDIRECTIONAL LINK, HIDDEN LINK AND LINK FAILURE

The node in discussion has to send data to some other node called destination, so it will send RREQ to all neighbor nodes, when the RREQ is received at neighbor nodes it will reply with Acknowledge Packet (ACK) back to source node, if the source node does not receive Acknowledgement (ACK) from any of the neighbor node it will have to check two scenarios under which the concern node did not reply.

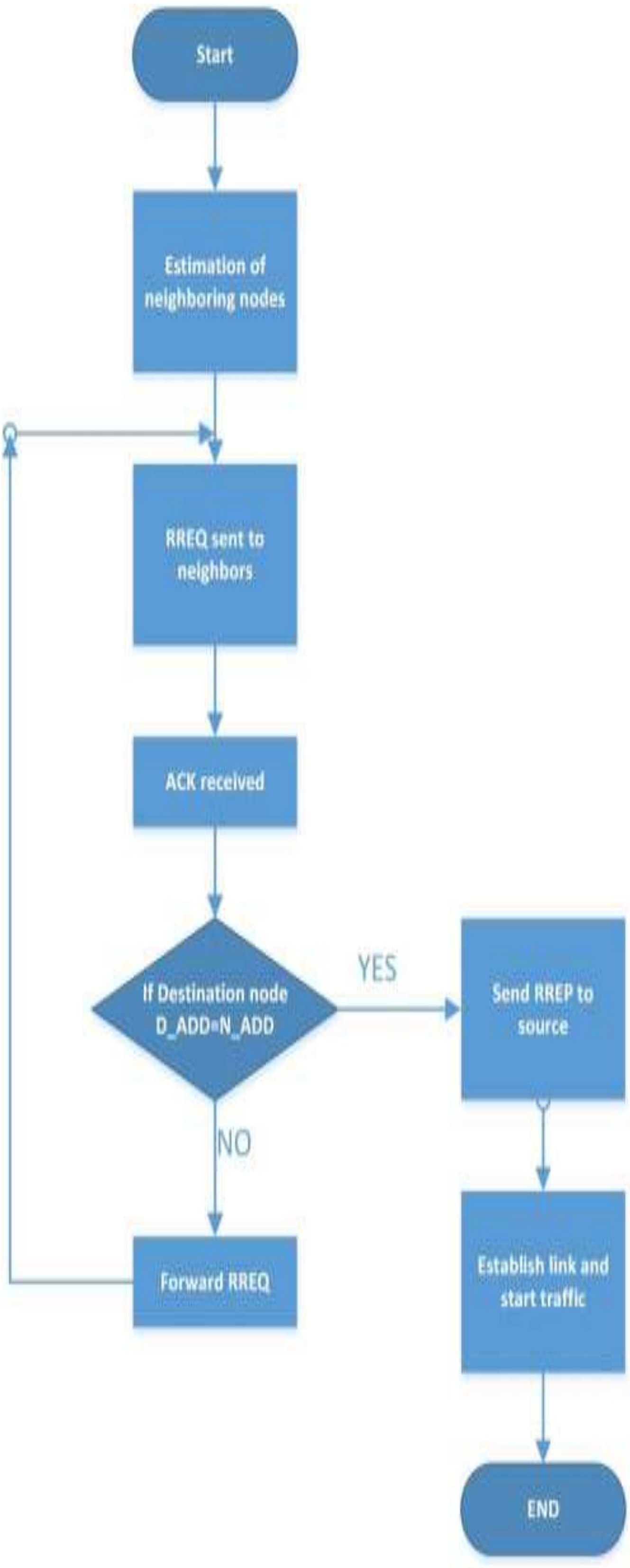

Figure 4. DSR protocol Process

A. Hidden node scenario

Another problem researcher's encounter while deploying adhoc network in a certain area is hidden nodes. This is a problem that occurs when a node A want to communicate with other node AP (access point) and at the same time some other node B is also trying to communicate with the same node (access point) as seen in "fig .5". If one of the nodes is trying to send a large number of data packets so we can encounter a lot of packet drops as neither of the packet will pass as both A and B are sending data packets. To handle this problem we can use different solutions.

1. RTS/CTS (Request to send/Clear to send). Node will send RTS to AP and when AP responds with CTS it will send its data.
2. By enhancing antenna range so the node will now not be a hidden node as we are using CSMA/CA, in which every node will wait for its due turn to send data.
3. We can also encounter this problem due to some obstacle so first we have to remove the obstacle is some cases or in other cases where we cannot move obstacle we will move the node location.

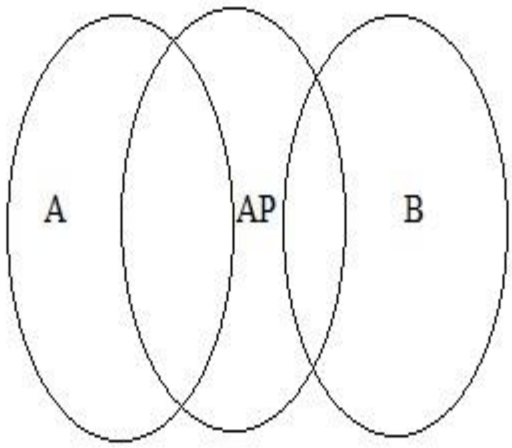

Figure 5. Hidden node

B. Unidirectional link scenario

In the second place if the node is not hidden node then the source node will check for the unidirectional link, for that, it will initiate a counter and will wait for Maximum Upper threshold each time it sends the RREQ to the specific node, when the counter reaches the count three and the node did reply with RREP packet so the node will go into its natural process. If the node did not reply with RREP packet the node will perform three processes there as shown in figure 4.

a) Blacklist the node
b) Update its routing table
c) Inform the concern nodes that this link has been blacklisted

If the Hello Packet (RREQ) is Acknowledge by the neighbor and it will compare its Address with the Destination Address send by source node, if the node Address matches with Destination Address it will send RREP packet and the source node will establish the link and will start traffic between them. If the neighbor node is not the destination node so it will send the RREQ Packet to its neighbor to find out the path to the destination node and the same process will be performed again and again till the RREQ Packet has reached the Destination node as shown in "fig. 6"[11][12]. Once the link is established between the source node and destination node there we can enconter link failure.

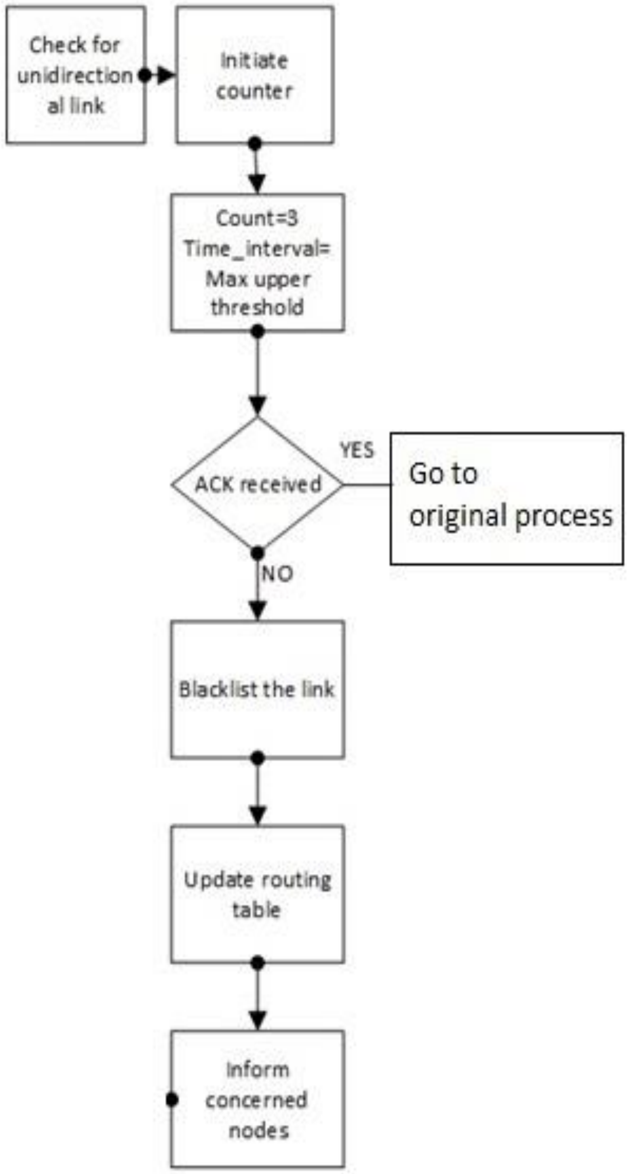

Figure 6. Black listing process

C. Link failure

When the source node and destination node transfer data there may be a link failure it can be due to many reasons.

I. Destination or Source node moves away from the range of each other.
II. Due to any interference between the Source and Destination nodes.
III. Due to frequencies variation of Source and Destination nodes.

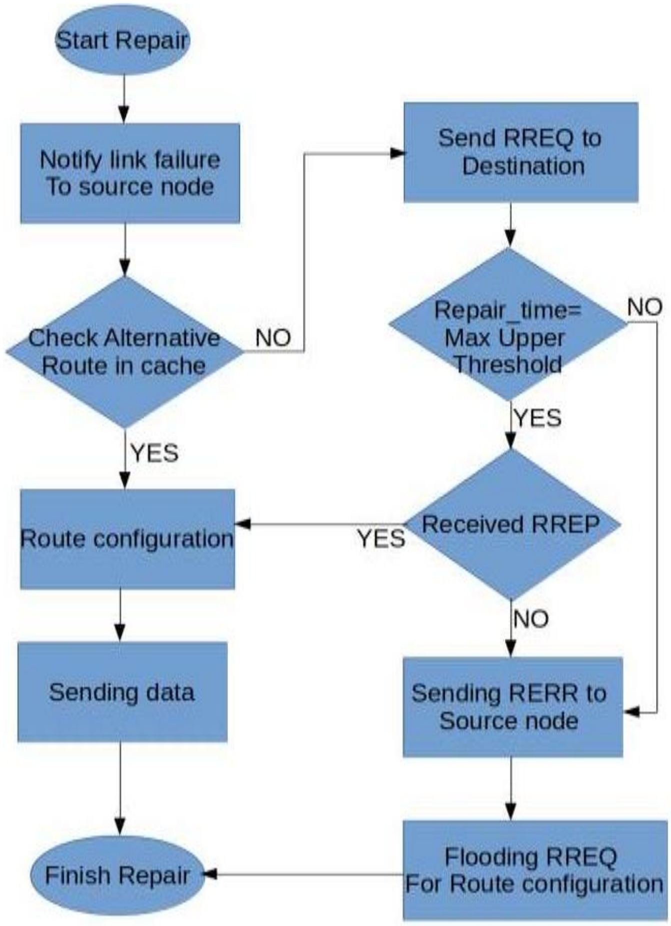

Figure 7. Link failure process

First the Source node will check the alternate route in its routing table to reach destination, if the route is found then the Source node will configure the route and after establishing the route it will start the traffic once again. But if the node don't have any route in its routing table, it will resend a RREQ packet towards the Destination node, it will wait till the Maximum upper threshold time, if the RREP is received so it will configure the route and establish the link and will start traffic but if the RREP is not received the at source the RERR packet will be sent to Source node and it will again start the main process by sending a RREQ packet to the neighbors as shown in "fig. 7".

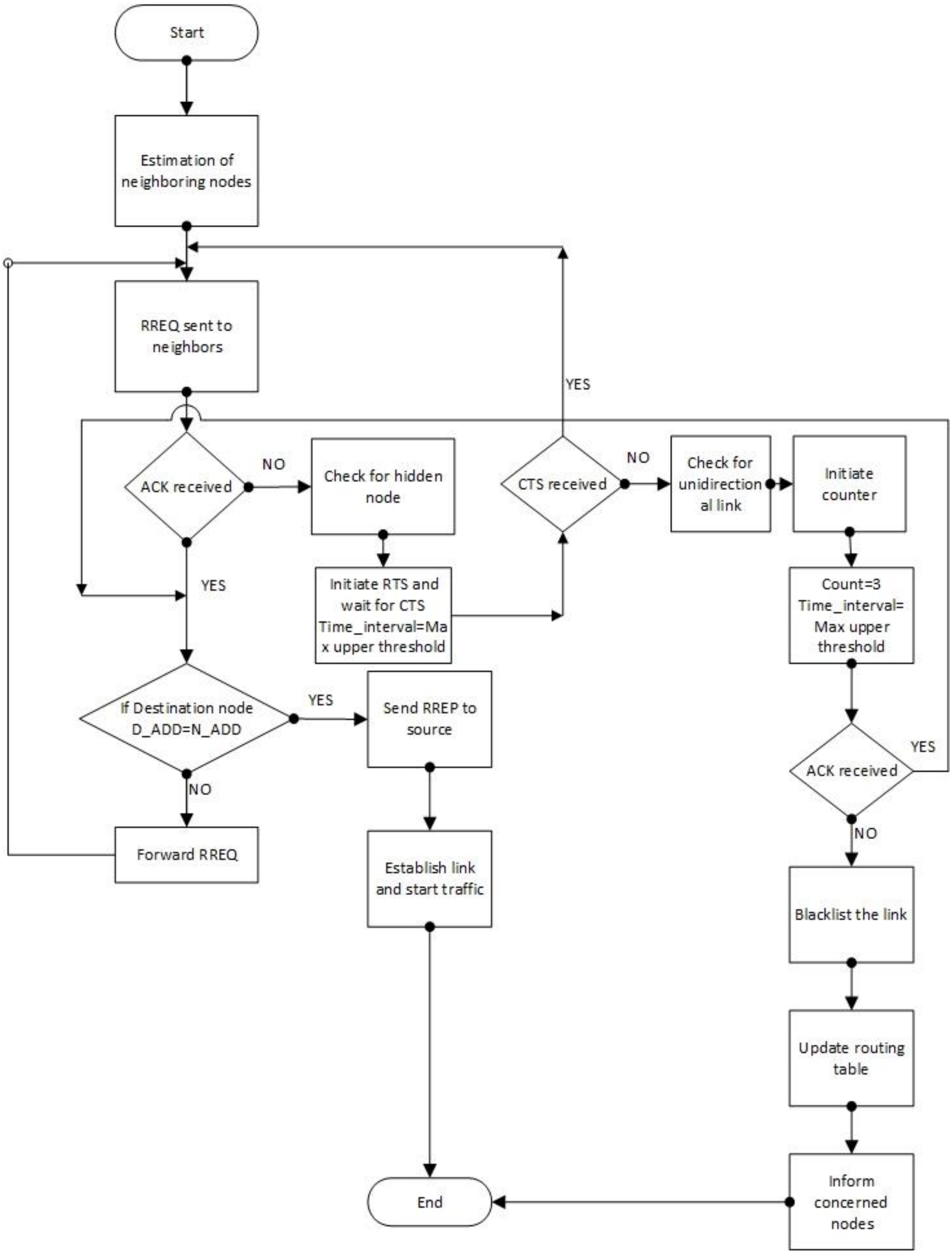

Figure 8. Flow chart of the whole process, Hidden node, unidirectional link and link failure

IV. SIMULATION RESULTS

In this chapter we will see into the simulations we had performed and evaluate the results. We had found during our research under the DSR protocol utilizing unidirectional links in adhoc networks. We are evaluating our results through four different parameters (1) Throughput (2) End-to-End delay (3) Network load (4) Packet Delivery ratio.

We will look into two sets of experiments i.e. (1) Comparison of DSR vs. DSR with unidirectional link and hidden nodes (2) Comparison of DSR with unidirectional Link and hidden nodes vs. DSR with unidirectional Link and hidden nodes including Link Failure recovery (Imp DSR with Link failure).

A. Comparison of DSR vs. DSR with unidirectional link and hidden nodes(Imp DSR)

We have used matlab as a simulation environment for our research purpose. We created a 100 nodes environment to find out the results. The result will be shown in two different scenarios mentioned above and there performance metrics. First we implemented the improved DSR protocol by including unidirectional link and hidden nodes scenarios. Then we compare their graphical response and we find out that throughput of the packets has shown improvement as shown in table. All other parameters such as End-to-End delay, Network load and Packet Delivery ratio has shown huge improvements it can be seen in the table and from the graphs.

Table 1: Throughput, End-to-End delay and Network load of DSR and Improved DSR

Rounds of data Packet sent	**Throughput of DSR**	**Throughput of Imp DSR**
1000	25%	75%
5000	3%	15%
	End-to-End Delay of DSR	**End-to-End Delay of Imp DSR**
1000	6ms	1ms
5000	9ms	3ms
	Network Load of DSR	**Network Load of Imp DSR**
1000	70%	10%
5000	90%	80%

Table 2: Packet Delivery ratio of DSR

Rounds of data Packet sent	**Packets received at destination (DSR)**	**Packets Drop (DSR)**
80000	43000 Approximately	37000 Approximately

Table 3: Packet Delivery ratio of Improved DSR

Rounds of data Packet sent	**Packets received at destination Imp DSR**	**Packets Drop Imp DSR**
80000	49000 Approximately	31000 Approximately

From the graphical response we can see that throughput has been incresed with avoidance of unidirectional links and hidden nodes adjustments. As here we are avoiding unnecessary data packets send on unidirectional links and then waiting for the response fro the specific node we are ncreasing our throughput ability and decresing the End-to-End Delay. Throughput in ths scenario has been achieved upto 12 to 10 percent more than simple DSR. The End-to-End Dealy has been minimsed upto 5 to 6 ms as shown in “fig10”. We can aslo see that the load on the network has been reduced upto 10 percent from DSR protocol. The packet Delivery ratio is another parameter that has been enhanced due to our proposed solutions, improved DSR has shown a increased upto 8 percent as shown in “fig .12”.

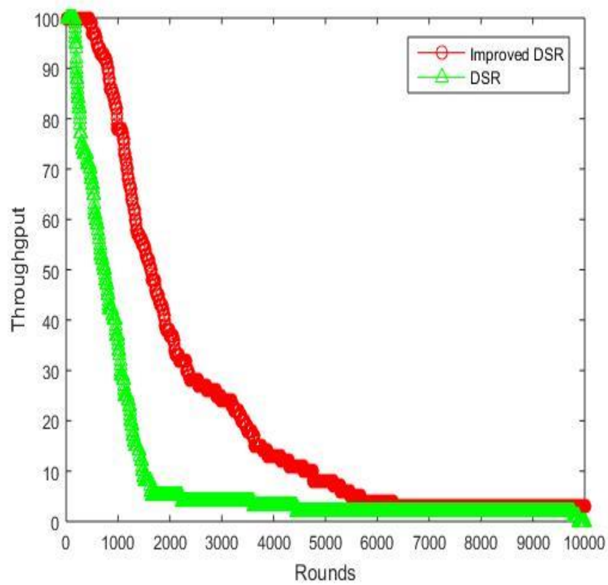

Figure 9: Throuput of DSR and Imp DSR

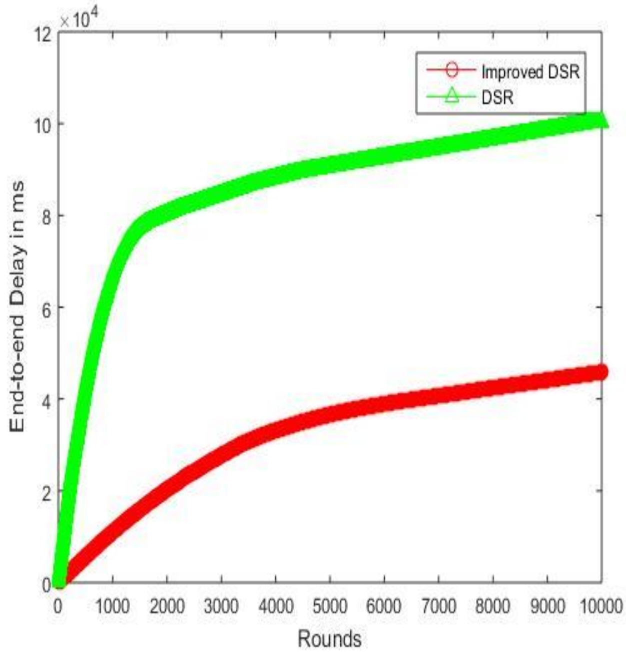

Figure 10: End-to-End Delay of DSR and Imp DSR

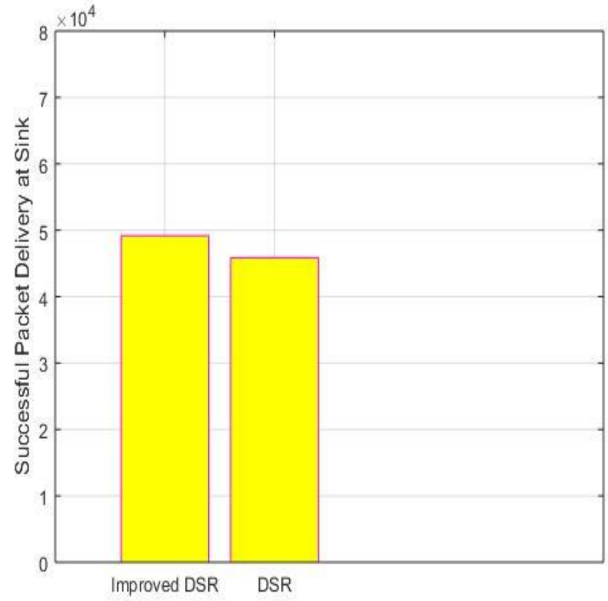

Figure 12:Packet Delivery Ratio of DSR and Imp DSR

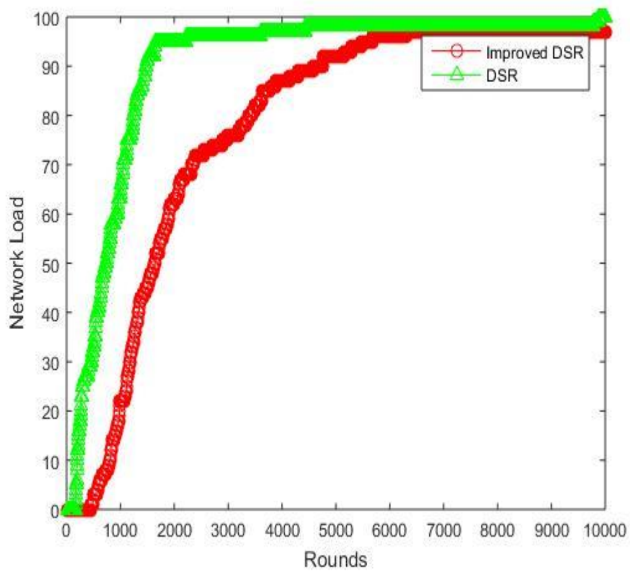

Figure 11: Network Load of DSR and Imp DSR

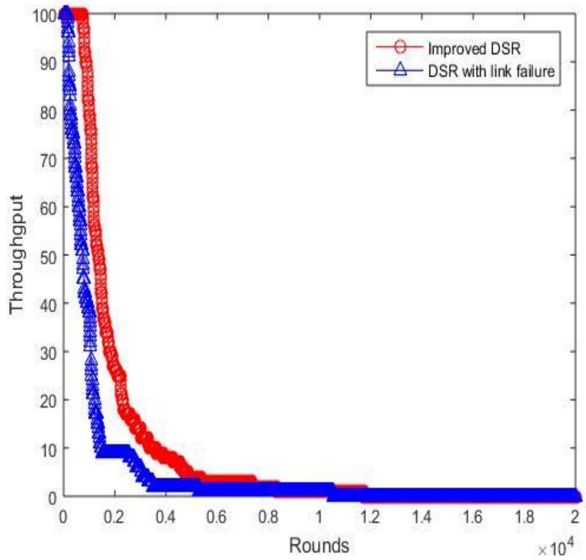

Figure 13: Throughput of Imp DSR and Imp DSR with link failure

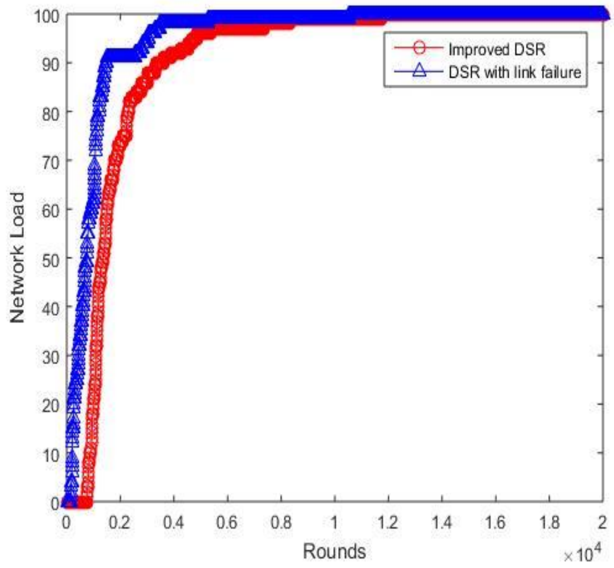

Figure 14: Network load of Imp DSR and Imp DSR with link failure

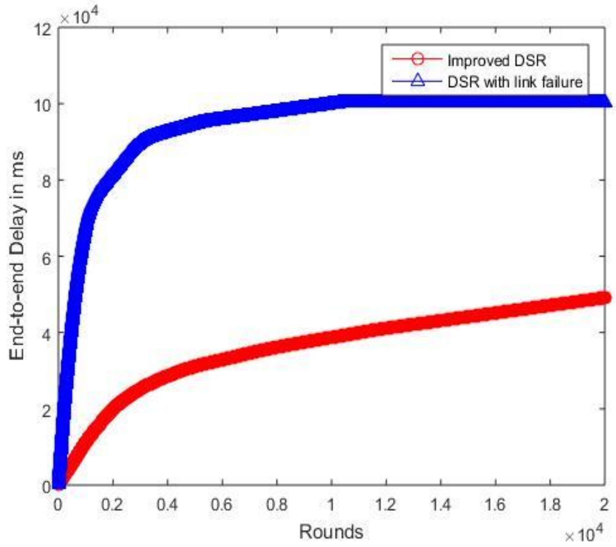

Figure 15: End-to-End Delay of Imp DSR and Imp DSR with link failure

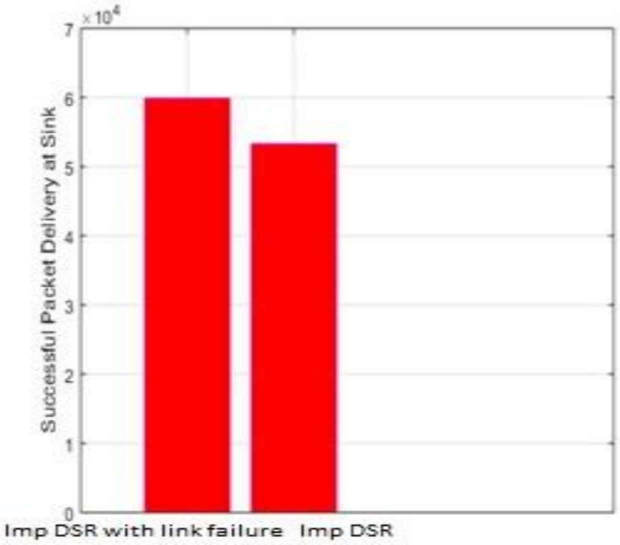

Figure 16: Packet Delivery ratio of Imp DSR and Imp DSR with link failure

Table 4: Throughput, End-to-End delay and Network load of Imp DSR and Imp DSR with link failure

Rounds of data sent	**Throughput of Imp DSR**	**Throughput of Imp DSR with link failure**
1000	75%	90%
4000	10%	15%
	End-to-End Delay of Imp DSR	**End-to-End Delay of Imp DSR with Link failure**
1000	1ms	3ms
4000	3ms	8ms
	Network Load of Imp DSR	**Network Load of Imp DSR with Link failure**
1000	10%	5%
4000	75%	70%

Table 5: Packet Delivery ratio of Imp DSR

Rounds of data sent	**Packets received at destination (Imp DSR)**	**Packets Drop (Imp DSR)**
70000	52000 Approximately	18000 Approximately

Table 6:. Packet Delivery ratio of Imp DSR With link failure

Rounds of data sent	**Packets received at destination (Imp DSR with link failure)**	**Packets Drop (Imp DSR with link failure)**
70000	61000 Approximately	8000 Approximately

B. *Comparison of DSR with unidirectional Link and hidden nodes (Imp DSR) vs. DSR with unidirectional Link and hidden nodes including Link Failure recovery (Imp DSR with Link failure).*

In the second part we established a link failure recovery when a link is gone down while transmitting data between the source and Destination node as shown in “fig. 8”. That gives a clear idea of how we will recover from a link failure by finding a shortest alternate path for data delivery, if we didn’t found any path in cache; we will send RREQ and look into if the link can established, if it did not established we will send a RERR and will start the process again. In the above tables we have shown the Comparison of DSR with unidirectional Link and hidden nodes (Imp DSR) vs. DSR with unidirectional Link and hidden nodes including Link Failure recovery (Imp DSR with Link failure).

From he graphical response the improvement can be seen up to 13% in Imp DSR with link failure. The total improvement in packet delivery ratio from DSR is 23% from the Imp DSR. In total which accumaletly gives us a value of 30 % from DSR protocol. The improvement is due to the alternate paths we find for data transfer and we don not wait for a long a time and we do not drop packets as our node is not sending any packets if the the link is broken.

C. *Trade off*

When we implemented the link failure recovery, so our End-to-End delay has been increased up to 4 to 5ms from the improved DSR that can be seen in Table 5 and “fig.15”. Due to looking into route cache for new shortest routes and may be restarting the process if we did not found the possible route, so this in return will increased our delay time.

CONCLUSION

In our thesis we are trying to enhance the capabilities of DSR routing protocol by implementing two main changes into it.

(1) DSR with hidden link and unidirectional links (improved DSR).

(2) Improved DSR with link failure recovery.

We are using the blacklisting technique to avoid the unidirectional links and RTS/CTS technique to avoid hidden links. Now the second problem was of link failure and its recovery. We used a simple technique of looking into any availale shortest path for communication is a specific time interval or else restart the whole process again after Max upper threshold time.

Our research of improving DSR routing protocol by the above mentioned techniques had shown a very good improvement in every performance parameter. It gives multiple advantages such as:

(1) Immunity from unidirectional links

(2) Avoiding hidden nodes

(3) Link failure recovery.

But we also have to face some tradeoffs in imp protocol with link failure regarding End-to- End delay.

REFERENCES

[1] Samir R. Das Mahesh K. Marina, "Routing Performance in the Presence of Unidirectional Links in Multihop Wireless Networks," Proceedings of the 3rd ACM international symposium on Mobile ad hoc networking & computing, pp. 12-23, 2002.

[2] Zygmunt J. Haas, Benjamin P. Manvell Marc R. Pearlman, "Using Multi-Hop Acknowledgements to Discover and Reliably Communicate over Unidirectional Links in Ad Hoc Networks," in IEEE Wireless Communications and Networking Conference, 2000.

[3] RAVI PRAKASH, "A Routing Algorithm forWireless Ad Hoc Networks with Unidirectional Links," Wireless Networks , vol. 7, no. 6, pp. 617-625, 2001.

[4] Daniel Mossé Venugopalan Ramasubramanian, "BRA: A Bidirectional Routing Abstraction for Asymmetric Mobile Ad Hoc Networks," IEEE/ACM TRANSACTIONS ON NETWORKING, pp. 116-129, 2008.

[5] SHIOW-FEN HWANG, CHYI-REN DOW YI-YU SU, "An Efficient Cluster-Based Routing Algorithm in Ad Hoc Networks with Unidirectional Links," JOURNAL OF INFORMATION SCIENCE AND ENGINEERING, pp. 1409-1428, 2008.

[6] Jian-de Lu, Jia-jia Tang Zhen-zhong Wang, "Neighbor Monitoring Mechanism to Solve Unidirectional Link Problem in MANET," in Wireless and Mobile Communications, International Conference, 2007, pp. 55-59.

[7] LIU Yuan-an, LIU Kai-ming, ZHAI Lin-bo, YANG Ming ZHUANG Lin, "An adaptive algorithm for connecting mobile ad hoc network to Internet with unidirectional links supported," The Journal of China Universities of Posts and Telecommunications, pp. 44-49, 2010.

[8] Sung-Ju Lee, Jun-Beom Lee Young-Bae Ko, "Ad Hoc Routing with Early Unidirectionality Detection and Avoidance," in IFIP International Conference on Personal Wireless Communications, 2004, pp. 132-146.

[9] Y. Hu, D. Maltz D. Johnson, "Request for Comments: 4728 (The Dynamic Source Routing Protocol (DSR))," Rice University, Microsoft Research, Experimental 2007.

[10] Jorg Nolte Reinhardt Karnapke, "Unidirectional Link Counter - A Routing Protocol for Wireless Sensor Networks with Many Unidirectional Links," in 14th Annual Mediterranean Ad Hoc Networking Workshop , 2015.

[11] Juan-Antonio Cordero , Jiazi Yi , Yuichi Igarashi Thomas Clausen, "Use ’em or lose ’em: On unidirectional links in reactive routing protocols," Elsevier Science Publishers, pp. 51-64, 2018.

[12] Y.Hui Y.Fengjie, "Research on DSDV routing protocol based on wireless mesh network," in Chinese control and decision conference, 2018.

IJEW 国际工程期刊 International Journal of Engineering Works انجینرنگ کاموں کا بین الاقوامی جرنل

International Journal of Engineering Works
ISSN-p: 2521-2419
ISSN-e: 2409-2770
Vol. 6, Issue 12, PP. 564-569, December 2019
https://www.ijew.io/
https://doi.org/10.34259/ijew.19.612564569

Device Modeling and Numerical Characterization of Perovskite/Si, Perovskite/CIGS and all-Perovskite Tandem Solar Cells

Saddam Hussain[1], Adnan Daud Khan[2]
[1] [1,2]US.Pakistan center for advanced studies in energy (USPCAS-E), University of engineering and technology (UET) Peshawar, Pakistan.
saddamahmad313@gmail.com[1]
Received: 16 December, Revised: 26 December, Accepted: 27 December

Abstract— From the past couple of years, the high-power conversion efficiency (PCE) of >25% and low-cost fabrication of single-junction perovskite photovoltaic cells have gained great attention from researchers. The bandgap tunability of these solar cells makes them an attractive and ideal candidate for tandem solar cell applications. The PCEs above than the single-junction solar cells theoretical Shockley-Queisser (SQ) radiative efficiency limit (31%-33%) can be achieved by harvesting a wide fraction of solar spectrum using multi-junction solar cells. In perovskite tandem (double-junction) solar cells, a wide-bandgap perovskite top cell is combined with either narrow-bandgap bottom cells of dissimilar materials like silicon (Si) and copper indium gallium selenide (CIGS) or with low bandgap perovskite solar cell. In this work, we have simulated perovskite/Si (PVK/Si), perovskite/CIGS (PVK/CIGS) and perovskite/perovskite (PVK/PVK) tandem solar cells and estimated 28.73%, 20.31% and 26.06% PCEs. The highest conversion efficiency is shown by PVK/Si tandem cells among others because of the suitable bandgap for tandem applications. Our work will guide the researchers for obtaining ultra-high conversion efficiency solar cells.

Keywords— Tandem solar cells, SunSolve, optical modeling, efficiencies, evaluation.

I. Introduction

The metal-halide perovskite solar cells have gained the attention of researchers in the past couple of years and became a hot topic of the photovoltaics (PV) community because at low manufacturing costs these solar cells have the potential to achieve a high PCEs [1][2][3]. The high performance of these solar cells is because of its remarkable optoelectronic properties like higher carrier mobility, longer diffusion lengths, high absorption and light to electrical conversion. Due to intense research efforts in the past few years from researchers in the photovoltaic community across the world have helped the conversion efficiencies of single-junction (SJ) PSCs to climb from <14% in 2013 to 25.2% in 2019[4]. The single-junction PSCs conversion efficiencies are approaching the Shockley-Queisser (SQ) theoretical limits (31-33%)[5]. In order to harvest the maximum fraction of the solar spectrum and go beyond the single junction S–Q limit, the multi-junction PSCs should be investigated. Due to this reason, the researchers are intended towards solar cells having double and triple junctions, which can achieve PCEs of greater than 42% under standard solar irradiance[6]. The multijunction tandem design aims to reduce energy losses due to the thermalization of light excited carriers by combining a stack of different bandgap semiconductor absorbers. The high energy photons are absorbed by the top subcell (wide-bandgap) of the stack and the bottom subcell (low bandgap) absorbs the low energy photons. In this way, the solar spectrum's wide portion is harvested. In the past 3-4 years, all the tandem cells have gained rapid progress due to the developments in low and high bandgap perovskite solar cells. In late 2014, for the first time, the PCE of 13.4% and 17% respectively reported by McGehee and Ballif groups separately for 4-T MAPI3/Si [7] and MAPbI3/multi-crystalline Si [8] tandem solar cells. More recently, the Ho-Baillie group combined (FAPbI3)0.83(MAPbBr3)0.17 with homojunction c-Si textured on the rear side in a monolithic architecture and showed a PCE of 21.8% having cell area of 16 cm2 [9]. Their work provides a path that leads to the commercialization of low-cost tandem solar cells. Perovskites are ideal partners of CIGS solar cells for tandem applications. Recently, for perovskite/CIGS tandems a PCE of 24.6% [10] and 21.6%[11] for 4-T and 2-T is achieved by researchers. All-perovskite based tandem cells are also fabricated in both 4-T and 2-T architecture. Recently, a PCE of 23% [12] and 24.8%[13] is reported for all-perovskite 4-T and 2-T tandems respectively. In our work, we used the SunSolve simulation tool from PV Lighthouse [14] for the optical simulation of monolithic 2-T PVK/c-Si, PVK/CIGS, and PVK/PVK tandem solar cells and estimated and compared their efficiencies. Our simulations are based on measured complex refractive indices (n and k) also known as optical constants for the different layers of the design stack. With our proposed device architectures, we have studied losses (reflection and parasitic absorption in each layer) and gains in absorber layers and have estimated a PCEs of 28.73%, 20.31% and 26.06% for PVK/c-Si, PVK/CIGS and PVK/PVK tandem solar cells under AM 1.5G 1000W m-2 and 300K temperature. In our simulations the PVK/c-Si tandem architecture exhibited greater efficiency compared to PVK/CIGS and PVK/PVK tandem architectures.

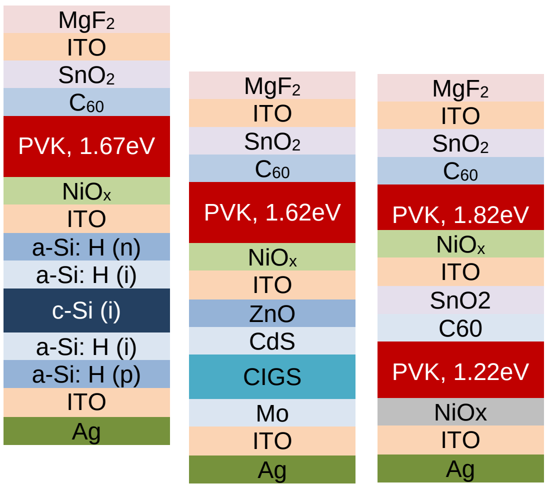

(a) (b) (c)

Figure 1: The device structure of monolithic 2-T PVK/c-Si (a), PVK/CIGS and (b) and PVK/PVK tandem solar cells (c) used in simulations.

Device Modeling and Simulations

The device architectures for the various tandem solar cells in our simulations are shown in figure 1. In the PVK/c-Si tandem architecture, the top subcell absorber bandgap is 1.67eV and the bottom subcell absorber (Si) bandgap is 1.1eV. Here the MgF2 is used as an anti-reflection layer to reduce reflection losses and improve the overall performance of the solar cell. The values of refractive indices (n and k) for each layer in the stack are obtained from the Refractive Index Library of SunSolve. The top and bottom subcells are serially interconnected using the recombination layer of indium tin oxide (ITO). In the PVK/CIGS architecture, the top subcell absorber bandgap is 1.62eV and the bottom subcell absorber (CIGS) bandgap is 1.15eV. The data for complex refractive indices of CIGS is obtained from the literature [15] and the remaining layers of the stack are obtained from the Refractive Index Library of SunSolve. The top and bottom subcells of the PVK/CIGS are interconnected by ITO as a recombination layer. Similarly, for PVK/PVK device stack, the front and rear absorbers used have a bandgap of 1.82eV and 1.22eV. The complex refractive indices data for the absorber layers is obtained from [16] and the remaining layers of the stack are obtained from the Refractive Index Library of SunSolve. The subcells are interconnected using ITO as a recombination layer (RL). Simulation software is known as SunSolve which is introduced by PV Lighthouse [14] for the solar cell optical simulations. The simulation method of SunSolve is based on the combination of Monte Carlo ray tracing (MRT) and thin-film optics which determines the optical losses and gains in various layers of solar cells for a chosen spectrum of light. For a user-defined spectrum, the magnitude of photon flux is calculated and integrated over the wavelength to determine the photon current density. The photo-generated current J_G in the stack of solar cells equates to the photo-current which can be pulled out with the help of electrodes. In simulations using SunSolve, we have used the perfect Lambertian reflector (Λ=1) scattering model at the bottom of the solar cell stack.

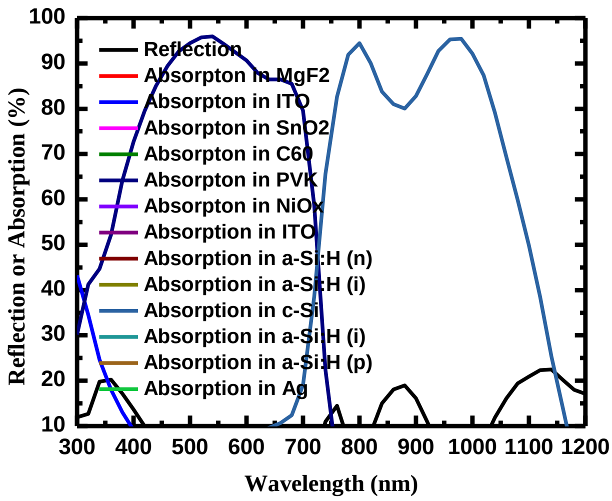

Figure 2: Reflection and absorption losses simulated in the device stack of PVK/c-Si tandem cell.

Results and Discussion

There are three different tandem architectures are simulated and compared in this research work. These are a) PVK/c-Si, b) PVK/CIGS and c) PVK/PVK tandem solar cells. Losses due to reflection and parasitic absorption in non-absorber layers are calculated and plotted. The quantum efficiencies for the proposed models are plotted whose detail is given below.

Perovskite-Silicon Tandem Solar Cell

Without substantial change in manufacturing costs, the output power of crystalline silicon solar panels can be increased by combining with wide bandgap PSCs. A ~1.1eV c-Si combined with wide bandgap perovskites of 1.6-1.75eV is an ideal tandem combination to achieve a PCE of more than 30% [17]. Here we have combined 1.67eV top subcell perovskite absorber with c-Si bottom subcell as shown in figure 1(a). All the layers of the stack are optimized using layer by layer optimization technique whose detail is listed in table 1 and a 20.4 mA cm-2 matched current density is obtained. The losses taking place in the device stack due to reflection from the front surface and parasitic absorption in the non-active layers which do not contribute to the electron-hole generation are plotted in figure 2 for the solar spectrum from 300nm to 1200nm. In the solar cell stack, about 7.87% (3.65 mA cm-2) of the incoming radiation is reflected from the front surface.

The perovskite/c-Si tandem stack photons to electrons conversion are higher than the individual subcells of the tandem stack. Because the solar spectrum large portion is harvested due to a combination of active layers of different bandgaps. The EQE plot in figure 3 shows that the photons of higher energy are absorbed by top subcells while the photons of lower energy i.e. greater wavelengths are absorbed by the bottom subcell of the tandem stack. The refinements made here in conjunction with the best-reported fill factor (FF=79%) and open-circuit voltage (V_{oc}=1.771V) and as reported in [18] along with our calculated matched current density, we estimate a PCE of 28.73%.

Table 1: Materials used in the optical simulation using SunSolve, their thicknesses range for optimization and optimized thicknesses of PVK/c-Si tandem solar cell. (MAPI= Methylammonium lead iodide)

Cell	Layers	Thickness range (nm)	Optimized thickness (nm)
Perovskite top subcell (1.67eV)	**MgF2**	50 – 250	100
	ITO	60 – 200	62
	SnO_2	5 – 50	15
	C_{60}	5 – 50	10
	MAPI	**100 – 1500**	**330**
	NiO_x	10 – 100	20
RL	**ITO**	10 – 300	20
Silicon bottom subcell (1.22eV)	**a-Si:H (n)**	10	10
	a-Si:H (i)	5	5
	c-Si	**1 – 1000 µm**	**130 µm**
	a-Si:H (i)	5	5
	a-Si:H (p)	10	10
	ITO	150	150
	Ag	300	300

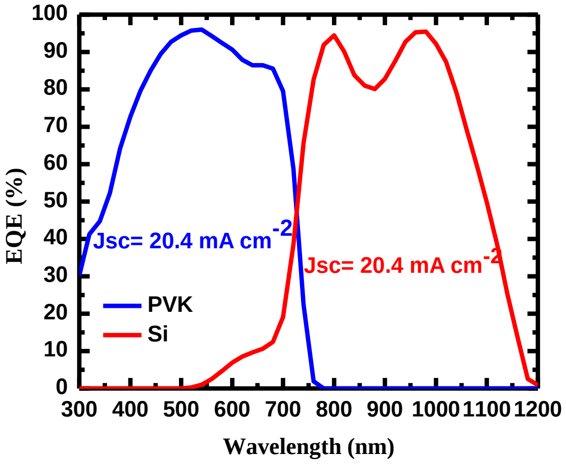

Figure 3: EQE of tandem PVK/c-Si solar cell stack for the solar spectrum of 300nm to 1200nm. Here the high energy photons are absorbed in the top subcell (blue line) and the low energy photons are absorbed by the bottom subcell (red line).

Perovskite-CIGS Tandem Solar Cell

In the tandem PVK/CIGS solar cell simulations, a perovskite solar cell having an absorber bandgap of 1.62eV is employed as a top subcell and CIGS solar cell with absorber bandgap=1.15eV is employed as bottom subcell as shown in figure 1(b). The detail of various layer thicknesses and their optimized values are listed in table 2. The tandem stack is optimized using layer by layer optimization technique and a 19.4 mA cm^{-2} matched current density is achieved. In figure 4 the breakdown of losses taking place in the tandem stack is plotted for a spectrum range of 300nm to 1200nm, which shows both reflection and parasitic absorption taking place in the proposed model of perovskite/CIGS tandem solar cell. Here about 6.30% (2.92 mA cm^{-2}) of the incoming solar spectrum (46.3 mA cm^{-2}) is reflected back from the front surface of the

Table 2: Materials used in the optical simulation of SunSolve, their thicknesses range for optimization and optimized thicknesses of perovskite/c-Si tandem solar cell. (MAPI= Methylammonium lead iodide)

Cell	Layers	Thickness range (nm)	Optimized thickness (nm)
Perovskite top subcell (1.62eV)	**MgF2**	50 – 250	100
	ITO	60 – 200	62
	SnO_2	5 – 50	15
	C_{60}	5 – 50	10
	MAPI	**100 – 1500**	**330**
	NiO_x	10 – 100	20
RL	**ITO**	10 – 300	20
CIGS bottom subcell (1.15eV)	**ZnO**	10	10
	Cds	5	5
	CIGS	**1 – 1000 µm**	**1.05 µm**
	Mo	10	10
	ITO	150	150
	Ag	300	300

device stack which is lower from reflection losses taking place in tandem PVK/c-Si stack (7.87%). This loss is reasonably reduced by the use of MgF_2 as an anti-reflection layer. Large parasitic losses are taking place in front of the transporting layers of the stack.

The tandem cell overall performance is limited by the less efficient subcell of the stack. The EQE of the perovskite/CIGS stack is the summation of its subcells EQEs. In figure 5, EQE of the perovskite/CIGS tandem stack is shown for the solar spectrum range from 300nm to 1200nm (absorbing region). The high bandgap top subcell harvest maximin photons near 550nm wavelength which is a high energy fraction of the incoming solar spectrum. The narrow bandgap (1.15eV) bottom subcell (CIGS) has high photons to electrons ratio near 850nm wavelength which is an intermediate energy fraction of incoming solar spectrum. By using these modifications and guidelines in conjunction with best-reported Voc = 1.49V, and FF =70.2% by [11] with our calculated J_{sc} of 19.5 mA cm^{-2} for tandem PVK/CIGS solar cell stack, we estimate a PCE of 20.31%.

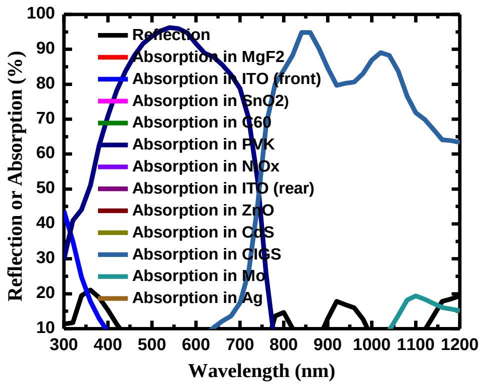

Figure 4: Reflection and absorption losses simulated in the device stack of PVK/CIGS tandem solar cell.

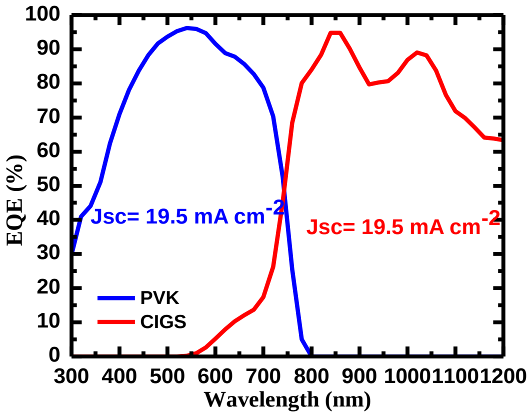

Figure 5: EQE of 2-T monolithic tandem PVK/CIGS solar cell is plotted. Here the high energy photons are absorbed by the top subcell (blue line) and the low energy photons are absorbed by the bottom subcell (red line).

All-Perovskite Tandem Solar Cells

The architecture used in the simulations of tandem PVK/PVK solar cells is given in figure 1(c). For the tandem architecture of PVK/PVK solar cells, a cell having high-Eg from ~1.7 to 1.9eV is used as a top subcell and a cell having low bandgap from ~1.1 to 1.3eV is used as bottom subcell [19]. The top subcell absorbs those photons whose energy is greater than its bandgap, while the bottom subcell absorbs those whose energy is greater from its bandgap and less than the top subcell bandgap. The final performance of the two-terminal tandem stack is greatly dependent on the matching of current between the subcells. The total current of the tandem cell is limited by a less efficient subcell of the stack. The low bandgap bottom subcell is relatively thicker and absorbs the infrared light passing from a wide bandgap top subcell. In our simulation, a perovskite cell with a wide-bandgap (1.82eV) absorber layer is employed as a top subcell and a perovskite with a narrow bandgap (1.22eV) absorber is employed as rear subcell in the PVK/PVK tandem stack. The subcells are interconnected through ITO which acts as a recombination layer. The thicknesses of both active layers in the tandem stack are varied until the current matching is achieved. A matched current density of 18mA cm^{-2} among the tandem stack subcells is achieved at thicknesses of 330nm and 1250nm for front and rear subcells respectively. The thickness range of each layer and optimized thickness values are listed in table 3. The breakdown of losses in the all-perovskite tandem stack for a solar spectrum range from 300nm to 1200nm is plotted in figure 6, which shows the reflection and parasitic absorptions along with absorption in active layers. The higher parasitic absorption occurs in MgF_2, front ITO and top subcell fullerene (C_{60}), which is 0.627, 0.456, and, 0.410 mA cm^{-2}. Nearly 6.17% corresponds to 2.86 mA cm^{-2} of the incoming radiation is reflected from the front of the tandem cell. In the design, 10.6% (4.89 mA cm^{-2}) of the incident radiation is escaped from the front of the solar cell. The recombination layer has very fewer absorption losses, which shows its significance to be used as a recombination layer. The all-perovskite tandem stack photons to electrons conversion are higher than the individual subcells of the tandem stack. Because the solar spectrum large portion is harvested due to a combination of active layers of different bandgaps.

Table 3: Materials used in the optical simulation of SunSolve, their thicknesses range for optimization and optimized thicknesses of perovskite/perovskite tandem solar cell.

Cell	Layers	Thickness range (nm)	Optimized thickness (nm)
Perovskite top subcell (1.82eV)	MgF2	50 – 250	100
	ITO	60 – 200	62
	SnO_2	5 – 50	15
	C_{60}	5 – 50	10
	$MA_{0.9}Cs_{0.1}Pb(I_{0.6}Br_{0.4})_3$	**100 – 1500**	**330**
	NiO_x	10 – 100	20
RL	ITO	10 – 300	20
Perovskite bottom subcell (1.22eV)	SnO_2	5 – 50	15
	C_{60}	5 – 50	10
	$CH_3NH_3Pb_{0.5}Sn_{0.5}I_3$	**100 – 1500**	**1250**
	NiO_x	10 – 100	20
	ITO	150	150
	Ag	300	300

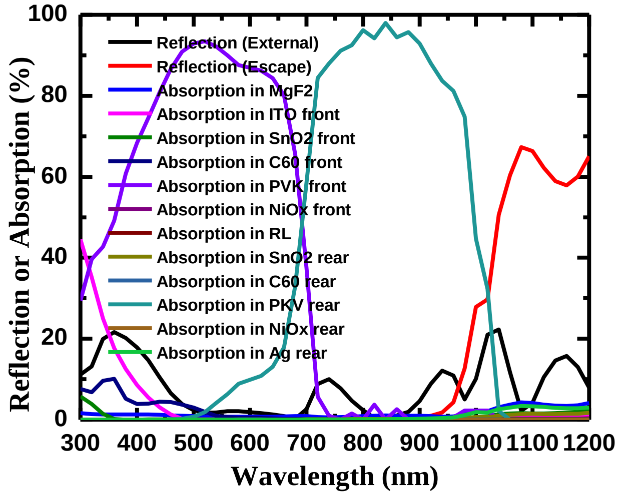

Figure 6: Reflection and absorption losses simulated in the device stack of perovskite/perovskite tandem solar cell.

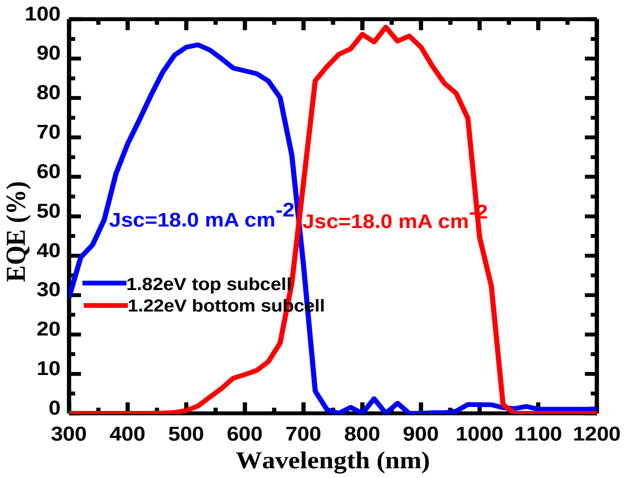

Figure 7: EQE of PVK/PVK tandem solar cell is plotted. Here the high energy photons are absorbed by the top subcell (blue line) and the low energy photons are absorbed by the bottom subcell (red line).

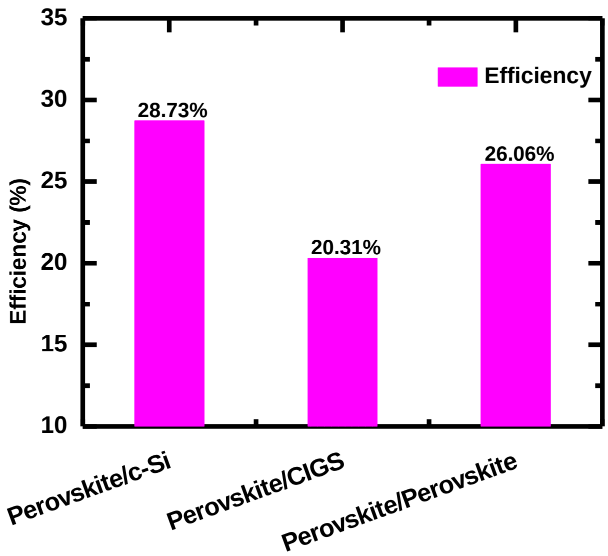

Figure 8: Comparison of three different tandem configurations that are simulated in our work.

The EQE plot in figure 7 shows that the photons of higher energy are absorbed by top subcell while the bottom subcell of the tandem stack absorbs photons of lower energy i.e. greater wavelengths. The fringes in the EQE plot of the rear subcell are due to interferences which leads to limit the light-generated current of the rear subcell and can be reduced by thinning the non-perovskite layers to 5nm [20]. By using these design guidelines in conjunction with Voc=1.98V and FF=73% from best-reported tandem PVK/PVK solar cell [16], we estimated a 26.06% PCE. Here the efficiency of tandem PVK/CIGS solar cell is inferior to the PVK/c-Si and tandem PVK/PVK solar cell as shown in figure 8.

Conclusion

In conclusion to this work, we optically simulated three types of 2-T monolithic tandem solar cells which are PVK/c-Si, PVK/CIGS, and PVK/PVK solar cells. For the simulation of tandem PVK/c-Si solar cell, we used a ~1.1eV c-Si bottom subcell and a 1.67eV perovskite top subcell and achieved a 20.4 mA cm-2 current density after optimization using layer by layer optimization and estimated a PCE of 28.73%. Then we optically simulated a 2-T monolithic tandem PVK/CIGS solar cell and determined various losses in the stack. A 19.4 mA cm-2 matched current density is achieved at 695nm and 1050nm optimized thicknesses of top and bottom absorber layers respectively and PCE of 20.31% is estimated. For modeling of the tandem PVK/PVK solar cell, a wide-bandgap (1.82eV) subcell on top of a narrow bandgap (1.22eV) subcell is employed to make a tandem PVK/PVK solar cell. An 18.0 mA cm-2 matched current density is calculated and a PCE of 26.06% is estimated. By reduction of the non-radiative recombination and optical losses in perovskite-based solar cells can lead the multijunction perovskite solar cells performances beyond the numbers we calculated here in our simulations.

Acknowledgment

I would like to acknowledge the support from USPCAS-E UET Peshawar, Arizona State University (ASU) and USAID during my research work.

References

[1] J.-P. Correa-Baena et al., "Promises and challenges of perovskite solar cells," Science (80-.)., vol. 358, no. 6364, pp. 739–744, 2017.

[2] T. Leijtens, K. A. Bush, R. Prasanna, and M. D. McGehee, "Opportunities and challenges for tandem solar cells using metal halide perovskite semiconductors," Nat. Energy, vol. 3, no. 10, p. 828, 2018.

[3] G. E. Eperon, M. T. Hörantner, and H. J. Snaith, "Metal halide perovskite tandem and multiple-junction photovoltaics," Nat. Rev. Chem., vol. 1, no. 12, p. 95, 2017.

[4] "Best Research-Cell Efficiencies, available online. [Accessed: 20 October 2019], 2019."

[5] W. Shockley and H. J. Queisser, "Detailed balance limit of efficiency of p‐n junction solar cells," J. Appl. Phys., vol. 32, no. 3, pp. 510–519, 1961.

[6] A. De Vos, "Detailed balance limit of the efficiency of tandem solar cells," J. Phys. D. Appl. Phys., vol. 13, no. 5, p. 839, 1980.

[7] P. Löper et al., "Organic-inorganic halide perovskite/crystalline silicon four-terminal tandem solar cells," Phys. Chem. Chem. Phys., vol. 17, no. 3, pp. 1619–1629, 2015.

[8] C. D. Bailie et al., "Semi-transparent perovskite solar cells for tandems with silicon and CIGS," Energy Environ. Sci., vol. 8, no. 3, pp. 956–963, 2015.

[9] J. Zheng et al., "21.8% efficient monolithic perovskite/homo-junction-silicon tandem solar cell on 16 cm2," ACS Energy Lett., vol. 3, no. 9, pp. 2299–2300, 2018.

[10] "Imec Perovskite/CIGS tandem cell with Record Efficiency of 24.6 percent Paves the Way for Flexible Solar Cells and High-Efficiency Building-Integrated PV 2018.[Online]. Available:(https://www.imec-int.com/en/articles/perovskite-cigs-tandem- cell-with-rec," 2018.

[11] M. Jost et al., "21.6%-Efficient Monolithic Perovskite/Cu (In, Ga) Se2 Tandem Solar Cells with Thin Conformal Hole Transport Layers for Integration on Rough Bottom Cell Surfaces," ACS Energy Lett., vol. 4, no. 2, pp. 583–590, 2019.

[12] D. Zhao et al., "Four-terminal all-perovskite tandem solar cells achieving power conversion efficiencies exceeding 23%," ACS Energy Lett., vol. 3, no. 2, pp. 305–306, 2018.

[13] S. Albrecht et al., "Monolithic perovskite/silicon-heterojunction tandem solar cells processed at low temperature," Energy Environ. Sci., vol. 9, no. 1, pp. 81–88, 2016.

[14] ""PVlighthouse,." [Online]. Available: https://www.pvlighthouse.com.au/sunsolve." .

[15] P. D. Paulson, R. W. Birkmire, and W. N. Shafarman, “Optical characterization of CuIn 1− x Ga x Se 2 alloy thin films by spectroscopic ellipsometry,” J. Appl. Phys., vol. 94, no. 2, pp. 879–888, 2003.

[16] A. Rajagopal et al., “Highly efficient perovskite–perovskite tandem solar cells reaching 80% of the theoretical limit in photovoltage,” Adv. Mater., vol. 29, no. 34, p. 1702140, 2017.

[17] [17] Z. Song, C. Chen, C. Li, R. A. Awni, D. Zhao, and Y. Yan, “Wide-bandgap, low-bandgap, and tandem perovskite solar cells,” Semicond. Sci. Technol., vol. 34, no. 9, p. 93001, 2019.

[18] J. Y. Zhengshan and Z. C. Holman, “Predicting the Efficiency of the Silicon Bottom Cell in a Two-Terminal Tandem Solar Cell,” in 2017 IEEE 44th Photovoltaic Specialist Conference (PVSC), 2017, pp. 3250–3253.

[19] D. Zhao et al., “Efficient two-terminal all-perovskite tandem solar cells enabled by high-quality low-bandgap absorber layers,” Nat. Energy, vol. 3, no. 12, p. 1093, 2018.

[20] M. T. Hörantner et al., “The potential of multijunction perovskite solar cells,” ACS Energy Lett., vol. 2, no. 10, pp. 2506–2513, 2017.

International Journal of Engineering Works
ISSN-p: 2521-2419
ISSN-e: 2409-2770
Vol. 6, Issue 12, PP. 534-542, December 2019
https://www.ijew.io/
https://doi.org/10.34259/ijew.19.612534542

A Comparative Study of Low-Voltage Ride-Through (LVRT) Control of Grid-Interfaced Doubly-Fed Induction Generator (DFIG)

Muhammad Naveed[1], Prof. Dr. Muhammad Naeem Arbab[2]
[1,2] University of Engineering and Technology, Peshawar Pakistan
naveedepe@gmail.com[1], mnarbab@yahoo.com[2]
Received: 15 December, Revised: 28 December, Accepted: 31 December

***Abstract*—** Due to the fast increase in energy of modern human being the desire for the clean renewable energy is increasing day by day. Electrical power generation from wind is promising source. But due to the large combination of wind forms in electrical power grid the stability and security are key issues for the electrical power engineers. Amongst the required grid codes for the power utilities LVRT is very important. According to LVRT the wind form should act as conventional power plant and connect to grid for some particular time to provide stability to grid at normal and fault time. In this paper we have developed a LVRT strategy for control of active, reactive power and DC link voltage of the variable speed wind turbine. The test bed system is 9 MW DFIG wind turbine attached to 120KV grid system by 30KM long 25 KV transmission line. The modelling and simulation is done by using MATLAB/SIMULINK. The control system is implemented by using PI controller using vector or field oriented control. The LVRT strategies implemented on test bed model are (STFCL), DC chopper, Rotor Crowbar and Hybrid strategy with using RSC control, GSC control and pitch control mechanisms. The hybrid strategy provides excellent solution for LVRT of DFIG wind turbine by controlling power (active and reactive) and voltage of DC link. The results of hybrid strategy during symmetrical fault is best and well suited to the LVRT requirements as compared of STFCL, DC chopper and crowbar.

***Keywords*—** DFIG, LVRT, STFCL, DC chopper.

I. INTRODUCTION

The usage of energy is growing due to the population increase and industrialization of the modern world. The use of traditional fossil fuel is increasing every day. This has created the energy shortage, environmental pollution, and the alarming situation of global warming. Due to these factors, todays the renewable energy is very much attractive and demanding type of energy. Amongst the renewable sources the wind power is widely and easily available. Therefore, there is rapid growth of using wind power technologies globally. The installations of wind power in 2018 was higher than 52GW. The expectation for wind power in 2019 is higher [1]. Due to the greater number of wind power plants present in power system grid and dynamic behavior of wind turbines there is serious issue of grid stability, security and control. So many countries have developed the new grid codes for the steady operation of grid system. The new codes of grids demand that the wind turbine well have to work like hydro and thermal plants during normal operations and at a time of fault to provide sustenance to grid system. In the latest grid codes, the main issue is (LVRT) or (FRT) ability when fault occurs on grid and is very essential for engineers in electrical power system [2], [3]. According to LVRT the wind turbine should be attached to grid during faults for a particular time after that it should be allowed to disconnect. Furthermore, the wind turbine will have to work as like the conventional power plants to provide back up to the grid [2], [3].

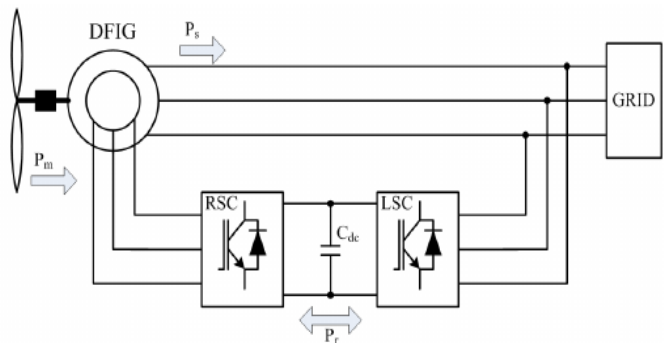

Fig. 1. DFIG based wind turbine configuration with partial scale convertors.

Among various wind turbines (WT), DFIG-WT as in Figure.1 is very well known due to its favorable features, such as (a) Greater efficiency , (b) greater speed variation, (c) active and reactive power is controlled without the effect of each other, (d) low Rating of Grid side converts (GSC)and Rotor side convertor (RSC), (e) reduced mechanical force and (f) better quality of power [4].However the dynamic behavior of the DFIG based WT is serious problem at the time of voltage dip because its stator is directly attached to grid [5], and due to the reduced scale convertors that are attached to the rotor of

DFIG. Therefore, when fault accrues at a far location from the DFIG WT the voltage at grid connection point GCP is reduced due to which the voltage of rotor, DC link and current increased [6]- [9]. So if we did not use any protection and control scheme these high voltage and currents would harm the power electronics convertor and the Wind turbine speed is increased to a danger level. This is also a great risk for the turbine operation Until we designed it suitably [6]-[12].Therefore the focus of this paper is to properly investigate the capability of LVRT of DFIG at the time of faults on grid and to give suitable control for LVRT solution that can provide safety and security to the DFIG WT during faulty grid condition. The proposed control strategy is Hybrid including Stator Type Fault Current Limiter (STFCL), DC Chopper, Rotor Side convertor (RSC) and Grid Side Convertor using PI controller.

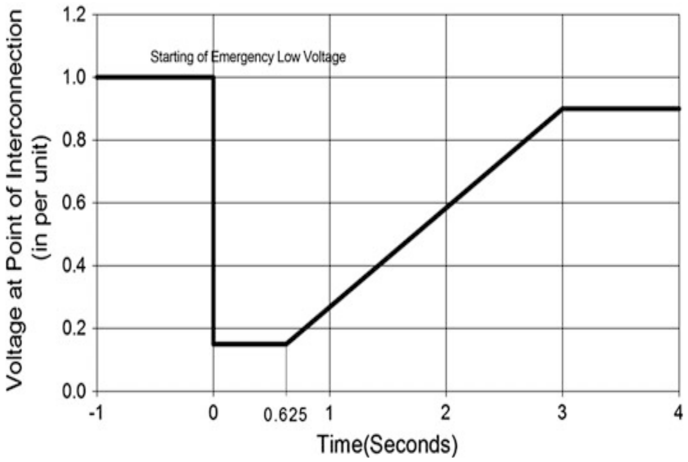

Fig. 2. The USA codes of grid for Low Voltage Ride Through [13].

II. DFIG Modelling

For the wind power industry, the improvement of LVRT of DFIG is very important challenge. The mathematical model of DFIG make us capable of analyzing the behavior during generic conditions.so here we want to know about the DFIG dynamic model. For the derivation of DFGIG model we use the equation the magnetic flux linkages. The equation of motion and voltages which are associated with stator and rotor of DFIG machine is also very important.

A. *Equation of Voltage for DFIG*

The Figure 3 shows the model which is equivalent of DFIG. This model is for synchronous speed.

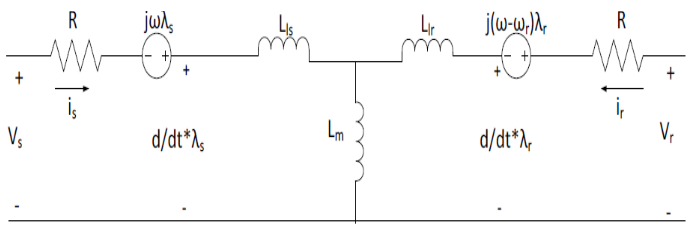

Fig. 3. DFIG space vector equivalent circuit model

From the above figure it is clear that the stator and rotor voltages are denoted as

$$V_s = R_s i_s + {d\lambda_s}/{dt} + j\omega\lambda_s \tag{1}$$

$$V_r = R_r i_r + {d\lambda_r}/{dt} + j(\omega - \omega_r)\lambda_r$$

In the above equation Vs,Vr are voltages.

The Rs,Rr represents the resistances. The Is,Ir are the currents a. The λs,λr is for the Flux linkages(Wb).ω is the rotating speed of arbitrary reference frame (rad/s). ω_r is used for angular speed in (rad/s).

In the above equations the subscript that have been used are s for stator and r for rotor. The terms j$\omega\lambda$s and J(ω_s-ω_r)λ_r are used to represents the voltage induced..

B. *Equation of Flux linkages*

The equation of the flux linkages can be represented as

$$\lambda_s = (L_{ls} + L_m)i_s + L_m i_r = L_s i_s + L_m i_r$$
$$\lambda_r = (L_{lr} + L_m)i_r + L_m i_s = L_m i_s + L_r i_r$$

Where

$$L_s = L_{ls} + L_m$$
$$L_r = L_{lr} + L_m \tag{2}$$

In the above equations λs, λr are used for the flux linkages of stator and rotor side. Ls is used to represent the stator self-induced flux in hennery (H). Lr is for Rotor self-induced flux in hennery (H).Lm is representing the inductance in (H) of magnetizing. The Lls, Llr are the leakage Inductances (H).

C. *Motion equation*

The Mechanical motion can be represented in terms of electromagnetic and mechanical torque using the following equation

$$J\frac{d\omega_m}{dt} = T_e - T_m$$
$$\mathrm{T_e} = \frac{3\mathrm{P}}{2}\mathrm{R_e}(\mathrm{j}\lambda_s \mathrm{i_s}) \tag{3}$$
$$\mathrm{T_e} = -\frac{3\mathrm{P}}{2}\mathrm{R_e}(\mathrm{j}\lambda_r \mathrm{i}_r)$$

In the above equations of (3) J is used for moment of inertia of rotor in the unit (Kgm^2). Te represents the electromagnetic torque.ω_r is used to represent rotor speed, and $\omega_m = \frac{\omega_r}{p}$. P is used to denote the poles pairs of DFIG. Tm denotes the Mechanical torque of generator shaft in the unit of Newton meter (Nm)

If we combine all the above equation, we can obtain the space vector model for the DFIG. The space vector model is changed to synchronous reference frame. The synchronous speed is given by

$$\omega_s = 2\pi f$$
$$\omega_{sl} = \omega_s - \omega_r \quad (4)$$

Where ω_{sl} is speed of slip and the ω_s is the synchronous speed at the electrical frequency f_s of stator. As the stationary reference is static therefore the value of ω is set to zero.

D. dq Reference frame Model

For the DFIG model we can use stationary or dq reference frames. In stationary reference frame the model parameters like inductance capacitances and resistances changes with time. For analyzing the performance of the DFIG we will have to use dq reference frame in which the equivalent circuit parameters such as inductance, resistances and voltages etc does not changes with time and remain constant with time. Using the dq reference frame the axes of d and q are separated at 90 degrees and therefore we can use the decoupled control.

The equations for different circuit parameters such as voltage, flux linkages and motion is derived if we divide Equations in to real and imaginary parts. Thus the new equation obtained in the form of

$$V_s = V_{ds} + jV_{qs}\,;\; i_s = i_{ds} + ji_{qs}\,;\; \lambda_s = \lambda_{ds} + j\lambda_{qs} \quad (5)$$

$$V_r = V_{dr} + jV_{qr}\,;\; i_r = i_{dr} + ji_{qr}\,;\; \lambda_r = \lambda_{dr} + j\lambda_{qr}$$

E. Voltage equation using dq reference frame

By splitting the real and imaginary parts the dq components of voltage will be

$$V_{sd} = R_s I_{sd} + {d\lambda_{sd}}/{dt} - \omega\lambda_{sq}$$
$$V_{sq} = R_s i_{sq} + {d\lambda_{sq}}/{dt} + \omega\lambda_{sd} \quad (6)$$
$$V_{rd} = R_r i_{rd} + {d\lambda_{rd}}/{dt} - (\omega - \omega_r)\lambda_{rq}$$
$$V_{rq} = R_r i_{rq} + {d\lambda_{rq}}/{dt} + (\omega - \omega_r)\lambda_{rd}$$

F. Equation for flux linkage in dq axis

The flux linkage equation for the dq components is given by

$$\begin{aligned}\lambda_{sd} &= L_s i_{sd} + L_m i_{rd}\\ \lambda_{sq} &= L_s i_{sq} + L_m i_{rq}\\ \lambda_{rd} &= L_m i_{sd} + L_r i_{rd}\\ \lambda_{rq} &= L_m i_{sq} + L_r i_{rq}\end{aligned} \quad (7)$$

G. Equation of motion in the dq axis

The torque (electromagnetic) is achieved in different ways. The mostly used expression in literature are below

$$T_e = \begin{cases} \dfrac{3P}{2}(I_{qs}\lambda_{ds} - I_{ds}\lambda_{qs}) \\ \dfrac{3PL_m}{2}(I_{qs}L_{dr} - I_{ds}I_{qr}) \\ \dfrac{3PL_m}{2L_r}(I_{qs}\lambda_{dr} - I_{ds}\lambda_{qr}) \end{cases} \quad (8)$$

The equivalent dq model of the DFIG is given below.

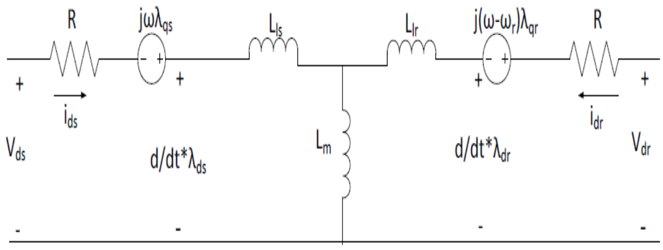

(a) d-axis model

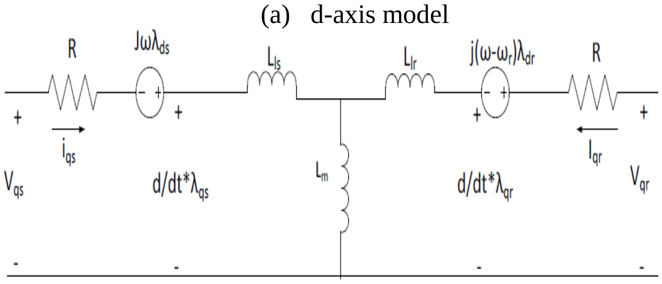

(b) q-axis model

Fig. 4. dq axis model for DFIG

H. Relation for speed, active power and torque

If we neglect the resistive losses, then the power of stator and rotor is

$$P_r \cong sP_s \quad (9)$$

And the mechanical power is also expressed as

$$P_m \cong P_s - sP_s \cong P_s(1 - s) \quad (10)$$

As we know that

$$(1 - s) = \omega_m/\omega_s \quad (11)$$

$$P_m \cong \frac{\omega_m}{\omega_s}P_s \cong T_{em}\omega_m/P \quad (12)$$

From the above Equation the relation between Ps and electromagnetic torque is given by (4.21)

$$P_s \cong T_{em}\omega_s/P \quad (13)$$

Similarly, the rotor power can be expressed as

$$P_r \cong T_{em}\omega_r / P \tag{14}$$

From the above equations it is clear that the DFIG can be operated in many ways. That is the DFIG can be operated in different modes. These are very important relation

III. PROPOSED LVRT STRATEGIES

As mentioned earlier that (DFIG) attached to grid must have to work as stated by the condition of (LVRT) when fault occurs. The LVRT condition required that the DFIG be attached to the grid system at faulty condition and provide assistance by providing active and reactive power to grid. Therefore, different LVRT strategies are discussed in literature. Amongst various hard ware strategies, the DC Chopper and (STFCL) are very effective.so our proposed LVRT strategy is the hybrid of these two strategies.

A. DC Chopper Circuit

This circuit is actually a combination of resistor, switch and freewheeling diode. These elements are attached in parallel of the capacitor of DC- link to supress the high voltage peaks of convertor DC bus as in shown in figure.5. At the time fault occurs on grid the high power flows to convertors and voltage level at DC bus increased [14]. In [15] the authors have also used the chopper control for over voltage protection.

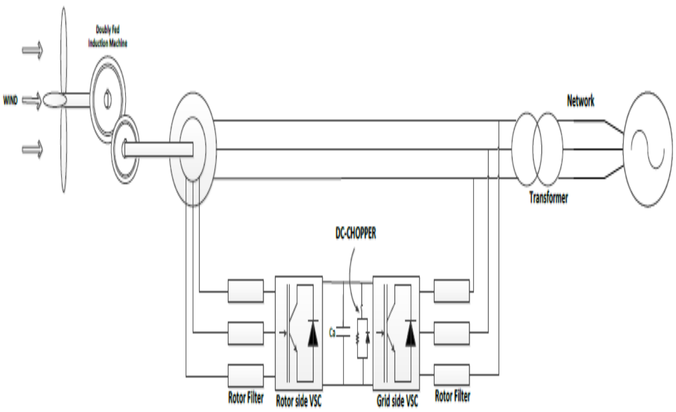

Fig. 5. DFIG Chopper circuitry [16]

At normal operation the switch is open when fault take place then the switch become closed and resistor is placed in circuit, this resistor dissipate the high extra energy and voltage peaks is filtered. The purpose of using Freewheeling diode is that it blocks the stress when the switch is off [17].

B. Stator type fault current limiter switch (STFCL)

STFCL as shown below worked for the improvement of the LVRT of DFIG. The purpose of using the STFCL is that it provides protection to the DFIG power electronics circuitry.it also provide safety to the grid system during fault when the torque is increased. From the figure below it is clear that it has a transformer for isolation purposes.it has a switch (S_d) which is a semiconductor type. This switch is normally closed switch. When the fault occurs at grid this switch detects the fault and the switch is opend.by opening this switch the fault current limiting circuitry is introduced to the fault. The STFCL circuit has also a bridge circuit consists of diodes. In parallel of the bridge it has a capacitor called snubber capacitor (Cf) and a resistor (Ra) and capacitor (Ca) which are in series to each other and parallel to snubber capacitor for the purposes of limiting the fault current as shown in Fig. 5.2.

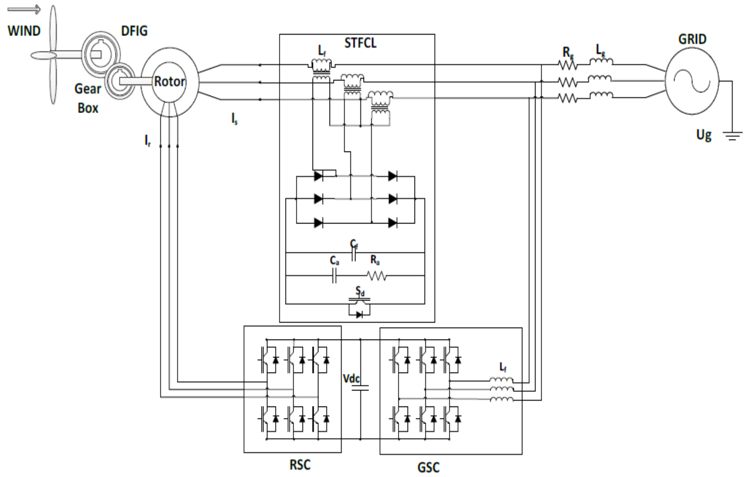

Fig. 6. DFIG Stator type fault current limiter switch [18]

At the time when there is not any fault, the switch is normally closed and the inductor L is not inserted in in the circuit. But when the fault occurs the switch is opened. At initial stage the current at fault is controlled by the L1, the (Ra) and the (Ca). At last time when the capacitor reaches to it full capacity the current flowing to bridge is stopped. At that time the inductor is fully placed in the stator for controlling current and the EMF is also weakens [19], [20],[21]

C. Hybrid strategy

This hybrid strategy is the combination of both the above strategies (DC Chopper + STFCL). This is our proposed strategy that is implemented in this paper as shown in the below figure.

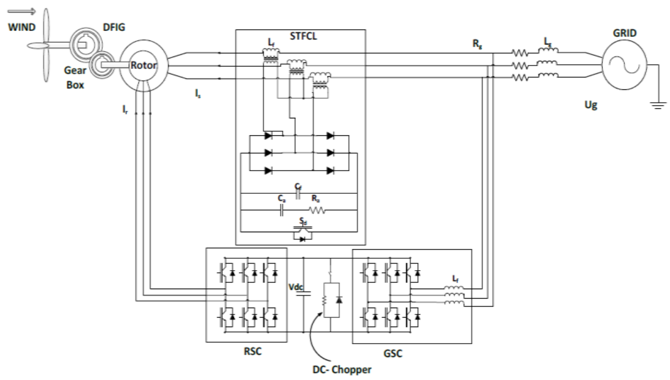

Fig. 7. DFIG Hybrid strategy

IV. CONTROL SYSTEM FOR DFIG

The control system makes us capable to regulate the flow of current of rotor. If we regulate current flow to rotor, then its output power is controlled and it is also possible to get maximum efficiency. We will use the Vector control system. It is very better control method and is widely used. In this method the real power is independently control without the effect of reactive control and vice versa. The generator and convertor in DFIG based WECS acts like a current regulated voltage source invertor.

In DFIG based WECS there are two power convertors (a) the rotor side convertor (RSC) and (b) the Grid side convertor (GSC). These convertors are attached by a capacitor called DC link capacitor. This DC link capacitor works for the storing the excessive energy and filters the voltage peaks. The purpose of RSC is to control the speed, torque and power. The GSC maintains the value of the voltage of DC link constant. It keeps control of reactive power as well [12].

A. Rotor side convertor (RSC) control system block diagram

The control system block diagram for RSC is shown in figure 8. The stator voltage oriented control (SVOC) is used for the RSC control. The Qs calculator calculate the stator position angle θ_s and θ_r is find out by the using of an encoder. The rotor slip angle θ_{sl} is

$$\theta_{sl} = \theta_s - \theta_r$$

Different variable can be transform by (abc to dq) block and similarly from the dq reference frame can be transform to abc by (dq to abc) block[22],[23]. The stator angle θ_s is find out by

$$\theta_s = tan^{-1}\frac{V\beta}{V\alpha} \tag{15}$$

And the stator dq voltage will be given by

$$\begin{bmatrix} V_\alpha \\ V_\beta \end{bmatrix} = \frac{2}{3}\begin{bmatrix} 1 & -\frac{1}{2} & -\frac{1}{2} \\ 0 & \frac{\sqrt{3}}{2} & -\frac{\sqrt{3}}{2} \end{bmatrix} \cdot \begin{bmatrix} V_{as} \\ V_{bs} \\ V_{cs} \end{bmatrix} \tag{16}$$

The Vas, Vbs and Vcs a re the three phase stator voltages.

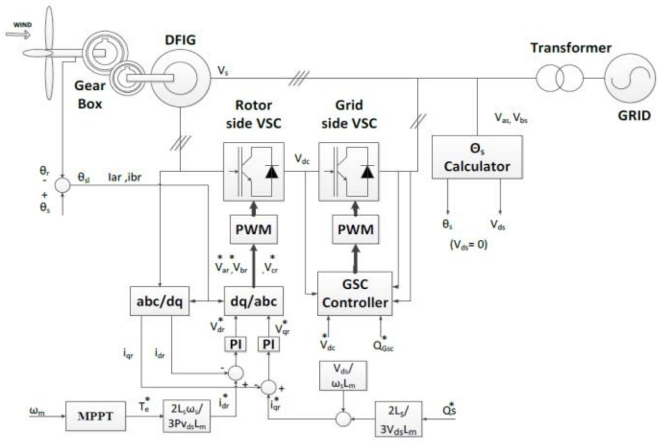

Fig. 8. (RSC) control system block diagram

The MPPT method (that is an optimum method) for torque production is utilized to find out reference torque (electromagnetic) Te. The i_{dr} is generated by the second block by tacking the reference torque T_e as input. The dq axis reference voltage V_{dr} and V_{qr} is transformed from the dq axis to (abc) reference frame v_a ,v_b, v_c. These v_a ,v_b, v_c act as a modulator signal for the PWM invertor. After that modulating signal is matched with carrier signal and the error signal worked as gating signal for the invertor device. Thus (RSC) control perform the two main functions. Controlling of power of the DFIG independently.

B. Grid side convertor (GSC) control for DFIG

This control system which is voltage oriented is one of the common scheme used for (GSC) control is shown in Fig. 9 below. In this control scheme the changing from the (abc) to (dq) reference is used [24], [25].

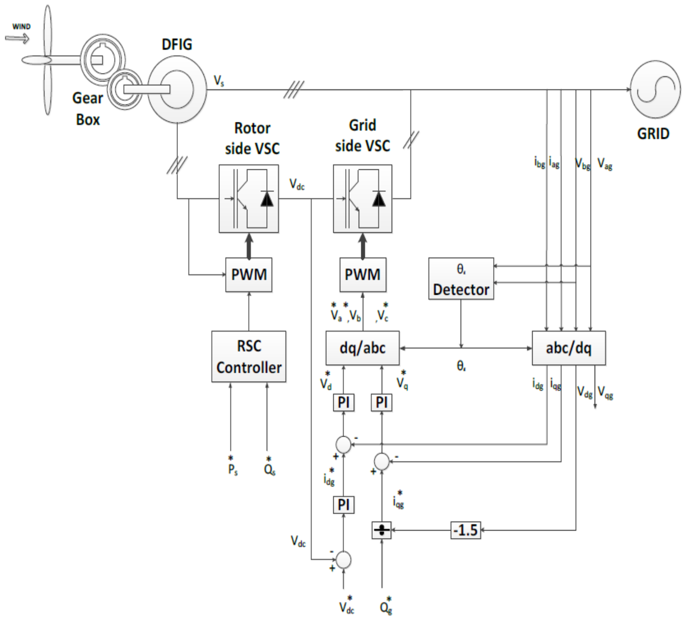

Fig. 9. (GSC) control system for DFIG

θ_g is needed for transferring (abc) to dq reference. For voltage angle θ_g calculation various methods are used but here we have used Phase locked loop (PLL) method. For the transformation from stationary (abc) reference to dq reference we need to measure the balance values for the three phase voltages v_a ,v_b, v_c [29].

We can find θ_g with following formula.

$$\theta_g = \tan^{-1}\frac{V_\beta}{V_\alpha} \tag{17}$$

Where V_α and V_β can be find by the following transformation

$$\begin{bmatrix} V_\alpha \\ V_\beta \end{bmatrix} = \frac{2}{3}\begin{bmatrix} 1 & -\frac{1}{2} & -\frac{1}{2} \\ 0 & \frac{\sqrt{3}}{2} & -\frac{\sqrt{3}}{2} \end{bmatrix} \cdot \begin{bmatrix} V_{ag} \\ V_{bg} \\ V_{cg} \end{bmatrix} \tag{18}$$

For the balance three phase voltages system we will have $V_{ag} + V_{bg} + V_{cg} = 0$. So we have

$$\begin{pmatrix} V_\alpha \\ V_\beta \end{pmatrix} = \frac{2}{3}\begin{pmatrix} V_{ag} - \frac{1}{2}V_{bg} - \frac{1}{2}V_{cg} \\ \frac{\sqrt{3}}{2}V_{bg} - \frac{\sqrt{3}}{2}V_{cg} \end{pmatrix} = \begin{pmatrix} V_{ag} \\ \frac{\sqrt{3}}{3}\left(V_{ag} + 2V_{bg}\right) \end{pmatrix} \tag{19}$$

From the above equation (19) it is clear that for VOC only two voltages V_{ag} and V_{bg} are enough. Practically the voltage signals from the grid are in distorted form having harmonics. So we use PLL practically to calculate the angle θ_g.

In VOC i_{ag}, i_{bg} and i_{cg} are calculated and transformed to dq components currents i_{dg} and i_{qg}. Then By using i_{dg} we control Ps and by using i_{qg} we control the Qs.

As we know that the in VOC V_{gd} is equal to zero.

$$V_{qg} = \sqrt{V_g^2 - V_{dg}^2} = 0 \tag{20}$$

And the power is

$$\begin{cases} P_s = \frac{3}{2}\left(V_{dg}I_{dg} + V_{qg}I_{qg}\right) = \frac{3}{2}V_{dg}I_{dg} \\ Q_s = \frac{3}{2}\left(V_{qg}I_{dg} - V_{dg}I_{qg}\right) = -\frac{3}{2}V_{dg}i_{qg} \end{cases} \tag{21}$$

Equation (21) clearly indicates that the Ps is controlled with i_{dg} and the Qs with i_{qg}. And the reference current of the q-axis is

$$i_{qg}^* = -\frac{Q_g^*}{1.5V_{dg}} \tag{22}$$

Q_g^* in the above equation represents the reference value of the grid reactive power. Its value is positive, negative or unity.

The PI controller produce the signal of i_{dg} according to the operating condition. That i_{dg} is used for the controlling of the active power Ps.

If we consider the ideal switch, then the DC active side power is equal to the invertor AC side power and mathematically it is represented as

$$P_g = \frac{3}{2}V_{dg}I_{dg} = V_{dc}I_{dc} \tag{23}$$

V. Simulation Results and Performance Evaluation

The results and behavior of the different LVRT strategies is tested using MATLAB SIMULINK software. The testing model is 9MW DFIG WT attached with grid. Which transmit electrical power to 120 KV power grid by 25 KV long transmission line. The wind is flowing with 11m/s. The fault (short circuit) is enforced at 30 KM transmission line. The duration of fault is 300ms.

Four LVRT strategies (1) Hybrid (2) (STFCL) (3) DC Chopper and (4) Crowbar are critically compared with (RSC) control, (GSC) control and pitch control is also implemented. The results are tested for symmetrical (three line to ground) (LLL-G) occurred on the transmission line and the voltage of DC Link is controlled using PI Controller.

A. Symmetrical faults

The figures (10) -(18) clearly gives the results of different LVRT strategies for the voltage of power Grid and current, voltage of DC link, active and reactive power, electromagnetic torque rotor current and voltage and the electromagnetic torque for the Symmetrical (three line to ground) fault of the grid interfaced DFIG. The fault occurs from 1 to 1.3 seconds (300ms) on 30 Km long transmission line.

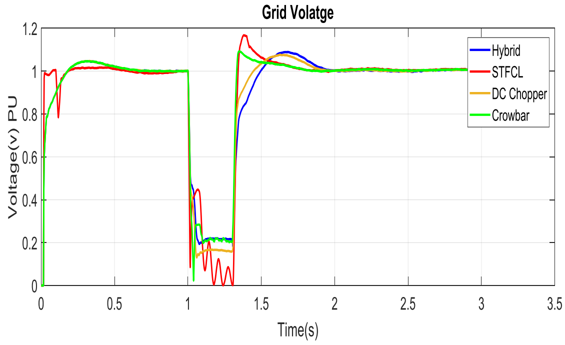

Fig 10. Grid Voltage

Figure 10 gives the grid voltage response of different strategies for the grid interfaced DFIG during symmetrical (LLL_G) fault. Sever voltage dip is for the STFCL.it is the lowest and has high oscillations. The hybrid strategy has lowest voltage dip of all and is smoother. The response of the DC chopper and Crowbar is in between hybrid and STFCL.

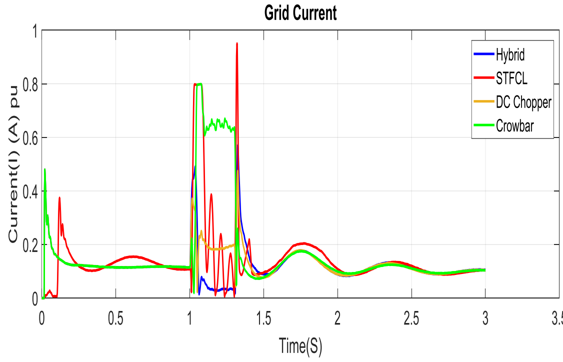

Fig 11: Grid current

The figures 11 shows the grid current response of different strategies for the grid interfaced DFIG during symmetrical (three line to ground) (LLL-G) fault. STFCL strategy has very high oscillations and peaks. The 2nd highest response is of the Crowbar and 3rd highest is of DC chopper strategy. The hybrid strategy has lowest current oscillations and peaks.so the hybrid is better of all the strategies.

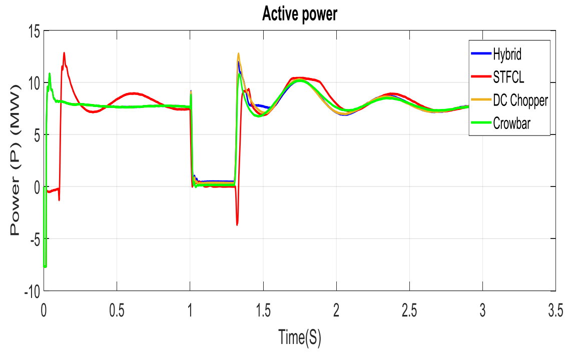

Fig 12: Active power

Figure 12 gives the Active power performance of different strategies for the grid interfaced DFIG during symmetrical (LLL-G) fault. It clearly shows the Hybrid strategy provide excellent results, the reaction of the STFCL is that it has below 0 MW power during grid fault. The crowbar and DC Chopper have approximately same active power response that is between the hybrid and STFCL.

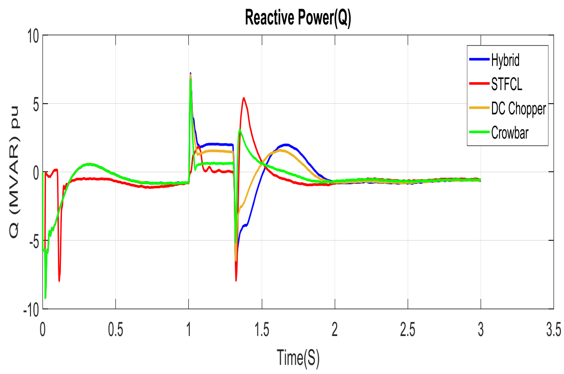

Fig 13: Reactive Power

Figure 13 shows the reactive power response of different strategies of grid interfaced DFIG during symmetrical (LLL-G) fault. The response of the Hybrid is again very good. It provides better MVAR as compared to the other strategies. The response of the STFCL is poor, it injects 0 MVAR to the grid during fault and after fault it has very great spikes. The DC chopper and Crowbar have better results than STFCL but poor than hybrid.

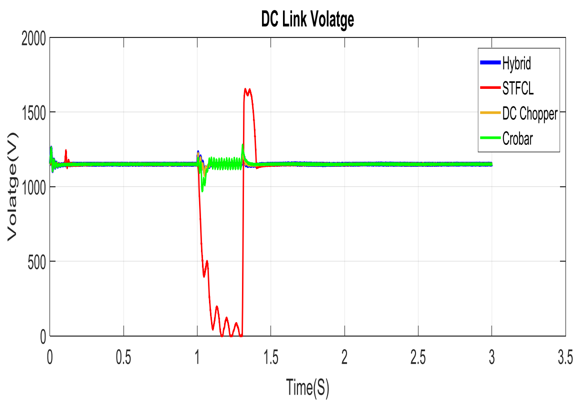

Fig 14: DC Link voltage

The figure 14 clearly indicates the voltage for the DC link response of different strategies of the grid interfaced DFIG during symmetrical (LLL-G) fault. The Hybrid strategy reduce the DC link voltage very effectively and have low oscillations. The STFCL voltage during grid faults falls to 0V and has spikes of above 1500 V. The voltage spikes of the crowbar and DC chopper have voltage spikes nearer to 1250V. The Hybrid have good response have lowest voltage spikes.

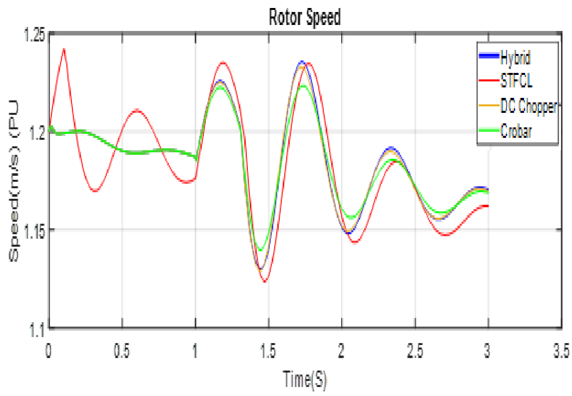

Fig 15: Rotor speed

Figure 15 clearly indicates the rotor speed reaction of different strategies for the grid interfaced DFIG during symmetrical (LLL-G) fault. The figure clearly indicates that hybrid has rotor speed nearer to per unit (pu) value and having low oscillations. The STFCL have very high and oscillatory rotor speed. The response of the DC chopper and crowbar is nearly same to the hybrid.

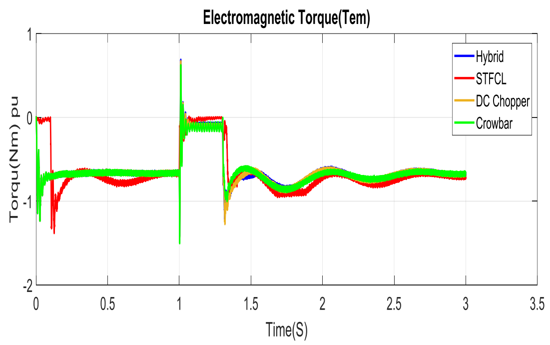

Fig 16: Electromagnetic Torque

Figure 16 shows the electromagnetic toque response during symmetrical (LLL-G) grid fault for the different strategies of grid interfaced DFIG. From the figure it is clear that the response of the STFCL is oscillatory and after fault it takes large time to stabilize. The response of hybrid is smoother and stabilize very soon after fault. DC chopper and crowbar have nearly same response as hybrid.

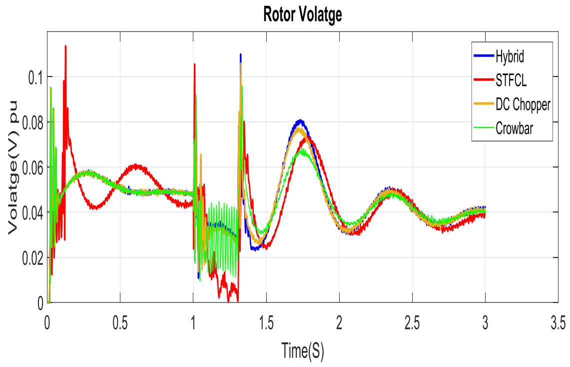

Fig 17: Rotor Voltage

Figure 17 shows the rotor voltage performance of different strategies for the grid interfaced DFIG during symmetrical (LLL-G) fault. STFCL has very high oscillations and peaks. The hybrid has lowest oscillation and smoother response of all strategies. The dc chopper and crowbar have response between the STFCL and hybrid.

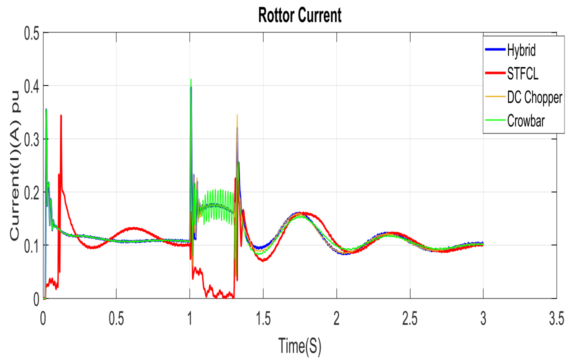

Fig 18: Rotor current

Figure 18 shows the rotor current response of different strategies for the grid interfaced DFIG during symmetrical (LLL-G) fault. The STFCL, DC chopper and Crowbar have very high oscillations and peaks but the Hybrid strategy has smooth and low oscillation and its current value is nearer to per unit (pu) value.

CONCLUSION

The LVRT strategies implemented on test bed model are (STFCL), DC chopper, Rotor Crowbar and Hybrid strategy with using RSC control, GSC control and pitch control mechanisms. The hybrid strategy provides excellent solution to the LVRT of DFIG based WT by controlling the active, reactive power and voltage of DC link. The results for the voltage of Grid and current, voltage of rotor and current, DC link voltage, active and reactive power, electromagnetic torque and rotor speed of hybrid strategy during symmetrical (three line to ground) (LLL-G) fault is best and well suited to the LVRT requirements as compared of STFCL, DC chopper and crowbar.

REFERENCES

[1] REN21. (2019). Renewables Global Status Report - REN21. [Online] Available at: http://www.ren21.net/status-of-renewables/global-status-report

[2] W. Qiao and R. G. Harley, "Grid Connection Requirements and Solutions for DFIG Wind Turbines," 2008 IEEE Energy 2030 Conference, 2008.

[3] FERC - Interconnection of Wind Energy, 18 CFR Part 35, Docket No. RM05-4-001; Order No. 661-A December 12, 2005.

[4] B. B. Ambati, P. Kanjiya, and V. Khadkikar, "A Low Component Count Series Voltage Compensation Scheme for DFIG WTs to Enhance Fault Ride-Through Capability," IEEE Transactions on Energy Conversion, vol. 30, no. 1, pp. 208–217, 2015

[5] D. A and S. A "Comparison of fault ride-through strategies for wind turbines with DFIM generators". IEEE European conference on power electronics and applications, New York ,2005, Dresden, pp. 1–8.:

[6] J. Morren and S.W.H. de Haan, "Ridet hrough of wind turbines with doubly-fed induction generator during a voltage dip," IEEE Trans.Energy Convers., vol. 20, no. 2, pp. 435 – 441, June 2005.

[7] J. Lopez, P. Sanchis, X. Roboam, and L. Marroyo, "Dynamic behaviour of the doubly fed induction generator during three-phase voltage dips," IEEE Trans. Energy Convers., vol. 22, no. 3, pp. 709 – 717, Sept. 2007.

[8] X. Kong, Z. Zhang, X. Yin and M. Wen, "Study of fault current characteristics of the DFIG considering dynamic response of the RSC," IEEE Trans. Energy Convers., vol. 29, no. 2, pp. 278-287, June. 2014

[9] W. Chen, F. Blaabjerg, N. Zhu, M. Chen and D. Xu, "Doubly fed induction generator wind turbine system subject to symmetrical recurring grid faults", IEEE Trans. Power Electron., early access, 2015.

[10] S. Seman, J. Niiranen, S. Kanerva, A. Arkkio, and J. Saitz, "Performance study of a doubly fed wind-power induction generator under network disturbances," IEEE Trans. Energy Convers., vol. 21, no. 4, pp. 883 – 890, December 2006.

[11] I. Erlich, H. Wrede, and C. Feltes, "Dynamic behavior of DFIG-based wind turbines during grid faults," in Proc. 38th IEEE Power Electronics Specialists Conference, Orlando, FL, USA, June 17-21, 2007, pp. 1195-1200.

[12] A. Hansen, G. Michalke, P. Sørensen, F. Iov, and T. Lund, "Coordinated voltage control of DFIG wind turbines in uninterrupted operation during grid faults," Wind & Solar Energy Journal, vol. 10, no. 1, Aug. 2006.

[13] P. Kumar and A. K. Singh." Grid Codes goals and challenges" Electrical Engineering Department, Motilal Nehru National Institute of Technology Allahabad, Uttar Pradesh 211004, India e-mail: pradeepkumar@ieee.orgA. K. Singh e-mail: asheesh@mnnit.ac.in

[14] K. E. Okedu, S. M. Muyeen, R. Takahashi, and J. Tamura, "Application of SDBR with DFIG to augment wind farm fault ride through," 2011 International Conference on Electrical Machines and Systems, 2011.

[15] R. Sarrias, L. M. Fernández, C. A. García, and F. Jurado, "Coordinate operation of power sources in a doubly-fed induction generator wind turbine/battery hybrid power system," Journal of Power Sources, vol. 205, pp. 354–366, 2012.

[16] F. Lima, A. Luna, P. Rodriguez, E. Watanabe, and F. Blaabjerg, "Rotor Voltage Dynamics in the Doubly Fed Induction Generator During Grid Faults," IEEE Transactions on Power Electronics, vol. 25, no. 1, pp. 118–130, 2010.

[17] S. Xiao, G. Yang, H. Zhou, and H. Geng, "Analysis of the control limit for rotor-side converter of doubly fed induction generator-based wind energy conversion system under various voltage dips," IET Renewable Power Generation, vol. 7, no. 1, pp. 71–81, 2013.

[18] W. Guo, L. Xiao, S. Dai, Y. Li, X. Xu, W. Zhou, and L. Li, "LVRT Capability Enhancement of DFIG With Switch-Type Fault Current Limiter," IEEE Transactions on Industrial Electronics, vol. 62, no. 1, pp. 332–342, 2015.

[19] K. Young, V. Utkin, and U. Ozguner, "A control engineers guide to sliding mode control," Proceedings. 1996 IEEE International Workshop on Variable Structure Systems. - VSS96 -.

[20] Mohan, Ned. Advanced electric drives: analysis, control, and modeling using MATLAB/Simulink. John wiley & sons, 2014.

[21] Niiranen, Jouko. "Voltage dip ride through of a doubly-fed generator equipped with an active crowbar." In Nordic wind power conference, vol. 1. Chalmers University of Technology Sweden, 2004.

[22] J. K. Huusom, N. K. Poulsen, S. B. Jørgensen, and J. B. Jørgensen, “ARX-Model based Model Predictive Control with Offset-Free Tracking,” Computer Aided Chemical Engineering 20th European Symposium on Computer Aided Process Engineering, pp. 601–606, 2010.

[23] J. K. Huusom, N. K. Poulsen, S. B. Jørgensen, and J. B. Jørgensen, “Tuning SISO offset-free Model Predictive Control based on ARX models,” Journal of Process Control, vol. 22, no. 10, pp. 1997–2007, 2012.

[24] R. Chudamani, C. Ramalingam, and K. Vasudevan, “Non-linear least-squares-based harmonic estimation algorithm for a shunt active power filter,” IET Power Electronics, vol. 2, no. 2, pp. 134–146, 2009.

[25] S. Hu, X. Lin, Y. Kang, and X. Zou, “An Improved Low-Voltage Ride-Through Control Strategy of Doubly Fed Induction Generator During Grid Faults,” IEEE Transactions on Power Electronics, vol. 26, no. 12, pp. 3653–3665, 2011.

Muhammad Naveed belongs to the Khyber Pakhtunkhwa province (KPK) Pakistan. He has got his bachelor degree in electrical power engineering from COMSATS University of science and Technology Islamabad (Abbottabad Campus) in 2015 and MSc Degree in electrical Power engineering from University of engineering and technology Peshawar Pakistan in 2019. His research area is Low voltage Ride through (LVRT) control of grid interfaced wind turbine (wind power generation in large grid system).

IJEW 国际工程期刊 International Journal of Engineering Works انجینئرنگ کاموں کا بین الاقوامی جرنل

International Journal of Engineering Works
ISSN-p: 2521-2419
ISSN-e: 2409-2770
Vol. 6, Issue 12, PP. 570-575, December 2019
https://www.ijew.io/
https://doi.org/10.34259/ijew.19.612570575

Prefeasibility Analysis of Electric Power Generation from Municipal Solid Waste using RETScreen: A Case Study of Peshawar City

Muhammad Shabir khan[1], Muhammad Raheel[2], Muhammad humayun[3], Muhammad Naeem khan[4]
[1,2]USPCAS-E, University of Engineering & Technology, Peshawar
[3,4]University of Engineering & Technology, Peshawar
shabiruet555@gmail.com[1], raheel_khan740@yahoo.com[2],
humayunchemist@nwfpuet.edu.pk[3], khattak1962@yahoo.com[4]

Received: 15 October , Revised: 20 November, Accepted: 27 December

Abstract**—**The escalation in the level of municipal solid waste generation by mankind is the index of using natural resources in an unsustainable and ineffective manner while that pattern has continued and paved its way to the exhaustion of the natural resources and environmental changes. Pakistan is not confronted solely by the increase in population growth like the other developing countries but it has also an escalation in its Municipal Solid waste (MSW) generation. The concerned municipal corporation authorities are incapable to cope up with due to a boost in the increased urbanization. Energy from waste being renewable energy can generate a good enough amount of electricity; reduces greenhouse gas emissions, solid waste minimization as well as it's a good source for a circular economy. RETScreen Expert Software support tool has been used in this study to determine the prefeasibility analysis of electricity generation from Peshawar city municipal solid wastes suggesting power plant having capacity assumed to be of 10 MW using city mix municipal solid waste it's being analyzed that for a 10 MW system which can export 74,816 MWh of electricity to the grid and the revenue generation from that will be 11,970,503 CAD. While the GHG emission reduction would be 32,598 tons of CO_2 having a simple payback period of 7.7 years with a cost to benefit ratio of 1.5 hence from the result its recommended to have a waste to energy facility for the Peshawar city municipal solid waste.

Keywords**—** RETScreen, waste to energy, incineration, Landfill gas to energy, Solid waste in Peshawar

I. Introduction

The significant intense growth in worldwide population is linked with the economic growth which is headed to swift urbanization as well as industrialization, this concerned situation of the population altered the pattern of consumption of goods which eventually at the end of the day it direct to the propagation of municipal solid waste at an upsetting degree [1].The study by the World Bank approximates that currently nearly 1.3 billion tonnes of MSW are produced every year around the world or 1.2 kg/capita/day. The exactly actual per capita rates however, vary highly as there are enormous diversities in the waste generation rates across the countries, between cities and even within the cities and localities [2]. by 2025 this amount will reach to 2.2 billion tonnes per year which represents the substantial escalation in the per capita waste generation rates from 1.2 kg to 1.42 kg/person/day in the coming next fifteen years [3] several techniques and practices are in operation around the world to generate energy and utilize the MSW in environmental and cost-effective manner such as landfill gas to energy, to make a compost out of it, electric power generation from MSW by incineration, pyrolysis, and plasma gasification, etc. [4]

II. Current Municipal Soild Waste Situation in Pakistan

Pakistan is not confronted solely by the increase in population growth like the other developing countries however it has likewise an escalation in its generation of MSW. The concerned corporation authorities who deal with municipal solid wastes are incapable to cope up with due to a boost in the increased urbanization. In the season of monsoon, the issues of managing the waste worsen to that level that the big city ceases because the drainage gets jammed, blocked sewers system and standing effluent ponds.

Pakistan is in the list of the world densest and congested countries but still, date in any big cities of the country here is no appropriate management system for solid waste exists. The major and the most vital discarding process for MSW in the country has been open- landfilling and open-air dumping for several decades, though after agreeing and complying in 2005 with the Kyoto Protocol, Pakistan has anticipated and planned several projects over Clean development mechanism CDM in order to shrink its way of landfilling their MSW however still one can observe that these initiatives are not so far driven in the region as compared to its nearby countries due to absence of interest by the provincial and federal governments, funds, expertise and by the public as well.

The solid waste per day generation in Pakistan according to an approximates is almost 67,500 tonnes in which the probably waste picked would be only 50-69 % and these picked and collected mix waste has been sent to open dumps and landfills areas usually located on the outside of the cities while the remaining waste left there as it as on the roadsides, in storm drains, open water sewers which pollute water, air and poses serious health concern to the public [5]

i. MSW current mechanism in Peshawar city

The city of Peshawar is considered one of the big cities of the country almost generates 800-1000 tonnes of solid waste per day whereas 40-50% gets collected in the unsegregated form and being landfilled in open dumping. There are four different organization working relevant to solid waste collection and disposal i.e. WSSP, TMA, PDA, local council Board.

In the city to date there is no proper segregation, collection and waste to energy setup.

ii. Composition of Peshawar city municipal solid waste

The Peshawar city municipal solid wastes predominantly comprises of food wastes which usually includes fruits and vegetables, wood, paper products, wood straws, and wood materials (boards, chips, and cardboards), plastics, textiles, rubbers and packing materials of different utility items, etc. Major waste type and its composition being provided in the table [5]

Table I. MSW COMPOSITION OF PESHAWAR CITY [5]

Type	**Waste composition (%)**
Fruits and vegetable wastes	31.9
Plastics	20.4
Papers	13.1
Wood straws and tree trimmings	12.3
Textiles	8.7
Leather and rubbers	4.1
Non-flammable materials i.e. clay debris etc.	9.1

III. Literature Review

MSW is a term commonly referred as a waste or litter which comprises of different daily practice items usually that are thrown away after usage such items contains furniture’s, food scraps, grass clippings, clothing’s, bottles, product packaging newspapers, varied appliances while some of the waste such as batteries waste, paints others hazardous and industrial wastes are not measured as MSW.

The global world population grows rapidly and the standard of living of peoples also get rises due to which a huge trends develop in the daily consumption usage of goods and increase in energy utilization as well along with that deforestation and change in the land usage, increase in the agriculture practices, industrialization, and energy usage from conventional fossil fuels sources. Since considering all of these as a whole and their impact have been so large in the immense increase in the potential contribution to ever-increasing levels of greenhouse gases in the atmosphere since the industrial era revolution.

Pakistan is not confronted solely by the increase in population growth like the other developing countries but it has an escalation in its generation of MSW. The concerned municipal corporation authorities are incapable to cope up with due to a boost in the increased urbanization [5].

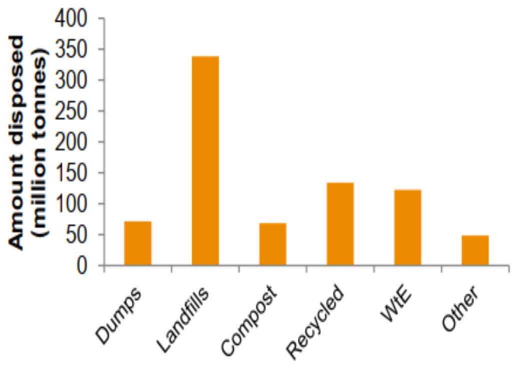

Figure 1: Quantity of waste disposed in 2012 by various processing techniques [9]

Countries like Pakistan which is the world sixth most populous country and its population increases rapidly but usually faces extreme level of energy crisis hence for Pakistan which has many environmental concern and energy issues the concept of electric power generation using waste to energy technology from municipal solid wastes would be a great matter of benefits, the electricity per unit price in Pakistan is almost higher due to a huge significant dependency on imported oil for power generation sectors as in the year 2011 oil import of the country were 40 % of the total imports such sort of situation has led the country trade deficit to 12 % in such circumstances where a country is running out of energy resources, the technology of energy generation from solid wastes which is considered as a renewable resource as well will be a good contribution to the energy mix of the country and can also bring down the energy cost per unit of electricity[6]MSW configuration differs greatly from country to country Depending on weather climate conditions, economic growth, culture, and energy sources utilization, where nation with low income have great portion of organic waste on the contrast MSW of high-income countries are greatly dominant by inorganic part [7].Different countries around the world have opted for and adopted the waste to energy technologies to produce energy, compost, and many useful products from solid waste as well as properly handling, disposing waste in sustainable and effective manner.

An approximation by the IRENA depicts that the world has a huge tremendous prospective of producing almost 1.3 Gigawatts of energy from the waste to the energy sector alone

[8] In the Fig 1. shown that the quantity of waste disposed/treated in millions of tons with the corresponding various treatment techniques the figure below clearly depicts that Landfilling is most common waste treatment techniques which is basically inefficient, environmentally polluting method.

A. *Waste to Energy*

The major and the most important aim of managing solid waste are material handling, collection, and recovering energy monitored by clearance of the residues, In waste processing technology the prime choice is not just to recover energy or waste demolition capacity or economic requirements but it's also to aspect and cater for environmental regulatory compliance of the relevant part that's why it's become mandatory to choose the finest accessible technology for treating wastes which have the tendency to match with the required standard criteria for a successful operation [10]. It's a great matter of concern and necessary to opt for a technology and usually selection of waste to energy technology depends on solid waste feedstock types, its composition, volatile components in the waste, end-use requirement, pollution control standards, economic and specific factors of the projects.

B. *Different Energy Recovery Pathways from MSW*

Several technologies developed around the globe in order to divert wastes from going to landfills the developing countries are focusing more on the innovation of the biological treatment (Composting) and incineration processes which can fit the MSW composition with high organic content. In order to obtain energy from MSW would greatly lessen solid waste, minimize the usage of conventional fuel which ultimately mitigate GHG emissions i.e. mitigating CH4 to CO2, Presently, in nearly 40 countries greater than 800 thermal WTE plants are functioned globally; which produces up to about a total of 429 TW h of power by treating approximately 11% of MSW generated worldwide [11]

Different WTE conversion processes exist in which the most important and greatly used processes are, a) thermal conversion which is further divided into incineration, gasification, pyrolysis b) biological conversion in which further it is classified into biomethanation or anaerobic digestion and composting process .c) landfilling with gas recovery [12]. Financial analysis and per kWh of energy generation of various waste treatments from MSW is provided in the Fig 2.

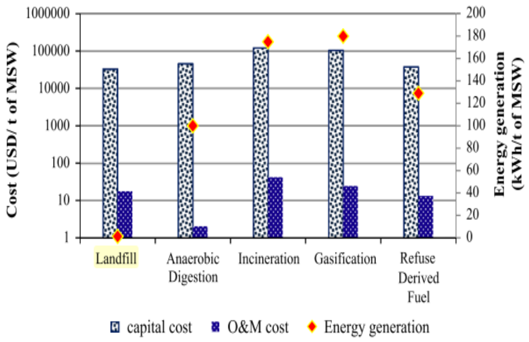

Figure 2: Energy production and financial analysis of WTE technologies [13]

IV. METHODOLOGY

a) *Study area of the Project*

The solid waste generation in the major cities of Pakistan has been trending due to huge urbanization and living standard of people. In this study Peshawar city as shown below in the map the provincial capital of Khyber-Pakhtunkhwa has been selected as a case study, as the city almost generates 800-1000 tonnes of solid wastes per day. RETScreen expert software analysis tool is used to assess the prefeasibility analysis of electric power generation from Peshawar city MSW.

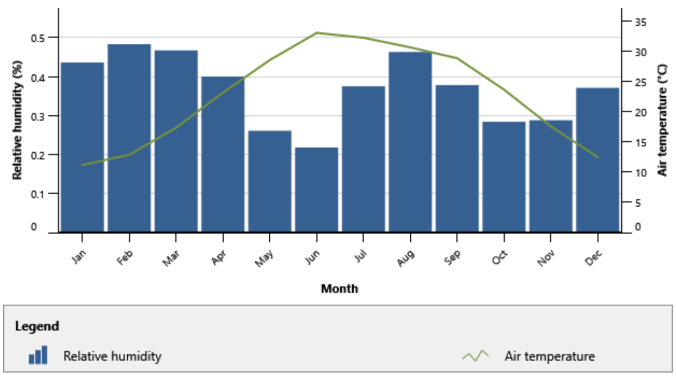

Figure 3.Peshawar city study area Climatic conditions

b) *Survey and data gathering*

In order to assess and direct about waste to energy plant, Composition of solid waste, the location of dumping grounds, waste to energy locality site selection, data from department of Tehsil Municipal Administration (TMA) Water and Sanitation Services Peshawar (WSSP), Local Governments has been gathered as much was possible.

c) *Studying different methods for energy recovery from municipal solid waste*

There are different Waste to energy plants operating around the world As in literature depicted that various methods for conversion of MSW to electricity generation i.e. Incineration, anaerobic digestion, pyrolysis, gasification and landfill gas to energy the type of technology selection greatly depends as it varies on the basis of the content it contained, type of solid waste, its economics and MSW processing capacity so based on the Peshawar region as it contained Mix of organic and inorganic fraction in combined as no proper solid waste management exists in the city and it also it get varies. Based upon the practices exists for waste to energy control incineration is considered to be one of the main techniques where the steam turbine is operating, along with the other reduce, reuse and recycle concept and RDF technologies can also be used as the solid waste also contain major fraction too of plastics waste.

d) Prefeasibility analysis through RETScreen

The RETScreen modeling tool is used for the Pre-feasibility analysis of the waste to energy generation from MSW of Peshawar city.

The ministry of natural resources Canada has developed clean energy management software called RETScreen Expert which provides Cost-effective and time-saving techniques to find the prefeasibility and feasibility analysis of any clean and green energy project rather than custom based conventional methods. The tool is used to assess the energy production of various renewables and clean energy technologies projects and it's used to find the integrated financial analysis of the project, Greenhouse gas emission reductions, different cash flows, sensitivity, and risk analysis. [14]. The concept of analysis in RETScreen Expert software workflow in the following manners as provided which contains the different parameters for the execution of any analysis type.

Figure 4: RETScreen analysis tool process cycle

V. Results And Discussion

RETScreen Expert as a decision support tool has been used to determine the prefeasibility analysis for a 10 MW power plant from the municipal solid waste of Peshawar city hence for the sake an analysis has been undertaken for the set up that either it is economically and environmentally viable or not.

1) Power plant type selection

Energy generation from Municipal solid waste is usually carried out using a steam turbine generator. Peshawar city MSW is a mix mixture of organic and inorganic content hence a detail prefeasibility analysis is carried out for a 10 MW capacity unit which will generate 74,816 MWh of electricity and fuel consumption is probably 63,707 tonnes.

2) Benchmark analysis

Benchmark analysis in RETScreen software is to make a comparative analysis of the proposed technology with base case technology in order to compare their energy performance, cost of a facility, GHG emissions, etc. These specific values of benchmark usually develop from the database of the software and clarify the view as an assumption of energy scenario, costs for the facility and GHG emissions and then after assuming benchmark values the most important then to estimate the performance and feasibility analysis, financial analysis, costs and revenue generated, greenhouse gas minimizations these can, later on, be updated as long as the data as an input obtained. In our case as a benchmark two types of the technology being selected by software using steam turbine i.e. one with fuel as coal and the other having MSW as a fuel and the benchmark unit appropriated as 0.22 CAD/KWh.

TABLE II: BENCHMARK ANALYSIS

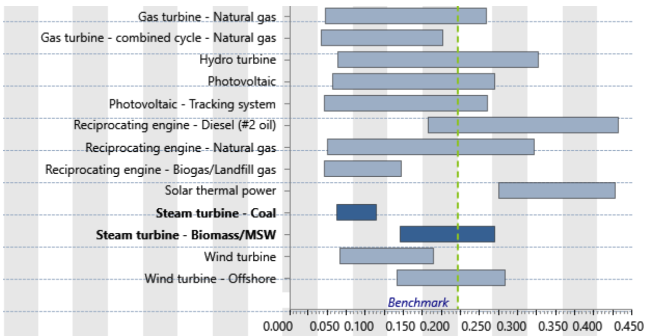

3) GHG emission reduction

The greenhouses gas mitigation by using proposed clean energy technology instead of conventional energy resources can be estimated from the emission analysis worksheet. In our study as we see that there are two cases i.e. one is the base case and other is the proposed case where there is a clear depiction that a huge quantity of GHG emission can be reduced using the proposed case .in a base case the GHG emission is 37,326 tCO_2 and can be minimized to a level in a proposed case to the extent is 4728.6t CO_2 hence the annual greenhouses gas (GHG) emission reduction potential is 32,598.1 tons of CO_2 which is as equivalent to 75809.5 barrels of crude oils being not consumed. The RETScreen provides a good platform to estimates how much greenhouses gases emission reduction cab be lessen if a clean energy being utilized instead of any conventional of fossil fuels based technology.it good compares in different format that is that much C02 can be reduced if number of cars and truck not to be used in transportation or that much of barrel of oils can be saved if that clean energy being used so it's a good foundation to estimate any green energy with various conventional technologies.

TABLE III. GHG EMISSIONS REDUCTION ANALYSIS

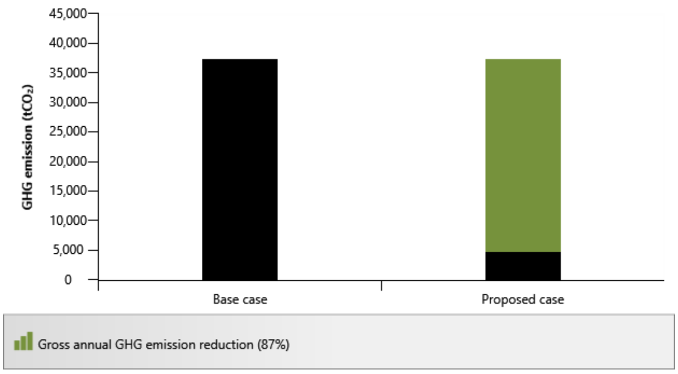

4) *Financial analysis of the project*

RETScreen decision support is one of the preliminary supportive tools in determining the financial analysis of any clean and green energy project hence it paves the way for investors or policymakers to proceed further with it or not. Different financial parameters as input exists from user input such as debt ratio, discount ratio, etc. and in return the software calculate internal rate of return IRR, net present value NPV, simple payback periods which allows the planners to have an overview of various financial parameters with great ease A description of these items relevance to the preliminary feasibility analysis, is included below. The fuel escalation rates are determined from current values of inflation rates as it gets varies in different range so Its opted an average of it is 9%. Discount rates are provided as being followed the range from various studies and NEPRA upfront tariff and the project life for such a project is usually considered for 25 years. Clean energy projects are usually majorly by government i.e. the government provides interest-free loan in the range of 40-70% so in our case its green project hence its opted to be 70 % and debt interest can be taken either zero as it interests free or in a range of 5-7%.

The different costs associated with it and the revenue that can be generated from the project is evaluated hence the parameters are not fixed as it gets vary the value should be varied as long as an optimum result are obtained and following the rules and regulation for the relevant energy projects is determined by each country.

TABLE IV. FINANCIAL VIABILITY ANALYSIS

Financial viability

Financial parameters

General		
Fuel cost escalation rate	%	9%
Inflation rate	%	9%
Discount rate	%	7%
Reinvestment rate	%	8%
Project life	yr	25
Finance		
Debt ratio	%	70%
Debt	$	63,300,909
Equity	$	27,128,961
Debt interest rate	%	7%
Debt term	yr	15
Debt payments	$/yr	6,950,100

Annual revenue

Electricity export revenue		
Electricity exported to grid	MWh	74,816
Electricity export rate	$/kWh	0.16
Electricity export revenue	$	11,970,503
Electricity export escalation rate	%	2%
Clean Energy (CE) production revenue		
CE production	MWh	74,816
CE production credit rate	$/kWh	0.04
CE production revenue	$	2,992,626
CE production credit duration	yr	0
CE production credit escalation rate	%	
Fuel type - Clean energy		Electricity exported to grid
Municipal solid waste	MWh	74,816

CONCLUSION

The Peshawar city MSW is increasing day by day due to huge urbanization in the city which poses serious health issues to the public, environment, soil and water contamination. Therefore, building a new WTE plant in Peshawar city is necessary in order to cope up with growing solid waste management and the energy crisis, is an urgent task for the local government. With incentives and support provided by the national government, waste to energy technologies exists in the world while the technology is usually based on the type of waste and moisture contents it contains hence from the literature studies steam turbine systems used for waste to energy projects Peshawar city generates almost 1000 ton/day hence for the first analysis base a 10 MW power plant set up is proposed in this study which yields a good amount of electricity and mitigates the potential greenhouse gases due to the high moisture and low heating value of MSW in Peshawar city a steam turbine generation unit has been proposed which will fetch to both the government and private investors a high financial benefit ultimately will consequence in several environmental benefits for the city of Peshawar.

REFERENCES

[1] A. Kumar and S. R. Samadder, "A review on technological options of waste to energy for effective management of municipal solid waste," *Waste Manag.*, vol. 69, pp. 407–422, 2017.

[2] P. Hoornweg, Daniel, Bhada-Tata, "What a waste - a global review on solid waste," vol. 1, no. 5, p. 116, 2012.

[3] D. Moya, C. Aldás, D. Jaramillo, E. Játiva, and P. Kaparaju, "ScienceDirect ScienceDirect Waste-To-Energy Technologies : an opportunity of energy recovery from Municipal Solid Waste, using Quito - Ecuador as case study," *Energy Procedia*, vol. 134, pp. 327–336, 2017.

[4] S. Aatif and M. Naeem Arbab, “Capacity Estimation of Power Generation from MSW of Peshawar City,” *Int. J. Comput. Appl.*, vol. 111, no. 15, pp. 40–45, 2015.

[5] M. J. S. Zuberi and S. F. Ali, “Greenhouse effect reduction by recovering energy from waste landfills in Pakistan,” *Renew. Sustain. Energy Rev.*, vol. 44, pp. 117–131, 2015.

[6] C. E. Palacio *et al.*, “Municipal Solid Waste Management and Energy Recovery José.”

[7] D. Moya, C. Aldás, G. López, and P. Kaparaju, “Municipal solid waste as a valuable renewable energy resource: A worldwide opportunity of energy recovery by using Waste-To-Energy Technologies,” in *Energy Procedia*, 2017.

[8] International Renewable Energy Agency (IRENA), 2016. Renewable EnergyStatistics.

[9] <http://www.irena.org/DocumentDownloads/Publications/IRENA_RE_Statistics_2016.pdf> (accessed 21.03.2017).

[10] World Energy Council, “World Energy Resources 2016,” *World Energy Counc. 2016*, pp. 6–46, 2016.

[11] G. Ali and N. A. Molla, “Selection of Appropriate Technology for Solid Waste Management: A Case of Thammasat Hospital, Thailand. Himalayan Adaptation, Water and Resilience (HI-AWARE) Research View project Climate change policies in Asia View project,” no. April, 2010.

[12] S. T. Tan, W. S. Ho, H. Hashim, C. T. Lee, M. R. Taib, and C. S. Ho, “Energy, economic and environmental (3E) analysis of waste-to-energy (WTE) strategies for municipal solid waste (MSW) management in Malaysia,” *Energy Convers. Manag.*, vol. 102, pp. 111–120, 2015.

[13] K. A. Kalyani and K. K. Pandey, “Waste to energy status in India: A short review,” *Renew. Sustain. Energy Rev.*, vol. 31, pp. 113–120, 2014.

[14] R. Intharathirat and P. Abdul Salam, “Valorization of MSW-to-Energy in Thailand: Status, Challenges and Prospects,” *Waste and Biomass Valorization*, vol. 7, no. 1, pp. 31–57, 2016.

[15] D. Moya, J. Paredes, and P. Kaparaju, “Technical , financial , economic and environmental pre-feasibility study of geothermal power plants by RETScreen – Ecuador ’ s case study,” *Renew. Sustain. Energy Rev.*, vol. 92, no. December 2017, pp. 628–637, 2018.

.